AD-A276 206

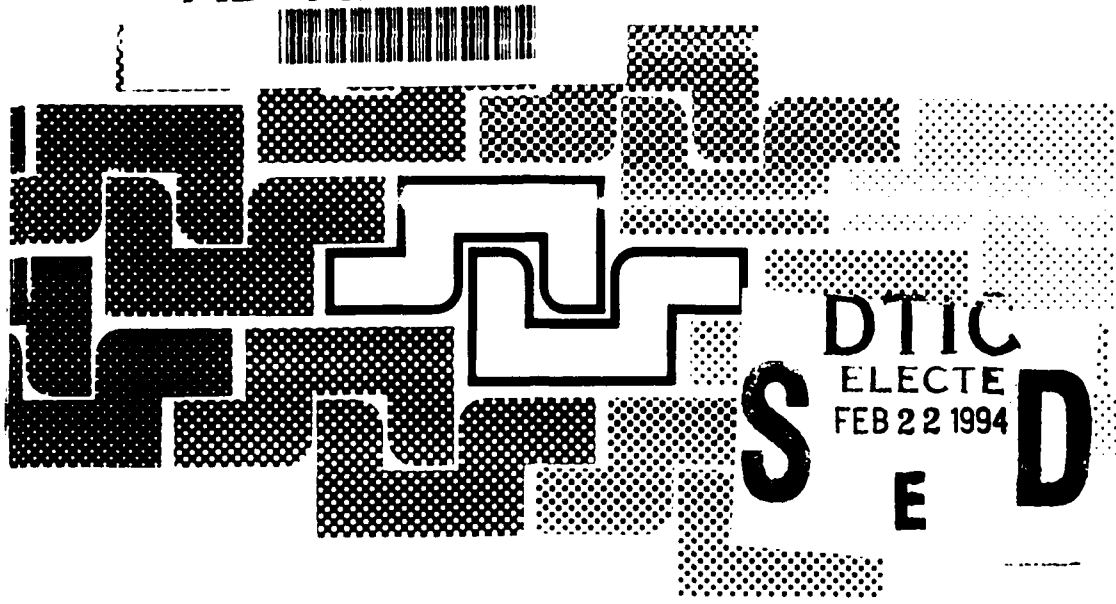

DTIC
ELECTE
FEB 22 1994
S E D

Approved for public release
Distribution unlimited

94-05421

Probabilistic and Stochastic Methods in Analysis, with Applications

Edited by

J. S. Byrnes, Jennifer L. Byrnes,
Kathryn A. Hargreaves and Karl Berry

94 2 18 029

NATO ASI Series

Series C: Mathematical and Physical Sciences - Vol. 372

Probabilistic and Stochastic Methods in Analysis, with Applications

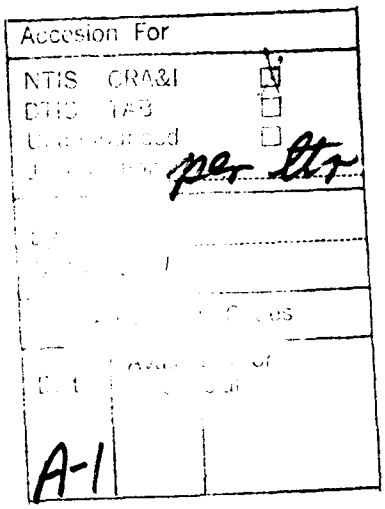

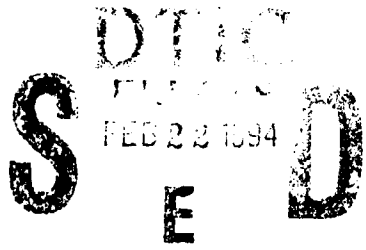

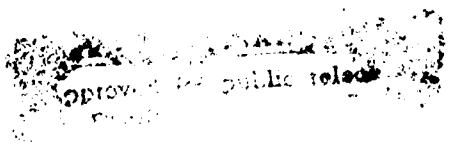

DISCLAIMER NOTICE

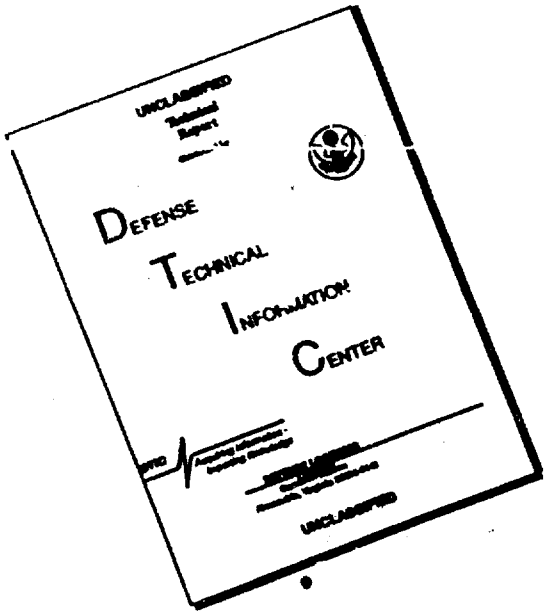

THIS DOCUMENT IS BEST QUALITY AVAILABLE. THE COPY FURNISHED TO DTIC CONTAINED A SIGNIFICANT NUMBER OF PAGES WHICH DO NOT REPRODUCE LEGIBLY.

NATO ASI Series

Advanced Science Institutes Series

A Series presenting the results of activities sponsored by the NATO Science Committee, which aims at the dissemination of advanced scientific and technological knowledge, with a view to strengthening links between scientific communities.

The Series is published by an international board of publishers in conjunction with the NATO Scientific Affairs Division

A Life Sciences **B Physics**	Plenum Publishing Corporation London and New York
C Mathematical and Physical Sciences **D Behavioural and Social Sciences** **E Applied Sciences**	Kluwer Academic Publishers Dordrecht, Boston and London
F Computer and Systems Sciences **G Ecological Sciences** **H Cell Biology** **I Global Environmental Change**	Springer-Verlag Berlin, Heidelberg, New York, London, Paris and Tokyo

NATO-PCO-DATA BASE

The electronic index to the NATO ASI Series provides full bibliographical references (with keywords and/or abstracts) to more than 30000 contributions from international scientists published in all sections of the NATO ASI Series.
Access to the NATO-PCO-DATA BASE is possible in two ways:

- via online FILE 128 (NATO-PCO-DATA BASE) hosted by ESRIN, Via Galileo Galilei, I-00044 Frascati, Italy.

- via CD-ROM "NATO-PCO-DATA BASE" with user-friendly retrieval software in English, French and German (© WTV GmbH and DATAWARE Technologies Inc. 1989).

The CD-ROM can be ordered through any member of the Board of Publishers or through NATO-PCO, Overijse, Belgium.

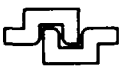

Series C: Mathematical and Physical Sciences - Vol. 372

Probabilistic and Stochastic Methods in Analysis, with Applications

edited by

J. S. Byrnes
Prometheus Inc., Newport, RI and
University of Massachusetts, Boston, MA, U.S.A.

Jennifer L. Byrnes
Harvard University, Cambridge, MA, U.S.A.

Kathryn A. Hargreaves
Free Software Foundation, Cambridge, MA and
Prometheus Inc., Newport, RI, U.S.A.

and

Karl Berry
Free Software Foundation, Cambridge, MA and
Prometheus Inc., Newport, RI, U.S.A.

Kluwer Academic Publishers

Dordrecht / Boston / London

Published in cooperation with NATO Scientific Affairs Division

Proceedings of the NATO Advanced Study Institute on
Probabilistic and Stochastic Methods in Analysis, with Applications
Il Ciocco, Italy
July 14–27, 1991

Library of Congress Cataloging-in-Publication Data

Probabilistic and stochastic methods in analysis, with applications
proceedings of the NATO advanced study institute, Il Ciocco, Italy,
July 14-27, 1991 / edited by J.S. Byrnes ... [et al.].
p. cm. -- (NATO ASI series. Series C, Mathematical and
physical sciences ; vol. 372)
"Published in cooperation with NATO Scientific Affairs Division."
Includes bibliographical references and index.
ISBN 0-7923-1804-8 (HB : acid-free paper)
1. Stochastic analysis--Congresses. 2. Probabilities--Congresses.
3. Mathematical analysis--Congresses. I. Byrnes, J. S. II. North
Atlantic Treaty Organization. Scientific Affairs Division.
III. Series: NATO ASI series. Series C, Mathematical and physical
sciences ; no. 372.
QA274.2.P77 1992
519.2--dc20 92-11225

ISBN 0-7923-1804-8

Published by Kluwer Academic Publishers,
P.O. Box 17, 3300 AA Dordrecht, The Netherlands.

Kluwer Academic Publishers incorporates the publishing programmes of
D. Reidel, Martinus Nijhoff, Dr W. Junk and MTP Press.

Sold and distributed in the U.S.A. and Canada
by Kluwer Academic Publishers,
101 Philip Drive, Norwell, MA 02061, U.S.A.

In all other countries, sold and distributed
by Kluwer Academic Publishers Group,
P.O. Box 322, 3300 AH Dordrecht, The Netherlands.

Printed on acid-free paper

All Rights Reserved
© 1992 Kluwer Academic Publishers
No part of the material protected by this copyright notice may be reproduced or utilized in any form or by any means, electronic or mechanical, including photocopying, recording or by any information storage and retrieval system, without written permission from the copyright owner.

Printed in the Netherlands

Acknowledgements

Financial support for the conference and this volume, from the following organizations and individuals, is gratefully acknowledged:

NATO, Dr. Louis V. da Cunha
AFOSR, Dr. Jon Sjogren and Dr. Arje Nachman
EOARD, Colonel Parris Neal
NSF, Dr. Anthony M. Boccanfuso
ONR, Dr. Neil Gerr
ONREUR, Dr. Robert Ryan
Prometheus Inc.
University of Massachusetts at Boston

This work relates to Department of the Navy Grant N00014-91-J-9031 issued by the Office of Naval Research European Office. The United States has a royalty-free license throughout the world in all copyrightable material contained herein.

Colophon

This book was designed by Karl Berry and Kathryn A. Hargreaves. They typeset it using TEX, developed by Donald E. Knuth. The text is set in Palatino, and the mathematics in Euler, both designed by Hermann Zapf. The heads are set in bold Helvetica, designed by Max Miedinger.

The camera-ready copy was produced in PostScript on a Hewlett Packard LaserJet IIP. Some figures were pasted in by hand.

Cross-referencing, indexing, and the various tables of contents were done automatically, using the Eplain macros written by Karl Berry and others, as well as (many) additional macros.

Preface

> *It is probably true quite generally that in the history of human thinking the most fruitful developments frequently take place at those points where two different lines of thought meet. Hence, if they actually meet, that is, if they are at least so much related to each other that a real interaction can take place, then one may hope that new and interesting developments may follow.*
>
> ***Werner Heisenberg***

This volume contains papers presented at the July 1991 NATO Advanced Study Institute *Probabilistic and Stochastic Methods in Analysis with Applications*. The conference was held at the beautiful Il Ciocco resort near Lucca, in the glorious Tuscany region of northern Italy. The dynamic interaction between world-renowned scientists from the usually disparate communities of pure mathematicians and applied scientists, which occurred at our 1989 ASI, *Fourier Analysis and its Applications*, continued at this meeting.

Probability has been an important part of mathematics for more than three centuries. Moreover, its importance has grown in recent decades with continuing increases in computational power. Faster and more powerful digital computers, now readily available to almost all scientists, have enabled them to use probabilistic and stochastic techniques to attack real-world problems not considered feasible only a few years ago. This approach has been used in such engineering areas as: speech and image processing, including the recent approaches employing wavelets, geophysical exploration, radar, sonar, etc.—and was a major focus of our ASI.

Among the papers to be found herein on these subjects are three exceptionally clear expositions on wavelets, frames, and their applications by John Benedetto, Stéphane Jaffard, and Stéphane Mallat; an illuminating description of holography and other image processing techniques by Walter Schempp; and interesting works on sampling theory and methods by Charly Gröchenig, Bill Heller, Christian Houdré, Keh-Shin Lii, and Tapan Sarkar.

Part of the conference was devoted to the connections between probability and partial differential equations, an area of extremely active current research. The reader will see how these fields have united, yielding new insight into known analytic facts, such as probabilistic representations of solutions to elliptic and parabolic PDE's. Furthermore, this unification is providing both new and simplified approaches to classical problems in probability, such as the PDE method for large deviation problems. Highlights of this section of the proceedings are in-depth introductions to stochastic optimal control and filtering theory—both new research fields of particular

interest for applications, presented by two recognized experts, Piermarco Cannarsa and Gopinath Kallianpur.

Another part of the conference dealt with the application of probabilistic techniques to mathematical analysis. The lovely paper by Jean-Pierre Kahane, a true pioneer in this field, is a standout among the many wonderful works in this volume. Babar Saffari, describing the use of probability methods in Fourier analysis, presents a very complex subject with exceptional clarity.

Finally, there are several papers which are difficult to categorize but a joy to read. Two such are Gavin Brown's clear explanation of normal numbers and dynamical systems, and Don Newman's thought-provoking foray into those aspects of probability which have a profound influence upon our daily lives.

The cooperation of many individuals and organizations was required in order to make the conference the success that it was. The financial sponsors are listed on the 'Acknowledgements' page. In addition, I wish to express my sincere appreciation to my assistants, Marcia and Jennifer Byrnes and Nicole Conte, for their invaluable aid. I am also grateful to Kathryn Hargreaves and Karl Berry, our TEXnicians, for their superlative work on all printed and emailed aspects of the conference, from the initial application to this volume. Their extraordinary effort in TEXing these proceedings, resulting in one of the few NATO proceedings where all papers are identically typeset, deserves special acclamation. Finally, my heartfelt thanks to the Il Ciocco staff, especially Bruno Giannasi and Alberto Suffredini, for offering an ideal setting, not to mention the magnificent meals, that promoted the productive interaction between the participants of the conference. All of the above, the other speakers, and the remaining conferees, made it possible for our Advanced Study Institute, and this volume, to fulfill the stated NATO objectives of disseminating advanced knowledge and fostering international scientific contacts.

December 25, 1991 *Jo Barry A. Cipra, Ria de Janeiro*

Contents

I

Wavelets and fractals

Wavelets and analysis of partial differential equations

Stéphane Jaffard
C.E.R.M.A.
Ecole Nationale des Ponts et Chaussées
La Courtine, 93167 Noisy-le-grand France
sj@antigone.enpc.fr

Abstract We describe the main properties of decompositions in orthonormal bases of wavelets. We then apply them to the theoretical and numerical study of some partial differential equations.

1. Introduction

In the seventies and the eighties, alternative methods to Fourier analysis appeared independently in many fields of science and technology. Let us mention oil detection, analysis of speech, quantum mechanics, image analysis, analysis of turbulent flows, multigrid methods, the theory of interpolation between functional spaces, the propagation of singularities of nonlinear partial differential equations PDE's, etc.

Wavelets comprise a mathematical tool which lies behind these new methods. We have two purposes in this paper. We give a survey of the construction of wavelets and related orthonormal bases, and we also show how certain specific properties of wavelets make them an important tool in the theoretical and numerical study of PDE's. We also give at the end a large bibliography.

2. Localization in the phase space

The mathematical evolution that led to wavelets and related constructions can be interpreted as the construction of successive bases of functions with the following aim: the decomposition on these bases yields the sharpest possible information on the time and frequency behavior of the analysed signal or function.

Such constructions are important in signal analysis (a recording of speech or music clearly contains localized parts which have a specific frequency), in quantum mechanics (to study probability waves) or in the study of partial differential operators.

J. S. Byrnes et al. (eds.), Probabilistic and Stochastic Methods in Analysis, with Applications, 3–13.
© 1992 *Kluwer Academic Publishers. Printed in the Netherlands.*

The first step was obtained by the Fourier series. The two main drawbacks of Fourier analysis are that it is not local and that it is difficult to use when dealing with other spaces than L^2 or the Sobolev spaces H^s.

The problem of having a stable decomposition for other spaces than L^2 led Alfred Haar to the so-called Haar system constructed as follows.

Let ϕ be the characteristic function of $[0, 1/2]$, and $\psi = \phi(x) - \phi(x-1/2)$. The collection of all the $\psi_{j,k}$ ($j \in Z$, $k \in Z$), defined by

$$\psi_{j,k}(x) = 2^{j/2}\psi(2^j x - k)$$

forms an orthonormal basis of $L^2(\mathfrak{R})$, and the decomposition makes sense also in the L^p spaces. The drawback is that the decomposition on this system does not give sharp frequency information, since the function ψ does not have a good frequency localization. Wavelets provide a way to avoid this.

Before describing the constructions of wavelet and wavelet-type bases, let us give some general results on "doubly-localized" orthonormal bases.

T. Steger proved [3] that L^2 does not admit a basis of the following form

$$f_j(x) = e^{ib_j x} g_j(x - a_j)$$

where the g_j would be such that $\sup \| g_j \|_\epsilon < \infty$, for an $\epsilon > 0$, where

$$\| g_j \|_\epsilon^2 = \int (1 + x^2)^{1+\epsilon} \, | g(x) |^2 \, dx + \int (1 + \xi^2)^{1+\epsilon} \, | \hat{g}(\xi) |^2 \, d\xi.$$

The optimal result was obtained by J. Bourgain who found a basis where this estimate holds with $\epsilon = 0$ (see [3]).

Actually, if we accept to mix in the same function positive and negative frequencies of the same value, this obstruction no more stands, and there exists an orthonormal basis of $L^2(\mathfrak{R})$ of the following form (see [9])

$$\psi_{0,n}(x) = \phi(x - n)$$
$$\psi_{l,n}(x) = \sqrt{2}\phi(x - \tfrac{n}{2}) \cos(2\pi l x) \text{ if } l \neq 0, l + n \in 2\mathbf{Z}$$
$$= \sqrt{2}\phi(x - \tfrac{n}{2}) \sin(2\pi l x) \text{ if } l \neq 0, l + n \in 2\mathbf{Z} + 1,$$

where ϕ and $\hat{\phi}$ have exponential decay.

The fact that we do not try to separate positive and negative frequencies of the same amplitude means, in the signal analysis terminology, that we study the real signal, and not the corresponding analytical signal.

Independently, H. Malvar (see [25]) obtained a basis of the following similar form

$$u_{k,l} = w(x - l) \sin[\pi(k + \tfrac{1}{2})(x - l)],$$

where w is compactly supported.

R. Coifman and Y. Meyer generalized this construction into the completely adaptative form that follows (see [4])

$$u_{k,l} = \sqrt{\frac{2}{L_l}} w_l(x) \sin\left[\pi(k+\tfrac{1}{2})\frac{x-a_l}{L_l}\right]$$

where a_l is an increasing sequence of real numbers such that $a_l \to +\infty$ when $l \to +\infty$ and $a_l \to -\infty$ when $l \to -\infty$; $L_l = a_{l+1} - a_l$ and w_l is compactly supported, essentially on the interval $[a_l, a_{l+1}]$.

More precisely, let ϵ_l satisfy $a_l + \epsilon_l < a_{l+1} - \epsilon_{l+1}$. Then one chooses w_l such that

- $0 \leqslant w_l(x) \leqslant 1$,
- $w_l(x) = 1$ on $[a_l + \epsilon_l, a_{l+1} - \epsilon_{l+1}]$,
- $w_l(x) = 0$ outside $[a_l - \epsilon_l, a_{l+1} + \epsilon_{l+1}]$,
- if $x \in [a_l - \epsilon_l, a_l + \epsilon_l]$, $w_l(x) = w_{l-1}(2a_l - x)$ and $w_l^2(x) + w_{l-1}^2(x) = 1$.

Notice that in order to compute the coefficients of a function on such a basis, we need to perform a pointwise multiplication, and then to compute Fourier coefficients. Clearly, the whole decomposition is obtained in $O(N \log(N))$ operations.

We have here a huge collection of orthonormal bases, roughly speaking, as many as the possible partitions of $\mathfrak{R}$ by segments of arbitrary length. This richness will be used for data compression: for a given signal, we want to determine a basis on which the signal has the "smallest" decomposition. For that, we need an algorithm which allows us to go easily from one basis to another. Let us describe the following recipe due to V. Wickerhauser ([5]).

Let A_l be the space spanned by the $(u_{k,l})_{k \in Z}$ (which are the functions corresponding to a given window). The space $A = A_l \cup A_{l+1}$ has exactly the same structure as a space A_m, with a window between a_l and a_{l+2}, and a function w which is

$$w(t) = \sqrt{w_l^2(x) + w_{l+1}^2(x)}.$$

Hence, we can replace two adjacent windows by a larger one without changing anything else.

The algorithm of representation of a function is the following: for a given f, we start by its decomposition using small windows all of the same width, and we merge two such windows, when there is an advantage in doing so. We iterate this procedure as long as needed, and obtain at the end a segmentation adapted to the signal. We still have to choose a criterion for deciding when we merge two windows together. The one chosen is given by a kind of "entropy minimization".

Suppose we have a familly of orthonormal bases $e_j^{(\alpha)}(t)$. For each α the signal f is decomposed on the corresponding orthonormal basis by

$$f(t) = \sum_j c_j^{(\alpha)} e_j^{(\alpha)}(t)$$

and we want to minimize the entropy

$$E^{(\alpha)} = -\sum_j \left|c_j^{(\alpha)}\right|^2 \log\left|c_j^{(\alpha)}\right|.$$

At each step, we calculate the entropy for the two windows and for the large one, and we merge the windows if the corresponding entropy decreases.

3. Construction of wavelets and wavelet packets

3.1. Multiresolution analysis

We shall now describe another collection of bases, which are a generalization of the classical wavelets, and will also supply a family of orthonormal bases for which the same entropy minimization algorithms are used. But let us first recall the construction of wavelets by a multiresolution analysis and the fast wavelet decomposition, both introduced by S. Mallat (see [24]). We shall stick to the dimension 1 for the sake of simplicity. A multiresolution analysis is an increasing sequence $(V_j)_{j\in Z}$ of closed subspaces of L^2 such that

- $\bigcap V_j = \{0\}$
- $\bigcup V_j$ is dense in L^2
- $f(x) \in V_j \Leftrightarrow f(2x) \in V_{j+1}$
- $f(x) \in V_0 \Leftrightarrow f(x+1) \in V_0$
- There is a function g in V_0 such that the $g(x-k)_{k\in Z}$ form a Riesz basis of V_0.

We also require g to be smooth and well localized.

A simple example of multiresolution analysis is obtained by taking for V_j the space of continuous and piecewise linear functions on the intervals $[k2^{-j}, (k+1)2^{-j}]$, $j,k \in Z$. A possible choice for g is the "hat" function, which is the function of V_0 taking the value 1 for $x = 0$ and vanishing at the other integers. It is easy to orthonormalise the set $g(x-k)$ by choosing

$$\hat{\phi}(\xi) = \hat{g}(\xi)\left(\sum |\hat{g}(\xi + 2k\pi)|^2\right)^{-1/2}.$$

Then, the $\phi(x-k)$ form an orthonormal basis of V_0.

Define W_j as the orthogonal complement of V_j in V_{j+1}. One immediately checks that the W_j are mutually orthogonal, and their direct sum is

equal to L^2. By a similar procedure which led to the construction of ϕ, we can obtain a function ψ such that the $\psi(x-k)$ form an orthonormal basis of W_0. Since the W_j are obtained from each other by dilation, and are mutually orthogonal, the functions $2^{j/2}\psi(2^j x-k)$ form an orthonormal basis of $L^2(\mathfrak{R})$.

Let us now come back to the orthogonal decomposition

$$V_0 = V_{-1} \bigoplus W_{-1}. \tag{3.1}$$

We have two orthonormal bases of V_1: the first one is the $\sqrt{2}\phi(2x-k)$, $k \in Z$, and the second one is the union of the $\phi(x-k)$ and $\psi(x-k)$.

The existence of two bases implies the existence of an isometry mapping the coordinates in the first basis on the coordinates in the second basis. Let us describe more precisely this isometry. Let h_k and g_k be

$$h_k = \frac{1}{2}\int \phi(x/2)\bar{\phi}(x-k)dx$$
$$g_k = \frac{1}{2}\int \psi(x/2)\bar{\phi}(x-k)dx.$$

Let $f \in V_0$ and let us write its decomposition on the two bases of V_0 given by (3.1).

$$\begin{aligned} f(x) &= \sum c_k^0 \phi(x-k) \\ &= \sum_l c_l^1 \tfrac{1}{\sqrt{2}}\phi\left(\frac{x}{2}-l\right) + \sum_l d_l^1 \tfrac{1}{\sqrt{2}}\psi\left(\frac{x}{2}-l\right), \end{aligned}$$

so that

$$\begin{aligned} c_l^1 &= \left\langle f \middle| \tfrac{1}{\sqrt{2}}\phi\left(\tfrac{x}{2}-l\right)\right\rangle \\ &= \sum_k c_k^0 \left\langle \phi(x-k) \middle| \tfrac{1}{\sqrt{2}}\phi\left(\tfrac{x}{2}-l\right)\right\rangle \\ &= \tfrac{1}{\sqrt{2}}\sum_k c_k^0 h_{k-2l}, \end{aligned}$$

and, similarly

$$d_l^1 = \tfrac{1}{\sqrt{2}}\sum_k c_k^0 g_{k-2l}$$

Suppose now that a signal is given by a sequence of discrete values c_k^0. We can consider that it is the coefficients of a function of V_0 on the $\phi(x-k)$. The isometry transforming the sequence c_k^0 into (c_k^1, d_k^1) can be written $F = (F_0, F_1)$ where F_0 and F_1 are commuting with even translations: they are discrete convolutions where we only keep each other term. In the terminology of signal analysis, F_0 and F_1 are said to be quadrature mirror filters. This notion

has been introduced in 1977 by D. Esteban and C. Galand for improving the quality of digital transmission of sound. Iterating $|j|-1$ times the filter F_0 and then applying once the filter F_1, we obtain the coefficients on the $\psi_{j,k}$ for $j \leqslant 0$. Each level requires only a discrete convolution. This algorithm constitutes the fast wavelet transform (see [24]). Of course the decision to apply F_0 n_j times and F_1 once is rather arbitrary, and we could decide to randomly apply F_0 and F_1 a certain number of times. This idea leads to wavelet packets which are a family of orthonormal bases of L^2 corresponding to all the "admissible" ways of applying these filters.

Let us come back to our initial problem of finding bases well localized in phase space. The adaptative Fourier windows and the wavelet packets do not give a satisfactory answer to this problem. It is therefore remarkable that, though they do not have this type of localization, they provide very efficient data compression algorithms. But the problem of finding an adaptative algorithm which gives good localization in phase space is still open (by good, we mean comparable to the localization of any of the commonly used wavelet bases). Because of this lack of localization, up to now only the "classical wavelets" have been used to study operators and PDE's, and therefore, only these bases will appear in the following.

4. Analysis of partial differential equations

4.1. Wavelet method for elliptic problems

Consider an elliptic problem, such as the Poisson problem, on a bounded domain. Let us first recall some properties of its resolution by Galerkin methods based on finite elements or of finite differences.

One of the main difficulties in these methods is that, once the problem has been properly discretized, one has to solve a system which is ill-conditioned. Typically, for a second order elliptic problem in two dimensions, one obtains a matrix M such that

$$\kappa = \|M\| \, \|M^{-1}\| = O(1/h^2)$$

where h is the size of the discretization (see [28]). Such ill-conditioning has two drawbacks; it leads to numerical instabilities and to slow convergence for iterative resolution algorithms. In order to avoid this problem, one usually uses a preconditioning, which amounts to finding an easily invertible matrix D such that $D^{-1}MD^{-1}$ (or $D^{-1}M$, depending on the method used) will have a better condition number κ. For the example we considered, the usual preconditioning methods on general domains (SSOR or DKR on a conjugate gradient method, for instance) make κ become $O(1/h)$. We shall give a wavelet method for which $\kappa = O(1)$ (see[13]). This result requires

the construction of wavelets adapted to the domain Ω (see [17]); they are an orthonormal basis of $L^2(\Omega)$ composed of functions $\psi_{j,k}$ ($j \geq 0$) such that

$$| \partial^\alpha \psi_{j,k}(x) | \leq C 2^{j\alpha} 2^{nj/2} \exp(-\gamma 2^j | x - k2^{-j} |)$$

for $| \alpha | \leq 2m - 2$, and a positive γ.

The decay estimates show that $\psi_{j,k}$ and its partial derivatives are essentially centered around $k2^{-j}$ with a width 2^{-j}. In the following, wavelets will be indexed by $\lambda = k2^{-j}$.

Actually, though these wavelets are not the same as in the case $\Omega = \mathfrak{R}^n$, they are "almost" the same; that is, numerically, only the wavelets that are close to the boundary are modified. Thus, we can essentially keep the fast decomposition algorithms, with only small modifications near the boundary.

Let us now describe the method of resolution for the Poisson equation. It is performed by a standard Galerkin method, keeping all the wavelets up to a frequency J_0. If we solve a Laplacian on a domain with Dirichlet boundary conditions, we have to invert a matrix

$$(M_{\lambda,\lambda'}) = (\langle \nabla \psi_\lambda \mid \nabla \psi_{\lambda'} \rangle).$$

We now renormalize the wavelets for the Sobolev H^1 norm, that is we consider that the functions on which the problem is discretized are the

$$\psi'_\lambda = 2^{-j} \psi_\lambda.$$

The condition number of the corresponding matrix is then bounded independently of the size discretization $h = 2^{-J_0}$. Thus, a conjugate gradient method will converge in a bounded number of steps, no matter how precise we require the solution to be. We shall explain this result in the next part by comparing it with multigrid algorithms. Let us also mention that, if we use smooth wavelets, the order of accuracy of the method is extremely good since it is driven by the *local* regularity of the problem (as opposed to spectral methods, for instance).

4.2. Wavelet and multigrid algorithms

A conjugate gradient method converges slowly when the condition number is large. Actually, the convergence is rather fast on the subspaces corresponding to the largest eigenvalues, but slow for the small eigenvalues. For an elliptic problem, small eigenvalues are associated to smooth, slowly oscillating functions (i.e., to wavelets indexed by a small j), and large eigenvalues to high frequency functions (i.e., to wavelets indexed by a large j).

Roughly speaking, in a multigrid method, one starts by making a few steps of conjugate gradient, until the high frequency component of the solution is well approximated; the error is then a comparatively low

frequency function, which can thus be accurately calculated on a grid with a double-size mesh. The resolution on the larger grid is performed again by the same method, and one iterates this procedure. The part of the solution which has frequencies around 2^i is thus calculated on the grid of size 2^{-i}. This is precisely what is performed on the wavelet method we described. The splitting on functions defined on meshes of different sizes (which is done in multigrid algorithms) is also performed by the wavelet decomposition. The essential difference is the following: it is the decomposition on wavelets and the recomposition which is iterative (by the fast algorithms described in section 2.2), but the resolution is just done once by a conjugate gradient. Actually, when the function is written in its wavelet decomposition

$$f = \sum_i \sum_k C_{j,k}\psi_{j,k},$$

each block $\sum_k C_{j,k}\psi_{j,k}$ has its frequencies around 2^i, so that the purpose of the renormalisation that we make (multiply the terms of this block by 2^{-i}) is to bring all the eigenvalues of the matrix M close together so that a conjugate gradient will converge fast. The multigrid method just works the other way round: the iterative decomposition according to the frequencies is performed during the resolution.

4.3. Analysis of singular operators

Let us mention a recent extension of the ideas developed in Section 4.1 to obtain estimates of the Green function of some singular elliptic operators (see [12]). Consider the following operator

$$A(u) = -\nabla(a\nabla u) + u$$

where the function a is positive, smooth, but may vanish. Suppose furthermore that a has a zero of order larger than 2 where it vanishes. Then the following estimates on the Green function of A and its derivatives hold

$$|\partial_x^\alpha \partial_y^\beta G(x,y)| \leq \frac{C}{|x-y|^{n-2+|\alpha|+|\beta|} \sup(\sqrt{a(x)a(y)}, |x-y|^2)}.$$

This is obtained, as in the case of elliptic operators, by showing that A and A^{-1} are "almost diagonal" in a wavelet basis.

5. Nonlinear evolution equations

The numerical study of nonlinear evolution equations is a field where wavelets should be very useful. The solutions of these equations often have singularities which then propagate (even when the initial value is

smooth). The local analysis of the regularity performed by wavelets and their properties of local approximation (see [16, 15]) can give ground to a justification of this hope. Several numerical experiments have been done for the one-dimensional Burgers equation (see for instance [11, 21, 22]). A recent extension to Korteweg de Vries equation has also been implemented ([18]). Consider the following Burgers equation to which is added a small viscosity term

$$\frac{\partial u}{\partial t} + \frac{\partial}{\partial x}(u^2) = \epsilon \frac{\partial^2 u}{\partial x^2}.$$

The methods used all consist of a finite difference discretization in time and a wavelet decomposition in space. A possible scheme is the following

$$\frac{U_{n+1} - U_n}{\Delta t} + U_n \frac{\partial U_n}{\partial x} = \epsilon \frac{\partial^2 U_n}{\partial x^2},$$

where U_n represents the solution at the time $n\Delta t$. Here the nonlinear term is treated explicitely, but the viscosity term appears implicitely. Knowing U_n by its wavelets coefficients, we want to calculate U_{n+1}. In order to compute the wavelet coefficients of the nonlinear term $U_n \frac{\partial U_n}{\partial x}$, we can either compute the values of U_n and $\frac{\partial U_n}{\partial x}$ on a regular grid (using the Fast Wavelet Transform) or try to obtain more or less explicit formulas for the wavelet coefficients of such products (this last issue is now studied). The choice of an implicit algorithm obliges us to compute $(\mathrm{Id} - \epsilon \Delta t \frac{\partial^2}{\partial x^2})^{-1}$ of a function given by its wavelet decomposition. This is performed by computing once for all

$$\left(\mathrm{Id} - \epsilon \Delta t \frac{\partial^2}{\partial x^2}\right)^{-1} (\psi_{j,k}) = \theta_{j,k}.$$

Since this computation is rather costly, it doesn't allow for changing the time scale Δt during the calculation. An explicit scheme using different time scales is being studied by Bacry, Mallat and Papanicolaou at the Courant Institute. These methods give the solution with a very good accuracy, especially near the shock where the oscillations are small and very well localized. Adaptative schemes with a local refinement around the shock are studied. The tracking of the shock is very easy since it takes place where the large wavelet coefficients are.

6. Bibliography

[1] E.H. Adelson, E. Simoncelli, and R. Hingorani. Orthogonal pyramid transforms for image coding. *Vision. Comm. and Image Proc.*, 845, 1987.

[2] F. Argoul, A. Arnéodo, G. Grasseau, Y. Gagne, E.J. Hopfinger, and U. Frisch. Wavelet analysis of turbulence data reveals the multifractal nature of the Richardson cascade. *Nature*, 338(6210), 1989.

[3] J. Bourgain. A remark on the uncertainty principle of Hilbertian basis. *J. Functional Analysis*, 79:136–143, 1988.

[4] R. Coifman and Y. Meyer. Remarques sur l'analyse de Fourier à fenêtres. *C.R.A.S.*, 312:259–261, 1991.

[5] R. Coifman, Y. Meyer, and V. Wickerhauser. Wavelet analysis and signal processing. Preprint, 1991.

[6] I. Daubechies. Orthonormal bases of compactly supported wavelets. *Comm. Pure Appl. Math.*, 41, 1988.

[7] I. Daubechies. The wavelet transform, time-frequency localization and signal analysis. *IEEE Trans. Information Theory*, 1989.

[8] I. Daubechies, A. Grossmann, and Y. Meyer. Painless nonorthogonal expansions. *J. Math and Physics*, 27:1271–1283, 1986.

[9] I. Daubechies, S. Jaffard, and J.L. Journé. A simple Wilson orthonormal basis with exponential decay. *SIAM J. Math. Anal.*, 22(2):554–572, 1991.

[10] M. Farge and D. Rabreau. Transformé en ondelettes pour détecter et analyser les structures cohérentes dans les écoulements turbulents bidimensionnels. *C.R.A.S.*, 307:1479–1486, 1988.

[11] R. Glowinski, W. Lawton, and M. Ravacho. Wavelet solution of linear and nonlinear elliptic, parabolic and hyperbolic problems in one space dimension. Preprint, June 1989.

[12] S. Jaffard. Analyse par ondelettes d'un problème elliptique singulier. *Journal de Mathématiques Pures et Appliquées*. To appear.

[13] S. Jaffard. Wavelet methods for fast resolution of elliptic problem. *SIAM Journal of Numerical Analysis*. To appear.

[14] S. Jaffard. Exposants de Holder en des points donnés et coefficients d'ondelettes. *C.R.A.S.*, 308:79–81, January 1989.

[15] S. Jaffard. Local order of approximation by wavelet. Preprint, 1991.

[16] S. Jaffard. Pointwise smoothness, two-microlocalization and wavelet coefficient. *Publicacions Matematiques*, 35:155–168, 1991.

[17] S. Jaffard and Y. Meyer. Bases d'ondelettes dans des ouverts de R^n. *Journal de Mathématiques Pures et Appliquées*, 68:95–108, 1989.

[18] Ph. Laurencot. Private communication, 1991.

[19] P.G. Lemarié. Ondelettes à localisation exponentielle. *Journal de Mathématiques Pures et Appliquées*, 67:227–236, 1988.

[20] P.G. Lemarié and Y. Meyer. Ondelettes et bases hilbertiennes. *Revista Math. Iberoamericana*, 1, 1986.

[21] Liandrat, V. Perrier, and P. Tchamitchian. Numerical resolution of the regularized Burgers equation using the wavelet transform. Preprint, 1990.

[22] Y. Maday, V. Perrier, and J.C. Ravel. Adaptativité dynamique sur bases d'ondelettes pour l'approximation d'équations aux dérivées partielles C.R.A.S., 1991.

[23] S. Mallat. Multiresolution approximations and wavelet orthonormal bases of $L^2(R)$. *Trans. Amer. Math. Soc.*, 1989.

[24] S. Mallat. A theory for multiresolution signal decomposition: The wavelet representation. *IEEE Trans. on Pattern Anal. and Machine Intel.*, II(7) December 1989.

[25] H. Malvar. Lapped transforms for efficient transform / subband coding. *IEEE Trans. Acoustics, Speech, Signal Processing*, 38(6):969–978, 1990.

[26] Y. Meyer. *Ondelettes et opérateurs*. Hermann, 1990.

[27] Y. Meyer. Wavelets and applications. To appear, 1990.

[28] G. Strang and G.J. Fix. *An analysis of the finite element method*. Prentice-Hall.

[29] J.-O. Stromberg. A modified Franklin system and higher-order spline systems on R^n as unconditional bases for Hardy spaces. Volume 2 of *Wadsworth Math Series*, pages 475–493. Conference in honor of Antoni Zygmund.

[30] J.-C. Wilson. Generalized Wannier functions. Preprint, 1987.

Methods of solving dilation equations†

Christopher Heil
Mathematics Department
Massachusetts Institute of Technology
Cambridge, MA 02139 USA
heil@math.mit.edu

Abstract. A *wavelet basis* is an orthonormal basis for $L^2(\mathbb{R})$, the space of square-integrable functions on the real line, of the form $\{g_{n,k}\}_{n,k\in\mathbb{Z}}$, where $g_{n,k}(t) = 2^{n/2} g(2^n t - k)$ and g is a single fixed function, the *wavelet*. Each *multiresolution analysis* for $L^2(\mathbb{R})$ determines such a basis. To find a multiresolution analysis, one can begin with a *dilation equation* $f(t) = \sum c_k f(2t-k)$. If the solution f (the *scaling function*) satisfies certain requirements, then a multiresolution analysis and hence a wavelet basis will follow. This paper surveys methods of achieving this goal. Two separate problems are involved: first, solving a general dilation equation to find a scaling function, and second, determining when such a scaling function will generate a multiresolution analysis. We present two methods for solving dilation equations, one based on the use of the Fourier transform and one operating in the time domain utilizing linear algebra. The second method characterizes all continuous, integrable scaling functions. We also present methods of determining when a multiresolution analysis will follow from the scaling function. We discuss simple conditions on the coefficients c_k which are "almost" sufficient to ensure the existence of a wavelet basis; in particular, they do ensure that $\{g_{n,k}\}_{n,k\in\mathbb{Z}}$ is a *tight frame*, and we present more complicated necessary and sufficient conditions for the generation of a multiresolution analysis. The results presented are due mainly to Cohen, Colella, Daubechies, Heil, Lagarias, Lawton, Mallat, and Meyer, although several of the results have been independently investigated by other groups, including Berger, Cavaretta, Dahmen, Deslauriers, Dubuc, Dyn, Erola, Gregory, Levin, Micchelli, Prautzsch, and Wang.

1. Introduction

The *Haar system* is the classical example of an *affine*, or *wavelet*, *orthonormal basis* for the space $L^2(\mathbb{R})$ of square-integrable functions on the real line.

† We thank David Colella of The MITRE Corporation, McLean, Virginia, for his collaboration on some of the results reported in this paper, and for his review of this document.

J. S. Byrnes et al. (eds.), Probabilistic and Stochastic Methods in Analysis, with Applications, 15–45.
© 1992 *Kluwer Academic Publishers. Printed in the Netherlands.*

It consists of a set of translations and dilations of a single function, the *Haar wavelet* $\psi(t) = \chi_{[0,1/2)} - \chi_{[1/2,1)}$, where χ_E is the characteristic function of the set E. Precisely, the Haar system has the form $\{\psi_{nk}\}_{n,k\in\mathbb{Z}}$, where $\psi_{nk}(t) = 2^{n/2}\psi(2^n t - k)$. Such a simply-generated orthonormal basis is very appealing; however, the fact that the Haar wavelet is discontinuous severely limits the usefulness of the Haar system in applications. Recently, examples of other, smooth *wavelets* which generate affine orthonormal bases have been given, the first by Meyer [28]. Meyer's example is an infinitely differentiable function which has a compactly supported Fourier transform. Additional examples have been given by Lemarié [26] and Battle [1] (k-times differentiable with exponential decay), Daubechies [12] (k-times differentiable with compact support), and others. Such smooth wavelets are better suited to applications than the Haar wavelet; for example, they have been used in speech compression [8, 7].

Soon after Meyer's initial example, Mallat and Meyer proved that each *multiresolution analysis* for $L^2(\mathbb{R})$ determines a wavelet basis [27]. Each of the wavelet bases mentioned above are determined by an appropriate multiresolution analysis (although not all wavelet bases are associated with multiresolution analyses). A multiresolution analysis $\{V_n, f\}$ is defined as a sequence of subspaces $\{V_n\}_{n\in\mathbb{Z}}$ of $L^2(\mathbb{R})$ such that

1) $V_n \subset V_{n-1}$ for all n,
2) $\cap V_n = \{0\}$,
3) $\cup V_n$ is dense in $L^2(\mathbb{R})$, and
4) $h(t) \in V_n \iff h(2t) \in V_{n-1}$,

together with a function $f \in V_0$ such that the collection of integer translates of f, $\{f(t-k)\}_{k\in\mathbb{Z}}$, forms an orthonormal basis for V_0. Given such a multiresolution analysis, we have $f \in V_0 \subset V_1$. As $\{2^{1/2}f(2t-k)\}_{k\in\mathbb{Z}}$ is an orthonormal basis for V_1, there must therefore exist scalars $\{c_k\}$ such that

$$f(t) = \sum_{k\in\mathbb{Z}} c_k\, 2^{1/2} f(2t-k). \tag{1.1}$$

This is referred to as the (induced) *dilation equation*, and its solution is the *scaling function*. It can be proved that if we define the *wavelet* g by

$$g(t) = \sum_{k\in\mathbb{Z}} (-1)^k c_{N-k}\, 2^{1/2} f(2t-k) \tag{1.2}$$

(where N is as defined below), then g will generate an orthonormal basis for $L^2(\mathbb{R})$ of the form $\{g_{nk}\}_{n,k\in\mathbb{Z}}$, cf. Section 4. From (1.2), it follows that properties of the wavelet g such as continuity, differentiability, etc., are determined by the corresponding properties of the scaling function f.

Remark 1.1. For the Haar system,

$$V_0 = \{h : h \text{ is constant on each interval}[k, k+1)\},$$

the induced dilation equation is $f(t) = f(2t) + f(2t-1)$ (i.e., $c_0 = c_1 = 1$ and all other $c_k = 0$), the scaling function is $f = \chi_{[0,1)}$, and the wavelet is the Haar wavelet $g(t) = \psi(t) = f(2t) - f(2t-1)$.

To find wavelet bases for $L^2(\Re)$, it suffices to construct multiresolution analyses. One method of achieving this is the following. Choose a set of coefficients $\{c_k\}$ and solve the corresponding dilation equation (1.1) for the scaling function f. If f is orthogonal to each of its integer translates then define V_0 to be the span of the integer translates of f and define V_n for $n \in \mathbb{Z}$ as the appropriate dilation of V_0 (i.e., $V_n = \text{span}\{f_{nk}\}_{k\in\mathbb{Z}}$). If $\bigcap V_n = \{0\}$ and if $\bigcup V_n$ is dense in $L^2(\Re)$ then $(\{V_n\}, f)$ is a multiresolution analysis, and therefore the wavelet g defined by (1.2) will generate an affine orthonormal basis for $L^2(\Re)$. If this is the case then we say that the coefficients $\{c_k\}$ have *determined* the multiresolution analysis $(\{V_n\}, f)$.

There are obviously two separate difficulties in this approach, namely,

1) solving a given dilation equation to find a scaling function, and
2) determining conditions under which a multiresolution analysis will follow from such a scaling function, i.e., conditions under which f will be orthogonal to its integer translates, etc.

We survey results on these two problems in this paper. A shorter survey, which also includes a discussion of the application of wavelets to fast signal processing algorithms, is [33].

The first problem, that of solving a general dilation equation, is not restricted in application to wavelet theory. In particular, dilation equations play a role in spline theory, interpolation and subdivision methods, and smooth curve generation [2, 4, 5, 17, 20, 19, 29, 30]. Although we focus in this paper on results by groups involved in wavelet research (including Cohen, Colella, Daubechies, Heil, Lagarias, Lawton, Mallat, and Meyer), many of the same or related results have been independently obtained by groups involved in these other areas (including Berger, Cavaretta, Dahmen, Deslauriers, Dubuc, Dyn, Eirola, Gregory, Levin, Micchelli, Prautzsch, and Wang). In some cases, results by these other groups were obtained earlier or are more complete than the ones we discuss.

In Sections 2 and 3 we consider two methods of solving general dilation equations. The methods in Section 2 are based on the use of the Fourier transform. We prove results due to Daubechies and Lagarias showing that every dilation equation has a solution in the sense of distributions and that integrable solutions, *if they exist*, are unique up to multiplication by a constant. We then present results of Daubechies and Mallat which show

when integrable solutions to dilation equations will exist, and results of Colella and Heil showing when they will not (these results do not completely characterize those dilation equations which have integrable solutions).

In Section 3 we present a time-domain based method for solving certain dilation equations, due to Daubechies and Lagarias, which utilizes linear algebra. This method produces continuous, integrable scaling functions if appropriate conditions hold. Colella and Heil have proved that this method characterizes those dilation equations which have continuous, integrable solutions.

In Section 4 we consider the second problem. We show that if the coefficients $\{c_k\}$ determine a multiresolution analysis then necessarily

$$\sum_k c_{2k} = \sum_k c_{2k+1} = 1 \tag{1.3}$$

and

$$\sum_k c_k c_{k+2l} = 2\delta_{0l} \qquad \text{for every} \quad l \in \mathbb{Z}, \tag{1.4}$$

where δ_{ij} is the Kronecker delta, i.e., $\delta_{ij} = 1$ if $i = j$ and 0 otherwise. We then prove a result due to Lawton which shows that (1.3) and (1.4) are "almost" sufficient to generate a wavelet orthonormal basis. In particular, Lawton has proved that if (1.3) and (1.4) are satisfied then $\{g_{nk}\}_{n,k\in\mathbb{Z}}$ will be a *tight frame*, i.e., the reconstruction property

$$h = \sum_{n,k} \langle h, g_{nk} \rangle g_{nk} \qquad \text{for all} \quad h \in L^2(\mathbb{R}) \tag{1.5}$$

will be satisfied, although $\{g_{nk}\}_{n,k\in\mathbb{Z}}$ need not be an orthogonal set. (The general theory of frames was developed by Duffin and Schaeffer in [18] in connection with nonharmonic Fourier series. The connection between frames and wavelet theory is surveyed in [23], and researched in depth in [13].) We also discuss more complicated conditions, independently derived by Lawton and Cohen, which are both necessary and sufficient to ensure that a multiresolution analysis, and therefore a wavelet orthonormal basis, is generated. Lawton has proved that almost all choices of coefficients $\{c_k\}$ which satisfy (1.3) and (1.4) also satisfy these conditions for orthogonality.

For simplicity of presentation, we assume throughout this paper that coefficients $\{c_k\}$ are given which are real with only $c_0, \ldots, c_N$ nonzero, i.e., we consider only Daubechies-type wavelets). In Sections 2 and 3, we assume in addition that (1.3) is satisfied. These conditions are not necessary for many of the proofs, and many of the results in which they are necessary can be modified for more general situations. The fact that the coefficients $\{c_k\}$ are real implies that the scaling function f will be real-valued.

Given these restrictions, the Haar system is of course the only example with $N = 1$. It can be shown that multiresolution analyses can be produced only when N is odd. We will use the case $N = 3$ to illustrate many of the results in this paper. For this case, assumption (1.3) reduces to the statement $c_0 + c_2 = c_1 + c_3 = 1$, i.e., the collection of four-coefficient dilation equations with the given restrictions is a two-parameter family. We select the independent parameters to be c_0 and c_3, and represent this collection of four-coefficient dilation equations as the (c_0, c_3)-plane. Figure 1.1 shows several geometrical objects in the (c_0, c_3)-plane. The following results regarding these geometrical objects are discussed in this paper.

1) There are no integrable solutions to dilation equations corresponding to points on or outside the ellipse, with the single exception of the point $(1, 1)$.
2) There do exist integrable solutions to dilation equations corresponding to points on and inside the circle, and inside the shaded region.
3) There are continuous, integrable solutions to dilation equations in a large portion of the triangle, and no continuous, integrable solutions outside the triangle.
4) There are differentiable, integrable solutions to dilation equations on the solid portion of the dashed line.
5) Each point on the circle, with the single exception of the point $(1, 1)$, determines a multiresolution analysis and therefore a wavelet basis for $L^2(\mathfrak{R})$. We refer to this circle as the *circle of orthogonality*.

Throughout this paper, $L^p(\mathfrak{R})$ will denote the *Lebesgue space* of p-integrable functions on the real line, with norm $\|f\|_p = \left(\int |f(t)|^p \, dt\right)^{1/p}$ for $1 \leq p < \infty$ and $\|f\|_\infty = \operatorname{ess\,sup} |f(t)|$. The *inner product* of functions f, g is $\langle f, g \rangle = \int f(t)\, \overline{g(t)}\, dt$. The Fourier transform of an integrable function f is $\hat{f}(\gamma) = \int f(t)\, e^{i\gamma t}\, dt$. Integrals with unspecified limits are over the entire real line.

2. Fourier methods

By considering the Fourier transform of the dilation equation, we can prove that every dilation equation has a solution in the sense of distributions. Consideration of the smoothness and decay of the Fourier transforms of these distributions can indicate whether or not these distributions are given by functions on the real line. We assume throughout this section that (1.3) is satisfied.

Some notation is required to adequately describe distributions. We let $S(\mathfrak{R})$ denote the Schwartz space of infinitely differentiable, rapidly decreasing functions on the real line, and let $S'(\mathfrak{R})$ denote its topological dual, the

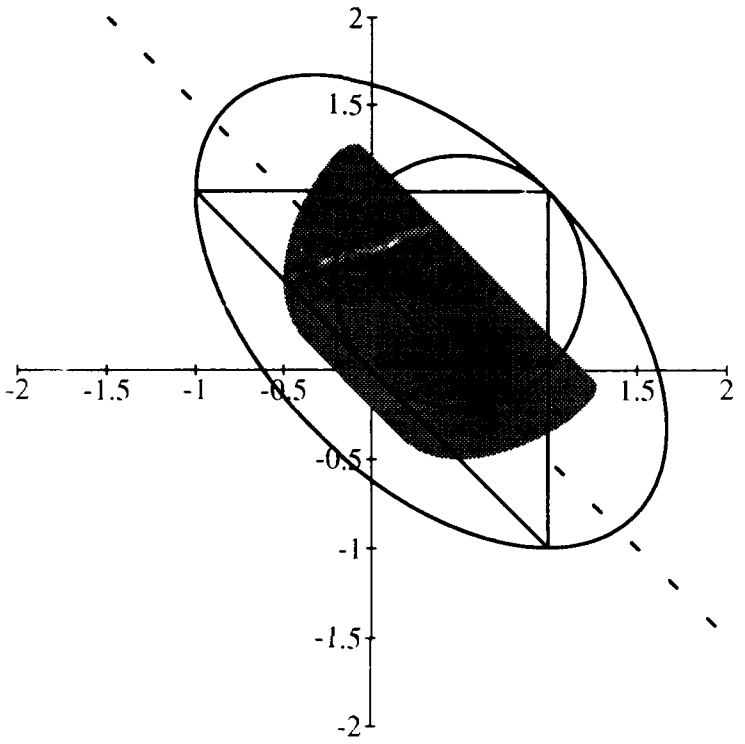

Figure 1.1: Circle of orthogonality, ellipse, line, triangle, and shaded region.

space of tempered distributions. For functions φ we define the *translation* operator $T_a\varphi(t) = \varphi(t - a)$ and the *dilation* operator $D_a\varphi(t) = \varphi(at)$. Translation and dilation of a distribution $\nu \in S'(\mathfrak{R})$ is defined by duality, i.e., $\langle T_a\nu, \varphi\rangle = \langle \nu, T_{-a}\varphi\rangle$ and $\langle D_a\nu, \varphi\rangle = a^{-1}\langle \nu, D_{a^{-1}}\varphi\rangle$. With this notation, the dilation equation (1.1) has the form $f = \sum c_k D_2 T_k f$. Therefore, we say that $\nu \in S'(\mathfrak{R})$ is a *scaling distribution* if

$$\nu = \sum_k c_k D_2 T_k \nu,$$

i.e., if $\langle \nu, \varphi\rangle = \sum c_k \langle D_2 T_k \nu, \varphi\rangle$ for all $\varphi \in S(\mathfrak{R})$. By taking Fourier transforms, we therefore have that ν is a scaling distribution if and only if

$$D_2\hat{\nu} = m_0\hat{\nu},$$

where $m_0(\gamma) = (1/2)\sum c_k e^{ik\gamma}$. If it is the case that $\hat{\nu}$ is a function on $\mathcal{R}$ then this is equivalent to

$$\hat{\nu}(2\gamma) = m_0(\gamma)\hat{\nu}(\gamma) \qquad \text{for a.e. } \gamma \in \mathcal{R}. \tag{2.1}$$

Assume now that $\hat{\nu}$ is a continuous function on $\mathcal{R}$. Then we can iterate (2.1), obtaining (formally) $\hat{\nu}(\gamma) = \hat{\nu}(\gamma/2^n)\prod_1^n m_0(\gamma/2^j) \to \hat{\nu}(0)\prod_1^\infty m_0(\gamma/2^j)$. Daubechies established that this infinite product converges, and proved with Lagarias the following result, cf. [12, 15].

Theorem 2.1.

1) $P(\gamma) = \prod_1^\infty m_0(\gamma/2^j)$ converges uniformly on compact sets to a continuous function which has polynomial growth at infinity.
2) Define f to be the tempered distribution such that $\hat{f} = P$. Then $\hat{f}(2\gamma) = m_0(\gamma)\hat{f}(\gamma)$ for all γ, so f is a scaling distribution. The support of f is contained in $[0, N]$.
3) If ν is another scaling distribution such that $\hat{\nu}$ is a function on $\mathcal{R}$ which is continuous at zero then $\nu = \hat{\nu}(0) f$.
4) If a nonzero integrable solution to (1.1) exists then it is f, up to multiplication by a constant, and $\int f(t)\,dt = 1$.

We call the distribution f defined in Theorem 2.1 the *canonical scaling distribution*. Other solutions to the dilation equation are given in [15], and certain classes of solutions are characterized in [11].

The proof of Theorem 2.1 requires only that $\sum c_k = 2$; if this is not the case then a canonical solution of the dilation equation can still be defined, but the uniqueness results of Theorem 2.1 will not hold. Even with the assumption $\sum c_k = 2$, uniqueness in function spaces other than $L^1(\mathcal{R})$ may not hold. For example, the Hilbert transform $H\nu$ of any solution ν of a dilation equation is also a solution of the same dilation equation. Since H maps $L^p(\mathcal{R})$ into $L^p(\mathcal{R})$ for $1 < p < \infty$, uniqueness cannot hold in any of these spaces. Additional uniqueness criteria and methods of generating new solutions to dilation equations from known solutions are given in [11].

Existence of an integrable solution of a dilation equation is not guaranteed. The following, from [11], is an easily checkable necessary condition for the existence of such solutions, based on the fact that the Fourier transform of an integrable solution must decay at infinity.

Theorem 2.2. Given $x \in [0, 2\pi)$. Assume that the set

$$\{x \bmod 2\pi, 2x \bmod 2\pi, \ldots, 2^{n-1}x \bmod 2\pi\}$$

is invariant mod 2π under multiplication by 2. If

$$\prod_{j=1}^{n-1} |m_0(2^j x)| \geq 1 \qquad \text{and} \qquad m_0(2^{-j}x) \neq 0 \qquad \text{for all } j \geq 1$$

then the canonical scaling distribution is not an integrable function, and therefore there do not exist any integrable solutions to (1.1).

Remark 2.3. Consider the case $N = 3$. The set $\{2\pi/3, 4\pi/3\}$ is invariant mod 2π under multiplication by 2, and $|m_0(2\pi/3)\, m_0(4\pi/3)| \geq 1$ for all (c_0, c_3) on and outside the ellipse shown in Figure 1.1. The additional hypotheses of Theorem 2.2 are also satisfied for all but countably many of these points, and therefore for almost no point on or outside the ellipse can an integrable solution to the corresponding dilation equation exist. All but one of the countably many remaining points are also eliminated when the 3-cycle $\{2\pi/7, 4\pi/7, 8\pi/7\}$ is checked in addition [11]. The remaining single point is $(1, 1)$; the integrable solution to the dilation equation corresponding to this point is $f = (1/3)X_{[0,3]}$.

Theorem 2.2 deals with non-existence of integrable solutions by establishing conditions under which the Fourier transform $P = \hat{f}$ of the canonical scaling distribution f will not decay at infinity. Alternatively, by imposing sufficient decay on $\hat{f}$ we can obtain $f \in L^2(\mathfrak{R})$, and therefore $f \in L^1(\mathcal{R})$ since f has compact support. This is made precise in the next theorem, due to Daubechies [12]. The notation used in the theorem is as follows. Since $2m_0(\pi) = \sum(-1)^k c_k = \sum c_{2k} - \sum c_{2k+1} = 0$, we can factor a term of the form $1 + e^{i\gamma}$ from $m_0(\gamma)$. If the zero at π has multiplicity at least L then $m_0(\gamma) = ((1 + e^{i\gamma})/2)^L\, Q(\gamma)$, and therefore

$$\hat{f}(\gamma) = \prod_{j=1}^{\infty} m_0(\gamma/2^j) = \left(\frac{\sin\gamma/2}{\gamma/2}\right)^L \prod_{j=1}^{\infty} Q(\gamma/2^j).$$

Theorem 2.4.

1) If $\|Q\|_\infty < 2^{L-1/2}$ then the canonical scaling distribution f is an integrable function.
2) If $\|Q\|_\infty < 2^{L-1}$ then the canonical scaling distribution f is a continuous, integrable function.

Proof. We prove only the first statement.

Set $M(\gamma) = \prod_1^\infty Q(\gamma/2^j)$; this is a continuous function. Define $R = \|M \cdot X_{[-1,1]}\|_\infty$; then since $M(2\gamma) = Q(\gamma)\, M(\gamma)$ we have $\|M \cdot X_{[-2^n, 2^n]}\|_\infty \leq \|Q\|_\infty^n R$, whence $|M(\gamma)| \leq C\,|\gamma|^{\log_2 \|Q\|_\infty}$ for some constant C. Therefore,

$$|\hat{f}(\gamma)|^2 \leq C' \left(\frac{\sin\gamma/2}{\gamma/2}\right)^{1+p},$$

where $p = 2L - 1 - 2\log_2 \|Q\|_\infty$ and C' is another constant. Since $p > 0$, $((\sin\gamma/2)/(\gamma/2))^{1+p}$ is integrable, and therefore $\hat{f} \in L^2(\mathfrak{R})$. Hence $f \in L^2(\mathfrak{R})$, and therefore f is integrable since it has compact support. ∎

Remark 2.5. For $N = 3$, the multiplicity L is one except for those points on the dashed line shown in Figure 1.1; for those points, $L = 2$.

The region of points (c_0, c_3) for which the hypotheses of the first part of Theorem 2.4 is satisfied with $L = 1$ is the shaded region shown in Figure 1.1, i.e., integrable scaling functions exist for all points in this region [11] (see also Remark 2.7 for an additional region).

No points in the (c_0, c_3)-plane satisfy the second part of Theorem 2.4 with $L = 1$. For $L = 2$, i.e., $c_3 = 1/2 - c_0$, Theorem 2.4 implies that continuous solutions exist for $-1/4 < c_0 < 3/4$. This result is inferior to the one obtained in Section 3, where it is shown that continuous scaling functions occur on this line precisely when $-1/2 < c_0 < 1$, and in fact are differentiable if $0 < c_0 < 1/2$ (i.e., on the solid portion of the line shown in Figure 1.1). Moreover, it is shown in Section 3 that continuous scaling functions occur over a large region of the (c_0, c_3)-plane, including the regions shown in Figures 3.1–3.6.

Eirola has taken a different (but still Fourier-based) approach in [21]. He obtains conditions under which scaling functions will be continuous and estimates for the Sovolev exponent of continuity for these scaling functions. In Section 3 we discuss a time-domain method for obtaining estimates for the Hölder exponent of continuity of scaling functions.

We end this section with an adaptation of an existence result due to Mallat [27]; part of the proof we give is due to Lawton [24].

Theorem 2.6. If

$$|m_0(\gamma)|^2 + |m_0(\gamma + \pi)|^2 \leqslant 1 \qquad \text{for all } \gamma,$$

then the canonical scaling distribution is an integrable function.

Proof. Set

$$u_n(\gamma) = \chi_{[-2^n\pi, 2^n\pi]}(\gamma) \cdot \prod_{j=1}^{n} m_0(\gamma). \tag{2.2}$$

By Theorem 2.1, u_n converges uniformly on compact sets to the Fourier

transform of the canonical scaling distribution f. Now,

$$\begin{aligned}
\|u_n\|_2^2 &= \int_{-2^n\pi}^{2^n\pi} \left| \prod_{j=1}^{n} m_0\left(\frac{\gamma}{2^j}\right) \right|^2 d\gamma \\
&= \int_0^{2^n\pi} \left| \prod_{j=1}^{n} m_0\left(\frac{\gamma}{2^j}\right) \right|^2 d\gamma \quad + \quad \int_0^{2^n\pi} \left| \prod_{j=1}^{n} m_0\left(\frac{\gamma+2^n\pi}{2^j}\right) \right|^2 d\gamma \\
&= \int_0^{2^n\pi} \left(\left| m_0\left(\frac{\gamma}{2^n}\right) \right|^2 + \left| m_0\left(\frac{\gamma}{2^n}+\pi\right) \right|^2 \right) \left| \prod_{j=1}^{n-1} m_0\left(\frac{\gamma}{2^j}\right) \right|^2 d\gamma \\
&\leqslant \int_{-2^{n-1}\pi}^{2^{n-1}\pi} \left| \prod_{j=1}^{n-1} m_0\left(\frac{\gamma}{2^j}\right) \right|^2 d\gamma \\
&= \|u_{n-1}\|_2^2,
\end{aligned}$$

and, by a similar argument, $\|u_1\|_2^2 = 2\pi$. Therefore $\{u_n\}$ is contained in the ball in $L^2(\mathfrak{R})$ of radius $\sqrt{2\pi}$ and therefore has a weak* accumulation point. Since $u_n(\gamma) \to \hat{f}(\gamma)$ pointwise, this accumulation point must be f, whence $f \in L^2(\mathfrak{R})$. Since f has compact support, it is therefore integrable as well. ∎

Remark 2.7. For $N = 3$, equation (2.2) is satisfied for all points (c_0, c_3) on and inside the circle shown in Figure 1.1. Therefore, there exist integrable solutions for all dilation equations corresponding to such points. By the remark following Theorem 2.4, integrable solutions also exist for points in the shaded region in Figure 1.1. The union of these two regions does not exhaust the set of four-coefficient dilation equations which have integrable solutions, cf. [11].

3. Matrix methods

In [16], Daubechies and Lagarias proved sufficient conditions under which a dilation equation has a continuous, integrable solution (or, more generally, an integrable and n-times differentiable solution). In particular, they proved that if the *joint spectral radius* $\rho(T_0|_V, T_1|_V)$ of two $N \times N$ matrices T_0, T_1 (whose entries contain only the coefficients $\{c_k\}$) restricted to a certain $N-1$ dimensional subspace V is less than one then the canonical scaling distribution f is a continuous and integrable function, and, moreover, is Hölder continuous with Hölder exponent $\alpha \geqslant -\log_2 \rho(T_0|_V, T_1|_V)$. We outline this result in this section. In [10], this result is extended to a necessary and sufficient condition; in particular, it is shown there that the canonical scaling distribution f is a continuous and integrable function if and only if $\rho(T_0|_W, T_1|_W) < 1$, where W is an appropriate subspace of V, and that in this case $\alpha = -\log_2 \rho(T_0|_W, T_1|_W)$. It is conjectured in [10] that $W = V$ in

general, except for a set of coefficients of measure zero, and it is proved in [9] that $\rho(T_0|_W, T_1|_W) = \rho(T_0|_V, T_1|_V)$ for all choices of coefficients with $N \leq 3$.

We assume throughout this section that (1.3) is satisfied.

Given the coefficients $\{c_k\}$, define the $N \times N$ matrices T_0 and T_1 by $(T_0)_{ij} = c_{2i-j-1}$ and $(T_1)_{ij} = c_{2i-j}$. For example, for $N = 3$ we have

$$T_0 = \begin{pmatrix} c_0 & 0 & 0 \\ c_2 & c_1 & c_0 \\ 0 & c_3 & c_2 \end{pmatrix} \qquad \text{and} \qquad T_1 = \begin{pmatrix} c_1 & c_0 & 0 \\ c_3 & c_2 & c_1 \\ 0 & 0 & c_3 \end{pmatrix}.$$

For $x \in [0, 1]$, $x \neq 1/2$, define

$$\tau x = \begin{cases} 2x, & 0 \leq x < 1/2, \\ 2x - 1, & 1/2 < x \leq 1, \end{cases}$$

i.e., if $x = .d_1 d_2 d_3 \ldots$ is the binary decimal expansion of x then $\tau x = .d_2 d_3 \ldots$. Although $\tau(1/2)$ is not uniquely defined, this ambiguity will not pose any problems in the analysis.

We say that a function f is *Hölder continuous* if there exist constants K, α such that $|f(x) - f(y)| \leq K|x - y|^\alpha$ for all $x, y \in \mathcal{R}$. The largest such exponent α is the *Hölder exponent* and the corresponding smallest constant K is the *Hölder constant*.

The relationship between the dilation equation (1.1) and the matrices T_0, T_1 is given in the following result from [16].

Proposition 3.1.

1) Assume f is a continuous and integrable scaling function. Define the vector-valued function $v(x)$ for $x \in [0, 1]$ by

$$v(x) = \begin{pmatrix} f(x) \\ f(x+1) \\ \vdots \\ f(x+N-1) \end{pmatrix}. \tag{3.1}$$

Then v is continuous on $[0, 1]$ and satisfies

$$v_1(0) = v_N(1) = 0,$$

$$v_{i+1}(0) = v_i(1) \qquad \text{for } i = 1, \ldots, N-1,$$

$$v(x) = T_{d_1} v(\tau x) \quad \text{for } x = .d_1 d_2 \ldots \in [0, 1], \ x \neq 1/2,$$

$$v(1/2) = T_0 v(1) = T_1 v(0), \tag{3.2}$$

where $v_i(x)$ is the i^{th} component of $v(x)$. Moreover, if f is Hölder continuous with Hölder exponent α then the same is true of v.

2) Assume v is a continuous vector-valued function on $[0,1]$ satisfying (3.2). Define the function f by

$$f(x) = \begin{cases} 0, & x \leqslant 0 \text{ or } x \geqslant N, \\ v_i(x), & i-1 \leqslant x \leqslant i,\ i = 1, \ldots, N. \end{cases} \tag{3.3}$$

Then f is a continuous and integrable scaling function. Moreover, if v is Hölder continuous with Hölder exponent α then the same is true of f.

The fundamental theorem on the existence of continuous, integrable scaling functions is the following result from [16]. The notation used in the theorem is as follows. Let V denote the subspace

$$V = \{u \in \mathcal{R}^N : u_1 + \cdots + u_N = 0\},$$

and let M be the $(N-1) \cdot (N-1)$ matrix $M_{ij} = c_{2i-j}$. A point $x = .d_1 \ldots d_m$ in $[0,1]$ with a finite binary decimal expansion is called a *dyadicpoint*.

Theorem 3.2. Fix any norm $\|\cdot\|$ on $\mathcal{R}^N$, and assume there exist constants $C > 0$ and $0 < \lambda < 1$ such that

$$\|(T_{d_1} \cdots T_{d_m})v\| \leqslant C\lambda^m \tag{3.4}$$

for every choice of $d_1, \ldots, d_m \in \{0,1\}$ and every $m > 0$. Then the following statements are true.

1) 1 is a simple eigenvalue of T_0, T_1, and M.
2) M has a right eigenvector $(a_1, \ldots, a_{N-1})^t$ for the eigenvalue 1 such that $a_1 + \cdots + a_{N-1} = 1$.
3) Set $v(0) = (0, a_1, \ldots, a_{N-1})^t$ and define $v(x)$ for $x = .d_1 \ldots d_m \in [0,1]$ by

$$v(x) = T_{d_1} \cdots T_{d_m} v(0). \tag{3.5}$$

Then $v_1(x) + \cdots + v_N(x) = 1$ for every such x.

4) v is bounded on the set of dyadic points in $[0,1]$.
5) v is Hölder continuous on the set of dyadic points in $[0,1]$ with Hölder exponent $\alpha \geqslant -\log_2 \lambda$, and has a unique continuous extension to $[0,1]$ which is Hölder continuous with the same exponent α.
6) v satisfies (3.2), and therefore the function f defined by (3.3) is a continuous, integrable scaling function and is Hölder continuous with exponent α.

Proof. Full details of the proof can be found in [16]; we sketch some selected points below.

1) follows from the fact that V has dimension $N-1$ in $\mathcal{R}^N$, and that M is a submatrix of both T_0 and T_1.

2) follows from 1) and the fact that $(1,\dots,1)$ is a left eigenvector for M for the eigenvalue 1.

3) Since $(1,\dots,1)$ is a common left eigenvector for T_0 and T_1 for the eigenvalue 1,

$$\begin{aligned} v_1(x)+\cdots+v_N(x) &= (1,\dots,1)v(x) \\ &= (1,\dots,1)T_{d_1}\cdots T_{d_m}v(0) \\ &= (1,\dots,1)v(0) \\ &= 1. \end{aligned}$$

5) Choose any dyadic $x = d_1\dots d_k \in [0,1]$ and assume $y > x$ is also dyadic. If $2^{-m-1} \leqslant y-x < 2^{-m}$ with $m > k$ then $x = .d_1\dots d_m$ and $y = .d_1\dots d_m d_{m+1}\dots d_{m+j}$ for some j. From 3), $v(\tau^m y) - v(0) \in V$, so

$$\begin{aligned} \|v(y)-v(x)\| &= \|T_{d_1}\cdots T_{d_m}(v(\tau^m y)-v(0))\| \\ &\leqslant \|(T_{d_1}\cdots T_{d_m})|_V\|\,\|v(\tau^m y)-v(0)\| \\ &\leqslant 2LC\lambda^m \\ &= 2LC\lambda^{-1}(2^{-m-1})^{-\log_2\lambda} \\ &\leqslant 2LC\lambda^{-1}|y-x|^{-\log_2\lambda}, \end{aligned}$$

where $L = \sup\{\|v(t)\| : \text{dyadic } t \in [0,1]\} < \infty$ by 4). Thus v is Hölder continuous from the right on the set of dyadic points in $[0,1]$ with Hölder exponent $\alpha \geqslant -\log_2\lambda$. A similar proof establishes Hölder continuity from the left.

6) Given $x = .d_1\dots d_m$ dyadic, we have $v(x) = T_{d_1}(T_{d_2}\cdots T_{d_m}v(0)) = T_{d_1}v(\tau x)$. By continuity, this holds for all $x \in [0,1]$. ∎

Examples of norms on $\mathcal{R}^N$ are $\|u\|_p = (|u_1|^p + \cdots + |u_N|^p)^{1/p}$ for $1 \leqslant p < \infty$ and $\|u\|_\infty = \max\{|u_1|,\dots,|u_N|\}$.

Condition (3.4) is most easily analyzed in a spectral form, as follows.

The *joint spectral radius* of a set of $N \times N$ matrices $\{A_0,\dots,A_n\}$ is the straightforward generalization of the usual spectral radius of a single matrix, namely,

$$\rho(A_0,\dots,A_n) = \limsup_{m\to\infty}\lambda_m,$$

where

$$\lambda_m = \max_{d_1\in\{0,\dots,n\}}\|A_{d_1}\cdots A_{d_m}\|^{1/m}.$$

The joint spectral radius was first introduced by Rota and Strang [32]. Recent articles are [3, 14].

Lemma 3.3.

1) For every $\lambda > \rho(A_0, \ldots, A_n)$ there exists a constant $C > 0$ such that $\lambda_m^m \leq C\lambda^m$ for every m.
2) If there exist C, $\lambda > 0$ such that $\lambda_m^m \leq C\lambda^m$ for every m then $\rho(A_0, \ldots, A_n) \leq \lambda$.

It follows from Lemma 3.3 that (3.4) is equivalent to $\rho(T_0|_V, T_1|_V) < 1$ (however, $\rho(T_0|_V, T_1|_V) = 1$ is not equivalent to $\lambda_m^m \leq C$ for every m).

The joint spectral radius can be difficult to compute, except in special cases. For a single matrix A, $\rho(A)$ is simply the usual spectral radius of A and is therefore the largest of the absolute values of the eigenvalues of A. This is not true in general, i.e., if we define

$$\sigma_m = \max_{d_i \in \{0, \ldots, n\}} \rho(A_{d_1} \cdots A_{d_m})^{1/m},$$

then $\rho(A_0, \ldots, A_n) \neq \sigma_1 = \max\{\rho(A_0), \ldots, \rho(A_n)\}$. However, we do have the following, cf. [16].

Lemma 3.4.

1) $\sigma_m \leq \rho(A_0, \ldots, A_n) \leq \lambda_m$ for every m.
2) $\rho(A_0, \ldots, A_n)$ is independent of the choice of basis, i.e., if B is any invertible matrix then $\rho(BA_0B^{-1}, \ldots, BA_nB^{-1}) = \rho(A_0, \ldots, A_n)$.
3) If there exists an invertible matrix B such that $BA_0B^{-1}, \ldots, BA_nB^{-1}$ are all simultaneously symmetric, then $\rho(A_0, \ldots, A_n) = \sigma_1$.

Berger and Wang have proved that $\rho(A_0, \ldots, A_n) = \limsup \sigma_m$, and therefore $\rho(A_0, \ldots, A_n) = \sup \sigma_m$ [3].

We return now to consideration of the matrices T_0, T_1. Since V has dimension $N-1$, an appropriate change of basis gives $\rho(T_0|_V, T_1|_V) = \rho(S_0, S_1)$, where S_0, S_1 are $(N-1) \times (N-1)$ matrices (not necessarily unique).

Remark 3.5. For $N = 3$ we can set

$$S_0 = \begin{pmatrix} c_0 & 0 \\ c_3 & 1 - c_0 - c_3 \end{pmatrix} \quad \text{and} \quad S_1 = \begin{pmatrix} 1 - c_0 - c_3 & c_0 \\ 0 & c_3 \end{pmatrix},$$

cf. [9]. The shaded area in Figure 3.1 shows the set SS of points (c_0, c_3) for which S_0 and S_1 can be simultaneously symmetrized with $\rho(S_0, S_1) < 1$. Continuous, integrable scaling functions therefore exist for all points in this region.

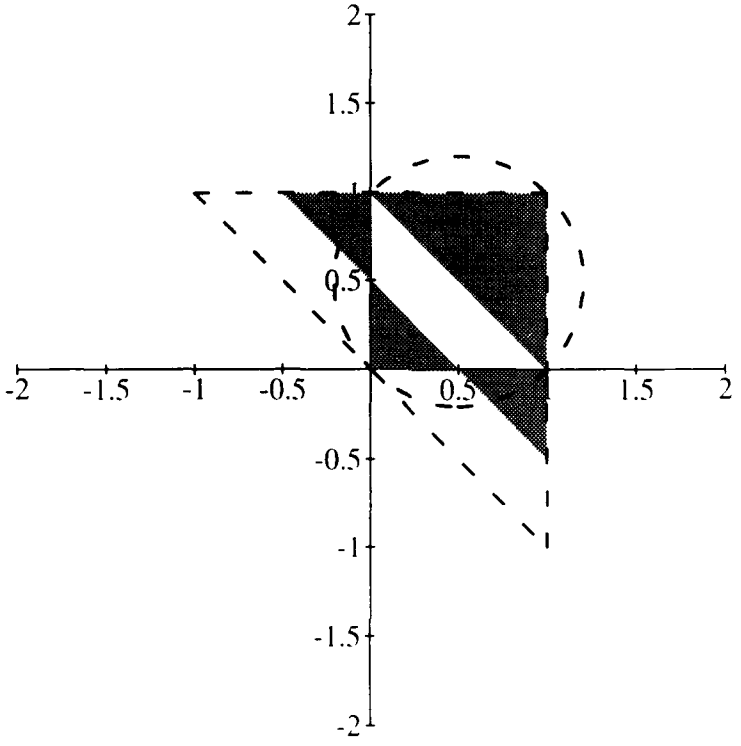

Figure 3.1: Region SS where simultaneous symmetrization is possible and leads to continuous scaling functions (shaded area).

In the regions where simultaneous symmetrization is not possible, Lemma 5.4 can be used to estimate the joint spectral radius.

Remark 3.6. Set $N = 3$, and let $C_{p,m}$ be the set of points (c_0, c_3) such that $\rho(S_0, S_1) \leq \lambda_m < 1$ with the choice of norm $\|\cdot\|_p$. By Theorem 3.2 continuous, integrable scaling functions exist for all points in any $C_{p,m}$. Figures 3.2–3.4 show $C_{p,1}$ for several choices of p, i.e., the sets obtained by considering the matrices S_0, S_1 directly (since $\lambda_1 = \max(\|S_0\|_p, \|S_1\|_p)$).

Figure 3.5 shows the region $C_{2,16}$ obtained by considering, for each point (c_0, c_3), the Euclidean space norm $\|\cdot\|_2$ of all 65536 possible products $S_{d_1} \cdots S_{d_{16}}$ of S_0 and S_1 of length 16.

The union of the regions shown in Figures 3.2–3.5, plus the region SS shown in Figure 3.1, is shown in Figure 3.6. Continuous, integrable scaling functions therefore exist for all points in the shaded area in Figure 3.6. By

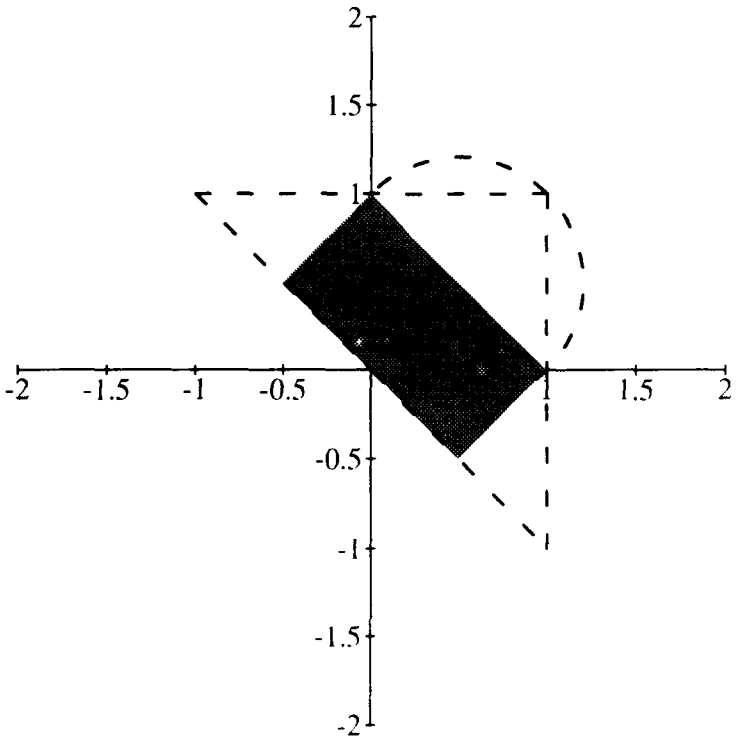

Figure 3.2: The set $C_{1,1}$ (shaded area).

Remark 3.10, there are no continuous, integrable scaling functions on or outside the solid boundary shown in Figure 3.6.

Note that half of the circle of orthogonality lies inside the shaded area in Figure 3.6, and half lies outside the solid line. Therefore there exist many wavelet bases with $N = 3$ for which the wavelet is continuous, cf. Figures 3.7 and 3.8.

For large m, direct computation of λ_m is impractical. The following algorithm can be used to select a subset of matrices which can be used to estimate $\rho(A_0, \ldots, A_n)$ [10], cf. [16].

Proposition 3.7. Given $\rho > \rho(A_0, \ldots, A_n)$. For each of the matrices $A_0, \ldots, A_n$ in turn, implement the following recursion.

- Given a product $P = A_{d_1} \cdots A_{d_m}$. If $\|P\|^{1/m} < \rho$ then keep P as a *building block*. Otherwise, repeat this step with each of the products $PA_0, \ldots, PA_n$ in turn.

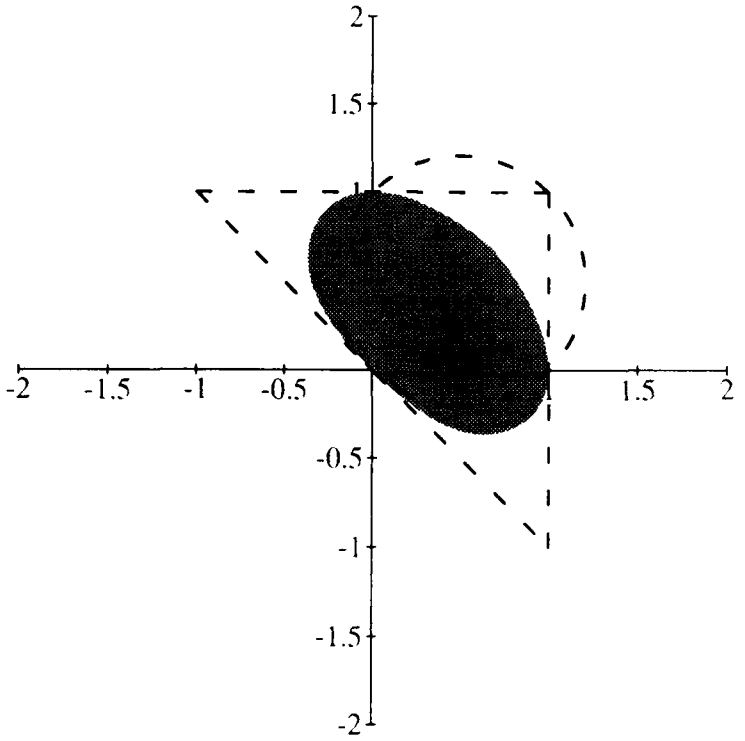

Figure 3.3: The set $C_{2,1}$ (shaded area).

Label the resulting set of building blocks $P_1, \ldots, P_L$, and let m_i be the length of the product P_i. Then the following statements hold.

1) There is an $r \geq 0$ such that if $P = A_{d_1} \cdots A_{d_m}$ is any product of the matrices $A_0, \ldots, A_n$, then $P = P_{i_1} \cdots P_{i_k} R$ where R is some product of at most r of the matrices $A_0, \ldots, A_n$.
2) $\rho(A_0, \ldots, A_n) \leq \max\{\|P_1\|^{1/m_1}, \ldots, \|P_L\|^{1/m_L}\}$.

This algorithm can be used to significantly shorten the time required to estimate a joint spectral radius.

Remark 3.8. For $N = 3$ and $(c_0, c_3) = (.6, -.2)$, for which simultaneous symmetrization is not possible, we compute (using the norm $\|\cdot\|_1$) $\lambda_1 = .737$ and $\lambda_{13} = .682$. The computation of λ_{13} required the calculation of 8192 matrix products; however, the algorithm given in Proposition 3.7 equals this estimate after only 94 matrix product computations. A deeper search,

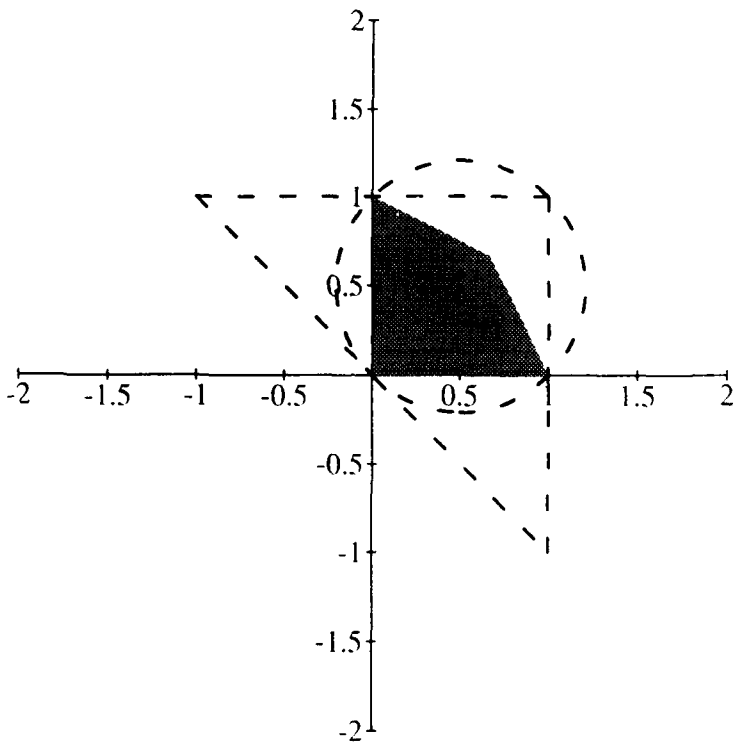

Figure 3.4: The set $C_{\infty,1}$ (shaded area).

with a maximum matrix product length of 73, required only 14156 matrix product computations and resulted in the estimate $\rho(S_0, S_1) \leq .661$. Even if λ_{73} could be computed it would not improve this estimate, e.g., $\|S_0^2 S_1 S_0^{14} S_1 S_0^{14} S_1 S_0^{13} S_1 S_0^{12} S_1 S_0^{12} S_1\|_1^{1/73} = .663$. These computations, and the significance of the point $(c_0, c_3) = (.6, -.2)$, are explained in detail in [9]; note, however, that the Hölder exponent of continuity for the scaling function determined by the coefficients $(c_0, c_3) = (.6, -.2)$ is at least $-\log_2 .661 \approx .598$, and therefore this scaling function is smoother than the standard four-coefficent example, the Daubechies scaling function D_4, which is determined by the coefficients $(c_0, c_3) = ((1 + \sqrt{3})/4, (1 - \sqrt{3})/4)$, and whose Hölder exponent of continuity is approximately .550. These two scaling functions are shown in Figures 3.7 and 3.8. Each of these two choices of coefficients lies on the circle of orthogonality and determines a multiresolution analysis for $L^2(\mathfrak{R})$.

Theorem 3.2 is extended to a necessary and sufficient condition in [10].

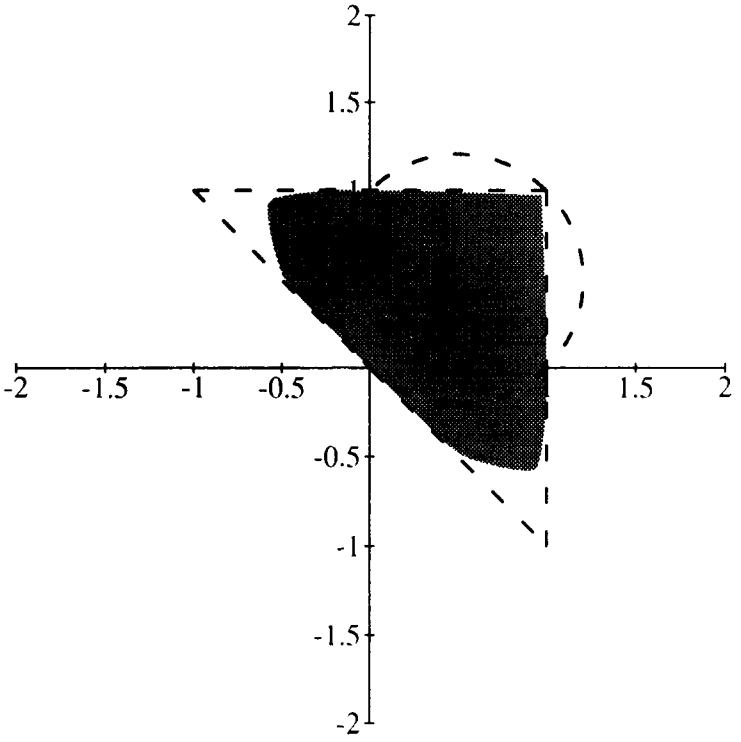

Figure 3.5: The set $C_{2,16}$ (shaded area).

We briefly indicate now the method used to obtain the converse result. Given an $N \times N$ matrix A and an eigenvalue λ of A, set $U_\lambda = \{u \in \mathcal{C}^N : (A - \lambda)^k u = 0 \text{ for some } k > 0\}$. By standard Jordan decomposition techniques we can write $\mathcal{C}^N = U_\lambda \oplus W$, where W is a unique A-invariant subspace of $\mathcal{C}^N$. Given $v \in \mathcal{C}^N$ we say that v *has a component in* U_λ if $v = u + w$ where $u \in U_\lambda$, $w \in W$, and $u \neq 0$. The following result is from [10].

Theorem 3.9. Assume v is a continuous vector-valued function on $[0,1]$ such that (3.2) holds, and let $T = T_{d_1} \cdots T_{d_m}$ be any fixed product of the matrices T_0, T_1. Let $x \in [0,1]$ be that point whose binary decimal expansion is $x = .d_1 \ldots d_m d_1 \ldots d_m \ldots$. If

1) λ is an eigenvalue of $T|_V$, and
2) there is some $z \in [0,1]$ such that $v(x) - v(z)$ has a component in U_λ,

then $|\lambda| < 1$ and the Hölder exponent of continuity of v is at most $-\log_2 |\lambda|^{1/m}$.

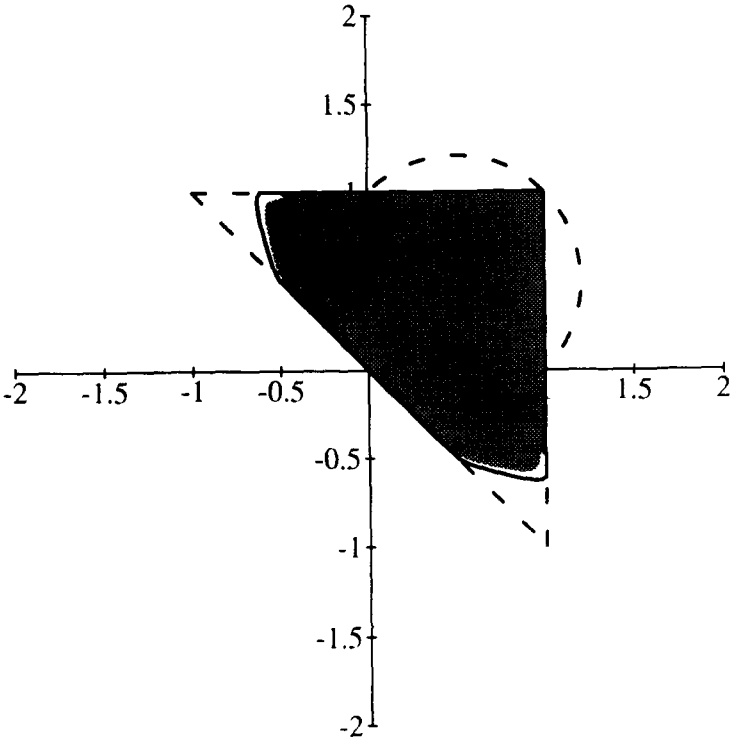

Figure 3.6: Union of the sets SS, $C_{1,1}$, $C_{2,1}$, $C_{\infty,1}$, and $C_{2,16}$ (shaded area); boundary of the set E_{16} (solid line).

Since $\rho(T_0|V, T_1|V) = \sup \sigma_m$ is the supremum of the absolute values of the eigenvalues of every $(T_{d_1} \cdots T_{d_m})|V$, it follows that if the hypotheses of Theorem 3.9 are satisfied for each product $T = T_{d_1} \cdots T_{d_m}$ then $\rho(T_0|V, T_1|V) \leqslant 1$ with $\sigma_m < 1$ for all m, and the Hölder exponent of ν satisfies $\alpha \leqslant -\log_2 \rho(T_0|V, T_1|V)$. Therefore, if the hypotheses of Theorem 3.9 are satisfied for each product $T = T_{d_1} \cdots T_{d_m}$ then Theorem 3.9 is the converse to Theorem 3.2, except for the possibility of one special case, namely,

$$\sup_m \sigma_m = 1 \qquad \text{and} \qquad \sigma_m < 1 \quad \text{for all } m.$$

It is unknown whether this special case can actually occur. It is proven in [9] that the hypotheses of Theorem 3.9 are always satisfied if $N \leqslant 3$ and it is conjectured in [10] that they are always satisfied in general except for a set of coefficients of measure zero. Methods for determining the validity of the

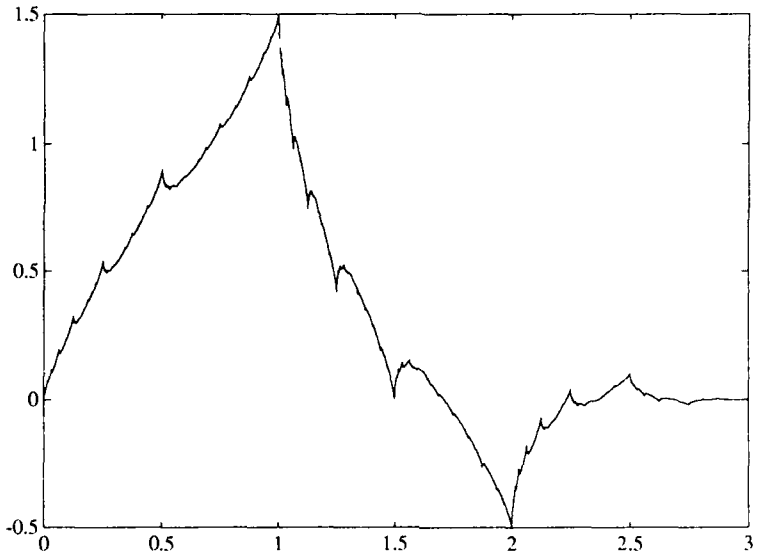

Figure 3.7: Scaling function corresponding to $(c_0, c_3) = (.6, -.2)$.

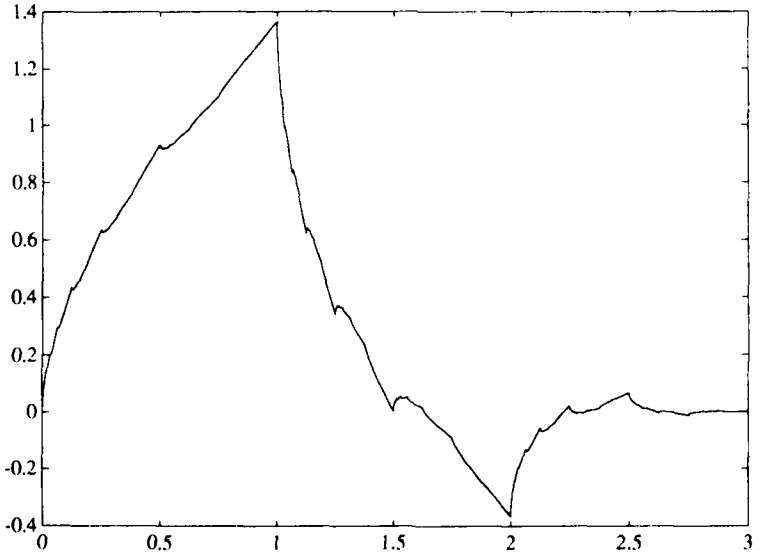

Figure 3.8: Daubechies scaling function D_4.

hypotheses of Theorem 3.9 for any specific choice of coefficients are given in [10].

Remark 3.10. Set $N = 3$ and define $E_m = \{(c_0, c_3) : \sigma_m \geq 1\}$. By Theorem 3.6, no dilation equation determined by a point in E_m can have a continuous, integrable solution. The set E_1 is precisely the boundary and exterior of the triangle shown in Figure 1.1. The solid line in Figure 3.6 shows a numerical approximation of the boundary of E_{16} [9]. By previous remarks, continuous, integrable scaling functions do exist in the shaded region in Figure 3.6.

The results of this section can be extended from consideration of continuous solutions to n-times differentiable solutions. If f is such a solution then its derivatives $f^{(j)}$ satisfy the dilation equations

$$f^{(j)}(t) = \sum_k 2^j c_k f^{(j)}(2t - k).$$

Therefore the vector $(f^{(j)}(1), \ldots, f^{(j)}(N-1))^t$ is a right eigenvector for the matrix M for the eigenvalue 2^{-j}. As M is an $(N-1) \times (N-1)$ matrix, f can therefore possess at most $N-2$ derivatives. This can always be achieved for an appropriate choice of coefficients [16].

The following modification of Theorem 3.2 for the case of higher derivatives is from [16].

Theorem 3.11. Assume that the coefficients $\{c_k\}$ satisfy the *sum rules* $\sum (-1)^k k^j c_k = 0$ for $j = 0, \ldots, n$. Define $V_n = \{u \in \mathcal{R}^N : e_j u = 0, j = 0, \ldots, n\}$, where $e_j = (1^j, 2^j, \ldots, N^j)$. If $\rho(T_0|_{V_n}, T_1|_{V_n}) < 2^{-n}$ then there exists an n-times differentiable solution f to (1.1), and the n-th derivative $f^{(n)}$ of f is Hölder continuous with exponent $\alpha \geq -\log_2 2^n \rho(T_0|_{V_n}, T_1|_{V_n})$.

Remark 3.12. For the case $N = 3$, differentiable solutions can exist only on the solid portion of the line shown in Figure 1.1. None of these solutions can be twice differentiable. In particular, for $N = 3$, no wavelet which generates an affine orthonormal basis can be differentiable since wavelets must be derived from points lying inside of the circle of orthogonality.

4. Orthogonality

In this section we consider the relationship between the choice of coefficents $\{c_k\}$ and frame or basis properties of the associated wavelet. We assume N is odd in this section.

We require the following lemmas. $C_c(\mathcal{R})$ denotes the space of all continuous functions on $\mathcal{R}$ which have compact support. The proof of the first lemma can be found in [27].

Lemma 4.1. If $(\{V_n\}, f)$ is a multiresolution analysis then $\int f(t)\,dt = 1$.

Lemma 4.2. *If (1.3) holds then the canonical scaling function f satisfies* $\sum f(t-k) = 1$ a.e.

Proof. Set $\theta_0 = \chi_{[0,1)}$ and $\theta_j(t) = \sum c_k\, \theta_{j-1}(2t-k)$. Since $\hat{\theta}$ is continuous, $\hat{\theta}(0) = 1$, and $\hat{\theta}_j(2\gamma) = m_0(\gamma)\,\hat{\theta}_{j-1}(\gamma)$, it follows that $\theta_j \to f$ weakly in $L^2(\mathfrak{R})$, i.e., $\langle \theta_j, h\rangle \to \langle f, h\rangle$ for all $h \in L^2(\mathfrak{R})$. Note that $\sum \theta_0(t-k) = 1$ a.e.; by induction, the same is true of θ_j, and hence of f. ∎

Next, we establish necessary conditions on the coefficients $\{c_k\}$ in order that a multiresolution analysis exist.

Proposition 4.3. If the coefficients $\{c_k\}$ determine a multiresolution analysis then (1.3) and (1.4) hold. The converse is not true.

Proof. Integrating both sides of the dilation equation implies that $\sum c_k = 2$, since $\int f(t)\,dt$ is nonzero by Lemma 4.1. Since f is orthogonal to its integer translates,

$$\begin{aligned} 2\,\delta_{0l} &= 2\int f(t)\,f(t+l)\,dt \\ &= 2\sum_{j,k} c_j\,c_k \int f(2t-j)\,f(2t+2l-k)\,dt \\ &= \sum_k c_k\,c_{k+2l}, \end{aligned}$$

so (1.4) holds. This, combined with the fact $\sum c_k = 2$, implies (1.3).

To see that (1.3) and (1.4) are not sufficient, consider the coefficient choice $c_0 = 1$, $c_1 = \cdots = c_{N-1} = 0$, $c_N = 1$. These coefficients satisfy (1.3) and (1.4), yet the canonical scaling function $f = (1/N)\chi_{[0,N)}$ is not orthogonal to its integer translates if $N > 1$. ∎

Remark 4.4. For $N = 3$, the set of points in the (c_0, c_2)-plane which satisfy both (1.3) and (1.4) is precisely the circle of orthogonality shown in Figure 1.1.

Equations (1.3) and (1.4) are equivalent to

$$m_0(0) = 1 \qquad \text{and} \qquad m_0(\pi) = 0 \tag{4.1}$$

and

$$|m_0(\gamma)|^2 + |m_0(\gamma+\pi)|^2 = 1 \qquad \text{for all} \quad \gamma. \tag{4.2}$$

Equation (4.2) implies that, in signal processing terms, $m_0(\gamma)$ and $m_0(\gamma+\pi)$ form a *quadrature mirror filter pair*. Such filter pairs induce fast digital signal

processing algorithms, e.g., *subband coding*. Daubechies has characterized those trigonometric polynomials m_0 which satisfy (4.1) and (4.2) in [12].

Although (1.3) and (1.4) are not sufficient to ensure that $\{c_k\}$ will generate a multiresolution analysis (and therefore that $\{g_{nk}\}_{n,k\in\mathcal{Z}}$ will be an orthonormal basis), Lawton has proven that (1.3) and (1.4) are sufficient to ensure that the sequence $\{g_{nk}\}_{n,k\in\mathcal{Z}}$ will satisfy the reconstruction property (1.5) of an orthonormal basis. Such a sequence is called a *tight frame*. (1.5) alone does not imply that $\{g_{nk}\}_{n,k\in\mathcal{Z}}$ is an orthogonal sequence or a basis, i.e., in general the summation in (1.5) is not unique. See [18] or [23] for exposition on frames and their properties.

The following theorem and proof are from [24].

Theorem 4.5. If the coefficients $\{c_k\}$ satisfy (1.3) and (1.4) then $\{g_{nk}\}_{n,k\in\mathcal{Z}}$ is a tight frame for $L^2(\mathfrak{R})$.

Proof. We proceed in four steps.

1) From (4.2) and Theorems 2.6 and 2.1, the canonical scaling distribution f is an integrable function with support contained in $[0, N]$ and satisfies $\int f(t)\,dt = 1$.

2) Define the operator $P_n : L^2(\mathfrak{R}) \to L^2(\mathfrak{R})$ by

$$P_n h = \sum_k \langle h, f_{nk}\rangle f_{nk}. \tag{4.3}$$

We claim that $P_n \to I$ as $n \to +\infty$ and $P_n \to 0$ as $n \to -\infty$, where I is the identity operator on $L^2(\mathfrak{R})$.

First, however, we show that the operators $\{P_n\}$ are uniformly bounded in norm. Since $\operatorname{supp}(f_{nk}) \subset I_{nk} = [k/2^n, (k+N)/2^n]$, with n fixed each set $\operatorname{supp}(f_{nk})$ can intersect at most N other $\operatorname{supp}(f_{nj})$. Therefore, for any scalars $\{a_k\}$,

$$\begin{aligned}\left\|\sum_k a_k f_{nk}\right\|_2 &\le N^{1/2}\left(\sum_k |a_k|^2 \|f_{nk}\|_2^2\right)^{1/2} \\ &= N^{1/2}\|f\|_2\left(\sum_k |a_k|^2\right)^{1/2},\end{aligned} \tag{4.4}$$

e.g., [22, Prop. 2.4.10]. Therefore,

$$\|P_n h\|_2 \le N^{1/2}\|f\|_2\left(\sum_k |\langle h, f_{nk}\rangle|^2\right)^{1/2}. \tag{4.5}$$

Now, for each $r = 0, \ldots, N-1$, the sequence $\{f_{n(lN+r)}\}_{l\in\mathcal{Z}}$ is an orthogonal collection of functions since their supports are disjoint. Therefore, by Bessel's

inequality, $\sum |\langle h, f_{n(kN+r)}\rangle|^2 \leqslant \|h\|_2^2 \|f\|_2^2$. Combining this with (4.5) we obtain $\|P_n h\|_2 \leqslant N \|f\|_2^2 \|h\|_2$, and therefore $\sup \|P_n\|_2 \leqslant N \|f\|_2^2 < \infty$.

Because the operators $\{P_n\}$ are uniformly bounded in norm, to prove $P_n h \to h$ as $n \to +\infty$ for all $h \in L^2(\mathfrak{R})$ it suffices to consider h in a dense subset of $L^2(\mathfrak{R})$, say $h \in C_c(\mathfrak{R})$. For such an h, since $\sum_k f_{nk}(t) = 2^{n/2}$ a.e. (Lemma 4.2), we can write

$$\begin{aligned} \|h - P_n h\|_2 &= \left(\int \left| \sum_k (2^{-n/2} h(t) - \langle h, f_{nk}\rangle) f_{nk}(t) \right|^2 dt \right)^{1/2} \\ &\leqslant N^{1/2} \left(\sum_k \|(2^{-n/2} h(t) - \langle h, f_{nk}\rangle) f_{nk}(t)\|_2^2 \right)^{1/2} \qquad (4.6) \\ &\leqslant N^{1/2} \|f\|_2 \left(\sum_k \alpha_{nk}^2 \right)^{1/2}, \end{aligned}$$

where we have used (4.4) again and where

$$\alpha_{nk} = \sup_{t \in I_{nk}} |2^{-n/2} h(t) - \langle h, f_{nk}\rangle|.$$

To see that $\sum \alpha_{nk}^2 \to 0$ as $n \to +\infty$, define

$$\beta_{nk} = \sup_{s,t \in I_{nk}} |h(s) - h(t)| \qquad \text{and} \qquad \tilde{h}_n = \sum_k \beta_{nk}^2 \chi_{I_{nk}}.$$

Note that $\tilde{h}_n(t) \to 0$ pointwise as $n \to +\infty$ since $h \in C_c(\mathfrak{R})$. Further, $\beta_{nk} \leqslant \beta_{n0}$ and $I_{nk} \subset I_{n0}$ for all k, so $\tilde{h}_n \leqslant \tilde{h}_0$ for $n \geqslant 0$. As $\tilde{h}_0$ is clearly integrable, it follows from the Lebesgue Dominated Convergence Theorem that $\int \tilde{h}_n(t)\, dt \to 0$ as $n \to +\infty$. Now, since $\int f_{nk}(t)\, dt = 2^{-n/2}$ (Lemma 4.1), we have for $t \in I_{nk}$ that

$$\begin{aligned} |2^{-n/2} h(t) - \langle h, f_{nk}\rangle| &= \left| \int_{I_{nk}} (h(t) - h(s)) f_{nk}(s)\, ds \right|^2 \\ &\leqslant \left(\int_{I_{nk}} |h(t) - h(s)|^2\, ds \right) \left(\int_{I_{nk}} |f_{nk}(s)|^2\, ds \right) \\ &\leqslant \|f\|_2^2 \beta_{nk}^2 \int \chi_{I_{nk}}(s)\, ds. \end{aligned}$$

Therefore, $\sum_k \alpha_{nk}^2 \leqslant \|f\|_2^2 \int \tilde{h}_n(s)\, ds \to 0$ as $n \to +\infty$, which, combined with (4.6), implies that $P_n h \to h$ in $L^2(\mathfrak{R})$ as $n \to +\infty$.

A similar proof shows that $P_n h \to 0$ as $n \to -\infty$.

3) Define the operator $F_n : L^2(\mathfrak{R}) \to L^2(\mathfrak{R})$ by

$$F_n h = \sum_k \langle h, g_{nk}\rangle g_{nk}.$$

We claim then that $F_n = P_{n+1} - P_n$ for each $n \in \mathbb{Z}$. Using the dilation equation (1.1) and the definition (1.2) we compute

$$\begin{aligned}
P_n h + F_n h &= \sum_k \langle h(t), 2^{n/2} f(2^n t - k)\rangle 2^{n/2} f(2^n t - k) \\
&\qquad + \sum_k \langle h(t), 2^{n/2} g(2^n t - k)\rangle 2^{n/2} g(2^n t - k) \\
&= 2^n \sum_{k,p,q} \langle h(t), c_p f(2^{n+1} t - 2k - p)\rangle c_q f(2^{n+1} t - 2k - q) \\
&\quad + 2^n \sum_{k,p,q} \langle h(t), (-1)^p c_{N-p} f(2^{n+1} t - 2k - p)\rangle \\
&\qquad \cdot (-1)^q c_{N-q} f(2^{n+1} t - 2k - q) \\
&= 2^n \sum_{p,q,k} \langle h(t), (c_p c_q + (-1)^{p+q} c_{N-p} c_{N-q}) f(2^{n+1} t - 2k - p)\rangle \\
&\qquad \times f(2^{n+1} t - 2k - q) \\
&= \sum_{j,l} \frac{1}{2} \sum_k (c_{j-2k} c_{l-2k} + (-1)^{j+l} c_{N-j+2k} c_{N-l+2k}) \\
&\qquad \cdot \langle h(t), 2^{(n+1)/2} f(2^{n+1} t - j)\rangle 2^{(n+1)/2} f(2^{n+1} t - l) \\
&= \sum_{j,l} C(j,l) \langle h, f_{(n+1)j}\rangle f_{(n+1)l},
\end{aligned}$$

where

$$C(j,l) = \frac{1}{2} \sum_k (c_{j-2k} c_{l-2k} + (-1)^{j+l} c_{N-j+2k} c_{N-l+2k}).$$

It suffices, therefore, to show that $C(j,l) = \delta_{jl}$. Note that by making the change of index $m = -k + j + l - (N-1)/2$ (recall N is odd) in the second summation, we obtain

$$\begin{aligned}
C(2j,2l) &= \frac{1}{2} \sum_k c_{2j-2k} c_{2l-2k} + \frac{1}{2} \sum_m c_{2j-2m+1} c_{2l-2m+1} \\
&= \frac{1}{2} \sum_k c_{2j-k} c_{2l-k} \\
&= \delta_{jl},
\end{aligned}$$

because of hypothesis (1.4). Similar calculations show that $C(2j, 2l+1) = C(2j+1, 2l) = 0$ and $C(2j+1, 2l+1) = \delta_{jl}$, as desired.

4) From steps 2) and 3), $\sum_n F_n = \lim_{n\to\infty}(P_n - P_{-n}) = I$. That is, for $h \in L^2(\mathfrak{R})$, $h = \sum_n F_n h = \sum_{n,k}\langle h, g_{nk}\rangle g_{nk}$, whence $\{g_{nk}\}_{n,k\in\mathfrak{Z}}$ is a tight frame. ∎

Corollary to 4.5. The coefficients $\{c_k\}$ determine a multiresolution analysis if and only if

1) (1.3) and (1.4) are satisfied, and
2) f is orthogonal to each of its integer translates.

In this case, $\{g_{nk}\}_{n,k\in\mathfrak{Z}}$ is an orthonormal basis for $L^2(\mathfrak{R})$.

Proof. Because of Proposition 4.3 we need only prove that if 1) and 2) hold then $\{c_k\}$ determines a multiresolution analysis. From (1.4) and the orthogonality of the integer translates of f,

$$\|f\|_2^2 = \int |f(t)|^2\,dt = \sum_{j,k} c_j c_k \int f(2t-j)\,f(2t-k)\,dt = \frac{1}{2}\sum_k c_k^2 = 1.$$

Therefore $\{f(t-k)\}_{k\in\mathfrak{Z}}$ is an orthonormal set and hence is an orthonormal basis for $V_0 = \operatorname{span}\{f(t-k)\}_{k\in\mathfrak{Z}}$. Defining $V_n = \operatorname{span}\{f_{nk}\}_{k\in\mathfrak{Z}}$, we have $V_n \subset V_{n+1}$ because f is a scaling function. The operator P_n defined by (4.3) is then the orthogonal projection of $L^2(\mathfrak{R})$ onto V_n. Since $P_n \to 0$ as $n \to -\infty$ we have $\cap V_n = \{0\}$, and similarly $\cup V_n$ is dense in $L^2(\mathfrak{R})$ since $P_n \to I$ as $n \to +\infty$. Thus $(\{V_n\}, f)$ is a multiresolution analysis.

To prove that $\{g_{nk}\}_{n,k\in\mathfrak{Z}}$ is an orthonormal basis, note that from (1.2), (1.4), and the orthogonality of the integer translates of f,

$$\|g\|_2^2 = \sum_{j,k}(-1)^{j+k} c_{N-j} c_{N-k} \int f(2t-j)\,f(2t-k)\,dt = \frac{1}{2}\sum_k c_k^2 = 1.$$

From the theorem, we know that $\{g_{nk}\}_{n,k\in\mathfrak{Z}}$ is a tight frame, so for $m, j \in \mathfrak{Z}$ fixed,

$$\begin{aligned} 1 &= \|g_{mj}\|_2^2 \\ &= \langle g_{mj}, g_{mj}\rangle \\ &= \Big\langle g_{mj}, \sum_{n,k}\langle g_{mj}, g_{nk}\rangle g_{nk}\Big\rangle \\ &= \sum_{n,k} |\langle g_{mj}, g_{nk}\rangle|^2. \end{aligned}$$

Thus $\langle g_{mj}, g_{nk}\rangle = \delta_{mn}\delta_{jk}$, i.e., $\{g_{nk}\}_{n,k\in\mathfrak{Z}}$ forms an orthonormal set. This, combined with the tight frame property, implies that $\{g_{nk}\}_{n,k\in\mathfrak{Z}}$ is an orthonormal basis. ∎

Lawton and Cohen have independently established necessary and sufficient conditions under which f will be orthogonal to its integer translates. Lawton's formulation is the following [24, 25]. ℓ^2 denotes the space of all square-summable sequences.

Theorem 4.6. Define the operator $G : \ell^2 \to \ell^2$ by

$$(Ga)_l = \frac{1}{2} \sum_{j,k} c_j c_k a_{2l+j-k} \qquad \text{for} \quad a \in \ell^2.$$

Then the coefficients $\{c_k\}$ determine a multiresolution analysis if and only if

1) (1.3) and (1.4) are satisfied, and
2) δ_{0l} is the only eigenvector for G for the eigenvalue 1.

Proof. Note that δ_{0l} is an eigenvector for G for the eigenvalue 1 because of (1.4), and the sequence a defined by $a_l = \int f(t) f(t + l)\, dt$ is also an eigenvector for G for the eigenvalue 1 since

$$\begin{aligned}
(Ga)_l &= \frac{1}{2} \sum_{j,k} c_j c_k \int f(t) f(t - 2l + j - k)\, dt \\
&= \frac{1}{2} \int \left(\sum_j c_j f(t - j) \right) \left(\sum_k c_k f(t - 2l - k) \right) dt \\
&= \frac{1}{2} \int f\left(\frac{t}{2}\right) f\left(\frac{t}{2} - l\right) dt \\
&= a_l.
\end{aligned}$$

Therefore, if δ_{0l} is the only eigenvector for G for the eigenvalue 1 then $a_l = c\,\delta_{0l}$ for some constant c, so f is orthogonal to its integer translates. The converse of this statement is proved in [25]. The proof is therefore complete by the corollary to Theorem 4.5. ∎

Lawton has proved, using a result of Pollen [31], that except for a set of measure zero, coefficients which satisfy (1.3) and (1.4) also satisfy the condition that δ_{0l} be the only eigenvector for G for the eigenvalue 1. Therefore almost all choices of coefficients satisfying (1.3) and (1.4) will determine a multiresolution analysis.

Cohen's formulation, which has been shown to be equivalent to Lawton's, is the following [6], cf. [25].

Theorem 4.7. The coefficients $\{c_k\}$ determine a multiresolution analysis if and only if

1) (1.3) and (1.4) are satisfied, and
2) there exists a $\gamma \in [-\pi/2, \pi/2]$ such that $\hat{f}(\gamma + 2k\pi) = 0$ for every $k \in \mathbb{Z}$.

Remark 4.8. For N = 3, the set of points satisfying (1.3) and (1.4) is the circle shown in Figure 1.1. Of these, every point with the single exception of the point (1, 1) does determine a multiresolution analysis [11].

5. Bibliography

[1] G. Battle. A block spin construction of ondelettes. *Comm. Math. Phys.*, 110:601–615, 1987.

[2] M.A. Berger. Random affine iterated function systems: smooth curve generation. Preprint.

[3] M.A. Berger and Y. Wang. Bounded semi-groups of matrices. Preprint.

[4] M.A. Berger and Y. Wang. Multi-scale dilation equations and iterated function systems. Preprint.

[5] A. Cavaretta, W. Dahmen, and C.A. Micchelli. Stationary subdivision. *Memoirs Amer. Math. Soc.* To appear.

[6] A. Cohen. Ondelettes, analyses multirésolutions et filtres miroirs en quadrature. *Ann. Inst. H. Poincare*, 7:439–459, 1990.

[7] R. Coifman, Y. Meyer, and M.V. Wickerhauser. Signal compression with wave packets. Preprint.

[8] R. Coifman and M.V. Wickerhauser. Best-adapted wave packet bases. Preprint.

[9] D. Colella and C. Heil. The characterization of continuous, four-coefficient scaling functions and wavelets. *IEEE Trans. Inf. Th., Special issue on Wavelet Transforms and Multiresolution Signal Analysis.* To appear.

[10] D. Colella and C. Heil. Characterizations of scaling functions, I. Continuous solutions. Preprint.

[11] D. Colella and C. Heil. Characterizations of scaling functions, II. Distributional and functional solutions. Preprint.

[12] I. Daubechies. Orthonormal bases of compactly supported wavelets. *Comm. Pure Appl. Math.*, 41:909–996, 1988.

[13] I. Daubechies. The wavelet transform, time-frequency localization and signal analysis. *IEEE Trans. Inf. Th.*, 1990.

[14] I. Daubechies and J. Lagarias. Sets of matrices all infinite products of which converge. *Lin. Alg. Appl.* To appear.

[15] I. Daubechies and J. Lagarias. Two-scale difference equations: I. Gobal regularity of solutions. *SIAM J. Math. Anal.* To appear.

[16] I. Daubechies and J. Lagarias. Two-scale difference equations: II. Local regularity, infinite products and fractals. *SIAM J. Math. Anal.* To appear.

[17] G. Deslauriers and S. Dubuc. Symmetric iterative interpolation processes. *Constr. Approx.*, 5:49–68, 1989.

[18] R.J. Duffin and A.C. Schaeffer. A class of nonharmonic Fourier series. *Trans. Amer. Math. Soc.*, 72:341–366, 1952.

[19] N. Dyn, J.A. Gregory, and D. Levin. Analysis of uniform binary subdivision schemes for curve design. *Const. Approx.*, 7:127–147, 1991.

[20] N. Dyn and D. Levin. Interpolating subdivision schemes for the generation of curves and surfaces. Preprint.

[21] T. Eirola. Sobolev characterization of solutions of dilation equations. *SIAM J. Math. Anal.* Submitted.

[22] C. Heil. *Wiener amalgam spaces in generalized harmonic analysis and wavelet theory.* Ph.D. thesis, University of Maryland, College Park, MD, 1990.

[23] C. Heil and D. Walnut. Continuous and discrete wavelet transforms. *SIAM Rev.*, 31:628–666, 1989.

[24] W. Lawton. Tight frames of compactly supported affine wavelets. *J. Math. Phys.*, 31:1898–1901, 1990.

[25] W. Lawton. Necessary and sufficient conditions for constructing orthonormal wavelet bases. *J. Math. Phys.*, 32:57–61, 1991.

[26] P.G. Lemarié. Ondelettes à localisation exponentielle. *Journ. de Math. Pures et Appl.*, 67:227–236, 1988.

[27] S.G. Mallat. Multiresolution approximations and wavelet orthonormal bases for $L^2(\mathbb{R})$. *Trans. Amer. Math. Soc.*, 315:69–87, 1989.

[28] Y. Meyer. Principe d'incertitude, bases hilbertiennes et algèbres d'opérateurs. *Séminaire Bourbaki*, 662, 1985–1986.

[29] C.A. Micchelli and H. Prautzsch. Refinement and subdivision for spaces of integer translates of compactly supported functions. In C.F. Griffiths and G. A. Watson, editors, *Numerical Analysis*, pages 192–222, 1987.

[30] C.A. Micchelli and H. Prautzsch. Uniform refinement of curves. *Lin. Alg. Appl.*, 114/115:841–870, 1989.

[31] D. Pollen. $SU_1(2, F[z, 1/z])$ for F a subfield of C. Preprint.

[32] G.C. Rota and G. Strang. A note on the joint spectral radius. *Indag. Math.*, 22:379–381, 1960.

[33] G. Strang. Wavelets and dilation equations: a brief introduction. *SIAM Rev.*, 31:614–627, 1989.

Characterization of singularities†

Stéphane Mallat
Courant Institute of Mathematical Sciences
251 Mercer Street
New York University
New York, NY 10012 USA
mallat@regard.nyu.edu

Wen Liang Hwang
(Same address.)

Abstract Most signal information is carried by irregular structures and transient phenomena. The mathematical characterization of singularities with Lipschitz exponents is reviewed. We explain the theorems that estimate local Lipschitz exponents of functions, from the evolution across scales of their wavelet transform. We then prove that the local maxima of a wavelet transform detect the locations of irregular structures and provide numerical procedures to compute their Lipschitz exponents. The wavelet transforms of singularities with fast oscillations have a different behavior that we study separately. The local frequency of the oscillations are measured from the wavelet transform local maxima. It has been shown numerically that one and two-dimensional signals can be reconstructed, with a good approximation, from the local maxima of their wavelet transform [16]. As an application, we develop an algorithm that removes white noise from signals, by analyzing the evolution of the wavelet transform maxima across scales.

† This research was supported by NSF grant IRI-890331, Air Force grant AFOSR-90-0040 and ONR grant N00014-91-J-1967.

We would like to thank Emmanuel Bacry for helping us with numerical computations and for interesting discussions.

J. S. Byrnes et al. (eds.), Probabilistic and Stochastic Methods in Analysis, with Applications, 47–100.
© 1992 *All Rights Reserved. Printed in the Netherlands.*

1. Introduction

Singularities and irregular structures often carry the most important information in signals. In images, the discontinuities of the intensity provide the locations of the object contours, which are particularly meaningful for recognition purposes. For many other types of signals, from electro-cardiograms to radar signals, the interesting information is given by transient phenomena such as peaks. In physics, it is also important to study irregular structures to infer properties about the underlying physical phenomena [17, 2, 1]. Until recently, the Fourier transform was the main mathematical tool for analyzing singularities. The Fourier transform is global and provides a description of the overall regularity of signals, but it is not well adapted for finding the location and the spatial distribution of singularities. This was a major motivation for studying the wavelet transform in mathematics [20] and in applied domains [11]. By decomposing signals into elementary building blocks that are well localized both in space and frequency, the wavelet transform can characterize the local regularity of signals. The wavelet transform and its main properties are briefly introduced in Section 2. In mathematics, the local regularity of a function is often measured with Lipschitz exponents. Section 3 is a tutorial review on Lipschitz exponents and their characterization with the Fourier transform and the wavelet transform. We explain the basic theorems that relate local Lipschitz exponents to the evolution across scales of the wavelet transform values. In practice, these theorems do not provide simple and direct strategies for detecting and characterizing singularities in signals. The following sections show that the wavelet transform local maxima give an efficient approach for studying these singularities.

The detection of singularities with multiscale transforms has been studied not only in mathematics but also in signal processing. In Section 4, we explain the relation between the multiscale edge detection algorithms used in computer vision and the approach of Grossmann [10] based on the phase of the wavelet transform. The detection of wavelet transform local maxima is strongly motivated by these techniques. Section 5 is a mathematical analysis of the local maxima properties. We prove that local maxima detect all singularities and that local Lipschitz exponents can often be measured from their evolution across scales. We derive practical algorithms to analyze isolated or non-isolated singularities in signals. Numerical examples illustrate the mathematical results. The wavelet transform has a different

behavior when singularities have fast oscillations. This particular case is studied separately. The local frequency of the oscillations can be measured from the points where the wavelet transform is locally maximum both along the scale and spatial variables. This approach is closely related to the work of Escudie and Torresani [9] for measuring the modulation law of asymptotic signals [8].

Another important issue is to understand whether one can reconstruct a signal from the local maxima of its wavelet transform. If it is possible, it allows us to process a signal's singularities by modifying the local maxima of its wavelet transform and then reconstruct the corresponding function. We review the most recent results of Meyer [21] on this completeness issue and describe a numerical algorithm developed by Zhong and one of us [16], which closely reconstructs a signal from the wavelet local maxima. One application is the removal of white noise from signals. In such problems, we often have some prior information on the differences between the signal singularities and the noise singularities. We describe an algorithm that differentiates the signal components from the noise, by selecting the wavelet transform local maxima that correspond to the signal singularities. After removing the local maxima of the noise fluctuations, we reconstruct a "denoised" signal.

1.1. Notation

- $L^p(\mathfrak{R})$ denotes the Hilbert space of measurable, functions such that
$$\int_{-\infty}^{+\infty} |f(x)|^p \, dx < +\infty.$$
- The norm of $f \in L^2(\mathfrak{R})$ is given by
$$\|f\|^2 = \int_{-\infty}^{+\infty} |f(x)|^2 \, dx.$$
- We denote the convolution of two functions $f \in L^2(\mathfrak{R})$ and $g \in L^2(\mathfrak{R})$ by
$$f * g(x) = \int_{-\infty}^{+\infty} f(u) g(x-u) \, du.$$
- The Fourier transform of a function $f(x)$ is written $\hat{f}(\omega)$ and defined by
$$\hat{f}(\omega) = \int_{-\infty}^{+\infty} f(x) e^{-i\omega x} \, dx.$$
- For any function $f(x)$, $f_s(x)$ denotes the dilation of $f(x)$ by the scale factor s:
$$f_s(x) = \frac{1}{s} f(x/s).$$

2. Continuous wavelet transform

This section reviews the main properties of the wavelet transform. The formalism of the continuous wavelet transform was first introduced by Morlet and Grossmann [11]. Let $\psi(x)$ be a complex valued function. The function $\psi(x)$ is said to be a wavelet if and only if its Fourier transform $\hat{\psi}(\omega)$ satisfies

$$\int_0^{+\infty} \frac{|\hat{\psi}(\omega)|^2}{\omega} d\omega = \int_{-\infty}^{0} \frac{|\hat{\psi}(\omega)|^2}{|\omega|} d\omega = C_\psi < +\infty. \tag{2.1}$$

This condition implies that

$$\int_{-\infty}^{+\infty} \psi(u)\, du = 0.$$

Let $\psi_s(x) = \frac{1}{s}\psi(x/s)$ be the dilation of $\psi(x)$ by the scale factor s. The wavelet transform of a function $f \in L^2(\mathfrak{R})$ is defined by

$$Wf(s,x) = f * \psi_s(x). \tag{2.2}$$

The Fourier transform of $Wf(s,x)$ with respect to the x variable is simply given by

$$\hat{Wf}(s,\omega) = \hat{f}(\omega)\hat{\psi}(s\omega). \tag{2.3}$$

The wavelet transform can easily be extended to tempered distributions, which is useful for the scope of this paper. For a thorough presentation of the theory of distributions, the reader might want to consult the book of Treves [26]. If $f(x)$ is a tempered distribution of order n and if the wavelet $\psi(x)$ is n times continuously differentiable, then the wavelet transform of $f(x)$ give by (2.2) is well defined. For example, a Dirac $\delta(x)$ is a tempered distribution of order 0 and $W\delta(s,x) = \psi_s(x)$, if $\psi(x)$ is continuous.

One can prove [11] that the wavelet transform is invertible and $f(x)$ is recovered with the formula

$$f(x) = \frac{1}{C_\psi} \int_0^{+\infty} \int_{-\infty}^{+\infty} Wf(s,u)\psi_s(u-x)\, du \frac{ds}{s}, \tag{2.4}$$

where $\psi_s(x)$ denotes the complex conjugate of $\psi_s(x)$. The wavelet transform $Wf(s,x)$ is a function of the scale s and the spatial position x. The plane defined by the ordered pair of variables (s,x) is called the scale-space plane [27]. An arbitrary function $F(s,x)$ is not a priori the wavelet transform of some function $f(x)$. One can prove that $F(s,x)$ is a wavelet transform if and only if it satisfies the reproducing kernel equation

$$F(s_0,x_0) = \int_0^{+\infty} \int_{-\infty}^{+\infty} F(s,x)K(s_0,s,x_0,x)\, dx \frac{ds}{s}, \tag{2.5}$$

with

$$K(s_0, s, x_0, x) = \frac{1}{C_\psi} \int_{-\infty}^{+\infty} \bar{\psi}_s(u - x)\psi_{s_0}(x_0 - u)\, du. \tag{2.6}$$

The reproducing kernel $K(s_0, s, x_0, x)$ expresses the intrinsic redundancy between the value of the wavelet transform at (s, x) and its value at (s_0, x_0).

3. Characterization of local regularity with the wavelet transform

As mentioned in the introduction, a remarkable property of the wavelet transform is its ability to characterize the local regularity of a function. In mathematics, the local regularity of functions is often measured with Lipschitz exponents.

Definition 3.1.

- Let n be a positive integer and $n \leqslant \alpha \leqslant n + 1$. A function $f(x)$ is said to be Lipschitz α, at x_0, if and only if there exists two constants A and $h_0 > 0$, and a polynomial $P_n(x)$ of order n such that for $h < h_0$

$$|f(x_0 + h) - P_n(h)| \leqslant A|h|^\alpha. \tag{3.1}$$

- The function $f(x)$ is uniformly Lipschitz α over the interval $]a, b[$ if and only if there exists a constant A such that for any $x_0 \in]a, b[$ there exists a polynomial of order n, $P_n(x)$, such that equation (3.1) is satisfied for any $x_0 + h \in]a, b[$.
- We call Lipschitz regularity of $f(x)$ at x_0 the sup of all values α such that $f(x)$ is Lipschitz α at x_0.
- We say that a function is singular at x_0 if it is not Lipschitz 1 at x_0.

A function $f(x)$ which is continuously differentiable at a point is Lipschitz 1 at this point. If the derivative of $f(x)$ is bounded but discontinuous at x_0, $f(x)$ is still Lipschitz 1 at x_0 and following Definition 3.1 we consider that $f(x)$ is not singular at x_0. One can easily prove that if $f(x)$ is Lipschitz α, for $\alpha > n$, then $f(x)$ is n times differentiable at x_0 and the polynomial $P_n(h)$ is the first $n + 1$ terms of the Taylor series of $f(x)$ at x_0. For $n = 0$, we have $P_n(h) = f(x_0)$. The Lipschitz regularity α_0 gives an indication of the differentiability of $f(x)$ but it is more precise. If the Lipschitz regularity α_0 of $f(x)$ satisfies $n < \alpha_0 < n + 1$, then we know that $f(x)$ is n times differentiable at x_0 but its n^{th} derivative is a distribution which is singular at x_0, and α_0 characterizes this singularity.

One can prove that if $f(x)$ is Lipschitz α then its primitive $g(x)$ is Lipschitz $\alpha + 1$. However, it is not true that if a function is Lipschitz α at a point x_0, then its derivative is Lipschitz $\alpha - 1$ at the same point. This is

due to oscillatory phenomena that are further studied in Section 5.3. On the opposite, one can prove that if α is not an integer and $\alpha > 1$, a function is *uniformly* Lipschitz α on an interval $]a, b[$ if and only if its derivative is uniformly Lipschitz $\alpha - 1$ on the same interval. This property enables us to define negative uniform Lipschitz exponents for tempered distributions. Integer Lipschitz exponents have a different behavior that is not studied in this article. It is necessary to define properly the notion of negative Lipschitz exponents for tempered distributions because they are often encountered in numerical computations.

Definition 3.2. Let $f(x)$ be a tempered distribution of finite order. Let α be a non-integer real number and $[a, b]$ an interval of $\mathfrak{R}$. The distribution $f(x)$ is said to be uniformly Lipschitz α on $]a, b[$ if and only if its primitive is uniformly Lipschitz $\alpha + 1$ on $]a, b[$.

For example, the second order primitive of a Dirac is a function which is piece-wise linear in the neighborhood $x = 0$. This function is uniformly Lipschitz 1 in the neighborhood of 0 and thus uniformly Lipschitz α for $\alpha < 1$. As a consequence of Definition 3.2, we can see that a Dirac is uniformly Lipschitz α for $\alpha < -1$ in the neighborhood of 0. Since Definition 3.2 is not valid for integer Lipschitz exponents, it does not allow us to conclude that a Dirac is Lipschitz -1 at 0 but we can derive that its Lipschitz regularity (see Definition 3.1) is -1 in the neighborhood of 0. Definition 3.2 is global because uniform Lipschitz exponents are defined over intervals but not at points. It is possible to make a local extension of Lipschitz exponents to negative values through the microlocalization theory of Bony [5, 15], but these sophisticated results go beyond the scope of this article. For isolated singularities, one can define pointwise Lipschitz exponents through Definition 3.2. We shall say that a distribution $f(x)$ has an isolated singularity Lipschitz α at x_0 if and only if $f(x)$ is uniformly Lipschitz α over an interval $]a, b[$, with $x_0 \in]a, b[$, and $f(x)$ is uniformly Lipschitz 1 over any sub-interval of $]a, b[$ that does not include x_0. For example, a Dirac centered at 0 has an isolated singularity at $x = 0$ whose Lipschitz regularity is -1.

A classical tool for measuring the Lipschitz regularity of a function $f(x)$ is to look at the asymptotic decay of its Fourier transform $\hat{f}(\omega)$. One can prove that a bounded function $f(x)$ is uniformly Lipschitz α over $\mathfrak{R}$ if it satisfies:

$$\int_{-\infty}^{+\infty} |\hat{f}(\omega)| (1 + |\omega|^{\alpha}) \, d\omega < +\infty. \tag{3.2}$$

This condition is sufficient but not necessary. It gives a global regularity condition over the whole real line but one cannot derive whether the function is locally more regular at a particular point x_0. This is because the Fourier transform unlocalizes the information along the spatial variable x. The

Fourier transform is therefore not well adapted to measure the local Lipschitz regularity of functions.

If the wavelet has compact support, the value of $Wf(s, x_0)$ depends upon the values of $f(x)$ on a neighborhood of x_0 of size proportional to the scale s. At fine scales, it provides localized information on $f(x)$. The following theorems relate the asymptotic decay of the wavelet transform at small scales to the local Lipschitz regularity. We suppose that the wavelet $\psi(x)$ is continuously differentiable and that it has compact support although this last condition is not strictly necessary. The first theorem is a well known result and a proof can be found in [13].

Theorem 3.3. Let $f(x) \in L^2(\mathfrak{R})$ and $[a, b]$ be an interval of $\mathfrak{R}$. Let $0 < \alpha < 1$. The function $f(x)$ is uniformly Lipschitz α over any interval $]a + \epsilon, b - \epsilon[$, with $b - a > \epsilon > 0$, if and only if there exists a constant A_ϵ such that for any $x \in]a + \epsilon, b - \epsilon[$ and any scale $s > 0$,

$$|Wf(s, x)| \leqslant A_\epsilon s^\alpha. \tag{3.3}$$

If $f(x) \in L^2(\mathfrak{R})$, for any scale $s_0 > 0$, by applying the Cauchy-Schwarz inequality, we can easily prove that the function $|Wf(s, x)|$ is bounded over the domain $s > s_0$. Hence, (3.3) is really a condition on the asymptotic decay of $|Wf(s, x)|$ when the scale s goes to zero. The sufficient condition (3.2) based on the Fourier transform implies that $|\hat{f}(\omega)|$ has a decay "faster" than $1/\omega^\alpha$. Equation (3.2) is similar if one considers the scale s as locally "equivalent" to $1/\omega$. However, in contrast to the Fourier transform condition, (3.3) is a necessary and sufficient condition and is localized on intervals and not over the whole real line.

In order to extend Theorem 3.3 to Lipschitz exponents α larger than 1, we must impose that the wavelet $\psi(x)$ has enough vanishing moments. A wavelet $\psi(x)$ is said to have n vanishing moments if and only if for all positive integers $k < n$, it satisfies

$$\int_{-\infty}^{+\infty} x^k \psi(x)\, dx = 0. \tag{3.4}$$

If the wavelet $\psi(x)$ has n vanishing moments, then Theorem 3.3 remains valid for any non-integer value α such that $0 < \alpha < n$. Let us see how this extension works, in order to understand the impact of vanishing moments. Since $\psi(x)$ has compact support $\hat{\psi}(\omega)$ is n times continuously differentiable, and one can derive from (3.4) that $\hat{\psi}(\omega)$ has a zero of order n at $\omega = 0$. For any integer $p < n$, $\hat{\psi}(\omega)$ can be factored into

$$\hat{\psi}(\omega) = (i\omega)^p \hat{\psi}^1(\omega). \tag{3.5}$$

In the spatial domain we have

$$\psi(x) = \frac{d^p \psi^1(x)}{d^p x}, \tag{3.6}$$

and the function $\psi^1(x)$ satisfies the wavelet admissibility condition (2.1). The p^{th} derivative of any function $f(x)$ is well defined in the sense of distributions. Hence,

$$Wf(s,x) = f * \psi_s(x) = \frac{d^p}{dx^p}(f * s^p \psi_s^1)(x) = s^p \left(\frac{d^p f}{dx^p} * \psi_s^1\right)(x). \tag{3.7}$$

The wavelet transform of $f(x)$ with respect to the wavelet $\psi(x)$ is thus equal to the wavelet transform of its p^{th} derivative, computed with the wavelet $\psi^1(x)$, and multiplied by s^p. Let p be an integer such that $0 < \alpha - p < 1$. The function $f(x)$ is uniformly Lipschitz α on an interval $]a, b[$, if and only if $\frac{d^p f}{dx^p}$ is uniformly Lipschitz $\alpha - p$ on the same interval. Since $0 < \alpha - p < 1$, Theorem 3.3 applies to the wavelet transform of $\frac{d^p f}{dx^p}$ defined with respect to the wavelet ψ^1. Theorem 3.3 shows that $\frac{d^p f}{dx^p}$ is uniformly Lipschitz $\alpha - p$ over intervals $]a + \epsilon, b - \epsilon[$ if and only if we can find constants $A_\epsilon > 0$ such that for $x \in]a + \epsilon, b - \epsilon[$,

$$\left|\frac{d^p f}{dx^p} * \psi_s^1(x)\right| \leq A_\epsilon s^{\epsilon - p}.$$

Equation (3.7) proves that this is true if and only if

$$|Wf(s,x)| \leq A_\epsilon s^\epsilon. \tag{3.8}$$

Equation (3.8) extends Theorem 3.3 for $\alpha < n$. If $\psi(x)$ has n vanishing moments but not $n + 1$, then the decay of $|Wf(s,x)|$ does not tell us anything about Lipschitz exponents for $\alpha > n$. For example, the function $f(x) = \sin(x)$ is uniformly Lipschitz $+\infty$ on any interval, but if $\psi(x)$ has exactly n vanishing moments one can easily prove that the asymptotic decay of $|Wf(s,x)|$ is equivalent to s^n on any interval. This decay does not allow us to derive anything on the regularity of the $n + 1^{st}$ derivative of $\sin(x)$. For $\alpha < 0$ and $\alpha \notin \mathbb{Z}$, (3.3) of Theorem 3.3 remains valid to characterize uniform Lipschitz exponents. In this case, we do not need to impose more than one vanishing moment on the wavelet $\psi(x)$. The proof can easily be derived from the statement of Definition 3.2.

For integer Lipschitz exponents α, (3.3) is necessary but not sufficient to prove that a function $f(x)$ is uniformly Lipschitz α over intervals $]a+\epsilon, b-\epsilon[$. If $\alpha = 1$ and the wavelet has at least two vanishing moments, the class of functions that satisfy (3.3), for any $x \in \mathbb{R}$, is called the *Zygmund class*. This class of functions is larger than the set of functions that are uniformly Lipschitz 1. For example, $x \log(x)$ belongs to the Zygmund class although

it is not Lipschitz 1 at $x = 0$. The reader is referred to Meyer's book [20] for more detailed explanations on the Zygmund class.

Theorem 3.3 gives a characterization of the Lipschitz regularity over intervals but not at a point. The second theorem proved by Jaffard [14] shows that one can also estimate the Lipschitz regularity of $f(x)$ precisely at a point x_0. The theorem gives a necessary condition and a sufficient condition but not a necessary and sufficient condition. We suppose that $\psi(x)$ has n vanishing moments, is n times continuously differentiable, and has compact support. Similar theorems on point-wise derivability have also been proved by Holschneider and Tchamitchian [13].

Theorem 3.4. Let n be a positive integer and $\alpha \leqslant n$. Let $f(x) \in L^2(\mathfrak{R})$. If $f(x)$ is Lipschitz α at x_0, then there exists a constant A such that for all points x in a neighborhood of x_0 and any scale s,

$$|Wf(s,x)| \leqslant A(s^\alpha + |x - x_0|^\alpha). \tag{3.9}$$

Conversely, let $\alpha < n$ be a non-integer value. The function $f(x)$ is Lipschitz α at x_0, if the two following conditions hold.

1) There exists $\epsilon > 0$ and a constant A such that for all points x in a neighborhood of x_0 and any scale s

$$|Wf(s,x)| \leqslant As^\epsilon. \tag{3.10}$$

2) There exists a constant B such that for all points x in a neighborhood of x_0 and any scale s

$$|Wf(s,x)| \leqslant B\left(s^\alpha + \frac{|x - x_0|^\epsilon}{|\log|x - x_0||}\right). \tag{3.11}$$

As a result of Theorem 3.3, we know that (3.10) implies that $f(x)$ is uniformly Lipschitz ϵ in some neighborhood of x_0. The value ϵ can be arbitrarily small. To interpret (3.9) and (3.11), let us define in the scale-space the cone of points (s,x) that satisfy

$$|x - x_0| \leqslant s.$$

For (s,x) inside this cone, (3.9) and (3.11) imply that when s goes to zero, $|Wf(s,x)| = O(s^\alpha)$. Below this cone, the value of $|Wf(s,x)|$ is controlled by the distance of x with respect to x_0, but the necessary and sufficient conditions have different upper bounds. Equation (3.11) means that for (s,x) below the cone,

$$|Wf(s,x)| = O\left(\frac{|x - x_0|^\epsilon}{|\log|x - x_0||}\right).$$

The behavior of the wavelet transform inside a cone pointing to x_0, and below this cone, are two components that must often be treated separately.

Theorems 3.3 and 3.4 prove that the wavelet transform is particularly well adapted to estimate the local regularity of functions. For example, Holschneider and Tchamitchian [13] used a similar result to analyze the differentiability of the Riemann-Weierstrass function. As mentioned in the introduction, we often want to detect and characterize the irregular parts of signals. Many interesting physical processes yield irregular structures that are currently being studied [2]. A well known example is the turbulence for high Reynolds numbers where there is still no comprehensive theory to understand the nature and repartition of irregular structures [4]. In signal processing, singularities often carry most of the signal information. In numerical experiments, it is however difficult to apply directly Theorems 3.3 and 3.4 in order to detect singularities and to characterize their Lipschitz exponents. Indeed, these theorems impose to measure the decay of $|Wf(s,x)|$ in a whole two-dimensional neighborhood of x_0 in the scale-space (s,x), which requires a lot of computation. The next section reviews briefly the different techniques that have been used to numerically detect singularities with a wavelet transform. We then explain how singular points are related to the wavelet transform local maxima.

4. Detection and measurement of singularities

The measurement of the wavelet transform decay, in a whole neighborhood of a point x_0 in the scale space (s,x), is numerically expensive. One technique that is often used in numerical applications, is to only compute the decay of $|Wf(s,x)|$ at a fixed abscissa $x = x_0$. This means that we measure the evolution of the wavelet transform along the vertical line that points to x_0 in the scale space (s,x). Although this approach can provide a good estimate of the local Lipschitz exponent in many cases, let us explain through a simple counterexample why it cannot be used reliably. We suppose that the wavelet $\psi(x)$ is symmetrical with respect to 0 and has compact support. Let $f(x) = 0$ for $x < x_0$ and $f(x) = 1$ for $x \geq x_0$. We can derive that $Wf(s,x) = \chi((x - x_0)/s)$, where $\chi(x)$ is the primitive of $\psi(x)$ with compact support. Since $\psi(x)$ is symmetrical, $\chi(x)$ is antisymmetrical and hence $\chi(0) = 0$. We thus derive that for any $s > 0$, $Wf(s,x_0) = 0$. Since $\chi(x)$ has compact support, for any $x \neq x_0$, there exists a scale $s_x > 0$ such that if $s < s_x$ then $Wf(s,x) = 0$. This proves that along each vertical line in the scale-space plane, the wavelet transform is uniformly zero for scales small enough. If we estimate the local Lipschitz exponents from the decay of the wavelet transform along vertical lines, it "looks like" the function $f(x)$ has no singularity although it does have a discontinuity at x_0. The mistake comes from the fact that we did not measure the decay of the wavelet transform inside a two-dimensional

neighborhood of x_0, as is required by theorems 3.3 and 3.4. Similar counter-examples are encountered in many usual signals. The function $\sin(1/x)$ is another type of counter-example which is studied in Section 5.3.

In his pioneering work on wavelets, Grossmann [10] gives an approach to detect singularities with a wavelet which is a Hardy function. A *Hardy function* $g(x)$ is a complex function whose Fourier transform satisfies

$$\hat{g}(\omega) = 0 \qquad \text{for } \omega < 0. \tag{4.1}$$

Let $f \in L^2(\mathfrak{R})$ and $Wf(s,x)$ be the complex wavelet transform built with a Hardy wavelet. For a fixed scale s, (2.3) implies that the Fourier transform $\widehat{Wf}(s,\omega)$ is also zero at negative frequencies, so it is also a Hardy function. Let $\phi(s,x)$ and $\rho(s,x)$ be respectively the argument and modulus of the complex number $Wf(s,x)$. The argument $\phi(s,x)$ is also called the phase of the wavelet transform. Grossmann [10] indicates that in the neighborhood of an isolated singularity located at x_0, the lines in the scale-space (s,x) where the phase $\phi(s,x)$ remains constant, converge to the abscissa x_0, when the scale s goes to 0. One can use this observation to detect singularities, but the phase $\phi(s,x)$ is not sufficient to measure their Lipschitz regularity. Moreover, the value of $\phi(s,x)$ is unstable when the modulus $\rho(s,x)$ is close to zero. It is thus necessary to combine the modulus and the phase information to characterize the different singularities, but no effective method has been derived yet.

In computer vision, it is extremely important to detect the edges that appear in images, and many researchers [25, 27, 18, 19, 6] have developed techniques based on multiscale transforms. These multiscale transforms are equivalent to a wavelet transform but have been studied before the development of the wavelet formalism. Let us call a *smoothing function* any real function $\theta(x)$ such that $\theta(x) = O(1/(1+x^2))$ and whose Fourier transform satisfies $\hat{\theta}(0) \neq 0$. The integral of a smoothing function is therefore nonzero. A smoothing function can be viewed as the impulse response of a low-pass filter. An important example often used in computer vision is the Gaussian function. Let $\theta_s(x) = 1/s\theta(x/s)$. Edges at the scale s are defined as local sharp variation points of $f(x)$ smoothed by $\theta_s(x)$. Let us explain how to detect these edges with a wavelet transform. Let $\psi^1(x)$ and $\psi^2(x)$ be the two wavelets defined by

$$\psi^1(x) = \frac{d\theta(x)}{dx} \quad \text{and} \quad \psi^2(x) = \frac{d^2\theta(x)}{dx^2}. \tag{4.2}$$

The wavelet transforms defined with respect to each of these wavelets are

given by:

$$W^1f(s,x) = f * \psi^1_s(x) \quad \text{and} \quad W^2f(s,x) = f * \psi^2_s(x). \tag{4.3}$$

$$W^1f(s,x) = f * \left(\frac{sd\theta_s}{dx}\right)(x) = s\frac{d}{dx}(f * \theta_s)(x) \tag{4.4}$$

and

$$W^2f(s,x) = f * \left(s^2\frac{d^2\theta_s}{dx^2}\right)(x) = s^2\frac{d^2}{dx^2}(f * \theta_s)(x). \tag{4.5}$$

The wavelet transforms $W^1f(s,x)$ and $W^2f(s,x)$ are proportional to, respectively, the first and second derivative of $f(x)$ smoothed by $\theta_s(x)$. For a fixed scale s, the local extrema of $W^1f(s,x)$ along the x variable correspond to the zero-crossings of $W^2f(s,x)$ and to the inflection points of $f * \theta_s(x)$ (see Figure 4.1).

If the wavelet $\psi^2(x)$ is continuously differentiable, the wavelet transform $W^2f(s,x)$ is a differentiable surface in the scale-space plane. Hence, the zero-crossings of $W^2f(s,x)$ define a set of smooth curves that often look like fingerprints [27]. Let us prove that one can define a particular Hardy wavelet such that the phase of the wavelet transform remains constant or changes sign along these fingerprints.

Let $\psi^3(x)$ be the Hilbert transform of $\psi^2(x)$ and $\psi^4(x) = \psi^2(x) + i\psi^3(x)$. The wavelet $\psi^4(x)$ is a Hardy wavelet. Let $W^4f(s,x) = f * \psi^4_s(x)$. The real part of $W^4f(s,x)$ is equal to $W^2f(s,x)$. Hence, the phase $\phi(s,x)$ is equal to $\pi/2$ or $-\pi/2$ if and only if $W^2f(s,x) = 0$. Since $W^4f(s,x)$ is a continuous function, the phase $\phi(s,x)$ cannot jump from $\pi/2$ to $-\pi/2$ along a connected line in the scale space, unless the modulus is equal to 0. If the modulus of $W^4f(s,x)$ is equal to 0, the phase is not defined and it can change sign at these points. Similarly to lines of constant phase, the zero-crossings "fingerprints" indicate the locations of sharp variation points and singularities but do not characterize their Lipschitz regularity. We need more information about the decay of $|W^2f(s,x)|$, in the neighborhood of these zero-crossings lines.

Detecting the zero-crossings of $W^2f(s,x)$ or the local extrema of $W^1f(s,x)$ are similar procedures but the local extrema approach has several important advantages. An inflection point of $f * \theta_s(x)$ can either be a maximum or a minimum of the absolute value of its first derivative. As in the abscissa x_0 and x_2 of Figure 4.1, the local maxima of the absolute value of the first derivative are sharp variation points of $f * \theta_s(x)$ whereas the minima correspond to slow variations (abscissa x_1). These two types of inflection points can be distinguished by looking whether an extremum of $|W^1f(s,x)|$ is a maximum or a minimum but they cannot be differentiated from the zero-crossings of $W^2f(s,x)$. For edge or singularity detection,

we are only interested in the local maxima of $|W^1f(s,x)|$. When detecting the local maxima of $|W^1f(s,x)|$, we can also keep the value of the wavelet transform at the corresponding location. With the results of theorems 3.3 and 3.4, we prove in the next section that the values of these local maxima often characterize the Lipschitz exponents of the signal irregularities.

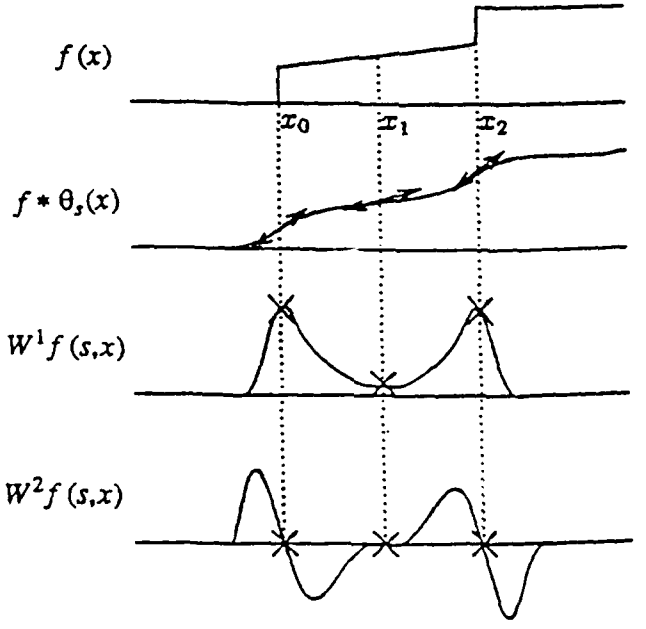

Figure 4.1: The extrema of $W^1f(s,x)$ and the zero-crossings of $W^2f(s,x)$ are the the inflection points of $f * \theta_s(x)$. The points of abscissa x_0 and x_2 are sharp variations of $f * \theta_s(x)$ and are local maxima of $|W^1f(s,x)|$. The local minimum of $|W^1f(s,x)|$ in x_1 is also an inflection point but it is a slow variation point.

5. Wavelet transform local maxima

5.1. General properties

By supposing that the wavelet $\psi(x)$ is the first derivative of a smoothing function, we impose that $\psi(x)$ has only one vanishing moment. In general, we do not want to impose only one vanishing moment because, as explained

in Section 3, then we cannot estimate Lipschitz exponents larger than 1. In this section, we study the mathematical properties of the wavelet local maxima and explain how to measure Lipschitz exponents. Let us first precisely define what we mean by local maximum.

Definition 5.1. *Let $Wf(s,x)$ be the wavelet transform of a function $f(x)$.*

- We call local extremum, any point (s_0, x_0) such that $\frac{\partial Wf(s_0,x)}{\partial x}$ has a zero-crossing at $x = x_0$, when x varies.
- We call local maximum, any point (s_0, x_0) such that $|Wf(s_0,x)| \leq |Wf(s_0,x_0)|$ when x belongs to either a right or the left neighborhood of x_0, and $|Wf(s_0,x)| \leq |Wf(s_0,x_0)|$ when x belongs to the other side of the neighborhood of x_0.
- We call maxima line, any connected curve in the scale space (s,x) along which all points are local maxima.

A local maximum (s_0, x_0) of the wavelet transform is strictly maximum either on the right or the left side of the x_0. To speak of local maximum of the wavelet transform is an abuse of language since we really mean a local maxima of the wavelet transform modulus, but it simplifies the explanations. The first theorem proves that if the wavelet transform has no maximum in a neighborhood, then the function is uniformly Lipschitz α, for $\alpha < n$.

Theorem 5.2. Let n be a strictly positive integer. Let $\psi(x)$ be a wavelet with compact support, n vanishing moments and n times continuously differentiable. Let $f(x) \in L^1([a,b])$.

- If there exists a scale $s_0 > 0$ such that for all scales $s < s_0$ and $x \in]a,b[$, $Wf(s,x)$ has no local maxima, then for any $\epsilon > 0$ and $\alpha < 0$, $f(x)$ is uniformly Lipschitz α on $]a+\epsilon, b-\epsilon[$.
- If $\psi(x)$ is the n^{th} derivative of a smoothing function, then $f(x)$ is uniformly Lipschitz n on any such interval $]a+\epsilon, b-\epsilon[$.

The proof of this theorem is in Appendix A. In the following, we suppose that $\psi(x)$ is the n^{th} derivative of a smoothing function. In this case we can prove that the function is locally Lipschitz α for the integer value $\alpha = n$ because the wavelet $\psi(x)$ has no more than n vanishing moments. Theorem 5.2 implies that on the intervals $]a+\epsilon, b-\epsilon[$, $f(x)$ has no singularity. Indeed, singularities were defined as points where the function is not Lipschitz 1. Let us define the closure of the wavelet transform maxima of $f(x)$ as the set of points x_0 such that for any $\epsilon > 0$ and scale $s_0 > 0$, there exists a wavelet transform local maxima at a point (s_1, x_1) that satisfy $|x_1 - x_0| < \epsilon$ and $s_1 < s_0$. This closure is the set of points on the real line that are arbitrarily close to some local maxima in the scale-space (s,x).

Corollary to 5.2. The closure of the set of points where $f(x)$ is not Lipschitz n is included in the closure of the wavelet transform maxima of $f(x)$.

This corollary is a straightforward implication of Theorem 5.2. It proves that all singularities of $f(x)$ can be located by following the maxima lines when the scale goes to zero. It is however not true that the closure of the points where $f(x)$ is not Lipschitz n is equal to the closure of the wavelet transform maxima. Equation (5.10) proves for example that if $\psi(x)$ is anti-symmetrical then for $f(x) = \sin(x)$, all the points $p\pi$, $p \in \mathbb{Z}$, belong to the closure of the wavelet local maxima, although $\sin(x)$ is infinitely continuously differentiable at these points. Let us now study how to use the value of the wavelet transform maxima in order to estimate the Lipschitz regularity of $f(x)$ at the points that belong to the closure of the wavelet transform maxima.

5.2. Non-oscillating singularities

In this section, we study the characterization of singularities when locally the function has no oscillations. The next section explains the potential impact of oscillations. We suppose that the wavelet $\psi(x)$ has compact support, is n times continuously differentiable and is the n^{th} derivative of a smoothing function. The following theorem characterizes a particular class of isolated singularities from the behavior of the wavelet transform local maxima.

Theorem 5.3. Let $f(x)$ be a tempered distribution whose wavelet transform is well defined over $]a, b[$ and let $x_0 \in]a, b[$. We suppose that there exists a scale $s_0 > 0$ and a constant C such that for $x \in]a, b[$ and $s < s_0$, all the maxima of $Wf(s, x)$ belong to a cone defined by

$$|x - x_0| \leq Cs. \tag{5.1}$$

Then, at all points $x_1 \in]a, b[$, $x_1 \neq x_0$, $f(x)$ is uniformly Lipschitz n in a neighborhood of x_1. Let $\alpha < n$ be a non-integer. The function $f(x)$ is Lipschitz α at x_0 if and only if there exists a constant A such that each local maxima (s, x) in the cone defined by (5.1) satisfies

$$|Wf(s, x)| \leq As^{\alpha}. \tag{5.2}$$

The proof of this theorem is given in Appendix B. Equation (5.2) is equivalent to

$$\log|Wf(s, x)| \leq \log(A) + \alpha \log(s). \tag{5.3}$$

If the wavelet transform maxima satisfy the cone distribution imposed by Theorem 5.3, (5.3) proves that the Lipschitz regularity at x_0 is the maximum slope of straight lines that remain above $\log|Wf(s, x)|$, on a logarithmic scale.

The fact that all local maxima remain in a cone that points to x_0 implies that $f(x)$ is Lipschitz n at all points $x \in]a, b[, \neq x_0$. Figures 5.2a through 5.2e show the wavelet transform of a function with isolated singularities that verify the cone localization hypothesis. To compute this wavelet transform we used a wavelet with only 1 vanishing moment. The graphs of $\psi(x)$ and its primitive $\theta(x)$ are shown in Figures 5.1a and 5.1b. The Fourier transform of $\psi(x)$ is

$$\hat{\psi}(\omega) = i\omega \left(\frac{\sin(\omega/4)}{\omega/4} \right)^4 . \tag{5.4}$$

This wavelet belongs to a class for which the wavelet transform can be computed with a fast algorithm [28].

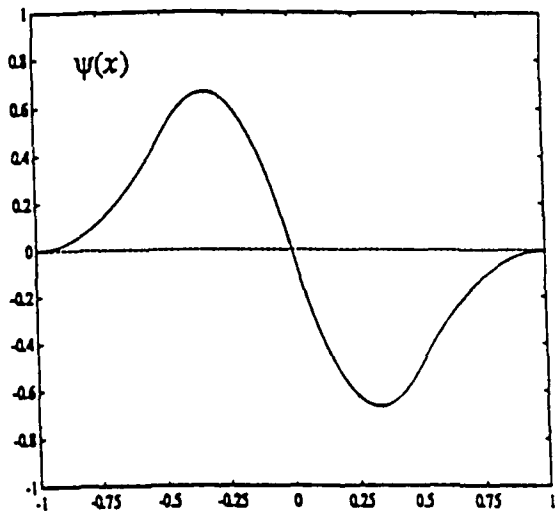

Figure 5.1a: Graph a wavelet $\psi(x)$ with compact support and one vanishing moment. It is a quadratic spline.

In numerical computations, the input function is not known at all abscissa x but is characterized by a uniform sampling which approximates $f(x)$ at a resolution that depends upon the sampling interval [16]. These samples are generally the result of a low-pass filtering of $f(x)$ followed by a uniform sampling. If we suppose for normalization purpose that the resolution is 1, then we can compute the wavelet transform of $f(x)$ only at scales larger than 1. When a function is approximated at a finite resolution, strictly speaking, it

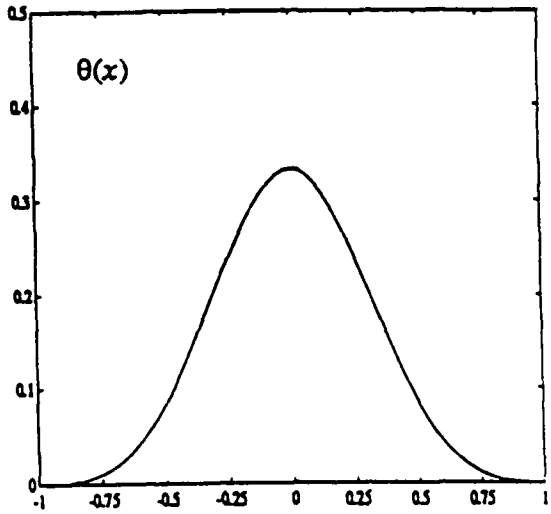

Figure 5.1b: Graph of the primitive $\theta(x)$ with compact support.

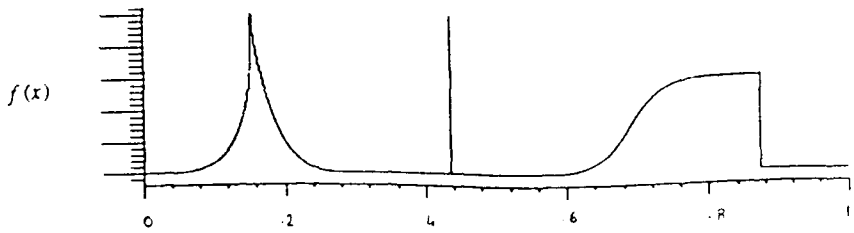

Figure 5.2a: In the left neighborhood of the abscissa 0.16, the signal locally behaves like $1 + (0.16 - x)^{0.2}$ whereas in the right neighborhood it behaves like $1 + (x - 0.16)^{0.6}$. At the abscissa 0.44 the signal has a discrete Dirac (Lipschitz regularity equal to -1). At 0.7, the Lipschitz regularity is 1.5 and at the abscissa 0.88 the signal is discontinuous.

is not meaningful to speak about singularities, discontinuities and Lipschitz exponents. This is illustrated by the fact that we cannot compute the asymptotic decay of the wavelet transform amplitude since we cannot compute the wavelet transform at scales smaller than 1. In practice, we still want to use the

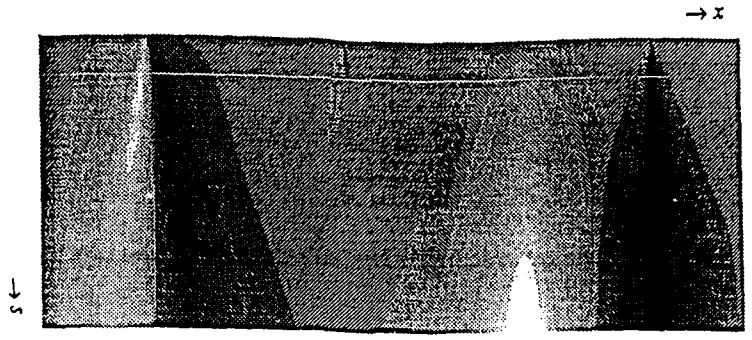

Figure 5.2b: Wavelet transform between the scales 1 and 2^8 computed with the wavelet shown in Figure 5.1a. The finer scales are at the top and the scale varies linearly along the vertical. Black, grey and white points indicate that the wavelet transform has respectively negative, zero and positive values.

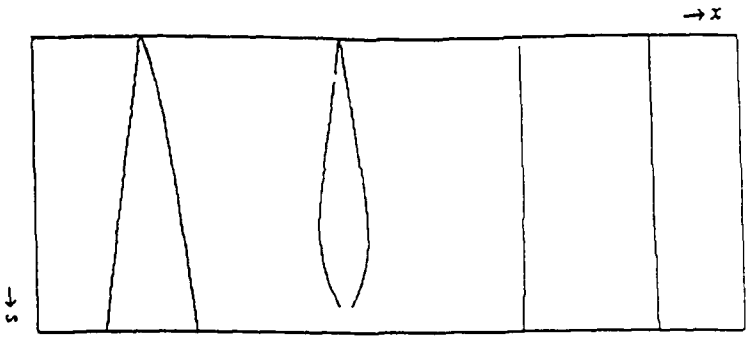

Figure 5.2c: Each black point indicates the position of a local maximum in the wavelet transform shown in Figure 5.2b The singularity of the derivative cannot be detected at the abscissa 0.7 because the wavelet has only one vanishing moment.

mathematical tools that describe singularities, even though we are limited by the resolution of measurements. Suppose that the approximation of $f(x)$ at the resolution 1 is given by a set of samples $(f_n)_{n\in\mathcal{Z}}$ with $f_n = 0$ for $n < n_0$ and $f_n = 1$ for $n \geqslant n_0$, like at the abscissa 0.88 of Figure 5.2a. We would

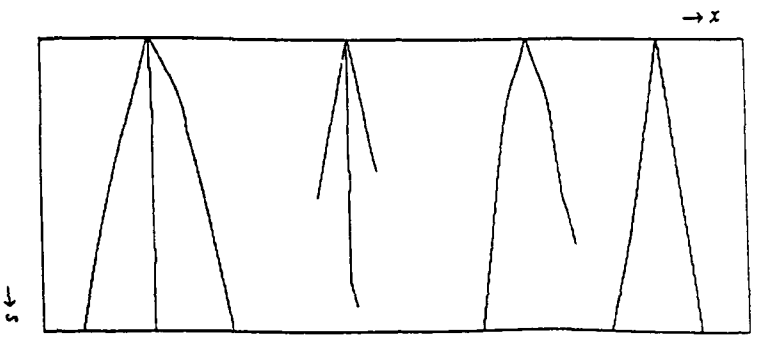

Figure 5.2d: Local maxima of the wavelet transform of the signal in Figure 5.2a, computed with a wavelet with two vanishing moments. The number of maxima line increases. The singularity of the derivative at 0.7 can now be detected from the decay of the wavelet local maxima.

like to say that at the resolution 1, $f(x)$ behaves as if it has a discontinuity at $n = n_0$ although it is possible that $f(x)$ is continuous at n_0 but has a sharp transition at that point which is not visible at the resolution 1. The characterization of singularities from the decay of the wavelet transform enables us to give a precise meaning to this discontinuity at the resolution 1. Since we cannot measure the asymptotic decay of the wavelet transform when the scale goes to 0, we measure the decay of the wavelet transform up to the finer scale available. The Lipschitz exponents are computed by finding the coefficient α such that As^α approximates at best the decay of $|Wf(s,x)|$ over a given range of scales larger than 1 (see Figure 5.2b). With this approach, we can use Lipschitz exponents to characterize the irregularities of discrete signals. In Figure 5.2b, the discontinuity appears clearly from the fact that $|Wf(s,x)|$ remains approximatively constant over a large range of scales, in the neighborhood of the abscissa 0.88. Negative Lipschitz exponents correspond to sharp irregularities where the wavelet transform modulus increases at fine scales. A sequence $(f_n)_{n\in\mathbb{Z}}$ with $f_n = 0$ for $n \neq n_0$, and $f_{n_0} = 1$, can be viewed as the approximation of a Dirac at the resolution 1. At the abscissa 0.44, the signal of Figure 5.2a has such a discrete Dirac. The wavelet transform maxima increase proportionally to s^{-1} over a large range of scales, in the corresponding neighborhood. In the rest of this paper, we suppose that all numerical experiments are performed on functions approximated at the resolution 1 and we consider that the decay of the wavelet transform at scales larger than 1 characterize the Lipschitz exponent of the function

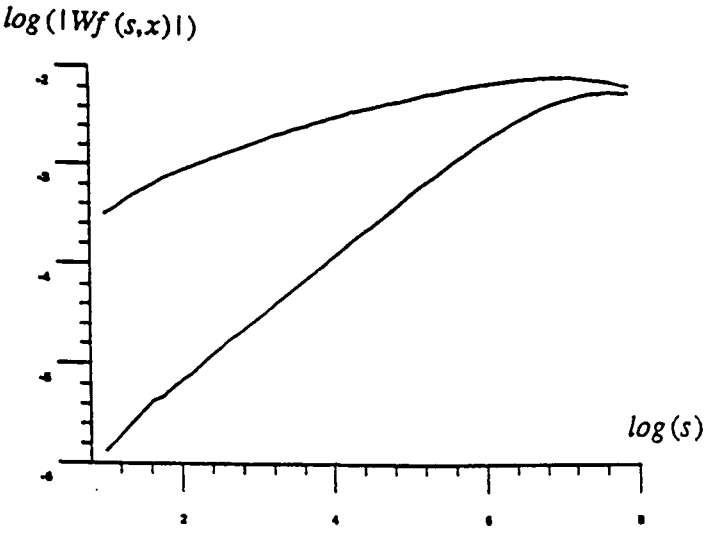

Figure 5.2e: Decay of $\log_2 |Wf(s,x)|$ as a function of $\log_2(s)$ along the two maxima lines that converge to the point of abscissa 0.16, computed with the wavelet of Figure 5.1a. The two different slopes show that the $f(x)$ has a different singular behavior in the left and right neighborhood of 0.16 and we can distinguish the two exponents 0.2 and 0.6.

up to the resolution 1. Fast algorithms to compute the wavelet transform are described in [16, 12]. We shall not worry anymore about the opposition between asymptotic measurements and finite resolution.

The local maxima of the wavelet transform of Figure 5.2b are shown in Figure 5.2c. The black lines indicate the position of the local maxima in the scale-space. Figure 5.2e gives the value of $\log_2 |Wf(s,x)|$ as a function of $\log_2(s)$ along each of the two maxima line that converge to the point of abscissa 0.16, between the scales 2^1 and 2^8. It is interesting to observe that at fine scales, the slopes of these two maxima lines are different and are approximatively equal to 0.2 and 0.6. This shows that $f(x)$ behaves like a function Lipschitz 0.2 in its left neighborhood and a function Lipschitz 0.6 in its right neighborhood. The Lipschitz regularity of $f(x)$ at 0.16 is 0.2 which is the smallest slope of the two maxima lines.

At this point one might wonder how to choose the number of vanishing moments to analyze a particular class of signals. If we want to estimate

the Lipschitz exponents up to a maximum value n, we know that we need a wavelet with at least n vanishing moments. In Figure 5.2c, there is one maxima line converging to the abscissa 0.7 along which the decay of $\log|Wf(s,x)|$ is proportional to $\log(s)$. The signal was built from a function whose derivative is singular but this cannot be detected from the slope of $\log|Wf(s,x)|$ because the wavelet has only one vanishing moment. Figure 5.2d shows the maxima line obtained from a wavelet which has two vanishing moments. The decay of the wavelet transform along the two maxima lines that converge to the abscissa 0.7 indicates that $f(x)$ is Lipschitz 1.5 at this location. Using wavelets with more vanishing moments has the advantage of being able to measure the Lipschitz regularity up to a higher order but it also increases the number of maxima lines as can be observed by comparing Figure 5.2c and Figure 5.2d. Let us prove this last observation. A wavelet $\psi(x)$ with $n+1$ vanishings moment is the derivative of a wavelet $\psi^1(x)$ with n vanishing moments. Similarly to (4.4), we obtain

$$Wf(s,x) = s\frac{d}{dx}(f * \psi^1_s)(x) = s\frac{\partial}{\partial x}W^1f(s,x). \tag{5.5}$$

The wavelet transform of $f(x)$ defined with respect to $\psi(x)$ is proportional to the derivative of the wavelet transform of $f(x)$ with respect to $\psi^1(x)$. Hence, the number of local maxima of $|Wf(s,x)|$ is always larger than the number of local maxima of $|W^1f(s,x)|$. The number of maxima at a given scale often increases linearly with the number of moments of the wavelet. In order to minimize the amount of computations, we want to have the minimum number of maxima necessary to detect the interesting irregular behavior of the signal. This means that we must choose a wavelet with as few vanishing moments as possible but with enough moments to detect the Lipschitz exponents of highest order that we are interested in. Another related property that influences the number of local maxima is the number of oscillations of the wavelet $\psi(x)$. For most types of singularities, the number of maxima lines converging to the singularity depends upon the number of local extrema of the wavelet itself. A Dirac $\delta(x)$ gives a simple verification of this property since $W\delta(s,x) = 1/s\psi(x/s)$. A wavelet with n vanishing moments has at least $n+1$ local maxima. In numerical computations, it is better to choose a wavelet with exactly $n+1$ local maxima. In image processing, we often want to detect discontinuities and peaks which have Lipschitz exponents smaller than 1. It is therefore sufficient to use a wavelet with only one vanishing moment. In signals obtained from turbulent fluids, interesting structures have a Lipschitz exponent between 0 and 2 [3]. We thus need a wavelet with two vanishing moments to analyze turbulent structures.

Let us suppose that the wavelet $\psi(x)$ has a symmetrical support equal to $[-K, K]$. We call the *cone of influence* of x_0 in the scale-space plane the set

of points (s,x) that satisfy

$$|x - x_0| \leqslant Ks.$$

It is the set of point (s,x) for which $Wf(s,x)$ is influenced by the value of $f(x)$ at x_0. In order to characterize the regularity of $f(x)$ at a point x_0, one might think that it is sufficient to measure the decay of the wavelet transform within the cone of influence of x_0. Theorem 3.4 proves that this is wrong in general and that one must also measure the decay of the wavelet transform below this cone of influence. This is due to oscillations that can create a singularity at x_0. The next theorem shows that if we suppose that $f(x)$ has no such oscillations, then the regularity of $f(x)$ at a point x_0 is characterized by the behavior of its wavelet transform along any line that belongs to a cone strictly smaller than the cone of influence. Section 5.3 explains why this property is wrong when $f(x)$ oscillates too much. In the following we suppose that $\psi(x)$ is a wavelet which is n times continuously differentiable, has a support equal to $[-K, K]$, and is equal to the n^{th} derivative of a function $\theta(x)$. We also impose that $\theta(x)$ is strictly positive on the interval $]-K, K[$.

Theorem 5.4. Let $x_0 \in \mathfrak{R}$, $f(x) \in L^2(\mathfrak{R})$. We suppose that there exists an interval $]a,b[$, with $x_0 \in]a,b[$, and a scale $s_0 > 0$ such that the wavelet transform $Wf(s,x)$ has a constant sign for $s < s_0$ and $x \in]a,b[$. Let us also suppose that there exists a constant B and $\epsilon > 0$ such that for all points $x \in]a,b[$ and any scale s

$$|Wf(s,x)| \leqslant Bs^{\epsilon}. \tag{5.6}$$

Let $x = X(s)$ be a curve in the scale space (s,x) such that $|x_0 - X(s)| \leqslant Cs$, with $C < K$. It there exists a constant A such that for any scale $s < s_0$, the wavelet transform satisfies

$$|Wf(s,X(s))| \leqslant As^{\gamma} \qquad \text{with } 0 \leqslant \gamma \leqslant n, \tag{5.7}$$

then $f(x)$ is Lipschitz α at x_0, for any $\alpha < \gamma$.

The proof of this theorem is in Appendix C. One can easily prove that the sign constraint over the wavelet transform of $f(x)$ is equivalent to imposing that the n^{th} derivative of $f(x)$ is a distribution whose restriction to $]a,b[$ has a constant sign. Theorem 5.4 shows that the regularity of $f(x)$ is controlled by the behaviour of its wavelet transform in the cone of influence, if its n^{th} derivative does not have an oscillatory behavior that accelerates in the neighborhood of x_0. A similar theorem can be obtained if we suppose that the n^{th} derivative of $f(x)$ has a constant sign over $]a,x_0[$ and $]x_0,b[$ but changes sign at x_0. This means that in the neighborhood of x_0, $Wf(s,x)$ has only one zero-crossing at any fixed scale s which is small enough. When s goes to zero, the zero-crossing curve converges to the abscissa x_0. In this case,

we need to control the decay of the wavelet transform along two lines that remain respectively in the left and the right part of the cone of influence of x_0.

From Theorem 5.4, one can compute the Lipschitz regularity of non-isolated singularities from the behavior of the wavelet transform maxima. We test whether the wavelet transform has a constant sign in the neighborhood of x_0 by testing the sign of the wavelet transform local maxima. It is also sufficient to verify (5.6) along the lines of maxima in the neighborhood of x_0. The Lipschitz regularity of $f(x)$ at x_0 is computed from the decay of the wavelet transform along one line of maxima that converges towards x_0. Let us emphasize again that if at each scale the wavelet transform has only one zero-crossing in a neighborhood of x_0, Theorem 5.4 can be extended by measuring the decay of the wavelet transform along two curves that are respectively in the left and the right parts of the cone of influence of x_0.

A "devil staircase" is an interesting example to illustrate the application of Theorem 5.4 to the detection of non-isolated singularities. The derivative of a devil staircase is a Cantor measure. For the devil staircase shown in Figure 5.4a, the Cantor measure is built recursively as follow. For $p = 0$, the support of the measure μ_0 is the interval [0,1], and it has a uniform density equal to 1 on $[0, 1]$. The measure μ_p is defined by subdividing each domain where μ_{p-1} has a uniform density equal to a constant $c > 0$, into three domains whose respective sizes are 1/5, 2/5 and 2/5. The density of the measure μ_p is equal to 0 in the central part, to $c/3$ in the first part and to $2c/3$ in last part (see Figure 5.3). One can verify that $\int_0^1 \mu_p(dx) = 1$. The limit measure μ_∞ obtained with this iterative process is a Cantor measure. The devil staircase is defined by:

$$f(x) = \int_0^x \mu_\infty(dx).$$

Figure 5.4a shows the graph of a devil staircase and Figure 5.4b its wavelet transform computed with the wavelet of Figure 5.1a. For a devil staircase, we can prove that the maxima lines converge exactly to the points where the function $f(x)$ is singular. There is no maxima line that converges to a point where the function is not singular.

Proof. By definition, the set of points where the maxima lines converge is the closure of the wavelet transform maxima, and the Corollary to 5.2 proves that it includes the closure of the points where $f(x)$ is singular. For a devil staircase, the support of the points where $f(x)$ is singular is equal to the support of the Cantor measure, which is a closed set. It is thus equal to its closure. For any point x_0 outside this closed set, we can find a neighborhood $]x_0 - \epsilon, x_0 + \epsilon[$ which does not intersect the support of $\mu_\infty(x)$. On this open interval, $f(x)$ is constant so for s small enough and $x \in]x_0 - \epsilon/2, x_0 + \epsilon/2[$, $Wf(s, x)$ is equal to zero. The point x_0 therefore cannot belong to the closure

of the wavelet transform maxima. This proves that the closure of the wavelet transform maxima is included in the singular support of $f(x)$. Since the opposite is also true, it implies that both sets are equal. ∎

For the particular devil staircase that we defined, the Lipschitz regularity of each singular point depends upon the location of the point. One can prove [3] that at all locations, Lipschitz exponent α satisfies

$$\frac{\log(2/3)}{\log(2/5)} \leq \alpha \leq \frac{\log(1/3)}{\log(1/5)}.$$

Hence, (5.6) of Theorem 5.4 is verified for $\epsilon < \log(2/3)/\log(2/5)$. Since a devil staircase is monotonically increasing and our wavelet is the derivative of a positive function, the wavelet transform remains positive. Theorem 5.4 proves that the local Lipschitz regularity of $f(x)$ at any singular point can be estimated from the decay of the wavelet transform along the maxima line that converges to that point. Figure 5.4c shows the position of the maxima lines in the scale-space. The renormalization properties of the Cantor set appear as renormalization properties of the graph of maxima lines. Muzy, Bacry and Arneodo [23] have shown that one can precisely compute the singularity spectrum $f(\alpha)$ of multifractal signals from the evolution across scales of the wavelet transform local maxima. These results are particularly interesting for studying irregular physical phenomena such as turbulences [23].

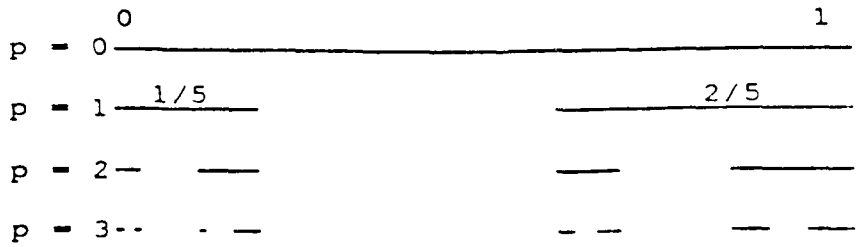

Figure 5.3: Recursive operation for building a multifractal Cantor measure. The Cantor measure is obtained at the limit of this iterative procedure.

5.3. Singularities with fast oscillations

If the function $f(x)$ is oscillating quickly in the neighborhood of x_0, then one cannot characterize the Lipschitz regularity of $f(x)$ from the behavior of its wavelet transform in the cone of influence of x_0. We say that a function $f(x)$

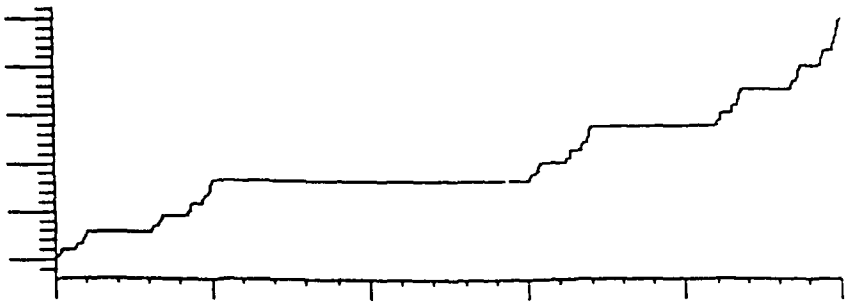

Figure 5.4a: Devil staircase.

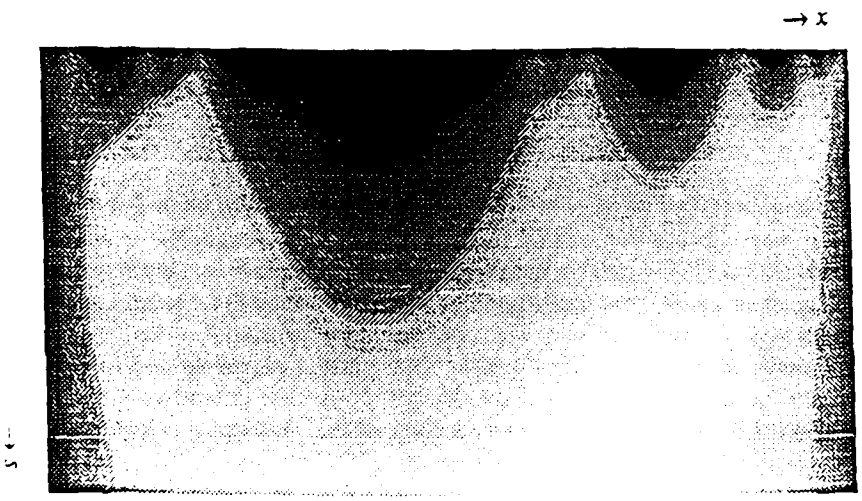

Figure 5.4b: Wavelet transform of the devil staircase computed with the wavelet of Figure 5.1a. Black and white points indicate respectively that the wavelet transform is zero or strictly positive.

has fast oscillations at x_0 if and only if there exists $\alpha > 0$ such that $f(x)$ is not Lipschitz α at x_0 but its primitive is Lipschitz $\alpha + 1$ at x_0. This situation occurs when $f(x)$ is a function which oscillates very quickly and whose singularity behavior at x_0 is dominated by these oscillations. The integral of $f(x)$ averages $f(x)$ so the oscillations are attenuated and the Lipschitz exponent at

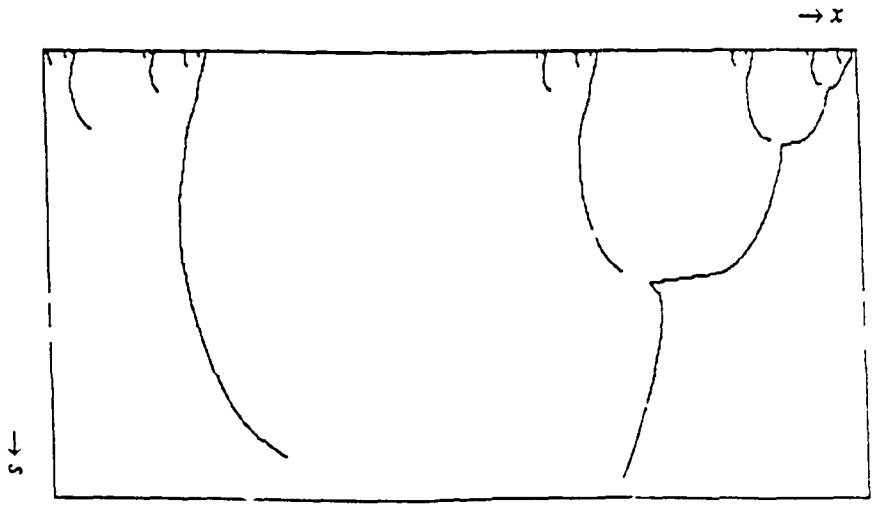

Figure 5.4c: Local maxima of the wavelet transform shown in Figure 5.4b.

x_0 increases by more than 1. Singularities with such an oscillatory behavior have been thoroughly studied in mathematics [29]. A classical example is the function $f(x) = \sin(1/x)$ in the neighborhood of $x = 0$. This function is not continuous at 0 but is bounded in the neighborhood of 0 so its Lipschitz regularity is equal to 0 at $x = 0$. Let $g(x)$ be a primitive of $\sin(1/x)$, one can easily prove that $|g(x) - g(0)| = O(x^2)$ in the neighborhood of $x = 0$, so $g(x)$ is Lipschitz 2 at this point. By computing the primitive of $f(x)$, we increase the Lipschitz exponent by 2 because the oscillations of $\sin(1/x)$ are attenuated by the averaging effect.

Let $f(x)$ be a function with fast oscillations at x_0 and let $g(x)$ be its primitive. Let $\psi^1(x)$ be the derivative of $\psi(x)$. Since $g(x)$ is Lipschitz $\alpha + 1$, the necessary condition (3.9) of Theorem 3.4 implies that in a neighborhood of x_0, the wavelet transform defined with respect to $\psi^1(x)$ satisfies

$$|W^1 g(s,x)| \leq A\,(s^{\alpha+1} + |x - x_0|^{\alpha+1})\,. \tag{5.8}$$

Similarly to (4.4) we can prove that

$$W^1 g(s,x) = g * \psi^1_s(x) = s(f * \psi_s)(x) = sWf(s,x).$$

We thus derive that

$$|Wf(s,x)| \leq A\,(s^{\alpha} + \tfrac{1}{s}|x - x_0|^{\alpha+1})\,. \tag{5.9}$$

This equation proves that although $f(x)$ is not Lipschitz α, in the cone of influence of x_0 $|Wf(s,x)| = O(s^c)$. The fact that $f(x)$ is not Lipschitz α cannot be detected from the decay of $|Wf(s,x)|$ inside the cone of influence of x_0, but by looking at its decay below the cone of influence, as a function of $|x - x_0|$. Since $f(x)$ is not Lipschitz α, the necessary condition (3.9) implies that for (s, x) below the cone of influence of x_0, the wavelet transform does not satisfy $|Wf(s,x)| = O(|x - x_0|^\epsilon)$. When a function has fast oscillations, its worst singular behavior at a point x_0 is observed below the cone of influence of x_0 in the scale-space plane.

Let us study in more detail the case of $f(x) = \sin(1/x)$. Since the primitive is Lipschitz 2, we can take $\alpha = 1$. Equation (5.9) implies that in the cone of influence of 0, the wavelet transform satisfies $|Wf(s,x)| = O(s)$. Figure 5.4e shows the wavelet transform of $\sin(1/x)$. It has a high amplitude along a curve in the scale space (s, x) which reaches $(0, 0)$ below the cone of influence of 0. It is along this path in the scale-space that the singular part of $f(x)$ reaches 0. Let us interpret this curve and prove that it is a parabola. Through this analysis we derive a procedure to estimate locally the size of the oscillations of $f(x)$.

The function $f(x) = \sin(1/x)$ can be written $f(x) = \sin(\omega_x x)$, where $\omega_x = 1/x^2$ can be viewed as an "instantaneous" frequency. Let us compute the wavelet transform of a sinusoidal wave of constant frequency ω_0. If we suppose that the wavelet $\psi(x)$ is antisymmetrical, as it is the case in our numerical computations, from (2.3) we derive that the wavelet transform of $h(x) = \sin(\omega_0 x)$ satisfies

$$|Wh(s,x)| = |\cos(\omega_0 x)||\hat{\psi}(s\omega_0)|. \tag{5.10}$$

For a symmetrical wavelet, the cosine is replace by a sine in the right-hand side of this equation. For a fixed abscissa x, the decay of $|Wh(s,x)|$ as a function of s is proportional to the decay of $|\hat{\psi}(s\omega_0)|$. If $|\hat{\psi}(\omega)|$ reaches its maxima at $\omega = \omega_m$, then for x fixed, $|Wh(s,x)|$ is maximum at $s_0 = \omega_m/\omega_0$. The scale where $|Wh(s,x)|$ is maximum is inversely proportional to the frequency of the sinusoidal wave. The value of $Wh(s,x)$ depends on the values of $h(x)$ in a neighborhood of size proportional to the scale s, so the frequency measurement is local. Since $f(x) = \sin(1/x)$ has an instantaneous frequency $\omega_x = 1/x^2$, for a fixed abscissa x, $|Wf(s,x)|$ is globally maximum for $s \approx \epsilon_m/\omega_x = \epsilon_m x^2$. This is why we see in Figure 5.4e that the wavelet transform has a maximum amplitude along a parabola that converges to the abscissa 0 in the scale-space. This "instantaneous" frequency measurement is based on an idea that has been developed previously by Escudie and Torresani [9] for measuring the modulation law of asymptotic signals. The results of Escudie and Torresani have also been refined by Delprat et al. [8], who explain how to precisely extract the amplitude and frequency modulation laws from a complex wavelet transform.

Let us now study the behavior of the wavelet transform maxima. The inflection points of $f(x)$ are located at $x = 1/(n\pi)$, for $n \in \mathcal{Z}$. Since the wavelet $\psi(x)$ has only one vanishing moment, all the maxima lines converge toward the points $x = 1/(n\pi)$. Since $f(x)$ is continuously differentiable in the neighborhood of $1/(n\pi)$, the wavelet transform along a maxima line converging to $1/(n\pi)$ satisfies

$$|Wf(s,x)| \leq A_n s. \tag{5.11}$$

The derivative of $f(x)$ at $1/(n\pi)$ is equal to $(-1)^{n+1}n^2$ so one can derive that $A_n = O(n^2)$. It is interesting to observe that along all maxima lines in the neighborhood of 0, the wavelet transform decays proportionally to the scale s although $f(x)$ is discontinuous in 0. This singularity in 0 can however be detected because the constants A_n grow to $+\infty$ when we get closer to 0. Figure 5.4f displays the local maxima of the wavelet transform of $\sin(1/x)$. In the neighborhood of 0, at fine scales, the maxima line have a different geometry in the scale space (s,x) due to the aliasing when sampling $\sin(1/x)$, for numerical computations. Let us now introduce the general maxima points and explain how they are related to the size of the oscillations of $f(x)$.

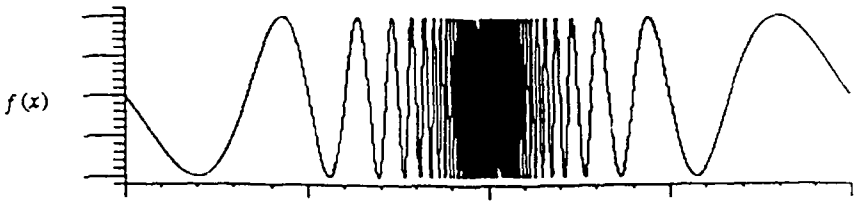

Figure 5.4d: Graph of $\sin(1/x)$.

Definition 5.5. We call *general maximum* of $Wf(s,x)$ a point (s_0, x_0) where $|Wf(s,x)|$ has a strict local maximum within a two-dimensional neighborhood in the scale-space plane (s,x).

Clearly, a general maxima point belongs to a local maxima line as defined by Definition 5.1. General maxima are points where $Wf(s,x)$ reaches a local maximum when the variables (s,x) vary along a maxima line. Equation (5.10) proves that the maxima lines of the wavelet transform of $\sin(\omega_0 x)$ are vertical lines in the scale-space plane (s,x) given by $x = n\pi$, for $n \in \mathcal{Z}$. If $|\psi(\omega)|$ has one global maxima, for $\omega > 0$, at ω_m and no other local maxima, then (5.10) implies that there is only one general maximum along each maxima line and it appears at the scale $s_0 = \omega_m/\omega_0$. A wavelet equal to the n^{th}

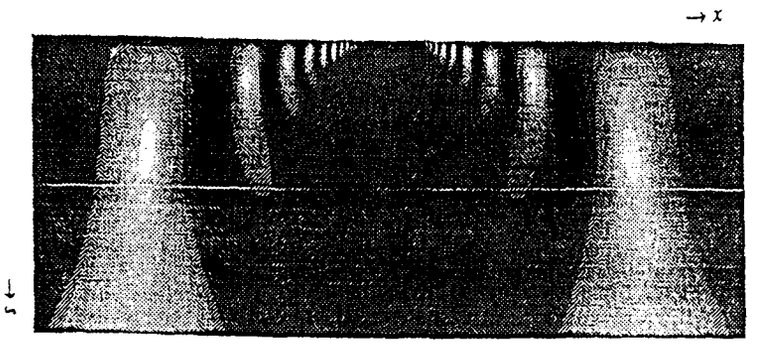

Figure 5.4e: Wavelet transform of $\sin(1/x)$. The amplitude is maximum along a parabola in the scale-space that converges to $(0,0)$ in the scale-space.

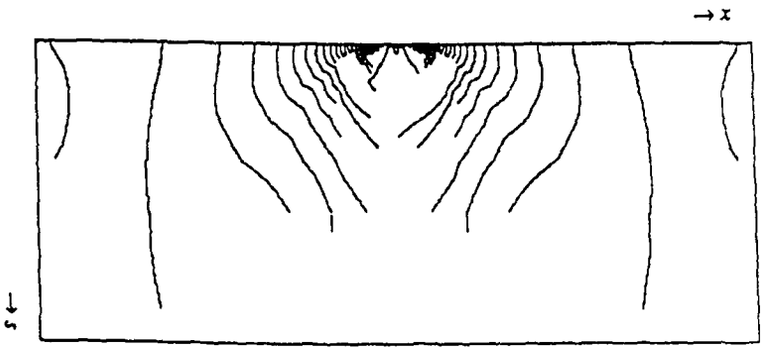

Figure 5.4f: Local maxima of the wavelet transform.

derivative of a Gaussian has such a property. If $|\psi(\omega)|$ has several local maxima, for $\omega > 0$, there are several general maxima along each maxima line but the one where $|Wf(s,x)|$ has the highest value is at the scale $s_0 = \omega_m/\omega_0$. One can thus recover the frequency ω_0 from the location of this general maxima. Figure 5.4g displays the sub-part of each maxima line that is below the general maxima of maximum amplitude. In the scale-space, these general maxima belong to a parabola whose equation is approximatively given by $s = \omega_m/\omega_x = Ax^2$. This equation is only an approximation because the

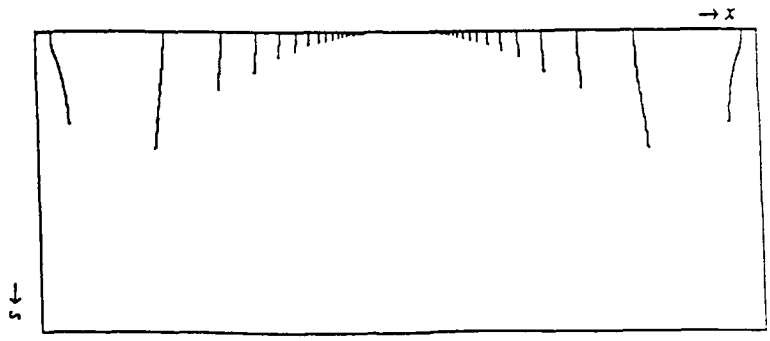

Figure 5.4g: The maxima line are displayed from the scale where is located the largest general maxima. The extremity of each maxima line indicates the position of a general maxima point and it belongs to a parabola in the scale-space (s, x).

frequency ω_x varies locally. A finer analysis of this type of property can be found in the work of Delprat et al. [8]. If $f(x)$ is locally equal to the sum of several sinusoidal waves whose frequency are well apart, so that they can be discriminated by $\hat{\psi}(s\omega)$ when s varies (see (5.10)), then we can measure the frequency of each of these sinusoidal waves from the scales of the general maxima that they produce. The efficiency of this method depends on how concentrated is the support of $\hat{\psi}(\omega)$. Here, we are limited by the uncertainty principle, which requires that $\psi(x)$ cannot have its energy well concentrated both in the spatial and frequency domains. To distinguish spectral lines that are too close, it is necessary to use more sophisticated methods as described by Delprat et al. [8].

Let us now give a spatial domain interpretation of this frequency measurement. We show that if the wavelet $\psi(x)$ has only one vanishing moment, the general maxima points provide measurements of the local oscillations even if the function is not locally similar to a sinusoidal wave. If $\psi(x)$ is the derivative of a smoothing function $\theta(x)$, (4.4) proves that

$$Wf(s,x) = s\frac{d}{dx}(f * \theta_s)(x),$$

hence

$$Wf(s,x) = \int_{-\infty}^{+\infty} \frac{df(u)}{du}\theta\left(\frac{x-u}{s}\right) du. \tag{5.12}$$

If locally $f(x)$ has a simple oscillation like in Figure 5.5, $\frac{df(x)}{dx}$ has a constant sign between the two top points x_1 and x_2 of the oscillation. The point

(s_0, x_0) is a general maximum if the support of $\theta((x_0 - x)/s_0)$ covers as much as possible the positive part of $\frac{df(x)}{dx}$, without paying the cost of covering a domain where $\frac{df(x)}{dx}$ is too negative. This means that the distance between the two top points of the oscillation is of the order of the size of the support of $\theta(x)$ multiplied by the scale s_0:

$$x_2 - x_1 \approx K s_0. \tag{5.13}$$

This spatial domain interpretation shows that even if the function is not locally similar to a sinusoidal wave, the size of the oscillation is approximately proportional to the scale s_0 of the general maxima point. If the wavelet $\psi(x)$ has more than one vanishing moment, this spatial interpretation is not valid.

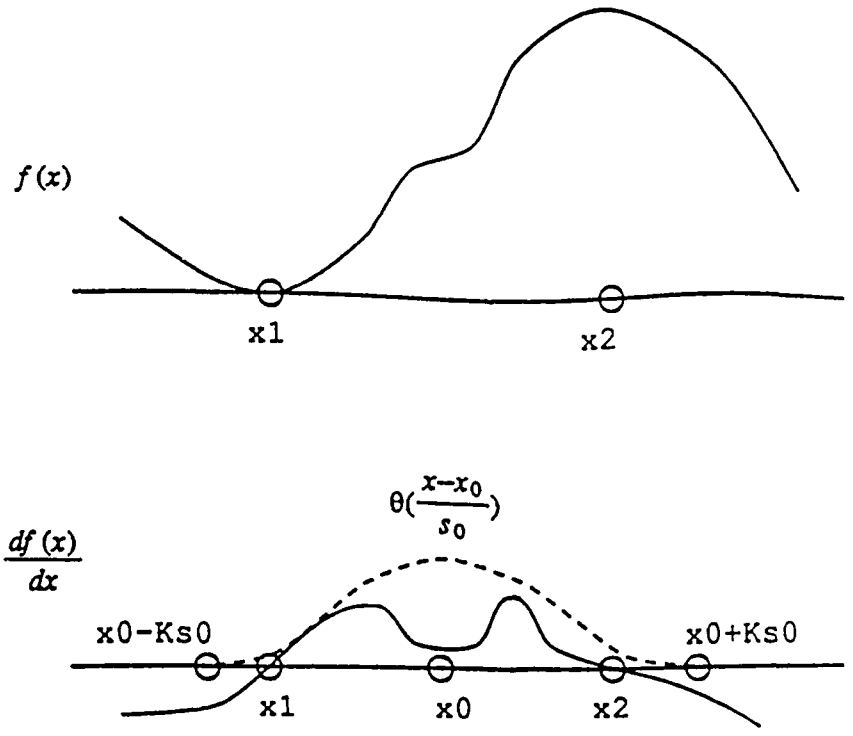

Figure 5.5: We suppose that the wavelet is the first derivative of a smoothing function $\theta(x)$. The point (s_0, x_0) is a general maxima of the wavelet transform of $f(x)$ if the function $\theta_{s_0}(x - x_0)$ covers a domain as large as possible where the function $f(x)$ has a positive derivative.

With (5.9), we saw that if a function $f(x)$ has fast oscillations in the neighborhood of x_0, then the regularity at x_0 depends upon the behavior of $Wf(s,x)$ below the cone of influence of x_0. To estimate this behavior, one approach is to measure the decay of $|Wf(s,x)|$ at the general maxima points that are below the cone of influence of x_0, when we converge towards x_0. Indeed, these general maxima points characterize the size of the oscillations of $f(x)$ and they give an upper bound for the value of the wavelet transform along each maxima line. Theorem 3.4 proves that $f(x)$ is Lipschitz α at x_0 only if $|Wf(s,x)| = O(|x - x_0|^\epsilon)$ below the cone of influence. Hence, $f(x)$ can be Lipschitz α at a point x_0 only if the general maxima point (s_i, x_i) below the cone of influence of x_0 satisfies

$$|Wf(s_i, x_i)| = O(|x_i - x_0|^\alpha). \tag{5.14}$$

This necessary condition gives an upper bound on the Lipschitz exponents at x_0. For $f(x) = \sin(1/x)$, (5.14) is satisfied only for $\alpha = 0$. We thus detect the discontinuity at $x = 0$ from the values of the general maxima points. In most situations, the general maxima points must be used in conjunction with the local maxima lines in order to estimate the decay of $|Wf(s,x)|$ inside and below the cone of influence of x_0.

6. Completeness of the wavelet maxima

We proved that the singularities of a function can be detected from the wavelet transform local maxima. One might wonder whether the positions and the values of the wavelet transform maxima provide a complete and stable representation of $f(x)$. The reconstruction of a function from the local maxima of its wavelet transform has been studied numerically by Zhong and one of us [16]. Local maxima are detected only along a dyadic sequence of scales $(2^j)_{j \in \mathbb{Z}}$ to obtain efficient numerical implementations. The reconstruction algorithm recovers signals with a relative precision approximatively equal to 10^{-2}. The remaining error is mostly concentrated in the highest frequencies. More recently Meyer [22] proved that the wavelet transform local maxima do not provide a complete signal representation. He constructed different functions whose wavelet transform have the same local maxima at all scales. However, these functions mostly differ at high frequencies and their relative $L^2(\mathbb{R})$ distance is of the same order as the precision of the numerical reconstruction algorithm. This seems to indicate that the wavelet transform local maxima is "complete" modulo a small high frequency error that remains to be identified mathematically. This section reviews briefly the properties of a dyadic wavelet transform as well as the algorithm that approximates a functions from local maxima. Section 7 describes an application to the suppression of white noise with a local estimation of Lipschitz exponents.

We call dyadic wavelet transform the sequence of functions of the variable x

$$(Wf(2^j, x))_{j \in \mathbb{Z}}. \tag{6.1}$$

Equation (2.3) implies that the Fourier transform of $Wf(2^j, x)$ is given by

$$\hat{Wf}(2^j, \omega) = \hat{\psi}(2^j \omega)\hat{f}(\omega). \tag{6.2}$$

The function $f(x)$ can be reconstructed from its wavelet transform and the reconstruction is stable [7, 16] if and only if there exists two constants $A > 0$ and $B > 0$ such that

$$A \leqslant \sum_{j=-\infty}^{+\infty} |\hat{\psi}(2^j \omega)|^2 \leqslant B. \tag{6.3}$$

Let us denote by $\|Wf(2^j, x)\|$ the $L^2(\mathfrak{R})$ norm of the function $Wf(2^j, x)$ along the variable x. As a consequence of (6.3), by applying the Parseval theorem, one can prove that a dyadic wavelet transform has finite energy

$$A\|f\|^2 \leqslant \sum_{j=-\infty}^{+\infty} \|Wf(2^j, x)\|^2 \leqslant B\|f\|^2. \tag{6.4}$$

This means that $(Wf(2^j, x))_{j \in \mathbb{Z}}$ belongs to the Hilbert space $l^2(L^2)$ of sequences of functions $(g_j(x))_{j \in \mathbb{Z}}$ that satisfy

$$\sum_{j=-\infty}^{+\infty} \|g_j(x)\|^2 < +\infty.$$

Similarly to the continuous wavelet transform, the dyadic wavelet transform is overcomplete. This means that any sequence $\{g_j(x)\}_{j \in \mathbb{Z}}$ is not a priori the dyadic wavelet transform of some function $f \in L^2(\mathfrak{R})$. The space **V** of all dyadic wavelet transforms of functions in $L^2(\mathfrak{R})$ is strictly included in $l^2(L^2)$. An orthogonal projection from $l^2(L^2)$ onto **V** is defined by a reproducing kernel equation similar to (2.5) [16].

If the wavelet satisfies the condition (6.3), the Lipschitz regularity of a function is also characterized by the decay across scales of the wavelet transform at the scales $(2^j)_{j \in \mathbb{Z}}$. Theorems 3.3 and 3.4 remain valid if we restrict the scale to the sequence $(2^j)_{j \in \mathbb{Z}}$ [14]. We can thus characterize the regularity of a function from the behavior of the wavelet transform local maxima at the dyadic scales. The results and theorems of Section 5 are valid if we restrict the scale parameter s to $(2^j)_{j \in \mathbb{Z}}$. Figure 6.1b is the dyadic wavelet transform of the signal in Figure 6.1a, computed with the wavelet shown in Figure 5.1a. The finer scale is limited by the resolution of the original discrete signal. We also stop the decomposition at a finite largest

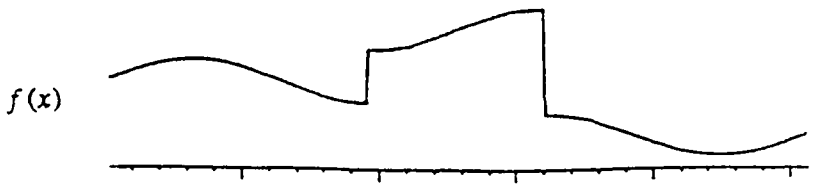

Figure 6.1a: Original signal.

scale. In Figure 6.1b, the largest scale is 2^6. The information provided by the dyadic wavelet transform at scales larger than 2^6 is given by one function [16], shown at the bottom. It carries the lower frequencies of f(x). Figure 6.1c displays the local maxima of the wavelet transform. Each Dirac indicates the position and value of $Wf(2^j, x)$ at a maxima location.

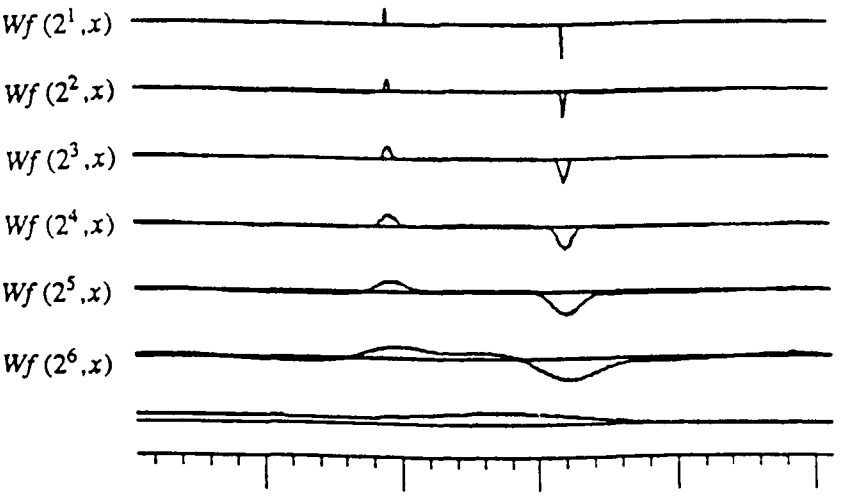

Figure 6.1b: Wavelet transform computed up to the scale 2^6.

Figure 6.1b gives the remaining low-frequencies at scales larger than 2^6.

Since the wavelet is the first derivative of a smoothing function, the wavelet transform maxima are located where the signal has sharp transitions. They provide an adaptive description of the signal information. The more irregularities in the signal, the more wavelet maxima. Let us now study

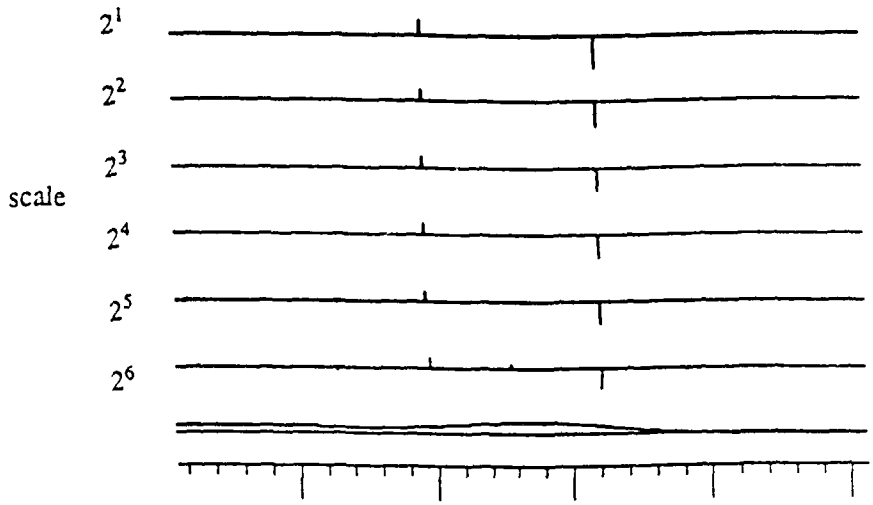

Figure 6.1c: Local maxima of the wavelet transform. At each scale, each Dirac indicates the position and value of a wavelet transform local maximum. We also keep the remaining low-frequency information shown at the bottom.

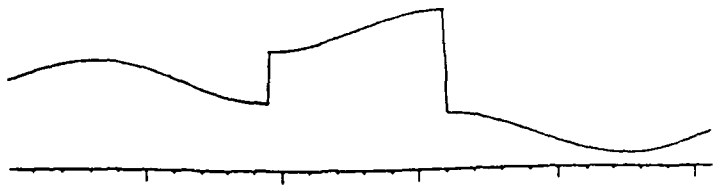

Figure 6.1d: Signal reconstructed from the wavelet transform local maxima shown in Figure 6.1c.

the completeness of this local maxima representation and briefly explain the reconstruction algorithm introduced by Zhong and one of us [16]. We want to characterize the set **S** of all possible wavelet transforms that have exactly the same local maxima as the wavelet transform of $f(x)$. The representation is complete if and only if the set **S** is reduced to the wavelet transform of $f(x)$. Clearly **S** is included in the space **V** of all dyadic wavelet transforms. The set **S** is also included in the set Γ of all sequences of functions $(g_j(x))_{j\in\mathbb{Z}}$

in $l^2(L^2)$ such that for each integer j, the local maxima of $g_j(x)$ occur at the same locations and have the same values as the local maxima of $Wf(2^j, x)$. For each $j \in \mathcal{Z}$, we require that $g_j(x)$ belongs to the space $H^1(\mathcal{R})$ of functions one-time differentiable in the sense of Sobolev so that their local maxima are well defined. This other constraint is justified if the wavelet $\psi(x) \in H^1(\mathcal{R})$ since it implies that $Wf(2^j, x) \in H^1(\mathcal{R})$. It is easy to verify that

$$\Gamma \cap \mathbf{V} = \mathbf{S}.$$

If the representation is not complete, then the set **S** is not reduced to the wavelet transform of $f(x)$. One can still recover a good approximation of this wavelet transform if the size of **S** is "small". The reconstruction algorithm is based on alternative projections on the set Γ and the Hilbert space **V**. We begin with an initial sequence of functions $(g_j(x))_{j \in \mathcal{Z}}$ arbitrarily chosen and then project successively this initial sequence on **V** and Γ, as illustrated by Figure 6.2. If the discrete signal has a total of N samples, the computational complexity of the projections on **V** and Γ is $O(N \log N)$ [16]. The convergence of the alternative projection algorithm to the intersection of Γ and **V** is not proved. However, in all our numerical experiments, the algorithm does converge fast. The root mean-square error to signal ratio of the reconstructed signal is of the order of 5×10^{-2} after 20 iterations on the projection operators [16]. Figure 6.1d is an example of signal reconstructed with 20 iterations. The differences with the original function are not visible on the graph. If we increase the number of iterations, the reconstruction error decrease but reaches a limit which is of the order of 10^{-2}. This limitation of precision is due to the non-completeness of the local maxima representation. Meyer proved recently [22] that for some particular functions $f(x)$, one can find high frequency perturbations $\epsilon(x)$ such that $Wf(2^j, x)$ and $W(f + \epsilon)(2^j, x)$ have the same local maxima at all scales 2^j. This means that the solution set **S** is not reduced to the wavelet transform of $f(x)$. However, the numerical experiments as well as the mathematical counter-examples seem to indicate that **S** is small. A precise mathematical characterization of the set **S** remains to be done. Once we recover a wavelet transform that belongs to **S**, we reconstruct the corresponding signal by applying the inverse wavelet transform operator. From a practical point of view, the numerical precision of this reconstruction algorithm is sufficient for a large class of signal processing applications. The next section describes an application to denoising.

7. Signal denoising based on wavelet maxima in one dimension

The properties of a signal can be modified by processing its wavelet transform maxima and then reconstructing the corresponding function. We describe an application to denoising based on a local estimation of the signal

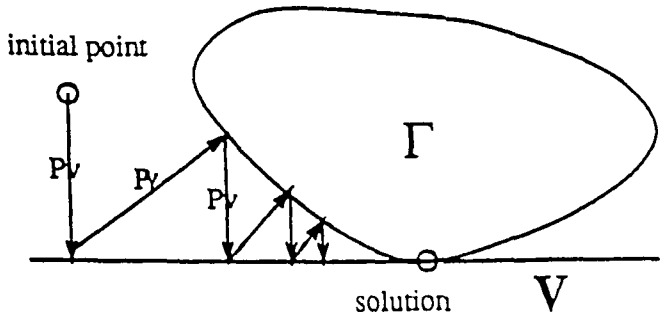

Figure 6.2: The reconstruction of the wavelet transform of $f(x)$ is done with alternative projections on the set Γ that expresses the constraints on the local maxima and on the space **V** of all dyadic wavelet transforms. The wavelet transform of $f(x)$ is included in the intersection Γ and **V**.

singularities. The most classical technique to remove white noise from a signal is to convolve the signal with a Gaussian filter. For a large class of important signals, the energy of the white noise dominates the signal at high frequencies whereas the energy of the signal dominates the noise at low frequencies. The Gaussian low-pass filtering attenuates the high frequencies and keeps the low frequencies. As a consequence, a large portion of the noise is removed but the sharp variations of the original signal are smoothed. The fact that most of the signal energy is concentrated in low-frequencies often indicates that most of the singularities have Lipschitz exponent that are positive. Our denoising algorithm discriminates the signal and the noise with a local analysis of the singularity types.

Let us first describe the properties of the wavelet transform of white noise. Let $n(x)$ be a real white noise random process and $Wn(s,x)$ be its wavelet transform. We denote by $E(X)$ the expected value of a random variable X. We suppose that the wavelet $\psi(x)$ is real. Grossmann et al. [10] have shown that the decay of $E(|Wn(s,x)|^2)$ is proportional to $1/s$. Indeed,

$$|Wn(s,x)|^2 = \int_{-\infty}^{+\infty}\int_{-\infty}^{+\infty} n(u)n(v)\psi_s(x-u)\psi_s(x-v)\,du\,dv.$$

Since $n(x)$ is a white noise, $E(n(u)n(v)) = \delta(u-v)$, hence

$$E(|Wn(s,x)|^2) = \int_{-\infty}^{+\infty}\int_{-\infty}^{+\infty} \delta(u-v)\psi_s(x-u)\psi_s(x-v)du\,dv.$$

We thus derive that

$$E(|Wn(s,x)|^2) = \frac{\|\psi\|^2}{s}. \tag{7.1}$$

At a given scale s, the wavelet transform $Wn(s,x)$ is a random process in x. If we suppose that the white noise $n(x)$ is Gaussian white noise then $Wn(s,x)$ is also a Gaussian process. From this property, we prove in Appendix D that at a scale s, the density of local maxima of the wavelet transform is

$$d_s = \frac{\lambda\|\psi^{(2)}\|}{\pi\|\psi^{(1)}\|}\frac{1}{s}, \tag{7.2}$$

where $\psi^{(n)}(x)$ is the n^{th} derivative of $\psi(x)$ and λ a constant between 0.5 and 1. The density of local maxima is inversely proportional to the scale s. The realization of white noise is a distribution which is almost everywhere singular. One can prove that the singularities of Gaussian white noise are Lipschitz $-1/2$. Figure 7.1a is a signal obtained by adding Gaussian white noise of variance 1 to the signal of Figure 6.1a. Figure 7.1b shows its dyadic wavelet transform.

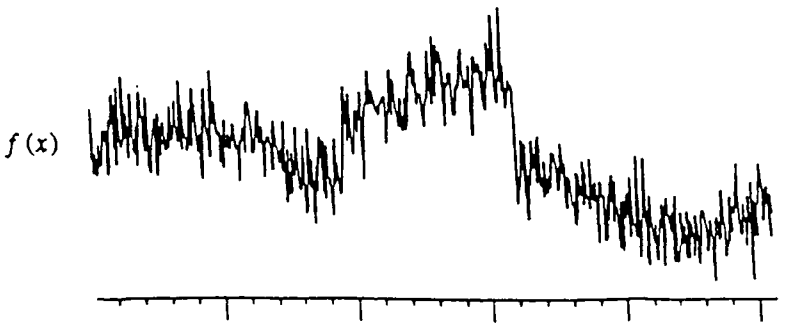

Figure 7.1a: Signal of Figure 6.1a to which we added Gaussian white noise of variance 1.

Let us suppose that the original signal has isolated singularities whose Lipschitz regularities are positive. Since the noise creates singularities whose Lipschitz regularity is negative, we can discriminate the local maxima created by the white noise from the ones produced by the signal, by looking at the evolution of their amplitude across scales. If the local maxima have an amplitude which increases when the scale decreases, it indicates that the corresponding singularities have negative Lipschitz exponents. These maxima

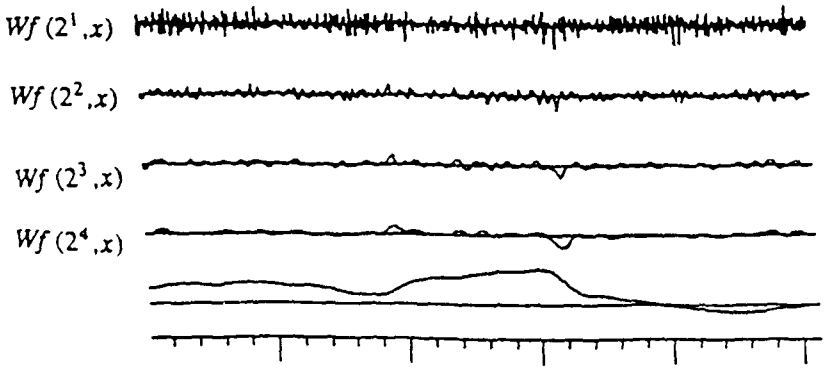

Figure 7.1b: Wavelet transform computed up to the scale 2^4.

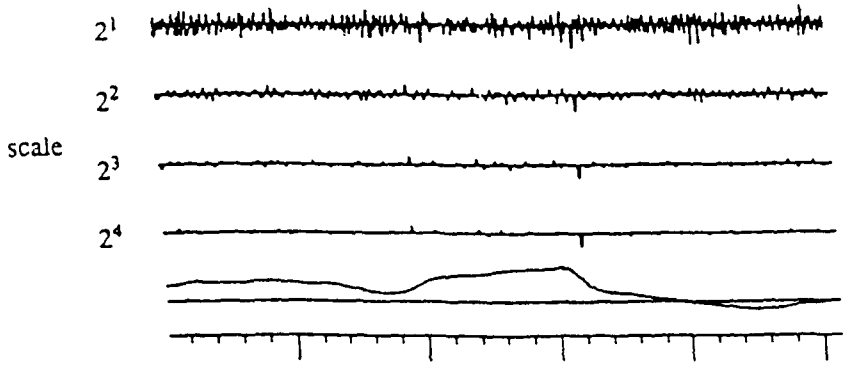

Figure 7.1c: Local maxima of the wavelet transform. At coarser scales the maxima of the signal discontinuities dominate the maxima of the white noise.

are mostly dominated by the white noise and thus are removed. At the locations where the signal has singularities with positive Lipschitz exponents, the noises adds singularities with negative Lipschitz exponents. Mathematically, the sum is a signal whose singularities have negative Lipschitz exponents. However, if the signal dominates the noise at low frequencies, wherever the signal is singular, at coarse scales the amplitude of the local maxima is mostly influenced by the signal variations. Since the signal sin-

gularities have positive Lipschitz exponents, at coarse scales the amplitude of the corresponding maxima do not increase when the scale decreases. This can be observed in the neighborhood of the discontinuities of the noisy signal shown in Figures 7.1a through 7.1c.

In order to evaluate the behavior of the wavelet maxima across scales, we need to make a correspondence between the maxima that appear at different scales 2^j. We say that a maxima at a scale 2^j propagates to another maxima at the coarser scale 2^{j+1} if both maxima belong to the same maxima line in the scale space (s, x). Equation (7.2) proves that for a white noise, on average, the number of maxima decreases by a factor 2 when the scale increases by 2. Half of the maxima do not propagate from the scale 2^j to the scale 2^{j+1}. In order to find which maxima propagate to the next scale, one should compute the wavelet transform on a dense sequence of scales. However, with a simple ad-hoc algorithm one can still try to find which maxima propagate to the next scale, by looking at their value and position with respect to other maxima at the next scale. The propagation algorithm supposes that the maxima that propagate from a scale 2^j to a coarser scale 2^{j+1} are the ones which locally have the largest amplitude and which have a location which is close to a maxima at the scale 2^j, whose amplitude has the same sign. Such an ad-hoc algorithm is not exact but saves computations since we do not need to compute the wavelet transform at any other scale. The denoising algorithm removes all maxima whose amplitude increase on average when the scale decreases, or which do not propagate at larger scales. These are the local maxima that are mostly influenced by the noise fluctuations. Figure 7.3a shows the local maxima that are kept by the denoising algorithm. As expected, these local maxima correspond to the signal discontinuities. The position and amplitude of the remaining local maxima is affected by the white noise components in the corresponding neighborhood. The white noise introduces more distortions at fine scales because the signal to noise ratio is smaller. The maxima selection algorithm is based on an analysis of singularity types and thus cannot be used to discriminate the low-frequency sinusoidal components of the signal from the white noise. Hence, we do not try to select local maxima below the scale 2^4, and keep both the signal and the noise components below this scale. This non-linear filtering algorithm, like a Gaussian smoothing, does not modify the lowest frequencies but it removes selectively the fine scales components depending upon the local singularity types.

After the maxima selection, we reconstruct a "denoised" signal with the alternative projection algorithm previously described. A priori, there is no guarantee that there exists a function whose wavelet transform has local maxima that correspond exactly to the maxima that we selected. This means that the set Γ that characterizes the maxima constraints might not intersect the space $\mathbf{V}$ of all wavelet transforms (see Figure 7.2). The reconstruction

algorithm thus does not converge but if we stop after enough iterations (20 in practice), we reconstruct a sequence of functions which is close to Γ and $\mathbf{V}$. The function shown in Figure 7.3b was obtained after 20 such iterations. As can be observed, the two discontinuities of the original function are still perfectly sharp. The overshoot is due to the white noise components that modified the values and positions of the original local maxima, at these locations. In the smooth signal variations, we can see the remaining components of the white noise that have been kept at scales larger than 2^4. This simple algorithm shows the feasibility to discriminate a signal from its noise with an analysis of the local maxima behavior across scales. Better strategies for selecting the maxima can certainly be developed depending upon the applications. This denoising procedure does not require that the noise is white but only that its singularities have Lipschitz exponents that can be differentiated from the signal singularities.

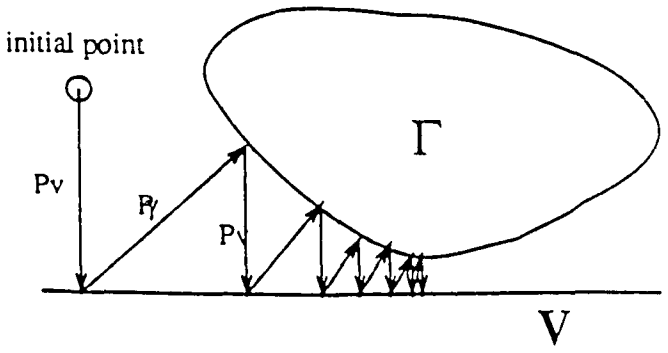

Figure 7.2: After a modification of the local maxima, in general there is no wavelet transform whose local maxima are exactly equal to the one that we selected. Hence, the set Γ that carries the constraints on local maxima does not intersect the space $\mathbf{V}$ of all dyadic wavelet transforms. The algorithm reconstructs a sequence of functions that is close to Γ and $\mathbf{V}$.

8. Conclusion

We proved that the wavelet transform local maxima detect all the singularities of a function and we described strategies to measure their Lipschitz regularity. This mathematical study provides algorithms for characterizing singularities of irregular signals such as the multifractal structures observed

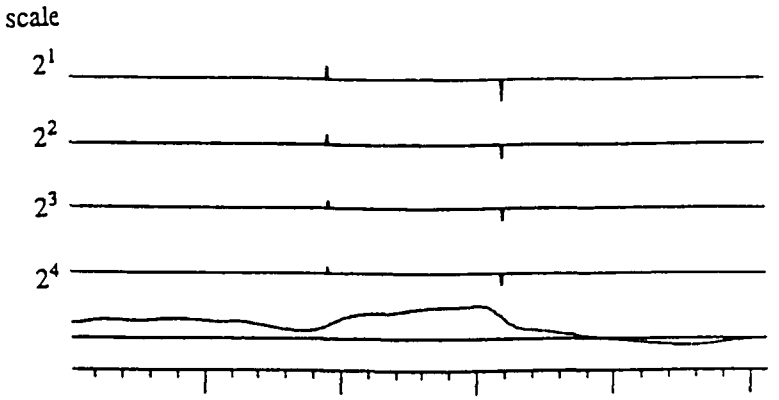

Figure 7.3a: Local maxima kept by the denoising algorithm.

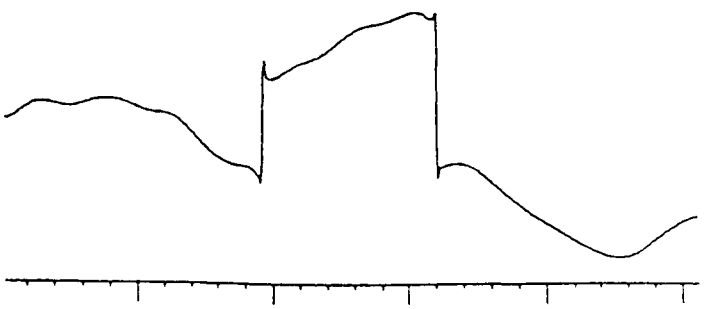

Figure 7.3b: Signal reconstructed from the local maxima shown in Figure 7.3a. The overshoot at the discontinuity locations is due to the modification of the maxima amplitude by the white noise.

in physics [23]. Oscillations can also be measured from the general maxima of the wavelet transform, with a technique similar to the approach of Escudie and Torresani [9].

From a numerical point of view, it is possible to reconstruct a close approximation of a signal from the local maxima of its wavelet transform. We studied an application to signal denoising. The prior information on the regularity of a signal versus the local properties of the noise are expressed through constraints on the behavior of the wavelet transform local maxima.

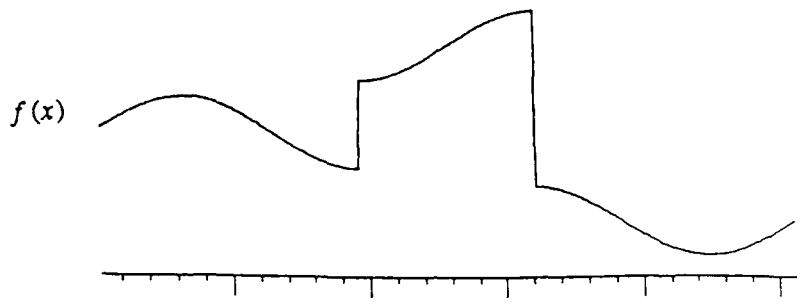

Figure 7.3c: Original signal.

The local maxima model has been extended to two dimensions in order to detect edges in images [16]. As in one dimension, images can be reconstructed from the wavelet transform local maxima. This representation of images with multiscale edges has applications in pattern recognition as well as compact image coding. An algorithm that selects the important edges for building a compact image code is described in [16].

9. Bibliography

[1] F. Argoul, A. Arneodo, J. Elezgaray, and G. Grasseau. Wavelet analysis of fractal growth process. In *Proc. of 4th EPS Liquid State Confer.*, Arcachon, France, May 1988.

[2] A. Arneodo, G. Grasseau, and H. Holschneider. On the wavelet transform of multifractals. In Combes and et al., editors, *Wavelets*. Springer-Verlag, Berlin, Heidelberg, New York, London, Paris, Tokyo, Hong Kong, 1988.

[3] E. Bacry. Transformation en ondelettes et turbulence pleinement developpee. In *Rapport de Magistere*, Univ. Paris VII, 1989.

[4] E. Bacry, A. Arneodo, U. Frisch, Y. Gagne, and E. Hopfinger. Wavelet analysis of fully developed turbulence data and measurement of scaling exponents. In M. Lesieur and O. Metais, editors, *Turbulence and Coherent Structure*. Kluwer Academic Publishers Group, Dordrecht, Boston, London, 1990. To appear.

[5] J. Bony. Propagation et interaction des singularites pour les solutions des equations au derivees paritelles non-lineaires. In *Proc. of the In-*

ternational Congress of Mathematicians, pages 1133–1147, Warszawa, 1983.

[6] J. Canny. A computational approach to edge detection. *IEEE Trans. on Pattern Anal. and Machine Intel.*, 8:679–698, 1986.

[7] I. Daubechies. The wavelet transform, time-frequency localization and signal analysis. *IEEE Trans. Information Theory*, 36:961–1005, September 1990.

[8] N. Delprat, B. Escudie, P. Guillemain, R. Kronland-Martinet, Ph. Tchamitchian, and B. Torresani. Asymptotic wavelet and Gabor analysis: extraction of instantaneous frequencies. Technical Report CPT-91/P.2512, CPT, CNRS Luminy, Marseilles, February 1991.

[9] B. Escudie and B. Torresani. Wavelet representation and time-scaled matched receiver for asymptotic signals. In *Proc. of 5th EUSIPCO Conf.*, pages 305–308, Barcelona, Spain, 1990.

[10] A. Grossmann. Wavelet transform and edge detection. In P. Blanchard, L. Streit, and M. Hazewinkel, editors, *Stochastic Processes in Physics and Engineering*. D. Reidel, Dordrecht, Boston, Lancaster, Tokyo, 1986.

[11] A. Grossmann and J. Morlet. Decomposition of Hardy functions into square integrable wavelets of constant shape. *SIAM J. Math.*, 15:723–736, 1984.

[12] M. Holschneider, R. Kronland-Martinet, J. Morlet, and P. Tchamitchian. A real-time algorithm for signal analysis with the help of the wavelet transform, 1988. Preprint.

[13] M. Holschneider and P. Tchamitchian. Regularite locale de la fonction non-differentiable de Riemann. In P.G. Lemarie, editor, *Les ondelettes en 1989*, Lecture notes in Mathematics. Springer-Verlag, Berlin, Heidelberg, New York, London, Paris, Tokyo, Hong Kong, 1989.

[14] S. Jaffard. Exposants de Holder en des points donnes et coefficients d'ondelettes. *Notes au Compte-Rendu de l'Academie Des Sciences*, 308, serie I:79–81, 1989.

[15] S. Jaffard. Pointwise smoothness, two microlocalisation and wavelet coefficients. *Publicacions Matematiques*, 35, 1991.

[16] S. Mallat and S. Zhong. Characterization of signals from multiscale edges. Computer science tech. report, NYU, December 1991.

[17] B. Mandelbrot. *The Fractal Geometry of Nature*. W.H. Freeman, San Francisco, New York, 1983.

[18] D. Marr. Vision. W.H. [illegible] 1982.

[19] D. Marr and E. Hildr[illegible] Proc. Roy. Soc. London, 207:187–217, [illegible]

[20] Y. Meyer. Ondelettes et [illegible]

[21] Y. Meyer. La 2-microlocalisation [illegible]

[22] Y. Meyer. Un contre-exemple [illegible] de Marr et a celle de S. Mallat. Preprint, 1991.

[23] J.F. Muzy, E. Bacry, and A. Arneodo. Wavelets and multifractal formalism for singular signals: application to turbulent data. Submitted to Physics Review Letters, July 1991.

[24] A. Papoulis. *Probability, Random Variables, and Stochastic Processes*. McGraw-Hill, 1984.

[25] A. Rosenfeld and M. Thurston. Edge and curve detection for visual scene analysis. *IEEE Trans. on Computers*, C-20:562–569, 1971.

[26] F. Treves. *Topological Vector Spaces, Distributions and Kernels*. Academic Press.

[27] A. Witkin. Scale space filtering. In *Proc. Int. Joint Conf. Artificial Intell.*, 1983.

[28] S. Zhong. *Edges representation from wavelet transform maxima*. PhD thesis, New York University, New York, September 1990.

[29] A. Zygmund. *Trigonometric Series*. Cambridge University Press, Cambridge, U.K., 1968.

A. Proof of Theorem 5.2

We prove Theorem 5.2 by proving by induction the following proposition.

Proposition A.1 ((P_n)). Let $\psi(x)$ be a wavelet that can be written $\psi(x) = \frac{d^n \phi(x)}{dx}$, where $\phi(x)$ is a continuous function of compact support. Let $f(x)$ be a function and we suppose that for any $\epsilon > 0$, there exists a constant K_ϵ, such that at all scales s

$$\int_{a-\epsilon}^{b+\epsilon} |f * \phi_s(x)|\, dx \leq K_\epsilon . \tag{A.1}$$

If $Wf(s,x)$ has no maxima for $x \in]a,b[$ and $s < s_0$, then for any $\epsilon > 0$, there exists a constant $A_{\epsilon,n}$ such that for any $x \in]a+\epsilon, b-\epsilon[$ and $s < s_0$,

$$|Wf(s,x)| \leq A_{\epsilon,n} s^n . \tag{A.2}$$

If we modify $f(x)$ by multiplying it by the indicator function of $[a, b]$, we do not modify its regularity on any interval $[a + \epsilon, b - \epsilon]$. We shall thus suppose that $f(x) = 0$ for $x \notin [a, b]$. Let us first prove that (A.1) is satisfied. Since $f(x) \in L^1([a, b])$ and $f(x) = 0$ for $x \notin [a, b]$,

$$\int_a^b |f * \phi_s(x)|\, dx \leqslant \int_a^b |f(x)|\, dx \int_{-\infty}^{+\infty} |\phi_s(x)|\, dx.$$

With a change of variable in the integral we obtain

$$\int_{-\infty}^{+\infty} |\phi_s(x)|\, dx = \int_{-\infty}^{+\infty} |\phi(x)|\, dx.$$

Hence, $\int_a^b |f * \phi_s(x)|\, dx$ is bounded by a constant independent of the scale s, as in (A.1). In order to prove the proposition (P_n) for $n = 1$, we introduce a lemma.

Lemma A.2. Let $[c, d]$ be an interval of $\mathfrak{R}$. Let K be a positive constant. Let $g(x)$ be a function which satisfies

$$\int_c^d |g(x)|\, dx < K, \tag{A.3}$$

and such that $\left|\frac{dg(x)}{dx}\right|$ has no local maxima on $[c, d]$. Let $\beta > 0$ with $\beta < (d - c)/4$. There exists two constants B_β and C_β such that

$$\forall x \in [c + \beta, d - \beta], \qquad |g(x)| < B_\beta \tag{A.4}$$

and

$$\forall x \in [c + \beta, d - \beta], \qquad \left|\frac{dg(x)}{dx}\right| < C_\beta. \tag{A.5}$$

The constants B_β and C_β only depends upon β, $d - c$ and K.

We denote $g'(x) = \frac{dg(x)}{dx}$. Although quite simple, this proof is long because it includes many sub-cases. We prove (A.4) and then (A.5). In the following, we only consider the values of $g(x)$ over the interval $[c, d]$. We first have two cases. Since $|g'(x)|$ has no local maximum, either $g'(x)$ has a constant sign or $g'(x)$ is monotonic.

1) If we suppose that $g'(x)$ has a constant sign then $g(x)$ is monotonic. Equation (A.3) yields

$$\int_c^{c+\beta} |g(x)|\, dx \leqslant K \quad \text{and} \quad \int_{d-\beta}^{d} |g(x)|\, dx \leqslant K. \tag{A.6}$$

Since, $g(x)$ is monotonic on $[c, d]$, these integral constraints imply that

$$|g(c + \beta)| \leqslant \frac{K}{\beta} \quad \text{and} \quad |g(d - \beta)| \leqslant \frac{K}{\beta}. \tag{A.7}$$

To prove (A.7) one must distinguish several cases. For example if $g'(x)$ is positive and $g(x)$ remains positive, the second integral of (A.6) implies that $|g(d-\beta)| \leqslant K/\beta$ and since $|g(c+\beta)| \leqslant |g(d-\beta)|$ (A.7) is valid. The other cases are treated similarly. Since $g(x)$ is monotonic, $|g(x)| \leqslant \text{Max}(|g(c+\beta)|, |g(d-\beta)|)$, hence (A.4) is satisfied for $B_\beta \geqslant \frac{K}{\beta}$.

2) Let us suppose that $g'(x)$ is monotonic, for example that it decreases. The function $g(x)$ is concave. The same proof is valid for a convex function.

   a) We first suppose that $g(x)$ does not change sign on $]c+\beta, d-\beta[$.

      i) If $g(x)$ is negative, since it is concave $|g(x)| \leqslant \text{Max}(|g(c+\beta)|, |g(d-\beta)|)$, for $x \in]c+\beta, d-\beta[$. Since $g'(x)$ is monotonically decreasing, either it is positive at all points of $[c, c+\beta]$ or it is negative at all points of $[c+\beta, d]$. We know that $g(x)$ remains negative and

$$\int_c^{c+\beta} |g(x)|\,dx \leqslant K, \qquad \int_{c+\beta}^{d} |g(x)|\,dx \leqslant K.$$

      We can thus derive that

$$|g(c+\beta)| \leqslant \text{Max}\left(\frac{K}{\beta}, \frac{K}{d-c-\beta}\right).$$

      Since $\beta \leqslant (b-c)/4$, we obtain $|g(c+\beta)| \leqslant K/\beta$. Similarly we can prove that $|g(d-\beta)| \leqslant K/\beta$. Hence $|g(x)| \leqslant K/\beta$.

      ii) If $g(x)$ remains positive, there exists $e \in]c+\beta, d-\beta[$ such that $g(x) \leqslant g(e)$ for all $x \in]c+\beta, d-\beta[$. Since $g(x)$ is concave, one can derive that

$$\int_{c+\beta}^{d-\beta} g(x)\,dx \geqslant \frac{g(e)(d-c-2\beta)}{2}.$$

      Since $\beta < (d-c)/4$, we obtain $g(e) \leqslant 4K/(d-c)$. Hence $|g(x)| \leqslant 4K/(d-c)$.

   b) Let us now suppose that $g(x)$ changes of sign over $[c+\beta, d-\beta]$. Either both $g(c+\beta)$ and $g(d-\beta)$ are negative or only one of them is negative. We only consider the case where both are negative. The other case can be treated with the same approach. Since $g(x)$ is concave, it has two zero-crossings at the locations z_0 and z_1, $z_0 < z_1$. For $x \in]c+\beta, z_0[\cup]z_1, d-\beta[$, $g(x)$ is negative and $|g(x)| \leqslant \text{Max}(|g(c+\beta)|, |g(d-\beta)|)$. Over $[c, c+\beta]$ and $[d-\beta, d]$ $g(x)$ is monotonic. With the same argument as in 1), we prove that

$$|g(c+\beta)| \leqslant K/\beta \quad \text{and} \quad |g(d-\beta)| \leqslant K/\beta.$$

For $x \in [z_0, z_1]$, $g(x) \geq 0$ and there exists $e \in]z_0, z_1[$ such that $g(x) \leq g(e)$ for $x \in]z_0, z_1[$. We must prove that $g(e)$ is bounded. Since $g(x)$ is concave over $[z_0, z_1]$, one can derive that

$$K \geq \int_{z_0}^{z_1} g(x)\,dx \geq \frac{g(e)(z_1 - z_0)}{2}. \tag{A.8}$$

Let us suppose that $g(e) \geq K/\beta$. Let $l(x)$ be the affine function which crosses 0 at the abscissa z_0, and is equal to $g(e)$ at the abscissa e. Before the abscissa z_0, $l(x)$ is negative and $l(x) > g(x)$ because $g(x)$ is concave. Hence, $|l(c+\beta)| \leq |g(c+\beta)| \leq K/\beta$. We know that

$$\frac{|l(c+\beta)|}{|l(e)|} = \frac{z_0 - c - \beta}{e - z_0}.$$

Since $|l(c+\beta)| \leq K/\beta$ and $l(e) = g(e) \geq K/2$, we obtain

$$e - z_0 \geq z_0 - c - \beta.$$

With the same argument applied between on the second zero-crossing z_1 and $d - \beta$, we can also prove that

$$z_1 - e \geq d - \beta - z_1.$$

Adding these two equations yields

$$z_1 - z_0 \geq \frac{d - c - 2\beta}{2} \geq \frac{d - c}{4}.$$

If we insert this equation into (A.8), we obtain

$$g(e) \leq \frac{8K}{d - c}.$$

Hence, $g(e) \leq \mathrm{Max}(8K/(d - c), K/\beta)$. This last case finishes the proof of (A.4) of Lemma A.2 for a constant B_β such that $B_\beta \geq \mathrm{Max}(8K/(d - c), k/\beta)$.

Let us now prove that $g'(x)$ is bounded. Since $|g'(x)|$ has no maxima on the interval $[c + \beta/2, d - \beta/2]$, we know that $|g'(x)| \leq \max(|g'(c+\beta)|, |g'(d - \beta)|)$ for $x \in [c + \beta, d - \beta]$. Let us suppose for example that $|g'(c + \beta)| \geq |g'(d - \beta)|$. Then, $|g'(x)|$ is monotonically decreasing on $[c + \beta/2, c + \beta]$ and $g'(x)$ does not change sign over this interval. Hence,

$$|g'(c+\beta)| \leq \frac{2}{\beta}\left|\int_{c+\beta/2}^{c+\beta} g'(x)\,dx\right| = \tfrac{2}{\beta}|g(c + \beta/2) - g(c + \beta)| \leq \tfrac{4}{\beta} B_{\beta/2}.$$

Since $|g'(x)| \leq \mathrm{Max}(|g'(c+\beta)|, |g'(d-\beta)|)$ for $x \in [c+\beta, d-\beta]$, we derive that $|g'(x)|$ is bounded by a constant C_β which only depends upon β, $b-c$ and K.

Lemma A.3. Let $[c,d]$ be an interval of $\mathfrak{R}$. Let K be a positive constant. Let $g(x)$ be a function which satisfies

$$\int_c^d |g(x)|\,dx < K,$$

and such that $\frac{|d^2 g(x)}{dx^2|}$ has no local maxima on $[c,d]$. Let $\beta > 0$ with $\beta < (d-c)/4$. There exists a constant D_β that only depends upon β, $d-c$ and K, such that

$$\forall x \in [c+\beta, d-\beta], \qquad |\tfrac{d^2 g(x)}{dx^2}| < D_\beta. \tag{A.9}$$

The proof of this lemma is mostly the same as that for Lemma A.2 and we leave it to the reader.

Let us now prove that the proposition (P_n) is true for $n = 1$. Since $\psi(x) = \frac{d\phi(x)}{dx}$, we derive that

$$Wf(s,x) = s\frac{d}{dx}(f * \phi_s)(x).$$

Our induction hypothesis supposes that $g(x) = f * \phi_s(x)$ satisfies (A.3) of Lemma A.2 for $c = a + \epsilon/2$ and $d = b - \epsilon/2$. The result of this lemma for $\beta = \epsilon/2$ and $s < s_0$ yields

$$|Wf(s,x)| \leq sC_{\epsilon/2}.$$

This concludes the proof of (A.2) for $n = 1$. The proof of (P_n) for $n = 2$ is based on Lemma A.3. Since $\psi(x) = \frac{d^2\phi(x)}{dx^2}$, we derive that

$$Wf(s,x) = s^2\frac{d^2}{dx^2}(f * \phi_s)(x).$$

We can apply the result of Lemma A.3 to $g(x) = f * \phi_s(x)$, with $\beta = \epsilon/2$, $c = a + \epsilon/2$ and $d = b - \epsilon/2$. Equation (A.9) yields

$$|Wf(s,x)| \leq s^2 D_{\epsilon/2},$$

which finishes to proof of (P_n) for $n = 2$.

Let us now prove that if (P_n) is true, for $n \geq 2$, then (P_{n+1}) is also true. Let $\psi(x)$ be a wavelet with $n+1$ vanishing moments and $f(x)$ a function that satisfies (A.8). The wavelet $\psi(x)$ can be written $\psi(x) = \frac{d\chi(x)}{dx}$ where the

wavelet $\chi(x)$ has n vanishing moments. Let $\frac{df(x)}{dx}$ be the derivative of $f(x)$ in the sense of distributions,

$$Wf(s,x) = s\frac{df}{dx} * \chi_s(x). \tag{A.10}$$

In order to apply our induction hypothesis (P_n) to $\frac{df(x)}{dx}$ with respect to the wavelet $\chi(x)$, we need provehat to for any $\epsilon > 0$, there exists a constant K_ϵ such that at all scales s

$$\int_{a+\epsilon}^{b-\epsilon} \left| \frac{df}{dx} * \phi_s(x) \right| dx \leq K_\epsilon. \tag{A.11}$$

Since the wavelet $\psi(x)$ has more than two vanishing moments, the proposition (P_2), that we just proved, implies that for any $\epsilon > 0$, if $x \in]a+\epsilon, b-\epsilon[$

$$|Wf(s,x)| \leq s^2 A_{\epsilon,2}.$$

From Theorem 3.3 we derive that $f(x)$ is uniformly Lipschitz α on the intervals $]a+\epsilon, b-\epsilon[$, for any $\alpha < 2$. Hence, $\frac{df(x)}{dx}$ is uniformly bounded on any such interval. One can then easily derive that the condition (A.11) is satisfied. Let now apply the induction hypothesis (P_n) to $\frac{df(x)}{dx}$ with respect to the wavelet $\chi(x)$. There exists a constant $A_{\epsilon,n}$ such that for any $x \in]a+\epsilon, b-\epsilon[$ and $s < s_0$,

$$\left| \frac{df}{dx} * \chi_s(x) \right| \leq A_{\epsilon,n} s^n.$$

Equation (A.10) implies that

$$|Wf(s,x)| \leq A_{\epsilon,n} s^{n+1}.$$

This finishes the proof of (P_{n+1}).

By applying Theorem 3.3 to the statement (P_n), we derive that the function $f(x)$ is Lipschitz α for any $\alpha < n$. For $\alpha = n$, Theorem 3.3 does not apply because it is an integer Lipschitz exponent.

Let us now prove that (A.2) implies that $f(x)$ is Lipschitz n if the wavelet $\psi(x)$ can be written

$$\psi(x) = \frac{d^n \theta(x)}{dx}, \tag{A.12}$$

where $\theta(x)$ is a smoothing function. Let $\frac{d^n f(x)}{dx^n}$ be the n^{th} derivative of $f(x)$ in the sense of distributions. Similarly to (A.10), (A.12) yields

$$Wf(s,x) = s^n \frac{d^n f}{dx^n} * \theta_s(x).$$

Equation (A.2) of the proposition (P_n) implies that for any $\epsilon > 0$ there exists a constant $A_{\epsilon,n}$ such that for any $x \in]a + \epsilon, b - \epsilon[$ and $s < s_0$

$$\left| \frac{d^n f}{dx^n} * \theta_s(x) \right| \leq A_{\epsilon,n}.$$

Since the integral of $\theta(x)$ is nonzero, this equation implies that $\frac{d^n f(x)}{dx^n}$ is a function which is bounded by $A_{\epsilon,n}$ over the interval $]a + \epsilon, b - \epsilon[$. Hence $f(x)$ is uniformly Lipschitz n over the interval $]a + \epsilon, b - \epsilon[$.

B. Proof of Theorem 5.3

We first derive from Theorem 5.2 that $f(x)$ is Lipschitz n at all points different than x_0. Let $x_1 \in]a, x_0[$. For $s < s_0$, $|Wf(s,x)|$ has maxima only in a cone pointing to x_0. Hence, for $\epsilon > 0$ such that $a + \epsilon < x_0 - \epsilon$, there exists s_ϵ such that for $s < s_\epsilon$, and $x \in]a + \epsilon/2, x_0 - \epsilon/2[$, $|Wf(s,x)|$ has no maxima. From Theorem 5.2 we derive that $f(x)$ is uniformly Lipschitz n in $]a + \epsilon, x_0 - \epsilon[$. From this result we easily derive that $f(x)$ is uniformly Lipschitz n in a neighborhood of any point $x_1 \in]a, x_0[$. The same proof is valid for $x_1 \in]x_0, b[$.

Let us now prove that the Lipschitz regularity at x_0 is characterized by the decay of the wavelet transform local maxima. Let $x_1 \in]a, x_0[$ and $x_2 \in]x_0, b[$. We proved that $f(x)$ is uniformly Lipschitz n in the neighborhood of x_1 and x_2. The necessary condition of Theorem 3.3 is valid for integer Lipschitz exponents and it implies that there exists s_0 such that for $s < s_0$,

$$|Wf(s,x_1)| \leq A_1 s^n \quad \text{and} \quad |Wf(s,x_2)| \leq A_2 s^n. \tag{B.1}$$

For $x \in]x_1, x_2[$ and $s < s_0$, the value of $|Wf(s,x)|$ is smaller or equal to the maximum value among $|Wf(s,x_1)|$, $|Wf(s,x_2)|$ and the wavelet transform modulus at all the local maxima that occur at the same scale inside the cone pointing to x_0. Theorem 5.3 supposes that all these local maxima have an amplitude smaller than As^α. Since $\alpha < n$, we derive from (B.1) that there exists a constant B such that if $x \in]x_1, x_2[$ and $s < s_0$,

$$|Wf(s,x)| \leq Bs^\alpha.$$

Since $x_0 \in]x_1, x_2[$, Theorem 3.3 implies that $f(x)$ is Lipschitz α at x_0.

C. Proof of Theorem 5.4

In order to apply Theorem 3.4, we want to prove that there exists a scale s_1 and $\epsilon > 0$ such that if $s < s_1$ and $x \in]x_0 - \epsilon, x_0 + \epsilon[$,

$$|Wf(s,x)| \leq B(s^\gamma + |x - x_0|^\gamma). \tag{C.1}$$

We prove this by showing separately that there exists two constants B_1 and B_2 such that

$$|Wf(s,x)| \leq B_1 s^\gamma, \tag{C.2}$$

when (s,x) is in the cone of influence of x_0 and

$$|Wf(s,x)| \leq B_2 |x - x_0|^\gamma, \tag{C.3}$$

when (s,x) is below the cone of influence of x_0. Once (C.1) is proved, Theorem 5.4 is a simple consequence of Theorem 3.4, for $\alpha < \gamma$. For $\alpha = \gamma$, we cannot apply Theorem 3.4 because we are missing the logarithmic term. Theorem 5.4 supposes that $Wf(s,x)$ has a constant sign in a neighborhood of x_0, and we shall suppose that it is positive. For $s < s_0$ and $|X(s) - x_0| < C\epsilon$, we have

$$|Wf(s, X(s))| \leq As^\gamma. \tag{C.4}$$

We first prove (C.2) and then (C.3) for $\epsilon = \frac{1}{4}(K - C)s_0$ and $s_1 = \frac{1}{4K}(K - C)s_0$.

The wavelet $\psi(x)$ is the n^{th} derivative of a positive function $\theta(x)$ of support equal to $[-K, K]$ and which is strictly positive on $]-K, K[$. Hence,

$$Wf(s,x) = s^n (f^{(n)} * \theta_s)(x) > 0, \tag{C.5}$$

where $f^{(n)}(x)$ is the n^{th} derivative of $f(x)$ in the sense of distributions. The function $\theta(x)$ is a positive function with a strictly positive integral. Since (C.5) is valid at all scales $s < s_0$, it implies that $f^{(n)}(x) > 0$ for $x \in [a,b]$ (positive in the sense of distributions). Equation (C.5) can be rewritten

$$Wf(s,x) = s^{n-1} \int_{-\infty}^{+\infty} \theta\left(\frac{x-u}{s}\right) f^{(n)}(u)\, du.$$

Let (s,x) be a point in the cone of influence of x_0, $|x - x_0| \leq Ks$. The support of $\theta((x-u)/s)$ is included in $[x_0 - 2Ks, x_0 + 2Ks]$ so

$$Wf(s,x) = s^{n-1} \int_{x_0 - 2Ks}^{x_0 + 2Ks} \theta\left(\frac{x-u}{s}\right) f^{(n)}(u)\, du. \tag{C.6}$$

Let $M = \max_{x \in [-K,K]} \theta(x)$. Since $\theta(x)$ is continuous and strictly positive over $]-K, K[$, there exists $\lambda > 0$ such that

$$\forall x \in [(-K + C)/2, (K + C)/2], \theta(x) > \lambda M.$$

Let $s' = 4Ks/(K-C)$. We know that $|x_0 - X(s')| \leqslant Cs'$. For $u \in [x_0 - 2Ks, x_0 + 2Ks]$, we derive that $|(X(s') - u)/s'| \leqslant (K + C)/2$ and therefore

$$\forall u \in [x_0 - 2Ks, x_0 + 2Ks], \theta\left(\frac{X(s') - u}{s'}\right) \geqslant \lambda M.$$

Since $0 \leqslant \theta((x-u)/s) \leqslant M$ and $f^{(n)}(x) \geqslant 0$,

$$\int_{x_0-2Ks}^{x_0+2Ks} \theta\left(\frac{x-u}{s}\right) f^{(n)}(u)\,du \leqslant 1/\lambda \int_{x_0-2Ks}^{x_0+2Ks} \theta\left(\frac{X(s')-u}{s'}\right) f^{(n)}(u)\,du.$$

Equation (C.6) yields

$$Wf(s,x) \leqslant s^{n-1}\frac{1}{\lambda}\int_{-\infty}^{+\infty} \theta\left(\frac{X(s')-u}{s'}\right) f^{(n)}(u)\,du$$

$$= \tfrac{1}{\lambda} Wf(s', X(s')). \tag{C.7}$$

We suppose that (C.4) holds so

$$Wf(s', X(s')) \leqslant A(s')^\gamma = \tfrac{A(4K)^\gamma}{(K-C)^\gamma} s^\gamma.$$

We thus derive from (C.7) that

$$Wf(s,x) \leqslant B_1 s^\gamma \qquad \text{with } B_1 = \tfrac{A(4K)^\gamma}{\lambda(K-C)^\gamma}. \tag{C.8}$$

Let us now prove that if (s,x) is below the cone of influence of x_0, $Wf(s,x) \leqslant B_2|x-x_0|^\gamma$.

$$Wf(s,x) = s^{n-1}\int_{-\infty}^{+\infty} \theta\left(\frac{x-u}{s}\right) f^{(n)}(u)\,du.$$

Let $s_2 = |x - x_0|/K$. Since (x,s) is below the cone of influence of x_0, $|x - x_0| \geqslant Ks$, so $s \leqslant s_2$. The support of $\theta((x-u)/s)$ is thus included in $[x_0 - 2Ks_2, x_0 + 2Ks_2]$ so

$$Wf(s,x) = s^{n-1}\int_{x_0-2Ks_2}^{x_0+2Ks_2} \theta\left(\frac{x-u}{s}\right) f^{(n)}(u)\,du. \tag{C.9}$$

Let us now define $s_2' = 4Ks_2/(K-C)$. With the same argument as for (C.7), we can prove that

$$Wf(s,x) \leqslant \tfrac{1}{\lambda} Wf(s_2', X(s_2')). \tag{C.10}$$

Equation (C.4) implies

$$Wf(s_2', X(s_2')) \leqslant A(s_2')^\gamma = \tfrac{A4^\gamma}{(K-C)^\gamma}|x - x_0|^\gamma. \tag{C.11}$$

By inserting (C.11) in (C.10) we obtain

$$Wf(s,x) \leqslant B_2|x-x_0|^\gamma \qquad \text{with } B_2 = \tfrac{A4^\gamma}{\lambda(K-C)^\gamma}. \tag{C.12}$$

One can verify that both (C.8) and (C.12) are valid for $x \in [x_0 - \epsilon, x_0 + \epsilon]$ and $s \leqslant s_1$ with $\epsilon = \frac{1}{4}(K-C)s_0$ and $s_1 = \frac{1}{4K}(K-C)s_0$.

D. White noise wavelet transform

It is well known [24] that the density of zero-crossings of a differentiable Gaussian process whose autocorrelation is $R(\tau)$ is

$$\sqrt{\frac{-R^{(2)}(0)}{\pi^2 R(0)}}, \tag{D.1}$$

where $R^{(n)}(\tau)$ is the n^{th} derivative of $R(\tau)$. If the process is twice differentiable, the density of local extrema is equal to the density of zero-crossings of the derivative of the process. The autocorrelation of the derivative is $-R^{(2)}(\tau)$. Hence, the density of extrema is

$$\sqrt{\frac{-R^{(4)}(0)}{\pi^2 R^{(2)}(0)}}. \tag{D.2}$$

The autocorrelation of the Gaussian process $Wn(s,x)$ is defined by

$$\begin{aligned} R(\tau) &= E\{Wn(s,x+\tau)Wn(s,x)\} \\ &= \int_{-\infty}^{+\infty}\int_{-\infty}^{+\infty} n(u)n(v)\psi_s(x+\tau-u)\psi_s(x-v)\,du\,dv. \end{aligned}$$

Since $n(x)$ is white noise, $E\{n(u)n(v)\} = \delta(u-v)$ and we obtain

$$R(\tau) = \int_{-\infty}^{+\infty} \psi_s(\tau+u)\psi_s(u)\,du. \tag{D.3}$$

From this equation, we can prove that $R^{(4)}(0) = \|\psi^{(2)}\|^2/s^5$ and $R^{(2)}(0) = -\|\psi^{(1)}\|^2/s^3$. From (D.2), we derive that the density of extrema of the process $Wn(s,x)$ is

$$\frac{\|\psi^{(2)}\|}{s\pi\|\psi^{(1)}\|}. \tag{D.4}$$

At least half of these local extrema are local maxima of $|Wn(s,x)|$. The number of local maxima depends upon the proportion of local extrema and zero-crossings of $Wn(s,x)$. Equations (D.1) and (D.3) prove that the density of zero-crossings of $Wn(s,x)$ is $\|\psi^{(1)}\|/(s\pi\|\psi\|)$. The proportion of local extrema and zero-crossings of $Wn(s,x)$ is independent of the scale, which proves that the density of local maxima of $|Wn(s,x)|$ is

$$d_s = \lambda\frac{\|\psi^{(2)}\|}{s\pi\|\psi^{(1)}\|}, \tag{D.5}$$

where λ is a constant between 0.5 and 1 that depends only on $\|\psi\|$, $\|\psi^{(1)}\|$ and $\|\psi^{(2)}\|$.

Complex analysis and frames in sampling theory†

William Heller
Department of Mathematics and Computer Science
Dartmouth College
6188 Bradley Hall
Hanover, NH 03755-3551 USA
heller@cannon.dartmouth.edu

Abstract. Regular and irregular sampling theorems are proved using frames of exponentials, Gabor frames, and nonharmonic Fourier series. These include the Shannon sampling theorem, the Yao-Thomas irregular sampling theorem, and a result dual to the Yao-Thomas theorem. An irregular sampling algorithm is presented that allows much more general sampling lattices. These ideas are then applied to the Gabardo-Walker uniqueness theorem to obtain a corresponding representation theorem.

1. Classical sampling theory using frames

Ordinary Fourier series in $L^2[-\frac{1}{2T}, \frac{1}{2T}]$, $T > 0$, that is expansions using exponentials of the form $\{e^{2\pi i n T \gamma}\}$, have been used in mathematics, engineering, and science for years. Here we give several applications of *nonharmonic Fourier series*, that is expansions using exponentials of the form $\{e^{2\pi i t_n \gamma}\}$ where the regular sequence of real numbers $\{nT\}$ has been replaced by the irregular sequence $\{t_n\}$. The difficulty with applying nonharmonic Fourier series is that they are not orthonormal bases and so the nonharmonic Fourier series must be interpreted carefully. The concept of a frame provides this interpretation.

Definition/Proposition 1.1. A sequence $\{g_n\} \subseteq H$, a separable Hilbert space, is a *frame* if there exists constants $A, B > 0$ such that

$$\forall\, h \in H, \quad A\|h\|^2 \leq \sum_n |\langle h, g_n\rangle|^2 \leq B\|h\|^2.$$

† The work presented here is a short exposition of joint work with John Benedetto, whose patience, friendship, and teachings have left a deep and positive mark on me. I would also like to thank Hans Feichtinger and Christian Houdré for insights, discussions, and preprints on the topics discussed herein.

J. S. Byrnes et al. (eds.), Probabilistic and Stochastic Methods in Analysis, with Applications, 101–116.
© 1992 *Kluwer Academic Publishers. Printed in the Netherlands.*

The constant A (resp. B) is called the *lower* (resp. *upper*) *frame bound.*

If $\{g_n\}$ is a frame, then we have the *reconstruction formulas*

$$\forall h \in H, \quad h = \sum_n \langle h, S^{-1}g_n\rangle g_n$$

and

$$\forall h \in H, \quad h = \sum_n \langle h, g_n\rangle S^{-1}g_n$$

where the *frame operator* S is given by

$$Sh = \sum_n \langle h, g_n\rangle g_n.$$

If $\{g_n\}$ is a frame in H, then $\{S^{-1}g_n\}$ is also a frame in H called the *dual frame.*

Proof. See [4, 9, 3]. ∎

Example 1.2.

1) Orthonormal bases in Hilbert spaces are frames with the reconstruction formulas being the orthonormal basis decomposition and the frame operator being the identity.
2) The exponentials $\{E_{t_n} = e^{-2\pi i t_n \gamma}\}$ where $\{t_n\}$ satisfies

$$|t_n - nT| \leq L < \frac{T}{4}$$

is a frame for $L^2[-\frac{1}{2T}, \frac{1}{2T}]$ (see Example 1.9). More generally, see Definition 2.1 and Theorems 2.2 and 2.3.

Remark 1.3. Duffin and Schaeffer invented the concept of a frame to deal with questions about spanning properties of sets of exponentials. That is, they were interested in whether a collection of exponentials $\{E_{t_n}\}$, $E_{t_n} = e^{-2\pi i t_n \gamma}$, $n \in \mathbb{Z}$, generated by a sequence of real or complex numbers $\{t_n\}$ was *complete* in $L^2[-\Omega, \Omega]$, $\Omega > 0$—i.e., whether each function in $L^2[-\Omega, \Omega]$ can be approximated arbitrarily closely by a linear combination of exponentials taken from the collection. Much work has been done on this and related questions as the interested reader may investigate by consulting [2, 17, 15, 20]. For our purposes completeness is not enough; we want to decompose functions as sums of exponentials or other functions. The reconstruction formulas permit this and represent, until the work on wavelets and related topics, a neglected aspect of the work of Duffin and Schaeffer. These formulas are at the heart of the sampling work which follows.

Definition/Proposition 1.4. A function f is *Ω-bandlimited*, $\Omega > 0$, i.e., $f \in PW_\Omega$, if $f \in L^2(\mathfrak{R})$ with $\operatorname{supp} \hat{f} \subseteq [-\Omega, \Omega]$, where $\hat{f}$ is the Fourier transform $\hat{f}(\gamma) = \int f(t)e^{-2\pi i t\gamma}\,dt$. The Ω-bandlimited functions are entire functions of *exponential type* Ω and conversely, i.e., there exists a constant A such that

$$\forall z \in \mathbb{C}, \qquad |f(z)| \leqslant Ae^{2\pi\Omega|z|}.$$

Theorem 1.5 (Shannon). Let $T, \Omega > 0$ for which $0 < \Omega \leqslant \frac{1}{2T}$. Then

$$\forall f \in PW_\Omega, \quad f(t) = T\sum_{n\in\mathcal{Z}} f(nT)\, d_{\frac{\pi}{T}}(t - nT) \quad \text{in } L^2(\mathfrak{R}),$$

where $f(nT)$ is the value of f at $nT \in \mathfrak{R}$, where $d_{\frac{\pi}{T}}$ is the $\frac{\pi}{T}$ dilation of the *Dirichlet (or "sinc") function*

$$d(t) = \frac{\sin t}{\pi t},$$

and where $d_{\frac{\pi}{T}}(t - nT)$ is the translation

$$d_{\frac{\pi}{T}}(t - nT) = \frac{\sin\frac{\pi}{T}(t - nT)}{\pi(t - nT)}.$$

The convergence is in $L^2(\mathfrak{R})$ and uniform over $\mathfrak{R}$.

Proof. Consider the frame of exponentials in $L^2[-\frac{1}{2T}, \frac{1}{2T}]$ given by $\{e^{-2\pi inT\gamma}\}_{n\in\mathcal{Z}}$. We know this collection is a frame as, upon normalization, it is an orthonormal basis in $L^2[-\frac{1}{2T}, \frac{1}{2T}]$. The frame operator is the constant multiplier $\frac{1}{T}$ as

$$\begin{aligned}\forall \hat{h} \in L^2[-\tfrac{1}{2T}, \tfrac{1}{2T}], \quad S(\hat{h}) &= \sum_n \langle \hat{h}(\zeta), e^{-2\pi inT\zeta}\rangle e^{-2\pi inT\gamma} \\ &= \frac{1}{T}\sum_n \langle \hat{h}(\zeta), \sqrt{T}e^{-2\pi inT\zeta}\rangle \sqrt{T}e^{-2\pi inT\gamma} \\ &= \frac{1}{T}\hat{h}.\end{aligned}$$

Hence both reconstruction formulas reduce to

$$f(\gamma) = T\sum_n \langle \hat{f}(\zeta), e^{-2\pi inT\zeta}\rangle_{(\frac{1}{2T})} e^{-2\pi inT\gamma}\mathbf{1}_{(\frac{1}{2T})}(\gamma). \tag{1.1}$$

where $\mathbf{1}_{(\frac{1}{2T})}$ is 1 on $[-\frac{1}{2T}, \frac{1}{2T}]$ and 0 elsewhere. The characteristic function $\mathbf{1}_{(\frac{1}{2T})}$ is necessary as (1.1) is an expansion in $L^2[-\frac{1}{2T}, \frac{1}{2T}]$, which we view as a subspace of $L^2(\hat{\mathfrak{R}})$. Applying the inverse Fourier transform and evaluating

the coefficients produces the desired expansion with $L^2(\mathfrak{R})$ convergence. The uniform convergence can be verified by an advanced calculus argument. ∎

Remark 1.6.

1) The coefficients are the function values at the points $\{nT\}_{n\in\mathcal{Z}}$, hence the name "sampling formula." Note that the sampling lattice $\{nT\}$ generated the frame of exponentials $\{e^{-2\pi inT\gamma}\}_{n\in\mathcal{Z}}$ in $L^2[-\frac{1}{2T}, \frac{1}{2T}]$.
2) The decomposing functions are tanslates of a single $\frac{1}{2T}$-bandlimited function, $d_{\frac{\pi}{T}}(t)$, the dilated sinc function.
3) The poor decay of the sinc function can be overcome by using an over–sampling argument that smooths out the discontinuities of $\mathbf{1}_{(\frac{1}{2T})}$. This is accomplished by multiplying both sides of (1.1) by a function $\hat{s} \in C_c^\infty(\mathfrak{R})$ with $\operatorname{supp}\hat{s} \subseteq [-\frac{1}{2T}, \frac{1}{2T}]$ and with $\hat{s}(\gamma) = 1$ for all $\gamma \in [-\Omega, \Omega]$.
4) Clearly one need not invoke the concept of a frame of exponentials in the proof above as the exponentials, upon normalization, form an orthonormal basis for $L^2[-\frac{1}{2T}, \frac{1}{2T}]$. The point is that the proof above is generalizable to a class of irregular sampling lattices, $\{t_n\}$ instead of $\{nT\}$, where $\{t_n\}$ is a sequence of real numbers. By doing this, we will be able to reproduce the classical irregular sampling formula of Yao and Thomas, obtain a new dual result, and finally produce an irregular sampling algorithm for sampling lattices with great generality. To accomplish this we will need a few more facts about frames.

Definition/Proposition 1.7 ([4]). A frame in a separable Hilbert space is *exact* if it ceases to be a frame upon the removal of any one element. Orthonormal bases are exact frames, but it can be shown that the union of two orthonormal bases is a frame that is not exact. Several less elementary examples are given in Example 1.9.

Definition/Proposition 1.8 ([4]). Let $\{g_n\}$ be an exact frame in a separable Hilbert space H. Then the frame $\{g_n\}$ and the dual frame $\{S^{-1}g_n\}$ are *biorthonormal*, i.e.,

$$\langle g_m, S^{-1}g_n\rangle = \delta_{mn}$$

where $\delta_{mn} = 1$ if $m = n$ and zero otherwise.

The point of this definition/proposition is that one can, in certain cases, explicitly construct the sequence orthonormal to $\{g_n\}$, that is the dual frame $\{S^{-1}g_n\}$, by methods other than an involved analysis of the inverse frame operator S^{-1}. For certain collections of exponentials this can be accomplished by using Lagrange interpolation theory and function theory. This is done in

the next example. For convenience we let $E_{t_n} = e^{-2\pi i t_n \gamma}$, $n \in \mathbb{Z}$, where γ is in $[-\frac{1}{2T}, \frac{1}{2T}]$ or in $\hat{\mathfrak{R}}$, depending on the context.

Example 1.9.

1) (Kadec-Levinson) If $\{t_n\}$ satisfies

$$|t_n - nT| \leq L < \frac{T}{4}$$

then $\{E_{t_n}\}$ is an exact frame for $L^2[-\frac{1}{2T}, \frac{1}{2T}]$ with dual frame $\{h_n = S^{-1}E_{t_n}\}$ given by

$$h_n^{\vee}(t) = r_n(t) = \frac{r(t)}{r'(t_n)(t - t_n)}$$

where

$$r(t) = (t - t_0)\prod_{n=1}^{\infty}\left(1 - \frac{t}{t_{-n}}\right)\left(1 - \frac{t}{t_n}\right).$$

See [20, 15, 12].

2) It can be shown [10, Section 5.3] that any finite modification of an exact frame of exponentials is also an exact frame—i.e., replacing any finite number of exponentials with exponentials at other points not already contained in the collection also produces an exact frame.

We now apply these ideas to obtain the Yao-Thomas irregular sampling theorem [19], which is the first expansion below, and a dual result.

Theorem 1.10. Assume $\{t_n\}$ satisfies the Kadec-Levinson condition

$$|t_n - nT| \leq L < \frac{T}{4}.$$

Then

$$\forall f \in PW_{\Omega}, \quad f(t) = \sum_n f(t_n) r_n(t)$$

and

$$\forall f \in PW_{\Omega}, \quad f(t) = \sum_n \langle f, r_n \rangle d_{\frac{\pi}{T}}(t - t_n)$$

where $\{r_n\}$ is as defined above. Both series converge uniformly to f on $\mathfrak{R}$ as well as in $L^2(\mathfrak{R})$.

Proof. By the first assertion of Example 1.9 and the reconstruction formulas we have

$$\forall f \in PW_\Omega, \quad \hat{f}(\gamma) = \sum_n \langle \hat{f}, E_{t_n} \rangle_{(\frac{1}{2T})} h_n(\gamma)$$

and

$$\forall f \in PW_\Omega, \quad \hat{f}(\gamma) = \sum_n \langle \hat{f}, h_n \rangle_{(\frac{1}{2T})} E_{t_n}(\gamma).$$

Applying the inversion formula to both expansions and the Parseval relation to the coefficients in the second, we obtain the $L^2(\mathfrak{R})$ convergent sums of the theorem. The uniform convergence follows as in [19] or by using an advanced calculus argument. ∎

Remark 1.11.

1) The first expansion in the previous theorem is the Yao-Thomas irregular sampling formula [19]. Yao and Thomas derived their sampling formula using the Lagrange interpolation work of Levinson [15, Chapter 4] and Levin [14, p. 198], providing an interpretation of it in terms of engineering considerations. However, the second expansion cannot be obtained directly from interpolation considerations and hence appears to be new.
2) Both of the expansions above can be produced using the idea of a Riesz basis of exponentials, as exact frames are Riesz bases and conversely. This approach is described in [10] (see also [20]).
3) The Kadec-Levinson condition and the other examples given above are restrictive and, as such, we seek sampling formulas for a wider class of sampling lattices $\{t_n\}$. So far we have employed orthonormal bases and Riesz bases (exact frames) of exponentials. By a *basis* we mean a collection in a Banach space by which every element of the space can be written uniquely as a (possibly infinite) linear combination of elements from the collection. One could ask whether it is possible to obtain sampling formulas employing bases of exponentials that are not Riesz bases or orthonormal bases. According to Young [20, p. 197], no example has yet been found of a basis of exponentials for $L^2[-\frac{1}{2T}, \frac{1}{2T}]$ that is not a Riesz basis. There are, however, examples of collections of exponentials which are complete and minimal but which are not known to be bases of exponentials [20, p. 126]. By *minimal* we mean a collection in which each element is not contained in the closed span of the other elements of the collection. A basis is necessarily minimal and complete but a minimal, complete set need not be a basis [10, Section 4.2]. Sampling formulas for these collections can be produced using Gram-Schmidt orthogonalization. This is discussed in [10, Section 4.2].

4) The expansions for $\hat{f}$ given in the proof can be multiplied by functions $\hat{s} \in C_c^\infty(\hat{\mathfrak{R}})$ with $\operatorname{supp} \hat{s} \subseteq [-\frac{1}{2T}, \frac{1}{2T}]$ and with $\hat{s}(\gamma) = 1$ for all $\gamma \in [-\Omega, \Omega]$, as described in Remark 1.6 (3). Upon inversion this gives $(s * r_n)(t)$ and $s(t - t_n)$, respectively, in the expansions of the previous theorem.

2. Modern sampling theory using frames

To take advantage of the full power of frames, we drop the requirement in the previous theorem that the frame be exact. Doing so creates two obstacles. The first is whether there are any sequences which generate frames of exponentials for $L^2[-\frac{1}{2T}, \frac{1}{2T}]$, $T > 0$, which are not exact. The second relates to the analysis of the inverse frame operator S^{-1}. In the previous theorem, we used the biorthonormality relation described in the proposition. This relation is not true if the frame is not exact. Hence we must find a realization of the inverse frame operator that is both useful and applies to frames which are not necessarily exact.

To answer the first question we describe the work of Duffin and Schaeffer and the work of Jaffard on this topic.

Definition 2.1. A sequence $\{t_n\}$ is *uniformly discrete* if there exists a constant d such that

$$\forall\, n \neq m, \quad |t_n - t_m| \geqslant d > 0.$$

A sequence $\{t_n\}$ is *uniformly dense* if it is uniformly discrete and there exist constants $\Delta, L > 0$ such that

$$\forall\, n \in \mathcal{Z}, \quad |t_n - \frac{n}{\Delta}| \leqslant L.$$

The constant Δ is called the *uniform density* for such sequences.

Theorem 2.2 ([4]). If $\{t_n\}$ has uniform density $\Delta > 0$, then $\{E_{t_n}\}$ is a frame for $L^2[-\Omega, \Omega]$ where $0 < 2\Omega < \Delta$ and where $E_{t_n} = e^{-2\pi i t_n \gamma}$, $n \in \mathcal{Z}$.

Theorem 2.3 ([11]). The sequence $\{t_n\}$ generates a frame of exponentials for $L^2(I)$ where I is an interval if and only if it can be written as the finite union of uniformly discrete subsequences at least one of which is uniformly dense.

Remark 2.4.

1) While not explicitly indicated in Jaffard's theorem, there is a relationship between the length of I and the uniform density of all uniformly dense subsequences of $\{t_n\}$ [11].
2) The *completeness radius* of a sequence $\{t_n\}$ is the supremum over all non-negative real numbers Ω such that $\{E_{t_n}\}$ is complete in $L^2[-\Omega, \Omega]$. This concept has a long history as the reader can investigate in [2, 13, 15, 16, 17]. The result of Jaffard above arose in his investigation of the concept of the *frame radius*, that is the supremum over all non-negative real numbers Ω such that $\{E_{t_n}\}$ is a frame in $L^2[-\Omega, \Omega]$.
3) The Duffin-Schaeffer and Jaffard theorems give the answer to the first question asked above. If we choose a sequence $\{t_n\}$ that is the union of a uniformly dense subsequence with a uniform density $\Delta > 2\Omega$, and a finite number of uniformly discrete subsequences, then $\{E_{t_n}\}$ is a frame for $L^2[-\Omega, \Omega]$. This gives a sufficiently rich class of sequences for us to investigate the existence of an irregular sampling algorithm employing them.
4) Uniformly discrete sequences generate upper frame bounds for sets of exponentials. Uniformly dense sequences generate upper frame bounds, as they are uniformly discrete, but also lower frame bounds. For the frame $\{E_{t_n}\}$ mentioned in the previous remark, explicit estimates for the upper frame bound always exists. Using the work of Plancherel and Pólya [20, pp. 93-98] one can show [10, Section 4.3] that for any uniformly discrete set $\{t_n\}$, the upper frame bound B for the set of exponentials $\{E_{t_n}\}$ in $L^2[-\Omega, \Omega]$ exists and satisfies

$$B \leqslant \frac{(e^{2\pi\Omega d} - 1)}{\pi^2 \Omega d^2}$$

where $d > 0$ is the minimum separation between sequence points $\{t_n\}$. If $\{t_n\}$ is the union of a finite number of uniformly discrete subsequences $\{t_n^1\}, \{t_n^2\}, \ldots, \{t_n^k\}$, then the upper frame bound for the exponentials $\{E_{t_n}\}$ in $L^2[-\Omega, \Omega]$ is the sum $B_1 + B_2 + \ldots + B_k$ where $B_1, \ldots, B_k$ satisfy an estimate of the form given above for each of the uniformly discrete subsequences $\{t_n^1\}, \{t_n^2\}, \ldots, \{t_n^k\}$.

Uniformly dense sequences $\{t_n\}$ impose lower frame bounds on the corresponding set of exponentials $\{E_{t_n}\}$ as well as upper frame bounds. (Recall that uniformly dense sequences are also uniformly discrete.) The lower frame bounds are also additive in the case that the sequence $\{t_n\}$ is composed of a finite number of uniformly dense subsequences. However, the lower frame bound is highly dependent on the distribution of the points and the density of the uniformly dense set. No simple relationship is known for the lower frame bound of

a uniformly dense set, as is the case for the upper frame bound for a uniformly discrete set. However, in certain useful cases explicit lower bounds can be given, as will be described latter (see Remark 3.3 (3)).

5) Note that in the definition of a uniformly dense set, the value of L could be any positive number. As such, it is possible to have large gaps in the sampling lattice—i.e., places where the distance between consecutive lattice points $\{t_n\}$ is large—by taking the value of L large enough. This is an advantage of the frame approach as compared to other approaches to irregular sampling (see the work of Karlheinz Gröchenig [7] in this volume).

To deal with the second problem associated with applying non-exact frames of exponentials to sampling problems—the problem of analyzing the inverse frame operator—we need the following fact about the frame operator. This proposition represents the Neumann expansion for the inverse frame operator.

Proposition 2.5 ([4, 3]). *If $\{g_n\} \subseteq H$, a separable Hilbert space, is a frame with frame bounds $A \leqslant B$, then*

$$\forall\, h \in H, \quad S^{-1}(h) = \frac{2}{A+B} \sum_{k=0}^{\infty} \left[\mathbf{1} - \frac{2S}{A+B}\right]^k (h).$$

where

$$\left\|\mathbf{1} - \frac{2S}{A+B}\right\| \leqslant \frac{B-A}{A+B} < 1.$$

Lemma 2.6. Let $\Gamma, \Omega > 0$ for which $0 < \Omega \leqslant \frac{1}{2\Gamma}$. Let $\{t_n\}$ generate a frame of exponentials $\{E_{t_n}\}$ for $L^2[-\frac{1}{2\Gamma}, \frac{1}{2\Gamma}]$. Then

$$\forall\, f \in PW_\Omega, \quad f(t) = \sum_n \langle \hat{f}, S^{-1}(E_{t_n})\rangle_{(\frac{1}{2\Gamma})} d_{\frac{\pi}{\Gamma}}(t - t_n)$$

where the series converges uniformly on $\mathfrak{R}$ to f and in $L^2(\mathfrak{R})$, and where the coefficients can be approximated by (infinite) linear combinations of the sample values by taking truncations of the Neumann series for S^{-1} given by

$$\begin{aligned} c_n &= \langle \hat{f}, S^{-1}(E_{t_n})\rangle_{(\frac{1}{2\Gamma})} \\ &= \frac{2}{A+B} \sum_{k=0}^{\infty} \left\langle \left[\mathbf{1} - \frac{2S}{A+B}\right]^k \hat{f}, E_{t_n} \right\rangle_{(\frac{1}{2\Gamma})}. \end{aligned}$$

Proof. Applying the appropriate reconstruction formula to the frame of exponentials $\{E_{t_n}\}$ we have

$$\forall\, f \in PW_\Omega, \qquad \hat{f}(\gamma) = \sum_n \langle \hat{f}, S^{-1}(E_{t_n})\rangle_{(\frac{1}{2\Gamma})} E_{t_n} \mathbf{1}_{(\frac{1}{2\Gamma})}(\gamma).$$

The first conclusion follows by applying the inversion formula to this, while the uniform convergence follows by either an advanced calculus argument or as in [19]. The second conclusion is an application of the previous proposition and the fact that S^{-1} is self-adjoint. ∎

The lemma appears to have nothing to do with sampling as the sample values do not appear in the expansion given above. However, when we analyze the coefficients $\{c_n\}$ by truncating the coefficient expansions, we see that the sample values of f appear. This produces the following algorithm.

Algorithm 2.7. We obtain an irregular sampling algorithm by truncating the Neumann expansion for the coefficients at various places. For example, if we take the $k = 0$ term only, we have

$$\begin{aligned} c_n &\approx \frac{2}{A+B}\langle f, E_{t_n}\rangle_{(\frac{1}{2T})} \\ &= \frac{2}{A+B} f(t_n). \end{aligned}$$

Note that if $t_n = nT$, $n \in \mathbb{Z}$, then $A = B = \frac{1}{T}$, and so $c_n \approx Tf(nT)$, as we would expect from the Shannon sampling theorem (Theorem 1.5). In fact, if we truncate after *any* value of k for $t_n = nT$, $n \in \mathbb{Z}$, with $A = B = \frac{1}{T}$, then the approximation to the coefficients is exactly $\frac{2}{A+B} f(t_n) = Tf(nT)$, so we can conclude that $c_n = Tf(nT)$ in this case.

If we keep only the $k = 0$ and $k = 1$ terms, we have

$$\begin{aligned} c_n &\approx \frac{4}{A+B} f(t_n) - \left(\frac{2}{A+B}\right)^2 \langle Sf, E_{t_n}\rangle_{(\frac{1}{2T})} \\ &= \frac{4}{A+B} f(t_n) - \left(\frac{2}{A+B}\right)^2 \sum_m \langle f, E_{t_m}\rangle_{(\frac{1}{2T})} \langle E_{t_m}, E_{t_n}\rangle_{(\frac{1}{2T})} \\ &= \frac{4}{A+B} f(t_n) - \left(\frac{2}{A+B}\right)^2 \sum_m f(t_m) T d_{\frac{1}{T}}(t_n - t_m). \end{aligned}$$

Again, if $t_n = nT$, $n \in \mathbb{Z}$, then $A = B = \frac{1}{T}$, and, since $T d_{\frac{1}{T}}(t_n - t_m) = \delta_{mn}$ in this case, we have

$$c_n \approx 2Tf(nT) - Tf(nT) = Tf(nT)$$

as we claimed above.

Remark 2.8.

1) As we take larger and larger values of k, we observe that the computation of the approximations to the coefficients falls into a pattern that is suitable for programming on a computer.

2) We can obtain versions of this algorithm with sampling kernels having more rapid decay than $d_{\frac{1}{T}}$ by multiplying both sides of the expansion in the proof of Lemma 2.6 by a function $\hat{s} \in C_c^\infty(\mathfrak{R})$ with $\operatorname{supp} \hat{s} \subseteq [-\frac{1}{2T}, \frac{1}{2T}]$ and with $\hat{s}(\gamma) = 1$ for all $\gamma \in [-\Omega, \Omega]$, as described in Remark 1.6 (3).
3) We have truncation error estimates for both the coefficient expansions and the sampling expansion. See [10, Sections 4.3].
4) One could also consider using the other reconstruction formula in the proof of Lemma 2.6, as the two reconstruction formulas produced two different sampling formulas when we assumed the Kadec-Levinson condition (Theorem 1.10). When using the Neumann expansion, the two reconstruction formulas do in fact produce the same sampling formula. This can be shown by an induction argument. See [10, Theorem 4.3.1].
5) The sampling theory presented above can be reproduced using Gabor frames (also called Weyl-Heisenberg, or weighted Fourier, frames). *Gabor frames* are frames for the separable Hilbert space $L^2(\mathfrak{R})$ composed of elements of the form $\{e^{2\pi i m b \gamma} g(\gamma - na)\}_{n,m \in \mathbb{Z}}$ where a, b are real numbers such that $ab \leq 1$ and $g \in L^2(\mathfrak{R})$. If a, b and g satisfy certain additional assumptions, then the collection above will be a frame for $L^2(\mathfrak{R})$ (see [9]). As indicated in [1] and [10, Chapters 2 and 3], one can generalize this construction to allow irregular sequences $\{t_m\}$ to take the place of the regular lattice $\{mb\}$. The central ingredient needed to accomplish this is that $\{e^{2\pi i t_m \gamma}\}$ be a frame of exponentials for $L^2[-\Omega, \Omega]$, $\Omega > 0$. The Shannon theorem, the Yao-Thomas theorem and its dual, and the irregular sampling algorithm can all be reproduced using Gabor frames. The chief advantage of this appproach is that while the coefficients c_n in the irregular sampling algorithm above contain the slowly decaying factors $d_{\frac{1}{T}}(t_n - t_m)$, the coefficients in the Gabor frame construction can have more rapidly decaying factors $s(t_n - t_m)$ where s is a function of the type mentioned in (2) above with the additional assumption that $\hat{s} > 0$ on $(-\frac{1}{2T}, \frac{1}{2T})$. This allows for more rapid convergence of the coefficient expansions and hence better numerical performance.

3. Application

As an application of these ideas, we prove the following theorem of Gabardo [6] and Walker [18] in all except the extreme case. As a bonus, we obtain a sampling theorem for entire functions of exponential type Ω.

Theorem 3.1 (Gabardo-Walker). Let $f \in L^2(\mathfrak{R})$ with $\operatorname{supp} \hat{f} \subseteq [-\Omega, \Omega]$,

$\Omega > 0$. Assume $f(t_n) = 0\ \forall\ n \in \mathbb{Z}$ where $\{t_n\}$ is a sequence of real numbers satisfying

1) $t_n < t_{n+1}$;
2) $\lim_{n\to\infty} t_n = \infty$ and $\lim_{n\to-\infty} t_n = -\infty$;
3) $\sup_{n\in\mathbb{Z}} |t_{n+1} - t_n| = B < \infty$.

If $2\Omega B \leq 1$, then f vanishes identically.

Proof (G-W). If $f \neq 0$, then Bernstein's inequality [20, pp. 84, 86-87] gives

$$\|f'\|_2 < 2\pi\Omega \|f\|_2.$$

On the other hand, by Wirtinger's inequality [8, p. 184], [5, p. 47],

$$\int_{t_n}^{t_{n+1}} |f(t)|^2\,dt \leq \frac{|t_{n+1} - t_n|^2}{\pi^2} \int_{t_n}^{t_{n+1}} |f'(t)|^2\,dt$$
$$\leq \frac{B^2}{\pi^2} \int_{t_n}^{t_{n+1}} |f'(t)|^2\,dt,$$

since $f(t_n) = 0\ \forall\ n$. Hence

$$\int_{\mathbb{R}} |f(t)|^2\,dt = \sum_n \int_{t_n}^{t_{n+1}} |f(t)|^2\,dt$$
$$\leq \frac{B^2}{\pi^2} \sum_n \int_{t_n}^{t_{n+1}} |f'(t)|^2\,dt$$
$$= \frac{B^2}{\pi^2} \|f'\|_2^2.$$

Combining these two inequalities, we have

$$\int_{\mathbb{R}} |f(t)|^2\,dt \leq \frac{B^2}{\pi^2} \int_{\mathbb{R}} |f'(t)|^2\,dt$$
$$< \frac{B^2(2\pi\Omega)^2}{\pi^2} \int_{\mathbb{R}} |f(t)|^2\,dt.$$

If $2\Omega B \leq 1$, this last series of inequalities is impossible. Hence, $f = 0$. ∎

Alternate proof (For $2\Omega B < 1$ only). Let $\Omega_1 > \Omega$ such that $B < \frac{1}{2\Omega_1} < \frac{1}{2\Omega}$. We show that the sequence $\{t_n\}$ contains a subsequence $\{t_{n_k}\}$ that generates a frame of exponentials for $L^2[-\Omega_1, \Omega_1]$, and hence for $L^2[-\Omega, \Omega]$ as well.

To begin, pick $\epsilon > 0$ small enough so that $B < \frac{1}{2\Omega_1 + \epsilon}$. Pick symmetric intervals around $\frac{n}{2\Omega_1 + \epsilon}\ \forall\ n$ of length $\frac{1}{2\Omega_1 + \epsilon} - \delta > B$ with $\delta > 0$ small. Since

$$\sup_{n\in\mathbb{Z}} (t_{n+1} - t_n) = B < \frac{1}{2\Omega_1 + \epsilon} - \delta,$$

each interval centered around a multiple of $\frac{1}{2\Omega_1+\epsilon}$ must contain at least one t_n. Discard all elements except one of the sequence $\{t_n\}$ in each symmetric interval, and discard all elements that fall between the intervals. Label the element remaining in the interval centered at $\frac{k}{2\Omega_1+\epsilon}$ by t_{n_k}. Then the subsequence $\{t_{n_k}\}$ of $\{t_n\}$ is a uniformly dense sequence with uniform density $2\Omega_1+\epsilon$—i.e., $\{t_{n_k}\}$ satisfies $|t_{n_k}-t_{n_m}|\geq\delta>0$ for $k\neq m$ and

$$\left|t_{n_k}-\frac{k}{2\Omega_1+\epsilon}\right|\leq L=\frac{1}{2}\left[\frac{1}{2\Omega_1+\epsilon}-\delta\right].$$

Hence, by the theorem of Duffin and Schaeffer (Theorem 2.2), the collection of exponentials $\{t_{n_k}\}$ is a frame for $L^2[-\Omega_1,\Omega_1]$. So, by applying Algorithm 2.7, we obtain a sampling expansion for entire functions of exponential type Ω employing the sample values $\{f(t_{n_k})\}$. ∎

Counterexample 3.2. We show by example that if we let $2\Omega B=1$, then there exist sequences that do *not* contain a subsequence which generates a frame of exponentials. Consider the sequence defined by $t_n=\frac{n}{2\Omega}$ for $n\leq 0$ and

$$t_n=\begin{cases}\frac{n+1}{4\Omega}+\delta\sum_{1}^{\frac{n-1}{2}}\frac{1}{k}, & \text{for } n>0 \text{ odd}\\ \frac{n}{4\Omega}+\delta\sum_{1}^{\frac{n}{2}}\frac{1}{k}, & \text{for } n>0 \text{ even}\end{cases}$$

for $\delta>0$. Consider the following observations:

1) Observe that the positively indexed terms are clustered together in pairs — an oddly indexed term and its following evenly indexed term. The two elements of each pair get infinitely close together as $n\to\infty$ as they differ by $\frac{2\delta}{n}$, where n is even. Hence if this sequence does contain a uniformly dense subsequence, a subsequence which, by definition, is also uniformly discrete, then only a finite number of terms of this subsequence can be taken from both elements of these pairs. So for $n>0$ large enough, then at most one element can come from each of these pairs in any uniformly dense subsequence.
2) Note that if a subsequence is uniformly dense, the subsequence can grow no faster or slower than $\frac{n}{\Delta}$ since, from the defintion of a uniformly dense sequence,

$$\frac{n}{\Delta}-L\leq|t_{n_k}|\leq\frac{n}{\Delta}+L$$

for some $L>0$.

We claim that we can not select a uniformly dense subsequence from $\{t_n\}$, as we can not find a suitable density for this subsequence that satisfies the growth condition (2). This is because any subsequence that obeys observation (1) will grow faster than the sequence $\{\frac{n}{2\Omega+\epsilon}\}$ for $\epsilon \geq 0$ by virtue of the $\frac{1}{2\Omega}$ factor added to the terms and by the unboundedness of the sequence $\delta, \frac{\delta}{2}, \frac{\delta}{3}, \ldots$. *However, any uniformly dense subsequence will grow slower* than $\frac{n}{2\Omega-\epsilon}$, for $\epsilon > 0$ since $t_{n+1} - t_n = B = \frac{1}{2\Omega}$ for n even. ∎

Remark 3.3.

1) In the alternate proof for $2\Omega B < 1$, we selected a subsequence $\{t_{n_k}\}$ of $\{t_n\}$ such that $\{t_{n_k}\}$ generated a frame of exponentials for $L^2[-\Omega_1, \Omega_1]$. By applying the algorithm, we obtain formulas enabling us to reconstruct the function f from its sample values at the points $\{t_{n_k}\}$. (The *remaining points of the sequence* $\{t_n\}$ not in the subsequence $\{t_{n_k}\}$ can be discarded, or, if they can be partitioned into a finite number of uniformly discrete subsequences, they can be incorporated into the frame of exponentials generated by $\{t_{n_k}\}$.) So we have obtained a representation theorem corresponding to the uniqueness theorem in the case $2\Omega B < 1$.
2) Note also that the work of Jaffard and Duffin and Schaeffer allow us to produce frames of exponentials, and hence uniqueness and representation theorems, for sequences which do not satisfy the restriction $2\Omega B < 1$. In particular, since in the definition of uniformly dense sequences L can be any positive number, we can generate uniformly dense sequences with large gaps—i.e., for which the distance between certain consecutive points is larger than $\frac{1}{2\Omega}$. Hence we can extend the Gabardo-Walker Theorem to irregular sampling lattices that do not satisfy all of the restrictions of the hypotheses of that theorem.
3) It can be shown [10, Corollary 4.4.4] that the lower frame bound for the frame of exponentials in $L^2[-\Omega_1, \Omega_1]$ generated in the alternate proof is $\frac{(1-2\Omega_1 B)^2}{B}$. (See also Remark 2.4 (4).)
4) For another approach to irregular sampling, see the paper by Karlheinz Gröchenig [7] in this volume. The method described there, and in the joint papers with Hans Feichtinger listed in the references of that paper, *applies in a wide variety of function spaces on various groups*. This is to be contrasted with the method described here which applies only in $L^2(\mathbb{R}^n)$, $n = 1$.

4. Notation

The Fourier transform $\hat{f}$ of $f \in L^1(\mathfrak{R})$ is defined as

$$\hat{f}(\gamma) = \int f(t)e^{-2\pi i t\gamma}\, dt,$$

where "$\int$" designates integration over the real line $\mathfrak{R}$; $\hat{f}$ is defined on $\hat{\mathfrak{R}}$ $(= \mathfrak{R})$ and $f^\vee$ is the inverse Fourier transform of f. The Fourier transform is defined on $L^2(\mathfrak{R})$, and, for fixed $\Omega > 0$,

$$PW_\Omega \equiv \{f \in L^2(\mathfrak{R}) : \operatorname{supp} \hat{f} \subseteq [-\Omega, \Omega]\},$$

where $\operatorname{supp} \hat{f}$ is the support of $\hat{f}$. Functions that are in the space PW_Ω are called *Ω-bandlimited*.

Besides the $L^p(\mathfrak{R})$–spaces , we deal with the space $C^\infty(\mathfrak{R})$ of infinitely differentiable functions and its subspace $C_c^\infty(\mathfrak{R})$ whose elements have compact support.

"$\sum$" designates summation over the whole discrete group in question, e.g., over $\mathcal{Z}$ where $\mathcal{Z}$ is the group of integers. The function $\mathbf{1}_S$ is the characteristic function of $S \subseteq \mathfrak{R}$, $|S|$ is the Lebesgue measure of S, and $\mathbf{1}_{[\Omega]} \equiv \mathbf{1}_{[-\Omega,\Omega]}$. The function δ_{mn} is defined as 0 if $m \neq n$ and as 1 if $m = n$. The dilation f_λ of the function f is $f_\lambda(t) = \lambda f(\lambda t)$. Finally, the exponential function E_a is $E_a(t) = e^{-2\pi i a t}$.

5. Bibliography

[1] J. Benedetto and W. Heller. Irregular sampling and the theory of frames, I. *Note Mat.*, 1991.

[2] A. Beurling and P. Malliavin. On the closure of characters and the zeros of entire functions. *Acta Math.*, 118:79–93, 1967.

[3] I. Daubechies. The wavelet transform, time–frequency localization, and signal analysis. *IEEE Trans. Inform. Theory*, 36:961–1005, 1990.

[4] R. Duffin and A. Schaeffer. A class of nonharmonic Fourier series. *Trans. Am. Math. Soc.*, 72:341–366, 1952.

[5] H. Dym and H. P. Mckean. *Fourier series and integrals.* Academic Press, New York, 1972.

[6] J.-P. Gabardo. *Spectral gaps and uniqueness problems in Fourier analysis.* PhD thesis, University of Maryland, College Park, MD, 1987.

[7] Karlheinz Gröchenig. Sharp results on random sampling of bandlimited functions. In J.S. Byrnes, Jennifer L. Byrnes, Karl Berry, and Kathryn A.

Hargreaves, editors, *Probabilistic and Stochastic Methods in Analysis, with Applications: Proceedings of the NATO Advanced Study Institute*, NATO ASI series C: Mathematical and physical sciences, Dordrecht, Boston, London, 1992. Kluwer Academic Publishers Group. Held at Il Ciocco Resort, Tuscany, Italy.

[8] G. H. Hardy, J. E. Littlewood, and G. Pólya. *Inequalities*. Cambridge University Press, 1952.

[9] C. Heil and D. Walnut. Continuous and discrete wavelet transforms. *SIAM Review*, 31:628–666, 1989.

[10] W. Heller. *Frames of exponentials and applications*. PhD thesis, University of Maryland, College Park, MD, 1991.

[11] S. Jaffard. A density criterion for frames of complex exponentials. *Mich. J. of Math.*, 38:339–348, 1991.

[12] M. Kadec. The exact value of the Paley-Wiener constant. *Sov. Math. Dokl.*, 5:559–561, 1964.

[13] H. Landau. Necessary density conditions for sampling and interpolation of certain entire functions. *Acta Math.*, 117:37–52, 1967.

[14] B. Ja. Levin. *Distribution of zeros of entire functions*, volume 5 of *Trans. of Math. Monographs*. Am. Math. Soc., Providence RI, rev. edition, 1980.

[15] N. Levinson. *Gap and density theorems*, volume 26 of *Am. Math. Soc. Colloq. Publ.* Am. Math. Soc., Providence RI, 1940.

[16] R. Paley and N. Wiener. *Fourier transforms in the complex domain*, volume 19 of *Am. Math. Soc. Colloq. Publ.* Am. Math. Soc., Providence, RI, 1934.

[17] R. Redheffer. Completeness of sets of complex exponentials. *Advances in Math.*, 24:1–62, 1977.

[18] W. Walker. The separation of zeros for entire functions of exponential type. *J. of Math. Analysis and Appl.*, 122:257–259, 1987.

[19] K. Yao and J. Thomas. On some stability and interpolatory properties of nonuniform sampling expansions. *IEEE Trans. Circuit Theory*, CT-14:404–408, 1967.

[20] R. Young. *An introduction to nonharmonic Fourier series*. Academic Press, New York, 1980.

Stationary frames and spectral estimation†

John J. Benedetto
Department of Mathematics
University of Maryland
College Park, Maryland 20742 USA
jjb@math.umd.edu
Also at Prometheus Inc.

Dedicated to Professor George Maltese on the occasion of his sixtieth birthday.

Abstract Kolmogorov's fundamental paper on stationary sequences (1941) played a major role in important problems dealing with stochastic processes. His results are reviewed here in the context of their relations with three topics in harmonic analysis. The topics are weighted Fourier transform norm inequalities, stationary frames, and Wiener-Plancherel formulas.

Kolmogorov's prediction theory lead to weighted Hilbert transform inequalities which, in turn, are characterized by A_p-weights. These weights identify a special collection of weighted Fourier transform inequalities, including results of Hardy, Littlewood, and Paley. The extension to more general Fourier transform inequalities leads to restriction theorems and uncertainty principle inequalities.

Stationary frames establish a conceptual distinction between wavelets and coherent states. They are developed from Kolmogorov's spectral characterization of minimal sequences.

Wiener-Plancherel formulas are used in the spectral estimation associated with the mathematical setting of both Kolmogorov's and Wiener's prediction theories.

† Supported in part by NSF Contract DMS-9002420 and the MITRE Corporation.

I would like to thank Professor Pesi Masani for providing me with a handwritten translation of Kolmogorov's paper [39] (given to him by Professor Kallianpur), as well as for his fascinating, wise comments on this topic. Even more, he has been an inspiration through the years with his first-rate contribution to mathematics, his high-minded intellectual independence, and his profound and thoroughly honest sense of scholarship.

I would also like to thank Professor Christian Houdré for directing me to [37], and for many insightful observations on this material.

J. S. Byrnes et al. (eds.), Probabilistic and Stochastic Methods in Analysis, with Applications, 117–161.
© 1992 *Kluwer Academic Publishers. Printed in the Netherlands.*

1. Introduction

Fifty years ago, in 1941, Kolmogorov published his monumental paper, *Stationary sequences in Hilbert space* [39]. As Cramér pointed out [17, p. 532],

> "The fundamental importance of this work by Kolmogorov lies in the fact that he showed how the abstract theory of Hilbert space (as well, of course, as of other types of spaces) could be applied to the theory of random variables and stochastic processes."

Moreover, in [39] and its sequel *Interpolation and extrapolation of stationary random sequences* (1941), Kolmogorov introduced the basic concepts of deterministic and purely nondeterministic stationary sequences, and posed and solved the primary problems in

A: Prediction theory
B: Spectral theory of minimal stationary sequences.

The setting for these two areas is based on the

C: Wiener-Khinchin theorem.

From the point of view of stationarity, the wonderful and influential ideas formulated in [39] are now standard fare in probability theory, and to some extent they have been played-out, especially in the (multivariate) discrete semi-infinite prediction theoretic case, e.g., [43], [47], [53, Volume III, including the updates by Masani (pp. 276–306), Salehi (pp. 307–338), Muhly (pp. 339–370), and Kallianpur (pp. 402–424)], cf. [20]. There is still a great deal to be done in the case of stationary fields, e.g., [15], [37], and Section 4.2.

Our goal in Sections 3–5 is to describe recent results from three topics of modern harmonic analysis which are in the intellectual lineage of the above items A, B, and C, respectively. A will lead to the topic of weighted Fourier transform norm inequalities, B to a topic in wavelet and coherent-states theory, and C to multidimensional Wiener-Plancherel theorems.

Section 2 is devoted to a commentary on parts of [39], and we have resisted the temptation to record much subsequent related material on stochastic processes and prediction theory. We have lectured on the relation between

prediction theory and weighted Fourier transform norm inequalities since the early 1980's; and most of the material in Section 3 is taken from those lectures. Section 4 records some of the preliminary ideas being used in our current work on stationary frames. Section 5 rounds out our view of the type of harmonic analysis affected by [39]; the format in Section 5 is just to state our recent published results [6].

Besides the usual notation in analysis as found in the books by Hörmander [35], Schwartz [49], and Stein and Weiss [50], we shall use the conventions and notation described at the end of the paper.

2. Kolmogorov and stationary sequences

2.1. The Wiener-Khinchin theorem

Definition 2.1. A sequence $\{x(n) : n \in \mathcal{Z}\}$ in a complex Hilbert space H is *stationary* if the inner product

$$R(n) = R_{xx}(n) = \langle x(n+k), x(k)\rangle, \qquad n \in \mathcal{Z},$$

is independent of k. R_{xx} is the *autocorrelation* of x. Two stationary sequences $\{x(n)\}$ and $\{y(n)\}$ are *stationarily correlated* if the inner product,

$$R_{xy}(n) = \langle x(n+k), y(k)\rangle, \qquad n \in \mathcal{Z},$$

is independent of k. Clearly,

$$\forall n \in \mathcal{Z}, \qquad R_{xy}(n) = \bar{R}_{xy}(-n).$$

Theorem 2.2 (Wiener-Khinchin).

1) Given a stationary sequence $\{x(n)\} \subseteq H$, there is $\mu \in M_+(\mathcal{T})$ for which $R_{xx} = \mu^\vee$. μ is the *power spectrum* of x, cf. Definition 5.9.
2) Given $\mu \in M_+(\mathcal{T})$, there is a stationary sequence $\{x(n)\}$ for which $R_{xx} = \mu^\vee$.

Remark 2.3.

1) Item 1 of Theorem 2.2 is immediate since R_{xx} is positive definite, thereby allowing us to apply Herglotz's theorem.
2) For Item 2 of Theorem 2.2, we first note that $\mu^\vee = R$ is positive definite. For the case of stationary stochastic processes x, e.g., [45], the problem is to construct x for which $R_{xx} = R$. This was done by Khinchin (1934) on $\mathcal{R}$, by Wold (1938) on $\mathcal{Z}$, and in a more general setting on both

$\mathfrak{R}$ and $\mathfrak{Z}$ by Cramér (1940) [16, p. 224]; the method is standard, e.g., [20, pp. 62–63 and pp. 72–73], [46, pp. 221–222], and the constructed process is Gaussian. In fact, in this Gaussian case there is a natural bijection between $M_+(\mathfrak{T})$ (or $M_{b+}(\hat{\mathfrak{R}})$) and stationary Gaussian processes subjected to a mild technical constraint. The argument in [20] uses the Kolmogorov extension theorem found in his classical book (1933). This should be compared with Kolmogorov's abstract "Hermitian extension" method [39, Lemma 1 and Lemma 2], which he used to prove Item 2 of Theorem 2.2 and its generalization for stationarily correlated sequences, viz., [39, Theorems 4, 5, and 6]. A footnote in [16, p. 221] as well as a reference in [39] indicate that both Cramér and Kolmogorov were aware of the other's similar results, which were proved by different methods and resulted in more generality in [39].

3) Wiener's contribution (1930) to the Wiener-Khinchin theorem was formulated in nonprobabilistic terms, cf. [27]; and lead to the constructive Wiener-Wintner theorem (1939) on $\mathfrak{R}$. Bass and Bertrandias made significant contributions to this result; and recently my student, R. Kerby, and I have proven the Wiener-Wintner theorem in $\mathfrak{R}^d$. One basic construction is given in [2] and two others, which are quite ingenious, are contained in [38].

Our result is

Theorem 2.4 (Wiener-Wintner). Given $\mu \in M_{b+}(\mathfrak{R}^d)$, there is a constructible function $x \in L_{loc}^{\infty}(\mathfrak{R}^d)$ such that, for all t,

$$\exists R(t) = \lim_{T \to \infty} \frac{1}{|B(0,T)|} \int_{B(0,T)} x(t+u)\bar{x}(u)du \tag{2.1}$$

and

$$R(t) = \mu^{\vee}(t).$$

The ordinary point function R in (2.1) and its probabilistic counterpart R_x, defined by a stationary stochastic process $x(t,\alpha)$, are essentially equivalent in correlation ergodic processes, e.g., [45]; the role of Theorem 2.4 in spectral estimation is discussed in [2], [5, Section 5], and Section 5.4 of this paper. Given $x \in L_{loc}^{1}(\mathfrak{R}^d)$ and R defined by (2.1); the converse of Theorem 2.4 is immediate by Bochner's theorem.

2.2. The fundamental isometry and structure theorems

In his work of 1941, as well as in an earlier *Comptes Rendus* note (1939), Kolmogorov solved the problem of predicting the future from the whole past, cf. Item 1 of Remark 2.10. The following elementary observation plays a role

in this solution by transferring a large class of statistical prediction problems into problems of trigonometric approximation in weighted Lebesgue spaces.

Theorem 2.5. Given a stationary sequence $\{x(n)\} \subseteq H$, with power spectrum μ. Let $H(x) = \overline{sp}\{x(n)\}$. The mapping,

$$Z : L^2_\mu(\mathfrak{T}) \to H(x),$$

defined linearly on $sp\{e^{2\pi i n\gamma}\}$ by $Z(e^{2\pi i n\gamma}) = x(n)$, extends to a linear isometric isomorphism, cf. [39, Lemma 4 and its proof in terms of the spectral representation of the shift operator U].

Proof. Since μ is a bounded Radon measure we have that $e^{2\pi i n\gamma} \in L^2_\mu(\mathfrak{T})$. For finite sums $p(\gamma) = \sum c_n e^{2\pi i n\gamma} \in L^2_\mu(\mathfrak{T})$ and $x = \sum c_n x(n) \in H(x)$, we compute

$$\begin{aligned}
\|p\|_{2,\mu} &= \left\| \sum c_n e^{2\pi i n\gamma} \right\|^2_{2,\mu} = \sum_{m,n} c_m \bar{c}_n \mu^\vee(m-n) \\
&= \sum_{m,n} c_m \bar{c}_n R(m-n) = \sum_{m,n} c_m \bar{c}_n \langle x(m-n+k), x(k) \rangle \\
&= \sum_{m,n} c_m \bar{c}_n \langle x(m), x(n) \rangle = \left\langle \sum c_n x(n), \sum c_n x(n) \right\rangle \\
&= \left\| \sum c_n x(n) \right\|^2_H = \|x\|^2_H,
\end{aligned}$$

and so Z is an isometry on $sp\{e^{2\pi i n\gamma}\}$.

Next, we see that $\overline{sp}\{e^{2\pi i n\gamma}\} = L^2_\mu(\mathfrak{T})$. In fact, for a given $\epsilon > 0$ and $f \in L^2_\mu(\mathfrak{T})$, there is a continuous function g on $\mathfrak{T}$ and a trigonometric polynomial p such that

$$\|f - g\|_{2,\mu} < \epsilon/2 \quad \text{and} \quad \|g - p\|_\infty < \frac{\epsilon}{2\|\mu\|_1^{1/2}}.$$

Consequently,

$$\begin{aligned}
\|f - p\|_{2,\mu} &< \frac{\epsilon}{2} + \|g - p\|_{2,\mu} \\
&< \frac{\epsilon}{2} + \left(\left(\frac{\epsilon}{2^2 \|\mu\|_1} \right) \int_{\mathfrak{T}} d|\mu|(\gamma) \right)^{1/2} = \epsilon.
\end{aligned}$$

Thus, by general considerations, Z is a linear isometry from $L^2_\mu(\mathfrak{T})$ onto a dense subspace of $H(x)$. In particular, Z is injective. Finally, taking $y \in H(x)$ and using the Cauchy sequences, $\{y_n\} \subseteq H(x)$ and $\{Z^{-1}y_n\} \subseteq L^2_\mu(\mathfrak{T})$, where $\lim y_n = y$ and $\lim Z^{-1}y_n = f$, it is easy to check that $Zf = y$; and so Z is a surjection onto $H(x)$. ∎

The verification in the proof of Theorem 2.5, that $\overline{\text{sp}}\{e^{2\pi i n\gamma}\} = L^2_\mu(\mathfrak{T})$, also works for stationary functions,

$$x : \mathfrak{R}^d \to H, \tag{2.2}$$

i.e., functions (2.2) for which $\langle x(t+s), x(s)\rangle$ is independent of s. In fact, we take $g \in C_c(\mathfrak{R}^d)$, with supp g contained in a cube Q, and choose $p\mathbf{1}_Q$ instead of p. Another elementary proof that

$$\overline{\text{sp}}\{e^{2\pi i t\cdot\gamma} : t \in \mathfrak{R}^d\} = L^2_\mu(\hat{\mathfrak{R}}^d),$$

where the power spectrum $\mu_x = \mu$ is an element of $M_{b+}(\hat{\mathfrak{R}}^d)$, utilizes the Hahn-Banach theorem instead of the Weierstrass approximation theorem. In this case, the argument is completed by the uniqueness theorem for the Fourier transform.

The structure of bounded measures on $\hat{\mathfrak{R}}$ (or $\mathfrak{T}$) is given by

Theorem 2.6. Each $\mu \in M_b(\hat{\mathfrak{R}})$ can be written in the form

$$\mu = f_{ac} + \mu_s = f_{ac} + \mu_{sc} + \mu_d,$$

where $f_{ac} \in L^1(\hat{\mathfrak{R}})$, μ_s is the singular part of μ, $\mu_{sc} \in M_b(\hat{\mathfrak{R}})$ is designated the continuous singular part of μ, and $\mu_d = \sum d_\gamma \delta_\gamma \in M_b(\hat{\mathfrak{R}})$, where $\sum |d_\gamma| < \infty$. Further,

$$\mu = F',$$

the distributional derivative of a function of bounded variation (BV), and

$$F = F_{ac} + F_{sc} + \sum d_\gamma H_\gamma,$$

where $F_{ac} \in$ BV is locally absolutely continuous, $F_{sc} \in$ BV is a continuous function whose ordinary derivative vanishes a.e., and H_γ is the Heaviside function with jump at γ. Finally,

$$F'_{ac} = f_{ac}, \qquad F'_{sc} = \mu_{sc}, \qquad \left(\sum d_\gamma H_\gamma\right)' = \sum d_\gamma \delta_\gamma,$$

under distributional differentiation.

2.3. The Wold decomposition and deterministic sequences

Definition 2.7.

1) Given a nonzero stationary sequence $\{x(n)\} \subseteq H$. Besides the notation

$$H(x) = \overline{\text{sp}}\{x(n)\} = H(x, \infty),$$

defined in Theorem 2.5 and which does not depend on stationarity, we now define the closed subspaces,

$$\forall n, \qquad H(x,n) = \overline{sp}\{x(k) : k \leqslant n\}$$

and

$$H(x,-\infty) = \cap H(x,n).$$

Clearly,

$$\forall n, \qquad H(x,-\infty) \subseteq H(x,n) \subseteq H(x,\infty).$$

- $\{x(n)\}$ is *deterministic* if

$$H(x,-\infty) = H(x,\infty);$$

- $\{x(n)\}$ is *nondeterministic* if

$$H(x,-\infty) \neq H(x,\infty);$$

- $\{x(n)\}$ is *purely nondeterministic* if

$$H(x,-\infty) = \{0\} \qquad (\neq H(x,\infty)).$$

2) In 1941, Kolmogorov was aware of the Wold decomposition (1938), whereas Wiener, in his independent development of prediction theory was not, e.g., [44, p. 193]. Because of the role of Wold's result in [39], we state the *Wold decomposition*, which, notwithstanding its origins, is a theorem about operators on a Hilbert space and nondeterministic sequences from Kolmogorov's point of view.

Let $\{x(n)\}$ be a nondeterministic stationary sequence with shift operator $U = U_x$ on $H(x,\infty)$ defined by $U(x(n)) = x(n+1)$ on $\{x(n)\}$. Then there are stationary sequences $\{u(n)\}$ and $\{v(n)\}$, and a unique decomposition,

$$\forall n, \qquad x(n) = u(n) + v(n),$$

such that

a) $\{u(n)\}$ is purely nondeterministic and $\{v(n)\}$ is deterministic,
b) $\forall n$, $H(u,n) \cup H(v,n) \subseteq H(x,n)$,
c) $H(u,\infty) \perp H(v,\infty)$,
d) $\forall n$, $v(n)$ is the projection of $\{x(n)\}$ onto $H(x,-\infty)$.

3) Given the hypotheses of the Wold decomposition in Item 2. Since $\{x(n)\}$ is nondeterministic, $H(x,0) \neq H(x,1)$. There is an essentially unique unit vector $z(1) \in H(x,1)$ such that $z(1) \perp H(x,0)$ and $\overline{sp}\{z(1), H(x,0)\} = H(x,1)$. Noting that U extends to a unitary operator on $H(x,\infty)$ and that U^{-1} is the adjoint operator, we define

$$\forall k \in \mathcal{Z}, \qquad z(k) = U^{k-1}(z(1)).$$

By U's definition it is easy to check that $\{z(k)\}$ is orthonormal and that

$$\forall k \in \mathcal{Z}, \qquad z(k) \perp H(x, k-1). \tag{2.3}$$

Writing the Fourier expansion of $x(1)$ with respect to $\{z(k)\}$ we compute

$$x(1) = \sum_{k=0}^{\infty} c_k z(1-k) + v(1), \tag{2.4}$$

noting that $c_k \equiv \langle x(1), z(1-k)\rangle = 0$ for $k < 0$ by (2.3). We have $\{c_k\} \in l^2(\mathcal{Z})$ and can verify that $v(1) \in H(x,-\infty)$. Applying the operator U^{n-1} to (2.4) we have

$$\forall n, \qquad x(n) = \sum_{k=-\infty}^{n} c_{n-k} z(k) + v(n),$$

and, in particular, the purely nondeterministic sequence $\{u(n)\}$ is a particular *moving average, viz.*,

$$\forall n, \qquad u(n) = \sum_{k=-\infty}^{n} c_{n-k} z(k). \tag{2.5}$$

The Wold decomposition is equivalent to the power spectral decomposition of μ_x into its absolutely continuous and singular parts. For example, if $\log f_{ac} \in L^1(\mathcal{T})$, where $\mu_x = f_{ac} + \mu_s$, cf. Theorem 2.6, then $\{u(n)\}$ corresponds to f_{ac} and $\{v(n)\}$ corresponds to μ_s, cf. Theorem 2.8. If $\log f_{ac} \notin L^1(\mathcal{T})$, where $\mu_x = f_{ac} + \mu_s$, then $\{v(n)\}$ corresponds to all of μ_x. This material is well-traveled and there are many points of view, e.g., [20, Chapter 4], [27, pp. 259–261], [42, pp. 62ff], [46, pp. 755-759]. We shall exposit Kolmogorov's original formulation from [39, Sections 8–10], which he points out is "more unfamiliar (than Sections 1–7) and seems to be really new."

2.4. Spectral characterizations of deterministic sequences

Theorem 2.8. [39, Theorem 22] Given a stationary sequence $\{x(n)\} \subseteq H$ with power spectrum μ. $\{x(n)\}$ is purely nondeterministic if and only if $\mu = f_{ac} \in L^1(\mathfrak{T})$ and

$$\log f_{ac} \in L^1(\mathfrak{T}).$$

(In particular, $\mu > 0$ a.e. and supp $\mu = \mathfrak{T}$.)

One of the features of such a result is that, when we know the autocorrelation of a process (which is often experimentally available), we can characterize the *prediction* theoretic properties of the underlying process. There are analogous results for related *filter* problems, e.g., [3, Theorem IV.2.1] and the thesis [55] of my student, G. Yang.

Theorem 2.9. [39, Theorem 23] Given a stationary sequence $\{x(n)\} \subseteq H$ with power spectrum $\mu = f_{ac} + \mu_s$.

1) If $f_{ac} = 0$ on a set of positive Lebesgue measure then $\{x(n)\}$ is deterministic.
2) If $f_{ac} > 0$ a.e. and $\log f_{ac} \notin L^1(\mathfrak{T})$ then $\{x(n)\}$ is deterministic.
3) If $f_{ac} > 0$ a.e. and $\log f_{ac} \in L^1(\mathfrak{T})$ then $\{x(n)\}$ is nondeterministic, cf. Item 2.

Remark 2.10.

1) Using the definition of a deterministic stationary sequence as well as the isometric isomorphism in Theorem 2.5, we can rewrite Theorem 2.9 in terms of trigonometric approximation as follows:

   Given $\mu = f_{ac} + \mu_s \in M_+(\mathfrak{T})$.

   $$\overline{\text{sp}}\{e^{2\pi i k\gamma} : k \leqslant 0\} = L^2_\mu(\mathfrak{T}) \tag{2.6}$$

   if and only if

   $$\log f_{ac} \notin L^1(\mathfrak{T}). \tag{2.7}$$

   Kolmogorov's proof was a consequence of the Szegö alternative, and there is an elementary presentation of this proof in [1, pp. 261–263]. The completeness statement (2.6) is the analytic formulation of the prediction theoretic statement, concerning prediction of the future from the whole past, which we made prior to Theorem 2.5. The result can first be proved for $\mu = f_{ac}$, and the "reduction" from arbitrary μ to f_{ac} uses the F. and M. Riesz Theorem.

The analogous result for $\mu \in M_{b+}(\hat{\mathfrak{R}})$ and $L^2_\mu(\hat{\mathfrak{R}})$ is due to Krein (1945). In this case, "$k \leqslant 0$" is replaced by "$t \leqslant 0$" in (2.6), "$\mathfrak{T}$" is replaced by "$\hat{\mathfrak{R}}$", and (2.7) is replaced by the condition,

$$\int \frac{|\log f_{ac}(\gamma)|}{1+\gamma^2} d\gamma = \infty.$$

2) The relation of Theorem 2.9 (as written in Item 1) to Wiener's Tauberian theorem, Beurling's spectral analysis, the Denjoy-Carleman theorem on quasi-analytic classes, and Harry Pollard's solution (1955) of the Bernstein approximation problem is discussed in [4]. Pollard's basic lemma on entire functions of exponential type was used by (his student) de Branges to prove uniqueness criteria in the spirit of work by the Rieszes, Levinson, and Beurling-Malliavin [4]. A deep, novel, and applicable distributional analysis of this latter body of work is due to my student, J.-P. Gabardo [25, 22, 24].

2.5. Spectral properties of minimal sequences

The final notion, which we wish to discuss and that was introduced by Kolmogorov in [39], is the following:

Definition 2.11.

1) Given a sequence $\{x(n)\} \subseteq H$ and define the closed subspace,

$$H(x, n) \equiv \overline{sp}\{x(k) : k \neq n\}.$$

$\{x(n)\}$ is *minimal* if

$$\forall n, \qquad x(n) \notin H(x, n). \tag{2.8}$$

In the case of stochastic processes, minimal sequences are "those for which the random function at any time ($t = n$) is outside the closed subspace spanned by the past and future functions of the process" [43, pp. 141–142].

2) If $\{x(n)\}$ is a stationary sequence then either $H(x, n) = H(x, \infty)$ for all n or $H(x, n) \not\subseteq H(x, \infty)$ for all n. For example, suppose $H(x, n) = H(x, \infty)$ and $m \neq n$. If $H(x, m) \neq H(x, \infty)$ then

$$\forall k \neq 0, \qquad \langle x(m), x(m+k) \rangle = 0,$$

so that by stationarity,

$$\forall k \neq 0, \qquad \langle x(n), x(n+k) \rangle = 0. \tag{2.9}$$

By hypothesis, (2.9) implies that $x(n) = 0$, a contradiction. Thus, for stationary sequences, the criterion (2.8) for minimality can be replaced by the condition,

$$H(x, \hat{0}) \neq H(x, \infty). \tag{2.10}$$

3) Minimality not only plays a natural role in prediction theory, but is an essential aspect of Köthe's theorem (1936) characterizing Riesz bases. Köthe's theorem and its role in irregular sampling constitute recent results with my student, W. Heller [11].

Theorem 2.12. [39, Theorem 24] Given a stationary sequence $\{x(n)\} \subseteq H$, with power spectrum $\mu = f_{ac} + \mu_s$. $\{x(n)\}$ is minimal if and only if

$$f_{ac}^{-1} \in L^1(\mathfrak{T}),$$

cf. the multivariate version $\mathbb{Z} \to H^d$ in [43, Theorem 2.8], [47].

Theorem 2.12 has had important modifications (even in the case $\mathbb{Z} \to H$) due to Masani [43] and Rozanov [47], e.g., Theorem 2.17; and these have stimulated and affected our observations in Section 4 concerning topic B.

Definition 2.13.

1) Given a separable complex Hilbert space H. Two sequences $\{x(n)\}$, $\{y(n)\} \subseteq H$ are *biorthonormal* if

$$\forall m, n, \qquad \langle x(m), y(n) \rangle = \delta_{m,n}.$$

2) Given a sequence $\{x(n)\} \subseteq H$. An Hahn-Banach argument shows that *there is a sequence* $\{y(n)\} \subseteq H$ *so that* $\{x(n)\}$, $\{y(n)\}$ *are biorthonormal if and only if* $\{x(n)\}$ *is minimal.* Furthermore, $\{y(n)\}$ *is uniquely determined if and only if* $\{x(n)\}$ *is not only minimal in* H *but also* $\overline{\text{sp}}\{x(n)\} = H$.

Using the fact stated in Item 2 of Definition 2.1 we can make the following definition.

Definition 2.14.

1) Given a minimal, complete sequence $\{x(n)\} \subseteq H$, and let $\{x(n)\}$, $\{y(n)\}$ be biorthonormal. $\{x(n)\}$ is a ***Bessel sequence*** if the ***Bessel map,***

$$\begin{aligned} B &: H \to l^2(\mathbb{Z}) \\ &x \mapsto \{\langle x, y(n) \rangle\}, \end{aligned} \tag{2.11}$$

is a well-defined linear map. $\{x(n)\}$ is a *Hilbert sequence* if

$$\forall \{c(n)\} \in l^2(\mathbb{Z}), \qquad \exists x_c \in H \text{ such that}$$
$$\forall n, \qquad c(n) = \langle x_c, y(n)\rangle.$$

Clearly, a Bessel sequence is a Hilbert sequence if and only if the Bessel map B is surjective.

2) If $\{x(n)\}$ is a Bessel sequence then, by the uniform boundedness principle, there is a constant $B > 0$ such that

$$\forall x \in H, \qquad \sum |\langle x, y(n)\rangle|^2 \leq B\|x\|^2. \tag{2.12}$$

Thus, the map B in (2.11) is not only well-defined and linear but also continuous.

If $\{x(n)\} \subseteq H$ is a minimal, complete sequence, and $\{x(n)\}, \{y(n)\} \subseteq H$ are biorthonormal then it is not necessarily true that $\overline{sp}\{y(n)\} = H$; an old example of Kaczmarz and Steinhaus (1935) provides a counterexample, e.g., [34, pp. 19–20]. On the other hand, Masani [43] and Rozanov [47] have used Theorem 2.5 to observe the following lemma.

Lemma 2.15. Given a stationary, minimal, complete sequence $\{x(n)\} \subseteq H$, and let $\{x(n)\}, \{y(n)\}$ be biorthonormal. Then $\overline{sp}\{y(n)\} = H$.

Theorem 2.16. Given a stationary, minimal, complete sequence $\{x(n)\} \subseteq H$, and let $\{x(n)\}, \{y(n)\}$ be biorthonormal. Assume $\{x(n)\}$ is both a Bessel sequence and a Hilbert sequence. Then there are constants $A, B > 0$ such that

$$\forall x \in H, \qquad A\|x\|^2 \leq \sum |\langle x, y(n)\rangle|^2 \leq B\|x\|^2. \tag{2.13}$$

Conversely, if (2.13) holds, then $\{x(n)\}$ is both a Bessel sequence and a Hilbert sequence.

Proof.

1) The second inequality of (2.13) is clear since $\{x(n)\}$ is a Bessel sequence, e.g., (2.12).

   To verify the first inequality of (2.13), first note that the Bessel map B is injective by Lemma 2.15. Since $\{x(n)\}$ is a Hilbert sequence, the Bessel map B is surjective, so that, by the open mapping theorem, $B^{-1} : l^2(\mathbb{Z}) \to H$, is continuous. This yields the first inequality.

2) For the converse, the second inequality of (2.13) implies $\{x(n)\}$ is a Bessel sequence.

Since $\{x(n)\}$ is a Bessel sequence, the Bessel map B has a well-defined continuous adjoint, $B^* : l^2(\mathcal{Z}) \to H$. Clearly,

$$\langle y, B^*c\rangle = \langle By, c\rangle = \sum \langle y, y(n)\rangle \bar{c}(n)$$
$$= \langle y, \sum c(n)y(n)\rangle.$$

Thus, for any $c \in l^2(\mathcal{Z})$, $B^*c = \sum c(n)y(n) \equiv x \in H$; and, by the biorthonormality, $c(n) = \langle x, y(n)\rangle$. Therefore, $\{x(n)\}$ is also a Hilbert sequence.

∎

Condition (2.13) in Theorem 2.16 defines $\{y(n)\}$ as a *frame*, cf. Section 4.

Theorem 2.17 ([47]). Given a stationary, minimal, complete sequence $\{x(n)\} \subseteq H$, with power spectrum $\mu = f_{ac}$.

1) $\{x(n)\}$ is a Bessel sequence if and only if $f_{ac}^{-1} \in L^\infty(\mathfrak{T})$.
2) $\{x(n)\}$ is a Hilbert sequence if and only if $f_{ac} \in L^\infty(\mathfrak{T})$.

Rozanov's Theorem 2.17 and Masani's related contributions utilize Theorem 2.5. This result, and similar ones by these authors, were proved in the multivariate case, $\mathcal{Z} \to H^d$, e.g., [53, Volume III]. There are significant problems in the multivariable case, $\mathcal{Z}^d \to H$, cf. Section 4.2.

Remark 2.18. As we have mentioned, prediction theory leads to our formulation of Section 3. At the end of Section 3 we shall discuss the role of the uncertainty principle inequalities in the context of weighted Fourier transform norm inequalities. With this in mind, we close this section with an intriguing observation by Norbert Wiener [54, p. 9].

> "The prediction of the future of a message is done by some sort of operator on its past, whether this operator is realized by a scheme of mathematical computation, or by a mechanical or electrical apparatus. In this connection, we found that the ideal prediction mechanisms which we had at first contemplated were beset by two types of error, of a roughly antagonistic nature. While the prediction apparatus which we at first designed could be made to anticipate an extremely smooth curve to any desired degree of approximation, this refinement of behavior was always attained at the cost of an increasing sensitivity. The better the apparatus was for smooth waves, the more it would be set into oscillation by small departures from smoothness, and the longer it would be before such oscillation would die out. Thus the good prediction of a smooth wave seems to require a more delicate and sensitive apparatus than

the best possible prediction of a rough curve, and the choice of the particular apparatus to be used in a specific case was dependent on the statistical nature of the phenomenon to be predicted. This interacting pair of types of error seemed to have something in common with the contrasting problems of the measure of position and of momentum to be found in the Heisenberg quantum mechanics, as described according to his Principle of Uncertainty."

3. Weighted Fourier transform norm inequalities

3.1. Prediction theory and weighted Hilbert transform norm inequalities

Kolmogorov's conception and characterization of deterministic sequences lead to a new prediction problem formulated by Helson and Szegö (1960) [33]. We shall describe this problem, its relation to the material in Section 2, and the role of the Hilbert transform. In light of Theorem 2.5, we shall deal with trigonometric approximation in $L^2_\mu(\mathfrak{T})$.

Notation 3.1. Given $\mu = f_{ac} + \mu_s \in M_1(\mathfrak{T})$, we define the following subspaces of $L^2_\mu(\mathfrak{T})$:

$$\mathcal{P}_0 = \text{sp}\{e^{2\pi i k\gamma} : k \leqslant 0\},$$
$$\mathcal{P} = \text{sp}\{e^{2\pi i k\gamma} : k \leqslant -1\},$$

and

$$\mathcal{F} = \text{sp}\{e^{2\pi i k\gamma} : k \geqslant 1\}$$

"$\mathcal{P}$" is for "past" and "$\mathcal{F}$" is for "future."

The results about deterministic and minimal sequences from Theorems 2.8, 2.9, and 2.12 in Section 2 are the consequences of the following formulas developed by Szegö and Kolmogorov, respectively.

Formulas 3.2.

$$\inf_{p\in\mathcal{P}} \int_{\mathfrak{T}} |1 + p(\gamma)|^2 d\mu(\gamma) = \exp\left(\int_{\mathfrak{T}} \log f_{ac}(\gamma) d\gamma\right); \tag{3.1}$$

$$\inf_{\substack{p\in\mathcal{P}\\ q\in\mathcal{F}}} \int_{\mathfrak{T}} |1 + p(\gamma) + q(\gamma)|^2 d\mu(\gamma) = \left(\int_{\mathfrak{T}} f_{ac}(\gamma)^{-1} d\gamma\right)^{-1}. \tag{3.2}$$

Remark 3.3. If $\log f_{ac} \notin L^1(\mathfrak{T})$ then the right side of (3.1) vanishes and so $1 \in \overline{\mathcal{P}}$; in fact, $\overline{\mathcal{P}} = L^2_\mu(\mathfrak{T})$. Similarly, if $f_{ac}^{-1} \notin L^1(\mathfrak{T})$ then the right side of (3.2) vanishes and so $1 \in \overline{(\mathcal{P} \cup \mathcal{F})}$.

In the converse direction, these formulas show that "if f_{ac} is not too small," i.e., if the right-sides of (3.1) and (3.2) are positive, "then the exponentials possess a certain kind of independence" [33, p. 108]. Intuitively, this means, for example, that $\overline{\mathcal{P}} \neq \overline{\mathcal{F}}$ in the case that the elements of $\mathcal{P}$ are linearly "independent" of $\mathcal{F}$, i.e., the nondeterministic case. Geometrically, this signifies that $\overline{\mathcal{P}}$ and $\overline{\mathcal{F}}$ are *at a positive angle* α to each other in the sense that

$$\begin{aligned} \rho &\equiv \cos\alpha \\ &\equiv \sup\{|\langle p, q\rangle| : p \in \mathcal{P}, q \in \mathcal{F} \text{ and } \|p\|_{2,\mu}, \|q\|_{2,\mu} \leqslant 1\} < 1. \end{aligned} \tag{3.3}$$

The definition (3.3) is the natural Hilbert space generalization of *angle* from the Euclidean case, where the law of cosines is used to evaluate an angle α between two lines (subspaces) through the origin. Clearly, in this case, if $\alpha = 0$ then the two lines are the same. It is in this spirit that we would have the deterministic result, $\overline{\mathcal{P}} = \overline{\mathcal{F}}$, when $\alpha = 0$ in (3.3).

Helson and Szegö noted that the notion of independence defined by the condition, $\rho < 1$, is stronger that the independence defined by Kolmogorov's nondeterminism [33, p. 109], and discovered the following remarkable role for the Hilbert transform in prediction theory when dealing with positive angles between subspaces.

Theorem 3.4. [33, Theorem 2, pp. 129–130] Given $\mu = f_{ac} \in L^1_+(\mathfrak{T})$, and define the *conjugate function* $\tilde{p}(\gamma) = -i\sum_{|n|\leqslant N} \hat{p}[n]\,(\operatorname{sgn} n)\, e^{2\pi i n\gamma}$ for every trigonometric polynomial $\sum_{|n|\leqslant N} \hat{p}[n] e^{2\pi i n\gamma}$. There is $\rho \in (0, 1)$ such that

$$\forall p \in \mathcal{P} \text{ and } q \in \mathcal{F},$$
$$\left|\operatorname{Re}\int_{\mathfrak{T}} p(\gamma) e^{2\pi i\gamma}\overline{q(\gamma)} f_{ac}(\gamma)\,d\gamma\right| \leqslant \rho\|p\|_{2,\mu}\|q\|_{2,\mu}$$

if and only if there is $C > 0$ such that

$$\|\tilde{p}\|_{2,\mu} \leqslant C\|p\|_{2,\mu} \tag{3.4}$$

for all trigonometric polynomials p. Equivalently, $\overline{\mathcal{P}}_0$ and $\overline{\mathcal{F}}$ are at a positive angle in $L^2_\mu(\mathfrak{T})$ if and only if (3.4) holds for every real trigonometric polynomial p.

Remark 3.5. If f is a trigonometric series, $\sum a_n e^{2\pi i n\gamma}$, with conjugate series $\tilde{f}$, then

$$f + i\tilde{f} = a_0 + 2\sum_1^\infty a_n e^{2\pi i n\gamma}$$

is a series of *analytic type*. If $f \in L^2(\mathfrak{T})$ then $\tilde{f} \in L^2(\mathfrak{T})$ and $f + i\tilde{f} \in H^2(\mathfrak{T})$. The famous theorem of Marcel Riesz (1927) asserts

$$\forall f \in L^p(\mathfrak{T}), \qquad \|\tilde{f}\|_p \leqslant C\|f\|_p, \tag{3.5}$$

where $p > 1$, cf. (3.4). Kolmogorov (1925) proved the $L^1(\mathfrak{T})$-version of (3.5):

$$\begin{aligned} &\exists C > 0 \text{ such that } \forall f \in L^1(\mathfrak{T}) \text{ and } \forall \lambda > 0, \\ &|\{\gamma : |\tilde{f}(\gamma)| > \lambda\}| \leqslant C\lambda^{-1}\|f\|_1, \end{aligned} \tag{3.6}$$

i.e., $\tilde{f}$ is of *weak* L^1*-type* if $f \in L^1(\mathfrak{T})$. Note that the constant C in (3.6) is independent of f.

Definition 3.6.

1) The *Hilbert transform* of $f \in L^2(\mathfrak{R})$ is the conjugate function $\tilde{f}$ defined by the formula

$$(\tilde{f})^\vee(\gamma) = -i(\operatorname{sgn}\gamma)f^\vee(\gamma).$$

2) Since $\operatorname{sgn}\gamma = 2H(\gamma) - 1$ ($H \equiv$ Heaviside function) and since the distributional Fourier transform of $\frac{-1}{\pi i}\operatorname{pv}\left(\frac{1}{t}\right)$ is $2H(\gamma) - 1$, then

$$\tilde{f}(t) = \frac{1}{\pi}\operatorname{pv}\left(\frac{1}{t}\right) * f(t).$$

Thus, prediction problems are intimately related to weighted Hilbert transform norm inequalities.

3.2. A_p-weights, the Hilbert transform, and the fundamental theorem of calculus

Definition 3.7. For each $f \in L_{loc}{}^1(\mathfrak{R})$, the *Hardy-Littlewood* (1930) *maximal function* Mf is defined as

$$\forall t \in \mathfrak{R}, \qquad (Mf)(t) = \sup_{t \in I} \frac{1}{|I|}\int_I |f(u)|du,$$

where I ranges over the nontrivial compact intervals containing t. The extension to $\mathfrak{R}^d$ was made and used by Wiener (1939) in work on the ergodic theorem.

Theorem 3.8.

1) If $f \in L^1(\mathfrak{R})$ then Mf is of weak L^1-type, i.e., there is a constant $C > 0$ such that

$$\begin{aligned} &\forall f \in L^1(\mathfrak{R}) \text{ and } \forall \lambda > 0 \\ &\quad |\{t : (Mf)(t) > \lambda\}| \leqslant C\lambda^{-1}\|f\|_1. \end{aligned} \tag{3.7}$$

Note that the constant C in (3.7) is independent of f.

2) If $1 < p \leqslant \infty$ and $f \in L^p(\mathfrak{R})$ then $Mf \in L^p(\mathfrak{R})$, and there is a constant $C = C_p > 0$ such that

$$\forall f \in L^p(\mathfrak{R}), \qquad \|Mf\|_p \leqslant C_p\|f\|_p$$

(Hardy-Littlewood, 1930).

3) If $f \in L^1(\mathfrak{R})$ then

$$\lim_{t \in I} \frac{1}{|I|} \int_I f(u)du = f(t) \text{ a.e.}$$

where for a given t, the measures of the compact intervals I tend to 0 (Lebesgue, 1910).

Remark 3.9. In Theorem 3.8, Item 3 is a corollary of Item 1. Item 3 is that direction of the fundamental theorem of the calculus which asserts that

$$\text{"D} \circ \int = \text{ Identity,"} \tag{3.8}$$

where "D" is the differentiation operator and "$\int$" is the integration operator; and so Item 1 of Theorem 3.8 can be viewed as a quantitative version of (3.8). Of course, we also know that

$$\text{"} \int \circ D = \text{ Identity."} \tag{3.9}$$

More precisely, for compact intervals, F is absolutely continuous on $[a, b]$ if and only if

$$\exists f \in L^1[a, b] \text{ such that } \forall t \in [a, b], \qquad F(t) - F(a) = \int_a^t f(u)du.$$

Definition 3.10. Given $1 < p < \infty$ and a Borel measurable function $v > 0$ a.e. *v is an A_p-weight A_p-weight, written $v \in A_p$, if there is a constant $C > 0$* such that

$\forall I$ (compact interval),

$$\left(\frac{1}{|I|}\int_I v(t)dt\right)\left(\frac{1}{|I|}\int_I v(t)^{-1/(p-1)}dt\right)^{p-1} \leqslant C.$$

For example, $v(t) = |t|^\alpha \in A_p$ if $-1 < \alpha < p - 1$.

The A_p condition is precisely what is needed to prove a weighted version of Item 2 of Theorem 3.8.

Theorem 3.11 (Muckenhoupt, 1972). Given $1 < p < \infty$ and a Borel measurable function $v > 0$ a.e. There is a constant $C > 0$ such that

$$\forall f \in L^p_v(\mathfrak{R}), \qquad \|Mf\|_{p,v} \leqslant C\|f\|_{p,v}$$

if and only if

$$v \in A_p.$$

The relation between the material of this subsection and Section 3.1 is made by the following result.

Theorem 3.12 (Hunt, Muckenhoupt, Wheeden, 1973). Given $1 < p < \infty$ and a Borel measurable function $v > 0$ a.e. There is a constant $C > 0$ such that

$$\forall f \in L^\infty_c(\mathfrak{R}), \qquad \|\tilde{f}\|_{p,v} \leqslant C\|f\|_{p,v}$$

if and only if

$$v \in A_p.$$

Besides the original papers, [26] provides an excellent treatment of Theorems 3.11 and 3.12, as well as subsequent related developments concerning A_p and maximal and singular integral operators.

3.3. A_p-weights and weighted Fourier transform norm inequalities

We have seen how prediction theory leads to weighted Hilbert transform norm inequalities and A_p weights, with an accompanying theme dealing with the fundamental theorem of calculus.

The following result illustrates how Fourier transform inequalities come into the picture.

Theorem 3.13. [10] Given $1 < p \leqslant q \leqslant p' < \infty$ and an even, non-negative, Borel measurable function v, which is nondecreasing on $(0, \infty)$. There is a constant $C > 0$ such that

$$\forall f \in C^\infty_c(\mathfrak{R}),$$

$$\left(\int |\hat{f}(\gamma)|^q |\gamma|^{\left(\frac{q}{p'}-1\right)} v\left(\frac{1}{\gamma}\right)^{\frac{q}{p}} d\gamma\right)^{\frac{1}{q}} \leqslant C\left(\int |f(t)|^p v(t)dt\right)^{\frac{1}{p}} \qquad (3.10)$$

if and only if

$$\nu^{\frac{q}{p}} \in A_{1+(\frac{q}{p'})},$$

cf. [5, Section 2.2.2] for a d-dimensional version.

Remark 3.14.

1) Depending on ν, the quantitative expression for $\hat{f}$ is not transparent in the case $f \notin L^p_\nu(\mathfrak{R})\backslash L^1(\mathfrak{R}) \cap L^p_\nu(\mathfrak{R})$, e.g., [5], [8], and recent work with my student, J. Lakey [41].
2) If $p = q = 2$ then (3.10) becomes

$$\|\hat{f}\|_{2,\nu(\frac{1}{\gamma})} \leqslant C\|f\|_{2,\nu(t)}. \tag{3.11}$$

If we define the *Kelvin operator,*

$$(Kf)(\gamma) = \frac{1}{\gamma}\hat{f}\left(\frac{1}{\gamma}\right),$$

then (3.11) becomes

$$\|Kf\|_{2,\nu} \leqslant C\|f\|_{2,\nu}.$$

There is a corresponding inequality in terms of K for the general case (3.10). Harmonicity in $\mathfrak{R}^2$ is invariant under any conformal mapping. This fact is not valid in $\mathfrak{R}^d$, $d > 2$, and Kelvin transformations are used to provide the invariance of harmonicity in these higher dimensions as well as $\mathfrak{R}^2$ (W. Thomson, Lord Kelvin, 1847).

Example 3.15.

1) If $p = q$ and $\nu = 1$ then (3.10) is the Hardy, Littlewood, Paley theorem (1931),

$$\left(\int |\hat{f}(\gamma)|^p |\gamma|^{p-2} d\gamma\right)^{1/p} \leqslant C\|f\|_p, \tag{3.12}$$

originally proved for Fourier series.
2) If $q = p'$ and $\nu = 1$ then (3.10) is the Hausdorff-Young (1923), Titchmarsh theorem (1924),

$$\|\hat{f}\|_{p'} \leqslant C\|f\|_p. \tag{3.13}$$

Hausdorff-Young proved (3.13) for Fourier series, and Titchmarsh proved it for Fourier transforms.

3) If $v(t) = |t|^\alpha$, $0 \leqslant \alpha < p - 1$, then (3.10) is Pitt's theorem (1937),

$$\left(\int |\hat{f}(\gamma)|^q |\gamma|^{-\beta} d\gamma\right)^{1/q} \leqslant C \left(\int |f(t)|^p |t|^\alpha dt\right)^{1/p}, \tag{3.14}$$

where $\beta = \frac{q}{p}(\alpha + 1) + 1 - q$. The result was originally proved for Fourier series. If $p = q$ and $\alpha = 0$ then (3.14) reduces to (3.12). If $q = p'$ and $\alpha = 0$ then $\beta = 0$ and (3.14) reduces to (3.13).

4) The result in Item 1 was first proved by Hardy and Littlewood, but in the same year Paley proved it for uniformly bounded orthonormal systems. Paley's ideas are significant and deal with rearrangements, cf. J.E. Littlewood, "On a theorem of Paley," JLMS, *29*(1954), 387–395. Salem and Zygmund proved (3.12) for $p = 1$ when the given Fourier series is of analytic type (BAMS, *55*(1949), 851–859).

3.4. Weighted Fourier transform norm inequalities and the uncertainty principle

Our path from prediction theory lead us in Section 3.3 to A_p weights which characterize special weighted Fourier transform norm inequalities. The next step is to see what is involved in establishing general weighted Fourier transform norm inequalities.

H. Heinig and I proved the following result during the summer of 1982 here in Toscana (as well as in North America). Similar results were being proved during the same period by Muckenhoupt and by Jurkat and Sampson.

Theorem 3.16 ([9]). Given $1 \leqslant p \leqslant q < \infty$ and two even, non-negative, Borel measurable functions u and v, which are nonincreasing and nondecreasing, respectively, on $(0, \infty)$. There is a constant $C = C(K) > 0$ such that

$$\forall f \in C_c^\infty(\mathfrak{R}) \qquad \|\hat{f}\|_{q,u} \leqslant C\|f\|_{p,v} \tag{3.15}$$

if and only if

$$\sup_{s>0} \left(\int_0^{1/s} u(\gamma) d\gamma\right)^{1/q} \left(\int_0^s v(t)^{-p'/p} dt\right)^{1/p'} \equiv K < \infty. \tag{3.16}$$

Remark 3.17.

1) Naturally, from general considerations, (3.15) allows us to define $\hat{f}$ for each $f \in L_v^p(\mathfrak{R})$, with the same caveat to which we alluded in Item 1 of Remark 3.14.

2) Our proof of the necessary conditions for (3.15), *viz.*, the implication that (3.15) implies (3.16), does not require monotonicity.
3) Given our present point of view of tracing mathematical paths from Kolmogorov's seminal work, we should point out that Theorem 3.16 was used in our proof of Theorem 3.13.

Qualitatively, the condition (3.16) is in the spirit of the uncertainty principle. In the early 1980s, Heinig and I verified an elementary weighted Heisenberg inequality by means of Theorem 3.16. In a recent NATO ASI, we developed a full theory of uncertainty principle inequalities, taking into account significant work of others, working in the context of weighted Fourier transform norm inequalities, and utilizing wavelets and coherent states [5].

Theorem 3.16 is just the starting point for weighted Fourier transform norm inequalities. The theory has been highly developed in the past decade by many harmonic analysts, and is naturally akin to the topic of restriction theorems where geometry plays such a critical role. The goal is to characterize norm inequalities such as (3.15) both effectively and computationally, and for the most general class of weights. Our most recent contribution [8] deals with effective criteria, i.e., no rearrangements, and measure weights; it also contains references to recent contributions by others, cf. [41].

4. Stationary frames

4.1. The theory of frames

Definition 4.1.

1) A sequence $\{x(n)\}$ in Hilbert space H is a *frame* if there exist $A, B > 0$ such that

$$\forall y \in H, \qquad A\|y\|^2 \leq \sum |\langle y, x(n)\rangle|^2 \leq B\|y\|^2,$$

where $\langle\ ,\ \rangle$ is the inner product on H and the norm of $y \in H$ is $\|y\| = \langle y, y\rangle^{1/2}$. A and B are the *frame bounds*, and a frame $\{x(n)\}$ is *tight* if $A = B$. A frame $\{x(n)\}$ is exact if it is no longer a frame when any one of its elements is removed. Clearly, if $\{x(n)\}$ is an orthonormal basis of H then it is a tight exact frame with $A = B = 1$.
2) The *frame operator* of the frame $\{x(n)\}$ is the function $S : H \to H$ defined as $Sy = \sum \langle y, x(n)\rangle x(n)$.

The theory of frames is due to Duffin and Schaeffer [19] in 1952. Expositions include the book by Young [56] and the article by my students C. Heil and D. Walnut [29]; the former is presented in the context of nonharmonic Fourier series and the latter in the setting of wavelet theory.

Theorem 4.2. Let $\{x(n)\} \subseteq H$ be a frame with frame bounds A and B.

1) S is a topological isomorphism with inverse $S^{-1} : H \to H$. $\{(S^{-1}x)(n)\}$ is a frame with frame bounds B^{-1} and A^{-1}, and

$$\forall y \in H, \qquad y = \sum \langle y, (S^{-1}x)(n)\rangle\, x(n)$$
$$= \sum \langle y, x(n)\rangle (S^{-1}x)(n).$$

The first expansion is the *frame expansion* and the second is the *dual frame expansion*.

2) If $\{x(n)\}$ is tight, $\|x(n)\| = 1$ for all n, and $A = B = 1$, then $\{x(n)\}$ is an orthonormal basis of H.
3) If $\{x(n)\}$ is exact, then $\{x(n)\}$ and $\{(S^{-1}x)(n)\}$ are biorthonormal, i.e.,

$$\forall m, n, \qquad \langle x(m), (S^{-1}x)(n)\rangle = \delta_{mn}.$$

Remark 4.3. We comment on Item 2 because it is surprisingly useful and because of a stronger result by Vitali (1921) [51].

To prove Item 2 we first use tightness and $A = 1$ to write,

$$\|x(m)\|^2 = \|x(m)\|^4 + \sum_{n \neq m} |\langle x(m), x(n)\rangle|^2;$$

and obtain that $\{x(n)\}$ is orthonormal since each $\|x(n)\| = 1$. To conclude the proof we then invoke the well-known result: if $\{x(n)\} \subseteq H$ is orthonormal then it is an orthonormal basis of H if and only if

$$\forall y \in H, \qquad \|y\|^2 = \sum |\langle y, x(n)\rangle|^2.$$

In 1921, Vitali proved that an orthonormal sequence $\{g_n\} \subseteq L^2[a, b]$ is complete, and so $\{g_n\}$ is an orthonormal basis, if and only if

$$\forall t \in [a, b], \qquad \sum \left| \int_a^t g_n(u)du \right|^2 = t - a. \tag{4.1}$$

For the case $H = L^2[a, b]$, Vitali's result is stronger than Item 2 since (4.1) is tightness with $A = 1$ for functions $f = \mathbf{1}_{[a,t]}$.

Definition 4.4. Let H be a complex separable Hilbert space. A sequence $\{x(n)\} \subseteq H$ is a *Schauder basis* or *basis* of H is each $y \in H$ has a unique decomposition $y = \sum c_n(y)x(n)$. A basis $\{x(n)\}$ is an *unconditional basis* if

$\exists C$ such that $\forall F \subseteq \mathcal{Z}$, where card $F < \infty$, and

$\forall b_n, c_n \in \mathcal{C}$, where $n \in F$ and $|b_n| \leqslant |c_n|$,

$$\left\| \sum_{n \in F} b_n x(n) \right\| \leqslant C \left\| \sum_{n \in F} c_n x(n) \right\| .$$

An unconditional basis $\{x(n)\}$ is *bounded* if

$\exists A, B > 0$ such that $\forall n, A \leqslant \|x(n)\| \leqslant B$.

Separable Hilbert spaces have orthonormal bases, and orthonormal bases are bounded unconditional bases.

Köthe (1936) proved the implication, Item 2 implies Item 3, of the following theorem. The implication, Item 3 implies Item 2, is straightforward; and the equivalence of Item 1 and Item 3 is found in [56, pp. 188–189].

Theorem 4.5. Let H be a complex separable Hilbert space and let $\{x(n)\} \subseteq H$ be a given sequence. The following are equivalent:

1) $\{x(n)\}$ is an exact frame for H;
2) $\{x(n)\}$ is a bounded unconditional basis of H;
3) $\{x(n)\}$ is a *Riesz basis*, i.e., there is an orthonormal basis $\{u(n)\}$ and a topological isomorphism $T : H \to H$ such that $(Tx)(n) = u(n)$ for each n.

Theorem 4.6. Let H be a separable Hilbert space and let $\{x(n)\} \subseteq H$ be a frame. $\{x(n)\}$ is an exact frame $\iff$ $\{x(n)\}$ is a minimal sequence.

Proof.

$\Rightarrow$ Since $\{x(n)\}$ is exact we have that $\{x(n)\}, \{(S^{-1}x)(n)\}$ are biorthonormal [19], cf. [29, p. 637]. By Item 2 of Definition 2.13b, $\{x(n)\}$ is minimal.

$\Leftarrow$ Since $\{x(n)\}$ is minimal then

$$\forall p, \qquad x(p) \notin \overline{\text{sp}}\{x(n) : n \neq p\} \tag{4.2}$$

To prove $\{x(n)\}$ is an exact frame we must show that each $\{x(n) : n \neq p\}$ is not a frame. If any $\{x(n) : n \neq p\}$ were a frame, then by Theorem 4.2 $x(p) = \sum_{n \neq p} c_n x(n)$, and this fails by (4.2). ∎

Corollary 4.7. Given a stationary, minimal, complete sequence $x : \mathcal{Z} \to H$. Then $\{x(n)\}$ is both a Bessel sequence and a Hilbert sequence if and only if $\{x(n)\}$ is a bounded unconditional basis.

Proof. Bessel-Hilbert sequences are frames by Theorem 2.16. Thus, $\{x(n)\}$ is a bounded unconditional basis by Theorems 4.5 and 4.6. The converse is immediate by Theorems 2.16 and 4.5. ∎

Example 4.8. Given $g \in L^2(\mathfrak{R}^d)$ and $a = (a_1, \ldots, a_d)$, $b = (b_1, \ldots, b_d) \in \mathfrak{R}^d$. Assume each $a_j, b_k > 0$. Define the translation and modulation maps,

$$T_{na}f(t) = f(t - na) \text{ and } E_{mb}f(t) = e^{2\pi it \cdot mb}f(t),$$

respectively, where $m, n \in \mathcal{Z}^d$, $f \in L^2(\mathfrak{R}^d)$, $na = (n_1a_1, \ldots, n_da_d)$, and $mb = (m_1b_1, \ldots, m_db_d)$. The *Weyl-Heisenberg system* $\{\phi_{m,n} : m, n \in \mathcal{Z}^d\}$ is defined by

$$\phi_{m,n} = E_{mb}T_{na}g,$$

cf. [11, Definition 2.6] for a generalization. If $\{\phi_{m,n}\}$ is a frame for $L^2(\mathfrak{R}^d)$ it is called a *Weyl-Heisenberg* or *Gabor frame* (of coherent states).

Remark 4.9. Given $g \in L^2(\mathfrak{R}^d)$ and $a, b > 0$ for which $ab = 1$. *If $\{\phi_{m,n}\}$ is a frame then it is an exact frame*, cf. Theorem 4.5. This remarkable fact (for $ab = 1$) can be proved using properties of the Zak transform, which we now define.

Definition/Property 4.10.

1) Given $a = (a_1, \ldots, a_d) \in \mathfrak{R}^d$, with each $a_j > 0$. The *Zak transform* of $f \in L_{loc}^1(\mathfrak{R}^d)$ is formally defined as

$$Gf(x, w) = a^{d/2} \sum_{k \in \mathcal{Z}^d} f(xa + ka)e^{2\pi ik \cdot w}, \quad (x, w) \in \mathfrak{T}^d \times \mathfrak{T}^d, \quad (4.3)$$

where multiplication is component-wise and $a^{d/2} = \Pi a_j^{1/2}$. Its history has been traced to Gauss, from whence the "G" in (4.3); and in recent times there have been independent formulations by Auslander-Tolimieri, Brezin-Weil, and, of course, Zak, cf. [36].

2) Formally, Gf is *quasi periodic* in the sense that

$$Gf(x + n, w) = e^{-2\pi in \cdot w}G(x, w) \text{ and } G(x, w + n) = G(x, w)$$

for $(x, w) \in \mathfrak{T}^d \times \mathfrak{T}^d$ and $n \in \mathcal{Z}^d$.

The proof of Theorem 4.11 is straightforward, beginning with an elementary calculation verifying that

$$\forall f \in C_c^\infty(\mathfrak{R}^d), \qquad \|Gf\|_{L^2(\mathfrak{T}^d \times \mathfrak{T}^d)} = \|f\|_2.$$

Theorem 4.11. $G : L^2(\mathfrak{R}^d) \to L^2(\mathfrak{T}^d \times \mathfrak{T}^d)$ is a unitary map.

Given $a, b \in \mathfrak{R}^d$ *with each* $a_j, b_k > 0$. *If* $g \in L^2(\mathfrak{R}^d)$ *and* $ab = 1$, *i.e,* $a_j b_j = 1$ *for each* $j = 1, \ldots, d$, *then*

$$\begin{aligned} G(E_{mb} T_{na} g)(x, w) &= E_m(x) E_n(w) G g(x, w) \\ &\equiv E_{m,n}(x, w) G g(x, w), \quad (x, w) \in \mathfrak{T}^d \times \mathfrak{T}^d. \end{aligned} \tag{4.4}$$

Note that $\{E_{m,n}\}$ is an orthonormal basis of $L^2(\mathfrak{T}^d \times \mathfrak{T}^d)$. By isolating Gg (from $G(E_{mb} T_{na} g)$) when considering $\{\phi_{m,n}\}$, it is clear that (4.4), in conjunction with Theorem 4.11 plays a role in the following result. This result (Theorem 4.12) has had partial formulations in the coherent states literature for many years, and seems to go back to the analysis of von Neumann found in [52, pp. 405ff.], cf. [18], [28, Proposition 7.3.4], [29, Theorem 4.3.3], [36].

Theorem 4.12. Given $g \in L^2(\mathfrak{R}^d)$ and $a, b \in \mathfrak{R}^d$ with each $a_j, b_k > 0$. Assume $ab = 1$ and consider the Weyl-Heisenberg system $\{\phi_{m,n}\}$ (defined in Example 4.8).

1) $\{\phi_{m,n}\}$ is complete in $L^2(\mathfrak{R}^d)$ if and only if $Gg \neq 0$ a.e.
2) $\{\phi_{m,n}\}$ is minimal and complete in $L^2(\mathfrak{R}^d)$ if and only if $1/Gg \in L^2(\mathfrak{T}^d \times \mathfrak{T}^d)$.
3) $\{\phi_{m,n}\}$ is an orthonormal basis of $L^2(\mathfrak{R}^d)$ if and only if $|Gg| = 1$ a.e.
4) $\{\phi_{m,n}\}$ is a frame for $L^2(\mathfrak{R}^d)$ with frame bounds A and B if and only if

$$A \leqslant |Gg|^2 \leqslant B \qquad \text{a.e.}$$

In this case, $\{\phi_{m,n}\}$ is an exact frame.

Item 1 of Theorem 4.12 should be compared with Corollary 4.7 and Section 4.3, where we note that $\{\phi_{m,n}\}$ is stationary in the case $ab = 1$.

Example 4.13. Given $\psi \in L^2(\mathfrak{R})$. The *wavelet system* $\{\psi_{m,n} : m, n \in \mathfrak{Z}\}$ is defined as

$$\psi_{m,n}(t) = 2^{m/2} \psi(2^m t - n).$$

If $\{\phi_{m,n}\}$ is a frame for $L^2(\mathfrak{R})$ it is called a *wavelet frame*.

4.2. Multidimensional analogues of classical analysis problems

The extension of the Kolmogorov or Szegö or Wiener prediction theory to multidimensional domains is a natural problem, and has been and is being pursued, e.g., [15, 37]. Chiang's work [15] precedes the well-known contribution of Helson and Lowdenslager. There has been a proliferation of results dealing with specific topics and diverse levels of abstraction. (For example,

[20, Preface] provides references for Markovian properties in this setting.) From the mathematical point of view, the work of Helson and Lowdenslager [31, 32, 30] is preeminent. One can reasonably argue its central position in the development of abstract analysis for a generation, and its influence on such topics as locally compact abelian groups, Dirichlet algebras, von Neumann algebras, and H^p-theory, e.g., [53, Volume III, pp. 347ff.] for what now are classical (or at least standard) references. With all of this, there are still *basic* multidimensional prediction problems.

Our goal in this section is to exhibit a little bit of the multidimensional evolution of one particular classical problem, which played a role in [39]. At the very least, it gives us the opportunity to advertise two recent and deep contributions by Benedicks [12] and Gabardo [23]. Our slightly broader goal in Section 4 is to suggest an interleaving of technology between the theories of frames and prediction, with the hope of bringing new techniques to bear on the problems in each area. Our method will become apparent in Section 4.3.

The role of the F. and M. Riesz theorem in one of Kolmogorov's spectral characterizations, viz., [39, Theorem 23], was discussed in Remark 2.10.

Theorem 4.14 (F. and M. Riesz, 1916). Given $\mu \in M(\mathfrak{T})$ and assume $\hat{\mu}(n) = 0$ for all $n < 0$. Then $\mu = f_{ac}$, i.e., $\mu \in L^1(\mathfrak{T})$.

Three years after Kolmogorov's paper [39], Bochner published the following result.

Theorem 4.15 (Bochner, 1944). Given $\mu \in M(\mathfrak{T}^2)$ and assume μ vanishes outside a sector $S \subseteq \mathfrak{Z}^2$ of opening $\alpha_S < \pi$. Then $\mu \in L^1(\mathfrak{T}^2)$. (Precisely, S is a closed sector of $\mathfrak{R}^2$.)

Bochner's work was not only an inspiration for Helson and Lowdenslager's program, in which they generalized Szegö's theorem dramatically, but in [31] they proved a generalization of the F. and M. Riesz Theorem of which Theorem 4.15 is a corollary, e.g., [48, Chapter 8], a book where many of us began. Instead of the duality between $\mathfrak{T}$ and $\mathfrak{Z}$, the setting in [31] is the duality between a compact connected abelian group Γ and its discrete dual group G in the case G is ordered, e.g., [48, pp. 193–194] for the definition of ordered group.

Ordered groups also arise in the theory of Bohr almost periodic functions, e.g., [53, Volume III, pp. 347-348].

4.3. Stationary frames

Definition/Remark 4.16.

1) A sequence $\{x(n) : n \in \mathcal{Z}^d\}$ in a complex Hilbert space H is *stationary* if the inner product,

$$R(m) = R_{xx}(m) = \langle x(m+k), x(k)\rangle, \quad m \in \mathcal{Z}^d,$$

is independent of $k \in \mathcal{Z}^d$, i.e.,

$$\forall m, n \in \mathcal{Z}^d, \qquad \langle x(m), x(n)\rangle = \langle x(m-n), x(0)\rangle.$$

Thus, $\{x(n)\}$ is stationary if the function $s : \mathcal{Z}^d \times \mathcal{Z}^d \to \mathcal{C}$, defined as

$$s(m,n) = \langle x(m), x(n)\rangle,$$

has the form $s(m,n) = s(m-n)$. In this case, $R_{xx}(m-n) = s(m-n)$, and $R_{xx}(m) = s(m-0) = s(m,0) = \langle x(m), x(0)\rangle$. R_{xx} is the *autocorrelation* of x and is a positive definite function on the group $\mathcal{Z}^d$. $\mu = R_{xx}^{\wedge} \in M_+(\mathcal{T}^d)$ is the *power spectrum* of x.

2) The analogue of Theorem 2.5 is valid for stationary sequences $x : \mathcal{Z}^d \to H$, where $H(x) = \overline{sp}\{x(n) : n \in \mathcal{Z}^d\}$: *the mapping*

$$Z : L^2_\mu(\mathcal{T}^d) \to H(x),$$

defined linearly on $sp\{e^{2\pi i n\cdot\gamma}\}$ *by* $Z(e^{2\pi i n\cdot\gamma}) = x(n)$, *extends to a linear isometric isomorphism.*

3) A stationary sequence $\{x(n) : n \in \mathcal{Z}^d\} \in H$ is a *stationary frame* if $\{x(n) : n \in \mathcal{Z}^d\}$ is a frame in H.

Example 4.17.

1) Given $g \in L^2(\mathcal{R}^d)$ and $a, b \in \mathcal{R}^d$ with each $a_j, b_k > 0$. Consider the Weyl-Heisenberg system $\{\phi_{m,n} : m, n \in \mathcal{Z}^d\}$, where

$$\phi_{m,n} = E_{mb} T_{na} g.$$

If $ab = 1$, *i.e.*, $a_j b_j = 1$ *for each* $j = 1, \ldots, d$, *then the sequence* $x : \mathcal{Z}^d \times \mathcal{Z}^d \to L^2(\mathcal{R}^d)$, *defined by* $x(m,n) = \phi_{m,n}$, *is a stationary sequence.* In fact,

$$\langle \phi_{m,n}, \phi_{p,q}\rangle = \int e^{2\pi i t\,(m-p)b} g(t - na)\overline{g}(t - qa)dt$$

$$= \int e^{2\pi i (u + qa)\,(m-p)b} g(u - (n-q)a)\overline{g}(u)du$$

$$= \int e^{2\pi i t\cdot(m-p)b} \exp\left\{2\pi i \sum_{j=1}^{d} q_j(m_j - p_j)a_j b_j\right\}$$
$$\times g(u-(n-q)a)\overline{g}(u)du$$

$$= \int e^{2\pi i u\cdot(m-p)b} g(u-(n-q)a)\overline{g}(u)du$$

$$= \langle \phi_{m-p,n-q}, g\rangle \equiv \langle \phi_{m-p,n-q}, \phi_{0,0}\rangle,$$

and this is the desired stationarity. Of course, the positive definiteness follows from general considerations, *viz.*,

$$\sum_{\substack{(m,n)\\(p,q)}} c_{m,n}\overline{c}_{p,q} R\Big((m,n)-(p,q)\Big)$$
$$= \sum_{\substack{(m,n)\\(p,q)}} c_{m,n}\overline{c}_{p,q}\langle \phi_{m,n}, \phi_{p,q}\rangle$$
$$= \sum_{\substack{(m,n)\\(p,q)}} \langle c_{m,n}\phi_{m,n}, c_{p,q}\phi_{p,q}\rangle$$
$$= \left\langle \sum_{(m,n)} c_{m,n}\phi_{m,n}, \sum_{(p,q)} c_{p,q}\phi_{p,q}\right\rangle \geq 0.$$

Thus, $R^{\wedge} = \mu \in M_1(\mathfrak{T}^d)$.

2) In the case of Item 1,

$$R(m,n) = \int e^{2\pi i u\cdot mb}(T_{na}g(u))\,\overline{g}(u)du.$$

Clearly, $|R(m,n)| \leq \|g\|^2_{L^2(\mathfrak{R}^d)}$ for $(m,n) \in \mathcal{Z}^d \times \mathcal{Z}^d$.

Also, for each $n \in \mathcal{Z}^d$, $(T_{na}g)\,\overline{g} \in L^1(\mathfrak{R}^d)$, and so

$$\forall n, \qquad \lim_{|m|\to\infty} |R(m,n)| = 0$$

by the Riemann-Lebesgue lemma. Here, thinking in terms of locally compact abelian groups, $\lim_{|m|\to\infty} r(m) = 0$ indicates that for all $\epsilon > 0$, there is a finite set $K \subseteq \mathcal{Z}^d$ such that

$$\forall m \in \mathcal{Z}^d\backslash K, \qquad |r(m)| < \epsilon.$$

Further, by Parseval's theorem,

$$R(m,n) = \int e^{-2\pi i n a\cdot\gamma}\hat{g}(\gamma)(T_{-mb}\hat{g})^{-}(\gamma)d\gamma;$$

and so, as above,

$$\forall m, \qquad \lim_{|n|\to\infty} |R(m,n)| = 0.$$

Example 4.18. Given $\psi \in L^2(\mathfrak{R})$ and the wavelet system $\{\psi_{m,n}\}$. We compute the following

$$\begin{aligned}\langle \psi_{m,n}, \psi_{p,q} \rangle &= 2^{\frac{m+p}{2}} \int \psi(2^m t - n)\overline{\psi}(2^p t - q)dt \\ &= 2^{\frac{m+p}{2}} \int \psi\left(2^{m-p}(u+q) - n\right)\overline{\psi}(u)2^{-p}du \\ &= 2^{\frac{m-p}{2}} \int \psi\left(2^{m-p}u - (n - 2^{m-p}q)\right)\overline{\psi}(u)du.\end{aligned}$$

Thus, $\{\psi_{m,n}\}$ is *not* a stationary sequence since $n - 2^{m-p}q \neq n - q$ unless $m = p$.

Besides Example 4.17, there is another relationship between Weyl-Heisenberg systems and power spectra which we first proved in the AMS series, *Contemporary Mathematics, 91*(1989), pp. 9–27.

Theorem 4.19. Given $g \in L^\infty(\mathfrak{R})$. Define the (analogue) *Weyl-Heisenberg system,*

$$\phi_{\omega,x}(t) = E_\omega T_x g(t) = e^{2\pi i t\omega} g(t - x),$$

$(x, \omega) \in \mathfrak{R} \times \hat{\mathfrak{R}}$, and the L^1*-Weyl-Heisenberg transform,*

$$\forall f \in L^1(\mathfrak{R}), \qquad W(f)(x,\omega) = \int f(t)\overline{\phi}_{\omega,x}(t)dt.$$

Assume g has a continuous autocorrelation,

$$\forall t \in \mathfrak{R}, \qquad R(t) = \lim_{T\to\infty} \frac{1}{2T} \int_{-T}^{T} g(t+u)\overline{g}(u)du$$

with $R(0) > 0$; and let $\{\rho_n\} \subseteq L^1(\hat{\mathfrak{R}})$ have the property that $\{\rho_n^\vee\} \subseteq L^1(\mathfrak{R})$ is an L^1-approximate identity. Then

$$\forall f \in L^1(\mathfrak{R}), \qquad \lim_{n\to\infty} \|f - f_n\|_1 = 0,$$

where

$$f_n(t) = \frac{1}{R(0)} \lim_{T\to\infty} \frac{1}{2T} \int\int_{-T}^{T} W(f)(x,\omega)\phi_{\omega,x}(t)\rho_n(\omega)dx\,d\omega.$$

Remark 4.20. If $g = 1$ then the L^1-Weyl-Heisenberg transform is the ordinary Fourier transform; and Theorem 4.19 is the usual L^1-inversion theorem for the Fourier transform.

The autocorrelation defined in Theorem 4.19 corresponds to the autocorrelation defined for stationary sequences in the case of correlation ergodic processes. Also, it is possible to substitute other modes of convergence in the definition of autocorrelation and still obtain Theorem 4.19.

Point of view. Given the stationary sequence

$$x : \mathcal{Z}^d \times \mathcal{Z}^d \to L^2(\mathfrak{R}^d),$$

where $x(m,n) = \phi_{m,n}$ for some $g \in L^2(\mathfrak{R}^d)$ and $ab = 1$; and suppose

$$H(x) = L^2(\mathfrak{R}^d),$$

where $H(x) = \overline{sp}\{x(m,n) : (m,n) \in \mathcal{Z}^d \times \mathcal{Z}^d\}$. If μ is the power spectrum of x then

$$Z : L^2_\mu(\mathcal{T}^d \times \mathcal{T}^d) \to L^2(\mathfrak{R}^d)$$

is a unitary map, as is the Zak transform,

$$G : L^2(\mathfrak{R}^d) \to L^2(\mathcal{T}^d \times \mathcal{T}^d),$$

and the induced map,

$$G \circ Z : L^2_\mu(\mathcal{T}^d \times \mathcal{T}^d) \to L^2(\mathcal{T}^d \times \mathcal{T}^d).$$

In this last case,

$$G \circ Z(E_{m,n})(x,\omega) = E_{m,n}(x,\omega)Gg(x,\omega),$$

cf. (4.4). Note that $\mu \geqslant 0$ is a periodic measure on $\hat{\mathfrak{R}}^d \times \hat{\mathfrak{R}}^d$, and Gf is quasi-periodic on $\hat{\mathfrak{R}}^d \times \hat{\mathfrak{R}}^d$ for each $f \in L^2(\mathfrak{R}^d)$.

The general problem we pose is to analyze and compare the periodic measure μ and quasi-periodic function Gg *vis a vis* obtaining results in multidimensional prediction theory and the decomposition theory for coherent states, e.g., Theorem 4.12.

In one direction it is natural to establish the role of μ in formulating criteria for expansions such as those given in Theorem 4.12, in the case the Zak transform of g is more intractable than μ. In the other direction, we envisage incorporating the Zak transform of g in obtaining "spectral" characterizations of deterministic properties of various complete Weyl-Heisenberg systems indexed by $g \in L^2(\mathfrak{R}^d)$. There are partial results, and, assuming further progress can be made, these will appear elsewhere.

5. The spherical Wiener-Plancherel formula

5.1. Wiener-Plancherel formulas

What exactly is a Wiener-Plancherel formula? Given a function ϕ defined on $\mathfrak{R}^d$ having Fourier transform $\hat{\phi}$ defined on $\hat{\mathfrak{R}}^d (= \mathfrak{R}^d)$. Suppose the distribution $\hat{\phi}$ is intractable, as is likely for poorly behaved ϕ. Let s be an operable integral of $\hat{\phi}$, i.e., suppose that s is a well-behaved function and that $Ls = \hat{\phi}$, distributionally, for some differential operator L. Wiener's idea was to deal with a computable function s instead of the more esoteric distribution $\hat{\phi}$, and to relate the quadratic behavior of ϕ and s. In particular, for the spherical case dealing with balls $B(0,R) = \{t \in \mathfrak{R}^d : |t| \leqslant R\}$ having volumes $|B(0,R)|$, a Wiener-Plancherel formula has the form

$$\lim_{R\to\infty} \frac{1}{|B(0,R)|} \int_{B(0,R)} |\phi(t)|^2 dt = Q(s),$$

where $Q(s)$ is an explicit quadratic expression and Q, s and L are interdependent, cf. (5.1) for the exact formula. In Wiener's original result ($d = 1$), Ls can be correctly formulated as a first distributional derivative of s, and

$$Q(s) = \lim_{\lambda\to 0} \frac{1}{2\lambda} \int_{-\infty}^{\infty} |s(\gamma + \lambda) - s(\gamma - \lambda)|^2 d\gamma.$$

The Plancherel formula allows one to define the Fourier transform of a square-integral function f, and, at certain levels of abstraction, it is considered as characterizing what is meant by an harmonic analysis of f. On the other hand, for most applications in $\mathfrak{R}^d$, the Plancherel formula assumes the workaday role of an effective tool used to obtain quantitative results. It is this latter role we envisage for Wiener-Plancherel formulas in the non-square-integrable case. After all, distribution theory (in $\mathfrak{R}^d$) gives the proper definition of the Fourier transform of tempered distributions. The real issue is to obtain quantitative results for problems where an harmonic analysis of a non-square-integrable function is desired. A host of such problems comes under the heading of an harmonic (spectral) analysis of signals containing non-square-integrable noise and/or random components, whether it be speech recognition, image processing, geophysical modeling, or turbulence in fluid mechanics. Such problems can be attacked by Beurling's profound theory of spectral synthesis, as well as by the extensive multifaceted theory of time series, e.g., [46]. Beurling's spectral synthesis does not deal with energy and power considerations, i.e., quadratic criteria, and time series relies on a stochastic point of view. Our goal is to implement Wiener-Plancherel formulas to address the above-mentioned group of problems. These formulas are well-suited to deal with energy and power; and they provide an analytic

device which should dovetail with spectral estimation methods (from time series) developed since Kolmogorov's and Wiener's time.

In Formula 5.1, we shall state our spherical Wiener-Plancherel formula, viz., (5.1), without going into any detail concerning hypotheses and motivation. We feel that the technicalities and hypotheses are sufficiently complex to warrant a displayed version at the outset. The relation between (5.1) and the Wiener-Khinchin theorem, as mentioned in Section 2, becomes apparent in Section 5.4.

Formula 5.1. The spherical Wiener-Plancherel formula is

$$\begin{aligned}&\lim_{R\to\infty}\frac{1}{|B(0,R)|}\int_{B(0,R)}|\phi(t)|^2dt\\&\quad=\lim_{\lambda\to 0}\frac{c(d,k)(2\pi)^{4k}}{\omega_{d-1}\lambda^{4k-d}}\int|D_\lambda s_k(\gamma)|^2d\gamma,\end{aligned}\tag{5.1}$$

cf. Theorem 5.6 for a precise statement of hypotheses for the validity of (5.1). The function s_k is the Wiener s-function,

$$s_k=\hat{\phi}*E_k,\tag{5.2}$$

where $\Delta^k E_k=\delta$, ω_{d-1} is the surface area of the unit sphere Σ_{d-1}, $c(d,k)^{-1}$ is the L^1-norm of a special function related to the Fourier transform of the restriction of surface measure σ_{d-1} to Σ_{d-1}, e.g., Example 5.4,

$$D_\lambda s_k=s_k-\mathcal{M}_\lambda s_k,$$

and $\mathcal{M}_\lambda$ is the spherical mean-value operator defined by

$$\mathcal{M}_\lambda s_k(\gamma)=\frac{1}{\omega_{d-1}}\int_{\Sigma_d}s_k(\gamma+\lambda\theta)d\sigma_{d-1}(\theta).$$

The integer k is related to the dimension d, and there must be control of the quadratic means of ϕ over spheres in order to verify (5.1). The operator L described above is the iterated Laplacian Δ^k.

Remark 5.2.

1) In previous work with my students G. Benke and W. Evans [7], we proved a rectilinear version of (5.1). The rectilinear result is easier to prove than the spherical one, although by no means elementary. Also, in the case of "rectilinear geometry" the operator L is the hyperbolic operator

$$L=\partial_1\partial_2\ldots\partial_d;$$

whereas, the "spherical geometry" of (5.1) gives rise to the elliptic operator $L = \Delta^k$. This remark indicates there is a range of Wiener-Plancherel formulas according to the number of degrees of freedom available in various convergence criteria.

2) It is natural to expect significant differences between the rectilinear and spherical cases.

The analogous situation with the convergence problem for multiple Fourier series makes this point clear. There are several natural rectilinear convergence criteria for multiple Fourier series, and there exist positive results in some cases. For example, using the Carleson-Hunt theorem for $d = 1$, C. Fefferman [21] (1971) proved that

$$\lim_{R\to\infty} \sum_{m\in RP\cap\mathcal{Z}^d} a_m e^{2\pi i t\cdot m} = \phi(t), \text{a.e.} \tag{5.3}$$

for $\phi \in L^p(\mathfrak{R}^d/\mathcal{Z}^d)$, $1 < p \leqslant \infty$, where $P \subseteq \mathfrak{R}^d$ is a d-dimensional polygon. The rectilinear convergence we used in [7] is analogous to the so-called "restricted rectangular" convergence criterion in the theory of multiple Fourier series; this criterion is different from that of (5.3). If the polygonal convergence of (5.3) is replaced by spherical convergence, then it is not known whether all the elements of $L^2(\mathfrak{R}^d/\mathcal{Z}^d)$, $d > 1$, have a Fourier series representation pointwise a.e.. There are negative results if $p < 2$. The problem of multiple Fourier series with spherical convergence criteria is closely related to deep problems associated with Bochner-Riesz multipliers. There are some positive results, and we close this discussion with one such theorem due to Carbery and F. Soria (1988): if $d \geqslant 2$, $\alpha > 0$, $2 \leqslant p < 2d/(d-1)$, and ϕ is an element of the Sobolev space $L^p_\alpha(\mathfrak{R}^d)$, then

$$\lim_{R\to\infty} \int_{B(0,R)} \hat{\phi}(\gamma) e^{2\pi i t\cdot\gamma} d\gamma = \phi(t), \text{a.e.}$$

Example 5.3. A formula such as (5.1) established a mapping between spaces of functions. For example, if the left side of (5.1) is finite then $\|\phi\|_{B^2(\mathfrak{R}^d)} < \infty$, where $B^2(\mathfrak{R}^d)$ consists of functions having bounded quadratic means over spheres. There is a hierarchy of Besicovich spaces $B(p,q)$ of which $B^2 = B(2,\infty)$. For the right side of (5.1) the corresponding hierarchy $V(p,q)$ is related to Besov spaces. In the case $d = 1$, the mappings $B(2,1) \to V(2,1)$ and $B(2,\infty) \to V(2,\infty)$, established by Wiener's original Wiener-Plancherel formula, are topological isomorphisms. The first mapping is a consequence of an important result by Beurling [13], coupled with an extraordinarily clever insight of my student C. Heil [28]. The second mapping is due to Chen and Lau [14]. Taking $d \geqslant 1$ and using the rectilinear Wiener-Plancherel formula in [7], Heil also proved that the mapping $B(2,q) \to V(2,q)$ is a topological isomorphism for $1 \leqslant q \leqslant \infty$.

5.2. The spherical Wiener-Plancherel formula

As mentioned in Formula 5.1, we need the following example in the basic formula (5.1) and in Theorem 5.6.

Example 5.4. For each dimension $d \geq 2$, we utilize the function,

$$K_k(r) = r^{4k-d}\left(1 - \frac{2\pi}{\omega_{d-1}}\left(\frac{1}{r}\right)^{-\frac{d-2}{2}} J_{\frac{d-2}{2}}\left(\frac{2\pi}{r}\right)\right)^2,$$

where $k \geq 0$ is an integer, $r > 0$, and J is a Bessel function of the first kind.

Definition/Remark 5.5.

1) The space $B^2(\mathfrak{R}^d)$ of functions having *bounded quadratic means over spheres* is the set of all functions $\phi \in L_{loc}{}^2(\mathfrak{R}^d)$ for which

$$\|\phi\|_{B^2(\mathfrak{R}^d)} = \sup_{R>0}\left(\frac{1}{|B(0,R)|}\int_{B(0,R)}|\phi(t)|^2 dt\right)^{1/2} < \infty. \qquad (5.4)$$

$B^2(\mathfrak{R}^d)$ is a Banach space with norm defined by (5.4).

2) Given $\phi \in L_{loc}{}^2(\mathfrak{R}^d)$. The *spherical average of* ϕ is the function Φ defined as

$$\Phi(r) = \frac{1}{\omega_{d-1}}\int_{\Sigma_{d-1}}|\phi(r\theta)|^2 d\sigma_{d-1}(\theta), \qquad r > 0. \qquad (5.5)$$

3) A basic property of spherical averages, and one that is relevant for comparison with the classical and rectangular Wiener-Plancherel formulas [7], is that

$$\Phi \in L^\infty \text{ implies } \phi \in B^2(\mathfrak{R}^d). \qquad (5.6)$$

The verification of (5.6) is immediate:

$$\frac{1}{|B(0,R)|}\int_{B(0,R)}|\phi(t)|^2 dt = \frac{\omega_{d-1}}{|B(0,R)|}\int_0^R r^{d-1}\Phi(r)dr$$
$$\leq \frac{\|\Phi\|_\infty}{d|B(0,R)|}\omega_{d-1}R^d = \|\Phi\|_\infty.$$

4) Clearly $B^2(\mathfrak{R}^d)\backslash L^\infty(\mathfrak{R}^d) \neq \emptyset$. In fact, we can choose a continuous radial element $\phi \in L^2(\mathfrak{R}^d)$ for which $\overline{\lim}_{r\to\infty}|\phi(r)| = \infty$. This function also shows that the converse of (5.6) fails since $\Phi(r) = |\phi(r)|^2$. Further, this observation shows that, for the class of radial continuous functions, $\Phi \in L^\infty$ if and only if $\phi \in L^\infty(\mathfrak{R}^d)$.

The following result is our spherical Wiener-Plancherel formula. Wiener's Tauberian theorem (for the multiplicative group of reals) plays an essential role in its proof.

Theorem 5.6. [6] Given $\phi \in L_{loc}{}^2(\mathfrak{R}^d)$, which is bounded in a neighborhood of the origin, and an integer k for which $4(k-1) < d < 4k$ and $d > 2k$ ($d > 4(k-1)$ implies $d > 2k$ for $k \geq 2$.) Assume the spherical average Φ of ϕ is an element of L^∞. Then $s_k = (\phi E_k^\vee)^\wedge \in \mathcal{S}'(\hat{\mathfrak{R}}^d)$, and the spherical Wiener-Plancherel formula (5.1) is valid in the sense that if the left side exists then the right side exists and they are equal. The constant $c(d,k)$ in (5.1) has the explicit representation,

$$c(d,k)^{-1} = \int_0^\infty K_k(r)\frac{dr}{r}.$$

Another technical ingredient in the proof of Theorem 5.6 is stated separately below as Theorem 5.7 because of its use in Example 5.4.

5.3. The Laplacian and spherical mean value operator

Theorem 5.7. Given $g \in L^2(\hat{\mathfrak{R}}^d)$, $\alpha \in \mathbb{C}$, and $f \in \mathcal{S}'(\hat{\mathfrak{R}}^d)$. Assume f satisfies the following conditions: $f^\vee \in \mathcal{S}'(\mathfrak{R}^d)$ is a Borel measurable function,

$$\exists R > 0, \text{ such that } f^\vee \in L_{loc}{}^2(B(0,R)^c),$$

and

$$|t|^2 f^\vee(t) \in L_{loc}{}^2(\mathfrak{R}^d).$$

Then $f - \mathcal{M}_\lambda f \in L^2(\hat{\mathfrak{R}}^d)$ and

$$\|g - \alpha(f - \mathcal{M}_\lambda f)\|_2 = \left\| g^\vee(t) - \alpha f^\vee(t)\left(1 - \frac{2\pi}{\omega_{d-1}}(|t|\lambda)^{-\frac{d-2}{2}} J_{\frac{d-2}{2}}(2\pi|t|\lambda)\right)\right\|_2. \tag{5.7}$$

Proof.

1) The hypothesis, $|t|^2 f^\vee(t) \in L_{loc}{}^2(\mathfrak{R}^d)$, implies that $f^\vee \in L_{loc}{}^2(\mathfrak{R}^d \setminus \{0\})$. In fact, if $K \subseteq \mathfrak{R}^d$ is compact and $0 \notin K$ then

$$\int_K |f^\vee(t)|^2 dt = \int_K \frac{|t|^4}{|t|^4}|f^\vee(t)|^2 dt \leq C \int_K |t|^4 |f^\vee(t)|^2 dt < \infty.$$

If we did not assume $f^\vee$ to be a Borel measurable function then it could contain terms of the form $\partial^\beta \delta$.

2) We now prove

$$f^\vee(t)\theta_\lambda(t) = f^\vee(t)\left(1 - \frac{2\pi}{\omega_{d-1}}(|t|\lambda)^{-\frac{d-2}{2}} J_{\frac{d-2}{2}}(2\pi|t|\lambda)\right) \in L^2(\mathfrak{R}^d). \tag{5.8}$$

Since $f^\vee(t) \in L^2(B(0,R)^\sim)$ and

$$\sup_{|t|\geq R} |t|^{-d+2} J_{\frac{d-2}{d}}(2\pi|t|\lambda)^2 \leq C \sup_{|t|\geq R} |t|^{-d+2}(2\pi|t|\lambda)^{-1} \leq C_\lambda \sup_{|t|\geq R} |t|^{-d+1} \leq C_\lambda R^{-d+1}$$

it is sufficient for (5.8) to dominate

$$I = \int_{B(0,R)^\sim} \left| f^\vee(t)\left(1 - \frac{2\pi}{\omega_{d-1}}(|t|\lambda)^{-\frac{d-2}{2}} J_{\frac{d-2}{d}}(2\pi|t|\lambda)\right)\right|^2 dt. \tag{5.9}$$

This integral is

$$\int_{B(0,R)^\sim} \left| f^\vee(t)\left\{\left(1 - \frac{2\pi}{\omega_{d-1}}(|t|\lambda)^{-\frac{d-2}{2}}\left(\frac{2\pi|t|\lambda}{2}\right)^{d-2+2} \frac{1}{\Gamma(d/2)}\right)\right.\right.$$
$$\left.\left. - \frac{2\pi}{\omega_{d-1}}(|t|\lambda)^{-\frac{d-2}{2}}\left(\frac{2\pi|t|\lambda}{2}\right)^{\frac{d-2}{2}} \sum_{k=1}^{\infty} \frac{(-\frac{1}{4}(2\pi|t|\lambda)^2)^k}{k!\Gamma(\frac{d-2}{2}+k+1)}\right\}\right|^2 dt$$
$$= \int_{B(0,R)^\sim} \left| f^\vee(t)\left\{\frac{2\pi}{\omega_{d-1}}^{\frac{d}{2}} \sum_{k=1}^{\infty} \frac{(-\pi^2|t|^2\lambda^2)^k}{k!\Gamma(\frac{d}{2}+k)}\right\}\right|^2 dt.$$

Thus, by Minkowski's inequality, we have

$$I^{1/2} \leq \sum_{k=1}^{\infty} \left\| f^\vee(t) \frac{2\pi}{\omega_{d-1}}^{d/2} \frac{(\pi|t|\lambda)^{2k}}{k!\Gamma(\frac{d}{2}+k)}\right\|_{L^2(B(0,R)^\sim)}$$
$$= \Gamma\left(\frac{d}{2}\right) \sum_{k=1}^{\infty} \frac{(\pi\lambda)^{2k}}{k!\Gamma(\frac{d}{2}+k)} \|f^\vee(t)|t|^{2k}\|_{L^2(B(0,R)^\sim)};$$

and this is finite since $|t|^2 f^\vee(t) \in L_{loc}{}^2(\mathfrak{R}^d)$. As a consequence, (5.8) is valid.

3) Distributionally, we have

$$\forall \psi \in \mathcal{S}(\mathfrak{R}^d), \qquad (f^\vee\theta_\lambda)(\overline{\psi}) = (f^\vee\theta_\lambda)^\wedge(\overline{\hat{\psi}}).$$

The left hand side is

$$\int f^{\vee}(t)(\theta_\lambda \overline{\psi})(t)dt = \int f^{\vee}(t)\overline{(\theta_\lambda(t)\psi(t))}dt = \overline{f(\theta_\lambda\psi)^{\wedge}}$$

$$= f(\gamma)\left(\int\left(1 - \frac{1}{\omega_{d-1}}\int_{\Sigma_{d-1}} e^{-2\pi i t\cdot\lambda\theta}d\sigma_{d-1}(\theta)\right)\psi(t)e^{-2\pi i t\cdot\gamma}dt\right)^{-}$$

$$= f(\gamma)\left(\hat{\psi}(\gamma)\right.$$

$$\left. -\frac{1}{\omega_{d-1}}\int_{\Sigma_{d-1}}\left(\int\psi(t)e^{-2\pi i t\cdot(\gamma+\lambda\theta)}dt\right)d\sigma_{d-1}(\theta)\right)^{-}$$

$$= f(\hat{\psi} - \mathcal{M}_\lambda\hat{\psi})^{-} = f(\hat{\psi})^{-} - (\mathcal{M}_\lambda^* f)(\hat{\psi})^{-} = (f - \mathcal{M}_\lambda f)(\overline{\hat{\psi}}).$$

Thus, $f - \mathcal{M}_\lambda f = (f^{\vee}\theta_\lambda)^{\wedge}$.

Since $f^{\vee}\theta_\lambda \in L^2(\mathfrak{R}^d)$ we know that $(f^{\vee}\theta_\lambda)^{\wedge} \in L^2(\mathfrak{R}^d)$, and, hence, that $f - \mathcal{M}_\lambda f \in L^2(\mathfrak{R}^d)$. (5.7) is a consequence of the Plancherel theorem.

■

The operator (on the function f),

$$\frac{-2d}{\lambda^2}(f - \mathcal{M}_\lambda f),$$

corresponds to the Laplacian in $\mathfrak{R}^d$ in the same way the difference operator,

$$\frac{1}{2\lambda}(\tau_{-\lambda}f - \tau_\lambda f), \tag{5.10}$$

corresponds to the ordinary derivative in $\mathfrak{R}$, cf. [7] for the rectangular generalization of (5.10) to $\mathfrak{R}^d$ and Item 1 of Remark 5.2 for the corresponding differential operator. Wiener made the following calculation for the case $d = 3$ [53, Volume III, pp. 718–727] (1927).

"Theorem" 5.8. Given $f \in \mathcal{S}'(\mathfrak{R}^d)$ for which $\Delta f \in L^2(\mathfrak{R}^d)$ and $f^{\vee}$ is Borel measurable. Then

$$\lim_{\lambda\to 0}\left\|\Delta f - \left(-\frac{2d}{\lambda^2}\right)(f - \mathcal{M}_\lambda f)\right\|_2 = 0. \tag{5.11}$$

"Proof". Since Δf is a convolution of $f \in \mathcal{S}'(\mathfrak{R}^d)$ and a distribution having compact support, the exchange formula is valid and $\Delta f^{\vee}(t) = -4\pi^2|t|^2 f^{\vee}(t) \in \mathcal{S}'(\mathfrak{R}^d)$. The hypothesis, $\Delta f \in L^2(\mathfrak{R}^d)$, allows us to

conclude that $-4\pi^2|t|^2 f^\vee(t) \in L^2(\mathfrak{R}^d)$. In particular, the hypotheses of Theorem 5.7 are satisfied and so we have

$$\begin{aligned}&\left\|\Delta f - \left(-\frac{2d}{\lambda^2}\right)(f - \mathcal{M}_\lambda f)\right\|_2 \\ &\quad = \left\| f^\vee(t)\left(\frac{2d}{\lambda^2}\left\{1 - \frac{2\pi^2|t|^2\lambda^2}{d}\right.\right.\right. \\ &\qquad \left.\left.\left. - \frac{2\pi}{\omega_{d-1}}(|t|\lambda)^{-\frac{d-2}{2}} J_{\frac{d-2}{2}}(2\pi|t|\lambda)\right\}\right)\right\|_2 .\end{aligned} \tag{5.12}$$

Using the series representation of J_ν, the right side of (5.12) becomes

$$\begin{aligned}&\left\| f^\vee(t)\left(\frac{2d}{\lambda^2}\left\{\left[1 - \frac{2\pi}{\omega_{d-1}}(|t|\lambda)^{-\frac{d-2}{2}}\left(\frac{2\pi|t|\lambda}{2}\right)^{\frac{d-2}{2}}\frac{1}{\Gamma\left(\frac{d}{2}\right)}\right]\right.\right. \\ &\qquad + \left[-\frac{2(\pi|t|\lambda)^2}{d}\right. \\ &\qquad\quad \left.\left. - \frac{2\pi}{\omega_{d-1}}(|t|\lambda)^{-\frac{d-2}{2}}\left(\frac{2\pi|t|\lambda}{2}\right)^{\frac{d-2}{2}}\left(\frac{-(\pi|t|\lambda)^2}{\Gamma\left(\frac{d}{2}+1\right)}\right)\right] \right. \\ &\qquad \left.\left. - \frac{2\pi^{d/2}}{\omega_{d-1}}\sum_{k=2}^{\infty}\frac{(-(\pi|t|\lambda)^2)^k}{k!\Gamma\left(\frac{d}{2}+k\right)}\right\}\right)\Bigg\|_2 \\ &\quad = 2d\Gamma\left(\frac{d}{2}\right)\left\| f^\vee(t)\frac{1}{\lambda^2}\sum_{k=2}^{\infty}\frac{(-(\pi|t|\lambda)^2)^k}{k!\Gamma\left(\frac{d}{2}+k\right)}\right\|_2 ,\end{aligned} \tag{5.13}$$

where we use the fact, $\Gamma(d/2 + 1) = d/2\,\Gamma(d/2)$, to eliminate the $k = 1$ term.

The right side of (5.13) *formally* tends to 0 as λ tends to 0 since $k \geq 2$.

5.4. Multidimensional spectral estimation

Definition 5.9. Given $\phi \in L^2_{loc}(\mathfrak{R}^d)$ and define

$$\forall R > 0, \qquad P_{\phi,R}(t) = \frac{1}{|B(0,R)|}\int_{B(0,R)} \phi(t + x)\overline{\phi(x)}\,dx.$$

Suppose that there is a continuous positive definite function P_ϕ for which $\lim_{R\to\infty} P_{\phi,R} = P_\phi$ in the $\sigma(M(\mathfrak{R}^d), C_c(\mathfrak{R}^d))$ topology, where $M(\mathfrak{R}^d)$ is the space of measures on $\mathfrak{R}^d$. Then $P_\phi \in L^\infty(\mathfrak{R}^d)$ is the *autocorrelation* of ϕ, and the positive measure $\mu_\phi = \hat{P}_\phi$ is the *power spectrum* of ϕ, cf. the Wiener-Khinchin theorem (Theorem 2.2).

Remark 5.10.

1) Depending on the particular problem, the weak topology in Definition 5.9 can be replaced by various other convergence criteria, including pointwise convergence.
2) Given $\phi \in L_{loc}{}^2(\mathfrak{R}^d)$ with power spectrum μ_ϕ, and assume there is an increasing function $i(R)$ on $(0,\infty)$ for which $\sup_{|t|\le R}|\phi(t)| \le i(R)$ and $\lim_{R\to\infty} i(R)^2/R = 0$. Then we can prove that

$$\forall \psi \in C_c(\mathfrak{R}^d), \tag{5.14}$$
$$\lim_{R\to\infty} \frac{1}{|B(0,R)|}\int_{B(0,R)} |\psi * \phi(t)|^2 dt = \int |\hat{\psi}(\gamma)|^2 d\mu_\phi(\gamma),$$

[2, Section 5].

If we take $\psi = \delta$ in (5.14) then the left side of (5.14) is the arithmetic mean on the left side of our Wiener-Plancherel formula (5.1). Given $\phi \in L_{loc}{}^2(\mathfrak{R}^d)$ and combining the formulas (5.1) and (5.14), it is then reasonable to expect that

$$\lim_{\lambda\to 0} \frac{c(d,k)(2\pi)^{4k}}{\omega_{d-1}\lambda^{4k-d}} |D_\lambda s_k|^2 = \mu_\phi \tag{5.15}$$

in some weak topology. In this same spirit we provide the following calculation which Wiener made for the case $d = 1$ [53, Volume II, pp. 219–223] (1930).

Formula calculation 5.11. Given $\phi \in L_{loc}{}^2(\mathfrak{R}^d)$ with autocorrelation P_ϕ. For $t \in \mathfrak{R}^d$,

$$\lim_{\lambda\to 0} \frac{c(d,k)(2\pi)^{4k}}{\omega_{d-1}\lambda^{4k-d}} \int |D_\lambda s_k(\gamma)|^2 e^{2\pi i t\cdot\gamma} d\gamma = P_\phi(t). \tag{5.16}$$

"Proof".

1) A direct calculation gives

$$\begin{aligned} P_\phi(t) &= \lim_{R\to\infty} \frac{1}{|B(0,R)|}\int_{B(0,R)} \phi(t+x)\overline{\phi(x)}dx \\ &= \frac{1}{4}\lim_{R\to\infty} \frac{1}{|B(0,R)|}\int_{B(0,R)} \{|\phi(t+x)+\phi(x)|^2 \\ &\quad - |\phi(t+x)-\phi(x)|^2 + i|\phi(t+x)+i\phi(x)|^2 \\ &\quad - i|\phi(t+x)-i\phi(t)|^2\}\,dt \\ &= \frac{1}{4}(K_1 - K_2 + iK_3 - iK_4). \end{aligned} \tag{5.17}$$

2) Let $\psi(x) = \phi(t + x) + c\phi(x)$, where $|c| = 1$; and write $s_k(\vartheta)(\gamma) = (\vartheta E_k^{\vee})^{\wedge}(\gamma)$, so that $s_k(\phi) = s_k$. By the Wiener-Plancherel formula we compute the following

$$\begin{aligned}
&\lim_{R\to\infty} \frac{1}{|B(0,R)|} \int_{B(0,R)} |\psi(x)|^2 dx \\
&= \lim_{\lambda\to 0} \frac{c(d,k)(2\pi)^{4k}}{\omega_{d-1}\lambda^{4k-d}} \int |D_\lambda s_k(\tau_{-t}\phi)(\gamma) + D_\lambda s_k(c\phi)(\gamma)|^2 \, d\gamma \\
&= \lim_{\lambda\to 0} \frac{c(d,k)(2\pi)^{4k}}{\omega_{d-1}\lambda^{4k-d}} \int |D_\lambda s_k(\tau_{-t}\phi)(\gamma) - e^{2\pi i t\cdot\gamma} D_\lambda s_k(\phi)(\gamma) \\
&\qquad + (c + e^{2\pi i t\cdot\gamma}) D_\lambda s_k(\phi)(\gamma)|^2 \, d\gamma \\
&= E + \lim_{\lambda\to 0} \frac{c(d,k)(2\pi)^{4k}}{\omega_{d-1}\lambda^{4k-d}} \int |D_\lambda s_k(\phi)(\gamma)|^2 \, |c + e^{2\pi i t\cdot\gamma}|^2 \, d\gamma,
\end{aligned} \tag{5.18}$$

where the "error" E is estimated by

$$\begin{aligned}
&\lim_{\lambda\to 0} \frac{c(d,k)(2\pi)^{4k}}{\omega_{d-1}\lambda^{4k-d}} \\
&\quad \cdot \int |D_\lambda s_k(\tau_{-t}\phi)(\gamma) - e^{2\pi i t\cdot\gamma} D_\lambda s_k(\phi)(\gamma)|^2 \, d\gamma.
\end{aligned} \tag{5.19}$$

Under natural hypotheses, and implementing Theorem 5.7 we can show that the limit in (5.19) vanishes, i.e., $E = 0$.

3) We now combine the right side of (5.17) and (5.18) with $E = 0$, for the four cases $c = \pm 1, \pm i$. Thus,

$$\begin{aligned}
P_\phi(t) = \frac{1}{4} \lim_{\lambda\to 0} \frac{c(d,k)(2\pi)^{4k}}{\omega_{d-1}\lambda^{4k-d}} \int |D_\lambda s_k(\gamma)|^2 \\
\cdot [(2 + e_{-t}(\gamma) + e_t(\gamma)) - (2 - e_{-t}(\gamma) - e_t(\gamma)) \\
+ i(2 + ie_{-t}(\gamma) - ie_t(\gamma)) - i(2 - ie_{-t}(\gamma) + ie_t(\gamma))] d\gamma,
\end{aligned}$$

where $e_u(\gamma) = e^{2\pi i u\cdot\gamma}$. Combining terms, we obtain (5.16).

Formally, (5.15) and (5.16) are compatible. If we are given data ϕ_S on a set S, these formulas lead us to consider multidimensional *spectral estimators* molded from expressions of the form

$$\frac{c(d,k)(2\pi)^{4k}}{\omega_{d-1}\lambda^{4k-d}} \left| D_\lambda(\phi_S * f_k) \right|^2. \tag{5.20}$$

Instead of continuing this section with a quodlibetic discussion of spectral estimation, we shall refer to the classical spectral estimation algorithms and results on evolutionary spectra for nonstationary processes, e.g., [46, Chapter 11].

6. Notation

Let G be a locally compact abelian group with dual group Γ, e.g., $G = \mathfrak{R}^d$ and $\Gamma = \hat{\mathfrak{R}}^d$, where $\mathfrak{R}^d = \hat{\mathfrak{R}}^d$ is d-dimensional Euclidean space, or $G = \mathcal{T} = \mathfrak{R}/\mathcal{Z}$ and $\Gamma = \mathcal{Z}$, the group of integers. $M_b(\Gamma)$, resp., $M_+(\Gamma)$, is the space of bounded, resp., positive, Radon measures on Γ; and $M_{b+}(\Gamma) = M_b(\Gamma) \cap M_+(\Gamma)$. $L^p_\mu(\mathfrak{R}^d)$ is the weighted L^p-space defined by its norm, $\|f\|_{p,\mu} = (\int |f|^p d\mu)^{1/p}$, where $1 \leqslant p < \infty$, $\mu \in M_+(\Gamma)$, and integration is over Γ.

The Fourier transform of $f \in L^1(\mathfrak{R}^d)$ is $\hat{f}(\gamma) = \int f(t)e^{-2\pi i t\cdot\gamma}dt$, where integration is over $\mathfrak{R}^d$; and $\mu^\vee$ designates the inverse Fourier transform of $\mu \in M_b(\Gamma)$.

If $S \subseteq G$ then $|S|$ is its Haar measure and 1_S is the characteristic function of S. $\delta_{m,n}$ is 1 if $m = n$ and 0 if $m \neq n$. Finally, if X is contained in a topological vector space H then spX is the linear span of X in H, and $\overline{\text{sp}}X$ is its closure in H.

7. Bibliography

[1] N. Akhiezer. *Theory of Approximation.* Ungar Publishing, New York, 1956.

[2] J.J. Benedetto. The multi-dimensional Wiener-Wintner theorem and spectrum estimation. *Trans. AMS*, 237. To appear.

[3] J.J. Benedetto. Harmonic analysis and spectral estimation. *J. Math. Analysis Appl.*, 91:444–509, 1983.

[4] J.J. Benedetto. Fourier uniqueness criteria and spectrum estimation theorems. *Fourier techniques and applications*, pages 149–170, 1985. Plenum Publishing, J.F. Price, ed.

[5] J.J. Benedetto. Uncertainty principle inequalities and spectrum estimation. In J.S. Byrnes and Jennifer L. Byrnes, editors, *Recent Advances in Fourier Analysis and its Applications: Proceedings of the NATO Advanced Study Institute*, volume 315 of *NATO ASI series C: Mathematical and physical sciences*, pages 143–182, Dordrecht, Boston, London, 1990. Kluwer Academic Publishers Group. Held at Il Ciocco Resort, Tuscany, Italy.

[6] J.J. Benedetto. The spherical Wiener-Plancherel formula and spectral estimation. *SIAM J. Math. Analysis*, 21, 1991.

[7] J.J. Benedetto, G. Benke, and W. Evans. An n-dimensional Wiener-Plancherel formula. *Advances in Applied Math*, 10:457–487, 1989.

[8] J.J. Benedetto and H. Heinig. Fourier transform inequalities with measure weights. *Advances in Math.* To appear.

[9] J.J. Benedetto and H. Heinig. Weighted Hardy spaces and the Laplace transform. In *Lecture Notes in Math*, **992**, pages 240–277. Harmonic Analysis Conf., Cortona Italy, 1982, Springer-Verlag, 1983.

[10] J.J. Benedetto, H. Heinig, and R. Johnson. Fourier inequalities with A_p-weights. *ISNM*, 80:217–232, 1987. Birkhäuser Verlag.

[11] J.J. Benedetto and W. Heller. Irregular sampling and the theory of frames, I. *Note. Mat*, Special Köthe volume, 1991.

[12] M. Benedicks. Supports of Fourier transform pairs and related problems on positive harmonic functions. *TRITA-MAT*, 10, 1980. Stockholm.

[13] A. Beurling. Construction and analysis of some convolution algebras. *Ann. Inst. Fourier*, 14:1–32, 1964. Grenoble.

[14] Y.-Z. Chen and K.-S. Lau. Harmonic analysis on functions with bounded means. *Contemp. Math*, 91:165–175, 1989. Commutative harmonic analysis, 1987, D. Collela, ed.

[15] T.-P. Chiang. On the linear extrapolation of a continuous homogeneous field. *Theory Prob. Appl*, 2:58–89, 1957.

[16] H. Cramér. On the theory of stationary random processes. *Annals of Math.*, 41:215–230, 1940.

[17] H. Cramér. Half a century with probability theory: some personal recollections. *Annals of Prob.*, 4:509–546, 1976.

[18] I. Daubechies. The wavelet transform, time-frequency localization and signal analysis. *IEEE Trans. Inf. Theory*, 39:961–1005, 1990.

[19] R. Duffin and A. Schaeffer. A class of nonharmonic Fourier series. *Trans. Am. Math. Soc*, 72:341–366, 1952.

[20] H. Dym and H. McKean. *Gaussian Processes, Function Theory, and the Iniverse Spectral Problem*. Academic Press, New York, 1976.

[21] C. Fefferman. On the convergence of multiple Fourier series. *Bull. AMS*, 77:744–745, 1971.

[22] J.-P. Gabardo. Tempered distributions supported on a half-space of R^n and their Fourier transforms. *Canad. J. Math.* To appear.

[23] J.-P. Gabardo. Two problems in multidimensional prediction theory. *Mich. J. Math.* To appear.

[24] J.-P. Gabardo. Weighted L^p spaces and the Fourier transform of functions with compact support. *To be submitted.*

[25] J.-P. Gabardo. Tempered distributions with spectral gaps. *Math. Proc. Camb. Phil. Soc.*, 106:143–162, 1989.

[26] J. García-Cuerva and J. Rubio de Francia. *Weighted Norm-inequalities and Related topics.* North-Holland, Elsevier Science Publishers, New York, 1985.

[27] W. Gardner. *Statistical Spectral Analysis—A Nonprobabilistic Theory.* Prentice Hall, New Jersey, 1988.

[28] C. Heil. *Wiener amalgam spaces in generalized harmonic analysis and wavelet theory.* PhD thesis, University of Maryland, College Park, 1990.

[29] C. Heil and D. Walnut. Continuous and discrete wavelet transforms. *SIAM Review*, 31:628–666, 1989.

[30] H. Helson. *Lectures on Invariant Subspaces.* Academic Press, New York, 1964.

[31] H. Helson and D. Lowdenslager. Prediction theory and Fourier series in several variables, I. *Acta. Math*, 99:165–202, 1958.

[32] H. Helson and D. Lowdenslager. Prediction theory and Fourier series in several variables, II. *Acta. Math*, 106:175–213, 1961.

[33] H. Helson and G. Szegö. A problem in prediction theory. *Annali di Mat.*, 51:107–138, 1960.

[34] J. Higgins. *Completeness and Basis Properties of Sets of Special Functions.* Cambridge University Press, 1977.

[35] L. Hörmander. The Analysis of Linear Partial Differential Operators, 1983. Volumes I and II, Springer-Verlag, New York.

[36] A. Janssen. The Zak transform: a single transform for sampled time-continuous signals. *Philips J. Research*, 43:23–69, 1988.

[37] G. Kallianpur, A. Miamee, and H. Niemi. On the prediction theory of two parameter stationary random fields. *J. Multivariate Analysis*, 32:120–149, 1990.

[38] R. Kerby. *The correlation function and the Wiener-Wintner theorem in higher dimensions.* PhD thesis, University of Maryland, College Park, 1990.

[39] A.N. Kolmogorov. Stationary sequences in Hilbert space. *Bull. Moscow State U,* Math. 2(6), 1941. 40 pages. (Translation by G. Kallianpur).

[40] G. Köthe. Das Trägheitsgesetz der quadratischen Formen im Hilbertschen Raum. *Math. Z,* 41:137–152, 1936.

[41] J. Lakey. *Weighted norm inequalities for the Fourier transform.* PhD thesis, University of Maryland, College Park, 1991.

[42] J. Lamperti. *Stochastic Processes.* Springer-Verlag, New York, 1977.

[43] P. Masani. The prediction theory of multivariate stochastic processes, III. *Acta Math.*, 104:141–162, 1960.

[44] P. Masani. *Norbert Wiener.* Birkhäuser Verlag, Boston, Massachusetts, 1990.

[45] A. Papoulis. *Probability, Random Variables, and Stochastic Processes.* McGraw-Hill, New York, second edition, 1984.

[46] M. Priestley. *Spectral Analysis and Time Series.* Academic Press, New York, 1981.

[47] Yu. Rozanov. On stationary sequences forming a basis, 1960. *Dokl. Akad. Nauk,* SSSR, 130:1199–1202, (Russian). Soviet Math. Dokl., 1:155–158, 1960.

[48] W. Rudin. *Fourier Analysis on Groups.* J. Wiley and Sons, New York, 1962.

[49] L. Schwartz. *Théorie des Distributions.* Hermann, Paris, 1966.

[50] E. Stein and G. Weiss. *Fourier Analysis on Euclidean Spaces.* Princeton University Press, Princeton, New Jersey, 1971.

[51] G. Vitali. Sulla condizione di chiusura di un sistema di funzioni ortogonali. *Atti R. Accad. Naz. Lincei, Rend. Cl. Sci. Fis. Mat. Nat,* 30:498–501, 1921.

[52] J. von Neumann. *Mathematical Foundations of Quantum Mechanics.* Princeton University Press, 1955. Also, 1932 and 1949.

[53] N. Wiener. *Collected Works.* M.I.T. Press, Cambridge, Massachusetts. (P. Masani, editor).

[54] N. Wiener. *Cybernetics.* M.I.T. Press, Cambridge, Massachusetts, second edition, 1961. Also 1948.

[55] G. Yang. *Applications of the Wiener Tauberian theorem to a filtering problem.* PhD thesis, University of Maryland, College Park, 1990.

[56] R. Young. *An Introduction to Nonharmonic Fourier Series.* Academic Press, New York, 1980.

Density of fuzzy attractors: A step towards the solution of the inverse problem for fractals and other sets

Carlos Cabrelli
Department of Applied Mathematics
University of Waterloo
Waterloo, Ontario N2L 3G1 Canada
ccabrelli@poppy.waterloo.edu
Also at Department of Mathematics, Universidad de Buenos Aires,
Pab.I Cdad. Universitaria (1428), Cap.Fed. Argentina

Ursula Molter
ummolter@poppy.waterloo.edu
(Other addresses the same.)

Abstract The theory of iterated fuzzy set systems, *IFZS*, was introduced by Cabrelli et al. in [4]. They showed that by combining the idea of representing an image as a fuzzy set with the theory of iterated function systems, it is possible to generate images with grey or colour levels as attractors of IFZS. The purpose of this paper is to show that the class of attractors of IFZS is dense in the class of images, i.e., each image can be approximated with the desired accuracy. A brief review of the main concepts of IFZS is presented first.

1. Introduction

We first want to present an overview of the theory of iterated fuzzy set systems (IFZS). Since a complete development of the theory can be found in [4], we are going to omit most of the proofs. We then show that the set of images that can be obtained using this approach, is dense in the set of all images.

The notion of self-similarity and its generalizations[1], has found a natural frame in the theory of iterated function systems (IFS): self-similar sets became attractors of certain systems of maps [10, 1, 8]. The generalization of the concept of self-similarity to a more general class of maps—other than similarities, introduced more flexibility in the model, widening the class of sets that have the property to be expressed as smaller copies of themselves.

[1] A subset S of an arbitrary set X, is said to be self-similar (in the wide sense) if there exist a finite number of maps $f_1, \ldots, f_N$, $f_i : X \to X$ such that $S = \bigcup_{1 \le i \le N} f_i(S)$

J. S. Byrnes et al. (eds.), Probabilistic and Stochastic Methods in Analysis, with Applications, 163–173.
© 1992 Kluwer Academic Publishers. Printed in the Netherlands.

On the other hand, the use of IFS enabled the construction of self-similar sets of fractional dimensions, and therefore this theory has found wide applications in computer graphics to generate fractal images on computers (see for example [3, 13]). The ergodicity involved in the process is another advantage that this method provides in image generation and representation, see [7].

One of the major applications of IFS theory in image processing, is in data compression: huge amounts of data can be squeezed into a few number of parameters. Two questions naturally arise:

- Which kind of images can be represented through this model, or, how big is the class of images that can be represented through IFS?
- Is there an efficient algorithm or method to find that representation?

Regarding the first question, in the case that the maps are contractive but not necessarily similarities, it has been shown [9] that this class is dense in the class of compact sets. In image processing language this means, that to any object in a black and white image, one can associate an IFS code. This result shows that the so-called inverse problem for fractals and other sets, that is to find the IFS code associated with any given black and white image, has at least one solution. It is well known however, that in most of the cases the solution that can be constructed from the proof of the theorem does not yield good compression rate. It is a very difficult problem to find an efficient IFS code for a given black and white image. Some results in that direction for the one dimensional case can be found in [2, 5, 16].

In the case of images with grey-levels, the IFS theory provides us with a class of measures that are generated by adding a probability vector to each IFS code. The ergodicity allows one to generate this measure through a random iterative algorithm. This approach however, seems to have two weak points: first, the relation between the parameters and the resulting measure is not straightforward, and this then becomes a serious difficulty for the inverse problem. Secondly, the class of measures that can be obtained through IFS, seems not to be as wide as desirable. The question of how big this class of measures is in relation to a suitable space of measures (here suitable refers to images) seems to be still open.

The IFZS approach to grey-level images considers images as functions rather than measures, and hereby tends to avoid these problems. In that direction, Theorem 3.1 of this paper shows that the class of images that can be generated using IFZS is dense in the class of images, i.e., given a grey-level image, we prove that for a given ε there exists an IFZS whose attractor is closer than ε to that image.

2. The iterated fuzzy set systems (IFZS)

2.1. Iterated function systems (IFS)

s Let us briefly recall the basic notions of IFS. Given a compact metric space (X, d) with distance d, let us consider N contraction mappings $w_i : X \to X$. The metric space X, together with the N contraction mappings is referred to as an Iterated Function System (IFS) and denoted by $\{X, \mathbf{w}\}$. Usually, in applications, X is a compact subset of $\Re^n$.

If $\mathcal{H}(\mathcal{X})$ denotes the set of all nonempty closed subsets of X, we can define N set-valued maps $\widehat{w}_i : \mathcal{H}(\mathcal{X}) \to \mathcal{H}(\mathcal{X})$, by $\widehat{w}_i(S) = \{w_i(x) : x \in S\}$, e.g. the image of S under the transformation w_i, for all $S \in \mathcal{H}(\mathcal{X})$. If h is the Hausdorff distance in $\mathcal{H}(\mathcal{X})$:

$$h(A, B) := \max\{D(A, B), D(B, A)\} \tag{2.1}$$

where

$$D(A, B) = \sup_{x \in A} \inf_{y \in B} d(x, y) \tag{2.2}$$

then $(\mathcal{H}(\mathcal{X}), h)$ is a compact metric space, and $\widehat{w}_i$ are contraction mappings of $\mathcal{H}(\mathcal{X})$. The map $W : \mathcal{H}(\mathcal{X}) \to \mathcal{H}(\mathcal{X})$ defined by:

$$W(S) = \bigcup_{i=1}^{N} \widehat{w}_i(S), \quad \forall S \in \mathcal{H}(\mathcal{X}) \tag{2.3}$$

is also a contraction on $\mathcal{H}(\mathcal{X})$. Therefore it possesses an unique fixed point (or invariant set) $\mathcal{A}$, called the *attractor* of the IFS;

$$\mathcal{A} = W(\mathcal{A}) = \bigcup_{i=1}^{N} \widehat{w}_i(\mathcal{A}). \tag{2.4}$$

This shows that $\mathcal{A}$ is self-similar with respect to $w_1, \ldots, w_N$. This property is sometimes referred to as the *self-tiling* property of IFS attractors, meaning that $\mathcal{A}$ can be built with smaller copies of itself. As well, the name *attractor* is justified by the following property:

$$h(W^n(S), \mathcal{A}) \longrightarrow 0 \qquad \text{as } n \to \infty, \forall S \in \mathcal{H}(\mathcal{X}). \tag{2.5}$$

2.2. Fuzzy sets as generalization of sets

The notion of fuzzy sets introduced by Zadeh in 1965 [17], has been widely used in different contexts. We want to use it here in the sense of a generalization of the concept of *set*: If X is an arbitrary (non empty) set, a *fuzzy set* (in X) is a function **u** with domain X and values in $[0, 1]$, i.e., $\mathbf{u} : X \to [0, 1]$.

In particular, if S is an ordinary subset of X, its characteristic function χ_S is a fuzzy set. To relate this concept with images, we think of a digitized picture as a set of pixels, each of which has associated a *grey-level*; the value 1 representing *black* or the foreground, the value 0 representing *white* or the background. The value $\mathbf{u}(x)$ then corresponds to the grey-level of the pixel x. If the image is black and white, we only have two values: 0 or 1, and therefore we can represent it by a characteristic function, or a "set."

If $\mathcal{F}(X)$ denotes the class of all fuzzy sets in a metric space (X, d), i.e., all functions $\mathbf{u} : X \to [0, 1]$, we are going to restrict ourselves to a subclass $\mathcal{F}^*(X) \subset \mathcal{F}(X)$: namely, $\mathbf{u} \in \mathcal{F}^*(X)$ if and only if:

1) $\mathbf{u} \in \mathcal{F}(X)$,
2) $\mathbf{u}$ is uppersemicontinuous (u.s.c) on (X, d),
3) $\mathbf{u}$ is *normal*, that is $\mathbf{u}(x_0) = 1$ for some $x_0 \in X$.

These properties yield the following results:

a: For each $0 < \alpha \leqslant 1$, the α–level set, defined as $[\mathbf{u}]^\alpha := \{x \in X : \mathbf{u}(x) \geqslant \alpha\}$ is a nonempty compact subset of X,

b: The closure of $\{x \in X : \mathbf{u}(x) > 0\}$, denoted by $[\mathbf{u}]^0$, is also a nonempty compact subset of X.

Note that the characteristic function of a closed set is in $\mathcal{F}^*(X)$. We also want to point out here that the level sets of the fuzzy set $\mathbf{u}$ completely characterize $\mathbf{u}$, i.e., knowing $\mathbf{u}(x), \forall x \in X$, is equivalent to knowing $[\mathbf{u}]^\alpha, 0 \leqslant \alpha \leqslant 1$.

By the above properties, $[\mathbf{u}]^\alpha \in \mathcal{H}(X), 0 \leqslant \alpha \leqslant 1$. We now introduce the metric d_∞ on $\mathcal{F}^*(X)$ (see [6]), which has been used in many applications of fuzzy set theory [11, 12, 15]:

$$d_\infty(\mathbf{u}, \mathbf{v}) = \sup_{0 < \alpha \leqslant 1} \{h([\mathbf{u}]^\alpha, [\mathbf{v}]^\alpha)\} \quad \forall \mathbf{u}, \mathbf{v} \in \mathcal{F}^*(X). \tag{2.6}$$

Here h is the Hausdorff metric introduced in (2.1). The metric space $(\mathcal{F}^*(X), d_\infty)$ is complete. This space represents the generalization of the space $(\mathcal{H}(X), h)$ to fuzzy sets.

At this point we want to incorporate the IFS theory into the fuzzy set frame. Therefore, we first use the *extension principle* for fuzzy sets [18, 14] in order to extend the set-valued maps $\tilde{w}_i$ defined in Section 2.1 to maps between fuzzy sets, i.e., we want to define a map from $\mathcal{F}^*(X)$ to $\mathcal{F}^*(X)$ which is equal to $\tilde{w}_i$ (with the earlier mentioned identification) when its domain is restricted to the characteristic function of a set. Therefore we define for each $\mathbf{u} \in \mathcal{F}^*(X)$ and each subset B of X,

$$\tilde{\mathbf{u}}(B) := \sup\{\mathbf{u}(y) : y \in B\}, \qquad \text{if } B \neq \emptyset$$

$$\tilde{\mathbf{u}}(\emptyset) := 0, \tag{2.7}$$

which implies, in particular, $\tilde{\mathbf{u}}(\{x\}) = \mathbf{u}(x)$ at each $x \in X$.

For each w_i, $i = 1, 2, \ldots, N$, and each $x \in X$ we now define

$$\tilde{\mathbf{u}}_i(x) := \tilde{\mathbf{u}}(w_i^{-1}(\{x\})), \tag{2.8}$$

where, of course, $w_i^{-1}(\{x\}) = \emptyset$ if $x \notin w(X)$. If $\mathbf{u} \in \mathcal{F}^*(X)$, then each of these functions $\tilde{\mathbf{u}}_i : X \to [0, 1]$ is a fuzzy set in $\mathcal{F}^*(X)$ (see [4]).

In fuzzy set theory, the union of two fuzzy sets $\mathbf{u}$,$\mathbf{v}$ is usually defined as the fuzzy set $\sup(\mathbf{u}, \mathbf{v})$. We could then generalize the contraction mapping W given by equation (2.3) to a map $\tilde{\mathbf{w}} : \mathcal{F}^*(X) \to \mathcal{F}^*(X)$ defined by:

$$\tilde{\mathbf{w}}(\mathbf{u})(x) = \sup_{1 \leq i \leq N} \tilde{\mathbf{u}}_i(x), \qquad \text{for each } \mathbf{u} \in \mathcal{F}^*(X). \tag{2.9}$$

In [4] it is shown that this is a contraction mapping on $\mathcal{F}^*(X)$ with the d_∞-metric. Therefore it has a unique fuzzy attractor $\mathbf{u}^* \in \mathcal{F}^*(X)$, e.g., $\tilde{w}(\mathbf{u}^*) = \mathbf{u}^*$. It turns out however, that this fuzzy attractor is the characteristic function of the attractor of the IFS $\{X, \mathbf{w}\}$. This means that the direct generalization of the IFS theory to Fuzzy Sets, does not provide us with a bigger class of attractors. We will see in the next section, how this class can be enlarged without losing the contractivity of the map $\tilde{\mathbf{w}}$.

2.3. Modification of the grey-levels of the attractor

In order to gain more generality with the fuzzy set model, the "grey-level maps" are introduced. To each $\tilde{\mathbf{u}}_i(x)$ defined in (2.8), a *grey-level map* $\varphi_i : [0, 1] \to [0, 1]$ is associated, in order to modify the values of $\tilde{\mathbf{u}}_i$, that is the grey-levels.

Now the supremum of (2.9) is taken over the functions $\tilde{\mathbf{u}}_i$ modified by the functions φ_i; e.g.,

$$\mathbf{u} \mapsto \sup_{1 \leq i \leq N} \varphi_i \circ \tilde{\mathbf{u}}_i. \tag{2.10}$$

In other words, an operator $T_s : \mathcal{F}^*(X) \to \mathcal{F}^*(X)$ is introduced:

$$(T_s\mathbf{u})(x) := \sup\{\varphi_1(\tilde{\mathbf{u}}_1(x)), \ldots, \varphi_N(\tilde{\mathbf{u}}_N(x))\}$$

$$= \sup\{\varphi_1(\tilde{\mathbf{u}}(w_1^{-1}(x))), \ldots, \varphi_N(\tilde{\mathbf{u}}(w_N^{-1}(x)))\}. \tag{2.11}$$

In order for the operator T_s to be well defined, the grey-level functions φ_i have to satisfy certain conditions, namely: for $i = 1, 2, \ldots, N$,

1) $\varphi_i : [0, 1] \longrightarrow [0, 1]$ is non-decreasing,
2) φ_i is right continuous on $[0, 1)$,
3) $\varphi_i(0) = 0$, and
4) for at least one $j \in \{1, 2, \ldots, N\}$, $\varphi_j(1) = 1$.

The fact that φ_i are non-decreasing and right continuous, guarantees the uppersemicontinuity of $\varphi_i \circ \mathbf{u}$ for any $\mathbf{u}$ in $\mathcal{F}^*(X)$, moreover they are necessary and sufficient conditions [4]. Property 3) is a natural assumption in the consideration of grey level functions: if the grey level of a point (pixel) $x \in X$ is zero (the pixel is in the background), then it should remain zero after being acted upon by the φ_i maps.

The set of maps $\Phi = \{\varphi_i, i = 1, 2, \ldots, N\}$, satisfying the above conditions, together with the N contraction maps w_i (which then yield $\tilde{\mathbf{u}}_i$) form the Iterated Fuzzy Set System (IFZS) denoted $\{X, \mathbf{w}, \Phi\}$.

In [4] it is shown that the operator T_s as defined in (2.11) is indeed a contraction mapping on $(\mathcal{F}^*(X), d_\infty)$, i.e., T_s maps $\mathcal{F}^*(X)$ into itself and there exists an s, $0 \leq s < 1$, such that

$$d_\infty(\mathbf{T}_s\mathbf{u}, \mathbf{T}_s\mathbf{v}) \leq s\, d_\infty(\mathbf{u}, \mathbf{v}) \quad \forall\, \mathbf{u}, \mathbf{v} \in \mathcal{F}^*(X). \tag{2.12}$$

Therefore, by the Contraction Mapping Principle, T_s possesses an unique fixed point $\mathbf{u}^*$, that is:

$$\mathbf{T}_s\mathbf{u}^* = \mathbf{u}^*. \tag{2.13}$$

This implies that there exists a unique solution to the functional equation in the unknown $\mathbf{u} \in \mathcal{F}^*(X)$,

$$\begin{aligned}\mathbf{u}(x) = \sup\{&\varphi_1(\tilde{\mathbf{u}}(w_1^{-1}(x))), \varphi_2(\tilde{\mathbf{u}}(w_2^{-1}(x))), \ldots, \\ &\varphi_N(\tilde{\mathbf{u}}(w_N^{-1}(x)))\},\end{aligned} \tag{2.14}$$

for all $x \in X$. The fuzzy set solution, $\mathbf{u}^*$, will be called the *attor* or *fuzzy attractor* of the IFZS, since it follows from the Contraction Mapping Principle that

$$d_\infty((\mathbf{T}_s)^n\mathbf{v}, \mathbf{u}^*) \to 0 \qquad \text{as } n \to \infty, \forall \mathbf{v} \in \mathcal{F}^*(X). \tag{2.15}$$

It is easy to find examples showing that these fuzzy attractors are not longer only characteristic functions of closed sets. Hence, using IFZS, the class of images that can be obtained using IFS has been widened. In section Section 3, we show in fact that any image can be obtained (up to an ε) as a fuzzy attractor of an IFZS. Note that in the case that all φ_i are the identity maps, the operator T_s reduces to the one defined in equation (2.9).

2.4. Properties of the fuzzy attractors

It is worth mentioning several properties of the *fuzzy attractors*. The proofs can be found in [4].

Property 2.1. If $\mathcal{A} \in \mathcal{H}(\mathcal{X})$ is the attractor of the IFS $\{X, \mathbf{w}\}$, and $\mathbf{u}^* \in \mathcal{F}^*(X)$ denotes the fuzzy attractor of the IFZS $\{X, \mathbf{w}, \Phi\}$, then $support(\mathbf{u}^*) \subseteq \mathcal{A}$, that is, $[\mathbf{u}^*]^0 \subseteq \mathcal{A}$.

This means, that using the grey-level maps, we are able to modify the support of our attractor, allowing for example a rough approximation through the w_i, and then a "fine-tuning" using the φ_i. This property may be used for applications, if we want to find the IFZS code for an image. Note that *support*$(\mathbf{u}^*)$ is exactly equal to A, in the following two cases:

- For all $i \in \{1, 2, \ldots, N\}$, $\varphi_i(1) = 1$, then $\mathbf{u}^* = \chi_A$.
- For all $i \in \{1, 2, \ldots, N\}$, φ_i are increasing at 0 (i.e., $\varphi_i^{-1}(0) = \{0\}$). Indeed, in this case $[\mathbf{u}^*]^0 = \bigcup_{i=1}^N w_i([\varphi_i \circ \mathbf{u}^*]^0) = \bigcup_1^N w_i(A) = W(A) = A$.

We should also point out that in the case that $\varphi_i(0) > 0$ for one $i \in \{1, 2, \ldots, N\}$, this inclusion is not longer true.

Property 2.2. The level sets of the fuzzy attractor satisfy a generalized self-tiling condition:

$$[\mathbf{u}^*]^\alpha = \bigcup_{i=1}^N w_i([\varphi_i \circ \mathbf{u}^*]^\alpha), \ 0 \leqslant \alpha \leqslant 1. \tag{2.16}$$

This condition is a consequence of the property of the operator T_s:

$$[\mathbf{Tu}]^\alpha = \bigcup_{i=1}^N w_i([\varphi_i \circ \mathbf{u}]^\alpha), \ \forall \mathbf{u} \in \mathcal{F}^*(X) \qquad \text{(see [4])}. \tag{2.17}$$

This property is interesting, since it shows that the fuzzy attractor is no longer self-similar, in the sense, that it is no longer the union of smaller copies of itself, but rather a union of *modified* copies of itself. The modification is given by the grey-level maps.

Property 2.3 (IFZS Collage Theorem). Let $\mathbf{u} \in \mathcal{F}^*(X)$ and suppose that there exists an IFZS $\{X, \mathbf{w}, \Phi\}$ so that

$$d_\infty(\mathbf{u}, \mathbf{T}_s\mathbf{u}) < \varepsilon, \tag{2.18}$$

where the operator $\mathbf{T}_s$ is defined by (2.11). Then

$$d_\infty(\mathbf{u}, \mathbf{u}^*) < \frac{\varepsilon}{1 - s}, \tag{2.19}$$

where $\mathbf{u}^* = \mathbf{T}_s\mathbf{u}^*$ is the invariant fuzzy set of the IFZS, and s is the maximum contraction factor of the w_i.

This means that if the w_i are very contractive (i.e., s is very small), every fuzzy set that remains relatively unchanged after the application of the operator T_s, is close to the fuzzy attractor.

This property, a direct consequence of the contractivity of T_s, is (as for IFS) very useful for the inverse problem.

3. Density of fuzzy attractors

In this section we will show that the class of fuzzy attractors is dense in $\mathcal{F}^*(X)$ with the d_∞- metric. In other words, given a fuzzy set $\mathbf{u}$ in $\mathcal{F}^*(X)$, and $\varepsilon > 0$, we can always find a natural number N, N contraction mappings $w_i : X \to X$, and N grey-level maps $\varphi_i : [0,1] \to [0,1]$, such that the fuzzy attractor $\mathbf{u}^*$ of the associated IFZS $\{X, \mathbf{w}, \Phi\}$ satisfies: $d_\infty(\mathbf{u}, \mathbf{u}^*) < \varepsilon$. We therefore have the following:

Theorem 3.1. If $X \subset \mathfrak{R}^n$ is compact and $(\mathcal{F}^*(X), d_\infty)$ is defined as above, then the class

$$\mathcal{D} = \{\mathbf{u}^* \in \mathcal{F}^*(X) : \mathbf{u}^* \text{ is attractor of some IFZS on X.}\}$$

is dense in $(\mathcal{F}^*(X), d_\infty)$.

Proof.

Let $\varepsilon > 0$ and $\mathbf{u} \in \mathcal{F}^*(X)$. The idea of the proof is to find $N \in \mathfrak{N}$, $\mathbf{w} = \{w_1, \ldots, w_N\}$ and $\Phi = \{\varphi_1, \ldots, \varphi_N\}$ such that:

1) $\sup c_i < \frac{1}{2}$ (c_i is the contractivity factor of w_i);
2) $d_\infty(T_s\mathbf{u}, \mathbf{u}) < \frac{\varepsilon}{2}$, where T_s is the operator associated to $\{X, \mathbf{w}, \Phi\}$.

Then, using the IFZS collage theorem (Property 2.3) from 1) and 2) we have:

$$d_\infty(\mathbf{u}, \mathbf{u}^*) < \frac{\varepsilon}{2}\left(\frac{1}{1 - 1/2}\right) = \varepsilon,$$

where $\mathbf{u}^*$ is the attractor of the IFZS $\{X, \mathbf{w}, \Phi\}$, i.e., $T_s\mathbf{u}^* = \mathbf{u}^*$. ∎

Let us now find $\mathbf{w}$ and Φ, such that 1) and 2) are satisfied: Let $N \in \mathfrak{N}$, and $x_1, \ldots, x_N$ be an $\frac{\varepsilon}{4}$ -net of $[\mathbf{u}]^0$, i.e., $[\mathbf{u}]^0 \subset \bigcup_1^N B_i$, where $B_i = B(x_i, \frac{\varepsilon}{4})$, are the open balls of radius $\frac{\varepsilon}{4}$ centered at x_i.

Let $w_i : X \to X$, $w_i(X) \subset B_i$, $i = 1, \ldots, N$ be contraction mappings with contraction factor c_i, with $c_i < \frac{1}{2}$. Choose now $\alpha_0 = 0$ and $\alpha_i = \sup_{x \in \overline{B_i}} \mathbf{u}(x)$.

Then for $0 \leq \alpha \leq 1$ we have $[\mathbf{u}]^\alpha \subset \bigcup_{\{i:\alpha < \alpha_i\}} B_i$.

We now choose φ_i non-decreasing, right continuous, such that $\varphi_i(x) \leq \alpha_i$, $\forall x \in [0,1]$, and $\varphi_i(1) = \alpha_i$, $i = 1, \ldots, N$. For example, the stepfunctions $\alpha_i \chi_{[\alpha_i, 1]}$ satisfy these conditions.

Then

$$[\varphi_i \circ \mathbf{u}]^\alpha = \begin{cases} \neq \emptyset & \alpha \leq \alpha_i; \\ \emptyset & \alpha > \alpha_i. \end{cases}$$

But using condition (2.17), we have

$$[T_s\mathbf{u}]^\alpha = \bigcup_{i=1}^{N} w_i([\varphi_i \circ \mathbf{u}]^\alpha) = \bigcup_{\{i:\alpha < \alpha_i\}} w_i([\varphi_i \circ \mathbf{u}]^\alpha).$$

Now, if the δ-dilatation $D_\delta(S)$ of a nonempty closed set S is $D_\delta(S) = \{x \in X : d(x,S) < \delta\}$, $\delta > 0$, we can observe that for $0 \leq \alpha \leq 1$

$$[\mathbf{u}]^\alpha \subset \bigcup_{(i:\alpha \leq \alpha_i)} B_i \subset D_\delta([\mathbf{u}]^\alpha) \tag{3.1}$$

and

$$w_i(S) = B_i \subset D_\delta(w_i(S))$$
$$\text{for } 1 \leq i \leq N, \forall S \text{ closed subset of } X. \tag{3.2}$$

We then have:

$$[\Gamma_\delta \mathbf{u}]^\alpha \subset \bigcup_{(i:\alpha \leq \alpha_i)} B_i \subset D_\delta([\mathbf{u}]^\alpha)$$
$$[\mathbf{u}]^\alpha \subset \bigcup_{(i:\alpha \leq \alpha_i)} B_i \subset D_\delta([\Gamma_\delta \mathbf{u}]^\alpha).$$

Using the above equations, we then obtain

$$h([\Gamma_\delta \mathbf{u}]^\alpha, [\mathbf{u}]^\alpha) \leq \frac{\delta}{2}, \quad \forall \alpha, 0 < \alpha \leq 1, \tag{3.3}$$

and hence

$$d_\infty(\Gamma_\delta \mathbf{u}, \mathbf{u}) \leq \frac{\delta}{2}. \tag{3.4}$$

■

4. Conclusions

The IFZS model represents a different and promising approach to the inverse problem for fractal construction and image encoding. The introduction of the grey-level maps allows one to enlarge the class of attractors. We prove that this class is dense in $(F^*(X), d_\infty)$, the space of uppersemicontinuous normal functions, a space which is large enough for image representation. Again, the proof of the density does not give an efficient algorithm to find the appropriate code, but it provides a theoretical justification for the fuzzy set approach.

We believe, that we might be able to relax several conditions of the model presented here, in order to efficiently solve the inverse problem. We have experimental results comforting our intuition.

5. Acknowledgements

We wish to acknowledge support from the CONICET (Argentina) and the Department of Applied Mathematics of the University of Waterloo. We want to express our gratitude to all the people of the Department who made our stay there so enjoyable. In particular we are enormously grateful to Profs. B. Forte and E. Vrscay for their continuous support and encouragement.

We were able to attend the NATO 1991 meeting, thanks to financial support granted from Profs. B. Forte, K. Hare and E. Vrscay all from University of Waterloo, and Prof. J. Byrnes/NATO 1991.

6. Bibliography

[1] Michael F. Barnsley and Steven Demko. Iterated function systems and the global construction of fractals. *Proc. Roy. Soc. Lond.*, A399:243–275, 1985.

[2] Michael F. Barnsley, V. Ervin, D. Hardin, and J. Lancaster. Solution of an inverse problem for fractals and other sets. *Proceedings of the National Academy of Sciences*, 83:1975–1977, 1985.

[3] Michael F. Barnsley and A.D Sloan. A better way to compress images. *BYTE Magazine*, January issue:215–223, 1988.

[4] Carlos A. Cabrelli, Bruno Forte, Ursula M. Molter, and Edward R. Vrscay. Iterated fuzzy set systems: A new approach to the inverse problem for fractals and other sets. *Journal of Mathematical Analysis and Applications*, 1992. To appear.

[5] Persi Diaconis and Mehrdad Shahshahani. Products of random matrices and computer image generation. In *Random Matrices and Their Applications*, volume 50 of *Contemporary Mathematics*, pages 173–182. American Mathematical Society, 1986. Proceedings of a Summer Research Conference, held June 17–23.

[6] P. Diamond and P. Kloeden. Metric spaces of fuzzy sets. *Fuzzy sets and systems*, 35:241–249, 1990.

[7] John Elton. An ergodic theorem for iterated maps. *Ergodic Theory and Dynamical Systems*, 7:481–488, 1987.

[8] Kenneth J. Falconer. *The geometry of fractal sets*. Cambridge University Press, 1985.

[9] Kenneth J. Falconer. *Fractal Geometry, Mathematical Foundations and Applications*. John Wiley & Sons, 1990.

[10] J. Hutchinson. Fractals and self-similarity. *Indiana University Journal of Mathematics*, 30:713–747, 1981.

[11] O. Kaleva. Fuzzy differential equations. *Fuzzy Sets and Systems*, 24:301–317, 1987.

[12] P.E Kloeden. Fuzzy dynamical systems. *Fuzzy Sets and Systems*, 7:275–296, 1982.

[13] Benoit B. Mandelbrot. *The Fractal Geometry of Nature*. W.H. Freeman and Company, New York, 1977.

[14] H.T Nguyen. A note on the extension principle for fuzzy sets. *Journal of Mathematical Analysis and Applications*, 64:369–380, 1978.

[15] M.L Puri and D.A Ralescu. The concept of normality for fuzzy random variables. *Ann. Prob.*, 13:1373–1379, 1985.

[16] Edward R. Vrscay and C.J Roehrig. Iterated function systems and the inverse problem of fractal construction using moments. In E. Kaltofen and S.M Watt, editors, *Computers and Mathematics*, pages 250–259. Springer Verlag, 1989.

[17] Lotfi A. Zadeh. Fuzzy sets. *Inform. Control*, 8:338–353, 1965.

[18] Lotfi A. Zadeh. The concept of linguistic variable and its application to approximate reasoning. *Information Sciences*, 8:199–249, 301–357, 1975.

Multifractal measures

Jacques Peyrière
Université Paris-Sud
Département de mathématiques, bât. 425
Unité associée au CNRS 757
91405 Orsay Cedex France
peyriere@matups.matups.fr

Abstract The present redaction is mainly an account of a joint work [6] with G. Brown, from the University of New South Wales, and G. Michon, from Dijon University. The multifractal formalism is described, and a setting in which it holds is given, as well as the Michon construction of Gibbs measures.

1. Introduction: the multifractal formalism

Let ν_n be an increasing sequence of positive integers. The interval $[\frac{j}{\nu_n}, \frac{j+1}{\nu_n}[$ is denoted by $I_{n,j}$. Let μ be a probability measure on $[0,1[$. Set

$$\tau_n(q) = -\frac{1}{\log \nu_n} \log \sum_{0 \le j < \nu_n}^{*} \mu(I_{n,j})^q$$

where $\sum^*$ means that the summation runs over the indices j such that $\mu(I_{n,j}) \neq 0$, and suppose that $\tau(q) = \lim_{n\to\infty} \tau_n(q)$ exists for every q in a certain interval $\mathcal{J}$ of $\mathfrak{R}$.

On the other hand, let us define $I_n(x)$ to be the interval of the family $(I_{n,j})_{0 \le j < \nu_n}$ which contains the point x of $[0,1[$, and set, for $\alpha > 0$,

$$E_\alpha = \left\{ x \in [0,1[\,\middle|\, \lim_{n\to\infty} -\frac{\log \mu(I_n(x))}{\log \nu_n} = \alpha \right\}.$$

Then the multifractal formalism, as asserted in various works [11, 12, 13], and proved [1, 2, 5, 9, 17] to hold in various contexts, says that the Hausdorff dimension of E_α can be computed in the following way:

$$\dim E_\alpha = \inf_{q \in \mathcal{J}} [\alpha q - \tau(q)]. \tag{1.1}$$

In the case where τ is differentiable at a point q_0 and $\alpha = \tau'(q_0)$, we have $\dim E_\alpha = \alpha q_0 - \tau(q_0)$.

J. S. Byrnes et al. (eds.), Probabilistic and Stochastic Methods in Analysis, with Applications, 175–186.
© 1992 *Kluwer Academic Publishers. Printed in the Netherlands.*

This article is organized as follows. In the next section, the setting is enlarged in order to deal with families of partitions the elements of which can have different lengths. Without any assumption on the measure, it is shown that the right hand side of (1.1) is always an upper bound for dim E_α. Moreover, the result is a bit stronger, in the sense that we can deal with the Tricot (packing) dimension instead of Hausdorff's. We can also majorize the dimension of a larger set than E_α.

The third section is devoted to getting lower bounds for dimensions once the existence of Gibbs measures is assumed.

In the fourth section, Michon's proof of the existence of Gibbs measures for homogeneous trees is given.

2. Upper bounds for dimensions

Let $\{\{I_{n,j}\}_{1\leqslant j\leqslant \nu_n}\}_{n>0}$ be a sequence of partitions of $[0,1[$ by intervals, semi-open to the right. These partitions need not be nested. If $x \in [0,1[$, $I_n(x)$ stands for the interval of the family $\{I_{n,j}\}_{1\leqslant j\leqslant \nu_n}$ which contains x. The length of an interval J is denoted by $|J|$. We suppose that, for any $x \in [0,1[$, $\lim_{n\to\infty} |I_n(x)| = 0$.

We consider two indices dim and Dim which are defined as Hausdorff and Tricot dimensions are, but by only considering coverings and packings by intervals in the family $\{\{I_{n,j}\}_{1\leqslant j\leqslant \nu_n}\}_{n>0}$. An account of several notions of dimension is given in the appendix.

We are given a probability measure μ on $[0,1[$ and a sequence $\{\lambda_n\}_{n>0}$ of positive integers such that $\sum_{n>0} \exp(-\eta\lambda_n) < \infty$ for any $\eta > 0$.

We define the following quantities:

$$C_n(x,y) = \frac{1}{\lambda_n} \log \sum_{1\leqslant j\leqslant \nu_n}^{*} \mu_n(I_{n,j})^{x+1} |I_{n,j}|^{-y}$$

and

$$C(x,y) = \limsup_{n\to\infty} C_n(x,y)$$

where $\sum^*$ means that the summation runs over the j's such that $\mu_n(I_{n,j}) \neq 0$.

We suppose that $C(x,y)$ is not constantly equal to 0 or ∞ (this imposes the growth of the sequence $\{\lambda_n\}$), and set $\Omega = \{(x,y) \in \mathfrak{R}^2 | C(x,y) < 0\}$. Since C is a convex function, non-decreasing as a function of x, and non-increasing as a function of y, there exists a concave and non-decreasing function φ from $\mathfrak{R}$ to $\mathfrak{R}$ such that the interior of Ω is identical to the set $\{(x,y) \in \mathfrak{R}^2 | y < \varphi(x-0)\}$. Of course, taking the limit to the left only matters at the left end of the interval $\mathcal{J}$ on which φ is finite. Besides, we assume that $0 \in \mathcal{J}$ and, for the sake of simplicity, that φ is differentiable on this interval (the complete discussion, in the case where it is not so, is given in [6]).

In the case described in the introduction, where all the intervals of the partition $\{I_{n,j}\}_{1\leqslant j\leqslant \nu_n}$ have the same length, $\lambda_n = \nu_n$ and the limit exists, we have $\varphi(x) = \tau(x+1)$, where τ is the function defined in the introduction.

Set $f(\alpha) = \inf[\alpha(x+1) - \varphi(x)]$.

On the other hand, we consider the following sets

$$B_\alpha = \left\{ x \in [0,1[\;\middle|\; \limsup \frac{\log \mu(I_n(x))}{\log |I_n(x)|} \leqslant \alpha \right\}$$

$$B_\alpha^* = \left\{ x \in [0,1[\;\middle|\; \liminf \frac{\log \mu(I_n(x))}{\log |I_n(x)|} \leqslant \alpha \right\}$$

$$V_\alpha = \left\{ x \in [0,1[\;\middle|\; \liminf \frac{\log \mu(I_n(x))}{\log |I_n(x)|} \geqslant \alpha \right\}$$

$$V_\alpha^* = \left\{ x \in [0,1[\;\middle|\; \limsup \frac{\log \mu(I_n(x))}{\log |I_n(x)|} \geqslant \alpha \right\}$$

We then have the following result.

Theorem 2.1.

1) For any α, we have $\operatorname{Dim} B_\alpha^* \leqslant -\varphi(-1)$ and $\operatorname{Dim} V_\alpha^* \leqslant -\varphi(-1)$.
2) If $\alpha \leqslant \varphi'(-1)$, then $\operatorname{Dim} B_\alpha \leqslant f(\alpha)$ and $\dim B_\alpha^* \leqslant f(\alpha)$.
3) If $\alpha \geqslant \varphi'(-1)$, then $\operatorname{Dim} V_\alpha \leqslant f(\alpha)$ and $\dim V_\alpha^* \leqslant f(\alpha)$.

Proof. Let us for instance consider the second case ($\alpha < \varphi'(-1)$), and set

$$B_\beta(n) = \{ t \in [0,1[\;|\; \mu(I_n(t)) \geqslant |I_n(t)|^\beta \}$$

We then have

$$B_\alpha = \bigcap_{\alpha < \beta < \varphi'(-1)} \bigcup_m \bigcap_{n \geqslant m} B_\beta(n).$$

Fix $\alpha < \beta < \varphi'(-1)$ and $\delta > f(\beta)$, and choose $t > 0$ such that $C(-1+t, -\delta + \beta t) < 0$. Then

$$\begin{aligned} \sum_{j,\mu(I_{n,j}) \geqslant |I_{n,j}|^\beta} |I_{n,j}|^\delta &= \sum_{\text{idem}} |I_{n,j}|^{\beta t} |I_{n,j}|^{-(-\delta+\beta t)} \\ &\leqslant \sum_j \mu(I_{n,j})^t |I_{n,j}|^{-(-\delta+\beta t)} \\ &\leqslant \exp \lambda_n C_n(-1+t, -\delta+\beta t). \end{aligned}$$

Therefore

$$\sum_n \sum_{j,\mu(I_{n,j}) \geqslant |I_{n,j}|^\beta} |I_{n,j}|^\delta < \infty.$$

So, if $\{I_j\}$ is a packing of $\bigcap_{n \geqslant m} B_\beta(n)$ by intervals from generations larger than m, we have $\sum |I_j|^\delta < \infty$. Therefore $\Delta\left(\bigcap_{n \geqslant m} B_\beta(n)\right) \leqslant \delta$ (cf. appendix) and $\operatorname{Dim} B_\alpha \leqslant \delta$. Finally $\operatorname{Dim} B_\alpha \leqslant f(\alpha)$.

The other cases are handled in a similar way. ∎

2.1. An alternate definition of φ

Consider the following quantity:

$$K(x,y) = \lim_{\varepsilon \to 0} \sup_{\varepsilon\text{-packing}} \sum \mu(I_j)^{x+1} |I_j|^{-y}.$$

The function K is convex, so the set $\Omega = \{K = 0\}$ is also convex. Moreover, if $K(a,b)$ is finite, then $K(a+t, y-u) = 0$ for positive t and u. Therefore, there exists a concave and non-decreasing function φ from $\mathfrak{R}$ to $\mathfrak{R}$ such that $\overset{\circ}{\Omega} = \{(x,y) | y < \varphi(x-0)\}$.

As previously, set $f(\alpha) = \inf_x (\alpha(x+1) - \varphi(x))$. In these conditions, we have the following result.

Theorem 2.2.

1) If $\alpha < \varphi'(-1)$, then $\operatorname{Dim} B_\alpha \leqslant f(\alpha)$.
2) If $\alpha > \varphi'(-1)$, then $\operatorname{Dim} V_\alpha \leqslant f(\alpha)$.

Proof. In the first case ($\alpha < \varphi'(-1)$), if $\delta > f(\alpha)$ the straight half line of slope α stemming from the point $(-1, -\delta)$ intersects $\overset{\circ}{\Omega}$. In other terms, there exists a positive number t such that $(-1+t, -\delta + \alpha t) \in \Omega$. There exists $\varepsilon > 0$ such that, for any ε-packing $\{I_j\}_{j>0}$ of $[0,1[$ by elements of the family $\{I_{n,j}\}_{n,j}$ we have $\sum_j \mu(I_j)^{x+1} |I_j|^{-y} \leqslant 1$.

As in the preceding section, we write

$$B_\alpha^* = \bigcap_{\alpha < \beta < \varphi'(-1)} \bigcap_{m \geqslant 1} \bigcup_{n \geqslant m} B_\beta(n).$$

Therefore, if n is such that $\sup_j |I_{n,j}| \leqslant \varepsilon$, if $\alpha < \beta < \varphi'(-1)$, and if $\{I_j\}_j$ is an ε-packing of the set $B_\beta(n)$, we have

$$\sum |I_j|^\delta = \sum |I_j|^{t\alpha} |I_j|^{\delta - t\alpha}$$
$$\leqslant \sum \mu(I_j)^{(-1+t)+1} |I_j|^{-(-\delta+\alpha t)} \leqslant 1$$

So, $\operatorname{Dim} B_\beta(n) \leqslant \delta$, and $\operatorname{Dim} B_\alpha \leqslant f(\alpha)$.

The second case is handled in the same way. ∎

Remark 2.3. We could also have defined $K(x,y)$ to be:

$$\lim_{\varepsilon \to 0} \inf \sum \mu(I_j)^{x+1} |I_j|^{-y}$$

where the inf is taken over the ε-coverings $\{I_j\}$ of $[0,1[$ by elements of the family $\{I_{n,j}\}_{n,j}$. The function K may be no longer convex, but the boundary of $\{K = 0\}$ is still defined by a non-decreasing function φ from $\mathfrak{R}$ to $\mathfrak{R}$. If f is defined as above, then a similar conclusion holds by replacing Dim by dim.

3. Lower bounds for dimensions

The notations are the same as in the previous section. If u and v are two functions, the relation $u \approx v$ means that there exists a positive constant K such that $K^{-1}u \leqslant v \leqslant Ku$.

Theorem 3.1. Let $\theta \in \mathfrak{R}$ and suppose that $\varphi'(\theta)$ exists and that there is a measure μ_θ such that $\mu_\theta(I_{n,j}) \approx \mu(I_{n,j})^{\theta+1}|I_{n,j}|^{-\varphi(\theta)}$. Then we have $\dim E_{\varphi'(\theta)} = f(\varphi'(\theta))$.

The measure μ_θ, in analogy with statistical mechanics, is called a Gibbs measure.

Proof. Consider the following quantities

$$\tilde{C}_n(x,y) = \frac{1}{\lambda_n} \log \sum_j{}^* \mu(I_{n,j})^x |I_{n,j}|^{-y} \mu_\theta(I_{n,j})$$

and

$$\tilde{C}(x,y) = \limsup \tilde{C}_n(x,y).$$

We have

$$\tilde{C}_n(x,y) = \frac{1}{\lambda_n} \log \sum{}^* \mu(I_{n,j})^{x+\theta+1} |I_{n,j}|^{-y-\varphi(\theta)} + o(1)$$

and

$$\tilde{C}(x,y) < 0 \Leftrightarrow C(x+\theta, y+\varphi(\theta)) < 0.$$

Therefore

$$\left\{\tilde{C} < 0\right\}^\circ = \left\{(x,y) \middle| y < \varphi(x+\theta) - \varphi(\theta)\right\}.$$

∎

Lemma 3.2. As n goes to infinity, $\frac{\log \mu(I_n(t))}{\log |I_n(t)|} \to \varphi'(\theta)$ for μ_θ-almost every t.

Proof. If $\alpha < \varphi'(\theta)$ then there exists $t > 0$ such that $\tilde{C}(t, \alpha t) < 0$. Then

$$\begin{aligned}
\mu_\theta \{t | \mu(I_n(t)) > |I_n(t)|^\alpha\} &= \sum_{j:\mu(I_{n,j}) > |I_{n,j}|^\alpha} \mu_\theta(I_{n,j}) \\
&= \sum_{\text{idem}} |I_{n,j}|^{\alpha t} |I_{n,j}|^{-\alpha t} \mu_\theta(I_{n,j}) \\
&\leqslant \sum_j \mu(I_{n,j})^t |I_{n,j}|^{-\alpha t} \mu_\theta(I_{n,j}) \\
&= \exp \lambda_n \tilde{C}_n(t, \alpha t).
\end{aligned}$$

(this inequality is a large deviation type result [7], as well as the analogous one in the proof of the theorem concerning upper bounds). Therefore

$$\sum_n \mu_\theta \left\{ \frac{\log \mu(I_n(t))}{\log |I_n(t)|} < \alpha \right\} < \infty$$

so, lim inf $\frac{\log \mu(I_n(t))}{\log |I_n(t)|} \geqslant \alpha$ for μ_θ-almost t. The upper limit is treated similarly.

We can now complete the proof of the theorem. It results from the above lemma first that $\mu_\theta(E_{\varphi'(\theta)}) = 1$ and secondly, taking into account the properties of μ_θ, that

$$\frac{\log \mu_\theta(I_n(t))}{\log |I_n(t)|} \to (\theta + 1)\varphi'(\theta) - \varphi(\theta)$$

for μ_θ-almost t. Therefore, due to the Billingsley-Kinney-Pitcher theorem, we have dim $E_{\varphi'(\theta)} \geqslant f(\varphi'(\theta))$. The equality then results from the previous section. ∎

As a consequence, the Hausdorff or Tricot dimensions of all the sets E_α, B_α, V_α, B^*_α, and V^*_α are equal to $f(\alpha)$ under the same conditions. This generalizes some results of Besicovitch [3], Eggleston [10], and Volkman [28] on the dimension of sets defined in terms of frequency of digits. This also accounts for some results in [9] and some work on 'cookie-cutters' [1, 5].

4. Existence of Gibbs measures

In this section we suppose that the sequence $\{\{I_{n,j}\}_{1 \leqslant j \leqslant \nu_n}\}_{n>0}$ of partitions has the following properties: each element of the $(n+1)$-st partition is contained in one element of the n-th one, and each element of the n-th partition is split into a fixed number p of elements of the $(n+1)$-st one. Obviously, this imposes $\nu_n = p^n$. We are going to use another indexation of the intervals $\{I_{n,j}\}$: the intervals $\{I_{2,j}\}$ will be denoted by $I_{i_1 i_2}$, with $0 \leqslant i_1, i_2 < p$, in such a way that $I_{i_1 i_2} \subset I_{i_1}$; and so on.

Let $\mathcal{A}$ be the set of words over the alphabet $\{0, 1, \ldots, p-1\}$. The concatenation, just denoted by juxtaposition, endows $\mathcal{A}$ with a semigroup structure. The empty word, which is the unit, is denoted by ϵ. The set of words of length n is denoted by $\mathcal{A}_n$; it indexes the elements of the n-th partition. If $a \in \mathcal{A}$, instead of writing $\mu(I_a)$ we shall simply write $\mu(a)$. In these conditions, for every $a \in \mathcal{A}$, we have $\sum_{0 \leqslant b < p} \mu(ab) = \mu(a)$.

We suppose that μ is quasi-Bernoulli, i.e., there exists a positive number M such that, for any a and b in $\mathcal{A}$, we have $M^{-1}\mu(a)\mu(b) \leqslant \mu(ab) \leqslant M\mu(a)\mu(b)$.

We also define a mapping l from $\mathcal{A}$ to $\mathfrak{R}$: $l(a) = |I_a|$. We assume that l is almost multiplicative, i.e., there exists a positive constant L such that, for any a and b in $\mathcal{A}$, we have $L^{-1}l(a)l(b) \leqslant l(ab) \leqslant L\, l(a)l(b)$.

Under these conditions, G. Michon [21, 22] proved that the 'free energy' exists and that there are Gibbs measures. We are going now to give his proof.

Proposition 4.1. For every x and y in $\mathfrak{R}$, the ratio

$$\frac{1}{n}\log\left[\sum_{a\in\mathcal{A}_n} l(a)^{-y}\mu(a)^{x+1}\right]$$

has a limit, denoted by $C(x,y)$, as n goes to infinity.

Proof. By replacing l by $l^{-y}\mu^x$, it is enough to consider the case $x = 0$, $y = -1$. Set

$$Z_n = \sum_{a\in\mathcal{A}_n} l(a)\mu(a) \quad \text{, and} \quad C_n = \frac{1}{n}\log(Z_n).$$

We have

$$Z_{m+n} = \sum_{a\in\mathcal{A}_m} l(a)\mu(a) \sum_{b\in\mathcal{A}_n} \frac{l(ab)}{l(a)l(b)} \frac{\mu(ab)}{\mu(a)\mu(b)} l(b)\mu(b).$$

Therefore, we have $|\log Z_{m+n} - \log Z_m - \log Z_n| \leqslant \log(ML)$. It results that C_n has a limit C as n goes to infinity. Moreover, we have $|C_n - C| \leqslant \frac{1}{n}\log ML$. ∎

Let us notice that if we set $l_a(b) = l(ab)/l(a)$, (for a and b in $\mathcal{A}$), we have $L^{-2}l_a(b)l_a(c) \leqslant l_a(bc) \leqslant L^2 l_a(b)l_a(c)$ for a, b, and c in $\mathcal{A}$. Similarly for μ.

For any a in $\mathcal{A}$, and s in $\mathfrak{R}$, set ${}_aZ_n = \sum_{b\in\mathcal{A}_n} l_a(b)\,\mu_a(b)$, and

$$Z_a(s) = \sum_{n\geqslant 0} {}_aZ_n e^{-ns} \tag{4.1}$$

It results from the above remark that, for any n and for any a, we have $K^{-1}Z_n \leqslant {}_aZ_n \leqslant KZ_n$, with $K = LM$. Therefore $\lim_{n\to\infty} \frac{1}{n}\log {}_aZ_n$ does not depend on a and is equal to what we called C in the proof of the above proposition. Moreover, $|\frac{1}{n}\log {}_aZ_n - C| \leqslant \frac{2}{n}\log K$ and $K^{-2}\exp nC \leqslant {}_aZ_n \leqslant K^2\exp nC$ for any n. So the series (4.1) converges for $s > C$. From these last inequalities it results also that

$$1 - \frac{K^2}{\exp(C-s)} \leqslant Z_a(s) \leqslant 1 - \frac{K^2}{\exp(C-s)}$$

Theorem 4.2. For every x and y in $\mathfrak{R}$, there exist a constant c and a measure $\mu_{x,y}$ such that, for any a in $\mathcal{A}_n$, we have

$$c^{-1}l(a)^{-y}\mu(a)^{x+1}e^{-nC(x,y)} \leqslant \mu_{x,y}(a) \leqslant c\,l(a)^{-y}\mu(a)^{x+1}e^{-nC(x,y)}$$

Proof. As previously, it is enough to consider the case $x = 0$, $y = -1$.

Let us denote by l_n the following mapping from $[0,1[$ to $\mathfrak{R}$: $l_n(t) = \log|I_n(t)|$. Let us define a family of functions from $[0,1]$ to $\mathfrak{R}^+$ in the following way $\varphi_s = l_0 + l_1 e^{-s} + l_2 e^{-2s} + \cdots$. Obviously, we have $\int \varphi_s \, d\mu = Z_\epsilon(s)$. This allows us to define the family $P_s = \frac{\varphi_s}{Z_\epsilon(s)} \mu$ $(s > C)$ of probability measures on $[0,1]$.

If $a \in \mathcal{A}_n$, we denote by a_i $(0 \leqslant i \leqslant n)$ the word formed by the i first letters of a. In these conditions, we have, denoting $P_s(I_a)$ simply by $P_s(a)$,

$$Z_\epsilon(s) P_s(a) = \mu(a) \sum_{0 \leqslant i \leqslant n} l(a_i) e^{-is} + \sum_{1 \leqslant i \leqslant n} \sum_{b \in \mathcal{A}} l(ab) \mu(ab_i) e^{-(i+n)s}$$

In other terms

$$P_s(a) = \frac{\mu(a)}{Z_\epsilon(s)} \sum_{0 \leqslant i \leqslant n} l(a_i) e^{-is} + l(a) \mu(a) e^{-ns} \frac{Z_a(s)}{Z_\epsilon(s)}.$$

When s goes to infinity, P_s has a weak limit point γ at least. But, we know that, as s goes to infinity, so does $Z_\epsilon(s)$ and that the ratio $Z_a(s) / Z_\epsilon(s)$ stays between K^{-1} and K. This means that we have, for $a \in \mathcal{A}_n$,

$$K^{-2} \leqslant \frac{\gamma(a)}{l(a)\mu(a) e^{-n\zeta}} \leqslant K^2.$$

∎

Remark 4.3. The case of Riesz products [8] is not handled by this proof.

5. Example

One of the paradigms of mutifractality is the multinomial measures of which we give a generalization in this section..

Let X be the simplex $\{(x_1, \ldots, x_p) : x_1 + \cdots + x_p = 1, x_i > 0$ for $i = 1, \ldots, p\}$, $(p \geqslant 2)$. Consider a sequence $\{m_n, l_n\}_{n \geqslant 0}$ of elements of $X \times X$. We assume that this sequence has a continuous measure of repartition ξ. This means that there exists a continuous probability measure ξ on the space $X \times X$ such that, for any open set $U \subset X \times X$ the boundary of which is of zero ξ-measure, we have

$$\lim_{n \to \infty} \frac{1}{n} \# \{i \leqslant n : (m_i, l_i) \in U\} = \xi(U).$$

Moreover we assume that the boundary of $X \times X$ is of zero ξ-measure.

As in the section concerning the construction of Gibbs measures, we consider subintervals of $[0,1[$ indexed by words over the alphabet $\{0, 1, \ldots, p-1\}$: $I_\epsilon = [0,1[$, and the length of $I_{x_1 \ldots x_{n+1}}$ is $l_{n+1, x_{n+1}} |I_{x_1 \ldots x_n}|$.

Define a measure μ on $[0,1[$ in the following way:

$$\mu(I_{x_1,\dots,x_n}) = \prod_{1\le j\le n} m_{j,x_j}.$$

It can be verified that we have

$$\lim_{n\to\infty} \frac{1}{n} \log \sum \mu(I_{x_1,\dots,x_n})^{x+1} |I_{x_1,\dots,x_n}|^{-y} = \int_{X\times X} \log \sum_{1\le k\le p} (u_k^{x+1} v_k^{-y})\, d\xi(u,v).$$

So we have an explicit expression for $C(x,y)$. On the other hand, if we keep the same l_n, but if m_n is replaced by $\frac{m_n^{x+1} l_n^{y}}{\sum_{1\le k\le p} m_{n,k}^{x+1} l_{n,k}^{y}}$ (where to exponentiate a vector means to exponentiate each of its components) and perform a similar construction, we get a measure $\nu_{x,y}$ which is the Gibbs measure corresponding to (x,y). Therefore in this situation the multifractal formalism holds.

6. Appendix: Hausdorff and Tricot dimensions

6.1. Hausdorff dimension

Let E be a subset of $[0,1[$ and α a positive number. Set

$$H_\alpha(E) = \lim_{\varepsilon\to 0} \inf \left\{ \sum |I_i|^\alpha \mid E \subset \bigcup I_i,\ |I_i| < \varepsilon \right\}.$$

If $H_\alpha(E) < \infty$ then $\beta > \alpha \Rightarrow H_\beta(E) = 0$. So there is a cutoff α_0 such that

$$\alpha < \alpha_0 \Rightarrow H_\alpha(E) = \infty \quad \text{and} \quad \alpha > \alpha_0 \Rightarrow H_\alpha(E) = 0.$$

This number α_0 is, by definition, the Hausdorff dimension of E.

Another dimensional index is of wide use. Let $N_\varepsilon(E)$ be the minimum number of elements of coverings of E by intervals of lengths less than ε, and set

$$\Delta(E) = \limsup_{\varepsilon\to 0} \frac{\log N_\varepsilon(E)}{\log \frac{1}{\varepsilon}}.$$

This index has been considered by many authors and bears several names: Bouligand-Minkowski dimension, entropy dimension, logarithmic index, box dimension ... In fact these indices differ in a general metric space. Obviously we have $\dim E \le \Delta(E)$.

The following observation gives a way of getting a lower bound for the Hausdorff dimension: if there exists a measure μ satisfying a Hölder condition of order α (i.e., $\mu(I) \le C|I|^\alpha$ for every interval I) and such that

$\mu(E) > 0$, then $\dim E \geqslant \alpha$. Indeed if $\{I_j\}$ is a covering of E by intervals, we have

$$0 < \mu(E) \leqslant \sum \mu(I_j) \leqslant C \sum |I_j|^\alpha$$

wich proves the above assertion. In fact a refinement of this argument gives the following lemma due to Kinney and Pitcher and, in a more general form, to Billingsley [4].

Lemma 6.1. Let μ be a probability measure. If

$$\mu(E) > 0 \quad \text{and} \quad E = \left\{ t \mid \liminf_{I \searrow \{t\}} \frac{\log \mu(I)}{\log |I|} \geqslant \alpha \right\}$$

then $\dim E \geqslant \alpha$.

6.2. Tricot dimension

An ε-packing of E is a collection of mutually disjoint intervals intersecting E. The following property of box dimension can be found in [26]:

$$\begin{aligned} \Delta(E) &= \inf \left\{ \alpha \mid \limsup_{\varepsilon \searrow 0} \left(\sum |I_j|^\alpha \mid \{I_j\} \text{ being an } \varepsilon\text{-packing of } E \right) = 0 \right\} \\ &= \sup \left\{ \alpha \mid \limsup_{\varepsilon \searrow 0} \left(\sum |I_j|^\alpha \mid \{I_j\} \text{ being an } \varepsilon\text{-packing of } E \right) = \infty \right\} \end{aligned}$$

One drawback of the box dimension is that it does not distinguish a set from its closure. For instance, it assigns 0 to the dimension of the rationals. This led Tricot [26, 25] to introduce the following concept:

$$\operatorname{Dim} E = \inf \left\{ \sup_n \Delta(E_n) \mid E \subset \bigcup E_n \right\}$$

Obviously $\dim E \leqslant \operatorname{Dim} E$. A related notion has been introduced by Sullivan [24]. An account of this notion of dimension and of connected outer measures can be found in [27].

The index Dim has the same regularity properties as Hausdorff dimension: if $E \subset F$ then $\operatorname{Dim} E \leqslant \operatorname{Dim} F$, and, if E is the union of a sequence $\{E_n\}$ of sets, then $\operatorname{Dim} E = \sup_n \operatorname{Dim} E_n$.

7. Final remarks

There are many developments which we are not going to discuss about multifractals, in particular concerning further interpretations [15, 16, 18, 19, 20] of the function $f(\alpha)$ especially when it assumes negative values.

In a recent work Muzy et al. [23] have adapted this formalism to handle another situation by replacing indicator functions of intervals by wavelets.

Finally, the thermodynamical formalism has been used to study harmonic measures [14].

8. Bibliography

[1] T. Bedford. Applications of dynamical systems theory to fractals: A study of cookie-cutter Cantor sets. Preprint, TU Delft (Netherlands).

[2] T. Bedford. Hausdorff dimension and box dimension in self-similar sets. In V. Binz, editor, *Proc. conf. Topology and Measure*, GDR, 1987.

[3] A.S. Besicovitch. On the sum of digits of real numbers represented in the dyadic system. *Math. Ann.*, 110:321–330, 1934.

[4] P. Billingsley. *Ergodic theory and information*. John Wiley & Sons, 1965.

[5] T. Bohr and D. Rand. The entropy function for characteristic exponents. *Physica*, 25D:387–398, 1987.

[6] G. Brown, G. Michon, and J. Peyriere. On the multifractal analysis of measures. *J. Stat. Phys.*, 66(3/4). To appear.

[7] H. Chernoff. A measure of asymptotic efficiency for tests of a hypothesis based on the sum of observations. *Ann. Math. Stat.*, 23:493–507, 1952.

[8] P. Collet. Preprint.

[9] P. Collet, J.L. Lebowitz, and A. Porzio. The dimension spectrum of some dynamical systems. *J. Stat. Phys.*, 47:609–644, 1987.

[10] H.G. Eggleston. The fractional dimension of a set defined by decimal properties. *Quarterly J. of Math. Oxford*, pages 31–46, 1949.

[11] U. Frisch and G. Parisi. Fully developed turbulence and intermittency in turbulence, and predictability in geophysical fluid dynamics and climate dynamics. In M. Ghil, editor, *International school of physics "Enrico Fermi"*, Course 88, page 84. North Holland-Elsevier Science Publishers, 1985.

[12] T.C. Halsey, M.H. Jensen, L.P. Kadanoff, I. Procaccia, and B.I. Shraiman. Fractal measures and their singularities: the characterisation of strange sets. *Phys. Rev. A*, 33:1141, 1986.

[13] H.G.E. Hentschel and I. Procaccia. The infinite number of generalized dimensions of fractals and strange attractors. *Physica*, 8D:435, 1983.

[14] N. Makarov. Preprint.

[15] B.B. Mandelbrot. A class of multifractal measures with negative (latent) value for the dimension $f(\alpha)$. In Luciano Pietronero, editor, *Fractals: physical origin and properties* (Erice, 1988). Plenum Press, New York, 1989.

[16] B.B. Mandelbrot. Limit log-normal multifractal measures. In Errol Gotsman, editor, *Frontiers of physics: Landau memorial conference*, pages 91–122, Tel Aviv (1988), 1989. Pergamon, New York.

[17] B.B. Mandelbrot. Multifractal measures, especially for the geophysicist. *Annual Rev. of Materials Sciences*, 19:514–516, 1989.

[18] B.B. Mandelbrot. New "anomalous" multiplicative multifractals: left sided $f(\alpha)$ and the modeling of DLA. In *Condensed matter physics, in honour of Cyrill Domb*, Bar Ilan (1990), 1990. Physica A.

[19] B.B. Mandelbrot. Two meanings of multifractality, and the notion of negative fractal dimension. In *Soviet-American chaos meeting*, Woods Hole (1989), 1990. American Institute of Physics.

[20] B.B. Mandelbrot, C.J.G. Evertsz, and Y. Hayakawa. Exactly self-similar "left-sided" multifractal measures. *Phys. Rev. A*. Submitted.

[21] G. Michon. Mesures de Gibbs sur les Cantor Réguliers. *Ann. Inst. Henri Poincaré*. Submitted.

[22] G. Michon. Une construction des mesures de Gibbs sur certains ensembles de Cantor. *C.R. Acad. Sci. Paris*, 308:315–318, 1989.

[23] J.-F. Muzy, E. Bacry, and A. Arneodo. Wavelets and multifractal formalism for singular signals: application to turbulence data. Preprint.

[24] D. Sullivan. Entropy, Hausdorff measures old and new, and limit sets of geometrically finite Kleinian groups. *Acta Math*, 153:259–277, 1984.

[25] C. Tricot. *Sur la classification des ensembles Boréliens de mesure de Lebesgue nulle*. PhD thesis, Faculté des Sciences de l'Université de Genève, 1980. No. 1921.

[26] C. Tricot. Two definitions of fractional dimension. *Math. Proc. Camb. Phil. Soc.*, 91:57–74, 1982.

[27] C. Tricot and S.J. Taylor. Packing measure and its evaluation for a Brownian path. *Trans. Amer. Math. Soc.*, 288(2):679–699, 1985.

[28] B. Volkman. Ober Hausdorffsche dimensionen von Mengen, die durch Zifferneigenschaften charakterisiert II, III & IV. *Math. Zeitschr*, 59:247–254. 259–270, 425–433, 1953-54.

Applications of Gabor and wavelet expansions to the Radon transform†

David Walnut
Department of Mathematical Sciences
George Mason University
Fairfax, VA 22030 USA
dwalnut@gmuvax2.gmu.edu

Abstract We investigate the relationship between the Radon transform and certain phase space localization functions, namely the continuous Gabor and wavelet transforms. We derive inversion formulas for the Radon transform based on the Gabor and wavelet transform. Some of these formulas give a direct reconstruction of f or of $\Delta^{\frac{1}{2}} f$ from the Radon transform data. Others show how the Gabor and wavelet transforms of f or $\Delta^{\frac{1}{2}} f$ can be recovered directly from the Radon transform data. We suggest ways in which these formulas can lead to efficient reconstruction algorithms and can be applied to noise reduction in reconstructed images.

1. Introduction

The *Radon transform* is a mathematical tool which is used to describe an image (which may be thought of as a function of several, typically two, variables) in terms of intensity averages over lines or hyperplanes in several directions. Typically such averages can be easily measured while the function itself is inaccessible. In computerized tomography (CT) scanners, for example, one wishes to determine the tissue density function in a cross-section of the human body from non-invasive measurements. The basic problem is the accurate recovery of the unknown function or at least relevant features of the unknown function in a stable fashion and requiring the fewest possible measurements. In addition to medical applications, the Radon transform has also been used in astronomy, electron microscopy, optics, geophysics [7]. The Radon transform has recently been proposed as the basis of a recovery instrument for space plasmas, and in determining the chemical composition of flames [23].

† This paper is a report of joint work being undertaken by the author together with Carlos Berenstein of the University of Maryland.

J. S. Byrnes et al. (eds.), Probabilistic and Stochastic Methods in Analysis, with Applications, 187–205.
© 1992 *Kluwer Academic Publishers. Printed in the Netherlands*

Given a function f defined on $\mathfrak{R}^d$, its Radon transform, Rf consists of the average of f over all hyperplanes in $\mathfrak{R}^d$. For example, the Radon transform in the plane (d = 2) would consist of the integrals over all lines of a function defined in the plane. In planar imaging, these averages can be found by measuring the attenuation of a beam passing through a two dimensional slice of the body. In some applications, one also needs to consider integration over k-planes in $\mathfrak{R}^d$. For instance, when d = 3, NMR scanners can be modelled in terms of the hyperplane Radon transform, but emission tomography leads naturally to integration on straight lines. This is usually called the X-ray transform. For simplicity, the rest of the discussion in this paper will be about the hyperplane transform. In this case, the hyperplane averages of f are organized as follows.

$$R_\theta f(s) = \int_{\theta^\perp} f(s\theta + y)\, dy$$

where $\theta \in S^{d-1}$ and $s \in \mathfrak{R}$.

The adjoint of the Radon transform is commonly referred to as the *backprojection* operator and is defined as follows. For a function h defined on $S^{d-1} \times \mathfrak{R}$,

$$R^\# h(x) = \int_{S^{d-1}} h(\theta, x \cdot \theta)\, d\theta$$

with $x \in \mathfrak{R}^d$.

In even dimensions, the Radon transform is non-local in the sense that the recovery of f(x) requires knowledge of the integrals of f over all hyperplanes. By contrast in odd dimensions recovery of f(x) requires only the integrals of f over hyperplanes passing through a neighborhood of x. This is an important consideration in medical imaging as one wants to expose the patient to as little radiation as possible.

An approach which tries to preserve locality in even dimensions has recently been proposed in [9]. This involves the recovery of Λf where $\Lambda = 1/2\pi(-\Delta)^{1/2}$ where Δ is the Laplacian. In even dimensions, it is possible to recover $\Lambda f(x)$ from integrals of f on hyperplanes passing through a neighborhood of x. Since Λ acts as a differentiation operator, the image Λf tends to highlight edges in f(x), i.e., regions of sharp changes in tissue density, and also to reveal more clearly details such as small blood vessels. This approach is known as *local tomography* or *Lambda tomography* [18, 9].

The *Gabor transform*, a variant of which is known as the short-time Fourier transform, was introduced in 1946 by D. Gabor [13] as a tool in communication theory. It and its variants have long been used by engineers in digital signal processing applications. More recently, the Gabor transform has been used as a tool in image analysis, compression, and segmentation

[6, 22]. The transform compares a given signal to shifts and modulations of a fixed window function, g, that is, to

$$g_{x,\xi}(t) = e^{2\pi i \xi \cdot (t-x)}\, g(t-x). \tag{1.1}$$

In this way, the transform gives a time-frequency picture of the signal. Gabor used a Gaussian as a window in order to achieve the best possible joint localization in time and frequency. With the short-time Fourier transform, a box function is used as a window. Discrete versions of the Gabor transform, known as frames [8], exist which permit stable and efficient expansions and reconstruction of functions [4]. However, such developments are necessarily overcomplete [1, 2]. Recently an orthonormal basis closely related to frames of Gabor functions has been discovered [5]. Such bases are known as *Wilson bases* and consist of linear combinations of pairs of Gabor functions. The Wilson basis functions are real valued, and their close relation to Gabor functions permits easy computation.

The *wavelet transform*, introduced in [16] has been an increasingly popular tool for signal and image analysis. The transform compares a signal to shifts and dilates of a fixed function, the mother wavelet ψ, that is, to

$$\psi_{a,b}(t) = a^{-d\ 2}\psi((t-b)/a) \tag{1.2}$$

with $a \in \mathfrak{R}$ and $b \in \mathfrak{R}^d$. As a time-frequency localization operator, the wavelet transform is fundamentally different from the Gabor transform. By using dilations the wavelet transform can achieve arbitrary fine time localization while still giving a complete representation of the signal. Remarkable wavelet orthonormal bases have been constructed consisting of smooth and rapidly decaying (even compactly supported) functions. The expansion and reconstruction of a signal in such a basis is very efficient numerically, and in fact is faster than the FFT.

In this paper, we investigate some of the connections between the Gabor and wavelet transforms and the Radon transform. We will derive inversion formulas for the Radon transform based on the Gabor and wavelet transforms. One type is a direct inversion formula based on the development of $R_\theta f(s)$ for each θ in a series of the form

$$R_\theta f(s) = \sum_{n,m} c_{n,m}(\theta)\, h_{n,m}(s) \tag{1.3}$$

where the $h_{n,m}$ can be a collection of Gabor functions, a Wilson basis, or a wavelet basis. In the case of Gabor or Wilson functions, the advantage lies in the fact that the basis functions are known explicitly so there are no problems of interpolation in the reconstruction scheme. In the wavelet case, the basis functions do not in general admit a closed form analytic expression, so numerical approximations must be used. In this case, however, the computation of the coefficients is extremely fast.

Another type of inversion formula presented here is based on the method of filtered backprojection which is essentially an implementation of the formula (see Proposition 2.4)

$$K * f = R^{\#}(k * Rf) \tag{1.4}$$

where $R^{\#}k = K$ [19]. The idea is to compute (1.4) for functions K which approximate the δ-function. Such K are often referred to as "point-spread functions." Since both the Gabor and wavelet transforms can be realized as convolution operators, it seems natural to ask whether one can recover these transforms directly from the Radon transform data. In the Gabor case, the kernels K are modulated Gaussians and in the wavelet case are dilates of a fixed mother wavelet. In Sections 2 and 3, formulas are derived which in some cases allow the recovery of the Gabor and wavelet transforms directly from the one-dimensional transforms applied to the data $R_\theta f$ for each θ.

In both cases, the formulas are local in odd dimensions and in even dimensions Λf can be recovered in a local fashion. Also, the formulas allow the selective recovery of f or Λf at certain frequencies (the Gabor case) or at certain resolutions (the wavelet case). This feature can be useful in the noise reduction of tomographic images [21].

In this paper we use the following notations. We denote by $\mathfrak{R}^d$, d dimensional Euclidean space and by $\mathfrak{R}^d$ its dual space. The Fourier transform in $\mathfrak{R}^d$ is defined by $\hat{f}(\xi) = \int_{\mathfrak{R}^d} e^{2\pi i \xi \cdot x} f(x)\,dx$ whenever f is integrable and as an appropriate limit when it is not. We denote by $S(\mathfrak{R}^d)$ the space of infinitely differentiable functions which, with all of their derivatives, decay faster than any polynomial. This space is commonly refered to as the Schwartz space.

We begin with a review of the definition and some basic properties of the Radon transform.

2. The Radon transform

2.1. Definitions and preliminaries

Definition 2.1. Given $f \in S(\mathfrak{R}^d)$, we define the *Radon transform*, Rf of f by

$$Rf(\theta, s) = R_\theta f(s) = \int_{\theta^\perp} f(s\theta + y)\,dy$$

where $\theta \in S^{d-1}$, $s \in \mathfrak{R}$.

Definition 2.2. Given h a bounded continuous function on $\mathfrak{R}$, we define for each $\theta \in S^{d-1}$, the operator $R_\theta^{\#}$ by

$$R_\theta^{\#} h(x) = h(x \cdot \theta).$$

For h bounded on $S^{d-1} \times \mathfrak{R}$, we define the operator $R^{\#}$ by

$$R^{\#}h(x) = \int_{S^{d-1}} h(\theta, x \cdot \theta).$$

Note that given $f \in \mathbf{S}(\mathfrak{R}^d)$ and $h \in \mathbf{S}(\mathfrak{R})$, we have that

$$\begin{aligned}\int_{\mathfrak{R}} R_\theta f(s)\, h(s)\, ds &= \int_{\mathfrak{R}} \int_{\theta^\perp} f(s\theta + y)\, dy\, h(s)\, ds \\ &= \int_{\mathfrak{R}^d} f(x)\, h(x \cdot \theta)\, dx = \int_{\mathfrak{R}^d} f(x)\, R_\theta^{\#} h(x)\, dx.\end{aligned}$$

Also, for $f \in \mathbf{S}(\mathfrak{R}^d)$, and $h \in \mathbf{S}(S^{d-1} \times \mathfrak{R})$, integrating the above over S^{d-1} gives

$$\int_{S^{d-1}} \int_{\mathfrak{R}} Rf(\theta, s)\, h(\theta, s)\, ds\, d\theta = \int_{\mathfrak{R}^d} f(x)\, R^{\#} h(x)\, dx.$$

In this sense, $R_\theta^{\#}$ and $R^{\#}$ are the formal adjoints of R_θ and R.

We now collect some basic properties of the Radon transform whose proofs can be found in any standard text on the subject, e.g., [19].

Proposition 2.3. Let $f, g \in \mathbf{S}(\mathfrak{R}^d)$. Then for a.e., θ and s,

$$R_\theta(f * g)(s) = R_\theta f * R_\theta g(s)$$

where the convolution on the left is in $\mathfrak{R}^d$ and that on the right is in $\mathfrak{R}$.

Proof. Suppose that $f, g \in \mathbf{S}(\mathfrak{R}^d)$.

$$\begin{aligned}R_\theta(f * g)(s) &= \int_{\theta^\perp} \int_{\mathfrak{R}^d} f(t)\, g(s\theta + y - t)\, dt\, dy \\ &= \int_{\mathfrak{R}} \int_{\theta^\perp} f(\tau\theta + t') \int_{\theta^\perp} g((s - \tau)\theta + y - t')\, dy\, dt'\, d\tau \\ &= \int_{\mathfrak{R}} R_\theta f(\tau) R_\theta g(s - \tau)\, d\tau = R_\theta f * R_\theta g(s).\end{aligned}$$

■

Proposition 2.4. Let $f \in \mathbf{S}(\mathfrak{R}^d)$, $g \in L^\infty(\mathfrak{R})$. Then for each $\theta \in S^{d-1}$,

$$(R_\theta^{\#} g) * f = R_\theta^{\#}(g * R_\theta f) \tag{2.1}$$

where the convolution on the left is in $\mathfrak{R}^d$ and that on the right is in $\mathfrak{R}$.

If $g \in L^\infty(S^{d-1} \times \mathfrak{R})$, then

$$R^{\#} g * f = R^{\#}(g * Rf). \tag{2.2}$$

Proof. Assume that $f \in S(\mathfrak{R}^d)$. For $\theta \in S^{d-1}$ fixed, let $t = \tau\theta + t'$ and $x = s\theta + x'$. Then

$$\begin{aligned}\int_{\mathfrak{R}^d} g(t\cdot\theta)\, f(x-t)\, dt &= \int_{\theta^\perp}\int_{\mathfrak{R}} g(\tau) f((s-\tau)\theta + (x'-t'))\, d\tau\, dt' \\ &= \int_{\mathfrak{R}} g(\tau)\int_{\theta^\perp} f((s-\tau)\theta + (x'-t'))\, dt'\, d\tau \\ &= \int_{\mathfrak{R}} g(\tau) R_\theta f(s-\tau)\, ds = g * R_\theta f(x\cdot\theta).\end{aligned}$$

This proves (2.1). Integrating the above formula over $\theta \in S^{d-1}$ gives (2.2) for $f \in S(\mathfrak{R}^d)$. ∎

2.2. Inversion of the Radon transform

Proposition 2.5 (The Fourier Slice Theorem). Let $f \in S(\mathfrak{R}^d)$. Then for $\theta \in S^{d-1}$, $\gamma \in \mathfrak{R}$,

$$(R_\theta f)^\wedge(\gamma) = \hat{f}(\gamma\theta). \tag{2.3}$$

Proof.

$$\begin{aligned}\int_{\mathfrak{R}} R_\theta f(s)\, e^{-2\pi i s\gamma}\, ds &= \int_{\mathfrak{R}}\int_{\theta^\perp} f(s\theta + y)\, e^{-2\pi i s\gamma}\, dy\, ds \\ &= \int_{\mathfrak{R}^d} f(x)\, e^{-2\pi i (x\cdot\gamma\theta)}\, dx = \hat{f}(\gamma\theta).\end{aligned}$$

∎

Corollary to 2.5 (Fourier inversion). Let $f \in S(\mathfrak{R}^d)$. Then

$$f(x) = \int_{S_+^{d-1}}\int_{-\infty}^{\infty} (R_\theta f)^\wedge(r)\, e^{2\pi i (x\cdot\theta) r} |r|^{d-1}\, dr\, d\theta. \tag{2.4}$$

where S_+^{d-1} denotes the upper-half sphere in $\mathfrak{R}^d$.

Proof. Writing the standard Fourier inversion formula

$$f(x) = \int \hat{f}(\xi)\, e^{2\pi i (x\cdot\xi)}\, d\xi$$

in polar coordinates and using (2.3) gives

$$\begin{aligned}f(x) &= \int_{S^{d-1}}\int_0^\infty (R_\theta f)^\wedge(r)\, e^{2\pi i (x\cdot\theta) r} r^{d-1}\, dr\, d\theta \\ &= \int_{S_+^{d-1}}\int_{-\infty}^{\infty} (R_\theta f)^\wedge(r)\, e^{2\pi i (x\cdot\theta) r} |r|^{d-1}\, dr\, d\theta\end{aligned}$$

since $(R_{-\theta}f)^\wedge(r) = (R_\theta f)^\wedge(-r)$. ∎

Definition 2.6. Let $f \in S(\mathfrak{R}^d)$, $\alpha \in \mathfrak{R}$. Then we define the *Riesz potential operator*, I^α by $(I^\alpha f)^\wedge(\xi) = |\xi|^{-\alpha}\hat{f}(\xi)$.

If $\alpha = -2$, then $I^\alpha = -1/(2\pi)^2\Delta$, and Δ is the Laplacian. If $\alpha = -1$, we refer to I^{-1} as the *Lambda operator*, Λ, which is important in local tomography. Note that $\Lambda f = 1/2\pi\,(-\Delta)^{1/2}f$, see [9, 18, 19, 7].

Proposition 2.7. Let $f \in S(\mathfrak{R}^d)$, $\alpha < n$. Then

$$f = \frac{1}{2} I^{-\alpha} R^\# I^{\alpha+1-d} R f. \tag{2.5}$$

Proof. See [19]. ∎

Corollary to 2.7. If $\alpha = 0$ then

1) if d is even,

$$f = \frac{1}{2(2\pi i)^{d-2}} R^\# H \partial_s^{d-1} R_\theta f$$

2) if d is odd,

$$f = \frac{1}{2(2\pi i)^{d-1}} R^\# \partial_s^{d-1} R_\theta f$$

where H is the Hilbert transform on $\mathfrak{R}$, i.e., for $\gamma \in \hat{\mathfrak{R}}$,

$$(Hf)^\wedge(\gamma) = \frac{1}{2\pi i}\sigma(\gamma)\hat{f}(\gamma) \tag{2.6}$$

(σ is the signum function) and ∂_s means differentiation with respect to s.

If $\alpha = -1$ and d is even,

$$\Lambda f = I^{-1} f = \frac{1}{2(2\pi i)^d} R^\# \partial_s^d R_\theta f. \tag{2.7}$$

Proof. For d even, $d - 1$ is odd, so for any $h \in S(\mathfrak{R})$,

$$\begin{aligned} I^{1-d}h(s) &= \int_{\mathfrak{R}} |\gamma|^{d-1}\hat{h}(\gamma)\, e^{2\pi i\gamma s}\, ds \\ &= 1/(2\pi i)^{d-2}\int_{\mathfrak{R}} \sigma(\gamma)/2\pi i\,(2\pi i\gamma)^{d-1}\hat{h}(\gamma)\, e^{2\pi i\gamma s}\, ds \\ &= 1/(2\pi i)^{d-2} H\partial_s^{d-1}h(s). \end{aligned}$$

Taking $h(s) = R_\theta f(s)$ gives 1) and 2).

Similarly for d odd,

$$I^{1-d}h(s) = 1/(2\pi i)^{d-1}\partial_s^{d-1}h(s).$$

Taking $h(s) = R_\theta f(s)$ gives (2.7). ∎

3. Radon transform inversion based on the Gabor transform

3.1. Background and preliminaries on the Gabor transform

Definition 3.1. We define the following operators. Given a function h defined on $\mathfrak{R}^d$,

1) $E_y h(t) = e^{2\pi i y\cdot t}h(t)$, $y \in \mathfrak{R}^d$.
2) $T_x h(t) = h(t-x)$, $x \in \mathfrak{R}^d$.
3) $D_a h(t) = h_a(t) = a^{-d/2}h(t/a)$, $a > 0$.

Given $f \in S(\mathfrak{R}^d)$, and h a real-valued even function on $\mathfrak{R}^d$ with $\|h\|_2 = 1$, we define for $x \in \mathfrak{R}^d$ and $\xi \in \mathfrak{R}^d$,

$$h_{x,\xi}(t) = e^{2\pi i \xi\cdot(t-x)}h(t-x).$$

The Gabor transform of f with respect to h is defined by

$$\Psi^{(d)}(h;f)(x,\xi) = \int_{\mathfrak{R}^d} f(y)\,h_{x,\xi}(y)\,dy = E_\xi h * f(x). \tag{3.1}$$

In what follows we will in general take the analyzing function h to be the Gaussian or a scaled version of the Gaussian. Therefore we define $g(x) = e^{-\pi|x|^2}$ for $x \in \mathfrak{R}^d$. We use the same notation for the Gaussian in different dimensions. The dimension will always be clear from the context.

The following facts are readily proved [4, 17].

Proposition 3.2.

$$\int_{\mathfrak{R}^d}\int_{\mathfrak{R}^d} |\Psi^{(d)}(h;f)(x,\xi)|^2\,dx\,d\xi = \int_{\mathfrak{R}^d} |f(t)|^2\,dt. \tag{3.2}$$

$$\Psi^{(d)}(h;f)(x,\xi) = \int_{\mathfrak{R}^d}\int_{\mathfrak{R}^d} \Psi^{(d)}(h;f)(x',\xi')\,e^{2\pi i(\xi-\xi')\cdot x}\,\Psi^{(d)}(h;h)(x-x',\xi-\xi')\,dx'\,d\xi'. \tag{3.3}$$

$$f(t) = \int_{\mathfrak{R}^d}\int_{\mathfrak{R}^d} \Psi^{(d)}(h;f)(x,\xi)\,h_{x,\xi}(t)\,dx\,d\xi. \tag{3.4}$$

(3.2) means that $\Psi^{(d)}$ is an isometry on L^2. That is, $\Psi^{(d)}$ is an injection from $L^2(\mathfrak{R}^d)$ into $L^2(\mathfrak{R}^d \times \mathfrak{R}^d)$ and is invertible on its range. The inversion formula (3.4) is valid as written when f has sufficient smoothness and

decay. Otherwise the integral on the right must be interpreted as an appropriate limit. This inversion formula is formally analogous to the Fourier inversion formula.

We now give a brief exposition of some of the sampling and interpolation properties of the Gabor transform which will be useful later on. Details and proofs may be found in the cited references.

The reproducing formula (3.3) characterizes the range of the map $\Psi^{(d)}$. It shows that this range is very small and hence that $\Psi^{(d)}f$ contains a lot of redundant information about f. This fact has been exploited in [10, 11] to show that in fact $f \in \mathbf{S}(\mathfrak{R}^d)$ is completely recoverable from any sufficiently dense sampling of its Gabor transform. This has also been shown in other contexts for regular lattices [4, 17, 20]. The necessary density of the lattice depends only on the analyzing function h and not on f. For example, it is known that when h is the Gaussian, then any $f \in \mathbf{S}(\mathfrak{R}^d)$ can be recovered completely from the samples $\Psi^{(d)}(g; f)(n/2, m)$ with $n, m \in \mathbb{Z}^d$ in the following sense [4, 5].

Proposition 3.3. Given $f \in \mathbf{S}(\mathfrak{R}^d)$, there is a function g with exponential decay in time and frequency such that

$$f(x) = \sum_{n \in \mathbb{Z}^d} \sum_{m \in \mathbb{Z}^d} \Psi^{(d)}(g; f)(n/2, m)\, g_{n/2,m}(x) \tag{3.5}$$

where the sum converges absolutely and uniformly.

Proposition 3.3 says in particular that the collection $\{g_{m,n/2}\}$ is a *frame* for the Fréchet space $\mathbf{S}(\mathfrak{R}^d)$ [14, 12]. In fact, g and g are very close in many senses (in particular, in the L^1 and L^∞ sense) and

$$f(x) \approx \sum_{n \in \mathbb{Z}^d} \sum_{m \in \mathbb{Z}^d} \Psi^{(d)}(g; f)(n/2, m)\, g_{n/2,m}(x) \tag{3.6}$$

is a good approximation.

In the case $d = 1$, even more can be said. In [5], it has been recently shown that the collection

$$h_{0,n}(x) = g(x - n), \qquad n \in \mathbb{Z}$$
$$h_{\ell,n}(x) = \sqrt{2}(g_{n/2,m} + (-1)^{\ell+n} g_{n/2,m}), \qquad \ell = 0, 1, \ldots; n \in \mathbb{Z}$$

is a non-orthogonal basis for $L^2(\mathfrak{R})$ and an unconditional basis for $\mathbf{S}(\mathfrak{R})$ (see also [12, 15, 20]). This basis can be rewritten in the following more convenient way.

$$h_{0,n}(x) = g(x - n), \qquad n \in \mathbb{Z}$$
$$h_{\ell,n}(x) = \sqrt{2}g(x - n/2)\cos(2\pi\ell x) \qquad \ell + n \text{ even}; n \in \mathbb{Z}$$
$$h_{\ell,n}(x) = i\sqrt{2}g(x - n/2)\sin(2\pi\ell x) \qquad \ell + n \text{ odd}; n \in \mathbb{Z}$$

As before,

$$f(x) \approx \sum_{\ell \geq 0} \sum_{n \in \mathbb{Z}} \langle f, h_{\ell,n} \rangle h_{\ell,n}(x)$$

is a good approximation. The advantage of such a basis is that a real-valued function f is developed as a series of real-valued functions. Also, its close relation to the Gabor functions allows for easy computation.

3.2. Inversion formulas

Proposition 3.4. Let $\lambda > 0$ and let the collection of functions $\{g^{\lambda}_{\ell,n}\}$ be defined by

$$g^{\lambda}_{0,n} = g_{\lambda}(x - \lambda^{1/2} n), \qquad n \in \mathbb{Z}$$
$$g^{\lambda}_{\ell,n} = \sqrt{2} g_{\lambda}(x - \lambda^{1/2} n/2) \cos(2\pi\lambda^{1/2}\ell x) \qquad \ell + n \text{ even}; n \in \mathbb{Z}$$
$$g^{\lambda}_{\ell,n} = \sqrt{2} g_{\lambda}(x - \lambda^{1/2} n/2) \sin(2\pi\lambda^{1/2}\ell x) \qquad \ell + n \text{ odd}; n \in \mathbb{Z}$$

Then $\{g^{\lambda}_{\ell,n}\}$ is an unconditional basis for $\mathbf{S}(\mathfrak{R})$. Moreover,

$$g^{\lambda}_{0,n} = 1/\sqrt{2\pi}\lambda^{1/2} \hat{g}_{\lambda} e_{n\lambda}, \qquad n \in \mathbb{Z}$$
$$g^{\lambda}_{\ell,n} = 1/\sqrt{2\pi}\lambda^{1/2} (T_{\lambda^{1/2}\ell} \hat{g} + T_{-\lambda^{1/2}\ell} \hat{g}) e_{n\lambda/2} \qquad \ell + n \text{ even}; n \in \mathbb{Z}$$
$$g^{\lambda}_{\ell,n} = 1/i\sqrt{2\pi}\lambda^{1/2} (T_{\lambda^{1/2}\ell} \hat{g} - T_{-\lambda^{1/2}\ell} \hat{g}) e_{n\lambda/2} \qquad \ell + n \text{ odd}; n \in \mathbb{Z}$$

Proof. The first part is merely a dilation of the Wilson basis defined previously. The second part is an easy computation. ∎

Proposition 3.5 (Inversion with Wilson bases). Let $f \in \mathbf{S}(\mathfrak{R}^d)$, and suppose that for each $\theta \in S^{d-1}$,

$$R_{\theta} f(s) = \sum_{\ell \geq 0} \sum_{n \in \mathbb{Z}} c_{\ell,n}(\theta)\, g^{\lambda}_{\ell,n}(s) \tag{3.7}$$

Then

1) If d is even,

$$f(x) = 1/(2\pi i)^{d-2} \sum_{\ell \geq 0} \sum_{n \in \mathbb{Z}} \int_{S^{d-1}} c_{\ell,n}(\theta) H\partial_s^{d-1} g^{\lambda}_{\ell,n}(x \cdot \theta)\, d\theta \tag{3.8}$$

and

$$\Lambda f(x) = 1/(2\pi i)^{d} \sum_{\ell \geq 0} \sum_{n \in \mathbb{Z}} \int_{S^{d-1}} c_{\ell,n}(\theta) \partial_s^{d} g^{\lambda}_{\ell,n}(x \cdot \theta)\, d\theta \tag{3.9}$$

2) If d is odd,

$$f(x) = 1/(2\pi i)^{d-1} \sum_{\ell=0}^{\infty} \sum_{n\in\mathbb{Z}} \int_{S^{d-1}} c_{\ell,n}(\theta) \partial_s^{d-1} g_{\ell,n}^{\lambda}(x\cdot\theta)\, d\theta \quad (3.10)$$

Proof. Note first that since the sum in (3.7) converges absolutely and uniformly and in L^2,

$$(R_\theta f)^\wedge(r) = \sum_{\ell=0}^{\infty} \sum_{n\in\mathbb{Z}} c_{\ell,n}(\theta)\, \hat{g}_{\ell,n}^{\lambda}(r). \quad (3.11)$$

By (2.4), we have

$$\begin{aligned} f(x) &= \int_{S^{d-1}} \int_{-\infty}^{\infty} (R_\theta f)^\wedge(r)\, e^{2\pi i r x\cdot\theta} |r|^{d-1}\, dr\, d\theta \\ &= \sum_{\ell=0}^{\infty} \sum_{n\in\mathbb{Z}} \int_{S^{d-1}} c_{\ell,n}(\theta) \int_{-\infty}^{\infty} \hat{g}_{\ell,n}^{\lambda}(r)\, e^{2\pi i r x\cdot\theta} |r|^{d-1}\, dr\, d\theta \\ &= 1/(2\pi i)^{d-2} \sum_{\ell=0}^{\infty} \sum_{n\in\mathbb{Z}} \int_{S^{d-1}} c_{\ell,n}(\theta) \int_{-\infty}^{\infty} \sigma(r)\, 2\pi i \hat{g}_{\ell,n}^{\lambda}(r) \\ &\qquad e^{2\pi i r x\cdot\theta} (2\pi i r)^{d-1}\, dr\, d\theta \\ &= 1/(2\pi i)^{d-2} \sum_{\ell=0}^{\infty} \sum_{n\in\mathbb{Z}} \int_{S^{d-1}} c_{\ell,n}(\theta) H\partial_s^{d-1} g_{\ell,n}^{\lambda}(x\cdot\theta)\, d\theta. \end{aligned}$$

This proves (3.8), and (3.10) follows similarly.

To prove (3.9), note that

$$\begin{aligned} \Lambda f(x) &= \int_{\mathbb{R}^d} |\xi| f(\xi)\, e^{2\pi i \xi\cdot x}\, d\xi \\ &= \int_{S^{d-1}} \int_0^{\infty} r (R_\theta f)^\wedge(r)\, e^{2\pi i r x\cdot\theta} r^{d-1}\, dr\, d\theta \\ &= \int_{S^{d-1}} \int_{-\infty}^{\infty} (R_\theta f)^\wedge(r)\, e^{2\pi i r x\cdot\theta} r^{d}\, dr\, d\theta. \end{aligned}$$

The result now follows just as in the proof of (3.8). ∎

Lemma 3.6. Let $\xi \in \mathbb{R}^d$, $\lambda > 0$. Then

$$R_\theta(E_\xi g_\lambda)(s) = \lambda^{1/2} e^{-\pi\lambda^{-1}|\xi|^2} e^{\pi\lambda^{-1}(\xi\cdot\theta)^2} E_{\xi\cdot\theta} g_\lambda(s). \quad (3.12)$$

Proof. With $\xi = t\theta + \eta$, $\eta \perp \theta$, $\xi' = s\theta + \eta$, we have

$$\begin{aligned}\int_{\theta^\perp} E_\xi g_\lambda(s\theta + y)\,dy &= \lambda^{d-2}\int_{\theta^\perp} e^{2\pi i\lambda(t-s)}\,e^{-\pi\lambda(s^2+|y|^2)}\,dy \\ &= e^{2\pi i\lambda t}e^{-\pi\lambda s^2}\lambda^{d-2}\int_{\theta^\perp} e^{-2\pi i\lambda\langle\eta,y\rangle}e^{-\pi\lambda|y|^2}\,dy \\ &= \lambda^{\frac{d}{2}-2}e^{2\pi i\lambda t}e^{-\pi\lambda s^2}e^{-\pi\lambda^{-1}|\xi|^2}\end{aligned}$$

Observing that $\xi'^2 = \xi^2 + (\xi\cdot\theta)^2$ completes the proof. ∎

Proposition 3.7.

1) For d even,

$$E_\xi g_\lambda(x) = \frac{1}{2(2\pi i)^{d-2}}\lambda^{\frac{d}{2}-2}e^{-\pi\lambda^{-1}|\xi|^2}\int_{S^{d-1}} e^{\pi\lambda^{-1}\langle\xi,\theta\rangle^2}H\partial_\xi^{d-1}E_\xi * g_\lambda(x\cdot\theta)\,d\theta$$

where H denotes the Hilbert transform, see (2.6).

2) For d odd,

$$E_\xi g_\lambda(x) = \frac{1}{2(2\pi i)^{d-1}}\lambda^{\frac{d}{2}-2}e^{-\pi\lambda^{-1}|\xi|^2}\int_{S^{d-1}} e^{\pi\lambda^{-1}\langle\xi,\theta\rangle^2}\partial_\xi^{d-1}E_\xi * g_\lambda(x\cdot\theta)\,d\theta.$$

Proof. Both (a) and (b) follow from the inversion formulas in the corollary to Proposition 2.7 and from Lemma 3.6. ∎

Corollary to 3.7. For d even

$$\Delta E_\xi g_\lambda(x) = \frac{1}{2(2\pi i)^d}\lambda^{\frac{d}{2}-2}e^{-\pi\lambda^{-1}|\xi|^2}\int_{S^{d-1}} e^{\pi\lambda^{-1}\langle\xi,\theta\rangle^2}\partial_\xi^d E_\xi * g_\lambda(x\cdot\theta)\,d\theta$$

Proposition 3.8 (Filtered backprojection). Let $f \in \mathcal{S}(\mathbb{R}^d)$, $\lambda > 0$.

1) If d is even,

$$\Psi^d(g_\lambda; f)(x,\xi) = \frac{1}{2(2\pi i)^{d-2}}\lambda^{\frac{d}{2}-2}e^{-\pi\lambda^{-1}|\xi|^2}\int_{S^{d-1}} e^{\pi\lambda^{-1}\langle\xi,\theta\rangle^2}H\partial_\xi^{d-1}E_\xi * g_\lambda * R_\theta f(x\cdot\theta)\,d\theta$$

2) If d is odd,

$$\Psi^{(d)}(g_\lambda; f)(x,\xi) = \frac{1}{2(2\pi i)^{d-1}} \lambda^{1/2} e^{-\pi\lambda^{-1}|\xi|^2} \int_{S^{d-1}} e^{\pi\lambda^{-1}(\xi\cdot\theta)^2} \partial_s^{d-1} E_{\xi,\theta} g_\lambda * R_\theta f(x\cdot\theta)\, d\theta$$

Proof. By Proposition 3.7,

$$E_\xi g_\lambda = \lambda^{1/2} e^{-\pi\lambda^{-1}|\xi|^2} R^\#(e^{\pi\lambda^{-1}(\xi\cdot\theta)^2} I^{1-d} E_{\xi,\theta} g_\lambda)(x).$$

By Proposition 2.4,

$$\begin{aligned}\Psi^{(d)}(g_\lambda; f)(x,\xi) &= E_\xi g_\lambda * f(x) \\ &= \lambda^{1/2} e^{-\pi\lambda^{-1}|\xi|^2} \int_{S^{d-1}} e^{\pi\lambda^{-1}(\xi\cdot\theta)^2} I^{1-d} E_{\xi,\theta} g_\lambda * R_\theta f(x\cdot\theta)\, d\theta.\end{aligned}$$

From this the result follows. ∎

Corollary to 3.8.

1) If d is even,

$$\Psi^{(d)}(g_\lambda; Af)(x,\xi) = \frac{1}{2(2\pi i)^d} \lambda^{1/2} e^{-\pi\lambda^{-1}|\xi|^2} \sum_{j=0}^{d} \alpha_j \int_{S^{d-1}} e^{\pi\lambda^{-1}(\xi\cdot\theta)^2} (\xi\cdot\theta)^j \Psi^{(1)}(\partial_s^{d-j} g_\lambda; R_\theta f)(x\cdot\theta, \xi\cdot\theta)\, d\theta$$

where $\alpha_j = \binom{d}{j}(2\pi i)^j$.

2) If d is odd,

$$\Psi^{(d)}(g_\lambda; f)(x,\xi) = \frac{1}{2(2\pi i)^{d-1}} \lambda^{1/2} e^{-\pi\lambda^{-1}|\xi|^2} \sum_{j=0}^{d-1} \alpha_j \int_{S^{d-1}} e^{\pi\lambda^{-1}(\xi\cdot\theta)^2} (\xi\cdot\theta)^j \Psi^{(1)}(\partial_s^{d-1-j} g_\lambda; R_\theta f)(x\cdot\theta, \xi\cdot\theta)\, d\theta$$

where $\alpha_j = \binom{d-1}{j}(2\pi i)^j$.

Proof. Both (a) and (b) follow by the same argument as in Proposition 3.8 together with an application of Leibnitz's rule. ∎

4. Radon inversion based on the wavelet transform

4.1. Background and preliminaries on the wavelet transform

Definition 4.1. Given g a real-valued, square-integrable radial function on $\mathfrak{R}^d$ which satisfies

$$\int_0^\infty |\hat{g}_0(s)|^2/s\, ds < \infty \tag{4.1}$$

(where $g(\xi) = \hat{g}_0(|\xi|)$), we define the wavelet transform of f by

$$\Phi^{(d)}(g;f)(u,v) = \int_{\mathfrak{R}^d} f(t)\, e^{-ud/2} g(e^{-u}t - v)\, dt = f * D_{e^u} g(e^u v) \tag{4.2}$$

where $u \in \mathfrak{R}$ and $v \in \mathfrak{R}^d$. Any function satisfying (4.1) is called *admissible*.

As with the Gabor transform, the following are easily proved [16].

Proposition 4.2.

$$\int_{\mathfrak{R}^d} \int_{\mathfrak{R}} |\Phi^{(d)}(g;f)(u,v)|^2\, du\, dv = \int_0^\infty |\hat{g}_0(s)|^2/s\, ds \int_{\mathfrak{R}^d} |f(t)|^2\, dt. \tag{4.3}$$

$$\Phi^{(d)}(g;f)(u,v) = \int_{\mathfrak{R}^d} \int_{\mathfrak{R}} \Phi^{(d)}(g;f)(u',v') \Phi^{(d)}(g;g)(u-u', v - e^{u'-u}v')\, du'\, dv'. \tag{4.4}$$

$$f(t) = \int_{\mathfrak{R}^d} \int_{\mathfrak{R}} \Phi^{(d)}(g;f)(u,v)\, e^{-ud/2}\, g(e^{-u}t - v)\, du\, dv. \tag{4.5}$$

When $d = 1$, it is possible to construct compactly supported, differentiable functions ψ such that the collection $\{2^{j/2}\psi(2^j x - k)\}_{j,k\in\mathfrak{Z}}$ is an orthonormal basis for $L^2(\mathfrak{R})$. Computing the expansion of a given f in this basis is extremely fast numerically [3].

4.2. Inversion formulas

Proposition 4.3 (Inversion with wavelets). Let $f \in S(\mathfrak{R}^d)$, and suppose that for each $\theta \in S^{d-1}$,

$$R_\theta f(s) = \sum_{j\in\mathfrak{Z}} \sum_{k\in\mathfrak{Z}} c_{j,k}(\theta)\psi_{j,k}(s) \tag{4.6}$$

where $\psi_{j,k}(s) = 2^{j/2}\psi(2^j s - k)$. Then

1) If d is even,

$$f(x) = 1/(2\pi i)^{d-2} \sum_{j\in\mathbb{Z}} \sum_{k\in\mathbb{Z}} \int_{S^{d-1}} c_{j,k}(\theta) H\partial_s^{d-1}\psi_{j,k}(x\cdot\theta)\, d\theta \quad (4.7)$$

and

$$\Lambda f(x) = 1/(2\pi i)^{d} \sum_{j\in\mathbb{Z}} \sum_{k\in\mathbb{Z}} \int_{S^{d-1}} c_{j,k}(\theta)\partial_s^{d}\psi_{j,k}(x\cdot\theta)\, d\theta \quad (4.8)$$

2) If d is odd,

$$f(x) = 1/(2\pi i)^{d-1} \sum_{j\in\mathbb{Z}} \sum_{k\in\mathbb{Z}} \int_{S^{d-1}} c_{j,k}(\theta)\partial_s^{d-1}\psi_{j,k}(x\cdot\theta)\, d\theta \quad (4.9)$$

Proof. This follows exactly as in Proposition 3.5. ∎

Lemma 4.4. $R_\theta(D_{e^u} g)(s) = e^{u(d-1)/2} D_{e^u} R_\theta g(s)$.

Proof.

$$\begin{aligned} e^{-ud/2}\int_{\theta^\perp} g(e^{-u}(s\theta + y))\, dy &= e^{-ud/2}\int_{\theta^\perp} g(e^{-u}s\theta + e^{-u}y))\, dy \\ &= e^{ud/2}e^{-u}\int_{\theta^\perp} g(e^{-u}s\theta + y))\, dy \\ &= e^{u(d-1)/2} D_{e^u} R_\theta g(s). \end{aligned}$$

∎

Proposition 4.5. For $g \in S(\mathfrak{R}^d)$,

$$D_{e^u} g(x) = 1/2 e^{-u(d-1)/2} \int_{S^{d-1}} D_{e^u} I^{1-d} R_\theta g(x\cdot\theta)\, d\theta.$$

Proof. Note first that for any $h \in S(\mathfrak{R})$, $\alpha \in \mathfrak{R}$,

$$\begin{aligned} I^\alpha D_{e^u} h(x) &= \int_{\mathfrak{R}} |\gamma|^{-\alpha} (D_{e^u} h)^\wedge(\gamma)\, e^{2\pi i\gamma x}\, d\gamma \\ &= e^{u/2}\int_{\mathfrak{R}} |\gamma|^{-\alpha} \hat{h}(e^u\gamma)\, e^{2\pi i\gamma x}\, d\gamma \\ &= e^{\alpha u} e^{-u/2}\int_{\mathfrak{R}} |\gamma|^{-\alpha} \hat{h}(\gamma)\, e^{2\pi i\gamma(e^{-u}x)}\, d\gamma \\ &= e^{\alpha u} D_{e^u} I^\alpha h(x). \end{aligned}$$

Thus,

$$\begin{aligned} D_{e^u} g(x) &= 1/2 R^{\#} I^{1-d} R D_{e^u} g(x) \\ &= 1/2 e^{u(d-1)/2} R^{\#} I^{1-d} D_{e^u} R g(x) \\ &= 1/2 e^{-u(d-1)/2} R^{\#} D_{e^u} I^{1-d} R g(x) \\ &= 1/2 e^{-u(d-1)/2} \int_{S^{d-1}} D_{e^u} I^{1-d} R_\theta g(x \cdot \theta)\, d\theta. \end{aligned}$$

■

Lemma 4.6. Let $g \in \mathbf{S}(\mathfrak{R})$ be real-valued and admissible. Then for any integer $j > 0$, $\partial_s^j g$ is admissible. Also, if $\hat{g} \in \mathbf{S}(\mathfrak{R}^d)$ is a radial function such that $R_\theta \hat{g}(s) = g(s)$ for all $\theta \in S^{d-1}$, then $\hat{g}$ is admissible.

Proof.

$$\begin{aligned} \int_0^\infty |(\partial_s^j g)^\wedge(\gamma)|^2/\gamma \, d\gamma &= (2\pi i)^{2j} \int_0^\infty |\gamma|^{2j} |\hat{g}(\gamma)|^2/\gamma \, d\gamma \\ &= (2\pi i)^{2j} \int_0^\infty \gamma^{2j-1} |\hat{g}(\gamma)|^2 \, d\gamma < \infty \end{aligned}$$

since $g \in \mathbf{S}(\mathfrak{R})$.

Since $\hat{g}$ is radial, so is $(\hat{g})^\wedge$ and by the Fourier slice theorem,

$$(\hat{g})^\wedge(\xi) = (\hat{g})^\wedge(|\xi| \xi/|\xi|) = (R_{\xi/|\xi|} \hat{g})^\wedge(|\xi|) = \hat{g}(|\xi|).$$

Thus, $\hat{g}$ is admissible since g is. ■

Proposition 4.7. Let $f \in \mathbf{S}(\mathfrak{R}^d)$, let $\hat{g} \in \mathbf{S}(\mathfrak{R}^d)$ be an admissible radial function, and let $g \in \mathbf{S}(\mathfrak{R})$ be such that $R_\theta \hat{g}(s) = g(s)$ for all $\theta \in S^{d-1}$.

1) If d is even,

$$\Phi^{[d]}(\hat{g}; f)(u, v) = \frac{1}{2(2\pi i)^{d-2}} e^{u(1-d)/2} \int_{S^{d-1}} \Phi^{[1]}(H \partial_s^{d-1} g; R_\theta f)(u, v \cdot \theta)\, d\theta$$

and

$$\Phi^{[d]}(\hat{g}; \Lambda f)(u, v) = \frac{1}{2(2\pi i)^d} e^{u(1-d)/2} \int_{S^{d-1}} \Phi^{[1]}(\partial_s^d g; R_\theta f)(u, v \cdot \theta)\, d\theta.$$

2) If d is odd,

$$\Phi^{[d]}(\hat{g}; f)(u, v) = \frac{1}{2(2\pi i)^{d-1}} e^{u(1-d)/2} \int_{S^{d-1}} \Phi^{[1]}(\partial_s^{d-1} g; R_\theta f)(u, v \cdot \theta)\, d\theta.$$

5. Conclusions

We have seen how the Gabor and wavelet transforms relate to the Radon transform. We have derived inversion formulas for the Radon transform based on Gabor and wavelet expansions either by a direct method, or by filtered backprojection. The second approach gives directly the Gabor or wavelet transform of f from knowledge of the one-dimensional transform of $R_\theta f$ for each θ.

The idea of using localizing transforms to invert the Radon transform may prove practical for the following reasons.

1) Discretization properties of the continuous parameter Gabor and wavelet transforms are well understood. Recovery of a signal from sparse and even irregular samples of its Gabor or wavelet transform have been studied in [11, 10, 20]. Moreover, an interpolation theory exists for the Gabor or wavelet transform which allows recovery of the continuous parameter transform from its samples at a regular or irregular lattice. This kind of built-in interpolation may enhance numerical stability.
2) Fast numerical algorithms exist for computing the Gabor and wavelet expansions of signals.
3) The spatial localization properties of the Gabor and wavelet transforms suggest efficiency in the odd dimension case and also for local tomography in the plane. The formulas for inversion of the Radon transform in both the Gabor and wavelet case are local in odd dimensions, and in even dimensions Λf can be recovered in a local fashion.
4) The inversion formulas allowing the recovery of the Gabor and wavelet transforms directly from the Radon transform data allow the selective recovery of f or Λf at certain frequencies (the Gabor case) or at certain resolutions (the wavelet case). This feature can be useful in the noise reduction of tomographic images [21].

6. Bibliography

[1] R. Balian. Un principe d'incertitude fort en théorie du signal ou en mécanique quantique. *C.R. Acad. Sci. Paris*, 292:1357–1362, 1981.

[2] G. Battle. Heisenberg proof of the Balian-Low theorem. *Lett. Math. Phys.*, 15:175–177, 1988.

[3] I. Daubechies. Wavelet orthonormal bases of compact support. *Comm. Pure Appl. Math.*, 41:909–996, 1988.

[4] I. Daubechies. The wavelet transform, time-frequency localization and signal analysis. *IEEE Trans. Information Theory*, 36:961–1005, 1990.

[5] I. Daubechies, S. Jaffard, and J.-L. Journé. A simple Wilson basis with exponential decay. To appear.

[6] J. Daugmann. Complete discrete 2-d Gabor transforms by neural networks for image analysis and compression. *IEEE Trans. Acoustics, Speech, Signal Processing*, 36:1169–1179, 1988.

[7] S. Deans. *The Radon Transform and Some of its Applications*. John Wiley & Sons, New York, 1983.

[8] R. J. Duffin and A. C. Schaeffer. A class of nonharmonic Fourier series. *Trans. Amer. Math. Soc.*, 72:341–366, 1952.

[9] A. Faridani, F. Keinert F. Natterer, E. L. Ritman, and K. T. Smith. Local and global tomography. Preprint.

[10] H. Feichtinger and K. Gröchenig. A unified approach to atomic decompositions through integrable group representations. In M. Cwikel et al., editor, *Function Spaces and Applications*, volume 1302 of *Lecture Notes in Math.*, pages 52–73. Springer-Verlag, Berlin, Heidelberg, New York, London, Paris, Tokyo, Hong Kong, 1988.

[11] H. Feichtinger and K. Gröchenig. Irregular sampling theorems and series expansions of bandlimited functions. *I.J. Funct. Anal.*, 86:307–340, 1989.

[12] H. Feichtinger, K. Gröchenig, and D. Walnut. Wilson bases in modulation spaces. *Math. Nachr.*, 1991.

[13] D. Gabor. Theory of communications. *J. Inst. Elec. Eng.*, 93:429–457, 1946.

[14] K. Gröchenig. Describing functions: Atomic decompositions vs. frames. Submitted.

[15] K. Gröchenig and D. Walnut. A Riesz basis for Bargmann-Fock space related to sampling and interpolation. *Arkiv. f. Math.*

[16] A. Grossmann, J. Morlet, and T. Paul. Transforms associated to square integrable group representations, I, General results. *Journal of Mathematics and Physics*, 26:2473–2479, 1985.

[17] C. Heil and D. Walnut. Continuous and discrete wavelet transforms. *SIAM Review*, 31:628–666, 1989.

[18] F. Keinert. Inversion of k-plane transforms and applications in computer tomography. *SIAM Review*, 31:273–298, 1989.

[19] F. Natterer. *The Mathematics of Computerized Tomography*. John Wiley & Sons, New York, 1986.

[20] K. Seip and R. Wallstén. Sampling and interpolation in the Bargmann-Fock space. Preprint.

[21] K.T. Smith, S.L. Wagner, and M.J. Bottema. Sharpening radiographs. *Proc. Nat. Acad. Sci. USA*, 81:5237–5241, 1984.

[22] M. Turner. Texture discrimination by Gabor functions. *Biological Cybernetics*, 55:71–82, 1986.

[23] Y. Zhang, M. Coplan, J. Moore, and C. Berenstein. Computerized tomographic imaging for space plasma physics. To appear.

Normal numbers and dynamical systems

Gavin Brown
School of Mathematics
University of New South Wales
P.O. Box 1
Kensington 2033 NSW Australia
gavin@hydra.maths.unsw.oz.au

Abstract Those dynamical systems generated by integer matrices operating on multidimensional tori are useful general exemplars. In particular, Bill Moran and I have recently explored notions of dependence between pairs of such systems.

It is well known that if the $m \times m$ integer matrix A is nonsingular and has no roots of unity as eigenvalues, then $\{A^n x\}$ is uniformly distributed for almost all vectors x on the m-torus (x is A-normal).

We have proved that given two such matrices A and B which commute, A-normality coincides with B-normality if and only if $A^r = B^s$ for some positive integers r and s. This confirms a longstanding number theory conjecture of Wolfgang Schmidt.

1. Introduction

Let me say at the outset that the main new result which eventually I will sketch is joint work with William Moran [2]. That, in turn, traces back through ideas of Schmidt [8, 9, 10], and Cassels [3], to a problem of Steinhaus which can be presented as pure number theory. It will, I hope, add interest to emphasize the connexion with ergodic theory and dynamical systems.

The dynamical systems in question have discrete time and are determined by the action of an $n \times n$ integer matrix T on the n-dimensional torus $\mathfrak{T}^n = \mathfrak{R}^n/\mathfrak{Z}^n$. From an initial vector x in $\mathfrak{T}^n$ the system evolves along the orbit $(T^k x)$ as time $k = 1, 2, \ldots$ varies.

The simplest example occurs when $n = 1$ and the operator T is multiplication by 2. We may think of the initial vector x being in]0,1] and having binary expansion $x = \sum_{k=1}^{\infty} x_k 2^{-k}$, or $x = .x_1 x_2 x_3 \cdots$ The evolution of the system amounts to shifting along the tail of the expansion of x. As we all know, this simple system illustrates some of the basic notions associated with chaos theory. In particular we may obviously choose x to exhibit cycles of arbitrary length, yet for almost all x the orbit is "randomly" distributed

J. S. Byrnes et al. (eds.), Probabilistic and Stochastic Methods in Analysis, with Applications, 207–216.
© 1992 *Kluwer Academic Publishers. Printed in the Netherlands.*

over $\mathfrak{T}$. This butterfly effect relates even to time averages, since, for almost all x and every continuous real-valued function f on $\mathfrak{T}$, we know that

$$\lim_{K\to\infty} \frac{1}{K} \sum_{k=1}^{K} f(2^k x) = \int f dm, \tag{1.1}$$

where m is Haar measure on $\mathfrak{T}$. In other words, x is normal in base 2.

That famous result of Borel [1] (in view of its place of publication, not inappropriate for a workshop on Italian soil!), has been extended to the multidimensional case by Rokhlin [7], and Cigler [4]. In fact we say that $(T^k x)$ is *uniformly distributed* if, for all real-valued continuous f on $\mathfrak{T}^n$,

$$\lim_{K\to\infty} \frac{1}{K} \sum_{k=1}^{K} f(T^k x) = \int f dm, \tag{1.2}$$

where m is now Haar measure on $\mathfrak{T}^n$. We then say that x is T- *normal*. Moreover we call the matrix T *ergodic* if m almost all x are T-normal. It turns out that T is ergodic if and only if T is invertible and has no root of unity as an eigenvalue.

The problem of Steinhaus, solved by Cassels, is: "Do there exist numbers normal to base 2 but not normal to base 3?" Schmidt [9] proved the definitive one-dimensional result. For integer bases s, t, all numbers normal to base s are normal to base t if and only if $s^a = t^b$ for integers a, b. (Otherwise there are uncountably many numbers not normal to either one of the bases and normal to the other.)

Cigler [4] proved that if the ergodic matrices S, T are rationally dependent in the sense that $S^a = T^b$, then S-normality and T-normality coincide. We are thus tempted to say that the dynamical systems generated by ergodic matrices S, T are *dependent* if S-normality and T-normality coincide. Is it too much to hope that dependence implies rational dependence? In fact Schmidt conjectured this in [10] and proved by a tour de force that the result holds under the additional hypotheses that (i) $ST = TS$ and that (ii) every eigenvalue of S has modulus strictly greater than one. It is hypothesis (ii) which Moran and I have removed so we have the result for all commuting systems. (It is interesting to note that dependence implies rational dependence when S, T are assumed to be *auto*morphisms of $\mathfrak{T}^2$. This nice result of Sigmund [11] is much simpler—and essentially disjoint because commuting automorphisms are automatically rationally dependent).

2. Schmidt's result in one dimension

Let us fix integer bases s, t. Maxfield's result that s-normality and t-normality coincide when $s^a = t^b$ is not difficult. Accordingly let us assume that s, t

are rationally independent. We seek to establish the existence of numbers which are s-normal but not t-normal.

We know how to tinker with a base t expansion to prevent normality and, intuitively, we feel this should not affect the base s expansion of such numbers. More precisely we may choose a probability measure μ with respect to which almost all numbers fail to be t-normal (e.g., if $t = 3$ we may take a uniform mass over the Cantor middle third set) and we may hope that μ almost all numbers are s-normal. In view of Weyl's criterion we may even expect to achieve that last step by estimating Fourier transforms. This recipe is very much the one used by both Cassels and Schmidt. Because they manipulated the base t expansion their measure μ is generically of infinite convolution type.

In a sequence of papers [2, 5, 6], Charles Pearce, Moran and I explored the possibility of choosing instead a Riesz product for μ. It turns out that there are significant technical gains although our first efforts were more than somewhat clumsy. Here, with the benefit of hindsight, is a cleaner version.

Choose

$$\mu = \lim_{K\to\infty} \prod_{k=1}^{K} (1 + \cos 2\pi t^k x) \cdot m,$$

where m is Haar measure on $\mathfrak{T}$. Then μ is a probability measure whose Fourier transform vanishes off words of the form $\sum \epsilon_k t^k$ with $\epsilon_k \in \{0, \pm 1\}$. Also

$$\mu\left(\sum \epsilon_k t^k\right) = \prod \left(\frac{1}{2}\right)^{|\epsilon_k|}.$$

Note, in particular, that

$$\frac{1}{K} \sum_{k=1}^{K} \exp(2\pi i t^k x) \to \frac{1}{2} \qquad (\mu \text{ a.e.})$$

Comparison with (1.1) or (1.2) with $f(x) = \exp(2\pi i x)$ shows that μ almost all numbers are not t-normal.

Next we claim (following the lines of Davenport, Erdös and Leveque):

Proposition 2.1. Suppose that, for all r,

$$\sum_{n=1}^{\infty} N^{-3} \sum_{k=1}^{N} \sum_{j=1}^{k-1} |\mu^{\wedge}(rs^k - rs^j)| < \infty \tag{2.1}$$

then μ almost all numbers are s-normal.

Proof. In view of Weyl's criterion (i.e., (1.2) with $n = 1$ and $f(x) = \exp(2\pi irx)$) it suffices to prove that, for all nonzero integers r,

$$\frac{1}{N}\sum_{k=1}^{N}\exp(2\pi irs^k x) \to 0 \quad (\mu \text{ a.e.}) \tag{2.2}$$

Because $|\exp(2\pi iy)| = 1$, it is in fact enough to show (2.2) along some mildly lacunary increasing sequence $N = N_j$. In fact provided that $N_{j+1} \leqslant (1+\epsilon)N_j$, we find

$$\left|\frac{1}{N}\sum_{k=1}^{N}\exp(2\pi irs^k x) - \frac{1}{M}\sum_{k=1}^{M}\exp(2\pi irs^k x)\right| \leqslant 2\epsilon,$$

whenever $N_j \leqslant N, M \leqslant N_{j+1}$.

Observe also that (2.1) gives

$$\sum_{N=1}^{\infty} N^{-1}\int\left|N^{-1}\sum_{k=1}^{N}\exp(2\pi irs^k x)\right|^2 d\mu(x) < \infty.$$

Choose $M_{j+1} = [(1+\epsilon)M_j]$, then

$$\sum_{j=1}^{\infty}\left(\frac{M_{j+1}-M_j}{M_j}\right)\min_{M_j < N \leqslant M_{j+1}}\int\left|N^{-1}\sum_{k=1}^{N}\exp(2\pi irs^k x)\right|^2 d\mu(x) < \infty$$

i.e.,

$$\sum_{j=1}^{\infty}\int\left|N_j^{-1}\sum_{k=1}^{N_j}\exp(2\pi irs^k x)\right|^2 d\mu(x) < \infty,$$

for some suitable increasing (N_j) and the result follows. ∎

It remains to establish (2.1). This we achieve crudely by counting the number of possible nonzero Fourier coefficients, i.e., by counting solutions of the equations

$$r(s^k - s^j) = \sum_{i=1}^{m}\epsilon_i t^i \qquad \epsilon_i \in \{0, \pm 1\}. \tag{2.3}$$

In fact let G_N be the number of $k \leqslant N$ such that for some j with $0 \leqslant j \leqslant k - \log N$ and some ϵ_i, equation (2.3) holds. In view of Proposition 2.1 it suffices to check that

$$\sum N^{-2}G_N < \infty. \tag{2.4}$$

This is because

$$\sum N^{-3}\sum_{k=1}^{N}\sum_{s=1}^{k-1}\mu\{rs^k \cdots rs^1\} \le \sum N^{-3}(NG_N + N\log N).$$

To check (2.4) we use the independence of s,t and Alan Baker's famous estimate that there is a constant C so that

$$|n\log s - m\log t| > C^{-\log N}, \tag{2.5}$$

whenever $0 < \max(|n|, |m|) < N$. We can replace s,t by $s^{\pm 1}, t^{\pm 1}$ without loss of generality and therefore can assume that $\min(s,t) > C^{-2}$.

Lemma 2.2. If (2.3) holds with $c_{m-1} = 1$ then $s^k t^m$ belongs to a union of at most $3^{\log N}$ discs of radius $O(C^{-2\log N})$, lying in some fixed disc.

Proof. $s^k t^m = r^{-1}(1 - s^{k-1})(1 + \sum_{i=1}^{m-1} c_i t^{i-m})$. The second term of the product is $1 + O(C^{-2\log N})$. The third term can be written (with c_{m-1} in place of c_i) as

$$\left(1 + \sum_{i=1}^{\log N} c_i t^{-i}\right)\left(1 + \left(1 + \sum_{i=1}^{\log N} c_i t^{-i}\right)^{-1} \sum_{\log N < i < m-1} c_i t^{-i}\right)$$

$$\left(1 + \sum_{i=1}^{\log N} c_i t^{-i}\right)\left(1 + t^{-\log N} R\right)$$

where

$$R = \left(\sum_{i=1}^{\infty} t^{-i}\right)\left[1 - \sum_{i=1}^{\infty} t^{-i}\right] < 2.$$

In view of the lemma and inequality (2.5), none of the discs can contain more than one element. It follows that G_N does not exceed $N^{\log 3}$ and (2.4) is established. ∎

3. N dimensions—underlying method

Following Schmidt we consider a somewhat wider class of matrices, the *almost integer* matrices. These are $n \times n$ invertible matrices with rational entries and all of whose eigenvalues are algebraic integers. Such a matrix is ergodic if and only no eigenvalue is a root of unity and it is these so-called *almost ergodic* matricesthat we use. Schmidt proved in [10] that for every almost ergodic matrix Γ there exists an integer d (the *denominator* of Γ) such

that dT^n is integral for all $n = 1, 2, \ldots$ This makes it possible to consider Riesz products of the form

$$\mu = \lim_{K \to \infty} \prod_{k=1}^{K} (1 + \cos 2\pi\alpha T^k x) \cdot m,$$

where m is Haar measure on $\mathfrak{T}^n$ and α is an integer vector multiplied by the denominator of T. Of course this makes sense only if there is a substitute for the lacunarity familiar in the one-dimensional case. We require *dissociateness* in the sense that equations

$$\sum_{i=1}^{K} \epsilon_i \alpha T^i = 0 \quad (\epsilon_i \in \{0, \pm 1, \pm 2\})$$

cannot arise unless all $\epsilon_i = 0$. Because T-normality and T^p-normality coincide we are at liberty to replace T by some suitable power to achieve dissociateness. The appropriate result is the next lemma.

Lemma 3.1. Let T be almost ergodic. Then there is a positive integer p such that (αT^{np}) is dissociate for all $\alpha \neq 0$ in $\mathfrak{Q}^n$.

Proof. If every eigenvalue of T had modulus one then Dirichlet's theorem would force some root of unity to be an eigenvalue in contradiction of ergodicity. Accordingly we may replace T by T^p to ensure that some eigenvalue λ_1 of T has modulus greater than, say, 5. (The integral nature of dT^n rules out the possibility that all eigenvalues are inside the unit circle).

Assume then that $|\lambda_1| > 5$ and λ_1 is an eigenvalue of T. First we decompose T over the rationals into a direct sum of matrices whose characteristic polynomials are of the form $q(x)^t$ where q is a monic irreducible over $\mathfrak{Q}$. At least one component of α in this decomposition will be nonzero and the entries of α remain rational. Replacing T by a suitable component matrix we can assume that the characteristic polynomial of T is a power of an irreducible. Next we consider T as a linear operator on $\mathfrak{C}^n$ and decompose $\mathfrak{C}^n$ as a direct sum of subspaces, $V_\lambda = \ker (\lambda - T)^t$ as λ ranges over the eigenvalues of T. The decomposition can be achieved over the splitting field of q and the automorphism group of this field will permute the components of α, leaving α unchanged since it is rational. Thus the component of α in each of these subspaces is nonzero. We may replace T and α by their components on the subspace V_{λ_1} and we choose s to be the largest integer such that $\beta = \alpha(\lambda_1 - T)^s \neq 0$. Now any equation

$$\sum \epsilon_i \alpha T^i = 0$$

leads to the equation

$$\sum \epsilon_i \alpha (\lambda_1 - T)^s T^i = 0$$

which is

$$\sum \epsilon_i \lambda_1^i \beta = 0$$

and that forces $\epsilon_i = 0$. ∎

Matters are now arranged so that analogues of the one-dimensional case may be employed. In particular it is straightforward to see that μ almost all vectors in $\mathfrak{T}^n$ are not T-normal. The challenge is to prove that μ almost all vectors are S-normal and this boils down to counting solutions of matrix Diophantine equations of the form

$$\beta S^k - \beta S^j = \sum_{m=1}^{M(m,j)} \epsilon_m \alpha T^m \quad (\epsilon_m \in \{0, \pm 1\}) \tag{3.1}$$

4. Irreducible case

For a workshop such as this it is inappropriate to plough through the technical details of the proof so let me discuss the simplest case, that in which the algebra $\mathcal{A}(S, T)$ generated by S, T is irreducible. That forms the basis for an induction proof of the general case and the reader is referred to [2] for the full details.

We assume then that $\mathfrak{Q}^n$ has no invariant subspace for the algebra $\mathcal{A}(S, T)$ and that for each α in $\mathfrak{Q}^n$ there exists β in $\mathfrak{Q}^n$ with $\sum N^{-2} G_N(\beta) = \infty$, where $G_N(\beta)$ is the number $k \leq N$ such that for some j with $0 \leq j \leq k - \log N$ and some $\epsilon_1, \epsilon_2, \epsilon_3, \ldots, \epsilon_{M(k,j)}$ $(\epsilon_m \in \{0, \pm 1\})$

$$\beta S^k - \beta S^j = \sum_{i=1}^{M(k,j)} \epsilon_i \alpha T^m.$$

Let us suppose further that for any eigenvalues λ of S and ρ of T with $\lambda^{n'} \neq \rho^{m'}$ and $\max(|m'|, |n'|) \leq N$ then

$$|n' \log \lambda - m' \log \rho| \geq C^{-\log N}$$

and (as a consequence of replacing S, T by suitable powers) that any eigenvalue of S or T with modulus ≥ 1 has, in fact, modulus $\geq C^2$.

Lemma 4.1. Under the prevailing conditions there exists an $n \times n$ matrix U over $\mathfrak{Q}$ such that if F_N is the number of all k for which

$$U(S^k - S^j) = \sum_{m=1}^{M(k,j)} \epsilon_m T^m \tag{4.1}$$

for some $0 \leq j \leq k - \log N$ and $\epsilon_m \in \{0, \pm 1\}$ then $\sum N^{-2} F_N = \infty$. Moreover U belongs to $\mathcal{A}(S, T)$.

Proof. We know that for each $\alpha \neq 0$ in Ω^n there exists some β in Ω^n such that

$$\beta(S^k - S^j) = \sum_{m=1}^{M(k,j)} \epsilon_m \alpha T^m, \tag{4.2}$$

for infinitely many pairs (k, j) corresponding to k in $G_N(\beta)$. Choose a cyclic vector α_0 for $\mathcal{A}(S, T)$ and let β_0 be the corresponding vector as in (4.2). Multiply both sides of (4.2) by an arbitrary element of $\mathcal{A}(S, T)$ to see that (4.2) does indeed establish a linear correspondence which we can express in the form $\beta = \alpha U$. Evidently U belongs to the algebra generated by S and T. ∎

Lemma 4.2. Let $\mathcal{A} \neq 0$ be an irreducible commutative subalgebra of $M(\Omega^n)$. There is a finite field extension F of Ω and a field isomorphism $\psi : \mathcal{A} \to F$ such that, for each A in $\mathcal{A}$, $\psi(A)$ is an eigenvalue of A. Moreover, given some fixed S in $\mathcal{A}$ and as eigenvalue λ_s of S, we may choose $\psi(S) = \lambda_s$.

Proof. If $A \in \mathcal{A}$ and $\ker A \neq 0$ then $\ker A$ would be a proper invariant subspace of $\mathcal{A}$. Accordingly each A in $\mathcal{A}$ is invertible and $\mathcal{A}$ is a field which is isomorphic to a finite extension F of Ω^n under some map $\psi : \mathcal{A} \to F$. We know from the Cayley-Hamilton theorem that A satisfies its own characteristic equation and therefore $\psi(A)$ is an eigenvalue of A. The minimal polynomial m_s of any nonzero S in $\mathcal{A}$ is irreducible and so the Galois group acts transitively on the roots of that polynomial. It follows that, given λ_s, we may indeed choose $\psi(S) = \lambda_s$. ∎

Proposition 4.3. Under the conditions of this section there are integers p, q such that $S^p = T^q$.

Proof. We apply the last lemma to choose $\psi : \mathcal{A}(S, T) \to F$ such that $\psi(S) \in C^2$. Now evaluate both sides of (4.1) under ψ to obtain an analogue of (2.3) with $\psi(U)$ in place of r, $\psi(S)$ in place of s, $\psi(T)$ in place of t. The one-dimensional methods of the previous section force

$$\psi(S)^q = \psi(T)^p, \text{ for some } p, q,$$

and we deduce that

$$S^p = T^q.$$

5. Forwards and sideways

The Riesz product technology makes it possible almost to separate the linear algebra from the Fourier analysis and number theory. That is why Moran and I have been able to push Schmidt's methods much further. We have also made further progress in the non-commutative case but that work is still in preparation and is still far from resolving the "big" conjecture.

Absolutely fundamental throughout the work is the possibility of raising S, T to suitable powers without affecting normality. This is very much a feature of the (almost) integral nature of the matrices. Even in the one-dimensional case there are difficult questions concerning non-integer bases. For example, is $\sqrt{2}$ normal to base 2?

In a forthcoming series of papers Berend, Moran, Pollington and myself will demonstrate several new results on normality to non-integer bases. For example we show how to construct generic examples of θ such that normality to base θ does not imply normality to base θ^p and normality to base θ^p does not imply normality to base θ. Moran, Pollington and I can also show, for example, that every number normal to base $\sqrt{10}$ is necessarily normal to base 10 but we believe that the converse fails. Riesz products play a key role there also.

6. Bibliography

[1] E. Borel. Les probabilitès dénombrables et leurs applications arithmétiques. *Rend. Circ. Mat. Palermo*, 27:247–271, 1909.

[2] G. Brown and W. Moran. Schmidt's conjecture on normality for commuting matrices. To appear.

[3] J.W.S. Cassels. On a problem of Steinhaus about normal numbers. *Colloquium Math.*, 7:95–101, 1959.

[4] J. Cigler. Ein gruppentheoretisches analogon zum begriff der normalen zahl. *J. für die Reine u. Angewandte Math.*, 206:3–8, 1961.

[5] W. Moran G. Brown and C.E.M. Pearce. Riesz products and normal numbers. *Journal London Math. Soc.*, 32:12–18, 1985.

[6] W. Moran G. Brown and C.E.M. Pearce. A decomposition theorem in which the summands have prescribed normality properties. *Journal of Number Theory*, 24:259–271, 1986.

[7] W.A. Rokhlin. On endormorphisms of compact abelian groups. *Izv. Akad. Nauk. USSR Ser. Mat.*, 13:329–340, 1949. In Russian.

[8] W.M. Schmidt. On normal numbers. *Pac. J. of Math.*, 10:661–672, 1960.

[9] W.M. Schmidt. Über die normalität von zahlen zu verschiedenen basen. *Acta Math*, 7:299–301, 1962.

[10] W.M. Schmidt. Normalität bezüglich matrizen. *J. für die Reine u. Angewandte Math.*, 214/5:227–260, 1964.

[11] K. Sigmund. Normal and quasiregular points for automorphisms of the torus. *Math. Systems Theory*, 8:251–255, 1975.

Linear and non-linear decomposition of images using Gabor wavelets

Bruce W. Suter
Department of Electrical and Computer Engineering
Air Force Institute of Technology
Wright-Patterson AFB, OH 45433 USA
bsuter@galaxy.afit.af.mil

Matthew Kabrisky
(Same address.)

Steven K. Rogers
(Same address.)

Erik J. Fretheim
(Same address.)

Dennis W. Ruck
(Same address.)

Michael Mueller
(Same address.)

Abstract This paper will contrast two wavelet-based image analysis techniques, one fundamentally non-linear and the other essentially linear, to process images arising from different physical sources and requiring fundamentally different processing outcomes. The intent is to emphasize the flexibility inherent in image processing algorithms even given the constraint that the initial feature extraction process is a wavelet analysis. (It should be noted that current physiological data from mammalian visual centers indicate that a Gabor-like wavelet analysis is one of the first steps in animal visual processing; in humans this becomes an exquisitely flexible, adaptable and programmable process, to match the specific visual task required.)

We will first describe a non-linear system to locate specific key landmarks on VLSI chip photomicrographs. These landmarks, easily visible to a human observer, are not extractable by any linear spatial filtering technique or any thresholding technique. However, if a series of Gabor correlation planes (using appropriately selected size, frequency and orientation parameters) are computed, it is possible merely by selecting the max or min value for each pixel in the registered set of planes to produce an "image" which clearly shows the desired landmarks. This is a non-linear

J. S. Byrnes et al. (eds.), Probabilistic and Stochastic Methods in Analysis, with Applications, 217–231.
© 1992 *Kluwer Academic Publishers. Printed in the Netherlands.*

rule-based system selection "filter" following the essentially linear process of Gabor correlation.

In a second case, we will show that actual infrared images can be filtered to select items of specific sizes and texture by a linear summation of Gabor correlation planes followed by a simple threshold rule.

The purpose of this work is to demonstrate that Gabor features seem to be intrinsically useful for image processing provided that flexibility in the use of its fruits is adopted by the system designer.

1. Introduction

This paper will describe two image segmenters specifically adapted to distinctly different types of images. Both, however, are based on an initial Gabor wavelet decomposition of their images and differ from each other only in their post-Gabor-processing details [4]. The fact that the images are derived from totally different sources and yet are both usefully processed by a wavelet analyzer suggests to us that this may be a broadly useful technique. We also note that the initial processing of images in the vertebrate brain stem and in the mammalian visual cortex also includes a close approximation to a Gabor wavelet decomposition of the scene being viewed by the animal, and are thus further encouraged to explore the consequences of Gabor decomposition of images. The first segmenter described is for photomicrographs of VLSI chips obtained for the purpose of reverse-engineering and circuit verification of the chips. The second segmenter is designed to locate potential targets in a FLIR image. Finally, we will conclude with an appendix outlining some Gabor-like processes now known to occur in animal visual systems.

2. VLSI chip image processing

Figure B.1 shows a typical photomicrograph of a portion of a VLSI circuit. This is a 512 × 480 array of pixels derived from a TV camera image. VLSI circuits are built up from a small repertoire of standardized circuit elements such as resistors, transistors, flip-flops, switches, etc, which are connected by straight metal conductors. Layers of the circuits are interconnected on the chip by vias or contacts which are round or toroidally shaped elements. Deriving the electrical circuit from such a photograph is a good candidate for automation because the chips consist of a very large number of iterated, stereotyped arrangements of a small set of possible elements. Frequently, thousands or even millions of each element can be found in currently used chips.

The first elements we chose to find are the round vias or contacts. Note that while these are visible in Figure B.1 to a human observer, it is virtually impossible to extract them with the usual image processing techniques. They

can be extracted, however, with a Gabor-wavelet-based process. The process begins by performing a two dimensional correlation between the image and an appropriate two dimensional Gabor wavelet. We use the term "Gabor filtering" or "Gabor transformation" for this operation [3, 2]. This process is described in the appendix of this paper.

Gabor transforms of the images are computed directly in the spatial domain. Several factors make this method attractive. The image size is 512×480 pixels so that high speed two-dimensional array processors are available, and spatial correlation allows control of the decimation of the scene. With this technique, the Gabor transform is defined as the dot product of the Gabor wavelet and the image at each point on the image.

The quality of images obtained from the chips varies among the different chips and regions of the same chip. Therefore, the images are first preprocessed so the Gabor filtering has the best chance to discriminate the contacts. We generally use a special normalization technique to do this preprocessing. The average brightness of a neighborhood of pixels around a selected center pixel is computed and the brightness of the center pixel is subtracted from this average. The result is then multiplied by 2 and added to 127, the middle of the total 0–255 brightness range in the system [7]. The effect is edge enhancement with a normalized, constant average background. Contacts, which typically appear as small bright regions surrounded by dark rings, are emphasized. This local computation technique is similar to some of the normalization processes performed by the vertebrate visual system [11]. Figure B.2 shows the results of this process applied to Figure B.1.

Pixel intensity values can range from 0–255 in our eight bit system: full black to full white. In some images, however, a histogram of pixel values shows the total intensity range to be very narrow. Linear contrast enhancement can be performed to spread the variations of image intensity over the full range available to the image system [5]. This allows easier visual examination of the image.

After this preprocessing, several Gabor transforms are taken of the image. The required Gabor wavelet parameters which must be specified are orientation, Gaussian envelope amplitude and width, sinusoidal modulation frequency and wave type (sine or cosine). Since this application uses spatial domain correlation, a decimation factor can also be specified.

Gabor filters respond strongly to linear features oriented parallel to the filter's principal axis. The strength of their response is also dependent on the relative size of the object and its components or texture compared to the modulation pitch of the Gabor wavelet. Figure B.3 is an example of correlating a Gabor pattern with a 45° orientation with the image in Figure B.2. The majority of features on the VLSI circuits are the metal connective "wires" and are horizontal and vertical; the vias and the contacts appear as circular features. Therefore, we used a set of Gabor filters with

rotations of 20, 45, 70, 110, 135, and 160 degrees. Orientations of 0 and 90 degrees and their multiples were avoided in order to suppress the wires and help enhance the circular elements. Not all rotations were required for all images.

The angles chosen cause the Gabor filters to respond strongly to the edges of the contacts and the corners of other features, but not to many of the other chip features. The Gaussian width and the sinusoidal modulation of the wavelets are chosen to match the expected contact size in the scene. This reduces the response of the filters to many corners and other distractors. When the set of Gabor filters of varied rotation is applied to the scene and combined correctly, the response of the contacts dominates the resulting feature set.

The transformed scenes are combined by a localized non-linear thresholding operation. In the Gabor-transformed scenes, the pixel values are limited to {−127 to 127}. Each input image will produce a set of intermediate transformed images which depend upon the rotation of the Gabor filters. For each pixel in the combined image, the pixels with the same (x, y) coordinates in each of the transformed images are individually examined. The pixel with the greatest absolute value is used for the feature set (and the sign is preserved). This technique selects the extreme values and assumes they contain the most information. Once the feature set is assembled the pixel values are shifted to range from 0 to 255. Figure B.4 shows the result of this process. The pixel array shown in Figure B.4 is then thresholded to select the maximum 5–10% pixels. Figure B.5 shows the superposition of Figure B.1, the original image, with these maximum pixels derived from thresholding Figure B.4. Each of the bright spots is a potential location for a via or contact. In typical scenes, the highlighted pixels represent only a few percent of the original 512 × 480 array (see Table 2.1).

Chip	Scene	Contacts Present	Contacts Detected	Area Covered
A	1	27	27	8.0%
A	2	45	45	7.2%
B	1	42	42	6.4%
B	2	54	54	8.3%
C	1	23	23	3.6%
C	2	11	11	0.5%
C	3	24	24	14.6%

Table 2.1: Segmentation results.

To determine which of the highlighted pixels actually represent vias or contacts, a video subimage from the original (or enhanced original) scene, about the same size as the vias or contacts, is extracted and correlated with a nominal template of the desired element. In this research, correlation

was usually performed by a trained neural net (connected in the back-propagation mode) [8].

By limiting the number of such locations to be searched to a small number of the 512 × 480 possible locations in the original image, the processing time is greatly reduced. Many fewer false positives result and in our experience, virtually all (96%) of the targeted forms are located.

In a sense the nonlinear Gabor analysis serves as an initial selector filter for points in an image which have a high likelihood of containing the sought image. Thus, the expensive correlation scheme to determine if the target image is actually at some location need be carried out only at a few locations in the scene. This type behavior seems to occur also in animal visual systems where actual eye motion consists of a sequence of jumps (saccades) driven by image content.

3. Segmentation of FLIR images

The second application discussed in this paper is the segmentation of potential targets in forward looking infrared (FLIR) images. The motivation is similar to that in the previous application. Given an image with a large number of pixels, is there some easy way to locate the coordinates of the most likely locations of targets prior to performing complex target analysis and identification procedures?

Figure B.6 shows a representative FLIR image. It was subsequently processed by correlating it with Gabor wavelets using four wavelet orientations: 0°; 45°; 90°; 135°. The pitch and orientation of the Gabor wavelet modulation is important for these images. A Gabor wavelet can be considered to be an anisotropic spatial filter and Gabor transformation is an approximation to spatially filtering an image.

Therefore, it is important to estimate the spatial frequency contact of the targets of interest and select Gabor filtering frequencies to highlight these frequencies. In the case of scenes containing targets, approximate range is frequently known as is the approximate size of the targets. Therefore, it is possible to estimate the angular extent of potential targets and hence select the appropriate Gabor wavelets for image plane processing. If not, then the images can be processed with a range of Gabor frequencies and then post-processed with extra-image information to analyze potential target sites.

The example in Figure B.7 shows the result of applying appropriate Gabor wavelet functions. Figure B.7 has had only one non-linear operation, namely the final thresholding of a new image created by simple addition of corresponding pixels in the four Gabor filtered images created from Figure B.6.

Figure B.8 shows the same image after Gabor filtering with sine rather than cosine modulation. Notice this is an effective edge finder without

the disadvantage of many derivative type edge finders, in that there is no enhancement of high spatial frequency noise. This is because the spatial frequency components of a Gabor wavelet are grouped about a narrow band of frequencies so that a Gabor-filter is actually an anisotropic band pass filter. This filter can be tuned to type of edge of interest as shown in Figure B.8. This image is also the result of final thresholding of the linear summation of four Gabor filtered images.

4. Bibliography

[1] Marianna Clark and Alan C. Bovik. Texture discrimination using a model of visual cortex. In *Proceedings of the IEEE International Meeting on Cybernetics and Society*, pages 1425–1430, 1986.

[2] John G. Daugman. Uncertainty relation for resolution in space, spatial frequency, and orientation optimized by two-dimensional visual cortical filters. *J. Optical Society of America A*, 2:1160–1169, July 1985.

[3] John G. Daugman. Complete discrete 2-d Gabor transforms by neural networks for image analysis and compression. *IEEE Trans. Acoustics, Speech, Signal Processing*, 36:1169–1179, July 1988.

[4] Dennis Gabor. Theory of communication. *J. of IEE*, 93:429–457, 1946.

[5] William B. Green. *Digital Image Processing*. Van Nostrand Reinhold Company, New York, 1983.

[6] Judson P. Jones and Larry A. Palmer. An evaluation of the two-dimensional Gabor filter model of simple receptive fields in cat striate cortex. *J. Neurophysiology*, 58:1233–1258, December 1987.

[7] Laurence Lambert. Evaluation and enhancement of the AFIT autonomous face recognition machine. Master's thesis, School of Engineering, Air Force Institute of Technology (AU), December 1987.

[8] R. Lippman. An introduction to computing with neural nets. *IEEE Trans. Acoustics, Speech, Signal Processing*, 4:4–22, April 1987.

[9] Steven L. Polyak. *The Vertebrate Visual System*. Chicago, 1957.

[10] M. R. Turner. Texture discrimination by Gabor functions. *Biological Cybernetics*, 55:71–82, 1986.

[11] Frank S. Werblin. The control of sensitivity in the retina. *Scientific American*, 228:70–79, January 1973.

A. Gabor-like processes in animal visual systems

The basic data input channels in the mammalian visual systems are well known [9]. See Figure B.9. There are three basic processing centers. The first of these is the retina, a five layer system in which the optical image is coded so that it may be transmitted through neuron channels to the brain. The retina performs local contrast and average intensity normalization, color coding, motion detection, spatial and dynamic range data compression, the first stage of log Z mapping of the two-dimensional retinal image, and then transmits local differential brightness data of points in the image compared to a local circular surround of image data.

These data are mapped in a six layer system in the brain stem (lateral geniculate nucleus (LGN)). Individual neurons can be instrumented in LGN by means of micro-electrodes, and it is here that we see that many of these neurons seem to view the world as though they were Gabor-like filters [6]. The visual data are then retransmitted in the form of a log Z map of the optical image to the primary visual center (VI) in the cortex and it is here that humans are first aware of visual data. Needless to say, instrumented cells in VI respond as though they are components of two-dimensional Gabor-like filters. Therefore, one concludes that the apparent world is in fact the real world viewed through a set of spatially distributed Gabor-like filters. These can obviously serve as texture and edge detectors for animals like us, as well as pattern recognition machines.

Several researchers have proposed models for the mammalian visual system which are based on Gabor's work (see [2, pp. 1164–5] and [6]). The idea that the human visual system optimizes the available information in both the spatial and spatial frequency domains makes intuitive sense [1, p. 1426]. A model of the visual system which uses Gabor filters may help resolve the long-running debate over whether the cortical (brain) cells involved in vision perform as local feature detectors in the spatial domain or spatial frequency components of a Fourier-like decomposition [2, p. 1160] or both.

Daugman modified Gabor's one-dimensional time-frequency "signals" into two-dimensional spatial filters. The filters consist of a two-dimensional sinusoid (grating pattern) multiplied by a two-dimensional Gaussian envelope. These filters were also shown to have optimal joint resolution in the spatial and frequency domains [2, pp. 1162–4]. Daugman's two-dimensional Gabor filter is a product of a two-dimensional sinusoid and a two-dimensional Gaussian envelope. The general form of the two-dimensional Gabor filter family in the space domain is:

$$\Gamma(x,y) = \exp[-(x_\gamma^2 + y_\gamma^2)/2(\alpha^2 + \beta^2)]\sin[-2\pi(U_\phi x + V_\phi y) - \Psi] \quad (A.1)$$

where (x_γ, y_γ) are coordinates for the Gaussian, α and β are the Gaussian decay terms, U_ϕ and V_ϕ express the modulation, and Ψ controls the phase

of the two-dimensional sine-wave. The resulting waveform is shown in Figure B.10.

One example of a visual system model is given by Jones and Palmer [6, pp. 1233–58]. The hypothesis in their paper is that the visual fields in a typical mammalian (cat) visual (brain) cells behave as though they were linear filters having the functional form of the two-dimensional Gabor filters. Jones and Palmer obtained the two-dimensional spatial response and temporal responses of 36 instrumented cells from cat cortices. They used a simplex algorithm to find Gabor filters which best fit the response profiles in a least-squared-error sense. The error between the spatial response profiles and their corresponding two-dimensional Gabor filters were then calculated.

The study showed that 33 of 36 spatial responses and 34 of 36 temporal responses showed no statistical difference from a Gabor filter. The authors concluded that the Gabor filter has appeared to evolve as an optimal strategy for sampling images simultaneously in the two-dimensional spatial and spatial frequency domains [6, p. 1233]. The brain visual system, however, is not necessarily a linear system, so it is possible that Jones' and Palmer's data may be a consequence of the specific and simple test stimuli applied to the cells rather than a general and robust description of the visual system. Nonetheless, their results strongly suggest that Gabor filtered images are part of the computational routines used by vertebrate animals to segment images.

Other authors have focused on texture discrimination, which requires simultaneous measurement in both space and frequency domains [10, p. 71]. Turner approaches the texture discrimination problem from the aspect of information representation [10, p. 72] If an image is represented as single-valued pixels, global texture information is not specifically demonstrated, but if a global Fourier transform is used, local texture information is missing. Turner therefore developed a set of spatially localized Gabor filters and used them to segment textural features. His filters were circularly symmetric and non-self-similar, that is the Gaussian envelope had fixed size but the frequency of the modulated sinusoid was allowed to vary [10, p. 74].

B. Figures

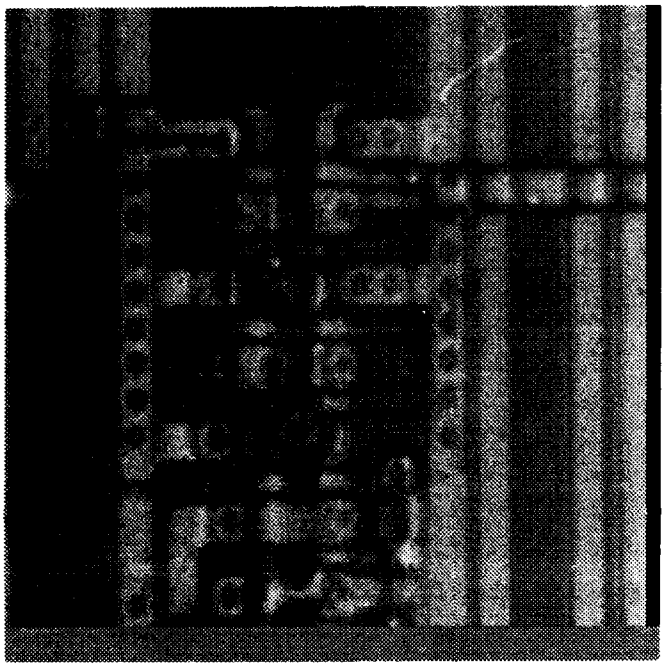

Figure B.1: Typical photomicrograph of a portion of a VLSI chip.

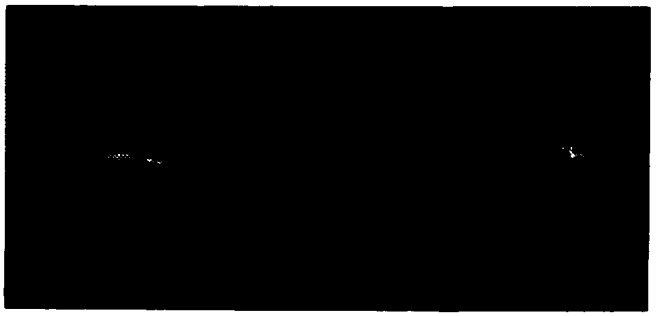

Figure B.6: Typical FLIR image showing a tank, APC, target board and truck.

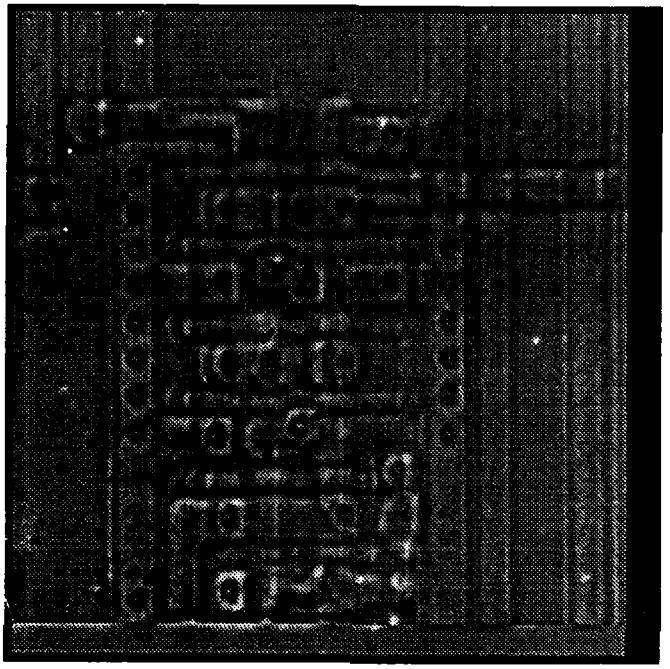

Figure B.2: Result of preprocessing the image in Figure B.1.

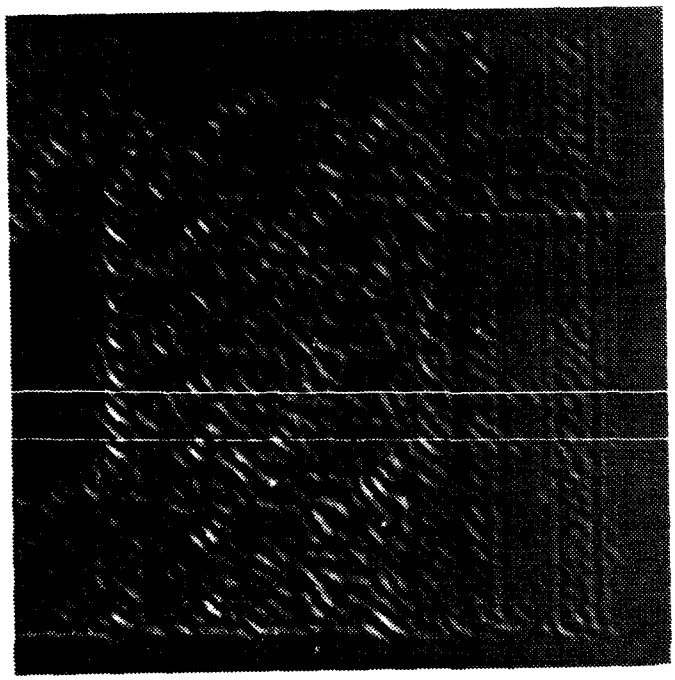

Figure B.3: The result of correlating ("Gabor transforming") the image in Figure B.2 with a two-dimensional Gabor pattern. Note that the image is printed on a 512 × 512 pixel space and that the Gabor patterns are 34 × 34 pixels; the pitch of the modulation is 17 pixels per cycle and is phased as a sine modulation (to provide edge enhancement). The orientation is 45°.

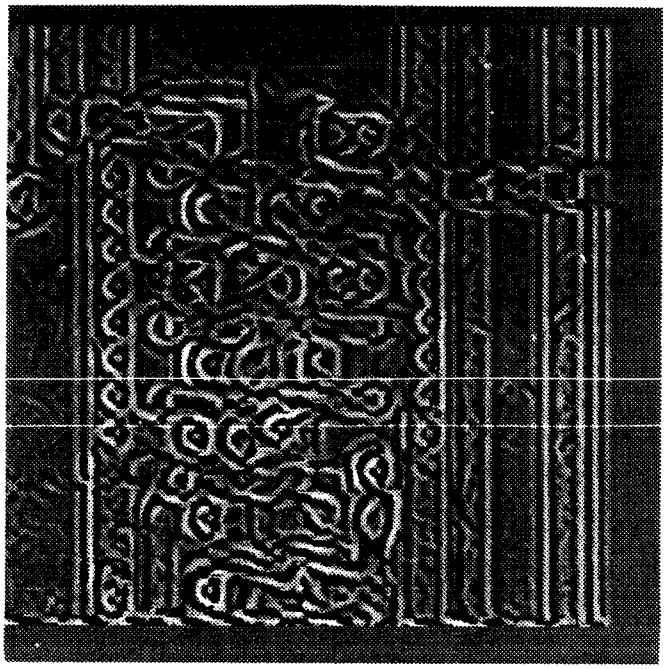

Figure B.4: Result of performing the non-linear min-max pixel selection procedure on Gabor filtered versions of Figure B.1. There were six of these images resulting from Gabor filtering at 20°, 45°, 70°, 110°, 135°, and 160°.

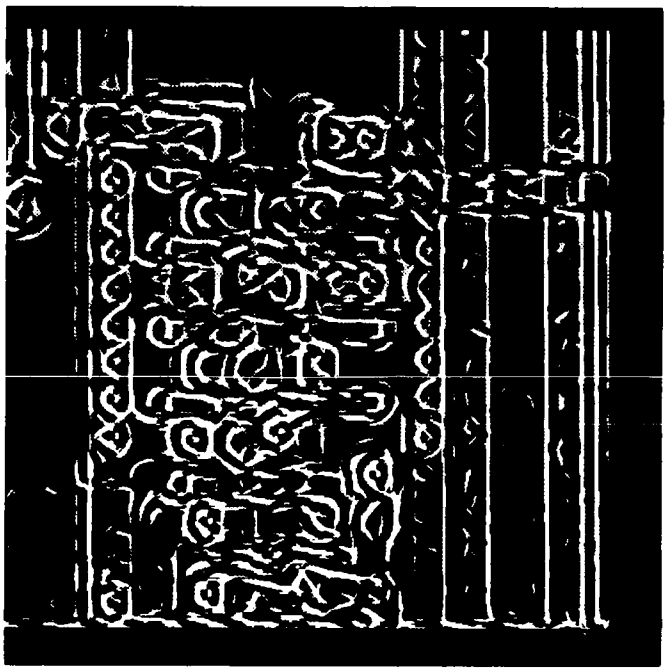

Figure B.5: Superposition of Figure B.1 with the maximum/minimum points thresholded from Figure B.4. Note that these points lie primarily on vias or contacts. They represent only a few percent of the original 512 × 480 array of pixels.

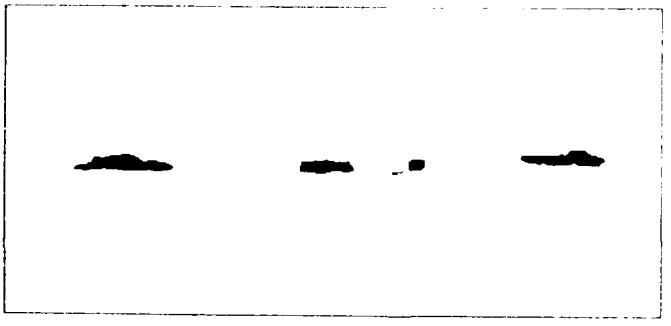

Figure B.7: The result of adding four (cosine) Gabor filtered images derived from Figure B.6 with subsequent thresholding.

Figure B.8: Same as Figure B.7 but with sine Gabor filtering.

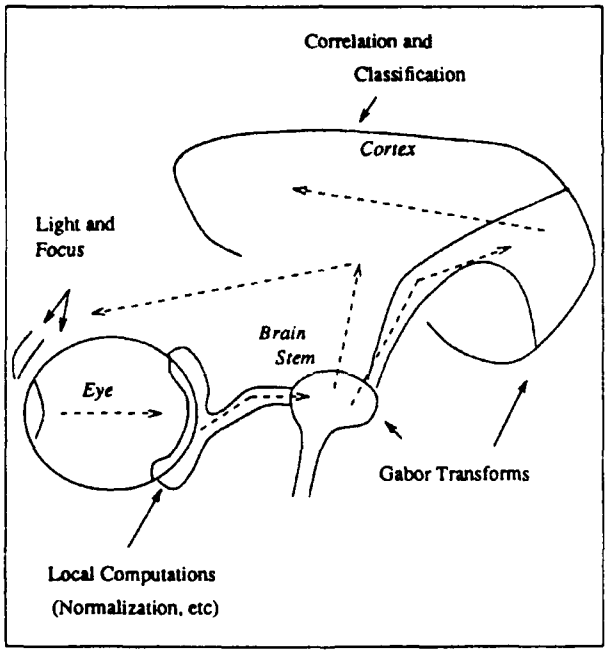

Figure B.9: Basic input data channels in the mammalian visual system.

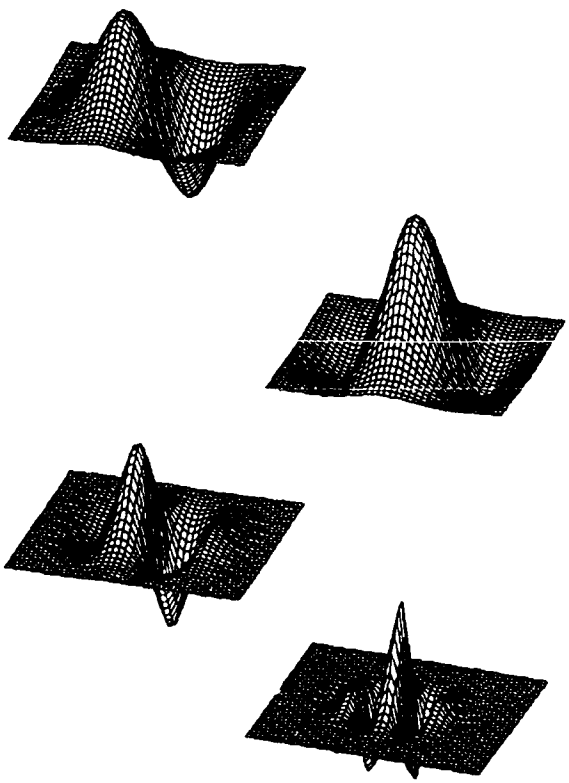

Figure B.10: Two-dimensional Gabor functions.

Multiresolution analyses, tiles, and scaling functions†

W.R. Madych
Department of Mathematics
University of Connecticut
Storrs, CT 06268 USA
madych@uconnvm.uconn.edu

Abstract Several, hopefully useful, observations concerning the topic in the title are discussed: (i) It is noted that the axiom of intersection is not essential in the definition of a multiresolution analysis. (ii) Several conditions, which are often easily verifiable, are given for scaling sequences which imply that such sequences generate scaling functions whose supports give rise to non-overlapping tilings of $\mathfrak{R}^n$.

1. Introduction

The point of this lecture is to communicate several observations which may be useful to investigators and other individuals who work with multiresolution analyses. These observations concern two topics: one pertains to the axiom list for a multiresolution analysis and the other has to do with the characterization of certain scaling functions.

Recall that a multiresolution analysis is a sequence $\{V_j\}_{j\in\mathbb{Z}}$ of closed subspaces of $L^2(\mathfrak{R}^n)$ which enjoy certain properties, see [1, 2, 3, 8, 9]. One of the properties is the following:

$$\bigcap_{j\in\mathbb{Z}} V_j = \{0\}. \tag{1.1}$$

Property (1.1) is often a nuisance to verify. For instance see [5, 7]. The reason for this may be the notion that the property depends intrinsically on the specific example. Fortunately this is not the case.

In this lecture we show that property (1.1) is a consequence of the other properties enjoyed by multiresolution analyses. Thus its appearance in the definition is unnecessary and redundant.

† Partially supported by a grant from the Air Force Office of Scientific Research, AFOSR-90-311.

J. S. Byrnes et al. (eds.), Probabilistic and Stochastic Methods in Analysis, with Applications, 233–243.
© 1992 *Kluwer Academic Publishers. Printed in the Netherlands.*

Another topic we will touch upon here concerns multiresolution analyses whose scaling functions are characteristic functions. This matter was recently studied in [3, 4]. The characterization of scaling sequences which give rise to such scaling functions is an important problem in these studies. Here we give several conditions which imply that a given sequence has the desired properties and which are relatively easy to verify for many examples.

2. On axioms for a multiresolution analysis

2.1. The main observation

Suppose A is a linear transformation on $\mathfrak{R}^n$. We say that A is an *acceptable dilation* for $\mathfrak{Z}^n$ if it satisfies the following properties:

- A leaves $\mathfrak{Z}^n$ invariant.
- All the eigenvalues λ_i of A satisfy $|\lambda_i| > 1$.

These properties imply that $q = |\det A|$ is an integer which is ≥ 2. In what follows we will always assume that A is an acceptable dilation for $\mathfrak{Z}^n$.

Proposition 2.1. Suppose $\{V_j\}_{j\in\mathfrak{Z}}$ is a sequence of close subspaces of $L^2(\mathfrak{R}^n)$ which enjoys the following properties:

- $f(x)$ is in V_j if and only if $f(Ax)$ is in V_{j+1}.
- There is a function φ in V_0 such that $\{\varphi(x-k)\}_{k\in\mathfrak{Z}^n}$ is a complete orthonormal system for V_0.

If $P_j f$ denotes the orthogonal projection of f into V_j then

$$\lim_{j\to-\infty} \|P_j f\| = 0 \tag{2.1}$$

for all f in $L^2(\mathfrak{R}^n)$.

Note that (2.1) implies

$$\bigcap_{j\in\mathfrak{Z}} V_j = \{0\}. \tag{2.2}$$

Since the properties enjoyed by the sequence of subspaces in Proposition 2.1 are also enjoyed by all multiresolution analyses, see [1, 2, 3, 8, 9], we may make the following conclusion:

Corollary to 2.1. If $\{V_j\}_{j\in\mathfrak{Z}}$ is a multiresolution analysis then property (2.2) is a consequence of the other properties enjoyed by $\{V_j\}_{j\in\mathfrak{Z}}$.

2.2. Details

Proposition 2.1 is an easy consequence of the formula for the Fourier transform of $P_j f$:

$$\widehat{P_j f}(\xi) = \sum_{k \in \mathbb{Z}^n} \left\{ \hat{f}(\xi - 2\pi B^j k) \overline{\hat{\varphi}(B^{-j}\xi - 2\pi k)} \right\} \hat{\varphi}(B^{-j}\xi) \tag{2.3}$$

where $B = A^*$ is the adjoint of A. Here $\hat{g}$ denotes the Fourier transform of g which, for an integrable function, is defined by

$$\hat{g}(\xi) = \int_{\mathfrak{R}^n} e^{-i\langle x, \xi \rangle} g(x) dx$$

and distributionally otherwise.

In what follows we will use the notation

$$\mathrm{per}_j(g(\xi)) = \sum_{k \in \mathbb{Z}^n} g(\xi - 2\pi B^j k).$$

With this notation (2.3) may be re-expressed as

$$\widehat{P_j f}(\xi) = \mathrm{per}_j(\hat{f}(\xi) \overline{\hat{\varphi}(B^{-j}\xi)}) \hat{\varphi}(B^{-j}\xi).$$

To see (2.1), use Plancherel's formula, formula (2.3), and the fact that P_j is an orthogonal projection to write

$$\|P_j f\|^2 = \langle P_j f, f \rangle$$

$$= \frac{1}{(2\pi)^n} \int_{\mathfrak{R}^n} \mathrm{per}_j(\hat{f}(\xi) \overline{\hat{\varphi}(B^{-j}\xi)}) \hat{\varphi}(B^{-j}\xi) \overline{\hat{f}(\xi)}\, d\xi \tag{2.4}$$

Observe that

$$\mathrm{per}_j(\hat{f}(\xi) \overline{\hat{\varphi}(B^{-j}\xi)}) \leq \{\mathrm{per}_j(|\hat{f}(\xi)|^2)\}^{1/2} \{\mathrm{per}_j(|\hat{\varphi}(B^{-1}\xi)|^2)\}^{1/2}$$

and since

$$\mathrm{per}_j(|\hat{\varphi}(B^{-j}\xi)|^2) = 1,$$

by virtue of the fact that $\{\varphi(x - k)\}_{k \in \mathbb{Z}^n}$ is a complete orthonormal system for $L^2(\mathfrak{R}^n)$, we may conclude that

$$\|P_j f\|^2 \leq \frac{1}{(2\pi)^n} \int_{\mathfrak{R}^n} \{\mathrm{per}_j(q^j |\hat{f}(\xi)|^2)\}^{1/2} |q^{-j/2} \hat{\varphi}(B^{-j}\xi) \hat{f}(\xi)| d\xi \tag{2.5}$$

where $q = |\det B|$.

Observe that $\mathrm{per}_j(q^j |\hat{f}(\xi)|^2)$ is essentially an approximating Riemann sum for $\int_{\mathfrak{R}^n} |\hat{f}(\xi - 2\pi\eta)|^2 d\eta$. Hence if $\hat{f}$ is continuous with compact support then if $j \leq 0$,

$$\mathrm{per}_j(q^j|\hat{f}(\xi)|^2) \leqslant C \tag{2.6}$$

where C is a constant which depends on f but not on j. Thus, in view of (2.5) and (2.6), for such f we may write

$$\|P_j f\|^2 \leqslant C \int_{\mathfrak{R}^n} |q^{-j/2}\hat{\phi}(B^{-j}\xi)\hat{f}(\xi)|d\xi. \tag{2.7}$$

whenever $j \leqslant 0$, where C is a constant independent of j. Now, if f vanishes in a neighborhood of the origin say $\{\xi : |\xi| < \varepsilon\}$, we may write

$$\int_{\mathfrak{R}^n} |q^{-j/2}\hat{\phi}(B^{-j}\xi)\hat{f}(\xi)|d\xi \leqslant \|\hat{f}\|_\infty \int_{|\xi|>\varepsilon} q^{-j}|\hat{\phi}(B^{-j}\xi)|^2 d\xi)^{1/2} \tag{2.8}$$

and note that, since $|\hat{\phi}(\xi)|^2$ is in $L^1(\mathfrak{R}^n)$, the integral involving ϕ on the right hand side of (2.8) goes to zero as $j \to -\infty$. Thus from (2.7) and (2.8) we may conclude that (2.1) holds for all f such that f is continuous, compactly supported, and vanishes in a neighborhood of the origin. Since such f are dense in $L^2(\mathfrak{R}^n)$ and $\|P_j\| \leqslant 1$, we may make the stronger conclusion that (2.1) holds for all f in $L^2(\mathfrak{R}^n)$.

3. Tiles and scaling functions

3.1. Background

Suppose A is an acceptable dilation for $\mathfrak{Z}^n$ and $\mathcal{K}$ is a collection of distinct representatives of $\mathfrak{Z}^n/A\mathfrak{Z}^n$. Recall that the number of elements in $\mathcal{K}$ is q, where $q = |\det A|$, and that

$$\mathfrak{Z}^n = \bigcup_{k\in\mathcal{K}} \{k + A\mathfrak{Z}^n\}$$

where the terms in this union are pairwise disjoint.

Let

$$Q = \{x \in \mathfrak{R}^n : x = \sum_{j=1}^{\infty} A^{-j}k_j,\ k_j \in \mathcal{K}\}. \tag{3.1}$$

The set Q satisfies the following properties:

$$AQ \simeq \bigcup_{k\in\mathcal{K}} \{k + Q\}, \tag{3.2}$$

$$\bigcup_{k\in\mathfrak{Z}^n} \{k + Q\} = \mathfrak{R}^n, \tag{3.3}$$

$$\{k_1 + Q\} \bigcap \{k_2 + Q\} \simeq \emptyset \qquad \text{whenever } k_1, k_2 \in \mathcal{K} \text{ and } k_1 \neq k_2. \tag{3.4}$$

Here, $S \simeq T$ means that $|T\backslash S| = |S\backslash T| = 0$ where $|S|$ denotes the Lebesgue measure of S. If Q enjoys

$$\{k + Q\} \bigcap Q \simeq \emptyset \qquad \text{for all } k \text{ in } \mathbb{Z}^n \backslash \{0\}, \tag{3.5}$$

which may be stronger than (3.4), then the characteristic function of Q is a scaling function for a multiresolution analysis.

In a recent paper [3] the authors studied such scaling functions and gave several conditions which are equivalent to (3.5). Unfortunately, in many interesting examples, none of these conditions may be particularly convenient to test. On the other hand, most of the time one is only interested in sufficient conditions on A and $\mathcal{K}$ to ensure that the set Q satisfies (3.5). In what follows we give several such sufficient conditions which, in appropriate cases, are relatively easy to verify.

3.2. Main results

To avoid unpleasant technical complications in what follows we always assume that $\mathcal{K}$ contains 0.

For any nonnegative integer N let

$$\mathcal{A}\mathcal{K}_N = \sum_{j=0}^{N} A^j \mathcal{K}. \tag{3.6}$$

Thus $\mathcal{A}\mathcal{K}_N$ is a finite subset of $\mathbb{Z}^n$ consisting of q^{N+1} sums k of the form

$$k = \sum_{j=0}^{N} A^j k_j \tag{3.7}$$

where the k_j's are in $\mathcal{K}$. Let

$$\mathcal{A}\mathcal{K}_\infty = \bigcup_{N=0}^{\infty} \mathcal{A}\mathcal{K}_N \tag{3.8}$$

and let

$$\mathcal{D}\mathcal{A}\mathcal{K}_\infty = \mathcal{A}\mathcal{K}_\infty - \mathcal{A}\mathcal{K}_\infty. \tag{3.9}$$

In other words every element in $\mathcal{A}\mathcal{K}_\infty$ is a finite sum of the form (3.7) for some N and every element k in $\mathcal{D}\mathcal{A}\mathcal{K}_\infty$ is of the form

$$k = k_1 - k_2 \tag{3.10}$$

where k_1 and k_2 are in $\mathcal{A}\mathcal{K}_\infty$. We are now ready to state the promised conditions.

Proposition 3.1. If $\mathcal{DAK}_\infty = \mathcal{Z}^n$ then Q satisfies (3.5).

Let $b = \max\{|k| : k \in \mathcal{K}\}$ where $|k|$ denotes the Euclidean norm of k, let

$$a^{-1} = \sup\{\|A^{-1}x\| : x \subset \mathcal{R}^n \quad \text{and} \quad |x| = 1\},$$

and let $\mathcal{B} = \{k \in \mathcal{Z}^n : |k| < 2ab/(a-1)\}$. In terms of this notation we may state the following:

Proposition 3.2. If $\mathcal{B} \subset \mathcal{DAK}_\infty$ then Q satisfies (3.5).

Sometimes it is possible to obtain an estimate of $|Q|$, the measure of Q. In such a case the following may be useful:

Proposition 3.3. If $|Q| < 2$ then Q satisfies (3.5).

3.3. Examples

We apply the above results to some of the examples considered in [3] where they where handled by verifiying Cohen's condition.

Example 3.4.

Let $n = 1$, $A = 3$, and $\mathcal{K} = \{0, 1, 5\}$. Then $a = 3$, $b = 5$, and $\mathcal{B} = \{k : |k| < 5\}$. Since $\{0, 1\} \subset \mathcal{K}$ and $\mathcal{DAK}_\infty = -\mathcal{DAK}_\infty$, it suffices to check that 2, 3 and 4 are in $\mathcal{DAK}_\infty$. The identities $2 = 5 - 3 \cdot 1$, $3 = 3 \cdot 1$, and $4 = 5 - 1$ imply that 2, 3 and 4 are in $\mathcal{DAK}_\infty$ so that we may apply Proposition 3.2 to conclude that the corresponding Q satisfies (3.5).

Example 3.5.

Let $n = 2$,

$$A = \begin{pmatrix} 1 & 1 \\ 1 & 1 \end{pmatrix}, \quad \text{and} \quad \mathcal{K} = \left\{\begin{pmatrix} 0 \\ 0 \end{pmatrix}, \begin{pmatrix} 1 \\ 0 \end{pmatrix}\right\}.$$

In this case $a = \sqrt{2}$ and $b = 1$. It is not difficult to verify that $\mathcal{B} = \mathcal{DAK}_\infty$. Hence the corresponding Q satisfies (3.5) by virtue of Proposition 3.2.

Let $n = 2$,

$$A = \begin{pmatrix} 2 & 0 \\ 0 & 2 \end{pmatrix}, \quad \text{and} \quad \mathcal{K} = \left\{\begin{pmatrix} 0 \\ 0 \end{pmatrix}, \begin{pmatrix} 1 \\ 0 \end{pmatrix}, \begin{pmatrix} 0 \\ 1 \end{pmatrix}, \begin{pmatrix} 1 \\ 1 \end{pmatrix}\right\}. \tag{3.11}$$

In this case it is quite transparent that $\mathcal{DAK}_\infty = \mathcal{Z}^2$ so that Proposition 3.1 can be applied directly to conclude that the corresponding Q satisfies (3.5).

Example 3.6.

Let $n = 2$,

$$A = \begin{pmatrix} 3 & 0 \\ 0 & 3 \end{pmatrix},$$

and let $\mathcal{K}$ be the set whose elements are the columns of

$$\begin{pmatrix} 0 & 1 & 2 & 0 & 0 & 1 & 2 & 2 & 4 \\ 0 & 0 & 0 & 1 & 2 & 2 & 1 & 2 & 4 \end{pmatrix}.$$

To see that $\mathcal{DAK}_\infty = \mathbb{Z}^2$ it suffices to show that

$$\begin{pmatrix} 1 \\ 1 \end{pmatrix}$$

is in $\mathcal{DAK}_\infty$. But this is clear since

$$\begin{pmatrix} 1 \\ 1 \end{pmatrix} = \begin{pmatrix} 2 \\ 1 \end{pmatrix} - \begin{pmatrix} 1 \\ 0 \end{pmatrix}$$

Hence Proposition 3.1 can be applied directly to conclude that the corresponding Q satisfies (3.5).

Remark 3.7. Numerical results corresponding to some of the above examples easily imply that $|Q| < 1$. For instance, in example (3.11) it is clear that Q is contained in a triangle of area 3/2. Hence in this case Proposition 3.3 can be applied to conclude that Q satisfies (3.5).

Example 3.8.

Let $n = 2$,

$$A = \begin{pmatrix} 2 & -1 \\ 1 & 2 \end{pmatrix},$$

let $\mathcal{K}_1$ be the set whose elements are the columns of

$$\begin{pmatrix} 0 & 0 & 0 & 1 & 1 \\ 0 & 1 & 2 & 1 & 2 \end{pmatrix},$$

let $\mathcal{K}_2$ be the set whose elements are the columns of

$$\begin{pmatrix} 0 & 0 & 0 & 1 & 1 \\ 0 & 1 & 2 & 1 & -1 \end{pmatrix},$$

and let $\mathcal{K}_3$ be the set whose elements are the columns of

$$\begin{pmatrix} 0 & 0 & 0 & 1 & 1 \\ 0 & -4 & 2 & 1 & -1 \end{pmatrix}.$$

The corresponding tiles are plotted in Figure 3.1, Figure 3.2, Figure 3.3. Property (3.5) can be verified by applying Proposition 3.1, Proposition 3.2, or Proposition 3.3.

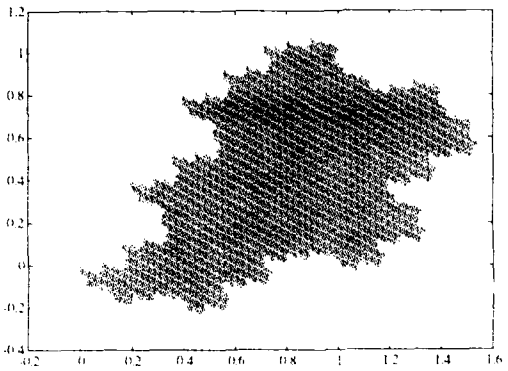

Figure 3.1: Tile generated by $\mathcal{K}_1$ in Example 3.8.

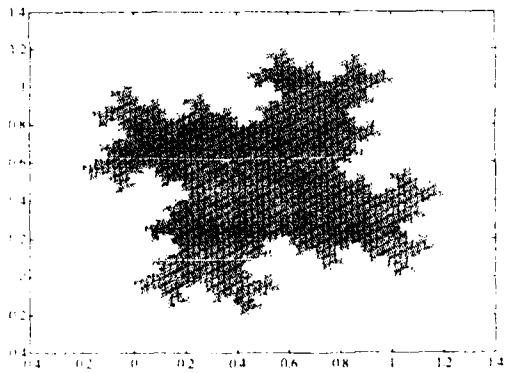

Figure 3.2: Tile generated by $\mathcal{K}_2$ in Example 3.8.

3.4. Details

Proof (of Proposition 3.1). Recall that (3.4) says that

$$\{k_1 + Q\} \bigcap \{k_2 + Q\} \simeq \emptyset \tag{3.12}$$

whenever k_1 and k_2 are in $\mathcal{AK}_0$ and $k_1 \neq k_2$. Hence

$$A\{k_1 + Q\} \bigcap A\{k_2 + Q\} \simeq \emptyset \tag{3.13}$$

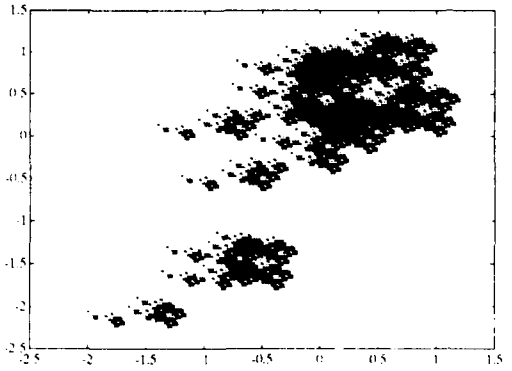

Figure 3.3: Tile generated by $\mathcal{K}_3$ in Example 3.8.

for such k_i. In view of (3.2) we may write

$$A(k_i + Q) = Ak_i + \bigcup_{k \in \mathcal{K}} (k + Q)$$

Since the union in the right hand side of the above identity is taken over pairwise disjoint sets, we may conclude that this identity together with (3.13) imply (3.12) whenever k_1 and k_2 are in $A\mathcal{K}_1$. By induction it is clear that (3.12) is valid whenever k_1 and k_2 are in $A\mathcal{K}_N$ for any non-negative integer N. In other words, since $k \in \mathcal{D}A\mathcal{K}_\infty$ can be expressed as $k = k_1 - k_2$ with k_1 and k_2 in $A\mathcal{K}_N$ for some N we may conclude the following:

Lemma 3.9. If $k \in \mathcal{D}A\mathcal{K}_\infty$ and $k \neq 0$ then

$$(k + Q) \bigcap Q \sim \emptyset$$

This implies the desired result. ∎

Proof (of Proposition 3.2). If $B_r = \{x \in \mathbb{R}^n : |x| \leq r\}$ then a routine estimate shows that $Q \subset B_r$ whenever $r \geq ab/(a - 1)$. Since

$$(k + B_r) \bigcap B_r \simeq \emptyset$$

whenever $|k| \geq 2r$, we may conclude that in order to show that Q satisfies (3.5) for all k in $\mathbb{Z}^n$ it suffices to check that Q satisfies (3.5) for all k in $\mathcal{B}$. This, of course, is the case when $\mathcal{B} \subset \mathcal{D}A\mathcal{K}_\infty$. ∎

Proof (of Proposition 3.3). The result is a transparent consequence of Theorem 2 in [3]. We recall some of the details. In what follows χ_S denotes the characteristic function of the set S.

Let $Q_N, N = 0, 1, 2, \ldots$, be the sequence of sets defined as follows:

- $Q_0 = [-1/2, 1/2]^n$
- $Q_N = \bigcup_{k \in K} A^{-1}(k + Q_{N-1}), \quad N = 1, 2, \ldots$

Then the characteristic functions of Q_N satisfy

- $\sum_{k \in \mathbb{Z}^n} \chi_{Q_N}(x - k) = 1$ a.e.
- for all functions φ which are continuous and bounded on $\mathbb{R}^n$

$$\lim_{N \to \infty} \int_{\mathbb{R}^n} \chi_{Q_N}(x)\varphi(x)dx = \frac{1}{|Q|} \int_{\mathbb{R}^n} \chi_Q(x)\varphi(x)dx$$

The last two items imply that

$$\frac{1}{|Q|} \sum_{k \in \mathbb{Z}^n} \chi_Q(x - k) = 1 \qquad \text{a.e.} \tag{3.14}$$

Since $1 \leq |Q| < \infty$ and the sum in (3.14) is integer-valued for all x, we may conclude the following:

Lemma 3.10. $|Q|$ is equal to a positive integer.

Hence the estimate $|Q| < 2$ implies that

$$|Q| = 1. \tag{3.15}$$

Since (3.15) is equivalent to (3.5), see Lemma 1 in [3], the argument is complete. ∎

4. Miscellaneous remarks

The observations leading to Proposition 2.1 were made while I was preparing a draft of [6] and was confronted with the task of verifying (1.1) for a particularly unpleasant example. A review of the literature indicates that the general idea however is at least implicit in earlier work on the subject. For example, a variant of (2.1) may be found in [2].

Some of the observations which eventually led to Proposition 3.1 and Proposition 3.2 were made during a discussion with Stuart Nelson who provided significant input. Wayne Lawton kindly provided me with a copy of [4], discussed some of the material therein, and brought Lemma 3.10 to my attention via a different argument.

5. Bibliography

[1] A. Cohen. Ondelettes, analyses multirésolutions et filtres miroirs en quadrature. *Ann. Inst. Henri Poincaré*, 7:439–459, 1990.

[2] I. Daubechies. Orthonormal bases of compactly supported wavelets. *Comm. Pure Appl. Math.*, 41:909–996, 1988.

[3] K. Gröchenig and W.R. Madych. Multiresolution analyses, Haar bases, and self-similar tilings of R^n. *IEEE Trans. Information Theory*. To appear, now BRC technical report.

[4] W.M. Lawton and H.L. Resnikoff. Multidimensional wavelet bases. *SIAM J. Math. Anal.* Submitted, now Aware Inc. technical report.

[5] R.A.H. Lorentz and W.R. Madych. Wavelets and generalized box splines. *Applicable Analysis*. To appear, now a GMD technical report.

[6] W.R. Madych. Wavelets and higher order multiresolution analyses. Technical report, BRC.

[7] W.R. Madych. Polyharmonic splines, multiscale analysis, and entire functions. In W. Haußmann and K. Jetter, editors, *Multivariate Approximation and Interpolation*, pages 205–216. Birkhäuser Verlag, Basel, 1990.

[8] S. Mallat. Multiresolution approximations and wavelet orthonormal bases of $L^2(R)$. *Trans. Amer. Math. Soc.*, 315:69–88, 1989.

[9] Y. Meyer. *Ondelettes et Opérateurs*. Hermann, Paris, 1990.

II

Applications in engineering

Innovations and entropy rate with applications in factorization, spectral estimation, and prediction

Athanasios Papoulis
Polytechnic University
Department of Electrical Engineering
Route 110
Farmingdale, NY 11735 USA

Abstract The concept of innovations is introduced as the base of the orthonormal representation of a random process and the result is used to simplify the estimation of the spectrum of an ARMA process. The ARMA model is conceptually justified in terms of the principle of maximum entropy generalized in the context of entropy rate.

1. Factorization and innovations

In the following, we present a number of fundamental concepts related to the orthonormal representation of stochastic processes and we illustrate the results with a variety of topics of theoretical and applied interest. The paper is mostly tutorial. To make it self-contained, we review briefly the early concepts [7].

A *discrete-time stochastic process* is a sequence $\underline{x}_n$ or $\underline{x}[n]$ of random variables (RVs) defined for every integer n. We shall assume that it is a real stationary process with zero mean. The autocorrelation $R[m]$ of $\underline{x}[n]$ is the expected value of the product $\underline{x}[n+m]\underline{x}[m]$:

$$R[m] = E\{\underline{x}[n+m]\underline{x}[n]\} \tag{1.1}$$

The power spectrum $S(e^{jw})$ of $\underline{x}[n]$ is the discrete Fourier transform (DFT) of $R[m]$:

$$S(e^{jw}) = \sum_{m=-\infty}^{\infty} R[m]e^{-jm\omega} \qquad R[m] = \frac{1}{2\pi}\int_{-\pi}^{\pi} S(\omega)e^{jm\omega}\,d\omega \tag{1.2}$$

The process $\underline{x}[n]$is called *white noise* if the RVs $\underline{x}[n]$ and $\underline{x}[n+m]$ are uncorrelated for every $m \neq 0$, that is, if

$$R[m] = P\delta[m] = \begin{cases} P, & m = 0 \\ 0, & m \neq 0 \end{cases} \tag{1.3}$$

$$S(e^{j\omega}) = P$$

J. S. Byrnes et al. (eds.), Probabilistic and Stochastic Methods in Analysis, with Applications, 247–261.
© 1992 *Kluwer Academic Publishers. Printed in the Netherlands.*

Systems A linear time-invariant system is an operator assigning to a given process $\underset{\sim}{x}[n]$ (input) the process (output)

$$\underset{\sim}{y}[n] = \sum_{k=-\infty}^{\infty} \underset{\sim}{x}[n-k]h[k] = \underset{\sim}{x}[n] * h[n] \tag{1.4}$$

Thus, $\underset{\sim}{y}[n]$ is the discrete convolution of $\underset{\sim}{x}[n]$ with the delta response $h[n]$ of the system.

The z-transform

$$H(z) = \sum_{n=-\infty}^{\infty} h[n]z^{-n} \tag{1.5}$$

of $h[n]$ is the system function.

With $R_{xy}[m] = E\{\underset{\sim}{x}[n+m]\underset{\sim}{y}[n]\}$ and $R_{yy}[m] = E\{\underset{\sim}{y}[n+m]\underset{\sim}{y}[n]\}$, it follows from (1.4) that

$$\begin{aligned} R_{xy}[m] &= R_{xx} * h[-m] \qquad & R_{yy} &= R_{xy}[m] * h[m] \\ S_{xy}(z) &= S_{xx}(z)H(1/z) & S_{yy}(z) &= S_{xy}(z)H(z) \end{aligned} \tag{1.6}$$

1.1. Spectral factorization

A function $L(z)$ is called *minimum phase* if it and its inverse $\Gamma(z) = 1/L(z)$ are analytic for $|z| < 1$:

$$L(z) = \sum_{n=0}^{\infty} l[n]z^{-n} \qquad \Gamma(z) = \sum_{n=0}^{\infty} \gamma[n]z^{-n} \tag{1.7}$$

If $S(e^{j\omega})$ is the spectrum of a regular process $\underset{\sim}{x}[n]$ satisfying the Paley-Wiener condition [4]

$$\int_{-\pi}^{\pi} |\ln S(e^{j\omega})|\, d\omega < \infty \tag{1.8}$$

then we can find a minimum-phase function $L(z)$ such that

$$S(z) = L(z)L(1/z) \tag{1.9}$$

The determination of the function $L(z)$ is simple if the given spectrum $S(z)$ is rational: $S(z) = A(z)/B(z)$. We factor the polynomials $A(z)$ and $B(z)$ and form the polynomials $N(z)$ and $D(z)$ using only the roots $|z^i| < 1$ (Fejer-Riesz theorem)

$$S(z) = \frac{A(z)}{B(z)} = \frac{N(z)N(1/z)}{D(z)D(1/z)} \qquad L(z) = \frac{N(z)}{D(z)} \tag{1.10}$$

Example 1.1. We wish to factor the spectrum

$$S(e^{j\omega}) = \frac{5 - 4\cos\omega}{10 - 6\cos\omega} \qquad S(z) = \frac{5 - 2(z + z^{-1})}{10 - 3(z + z^{-1})}$$

Clearly,

$$S(z) = \frac{2(z - 1/2)(z - 2)}{3(z - 1/3)(z - 3)} \quad \text{hence} \quad L(z) = \frac{2z - 1}{3z - 1}$$

1.1.1. Innovations

From (1.6) and (1.9) it follows that if $\underset{\sim}{x}[n]$ is the input to the system $\Gamma(z)$ (Figure 1.1) the spectrum $S_{ii}(z)$ of the resulting output $\underset{\sim}{i}[n]$ is white noise:

$$S_{ii}(z) = S(z)\Gamma(z)\Gamma(1/z) = 1 \qquad R_{ii}[m] = \delta[m] \tag{1.11}$$

The process $\underset{\sim}{i}[n]$ so formed is called the *innovations* of $\underset{\sim}{x}[n]$. Thus,

$$\underset{\sim}{i}[n] = \sum_{k=0}^{\infty} \gamma[k]\underset{\sim}{x}[n - k] \qquad E\{\underset{\sim}{i}[n + m]\underset{\sim}{i}[n]\} = \begin{cases} 1, & m = 0 \\ 0, & m \neq 0 \end{cases} \tag{1.12}$$

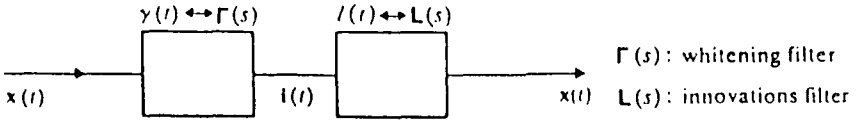

Figure 1.1: Whitening and innovations filter.

Cascading the system $\Gamma(z)$ (whitening filter) with its inverse $I(z)$ (innovations filter) as in Figure 1.1, we conclude that the resulting output equals $\underset{\sim}{x}[n]$. This shows that $\underset{\sim}{x}[n]$ is the output of the filter $L(z)$ with input $\underset{\sim}{i}[n]$:

$$\underset{\sim}{x}[n] = \sum_{k=0}^{\infty} l[k]\underset{\sim}{i}[n - k] \tag{1.13}$$

We have thus shown that a regular process $\underset{\sim}{x}[n]$ is linearly equivalent to a white noise process $\underset{\sim}{i}[n]$ in the sense that each can be expressed linearly in terms of the other and its past, as in (1.12) and (1.13). This is the extension of the Gram-Schmidt orthonormalization to stochastic processes. We give next several applications.

2. Linear prediction

Linear prediction is the LMS estimation of the present value $\underline{x}[n]$ of a stochastic process by a linear function of its past values. The result is a direct application of the projection theorem in Hilbert space. In terms of RVs this theorem can be phrased as follows:

We wish to estimate an RV $\underline{x}_0$ in terms of n RVs, $\underline{x}_1, \ldots, \underline{x}_n$ (data). The desired estimate is the sum

$$\hat{\underline{x}}_0 \stackrel{\Delta}{=} a_1\underline{x}_1 + \cdots + a_n\underline{x}_n \tag{2.1}$$

Our objective is to determine the constants a_i so as to minimize the MS value

$$P = E\{(\underline{x}_0 - \hat{\underline{x}}_0)^2\} \tag{2.2}$$

of the estimation error $\underline{x}_0 - \hat{\underline{x}}_0$. Clearly, P is minimum if

$$\frac{\partial P}{\partial a_i} = -E\{[\underline{x}_0 - (a_1\underline{x}_1 + \cdots + a_n\underline{x}_n)]\underline{x}_i\} = 0 \qquad i = 1, \ldots, n \tag{2.3}$$

This yields a system of n equations expressing the unknowns a_i in terms of the second order moments $E\{\underline{x}_i\underline{x}_j\}$ of the $n + 1$ RVs $\underline{x}_0, \ldots, \underline{x}_n$.

The system (2.3) can be written in the following form:

$$E\{\underline{\epsilon}\underline{x}_i\} = 0 \qquad i = 1, \ldots, n \quad \text{and} \quad \underline{\epsilon} = \underline{x}_0 - \hat{\underline{x}}_0 \tag{2.4}$$

This result, known as the orthogonality principle, states that P is minimum if the estimation error $\underline{\epsilon}$ is orthogonal to the data $\underline{x}_i$.

Note that

$$E\{\underline{\epsilon}\underline{x}_0\} = 0 \qquad P = E\{(\underline{x}_0 - \hat{\underline{x}}_0)\underline{x}_0\} \tag{2.5}$$

2.1. The Yule-Walker equations

Now we consider the problem of estimating the present value $\underline{x}[n]$ of a stochastic process in terms of its N most recent past values $\underline{x}[n-k]$. Our estimate is the sum

$$\hat{\underline{x}}_N[n] = \sum_{k=1}^{N} a_{N,k}\,\underline{x}[n-k] \tag{2.6}$$

as in (2.1). This is the output of the FIR (finite impulse response) filter

$$H_N(z) = a_{N,1}\,z^{-1} + \cdots + a_{N,N}\,z^{-N} \tag{2.7}$$

with input $\underline{x}[n]$. To find the coefficients $a_{N,k}$, we apply (2.5). This yields

$$E\{(\underline{x}[n] - \hat{\underline{x}}_N[n])\underline{x}[n-m]\} = 0 \qquad m = 1, \ldots, N \tag{2.8}$$

Hence,

$$\sum_{k=1}^{N} a_{N,k} R[m-k] = R[m] \qquad m = 1, \ldots, N \tag{2.9.1}$$

The above is a system of N equations (Yule-Walker) and its solution yields the N unknowns $a_{N,k}$.

With $a_{N,k}$ so determined, the resulting LMS error P_N equals (see (2.5) and (2.6))

$$P_N = R[0] - \sum_{k=1}^{N} a_{N,k} R[k] \tag{2.9.2}$$

2.1.1. Levinson's algorithm

To solve the system (2.9) directly, we must invert the matrix of its coefficients (covariance matrix). This is a Toeplitz matrix whose inversion can be simplified. Next we present a simple recursive method (Levinson's algorithm [3]) yielding the N + 1 unknowns P_N and $a_{N,k}$. Following the standard notation, we set $K_N = a_{N,N}$. It follows from (2.9) that

$$a_{1,1} = \frac{R[1]}{R[0]} = K_1 \qquad P_1 = R[0] - a_{1,1}R[1] \tag{2.10}$$

Suppose that we have determined the N − 1 coefficients $a_{N-1,k}$ and the corresponding LMS error P_{N-1}. It can be shown that [6]

$$P_{N-1}K_N = R[N] - \sum_{k=1}^{N-1} a_{N-1,k}R[N-k] \tag{2.11.1}$$

$$a_{N,N} = K_N \quad a_{N,k} = a_{N-1,k} - K_N a_{N-1,N-k} \qquad 1 \leqslant k \leqslant N-1 \tag{2.11.2}$$

$$P_N = (1 - K_N^2)P_{N-1} \tag{2.11.3}$$

The first equation yields K_N; the second is used to find the N parameters $a_{N,k}$; the third equation determines P_N. The iteration starts with (2.10).

Note that $|K_N| \leqslant 1$ because $P_N \geqslant 0$. Thus, P_N is a decreasing sequence of numbers tending to a positive limit P.

2.2. The Wiener filter

As $N \to \infty$, the FIR predictor of $\underset{\sim}{x}[n]$ tends to the predictor

$$\hat{\underset{\sim}{x}}[n] = \sum_{k=1}^{\infty} h[k]x[n-k] \qquad H(z) = \sum_{n=1}^{\infty} h[n]z^{-n} \tag{2.12}$$

and, (2.9) tends to the infinite system (Wiener-Hopf equations)

$$\sum_{k=1}^{\infty} h[k]R[m-k] = R[m] \qquad m \geq 1 \tag{2.13.1}$$

$$P + \sum_{k=1}^{\infty} h[k]R[k] = R[0] \tag{2.13.2}$$

involving the unknowns $h[k]$ and P. We shall solve the system (2.13) indirectly using innovations. From the linear equivalence of the process $\underset{\sim}{x}[n]$ and its innovations $\underset{\sim}{i}[n]$ it follows that the predictor $\hat{\underset{\sim}{x}}[n]$ of $\underset{\sim}{x}[n]$ can be written as the response of a linear filter $H_i(z)$ with input $\underset{\sim}{i}[n]$:

$$\hat{\underset{\sim}{x}}[n] = \sum_{k=1}^{\infty} h_i[k]\underset{\sim}{i}[n-k] \qquad H_i(z) = \sum_{n=1}^{\infty} h_i[n] \tag{2.14}$$

To find $h_i[k]$, we apply the orthogonality principle (2.4):

$$E\left\{\left(\underset{\sim}{x}[n] - \sum_{k=1}^{\infty} h_i[k]\underset{\sim}{i}[n-k]\right)\underset{\sim}{i}[n-m]\right\} = 0 \qquad m \geq 1 \tag{2.15}$$

Since (see (1.12) and (1.13))

$$E\{\underset{\sim}{x}[n]\underset{\sim}{i}[n-m]\} = l[m] \qquad E\{\underset{\sim}{i}[n-k]\underset{\sim}{i}[n-m]\} = \delta[m-k]$$

(2.15) yields

$$h_i[m] = l[m] \qquad \hat{\underset{\sim}{x}}[m] = \sum_{k=1}^{\infty} l[k]\underset{\sim}{i}[n-k] \tag{2.16}$$

This shows that the estimate $\hat{\underset{\sim}{x}}[n]$ of $\underset{\sim}{x}[n]$ is the response of the filter

$$H_i(z) = \sum_{k=1}^{\infty} l[k]z^{-k} = L(z) - l[0] \tag{2.17}$$

to the input $\underset{\sim}{i}[n]$.

To complete the specification of the Wiener filter $H(z)$ it suffices to express $\underset{\sim}{i}[n]$ in terms of $\underset{\sim}{x}[n]$. The process $\underset{\sim}{i}[n]$ is the response of the whitening filter $1/L(z)$ to the input $\underset{\sim}{x}[n]$. Cascading with $H_i(z)$ we obtain Figure 2.1

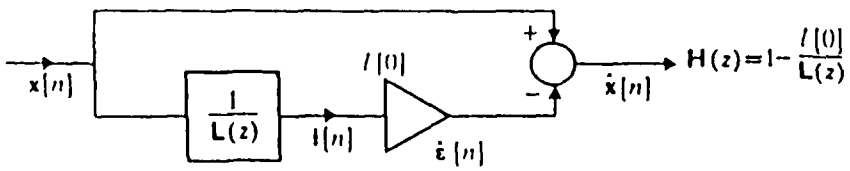

Figure 2.1: One-step predictor.

Example 2.1. Suppose that $\underline{x}[n]$ is the process of Example 1.1. In this case,

$$L(z) = \frac{2z-1}{3z-1} \qquad l[0] = \lim_{z\to\infty} L(z) = 2/3$$

$$H(z) = \frac{-z^{-1}}{6-3z^{-1}} \qquad \hat{\underline{x}}[n] = \frac{1}{2}\hat{\underline{x}}[n-1] + \frac{1}{6}\underline{x}[n-1]$$

2.2.1. The Kolmogoroff-Szego MS error formula

From (2.16) and (1.13) it follows that the estimation error equals

$$\underline{\epsilon}[n] = \underline{x}[n] - \hat{\underline{x}}[n] = l[0]\underline{i}[n]$$

And since $E\{\underline{i}^2[n]\} = 1$, this yields

$$P = E\{\underline{\epsilon}^2[n]\} = l^2[0] \tag{2.18}$$

We shall express this error directly in terms of the power spectrum $S(e^{j\omega}) = |L(e^{j\omega})|^2$ of $\underline{x}[n]$. The function $\ln L(z)$ is analytic for $|z| > 1$. From this it follows that [1]

$$\ln l^2[0] = \frac{1}{2\pi}\int_{-\pi}^{\pi} \ln |L(e^{j\omega})|^2 \, d\omega$$

hence

$$p = \exp\left\{\frac{1}{2\pi}\int_{-\pi}^{\pi} \ln S(e^{j\omega})\, d\omega\right\} \tag{2.19}$$

3. Spectral estimation

A process $\underline{x}[n]$ is called ARMA (autoregressive-moving average) if its spectrum $S(z)$ is rational as in (1.10):

$$S(z) = L(z)L(1/z) \qquad L(z) = \frac{b_0 + b_1 z^{-1} + \ldots + b_M z^{-M}}{1 + a_1 z^{-1} + \ldots + a_N z^{-N}} = \frac{N(z)}{D(z)} \tag{3.1}$$

In this case, $\underline{x}[n]$ satisfies the recursion equation

$$\underline{x}[n] + a_1\underline{x}[n-1] + \ldots + a_N\underline{x}[n-N] = b_0\underline{i}[n] + \ldots + b_M\underline{i}[n-M] \tag{3.2}$$

where $\underline{i}[n]$ is its innovations. We shall determine the $N + M + 1$ parameters a_i and b_k of $L(z)$ in terms of the first $N + M + 1$ values $R[0], \ldots, R[M+N]$ of the autocorrelation $R[m]$ of $\underline{x}[n]$.

The process $\underline{x}[n-m]$ is linearly dependent on $\underline{i}[n-m]$ and its past; furthermore $\underline{i}[n]$ is white noise with $E\{\underline{i}^2[n]\} = 1$. Multiplying (3.2) by $\underline{x}[n-m]$ and taking expected values, we conclude that

$$R[m] + a_1 R[m-1] + \ldots + a_N R[m-N] = 0 \qquad m > M \tag{3.3}$$

Setting $m = M + 1, \ldots, M + N$, we obtain a system of N equations. Its solution yields the N unknowns a_k. To complete the specification of $L(z)$ we need to find its numerator $N(z)$.

AR processes If $M = 0$, then $\underset{\sim}{x}[n]$ is an autoregressive process and

$$L(z) = \frac{b_0}{D(z)} \qquad b_0 = \lim_{z\to\infty} L(z) \tag{3.4}$$

In this case (see (3.2))

$$\underset{\sim}{x}[n] + a_1\underset{\sim}{x}[n-1] + \cdots + a_N\underset{\sim}{x}[n-N] = b_0\underset{\sim}{i}[n] \tag{3.5}$$

and (3.3) is reduced to the Yule-Walker equations (2.9.1) if we set $a_{N,k} = -a_k$. Solving, we obtain $D(z)$. To determine the constant b_0, we multiply (3.5) by $\underset{\sim}{i}[n]$ and take expected values. This yields $E\{\underset{\sim}{x}[n]\underset{\sim}{i}[n]\} = b_0E\{\underset{\sim}{i}^2[n]\} = b_0$. Multiplying (3.5) by $\underset{\sim}{x}[n]$ and using the above, we obtain

$$R[m] + a_1R[m-1] + \cdots + a_NR[m-N] = b_0 \tag{3.6}$$

This completes the determination of $L(z)$.

MA processes If $N = 0$, then $\underset{\sim}{x}[n]$ is the moving average of its innovations:

$$\underset{\sim}{x}[n] = b_0\underset{\sim}{i}[n] + \cdots + b_M\underset{\sim}{i}[n-M] \tag{3.7}$$

$$L(z) = b_0 + b_1z^{-1} + \cdots + b_Mz^{-M} \tag{3.8}$$

In this case (see (3.3)), $R[m] = 0$ for $m > M$; hence, $S(z)$ can be expressed directly in terms of $R[m]$:

$$S(e^{j\omega}) = \sum_{m=-M}^{M} R[m]D(e^{-jm\omega}) = |L(e^{j\omega})|^2 = \left|\sum_{m=0}^{M} b_me^{-jm\omega}\right|^2$$

Thus to find $L(z)$, it suffices to factor the function $S(z)$ as in (1.9). This method involves the determination of the roots of $S(z)$. We discuss later a method that avoids factorization.

ARMA processes Suppose, finally, that $\underset{\sim}{x}[n]$ is an ARMA process as in (3.1). As we have shown, the denominator $D(z)$ can be determined from (3.6) in terms of the N values $R[M+1], \ldots, R[M+N]$ values of $R[m]$. With a_k so determined, we form the process [2]

$$\underset{\sim}{y}[n] = \underset{\sim}{x}[n] + a_1\underset{\sim}{x}[n-1] + \cdots + a_N\underset{\sim}{x}[n-N] \tag{3.9}$$

This is the left side of (3.2). Clearly, $\underset{\sim}{y}[n]$ is the response of a system with input $\underset{\sim}{x}[n]$ and system function $D(z)$. Hence,

$$S_{yy} = S_{xx}(z)D(z)D(1/z) = N(z)N(1/z) \tag{3.10}$$

From the above it follows that $N(z)$ is the innovations filter of $\underset{\sim}{y}[n]$ and it shows that $\underset{\sim}{y}[n]$ is an MA process. To find $N(z)$, it suffices, therefore, to find the autocorrelation of $\underset{\sim}{y}[n]$ and proceed as in the MA case. Clearly,

$$D(z)D(1/z) = \sum_{m=-M}^{N} \rho[m]z^{-m} \tag{3.11}$$

To determine $\rho[m]$, we form the product on the left and equate coefficients. This yields

$$\rho[m] = \sum_{k=m}^{N} a_{k-m}a_k \qquad \text{for } |m| \leqslant N \text{ and 0 otherwise.}$$

Convolving with the inverse $R[m]$ of $S_{xx}(z)$, we obtain

$$R_{yy} = \sum_{k=-N}^{N} R[m-k]\rho[k] \qquad \text{for } |m| \leqslant M \text{ and 0 otherwise,} \tag{3.12}$$

The determination of an ARMA spectrum involves thus the following steps:

1) We find the constants a_k solving the system (3.3).
2) We compute $R_{yy}[m]$ from (3.12).
3) We factor the corresponding spectrum.

$$S_{yy}(z) = \sum_{m=-M}^{M} R_{yy}[m]z^{-m} = N(z)N(1/z)$$

Note that the system (3.3) cannot be solved with Levinson's algorithm because it holds only for $m > M \geqslant 2$.

4. Entropy rate

Given a partition A of a probability space S, consisting of N events A_i, we form the sum

$$H(A) = -\sum_{i=1}^{N} p_i \ln(p_i) \qquad p_i = P(A_i) \tag{4.1}$$

This sum is by definition the entropy of the partition A. Since $p_1 + \cdots + p_N = 1$ and $p_i \geqslant 0$, it follows that

$$0 \leqslant H(A) \leqslant \ln N$$

The maximum is reached if $p_1 = \ldots = p_N = 1/N$ and the minimum if $p_r = 1$ for some r. This justifies the use of the entropy as a measure of uncertainty about the occurrence of the events A_i in a single trial: if $p_r = 1$, then our uncertainty is zero because, almost certainty, only the event A_r will occur. If $p_i = 1/N$, our uncertainty is maximum. We give next an empirical interpretation of the concept of entropy. Our objective, however, is a method of estimating the spectrum of a process based on the principle of maximum entropy.

4.1. Typical sequences

In the space S_n of repeated trials, we form the event

$$B = \{A_i \text{ occurs } n_i \text{ times in a specific order}\} \tag{4.2}$$

The probability of this event equals

$$P(B) = p_1^{n_1} \cdots p_N^{n_N} \tag{4.3}$$

If we perform the underlying physical experiment n times and the event A_i occurs n_i times, then, almost certainly

$$p_i \simeq n_i/n \tag{4.4}$$

provided that n is sufficiently large. In the space S_n there are N^n sequences of the form (4.2). From (4.4) it follows that almost certainly, the elements $t \in T$ of the subset

$$T = \{A_i \text{ occurs } n_i \simeq np_i \text{ times in a specific order}\} \tag{4.5}$$

of B occur. These elements will be called *typical sequences*.

With $n_i \simeq np_i$, (4.3) yields

$$P(t) \simeq p_1^{np_1} \cdots p_N^{np_N} = e^{np_1 \ln p_1} \cdots e^{np_N \ln p_N} = e^{-nH(A)} \tag{4.6}$$

Thus, all typical sequences have the same probability. Denoting by n_t the total number of such sequences, we conclude from (4.6) that

$$n_t P(t) \simeq P(T) \simeq 1 \qquad n_t = e^{nH(A)} \tag{4.7}$$

If the events A_i are not equally likely, then $H(A) < \ln N$; hence, for large n, $nH(A) \ll n \ln N$. From this it follows that

$$n_t \ll e^{n \ln N} = N^n$$

Thus, the number of typical sequences is much smaller than the number N^n of all possible sequences even though almost certainly, only typical sequences will occur because the probability $P(T)$ of their union T is almost one. This property of typical sequences is important in coding theory [8] and it gives an empirical interpretation of the principle of maximum entropy.

4.2. Entropy of RVs

Suppose that $\underset{\sim}{x}$ is a discrete-type RV taking the values x_i with probability p_i. The events A_i form a partition A_x of S. The entropy of this partition is by definition the entropy $H(\underset{\sim}{x})$ of the RV $\underset{\sim}{x}$:

$$H(\underset{\sim}{x}) = H(A_x) = -\sum_i p_i \ln p_i \tag{4.8}$$

From this it follows that

$$H(\underset{\sim}{x}) = -E\{\ln f(\underset{\sim}{x})\} \tag{4.9}$$

where $f(x)$ is a function equal to p_i for $x = x_i$ and 0 elsewhere. Extending (4.9) to continuous-type RVs, we defined the entropy of an RV $\underset{\sim}{x}$ similarly:

$$H(\underset{\sim}{x}) = -E\{\ln f(\underset{\sim}{x})\} = -\int_{-\infty}^{\infty} \ln f(x)\, dx \tag{4.10}$$

where $f(x)$ is the density of $\underset{\sim}{x}$.

Example 4.1. If $\underset{\sim}{x}$ is a normal RV with zero mean and variance σ^2, then

$$H(\underset{\sim}{x}) = -E\left\{\ln \frac{1}{\sigma\sqrt{2\pi}} - \frac{\underset{\sim}{x}^2}{2\sigma^2}\right\} = \ln \sigma\sqrt{2\pi} + 1/2 = \ln \sigma\sqrt{2\pi e}$$

Example 4.2. If $f(x) = ce^{-cx}$ for $X > 0$ and 0 otherwise then $E\{c\underset{\sim}{x}\} = 1$, hence

$$H(\underset{\sim}{x}) = -E\{\ln c - c\underset{\sim}{x}\} = -\ln c + 1$$

The conditional entropy of $\underset{\sim}{y}$ assuming $\underset{\sim}{x}$ is by definition

$$H\{\underset{\sim}{y}|\underset{\sim}{x}\} = -E\{\ln f(\underset{\sim}{y}|\underset{\sim}{x})\} = -\iint_{-\infty}^{\infty} f(x, y) \ln f(y|x)\, dx\, dy \tag{4.11}$$

This is the measure of uncertainty about $\underset{\sim}{y}$ assuming that $\underset{\sim}{x}$ has been observed.

The entropy of a random vector $\underset{\sim}{X} = [\underset{\sim}{x}_1, \ldots, \underset{\sim}{x}_n]$ and the conditional entropy of $\underset{\sim}{Y} = [\underset{\sim}{y}_1, \ldots, \underset{\sim}{y}_n]$ assuming $\underset{\sim}{X}$ are defined similarly:

$$H(\underset{\sim}{X}) = -E\{\ln f(\underset{\sim}{X})\} \qquad H(\underset{\sim}{Y}|\underset{\sim}{X}) = -E\{\ln f(\underset{\sim}{Y}|\underset{\sim}{X})\} \tag{4.12}$$

4.3. Entropy rate

The m-th order entropy of a stochastic process $\mathbf{x}_n$ is the entropy of $H(\mathbf{x}_n, \mathbf{x}_{n-1}, \ldots, \mathbf{x}_{n-m+1})$ of a block of m consecutive samples $\mathbf{x}_{n-k}$, $k = 1, \ldots, m$ of $\mathbf{x}_n$. The ratio $H(\mathbf{x}_n, \ldots, \mathbf{x}_{n-m+1})/m$ is the average uncertainty per sample in a block of m consecutive samples. The limit

$$H(\mathbf{x}) = \lim_{m \to \infty} \frac{1}{m} H(\mathbf{x}_n, \ldots, \mathbf{x}_{n-m}) \tag{4.13}$$

is the *entropy rate* of the process $\mathbf{x}_n$.

It can be shown that [7]

$$H(\mathbf{x}) = \lim_{m \to \infty} H(\mathbf{x}_n | \mathbf{x}_{n-1}, \ldots, \mathbf{x}_{n-m}) \tag{4.14}$$

Thus $H(\mathbf{x})$ is the uncertainty about the present of $\mathbf{x}_n$ assuming that its entire past is observed.

If $\mathbf{x}_n$ is a normal process, then

$$H(\mathbf{x}) = \ln \sqrt{2\pi e} + \frac{1}{2\pi} \int_{-\pi}^{\pi} \ln S(e^{j\omega})\, d\omega \tag{4.15}$$

Note finally that if $\mathbf{x}_n$ is the input to a linear system with system function $L(z)$, then the entropy rate $H(\mathbf{y})$ if the resulting output $\mathbf{y}_n$ equals

$$H(\mathbf{y}) = H(\mathbf{x}) + \frac{1}{2\pi} \int_{-\pi}^{\pi} \ln |L(e^{j\omega})|\, d\omega \tag{4.16}$$

For normal processes, this follows readily from (4.15) because $S_y(e^{j\omega}) = S_x(e^{j\omega}) |L(e^{j\omega})|^2$. The proof of the general case is more difficult [5].

4.4. The principle of maximum entropy

Consider a partition A consisting of N events A_i as in (4.1). Suppose that we know nothing about the probabilities p_i of these events. The maximum entropy (ME) principle states that in this case, the unknowns p_i must be such as to maximize the entropy $H(A)$ of A. Since $p_1 + \cdots + p_N = 1$, this leads to the conclusion that the events A_i must be equally likely. If prior information about the probabilities p_i is available, then p_i must be such as to maximize $H(A)$ subject to the constraints resulting from the prior information.

Example 4.3. We are given a die and we wish to estimate the probability p_i of its faces. In the absence of any prior information, we conclude that $p_i = 1/6$. Suppose, however, that the probability that {even} shows equals 0.4. In this case, the constants p_i are such as to maximize the sum $-p_1 \ln p_1 - \cdots - p_6 \ln p_6$ subject to the conditions

$$p_1 + p_2 + \cdots + p_6 = 1 \qquad p_2 + p_4 + p_6 = 0.4$$

This yields

$$p_2 = p_4 = p_6 = 2/15 \qquad p_1 = p_3 = p_5 = 1/5$$

The empirical justification of the ME principle can be expressed in terms of the concept of typical sequences: the unknown constants p_i must be such as to maximize the number n_t of the sequences formed with the elements A_i of the partition A that are likely to occur (see (4.7)).

4.4.1. Constraints as expected values

We shall use the ME principle to estimate the density $f(x)$ of an RV $\underset{\sim}{x}$ under the assumption that the expected values η_i of n known functions $g_i(\underset{\sim}{x})$ of $\underset{\sim}{x}$ are given:

$$E\{g_i(\underset{\sim}{x})\} = \int_{-\infty}^{\infty} g_i(x) f(x)\, dx = \eta_i \qquad i = 1, \ldots, n \tag{4.17}$$

In this case, our problem is to find a positive function $f(x)$ of unit area such as to maximize the integral

$$H(\underset{\sim}{x}) = -\int_{-\infty}^{\infty} f(x) \ln f(x)\, dx \tag{4.18}$$

subject to the constraints (4.17). It is easy to show that the solution to this problem is an exponential:

$$f(x) = \frac{1}{Z} \exp\{-\lambda_1 g_1(x) - \cdots - \lambda_n g_n(x)\} \tag{4.19}$$

where

$$Z = \int_{-\infty}^{\infty} \exp\{-\lambda_1 g_1(x) - \cdots - \lambda_n g_n(x)\}\, dx \tag{4.20}$$

The n parameters λ_i are determined from (4.17).

Example 4.4. Estimate the density $f(x)$ of a positive RV $\underset{\sim}{x}$ with known mean.

In this problem, $n = 1$

$$g(x) = x \quad E\{\underset{\sim}{x}\} = \eta \quad f(x) = 0 \qquad \text{for } x < 0$$

and (4.19) yields

$$f(x) = \frac{1}{Z} e^{-\lambda x} \qquad \lambda = \tfrac{1}{\eta} Z + \eta$$

Example 4.5. Estimate $f(x)$ if $E\{\underset{\sim}{x}^2\} = m_2$. With $g(x) = \underset{\sim}{x}^2$, (4.19) yields

$$f(x) = \frac{1}{z}e^{-\lambda x^2} \qquad \lambda = \frac{1}{2m_2} \qquad Z = \frac{1}{\sqrt{2\pi m_2}}$$

Thus, if the second moment of an RV is known, then its ME density is normal with zero mean.

The preceding results can be readily extended to random vectors.

4.4.2. Spectral estimation

Using the ME principle, we shall estimate the power spectrum $S(z)$ of a stochastic process $\underset{\sim}{x}_n$ under the assumption that the first $2N + 1$ values

$$R[m] = E\{\underset{\sim}{x}_n \underset{\sim}{x}_{n-m}\} \qquad |m| \leqslant N \tag{4.21}$$

of its autocorrelation are known. This problem was solved in Section 3 under the assumption that $S(z)$ is rational (see (3.1)). In the following, we make no prior assumptions. We show that, under the given constraints, the ME principle leads to the conclusion that the process $\underset{\sim}{x}_n$ is normal and autoregressive.

In this problem, the constraints (4.21) are second order moments. From this it follows as in Example 4.5 that $\underset{\sim}{x}_n$ is a normal process and its entropy rate equals (see (4.15)).

$$H(x) = \ln\sqrt{2\pi e} + \frac{1}{2\pi}\int_{-\pi}^{\pi} \ln S(e^{j\omega})\, d\omega \tag{4.22}$$

The maximization of the entropy of $\underset{\sim}{x}_n$ of any order is equivalent to the maximation of its entropy rate $H(\underset{\sim}{x})$. Hence, to solve our problem, it suffices to maximize the integral in (4.22) subject to the constraints (4.21). Since

$$S(e^{j\omega}) = \sum_{m=-\infty}^{\infty} R[m]e^{-jm\omega} \qquad \frac{\partial S}{\partial R[m]} = \frac{1}{S(e^{j\omega})}e^{-jm\omega}$$

we conclude differentiating (4.22) that $H(\underset{\sim}{x})$ is maximum if

$$\frac{\partial H}{\partial R[m]} = \frac{1}{2\pi}\int_{-\pi}^{\pi} \frac{1}{S(e^{j\omega})}e^{-jm\omega}\, d\omega = 0 \qquad |m| > N \tag{4.23}$$

This shows that the Fourier series coefficients of the function $1/S(e^{j\omega})$ are 0 for $|m| > N$, hence, $1/S(e^{j\omega})$ is a trigonometric polynomial:

$$\frac{1}{S(e^{j\omega})} = \sum_{m=-N}^{N} c_m e^{-jm\omega} \tag{4.24}$$

To complete the estimation of $S(z)$, it suffices to determine the coefficients c_n. We can do so, using Levinson's algorithm as in Section 3.

5. Bibliography

[1] U. Grenander and G. Szego. *Toeplitz Forms and Their Applications.* Berkley University Press, 1958.

[2] M. Kaveh. High resolution spectral estimation for noisy signals. *IEEE Trans. Acoustics, Speech, Signal Processing*, 27, 1979.

[3] N. Levinson. The Wiener RMS error criterion in filter design and prediction. *Journal of Mathematics and Physics*, 25, 1947.

[4] A. Papoulis. *The Fourier Integral and its Applications.* McGraw-Hill, New York, 1962.

[5] A. Papoulis. Maximum entropy and spectral estimation: A review. *IEEE Trans. Acoustics, Speech, Signal Processing*, 29, 1981.

[6] A. Papoulis. Levinson's algorithm, Wold's decomposition, and spectral estimation. *SIAM Review*, 27, 1985.

[7] A. Papoulis. *Probability, Random Variables, and Stochastic Processes.* McGraw-Hill, New York, 3rd edition, 1991.

[8] C. E. Shannon and W. Weaver. *The Mathematical Theory of Communication.* University of Illinois Press, 1949.

Generation of accurate broadband information from narrowband data using the Cauchy method†

T.K. Sarkar
Department of Electrical Engineering
Syracuse University
Syracuse, NY 13210 USA
tksarkar@sunrise.acs.syr.edu

R.S. Adve
rsadve@sunrise.bitnet
(Other address the same.)

Abstract

The Method of Cauchy has been used to extrapolate a desired parameter over a broad range of frequencies. This information is generated using some information about the parameter over a narrow band of frequencies or at some discrete frequency points.

The approach is to assume that the parameter, as a function of frequency, is a ratio of two polynomials. The problem is to determine the order of the polynomials and the coefficients that define them.

This method can be coded as a standalone program or incorporated as part of a larger program. This technique has yielded accurate results while in use in conjunction with a Method of Moments program and as a independent program in filter analysis.

1. Introduction

In a host of problems in electromagnetics, it is necessary to obtain information about a system over a broad range of frequencies. In most cases it is not possible to evaluate the desired parameter in closed form. The sixties saw the development of the Method of Moments to overcome this difficulty. It was shown that the Method of Moments generated remarkably accurate solutions for a broad class of problems. The later years saw this method being refined into a popular algorithm in electromagnetics research.

The Method of Moments is an approximation technique, which converts interactions of complicated bodies into a set of smaller, easily solvable

† We would like to acknowledge the support of Scientific Atlanta for their partial support for the completion of this project.

J. S. Byrnes et al. (eds.), Probabilistic and Stochastic Methods in Analysis, with Applications, 263–271.
© 1992 *Kluwer Academic Publishers. Printed in the Netherlands.*

interactions. This method finds its major advantage in the widespread use of the computer. But its major drawback lies in that for broadband analysis the program has to be run at many frequency points. In a large system the execution time may be as long as days. Also the memory requirements in large systems can be too much for many available computer systems. Hence the time required to generate currents over a broad spectrum of frequencies may be prohibitive. In the laboratory it is not always possible to make accurate broadband measurements. This problem is especially severe in the case of measuring the transfer function of a filter in the stop band. In some cases the signal to noise ratio is too low to be confident about the measurements of filter characteristics.

These drawbacks in current methods have created a need for a technique that would generate the required information without using too much time and still yield accurate results. One possible technique is the Method of Cauchy. The approach is to approximate the currents as a function of a frequency. The function chosen is a ratio of two polynomials. The problem therefore reduces to the determination of the order of the polynomials and the coefficients therein. With the polynomial coefficients at hand, one can evaluate the currents at an arbitrary number of frequency points.

A successful application of this method would result in saving significant amounts of program execution time.

2. The Cauchy Method

Let us represent the current as a ratio of two polynomials. Hence the current (H), as a function of frequency (s), is

$$H(s) = \frac{A(s)}{B(s)} \tag{2.1}$$

The numerator polynomial is of order P and the denominator of order Q. Hence we have $P + Q + 2$ unknown coefficients. Cauchy's problem is: given $H^n(sj)$ for $j = 1, \ldots, J$ and $n = 1, \ldots, N_j$, to find P, Q, A(s) and B(s).

We need the values of the current and its N_j derivatives at frequency points s_j, $j = 1, \ldots, J$.

The solution for the coefficients is unique if the total number of samples is equal to the total number of unknown coefficients $P + Q + 2$, i.e.,

$$N = \sum_{j=1}^{J} (N_j + 1) = P + Q + 2 \tag{2.2}$$

From (2.1)

$$A(s) = H(s)B(s) \tag{2.3}$$

Differentiating the above equation n times results in the binomial expansion,

$$A^{(n)}(s_j) = \sum_{i=0}^{n} {}^{n}C_i H^{(n-i)}(s_j) B^{i}(s_j) \tag{2.4}$$

where ${}^{n}C_i = \frac{n!}{(n-i)!i!}$. Consider $A(s) = \sum_{k=0}^{P} a_k s^k$ and $B(s) = \sum_{k=0}^{Q} b_k s^k$.

Equation (2.4) can be rewritten as

$$\sum_{k=0}^{P} A_{j,n,k} a_k = \sum_{k=0}^{Q} B_{j,n,k} b_k \tag{2.5}$$

where

$$\mathbf{A}_{j,n,k} = \frac{k!}{(k-n)!} s_j^{(k-n)} u(k-n), \tag{2.6}$$

$$\mathbf{B}_{j,n,k} = \sum_{i=0}^{n} {}^{n}C_i H^{(n-i)}(s_j) u(k-i), \tag{2.7}$$

$j = 1, \ldots, J$, and $n = 0, 1, \ldots, N_j$, and $u(k) = 0$ for $k < 0$ and 1 otherwise.

Define

$$\mathbf{A} = \left[A_{j,n,0}, A_{j,n,1}, \ldots, A_{j,n,P}\right] \tag{2.8}$$

$$\mathbf{B} = \left[B_{j,n,0}, B_{j,n,1}, \ldots, B_{j,n,Q}\right] \tag{2.9}$$

The order of matrix **A** is $N \times (P + 1)$ and that of **B** is $Nx(Q + 1)$.

$$[\mathbf{a}] = [a_0, a_1, a_2, \ldots, a_P]^T \tag{2.10}$$

$$[\mathbf{b}] = [b_0, b_1, b_2, \ldots, b_Q]^T \tag{2.11}$$

Then, equation (2.5) becomes

$$[\mathbf{A}| - \mathbf{B}]\begin{bmatrix} a \\ b \end{bmatrix} = 0 \tag{2.12}$$

Now one can do a singular value decomposition of the matrix $[\mathbf{A}| - \mathbf{B}]$. This results in the equation:

$$[\mathbf{U}][\mathbf{\Sigma}][\mathbf{V}]^H[\begin{bmatrix} a \\ b \end{bmatrix}] = 0 \tag{2.13}$$

The matrices **U** and **V** are unitary matrices and **Σ** is a diagonal matrix with the singular values of $[\mathbf{A}|-\mathbf{B}]$ as its entries. Given the number of nonzero singular

entries, we can estimate the order of the two polynomials. Given these better estimates of the polynomial orders one can recalculate the matrices **A** and **B**. Now one can rewrite the above equation as:

$$[\mathbf{A}] - \mathbf{B}] \begin{bmatrix} a \\ b \end{bmatrix} = 0 \tag{2.14}$$

One solution is to choose the eigenvector corresponding to the minimum eigenvalue. Since the eigenvalues are in general complex, the minimum is defined as the one with the lowest absolute value.

In a computer realization of the Cauchy method, this technique could lead to errors since we may have multiple zero eigenvalues which show up as being only close to zero. The desired solution would be a linear combination of the eigenvectors corresponding to these near zero eigenvalues. This is specially true in the applications to filter analysis because the orders of the filters are important. Choosing the orders of the numerator and denominator polynomials as high values can lead to errors. One way of getting around this problem is to assume that $a_0 = 1.0$. Now equation (2.12) can be written as

$$[\mathbf{A}_1] - \mathbf{B}] \begin{bmatrix} a_1 \\ b \end{bmatrix} = -\mathbf{A}_0 \tag{2.15}$$

where $\mathbf{A}_1$ is the matrix **A** without its first column, a_1 is the column vector of numerator coefficients other than the a_0 and $\mathbf{A}_0$ is the first column of matrix **A**.

Now one does a singular value decomposition of the matrix $[\mathbf{A}_1] - \mathbf{B}]$ The resulting equation is:

$$[\mathbf{U}][\mathbf{\Sigma}][\mathbf{V}^H] \begin{bmatrix} a_1 \\ b \end{bmatrix} = -\mathbf{A}_0 \tag{2.16}$$

where $\mathbf{\Sigma}$ is the diagonal matrix with entries the singular values of the matrix $[\mathbf{A}_1] - \mathbf{B}]$. Now the solution can be written as

$$\begin{bmatrix} a_1 \\ b \end{bmatrix} = -[\mathbf{V}][\mathbf{\Sigma}^{-1}][\mathbf{U}^H]\mathbf{A}_0 \tag{2.17}$$

Hence we now have the coefficients of the polynomials at hand. We can now approximate the current at any frequency of interest. Any parameter we are interested in can be evaluated from the current.

It must be pointed out that the Cauchy method can be used for the extrapolation of a function with respect to any variable. In electromagnetics, frequency is often the variable of interest.

3. Interfacing with the Method of Moments

The usefulness of the above method is the ease with which it can be incorporated into a Method of Moments program. The Method of Moments results in a equation of the form

$$[V] = [Z][I] \tag{3.1}$$

Differentiating the above equation with respect to frequency results in a binomial expansion

$$[V]' = [Z]'[I] + [Z][I]' \tag{3.2}$$

$$\Rightarrow [I]' = [Z]^{-1}\left[[V]' - [Z]'[I]\right] \tag{3.3}$$

$$[V]'' = [Z]''[I] + 2[Z]'[I]' + [Z][I]'' \tag{3.4}$$

$$\Rightarrow [I]'' = [Z]^{-1}\left[[V]'' - 2[Z]'[I]' - [Z]''[I]\right] \tag{3.5}$$

In general,

$$[V]^n = \sum_{i=1}^{n} {}_nC_i [Z]^{n-i}[I]^i \tag{3.6}$$

$$\Rightarrow [I]^n = [Z]^{-1}\left[[V]^n - \sum_{i=1}^{n-1} {}_nC_i [Z]^{n-i}[I]^i\right] \tag{3.7}$$

In the above equations, $[V]^{(n)}$ is the vector with each element of [V] differentiated with respect to frequency n times. Similarly $[Z]^{(n)}$ is the matrix generated by differentiating each element of the Z-matrix with respect to frequency n times.

Hence, using a Method of Moments program, we can generate all the information needed to apply the Cauchy Method. Each element in the solution [I] matrix can be treated as our function H(s). Given the function and its derivatives at some frequency points, one can evaluate the function at many more points.

4. The method in filter analysis

The Cauchy method can also be used in analysis of filters over broad frequency ranges. This is particularly useful in generating the stop band response given the pass band response and some stop band information. Also one can produce the pass band response given some stop band information and a little of the pass band response. A filter response is a ratio of two polynomials and hence lends itself easily for application in a Cauchy program.

5. Results

5.1. With the Method of Moments

To test the Cauchy method, the RCS of a sphere was plotted over a wide frequency band. A program to calculate the RCS of an arbitrarily shaped body using triangular patching was used. It was modified to calculate the derivatives of currents as well. This information was used in the Cauchy subroutine. Also the same program was used to calculate the RCS without the Cauchy method. The RCS of a sphere was plotted as a function of $\frac{a}{\lambda}$, where a is the radius of the sphere.

The points chosen for the Method of Moments program were between $\lambda = 0.8\,\text{m}$ and $\lambda = 1.4\,\text{m}$ at intervals of $0.1\,\text{m}$ Using the above method, currents at 300 frequency points in this range were evaluated.

The major saving arising from the Cauchy Method is in execution time. The time taken for the above extrapolation, as compared to the time taken to evaluate the RCS at ten frequency points in the same range is shown below. The program was executed on a VAXstation 3100.

Method of Moments at 10 points:	3 hr 38 min 57.69 sec
Cauchy Method:	1 hr 50 min 06.12 sec.

Of the time taken for the Cauchy program to execute, 1 hr 31 min 45.14 sec was taken by the Method of Moments program to evaluate the current and its four derivatives at three frequency points. The time taken for the evaluation of currents at 300 frequency points was just 18 min 20.98 sec.

Figure A.1 shows the results from the Method of Cauchy and the Method of Moments program. As can be seen from the figure, the approximation is very accurate over this broad frequency range.

5.2. In filter analysis

Another application of the Cauchy method is in filter analysis. A filter transfer function was measured using a network analyzer. A few of these points were chosen as inputs to a Cauchy program. Two different cases were tested. One was the generation of the pass band response using stop band information. The other was the reverse, i.e., the generation of the stop band response using the pass band information. In each case a little of the unknown band response was required. As seen from Figures A.3 and A.4 the interpolation and extrapolation was extremely accurate.

6. Bibliography

[1] R.F. Harrington. *Time Harmonic Electromagnetic Fields.* McGraw-Hill, New York, 1961.

[2] K. Kottapalli, T.K. Sarkar, T. Hua, E. Miller, and G.J. Burke. Accurate computation of wide-band response of electromagnetic systems utilizing narrowband information. *IEEE Trans. on MTT*, 39:682–688, April 1991.

[3] S.M. Rao. *Electromagnetic Scattering and Radiation of Arbitrarily Shaped Surfaces By Triangular Patch Modeling.* PhD thesis, University of Mississippi, School of Engineering.

A. Figures

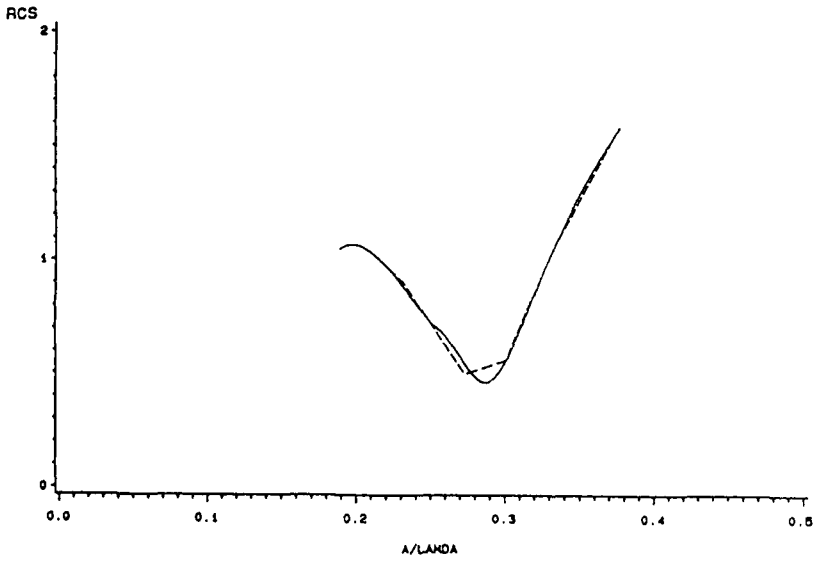

Figure A.1: RCS of a sphere.

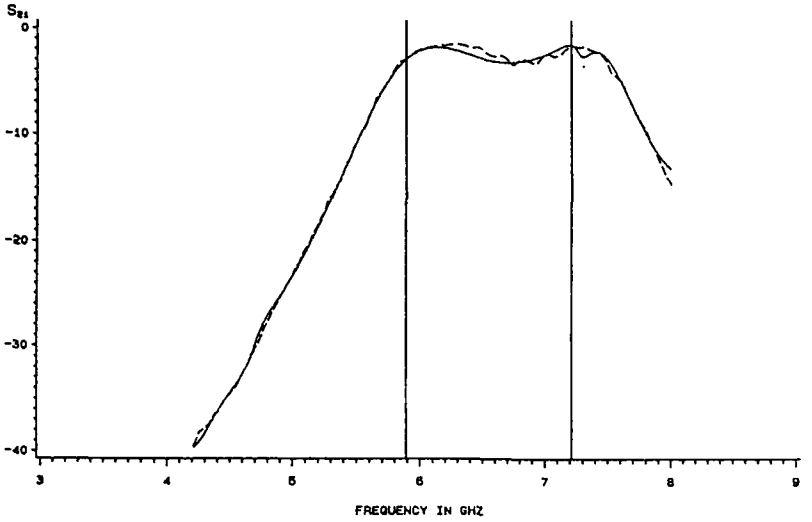

Figure A.2: S_{21} of a microstrip filter. Information up to 5.89 GHZ and from 7.21 GHZ used.

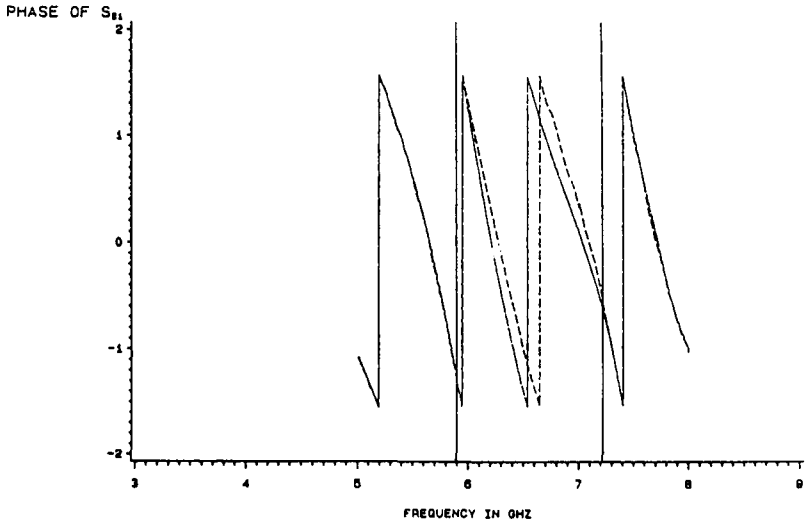

Figure A.3: Phase of S_{21} of a microstrip filter. Information up to 5.89 GHZ and from 7.21 GHZ used.

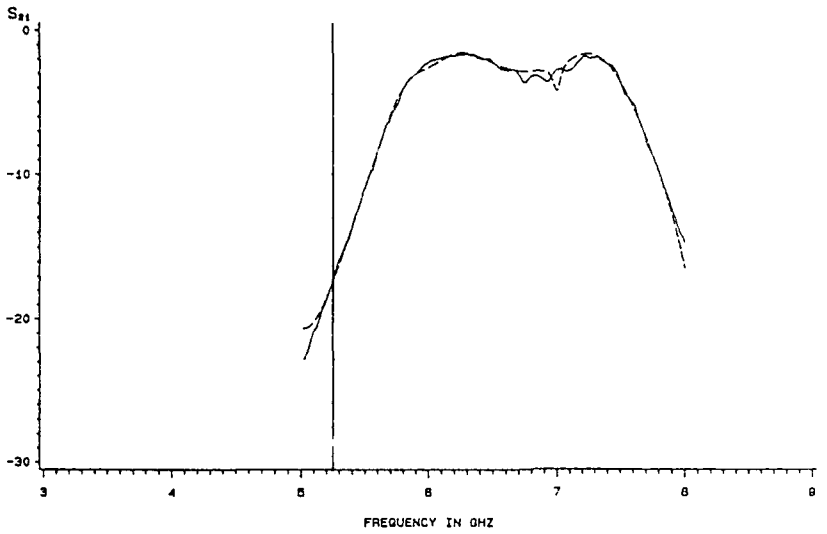

Figure A.4: S_{21} of a microstrip filter. Information up to 5.25 GHZ used.

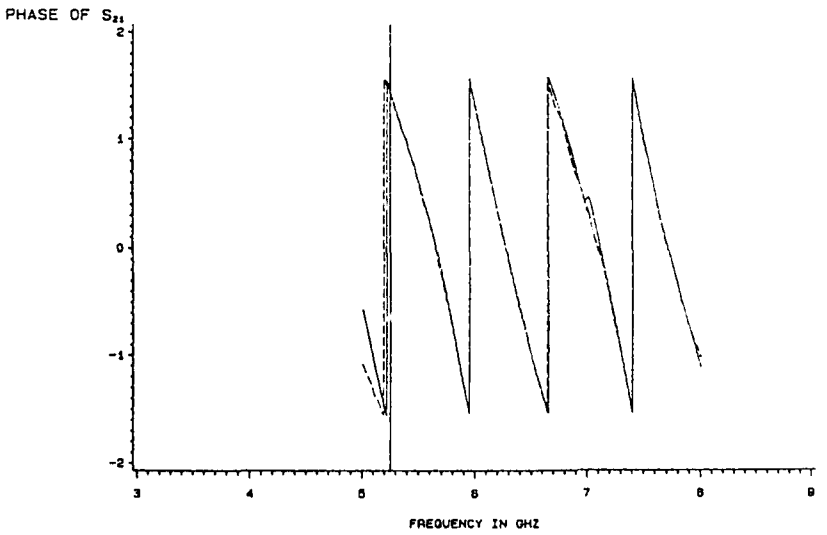

Figure A.5: Phase of S_{21} of a microstrip filter. Information up to 5.25 GHZ used.

Infinite divisibility and the identification of singular waveforms

Alfred S. Carasso
Computing and Applied Mathematics Laboratory
National Institute of Standards and Technology
Gaithersburg, MD 20899 USA
alfred@cam.nist.gov

Abstract Infinitely divisible probability density functions on the half-line $t \geq 0$ form a convolution semigroup on $t \geq 0$, as they describe stochastic processes with stationary, non-negative, independent increments. A subclass $\mathcal{D}$ of such densities are C^∞ functions on the whole t-line when extended by zero for $t < 0$. Such functions may be viewed as physically realizable, causal, C^∞ approximations to the Dirac δ-function, with further positivity properties. The use of such probe waveforms for system identification is particularly advantageous in transient wave propagation problems, where the system's impulse response is typically highly singular. An ill-posed deconvolution problem must be solved to recover the system's response; the semigroup and positivity properties of the input probe enable this deconvolution problem to be implemented as a Cauchy problem for a diffusion equation. This approach allows the analyst to monitor the gradual and systematic development of sharp singularities in the presence of noise. One important context where this theory applies is ultrasonic flaw detection in nondestructive evaluation.

Perturbations of the originally designed pulse shape, due to amplifiers, transducers, and other interfacing devices, may destroy infinite divisibility and lead to waveforms with large negative oscillations. A much wider class of probe waveforms can be constructed, the class $\mathcal{B}$, with $\mathcal{D} \subset \mathcal{B}$, that includes such waveforms. Moreover, if the perturbed pulse lies in $\mathcal{B}$, a simple linear transformation of the noisy output data can be found that reduces the perturbed deconvolution problem to one with a class $\mathcal{D}$ kernel. The search for this transformation is accomplished in the Fourier domain, by comparing the perturbed pulse with the originally designed pulse. The practical significance of this observation lies in enabling the experimentalist to correct for unintended effects of interfacing black boxes and recover a tractable deconvolution problem. The procedure is illustrated with a numerical experiment.

J. S. Byrnes et al. (eds.), Probabilistic and Stochastic Methods in Analysis, with Applications, 273–286.
© 1992 *Kluwer Academic Publishers. Printed in the Netherlands.*

1. Introduction

Determination of the impulse response of a linear time invariant system is an important objective in many areas of system identification. Frequently, the system's complexity together with incomplete knowledge of its physical characteristics preclude an analytical calculation, [4]. In other cases, the impulse response is needed to infer unknown inhomogeneities or other properties of the system. One such example, [5], is the use of impulse responses for flaw size estimation and characterization in ultrasonic nondestructive evaluation of materials. In such contexts, the impulse response may be obtained experimentally by pulsing the system with a physically realizable, smooth approximation to the Dirac δ-function. The present synopsis focuses on analytical considerations underlying the choice of probing pulse and its impact on the subsequent deconvolution problem. A detailed discussion, with further references to applications, is given in [2] and [3].

In one idealized experiment, an impulse of force $\delta(t)$ is applied at a point x on the surface of an infinite elastic plate; the output displacement response at some other point y, not necessarily on the same side of the plate as x, is called the *dynamic Green's function* $g(x,y,t)$. Non-dispersive elastic wave propagation between the source and receiver causes $g(x,y,t)$ to be a highly singular function of t for fixed x,y. Sharp features, including jumps, cusps, spikes, and the like, signal the arrivals of various reflected waves, and characterize the object in the test configuration x,y. However, if a smooth pulse waveform, $p(t)$, is applied at x, the output response at y is given by

$$b(t) = (p * g)(t) = \int_0^t p(t-\tau)g(x,y,\tau)\,d\tau, \qquad t \geq 0. \tag{1.1}$$

Such convolution severely distorts and blurs the sharp features in $g(t)$, and $b(t)$ cannot be used to identify the medium in that important singularities may have been smoothed out. An *ill-posed* deconvolution problem must be carefully solved to reconstruct $g(t)$, given $p(t)$ and the measured noisy output $b_\eta(t)$ in lieu of $b(t)$. Moreover, *a priori smoothness* constraints on $g(t)$ cannot be used to stabilize the inversion in the presence of noise. Weaker constraints, such as an *a priori* bound, M, on the L^2 norm of $g(t)$, together with an estimate, ϵ, for the L^2 norm $\| b - b_\eta \|$, must suffice. The noise to signal ratio $\omega = \epsilon^2/M^2 < 1$, used as an adjustable regularization parameter in (3.4) below, is the only *a priori* constraint in our deconvolution procedure. As a consequence, although the L^2 error in the reconstructed $g(t)$ tends to zero as $\epsilon \downarrow 0$, there is no information on the rate of convergence, [7], and error bounds in terms of the estimated noise level in $b_\eta(t)$, are not possible

2. Infinitely divisible probe pulses

A way of compensating for the lack of an error bound on $g(t)$ lies in performing the deconvolution in *slow motion*. Here, the notion of infinite divisibility plays a key role. We consider smooth pulses $p(t)$ satisfying

$$p(t) \in C^\infty; \quad p(t) = 0, \ t \leqslant 0; \quad p(t) \geqslant 0, \ t > 0; \quad \int_0^\infty p(t)\,dt = 1. \quad (2.1)$$

Such pulses represent one-sided (or causal) probability density functions. Infinite divisibility of $p(t)$ requires the following additional property: for every positive integer m, there exists a one-sided density $q_m(t)$ satisfying (2.1), such that $p(t)$ is the m-fold convolution of $q_m(t)$ with itself, i.e.,

$$p(t) = \{q_m(t)\}^{*m} \quad (2.2)$$

For large m, $q_m(t)$ is a narrow pulse concentrated near $t = 0$, and $q_m(t)$ approaches $\delta(t)$ as $m \uparrow \infty$. The inverse Gaussian pulse $p(\sigma, t)$, $\sigma > 0$, defined by

$$p(\sigma, t) = \frac{\sigma e^{-\sigma^2/4t}}{\sqrt{4\pi t^3}}, \qquad t \geqslant 0, \quad (2.3)$$

is an example of (2.1) for which $q_m(t)$ can be written down explicitly; we have $q_m(t) = p(\sigma/m, t)$. The pulse $s(\sigma, t)$, for $\sigma > 0$, given by

$$s(\sigma, t) = \frac{e^{\sigma - t} e^{-\sigma^2/4t}}{\sqrt{\pi t}}, \qquad t \geqslant 0, \quad (2.4)$$

is also infinitely divisible, has much the same shape as (2.3), but the m^{th} convolution root of $s(\sigma, t)$ is *not* $s(\sigma/m, t)$. Although relatively few C^∞ infinitely divisible densities can be writen down explicitly, a rich variety of such functions exists, as the convolution of any two causal infinitely divisible densities is again causal and infinitely divisible. While (2.3) and (2.4) are unimodal pulses (see Figure A.1), quite complicated multimodal pulses can be created by convolving (2.3) or (2.4) with discrete Poisson densities. All such pulses belong to the class $\mathcal{D}$ defined as follows: A one-sided infinitely divisible density $p(t) \in \mathcal{D}$ if and only if there exist positive constants, A, c, β, with $A \geqslant 1$, and $\beta < 1$, such that

$$\sqrt{2\pi}|\hat{p}(\xi)| \leqslant A e^{-c|\xi|^\beta}. \quad (2.5)$$

Here,

$$\hat{f}(\xi) = \mathcal{F}\{f(t)\} = \frac{1}{\sqrt{2\pi}} \int_{-\infty}^{\infty} f(t) e^{-i\xi t}\,dt, \quad (2.6)$$

denotes the Fourier transform of $f(t)$. Thus, (2.3) and (2.4) respectively satisfy

$$\sqrt{2\pi}|\hat{p}(\sigma,\xi)| = e^{-a|\xi|^{1/2}}, \qquad a = \sigma/\sqrt{2}, \tag{2.7}$$

and

$$e^{-e^{-1}}e^{-(\sigma+e^{-1})|\xi|^{1/2}} \leqslant \sqrt{2\pi}|\hat{s}(\sigma,\xi)| \leqslant e^{\sigma}e^{-a|\xi|^{1/2}}. \tag{2.8}$$

Note that infinite divisibility of $p(t)$ implies that $|\hat{p}(\xi)| > 0$ for all real ξ. See, e.g., [6, p. 557].

3. Deconvolution of class $\mathcal{D}$ probes

We now consider (1.1) when $p(t) \in \mathcal{D}$. If the exact data $b(t)$ were known, solving for $g(t)$ would be equivalent to finding $u(0,t)$ in the following Cauchy problem:

$$\begin{aligned} &\partial u/\partial x = \mathcal{P}u, && x > 0,\ t > 0, \\ &u(x,0) = 0, && x \geqslant 0, \\ &u(1,t) = b(t), && t \geqslant 0, \end{aligned} \tag{3.1}$$

where $\mathcal{P}$ is a linear pseudo-differential operator in the t variable determined by the input probe $p(t)$, and given by

$$(\mathcal{P}u)(x,t) = \mathcal{F}^{-1}\left\{\hat{u}(x,\xi)\log[\sqrt{2\pi}\hat{p}(\xi)]\right\}. \tag{3.2}$$

Indeed, Fourier analysis of (3.1) gives

$$u(x,t) = \mathcal{F}^{-1}\left\{[\sqrt{2\pi}\hat{p}(\xi)]^{x-1}\hat{b}(\xi)\right\}, \qquad 0 \leqslant x \leqslant 1,\ t \geqslant 0, \tag{3.3}$$

which reduces to $g(t)$ at $x = 0$. Infinite divisibility of $p(t)$ ensures that (3.2) is well-defined, while (2.5) gives the Cauchy problem (3.1) a parabolic character. The evolution of $u(x,t)$ as x decreases from $x = 1$ to $x = 0$ is termed *continuous deconvolution*, and represents the progressive undoing of smoothing caused by diffusion.

In the presence of noise, $b_n(t)$ replaces $b(t)$ on the left side of (1.1), and a direct inversion is not feasible in that error amplification overwhelms the reconstruction process. However, Tikhonov regularization of the ill-posed

Cauchy problem (3.1) leads to the following approximation for $u(x,t)$ on $0 \leqslant x \leqslant 1,\ t \geqslant 0$:

$$v(x,t) = \mathcal{F}^{-1}\left\{ \frac{[\sqrt{2\pi}\hat{p}(\xi)]^{x-1}|\hat{p}(\xi)|^2 \hat{b}_n(\xi)}{|\hat{p}(\xi)|^2 + (\omega^2/2\pi)} \right\}. \tag{3.4}$$

Here, $\omega = \epsilon/M \ll 1$ is the L^2 noise to signal ratio. For small fixed $x > 0$, $v(x,t)$ is a smooth approximation to the singular signal $g(t)$ and represents a *partial* deconvolution. One has the following 'log-convex' error bound, which, apart from a factor of 2, is the best possible in the L^2 norm,

$$\| u(x,\cdot) - v(x,\cdot) \| \leqslant 2M^{1-x}\epsilon^x, \qquad 0 \leqslant x \leqslant 1. \tag{3.5}$$

The parabolic nature of (3.1) can be exploited, [2], to obtain L^∞ error bounds for the partial deconvolution and its time derivatives at any fixed $x > 0$, in terms of ϵ, M, A, c, and β. All of these estimates degenerate at $x = 0$. However, for small ϵ, one can validate the sharp singularities in the total deconvolution $v(0,t)$, by observing their early genesis at some $x > 0$ and following their systematic development as $x \downarrow 0$.

An effective computational algorithm for obtaining the evolution of $v(x,t)$ as $x \downarrow 0$ has been developed [2]. The algorithm is based on the Poisson summation formula and is implemented in Laplace transform space using FFT routines. Input to the algorithm consists of time-domain data; namely, the recorded histories of the actual probe $p(t)$ and of the response $b_n(t)$, digitized at 2N equispaced points on the finite interval $[0, 2T]$, with N and T sufficiently large. The 'optimal' value of the regularization parameter ω is best found interactively, starting from a plausible first guess for the ratio ϵ/M.

4. Perturbations and the class $\mathcal{B}$

An explicitly known class $\mathcal{D}$ pulse such as (2.3) or (2.4) can be synthesized as an electrical voltage using a computer-driven digital to analog (D/A) converter. (It is advantageous to use the lowest value of σ compatible with the instrumentation bandwidth). To produce a dynamic force pulse having a prescribed time dependence, a high fidelity transducer is necessary. However, the electrical signal must first be amplified to a level sufficient to drive the transducer. The cumulative effects of the amplifier and transducer may result in an actual mechanical pulse $q(t)$ markedly different from the ideal, narrow, unimodal shape, [1]. We will show how to get around this difficulty in a large number of cases.

It is an interesting fact that there exist transformations of such prototypical class $\mathcal{D}$ pulses as (2.3) and (2.4) that may drastically change the time-domain character of these waveforms, while preserving the non-vanishing

property of their Fourier transforms. In particular, the distorted waveforms may develop large negative oscillations and cease to be probability densities altogether, let alone infinitely divisible ones. Convolution of $\mathcal{D}$ with the one-sided functions $h(t)$ described below, represents *only one* such class of transformations. Other transformations, linear or nonlinear, may produce similar results.

Consider any analytic function of the complex variable z of the form

$$\Lambda(z) = \sum_{n=0}^{\infty} a_n z^n, \qquad a_n \text{ real}, \; a_0 \neq 0, \tag{4.1}$$

such that for some $R > 0$,

$$0 < b_0 \leqslant |\Lambda(z)| \leqslant b_1 < \infty, \qquad |z| \leqslant R. \tag{4.2}$$

Let $f(t)$ be any real one-sided function (including linear combinations of Dirac δ-functions) such that $\sqrt{2\pi}|\hat{f}(\xi)| \leqslant R$, and let

$$h(t) = \sum_{n=0}^{\infty} a_n \{f(t)\}^{*n}, \qquad \left(\{f(t)\}^{*0} \equiv \delta(t)\right). \tag{4.3}$$

Then $h(t)$ *is a one-sided function, and*

$$0 < b_0 \leqslant \sqrt{2\pi}|\hat{h}(\xi)| \leqslant b_1 < \infty. \tag{4.4}$$

One may also rescale the time variable and form

$$h_1(t) = \sum_{n=0}^{\infty} a_n \{\theta f(\theta t - \psi)\}^{*n}, \qquad \theta > 0, \; \psi \geqslant 0, \tag{4.5}$$

while still retaining (4.4). The interesting case occurs when $f(t)$ includes a finite sum $\sum c_k \delta(t - \tau_k)$, with τ_k positive and c_k real.

With arbitrariness in both $\Lambda(z)$ and $f(t)$, a bewildering variety of pulse shapes can be created by iterated convolutions of $p(t) \in \mathcal{D}$ with such $h(t)$'s. The resulting waveform is always causal and C^∞ on the whole line. As a simple example, consider

$$\begin{aligned} \Lambda(z) &= e^{\lambda(z-1)}, \qquad \lambda \text{ real}, \\ f(t) &= \delta(t-1), \\ h_\lambda(t) &= e^{-\lambda} \sum_{n=0}^{\infty} \frac{\lambda^n}{n!} \delta(t-n), \end{aligned} \tag{4.6}$$

so that

$$\sqrt{2\pi}\,\hat{h}_\lambda(\xi) = e^{-\lambda} e^{\lambda e^{-i\xi}}. \tag{4.7}$$

Let

$$a = \sqrt{2}, \quad b = \sqrt{10}, \quad \lambda = -0.5, \quad \mu = -1.5, \tag{4.8}$$

and let $s(0.5, t)$ be the unimodal pulse (2.4) with $\sigma = 0.5$, shown in Figure A.1. Form successively,

$$q_1(t) = as(0.5, at), \qquad q_2(t) = (q_1 * h_\lambda)(t)$$

$$q_3 \quad = bq_2(bt), \qquad q_4 = (q_3 * h_\mu)(t). \tag{4.9}$$

Then, $q_4(t)$ is the pulse shown in Figure A.2.

Let $\gamma = (4a^2b^2)^{1/4}$, $\alpha = 2|\lambda + \mu|$. Using (4.8) and (4.7), we have

$$e^{-e^{-1}} e^{-\{(\sigma + e^{-1}/\gamma)|2\xi|\}^{1/2}} \leqslant \sqrt{2\pi}|\hat{q}_4(\xi)| \leqslant e^{\sigma+\alpha} e^{-(\sigma/\gamma)|\xi|^{1/2}}. \tag{4.10}$$

Next, let $p(\nu, t)$ be the inverse Gaussian pulse (2.3). We observe from (2.7) and (4.10) that if $\nu > (2\sigma + 2e^{-1}/\gamma \approx 0.58$, then

$$\frac{|\hat{p}(\nu, \xi)|}{|\hat{q}_4(\xi)|} \leqslant e^{e^{-1}}. \tag{4.11}$$

Choosing $\nu = 0.6$, we see from (4.11) that the complicated non-positive pulse in Figure A.2 is bounded below in Fourier space by the narrow inverse Gaussian shown in Figure A.1. This relationship is shown graphically in Figure A.3 where $|\hat{q}_4(\xi)|^{-1}$ (solid curve), and $2.5|\hat{p}(0.6, \xi)|^{-1}$ (dashed curve), are plotted as functions of discrete frequency $\xi_k = k\pi/10.24$, $k = 1, \ldots, 650$, using FFT routines. These considerations serve to motivate the following definition.

Definition 4.1. A function $q(t)$ is in class $\mathcal{B}$ if and only if $q(t)$ is causal and C^∞ on the whole line, with $|\hat{q}(\xi)| > 0$ for all real ξ and there exist an infinitely divisible density $p(t) \in \mathcal{D}$ and a positive constant $K = K(q, p)$, such that

$$\frac{|\hat{p}(\xi)|}{|\hat{q}(\xi)|} \leqslant K, \qquad \xi \text{ real}. \tag{4.12}$$

$\mathcal{B}$ *includes* all functions of the form $q(t) = (p * h)(t)$ with $p(t) \in \mathcal{D}$ and $h(t)$ of the form (4.3), and we have $|\hat{p}(\xi)|/|\hat{q}(\xi)| \leqslant 1/b_0$. In particular, choosing $h(t) = \delta(t)$, it follows that $\mathcal{D} \subset \mathcal{B}$. Other transformations of $p(t) \in \mathcal{D}$, possibly nonlinear, may also produce objects $q(t) \in \mathcal{B}$.

5. Deconvolution of class $\mathcal{B}$ probes

We view membership in $\mathcal{B}$ as resulting from perturbations of the originally intended class $\mathcal{D}$ probe, caused by interfacing devices. Assuming the actual mechanical pulse $q(t) \in \mathcal{B}$, we use Fourier analysis to find $p(t) \in \mathcal{D}$ such that (4.12) is satisfied. As in Figure A.3, this may be accomplished by plotting $|\hat{q}(\xi)|^{-1}$ and adjusting the width parameter of the candidate pulse $p(t)$ so that with a reasonable constant K, the curve $K|\hat{p}(\xi)|^{-1}$ lies above the q curve. We then let $\hat{d}(\xi) = \hat{p}(\xi)/\hat{q}(\xi)$, and refer to $p(t)$ as the *exchange* pulse.

Suppose

$$(q * g)(t) = e(t), \qquad t \geq 0, \tag{5.1}$$

where $e(t)$ is the output response that would have been recorded in the absence of noise. Let $e_n(t)$ be the noisy output data. As before, we assume

$$\| g \| \leq M, \qquad \| e - e_n \| \leq \eta, \tag{5.2}$$

where $\eta \ll M$. Let

$$b(\xi) = \hat{d}(\xi)\hat{e}(\xi), \qquad b_n(\xi) = \hat{d}(\xi)\hat{e}_n(\xi). \tag{5.3}$$

From (5.2), (4.12),

$$\| b - b_n \| \leq \epsilon, \qquad \epsilon = K\eta. \tag{5.4}$$

Fourier transforming (5.1) and using (5.3), we see that $(p * g)(t) = b(t)$, while $b_n(t)$ is the noisy output data corresponding to the exchange pulse $p(t) \in \mathcal{D}$. Thus, if $q(t) \in \mathcal{B}$, multiplication of the output $\hat{e}_n(\xi)$ by the bounded function $\hat{d}(\xi)$, reduces the deconvolution problem to the class $\mathcal{D}$ case, with bounded noise magnification, $\epsilon = K\eta$. With $\omega = \epsilon/M$, we may now construct the family of partial deconvolutions $v(x,t)$ in (3.4) for which the error bound (3.5) holds.

6. A numerical experiment

We now illustrate the foregoing development with a numerical reconstruction experiment using synthetic noisy data. Figure A.4 represents the theoretically calculated impulse response $g(t)$ of a homogeneous infinite elastic plate, where the source and receivers are on opposite sides of the plate, with the receiver located at the epicenter [8]. The sharp spikes are numerical δ-functions, with support equal to one mesh interval Δt, and with height $a/\Delta t$, the weights a being determined by the physics. The spikes, and other singularities, indicate the arrivals of elastic disturbances and their subsequent

multiple reflections from the plate faces. The drawing displays normalized displacement versus normalized time where

$$\text{Normalized displacement} = \pi \times \text{shear modulus} \times \text{plate thickness} \times \text{actual displacement/force},$$

$$\text{Normalized time} = \text{actual time} \times \text{shear wave speed/plate thickness}$$

The presence of flaws would generate additional reflections, resulting in a signature different from that shown in Figure A.4.

The pulse $q_4(t)$ shown in Figure A.2, with t measured in normalized time units, was used to simulate a distorted mechanical pulse applied at the plate surface. While such distortion is substantially worse than is typically the case in experimental work, the robustness of the deconvolution procedure is best demonstrated by considering extreme cases. The corresponding epicentral response $e(t) = (q_4 * g)(t)$, evaluated by numerical quadratures, is shown in Figure A.5. Each of $g(t)$, $q_4(t)$, and $e(t)$, were calculated at 500 equispaced points on the normalized time interval $[0, 5]$. Evidently, there is little correlation between Figures A.4 and A.5.

Next, noisy data $e_n(t)$ were constructed by adding to each data value y in $e(t)$, a random number drawn from a uniform distribution in the range $\pm 0.005y$. A noise level of between 0.1% and 1% is believed to be representative of experimental conditions. The inverse Gaussian shown in Figure A.1 was used as the exchange pulse, with corresponding data $b_n(t)$ obtained from (5.3). With $\omega = 1.0 \cdot 10^{-5}$, the family $v(x, t)$ was evaluated using (3.4) at 16 equispaced values of x on the interval $0 \leq x \leq 1$. The evolution is shown in Figure A.6. In that drawing, the first trace, in the foreground, is $b_n(t)$; the last trace, in the background, is the reconstructed $g(t)$. Although there is no visual hint of spikes in the foreground trace $b_n(t)$, early genesis of these singularities and their subsequent systematic development as $x \downarrow 0$, are noteworthy features in Figure A.6. There is also an easily assimilated visual relationship between successive traces, which facilitates pattern recognition. These effects are a reflection of the diffusion process associated with the exchange pulse $p(t)$.

We remark that it is possible to apply the deconvolution algorithm directly to $(q_4 * g)(t) = e(t)$, foregoing the exchange option, by substituting q_4 and e_n for p and b_n in (3.4). In that case, the underlying Cauchy problem (3.1) is not of parabolic type. The resulting evolution is shown in Figure A.7. While the last trace in that drawing is a good approximation to $g(t)$, the development of singularities is not easily discernible, as the non-positivity properties of $q_4(t)$ result in a tortuous evolution of the data $e_n(t)$ into $g(t)$. In the presence of flaws, where additional reflections can be expected to produce fairly complex signatures, pattern recognition may not be feasible.

7. Bibliography

[1] F.R. Breckenridge, T.M. Proctor, N.N. Hsu, S.E. Fick, and D. G. Eitzen. Transient sources for acoustic emission work. In K. Yamaguchi, H. Takahashi, and H. Niitsuma, editors, *Progress in Acoustic Emission V; Proceedings of the 10th International Acoustic Emission Symposium*. The Japanese Society for NDI, October 1990.

[2] A.S. Carasso. Infinitely divisible pulses, continuous deconvolution, and the characterization of linear time invariant systems. *SIAM J. of Applied Math.*, 47:892–927, 1987.

[3] A.S. Carasso. Impulse response acquisition as an inverse heat conduction problem. *SIAM J. of Applied Math.*, 50:74–90, 1990.

[4] A.S. Carasso. Probe waveforms and the reconstruction of structural dynamic Green's functions. *AIAA Journal*, 29:114–118, 1991.

[5] C.H. Chen. High resolution spectral analysis nde techniques for flaw characterization, prediction, and discrimination. In C.H. Chen, editor, *Signal Processing and Pattern Recognition in Nondestructive Evaluation of Materials*, volume F44 of *NATO ASI*, pages 155–173, New York, 1988. Springer-Verlag.

[6] W. Feller. *An Introduction to Probability Theory and its Applications*, volume 2. John Wiley & Sons, New York, second edition, 1971.

[7] J.N. Franklin. On Tikhonov's method for ill-posed problems. *Math. Comp.*, 28:889–907, 1974.

[8] N.N. Hsu. Dynamic Green's functions of an infinite plate; a computer program. Technical Report NISTIR 85-3234, U.S. Department of Commerce, National Institute of Standards and Technology, Gaithersburg, MD 20899, 1985.

A. Figures

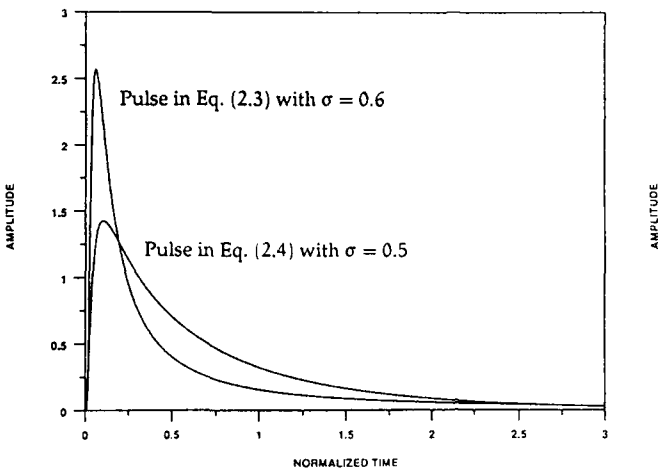

Figure A.1: Examples of unimodal pulses in class $\mathcal{D}$.

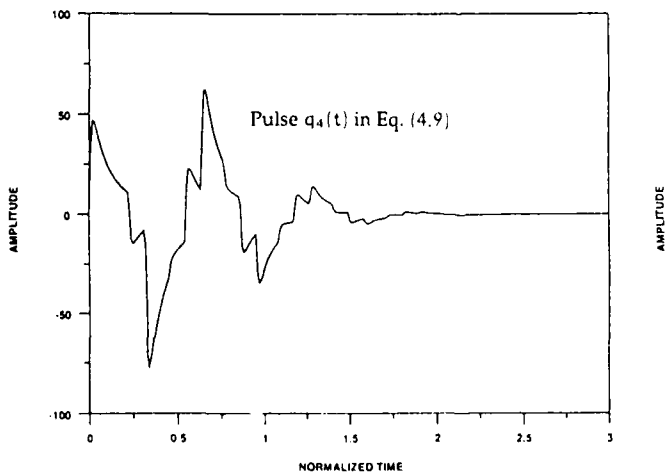

Figure A.2: Example of probing pulse in class $\mathcal{B}$.

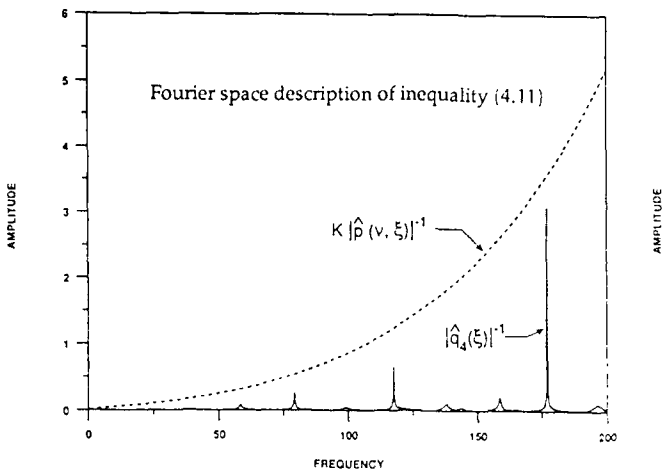

Figure A.3: Graphical idea behind Definition 4.1.

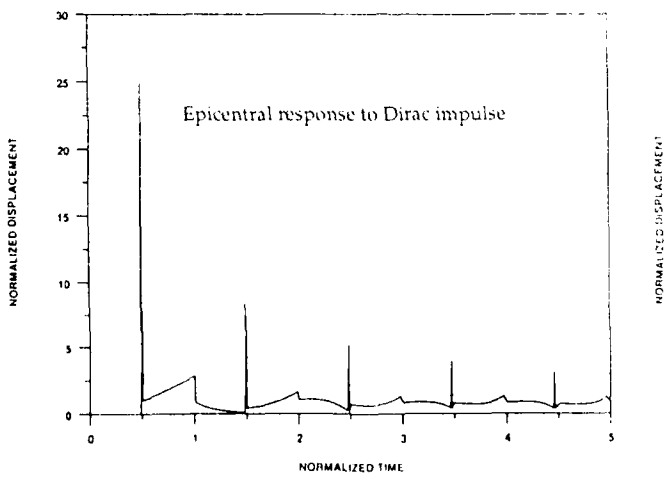

Figure A.4: Response of homogenous elastic plate to Dirac δ-function source, when source and receiver are on opposite sides of plate, with receiver located at epicenter.

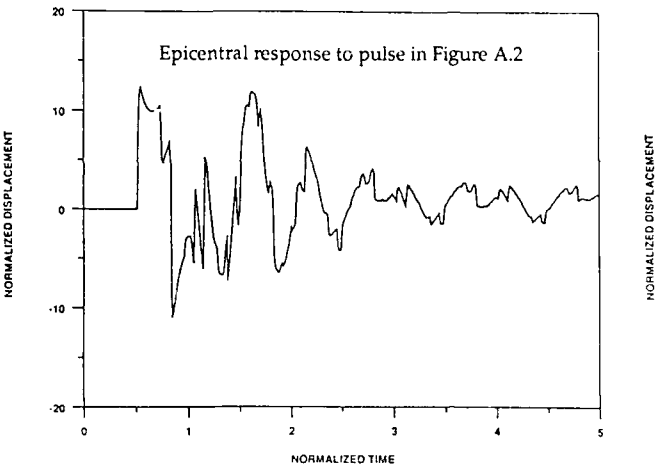

Figure A.5: Response to probe pulse of Figure A.2 with test configuration as in Figure A.4.

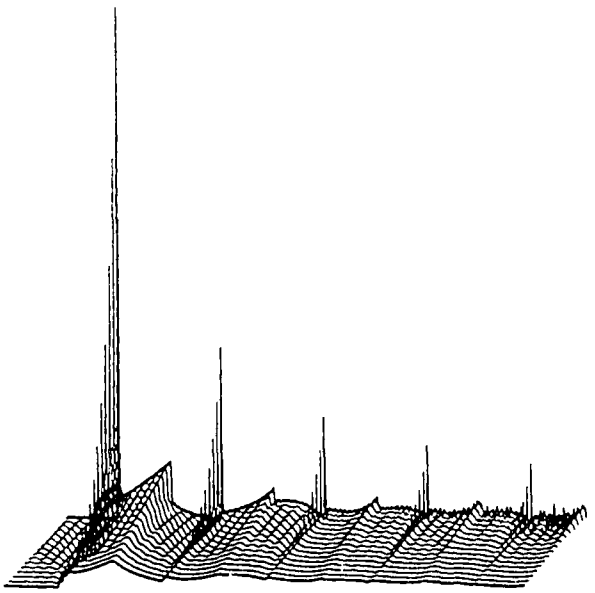

Figure A.6: Continuous deconvolution of response in Figure A.5 after using exchange option.

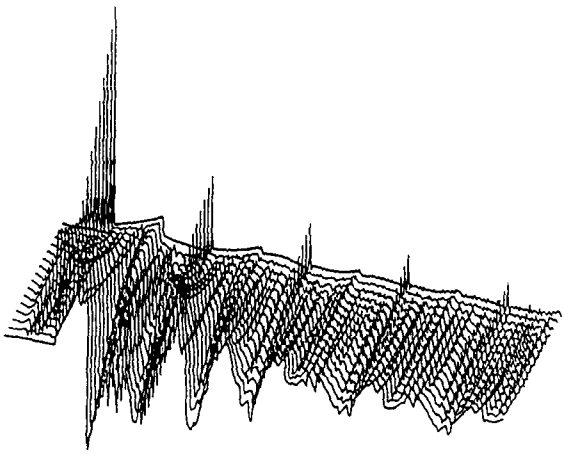

Figure A.7: Continuous deconvolution of response in Figure A.5 without use of exchange option.

Certain results on spatiotemporal random fields and their applications in environmental research†

George Christakos
University of North Carolina
CB#7400, 131 Rosenau Hall
Chapel Hill, NC 27599 USA
uncgch@unc.bitnet

Abstract This work is about spatiotemporal random fields and their applications in environmental research. Ordinary and generalized random fields are studied, and certain important classes of space nonhomogeneous/time nonstationary random fields are derived. Results are obtained regarding the optimal estimation and simulation of such fields in space and time.

1. Introduction

This presentation studies spatiotemporal natural processes, that is, processes which develop simultaneously in space and in time. In Section 2 we discuss the emergence of spatiotemporal natural processes in various branches of physical sciences and address the fundamental hypotheses and problems regarding the quantitative description of such processes. Several practical issues of spatiotemporal data analysis and processing are presented and the variety of potential applications is reviewed. The latter is followed by a critical discussion of the inadequacies of previous works on the subject.

In order to proceed with the rigorous mathematical modelling of natural processes which change in space and time, one must elaborate on a theory of spatiotemporal random field (S/TRF). This theory is presented in Sections 3 through 6. The preceding mathematical results act then as the theoretical support for the discrete parameter representations, as well as the optimal space-time estimation and simulation methods which are discussed in a more practical context in Sections 7, 8 and 9.

† The research was supported in parts by the R.J. Reynolds Fund, University of North Carolina at Chapel Hill.

J. S. Byrnes et al. (eds.), Probabilistic and Stochastic Methods in Analysis, with Applications, 287–322.
© 1992 *Kluwer Academic Publishers. Printed in the Netherlands.*

2. Spatiotemporal natural processes

Spatiotemporal processes, that is, processes which develop simultaneously in space and time, occur in nearly all the areas of applied sciences, such as: hydrogeology (e.g., water vapor concentrations, soil moisture content); environmental engineering (e.g., concentrations of pollutants in environmental media—water/air/soil/biota); climate predictions and meteorology (e.g., variations of atmospheric temperature, density, and velocity); and oil reservoir engineering (e.g., porosities, permeabilities and fluid saturations during the production phase).

In this context, important issues include: the assessment of the spatiotemporal variability of the earth's surface temperature and the prediction of extreme conditions; the assessment of space-time trends in runoff on the basis of a spatially and temporally sparse data base; the estimation of the soil moisture content at unmeasured locations in space and instants in time; the reconstruction of the whole field of a climate parameter using all the space-time data efficiently; the study of the transport of pollutants through porous media; the elucidation of the spatiotemporal distribution of rainfall for satellite remote-sensing studies; the optimal sampling design of meteorological observations; and the simulation of oil reservoir characteristics as a function of the spatial position and the production time.

The issues above are parts of the general problem of *analysis and processing of data from space-time physical phenomena*. In all these situations, the spatiotemporal pattern of change of the natural processes involved possesses a certain structure at the macroscopic level and a purely random character at the microscopic level. The latter implies a significant amount of uncertainty in spatiotemporal variation. Moreover, this variation is, in general, space nonhomogeneous and time nonstationary (there may exist complex trends in space, time varying correlation structures, significant space-time cross-effects, etc.). Spatiotemporal variability plays an extremely substantial role in the understanding, modelling and prediction of surficial processes in space-time. It is, also, very important in improving our basic knowledge regarding the climatological influences on the hydrogeology of a region. If neglected, spatiotemporal-parameter variability of water management models may adversely influence management decisions.

Typically, space-time data analysis and processing problems have been handled under some convenient but rather simplistic assumptions. In *hydrogeology and water resources research*, common statistical methods of analysis create artificial decompositions of hydrologic processes—one in space and one in time—and study them separately [25, 10]; or focus on time averages (monthly, seasonal, annual) of the hydrologic parameters; or make additional assumptions, like space homogeneity and weak time dependency (e.g., [4]). The multivariate analysis concept which has been used in a num-

ber of hydrologic problems (e.g., [11]) accounts for the vector formulation of the scalar time series model, where the component time series are correlated to each other. Variability in space is not taken into consideration and the modelling of the combined evolution of theses series in space and in time is clearly not an issue addressed by multivariate analysis. Similar decompositions has been applied on some recent studies on the assessment of Ireland's wind power resource (e.g., [17]). Moreover, classical statistics and time-series methods have failed to provide a conceptual framework determining the correlation structure of the spatiotemporal heterogeneity of soil-water properties from local to global scales.

In *environmental research* the existing models (e.g., [2, 15]) either apply traditional methods of classical statistics which are incapable of capturing important features of the space-time structure, or have been designed to handle problems that are significantly different in nature than those arising in the spatiotemporal data analysis and processing context considered above. In particular, the class of classical statistics models does not determine any law of change of the environmental parameters, and the relative distances of the sample locations/instances over space-time do not enter the analysis of the correlation structure. The second class of environmental models available concern, either specific space-time interaction systems where the input/output physical parameters are treated at each spatial location as separate time series, or the description of the system's transfer function by means of some special space-time patterns. These models do not provide an adequate quantitative assessment of spatiotemporal variability in general, and they do not account for the space nonhomogeneous and/or time nonstationary characteristics of the environmental parameters in particular. In some recent environmental studies the spatio-chronological order of the data is not properly considered, and arbitrary but not well justified decompositions of the correlation functions are assumed. Moreover, optimal reconstruction schemes, which are general enough to cover the majority of applications have not been developed; see, e.g., comments made in [28]; also by Bilonick [3]; and by Rouhani and Hall [26] in a geostatistical framework. Space-time models which are based on the distributed parameter concept [30] are not in general appropriate for most environmental problems. These models are assumed to be governed by a differential equation of a particular form that does not represent adequately the majority of the spatiotemporal natural processes of interest; issues of stability, controlability and observability involve serious difficulties.

In *reservoir characterization*, space-time data processing does not exist at present. Most of the techniques available exclusively account for the spatial variation of geological reservoir processes, when in reality these processes are simultaneously a function of spatial location and production time (e.g., [20]). Also, current practices in data collection—with the exception of some

oil sand deposits—do not account for time. The reasons that space-time models do not exist at present in reservoir characterization is due to the fact that the need for detailed and advanced reservoir characterization has been recognized only recently.

The methods used for *statistical climate modelling and prediction* are usually somewhat primitive versions of the methods used for *weather analysis and prediction* (e.g., [12, 21, 31]). Many of them suffer the same limitations with the methods used in hydrology. For example, the basic ansatz of multivariate techniques such as "principal oscillation pattern" and "principal interaction pattern" [31] is based on the arbitrary assumption that the space-time characteristics of a low-order system are the same as those of the full system. Also, important issues such as the characterization of spatiotemporal intermittency or spottiness in rainfall as it pertains to various notions of scaling as well as the physically observed features of clustering, growth, and decay of convective cells, and larger-scale spatiotemporal forms observed in mesoscale rainfall systems cannot be addressed by the existing statistical methods (see, e.g., [9]).

In *global warming research*, aspects of current interest are as follows:

1) Many eminent authors claim that while one certainly cannot assert that no warming occured, the existing statistical analysis of earth's surface temperature data is unable of providing adequate assessments regarding temperature's space-time variability and it does not lead to convincing arguments supporting the concept that changes at the macroscopic level are due to greenhouse warming rather than to space-time natural variability (e.g., [21]).
2) In water resources management the existence of a warming trend raises the question whether the global warming has been sufficient as to translate into a corresponding change in the spatiotemporal structure of runoff series. Again, current statistical analyses of runoff series are subject to serious question given that they are based on observations relating to a spatially and temporally sparse data base and they assume no model about the underlying spatiotemporal evolution of the runoff series.

Clearly, the temperature data in Item 1) and the rainfall series studies in Item 2) above are typical examples of analyses where the theoretical models used are incapable to provide adequate representations of the spatiotemporal variability and, hence, they cannot give satisfactory answers to crucial questions concerning climate and water resources problems.

The main reasons for such—clearly inadequate from various viewpoints—analyses of spatiotemporal data should be attributed to the following facts: (i) the importance of spatiotemporal variability in the study of space-time phenomena was not fully appreciated until recently; and (ii) most

of the theoretical tools and mathematical techniques of data processing available have been designed to operate exclusively in time (time series methods; e.g., [16]) or exclusively in space (random fields, geostatistics; e.g., [22, 32, 33]). Undoubtedly, the literature on the subject of applied space-time data analysis and processing is very limited and most aspects of importance in the analysis, modelling and estimation of spatiotemporal parameters have not been studied adequately.

In view of the foregoing, the following conclusions are drawn:

1) Any modelling assumption should reflect adequately the macroscopic and microscopic evolution characteristics of the underlying processes over space and time. The latter is a requisite for the understanding and prediction of spatiotemporal processes in hydrogeology, climate modelling and environmental pollution monitoring and control.
2) Due to the random character in the variability of the data at the microscopic level, these processes must naturally be described stochastically; the concept of randomness should be viewed as an intrinsic part of the space-time evolution, and not only as a statistical description of possible states.
3) The proper model should be capable of assessing quantitatively any space nonhomogeneous/time nonstationary variability features and to provide efficient solutions to practical problems, such as space-time estimation.

Taking these issues into account, it seems quite reasonable that the concept of an S/TRF is the appropriate stochastic model for spatiotemporal processes. Within the framework of the S/TRF model, space and time form a combined process having simultaneous and interrelated effects on the evolution of the natural variable it represents. Suitable methodological hypotheses and operational tools assure that the mathematical concept of S/TRF is compatible with the physics of the variate it describes and, thus, it is applicable in practice. Lastly, conclusions regarding the spatiotemporal variability (trends in space, periodicities in time, nonhomogeneous/nonstationary correlations, etc.) can be established in terms of duality principles that relate the mathematical notions and the physical behavior of the process they model. Here, stochastic spatiotemporal correlation functions provide the means for structural inferences.

In general, the objectives of spatiotemporal data analysis and processing are: (a) to assess quantitatively the spatiotemporal variability of the natural processes of interest (degree of regularity, continuity, non- homogeneous spatial features, nonstationary characteristics, etc.); and (b) to provide efficient and computationally attractive procedures for deriving optimal (in a well defined mathematical sense) and physically meaningful estimation

maps of the natural process, at unknown points in space and/or instants in time, based on fragmentary space-time data.

Of course, the outcomes of space-time data analysis and processing may be not an end in themselves. Several important consequences will emerge in the context of earth sciences. More specifically:

1) A deeper understanding of the physics of the space-time processes will be obtained. For instance, knowledge about the spatiotemporal variability of the various climate parameters will improve our basic understanding of how the global climate actually functions.
2) The predictive capabilities of many computer-based differential equation models in hydrology and environmental research, are limited because the parameters of the models are difficult to determine. Much of this difficulty may stem: (a) from the spatiotemporal variability of the media, and (b) from identifiable differences in initial physical assumptions. It is, hence, of significant importance to understand how (a) and (b) influence the outcomes of modelling.
3) Space-time data analysis and processing will provide the necessary means for solving important problems in various areas of water resources. Information about the spatiotemporal-parameter variability of a water resource system will allow the detailed simulation of the system and will influence considerably management decisions. The assessment of the spatiotemporal variability of pollutant concentrations will provide the knowledge needed to monitor and control environmental pollution. S/TRF simulations of the anticipated effects on surface temperature due to the increase of carbon dioxide in the atmosphere over a specific time period will provide valuable insight into the study of global warming issues. In connection to this, the possible effects of the coupled increase of precipitation and temperature on the hydrology of a particular region can be determined; then, conclusions could be derived about the incorporation of climatic changes into the planning of future earth systems, and the modification of the operating rules of existing water resource systems.

A S/TRF is termed *continuous parameter* or *discrete parameter* according to whether its space-time arguments of an S/TRF take continuous or discrete sets of values.

3. Ordinary spatiotemporal random fields

3.1. The basic space-time notions

Let $\underline{s} = (s_1, s_2, \ldots, s_n) \in \mathfrak{R}^n$ ($\mathfrak{R}^n$ is the Euclidean space of dimensionality $n \geq 1$) with $|\underline{s}| = \sqrt{\sum_{i=1}^{n} \underline{s}_i^2}$, and $t \in T$ ($T \subseteq \mathfrak{R}^1_{t,0} = \{t \in \mathfrak{R}^1 : t \geq 0\}$).

In the Cartesian product $\mathfrak{R}^n \times T$ let $(\underline{s}, t \in \mathfrak{R}^n \times T)$ denote space-time coordinates, such that $|(\underline{s}, t)|^2 = |\underline{s}|^2 + t^2$. We also define $(\underline{s}, t)^{\underline{\alpha}, \beta} = \underline{s}^{\underline{\alpha}} t^{\beta} = s_1^{\alpha_1} s_2^{\alpha_2} \ldots s_n^{\alpha_n} t^{\beta}$, where β is a nonnegative integer and $\underline{\alpha} = (\alpha_1, \alpha_2, \ldots, \alpha_n)$ is a multi-index of nonnegative integers such that $|\underline{\alpha}| = \sum_i^n {}_1 \alpha_i$ and $\underline{\alpha}! = \alpha_1! \alpha_2! \ldots \alpha_n!$.

We define some spaces of spatiotemporal functions $X(\underline{s}, t)$ in $\mathfrak{R}^n \times T$, which are useful within the framework of the present study: The space **C** of all real and continuous space-time functions with compact support (i.e., they vanish outside some bounded region). The space **K** of all real, continuous and infinitely differentiable functions in space and time with compact support. The space **S** of all real, continuous and infinitely differentiable functions which, together with their derivatives of all orders, approach zero more rapidly than any power of $1/|(\underline{s}, t)|$ as $|(\underline{s}, t)| \to \infty$. Notice that $\mathbf{S} \supset \mathbf{K}$, as all functions in **K** vanish identically outside a finite support, whereas those in **S** merely decrease rapidly at infinity. Spaces **K** and **S** are of particular importance in this study. The topology in **K** and **S** is in the sense of [27] where, in view of the aforementioned space-time considerations, the argument is now $(\underline{s}, t) \in \mathfrak{R}^n \times T$.

3.2. *Definition of ordinary spatiotemporal random fields*

Let (Ω, F, P) be a probability space, where Ω is the sample space, F is the σ-field of subsets of Ω and P is the probability measure on the measurable space (Ω, F) satisfying Kolmogorov's axioms; let $\underline{z} = (\underline{s}, t)$. We denote by $\mathcal{H}_x = L_2(\Omega, F, P)$ the Hilbert space of all continuous-parameter random variables $x_1, \ldots, x_m$ defined at $\underline{z}_1, \ldots, \underline{z}_m$ and endowed with the scalar product

$$(x_1, x_2) = E[x_1 x_2] = \iint \chi_1 \chi_2 \, dF_x(\chi_1, \chi_2) \tag{3.1}$$

where $F_x(\chi_1, \chi_2)$ denotes the joint probability distribution of the random variables x_1 and x_2, while

$$\|x\|^2 = E|x|^2 = \int \chi^2 \, dF_x(\chi) < \infty, \tag{3.2}$$

where $F_x(\chi)$ denotes the probability distribution of x. Usually $F_x(\chi)$ and $F_x(\chi_1, \chi_2)$ are assumed to be differentiable so that they can be replaced by the probability densities $f_x(\chi)$ and $f_x(\chi_1, \chi_2)$.

Definition 3.1. The ordinary S/TRF (OS/TRF) $X(\underline{s}, t)$ is defined as the function on the Cartesian product $\mathfrak{R}^n \times T$ with values in the Hilbert space $L_2(\Omega, P, F)$, viz.

$$X : \mathfrak{R}^n \times T \to L_2(\Omega, F, P) \tag{3.3}$$

Just as for purely spatial RF (SRF), a S/TRF $X(\underline{z}) = X(\underline{s}, t)$ is specified completely by means of all finite dimensional probability measures $\mu_x(B)$ associated with the families of random variables $x_1, \ldots, x_m$ at $\underline{z}_1, \ldots, \underline{z}_m$:

$$\mu_x(B) = \mu_{\underline{z}_1, \ldots, \underline{z}_m}(B) = P[(x_1, \ldots, x_m) \in B] \qquad \text{for every } B \in \mathfrak{I}^m$$

($\mathfrak{I}^m$ is a suitably chosen σ-field of subsets of $\mathfrak{R}^n$) and all $m = 1, 2, \ldots$ The corresponding probability density functions are written as

$$f_x(\chi_1, \ldots, \chi_m)\, d\chi_1 \ldots d\chi_m = f_{\underline{z}_1, \ldots, \underline{z}_m}(\chi_1, \ldots, \chi_m)\, d\chi_1 \ldots d\chi_m$$
$$P[\chi_1 \leqslant x(\underline{z}_1) \leqslant \chi_1 + d\chi_1, \ldots, \chi_m \leqslant x(\underline{z}_m) \leqslant \chi_m + d\chi_m]. \qquad (3.4)$$

for all m. All OS/TRF to be considered will be *continuous* in the mean square sense, i.e., $E|X(\underline{s}', t') - X(\underline{s}, t)|^2 \to 0$, when $\underline{s}' \to s$ and $t' \to t$. Moreover, OS/TRF are, in general, taken to represent *space nonhomogeneous/time nonstationary* natural processes (e.g., spatiotemporal history of soil shear stresses during an earthquake, oil reservoir porosity distribution in space-time during the production phase). The space of all continuous OS/TRF will be denoted by $\mathfrak{K}$.

In the sequel we will consider *second-order OS/TRF*, that is, the analysis will be based on second order statistical moments which are assumed to be continuous and finite. More precisely, an OS/TRF $X(\underline{s}, t)$ will be characterized in terms of its *spatiotemporal mean value*

$$m_x(\underline{s}, t) = E[X(\underline{s}, t)] = \int \chi f_x(\chi)\, d\chi, \qquad (3.5)$$

the *centered spatiotemporal covariance function*

$$c_x(\underline{s}, t; \underline{s}', t') = E\big[(X(\underline{s}, t) - m_x(\underline{s}, t))(X(\underline{s}', t') - m_x(\underline{s}', t'))\big]$$
$$= \iint (\chi_1 - m_1)(\chi_2 - m_2) f_x(\chi_1, \chi_2)\, d\chi_1\, d\chi_2 \qquad (3.6)$$

and the *spatiotemporal semivariogram* or *structure function*

$$\gamma_x(\underline{s}, t; \underline{s}', t') = \tfrac{1}{2} E[X(\underline{s}, t) - X(\underline{s}', t')]^2$$
$$= \tfrac{1}{2} \iint (\chi_1 - \chi_2)^2 f_x(\chi_1, \chi_2)\, d\chi_1\, d\chi_2. \qquad (3.7)$$

A continuous function $c_x(\underline{s}, t; \underline{s}', t')$ is the covariance function of an OS/TRF if and only if it satisfies the *nonnegative-definiteness condition*

$$\sum_{i}^{m} \sum_{1}^{k_1} \sum_{j}^{m} \sum_{1}^{k_1} q_{ij} q_{i'j'} c_x(\underline{s}_i, t_j; \underline{s}_{i'}, t_{j'}) \geqslant 0 \qquad (3.8)$$

for all m, k_i, $k_{i'}$ (= 1, 2, ...), all $(\underline{s}_i, t_j) \in \mathfrak{R}^n \times T$ and all numbers (real or complex) q_{ij}, $q_{i'j'}$; here k_i denotes the number of time instants t_j, $j = 1_i, 2_i, \ldots, k_i$ used, given that we are at the spatial position $\underline{s}_i$.

Instead of the centered covariance function one may also define the *non-centered* spatiotemporal covariance function

$$\sigma_X(\underline{s}, t; \underline{s}', t') = E[X(\underline{s}, t)X(\underline{s}', t')]$$

$$= c_X(\underline{s}, t; s', t') + m_X(\underline{s}, t)m_X(\underline{s}', t'). \tag{3.9}$$

The other mode of second-order analysis is that in the *frequency domain*. The harmonic expansions of $X(\underline{s}, t)$ can be considered as an extension in the space-time context of the relevant results for SRF (e.g., [7]). In particular (for simplicity's sake, the symbol $\mathfrak{R}^n T$ under the integrals will be omitted in the following)

$$X(\underline{s}, t) = \iint \exp[i(\underline{w} \cdot \underline{s} + \lambda t)]\tilde{X}(\underline{w}, \lambda)\, d\underline{w}\, d\lambda, \tag{3.10}$$

where $i = \sqrt{-1}$, and $\tilde{X}(\underline{w}, \lambda)$ is the so-called *spectral amplitude* of $X(\underline{s}, t)$. The corresponding *spectral density function* $C_X(\underline{w}, \lambda; \underline{w}', \lambda')$ is defined by

$$c_X(\underline{s}, t; \underline{s}', t') = \iiiint \exp[i(\underline{w} \cdot \underline{s} + \underline{w}' \cdot s' + \lambda t + \lambda' t')]$$

$$C_X(\underline{w}, \lambda; \underline{w}', \lambda')\, d\underline{w}\, d\lambda\, d\underline{w}'\, d\lambda', \tag{3.11}$$

where $C_X(\underline{w}, \lambda; \underline{w}', \lambda')$ is a positive summable function in $\mathfrak{R}^n \times T$. The $C_X(\underline{w}, \lambda; \underline{w}', \lambda')$ forms an $\mathfrak{R}^n \times T$-fold Fourier transform pair with the spatiotemporal covariance $c_X(s, t; s', t')$.

3.3. Space homogeneous/time stationary spatiotemporal random fields

An OS/TRF $X(\underline{s}, t)$, $(\underline{s}, t) \in \mathfrak{R}^n \times T$ will be called *space homogeneous/time stationary in the strict sense* if all the multidimensional probability densities are invariant under the translation $\underline{z} \to \underline{z} + \delta\underline{z}$ (where, as before, $\underline{z} = (\underline{s}, t)$):

$$P[\chi_1 \leq x(\underline{z}_1) \leq \chi_1 + d\chi_1, \ldots, \chi_m \leq x(\underline{z}_m) \leq \chi_m + d\chi_m] =$$
$$P[\chi_1 \leq x(\underline{z}_1 + \delta\underline{z}) \leq \chi_1 + d\chi_1, \ldots, \chi_m \leq x(\underline{z}_m + \delta\underline{z})$$
$$\leq \chi_m + d\chi_m], \tag{3.12}$$

or

$$f_{\underline{z}_1, \ldots, \underline{z}_m}(\chi_1, \ldots, \chi_m) = f_{\underline{z}_1 + \delta\underline{z}, \ldots, \underline{z}_m + \delta\underline{z}}(\chi_1, \ldots, \chi_m) \tag{3.13}$$

for all $m = 1, 2, \ldots$ Space homogeneous/time stationary RF occur, for example, in the case of blackbody radiation within a large cavity maintained at a constant temperature.

An OS/TRF $X(\underline{s}, t)$ will be called *space homogeneous/time stationary in the wide sense* if its mean and covariance do not change under a shift of the parameters, i.e.,

$$m_x(\underline{s}, t) = \text{constant} \tag{3.14}$$

and

$$c_x(\underline{s}, t; \underline{s}', t') = c_x(\underline{h}, \tau), \tag{3.15}$$

where $\underline{h} = \underline{s} - \underline{s}'$ and $\tau = t - t'$. In other words, there exist in the closed linear subspace H spanned by the random variables x in $L_2(\Omega, P, F)$ a group of unitary operators $U_{\underline{h},\tau}$ such that

$$U_{\underline{h},\tau} X(\underline{s}, t) = S_{\underline{h},\tau} X(\underline{s}, t), \tag{3.16}$$

where $\underline{s}, \underline{h} \in \mathfrak{R}^n$ and $t, \tau \in T$ (here, $S_{\underline{h},\tau} X(\underline{s}, t) = X(\underline{s} + \underline{h}, t + \tau)$ is the shift operator). It is easily seen that in the case of space homogeneous/time stationary fields the covariance (3.6) and the semivariogram (3.7) are related by (assuming a zero mean field)

$$c_x(\underline{h}, \tau) = c_x(\underline{0}, 0) - \gamma_x(\underline{h}, \tau). \tag{3.17}$$

The set of all space homogeneous/time stationary ordinary fields will be denoted by $\mathcal{K}_0 \subset \mathcal{K}$.

The space homogeneous/time stationary RF $X(s, t)$ admits the Fourier-Stieltjes representation

$$X(\underline{s}, t) = \iint \exp[i(w \cdot s) + \lambda t]\, d\aleph_x(\underline{w}, \lambda), \tag{3.18}$$

where $\aleph_x(\underline{w}, \lambda)$ is a random field such that $C_x(w, \lambda)\delta(w - w')\delta(\lambda - \lambda') = E[d\aleph_x(\underline{w}, \lambda) d\bar{\aleph}_x(\underline{w}', \lambda')]$, where $C_x(\underline{w}, \lambda)$ is the spectral function satisfying the spectral representation of the covariance $c_x(\underline{h}, \tau)$, viz.

$$c_x(\underline{h}, \tau) = \iint \exp[i(\underline{w} \cdot \underline{h} + \lambda\tau)] C_x(\underline{w}, \lambda)\, d\underline{w}\, d\lambda, \tag{3.19}$$

and

$$C_x(\underline{w}, \lambda) = \frac{1}{(2\pi)^{n+1}} \iint \exp[-i(\underline{w} \cdot \underline{h} + \lambda\tau)] c_x(\underline{h}, \tau)\, d\underline{h}\, d\tau. \tag{3.20}$$

Since the covariance $c_x(\underline{h}, \tau)$ is a nonnegative-definite function, according to *Bochner's theorem*

$$C_x(\underline{w}, \lambda) \geq 0 \tag{3.21}$$

for all $\underline{w}$, λ.

The $c_x(\underline{h},\tau)$ will be termed *space-time separable* if

$$c_x(\underline{h},\tau) = c_x(\underline{h})c_x(\tau). \tag{3.22}$$

Clearly, this implies $C_x(\underline{w},\lambda) = C_x(\underline{w})C_x(\lambda)$. When physically justified, separability is an extremely convenient property from a mathematical point of view.

In practice, one usually makes an additional assumption, namely that of *space isotropic/time stationary* RF: the covariance and spectral functions are

$$c_x(\underline{h},\tau) = c_x(r,\tau), \tag{3.23}$$

and

$$C_x(\underline{w},\lambda) = C_x(\omega,\lambda), \tag{3.24}$$

where $r = |\underline{h}|$ and $\omega = |\underline{w}|$.

In order that $c_x(r,\tau)$ be a covariance function of a space isotropic/time stationary RF, it is necessary and sufficient that this function admits a representation of the form

$$c_x(r,\tau) = 2\pi^{n/2}\int_{-\infty}^{\infty}\int_0^{\infty}\frac{J_{n/2-1}(\omega r)}{(\omega r)^{n/2-1}}\exp(i\lambda\tau)\omega^{n/2}\,C_x(\omega,\lambda)\,d\omega\,d\lambda, \tag{3.25}$$

where $C_x(\omega\lambda) \geq 0$ on the half-plane (ω,λ), $\omega \in [0,\infty)$, $\lambda \in (-\infty,\infty)$. A similar condition holds true in terms of the semivariogram in (3.17).

Other combinations of spatial homogeneity and temporal stationarity, in the strict or the wide sense, are also possible [7]. Lastly, the space-time covariances satisfy relationships similar to those for purely SRF; for example, for a time stationary S/TRF (in the wide sense) it is valid that

$$|c_x(\underline{s},\underline{s}';\tau)| \leq \sqrt{c_x(\underline{s},\underline{s};0)c_x(\underline{s}',\underline{s}';0)}.$$

4. Generalized spatiotemporal random fields

4.1. Definition and basic properties

In dealing with space nonhomogeneous and/or time nonstationary natural processes it will be useful to introduce the notion of generalized S/TRF. The latter is an extension in the space-time context of the notion of random distribution due to Ito [18] and Gel'fand [13]. Let Q be some specified linear

space of elements q and let $\mathcal{H}_2 = L_2(\Omega, \mathcal{F}, P)$ be the Hilbert space of all random variables $x(q)$ on Q endowed with the scalar product

$$(x(q_1), x(q_2)) = E[x(q_1)x(q_2)] = \iint \chi_1 \chi_2 \, dF(\chi_1, \chi_2), \tag{4.1}$$

where $F(\chi_1, \chi_2)$ denotes the joint probability distribution of the random variables $x(q_1), x(q_2)$ with $\|x(q)\|^2 = E[x(q)^2] < \infty$ and satisfying the following linearity condition

$$x\left(\sum_{i=1}^{N} \lambda_i q_i\right) = \sum_{i=1}^{N} \lambda_i x(q_i) \tag{4.2}$$

for all $q_i \in Q$ and all (real or complex) numbers $\lambda_1, \ldots, \lambda_N$. The elements $q \in Q$ are in $\mathcal{R}^n \times T$, i.e., $q = (s, t)$. Among the Q spaces which are suitable for the purpose of this study, are the spaces $\mathbf{K}$ and $\mathbf{S}$ of Section 3.1.

Definition 4.1. A *generalized S/TRF* (GS/TRF) on Q, $X(q)$, is the random mapping

$$X : Q \to L_2(\Omega, \mathcal{F}, P). \tag{4.3}$$

The GS/TRF considered will always assumed to be continuous in the sense that $E[X(q_n) - X(q)]^2 \to 0$ when $q_n \to q$. The set of all continuous GS/TRF on Q will be denoted by $\mathcal{G}$.

The second order characteristics of the GS/TRF are the *spatiotemporal mean value*

$$m_x(q) = E[X(q)] = \int \chi \, dF_x(\chi), \tag{4.4}$$

where $F_x(\chi)$ denotes the probability distribution of $X(q)$, and the

$$c_x(q_1, q_2) = E[(X(q_1) - m_x(q_1))(X(q_2) - m_x(q_2))] \tag{4.5}$$

which will be called the *(centered) spatiotemporal covariance functional* of the GS/TRF $X(q)$. Both the mean and the covariance functional will be assumed to be real-valued and continuous relative to the topology of Q. Also, a useful second-order characteristic is the *spatiotemporal structure* or *semivariogram functional* which is defined by

$$\gamma_x(q_1, w_2) = \tfrac{1}{2} E[X(q_1) - X(q_2)]^2. \tag{4.6}$$

Finally, mathematically equivalent space-time second order functionals may be constructed in the frequency domain by taking the Fourier transform of the covariance and the semivariogram functionals.

4.2. Continuous linear functional representation of generalized spatiotemporal random fields

In the sequel we will concentrate on GS/TRF which are of the *continuous linear functional form (CLF)*

$$X(q) = \langle q(\underline{s},t), X(\underline{s},t)\rangle = \iint q(\underline{s},t)X(\underline{s},t)\,d\underline{s}\,dt, \tag{4.7}$$

where $q \in Q$ and $X(\underline{s},t)$ is an OS/TRF in the sense of Definition 3.1 above. Depending on the choice of the function q, the CLF (4.7) may admit a variety of physical interpretations. Let us consider the following example.

Example 4.2. Assume that $X(\underline{s},t)$ represents the concentration of an aerosol substance in the atmosphere. By choosing $q(\underline{s},t) = \delta(\underline{s}-\underline{s}^*)\delta(t-t^*)$, (4.7) gives the value of the substance at the point/instant $\underline{s},t$. If one let

$$q(\underline{s},t) = \begin{cases} 1, & \text{if } \underline{s} \in V \text{ and } t \in [t_1,t_2] \\ 0, & \text{otherwise,} \end{cases}$$

(4.7) provides the total amount of substance in the volume V during the time period $[t_1,t_2]$.

Since a GS/TRF $X(q)$ cannot be assigned values at isolated points/instances $(\underline{s},t)$ (unless q is a delta function), we introduce the following field.

Definition 4.3. A *convoluted S/TRF (CS/TRF)* is defined as the S/TRF

$$Y_q(\underline{s},t) = \langle q(\underline{s}',t'), S_{\underline{s},t}X(\underline{s}',t')\rangle$$

$$= \iint q(\underline{s}',t')S_{\underline{s},t}X(\underline{s}',t')\,d\underline{s}'\,dt'. \tag{4.8}$$

We can now make the following observations: The CS/TRF (4.8) is characterized by $Y_q(\underline{0},0) = X(q)$ for all $q \in Q$. Also, it holds true that $Y_q(\underline{s},t) = S_{\underline{s},t}X(q) = X(S_{-\underline{s},-t})$ for all $q \in Q$ and all $(\underline{s},t) \in \mathfrak{R}^n \cdot T$. The space $\mathcal{K}$ of OS/TRF may be considered as a subset of the space $\mathcal{G}$ of GS/TRF, viz. $\mathcal{K} \subset \mathcal{G}$. Moreover, the fields $X(q)$ and $Y_q(\underline{s},t)$ have certain important properties, as follows.

Property 4.4. The means and covariances of $X(q)$ and $Y_q(\underline{s},t)$ write

$$m_X(q) = E[X(q)] = \langle m_X(\underline{s},t), q(\underline{s},t)\rangle, \tag{4.9}$$

$$m_Y(\underline{s},t) = E[Y_q(\underline{s},t)] = \langle m_{S_{\underline{s},t}X}(\underline{s}',t'), q(\underline{s}',t')\rangle, \tag{4.10}$$

and

$$c_X(q_1, q_2) = E\left[(X(q_1) - m_X(q_1))(X(q_2) - m_X(q_2))\right]$$

$$= \langle (c_X(\underline{s}, t; \underline{s}', t'), q_1(\underline{s}, t)), q_2(\underline{s}', t') \rangle, \tag{4.11}$$

$$c_Y(\underline{s}, t; \underline{s}', t') = E\left[(Y_{q_1}(\underline{s}, t) - m_Y(\underline{s}, t))(Y_{q_2}(\underline{s}', t') - m_Y(\underline{s}', t'))\right]$$

$$= \langle (c_X(S_{\underline{s},t} X(\underline{s}'', t''), S_{\underline{s}',t'} X(\underline{s}''', t''')), q_1(\underline{s}'', t'')),$$

$$q_2(\underline{s}''', t''') \rangle. \tag{4.12}$$

The means and covariances of the GS/TRF and CS/TRF are linearly related to those of the corresponding OS/TRF. From (4.10) and (4.12) we find that the corresponding mean values and covariances functions write, respectively,

$$m_X(q) = m_Y(\underline{0}, 0), \tag{4.13}$$

$$c_X(q_1, q_2) = c_Y(\underline{0}, 0; \underline{0}, 0). \tag{4.14}$$

Property 4.5. The covariance functional of the GS/TRF X(q) is a *nonnegative-definite bilinear functional* in the sense that

$$c_X(q, q) = \langle |X(q) - m_X(q)|^2 \rangle \geq 0 \tag{4.15}$$

for all $q \in Q$. Conversely, every continuous nonnegative-definite bilinear functional $c_X(q_1, q_2)$ in Q is a covariance functional of some GS/TRF X(q).

Property 4.6. The fields X(q) and $Y_q(\underline{s}, t)$ are always *differentiable*, even when X(s, t) is not. To see this assume $Q = K$ and let

$$X^{(\underline{\rho}, \zeta)}(q) = \langle q(\underline{s}, t), X^{(\underline{\rho}, \zeta)}(\underline{s}, t) \rangle$$

$$= \iint q(s, t) X^{(\underline{\rho}, \zeta)}(s, t)\, ds\, dt, \tag{4.16}$$

where ζ is a nonnegative integer and $\underline{\rho} = (\rho_1, \rho_2, \ldots, \rho_n)$ is a multi-index of nonnegative integers; i.e., the superscript $(\underline{\rho}, \zeta)$ denotes partial differentiation of the order ρ in space and differentiation of order ζ in time

$$X^{(\underline{\rho}, \zeta)}(s, t) = D^{(\underline{\rho}, \zeta)} X(s, t) = \frac{\partial^{|\underline{\rho}|}}{\partial s_1^{\rho_1} \ldots \partial s_n^{\rho_n}} \left[\frac{\partial^\zeta}{\partial t^\zeta} X(s, t)\right], \tag{4.17}$$

where $\rho = |\underline{\rho}, \zeta| = \sum_{i=1}^{n} \rho_i$. By applying integration by parts (4.16) writes,

$$X^{(\underline{\rho},\zeta)}(q) = (-1)^{\rho+\zeta} X(q^{(\underline{\rho},\zeta)}). \tag{4.18}$$

Similarly for the CS/TRF,

$$Y_q^{(\underline{\rho},\zeta)}(\underline{s}, t) = (-1)^{\rho+\zeta} S_{\underline{s},t} X(q^{(\underline{\rho},\zeta)}). \tag{4.19}$$

Therefore, although there may exist no $X^{(\underline{\rho},\zeta)}$ as such, we can always obtain $X^{(\underline{\rho},\zeta)}(q)$ and $Y_q^{(\underline{\rho},\zeta)}$ in the sense defined above.

Property 4.7. By applying the Riesz-Radon theorem in terms of generalized functions we find that the mean $m_x(q)$ can be written as

$$m_x(q) = \left\langle \sum_{\rho \le \nu} \sum_{\zeta \le \mu} q^{(\underline{\rho},\zeta)}(\underline{s}, t), f_{\underline{\rho},\zeta}(\underline{s}, t) \right\rangle, \tag{4.20}$$

where ν and μ are nonnegative integers, $q(\underline{s}, t) \in \mathbf{K}$ and $f_{\underline{\rho},\zeta}(\underline{s}, t)$ are continuous functions in $\mathfrak{R}^n \times T$, only a finite number of which are different than zero on any given finite support $\mathbf{U}$ of $\mathbf{K}$. Integration by parts yields

$$m_x(q) = \left\langle \sum_{\rho \le \nu} \sum_{\zeta \le \mu} (-1)^{\rho+\zeta} f_{\underline{\rho},\zeta}^{(\underline{\rho},\zeta)}(\underline{s}, t), q(\underline{s}, t) \right\rangle. \tag{4.21}$$

A similar expression may be derived for the mean $m_Y(\underline{s}, t)$ of $Y_q(\underline{s}, t)$, namely

$$m_Y(\underline{s}, t) = \left\langle \sum_{\rho \le \nu} \sum_{\zeta \le \mu} (-1)^{\rho+\zeta} S_{\underline{s},t} f_{\underline{\rho},\zeta}^{(\underline{\rho},\zeta)}(\underline{s}', t'), q(\underline{s}', t') \right\rangle. \tag{4.22}$$

For convenience in the subsequent analysis let us put $g_{\underline{\rho},\zeta}(\underline{s}, t) \quad f_{\underline{\rho},\zeta}^{(\underline{\rho},\zeta)}(\underline{s}, t)$. Closely related to Property 4.7 is the following section.

4.3. Space homogeneous/time stationary generalized spatiotemporal random fields

A GS/TRF $X(q)$, $q(\underline{s}, t) \in Q$, $(\underline{s}, t) \in \mathfrak{R}^n \times T$ will be called *space homogeneous/time stationary in the wide sense* if its mean value $m_x(q)$ and covariance functional $c_x(q_1, q_2)$ are invariant with respect to any shift of the parameters, that is

$$m_x(q) \quad = m_x(S_{\underline{h},\tau} q), \tag{4.23}$$

$$c_x(q_1, q_2) = c_x(S_{\underline{h},\tau} q_1, S_{\underline{h},\tau} q_2), \tag{4.24}$$

for any $(\underline{h},\tau) \in \mathfrak{R}^n \times T$. Clearly, when the $X(q)$ is space homogeneous/time stationary the $c_x(q_1,q_2)$ is a translation-invariant, nonnegative-definite bilinear functional on Q, and the following proposition can be proven [6].

Proposition 4.8. If $X(q)$ is a space homogeneous/time stationary, GS/TRF on Q, there exists one and only one generalized functional $c_x(q_1,q_2) \in Q'$ such that $\langle X(q_1), X(q_2)\rangle = c_x(q_1,q_2)$, $q_1,q_2 \in Q$.

We shall denote by $\mathcal{G}_0$ the set of all space homogeneous/time stationary generalized fields. Note that $\mathcal{K}_0 \subset \mathcal{G}_0 \subset \mathcal{G}$. Similarly, the CS/TRF $Y_q(\underline{s},t)$ is called *space homogeneous/time stationary* if

$$m_Y(\underline{s},t) = \text{constant}, \tag{4.25}$$

and

$$c_Y(\underline{s},t;\underline{s}',t') = c_Y(\underline{h},\tau), \tag{4.26}$$

where $\underline{h} = \underline{s} - \underline{s}'$, $\tau = t - t'$, for any $(\underline{h},\tau) \in \mathfrak{R}^n \times T$. In view of (4.22) and condition (4.23) it follows that the functions $f_{\rho,\zeta}(\underline{s},t)$ are constants. Therefore

$$\begin{aligned} g_{\rho,\zeta}(\underline{s},t) = f^{(\rho,\zeta)}_{\rho,\zeta}(\underline{s},t) = 0 \qquad & \text{for all } \rho \geqslant 1, \zeta \geqslant 1 \\ = f^{(0,0)}_{0,0}(\underline{s},t) = m \qquad & \text{for } \rho = \zeta = 0 \end{aligned} \tag{4.27}$$

and the $m_x(q)$ will have the form

$$m_x(q) = m \iint q(\underline{s},t)\, d\underline{s}\, dt = m\langle q(\underline{s},t), 1\rangle. \tag{4.28}$$

The $c_x(q_1,q_2) \in Q'$ can be expressed in terms of the corresponding $c_x(\underline{h},\tau)$ as follows

$$c_x(q_1,q_2) = \langle c_x(\underline{h},\tau), q_1 * \check{q}_2(\underline{h},\tau)\rangle = c_x(q_1 * \check{q}_2), \tag{4.29}$$

for all $q_1,q_2 \in Q$, where $*$ denotes convolution and $\check{}$ denotes inversion (i.e., $\check{q}_2(\underline{h},\tau) = q_2(-\underline{h},-\tau)$).

Example 4.9. Let us define in $R^1 \times T$ a zero mean *Wiener S/TRF* $W(s,t)$, $s \in [s_1,s_2]$, $t \in [0,\infty)$ as a *Gaussian* S/TRF with covariance function

$$c_x(s,t;s',t') = \min(s - s_1, s' - s_2)\min(t,t'). \tag{4.30}$$

The $X(s,t) = \frac{\partial W(s,t)}{\partial s \partial t}$ will be zero mean *white noise* S/TRF with covariance function

$$c_x(h,\tau) = \delta(h,\tau), \tag{4.31}$$

where $h = s - s'$, $\tau = t - t'$ and $\delta(h, t)$ is the spatiotemporal delta function. The corresponding GS/TRF $X(q) = \langle X(s,t), q(s,t)\rangle$ has covariance

$$c_x(q_1, q_2) = \delta(q_1 * \check{q}_2). \tag{4.32}$$

The above results can be generalized to more than one spatial dimension. More specifically, one may define in $\mathfrak{R}^n \times T$ the so-called *Brownian sheet* $W(\underline{s}, t)$ which is a zero mean Gaussian S/TRF with covariance

$$c_w(\underline{s}, t; \underline{s}', t') = \min(s_1, s_1') \ldots \min(s_n, s_n') \min(t, t'). \tag{4.33}$$

Brownian sheet has important applications in the context of stochastic partial differential equations.

In the light of the Fourier transform properties of generalized functions, it is valid that $c_x(q_1, q_2) = \langle c_0, q_1 * \check{q}_2\rangle = \langle \phi, \hat{q}_1 \hat{q}_2\rangle$, which yields the following result (see also [6]).

Proposition 4.10. Let $X(q)$ be a GS/TRF in $\mathfrak{R}^n \times T$. The covariance functional writes

$$c_x(q_1, q_2) = \iint \hat{q}_1(\underline{w}, \lambda) \hat{q}_2(\underline{w}, \lambda)\, d\phi(\underline{w}, \lambda), \tag{4.34}$$

where $\hat{q}_1(\underline{w}, \lambda)$ and $\hat{q}_2(\underline{w}, \lambda)$ are the Fourier transform of the $q_1(\underline{s}, t)$ and $q_2(\underline{s}, t)$ respectively, and $\phi(\underline{w}, \lambda)$ is some positive tempered measure in $\mathfrak{R}^n \times T$. In this case the $\phi(\underline{w}, \lambda)$ is called the *spectral measure* of the GS/TRF $X(q)$.

Example 4.11. Consider once more Example 4.9 above. Since $c_x(q_1, q_2) = \langle c_0, q_1 * \check{q}_2\rangle = \langle \phi, \hat{q}_1 \hat{q}_2\rangle$, and the Fourier transform of $c_0 = \delta$ is $d\underline{w}\, d\lambda$ (Lebesgue space-time measure), we conclude that the spectral measure of $X(q)$ is $d\phi(\underline{w}, \lambda) = d\underline{w}\, d\lambda$.

Space homogeneous/time stationary analysis yields the next property.

Property 4.12. The CS/TRF $Y_q(\underline{s}, t)$ can be zero mean space homogeneous/time stationary even when the associated OS/TRF $X(\underline{s}, t)$ is space nonhomogeneous/time nonstationary. This can happen under certain conditions concerning the choice of the functions $q(\underline{s}, t)$ as well as the form of the functions $g_{\rho,\zeta}(\underline{s}, t)$. More specifically, we must define spaces

$$Q_{\nu/\mu} = \{q \in Q : \langle q(\underline{s}, t), g_{\rho,\zeta}(\underline{s}, t)\rangle = 0 \quad \text{for all } \rho \leqslant \nu, \zeta \leqslant \mu\}, \tag{4.35}$$

and

$$\mathcal{C}_{\nu/\mu} = \{g_{\rho,\zeta}(\underline{s}, t) \in \mathbf{C} : \langle q(\underline{s}, t), g_{\rho,\zeta}(\underline{s}, t)\rangle = 0 \Rightarrow \langle q(\underline{s}, t), S_{\underline{h},\tau} g_{\rho,\zeta}(\underline{s}, t)\rangle = 0 \text{ for all } \rho \leqslant \nu, \zeta \leqslant \mu\}, \tag{4.36}$$

where $\mathbf{C}$ is the space of continuous functions in $\mathfrak{R}^n \times T$ with compact support. (4.35) assures a zero mean value for the CS/TRF $Y_q(\underline{s}, t)$ at $(\underline{s}, t) = (\underline{0}, 0)$,

while the closeness of $\mathcal{C}_{\nu/\mu}$ to translation (equation (4.36)) is necessary in order that stochastic inference about $X(q)$ makes sense (i.e., in order that the stochastic correlation properties of $X(q)$ remain unaffected by a shift $S_{\underline{h},\tau}$ of the space/time origin). Functions that satisfy these conditions are of the form

$$g_{\underline{\rho},\zeta}(\underline{s},t) = \underline{s}^{\underline{\rho}} t^{\zeta} \exp[\underline{\alpha} \cdot \underline{s} + \beta t], \tag{4.37}$$

where $\underline{\alpha}$ and β are (real or complex) vector and number, respectively.

From a practical point of view, the modelling of spatio-chronological variations and the estimation of spatiotemporal processes is easier and more efficiently carried out when the $g_{\underline{\rho},\zeta}(\underline{s},t)$ are *pure polynomials*, viz.

$$g_{\underline{\rho},\zeta}(\underline{s},t) = \underline{s}^{\underline{\rho}} t^{\zeta} = s_1^{\rho_1} s_2^{\rho_2} \dots s_n^{\rho_n} t^{\zeta}, \tag{4.38}$$

where $\rho = |\underline{\rho}| = \sum_{i=1}^{n} \rho_i$. This is due mainly to convenient invariance and linearity properties that the latter satisfy. In conclusion, the "derived" fields $X(q)$ and $Y_q(\underline{s},t)$ have a very convenient mathematical structure. From a physical viewpoint this means that even if $X(\underline{s},t)$ represents an actual natural process which has, in general, very irregular, space nonhomogeneous/time nonstationary features, we can derive fields $X(q)$ and $Y_q(s,t)$ which have regular, space homogeneous/time stationary features. Hence, analysis and processing are much easier.

5. Spatiotemporal random fields of order-ν/μ (ordinary and generalized)

5.1. Random fields with space homogeneous/time stationary increments

We now come to what is, for our present concern, the most interesting aspect of S/TRF, namely the concept of S/TRF with space homogeneous/time stationary increments of orders ν in space and μ in time, in the ordinary or in the generalized sense.

Definition 5.1. A CS/TRF $Y_q(\underline{s},t)$ will be called a *CS/TRF of order ν in space/μ in time (CS/TRF-ν/μ)* if $q \in Q_{\nu,\mu}$. In this case the space $Q_{\nu,\mu}$ will be termed an *admissible space of order ν/μ (AS-ν/μ)*.

Definition 5.2. Let $Q_{\nu/\mu}$ be an AS-ν/μ. A *GS/TRF $X(q)$ with space homogeneous of order ν/time stationary of order μ increments (GS/TRF-ν/μ)* is a linear mapping

$$X : Q_{\nu,\mu} \to L_2(\Omega, F, P), \tag{5.1}$$

where the corresponding CS/TRF $Y_q(\underline{s},t)$ is a zero mean space homogeneous/time stationary for all $q \in Q_{\nu/\mu}$ and all $(\underline{h},\tau) \in \mathfrak{R}^n \times T$.

The set of all continuous GS/TRF-ν/μ will be denoted by $\mathcal{G}_{\nu/\mu}$. The definition above is equivalent to the following one, which we unfold in an extended Ito-Gel'fand spirit:

Definition 5.3. A GS/TRF-ν/μ $X(q)$ is a GS/TRF for which all differential operators of the form

$$Y(q) = D^{(\nu+1,\mu+1)}X(q), \tag{5.2}$$

where $D^{(\nu+1,\mu+1)}X(q) = X^{(\nu+1,\mu+1)}(q) = (-1)^{\nu+\mu+2}X(q^{(\nu+1,\mu+1)})$ are zero mean space homogeneous/time stationary generalized fields.

The OS/TRF associated with the space $\mathcal{G}_{\nu/\mu}$ will be defined as follows.

Definition 5.4. An OS/TRF $X(\underline{s},t)$ is called an *OS/TRF of order* ν/μ *(OS/TRF-*ν/μ*)* if for all $q \in Q_{\nu/\mu}$ the corresponding CS/TRF $Y_q(\underline{s},t)$ is a zero mean space homogeneous/time stationary.

In light of Definition 5.4, if the

$$Y(\underline{s},t) = D^{(\nu+1,\mu+1)}X(\underline{s},t) = X^{(\nu+1,\mu+1)}(\underline{s},t) \tag{5.3}$$

exist and are zero mean space homogeneous/time stationary fields, then the $X(\underline{s},t)$ is an OS/TRF-ν/μ.

In connection with this, the following propositions can be proven [6].

Proposition 5.5. The solutions of the stochastic partial differential equation in $R^1 \times T$

$$D^{(\nu+1,\mu+1)}X_{\nu,\mu}(s,t) = Y(s,t), \tag{5.4}$$

where $Y(s,t)$ is a zero mean space homogeneous/time stationary, are OS/TRF-ν/μ. Note that in this case the

$$\begin{aligned} Y(q) &= \langle q(s,t), Y(s,t)\rangle \\ &= \langle q(s,t), X^{(\nu+1,\mu+1)}_{\nu,\mu}(s,t)\rangle \\ &= Y_q^{(\nu+1,\mu+1)}(0), \end{aligned} \tag{5.5}$$

is a space homogeneous/time stationary generalized field.

Proposition 5.6. The OS/TRF

$$X(\underline{s},t) = \sum_{\rho=0}^{\nu}\sum_{\zeta=0}^{\mu}\beta_{\rho,\zeta}g_{\rho,\zeta}(\underline{s},t), \tag{5.6}$$

where $\beta_{\rho,\zeta}$ ($\rho \leqslant \nu$ and $\zeta \leqslant \mu$) are random variables in $\mathcal{H}_k = L_2(\Omega, F, P)$, is an OS/TRF-$\nu/\mu$.

In view of (4.7) and (4.8), to each generalized $X(q)$ correspond various ordinary $X(\underline{s}, t)$, all having the same CS/TRF $Y_q(\underline{s}, t) = X(S_{-\underline{s},-t}q)$; that is, we can write

$$\begin{array}{ccccc} & & X(q) & \leftrightarrow & \{X^a(\underline{s},t), a = 1,2,\ldots\} \\ & & \downarrow\uparrow & & \downarrow\uparrow \\ q) & = & X(S_{-\underline{y},-t} & & {}_q(\underline{s},t) \end{array} . \tag{5.7}$$

Hence,

Definition 5.7. The set $\mathfrak{X}_q = \{X^a(\underline{s}, t), a = 1, 2, \ldots\}$ of all OS/TRF-ν/μ which have the same CS/TRF-ν/μ $Y_q(\underline{s}, t)$ in Q will be termed the *generalized representation set of order* ν/μ *(GRS-*ν/μ*).* Each member of the GRS-ν/μ will be called a representation of the $X(q)$.

We can now state the proposition below [6].

Proposition 5.8. Let $X^0(\underline{s}, t)$ be a representation $\in \mathfrak{X}_q$ of $X(q)$. The OS/TRF $X^a(\underline{s}, t)$ is another representation if and only if it can be expressed as

$$X^a(\underline{s}, t) = X^0(\underline{s}, t) + \sum_{\rho} \sum_{|\underline{\rho}| \leqslant \nu} \sum_{\zeta \leqslant \mu} c_{\rho,\zeta} g_{\rho,\zeta}(\underline{s}, t), \tag{5.8}$$

where the $c_{\rho,\zeta}$, $\rho \leqslant \nu$ and $\zeta \leqslant \mu$ are random variables in $L_2(\Omega, F, P)$ s.t.

$$c_{\rho,\zeta} = \langle \eta_{\rho,\zeta}(\underline{s}, t), X^a(\underline{s}, t) \rangle, \tag{5.9}$$

where the $\eta_{\rho,\zeta}(\underline{s}, t)$ satisfy the

$$\langle \eta_{\rho,\zeta}(\underline{s}, t), g_{\rho',\zeta'}(\underline{s}, t) \rangle = \begin{cases} 1 & \text{if } \rho = \rho' \text{ and } \zeta = \zeta' \\ 0 & \text{otherwise.} \end{cases} \tag{5.10}$$

An OS/TRF-ν/μ is not always differentiable. It can, however, be expressed in terms of a differentiable OS/TRF-ν/μ as shown in the proposition below [6].

Proposition 5.9. Let $X(\underline{s}, t)$be a continuous OS/TRF-ν/μ. Then it follows

$$X(\underline{s}, t) = X^*(\underline{s}, t) + Y_q(\underline{s}, t), \tag{5.11}$$

where $X^*(\underline{s}, t)$ is an infinitely differentiable OS/TRF-ν/μ and $Y_q(\underline{s}, t)$ is a space homogeneous/time stationary random field.

5.2. The correlation structure of spatiotemporal random fields of order-ν/μ

In this subsection, we will study the spatiotemporal trend and correlation structure of a S/TRF-ν/μ. In view of the preceding results, the generalized field $X^{(\nu,\mu)}(q) = (-1)^{\nu+\mu}X(q^{(\nu,\mu)})$ has *constant mean*, i.e., we can write

$$E[X^{(\nu,\mu)}(q)] = m_x^{(\nu,\mu)}(q) = (-1)^{\nu+\mu}m_x(q^{(\nu,\mu)}) = a\tilde{q}(\underline{0},0), \tag{5.12}$$

while the covariance functional is expressed as

$$\begin{aligned} c_x(q_1^{(\nu+1,\mu+1)}, q_2^{(\nu+1,\mu+1)}) &= E[X(q_1^{(\nu+1,\mu+1)})X(q_2^{(\nu+1,\mu+1)})] \\ &= E[X^{(\nu+1,\mu+1)}(q_1)X^{(\nu+1,\mu+1)}(q_2)] \\ &= c_Y(q_1, q_2). \end{aligned} \tag{5.13}$$

But as was shown above, the $c_Y(q_1, q_2)$ in (5.13) is a translation-invariant bilinear functional and, therefore, so is $c_x(q_1^{(\nu+1,\mu+1)}, q_2^{(\nu+1,\mu+1)})$. Taking into account the properties of bilinear functionals (for the relevant theory see [14]), (5.12) and (5.13) lead to the proposition below.

Proposition 5.10. Let $X(q)$ be a GS/TRF-ν/μ in $\mathfrak{R}^n \times T$. Its mean value and covariance functional have the following forms

$$\begin{aligned} m_x(q) &= \sum_{0\leqslant|\underline{\rho}|\leqslant\nu} \sum_{0\leqslant\zeta\leqslant\mu} a_{\rho,\zeta}\langle \underline{s}^{\underline{\rho}}t^{\zeta}, q(\underline{s},t)\rangle \\ &= \sum_{\rho_1}\sum_{\rho_2}\cdots\sum_{\rho_n}\sum_{\zeta} a_{\rho_1\rho_2\ldots\rho_n\zeta}\langle s_1^{\rho_1}s_2^{\rho_2}\ldots s_n^{\rho_n}t^{\zeta}, q(\underline{s},t)\rangle, \end{aligned} \tag{5.14}$$

where $a_{\rho,\zeta}$ are suitable coefficients, $0 \leqslant \rho = |\underline{\rho}| = \sum_{i=1}^{n}\rho_i \leqslant \nu$; and

$$\begin{aligned} c_x(q_1, q_2) = &\iint_{\mathfrak{R}\times\mathfrak{I}} \tilde{q}_1(\underline{w},\lambda)\tilde{q}_2(\underline{w},\lambda)\,d\phi_x(\underline{w},\lambda) \\ &+G(\tilde{q}_1^{(\nu+1,\mu+1)}(\underline{0},0), \tilde{q}_2^{(\nu+1,\mu+1)}(\underline{0},0)), \end{aligned} \tag{5.15}$$

where $\mathfrak{R} = \mathfrak{R}^n - \{\underline{0}\}$ and $\mathfrak{I} = T - \{0\}$, ϕ_x is certain positive tempered measure and G is some function in $\tilde{q}_1^{(\nu+1,\mu+1)}(\underline{0},0)$ and $\tilde{q}_2^{(\nu+1,\mu+1)}(\underline{0},0)$.

We proceed with the analysis of the spatiotemporal correlation structure of OS/TRF-ν/μ by introducing the following definition.

Definition 5.11. Consider a continuous OS/TRF-ν/μ $X(\underline{s},t)$. A continuous and symmetric function $k_x(\underline{h},\tau)$ in $\mathfrak{R}^n \times T$ is termed a *generalized spatiotemporal covariance of order* ν *in space and* μ *in time (GS/TC-*ν/μ*)* if and only if

$$\langle X(q_1), X(q_2)\rangle = \langle k_x(\underline{h},\tau), q_1(\underline{s},t)q_2(\underline{s}',t')\rangle \geqslant 0, \tag{5.16}$$

where $\underline{h} = \underline{s} - \underline{s}'$ and $\tau = t - t'$, for all $q_1, q_2 \in Q_{\nu/\mu}$.

In other words, in order that a given function be a *permissible* model of some GS/TC-ν/μ it is necessary and sufficient that the condition (5.16) is satisfied. We saw above that with a particular GS/TRF-ν/μ $X(q)$ we can associate a GRS-ν/μ $\mathfrak{X}_q$ whose elements are the corresponding OS/TRF-ν/μ $X(\underline{s},t)$. Similarly, with a particular $X(q)$ we can associate a set of GS/TC-ν/μ satisfying Definition 5.11; this set will be called the *generalized spatiotemporal covariance representation set of order* ν/μ *(GS/TCRS-*ν/μ*)*, and will be denoted by $\mathcal{F}^X_{\nu/\mu}$. The concept of the GS/TC-ν/μ $k_x(\underline{h},\tau)$ can be considered as the space-time extension of the purely spatial generalized covariance in the sense of [22].

We will see below that some interesting properties of $\mathcal{F}^X_{\nu/\mu}$ may be obtained by assuming that the GS/TC-ν/μ is *space isotropic*, that is

$$k_x(\underline{h},\tau) = k_x(r,\tau), \tag{5.17}$$

where $r = |\underline{h}|$.

Let us now explore (5.13) some more in light of Definition 5.11. We have

$$c_x(q_1^{(\nu+1,\mu+1)}, q_2^{(\nu+1,\mu+1)}) = \langle c_Y(\underline{s}-\underline{s}', t-t'), q_1(\underline{s},t)q_2(\underline{s}',t')\rangle;$$

it also is true that

$$D^{(2\nu+2,2\mu+2)}c_x(\underline{s},t;\underline{s}',t') = c_Y(\underline{s}-\underline{s}', t-t'). \tag{5.18}$$

The above partial differential equation can be solved with respect to $c_x(\underline{s},t;\underline{s}',t')$. For illustration consider first the $\mathfrak{R}^1 \times T$ case: according to Proposition 5.5 above, if $X(\underline{s},t)$ is a differentiable OS/TRF-ν/μ in $\mathfrak{R}^1 \times T$ such that $D^{(\nu+1,\mu+1)}X(s,t) = Y(s,t)$, the $Y(s,t)$ is space homogeneous/time stationary. The corresponding covariances of $X(s,t)$ and $Y(s,t)$ are related by $D^{(2\nu+2,2\mu+2)}c_x(s,t;s',t') = c_Y(r,\tau)$, where $r = s - s'$ and $\tau = \tau - t'$. The solution of this partial differential equation is

$$c_x(s,t;s',t') = k_x(r,\tau) + p_{\nu,\mu}(s,t;s',t'), \tag{5.19}$$

where

$$k_x(r,\tau) = (-1)^{(\nu+\mu)}\int_0^r\int_0^\tau \frac{(r-u)^{2\nu+1}(\tau-v)^{2\mu+1}}{(2\nu+1)!(2\mu+1)!}c_Y(u,v)\,du\,dv \tag{5.20}$$

is the corresponding GS/TC-ν/μ and $p_{\nu,\mu}(s,t;s',t')$ is a polynomial of degree ν in s, s' and μ in t, t'. (5.20) can be solved with respect to $c_Y(\tau,\tau)$, viz.

$$c_Y(\tau,\tau) = (-1)^{(\nu+\mu+2)} D^{(2\nu+2,\mu+2)} k_x(\tau,\tau). \tag{5.21}$$

In $\mathfrak{R}^n \times T$ the analysis above leads to the following proposition [6].

Proposition 5.12. Let $X(\underline{s},t)$ be an OS/TRF-ν/μ in $\mathfrak{R}^n \times T$. Its covariance function can be expressed in the following form

$$c_x(\underline{s},t;\underline{s}',t') = k_x(\underline{h},\tau) + p_{\nu,\mu}(\underline{s},t;\underline{s}',t'), \tag{5.22}$$

where $k_x(\underline{h},\tau)$ ($\underline{h} = \underline{s} - \underline{s}'$ and $\tau = t - t'$) is the associated GS/TC-ν/μ and $p_{\nu,\mu}(\underline{s},t;s',t')$ is a polynomial with variable coefficients of degree ν in $\underline{s}$, $\underline{s}'$, and degree μ in t, t'.

Proposition 5.12 together with the definition of GS/TRF-ν/μ conclude the following result.

Corollary to 5.12. If $X(q)$ is a GS/TRF-ν/μ in $\mathfrak{R}^n \times T$, then

$$c_x(q_1,q_2) = \langle c_x(\underline{s},t;\underline{s}',t'), q_1(\underline{s},t)q_2(\underline{s}',t')\rangle$$

$$= \langle k_x(\underline{h},\tau), q_1(\underline{s},t)q_2(\underline{s}',t')\rangle. \tag{5.23}$$

In view of the Corollary to 5.12, condition (5.16), satisfied by all GS/TC-ν/μ $k_x(\underline{h},\tau)$, can also emerge from the fact that $c_x(q_1,q_2)$ is a nonnegative-definite bilinear in functional $Q_{\nu/\mu}$ which satisfies (5.23). A continuous and symmetric function $k_x(\underline{h},\tau)$ in $\mathfrak{R}^n \times T$ is a permissible GS/TC-ν/μ if and only if

$$\langle k_x(\underline{h},\tau), q(\underline{s},t)q(\underline{s}',t')\rangle \geqslant 0, \tag{5.24}$$

for all $q \in Q_{\nu/\mu}$. We will also say that the $k_x(\underline{h},\tau)$ is a *conditionally nonnegative-definite function* of order ν/μ.

Let $X(\underline{s},t)$ be a differentiable OS/TRF-ν/μ. By definition the

$$Y_a(\underline{s},t) = D_a^{(\nu+1,\mu+1)} X(\underline{s},t) \tag{5.25}$$

is a zero mean space homogeneous/time stationary random field for all $a \in A$, with

$$A = \{a = (\underline{\nu}^*, \mu+1) = (\nu_1,\nu_2,\ldots,\nu_n,\mu+1) : \sum_{i=1}^{n} \nu_i = \nu+1\}$$

The spectral representation of the covariance of each $Y_a(\underline{s},t)$ writes $c_{Y_a}(\underline{h},\tau) = \int\int \exp[i(\underline{w}\cdot\underline{h} + \lambda\tau)]\, d\phi_{Y_a}(\underline{w},\lambda)$, where $\phi_{Y_a}(\underline{w},\lambda)$, $a \in A$

are positive summable measures in $\mathfrak{R}^n \times T$, without atom at the origin. We define the covariance

$$\begin{aligned} c_Y(\underline{h},\tau) &= \sum_{a\in A} c_{Y_a}(\underline{h},\tau) \\ &= E\left[\sum_{a\in A} D_a^{(\nu+1,\mu+1)}X(\underline{s},t)D_a^{(\nu+1,\mu+1)}X(\underline{s}',t')\right] \\ &= \sum_{a\in A} D_a^{(2\nu+2,2\mu+2)}c_x(\underline{s},t;\underline{s}',t') \\ &= \iint \exp[i(\underline{w}\cdot\underline{h}+\lambda\tau)]\,d\phi_Y(\underline{w},\lambda), \end{aligned} \tag{5.26}$$

where $\phi_Y(\underline{w},\lambda) = \sum_{a\in A}\phi_{Y_a}(\underline{w},\lambda)$ is, also, a positive summable measure in $\mathfrak{R}^n \times T$, without atom at the origin.

A function $k_x(\underline{h},\tau)$ is a permissible GS/TC-ν/μ in the sense of Definition 5.11 if and only if it admits the following spectral representation

$$k_x(\underline{h},\tau) = \iint \frac{[\exp[i(\underline{w}\cdot\underline{h})] - p_{2\nu+1}[i(\underline{w}\cdot\underline{h})]]\,[\exp[i(\lambda\tau) - p_{2\mu+1}(i\lambda\tau)]]}{\underline{w}^{2\nu+2}\lambda^{2\mu+2}} d\phi_Y(\underline{w},\lambda) + p_{2\nu,2\mu}(\underline{h},\tau), \tag{5.27}$$

where

$$p_{2\nu+1}[i(\underline{w}\cdot\underline{h})] = \sum_{\rho=0}^{2\nu+1} i^\rho \frac{(\underline{w}\cdot\underline{h})^\rho}{\rho!},$$

and

$$p_{2\mu+1}(i\lambda\tau) = \sum_{\zeta=0}^{2\mu+1} i^\zeta \frac{(\lambda\tau)^\zeta}{\zeta!},$$

and $p_{2\nu,2\mu}(\underline{h},\tau)$ is an arbitrary polynomial of degree $\leqslant 2\nu$ in $\underline{h}$ and $\leqslant 2\mu$ in τ.

On the basis, now, of the obvious inequality

$$|\exp[i(\underline{w}\cdot\underline{h})] - p_{2\nu+1}[i(\underline{w}\cdot\underline{h})]|\,|\exp[i\lambda\tau] - p_{2\mu+1}(i\lambda\tau)| \leqslant \frac{(\underline{w}\cdot\underline{h})^{2\nu+2}(\lambda\tau)^{2\mu+2}}{(2\nu+2)!(2\mu+2)!},$$

and, since a OS/TRF$-\nu/\mu$ is also a OS/TRF $-\nu'/\mu'$ for all $\nu' > \nu$ and $\mu' > \mu$, it follows that

$$\lim_{|\underline{h}|\to\infty,\tau\to\infty} \frac{k_x(\underline{h},\tau)}{|\underline{h}|^{2\nu+2}\tau^{2\mu+2}} = 0, \tag{5.28}$$

which assures the existence of the integral (5.27). In view of the foregoing considerations, if $k_x(\underline{h},\tau) \in \mathcal{F}^X_{\nu/\mu}$, then $k_x(\underline{h},\tau) + p_{2\nu,2\mu}(\underline{h},\tau) \in \mathcal{F}^X_{\nu/\mu}$ too.

Clearly, the GS/TC-ν/μ satisfies the relation

$$\nabla^{2\nu+2}_{\underline{h}} \frac{\partial^{2\mu+2}}{\partial\tau^{2\mu+2}} k_x(\underline{h},\tau) = (-1)^{\nu+\mu} c_Y(\underline{h},\tau). \tag{5.29}$$

In relation to (5.29), the measure $\phi_Y(\underline{w},\lambda)$ is the Fourier transform of

$$(-1)^{\nu+\mu}\nabla^{2\nu+2}_{\underline{h}} \frac{\partial^{2\mu+2}}{\partial\tau^{2\mu+2}} k_x(\underline{h},\tau).$$

Employing Proposition 5.9 it is not difficult to show that the representation (5.29) is in general true for any $X(\underline{s},t)$not necessarily differentiable.

In the case now where $\phi_Y(\underline{w},\lambda)$ is differentiable, we can define the *generalized spectral density function of order* ν/μ $K_x(\underline{w},\lambda)$ as the n-fold space/time Fourier transform of $k_x(\underline{h},\tau)$. The lemma below is a immediate consequence of the preceding spectral analysis.

Lemma 5.13. Let $X(\underline{s},t)$ be a differentiable OS/TRF-ν/μ. A continuous function $k_x(\underline{h},\tau)$ in $\mathcal{R}^n \times T$ is a permissible GS/TC-ν/μ if and only if (5.28) holds true and the corresponding $K_x(\underline{w},\lambda)$ exists (in the sense of generalized functions), includes no atom at origin and is such that the $|\underline{w}|^{2\nu+2}\lambda^{2\mu+2}K_x(\underline{w},\lambda)$ is a nonnegative measure.

Note that if the space isotropic $c_Y(r,\tau)$, $r = |\underline{h}|$ is *space-time separable*, i.e., $c_Y(r,\tau) = c_Y(r)c_Y(\tau)$, then the $k_x(r,\tau)$ is separable too, i.e., $k_x(r,\tau) = k_x(r)k_x(\tau)$. We shall examine a series of cases of this type below.

Example 5.14. Consider the stochastic partial differential equation (5.4), where $Y(s,t)$ is a zero mean white noise S/TRF in $R^1 \times T$ with covariance

$$c_Y(r,\tau) = \delta(r,\tau) = \delta(r)\delta(\tau), \tag{5.30}$$

(5.20) gives

$$k_x(r,\tau) = (-1)^{\nu+\mu} \frac{r^{2\nu+1}\tau^{2\mu+1}}{(2\nu+1)!(2\mu+1)!}. \tag{5.31}$$

A generalization of the covariance (5.31) in $\mathcal{R}^n \times T$ is the isotropic GS/TC-ν/μ

$$k_x(r,\tau) = \sum_{\rho=0}^{\nu}\sum_{\zeta=0}^{\mu}(-1)^{\rho+\zeta}a_{\rho\zeta}r^{2\rho+1}\tau^{2\zeta+1}, \tag{5.32}$$

where the coefficients $a_{\rho\zeta}$ should satisfy certain permissibility conditions so that the $k_x(r,\tau)$ is a conditionally nonnegative-definite function in the sense

of (5.16); see also Lemma 5.13. More precisely the coefficients $a_{\rho\zeta}$ must be such that the following condition is satisfied:

$$\sum_{\rho=0}^{\nu}\sum_{\zeta=0}^{\mu}\frac{\Gamma((2\rho+n+1)/2)[(2\rho+1)!!][(2\zeta+1)!!]}{\rho!}a_{\rho\zeta}\omega^{2\rho-\nu}\lambda^{2\zeta-\mu}\geq 0, \tag{5.33}$$

where $\Gamma(\cdot)$ is the gamma function, for all $\omega \geq 0$ and $\lambda \geq 0$.

Based now on the observation that an OS/TRF-ν/μ of the form (5.4) can be assigned a GS/TC-ν/μ of the polynomial form (5.31), the proof of the following proposition is straightforward.

Proposition 5.15. Assume an OS/TRF-ν/μ in $\mathfrak{R}^1 \cdot T$ can be expressed by

$$X(s,t) = \sum_{\rho=0}^{\nu}\sum_{\zeta=0}^{\mu}\alpha_{\rho\zeta}\int_0^s\int_0^t\frac{(s-u)^{\rho}(t-v)^{\zeta}}{\rho!\zeta!}Y(u,v)\,du\,dv, \tag{5.34}$$

where $\alpha_{\rho\zeta}$, $\rho = 0, 1, \ldots, \nu$ and $\zeta = 0, 1, \ldots, \mu$ are suitable coefficients and $Y(s,t)$ is a zero mean white noise S/TRF in $\mathfrak{R}^1 \cdot T$. Then its GS/TC-ν/μ is of the form (5.32).

6. Stochastic partial differential equations

Stochastic differential equations over space-time have the general form

$$L[X(s,t)] = Y(s,t), \tag{6.1}$$

where $X(s,t)$ is the unknown S/TRF, $L[\cdot]$ is a given operator, and $Y(s,t)$ is a known S/TRF—also called a forcing function. Despite significant progress over the last decade or so, much work remains to be done in the theory of stochastic partial differential equations (SPDE). A partial list of references is given in [29].

We saw above that, by definition, a continuous-parameter OS/TRF-ν/μ obeys certain SPDE and the corresponding covariances (ordinary and generalized) satisfy the corresponding deterministic differential equations: If $X(s,t)$ is an OS/TRF-ν/μ, by definition, all

$$Y_i(s,t) = \frac{\partial^{\nu+\mu+2}}{\partial s_i^{\nu+1}\partial t^{\mu+1}}X(s,t) \tag{6.2}$$

are space homogeneous/time stationary, S/TRF. Let $\nu = 2m - 1$; the field

$$Y(s,t) = \sum_{i=1}^{n}Y_i(s,t) = \nabla^{\nu+1}\frac{\partial^{\mu+1}}{\partial t^{\mu+1}}X(s,t), \tag{6.3}$$

where $L[\cdot] = \nabla^{\nu+1}\frac{\partial^{\mu+1}}{\partial t^{\mu+1}}[\cdot]$, is space homogeneous/time stationary, too. This observation leads to the following result [7].

Proposition 6.1. Let $Y(\underline{s},t)$ be a space homogeneous/time stationary field. Then, there is one and only one OS/TRF-ν/μ $X(\underline{s},t)$ with representations satisfying the differential equation

$$Y(\underline{s},t) = \nabla^{\nu+1}\frac{\partial^{\mu+1}}{\partial t^{\mu+1}}X(\underline{s},t), \tag{6.4}$$

where $\nu = 2m - 1$.

An immediate consequence of Proposition 6.1 is the corollary below.

Corollary to 6.1. If $X(\underline{s},t)$ is an OS/TRF-ν/μ, then there exists an OS/TRF-$(\nu+2k)/(\mu+2\lambda)$ $Z(\underline{s},t)$ such that

$$X(s,t) = \nabla^{2k}\frac{\partial^{2\lambda}}{\partial t^{2\lambda}}Z(\underline{s},t). \tag{6.5}$$

The covariances associated with (6.2) and (6.3) are, respectively

$$c_Y = \frac{\partial^{2\nu+2\mu+4}}{\partial s_i^{\nu+1}\partial s_i'^{\nu+1}\partial t^{\mu+1}\partial t'^{\mu+1}}c_X(s,t;s',t'), \tag{6.6}$$

and

$$c_Y(\underline{h},\tau) = (-1)^{\nu+\mu}\nabla^{2\nu+2}\frac{\partial^{2\mu+2}}{\partial\tau^{2\mu+2}}k_X(h,\tau) \tag{6.7}$$

7. Discrete linear representations of spatiotemporal random fields

The key element in passing from abstract theory to a practical analysis of spatiotemporal data is the development of suitable *discrete linear representations* of the S/TRF model. This is necessary because real data are usually discretely distributed in space-time.

Let $X(s_i,t_j)$, where $(s_i,t_j) \in \mathfrak{R}^n \times T$, $i = 1,2,\ldots,m$ and $j = 1,2,\ldots,k$, be a discrete-parameter OS/TRF. Let $q \in Q = Q_m$, where Q_m is the space of real measures on $\mathfrak{R}^n \times T$ with finite support and such that

$$q(s,t) = \sum_{i=1}^{m}\sum_{j=1}^{p_i} q(s_i,t_j)\delta(s_i - \underline{s}, t_j - t)$$

$$= \sum_{i=1}^{m}\sum_{j=1}^{p_i} q_{ij}\delta_{ij}(\underline{s},t), \tag{7.1}$$

where p_i denotes the number of time instances t_j ($j = 1_i, 2_i, \ldots, p_i$) used, given that we are at the spatial position $\underline{s}_i$.

The corresponding discrete GS/TRF and CS/TRF are, respectively

$$X(q) = \left\langle \sum_{i=1}^{m} \sum_{j=1}^{p_i} q_{ij} \delta_{ij}(\underline{s}, t) X(\underline{s}, t) \right\rangle$$

$$= \sum_{i=1}^{m} \sum_{j=1}^{p_i} q_{ij} X(\underline{s}_i, t_j), \tag{7.2}$$

and

$$Y_q(\underline{s}, t) = \left\langle \sum_{i=1}^{m} \sum_{j=1}^{p_i} q_{ij} \delta_{ij}(\underline{s}', t'), S_{\underline{s},t} X(\underline{s}', t') \right\rangle$$

$$= \sum_{i=1}^{m} \sum_{j=1}^{p_i} q_{ij} S_{\underline{s},t} X(\underline{s}_i, t_j). \tag{7.3}$$

Definition 7.1. The discrete S/TRF $Y_q(\underline{s}, t)$ of (7.3) is called a *spatiotemporal increment of order* ν *in space and* μ *in time (S/TI-*ν/μ*)* on $Q_{\nu,\mu}$ if

$$\sum_{i=1}^{m} \sum_{j=1}^{p} q_{ij} s_i^{\rho} t_j^{\sigma} = 0, \tag{7.4}$$

for all $\rho \leq \nu$ and $\sigma \leq \mu$. In this case the coefficients $\{q_{ij} : Q_{\nu,\mu} = Q_m, i = 1, 2, \ldots, m \text{ and } j = 1_i, 2_i, \ldots, p_i\}$ will be termed *admissible coefficients of order* ν, μ *(AC-*ν, μ*)*.

Definition 7.2. The discrete OS/TRF $X(s, t)$ will be called a *OS/TRF-*ν, μ on $Q_{\nu,\mu}$ if the corresponding S/TI-ν, μ $Y_q(s, t)$ is a zero mean space homogeneous/time stationary RF.

A summary of continuous S/TRF-related notions and their discrete analogues are given in Figure 7.1.

Example 7.3. Consider the case illustrated in Figure 7.2, where $(\underline{s}, t) \in \mathbb{R}^2 \times I$ and $\underline{s} = (s_1, s_2)$. Let

$$Y_q(s_1, s_2, t) = \sum_{i=1}^{5} \sum_{j=1}^{3} q_{ij} X(s_{i1}, s_{i2}, t_j)$$

$$= X(s_1 + \Delta s, s_2, t + \Delta t) - 2X(s_1 + \Delta s, s_2, t) + X(s_1 + \Delta s, s_2, t - \Delta t)$$
$$+ X(s_1 + \Delta s, s_2, t + \Delta t) - 2X(s_1, s_2 + \Delta s, t) + X(s_1, s_2 + \Delta s, t - \Delta t)$$
$$+ X(s_1 - \Delta s, s_2, t + \Delta t) - 2X(s_1 - \Delta s, s_2, t) + X(s_1 - \Delta s, s_2, t - \Delta t)$$
$$+ X(s_1, s_2 - \Delta s, t + \Delta t) - 2X(s_1, s_2 - \Delta s, t) + X(s_1, s_2 - \Delta s, t - \Delta t)$$
$$- 4[X(s_1, s_2, t + \Delta t) - 2X(s_1, s_2, t) + X(s_1, s_2, t - \Delta t)]. \tag{7.5}$$

$$q(\underline{s},t)\in Q_{\nu/\mu} : q(\underline{s},t)=\sum_{i=1}^{m}\sum_{j=1_i}^{l_i} q\left(\underline{s}_i,t_j\right)\delta\left(\underline{s}_i-\underline{s},t_j-t\right)$$

THEORY	PRACTICE
$X(q)=\langle q(\underline{s},t),X(\underline{s},t)\rangle$	$X(q)=\sum_{i=1}^{m}\sum_{j=1_i}^{l_i} q_{ij}X\left(\underline{s}_i,t_j\right)$
$Y_q(\underline{s},t)=X(S_{\underline{s},t}\,q)$ $=\langle q(\underline{s}',t'),S_{\underline{s},t}\,X(\underline{s}',t')\rangle$	$Y_q(\underline{s},t)=X\left(S_{\underline{s},t}\,q\right)$ $=\sum_{i=1}^{m}\sum_{j=1_i}^{l_i} q_{ij}\,X\left(\underline{s}_i+\underline{s},t_j+t\right)$
$m_x(q)=\langle q(\underline{s},t),m_x(\underline{s},t)\rangle$	$m_x(q)=\sum_{i=1}^{m}\sum_{j=1_i}^{l_i} q_{ij}\,m_x\left(\underline{s}_i,t_j\right)$
$\langle q(\underline{s},t),g_{\rho\zeta}(\underline{s},t)\rangle=0$ $\rho\le\nu$ $\zeta\le\mu$	$\sum_{i=1}^{m}\sum_{j=1_i}^{l_i} q_{ij}\,g_{\rho\zeta}\left(\underline{s}_i,t_j\right)=0$ $\rho\le\nu$ $\zeta\le\mu$
$m_x(q)=\sum_{0\le\rho\le\nu}\sum_{0\le\zeta\le\mu}\alpha_{\rho\zeta}\langle g_{\rho\zeta}(\underline{s},t),q(\underline{s},t)\rangle$	$m_x(q)=\sum_{0\le\rho\le\nu}\sum_{0\le\zeta\le\mu} b_{\rho\zeta}\,g_{\rho\zeta}(\underline{s},t)$
$\langle k_x(\underline{s}-\underline{s}',t-t'),q(\underline{s},t)q(\underline{s}',t')\rangle\ge 0$ $q\in Q_{\nu/\mu}$	$\sum_{i=1}^{m}\sum_{j=1_i}^{l_i}\sum_{i'=1}^{m}\sum_{j'=1_{i'}}^{l_{i'}} q_{ij}\,q_{i'j'}\,k_x\left(\underline{s}_i-\underline{s}_{i'},t_j-t_{j'}\right)\ge 0$ $\{q_{ij}\}$ AC − ν/μ

Figure 7.1: S/TRF-related notions and their discrete analogues.

It is easily shown that

$$\sum_{i=1}^{5}\sum_{j=1}^{3} q_{i1,i2,j}\,s_{i1}^{\rho_1}\,s_{i2}^{\rho_2}\,t_j^{\zeta}=0$$

for all $\rho_1+\rho_2\leqslant 1$ and $\zeta\leqslant 1$. Therefore, the $Y_q(s_1,s_2,t)$ above is a S/TI-1/1.

Proposition 7.4. Let $X(\underline{s},t)$ be an OS/TRF on $Q_{\nu/\mu}$ and let

$$\hat{X}(\underline{s}_0,t_0)=\sum_{i=1}^{m}\sum_{j=1_i}^{p_i}\lambda_{ij}X(\underline{s}_i,t_j) \tag{7.6}$$

be the linear estimator of $X(\underline{s},t)$ at point/instant $\underline{s}_0,t_0$ such that

$$E[\hat{X}(\underline{s}_0,t_0)]-X(\underline{s}_0,t_0)]=0 \tag{7.7}$$

and

$$E[\hat{X}(\underline{s}_0,t_0)]=\sum_{\rho\le\nu}\sum_{\zeta\le\mu}\eta_{\rho\zeta}\underline{s}_0^{\rho}t_0^{\zeta}, \tag{7.8}$$

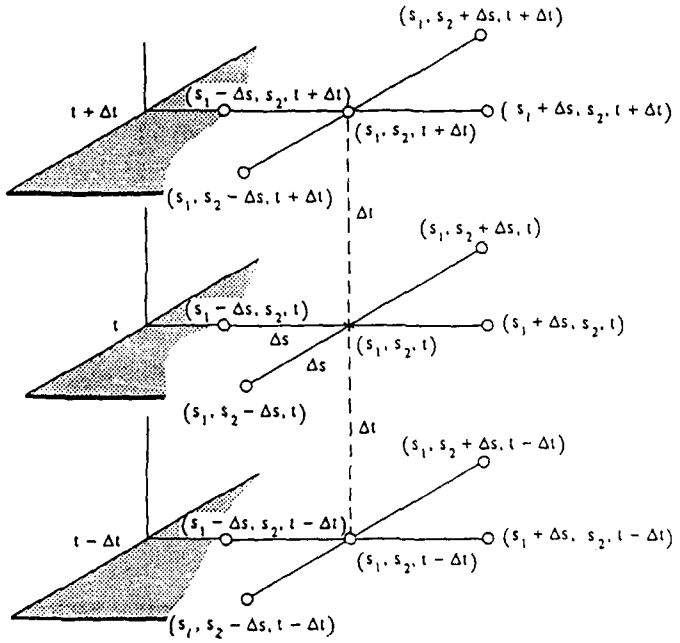

Figure 7.2: The $(\underline{s}, t) \in \Re^2 \times T$ case.

where $\eta_{\rho\zeta}$ are suitable coefficients. Then the difference

$$Y_a(\underline{s}_0, t_0) = X(\underline{s}_0, t_0) - X(\underline{s}_0, t_0) = \sum_{i=0}^{m} \sum_{j=0}^{p_i} \lambda_{ij} X(\underline{s}_i, t_j), \tag{7.9}$$

where $\lambda_{00} = -1$ and $\lambda_{i0} = \lambda_{0j} = 0$ $(i, j \neq 0)$, is an S/TI-ν/μ on $Q_{\nu,\mu}$.

Proof. See [6]. ∎

In the discrete framework, a function $k_x(\underline{h}, \tau)$ in $\Re^n \times T$ is a *generalized spatiotemporal covariance of order* ν *in space and* μ *in time (GS/TC-*ν/μ*)* if

and only if for all AC-ν/μ $\{q_{ij}\}$

$$E[X(q)]^2 = E[Y_q(\underline{0},0)]^2$$

$$= E\left[\sum_{i=1}^{m}\sum_{j=1_i}^{p_i} q_{ij}X(\underline{s}_i,t_j)\right]^2$$

$$= \sum_{i=1}^{m}\sum_{j=1_i}^{p_i}\sum_{i'=1}^{m}\sum_{j'=1_{i'}}^{p_{i'}} q_{ij}q_{i'j'}k_x(\underline{h}_{ii'},\tau_{jj'})$$

$$\geq 0, \tag{7.10}$$

where $\underline{h}_{ii'} = \underline{s}_i - \underline{s}_{i'}$, and $\tau_{jj'} = t_j - t_{j'}$.

8. Optimal estimation of spatiotemporal random fields

8.1. General considerations

In this section, we will deal with the spatiotemporal estimation problem, which has various applications in almost any scientific discipline.

In general, the spatiotemporal estimation problem can be summarized as follows:

Problem 8.1. Let $X(q)$ be a GRS-ν/μ, and let $\mathcal{H}_{\nu/\mu}$ be the Hilbert space generated by the representations $X(\underline{s},t)$ of $X(q)$ (the $X(\underline{s},t)$ may represent, for instance, the precipitation, the atmospheric pollution or a meteorologic element at position $\underline{s}$ at time t). Let $X(\underline{s}_k,t_q) \in \mathcal{H}_{\nu/\mu}$. We want to find estimates $\dot{X}(\underline{s}_k,t_q)$ of the actual values $X(\underline{s}_k,t_q)$ of the natural process of interest at unknown positions $\underline{s}_k$ and time instances t_q. The calculations are to be made on the basis of experimental data (observations) $X(\underline{s}_i,t_j)$, $i = 1, 2, \ldots, m$ and $j = 1_i, 2_i, \ldots, p_i$. More precisely, an estimate $\dot{X}(\underline{s}_k,t_q)$ is defined as an element of $\mathcal{H}_{\nu/\mu}$ which fulfills the following requirements:

1) *Linearity*, viz.

$$\dot{X}(\underline{s}_k,t_q) = \underline{\underline{\Xi}}^{\mathsf{T}}\,\underline{\underline{X}}, \tag{8.1}$$

where $\underline{\underline{\Xi}}^{\mathsf{T}} = [\xi_{ij}]$ $(i = 1, 2, \ldots, m;\ j = 1_i, \ldots, p_i)$ is a vector of real coefficients ξ_{ij} to be calculated during the estimation process, and $\underline{\underline{X}}^{\mathsf{T}} = [X(\underline{s}_i,t_j)]$ is a vector of known elements $X(\underline{s}_i,t_j) \in \mathcal{H}_{\nu/\mu}$, $(\underline{s}_i,t_j) \in A$,

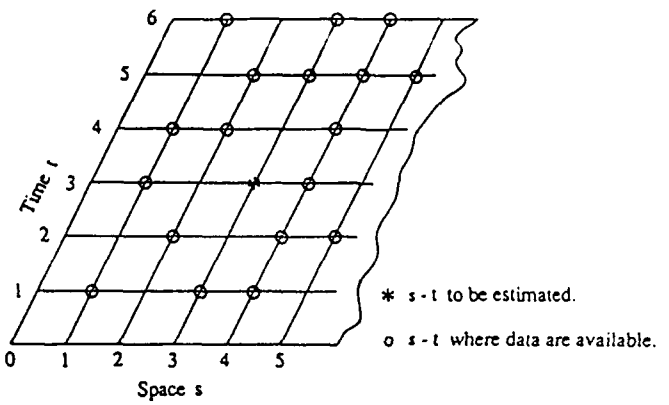

$$\hat{X}(s_3,t_3) = \sum_{i=1}^{4} \sum_{j=1_i}^{t_i} \lambda_{ij} X(s_i,t_j). \quad \text{(LINEAR)}$$

SPACE s	TIME INSTANCES t	j	t_i
1	1, 3, 4, 6	$1_1, 2_1, 3_1, 4_1$	4
2	2, 4, 5	$1_2, 2_2, 3_2$	3
3	1, 5, 6	$1_3, 2_3, 3_3$	3
4	1, 2, 3, 4, 5, 6	$1_4, 2_4, 3_4, 4_4, 5_4, 6_4$	6
5	2, 5	$1_5, 2_5$	2

Figure 8.1: The $\mathfrak{R}^1 \times T$ case of linear space-time estimation.

where A is a compact set of data points/time instances. (Figure 8.1 illustrates the $\mathfrak{R}^1 \times T$ case of such a linear estimator.)

2) *Unbiasedness*, i.e.,

$$E[Z(\underline{s}_k, t_q)] = 0, \tag{8.2}$$

where $Z(\underline{s}_k, t_q) = \hat{X}(\underline{s}_k, t_q) - X(\underline{s}_k, t_q)$.

3) *Optimality* (minimum mean square error), i.e., it must minimize the estimation error

$$\sigma_x^2(\underline{s}_k, t_q) = E[Z(\underline{s}_k, t_q)]^2. \tag{8.3}$$

$\underline{K} = [k$

This is a constrained optimization problem in $\mathfrak{R}^n \times T$ whose solution depends upon the regularity properties of the random field $X(\underline{s}, t)$ over space-time.

8.2. Optimal estimation of space nonhomogeneous/time nonstationary processes

Suppose now that the natural process can be represented by a S/TRF-ν/μ $X(\underline{s}, t)$. On the basis of Proposition 7.4, the $Z(\underline{s}_k, t_q) = \hat{X}(\underline{s}_k, t_q) - X(\underline{s}_k, t_q)$ is a S/TI-ν/μ, and its variance is given by

$$\sigma_x^2(\underline{s}_k, t_q) = \sum_{i=1}^{m} \sum_{j=1_i}^{p_i} \sum_{i'=1}^{m} \sum_{j'=1_{i'}}^{p'_i} \xi_{ij}\xi_{i'j'} k_x(\underline{h}_{ii'}, \tau_{jj'}) - 2 \sum_{i=1}^{m} \sum_{j=1_i}^{p_i} \xi_{ij} k_x(\underline{h}_{ki}, \tau_{qj}) + k_x(\underline{0}, 0), \tag{8.4}$$

($\xi_{kq} = -1$ and $\xi_{iq} = \xi_{kj} = 0$ $(i \neq k, j \neq q)$). The fact that $Z(\underline{s}_k, t_q)$ is a S/TI-ν/μ implies that

$$\sum_{i=1}^{m} \sum_{j=1_i}^{p_i} \xi_{ij} \underline{s}_i^{\rho} t_j^{\zeta} = \underline{s}_k^{\rho} t_q^{\zeta} \tag{8.5}$$

for all $0 \leqslant |\underline{\rho}| \leqslant \nu$ and $0 \leqslant \zeta \leqslant \mu$. (Note that (8.5) is, also, the unbiasedness condition (8.2)). The minimization of (8.4) with respect to ξ_{ij}'s subject to the constraint (8.5) yields the system of equations

$$\underline{\underline{K}}\,\underline{\underline{\Xi}}^* = \underline{\underline{\Theta}}; \tag{8.6}$$

$\underline{\underline{K}} = [k_x(\underline{s}_i, t_j; \underline{s}_{i'}, t_{j'}), \underline{s}_i^{\rho} t_j^{\zeta}$ $i, i' = 1, 2, \ldots, m$; $j = 1_i, \ldots, p_i$; $j' = 1_{i'}, \ldots, p_{i'}$; $|\underline{\rho}| \leqslant \nu$, $\zeta \leqslant \mu]$ is a matrix of GS/TC-ν/μ and space-time polynomials; $\underline{\underline{\Xi}}^{*\top} = [\xi_{ij}, \psi_{\rho\zeta}$, $i = 1, 2, \ldots, m$; $j = 1_i, \ldots, p_i$; $\rho = |\underline{\rho}| \leqslant \nu$; $\zeta \leqslant \mu]$ is a vector of coefficients ξ_{ij} which includes the Lagrange multipliers $\psi_{\rho\zeta}$; and the vector $\underline{\underline{\Theta}}^{\top} = [k_x(\underline{s}_k, t_q; \underline{s}_i, t_j), \underline{s}_k^{\rho} t_q^{\zeta}$; $i = 1, 2, \ldots, m$; $j = 1_i, \ldots, p_i$, $|\underline{\rho}| \leqslant \nu$, $\zeta \leqslant \mu]$.

9. Simulation in space-time

Several of the spatial simulation approaches can be extended in order to produce realizations of spatiotemporal random fields (S/TRF).

By means of the ST simulation concept [5, 8] the space n-dimensional × time random field $X_n(\underline{s}, t)$, where $(\underline{s}, t) \in \mathfrak{R}^n \times T$, can be simulated by

summing contributions from several random processes $X_{1,\underline{\theta}_i}(s_i,t)$, where $s = \underline{s}\cdot\underline{\theta}_i$, $(s_i,t)\in\Re^1\times T$; viz.

$$X_n(\underline{s},t) = \frac{1}{\sqrt{N}}\sum_{i=1}^{N} X_{1,\underline{\theta}_i}(s_i,t). \tag{9.1}$$

in which N is the number of simulation lines.

On-line realizations of the S/TRF $X_{1,\underline{\theta}_i}(s_i,t)$ can be generated in terms of its spectral density function

$$C_{1,\underline{\theta}}(\omega,\lambda) = \Psi_n^1[C_n(\underline{w},\lambda)], \tag{9.2}$$

where $\underline{w} = \omega\underline{\theta}$, by using the simulation formula

$$X_1(s,t) = \sum_{j=1}^{m}\sum_{k=1}^{K}\sqrt{2C_{1,\underline{\theta}}(\omega_j,\lambda_k)\Delta\omega_j\Delta\lambda_k}$$

$$\cos(\omega_j s - 2\pi\lambda_k t + \phi_{j,k}), \tag{9.3}$$

where the phase angles $\phi_{j,k}$ are distributed randomly but uniformly within $[0,2\pi]$.

Spatiotemporal simulation is a valuable tool in the context of random moving surfaces studies, such as sea waves and their action on structures, atmospheric pollutants and meteorological elements. Also, the simulation method may be used to develop a spatiotemporal model for rainfall generation. Space-time rainfall simulations can be used in evaluating strategies for satellite remote sensing of rainfall and for studying storm runoff problems.

10. Bibliography

[1] T.L. Bell. A space-time stochastic model of rainfall for satellite remote-sensing studies. *J. of Geophysical Research*, 92(D8):9631–9643, 1987.

[2] R.J. Bennett and R.J. Chorley. *Enviromental Systems*. Princeton University Press, Princeton, 1978.

[3] R.A. Bilonick. The space-time distribution of sulfate deposition in the northeastern United States. *Atmospheric Environment*, 19(11):1829–1845, 1985.

[4] R.L. Bras and I. Rodriguez-Iturbe. *Random Functions and Hydrology*. Addison-Wesley, Reading, MA, 1985.

[5] G. Christakos. Space transformations in the study of multidimensional functions in the hydrologic sciences. *Advances in Water Resources*, 9(1):42–48, 1986.

[6] G. Christakos. A theory of spatiotemporal random fields and its application to space-time data processing. *IEEE Trans. Systems, Man, and Cybernetics*, 21(4), 1991.

[7] G. Christakos. *Random Field Modeling in Earth Sciences*. Academic Press, Orlando, San Diego, New York, Austin, Boston, London, Sydney, Tokyo, Toronto, 1992.

[8] G. Christakos and C. Panagopoulos. Space transformation methods in the representation of random fields. *IEEE. Trans. Remote Sensing and Geosciences*, 30(1), 1992.

[9] National Research Council. *Opportunities in the Hydrologic Sciences*. National Academic Press, Washington, DC, 1991.

[10] J.P. Delhomme. Modeles de simulation et de gestion des resources en eau des basins de l'orne, la dives, et la seulles. Technical report, CIC, Centre de Geostatistique, France, 1977.

[11] M.B Fiering. Multivariate techniques for synthetic hydrology. *J. Hydraulic Div.*, pages 43–60, 1964. ASCE.

[12] L.S. Gandin. *Objective analysis of meteorological fields*. Gidrometeorologicheskoe Izdatel'stvo, Leningrad, 1963.

[13] I.M. Gel'fand. Generalized random processes. *Dokladi Akad. Nauk SSSR*, 100:853–856, 1955.

[14] I.M. Gel'fand and N.Y. Vilenkin. *Generalized Functions, 4*. Academic Press, Orlando, San Diego, New York, Austin, Boston, London, Sydney, Tokyo, Toronto, 1964.

[15] R.O. Gilbert. *Statistical Methods for Environmental Pollution Monitoring*. Van Nostrand Reinhold Company, New York, NY, 1987.

[16] U. Grenander and M. Rosenblatt. *Statistical Analysis of Stationary Time Series*. John Wiley & Sons, New York, London, Sydney, 1957.

[17] J. Haslett and A.E. Raftery. Space-time modelling with long-memory dependence: Assessing Ireland's wind power resource. *Applied Statistics*, 38(1):1–50, 1989.

[18] Ito K. Stationary random distributions. Memoirs, Series A 3, U. of Kyoto, Kyoto, Japan, 1954.

[19] R.P. Kanwal. *Generalized Functions—Theory and Technique*. Academic Press, Orlando, San Diego, New York, Austin, Boston, London, Sydney, Tokyo, Toronto, 1983.

[20] L.W. Lake and H.B. Carrol. *Reservoir Characterization*. Academic Press, Orlando, San Diego, New York, Austin, Boston, London, Sydney Tokyo, Toronto, 1986.

[21] R.S. Lindzen. Greenhouse warming: Science vs. consensus. Technical report, Center for Meteorology and Physical Meteorology, M.I.T., 1989.

[22] G. Matheron. The intrinsic random functions and their applications. *Adv. Appl. Prob.*, 5:439–468, 1973.

[23] S. Omatu and J.H. Seinfeld. Filtering and smoothing for linear discrete-time distributed parameter systems based on Wiener-Hopf theory with application to estimation of air pollution. *IEEE Trans. Systems, Man, and Cybernetics*, 11(12):785–801, 1981.

[24] A. Orlowski and K. Sobczyk. Solitons and shock waves under random external noise. *Reports on Math. Physics*, 27(1):59–71, 1989.

[25] I. Rodriguez-Iturbe and J.M. Mejia. The design of rainfall networks in time and space. *Water Resources Research*, 10(4):713–728, 1974.

[26] S. Rouhani and T.J. Hall. Space-time kriging of groundwater data. In M. Armstrong, editor, *In Geostatistics*, volume 2, pages 639–650. Kluwer Academic Publishers Group, Dordrecht, Boston, London, 1989.

[27] L. Schwartz. *Theorie des Distributions 1,2*. Paris, France, 1950-51.

[28] J.H. Shinn and S. Lynn. Do man-made sources affect the sulfur cycle of northeastern states? *Envir. Sci. Technol.*, 13:1062–1067, 1979.

[29] K. Sobczyk. *Stochastic Differential Equations*. Kluwer Academic Publishers Group, Dordrecht, Boston, London, 1991.

[30] P. Stavroulakis, editor. *Distributed Parameter Systems 1,2*. Hutchinson Ross Publishing Co., Colorado, USA, 1983.

[31] H. Von Storch, U. Weese, and J.S. Xu. Simultaneous analysis of space-time variability: Principal oscillation patterns and principal interaction patterns with applications to the southern oscillation. Technical Report 34, Max Planck Institüt für Meteorologie, Hamburg, Germany, 1989.

[32] A.M. Yaglom. Correlation theory of processes with stationary random increments of order n. *Math. USSR Sbornik*, pages 37–141, 1955. English translation in Am. Math. Soc. Trans. Ser. 2, pages 8–87, 1958.

[33] A.M. Yaglom. *Correlation Theory of Stationary and Related Random Functions: Basic Results*. Springer-Verlag, Berlin, Heidelberg, New York, London, Paris, Tokyo, Hong Kong, 1986.

Sharp results on irregular sampling of bandlimited functions†

Karlheinz Gröchenig
Dept. of Mathematics U-9
University of Connecticut
Storrs, CT 06268-3009 USA
groch@uconnvm.bitnet

Abstract We discuss the reconstruction of bandlimited functions for randomly sampled values and give an algorithm that works provided the sampling density is above the Nyquist rate.

Let f be of finite energy and bandlimited with bandwidth 2ω, i.e., $f \in L^2(\mathbb{R})$, $\operatorname{supp} \hat{f} \subseteq [-\omega, \omega]$, and let $\ldots < x_{i-1} < x_i < x_{i+1} < \ldots$ be a random sampling set, such that its density $\delta := \sup_i (x_{i+1} - x_i) < \pi/\omega$, i.e., arbitrarily close to the Nyquist rate. If f_n is the result of the algorithm after n iterations, then the rate of convergence of f_n to the original function f is $\|f - f_n\|_2 \leq (\delta\omega/\pi)^{n+1}(\pi + \delta\omega)(\pi - \delta\omega)^{-1}\|f\|_2$. This allows for good estimates of the number of iterations required to achieve a certain reconstruction accuracy.

In contrast to recent reconstruction methods: (1) an explicit and optimal estimate for the sampling density required for the convergence of the algorithm is derived, and (2) the algorithm functions independently of the sampling geometry—as long as the sampling density is higher than the Nyquist rate.

1. Introduction

In many applications the problem arises of whether a bandlimited function f is uniquely determined by its nonuniformly sampled values $f(x_n)$ and how it can be reconstructed from these samples.

In this article we discuss and compare various quantitative results on nonuniform sampling. At the 1989 ASI we outlined a new approach to nonuniform sampling which contains a new generation of iterative reconstruction algorithms [10]. In theory, these algorithms have all properties that are required for a good reconstruction algorithm: they are stable, converge for a large class of norms, possess good localization properties and

† The author acknowledges partial support by grant AFOSR-90-0311.

J. S. Byrnes et al. (eds.), Probabilistic and Stochastic Methods in Analysis, with Applications, 323–335.
© 1992 *Kluwer Academic Publishers. Printed in the Netherlands.*

work in any dimension [7, 6, 5]. However, for the algorithm to work, the sampling set was required to be "sufficiently dense." Thus it was not at all clear whether the algorithms would converge for realistic sampling sets close to the Nyquist density, and it was unknown how they would perform in practice.

Since then the numerical implementation and comparison with other methods has produced very convincing results in favor of this new class of reconstruction algorithms [2, 9].

The objective of this article is to provide some sharp estimates which explain the success of the new method. In Section 4 it is shown that for the version of the algorithm that has been implemented, the required sampling density is arbitrarily close to the Nyquist rate. Explicit estimates are given for the rate of convergence of the iterative algorithm. It is then compared with other methods that have been proposed for the complete reconstruction of bandlimited functions.

Let $L^2(\mathfrak{R})$ denote the Hilbert space of square-integrable functions on $\mathfrak{R}$ with norm $\|f\| = (\int_{-\infty}^{\infty} |f(x)|^2\, dx)^{1/2}$. For $\omega > 0$,

$$B_\omega^2 = \{f \in L^2(\mathfrak{R}) : \operatorname{supp} \hat{f} \subseteq [-\omega, \omega]\}$$

denotes the closed subspace of square-integrable bandlimited functions with bandwidth ω. Here the Fourier transform is defined by $\hat{f}(\xi) = \int_{\mathfrak{R}} f(x) e^{-ix\xi}\, dx$. $\chi_A(x)$ is the characteristic function of a set A.

B_ω^2 is a Hilbert space with reproducing kernel $L_y \operatorname{sinc} \omega(x) = \sin \omega(x - y)/\omega(x - y)$, where $\operatorname{sinc} x = \sin x/x$ and $L_y f(x) = f(x - y)$ denotes the shift operator. In other words,

$$f(y) = \int_{\mathfrak{R}} f(x) \operatorname{sinc} \omega(x - y)\, dx. \tag{1.1}$$

B_ω^2 has the orthonormal basis $\{\operatorname{sinc} \omega(x - \pi n/\omega), n \in \mathfrak{Z}\}$. A combination of both facts yields the cardinal series for $f \in B_\omega^2$

$$f(x) = \sum_{n \in \mathfrak{Z}} f(\pi n/\omega) \operatorname{sinc} \omega(x - \pi n/\omega)$$

The sampling rate $(\pi/\omega)^{-1}$ is the so-called Nyquist density. It is the lowest density at which complete reconstruction is possible in a stable way [16].

Since $L_y \operatorname{sinc} \omega x$ is the reproducing kernel, the reconstruction of f from $f(x_n) = \int f(x) \operatorname{sinc} \omega(x - x_n)\, dx$ is a version of the moment problem. Statements about sampling are therefore equivalent to statement about spanning properties of the sequence $L_{x_n} \operatorname{sinc} \omega x$. Thus conditions when a sequence $L_{x_n} \operatorname{sinc} \omega x, n \in \mathfrak{Z}$, or equivalently $e^{ix_n\xi} \chi_{[-\omega,\omega]}(\xi) = (L_{x_n} \operatorname{sinc} \omega x)\hat{}(\xi)$, constitutes (1) a Riesz basis, or (2) a frame, or (3) a weighted frame for B_ω^2 ($L^2([-\omega, \omega])$ respectively) lead naturally to sampling theorems.

Sections 2 through 4 explain the reconstruction methods related to these possibilities and discuss their advantages and disadvantages in the numerical treatment of nonuniform sampling. Section 5 contains the proof of Theorem 4.1, which is the most recent and currently most efficient algorithm.

2. Kadec's 1/4-Theorem

The first sampling theorem is implicit in the work of Paley and Wiener [20] on nonharmonic Fourier series and deals with the question when a sequence $e^{ix_n t}$ forms a basis for $L^2(-\omega, \omega)$. The sharp constant $1/4$ is due to Kadec [15]. For statements in the engineering literature see [1, 13, 19, 23].

Recall that a sequence $e_n, n \in \mathbb{Z}$ is called a Riesz basis of a Hilbert space $\mathcal{H}$, if it is the image of an orthonormal basis of $\mathcal{H}$ under a bounded, invertible, linear operator.

Theorem 2.1. If $x_n, n \in \mathbb{N}$ is a nonuniform sampling set for which

$$\left| x_n - \frac{\pi n}{\omega} \right| \leq L < \frac{\pi}{4\omega}, \qquad n \in \mathbb{Z} \tag{2.1}$$

then there exists a sequence g_n in B^2_ω, such that for every $f \in B^2_\omega$

$$f(x) = \sum_{n \in \mathbb{Z}} f(x_n) g_n(x) \tag{2.2}$$

where the series converges in the L^2-norm. The collection $\operatorname{sinc} \omega(x - x_n), n \in \mathbb{Z}$ is an Riesz basis for B^2_ω with biorthogonal system g_n.

2.1. Advantages

- The required sampling rate is exactly the Nyquist rate.
- Since the proof of this theorem is based on the inversion of a linear operator by a Neumann series [24], the reconstruction of f from the samples $f(x_n)$ could be formulated as an iterative algorithm, see Section 3 and Section 4.
- The functions $\{g_n\}$ of the biorthogonal basis are known explicitly in terms of Lagrange interpolation functions [17]. Let $g(x) = (x - x_0) \prod_{n=1}^{\infty} (1 - x/x_n)(1 - x/x_{-n})$, then $g_n(x) = g(x)/((x - x_n) g'(x_n))$.
- Both collections $\operatorname{sinc} \omega(x - x_n), n \in \mathbb{Z}$ and $g_n, n \in \mathbb{Z}$ are linearly independent. This fact has two important consequences:

  1) The coefficients c_i in the expansion $f = \sum_n c_n g_n$ are uniquely determined, namely $c_n = f(x_n)$.
  2) *Interpolation:* For every sequence $\lambda_n \in l^2$ there is a $f \in B^2_\omega$, such that $f(x_n) = \lambda_n$, specifically $f = \sum_n \lambda_n g_n$.

2.2. Disadvantages

- The sampling sets $x_n, n \in \mathbb{Z}$ are restricted to jittered versions of regular sampling.
- Although "explicitly" known, the g_n's are too complicated for use in numerical work.
- The sinc $\omega(x - x_n), n \in \mathbb{Z}$ are linearly independent. This implies that a function cannot be reconstructed completely if even only one sample is missed.
- *Instability:* If only one sampling location is changed, then all g_n's change drastically [21].

The applicability of Kadec's theorem in numerical work seems to be limited.

3. Duffin-Schaeffer's theorem on frames

The requirement that translates of sinc form a basis for B^2_ω is too strong to allow random sampling. A more realistic approach to sampling demands:

- the signal is uniquely determined by the samples, in other words, L_{x_n} sinc ωx spans B^2_ω, and
- the sampling is stable.

Both requirements can be expressed by

$$\|f\| \leq C \left(\sum_{n \in \mathbb{Z}} |f(x_n)|^2 \right)^{1/2} \tag{3.1}$$

The underlying abstract concepts were introduced in the fundamental paper by Duffin and Schaeffer [3]. For an exposition of this and related material in the context of nonharmonic Fourier series see also the monograph of R. Young [24].

A sequence $e_n, n \in \mathbb{Z}$ in a (separable) Hilbert space $\mathcal{H}$ is called a *frame* for $\mathcal{H}$, if there are two constants $A, B > 0$, such that for all $f \in \mathcal{H}$

$$A\|f\|^2_{\mathcal{H}} \leq \sum_n |\langle e_n, f\rangle|^2 \leq B\|f\|_{\mathcal{H}} \tag{3.2}$$

The constants A and B are called the *frame bounds*. From (3.2) follows that f is uniquely determined by the frame coefficients $\langle e_n, f\rangle$. It is remarkable that the equivalence of norms (3.2) implies a simple iterative reconstruction method. Define the frame operator S by

$$Sf = \sum_{n \in \mathbb{Z}} \langle e_n, f\rangle e_n \tag{3.3}$$

then by (3.2) S is bounded below and above and consequently S is invertible on $\mathcal{H}$. Setting $\alpha = 2/(A + B)$, f can be reconstructed recursively by

$$\phi_0 = \alpha S f \qquad \phi_{n+1} = \phi_n - \alpha S \phi_n \qquad f = \sum_{n=0}^{\infty} \phi_n \tag{3.4}$$

If $f_n = \sum_{k=0}^{n} \phi_k$ is the result after n iterations, then

$$\|f - f_n\|_{\mathcal{H}} \leq \left(\frac{B-A}{B+A}\right)^{n+1} \frac{B}{A} \|f\|_{\mathcal{H}} \tag{3.5}$$

and f_n converges to f at a geometric rate. α is called the *relaxation parameter*. The precise value of α in (3.4) is not crucial, the algorithm converges for all values of α between 0 and $2/\|S\|$. The choice $\alpha = 2/(A + B)$ yields the fastest convergence and the best numerical results.

In [3], Duffin and Schaeffer give conditions under which the sequence $\{\operatorname{sinc} \omega(x - x_n)\}$ is a frame for B^2_ω. For a converse see [14]. Most algorithms that were considered in engineering are reformulations or slight modifications of the frame method [19, 18, 22, 23].

Theorem 3.1. If for some constants α, D and $\gamma < 1$ the sampling set $x_n, n \in \mathbb{Z}$ satisfies $|x_n - x_m| \geq \alpha > 0$ for $m \neq n$ and

$$\left|x_n - \gamma \frac{\pi n}{\omega}\right| \leq D, \qquad n \in \mathbb{Z} \tag{3.6}$$

then sequence $\{\operatorname{sinc} \omega(x - x_n)\}$ is a frame for B^2_ω. There exist $A, B > 0$ such that for all $f \in B^2_\omega$

$$A\|f\|_2^2 \leq \sum_{n \in \mathbb{Z}} |f(x_n)|^2 \leq B\|f\|_2^2. \tag{3.7}$$

Consequently $f \in B^2_\omega$ can be reconstructed by the algorithm (3.4) with the frame operator

$$Sf(x) = \sum_n f(x_n) \operatorname{sinc} \omega(x - x_n) \tag{3.8}$$

3.1. Advantages

- The sampling rate in (3.6), i.e., the average number of samples in an interval of length 1, is $(\gamma\pi/\omega)^{-1}$ and thus arbitrarily close to the Nyquist rate.
- The sampling set may be fairly irregular and may have gaps of a fixed maximal length D, provided that they are compensated by more samples between the gaps.

- The sequence L_{x_n} sinc ωx is *overcomplete* in B^2_ω, and linearly dependent. The practical consequence of the overcompleteness cannot be overestimated. It means that even if a finite number of samples is missed, the signal f can still be completely recovered (possibly at a slower rate of convergence of the algorithm). It is this property which makes "inexact" frames so useful and often preferable to orthogonal or Riesz bases.

3.2. Disadvantages

- Since the proof in [3] uses heavy complex analysis, explicit numerical estimates for the frame bounds A and B are hard to come by. Therefore a suitable relaxation parameter has to be determined by experiment. Thus estimate (3.5) is not as useful as it looks at first glance.
- The sampling set is still just a perturbation of the regular sampling set $\gamma\pi n/\omega, n \in \mathbb{Z}$. The average number of samples in an interval of length 1 is $(\gamma\pi/\omega)^{-1}$. This excludes sampling sets with local variations of the density and thus many situations of practical interest. For instance, in sections of high interest one might want to sample at 10-fold the Nyquist rate, in sections of less interest just above the Nyquist rate. Of course, in order to satisfy (3.6), the excess samples could be dropped. But in most applications it seems quite unreasonable to throw away substantial information just to make the algorithm converge. Rather, one would look for a better algorithm.

  Let us also mention that from numerical experiments it is known that when gaps alternate with bunches of samples in accordance with (3.6), then the algorithm converges rather slowly.
- Since the functions sequence L_{x_n} sinc ωx are linearly dependent, the interpolation problem $f(x_n) = \lambda_n$ does not have a solution $f \in B^2_\omega$ for all sequences $\lambda_n \in l^2$.

4. A new algorithm and weighted frames

This section explains a new algorithm which overcomes most of the difficulties of the methods in Section 2 and Section 3. This algorithm emerges as a simplified version of a new generation of reconstruction algorithms which were explored in [4, 7, 6, 8, 5]. The material on the quantitative theory with sharp estimates is taken from [11].

Let the sampling set $x_n, n \in \mathbb{Z}$, be arranged in increasing order, $\ldots \leq x_{n-1} \leq x_n \leq x_{n+1} \leq \ldots$. Denote the midpoints by $y_n = (x_{n+1} + x_n)/2$ and set $\chi_n = \chi_{[y_{n-1}, y_n)}$. Then $y_n - x_n \leq \delta/2$, $x_n - y_{n-1} \leq \delta/2$ and $\sum_{n=-\infty}^{\infty} \chi_n(x) = 1$ for all x. P denotes the orthogonal projection from $L^2(\mathbb{R})$ onto B^2_ω, and is defined by $(Pf)^\wedge = \chi_{[-\omega,\omega]} \cdot \hat{f}$ a.e.

Theorem 4.1.

Reconstruction: *If*

$$\delta = \sup_{n\in\mathbb{Z}}(x_{n+1} - x_n) < \pi/\omega, \tag{4.1}$$

then every $f \in B_\omega^2$ can be completely reconstructed from the sampling values $f(x_n)$ by the following algorithm:

$$\phi_0 = P\left(\sum_{n\in\mathbb{Z}} f(x_n)\chi_n\right) \tag{4.2}$$

$$\phi_{k+1} = \phi_k - P\left(\sum_{n\in\mathbb{Z}} \phi_k(x_n)\chi_n\right) \tag{4.3}$$

and

$$f = \sum_{k=0}^{\infty} \phi_k \tag{4.4}$$

where all sums converge in L^2

Rate of convergence: Let $f_n = \sum_{k=0}^{n} \phi_k$ be the resulting approximation of f after n iterations of (4.3). Then

$$\|f - f_n\| \leq \left(\frac{\delta\omega}{\pi}\right)^{n+1} \frac{\pi + \delta\omega}{\pi - \delta\omega}\,\|f\| \tag{4.5}$$

From the estimates in the proof, we obtain the following important corollary on the stability of the algorithm and an alternate reconstruction method.

Corollary to 4.1. If w_n denotes the weights $w_n = \int \chi_n(x)\,dx = y_{n+1} - y_n$, then

$$\left(1 - \frac{\delta\omega}{\pi}\right)^2 \|f\| \leq \sum_{n\in\mathbb{Z}} |f(x_n)|^2 w_n \leq \left(1 + \frac{\delta\omega}{\pi}\right)^2 \|f\|. \tag{4.6}$$

In other words, the sequence

$$\sqrt{w_n}\,\operatorname{sinc}\omega(x - x_n) \qquad n \in \mathbb{Z}$$

is a (weighted) frame for B_ω^2 with the explicit frame bounds $A = (1 - \delta\omega/\pi)^2$ and $B = (1 + \delta\omega/\pi)^2$. According to (3.4), this yields the following reconstruction of f. Let

$$(S_w f)(x) = \left(1 + \frac{\delta^2\omega^2}{\pi^2}\right)^{-1} \sum_{n\in\mathbb{Z}} f(x_n) w_n \operatorname{sinc}\omega(x - x_n) \tag{4.7}$$

be the weighted frame operator, then

$$\phi_0 = S_w f \qquad \phi_{k+1} = \phi_k - S_w \phi_k \qquad f = \sum_{k=0}^{\infty} \phi_k \tag{4.8}$$

Since $2/(A+B) = (1+\frac{\delta^2\omega^2}{\pi^2})^{-1}$, $\gamma = (B-A)/(B+A) = 2\delta\omega/(\pi+\delta^2\omega^2/\pi)$, and $B/A = (\pi+\delta\omega)^2/(\pi-\delta\omega)^2$, the rate of convergence of $f_n = \sum_{k=0}^{n} \phi_k$ to f is as in (4.5)

$$\|f - f_n\| \leq \gamma^{n+1} \frac{(\pi+\delta\omega)^2}{(\pi-\delta\omega)^2} \|f\|$$

The proofs of Theorem 4.1 and its corollary are given in the final section.

Besides the general advantages and disadvantages of the frame method which were discussed in the previous section, we would like to emphasize the following peculiarities of the new method.

4.1. Advantages

- The algorithm converges whenever the largest gap between the samples is smaller than the Nyquist distance π/ω.
- Since no other conditions are imposed, the sampling set may be truly random; in particular, the algorithm handles local variations of the density quite well. Because of the use of the weights w_n the sequence $\sqrt{w_n}L_{x_n}$ sinc ωx is a frame in many situations, where Theorem 3.1 does not apply; for instance, when there is no positive minimal distance between the sampling points.
- The proof is much simpler than for the theorems of Kadec and Duffin-Schaeffer. All constants are explicit in terms of the maximal gap length and the size of the spectrum. The explicit calculation of the frame bounds and of the rate of convergence allows the number of iterations that are necessary to achieve a given accuracy to be determined a priori. For instance, in order to obtain an accuracy of 0.1% on a CD-player with 4-fold oversampling ($\delta\omega/\pi = 1/4$), only five iterations are necessary.
- Since after the removal of a finite number of points the sampling set still satisfies either (4.1) or (3.6), the algorithm provides a complete reconstruction of the signal even when a finite number of samples are missing or lost.

4.2. Disadvantages

Condition (4.1) is stronger than (3.6) and does not allow any gaps in the sampling set. If gaps do occur, the frame algorithm is still applicable, however at the cost of a slower rate of convergence.

Remark 4.2. The algorithms of Section 3 and Section 4 have been implemented and tested intensively by H.G. Feichtinger and his collaborators at the University of Vienna [2, 9]. From these experiments, it became clear that the best currently available reconstruction algorithm is (4.7) and (4.8), the "adaptive weights method." Since it is much easier to implement than the recursion of Theorem 4.1, it requires less time for the same number of iterations.

The performance of the ordinary frame method gets worse with increasing randomness of the sampling set.

Remark 4.3. A detailed error analysis that applies for an large class of reconstruction algorithms will appear in [5].

Remark 4.4. Theorem 4.1 has several interesting variations: complete reconstruction from local averages, random sampling with derivatives, and higher convergence rate through smoother approximation operators. We refer to [11] for detailed statements.

5. Proof of Theorem 4.1 and its corollary

For the proof of Theorem 4.1 we need the following well-known inequalities.

Lemma 5.1 (Wirtinger's inequality). If $f, f' \in L^2(a,b)$ and either $f(a) = 0$ or $f(b) = 0$, then

$$\int_a^b |f(x)|^2\,dx \leqslant \frac{4}{\pi^2}(b-a)^2 \int_a^b |f'(x)|^2\,dx \tag{5.1}$$

The lemma follows from [12, p. 184], by a change of variables. We use Wirtinger's inequality in the following form: If $f(c) = 0$ for $a < c < b$, then

$$\int_a^b |f(x)|^2\,dx \leqslant \frac{4}{\pi^2}\max\left((c-a)^2,(b-c)^2\right)\int_a^b |f'(x)|^2\,dx \tag{5.2}$$

which follows immediately from writing $\int_a^b = \int_a^c + \int_c^b$ and applying (5.1) to each term.

Lemma 5.2 (Bernstein's inequality). If $f \in B_\omega^2$, then $f' \in B_\omega^2$ and

$$\|f'\| \leqslant \omega\|f\| \tag{5.3}$$

Proof (of Theorem 4.1). Define

$$Af = P\left(\sum_{n\in\mathfrak{L}} f(x_n)\chi_n\right) \tag{5.4}$$

It is easily seen that A is a bounded linear operator from B^2_ω into B^2_ω (see also (5.7) below). The iteration step (4.3) requires an estimate on $\|f-Af\|$ for $f \in B^2_\omega$. By writing $f \in B^2_\omega$ as $f = Pf = P(\sum f\chi_n)$ one obtains

$$\begin{aligned}\|f - Af\|^2 &= \left\| P\left(\sum_{n\in\mathfrak{Z}} (f - f(x_n))\,\chi_n\right)\right\|^2 \\ &\leqslant \left\|\sum_{n\in\mathfrak{Z}} (f - f(x_n))\chi_n\right\|^2 \\ &= \int_{\mathfrak{R}} \left|\sum_n (f(x) - f(x_n))\chi_n\right|^2 dx \qquad (5.5)\end{aligned}$$

Since the χ_n's are characteristic functions and have mutually disjoint support, the last expression equals

$$\int_{\mathfrak{R}} \left(\sum_n |f(x) - f(x_n)|^2 \chi_n(x)\right) dx = \sum_n \int_{y_{n-1}}^{y_n} |f(x) - f(x_n)|^2\, dx \qquad (5.6)$$

Next one applies Wirtinger's inequality (5.2) to each term:

$$\begin{aligned}&\int_{y_{n-1}}^{y_n} |f(x) - f(x_n)|^2\, dx \\ &\quad\leqslant \frac{4}{\pi^2} \max\{(x_n - y_{n-1})^2, (y_n - x_n)^2\} \int_{y_{n-1}}^{y_n} |f'(x)|^2\, dx \\ &\quad\leqslant \frac{\delta^2}{\pi^2} \int_{y_{n-1}}^{y_n} |f'(x)|^2\, dx\end{aligned}$$

since $y_n - x_n \leqslant \delta/2$ and $x_n - y_{n-1} \leqslant \delta/2$.

Summing over n and using Bernstein's inequality, one obtains

$$\|f - Af\|^2 \leqslant \frac{\delta^2}{\pi^2} \sum_n \int_{y_{n-1}}^{y_n} |f'(x)|^2\, dx = \frac{\delta^2}{\pi^2} \|f'\|^2 \leqslant \frac{\delta^2\omega^2}{\pi^2} \|f\|^2$$

Thus we have obtained the basic estimate

$$\|f - Af\| \leqslant \frac{\delta\omega}{\pi} \|f\| \qquad \text{for all } f \in B^2_\omega \qquad (5.7)$$

This means that for $\delta\omega/\pi < 1$ the operator A is invertible on B^2_ω with the inverse

$$A^{-1} = \sum_{n=0}^{\infty} (Id - A)^n \qquad (5.8)$$

and

$$f = A^{-1}Af = \sum_{n=0}^{\infty} (Id - A)^n Af \tag{5.9}$$

Setting $\phi_0 = Af$ and

$$\phi_n = (Id - A)^n Af = (Id - A)(Id - A)^{n-1} Af$$

$$= \phi_{n-1} - A\phi_{n-1} \tag{5.10}$$

yields the algorithm (4.2)–(4.4). Since the start of the iteration is ϕ_0, the reconstruction indeed contains only the information on the samples $f(x_n)$.

For the error estimate (4.5) we observe that with (4.4), (5.9) and (5.10)

$$f - f_n = \sum_{k=n+1}^{\infty} \phi_k = \sum_{k=n+1}^{\infty} (Id - A)^k Af \tag{5.11}$$

From (5.7) one deduces

$$\|(Id - A)^k Af\| \leqslant \left(\frac{\delta\omega}{\pi}\right)^k \|Af\|_2 \tag{5.12}$$

and

$$\|Af\| \leqslant \|f\| + \|Af - f\| \leqslant \left(1 + \frac{\delta\omega}{\pi}\right) \|f\|_2 \tag{5.13}$$

Combining these estimates yields

$$\|f - f_n\| \leqslant \sum_{k=n+1}^{\infty} \left(\frac{\delta\omega}{\pi}\right)^k \left(1 + \frac{\delta\omega}{\pi}\right) \|f\|$$

$$= \left(\frac{\delta\omega}{\pi}\right)^{n+1} \frac{\pi + \delta\omega}{\pi - \delta\omega} \|f\| \tag{5.14}$$

∎

Proof (of Corollary to 4.1). The upper frame bound $B = 1 + \delta\omega/\pi$ in (4.6) follows from (5.13).

For the lower bound $A = 1 - \delta\omega/\pi$, we observe that by (5.8) and (5.7) A^{-1} has the operator norm $\|A^{-1}\| \leqslant (1 - \delta\omega/\pi)^{-1}$. The equality $\|\sum_{n\in\mathcal{Z}} f(x_n)\chi_n\|^2 = \sum_{n\in\mathcal{Z}} |f(x_n)|^2 w_n$ follows from a simple computation similar to (5.6). Altogether we obtain

$$\|f\| = \|A^{-1}Af\| \leqslant \|A^{-1}\| \, \|P\| \, \|\sum_{n\in\mathcal{Z}} f(x_n)\chi_n\|$$

$$\leqslant \left(1 - \frac{\delta\omega}{\pi}\right)^{-1} \left(\sum_{n\in\mathcal{Z}} |f(x_n)|^2 w_n\right)^{1/2}$$

and everything is proved. ∎

6. Bibliography

[1] F. Beutler. Sampling theorems and bases in Hilbert space. *Inform. Contr.*, 4:97–117, 1961.

[2] C. Cenker, H.G. Feichtinger, and M. Herrmann. Iterative algorithms in irregular sampling: a comparison of methods. In *Proc. IPCCC*, pages 483–489, Scottsdale, Arizona, 1991. IEEE Comp. Soc.

[3] R. Duffin and A. Schaeffer. A class of nonharmonic Fourier series. *Trans. Amer. Math. Soc.*, 72:341–366, 1952.

[4] H.G. Feichtinger. Discretization of convolution and reconstruction of bandlimited functions. *J. Approx. Th.* To appear.

[5] H.G. Feichtinger and K. Gröchenig. Error analysis in regular and irregular sampling theory. *Applicable Analysis.* To appear.

[6] H.G. Feichtinger and K. Gröchenig. Irregular sampling theorems and series expansions of bandlimited functions. *J. Math. Anal. Appl.* To appear.

[7] H.G. Feichtinger and K. Gröchenig. Iterative reconstruction of multivariate band-limited functions from irregular sampling values. *SIAM J. Math. Anal.* To appear.

[8] H.G. Feichtinger and K. Gröchenig. Multidimensional irregular sampling of bandlimited functions in L^p-spaces. In *Proc. Conf. Oberwolfach*, ISNM 90, pages 135–142, Birkhäuser, February 1989.

[9] H.G. Feichtinger, K. Gröchenig, and M. Hermann. Iterative methods in irregular sampling theory. In *Aachener Symposium für Signaltheorie, ASST 1990*, Informatik Fachber. 253, pages 160–166, Aachen. Springer.

[10] K. Gröchenig. A new approach to irregular sampling of bandlimited functions. In J.S. Byrnes and Jennifer L. Byrnes, editors, *Recent Advances in Fourier Analysis and its Applications: Proceedings of the NATO Advanced Study Institute*, volume 315 of *NATO ASI series C: Mathematical and physical sciences*, pages 251–260, Dordrecht, Boston, London, 1990. Kluwer Academic Publishers Group. Held at Il Ciocco Resort, Tuscany, Italy.

[11] K. Gröchenig. Reconstruction algorithms in irregular sampling. *Math. Comp.*, 1992. To appear.

[12] G. Hardy, J.E. Littlewood, and G. Pólya. *Inequalities.* Cambridge University Press, second edition, 1952.

[13] J.R. Higgins. A sampling theorem for irregularly sampled points. *IEEE Trans. Information Theory*, pages 621–622, September 1976.

[14] S. Jaffard. *A density criterium for frames of complex exponentials.* PhD thesis, L'Ecole Polytechnique, 1989.

[15] M.I. Kadec. The exact value of the Paley-Wiener constant. *Soviet Math. Dokl.*, 5:559–561, 1964.

[16] H. Landau. Necessary density conditions for sampling and interpolation of certain entire functions. *Acta Math*, 117:37–52, 1967.

[17] N. Levinson. Gap and density theorems. *Coll. Publ.*, 26, 1940.

[18] F. Marvasti and M. Analoui. Recovery of signals from nonuniform samples using iterative methods. In *Proc. Int. Symp. Circuits Syst.*, Portland, OR, May 1989.

[19] F.A. Marvasti. *A unified approach to zero-crossing and nonuniform sampling of single and multidimensional systems.* Nonuniform, P.O. Box 1505, Oak Park, IL 60304, 1987.

[20] R.E.A.C. Paley and N. Wiener. Fourier transforms in the complex domain. *AMS Coll. Publ.*, 19, 1934.

[21] W. Splettstößer. Unregelmäßige Abtastungen determinierter und zufälliger Signale. In H.G. Zimmer and V. Neuhoff, editors, *Kolloquium DFG-Schwerpunktprogramm Digitale Signalverarbeitung*, pages 1–4, Göttingen, 1981.

[22] R.G. Wiley. Recovery of bandlimited signals from unequally spaced samples. *IEEE Trans. Communications*, 26:135–137, 1978.

[23] K. Yao and J.O. Thomas. On some stability and interpolatory properties of nonuniform sampling expansions. *IEEE Trans. Circuit Theory*, 14:404–408, 1967.

[24] R. Young. *An Introduction to Nonharmonic Fourier Series.* Academic Press, New York, 1980.

Some recent results on the sampling theorem†

Christian Houdré
Department of Mathematics
University of Maryland
College Park, MD 20742 USA
ch@hilda.umd.edu

Abstract We study the a.s. convergence in the irregular sampling theorem. For bandlimited processes, we obtain necessary and sufficient conditions for exact recovery of almost all sample paths of the signal. No stationarity assumption is needed, but a spectral representation is.

1. Introduction

The sampling theorem, variously attributed in the regular case to Kotel'nikov, Shannon and Whittacker, has been the subject of numerous studies with both theoretical and applied flavors. This is reflected in the extensive bibliography available in the comprehensive works of Jerri [7] and Higgins [3]. However, as far as path reconstruction of stochastic processes is concerned, rather few results are available. Under the assumption of a stochastic model, the usual approach in the literature is to obtain, say, mean square reconstruction which follows quite directly from the deterministic sampling results. When a path of a process is observed and sampled, reconstruction "on average," i.e., in mean square, might be inadequate and path reconstruction has to be considered.

Only a few papers are concerned with reconstructing the paths of a process. Firstly, Belayev [1] obtained exact reconstruction via the cardinal series for stationary processes under a guard band assumption, i.e., the process is bandlimited to $(-\pi, \pi)$ while the sampling rate is greater than $1/\pi$. Secondly Piranashvili [10], still under a guard band assumption, extended Belayev's result to include some classes of nonstationary processes. Thirdly, Gaposhkin [2] gave, as a consequence to a general theorem on the almost sure convergence of stochastic integrals, a necessary and sufficient condition for path reconstruction of stationary processes bandlimited to $(-\pi, \pi)$, the

† Research supported by ONR Contracts No. N00014-91-J-1003 and N00014-89-C-0310.

J. S. Byrnes et al. (eds.), Probabilistic and Stochastic Methods in Analysis, with Applications, 337–341.
© 1992 *Kluwer Academic Publishers. Printed in the Netherlands.*

sampling rate being $1/\pi$. Gaposhkin's result is also limited to uniform sampling points and so the recovery is achieved via the cardinal series.

In the work presented below, both the assumptions on the stationarity of the process and the regularity of the samples are relaxed, and no moment condition is needed. A criterion is provided for the path recovery of some classes of nonstationary bandlimited processes using irregularly spaced samples.

2. Preparation

Let $(\Omega, \mathcal{B}, \mathcal{P})$ be a probability space. For $0 \leqslant \alpha \leqslant 2$, let $L^\alpha(\Omega, B, \mathcal{P})(L^\alpha(\mathcal{P})$ for short) be the corresponding space of complex-valued random variables equipped for $0 < \alpha \leqslant 2$ with the (quasi-)norms $(\mathcal{E}|\cdot|^\alpha)^{1/\alpha}$, while on $L^0(\mathcal{P})$, the topology is the one induced by convergence in probability. The main class of processes considered here have a spectral representation, namely, $X_t = \int_{\mathfrak{R}} e^{i\lambda t}\, dZ(\lambda)$, $t \in \mathfrak{R}$, where the random measure, $Z : \mathcal{B}(\mathfrak{R}) \to L^\alpha(\mathcal{P})$, $0 \leqslant \alpha \leqslant 2$ is σ-additive. Using the terminology of [4, 5] (where the reader can find more details, examples, references) these processes are (bounded continuous) (α, ∞)-bounded. Essential to our approach is the following result (again see [4, 5]).

Lemma 2.1. Let $X = \{X_t\}_{t\in\mathfrak{R}}$, $X_t \in L^\alpha(\Omega, B, \mathcal{P})$, be (α, ∞)-bounded, $0 \leqslant \alpha \leqslant 2$, with random measure Z_X. Then, there exists a probability space $(\dot{\Omega}, \dot{B}, \dot{\mathcal{P}})$ with $L^2(\mathcal{P}) \subset L^2(\dot{\mathcal{P}})$, a stationary process $Y = \{Y_t\}_{t\in\mathfrak{R}}$, $Y_t \in L^2(\dot{\mathcal{P}})$ and a random variable $\Lambda \in L^{2\alpha/2-\alpha}(\mathcal{P})$ such that $X_t = \Lambda P Y_t$, $t \in \mathfrak{R}$, where P is the orthogonal projection from $L^2(\dot{\mathcal{P}})$ to $L^2(\mathcal{P})$.

In Lemma 2.1 Z_Y, the random measure of Y, is orthogonally scattered; hence there exists a finite positive measure F such that

$$\mathcal{E}\left|\int_{\mathfrak{R}} f\, dPZ_Y\right|^2 \leqslant \|P\|^2 \mathcal{E}\left|\int_{\mathfrak{R}} f\, dZ_Y\right|^2 = \|P\|^2 \int_{\mathfrak{R}} |f|^2\, dF$$

for all $f \in L^2(F)$.

Now that the probability material has been given let us state another lemma which is a particular case of a beautiful and important result of Levinson [8, IV].

Lemma 2.2. Let $\{t_k\}_{k\in\mathfrak{Z}}$ be a sequence of reals such that $\sup_k |t_k - k| < 1/4$. Then the set $\{e^{i\lambda t_k}\}_{k\in\mathfrak{Z}}$ is complete in $L^2(-\pi, \pi)$ and there exists a unique biorthogonal set $\{h_k\}_{k\in\mathfrak{Z}} \subset L^2(-\pi, \pi)$ such that, for any $g \in L^2(-\pi, \pi)$, the ordinary Fourier series $\sum_{-\infty}^{+\infty} e^{i\lambda k}\hat{g}(k)$ and the nonharmonic Fourier

series $\sum_{-\infty}^{+\infty} e^{i\lambda t_k} \int_{-\pi}^{\pi} h_k(x)g(x)\,dx$ are uniformly equiconvergent on every compact subset of $(-\pi,\pi)$. The h_k are given by:

$$\Psi_k(t) = \int_{-\pi}^{\pi} h_k(x)e^{itx}dx = \frac{G(t)}{G'(t_k)(t-t_k)},$$

where

$$G(t) = (t-t_0)\prod_{n=1}^{\infty}\left(1-\frac{t}{t_n}\right)\left(1-\frac{t}{t_{-n}}\right), \qquad t \in \mathfrak{R}.$$

As mentioned above, Lemma 2.2 is a particular case (for $L^2(-\pi,\pi)$) of convergence results for non-harmonic Fourier series, which have their origins in Paley-Wiener [9]. The bound 1/4 is tight and is a sufficient condition for $\{e^{i\lambda t_k}\}_{k\in\mathfrak{Z}}$ to form a bounded unconditional basis of $L^2(-\pi,\pi)$. The functions Ψ_k are called Lagrangia interpolating functions since

$$\Psi_k(t_n) = \begin{cases} 0, & \text{for } k \neq n \\ 1, & \text{for } k = n. \end{cases}$$

When $t_k = k$, $G(t) = \sin \pi t/\pi$ but, in general, no closed form expression is available for G.

3. Reconstruction

Throughout the next two sections, by a process $X = \{X_t\}_{t\in\mathfrak{R}}$ we mean that X is (bounded continuous) (α,∞)-bounded, $0 \leqslant \alpha \leqslant 2$, i.e., $X(t) = \int_{\mathfrak{R}} e^{i\lambda t}\,dZ(\lambda)$, $t \in \mathfrak{R}$. Furthermore, X is said to be bandlimited to $(-\pi,\pi)$ (the bounds $\pm\pi$ are just chosen for notational convenience) if $Z = 0$ a.s. $\mathcal{P}$, outside of $(-\pi,\pi)$.

Theorem 3.1. Let X be bandlimited to $(-\pi+\epsilon,\pi-\epsilon)$, let $\{t_k\}_{k\in\mathfrak{Z}} \subset \mathfrak{R}$ with $\sup_k |t_k - k| < 1/8$, and let $G(t) = (t-t_0)\prod_{n\neq 0}^{\infty}(1-\frac{t}{t_n})(1-\frac{t}{t_{-n}})$. Then, $X(t) = \sum_{-\infty}^{+\infty} \frac{X(t_k)G(t)}{G'(t_k)(t-t_k)}$, a.s. $\mathcal{P}$, uniformly on every compact subset of $\mathfrak{R}$.

When the dominating measure F in Lemma 2.1 has some degree of smoothness, reconstruction is also always possible.

Theorem 3.2. Let X be second order stationary, bandlimited to $(-\pi,\pi)$. If for some $0 < \delta < 2$,

$$\int_{0<|\lambda\pm\pi|<\delta} \left(\log\log\frac{1}{\pi^2-\lambda^2}\right)^2 dF < +\infty.$$

Then,

$$X(t) = \sum_{-\infty}^{+\infty} \frac{X(t_k)G(t)}{G'(t_k)(t-t_k)}, \qquad \text{a.s. } \mathcal{P}.$$

Although reconstruction in $L^\alpha(\mathcal{P})$ is always possible, the next result shows that when the paths are concerned, things can go very wrong.

We also note that the result below provides a bandlimited stationary process for which

$$\limsup_{n\to+\infty}\left|\sum_{-n}^{n}\frac{X(t_k)G(t)}{G'(t_k)(t-t_k)}\right| = +\infty \qquad \text{a.s. } \mathcal{P}.$$

This is in sharp contrast to Theorem 3.1.

Theorem 3.3. Let $\{a_n\}_{n\geq 1}$ be a nondecreasing sequence of positive reals such that

1) $a_n = o(\log\log n)$,
2) there exists $C_1 > 0$ such that $a_{2^{n+1}} \leq C_1 a_{2^n}$, n large enough.

Let $\{t_k\}$ be any sampling sequence. Then, there exists a probability space $(\Omega_1, \mathcal{B}_1, \mathcal{P}_1)$ and a bandlimited stationary process X defined on this space such that with probability one $(\mathcal{P}_1)$,

$$\limsup_{n\to+\infty}\frac{1}{a_n}\left|\sum_{-n}^{n}\frac{X(t_k)G(t)}{G'(t_k)(t-t_k)}\right| = +\infty.$$

This work is still in progress. Extensions of these results, including the case of more general sampling sequences, will be published in [6].

4. Bibliography

[1] Yu.K. Belayev. Analytic random processes. *Theor. Probability Appl.*, 4:402–409, 1959.

[2] V.F. Gaposhkin. A theorem on the convergence almost everywhere of measurable functions, and its applications to sequences of stochastic integrals. *Math. USSR Sbornik*, 33:1–17, 1977.

[3] J.R. Higgins. Five short stories about the cardinal series. *Bull. AMS*, 12:45–89, 1985.

[4] C. Houdré. Linear Fourier and stochastic analysis. *Prob. Th. Rel. Fields*, 87:167–188, 1990.

[5] C. Houdré. On the spectral SLLN and pointwise ergodic theorem in L^α. *Annals of Probability*, 1992. To appear.

[6] C. Houdré. Path reconstruction of processes from irregular samples. In preparation.

[7] A.J. Jerri. The Shannon sampling theorem—its various extensions and applications: a tutorial review. *Proc. IEEE*, 65:1565–1596, 1977.

[8] N. Levinson. *Gap and Density Theorems*. American Mathematical Society, New York, 1940.

[9] R.E.A.C. Paley and N. Wiener. *Fourier transforms in the complex domain*. American Mathematical Society, Rhode Island, 1934.

[10] P.A. Piranashvili. The problem of interpolation of random processes. *Theor. Probability Appl.*, 12:647–657, 1967.

Spectral analysis of random fields with random sampling†

I-Shang Chou
Department of Statistics
University of California, Riverside
Riverside, California 92521 USA
chou@ucrstat.ucr.edu

Keh-Shin Lii
ksl@ucrstat.ucr.edu (Other addresses the same.)

Abstract We discuss the problem of estimating the spectral density function of a continuous 2-dimensional stationary random field when the data set is obtained from a point process on the plane. Second order spectral analysis of irregularly spaced data on a real line was first considered by Shapiro and Silverman [20]. General results of stationary interval functions were studied by Brillinger [5]. He established consistency results for general polyspectral estimates of the stationary interval functions. Consistency results and alias-free sampling schemes for the second-order case in the estimation of the spectral density function of a continuous time series were obtained by Masry [12, 11, 14]. We generalize these results to the estimation of spectral density functions on higher dimensions. Special attention is directed to the 2-dimensional case although general k-dimensional cases are considered also. Asymptotic bias and covariances are studied. In particular, it is shown explicitly how the information of the sampling process come into play in obtaining a consistent estimate of the density function of a continuous random field. Estimates under Poisson's sampling scheme are studied in detail. A few simulation examples are given as illustrations.

1. Introduction

Statistical analysis of the stationary spatial series has been given considerable attention in recent years with applications in many areas (see [8] and [19]). General discussions of spectral analysis of spatial series have been given by Brillinger [4] and Whittle [22]. This research is based on the data which is

† This research is supported by CNR contract N00014-85-k-0468 and USDA contract PSW-91-0003CA.

J. S. Byrnes et al. (eds.), Probabilistic and Stochastic Methods in Analysis, with Applications, 343–368.
© 1992 *Kluwer Academic Publishers. Printed in the Netherlands.*

sampled at equally spaced grid. In most applications, observation stations are often irregularly spaced. Masry [15, 16] introduced random acoustic arrays placed by an independent sampling from a given multidimensional probability density function to estimate the frequency-wave number spectrum of the ambient noise field. Inference of the spectral density function of a 2-dimensional point process is of interest also [2, 9]. This paper is concerned with the estimation of the spectral density function of a continuous 2-dimensional stationary random field which is sampled by an independent 2-dimensional point process.

Spectral analysis of irregularly spaced data on a real line was first considered by Shapiro and Silverman [20]. Brillinger [5] studied the general results of stationary interval function. Consistency results and alias-free sampling schemes for estimating the spectral density function of a continuous time series were obtained by Masry [11, 14, 15]. Masry [13] provided an alternative way to estimate the spectral density function by using an orthogonal series method. These results are based on the 1-dimensional case. We generalize these results to the estimation of spectral density functions on higher dimensions. Our purpose is to find the spectral density function of a stationary spatial process $Y = \{Y(t),\ t \in R^p\}$. Special attention is directed to the 2-dimensional case. The results obtained will be applicable to the analysis of data recorded at points in some region of a surface. This kind of data can be found in optics, forestry and geology.

Let $Y = \{Y(t),\ t \in R^p\}$ be a stationary, zero-mean spatial process with finite fourth-order moments, continuous covariance function $R_Y(t)$, $t \in R^p$, spectral density function $\phi_Y(\lambda)$, $\lambda \in R^p$ and k^{th}-order cumulants $Q_Y^k(u_1, \ldots, u_{k-1})$, $u_1, \ldots, u_{k-1} \in R^p$; $k = 2, \ldots$, where R^p denotes real Euclidean p-space. The point process $\{\tau_k, k = \ldots, -1, 0, 1, \ldots\}$, $\tau_k \in R^p$ is stationary and orderly, independent of Y, with finite fourth order moments. If $N(\cdot)$ is the counting process associated with $\{\tau_k\}$, then

- For any positive integer k and any collection $\{B_1, \ldots, B_k\}$ of subsets in R^p, with $B_i = \{(x_1, \ldots, x_p) : a_{ij} < x_i \leq b_{ij},\ a_{ij}, b_{ij} \in R$, for $i = 1, \ldots, p\}$, the joint distribution of the random variables $\{N(B_1 + h), \ldots, N(B_k + h)\}$ is independent of $h \in R^p$
- $P\{N(|B|) \geq 2\} = o(|B|)$ as $|B| \downarrow 0$.
- $E\{N^4(B)\} < \infty$, for all bounded B.

The results are true for $B_i \in \mathcal{B}^p$ where $\mathcal{B}^p$ is the Borel sets in R^p. From now on we will concentrate on $p = 2$ (i.e., in the 2-dimensional case). Let β be the

mean intensity of the point process $N(\cdot)$. Then

$$E[N(dt)] = \beta dt \tag{1.1}$$

$$\mathrm{cov}\{N(dt), N(du)\} = C_N(du)dt \tag{1.2}$$

where E denotes expectation and $N(dt)$ denotes the number of points in the region $[t_x, t_x + dt_x] \times [t_y, t_y + dt_y]$. C_N is called the reduced covariance measure; C_N has an atom at the origin, $C_N(\{0\}) = \beta$. The "sampled" process is taken to be

$$Z(B) = \sum_{\tau_i \in B} Y(\tau_i) \qquad B \in \mathcal{B}^2.$$

or in differential form

$$Z(dt) = Y(t)N(dt).$$

An estimate of the spectral density function of the random field $Y(t)$ is proposed when the observed process $Z(dt)$ and the sampling process $N(dt)$ are observed.

If $N(\cdot)$ is a 2-dimensional Poisson process with events randomly occurring in the plane, then the number of events occurs in any region of area A has the Poisson distribution, with mean $\beta|A|$ and the events in the non-overlapping area are independent. The probability density function of $N(A)$ is given by

$$P(N(A) = n) = \frac{e^{-\beta|A|}(\beta|A|)^n}{n!} \qquad n = 0, 1, 2, \ldots$$

In section 2, second order cumulants and the spectrum of a continuous 2-dimensional random processes $Y(t)$ are introduced. Its relation with the sampled process and the sampling point process is derived. Consistent estimates of 2nd-order spectrum of $Y(t)$ are proposed in Section 3 based on the 2-dimensional Poisson sampling scheme. A simple simulation example is presented in Section 4.

2. 2nd order cumulant and spectrum

Assumption 2.1. The process $Y = \{Y(t),\ t = (t(1), t(2)) \in R^2\}$, is a continuous 2-dimensional stationary random process with mean $m_Y = 0$, autocovariance function $R_Y(u)$, $u = (u(1), u(2)) \in R^2$, and has finite fourth order

moments, and the fourth order cumulants $Q_Y^{(4)}(t_1,t_2,t_3),t_1,t_2,t_3 \in R^2$. The 2nd order cumulant function of $Y(t)$ is

$$R_Y(u) = \mathrm{Cov}\{Y(t),Y(t+u)\}$$

$$= \mathrm{Cum}\{Y(t),Y(t+u)\} \tag{2.1}$$

which satisfies

$$\int |u(i)|\,|R_Y(u(1),u(2))|\,du(1)du(2) < \infty, \qquad i = 1,2.$$

The spectrum of $Y(t)$ is given by

$$\phi_Y(\lambda) = \frac{1}{(2\pi)^2}\int R_Y(u)e^{-iu\cdot\lambda}du, \qquad \lambda = (\lambda(1),\lambda(2)) \in R^2. \tag{2.2}$$

We are concerned with the estimation of $\phi_Y(\lambda),\lambda \in R^2$ given random samples of $Y(t),t \in R^2$ from a 2-dimensional point process $N(\cdot)$.

Under our assumptions in the introduction, the "sampled" process Z has finite fourth order moments. In particular

$$E\{Z(dt)\} = E\{Y(t)\}E\{N(dt)\} = 0$$

and

$$\mu_Z(du)dt \overset{\Delta}{=} E\{Z(dt)Z(du)\} \tag{2.3}$$

$$= E\{Y(t)N(dt)Y(t+u)N(du)\}$$

$$= R_Y(u)\{\beta^2 du + C_N(du)\}dt \tag{2.4}$$

so that

$$\mu_Z(B) = \int_B R_Y(u)\{\beta^2 du + C_N(du)\}, \qquad B \in \mathcal{B}^2 \tag{2.5}$$

is a σ-finite signed measure on $\mathcal{B}^2$. If we define the σ-finite measure

$$\mu_N(B) \overset{\Delta}{=} \int_B |\beta^2 du + C_N(du)|, \qquad B \in \mathcal{B}^2$$

then we can rewrite $\mu_Z(B)$ as

$$\mu_Z(B) = \int_B R_Y(u)\mu_N(du).$$

If the covariance density function $c_N(u)$ exists, i.e.,

$$C_N(B) = \beta\delta_0(B) + \int_B c_N(u)du, \qquad B \in \mathcal{B}^2 \tag{2.6}$$

then

$$\mu_Z(B) = \beta R_Y(0)\delta_0(B) + \int_B R_Y(u)[\beta^2 + c_N(u)]du \tag{2.7}$$

where

$$\delta_0(B) = \begin{cases} 1, & \text{if } 0 \in B \\ 0, & \text{otherwise.} \end{cases}$$

We define the spectral density $\phi_Z(\lambda)$ of the "sampled" process Z by

$$\phi_Z(\lambda) \triangleq \frac{1}{(2\pi)^2}\int e^{-iu\cdot\lambda}\mu_Z(du) \tag{2.8}$$

$$= \beta^2\phi_Y(\lambda) + \frac{\beta R_Y(0)}{(2\pi)^2} + \frac{1}{(2\pi)^2}\int R_Y(u)c_N(u)e^{-iu\cdot\lambda}du. \tag{2.9}$$

If we assume that $c_N(u) \in L_1$ with

$$\psi_N(\lambda) \triangleq \frac{1}{(2\pi)^2}\int e^{-iu\cdot\lambda}c_N(u)du$$

then

$$c_N(u) = \int \psi_N(\lambda)e^{iu\cdot\lambda}d\lambda$$

and

$$\begin{aligned}\frac{1}{(2\pi)^2}\int R_Y(u)c_N(u)e^{-iu\cdot\lambda}du &= \frac{1}{(2\pi)^2}\int R_Y(u)e^{-iu\cdot(\lambda-\nu)}e^{-iu\cdot\nu}c_N(u)du \\ &= \frac{1}{(2\pi)^2}\int R_Y(u)e^{-iu\cdot(\lambda-\nu)}e^{-iu\cdot\nu}\int \psi_N(\nu)e^{iu\cdot\nu}d\nu du \\ &= \frac{1}{(2\pi)^2}\iint R_Y(u)e^{-iu\cdot(\lambda-\nu)}du\psi_N(\nu)d\nu \\ &= \int \phi_Y(\lambda-\nu)\psi_N(\nu)d\nu.\end{aligned}$$

Hence we can rewrite $\phi_Z(\lambda)$ as

$$\phi_Z(\lambda) = \beta^2\phi_Y(\lambda) + \frac{\beta R_Y(0)}{(2\pi)^2} + \int \phi_Y(\lambda-u)\psi_N(u)du. \tag{2.10}$$

Note that for a 2-dimensional Poisson point process, $c_N(u) \equiv 0$, so that

$$\phi_Z(\lambda) = \beta^2 \left[\phi_Y(\lambda) + \frac{R_Y(0)}{(2\pi)^2\beta}\right]$$

and

$$\phi_Y(\lambda) = \frac{1}{\beta^2}\phi_Z(\lambda) - \frac{R_Y(0)}{(2\pi)^2\beta}. \tag{2.11}$$

However, if $c_N(u) \neq 0$, then we need to solve

$$\phi_Z(\lambda) = \beta^2\phi_Y(\lambda) + \frac{\beta R_Y(0)}{(2\pi)^2} + \int \phi_Y(\lambda - u)\psi_N(u)du.$$

We note that when the point process $N(\cdot)$ is Poisson then the problem is reduced to the case in [15, 16] with uniform density function and ignoring the time-frequency part. We will derive the following proposition.

Proposition 2.2. If

$$\gamma(u) \triangleq \frac{c_N(u)}{\beta^2 + c_N(u)} \in L_1 \tag{2.12}$$

with Fourier transform

$$\Gamma(\lambda) = \frac{1}{(2\pi)^2}\int e^{-iu\cdot\lambda}\gamma(u)du \in L_1,$$

then (2.10) can be inverted and we have

$$\phi_Y(\lambda) = \frac{1}{\beta^2}\left\{\left[\phi_Z(\lambda) - \frac{\beta R_Y(0)}{(2\pi)^2}\right] - \int \Gamma(\lambda - u)\left[\phi_Z(u) - \frac{\beta R_Y(0)}{(2\pi)^2}\right]du\right\}. \tag{2.13}$$

Proof. From (2.7) and (2.12) we can obtain

$$\mu_Z(du) = \beta R_Y(0)\delta_0(du) + R_Y(u)\{\beta^2 + c_N(u)\}du,$$

$$\begin{aligned} R_Y(u)du &= \frac{1}{\beta^2 + c_N(u)}[\mu_Z(du) - \beta R_Y(0)\delta_0(du)] \\ &= \frac{1}{\beta^2}[1 - \gamma(u)][\mu_Z(du) - \beta R_Y(0)\delta_0(du)]. \end{aligned}$$

Then we take the Fourier transform on both sides, and we have

$$\begin{aligned}
&\frac{1}{(2\pi)^2}\int R_Y(u)e^{-iu\cdot\lambda}du \\
&\quad = \frac{1}{\beta^2}\left\{\left[\frac{1}{(2\pi)^2}\int e^{-iu\cdot\lambda}\mu_Z(du) - \frac{1}{(2\pi)^2}\beta R_Y(0)\right]\right. \\
&\qquad - \left[\frac{1}{(2\pi)^2}\int \gamma(u)e^{-iu\cdot\lambda}\mu_Z(du)\right. \\
&\qquad \left.\left. - \frac{1}{(2\pi)^2}\int \gamma(u)\beta R_Y(0)e^{-iu\cdot\lambda}\delta_0(du)\right]\right\}
\end{aligned}$$

and

$$\begin{aligned}
\phi_Y(\lambda) = \frac{1}{\beta^2}\left\{\left[\phi_Z(\lambda) - \frac{\beta R_Y(0)}{(2\pi)^2}\right]\right. \\
\left. - \int \Gamma(\lambda - u)\left[\phi_Z(u) - \frac{\beta R_Y(0)}{(2\pi)^2}\right]du\right\}. \qquad (2.14)
\end{aligned}$$

Note that, if $N(\cdot)$ is a 2-dimensional Poisson point process, then the power spectrum of the continuous spatial series $Y(t)$, $t \in R^2$, can be calculated from the power spectrum of the "sampled" process Z by substracting a constant and multiplying a constant. In the general case (2.14) can be used to obtain estimate of $\phi_Y(\lambda)$. ∎

3. Estimation of 2-dimensional power spectrum

For simplicity, we assume that the sampling scheme $N(dt)$ is a 2-dimensional Poisson process which is independent of the 2-dimensional continuous random process $Y(t)$, $t \in R^2$. If the continuous random process $Y(t)$ satisfies the Assumption 2.1 and a realization of the process $N(\cdot)$ at $\tau_1, \tau_2, \ldots, \tau_{N(T)}$ in the region $\mathfrak{R}_T^2 = (0, T] \times (0, T], 0 < T < \infty$, where $\mathfrak{R}_T^2$ is an expanding subregion of R^2. The observed process is $Z(dt) = Y(t)N(dt)$. We propose the following statistics to estimate the spectral density function $\phi_Y(\lambda)$ (see (2.11))

$$\hat{\phi}_Y(\lambda) = \frac{1}{\hat{\beta}^2}\left(\hat{\phi}_Z(\lambda) - \frac{1}{(2\pi)^2}\hat{R}_Y(0)\hat{\beta}\right)$$

where

$$\hat{\beta} = \frac{N(T)}{T^2}, \tag{3.1}$$

$$\hat{\phi}_Z(\lambda) = \int W_T(\lambda - u) I_T(u)\, du, \tag{3.2}$$

$$\hat{R}_Y(0) = \frac{\sum_{j=1}^{N(T)} Y^2(\tau_j)}{N(T)}, \tag{3.3}$$

$$I_T(\lambda) = \frac{1}{(2\pi T)^2} \left| \sum_{k=1}^{N(T)} Y(\tau_k) e^{-i\tau_k \cdot \lambda} \right|^2 \tag{3.4}$$

where W_T is a spectral window which satisfies certain regularity conditions as Assumption 4.2 in [5] for some appropriate bandwidth B_T and is given by

$$W_T(\theta) = \frac{1}{(B_T)^2} W\left(\frac{\theta}{B_T}\right), \qquad \theta \in R^2.$$

Lemma 3.1. Let $N(\cdot)$ be a 2-dimensional Poisson process with mean intensity β which is a process of events randomly occurring in the plane then

- For any bounded region A of area $|A|$ the number of events in that region has a Poisson distribution with mean $\beta|A|$;
- The number of events in nonoverlapping regions are independent;

and

$$\begin{aligned} EN(A) &= \beta|A|, \\ Cum\{N(A), N(A)\} &= \beta|A|, \\ Cum\{N(A), N(A), N(A)\} &= \beta|A|, \\ Cum\{N(A), N(A), N(A), N(A)\} &= \beta|A|. \end{aligned}$$

Lemma 3.2. Assume $t(j)R_Y(t(1), t(2)) \in L_1$, $j = 1, 2$, then

$$\begin{aligned} E[I_T(\lambda)] &= \left[\beta^2 \phi_Y(\lambda) + \frac{\beta R_Y(0)}{(2\pi)^2}\right] + O\left(\frac{1}{T}\right) \\ &= \phi_Z(\lambda) + O\left(\frac{1}{T}\right). \end{aligned} \tag{3.5}$$

Proof. See Appendix B. ∎

Lemma 3.3. Assume $|t_j|^k Q_Y^{(4)}(t_1,t_2,t_3) \in L_1$, $t_j \in R^2$, $j = 1,2,3$, $k = 0,1$. Then

$$\begin{aligned}&\mathrm{Cov}\{I_T(\lambda(1),\lambda(2)), I_T(\mu(1),\mu(2))\}\\ &= \frac{1}{T^2}\phi_Z^2(\lambda(1),\lambda(2))\{\Delta_T(\lambda(1)+\mu(1))\Delta_T(\lambda(2)+\mu(2))\\ &\quad +\Delta_T(\lambda(1)-\mu(1))\Delta_T(\lambda(2)-\mu(2))\}\\ &\quad +O\left(\frac{1}{T^2}\right) \qquad (3.6)\end{aligned}$$

where

$$\Delta_T(\omega) = \frac{1}{T}\left(\frac{\sin\frac{T\omega}{2}}{\frac{\omega}{2}}\right)^2, \qquad \omega \in R.$$

Proof. See Appendix B. ∎

From Lemma 3.3, we see that $\mathrm{Cov}(I_T(\lambda), I_T(\mu))$ is asymptotically zero when $\lambda \neq \mu (\neq 0)$. To obtain consistent estimates of $\phi_Y(\lambda)$ we need to obtain consistent estimates of $\phi_Z(\lambda)$ in (2.11). One can use the usual smoothing periodogram given in (3.2). Details are omitted here. Or one can partition the region $(0,T] \times (0,T]$ into $m^2(T)$ subregions with size $(0, \frac{T}{m(T)}] \times (0, \frac{T}{m(T)}]$ each. If $m(T) \to \infty$ and $\frac{T}{m(T)} \to \infty$ when $T \to \infty$ then the average of $m^2(T)$ periodograms $I_{\frac{T}{m(T)}}$ is a consistent estimate of $\phi_Z(\lambda)$. This is used in the following example.

4. An example

Here is a simple 2-dimensional AR(2) process which is generated with a given spectrum

$$S(\lambda_1,\lambda_2) = (2\pi)^{-2}|1 + 0.2e^{-i\lambda_1} + 0.3e^{-i\lambda_2} - 0.24e^{-i(\lambda_1+\lambda_2)}|^{-2},$$
$$|\lambda_1|, |\lambda_2| \leqslant \pi.$$

A plot of SAS is given in Figure A.1. There are different ways to generate a stationary process with a given spectrum. We use the one described in [7]. A realization $Z(x,y)$ at $(x,y) \in R^2$ is given by

$$Z(x,y) = \sqrt{2}\sum_{i,j}(S(\lambda_i,\lambda_j)\cdot\Delta\lambda_i\cdot\Delta\lambda_j)^{\frac{1}{2}}\cdot\cos(x\cdot\lambda_i' + y\cdot\lambda_j' + u_{i,j})$$

where λ_i, λ_j are a discretization of the "support" of $S(\lambda_1,\lambda_2)$; λ_i', λ_j' are a jittered version of λ_i, λ_j and $u_{i,j}$ is i.i.d. uniform in $(0, 2\pi)$.

A Poisson sample is obtained on $(0,32] \times (0,32]$ with $N(32) = 1024$. The periodogram is given in Figure A.2. The average of 10 periodograms from 10 independent realizations of a Poisson sampling process is given in Figure A.3. We see that the estimate is close to the true one.

5. Bibliography

[1] M.S. Bartlett. The spectral analysis of point processes. *J.R. Statist. Soc. B*, 25:264–96, 1963.

[2] M.S. Bartlett. The spectral analysis of two-dimensional point process. *Biometrika*, 51(3–4):299, 1964.

[3] F.J. Beutler. Alias free randomly timed sampling of stochastic processes. *IEEE Trans. Information Theory*, 16:147–152, 1970.

[4] D.R. Brillinger. The frequency analysis of relations between stationary spatial series. In R.Pyke, editor, *Proc. Twelfth Bien. Sem. Canadian Math. Congr.*, pages 39–81, Montreal, 1970. Canadian Mathematical Congress.

[5] D.R. Brillinger. The spectral analysis of stationary interval functions. In *Proc. Sixth Berkeley Symp. Prob. Statist.*, pages 483–513, Berkeley, CA, 1972.

[6] D.R. Brillinger. *Time series: Data analysis and Theory*. Holt, Rinehart and Winston, New York, 1975.

[7] G. Christakos. Stochastic simulation of spatially correlated geo-processes. *Mathematical Geology*, 19(8):807–831, 1987.

[8] N. Cressie, C. A. Gotway, and M. O. Grondona. Spatial prediction from networks. *Chemometrics and Intelligent Laboratory System*, 7:251–271, 1990.

[9] D.J. Daley and D. Vere-Jones. A summary of the theory of point processes. In P.A.W. Lewis, editor, *In Stochastic Point processes*. John Wiley & Sons, New York, 1972.

[10] D.J. Daley and D. Vere-Jones. *An Introduction to the Theory of Point Processes*. Springer-Verlag, New York, 1988.

[11] E. Masry. Alias-free sampling: An alternative conceptualization and its applications. *IEEE Trans. Information Theory*, 24:317–324, 1978.

[12] E. Masry. Poisson sampling and spectral estimation of continuous-time processes. *IEEE Trans. Information Theory*, 24:173–183, 1978.

[13] E. Masry. Discrete-time spectral estimation of continuous-time processes: the orthogonal series method. *Annals of Statistics*, 8:1100–1109, 1980.

[14] E. Masry. Non-parametric covariance estimation from irregularly-spaced data. *Adv. Appl. Prob.*, 15:113–132, 1983.

[15] E. Masry. The estimation of the frequency-wavenumber spectrum using random acoustic arrays—Part I: Performance of beampower pattern estimators. *J. Acoust. Soc. Am.*, 76:139–149, 1984.

[16] E. Masry. The estimation of the frequency-wavenumber spectrum using random acoustic arrays—Part II: A class of consistent estimations. *J. Acoust. Soc. Am.*, 76, 1984.

[17] E. Masry and M. C. Liu. Discrete-time spectral estimation of continuous-parameter processes—a new consistent estimate. *IEEE Trans. Information Theory*, 22:298–312, May 1976.

[18] M.B. Priestley. *Spectral Analysis and Time Series.* Academic Press, 1981.

[19] B. D. Ripley. *Spatial statistics.* John Wiley & Sons, New York, 1981.

[20] H.S. Shapiro and R.A. Silverman. Alias-free sampling of random noise. *J. Soc. Indust. Appl. Math.*, 8:225–248, 1960.

[21] A.V. Vecchia. A general class of models for stationary two-dimensional random processes. *Biometrika*, 72(2):281–91, 1985.

[22] P. Whittle. On stationary processes in the plane. *Biometrika*, 41:434–449, 1954.

A. Figures

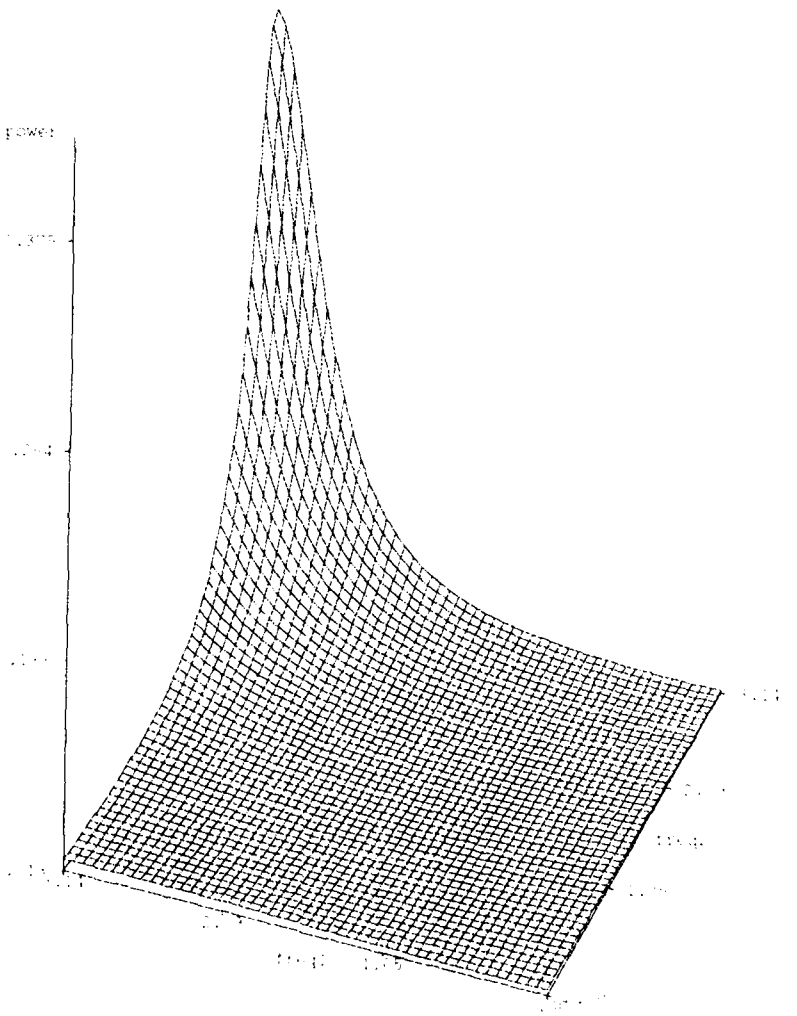

Figure A.1: 2-d theoretical power spectrum

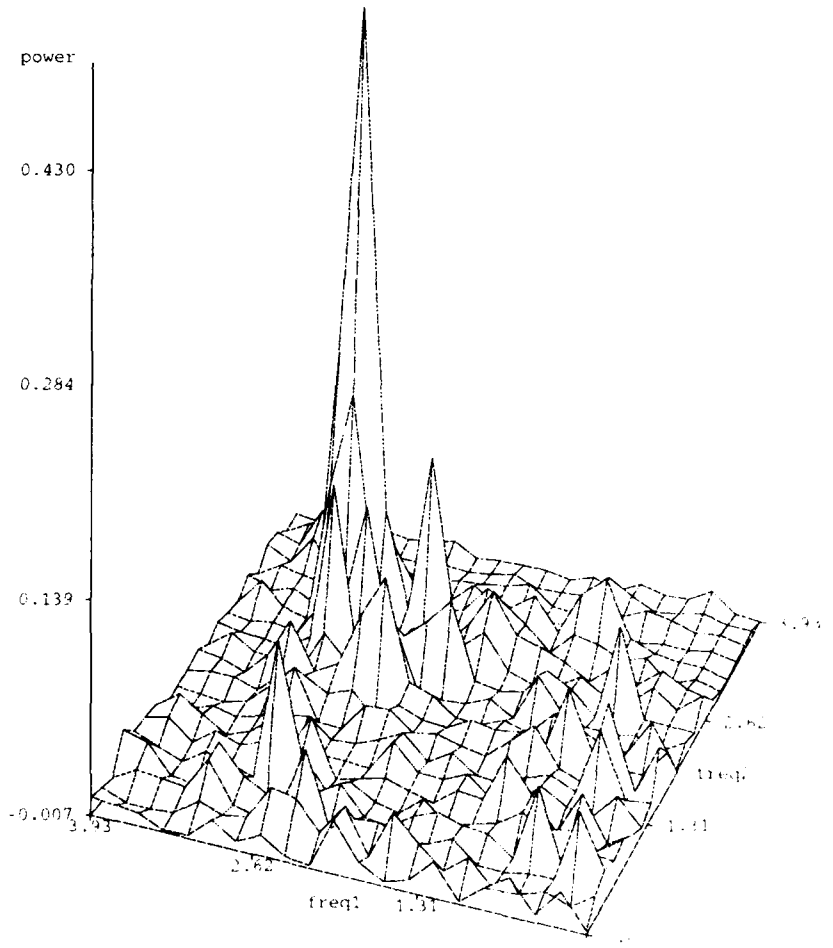

Figure A.2: 2-d power spectrum using Poisson sampling scheme

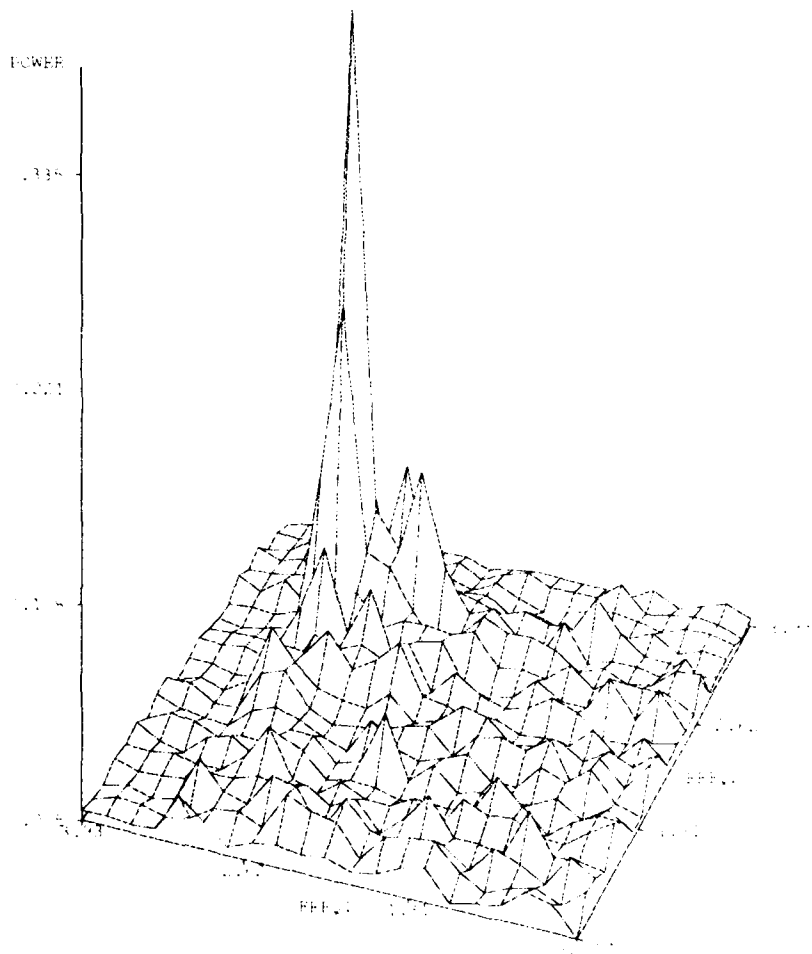

Figure A.3: 2-d smoothed periodogram using Poisson sampling scheme

B. Proofs

Proof (of Lemma 3.2).

$$E[I_T(\lambda)] = E\left[\frac{1}{(2\pi T)^2}\left|\sum_{k=1}^{N(1)} Y(\tau_k)e^{-i\tau_k\cdot\lambda}\right|^2\right]$$

$$= \frac{1}{(2\pi T)^2}E\left[\left|\int_{\mathfrak{R}_T^2} e^{-it\cdot\lambda}Z(dt)\right|^2\right]$$

$$= \frac{1}{(2\pi T)^2}E\left[\int_{\mathfrak{R}_T^2} e^{-it\cdot\lambda}Z(dt)\int_{\mathfrak{R}_T^2} e^{is\cdot\lambda}Z(ds)\right]$$

$$= \frac{1}{(2\pi T)^2}\int_{\mathfrak{R}_T^2}\int_{\mathfrak{R}_T^2} e^{-i(t-s)\cdot\lambda}E[Z(dt)Z(ds)]$$

where $\mathfrak{R}_T^2 = (0,T]\times(0,T]$. Note that

$$\begin{aligned}E[Z(dt)Z(ds)] &= E[Y(t)Y(s)N(dt)N(ds)]\\ &= E[Y(t)Y(s)]E[N(dt)N(ds)]\\ &= R_Y(t-s)[\beta^2 dtds + \beta\delta(t-s)dtds]\end{aligned}$$

where $\delta(x)$ is the 2-dimensional Dirac delta function. Thus we have

$$\begin{aligned}E[I_T(\lambda)] &= \frac{1}{(2\pi T)^2}\int_{\mathfrak{R}_T^2}\int_{\mathfrak{R}_T^2} e^{-i(t-s)\cdot\lambda}R_Y(t-s)[\beta^2 dtds + \beta\delta(t-s)dtds]\\ &= \frac{\beta^2}{(2\pi T)^2}\int_{\mathfrak{R}_T^2}\int_{\mathfrak{R}_T^2} e^{-i(t-s)\cdot\lambda}R_Y(t-s)dt\,ds + \frac{\beta k_Y(0)}{(2\pi)^2}\end{aligned}$$

where

$$\frac{\beta^2}{(2\pi T)^2}\int_{\mathfrak{R}_T^2}\int_{\mathfrak{R}_T^2} e^{-i(t-s)\cdot\lambda}R_Y(t-s)dt\,ds = \frac{\beta^2}{(2\pi T)^2}\int_0^T\int_0^T\int_0^T$$

$$\int_0^T e^{-i(t(1)-s(1))\lambda(1)-i(t(2)-s(2))\lambda(2)}$$
$$\times R_Y(t(1)-s(1),t(2)-s(2))dt(1)dt(2)ds(1)ds(2)$$

$$= \frac{\beta^2}{(2\pi T)^2}\int_0^T\int_0^T e^{-i(t(2)-s(2))\lambda(2)} \times\left[\int_0^T\int_0^T e^{-i(t(1)-s(1))\lambda(1)}R_Y(t(1)-s(1),t(2)-s(2))dt(1)ds(1)\right] dt(2)ds(2)$$

$$= \frac{\beta^2}{(2\pi T)^2}\int_0^T\int_0^T e^{-i(t(2)-s(2))\lambda(2)} \times\left[\int_{-T}^T (1-|u(1)|)e^{-iu(1)\lambda(1)}R_Y(u(1),t(2)-s(2))du(1)\right] dt(2)ds(2)$$

$$= \frac{\beta^2}{(2\pi T)^2}\int_{-T}^T\int_{-T}^T (T-|u(1)|)(T-|u(2)|)e^{-iu(1)\lambda(1)-iu(2)\lambda(2)} \times R_Y(u(1),u(2))du(1)du(2)$$

$$= \frac{\beta^2}{(2\pi)^2}\int_{-T}^T\int_{-T}^T \left(1-\frac{|u(1)|}{T}-\frac{|u(2)|}{T}+\frac{|u(1)||u(2)|}{T^2}\right) \times e^{-iu(1)\lambda(1)-iu(2)\lambda(2)}R_Y(u(1),u(2))du(1)du(2)$$

$$= \frac{\beta^2}{(2\pi)^2}\left[\int_{-T}^T\int_{-T}^T e^{-iu(1)\lambda(1)-iu(2)\lambda(2)}R_Y(u(1),u(2))du(1)dv\right.$$

$$-\int_{-T}^T\int_{-T}^T \frac{|u(1)|}{T}e^{-iu(1)\lambda(1)-iu(2)\lambda(2)}R_Y(u(1),u(2))du(1)du(2)$$

$$-\int_{-T}^T\int_{-T}^T \frac{|u(2)|}{T}e^{-iu(1)\lambda(1)-iu(2)\lambda(2)}R_Y(u(1),u(2))du(1)du(2)$$

$$+\frac{1}{T^2}\int_{-T}^T\int_{-T}^T e^{-iu(1)\lambda(1)-iu(2)\lambda(2)}|u(1)||u(2)| \times R_Y(u(1),u(2))|du(1)du(2)|\,.$$

Then as $T \to \infty$ and the assumption that we have the following asymptotic results:

$$\frac{\beta^2}{(2\pi)^2}\int_{\mathfrak{R}_1^2}\int_{\mathfrak{R}_1^2} e^{-i(t-s)\cdot\lambda}R_Y(t-s)dtds$$

$$= \beta^2 \phi_Y(\lambda) + O\left(\frac{1}{T}\right) + O\left(\frac{1}{T}\right) + O\left(\frac{1}{T}\right) + O\left(\frac{1}{T}\right)$$

$$= \beta^2 \phi_Y(\lambda) + O\left(\frac{1}{T}\right).$$

Hence,

$$E[I_T(\lambda)] = \beta^2 \phi_Y(\lambda) + \frac{\beta R_Y(0)}{(2\pi)^2} + O\left(\frac{1}{T}\right)$$

$$= \phi_Z(\lambda) + O\left(\frac{1}{T}\right)$$

where the $O(\frac{1}{T})$ term is uniform in λ. ∎

Proof (of Lemma 3.3).

$$\mathrm{Cov}(I_T(\lambda), I_T(\mu))$$

$$= \left(\frac{1}{2\pi T}\right)^4 \mathrm{Cov}\left\{\left|\int_{\mathfrak{R}_T^2} e^{-ir\cdot\lambda} Z(dr)\right|^2, \left|\int_{\mathfrak{R}_T^2} e^{-is\cdot\mu} Z(ds)\right|^2\right\}$$

$$= \left(\frac{1}{2\pi T}\right)^4 \left[E\left|\int_{\mathfrak{R}_T^2} e^{-ir\cdot\lambda} Z(dr)\right|^2 \left|\int_{\mathfrak{R}_T^2} e^{-is\cdot\mu} Z(ds)\right|^2 - E\left|\int_{\mathfrak{R}_T^2} e^{-ir\cdot\lambda} Z(dr)\right|^2 E\left|\int_{\mathfrak{R}_T^2} e^{-is\cdot\mu} Z(ds)\right|^2\right],$$

$$E\left|\int_{\mathfrak{R}_T^2} e^{-ir\cdot\lambda} Z(dr)\right|^2 \left|\int_{\mathfrak{R}_T^2} e^{-is\cdot\mu} Z(ds)\right|^2$$

$$= E\int_{\mathfrak{R}_T^2}\int_{\mathfrak{R}_T^2}\int_{\mathfrak{R}_T^2}\int_{\mathfrak{R}_T^2} e^{-i(r-r^*)\cdot\lambda} e^{-i(s-s^*)\cdot\mu} Z(dr) Z(dr^*) Z(ds) Z(ds^*)$$

$$= \int_{\mathfrak{R}_T^2}\int_{\mathfrak{R}_T^2}\int_{\mathfrak{R}_T^2}\int_{\mathfrak{R}_T^2} e^{-i(r-r^*)\cdot\lambda} e^{-i(s-s^*)\cdot\mu} E[Z(dr) Z(dr^*) Z(ds) Z(ds^*)],$$

$$E\left|\int_{\mathfrak{R}_T^2} e^{-ir\cdot\lambda} Z(dr)\right|^2 E\left|\int_{\mathfrak{R}_T^2} e^{-is\cdot\mu} Z(ds)\right|^2$$

$$= E\left[\int_{\mathfrak{R}_T^2}\int_{\mathfrak{R}_T^2} e^{-i(r-r^*)\cdot\lambda} Z(dr)Z(dr^*)\right]$$
$$\times E\left[\int_{\mathfrak{R}_T^2}\int_{\mathfrak{R}_T^2} e^{-i(s-s^*)\cdot\mu} Z(ds)Z(ds^*)\right]$$

$$= \int_{\mathfrak{R}_T^2}\int_{\mathfrak{R}_T^2} e^{-i(r-r^*)\cdot\lambda} R_Y(r-r^*)E[N(dr)N(dr^*)]$$
$$\times \int_{\mathfrak{R}_T^2}\int_{\mathfrak{R}_T^2} e^{-i(s-s^*)\cdot\mu} R_Y(s-s^*)E[N(ds)N(ds^*)]$$

$$= \int_{\mathfrak{R}_T^2}\int_{\mathfrak{R}_T^2} e^{-i(r-r^*)\cdot\lambda} R_Y(r-r^*)\left[\beta^2 dr dr^* + \beta\delta(r-r^*)dr dr^*\right]$$
$$\times \int_{\mathfrak{R}_T^2}\int_{\mathfrak{R}_T^2} e^{-i(s-s^*)\cdot\mu} R_Y(s-s^*)\left[\beta^2 ds ds^* + \beta\delta(s-s^*)ds ds^*\right]$$

$$= \beta^4 \int_{\mathfrak{R}_T^2}\int_{\mathfrak{R}_T^2} e^{-i(r-r^*)\cdot\lambda} R_Y(r-r^*)dr dr^*$$
$$\times \int_{\mathfrak{R}_T^2}\int_{\mathfrak{R}_T^2} e^{-i(s-s^*)\cdot\mu} R_Y(s-s^*)ds ds^*$$

$$+\beta^3 T^2 R_Y(0)\int_{\mathfrak{R}_T^2}\int_{\mathfrak{R}_T^2} e^{-i(r-r^*)\cdot\lambda} R_Y(r-r^*)dr dr^* + \beta^3 T^2 R_Y(0)$$
$$\times \int_{\mathfrak{R}_T^2}\int_{\mathfrak{R}_T^2} e^{-i(s-s^*)\cdot\mu} R_Y(s-s^*)ds ds^*$$

$$+T^4\beta^2 R_Y^2(0)$$

where $\delta(u)$ is the 2-dimensional Dirac delta function.

Note that

$$E[Z(dr)Z(dr^*)Z(ds)Z(ds^*)]$$
$$= E[Y(r)Y(r^*)Y(s)Y(s^*)N(dr)N(dr^*)N(ds)N(ds^*)]$$
$$= E[Y(r)Y(r^*)Y(s)Y(s^*)]E[N(dr)N(dr^*)N(ds)N(ds^*)]$$

Because the mean of the stationary process is zero, we have

$$E[Y(r)Y(r^*)Y(s)Y(s^*)]$$
$$= Q_Y^{(4)}(r-s^*, r^*-s^*, s-s^*) + R_Y(r-r^*)R_Y(s-s^*) \qquad (B.1)$$
$$+R_Y(r-s)R_Y(r^*-s^*) + R_Y(r-s^*)R_Y(r^*-s)$$

and

$$
\begin{aligned}
&E\{N(dr)N(dr^*)N(ds)N(ds^*)\} && \text{(B.2.1)}\\
&= \mathrm{Cum}\{N(dr), N(dr^*), N(ds), N(ds^*)\} && \text{(B.2.2)}\\
&\quad +\beta dr\,\mathrm{Cum}\{N(dr^*), N(ds), N(ds^*)\} && \text{(B.2.3)}\\
&\quad +\beta dr^*\,\mathrm{Cum}\{N(dr), N(ds), N(ds^*)\}\\
&\quad +\beta ds\,\mathrm{Cum}\{N(dr), N(dr^*), N(ds^*)\}\\
&\quad +\beta ds^*\,\mathrm{Cum}\{N(dr), N(dr^*), N(ds)\}\\
&\quad +\mathrm{Cum}\{N(dr), N(dr^*)\}\mathrm{Cum}\{N(ds), N(ds^*)\} && \text{(B.2.4)}\\
&\quad +\mathrm{Cum}\{N(dr), N(ds)\}\mathrm{Cum}\{N(dr^*), N(ds^*)\} && \text{(B.2.5)}\\
&\quad +\mathrm{Cum}\{N(dr), N(ds^*)\}\mathrm{Cum}\{N(dr^*), N(ds)\} && \text{(B.2.6)}\\
&\quad +\beta^2 dr dr^*\,\mathrm{Cum}\{N(ds), N(ds^*)\} && \text{(B.2.7)}\\
&\quad +\beta^2 dr ds\,\mathrm{Cum}\{N(dr^*), N(ds^*)\} && \text{(B.2.8)}\\
&\quad +\beta^2 dr ds^*\,\mathrm{Cum}\{N(dr^*), N(ds)\} && \text{(B.2.9)}\\
&\quad +\beta^2 dr^* ds\,\mathrm{Cum}\{N(dr), N(ds^*)\} && \text{(B.2.10)}\\
&\quad +\beta^2 dr^* ds^*\,\mathrm{Cum}\{N(dr), N(ds)\} && \text{(B.2.11)}\\
&\quad +\beta^2 ds ds^*\,\mathrm{Cum}\{N(dr), N(dr^*)\}\\
&\quad +\beta^4 dr dr^* ds ds^*. && \text{(B.2.12)}
\end{aligned}
$$

We partition (B.1) into four parts. First, we compute

$$
\left(\frac{1}{2\pi T}\right)^4 \int_{\mathfrak{R}_T^2}\int_{\mathfrak{R}_T^2}\int_{\mathfrak{R}_T^2}\int_{\mathfrak{R}_T^2} e^{-i(r-r^*)\cdot\lambda} e^{-i(s-s^*)\cdot\mu} \times Q_Y^{(4)}(r-s^*, r^*-s^*, s-s^*)E\{N(dr)N(dr^*)N(ds)N(ds^*)\}.
$$

Equation (B.2.1) has 15 terms. Computations of these terms are very similar. Here we consider $Q_Y^{(4)}(r-s^*, r^*-s^*, s-s^*)$ multiplying (B.2.2), (B.2.3), (B.2.4), (B.2.7) and (B.2.12) only.

$$
\begin{aligned}
&\left(\frac{1}{2\pi T}\right)^4 \int_{\mathfrak{R}_T^2}\int_{\mathfrak{R}_T^2}\int_{\mathfrak{R}_T^2}\int_{\mathfrak{R}_T^2} e^{-i(r-r^*)\cdot\lambda} e^{-i(s-s^*)\cdot\mu}\\
&\quad \times Q_Y^{(4)}(r-s^*, r^*-s^*, s-s^*)\mathrm{Cum}\{N(dr), N(dr^*), N(ds), N(ds^*)\}\\
&= \left(\frac{1}{2\pi T}\right)^4 \beta \int_{\mathfrak{R}_T^2} Q_Y^{(4)}(0,0,0)dr\\
&= \left(\frac{1}{2\pi}\right)^4 \frac{\beta}{T^2} Q_Y^{(4)}(0,0,0)
\end{aligned}
$$

$$= O\left(\frac{1}{T^2}\right),$$

$$\left(\frac{1}{2\pi T}\right)^4 \beta \int_{\mathfrak{R}_T^2}\int_{\mathfrak{R}_T^2}\int_{\mathfrak{R}_T^2}\int_{\mathfrak{R}_T^2} e^{-i(r-r^*)\cdot\lambda} e^{-i(s-s^*)\cdot\mu} \times Q_Y^{(4)}(r-s^*, r^*-s^*, s-s^*)\,\mathrm{Cum}\{N(dr^*), N(ds), N(ds^*)\}dr$$

$$= \left(\frac{1}{2\pi T}\right)^4 \beta^2 \int_{\mathfrak{R}_T^2}\int_{\mathfrak{R}_T^2} e^{-i(r-r^*)\cdot\lambda} Q_Y^{(4)}(r-r^*, 0, 0)\,dr\,dr^*$$

$$= O\left(\frac{1}{T^2}\right),$$

$$\left(\frac{1}{2\pi T}\right)^4 \int_{\mathfrak{R}_T^2}\int_{\mathfrak{R}_T^2}\int_{\mathfrak{R}_T^2}\int_{\mathfrak{R}_T^2} e^{-i(r-r^*)\cdot\lambda} e^{-i(s-s^*)\cdot\mu} \times Q_Y^{(4)}(r-s^*, r^*-s^*, s-s^*) \cdot \mathrm{Cum}\{N(dr), N(dr^*)\}\mathrm{Cum}\{N(ds), N(ds^*)\}$$

$$= \left(\frac{1}{2\pi T}\right)^4 \beta^2 \int_{\mathfrak{R}_T^2}\int_{\mathfrak{R}_T^2} Q_Y^{(4)}(r-s, r-s, 0)\,dr\,ds$$

$$= O\left(\frac{1}{T^2}\right),$$

$$\left(\frac{1}{2\pi T}\right)^4 \beta^2 \int_{\mathfrak{R}_T^2}\int_{\mathfrak{R}_T^2}\int_{\mathfrak{R}_T^2}\int_{\mathfrak{R}_T^2} e^{-i(r-r^*)\cdot\lambda} e^{-i(s-s^*)\cdot\mu} \times Q_Y^{(4)}(r-s^*, r^*-s^*, s-s^*)\,\mathrm{Cum}\{N(ds), N(ds^*)\}dr\,dr^*$$

$$= \left(\frac{1}{2\pi T}\right)^4 \beta^3 \int_{\mathfrak{R}_T^2}\int_{\mathfrak{R}_T^2}\int_{\mathfrak{R}_T^2} e^{-i(r-r^*)\cdot\lambda} Q_Y^{(4)}(r-r^*, r^*-s^*, 0)\,dr\,dr^*\,ds^*$$

$$= O\left(\frac{1}{T^2}\right),$$

$$\left(\frac{1}{2\pi T}\right)^4 \beta^4 \int_{\mathfrak{R}_T^2}\int_{\mathfrak{R}_T^2}\int_{\mathfrak{R}_T^2}\int_{\mathfrak{R}_T^2} e^{-i(r-r^*)\cdot\lambda} e^{-i(s-s^*)\cdot\mu}$$
$$\times Q_Y^{(4)}(r-s^*, r^*-s^*, s-s^*)\,dr\,dr^*\,ds\,ds^*$$
$$= O\left(\frac{1}{T^2}\right).$$

The result of the first part is $O\left(\frac{1}{T^2}\right)$ uniformly in λ and μ.

Now we compute

$$\left(\frac{1}{2\pi T}\right)^4 \int_{\mathfrak{R}_T^2}\int_{\mathfrak{R}_T^2}\int_{\mathfrak{R}_T^2}\int_{\mathfrak{R}_T^2} e^{-i(r-r^*)\cdot\lambda} e^{-i(s-s^*)\cdot\mu} R_Y(r-r^*)R_Y(s-s*)$$
$$\times E[N(dr)N(dr^*)N(ds)N(ds^*)]$$
$$-\left(\frac{1}{2\pi T}\right)^4 \left\{ E\left|\int_{\mathfrak{R}_T^2} e^{-ir\cdot\lambda} Z(dr)\right|^2 E\left|\int_{\mathfrak{R}_T^2} e^{-is\cdot\mu} Z(ds)\right|^2 \right\}$$

$$= \left(\frac{1}{2\pi T}\right)^4 \int_{\mathfrak{R}_T^2}\int_{\mathfrak{R}_T^2}\int_{\mathfrak{R}_T^2}\int_{\mathfrak{R}_T^2} e^{-i(r-r^*)\cdot\lambda} e^{-i(s-s^*)\cdot\mu}$$
$$\times R_Y(r-r^*)R_Y(s-s*)E[N(dr)N(dr^*)N(ds)N(ds^*)]$$

$$-\left(\frac{1}{2\pi T}\right)^4 \left\{ \beta^4 \int_{\mathfrak{R}_T^2}\int_{\mathfrak{R}_T^2} e^{-i(r-r^*)\cdot\lambda} R_Y(r-r^*)\,dr\,dr^* \right.$$
$$\times \int_{\mathfrak{R}_T^2}\int_{\mathfrak{R}_T^2} e^{-i(s-s^*)\cdot\mu} R_Y(s-s^*)\,ds\,ds^*$$

$$+\beta^3 T^2 R_Y(0) \int_{\mathfrak{R}_T^2}\int_{\mathfrak{R}_T^2} e^{-i(r-r^*)\cdot\lambda} R_Y(r-r^*)\,dr\,dr^*$$

$$\left. +\beta^3 T^2 R_Y(0) \int_{\mathfrak{R}_T^2}\int_{\mathfrak{R}_T^2} e^{-i(s-s^*)\cdot\mu} R_Y(s-s^*)\,ds\,ds^* + T^4\beta^2 R_Y^2(0) \right\}.$$

Because we subtracted dominant terms, the second part has 11 terms left. We consider $R_Y(r-r^*)R_Y(s-s^*)$ multiplying (B.2.2), (B.2.3), (B.2.5),

(B.2.11) only.

$$\left(\frac{1}{2\pi T}\right)^4 \int_{\mathfrak{R}_T^2}\int_{\mathfrak{R}_T^2}\int_{\mathfrak{R}_T^2}\int_{\mathfrak{R}_T^2} e^{-i(r-r^*)\cdot\lambda} e^{-i(s-s^*)\cdot\mu}$$
$$\times R_Y(r-r^*)R_Y(s-s^*)\,\mathrm{Cum}\{N(dr), N(dr^*), N(ds), N(ds^*)\}$$

$$= \left(\frac{1}{2\pi T}\right)^4 \int_{\mathfrak{R}_T^2} R_Y^2(0)\beta\,dr$$

$$= \left(\frac{1}{2\pi T}\right)^4 R_Y^2(0)\beta T^2$$

$$= O\left(\frac{1}{T^2}\right),$$

$$\left(\frac{1}{2\pi T}\right)^4 \int_{\mathfrak{R}_T^2}\int_{\mathfrak{R}_T^2}\int_{\mathfrak{R}_T^2}\int_{\mathfrak{R}_T^2} e^{-i(r-r^*)\cdot\lambda} e^{-i(s-s^*)\cdot\mu}$$
$$\times R_Y(r-r^*)R_Y(s-s^*)\beta\,\mathrm{Cum}\{N(dr^*), N(ds), N(ds^*)\}dr$$

$$= \left(\frac{1}{2\pi T}\right)^4 \beta^2 \int_{\mathfrak{R}_T^2}\int_{\mathfrak{R}_T^2} e^{-i(r-r^*)\cdot\lambda} R_Y(r-r^*)R_Y(0)\,dr\,dr^*$$

$$= \left(\frac{1}{2\pi T}\right)^4 \beta^2 R_Y(0) \int_{\mathfrak{R}_T^2}\int_{\mathfrak{R}_T^2} e^{-i(r-r^*)\cdot\lambda} R_Y(r-r^*)\,dr\,dr^*$$

$$= O\left(\frac{1}{T^2}\right),$$

$$\left(\frac{1}{2\pi T}\right)^4 \int_{\mathfrak{R}_T^2}\int_{\mathfrak{R}_T^2}\int_{\mathfrak{R}_T^2}\int_{\mathfrak{R}_T^2} e^{-i(r-r^*)\cdot\lambda} e^{-i(s-s^*)\cdot\mu}$$
$$\times R_Y(r-r^*)R_Y(s-s^*)\,\mathrm{Cum}\{N(dr), N(ds)\}\,\mathrm{Cum}\{N(dr^*), N(ds^*)\}$$

$$= \left(\frac{1}{2\pi T}\right)^4 \int_{\mathfrak{R}_T^2}\int_{\mathfrak{R}_T^2} e^{-i(r-r^*)\cdot\lambda} e^{-i(r-r^*)\cdot\lambda} R_Y(r-r^*)R_Y(r-r^*)\beta^2\,dr\,dr^*$$

$$= \left(\frac{1}{2\pi T}\right)^4 \beta^2 \int_{\mathfrak{R}_T^2}\int_{\mathfrak{R}_T^2} e^{-i(r-r^*)\cdot(\lambda+\mu)} R_Y^2(r-r^*)\,dr\,dr^*$$

$$= O\left(\frac{1}{T^2}\right),$$

$$\left(\frac{1}{2\pi T}\right)^4 \int_{\mathfrak{R}_T^2}\int_{\mathfrak{R}_T^2}\int_{\mathfrak{R}_T^2}\int_{\mathfrak{R}_T^2} e^{-i(r-r^*)\cdot\lambda} e^{-i(s-s^*)\cdot\mu}$$
$$\times R_Y(r-r^*)R_Y(s-s^*)\beta^2 \operatorname{Cum}\{N(dr), N(ds)\}dr^*ds^*$$

$$= \left(\frac{1}{2\pi T}\right)^4 \int_{\mathfrak{R}_T^2}\int_{\mathfrak{R}_T^2}\int_{\mathfrak{R}_T^2} e^{-i(r-r^*)\cdot\lambda} e^{-i(r-s^*)\cdot\mu}$$
$$\times R_Y(r-r^*)R_Y(r-s^*)\beta^3 dr dr^* ds^*$$

$$= O\left(\frac{1}{T^2}\right).$$

The result of part 2 is $O\left(\frac{1}{T^2}\right)$ uniformly in λ and μ. For the third part, we compute

$$\left(\frac{1}{2\pi T}\right)^4 \int_{\mathfrak{R}_T^2}\int_{\mathfrak{R}_T^2}\int_{\mathfrak{R}_T^2}\int_{\mathfrak{R}_T^2} e^{-i(r-r^*)\cdot\lambda} e^{-i(s-s^*)\cdot\mu}$$
$$\times R_Y(r-s)R_Y(r^*-s^*)E[N(dr)N(dr^*)N(ds)N(ds^*)].$$

Here we still have 15 terms, we compute the dominant terms only,the others can be obtained by using the method in Part 2. The dominant terms are (B.2.5), (B.2.8), (B.2.11), (B.2.12).

$$\left(\frac{1}{2\pi T}\right)^4 \int_{\mathfrak{R}_T^2}\int_{\mathfrak{R}_T^2}\int_{\mathfrak{R}_T^2}\int_{\mathfrak{R}_T^2} e^{-i(r-r^*)\cdot\lambda} e^{-i(s-s^*)\cdot\mu}$$
$$\times R_Y(r-s)R_Y(r^*-s^*)\operatorname{Cum}\{N(dr), N(ds)\}\operatorname{Cum}\{N(dr^*), N(ds^*)\}$$

$$= \left(\frac{1}{2\pi T}\right)^4 \beta^2 \int_{\mathfrak{R}_T^2}\int_{\mathfrak{R}_T^2} e^{-i(r-r^*)\cdot(\lambda+\mu)} R_Y^2(0)dr dr^*$$

$$= \left(\frac{1}{2\pi T}\right)^4 \beta^2 R_Y^2(0) \int_{\mathfrak{R}_T^2}\int_{\mathfrak{R}_T^2} e^{-i(r-r^*)\cdot(\lambda+\mu)} dr dr^*$$

$$= \left(\frac{1}{2\pi T}\right)^4 \beta^2 R_Y^2(0) \left[\frac{\sin^2\frac{T(\lambda(1)+\mu(1))}{2}}{\left(\frac{\lambda(1)+\mu(1)}{2}\right)^2}\right]\left[\frac{\sin^2\frac{T(\lambda(2)+\mu(2))}{2}}{\left(\frac{\lambda(2)+\mu(2)}{2}\right)^2}\right]$$

$$= \frac{1}{T^4}\frac{\beta^2 R_Y^2(0)}{(2\pi)^4}\left[\frac{\sin^2\frac{T(\lambda(1)+\mu(1))}{2}}{\left(\frac{\lambda(1)+\mu(1)}{2}\right)^2}\right]\left[\frac{\sin^2\frac{T(\lambda(2)+\mu(2))}{2}}{\left(\frac{\lambda(2)+\mu(2)}{2}\right)^2}\right],$$

$$\left(\frac{1}{2\pi T}\right)^4\int_{\mathfrak{R}_T^2}\int_{\mathfrak{R}_T^2}\int_{\mathfrak{R}_T^2}\int_{\mathfrak{R}_T^2} e^{-i(r-r^*)\cdot\lambda}e^{-i(s-s^*)\cdot\mu}R_Y(r-s)R_Y(r^*-s^*)\beta^2$$
$$\times \mathrm{Cum}\{N(dr), N(ds)\}dr^*ds^*$$

$$= \left(\frac{1}{2\pi T}\right)^4\int_{\mathfrak{R}_T^2}\int_{\mathfrak{R}_T^2}\int_{\mathfrak{R}_T^2} e^{-i(r-r^*)\cdot\lambda}e^{-i(r-s^*)\cdot\mu}$$
$$\times R_Y(0)R_Y(r^*-s^*)\beta^3 dr dr^* ds^*$$

$$= \left(\frac{1}{2\pi T}\right)^4\beta^3 R_Y(0)\int_{\mathfrak{R}_T^2}\int_{\mathfrak{R}_T^2}\int_{\mathfrak{R}_T^2} e^{i(r^*-s^*)\cdot\lambda}$$
$$\times R_Y(r^*-s^*)e^{-i(r-s^*)\cdot(\lambda+\mu)}dr dr^* ds^*$$

$$= \frac{1}{T^2}\left(\frac{1}{2\pi T}\right)^2\phi_Y(\lambda)\beta^3 R_Y(0)\left[\frac{\sin^2\frac{T(\lambda(1)+\mu(1))}{2}}{\left(\frac{\lambda(1)+\mu(1)}{2}\right)^2}\right]$$
$$\times\left[\frac{\sin^2\frac{T(\lambda(2)+\mu(2))}{2}}{\left(\frac{\lambda(2)+\mu(2)}{2}\right)^2}\right] + O\left(\frac{1}{T^2}\right),$$

$$\left(\frac{1}{2\pi T}\right)^4\int_{\mathfrak{R}_T^2}\int_{\mathfrak{R}_T^2}\int_{\mathfrak{R}_T^2}\int_{\mathfrak{R}_T^2} e^{-i(r-r^*)\cdot\lambda}e^{-i(s-s^*)\cdot\mu}$$
$$\times R_Y(r-s)R_Y(r^*-s^*)\beta^2\,\mathrm{Cum}\{N(dr^*), N(ds^*)\}dr ds$$

$$= \left(\frac{1}{2\pi T}\right)^4\beta^3 R_Y(0)\int_{\mathfrak{R}_T^2}\int_{\mathfrak{R}_T^2}\int_{\mathfrak{R}_T^2} e^{-i(r-s)\cdot\lambda}$$
$$\times R_Y(r-s)e^{i(r^*-s)\cdot(\lambda+\mu)}dr dr^* ds$$

$$= \frac{1}{T^2}\left(\frac{1}{2\pi T}\right)^2 \phi_Y(\lambda)\beta^3 R_Y(0)\left[\frac{\sin^2\frac{T(\lambda(1)+\mu(1))}{2}}{\left(\frac{\lambda(1)+\mu(1)}{2}\right)^2}\right]$$

$$\times\left[\frac{\sin^2\frac{T(\lambda(2)+\mu(2))}{2}}{\left(\frac{\lambda(2)+\mu(2)}{2}\right)^2}\right] + O\left(\frac{1}{T^2}\right),$$

$$\left(\frac{1}{2\pi T}\right)^4 \beta^4 \int_{\mathfrak{R}_T^2}\int_{\mathfrak{R}_T^2}\int_{\mathfrak{R}_T^2}\int_{\mathfrak{R}_T^2} e^{-i(r-r^*)\cdot\lambda} e^{-i(s-s^*)\cdot\mu}$$
$$\times R_Y(r-s)R_Y(r^*-s^*)drdr^*dsds^*$$

$$= \left(\frac{1}{2\pi T}\right)^4 \beta^4 \int_{\mathfrak{R}_T^2}\int_{\mathfrak{R}_T^2}\int_{\mathfrak{R}_T^2}\int_{\mathfrak{R}_T^2} e^{-i(r-s)\cdot\lambda} e^{i(r^*-s^*)\cdot\lambda}$$
$$\times R_Y(r-s)R_Y(r^*-s^*)e^{-i(s-s^*)\cdot(\lambda+\mu)}drdr^*dsds^*$$

$$= \left(\frac{1}{2\pi T}\right)^4 \phi_Y^2(\lambda)\beta^4\left[\frac{\sin^2\frac{T(\lambda(1)+\mu(1))}{2}}{\left(\frac{\lambda(1)+\mu(1)}{2}\right)^2}\right]\left[\frac{\sin^2\frac{T(\lambda(2)+\mu(2))}{2}}{\left(\frac{\lambda(2)+\mu(2)}{2}\right)^2}\right]$$
$$+ O\left(\frac{1}{T^2}\right).$$

Hence the third part equals to

$$\frac{1}{T^2}\phi_Z^2(\lambda)\left[\frac{\sin^2\frac{T(\lambda(1)+\mu(1))}{2}}{T\left(\frac{\lambda(1)+\mu(1)}{2}\right)^2}\right]\left[\frac{\sin^2\frac{T(\lambda(2)+\mu(2))}{2}}{T\left(\frac{\lambda(2)+\mu(2)}{2}\right)^2}\right] + O\left(\frac{1}{T^2}\right)$$

where

$$\phi_Z(\lambda) = \beta^2\phi_Y(\lambda) + \frac{\beta R_Y(0)}{(2\pi)^2}.$$

The proof of the fourth part will be the same as part three, we will find only four dominant terms which are (B.2.2), (B.2.9), (B.2.10), (B.2.12). The fourth part equals to

$$\frac{1}{T^2}\phi_Z^2(\lambda)\left[\frac{\sin^2\frac{T(\lambda(1)-\mu(1))}{2}}{T\left(\frac{\lambda(1)-\mu(1)}{2}\right)^2}\right]\left[\frac{\sin^2\frac{T(\lambda(2)-\mu(2))}{2}}{T\left(\frac{\lambda(2)-\mu(2)}{2}\right)^2}\right] + O\left(\frac{1}{T^2}\right).$$

Hence

$$\begin{aligned}&\mathrm{Cov}\{I_T(\lambda(1),\lambda(2)), I_T(\mu(1),\mu(2))\}\\&\quad=\frac{1}{T^2}\phi_Z^2(\lambda(1),\lambda(2))\{\Delta_T(\lambda(1)+\mu(1))\Delta_T(\lambda(2)+\mu(2))\\&\qquad+\Delta_T(\lambda(1)-\mu(1))\Delta_T(\lambda(2)-\mu(2))\}+O\left(\frac{1}{T^2}\right)\end{aligned}$$

where

$$\Delta_T(\omega)=\frac{1}{T}\left(\frac{\sin\frac{T\omega}{2}}{\frac{\omega}{2}}\right)^2, \qquad \omega\in R.$$

■

Application of probabilistic and self-organising neural networks in pattern recognition: a tutorial paper

D. Nandagopal
Guided Weapons Division
Defence Science and Technology Organisation
Salisbury, South Australia 5108
nan@dstos3.dsto.oz.au

Abstract Automatic target recognition in images from sources such as video cameras, infrared cameras, radar, satellites, etc., is an area of increasing importance and growing concern. Pattern recognition in images largely depends on two important factors: (a) a good feature extraction technique, and (b) good feature recognition and classification. Many image processing techniques and tools are available today to improve the quality of acquired images and thereby enhance the feature extraction process. Feature extraction depends on the nature of the image data and application. Statistical feature extraction methods treat patterns as points in a multidimensional measurement space. The statistical methods normally consider relationships—such as joint probability distribution, interpoint distances, and scatter matrices—to define patterns. There is, however, another approach. Recently there has been a sudden surge in research activity in the area of feature detection and recognition using neural networks. We will discuss the application of two interesting neural network structures based on (a) probabilistic neural networks (PNNs) and (b) self-organising neural networks. The self-organising neural net structure is built on adaptive resonance theory (ART), as propounded by Grossberg and Carpenter [1].

1. Introduction

Artificial neural networks (ANN) are computational models built around massively parallel interconnected processing elements, as in biological nervous systems. ANN models attempt to achieve human-like performance in real time. There has been a sudden surge in the development and use of ANN models to solve a wide variety of information processing problems, leading to the emergence of a fundamentally new and different approach to information processing and, hence, computing. This new approach—called *neurocomputing*—seems to be the alternative to "programmed computing" which has dominated information processing for the last 45 years. Robert Hecht-Nielsen defines neurocomputing as the new technological discipline

J. S. Byrnes et al. (eds.), Probabilistic and Stochastic Methods in Analysis, with Applications, 369–382.
© 1992 *Kluwer Academic Publishers. Printed in the Netherlands.*

concerned with information processing systems that autonomously develop operational capabilities in adaptive response to an information environment [5]. The following section briefly discusses some fundamental aspects of neurocomputing, while the later sections discuss the applications of two ANN models, viz, the adaptive resonance theory (ART) based structure and the probabilistic neural network (PNN), in pattern recognition.

2. Fundamentals of ANN

The fundamental unit of the complete information processing system in our brain is the *neuron*, which is a stand-alone analogue logical processing unit. Each neuron is a simple microprocessing unit which receives and combines signals from many other neurons through input processes called *dendrites*. See Figure 2.1 for the structure of a neuron. Signals to dendrites are communicated through specialised neuromuscular junctions called *synapses*. The input signals are weighted at these junctions. The synaptic strength determines the weight. The input signals are combined at the cell body (nucleus). If the combined signal is strong enough, it activates the firing of the neuron. This produces an output signal which travels along a long transmission line like structure, called an *axon*, which could be many meters long. The information transfer is chemical in nature but we can measure the effect as an electrical potential. This chemical is sometimes called a *neurotransmitter* and is released whenever the connection is made. The synaptic strengths (as determined by the amount of neurotransmitter release) are what is modified when the brain learns! The synapses along with the processing information of the neuron form the basic memory mechanism of the brain. The brain consists of tens of billions of neurons—all interconnected to form the biological neural network.

The neuron therefore, is a basic computing element in the brain. The neuron, like a microprocessor, receives many inputs, weights them, combines them and finally outputs through a threshold function.

2.1. Artificial (electronic) neurons

In an artificial neural network, the unit analogous to the neuron is called a *processing element* (electronic neuron). A processing element (PE) may have many inputs and only one output. The inputs are algebraically summed. The combined input is then modified by a nonlinear activation function or a transfer function. The activation function could also be a threshold function. The output of a PE can be connected to inputs of other PE's through connection weights (synaptic strength). Figure 2.2 illustrates this basic building block of an ANN.

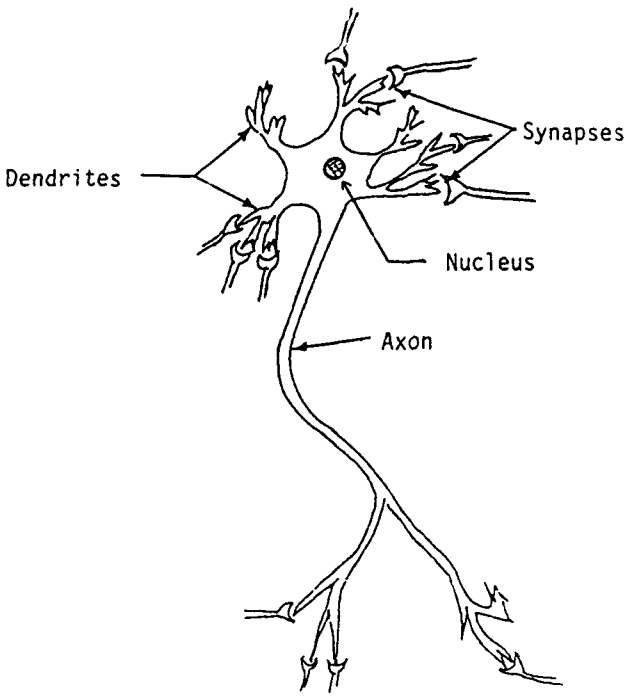

Figure 2.1: The biological neuron

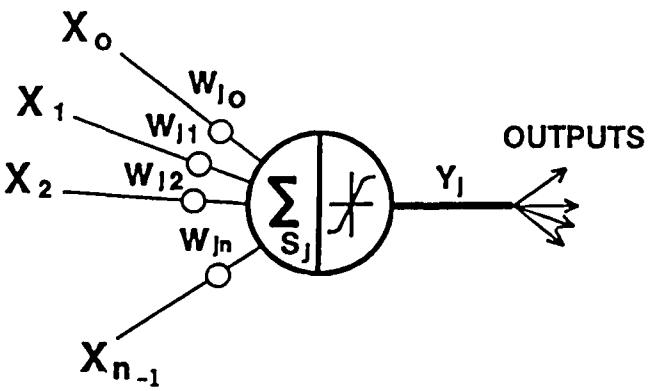

Figure 2.2: An artificial neuron. $S_j = \sum_i W_{ji} X_i$ and $Y_j = f(S_j)$ · (activation function).

If there are N inputs to a neuron, then the net input to the neuron is given by:

$$S_j = \sum_{i=0}^{N-1} W_{ij} X_i - \theta_j \tag{2.1}$$

where

S_j: the net input to j-th neuron.
X_i: inputs to the neuron.
W_{ij}: connection weights between the i-th input and j-th neuron.
θ_j: the bias value above which the neuron fires.

The output of the neuron is a function of a nonlinear activation function. A common activation function is the sigmoid function. The output Y_j of the j-th neuron can be described as:

$$Y_j = f(S_j) \tag{2.2}$$

$$= \frac{1}{1 + e^{-S_j}} \quad \text{for a sigmoid function} \tag{2.3}$$

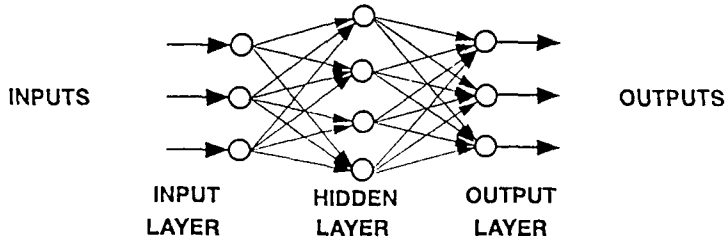

Figure 2.3: An ANN structure

2.2. ANN structure

A *neural network* consists of many interconnected processing elements. The PEs are normally organised into groups called *layers* or *slabs*. There are typically two layers which connect an ANN to the outside world. An input layer of neurons where the data is presented to the network as input and an output layer of neurons which hold the result. Figure 2.3 illustrates an ANN formed using the PEs as basic building blocks. Any layer(s) of neurons between the input and output slabs is(are) known as hidden layer(s).

2.3. ANN operation

The neural network operation depends largely on its "learning" process. *Learning* is the process of adapting or modifying the connection weights in response to stimuli being presented at the input and possibly the output. A stimulus at the output corresponds to a desired output or response to a given input, in which case the learning is *supervised*. If no desired output is shown, the learning is called *unsupervised learning*.

In summary, neural networks in general are nonprogrammed adaptive systems which process information in response to an excitation. Neural networks are normally trained to respond to an input and are adaptive or self-organising, i.e., they learn to solve problems purely on the basis of the training data presented to them. Several neural network paradigms, such as multi-layer perception, Hopfield net, back propagation, Kohonen's self-organising neural nets, etc., have been proposed to solve pattern recognition and other signal processing problems.

3. Pattern recognition

Neural networks are being applied to process a wide variety of sensor data. The sensor may be a microphone, a pair of electrodes, a radar, a TV or an infra-red camera, etc. The main aim of processing sensor signals is to extract information about the signal source and/or the medium through which the signals have travelled before detection by the sensors. One aspect of sensor signal processing is to detect and recognise certain "known" features of the signal. This process is often termed *pattern recognition*. Examples include:

- recognising a particular word or a speaker from speech signals;
- detecting waveform shapes (ECG waveforms);
- detecting and identifying a radar signature from a particular aircraft;
- recognising a particular class of ship using infra-red images, etc.

The recognition process may be illustrated schematically as stages in a signal processor, as indicated in Table 3.1. The functions in each block differ significantly depending on the type of sensors used.

Detection	Preprocessing	Feature extraction	Classificati	Identification
Sensor Signal	Distinguish signals from noise and clutter	Data reduction	Determine class membership	Determine specific type

Table 3.1 The pattern recognition process

3.1. Pattern recognition in images

Pattern recognition in images largely depends on two important factors: (a) good feature extraction techniques and (b) feature recognition and classification. A number of image processing techniques and tools are available today to improve the quality of acquired images and thereby enhance the feature extraction process. The feature extraction process depends on the nature of the image data and application. Conventional classifiers treat patterns as points in a multi-dimensional measurement space, using relationships such as joint probability distribution, interpoint distances and scatter matrices to define classes. Neural networks have been proved to be suitable for solving pattern recognition problems. The following sections briefly describe the application of two different neural network structures to pattern recognition of infrared images (IR) of ships. One of the neural networks is a self-organising type while the other is a probabilistic neural network based on the Bayesian classifier. The self-organising neural network considered here is based on adaptive resonance theory (ART) proposed by Grossberg [3, 4]. According to Grossberg, the adaptive resonance architectures are neural networks that self-organise stable recognition codes in real time in response to arbitrary sequences of input patterns. The probabilistic neural networks (PNN) for classification was introduced by Specht [8].

4. Probabilistic neural network (PNN)

The PNN is a neural network implementation of the Bayesian classifier and provides a general structure for solving pattern recognition problems. The PNN is basically a three-layer feed-forward network that uses the sums of Gaussian distributions to estimate the probability density functions (PDF) for various classes as learned from training data sets. Although the PNN structure resembles the back propagation network (BPN), the activation function of its processing elements is different from that of BPNs. In the processing elements of PNN, the commonly used sigmoidal activation is replaced by one of a class of exponential functions. The PNN provides probability and reliability measures for each of its classifications. A generalised structure of the PNN is illustrated in Figure 4.1. The neurons in the input layer simply span out the input data to neurons in the pattern layer where the data are weighted, summed and passed through an exponential activation function, as shown in Figure 4.2.

There are as many pattern units for each class as there are training vectors for each class.

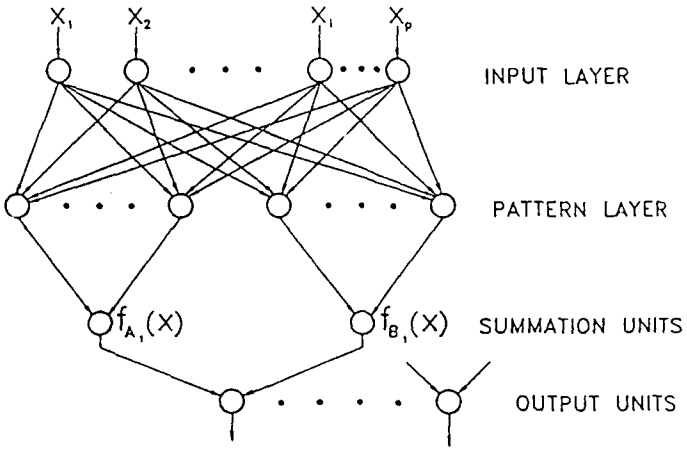

Figure 4.1: Generalised PNN structure

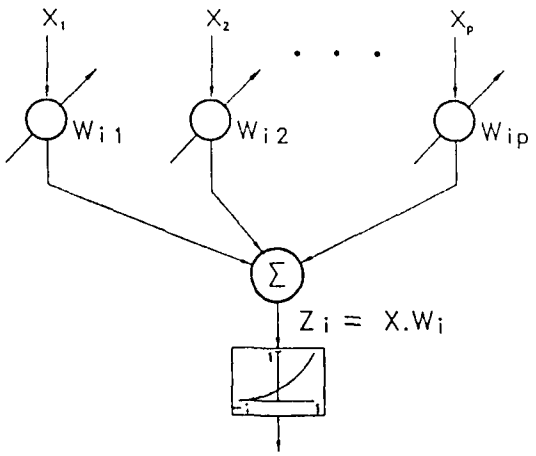

Figure 4.2: Pattern unit in PNN

5. Parzen estimator

Parzen estimation is used to build the PDF over the feature space for each

category. The Parzen estimator used in the PNN is given below.

$$f_A(X) = \frac{1}{(2\pi)^{p/2}\sigma^p}\frac{1}{N}\sum_{i=1}^{N} PK(X) \tag{5.1}$$

where

$$PK(X) = \text{Parzen kernel} \qquad = \exp(-(X - X_{ai})^T(X - X_{ai})/2\sigma^2) \tag{5.2}$$

and

$f_A(X)$: Probability density function for class A.
X: Input pattern vector of dimension p.
X_{ai}: i-th training pattern from class A.
σ: smoothing parameter.
N: total number of training patterns.
T: represents transpose.

The equation (5.2) can be simplified as:

$$PK(X) = \exp(X^T X_{ai} - 1)/\sigma^2) \qquad (\text{since } X^T X = 1) \tag{5.3}$$

The term $X^T X_{ai}$ is the dot product of the feature vector to be classified with a training vector. If the input paths to a processing element in the pattern layer have their weights set to the training vector, then the standard summation produces that dot product. If the activation function of the processing element is of the form

$$\exp(Z - 1)/\sigma^2 \tag{5.4}$$

where

$$Z = X \cdot W \tag{5.5}$$

and W is the training vector, the processing element then implements the Parzen kernel as in (5.3). The summation layer of the PNN sums the Parzen kernels for each class, and the output layer finally chooses the class with the largest PDF to the input. The output layer also includes weighting to implement the a priori class probabilities, thus providing the full Bayesian classification process.

Normally, the PNN calculates

$$f_A(X) \qquad \frac{1}{N}\sum_{i=1}^{N} \exp(Z_i - 1)/\sigma^2 \tag{5.6}$$

when each class has the same number of training examples. The fixed term in (5.1) can be set to have any value for each category for scaling purposes. Some commercially available ANN software normally implement (5.6) [6].

The accuracy of PNN depends on the smoothing factor used in the estimation of Parzen's PDF. The PNN is trained by placing the training samples for each class directly in memory and then testing the network on the testing samples at different values of smoothing factor σ. Training involves finding an optimal value for the smoothing factor which gives the peak accuracy.

6. ART neural network

The ART architecture is highly adaptive and evolved from the simpler adaptive pattern recognition networks known as the competitive learning models. Figure 6.1 illustrates the ART structure schematically [2].

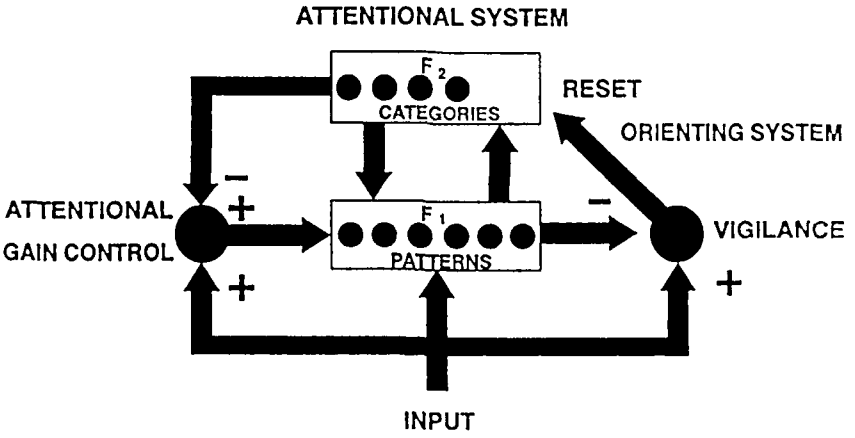

Figure 6.1: ART structure

There are two classes of ART structures: ART1 handles binary input patterns while ART2 can process both binary and analog patterns. The ART system basically consists of two layers of neurons called F1 and F2. The input sequence activates the neurons in the F1 layer and the activity passes through synaptic connections (weights) to neurons in the F2 layer where they compete with each other and finally one node fires (winner-take-all). The F1 layer is known as the *feature detection layer* and each neuron in the F2 layer represents a different "category." Each neuron in F1 is connected to every neuron in F2 by a *bottom-up pathway* and similarly a *top-down pathway* exists between neurons in the F2 and F1 layers. The activated node in the F2 layer reinforces activity in the F1 layer through *top-down priming*.

The neurons in F1 therefore receive two inputs. The flow of bottom-up and top-down information leads to a resonance in neural activity. If a particular feature is present in both the bottom-up and the top-down signals, then a reinforcement of F1 occurs. The attentional gain control system regulates the top-down signal when there is no bottom-up activity by setting the gain low and thus stopping the resonance when there is no input. The orienting system generates a reset signal to F2 whenever the input pattern to F1 is considerably different from the top-down information. The orienting system or the *novelty detector* receives an inhibitory input corresponding to the overall activity of F1 and an excitatory input from the input pattern, thus keeping a vigilance on the input pattern and the categories. When a novel pattern is detected, a reset signal is sent to F2 shutting off the active neurons and the network hunts for another neuron to be active through a new resonance. When a new neuron in F2 becomes active, then that node codes the input pattern. The detailed description of ART structure is well documented by Carpenter and Grossberg [2, 1].

7. Application of ART and PNN in pattern recognition

Infra-red (IR) images of navy vessels have been used to test the relative efficacies of ART and PNN in pattern recognition. Target images were obtained by a thermal imager operating in the 8–12μ region, recorded using a standard videotape recorder, and then digitised using a frame grabber to a resolution of 512 · 512 pixels with 8 bits per pixel depth.

7.1. Image processing

An edge-based image processing technique to localise and segment the target from its immediate surrounding background has been established in the Guided Weapons Division. The technique prefilters the IR image with the standard 3 · 3 median filter and then processes the image with the Prewitt 5 · 5 edge detector. The search for the targets is conducted in those regions of image that have relatively high edge strengths. Isothermal contours are extracted from areas of interest by an adaptive contour tracing algorithm at a number of thresholds. The details of image processing steps for IR images of ships can be found elsewhere [7].

7.2. Feature vector extraction

Two methods have been investigated to extract feature vectors. The fast Fourier transform (FFT) and the 1D Hadamard transform (HT) have been applied to extract the feature vectors from preprocessed IR images. The FFTs of the top profiles of ships (above the water line boundary) are computed

and the amplitudes of the first 12 Fourier coefficients are used as the input feature vectors to the Neural Network classifiers.

The 1D HT is applied to the whole of an object along its major axis (normally the horizontal axis). This process is suitable for images in which reflection of the vessel radiation from the sea surface is not a significant consideration. Objects are extracted using a local thresholding technique and the HT is applied between object extremities detected using a 1D Marr-Hildreth vertical edge detector. The HT is generated by sampling the area of the thresholded object through a series of binary masks generated from Walsh functions [9]. Feature vectors in a form suitable for input to the ART2 and PNN are obtained by normalising the 8 lowest order components to remove scale dependence and to retain a representation of their polarity.

7.3. Training of ART2 and PNN

Two sets of feature vectors were extracted using the FFT and 1D HT, as described above, from 80 IR images of ships belonging to 4 different classes. Each class of ship had 20 IR images obtained at various ranges. In each class, 10 images were used as training data and the remaining 10 as test data. The ART2 network was trained in an unsupervised incremental learning mode on a training set containing 10 feature vectors of each of 4 classes of ships. Thus, the ART2 network was trained separately on FFT and 1D HT feature vectors.

The PNN was trained by placing the training vectors for each class directly in memory and then testing the network on the test vectors at different values of the smoothing factor.

7.4. Recognition of ships by ART2 and PNN

We have investigated the efficacy of the two neural network structures in classifying IR images of ships belonging to 4 classes. We have also investigated two techniques (FFT and 1D HT) to extract feature vectors from the raw IR images. Both ART2 and PNN were presented with feature vectors from the test data set. Figure 7.1 shows the confusion matrices yielded by the ART2 in classifying the test data set (feature vectors were extracted using both the FFT and the 1D HT). The ART2 results have been presented at the Second Australian Conference on Neural Networks [7]. Refinements of the training technique have resulted in a significant improvement in the results from those reported earlier. It is obvious from the matrices that the ART2 Neural Net was able to classify the feature vectors obtained by the 1D HT far better than it could those obtained by the FFT. The ART2 classified 97.5% of 1D HT data with 100% classification accuracy.

		Input ship classes			
		A	B	C	D
Active	a	6	1	0	0
F2	b	0	9	0	0
Neurons	c	4	0	10	0
(Categories)	d	0	0	0	10
	u	0	0	0	0

Table 7.1: Using FFT generated feature vectors.

		Input ship classes			
		A	B	C	D
Active F2	a	9	0	0	0
Neurons	b	0	10	0	0
(Categories)	c	0	0	10	0
	d	0	0	0	10
	u	1	0	0	0

Table 7.2: Using 1D HT generated feature vectors.

Figure 7.1: Confusion matrices for ART2 pattern classification.

The PNN was tested using the same set of feature vectors as that of the ART2. The work on the PNN was carried out by the Department of Electrical and Electronic Engineering at the University of Western Australia through a research contract with the Guided Weapons Division for the purpose of comparing the performances of ART2 and PNN. Figure 7.2 shows the confusion matrix produced by the PNN in classifying 4 ship classes [10]. It is interesting to note that the PNN has also classified 97.5% (1D HT) of data correctly. Although the classification results of the PNN appear to be the same as those of ART2, the PNN has put some ship classes into wrong bins—thereby producing confusion. The ART2 did not cause such confusion (for 1D HT).

		Input ship class			
		A	B	C	D
PNN	a	8	0	0	2
Output	b	0	10	0	0
Class	c	0	0	10	0
	d	1	0	0	9

Table 7.3: Using FFT generated feature vectors.

		Input ship classes			
		A	B	C	D
PNN	a	10	1	0	0
Output	b	0	9	1	0
Class	c	0	0	10	0
	d	0	0	0	10

Table 7.4: Using 1D HT generated feature vectors.

Figure 7.2: Confusion matrices for PNN pattern classification.

8. Conclusions

A brief introduction to Artificial Neural Networks has been presented. The application of ANNs in pattern recognition has been examined. Two interesting Neural Network paradigms (ART2 and PNN) have been investigated,

yielding interesting results. The performances of the PNN and the ART2 have been compared. The PNN achieved classification accuracy similar to ART2's, but the ART2 produces less or no confusion compared to the PNN. In the case of the 1D Hadamard transform, the ART2 produced no confusion at all among the 4 ship classes. ART2 placed unclassified inputs into an unknown class, thus creating a new class. This is a desirable feature. The PNN, on the other hand, was insensitive to the value of sigma meaning that the classes are well separated. The data sets used are insufficient to draw definitive conclusions. However, the preliminary investigation has established the potential application of the ART2 and the PNN to pattern recognition of IR images of ships.

9. Bibliography

[1] G.A. Carpenter and S. Grossberg. ART2: Self-organisation of stable category recognition codes for analog input patterns. *Applied Optics*, 26:4919–4930, December 1987.

[2] G.A. Carpenter and S. Grossberg. A massively parallel architecture for a self-organising neural pattern recognition machine. *Computer Vision, Graphics and Image Processing*, 37:54–115, 1987.

[3] S. Grossberg. Adaptive pattern classifications and universal recording, I: Parallel development and coding of neural feature detectors. *Biological Cybernetics*, 23:121–134, 1976.

[4] S. Grossberg. Adaptive pattern classifications and universal recording, II: Feedback, expectation, olfaction and illusions. *Biological Cybernetics*, 23:187–202, 1976.

[5] R. Hecht-Nielsen. *Neurocomputing*. Addison-Wesley Publishing Company, USA, 1990.

[6] NeuralWare Inc. *NeuralWorks Professional II Users Guide*. USA, 1989.

[7] P. Lozo, R.P. Johnson, D. Nandagopal, G. Nussey, and T. Zyweck. An adaptive resonance theory (ART) based neural network approach to classifying targets in infrared images. In *Proceedings of the Second Australian Conference on Neural Networks (ACNN'91)*, pages 22–25, Sydney, 1991.

[8] D.F. Specht. Probabilistic neural networks for classification, mapping, or associative memory. In *Proceedings of International Conference on Artificial Neural Networks (ICNN-88)*, volume 1, pages 525–532, 1988.

[9] T.Y. Young and T.W. Calvert. *Classification, Estimation and Pattern Recognition.* Elsevier Publishing Co., 1974.

[10] A. Zaknich, C. deSilva, and Y. Attikiouzel. Comparative evaluation of the multi-class PNN and ART2 neural networks for classification of infra-red ship images—Parts I and II. In *The University of Western Australia Research Report to the Guided Weapons Division.* University of Western Australia, 1991.

Quantum holography and neurocomputer architectures†

Walter Schempp
Lehrstuhl fuer Mathematik I
University of Siegen
D-5900 Siegen Germany
schempp@hrz.uni-siegen.dbp.de

† This research was supported in part by the Institute for Mathematics and its Applications (IMA) at the University of Minnesota, with funds provided by the National Science Foundation. The author is grateful to Professors Avner Friedman, F. Alberto Grunbaum, and Willard Miller, Jr. for inviting him to participate in the IMA Summer Program 1990 on Radar and Sonar, and to Patricia V. Brick and Kaye Smith of IMA for their active assistance in producing the final version of the text.

Moreover, the author has many people to thank for giving him insights from alternate points of view. He especially wants to thank Professors Emmett N. Leith (University of Michigan at Ann Arbor) and Leonid P. Yaroslavsky (Institute of Information Transmission Problems of the Academy of Sciences of the USSR at Moscow) for technical discussions on optical holography, and to Professors Sing H. Lee (University of California at San Diego) and Jun Uozumi (Hokkaido University at Sapporo) for valuable conversations on computer-generated holography and holofractals, respectively. Finally, discussions with Professors Gheorghe Nemes (Central Institute of Physics at Bucharest) and Alexander G. Ramm (Kansas State University at Manhattan) on phase-space optics are greatly appreciated.

J. S. Byrnes et al. (eds.), Probabilistic and Stochastic Methods in Analysis, with Applications, 383–467.
© 1992 *Kluwer Academic Publishers. Printed in the Netherlands.*

The digital computer is extremely effective at producing precise answers to well-defined questions. The nervous system accepts fuzzy, poorly conditioned input, performs a computation that is ill-defined, and produces approximate output. The systems are thus different in essential and fundamentally irreconcilable ways. Our struggles with digital computers have taught us much about how neural computation is not done; unfortunately, they have taught us relatively little about how it is done. Part of the reason for this failure is that a large proportion of neural computation is done in an analog rather than in a digital manner.

Carver A. Mead (1989)

The actions of digital computers themselves depend vitally upon quantum effects—effects that are not, in my opinion, entirely free of difficulties inherent in the quantum theory. What is this 'vital' quantum dependence? In modern electronic computers, the existence of discrete states is needed (say, coding the digits 0 and 1), so that it becomes a clear-cut matter when the computer is in one of these states and when in another. This is the very essence of the 'digital' nature of computer operation. This discreteness depends ultimately on quantum mechanics.

Roger Penrose (1989)

1. Overview

The development of faster and more efficient computers in recent years has been driven by a seemingly unending thirst for communication, interaction, automation, control issues, information availability, and a yearning for new understanding of the self-organization principles of ourselves and our environment. The challenges of the future force us to create and study new concepts of adaptive information processing and to implement for faster communication novel computer architectures based on fundamental quantum theoretical principles.

Until now the increased power has been driven largely by continued refinements to microelectronic fabrication techniques, such as electronic switches (miniaturized transistors) with higher switching speeds and associated integrated circuits (ICs) with increased levels of integration on silicon chips. Although the advancements in the IC hardwiring and packaging functions have been significant, their prospect for continuing at the same steady rates from very large scale integration (VLSI) to ultra large scale integration (ULSI) are being dimmed by physical limitations associated with further miniaturization. Limitations of electronics include:

- electromagnetic interference at high speed,
- distorted edge transitions,

- complexity of metal connections,
- drive requirements for pins,
- large peak power levels,
- impedance matching effects.

Electromagnetic interference arises because the inductances of two current carrying wires are coupled. Sharp edge transitions must be maintained for proper switching, but higher frequencies are attenuated greater than lower frequencies, resulting in sloppy edges at high speeds. The complexity of metal connections on chips, on circuit boards, and between system components affects interconnection topology and introduces fields and unequal path lengths. This translates to signal skews that are overcome by slowing the system clock rate so that signals overlap sufficiently in time. Large peak power levels are needed to overcome residual capacitances, and impedance matching effects at connections require high currents which result in lower system speeds. Even if much smaller logic gates are produced by utilizing new techniques such as X-ray lithography yielding an order-of-magnitude reduction in feature size, the speed of the IC will be limited by the interconnection delays between transistors. Unlike transistor response times, these time lags are reluctant to scale down with size. As a result there is a 10^3 factor disparity between the speed of the fastest electronic switching components, presently transistors that can switch in 5 ps, and the clock rates of 5 ns of the fastest digital electronic computers.

To ensure further progress, it is prudent not to rely upon continued refinements to hardware and software implementations. In fact, computer architects are turning to the design of parallel processors to continue the drive toward faster and more powerful computers. The massively parallel organization principles which distinguish analog neural systems from the small scale interconnection architectures of special-purpose parallel electronic processors and even more from the von Neumann architecture of standard digital computer hardware are one of the main reasons for the largely emerging interest in neurocomputer science. Since presently some areas of microelectronics are approaching their natural physical limitations, it is necessary to examine other technologies that may offer denser, faster communication between chips or logic gate arrays or even provide alternatives to the gates themselves. If light could be used to transfer data between chips or gates, the interconnection-delay problems of electronics would be avoided and the communication would occur at the speed of light itself.

The system of linear interconnects by which nonlinear processing elements can share information among themselves is the most important component of any parallel computer. Just as photonics is becoming the technology of the future for telecommunication and machine-to-machine interconnects, it also penetrates computer hardware and affects communications

within a single computer, especially for processor-to-processor interconnects and board-to-board interconnects of parallel computer architectures, and even more of neurocomputer architectures. Not only does coherent light emitted by a laser have a much higher information capacity than electrical hardwires, but due to their boson character optical photons do not interfere during free-space propagation. Thus optical beams can occupy the same region of space without mutual interaction, allowing data streams to pass through one another without crosstalk and quantum interference, hence allowing multiple signals to travel the same channel in parallel. Indeed, a good lens can image tens of thousands of fully resolved points from one plane to another, each of these parallel channels having a theoretical bandwidth far in excess of 1 THz. Thus a single lens could easily carry all the telephone conversations simultaneously going on in the world at any moment in time. In this way, holographic optical interconnect technology leads to a very high packing density, to a simplified connection complexity, and to reduced drive requirements.

In summary of these arguments, optical technology includes the following advantages:

- high connectivity through coherent imaging,
- no physical contact for interconnects,
- non-interference of free-space propagating signals,
- high spatial and temporal bandwidth,
- no feedback to the power source,
- inherently low signal dispersion.

High bandwidth is achieved in space because of the non-interference of optical signals, and high bandwidth is achieved in time because propagating wavefronts do not mutually interact. There is no feedback to the power source as in electronics, so that there are no data dependent loads. Finally, inherently low signal dispersion means that the shape of a pulse as it leaves its source is virtually unchanged when it reaches its destination.

At the interchip level of the interconnection hierarchy, two types of holographic optical interconnects are available: free-space and guided-wave optical technology. In the free-space type, a large array of optical signal beams emitted from a light source is distributed by imaging it to a planar array of optical detectors using a holographic optical element (HOE) as a flat light diffracting device. This type of holographic optical interconnect is three-dimensional and provides flexible implementation of wiring schemes which are impossible to fabricate with conventional refractive/optical technology. However, it requires space because the HOE must be located above the arrays in the optical module. In the guided-wave type, an optical signal is transmitted and distributed from a coherent light source to an array of optical detectors via a guided-wave optical medium such as optical fibers

or integrated waveguides. This type of holographic optical interconnect is more compact and more mechanically stable than the free-space type. Its compactness is due to the planar layout of the optical elements and the use of small waveguides. Its stability is due to the fact that all optical elements are fixed on a common substrate. A hybrid integration procedure then enables integration of laser diodes and photodiodes at any position on the guided-wave circuit surface.

As an example of massively parallel extrinsic connections between hologram planes implemented by free space optics, the information throughput in one cycle of the AT&T Bell Laboratories' looped digital optical pipeline processor is higher than that of all the hardwired telephone nets on the whole world together. The processor is based on a family of optical modules which creates by split-and-shift hologratings from a pair of laser beams the array of power supply beams to read chips containing large arrays of self-electro-optic effect devices (SEEDs) of 5μm square. It operates at 1 million cycles per second, slower than most personal computers, but the most optimistic perspectives predict the implementation of an all-optical processor operating at several hundred million cycles per second—faster than most supercomputers—within the next five years.

Remark 1.1. The SEED processing elements form very-low-energy electo-optic modulators and optical logic gates based on multiple quantum well (MQW) structures that are fabricated by gallium arsenide GaAs-gallium aluminum arsenide GaAlAs technology utilizing molecular beam epitaxy (MBE). Large arrays of a family of SEEDs control the intensity of a beam of 850 nm-wavelength laser light passing through them by making use of the quantum confined Stark effect (QCSE). This quantum phenomenon causes an electrical voltage of a few volts applied normal to the plane of the quantum wells to decrease the material's ability to absorb light at 850nm wavelength. Thus an electrical signal can be converted to an optical signal carried by a laser beam. In a symmetric SEED (S-SEED) the quantum-well material is grown inside the intrinsic region of a PIN photodiode structure, and two such diodes are connected in series with a dc bias voltage applied. If laser light is incident on one of the diodes, a photocurrent is generated, the other diode acts as an electrical load, and the voltage across the first diode drops. This voltage drop causes an increase in optical absorption via the QCSE, thus generating more carriers and increasing the photocurrent. Positive feedback ensues, and the S-SEED switches into a stable state in which the first diode has a maximum absorption and transmits only a little light, while the second diode has low adsorption and high transmission. If a higher light intensity is applied to the second diode, the S-SEED will flip into the opposite state with the first diode absorbing and the second diode transmitting. The logic state of the device depends only upon the ratio of the input beams, and the state

of the device can be read out by a pair of equally powered beams without altering its condition, thus providing time-sequential gain. In this way the S-SEEDs can be used as fully cascadable optical differential logic devices with low switching energies (currently subpicojoule) and the potential speed of a billion operations per second. In fact, they are the first optical logic gates that are competitive with microelectronic processing elements in terms of switch energy and cascadability. Arrays of thousands of highly uniform S-SEEDs contained in GaAs chips can be addressed by arrays of laser beams incident normal to the plane of the chip. The beams can set and read out the logic state of the gates and transfer the data to subsequent similar arrays using imaging optics [83, 130 131].

Another example of massively parallel extrinsic connections between hologram planes is the guided-wave optical interconnection technology used in the field of amacronics. Amacronic structures are hybrid analog neural processors formed by layers of optics, electronics, and detector arrays organized in a parallel way similar to the amacrine clustered processing layers in front of the human retina. Like diurnal insects, amacronic sensor technology finally may be able to dynamically trade sensitivity for resolution.

All the holographic optical interconnect technology underlies the fundamental fact that in the quantized theory of the electromagnetic field the bosons (integral-spin particles) present in a beam of coherent light traveling in a well-defined direction are the photons. For light quanta, however, the quantum parallelism occurs according to which different alternatives at the quantum level are allowed to coexist in quantum complex linear superposition. The key idea of quantum holography is to mathematically model the quantum parallelism by the Kirillov quantization. This procedure allows to identify in a first step the hologram plane with the three-dimensional Heisenberg nilpotent Lie group quotiented by its one-dimensional center, then to restrict in a second step the sesquilinear holographic transform

$$\psi(t')dt' \otimes \varphi(t)dt \mapsto H_1(\psi, \varphi; x, y) \cdot dx \wedge dy$$

to the holographic lattices which form two-dimensional pixel arrays inside the hologram plane, and finally to recognize in a third step the hologram plane as a neural plane of local neural networks.

Quantum or photon holography as a part of quantum optics or photonics is the procedure of mathematically modeling the quantum parallelism by the Kirillov quantization. It allows a unified approach to planar optical components of digital optical computers and analog amacronic processors. Based on the beam splitter quantum interference experiment as an elementary building unit, the quantum holographic approach is also applicable to the Soffer optical resonator and the optical processing of synthetic aperture radar (SAR) data which represent particularly important examples of optical neurocomputer architectures.

Utilizing a unified quantum holographic approach to artificial neural network models implemented with coherent optical, optoelectronic, or analog electronic neurocomputer architectures, the paper establishes a new identity for the matching polynomials of complete bichromatic graphs which implement the intrinsic connections between neurons of local networks located in the neural plane. In microoptics and nanotechnology, the quantum theoretical treatment of optical holography is imperative because it involves only small differences of energy and not because atoms coherently excited by short laser pulses may be as large as some transistors of microelectronic ICs and the pathways between them inside the hybrid VLSI neurochips of amacronics. Actually, quantum effects can occur over distances of several meters or even billion of light years for quasars.

> *Until recently optical computing was looked upon as an alternative technology for performing an old task. Now, a paradigm shift is coming about as a result of the realization that optical computers are fundamentally different from, and in many senses superior to, any electronic computer. Certain optical computers are the only available ones that are intrinsically quantum mechanical processors.*
>
> ***H. John Caulfield and Joseph Shamir (1990)***

> *Not enough has been written about the philosophical problems involved in the application of mathematics, and particularly of group theory, to physics. On the one hand, mathematics is created to solve specific problems arising in physics, and, on the other hand, it provides the very language in which the laws of physics are formulated. One need only think of calculus or of Fourier analysis as examples of this dual relationship.*
>
> *We are all familiar with the exploitation of symmetry in the solution of a mathematical problem. On the other hand, the very assertion of symmetry is often the most profound formulation of a physical law or the key step in the development of a new theory.*
>
> ***V. Guillemin and S. Sternberg (1984)***

2. Introductory comments

Real-time image analysis and processing, computer vision, automatic target recognition for intelligent robots, remote surveillance, autonomous navigation, sound localization, speech processing and understanding, smart sensors processing, and various other application areas of artificial intelligence (AI) need to process an immense amount of data with very high velocity. The computational power required exceeds by many orders of magnitude

the capabilities of sequential digital computers. The Space Station program's Earth Observing System (Eos) polar orbiting platforms, for instance, require to process data rates up to 1.5 gigabits per second. High resolution color images running at frame rates as low as 30 frames per second will require 10^8 bits per second. If one adds some form of autonomous feature identification to the system, the processing requirement will be between 10^{10} and 10^{13} operations per second. As a final example, a human-like speech recognizer must simultaneously perform phonetic, phonemic, syntactic, semantic, and pragmatic analyses of its inputs and match them to $5 \cdot 10^4$ words in real time. These processing throughputs exceed even the most optimistic projections for sequential supercomputers.

The problem of large-volume and high-speed computations can be solved by

- data compression techniques,
- parallel data processing.

Since their very beginning, artificial neural networks have been considered as massively parallel computing paradigms. Indeed, neural nets offer the potential of providing massive parallelism, adaption to dynamic data structures, and new algorithmic approaches to problems in image processing, computer vision, speech recognition, robotic control, knowledge processing, among other application fields of AI. Ever the fastest sequential digital electronic computers (including advanced parallel architectures) typically require processing times ranging from many minutes to several hours for non-complex low-level image processing tasks on large image arrays.

The advantages of neural computation are now widely recognized and neural networks form one of the most rapidly expanding areas of contemporary research. In fact, research in neurocomputer science, stimulated by major advancements in neurophysiological studies, neurosynergetic understanding, optoelectronic technology, molecular engineering, and bioelectronic material processing is currently in the midst of a gold rush period, an intense period of rapid discovery and exploitation. Everywhere new veins of gold are being uncovered and mined by thousands of prospectors, most of whom have crossed over into this exciting new research area from a diversity of other disciplines—neurobiology, neurosynergetics, quantum physics, imaging optics, electrical engineering, mathematics, and computer science.

The fundamental characteristics of all known neurocomputer architectures are the linear synaptic interconnections between simple nonlinear processing elements, called neurons, to form a concurrent distributed processing pattern of extensive connectivity. The processing units like the S-SEED logic devices (cf. Remark 1.1 supra) are arranged as two-dimensional arrays of neurons in the neural plane. Information is stored in the neurocomputer almost exclusively in the interconnection pattern, called neural network.

Large scale (LS) collective systems like artificial neural networks exhibit many properties, including robustness, reliability, and fault tolerance, an ability to deal with ill-posed problems and noisy data, which conventional digital computer architectures do not. Adopting the synergetic point of view, neurobiology provides existence theorems on effectiveness of neural network parallel algorithms on appropriate problems.

For artificial neural networks to become ultimately useful, neuromorphic hardware must be developed. The effectiveness of neuromorphic hardware is in direct proportion to the attention it pays to the guiding neurobiological metaphor. Development efforts in the field of sixth generation computers have concentrated on one of two goals: to build

- efficient hardware that effectively executes software simulations,
- actual hardware emulators for specific neural network models.

Examples of the first are the Hecht-Nielsen Neurocomputer (HNC) accelerator board for conventional serial personal computers, and the Delta board by Science Applications International Corporation (SAIC). HNC is also pioneering a new computer language, AXON, that is designed for programming digital computers to simulate advanced neural networks. An important application of the SAIC neural network software simulation is the detection of explosives in checked airline baggage: the luggage is bathed in low energy (thermal) neutrons and the gamma rays resulting from neutron absorption by atomic elements in the luggage are analyzed. The artificial neural network software then searches for specific combinations of atomic elements that characterize explosives including dynamites and water gels.

Examples of the second can be viewed hierarchically. On the simplest level, the information is recorded and retrieved from an erasable magneto-optic disk by optical techniques. Higher-level building-blocks are two-dimensional arrays of coherent optical processors [2, 3, 4, 5, 7, 126, 127, 129, 128, 142, 145, 144, 143, 146] for the analog implementation of neural network models by holographic optical interconnects, and neural network analog VLSI chips. For instance, the analog silicon models of the orientation-selective retina for pattern recognition [1, 115, 117], and the analog electronic cochlea for auditory localization [92, 115, 116] belong to this category. The amacronic and the cochlea VLSI neurochips are made with a standard complementary metal oxide semiconductor (CMOS) process [189].

Although the implementation of the various neural network models needs to overcome many difficult optical, optoelectronic, and analog electronic design problems, their performance is modest compared with the powerful organizing principles found in biological neural wetware. The visual system of a single human being does more image processing than do the entire world's supply of supercomputers, and the nervous system of even a very simple animal like the common house fly (Musca domestica) contains

computing paradigms that are orders of magnitude more effective than are those found in systems made by humans. Unlike conventional computer hardware, neural circuitry is not hardwired or specified as an explicit set of point-to-point connections. Instead it develops under the influence of a genetic specification and epigenetic factors, such as electrical activity, both before and after birth. How this happens is in large part unknown.

Neurobiological development processes are far too complex to hope that a relatively complete understanding of how a perceptual system develops and functions will soon emerge. But we are familiar with complex synthetic systems whose principles of neural organization can be understood without one's knowing in detail how the components work. Furthermore, the same principles can be used to build neurocomputers in any of several different technologies. Presently the most advanced neural network analog CMOS VLSI chips model, to a first approximation, the time-frequency domain processing of two highly spectacular biological neural systems: the active echolocating system of the horseshoe bats (Rhinolophidae), and the passive auditory localization system of the barn owl (Tyto alba) which both produce complete maps of the auditory space from the time-frequency coding pathways. Continuing evolution, however, of hybrid submicron optoelectronic technology combined with neurocomputer science, the highly promising and exciting new field of studying how computations can be carried out in extensive networks formed by two-dimensional arrays of heavily interconnected simple processing elements, will create advanced neurocomputers within the next decade which will be able to solve problems intractable for even the largest conventional digital computers.

This paper concentrates on a unified quantum holographic approach to massively parallel coherent optical, optoelectronic, and analog electronic neurocomputer architectures. Notice that the borders between physical optics, electronics, and solid state physics are getting more and more fuzzy. The primary assumption of quantum or photon holography is that the energy transmitted by a beam of coherent radiation is divided into discrete wave packets, or photons, much as an electric current is made up of a flow of electrons. Detailed analysis shows that the arrival times at a photodetector of photons from a classical coherent radiation source such as a laser, exhibit the same Poissonian statistics as does the thermionic emission of electrons from the hot cathode of a vacuum tube. Thus, the photocurrent exhibits fluctuations which resemble the shot noise of the current in the vacuum tube. The quantum noise produced by a photoelectric detector is therefore an intrinsic property of the radiation itself, rather than of the photon detector.

The concept of photon arises from the quantization of the electromagnetic field. The spatial part of Maxwell's equations in vacuo

$$dF = 0 \quad \text{and} \quad d * F = 4\pi j$$

(differential 2-form $F = B + E \wedge dt$ on the Lorentz space $\mathfrak{R}^4$, d = exterior derivative, $*$ = Hodge star operator on $\Lambda^2(\mathfrak{R}^4)$) and the boundary conditions determine the possible frequencies ν, direction and spatial wavefront profile of the field, collectively referred to as the mode. The field modes are described by wave vectors $\mathbf{k} \neq 0$ in $\mathfrak{R}^3$. In spite of warnings, sometimes the suggestion occurs that the Maxwell waves do form the wave functions of the photon. This suggestion, however, is a false idea. Although a single photon can have a definite position at one time, it is impossible to construct a position operator for the photon. Therefore it cannot have definite positions at all times in a specified time interval, i.e., it cannot have a definite trajectory (Bohr's indeterminacy principle; see [139, 180]). Since in the presence of sources, photons can be absorbed or emitted, one cannot introduce a linear Schrödinger evolution equation for a single photon. In fact, the modes of the electromagnetic field must be quantized and photons of energy $h\nu$ then occur as elementary excitations driven by the quantized Maxwell field modes of frequency ν and label $\mathbf{k}$.

In quantum optics or photonics, the quantization of the Maxwell field modes is done by expressing the time dependent part of Maxwell's equations in the form of the equation of motion for a classical harmonic oscillator and then replacing the classical harmonic oscillator by its quantum-mechanical counterpart. In this way, the electromagnetic field is considered as an assemblage of driven harmonic oscillators. As a consequence, the energy of the radiation field is quantized and the quanta are referred to as photons. The state of the field can be expressed in terms of number states $|n_{\mathbf{k}}\rangle$ which are states with $n_{\mathbf{k}}$ quanta occupying the mode $\mathbf{k}$. These number states are eigenstates of the Hamiltonian of the quantum-mechanical harmonic oscillator. However, they are not a realistic description of a coherent radiation field, as emitted by a laser. One formal series of number states, the so called coherent state $|\alpha_{\mathbf{k}}\rangle$, is used to represent the coherent radiation field produced by an ideal source such as an ideal laser operating well above threshold. In the Dirac notation, the Glauber formal series expansion [134]

$$|\alpha_{\mathbf{k}}\rangle = \exp\left(-\frac{1}{2}|\alpha_{\mathbf{k}}|^2\right) \cdot \sum_{n=0} \frac{(\alpha_{\mathbf{k}})^n}{\sqrt{n!}} |n_{\mathbf{k}}\rangle$$

describes a state $|\alpha_{\mathbf{k}}\rangle$ where the probability of finding the mode occupied by $n_{\mathbf{k}}$ photons exhibits a Poisson distribution about a mean of $|\alpha_{\mathbf{k}}|^2$ with a width $|\alpha_{\mathbf{k}}|$. Ignoring the slowly time varying phase diffusion, the coherent state is considered to be a good approximation to the field produced by a coherent radiation source as a laser.

A mathematical description of photons or, more generally, of bosons is given by the Bargmann-Fock model of quantics [23, 78]. Actually, the Bargmann-Fock model is based on the quantum-field-theory annihilation

and creation operators for bosons and therefore on harmonic analysis of the three-dimensional isotropic Heisenberg nilpotent Lie group G. A first important advantage of the Heisenberg group approach is that it allows to define two-time averages, that is to say, mean values of mixed boson states taken at two different times t and $t' = t - x$ of fixed difference $t - t' = x$. A second important advantage is that the Kirillov quantization reveals the planar geometry of the unitary dual of the Heisenberg group G, that is to say, the planarly multilayered structure of the unitary dual manifold. To each flat layer, the Kirillov correspondence associates representations of G of linear Schrödinger type, or representations of G of linear Fraunhofer type, respectively. Because in the quantized theory of the electromagnetic field the bosons present in a beam of coherent light traveling in a well-defined direction are the photons, the Kirillov quantization approach allows to model, among other basic optical phenomena, the quantum parallelism performed by the beam splitter quantum interference experiment and optical holography, the functionality of holographic optical interconnects, optical phase conjugation, three-dimensional planarly multilayered optical devices like display holograms, and spatial light modulators (SLMs).

Display holograms are probably one of the most impressive realizations of the unitary dual manifold of G. Starting with the beam splitter quantum interference experiment as an elementary building unit, the key idea of quantum holography is to identify the symplectic hologram plane $\mathfrak{R} \dotplus \mathfrak{R}$ with G quotiented by its one-dimensional center C_G and to recognize via the Kirillov quantization procedure the symplectic hologram plane $\mathfrak{R} \dotplus \mathfrak{R}$ as a neural plane of local neural networks. As a result, harmonic analysis on the central projection G-slice G/C_G provides filtered backpropagation formulae which are at the base of the holographic reciprocity principle. Moreover, it gives rise to the elementary holograms and the Gabor wavelets which form total families of approximating functions in $L^2(\mathfrak{R} \dotplus \mathfrak{R})$ of decorrelating and correlating code primitives of artificial neural networks. The neural network implemented in the symplectic hologram plane $\mathfrak{R} \dotplus \mathfrak{R}$ explains the robust "associative" optical memory realized by optical holograms by the distributed nature of holographic recordings. Finally, a series of new identities for theta-null values which arises from artificial neural network identities shows that studies in computational mathematics combined with synthetic neurobiology may have an unexpected spin-off in pure mathematics.

Emphasis throughout the paper is placed on the application of quantum holography to neural computer architectures. For the fairly deep details of the Mackey machinery and the Kirillov quantization procedure underlying the harmonic analysis of the half-line bundle G over the two-sided symplectic hologram plane $\mathfrak{R} \dotplus \mathfrak{R}$, the reader is referred to the monograph [155]. Technological details of the implementations are described in the references indicated below and in the references listed in the monograph [52].

The double-slit experiment is a phenomenon which has in it the heart of quantum-mechanics; in reality it contains the only mystery of the theory.

Richard P. Feynman (1918–1988)

In any attempt of a pictorial representation of the behaviour of the photon we would meet with the difficulty: to be obliged to say, on the one hand, that the photon always chooses one of the two ways and, on the other hand, that it behaves as if it had passed both ways.

Niels Bohr (1885–1962)

The unitary Schrödinger evolution is totally deterministic, maintains quantum complex superposition, and acts in a continuous way, but the completely different procedure of forming the squared moduli of quantum amplitudes and only this non-deterministic reduction of the state-vector (or, as it is sometimes graphically described: collapse of the wavefunction) introduces uncertainties and probabilities into quantum theory. It is a probabilistic law which grossly violates quantum complex superposition and is blatantly discontinuous.

Roger Penrose (1989)

3. Quantum holography

The vertebrate vision system is perhaps the most complex neural assembly known. Although more details are known about vision than about any other neural system, it is by far not yet fully understood. On the deepest level of molecular operation, visual imaging is a quantum process. A solid object is seen because light scattered by the object causes chemical changes in the retinal cells of the eye. The eye is quite a good light detector: Experiments have shown that the vertebrate's retinal rod photoreceptors can respond to the absorption of even a single photon [14]. In general, however, many photons are absorbed by the eye without reaching a light sensitive cell. For this reason only a few photons in every hundred that enter the eye are detected. Obviously the chemical changes involved in seeing an object must be reversible. In fact, the cell reverts to its normal state after about one-tenth of a second. It is this short light storage period that limits the sensitivity of the eye for detecting faint objects. Photography can overcome this limitation of the eye by storing the changes in a permanent way on photographic emulsion.

Photographic emulsion consists of individual grains of a silver halide compound, in which the silver atoms are ionized. When a photon is absorbed by the photographic emulsion, an electron is emitted, in the same way as

electrons are knocked out of a metallic surface in the photo-electric effect. This electron can now be attracted by a silver ion to form a neutral atom of silver. Left to itself, the neutral silver atom, surrounded by the ionic silver halide compound, is unstable, and will eventually eject the electron and revert back to an ion. However, if before this happens, other photons have produced several other neutral silver atoms nearby, a stable development center consisting of a small number of atoms can be formed. In contrast, each grain of the photographic emulsion contains billions of silver ions. However, when the photographic emulsion is developed, this assembly of neutral silver atoms induces all the remaining silver ions in the grain to be deposited as opaque metallic si' 'er.

Figure 3.1

Figure 3.1 shows several photographs of the same person taken at different exposures. In the top left picture about $3 \cdot 10^3$ photons enter the camera. Most of these photons are absorbed without causing permanent change in the photographic emulsion. It is evident that $3 \cdot 10^3$ photons are not enough to generate a recognizable image and the photograph appears like random clusters of light dots. However, when the exposure increases the number of photons entering the camera increases. The top right picture involves about 10^4 photons and already, although there is no clear image, a blurred impression of an image is beginning to show up within the clusters of light dots. The improvement continues as the number of photons increases,

and the final exposure involves more than $3 \cdot 10^7$ photons. In this last picture, the image intensity seems to vary smoothly although it is built up out of individual development centers created by the arrival of individual photons. Although in the lowest exposure photograph the positions of the bright dots, signifying the presence of a development center in that grain emulsion, seem to be random, they are not. Centers are more likely to develop in places where the image will eventually be bright. Thus, even in a photograph, the quantum theoretical, probabilistic nature of light detection can be seen. It is not possible to predict with certainty where any particular photon will land, or in which grain of the photographic emulsion a development center will be produced.

Photographic emulsions are not sensitive to individual photons. Several neutral atoms must be produced in the photographic detector to form a development center. More efficient for imaging applications than photographic plates are the CCD (charge coupled device) detectors. They are formed by a two-dimensional array of photon detectors laid out on a single silicon chip typically comprising $2^9 \cdot 2^9$ pixels of size 20 μm · 20 μm. In fact, there are many formats for CCDs available. The arrival of single photons is detected directly by CCDs by converting them to electron-hole pairs, and then collecting the electrons into a potential well created by a depletion region. The accumulated charge at each position over the detector array then corresponds to the pattern of photons striking the CCD. The charge is read out by clocking the potential so that buckets of electrons transfer from well to well until they reach an integrating capacity and an on-chip preamplifier. An important feature of the device is that each pixel can be separately addressed, making CCDs extremely powerful for imaging applications.

Whereas photography first processes the optical information to form an image which is then recorded on the emulsion of a photographic plate or a CCD detector array, it is also possible to record the raw optical data in a non-localized way on the photographic emulsion or CCD and then place the processing in the future with the viewer. The method for recording the complete raw optical data is called optical holography. It is a two-step processing method which involves the phenomena of

- scattering,
- stationary quantum interference,
- diffraction.

In the first processing step, the holographic image encoding procedure, the beams scattered by the solid object are mixed with the coherent reference beam and the generated stationary quantum interference pattern is recorded as an optical hologram. In the second processing step, the holographic image decoding procedure, the quantum interference pattern is read out.

The quantum interference patterns are not stationary unless the interfering light wavelets are coherent. There are two types of coherence, both of which are required at least to some extent, to get a stationary interference fringe pattern. One is temporal (longitudinal or axial) coherence, which is the requirement that the light wavelets all travel in the same time or same frequency, i.e., monochromatic light. The other is spatial (transverse or lateral) coherence, which is the requirement that the light wavelets are moving together in phase as if they started from a single point in space. The laser produces a high degree of both temporal and spatial coherence.

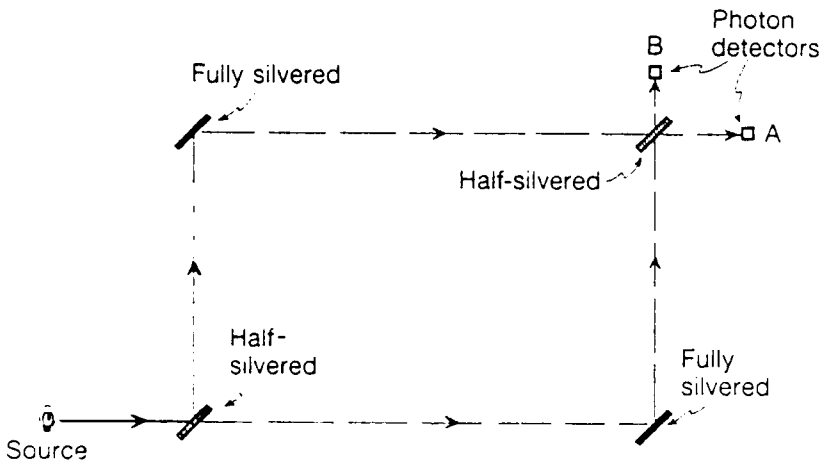

Figure 3.2

The basic experimental set-up to generate optical holograms is a modified version of the archetypical double-slit quantum interference experiment by which Thomas Young in 1803 conclusively verified the wave character of monochromatic light, and G.P. Thomson, the son of J.J. Thomson who first demonstrated that electrons behave like particles, and also Davisson and Germer in 1927 conclusively revealed that electrons also behave like waves: downstream, the primary wave is divided by a beam splitter into two coherent wavelets which travel different paths before recombination and detection; see Figure 3.2. If in the beam splitter quantum interference experiment the two photon routes possible in the linear Mach-Zehnder interferometer are exactly equal in length, there is 100% probability that the photon reaches the detector A and a 0% probability that it reaches the other detector B. In other words: the photon is certain to strike the detector A. If

an absorbing screen is placed in the way of either of the two interferometer routes, then it becomes equally probable that the photon reaches A or B; but when both paths are open and of the same lengths only detector A can be reached. Blocking off one of the two routes allows B to be reached. Therefore the photon must have actually traveled both routes at once. If a scattering object is placed in the way either of the two interferometer routes, a stationary quantum interference pattern is generated in the hologram plane due to the incremental measuring principle of the linear Mach-Zehnder interferometer. The organization of random clusters to stationary quantum interference fringe patterns in the hologram plane can be visualized by the photon-counting image acquisition system (PIAS-TI) which is capable to detect even single photons like the vertebrate's retinal rod and to obtain images at a level of darkness not obtainable even by ultra-high sensitivity video cameras.

Theorem 3.1. The holographic image encoding procedure is formed by a complex linear superposition of beam splitter quantum interference experiments. Conversely, the beam splitter quantum interference experiment performed by a linear Mach-Zehnder interferometer forms a degenerate holographic image encoding procedure.

From this result it follows that the basic quantum phenomenon of optical holography is the quantum parallelism according to which different alternatives at the photon level are allowed to coexist in quantum complex linear superposition. The great thirty-year dialogue between Bohr and Einstein [190, 191, 192, 194, 193, 195, 177] concerning the issues of the beam splitter quantum interference experiment demonstrates the fundamental importance of the basic holographic image encoding procedure (see Theorem 11.3 infra).

> *Die kodierte Form der Amplituden-und Phasenverteilung trägt die Bezeichnung Hologramm. Im Grunde genommen stellt das Hologramm ein Interferenzmuster dar, daß durch die Überlagerung der vom Objekt gestreuten Wellen mit der Referenzwelle zustande kommt. Die Funktion der Referenzwelle kann man sich auch so verdeutlichen, daß durch sie eine Lichtwelle im Raum "eingefroren" wird. Es addieren sich die Amplituden unter Berücksichtigung ihrer Phasenbeziehungen und nicht die Intensitäten.*
>
> ***Jurij I. Ostrovskij (1988)***

> *The various descriptions, Doppler filtering, aperture synthesis, holography, and cross-correlation, diverse as they are when described physically, become identically when formulated mathematically.*
>
> ***Emmett N. Leith (1978)***

4. The holographic image encoding procedure

The fundamental fact about optical holograms is that they are light diffracting elements. As planar diffractive optical elements (DOEs) they are of central importance for the implementation of neurocomputer architectures by holographic optical interconnects. The starting point of the holographic principle is the important fact that all detectors are phase-blind at the frequency range of the visible light. To overcome the phase-blindness, optical holography encodes in the writing step the phase information of the optical signals by a geometric encoding procedure. The word *holography* comes from the Greek *holos* meaning entire, complete and *graphein* meaning to write, to record. Subsequently, optical holographic technique decodes in the readout step the phase information by light diffraction. The holographic reciprocity principle mathematically describes the decoding procedure.

In order to get mathematical insight into the geometric encoding procedure of optical holography by sesquilinearization of the multiplexed signal energy, let $\mathcal{S}(\mathfrak{R})$ denote the Schwartz space of complex-valued $\mathcal{C}^\infty$ wavelet packet amplitude densities on the real line $\mathfrak{R}$ rapidly decreasing at infinity. Consider $\mathcal{S}(\mathfrak{R})$ as a dense vector subspace of the complex Hilbert space $L^2(\mathfrak{R})$ of square integrable complex-valued densities with respect to Lebesgue measure dt of $\mathfrak{R}$ under its natural isometric embedding. Endow $\mathcal{S}(\mathfrak{R})$ with the standard scalar product $\langle \, . \mid . \, \rangle$ and the associated total signal energy norm $\| \, . \, \|_2$. In optical holography, a square-law detector encodes in a massively parallel way the optical path length difference $x \in \mathfrak{R}$ and the phase difference $y \in \mathfrak{R}$ of two coherent signals having the same center frequency $\nu \neq 0$. Assuming that the writing complex-valued wavelet packet amplitude densities $\psi(t')dt'$ and $\varphi(t)dt$ with respect to Lebesgue measure $dt' = dt$ belong to the space $\mathcal{S}(\mathfrak{R})$, the coordinates (x, y) of the stationary quantum interference pattern are simultaneously recorded in the hologram plane $\mathfrak{R} \times \mathfrak{R}$ by the coherent two-wavelet mixing $\psi(t')dt' \times \varphi(t)dt$. In view of the phase-conjugate cross terms or interference terms $\langle \psi | \varphi \rangle$ and $\langle \overline{\psi} | \overline{\varphi} \rangle$ of the total signal energy distribution identity or signal intensity relation

$$\|v\psi + w\varphi\|_2^2 = \langle v\psi + w\varphi \mid v\psi + w\varphi \rangle$$

with complex weights $v, w \in \mathbb{C}$, the sesquilinear extension to $\mathcal{S}(\mathfrak{R}) \times \mathcal{S}(\mathfrak{R})$ of the mapping

$$\psi \times \varphi \mapsto H_\nu(\psi, \varphi; x, y) = \int_{\mathfrak{R}} \psi(t - x)\overline{\varphi}(t)e^{2\pi i \nu y t} dt \qquad (\nu \neq 0)$$

describes by quantum complex linear superposition of the phased two-time average the first step of the angle image encoding procedure of optical holography. In this first processing step, each object to be globally stored by the

coherent object signal beam is encoded in the hologram prior to its recording by mixing (or multiplexing or heterodyning) an unfocused linearly polarized coherent non-object-bearing reference signal beam having a particular angle between its wave vector and the normal vector of the hologram plane $\mathfrak{R} \div \mathfrak{R}$. Therefore the sesquilinear mapping defined by the assignment

$$\boxed{\psi(t')dt' \times \varphi(t)dt \mapsto H_1(\psi, \varphi; x, y) \cdot dx \wedge dy}$$

is called the holographic transform of the complex-valued writing wavelet packet amplitude densities [162, 150, 151]. It should be observed that unlike sequential data processing, the holographic transform of mixed wavelet packet amplitude densities as indicated above does not treat time as a sequencer but as an expresser of information similarly to biological neural systems where time is used throughout as one of the fundamental representational coordinates. Moreover, it should be noticed that the coordinates (x, y) of the stationary quantum interference pattern are independent of the distance between the object to be globally recorded and the square-law detector located in the hologram plane. It follows by quantum theoretical state-vector reduction which is a nonlinear procedure:

Theorem 4.1. Let ψ and φ be wavelets in $\mathcal{S}(\mathfrak{R})$ of unit energy $\|\psi\|_2 = \|\varphi\|_2 = 1$. Then the phased two-time average

$$|H_1(\psi, \varphi; x, y)|$$

which records the stationary quantum interference pattern generated by the coherent two-wavelet mixing $\psi(t')dt' \times \varphi(t)dt$ provides the probability of detecting a photon within a unit area attached to the point (x, y) of the hologram plane $\mathfrak{R} \div \mathfrak{R}$.

The method of optical holography or coherent wavefront reconstruction applies to all waves: to electron waves, X-rays, light waves, acoustic waves, and seismic waves, providing the wavelets are coherent enough to form the required stationary quantum interference patterns in the hologram plane [161]. Therefore a laser is not really needed for optical holography; it is merely the use of solid, three-dimensional objects that calls for light wavelets whose coherence length exceeds the path differences due to the unevenness of such objects. Dennis Gabor used in 1947 a filtered mercury arc lamp to get temporal coherence and a pinhole to get spatial coherence in the first optical hologram. The main reason for the discouraging quality of his optical holograms was that no light source existed at that time with the combined intensity and coherence that was needed. When laser light became available, the quantum interference experiments by Emmett N. Leith and Juris Upatnieks at the University of Michigan in 1962 resulted in excellent optical display holograms that astonished the scientific community.

In radar analysis, the mapping $(x,y) \mapsto H_\nu(\psi,\varphi;x,y)$ is called the narrowband cross-ambiguity function [16, 48, 94, 186, 122, 125, 153, 155] and is used to characterize the resolution performance of radar signals. In the following it will be convenient to define the narrowband auto-ambiguity function by $H_\nu(\psi;.,.) := H_\nu(\psi,\psi;.,.)$. The mapping

$$\psi(t)dt \mapsto H_1(\psi;x,y)\cdot dx \wedge dy$$

which describes the self-interference of photons is called the holographic trace transform. In view of Theorems 3.1 and 4.1 supra, the holographic trace transform models the classical beam-splitter quantum interference experiment.

Remark 4.2. The only examples of strictly convex objects for which the scattering amplitude density has been analyzed fairly completely for high frequencies ($|\nu| \to \infty$) are the compact spheres of the Euclidean space $\mathfrak{R}^3$. According to the synergetic point of view, however, optical holography does not attempt to mathematically predict the scattering amplitude densities but geometrically encodes and decodes the scattering amplitude densities and their phases as an experimental result utilizing coherent reference beams.

Remark 4.3. A vital element of optical neurocomputer architectures is the medium for optical hologram recording because it plays the role of an optical holographic associative memory. An associative memory has the basic capability of storing a number of associated information patterns (u,v), so that subsequent presentation of one pattern u recalls its paired pattern v. This is an inherently parallel procedure, and the attractiveness of optical implementations of holographic associative memories has been recognized for some time. Electro-optical photorefractive crystals (PRCs) are known to form reusable optical holographic storage materials that can be infinitely recycled and do not require additional processing. The crystals of the sillenite family, bismuth silicon oxide $Bi_{12}SiO_{20}$ (BSO), bismuth titanium oxide $Bi_{12}TiO_{20}$ (BTO), and bismuth germanium oxide $Bi_{12}GeO_{20}$ (BGO) exhibit the highest sensitivity to light among presently known PRCs [178]. Optical holograms are recorded inside PRCs directly by illuminating the crystal with laser light. The light induces a charge redistribution inside the crystal [49, 50] and in a certain characteristic time interval a dynamic equilibrium between distributions of the recording light intensity and internal electric charge is established. The electric charge induces an internal electrostatic field that changes the refractive index of the crystal by the electro-optical (Pockels or Kerr) effect and forms a volume holographic optical element (VHOE). As the interference pattern undergoes changes, a new charge distribution is formed, hence a new optical hologram is recorded. This charge

distribution again comes to a dynamic equilibrium with the recording quantum interference pattern. If the period during which the interference pattern changes is sufficiently long, the electro-optical crystal rerecords an optical hologram. Hence the electro-optical PRCs can adapt itself to varying external conditions, such as occasional temperature-induced changes of the phase difference between the writing object signal beam and reference signal beam, or mechanical instabilities. This is an extremely important feature because it allows more reliable storage of scattering objects by almost-real-time quantum holography.

Research in the area of real-time quantum holography in electro-optical PRCs needs to focus on materials in order to achieve a faster speed of photoresponse (< 1 msec), greater photorefractive sensitivity, control over image decay, and reduced fanning. Molecular engineering recently developed the highly interesting and promising organic crystals. As an alternative, bioelectronics or molecular electronics are offering photochemically sensitive materials like biopolymers of the chlorophyll-protein complex and the retinal-protein complex for real-time holographic recording. It has been discovered that specifically bacteriorhodopsin which belongs to the retinal-protein complex and which can be extracted from the purple membrane of Halobacterium halobium is a very attractive recording material for real-time optical signal processing. Depending on the preparation procedure, these materials have a very wide range of photoresponse time running from 100 sec down to 10 psec, and an extremely high spatial resolution limited by the dimensions of the molecules. However, research in this area is still in the early stage of development and for the present the studies are far from the practical implementation of potential biological neurocomputers. Nevertheless, investigations of the simplest optical processors and of associative memory elements based on biopolymers are being intensively developed in various laboratories all over the world so that it is expected that on the basis of purple membranes of halobacteria an optical memory with a capacity of 10^9 bits/cm^2 will be created in near future [148].

Remark 4.4. According to the rules of quantum theory, any two states whatever, irrespective of how different from one another they might be, can coexist in any quantum complex linear superposition. This is the deep and decisive reason for the fact that high-resolution radar imagery of the terrain and optical holographic imaging are closely related concepts. In fact, airborne and spaceborne SAR imaging systems are active remote sensing systems which illuminate the terrain with electromagnetic energy at relatively long wavelengths (radar L-band center wavelength $\lambda = 23$ cm, C-band center wavelength $\lambda = 5.7$ cm, X-band center wavelength $\lambda = 3.1$ cm) as the platform moves with respect to the ground being mapped. SAR imaging systems coherently detect the signals returning from the terrain (called radar return)

in order to store them in amplitude density including phase until all of the returns are collected. Simultaneous amplitude density and phase recording is performed by multiplexing or heterodyning the radar returns with a reference signal in order to generate microwave holograms [55, 93]. The signals that are collected and coherently superposed in SAR systems by small antennas are not already focused, as is the case in real aperture systems like radar altimeters. Because extensive processing is required to form the SAR image from the radar return, optical signal processing techniques have been applied to the collection and processing of SAR data. Chronologically, the coherent optical systems developed at the University of Michigan regarding applications to the processing of SAR data form the oldest branch in the family tree of optical computing [32, 33, 62, 90, 94]. SAR coherent imaging systems can be regarded as optical neurocomputers which implement a Doppler filter bank by a relatively static reflection pattern of the architecture mirror [26, 88]. The two-dimensional quantum parallelism inherent to the optical data processing approach is in large part responsible for the success of SAR coherent imaging.

Remark 4.5. Since the advent of optical holography there has been a strong interest in replacing lenses and other crucial parts of optical systems by high performance HOEs. In particular, optical SAR data processing systems may be realized by optical heads which include high performance hololenses. Many HOEs are fabricated by recording the stationary quantum interference pattern between two mixing laser beams. The use of digital computer-generated hologram (CGH) techniques, however, avoids the technological difficulties involved in the interferometric HOE fabrication. Moreover, one benefit that digital CGHs can offer that is not available with optical holography is the ability to deal with objects that exist only mathematically. Finally, high quality digital CGHs to implement holographic optical interconnects of high circuit density may be fabricated with the same technology used in the manufacture of CMOS VLSI circuit chips [79, 81, 82, 87, 89, 124, 175, 176]. The geometrical CGH encoding computations for specific HOE pattern parameters are performed with a standard computer aided design (CAD) station. Upon completion of the HOE pattern database generation and conversion of the pattern by a subroutine to the required formatted data, a digital computer controlled output device such as a Perkin-Elmer electron-beam high-resolution micro-lithographic system then writes the desired geometric pattern on photoresist, which is subsequently processed to produce the finished transmissive or reflective holographic element. It is at this intermediate level of lower throughput requirements where sequential processors play a role in vision and image processing. Alternately, digital CGHs may be realized by writing the appropriate geometrical pattern on a SLM. In any case, digital CGHs are at the base of a technology trans-

fer from microelectronics to microoptics or amacronics and form a bridge between digital computer and optical neurocomputer architectures. Since atoms coherently excited by short laser pulses (Rydberg atoms) may be as large as some transistors of microelectronic ICs and the pathways between them inside the CMOS VLSI chips [10, 202, 203], the quantum theoretical treatment of optical holography is of particular importance for amacronics (see Section 10 infra) and nanotechnology.

> *Investigators in one field may very well never have been aware that the Heisenberg group had been found in some field not seemingly related to theirs. Another factor certainly contributory to its relative obscurity is that what I call "the Heisenberg group" is not in fact one object, but a collection of similar objects, rather like a functor, or a scheme in algebraic geometry, or even a combination of several overlapping functors. Thus one has to look with a certain pair of spectacles in order to see the topics as being united via a single common phenomenon.*
>
> ***Roger Howe (1980)***

> *Perhaps the most rewarding aspect of analog computation is the extent to which elementary computational primitives are a direct consequence of fundamental laws of physics.*
>
> ***Carver A. Mead (1989)***

> *I would like to express my belief that the holographic concept of Gabor is as fundamental as the general relativity theorem of Einstein, and it has to be explored further for a better understanding of nature in which we live.*
>
> ***Pál Greguss (1970)***

> *Man sollte alles so einfach wie möglich machen, aber nicht einfacher.*
>
> ***Albert Einstein (1879–1955)***

5. The Kirillov quantization

Let G denote the multiplicative group of all unipotent real matrices

$$\begin{pmatrix} 1 & x & z \\ 0 & 1 & y \\ 0 & 0 & 1 \end{pmatrix} := (x, y, z)$$

with unit element $(0, 0, 0)$. Then G is a simply connected two-step nilpotent Lie group, diffeomorphic to the differential manifold $(\mathfrak{R} \times \mathfrak{R}) \cdot \mathfrak{R}$, with one-dimensional center $C_G = \{(0, 0, z) | z \in \mathfrak{R}\}$. The polarized presentation

$$(x_1, y_1, z_1) \cdot (x_2, y_2, z_2) = (x_1 + x_2, y_1 + y_2, z_1 + z_2 + x_1 y_2)$$

and the equivalent isotropic presentation

$$(x_1,y_1,z_1)\cdot(x_2,y_2,z_2)=(x_1+x_2,y_1+y_2,z_1+z_2+\frac{1}{2}(x_1y_2-x_2y_1))$$

show that G is a realization of the three-dimensional Heisenberg group [23, 56, 186, 155]. The Haar measure of G is Lebesgue measure $dx \otimes dy \otimes dz$ of the underlying differential manifold $\mathfrak{R}^3$. The Lie algebra $\mathfrak{g}=T_{(0,0,0)}(G)$ of G is formed by the upper triangular matrices $\{(x,y,z)-(0,0,0)|x,y,z\in\mathfrak{R}\}$. In terms of the canonical basis $\{P,Q,Z\}$ of $\mathfrak{g}$ which is given by the matrices

$$P:=\begin{pmatrix}0&1&0\\0&0&0\\0&0&0\end{pmatrix},\ Q:=\begin{pmatrix}0&0&0\\0&0&1\\0&0&0\end{pmatrix},\ Z:=\begin{pmatrix}0&0&1\\0&0&0\\0&0&0\end{pmatrix},$$

the Heisenberg commutation relations read as follows:

$$[P,Q]=PQ-QP=Z,\ [P,Z]=0,\ [Q,Z]=0.$$

Thus the center $\mathfrak{c}=\mathfrak{R}.Z$ of the Heisenberg Lie algebra $\mathfrak{g}$ is one-dimensional and satisfies $\exp(\mathfrak{c})=C_G$. Obviously

$$ad_{\mathfrak{g}}\begin{pmatrix}0&a&c\\0&0&b\\0&0&0\end{pmatrix}=\begin{pmatrix}0&0&0\\0&0&0\\-b&a&0\end{pmatrix}$$

for $a,b,c\in\mathfrak{R}$. The adjoint action $(x,y,z)\mapsto Ad_G(x,y,z)$ of G on $\mathfrak{g}$ linearizes the action of G on itself by inner automorphisms and is therefore defined by conjugation:

$$\begin{pmatrix}1&x&z\\0&1&y\\0&0&1\end{pmatrix}\begin{pmatrix}0&a&c\\0&0&b\\0&0&0\end{pmatrix}\begin{pmatrix}1&x&z\\0&1&y\\0&0&1\end{pmatrix}^{-1}=\begin{pmatrix}0&a&c+bx-ay\\0&0&b\\0&0&0\end{pmatrix}$$

With respect to the basis $\{P,Q,Z\}$ of $\mathfrak{g}$ it follows

$$Ad_G(x,y,z)=\begin{pmatrix}1&0&0\\0&1&0\\-y&x&1\end{pmatrix}\qquad((x,y,z)\in G).$$

Consequently the identity

$$Ad_G\circ\exp=\exp\circ ad_{\mathfrak{g}}$$

holds as usual on $\mathfrak{g}$. If $\{P^*,Q^*,Z^*\}$ denotes the dual basis of $\{P,Q,Z\}$, the coadjoint action $(x,y,z)\mapsto CoAd_G(x,y,z)$ of G in the dual vector space $\mathfrak{g}^*=T^*_{(0,0,0)}(G)$ of $\mathfrak{g}$ is given by the formula

$$CoAd_G(x,y,z)=\begin{pmatrix}1&0&y\\0&1&-x\\0&0&1\end{pmatrix}\qquad((x,y,z)\in G).$$

Hence

$$\mathrm{CoAd}_G(x,y,z)(\xi P^* + \eta Q^* + \nu Z^*) = (\xi + \nu y)P^* + (\eta - \nu x)Q^* + \nu Z^*,$$

where the triple (ξ, η, ν) denotes real coordinates. From this identity the Kirillov coadjoint orbit picture of G becomes apparent: For each center frequency $\nu \neq 0$ the orbit of the point $(0,0,\nu)$ under the CoAd_G-action of G is the affine plane $\mathcal{O}_\nu$ in $\mathfrak{g}^*$ through the point νZ^* parallel to the plane spanned by $\{P^*, Q^*\}$ through the origin of $\mathfrak{g}^*$. For $\nu = 0$ the points $(\xi, \eta, 0)$ are zero-dimensional coadjoint orbits $\mathcal{O}_{(\xi,\eta)}$ of G located in the plane spanned by $\{P^*, Q^*\}$ through the origin of $\mathfrak{g}^*$. Notice that the symplectic plane $\mathcal{O}_\nu (\nu \neq 0)$ carries the canonical differential 2-form

$$\omega_{\mathcal{O}_\nu} = \nu \cdot d\xi \wedge d\eta$$

which endows $\mathcal{O}_\nu$ with a well-defined orientation. The point-orbit $\mathcal{O}_{(\xi,\eta)}((\xi,\eta) \in \mathfrak{R} \times \mathfrak{R})$ can be identified with the Dirac measure $\varepsilon_{(\xi,\eta)}$ located at the point (ξ, η) of the "singular" plane $\nu = 0$.

In terms of the Heisenberg nilpotent Lie group G, the Kirillov quantization procedure means the choice of an irreducible unitary linear representation U of G acting in a complex Hilbert space $\mathcal{H}$ and the coadjoint orbit $\mathcal{O}_U$ associated with the isomorphy class of U. Recall that U is a continuous homomorphism of G into the unitary group $\mathbf{U}(\mathcal{H})$ of $\mathcal{H}$, i.e., $U : G \to \mathbf{U}(\mathcal{H})$ is a mapping such that

$$U((x_1,y_1,z_1)\cdot(x_2,y_2,z_2)) = U(x_1,y_1,z_1) \circ U(x_2,y_2,z_2),$$
$$U(0,0,0) = \mathrm{id}_{\mathcal{H}},$$

and such that the mapping $G \times \mathcal{H} \ni ((x,y,z),\psi) \mapsto U(x,y,z)\psi \in \mathcal{H}$ is continuous. Irreducibility means that $(U, \mathcal{H})$ is not obtained as a direct sum of two nontrivial linear subrepresentations of G. Equivalently, there exists no proper closed vector subspace $\neq \{0\}$ of $\mathcal{H}$ invariant under the action of G by U in $\mathcal{H}$.

According to the Stone-von Neumann-Mackey theorem [155] the Kirillov quantization problem has a solution unique up to unitary isomorphy: For any given center frequency $\nu \neq 0$, the central character

$$\chi_\nu : C_G \ni (0,0,z) \mapsto e^{2\pi i \nu z}$$

determines up to a unitary isomorphism a unique infinite-dimensional irreducible unitary linear representation U_ν of G in the standard Hilbert space $\mathcal{H} = L^2(\mathfrak{R})$ which acts on the vector subspace $\mathcal{S}(\mathfrak{R})$ according to the rule

$$U_\nu(x,y,z)\psi(t) = e^{2\pi i \nu (z + yt)}\psi(t - x) \qquad (t \in \mathfrak{R}).$$

Thus for all elements $(x, y, z) \in G$, the transition amplitude

$$U_\nu(x, y, z)\psi \in \mathcal{S}(\mathfrak{R})$$

is obtained by time shifting and phasor multiplication with respect to the frequency $\nu \neq 0$ of the wavelet $\psi \in \mathcal{S}(\mathfrak{R})$.

Linear representations of G that are unitarily isomorphic to one of the representations $(U_\nu, L^2(\mathfrak{R}))(\nu \neq 0)$ of G are called linear representations of Schrödinger type. The Kirillov correspondence assigns to the coadjoint orbit $(\mathcal{O}_\nu, \omega_{\mathcal{O}_\nu}) \in \mathfrak{g}^*/\mathrm{CoAd}_G(G)$ $(\nu \neq 0)$ of the point $(0, 0, \nu)$ in $\mathfrak{g}^*$ the isomorphy class of $(U_\nu, L^2(\mathfrak{R}))$. Notice that this isomorphy class contains the Bargmann-Fock model of quantics describing bosons by annihilation and creation operators (cf. Section 1 supra), and also the linear lattice representation of G (see Section 11 infra). Each element of the isomorphy class, i.e., each linear representation of Schrödinger type of G realizes $(U_\nu, L^2(\mathfrak{R}))$ by quantum complex linear superposition.

Notice that the complex vector space of $\mathcal{C}^\infty$-vectors for the linear representation U_ν $(\nu \neq 0)$ of G acting on $\mathcal{H} = L^2(\mathfrak{R})$ is given by the Schwartz space $\mathcal{S}(\mathfrak{R})$ on $\mathfrak{R}$, and that the differentiated form of U_ν reads

$$U_\nu(P) = \frac{d}{ds} U_\nu(\exp(sP))_{s=0} = -\frac{\partial}{\partial t},$$

$$U_\nu(Q) = \frac{d}{ds} U_\nu(\exp(sQ))_{s=0} = 2\pi i \nu t,$$

$$U_\nu(Z) = \frac{d}{ds} U_\nu(\exp(sZ))_{s=0} = 2\pi i \nu.$$

The linear operators $\{-\partial/\partial t, 2\pi i \nu t\}$ determine a representation of the Schrödinger operators by skew-symmetric operators. In particular, these operators satisfy the Heisenberg commutation relation [23, 155]

$$[P, Q] = PQ - QP = 2\pi i \nu . \mathrm{id} \qquad (\nu \in \mathfrak{R}, \nu \neq 0).$$

Shortly after Werner Heisenberg introduced the commutation relations in quantics, Hermann Weyl discovered in 1928 that they could be interpreted as the structure relations for the real Heisenberg Lie algebra $\mathfrak{g}$. The commutation relations combined with the Parseval-Plancherel theorem and the Cauchy-Schwarz inequality provide the Heisenberg inequality [15]

$$\int_{\mathfrak{R}} t^2 |\psi(t)|^2 dt . \int_{\mathfrak{R}} s^2 |\mathcal{F}\psi(s)|^2 ds \geq \frac{1}{16\pi^2} \left(\int_{\mathfrak{R}} |\psi(t)|^2 dt \right)^2$$

which expresses the local/global duality between the wavelet $\psi \in \mathcal{S}(\mathfrak{R})$ and its Fourier transform $\mathcal{F}\psi \in \mathcal{S}(\mathfrak{R})$. A standard density argument shows that the Heisenberg inequality extends to all elements of the complex Hilbert space $\mathcal{H} = L^2(\mathfrak{R})$. It implies the classical Heisenberg Uncertainty Principle

$$\Delta U_\nu(P) \cdot \Delta U_\nu(Q) \geq \pi |\nu| \qquad (\nu \in \mathfrak{R}, \nu \neq 0)$$

in terms of the standard root-mean-square deviations of the operators $U_\nu(P)$ and $U_\nu(Q)$ acting in $\mathcal{H} = L^2(\mathfrak{R})$. Expressed in terms of the canonical basis $\{P, Q, Z\}$ of the Heisenberg Lie algebra $\mathfrak{g}$, the classical Uncertainty Principle takes the form of the Robertson relation [149]

$$\Delta U_\nu(P) \cdot \Delta U_\nu(Q) \geq 1/2|U_\nu(Z)| \qquad (\nu \in \mathfrak{R}, \nu \neq 0).$$

The Uncertainty Principle has been one of the key relationships in quantum theory for over sixty years. In his Chicago lectures of spring 1929, Werner Heisenberg regarded this inequality as the precise mathematical expression of the Uncertainty Principle within the formalism of quantics [69]. Moreover, it has been recognized as one of the fundamental results in signal processing [13, 40, 140, 198]. Nevertheless, in the context of quantum holography it is very important to appreciate that the Heisenberg Uncertainty Principle does have a number of serious weaknesses. These are particularly related to the fact that the standard deviations $\Delta U_\nu(P)$ and $\Delta U_\nu(Q)$ which are defined by the square root of the expectation values only give very general information about the spreads of the probability density functions and are insensitive to the fine structure of quantum interference patterns [139, 180, 181]. The structure of the Heisenberg group G, however, includes the Poisson summation formula and is therefore rich enough to getting around this inadequacy of the Heisenberg Uncertainty Principle. Indeed, an application of the linear lattice representation δ_1 of G to the interfering wavelet packet amplitude densities enables the rigorous establishment of the quantum parallelism according to which different alternatives at the photon level are allowed to coexist in quantum complex linear superposition (see Theorem 11.3 infra).

Let $\overline{U}_\nu$ denote the contragradient representation of U_ν so that

$$\overline{U}_\nu(x, y, z) = {}^t U_\nu((x, y, z)^{-1})$$

holds for all elements $(x, y, z) \in G$. Obviously

$$U_\nu|C_G = \chi_\nu, \quad \overline{U}_\nu|C_G = \chi_{-\nu} \qquad (\nu \in \mathfrak{R}, \nu \neq 0).$$

In terms of neural network theory, $\overline{U}_\nu$ is the feedback or backprojection representation of G associated to U_ν $(\nu \neq 0)$. The flatness of the coadjoint orbits $(\mathcal{O}_\nu, \omega_{\mathcal{O}_\nu}) \in \mathfrak{g}^*/\mathrm{CoAd}_G(G)$ and $(\mathcal{O}_{-\nu}, \omega_{\mathcal{O}_{-\nu}}) \in \mathfrak{g}^*/\mathrm{CoAd}_G(G)$ $(\nu \neq 0)$ in the dual vector space $\mathfrak{g}^*$ of the Heisenberg Lie algebra $\mathfrak{g}$ associated by the Kirillov correspondence with the isomorphy classes of U_ν and $\overline{U}_\nu$, respectively, is equivalent to the square integrability modulo C_G of U_ν and $\overline{U}_\nu$. If G/C_G is endowed with the differential 2-form

$$\omega_1 = dx \wedge dy,$$

induced by the form $\omega_{\mathcal{O}_1}$ on $\mathcal{O}_1$, the central projection and backprojection G-slice theorem follows:

Theorem 5.1. The holographic transform is the coefficient form of the linear Schrödinger representation U_1 of the polarized *Heisenberg* group G projected along the center C_G onto $(G/C_G, \omega_1)$. Thus the *Kirillov* quantization identities

$$\begin{cases} \int H_1(\psi', \varphi'; x, y) \cdot dx \wedge dy = (U_1(x, y, 0)\psi'|\varphi') \cdot \omega_1 \\ \overline{H_1(\psi, \varphi; x, y)} \cdot dx \wedge dy = (U_1(x, y, 0)\psi, \varphi) \cdot \omega_1 \end{cases}$$

hold.

The irreducibility combined with the unitarity of the linear Schrödinger representation U_1 of G implies that the commutant of U_1 is isomorphic to the compact torus group $\mathfrak{T}$. Hence from the central projection G-slice theorem it follows:

Corollary 5.2. The holographic trace transform

$$\psi(t)dt \cdot \mathfrak{T} \to H_1(\psi; x, y) \cdot dx \wedge dy$$

extends to a mapping of $L^2(\mathfrak{R})$ into $L^2(\mathfrak{R} \times \mathfrak{R})$ such that the identity

$$H_1(\psi; x, y) \cdot dx \wedge dy = H_1(\varphi; x, y) \cdot dx \wedge dy$$

implies $\psi(t)dt = c\varphi(t)dt$ where $c \in \mathfrak{T}$ denotes a constant phase factor.

The free choice of the phase factor $c \in \mathfrak{T}$ reflects the fact that only the phase difference is of physical importance. Therefore the holographic image encoding procedure needs the mixing of a coherent reference signal beam by a linear Mach-Zehnder interferometer to incrementally record the phase of the object signal beam in the hologram plane $\mathfrak{R} \times \mathfrak{R}$.

> *Holograms are recordings of the intensities of interference patterns said to be formed with a "subject wave" and a "reference wave." Yet in the mathematical representation of the interference pattern intensity there is nothing except arbitrary notation to distinguish one wave from the other. We find the hologram transmittance of a plane hologram to be symmetric in the complex amplitudes of the two forming waves.*
>
> ***Robert J. Collier, Christoph B. Burkhardt, and Lawrence H. Lin (1971)***

> *The cross-correlation viewpoint, however, better than any other, renders understandable the well known all-range-focusing capability of the synthetic aperture radar system, implied in our holographic viewpoint.*

Since the form of the recorded signal, as manifested in the quadratic phase factor, is a function of range, it is apparent that each range element must be processed differently, for example, by correlation with a reference function which is different for each range. Since the pulsing provides resolution in range, we can store the data from each range separately and process them differently, so that each range is cross-correlated with the reference function proper for that range. Thus, the synthetic antenna is in effect focused simultaneously at all ranges, a most remarkable feat when viewed in terms of the capabilities of conventional antennas.

Emmett N. Leith (1978)

6. Metaplectic covariance

Another important advantage of the Kirillov quantization approach lies in the fact that the hidden symmetries of the holographic transform

$$\psi(t')dt' \cdot \varphi(t)dt \mapsto H_1(\psi, \varphi; x, y) \cdot dx \wedge dy$$

can be expressed by the group of automorphisms of the Heisenberg nilpotent Lie group G keeping the center C_G pointwise fixed. This group, the metaplectic group $\mathbf{Mp}(1, \mathfrak{R})$, forms a twofold cover of the symplectic group $\mathbf{Sp}(1, \mathfrak{R}) = \mathbf{SL}(2, \mathfrak{R})$. Its natural action on the hologram plane $\mathfrak{R} \times \mathfrak{R}$ preserves the center frequencies $\nu \neq 0$ [155, 165, 187]. Its action on the complex Hilbert space $L^2(\mathfrak{R})$ is performed by the metaplectic representation σ. The representation σ of $\mathbf{Mp}(1, \mathfrak{R})$ is a projective unitary linear representation of $\mathbf{Sp}(1, \mathfrak{R})$ in $L^2(\mathfrak{R})$ and satisfies the metaplectic covariance condition of the Kirillov quantization

$$\sigma(g)^{-1} \cdot U_\nu(x, y, 0) \cdot \sigma(g) = U_\nu((g^{-1}(x, y), 0))$$

$((x, y) \in \mathfrak{R} \times \mathfrak{R})$, for all $g \in \mathbf{Sp}(1, \mathfrak{R})$. It follows

Theorem 6.1. The holographic transform satisfies the metaplectic covariance identity

$$H_1(\sigma(g)\psi, \sigma(g)\varphi; x, y) \cdot dx \wedge dy = H_1(\psi, \varphi; g^{-1}(x, y)) \cdot dx \wedge dy$$

for all complex-valued wavelet packet amplitude densities $\psi(t')dt'$ and $\varphi(t)dt$ belonging to $\mathcal{S}(\mathfrak{R})$ and all elements $g \in \mathbf{Sp}(1, \mathfrak{R})$.

Notice that the action of $\mathbf{Sp}(1, \mathfrak{R})$ in $L^2(\mathfrak{R})$ by the metaplectic representation σ includes the dilations by real scaling factors $a \neq 0$, and the

one-dimensional Fourier transform $\mathcal{F}$, both being of importance for the Gabor wavelet transform. Indeed, for the diagonal matrix

$$g_a = \begin{pmatrix} a & 0 \\ 0 & a^{-1} \end{pmatrix}$$

in $\mathbf{Sp}(1,\mathfrak{R})$, the scaling (or zooming) identity

$$\sigma(g_a)\psi(t)dt = |a|^{-1/2}\psi(a^{-1}t)dt$$

follows, and similarly for the Weyl matrix

$$g_0 = \begin{pmatrix} 0 & 1 \\ -1 & 0 \end{pmatrix}$$

of $\mathbf{Sp}(1,\mathfrak{R})$ the relation

$$\sigma(g_0)\psi(t)dt = \mathcal{F}\psi(t)\,dt$$

holds for all $\psi \in \mathcal{S}(\mathfrak{R})$.

A Fourier transform hologram is an optical hologram which records the stationary quantum interference pattern of two coherent wavelets whose complex-valued wavelet packet amplitude densities at the symplectic hologram plane $\mathfrak{R} \times \mathfrak{R}$ are the Fourier transforms of both the object and the reference wavelet. It follows as a special case of the metaplectic covariance identity of the holographic transform:

Corollary 6.2. For the complex-valued wavelet packet amplitude densities $\psi(t')dt'$ and $\varphi(t)dt$ in $\mathcal{S}(\mathfrak{R})$ the 90° rotation identity

$$H_1(\mathcal{F}\psi, \mathcal{F}\varphi; x, y) \cdot dx \wedge dy = H_1(\psi, \varphi; -y, x) \cdot dx \wedge dy$$

holds.

If $\psi^-(t)dt = \psi(-t)dt$ denotes the complex-valued wavelet packet amplitude density of the time-reversed optical signal, the Fourier inversion theorem yields the identity

$$\sigma(g_0^2)\psi(t)dt = \psi^-(t)dt.$$

Thus the hologram plane rotated through 180° corresponds to the time-reversed writing signals.

It should be observed that the Weyl matrix g_0, the diagonal matrices $g_a (a \neq 0)$, and the unipotent matrices

$$g^u = \begin{pmatrix} 1 & 0 \\ u & 1 \end{pmatrix}$$

for $u \in \mathfrak{R}$ are generators of the group $\mathbf{Sp}(1,\mathfrak{R})$. In fact they give rise to an Iwasawa decomposition

$$\mathbf{Sp}(1,\mathfrak{R}) = \mathrm{KAN}$$

into compact, diagonal, and unipotent subgroups. As a paraxial ray-transfer matrix, $g^u \in \mathbf{Sp}(1,\mathfrak{R})$ defines a thin cylindrical lens of focal length $f = -1/u$ and $\sigma(g^u)$ defines the chirp modulation operator

$$\sigma(g^u)\psi(t)dt = e^{-i(u/2)t^2}\psi(t)dt$$

of chirp rate $u \neq 0$. For $u < 0$ the chirp modulation operator $\sigma(g^u) \in \mathbf{U}(L^2(\mathfrak{R}))$ defines an up chirp amplitude density modulation and for $u > 0$ a down chirp amplitude density modulation.

Corollary 6.3. The chirp amplitude density modulation $\sigma(g^u)$ of chirp rate $u \neq 0$ can be corrected by a thin cylindrical lens of focal length $f = 1/u$.

Finally, for the drift-length transfer matrix

$$g = \begin{pmatrix} 1 & u \\ 0 & 1 \end{pmatrix}$$

the identity

$$\mathcal{F}(\sigma(g)\psi)(t)dt = e^{-i(\pi/4)\,\mathrm{sign}\ u}\sigma(g^{-u})\mathcal{F}\psi(t)dt$$

follows where $\mathrm{sign}\ u = u/|u|$. The phasor occurring in this formula arises by the Maslov index which is responsible for the fact that $\mathbf{Mp}(1,\mathfrak{R}) = \widetilde{\mathbf{Sp}}(1,\mathfrak{R})$ forms a twofold cover of $\mathbf{Sp}(1,\mathfrak{R})$. Since optical holography is phase sensitive, it is exactly this sudden change in phase (Gouy effect) of

$$\pi/2 = \pi/4 - (-\pi/4)$$

which makes it not appropriate to place the hologram plane in the focal planes of the beam expanding lenses of the basic interferometric set-up.

It should be observed that the construction of the metaplectic representation σ of $\mathbf{Mp}(1,\mathfrak{R})$ is completely analogous to the construction of the spin representations of the orthogonal groups (symmetric tensors taking place of anti-symmetric tensors).

Example 6.4. Let $T > 0$ be given and denote by

$$\psi_T(t) = \begin{cases} 1 & |t| \leqslant \frac{1}{2}T \\ 0 & |t| > \frac{1}{2}T \end{cases}$$

the rectangular pulse of duration T. In terms of the triangular pulse

$$\Lambda(t) = \begin{cases} 1 - |t| & |t| \leqslant 1 \\ 0 & |t| > 1 \end{cases}$$

and the cardinal sine mother wavelet

$$\operatorname{sinc} x = \begin{cases} \frac{\sin \pi x}{\pi x} & x \neq 0 \\ 1 & x = 0 \end{cases}$$

the holographic trace transform of $\psi_T(t)dt$ takes the form

$$H_1(\psi_T; x, y) \cdot dx \wedge dy = \Lambda\left(\frac{x}{T}\right) \operatorname{sinc} y(T - |x|) \cdot dx \wedge dy.$$

An application of Theorem 6.1 supra shows that the chirp pulse density $\sigma(g^u)\psi_T(t)dt$ of duration T and chirp rate $u \neq 0$ admits the holographic trace transform

$$H_1(\sigma(g^u)\psi_T; x, y) \cdot dx \wedge dy = \Lambda\left(\frac{x}{T}\right) \operatorname{sinc}(y - ux)(T - |x|) \cdot dx \wedge dy.$$

Satellite altimetry uses the ranging capability of radar sensors to measure the surface topographic profile. An example of an advanced-type system is the SEASAT altimeter which was put into orbit in June, 1978. The satellite orbital altitude was 790 km and the platform velocity (ground track) v 6.6 km/sec. SEASAT was in operation for a total of 105 days. During that time, the altimeter provided profiles of the ocean surface with an accuracy of a fraction of a meter. In the altimetry mode, SEASAT operated at a center frequency of 13.5 GHz. The stable local oscillator (STALO) generated a sequence of 12.5 nanosec pulses at a 250 MHz center frequency which has been applied to the chirp generator. The SEASAT chirp generator was a surface acoustic wave (SAW) device fabricated on a lithium tantalate substrate. The resulting chirp modulated pulse had a linearly decreasing frequency with an 80 MHz bandwidth and a pulse duration $T = 3.2$ μsec. The pulse repetition frequency (PRF) was 1020 Hz. During the transmit mode, the chirp pulse at 250 MHz has been upconverted to 3375 MHz, amplified to a 1 W level, and multiplied by 4 to 13.5 GHz. This also multiplied the bandwidth by 4 in order to achieve the desired 320 MHz bandwidth and height measurement accuracy of 0.47 m. In the receive mode the chirp pulse have been upconverted to 3250 MHz, amplified to 0.1 W, multiplied by 4 to 13.0 GHz, and used for mixing with the received echo signal.

Example 6.5. In SAR remote sensing systems (see Remark 4.4 supra), a target at distance r_0 with velocity v relative to the moving platform induces a relativistic chirp amplitude density modulation $\sigma(g^u)$ of the received echo signal of chirp rate

$$u = \frac{4\pi v^2}{\lambda r_0}$$

where $\lambda = c/|v|$ denotes the center wavelength of the coherent radar. The dependence of the chirp rate u of the range r_0 is called the range-azimuth coupling.

In the SAR optical signal processor, let λ' denote the wavelength of the coherent light scanning the holographic film of transport velocity v'. If

$$v_0 = v/v' \ , \ \lambda_0 = \lambda/\lambda'$$

are the relative SAR platform velocity and the relative radar wavelength, respectively, then the radar return focuses at distance

$$f = \frac{\lambda_0 r_0}{4\pi v_0^2}$$

from the hologram plane. It follows that the relativistic effect of the platform motion generates an axial astigmatism. To compensate the linear range variation of the focal length f, a wide-screen equalizer is introduced in the hologram plane. Such an equalizer takes the form of a conical lens or a tilted cylindrical lens [90, 93, 94] which are components of a correcting anamorphic optical system (cf. Corollary 6.3 supra). The recent developments of SLMs have supplied an attractive replacement for the holographic film as an input medium. Moreover, two-dimensional optical data processors using laser diode illumination, acousto-optic (AO) cell data input and a CCD detector array for the output have been designed. For each realization of the SAR data processor, however, it is important to notice that the spatial resolution of SAR imaging systems is independent of the range r_0 to the target and the velocity v of the radar platform.

In the imaging mode, SEASAT SAR operated at a center frequency of 1275 MHz (L-band, $\lambda = 23.5$ cm) with pulse duration $T = 34$ μsec and PRF selections of 1464, 1537, 1580, and 1647 Hz admitting a spatial resolution of 25 m. The depression angle ranged between 67° to 73° and produced an image-swath width of 100 km. The antenna was a 10.74 m by 2.16 m phased array system deployed after orbit insertion. The microwave holographic data for each 100 km wide image-swath have been optically processed to produce four film strips each of which covered a width of 25 km and a length of several thousand kilometers.

The first Shuttle imaging radar (SIR-A) experiment was launched on the second flight of Columbia in November, 1981. The satellite orbital altitude was 250 km and the image-swath width 50 km in order to cover a surface area of about 10 million km^2. The SAR antenna of 9.44 m by 2.09 m radiating area was stowed inside the Shuttle cargo bay and operated when the Shuttle was in an inverted attitude. As in the SEASAT SAR, the transmitted pulse was a chirp pulse of 1275 MHz center frequency admitting a spatial resolution of 38 m. The image data were recorded as holographic film on board the Shuttle. The data film was developed and then processed at the laboratory by coherent laser light to generate the original image film at a scale of 1 : 500,000.

A second Shuttle imaging radar (SIR-B) experiment was conducted in October, 1984. For SIR-B the SAR antenna was modified, however, to permit

the depression angle to be changed during the mission within a range of 30° to 75°. The center wavelength λ was the same as in the earlier missions. The satellite orbital altitude was 225 km and the spatial resolution improved to 25 m.

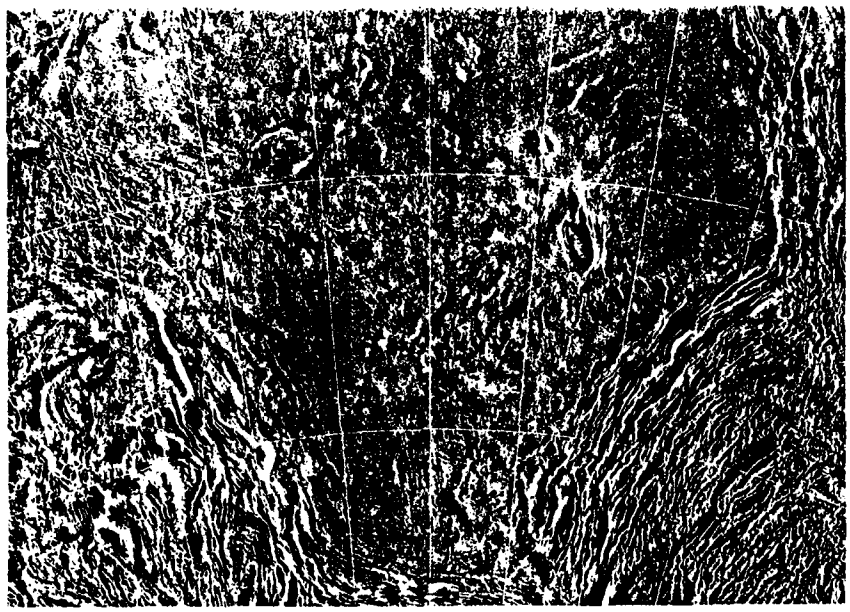

Figure 6.1

As an example, Figure 6.1 shows a SAR image of the Lakshmi region of the planet Venus. It has been generated by the Soviet Union VENERA 15 and 16 orbiters through the cloud-shrouding atmosphere of Venus which is impenetrable for visible light. NASA flew a SAR around Venus in 1990 for the Magellan mission. The radar is operating at a center frequency of 2385 MHz and provides a resolution down to 250 m; see Figures 6.2 and 6.3. By the late 1990s the Cassini spacecraft may be put in an orbit around Saturn and image its moon, Titan, at L-band and K-band on flybys.

Remark 6.6. The Heisenberg group G carries a sub-Riemannian metric and a sub-Laplacian [174]. On the fibre $T^*_{(x,y,z)}(G)$ with base point $(x,y,z) \in G$ of the cotangent bundle $T^*(G)$ of G, the associated bundled quadratic form Q is given by

$$Q_{(x,y,z)}(\xi,\eta,\nu) = (\xi + \nu y)^2 + (\eta - \nu x)^2.$$

Figure 6.2

Figure 6.3

Thus $Q_{(x,y,z)}$ is a parabolic quadratic form with one-dimensional null-space spanned by the vector $(-y, x, 1) \in \mathcal{O}_1$, $(\mathcal{O}_1, \omega_{\mathcal{O}_1}) \in \mathfrak{g}^*/\mathrm{CoAd}_G(G)$. The sub-Laplacian $\Box_G$ of G forms a sub-elliptic linear differential operator given by

$$\Box_G = \left(\frac{\partial}{\partial x} + y\frac{\partial}{\partial z}\right)^2 + \left(\frac{\partial}{\partial y} - x\frac{\partial}{\partial z}\right)^2 .$$

The Heisenberg helix is the analog of a geodesic for the sub-Riemannian geometry of G defined by the sub-elliptic bundled quadratic form Q on $T^*(G)$. This fact corresponds to the "expansion theorem" discovered by Dennis Gabor in 1965 which says that information attached to an optical signal pattern is not carried by "rays", but by a certain "tube of rays" the cross-section of which is proportional to the square of the center wavelength λ of the optical signal [57].

> *I have no doubt that my latest publication is my luckiest find yet. I have also much perfected the experimental method, and I can now produce really pretty reconstructions from apparently hopelessly muddled diffraction patterns.*
>
> ***Dennis Gabor (1900–1979) to Max Born (1882–1970) on 15th June, 1948***

> *The coherence of laser light finds a spectacular application in the making of holograms. A typical hologram looks like a gray piece of plastic with no evident image on it. However, the hologram actually has a microscopically fine and highly complex pattern of lines and spaces. Now illuminate the developed hologram by the same laser system, except that the object has been removed. The pattern on the hologram converts the pure laser beam into a precise replica of the pattern of ordinary light that would be obtained if the object were still there. In this way, the hologram acts as a window. Each eye looking at the illuminated hologram sees a different point of view, thus creating a three-dimensional image by an illusion of depth and solidity. By changing one's vantage point, it is possible to see behind things and around corners, just as if one was looking at the real object through an ordinary window. The image has a realistic three-dimensional appearance. Holography resulted in a whole new concept in the development of imaging systems and technology.*
>
> ***Enders A. Robinson (1989)***

7. The holographic image decoding procedure

In the following, the symplectic homogeneous G-manifolds

$$(\mathcal{O}_1, \omega_{\mathcal{O}_1}) \in \mathfrak{g}^*/\mathrm{CoAd}_G(G),$$
$$(\mathcal{O}_{-1}, \omega_{-1}) \in \mathfrak{g}^*/\mathrm{CoAd}_G(G),$$

and the central projection G-slice G/C_G will be identified with the two-sided symplectic hologram plane $\mathfrak{R} \oplus \mathfrak{R}$. Then the Heisenberg nilpotent Lie group G is a half-line bundle over the symplectic hologram plane $\mathfrak{R} \oplus \mathfrak{R}$, the two sides of which carry the canonical differential 2-forms $\omega_1 = dx \wedge dy$ and $\omega_{-1} = -dx \wedge dy = dy \wedge dx$, respectively. In view of the square integrability modulo C_G of the irreducible unitary linear representations U_1 and $\overline{U}_1$ of G, an application of Schur's lemma provides the biorthogonality relations [119, 136, 155, 168]

$$\iint_{\mathfrak{R}\dot{+}\mathfrak{R}} H_1(\psi', \varphi'; x, y)\overline{H}_1(\psi, \varphi; x, y)dxdy = (\psi' \otimes \varphi | \psi \otimes \varphi')$$

for the complex valued wavelet packet amplitude densities $\psi'(t)dt$, $\varphi'(t)dt$, $\psi(t)dt$, $\varphi(t)dt$ in $\mathcal{S}(\mathfrak{R})$. Therefore the dyads

$$\begin{cases} E(\psi', .; x, y) : \varphi' \mapsto H_1(\psi', \varphi'; x, y)\overline{U}_1(x, y, 0)\overline{\psi}' \\ \overline{E}(\psi, .; x, y) : \varphi \mapsto \overline{H}_1(\psi, \varphi; x, y)U_1(x, y, 0)\psi \end{cases}$$

($(x, y) \in \mathfrak{R} \dot{+} \mathfrak{R}$), which embed $\psi' \in \mathcal{S}(\mathfrak{R})$ and $\psi \in \mathcal{S}(\mathfrak{R})$, respectively, into the Hilbert-Schmidt (HS) operator-valued differential 2-forms acting on $L^2(\mathfrak{R})$, define a U_1-system $(E(., .; x, y))_{(x,y)\in\mathfrak{R}\dot{+}\mathfrak{R}}$, and a $\overline{U}_1$-system $(\overline{E}(., .; x, y))_{(x,y)\in\mathfrak{R}\dot{+}\mathfrak{R}}$ of coherent states based on the symplectic hologram plane $\mathfrak{R} \dot{+} \mathfrak{R}$ [120, 134]. Observe that these coherent state systems provide a quantum theoretical description of nonspreading wavelet packets [57, 134, 162] and therefore of the Gabor tubes of rays (see Remark 6.6 supra).

Theorem 7.1. For all complex-valued writing wavelet packet amplitude densities

$$\psi'(t)dt,\ \varphi'(t)dt,\ \psi(t)dt,\ \varphi(t)dt$$

in $\mathcal{S}(\mathfrak{R})$ the gain equations

$$\iint_{\mathfrak{R}\dot{+}\mathfrak{R}} E(\psi', \varphi'; x, y)dxdy = \|\psi'\|_2\overline{\varphi}',$$

$$\iint_{\mathfrak{R}\dot{+}\mathfrak{R}} \overline{E}(\psi, \varphi; x, y)dxdy = \|\psi\|_2\varphi$$

hold.

Remark 7.2. Similar inversion formulas can be established for the affine coherent states defined by the wavelet transform and the irreducible unitary linear representations of the non-unimodular affine Lie group

$$G_+ = \{(\alpha, \beta) | \alpha > 0,\ \beta \in \mathfrak{R}\}$$

of the real line $\mathfrak{R}$ ("$\alpha t + \beta$ group"). The affine wavelets are particularly useful code primitives for voice decomposition [65].

The non-abelian solvable Lie group G_+ has the presentation

$$(\alpha_1, \beta_1) \cdot (\alpha_2, \beta_2) = (\alpha_1 \alpha_2, \alpha_1 \beta_2 + \beta_1).$$

Of course, G_+ may also be represented as the group of real matrices

$$\begin{pmatrix} \alpha & \beta \\ 0 & 1 \end{pmatrix} \qquad (\alpha > 0,\ \beta \in \mathfrak{R})$$

under matrix multiplication. The left Haar measure of G_+ is given by $d\alpha \otimes d\beta/\alpha^2$ and the right Haar measure by $d\alpha \otimes d\beta/\alpha$. Apart from the trivial one-point coadjoint orbits located on the real line $\mathfrak{R}$, the affine group G_+ of $\mathfrak{R}$ admits exactly two non-trivial coadjoint orbits, the open upper half-plane $\mathcal{O}_+$ and the open lower half-plane $\mathcal{O}_-$. It follows from the Kirillov coadjoint orbit picture of G_+ that every irreducible unitary linear representation of G_+ of dimension > 1 is unitarily isomorphic to either U or its contragradient representation $\overline{U}$, where U can be realized on the complex Hilbert space $L^2(\mathfrak{R})$ by the assignment

$$U(\alpha, \beta)\psi(t) = e^{i\beta e^t}\psi(t + \log \alpha) \qquad (t \in \mathfrak{R}),$$

and $\overline{U}$ by the action

$$\overline{U}(\alpha, \beta)\psi(t) = e^{-i\beta e^t}\psi(t + \log \alpha) \qquad (t \in \mathfrak{R})$$

on $\psi \in \mathcal{S}(\mathfrak{R})$. More convenient are the realizations on $L^2(\mathfrak{R}_+)$ given by

$$U(\alpha\,\beta)\psi(t) = e^{\,i\beta t}\sqrt{\alpha}\,\psi(\alpha t) \qquad (t > 0),$$

and on $L^2(\mathfrak{R}_-)$ given by

$$\overline{U}(\alpha, \beta)\psi(t) = e^{-i\beta t}\sqrt{\alpha}\,\psi(\alpha t) \qquad (t < 0).$$

Notice that the irreducible unitary linear representations U and $\overline{U}$ of G_+ are square integrable and that their coefficient functions form the wideband ambiguity functions [48, 122].

Remark 7.3. One of the most dramatic deployments of computer technology in radiological diagnostic imaging is the development of computer-aided tomography (CT). In this case and, more recently, in magnetic resonance imaging (MRI) systems, the computational capability made possible by the advent of high speed computers has been an absolutely essential ingredient in the process of image formation. Similarly to holography, the raw data provided by the physical imaging system in CT or MRI is in an encoded form which bears no discernible resemblance to the two-dimensional array

of information comprising an image that can be visually perceived. CT generates an image of a cross-sectional slice of the body lying perpendicular to the long axis of the patient being examined. Unlike optical holography, in which the symplectic hologram plane $\mathfrak{R} \oplus \mathfrak{R}$ is transversal to the direction of laser irradiation, CT is based upon the measurement of the attenuation of X-ray beams lying entirely within the plane of the section being imaged. Turning from optical holography to CT [121], the preceding identities give rise by an application of the spectral theory of the irreducible reductive dual pair $(\widetilde{\mathbf{Sp}}(1,\mathfrak{R}), \widetilde{\mathbf{O}}(n,\mathfrak{R}))$ inside $\widetilde{\mathbf{Sp}}(n,\mathfrak{R})$ [78, 159], to the singular value decomposition of the Radon transform $\mathcal{R} : \mathcal{S}(\mathfrak{R}^n) \to \mathcal{S}(\mathfrak{R} \times \mathbf{S}_{n-1})$ acting on functions $f \in \mathcal{S}(\mathfrak{R}^n)$ according to

$$\mathcal{R}f(r,\omega) = \int_{\mathfrak{R}^n} f(x)\varepsilon_{(r-(\omega|x))}dx$$

(ε_p = Dirac measure located at the point $p \in \mathfrak{R}$). It follows that the inversion problem for the Radon transform $\mathcal{R}$ which underlies CT, MRI, and tomographic reconstruction for geophysical applications is ill-posed. Neurocomputers, however, seem to be more appropriate to solve ill-posed problems than conventional digital computers.

As a special case we obtain from Theorem 7.1 supra the following result which describes the readout procedure of optical holograms, i.e., the retrieval of geometrically encoded information by adaptive resonance. It is important to appreciate that the energy normalization is a nonlinear procedure.

Corollary 7.4. Let $\varphi \in \mathcal{S}(\mathfrak{R})$ and assume that $\psi \in \mathcal{S}(\mathfrak{R})$ satisfies the normalization condition $\|\psi\|_2 = 1$. If $\mathcal{F}$ denotes the Fourier transform acting on $\mathcal{S}(\mathfrak{R})$ then the filtered backpropagation formulae of degenerate coherent four-wavelet mixing

$$\begin{cases} \iint_{\mathfrak{R}\dot{+}\mathfrak{R}} H_1(\psi,\varphi;x,y)e^{-2\pi i y t}\,\overline{\psi}(t-x)\,dx\,dy & = \overline{\varphi}(t) \\ \iint_{\mathfrak{R}\dot{+}\mathfrak{R}} H_1(\psi,\varphi;-y,x)e^{-2\pi i y t}\mathcal{F}\,\overline{\psi}(t-x)\,dx\,dy & = \mathcal{F}\,\overline{\varphi}(t) \end{cases} \quad (t \in \mathfrak{R})$$

hold.

The preceding reproducing diffraction integrals prove the fundamental law of optical holography, or holographic reciprocity principle, which governs the angle image decoding procedure of optical holograms: The complex-valued wavelet packet amplitude density, including the magnitude and the phase of the conjugate object signal recorded in the hologram, can be read out simultaneously by illuminating the hologram with the conjugate to the original reference signal beam. The conjugate beam which becomes unfocused by a beam expander provides the illuminating wavelets with their

proper phase factors for adaptive resonance. Thus the geometric encoding procedure of optical holography is able to overcome the phase-blindness of the detectors at the frequency range of visible light: the holographic decoding procedure reconstructs the complete wavefront creating a real pseudoscopic image of the object. The reconstruction of a Fourier transform hologram establishes the 90° rotation identity of the Corollary 6.2 supra.

A complex-valued wavefront recorded in a planar optical hologram is effectively stored for future reconstruction by an application of the fundamental law of optical holography. Holographic interferometry is concerned with the formation and interpretation of the stationary quantum interference patterns which are created when a coherent wavelet, generated at some earlier time and stored in an optical hologram, is later reconstructed according to the holographic reciprocity principle, and caused to interfere with a phase-related comparison wavelet. It is the storage or time delay aspect which gives the holographic procedure a unique advantage over conventional optical interferometry. It permits diffusely reflecting or scattering objects which are subjected to stress to be interferometrically compared with their non-deformed state. Actually, the holographic interferometry has become one of the most important applications of the fundamental law of optical holography.

> *After the quantum of energy has already gone through the double slit screen, a last-instant free choice on our part gives at will a double-slit interference record or a one-slit-beam count. Does this result mean that present choice influences past dynamics, in contravention of every formulation of causality? Or does it mean, calculate pedantically and don't ask questions? Neither; the lesson presents itself rather as this, that the past has no existence except as it is recorded in the present.*
>
> ***John A. Wheeler (1978)***

> *I argue that the very structure of all quantum theories suggests a revision of the classical notion of space and time. I will present evidence that two copies of space-time, rather than one, are the proper arena for quantum processes. At the heart of this observation lies the very well known fact that every set of equations and formulae in quantum theory, from which all the transition amplitudes are determined, may always be written in two equivalent forms, differing by complex conjugation. We obtain one set from the other by reversing the sign of the imaginary unit* i.
>
> ***Iwo Bialynicki-Birula (1986)***

8. Optical wavefront conjugation

The pair of reproducing diffraction integrals of the Corollary to Theorem 7.1 supra describing the holographic filter bank is also at the basis of optical wavefront conjugation by means of real-time quantum holography [49, 50] in electro-optical PRCs. Two of the beams are referred to as pump beams and are arranged such that they are co-linear and counter-propagating and overlap both spatially and temporally in the symplectic hologram plane $\mathfrak{R} \dotplus \mathfrak{R}$. The third beam, commonly called the probe beam, can interfere with each of the pump beams to generate transient phase gratings within the electro-optical PRC. These gratings arise because the refractive index of the PRC changes in response to the intensity of laser light: as the pump beams interfere with each other, the regions of constructive and destructive interference cause a corresponding modulation of the refractive index. The pump beams then entering the PRC can be deflected by the induced gratings to produce the fourth, wave-front conjugate beam. The wavefront conjugate beam propagates back along the path of the probe beam with a wave vector opposite to the wave vector of the probe beam.

Recall that neurocomputers consist of weighted linear interconnections between arrays of simple nonlinear processing units, the neurons. Information is stored in the neurocomputer almost exclusively in the interconnection pattern. Learning dynamics are used to evolve the interconnection strength pattern as a succession of small perturbations. Because degenerate four-wavelet-mixing wavefront conjugate mirrors, as described above, provide retroreflection and optical tracking novelty filters, Theorem 7.1 is at the basis of neural network models implemented by local neural networks of reconfigurable holographic optical interconnect patterns in optical neurocomputer architectures [2, 3, 4, 5, 7, 79, 81, 82, 83, 124, 126, 127, 129, 128, 130, 131, 142, 145, 144, 143, 146]. In the long term, real-time holography in PRCs appears to be the most appealing reconfigurable optical interconnection technique. If the holographic associative memory has net gain comparable with the losses in the resonator cavity, the output will converge to a real image of the globally stored object: the expanded conjugate reference signal beam acts as an optical scanner for readout of the associate information. In case of a linear resonator memory, gain is supplied by the wavefront conjugate mirror which provides regenerative feedback, whereas in case of a loop resonator memory, gain is supplied by an externally pumped electro-optical PRC.

The Soffer optical resonator forms an implementation of an optical neurocomputer architecture which includes two degenerate four-wavelet-mixing wave-front conjugate mirrors. For more details, the reader is referred to Section 15 infra.

Geometric quantization provides the structure for the geometric realizations of the irreducible unitary representations of the groups involved in physics.

Norman E. Hurt (1983)

9. Radial isotropy

The vast majority of optical systems are designed to operate over a field of view that is radially isotropic. If the processing elements of an optical system are constrained to be radially symmetric, it is only necessary to optimize the performance over a radial slice of the field of view. The system is then guaranteed to have the same performance over any radial slice of the field of view. The advantages to optimizing over a radial slice as compared with the full field of view are speed and cost. Each additional field point used in the automatic design routine such as CODE V increases the computation time, and, therefore, the expense [67].

A complex-valued writing wavelet packet amplitude density $\psi(t)dt$ in $\mathcal{S}(\mathfrak{R})$ is called radially isotropic if its holographic trace transform $H_1\{\psi; x, y\} \cdot dx \wedge dy$ is a radial differential 2-form on the symplectic hologram plane $\mathfrak{R} \times \mathfrak{R}$, i.e., if $H_1\{\psi; x, y\} \cdot dx \wedge dy$ is invariant under the natural action of the orthogonal group $\mathbf{O}(2, \mathfrak{R})$ in $\mathfrak{R} \times \mathfrak{R}$.

Theorem 9.1. The complex-valued wavelet packet amplitude density $\psi(t)dt$ on $\mathfrak{R}$ is radially isotropic if and only if $\psi \in \mathcal{S}(\mathfrak{R})$ admits the form of Hermite-Gaussian eigenmodes

$$\psi = c_n H_n$$

where $c_n \in \mathbb{C}$ is a constant and $H_n(t) = e^{-t^2/2} h_n(t)$ is the Hermite function of degree $n \geq 0$.

The proof follows by Kirillov quantization: There is a complete classification of the irreducible unitary linear representations of the diamond solvable Lie group $\mathfrak{T} \cdot G$ having U_χ as their restrictions to G. The Kirillov corresponding coadjoint orbits in the dual of the non-exponential diamond Lie algebra are parabaloids of revolution [154].

It follows from the preceding theorem that a quantum mechanical harmonic oscillator is equivalent to an assembly of bosons each having one polarization state. Notice that the Hermite-Gaussian eigenmodes $(H_n)_{n \geq 0}$ are crucial for the phenomenon of daydreaming in optical resonator neurocomputers [5, 162].

Corollary 9.2. The elementary holograms $(H_1(H_m, H_n; \cdot, \cdot))_{m \geq 0, n \geq 0}$ form a Hilbert basis of the complex Hilbert space $L^2(\mathfrak{R} \times \mathfrak{R})$.

The orthogonality of the elementary holograms

$$(H_1(H_m, H_n; .,.))_{m \geq 0, n \geq 0}$$

in the complex Hilbert space $L^2(\mathfrak{R} \times \mathfrak{R})$ implies that in the Shannon sense the mutual information of the code coefficients is zero. Thus the code coefficients are non-redundant, they form a statistically independent ensemble, and image coding in terms of the decorrelating family of code primitives $(H_1(H_m, H_n; .,.))_{m \geq 0, n \geq 0}$ is optimally efficient. Let the element $\psi \in L^2(\mathfrak{R} \times \mathfrak{R})$ admit the expansion

$$\psi = \sum_{m \geq 0, n \geq 0} c_{m,n} H_1(H_m, H_n; .,.)$$

with complex coefficients given by

$$c_{m,n} = \langle \psi, H_1(H_m, H_n; .,.) \rangle \qquad (m \geq 0, n \geq 0).$$

It follows

$$\|\psi\|_2^2 = \sum_{m \geq 0, n \geq 0} |c_{m,n}|^2$$

and by switching to the time-asymmetric state-vector reduction procedure of quantics, the probability that $\psi \neq 0$ in $L^2(\mathfrak{R} \times \mathfrak{R})$ collapses to the elementary hologram $H_1(H_m, H_n; .,.)$ is given by the ratio

$$|c_{m,n}|^2 / \|\psi\|_2^2 \qquad (m \geq 0, n \geq 0).$$

The non-deterministic collapse of the wavefunction $\psi \in L^2(\mathfrak{R} \times \mathfrak{R})$ represents the nonlinear aspect of the Kirillov quantization procedure because it violates the quantum complex superposition principle. It is complementary to the linear aspects of quantum holography.

Corollary 9.3. The quantum mechanical mode competition in recognizing $\psi \neq 0$ in $L^2(\mathfrak{R} \times \mathfrak{R})$ is determined by the probabilities $(|c_{m,n}|^2 / \|\psi\|_2^2)_{m \geq 0, n \geq 0}$.

> *Amacronics is a name coined for layered structures of processing electronics, binary microoptics, and detector arrays, with applications in imaging systems with processing right at the focal plane. Amacronic structures are based on lessons that we learned from Mother Nature. Human beings live quite happily with a data transfer rate of a few kilocycles, massively parallel yes, but not very fast. All imaging systems suffer from the Von Neumann bottleneck in electro-optics (in computer systems all the processing functions go through a single* CPU, *the central processor unit; it slows down the overall system). Electro-optical systems are similar; all the optical information goes through a detector*

array at the focal plane which is the bottleneck. We are developing layered structures of optics and electronics in a parallel form (a processing unit per pixel), somewhat like what happens in front of the retina of your eye where you have similar amacrine clustered processing layers. The word "amacrine" comes from the Greek a macros meaning short range. The idea is to couple dynamically clusters of detector arrays. With binary optics we may be able to build systems with peripheral vision much more motion-sensitive than on-axis fovial view, or systems tuned for edge detection or noise reduction.

Wilfrid B. Veldkamp (1989)

Binary optics: The optics technology of the 1990s.

Wilfrid B. Veldkamp (1990)

10. Amacronics: the microoptics layer

The one-dimensional unitary linear representations of the polarized Heisenberg group G are given by the assignment

$$U_{(\xi,\eta)}(x,y,z)\psi(t) = e^{2\pi i(\xi x+\eta y)}\psi(t) \qquad (t \in \mathfrak{R}).$$

These representations which are, of course, irreducible are called representations of linear Fraunhofer type of G. Under the Kirillov correspondence they admit one-point coadjoint orbits $\{\mathcal{O}_{(\xi,\eta)} = \varepsilon_{(\xi,\eta)} | (\xi,\eta) \in \mathfrak{R} \dotplus \mathfrak{R}\}$ in the "singular" plane $\nu = 0$ spanned by $\{P^*, Q^*\}$ in $\mathfrak{g}^* = T^*_{(0,0,0)}(G)$ which form a set of Plancherel measure zero. The Plancherel measure π_G of G is uniquely determined by the Haar measure $dx \odot dy \odot dz$ and concentrated on $\mathfrak{R} - \{0\}$. It is given by

$$\pi_G = |\nu|\, d\nu.$$

The character formula of G [155] provides the radial fanin/fanout distribution on the symplectic hologram plane $\mathfrak{R} \dotplus \mathfrak{R}$:

$$\boxed{\varepsilon_{(0,0)} = \int_{\mathfrak{R}} \mathrm{Tr}_{G/C} U_\nu \, d\pi_G(\nu)}$$

The tempered distributions $\mathrm{Tr}_{G/C} U_\nu$ $(\nu \neq 0)$ follow from the trace identity for the linear Schrödinger representation U_1 of the Heisenberg group G

$$\mathrm{Tr}_{G/C}\, U_1 = \sum_{n \geq 0} H_1(H_n;.,.)$$

by time scaling $t \mapsto \sqrt{|\nu|}\, t$. Projection of the Kirillov corresponding paraboloids of revolution in the dual of the diamond Lie algebra along the

axis allows to create microscopic multi-level surface relief patterns of high quality diffractive HOEs [175, 176]; see Figure 10.1. The focal length of the diffractive microlenses in the HOE arrays is given by

$$f = |v|,$$

and therefore inversely proportional to the center wavelength λ. The plane $v = 0$ in $\mathfrak{g}^*$ forms therefore the focal plane layer of the amacrine structure. The quantization of the continuous phase profile into discrete phase levels is performed by using the VLSI ion-etching technology.

Both digital and analog optical computing requires sufficiently powerful and bright sources of radiation characterized by a small size and a highly efficient transformation of pumping energy into coherent radiation output. Diode or injection lasers provide the best choice in terms of power consumption and size. The coherence length of their radiation output is sufficient for optical computing purposes.

In the AT&T Bell Laboratories' looped digital optical pipeline processor the array of power supply beams to read the optical logic devices is created from a pair of laser beams by a HOE component. This holograting of Dammann type [82, 173, 185] is a multi-beam splitting DOE the pattern of which is computed to generate a uniform 4×8 array of wavelets from one incident laser beam. The two 850 nm diode lasers can therefore be used to generate two interleaved 4×8 arrays so that one array illuminates all the upper S-SEED diodes and the other illuminates all the lower ones. There are two advantages in this scheme: two lasers can supply twice as much power as one laser, and, by pulsing one of the pair of lasers, all of the devices in the array can be preset into the same logic state. The two beams from the laser pair are combined at a "knife-edge." The two counterpropagating beams are focused to two adjacent spots, one of which is reflected, the other transmitted. This pair of spots is imaged via the holograting onto the device array.

Presently the most advanced implementation of two-dimensional matrix-addressable arrays of laser diodes for free-space holographic optical interconnect patterns and photonic switching in optical computers is formed by a hybrid optoelectronic chip recently developed by the AT&T Bell Laboratories in collaboration with Bellcore. It includes more than 2 million electrically pumped vertical-cavity surface-emitting lasers (VCSELs) arranged on a GaAs substrate of size less than 1 cm^2. The active area of the micro-lasers emitting infrared laser light of about $\lambda = 8500\,0317$ wavelength consists of thin indium gallium arsenide (InGaAs) layers sandwiched between more than 600 successive molecular beam epitaxial (MBE) or epi layers of GaAs and aluminum arsenide AlAs. Each of the cylindrical microlasers has cross-section of about 5 mm and has been etched by a photolithographic process. The lengths of the microlasers are about 5.5 μm,

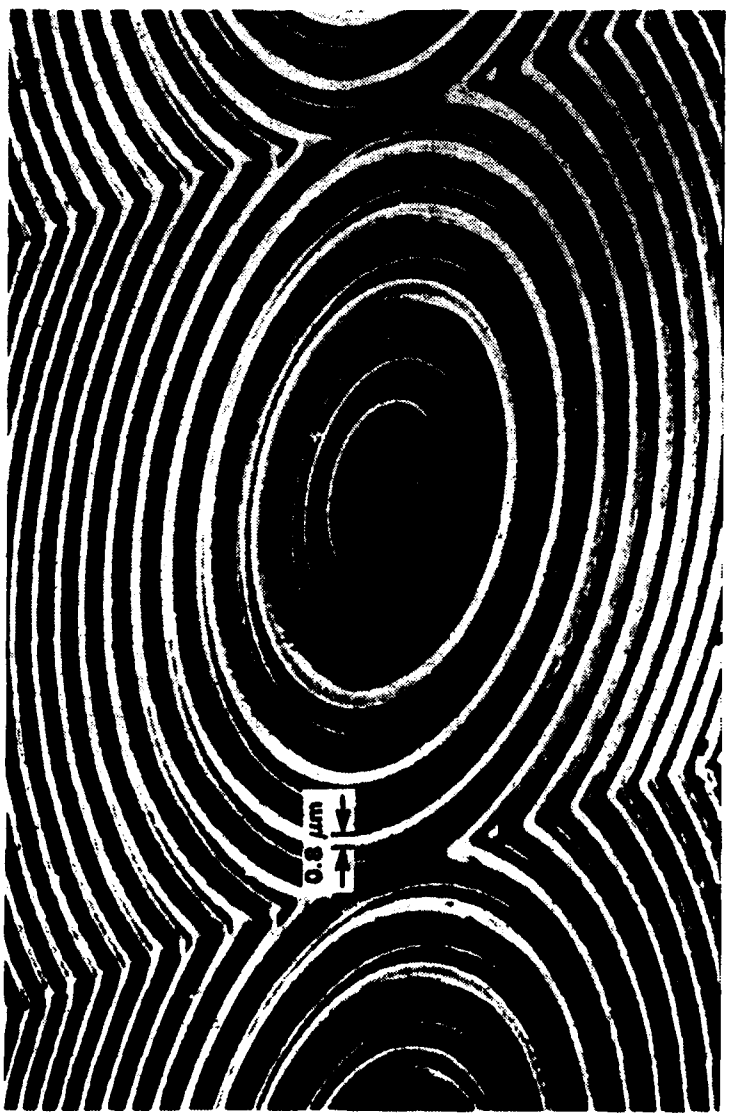

Figure 10.1

and greater than 99.5% of that is passive material. All the laser diodes are individually addressable, independently of the other ones by a current of about 1 mA and therefore are particularly suitable for performing the angle image encoding and decoding procedures of optical holograms. In practice, a simple 4×4 matrix-addressable surface-emitting laser (SEL) array (MASELA) was used to address an optical hologram containing 16 distinct images, each microlaser reading out a separate image. The two-dimensional MASELA is a technology to which conventional edge-emitting diode lasers have no practical counterpart. It is the aim of the present development in amacronic sensor technology to integrate the optical source chip into a hybrid VLSI neurochip.

The Heisenberg group is a natural setting for defining and analyzing certain continuous and discrete concepts arising from the Fourier transform and associated with nonstationary image representation.

Richard Tolimieri (1990)

Now it is together, blinking happily.

Alan Huang (1990)

Fractals or fractal objects are self-similar structures or scale-invariant. It can be understood as a form of symmetry.

Barry R. Masters (1990)

11. Hololattices and holofractals

The implementation of two-dimensional pixel arrays by holographic optical interconnect patterns [79, 81, 82, 83, 185] and analog VLSI wavefront arrays [1] suggests to look at the restrictions of the sesquilinear holographic transform

$$\psi(t')dt' \otimes \varphi(t)dt \mapsto H_1(\psi, \varphi; x, y) \cdot dx \wedge dy$$

to lattices located inside the symplectic hologram plane $\mathfrak{R} \oplus \mathfrak{R}$ [23, 157]. The quadratic lattice $\mathcal{Z} \oplus \mathcal{Z}$ embedded in the symplectic hologram plane $\mathfrak{R} \oplus \mathfrak{R}$ may be considered as the projection onto G/C_G of the 3-cubic (uniform) lattice

$$L_0 := \{(\mu, \mu', \zeta) | \mu \in \mathcal{Z},\ \mu' \in \mathcal{Z},\ \zeta \in \mathcal{Z}\}$$

and the normal subgroup

$$L := \mathcal{Z} \oplus \mathcal{Z} \oplus C_G$$

inside the three-dimensional Heisenberg nilpotent Lie group G along its center C_G. Form the compact Heisenberg nilmanifold $L_\Theta\backslash G$ associated to G which is a circle bundle over the two-dimensional compact torus $\mathcal{T}^2$. An application of the Weil-Zak isomorphism

$$w_1 : \psi \mapsto \{(x,y,z) \mapsto e^{2\pi i z} \sum_{m\in\mathcal{Z}} e^{2\pi i m y}\psi(m-x)\} \qquad (\psi \in \mathcal{S}(\mathfrak{R}))$$

allows to realize the linear Schrödinger representation U_1 of G as the linear lattice representation

$$\delta_1 = \mathrm{Ind}_L^G(\chi_1)$$

of G [59, 152, 153, 155]. Thus, δ_1 is a representation of G of linear Schrödinger type which reveals to be of extreme importance in quantum holography.

Remark 11.1. The projection of the Weil-Zak isomorphism w_1 onto the first coordinate axis gives rise to the periodization map

$$\mathfrak{p} : \psi \mapsto (x \mapsto w_1(\psi)(x,0,0)) \qquad (\psi \in \mathcal{S}(\mathfrak{R})).$$

Combined with the one-dimensional Fourier transform $\mathcal{F} = \sigma(g_\Theta)$, the periodization map $\mathfrak{p}$ gives rise to the Poisson summation formula for the elements of the space $\mathcal{S}(\mathfrak{R})$ and therefore to the Whittaker-Shannon-Nyquist-Kotel'nikov sampling theorem which allows the reconstruction of a band-limited signal from its uniformly distributed samples utilizing translates of the cardinal sine mother wavelet (cf. Example 6.4 supra). Interleaving in the Cross Interleave Reed-Solomon Code (CIRC) is employed to redistribute data symbols in the bit stream prior to recording so that consecutive words are never adjacent. Recording in a non-localized way guards against the very likely occurrence of burst errors. Upon de-interleaving during the CIRC decoding procedure, the shuffled words are placed back in their original and rightful position in the stream, and the errors are distributed in time.

Remark 11.2. For the affine Lie group $G_{\mathfrak{a}}$ of the real line $\mathfrak{R}$ (see Remark 7.2 supra), however, there exists no analog of the linear lattice representation δ_1 of G. Therefore, there is no summation formula of Poisson type for $G_{\mathfrak{a}}$.

From the isomorphy performed by w_1 between the linear Schrödinger representation U_1 and the linear lattice representation δ_1 of G follows the identity

$$H_1(\psi,\varphi;x,y)\cdot dx\wedge dy = \langle \delta_1(x,y,0)w_1(\psi)|w_1(\varphi)\rangle \cdot dx\wedge dy$$

inside the pixel $]-1/2,+1/2[\times]-1/2,+1/2[$ in the symplectic hologram plane $\mathfrak{R}\dotplus\mathfrak{R}$.

As a first application, the preceding identity allows to decide in a mathematically rigorous way the Bohr-Einstein dialogue [190, 191, 192, 194, 193, 195, 177] in favor of quantum theory. Thus the linear lattice representation δ_1 of G allows to overcome the inadequacy of the classical Heisenberg Uncertainty Principle in describing by standard root-mean-square deviations the beam-splitter quantum interference experiment and its application to the holographic image encoding procedure. In fact, Bohr's intuitive argument cannot be rigorously based on any of the known uncertainty relations. The comprehensive structure of the Heisenberg nilpotent Lie group G, however, is ideally suited for the purposes of quantum holography: An application of the preceding identity establishes the quantum parallelism in a mathematically conclusive way. In fact it proves.

Theorem 11.3. The holographic image encoding procedure implemented by a linear Mach-Zehnder interferometer generates an optical hologram if and only if quantum parallelism holds between the reference and object wavelets.

Quantum parallelism, according to which any two states of correlated photons must be considered as taking place simultaneously in quantum complex linear superposition, irrespective of how far from one another they might be, is a consequence of the Einstein-Podolsky-Rosen (EPR) type nonlocality of quantics. It has been verified by sophisticated and highly accurate laser experiments, the results of all of which are in excellent agreement with the quantum theoretical predictions [8, 10, 9, 11, 12]. The quantum interference pattern has been observed even when the time interval between the arrivals of individual photons was around 30,000 times longer than the time for an individual photon to pass through the linear Mach-Zehnder interferometer [135, 139]. Therefore, in the context of quantum holography the parallelism of firing neurons (cf. [123]) located at different columns of the visual cortex, which has been recently observed at the Max Planck Institute for Brain Research in Frankfurt am Main, is highly remarkable.

A second application is the computation of hologratings of Dammann type [82, 185] which are based on planar fabrication techniques, such as photolithography and reactive ion etching [189], now standard in VLSI electronic technology. They act as multi-beam splitting DOE components in the AT&T Bell Laboratories' looped digital optical pipeline processor.

A third important consequence is the Parseval-Plancherel type pixel identity

$$\sum_{(\mu,\mu')\in\mathfrak{Z}\dotplus\mathfrak{Z}} H_1(\psi;\mu,\mu')\overline{H}_1(\varphi;\mu,\mu') = \sum_{(\mu,\mu')\in\mathfrak{Z}\dotplus\mathfrak{Z}} |H_1(\psi,\varphi;\mu,\mu')|^2$$

which holds for all complex-valued writing wavelet packet amplitude densities $\psi(t)dt$, $\varphi(t)dt$ in the space $\mathcal{S}(\mathfrak{R})$. If the Hermite-Gaussian eigenfunctions

H_m and H_n $(m \geqslant n \geqslant 0)$ are inserted for ψ and φ, respectively, the radial symmetry of the terms of the left-hand side implies by a trace argument the following result [156, 157, 150].

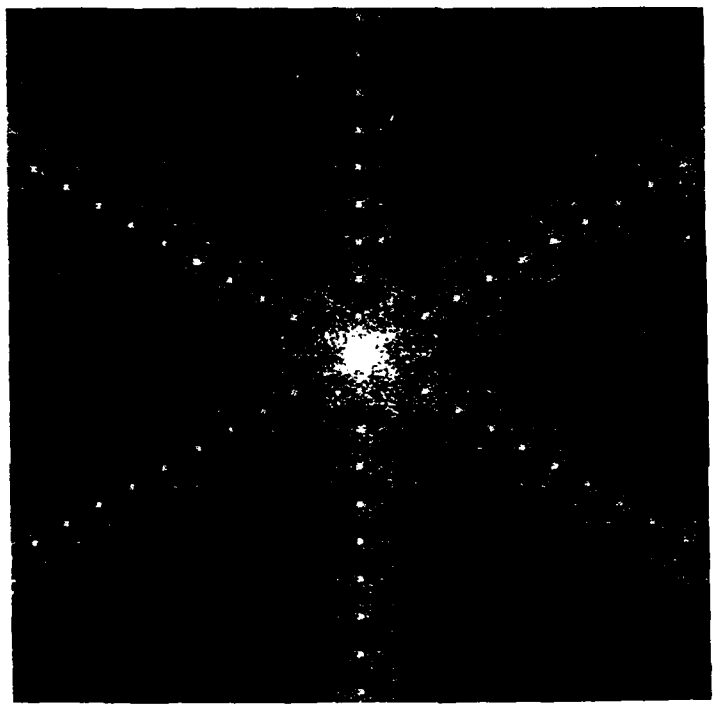

Figure 11.1

Theorem 11.4. The non-oriented lattices of two-dimensional pixel arrays in the symplectic hologram plane $\mathfrak{R} \dotplus \mathfrak{R}$ have the crystallographic dihedral groups $D_k (k \in \{1,2,3,4,6\})$ of order 2k as their groups of symmetry.

An application of the representations of linear Fraunhofer type of G yields the following

Corollary 11.5. The diffraction patterns of the non-oriented lattices located in the hologram plane are the reciprocal lattices.

Snowflake fractals, i.e., self-similar planar von Koch curves admitting locally the symmetry groups D_k $(k \in \{1,2,3,4,6\})$ are called holographic fractals or holofractals, for short. The validity of the preceding

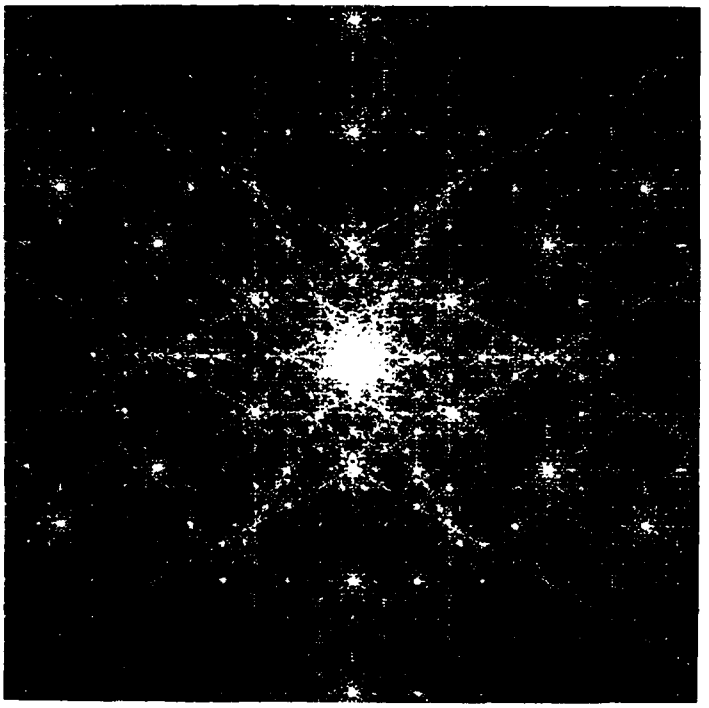

Figure 11.2

results can be experimentally demonstrated by means of optical holofractals readout by the representations of G of linear Fraunhofer type [150, 183, 182]. For the case $k = 3$ of triadic holofractals having Hausforff dimension $\log 4 / \log 3 = 1.2619\ldots$, a line segment of unit length serves as the initiator and an equilateral triangle becomes the generator; see Figures 11.1, 11.2, and 11.3. Readout of randomly distorted holofractals by the representations of G of linear Fraunhofer type generates radial speckle patterns [171, 172].

An application of the Weil-Zak isomorphism w_1 to the readout formulae of the Corollary to Theorem 7.1 supra shows that the scanout of the two-dimensional pixel arrays of the holographic lattices (or hololattices, for short) may be performed by a time-multiplexing procedure.

Remark 11.6. It is a highly remarkable observation of neurophysiology that the presynaptic vesicular grids of the mammalian brain are hexagonal hololattices. The thickness of the presynaptic membrane by which the

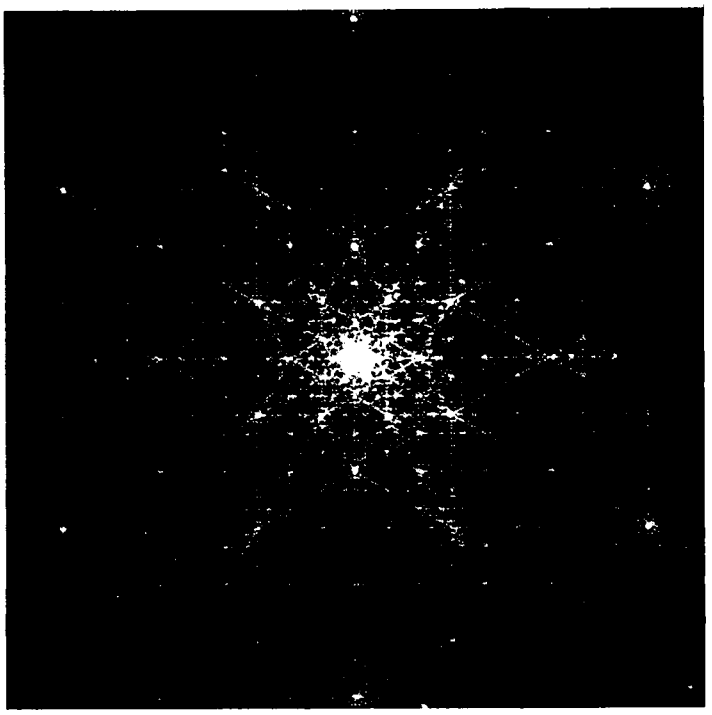

Figure 11.3

synaptic vesicles emit their specific neurotransmitter substances is about 50 0317 whereas the uncertainty of the position of a synaptic vesicle due to the Heisenberg Uncertainty Principle is about 50 0317 per millisecond [42, 36]. Of course, this observation and its consequences are also interesting from the philosophical point of view [43, 197].

Remark 11.7. The hololattices are at the basis of the detour phase method [158, 163] of writing digital CGHs of sampled images by use of the fast Fourier transform (FFT) algorithm. The height and the displacement of a single aperture centered at the sampling points of the hololattice are used to encode the complex-valued wavelet packet amplitude density including the phase of the wavefront. Thus the actual encoding of detour phase CGHs is performed without the explicit use of a reference wavelet. The hololattice corresponding to the crystallographic group D_6 of twelvefold symmetry offers substantial computational efficiency and a significant reduction of

required data storage compared with rectangular sampling: the hexagonal FFT is 25% more efficient than the most efficient rectangular FFT algorithm. The scanout of the wavefront is achieved when the CGH is illuminated with a plane wave and focused with a Fourier-transforming lens.

Remark 11.8. Compact disks (CDs) may be regarded as one-dimensional digital CGHs that may be scanned out by the holographic optical read-head of a CD digital audio player. The scanning laser beam which is focused on the surface of the CD is focused on its return path on a quadrant detector located near the laser diode chip. The detector converts the arrays of minute optical holograms which are coherently encoded by mixing the scanning beam with the beam scattered by the pits into a sequence of electric pulses. Thus the massive amount of information arising by scanning the simple interference patterns of pits and lands has to be serially pumped off the symplectic hologram plane $\mathfrak{R} \oplus \mathfrak{R}$ and then fed into the bit-stream chip or the multi stage noise shaping (MASH) IC of the CD player's microelectronic circuitry. It is the focal plane of the collimating lens which forms the optoelectronic von Neumann bottleneck of the hybrid device. Erasable magneto-optic technology uses laser light both to record and to read data. A blank disk has all its magnetic domains oriented north-pole-down. To record information, a burst of a few nanoseconds of high-intensity light from an infrared laser heats a spot about 1μm across in one magnetic layer of the disk. The coercive force required to change the magnetic orientation of all the domains in the spot from north-pole-down to north-pole-up falls to almost zero as the temperature of the spot increases to 150°C, and the bias magnetic field created by a coil flips the magnetic field. The data are read by a lower-powered beam from the same laser, whose polarization depends, by the Kerr magneto-optic effect on whether the magnetic orientation of the spot is north-pole-up or north-pole-down. Optoelectronic ICs in the magneto-optic write-read-head senses the polarization, and the magnetic orientation is interpreted as a digital 1 or 0. The magneto-optic switching technology suggests to consider the spin variables of an erasable CD as a one-dimensional artificial neural network.

> *The single most important principle in the analysis of electrical circuits is the principle of linear superposition. For an arbitrary network containing resistors and voltage sources, we can find the solution for the network (the voltage at every node and the current through every resistor) by the following procedure. We find the solution for the network in response to each voltage source individually, with all other voltage sources reduced to zero. The full solution, including the effects of all voltage sources, is just the sum of the solutions for the individual voltage sources. In addition to linearity of the component characteristics, there*

must be a well-defined reference value for voltages (ground), to which all node potentials revert when all sources are reduced to zero. This principle applies to circuits containing current sources as well as to those containing voltage sources. It applies even if the sources are functions of time. It also applies to circuits containing capacitors, provided that any initial charge on a capacitor is treated as though it were a voltage source in series with the capacitor.

Carver A. Mead (1989)

12. Amacronics: the processing electronics layer

Recall from the theory of electrical networks that a simple closed path in the plane $\mathfrak{R}\oplus\mathfrak{R}$ is called a mesh. A mesh is called hexagonal if it has the dihedral group D_6 as its symmetry group (see Theorem 11.4 supra). Let us assume that the processing electronics layer is implemented by a linear network of local resistive circuits and that the voltage is constant around the perimeter of each concentric hexagonal mesh about the driven node. Consider the nth concentric hexagonal mesh where all of its $6n$ nodes have the same voltage V_n. On its perimeter there are 6 vertices, and the remaining $6(n-1)$ nodes lie along the edges. Each of the 6 vertex nodes makes 3 outside interconnections, while each of the $6(n-1)$ edge nodes makes 2 outside interconnections. Thus the nth hexagonal mesh connects to the $(n+1)$st concentric hexagonal mesh through $(12n+6)$ parallel resistors. Each of the resistors has resistance R and conductance R_0^{-1}. Therefore the impedance connecting the nth mesh to the $(n+1)$th concentric mesh is $R/(12n+6)$. Similarly the impedance connecting the nth mesh to the $(n-1)$st concentric mesh is $R/(12n-6)$. Along the nth mesh there are $6n$ conductances to ground, making a net admittance to ground of $6nR_0^{-1}$. According to Kirchhoff's current law, the current flowing into the nth mesh from its neighbours balances with the current flowing out of the nth mesh to ground. It follows the forward recursion

$$\frac{V_{n+1}-V_n}{R/(12n+6)}+\frac{V_{n-1}-V_n}{R/(12n-6)}=6nR_0^{-1}V_n \qquad (n\geqslant 1).$$

Introducing the parameter $a = RR_0^{-1}$, Kirchhoff's current law takes the more convenient form [51, 115]

$$(2n+1)V_{n+1}-n(a+4)V_n+(2n-1)V_{n-1}=0 \qquad (n\geqslant 1).$$

It describes the voltage on a given hexagonal mesh in terms of the voltages on the two smaller concentric hexagonal meshes. For any number $w\in\mathbb{C}$ the identity

$$\sum_{n\geqslant 1}(w^n(2n+1)V_{n+1}-w^n n(4+a)V_n+w^n(2n-1)V_{n-1})=0$$

follows. For the power series $G(w) = \sum_{n \geq 1} V_n w^n$, the relations

$$\sum_{n \geq 1} w^{n+1} V_{n+1} = G(w) - wV_1,$$
$$\sum_{n \geq 1} w^{n-1} V_{n-1} = G(w) + V_0$$

yield the inhomogeneous linear differential equation of the first order

$$2\left(w^2 - \left(2 + \frac{a}{2}\right)w + 1\right)\frac{dG}{dw} + \left(w - \frac{1}{2}\right)G = V_1 - wV_0.$$

The linearity of the ordinary differential equations reflects the linearity of the network. Decompose the quadratic factor

$$w^2 - \left(2 + \frac{a}{2}\right)w + 1 = (w - r_+)(w - r_-)$$

into linear factors. Then the voltage of the first hexagonal mesh takes the form

$$V_1 = \left(1 - \frac{E(r_-^2)}{K(r_-^2)}\right) r_+ V_0$$

in terms of the voltage V_0 at the center of the network and the complete elliptic integrals of the first and second kind $E(r_-^2)$ and $K(r_-^2)$, respectively, evaluated at the parameter value r_-^2. The arithmetic-geometric mean algorithm presents an efficient tool to compute V_1 in terms of V_0 and then to apply the forward recursion to compute all the voltages V_n $(n \geq 1)$.

> *Although a cell's response function is in general nonlinear, visual neurophysiologists have found that for many cells, a linear summation approximation is appropriate.*
>
> ***Ralph Linsker (1988)***

13. Gabor wavelets attached to a hololattice

In biological vision, the center-surround receptive field profiles of the retinal neurons [35, 37, 38, 39, 41, 111] and the cells of the lateral geniculate nucleus are far from forming an orthogonal family in $L^2(\mathfrak{R} \oplus \mathfrak{R})$. Therefore the resulting neural representation remains highly correlated. Theorem 7.1 supra suggests to implement a matching filter bank by an adaptive artificial neural network model which is based for $(y, y') \in \mathfrak{R} \oplus \mathfrak{R}$ on the central projection and backprojection G-slice orbits

$$G^{(\mu,\mu')}_{(y,y')} : (x, x') \mapsto (U_1(x, y, 0) \otimes \overline{U}_1(x', y', 0)(H_0 \otimes H_0))(\mu, \mu')$$

$((\mu, \mu') \in \mathbb{Z} \dotplus \mathbb{Z})$, of the Gaussian mode $H_0 \otimes H_0$ in $L^2(\mathfrak{R} \dotplus \mathfrak{R})$. The irreducibility of the linear Schrödinger representation U_1 of G combined with the Weil-Zak isomorphism w_1 implies:

Theorem 13.1. The approximating family of Gabor wavelets

$$\left\{ G^{(\mu,\mu')}_{(y,y')} \mid (\mu, \mu') \in \mathbb{Z} \dotplus \mathbb{Z}, (y, y') \in \mathfrak{R} \dotplus \mathfrak{R} \right\}$$

attached to the hololattice $\mathbb{Z} \dotplus \mathbb{Z}$ inside the symplectic hologram plane $\mathfrak{R} \dotplus \mathfrak{R}$ is total in the complex Hilbert space $L^2(\mathfrak{R} \dotplus \mathfrak{R})$.

Notice that the Gabor wavelets form a non-orthogonal family in the Hilbert space $L^2(\mathfrak{R} \dotplus \mathfrak{R})$. L^2 expansions in terms of Gabor wavelets offer high code compression rates appropriate for image processing purposes [37]. Early stages of biological visual systems pay for keeping $m = n = 0$ by the non-orthogonality of the center-surround receptive field profiles. The family of Gabor wavelets give excellent fits in the chi-squared statistical sense to the correlating simple cell field profiles empirically studied in the cat striate cortex [85, 84, 111]. The retina [41], an outpost of the central nervous system, and the lateral geniculate nucleus, however, act as decorrelators of the incoming signals. At the level of the mammalian visual cortex, the introduction of orientation selectivity through localized wave modulation combined with quadrature phase relations among paired cells results in a decorrelated neural representation with optimal image compression performance by the Hilbert basis of $L^2(\mathfrak{R} \dotplus \mathfrak{R})$ of elementary holograms $(H_1(H_m, H_n; \ldots))_{m,n \in \mathbb{O}}$. Signal preprocessing and processing in the auditory parts of the cortex follow similar basic lines.

> *I saw my first hologram at the Ontario Science Centre in Canada, and have been obsessed with holography ever since.*
>
> ***Sunny Bains (1987)***

> *The resolution can indeed be very good, since the effective aperture for the system is not the aperture of the object-bearing system but is instead the aperture of the other branch of the interferometer*
>
> ***Emmett N. Leith (1986)***

14. Optical display holograms and superresolution imaging

Optical phase conjugation by degenerate four-wavelet-mixing requires a coherent light source. Due to the degrading effects of coherent artifact noise which results from the quantum stationary interference between the light scattered by imperfections in the optical path and the unscattered light

representing the optical signal, a considerable amount of research interest has been directed towards the use of partially coherent illumination.

In case of a spatially incoherent light source, the coherent holographic transform as defined above has to be modified. The canonical differential 2-form on G/C_G has to be replaced by

$$\omega_\nu = \nu \cdot dx \wedge dy \qquad (\nu \neq 0)$$

inherited from the symplectic form $\omega_{\mathcal{O}_\nu}$ of the coadjoint orbit $\mathcal{O}_\nu$ in the real dual of the Heisenberg Lie algebra. For different center frequencies $\nu \neq 0, \nu' \neq 0$, the symplectic affine planes $(\mathcal{O}_\nu, \omega_\nu)$, $(\mathcal{O}_{\nu'}, \omega_{\nu'})$ are different. Therefore the associated irreducible unitary linear representations U_ν, $U_{\nu'}$ of G are non-isomorphic. Consequently the orthogonality relations

$$\langle H_\nu(\psi, \varphi; ., .) | H_{\nu'}(\psi', \varphi'; ., .) \rangle = 0 \qquad (\nu \neq \nu')$$

hold on the symplectic plane $\mathfrak{R} \times \mathfrak{R}$ for $\psi, \varphi, \psi', \varphi'$ in $\mathcal{S}(\mathfrak{R})$. Instead of the coherent holographic transform, the transform defined by quantum complex linear superposition of the mapping

$$\psi(t')dt' \otimes \varphi(t)dt \mapsto H(\psi, \varphi; x, y) \cdot dx \wedge dy$$

has to be considered. The form coefficient

$$\boxed{H(\psi, \varphi; x, y) = \int_{\mathfrak{R}} \nu \cdot H_\nu(\psi, \varphi; x, y) d\nu}$$

is performed by integrating over the spatial frequencies ν emitted by the light source.

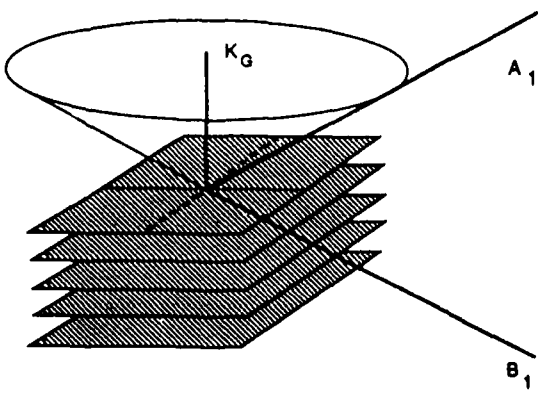

Figure 14.1

As a first application of the preceding identity, the various kinds of optical display holograms should be mentioned. A combination of the discretized frequency scale (ν scale dual to the z coordinate axis) with the Bragg frequency selection law for the generated diffractive planar multilayers explains the volume holograms (à la Denisyuk), the rainbow holograms (à la Benton), the multiplex holograms (à la Cross), and the waveguide holograms (à la Caulfield); see Figure 14.1 for the cone of Bragg angles associated to the multilayered dual manifold of G. The holographic angle decoding procedure can be restated in the following form:

Theorem 14.1. The choice of the hologram plane as a Kirillov orbit $\nu \neq 0$ within the multilayered unitary dual manifold of the Heisenberg nilpotent Lie group G is performed by the Bragg frequency selection law.

Corollary 14.2. The coordinates of a page oriented holographic memory are given by the coordinates $(x, y) \in \mathfrak{R} \oplus \mathfrak{R}$ of the hologram plane and the reference beam angle to $dx \wedge dy$.

Since the slit device in processing Benton holograms defines the axis directions of the coordinate system in the hologram plane $\mathfrak{R} \oplus \mathfrak{R}$, a movement of the illuminating white light source changes the rainbow colours of the optical display hologram.

One of the most common defects in optical display holograms is blurring of the image. It is important to appreciate the fundamental difference between optical holography and photography in this respect. A photograph as a two-dimensional recording of an image formed by a lens can be blurred from the start; the sharpness of the image is not affected by the light source used to illuminate it. The situation, however, is completely reversed for an optical hologram, which is a recording of a stationary quantum interference pattern, not an image. If the interference pattern is blurred at recording, only the brightness of the replay is affected, not the sharpness of the image. The sharpness of the image depends on the direction of the light wavelet packet amplitude densities diffracted by the hologram, which is determined by the spatial frequency of the recorded interference pattern, and also by the direction, size and wavelength of the readout source. In fact it is not possible to record an optical hologram of a blurred object. If any optical hologram is illuminated with an ideal light source, i.e., a point source at the correct wavelength, angle and distance, then the image will be pin sharp, no matter how it was recorded.

The conclusion that if an optical hologram is read out with a point monochromatic source, then the image would not be blurred at all, is only true if the observer does not look beyond the resolution of the human eye. The eye has only a very small aperture and intercepts only a very small cone of rays from the hologram at any time. If the image in an optical hologram

is inspected with larger aperture optics, or if a real image is projected on a screen, the observer will start to see blurring due to the geometric distortion of the light wavelets emanating from each image point. This arises if the replay wavelength is different from the recording wavelength which for a white-light reflection hologram means any change in layer thickness or refractive index, or if the replay angle is not exactly equal to the recording angle, or if a real-image hologram is replayed with an inexact conjugate beam.

Another application of the preceding identity is the superresolution imaging technique [30, 31, 97, 98, 99, 100]. The superresolution effect is achieved by incoherent to coherent conversion. In this procedure the aperture of the imaging system is reduced and the aperture reduction is compensated by reducing the spatial coherence of the light source. In view of the quantum parallelism, a reduced aperture like a pinhole spatial filter can be inserted also in the reference wavelet channel of the interferometer without limiting the effective resolution of the two-parallel-channel optical imaging system. In the readout step, the stationary quantum interference pattern generated in the symplectic hologram plane $\mathfrak{R} \dotplus \mathfrak{R}$ can be decoded as an optical hologram by using an expanded laser beam.

> *Neural network models offer a data-driven unsupervised computational approach which is complementary to the algorithm-driven approaches of traditional information processing and artificial intelligence. The fine granularity, massive interconnectivity, and high degree of parallelism set neural network models apart from traditional electronic serial computing. These same features are the hallmarks of optical computing architectures which have led many workers to consider optical implementations of neural network models.*
>
> ***Bernard H. Soffer (1988)***

> *The resonator memory and novelty filter must be considered as prototypes, not merely because they are rather primitive by neural network model standards but also because their relationship to any existing neural model has yet to be properly established; in several ways, the relationship is a distant one, at best. Many of the features of these devices are nevertheless strikingly reminiscent of neural models. In the resonator memory, for example, it is appropriate to use the term "competition" as it is used in some neural models.*
>
> ***Dana Z. Anderson and Marie C. Erie (1987)***

15. The Soffer optical resonator

In order to identify explicitly the terms of the Parseval-Plancherel type pixel identity indicated above, we denote by $K_{m,n}$ the complete bichromatic graph

of $m+n$ vertices. Define $c(K_{m,n}, 0) := 1$ and let $c(K_{m,n}, l)$ denote the number of choices of $l \geqslant 1$ disjoint edges in $K_{m,n}$ each linking two vertices of different colours. Then

$$\phi_{m,n}(X) := \sum_{0 \leqslant l \leqslant [(m+n)/2]} (-1)^l c(K_{m,n}, l) X^{m+n-2l}$$

denotes the matching polynomial [47, 60, 77, 162] of variable X associated to the bipartite graph $K_{m,n}$. For any number $w \in \mathbb{C}$ the radial evaluation of $\phi_{m,n}(X)$ at w is defined by the rule

$$\phi_{m,n}(w) := \sum_{0 \leqslant l \leqslant [(m+n)/2]} (-1)^l c(K_{m,n}, l) w^{m+n} (w\overline{w})^{-l}.$$

Theorem 15.1. The coefficients of the matching polynomial $\phi_{m,n}(X)$ are the elementary synaptic strengths $(-1)^l c(K_{m,n}, l)$, $0 \leqslant l \leqslant [(m+n)/2]$, where the matching coefficients $c(K_{m,n}, l)$ denote the number of disjoint synaptic interconnects of the local neural network $K_{m,n}$ $(m \geqslant n \geqslant 0)$ activated by l coherently firing neurons.

Example 15.2. In the case $m = n = 3$ the matching coefficients

$$c(K_{3,3}, 0) = 1$$
$$c(K_{3,3}, 1) = 9$$
$$c(K_{3,3}, 2) = 18$$
$$c(K_{3,3}, 3) = 6$$

arise. Thus the matching polynomial of the Thomsen graph $K_{3,3}$ is given by

$$\phi_{3,3}(X) = X^6 - 9X^4 + 18X^2 - 6.$$

Notice that the local network $K_{3,3}$ forms a non-planar graph.

In terms of Laguerre polynomials of order $m-n \geqslant 0$ and degree $n \geqslant 0$, it follows explicitly [77, 162]

$$\phi_{m,n}(X) = (-1)^n n! X^{m-n} L_n^{m-n}(X^2) \qquad (m \geqslant n \geqslant 0).$$

By radial evaluation of the matching polynomials $\phi_{m,n}(X)$ defined above, the next theorem describes the relationship between the elementary holograms and the matching polynomials attenuated by the Gaussian $(H_0 \hat{\otimes} H_0) \in L^2(\mathfrak{R} \oplus \mathfrak{R})$ with distance: the farther away an input is from a point in the neural network, the less synaptic strength it is given.

Theorem 15.3. Let $m \geqslant n \geqslant 0$. Then the elementary holograms admit the form of radially evaluated quasipolynomials

$$H_1(H_m, H_n; x, y) = \frac{(-1)^n}{\sqrt{m!n!}} e^{-\pi(x^2+y^2)/2} \phi_{m,n}(\sqrt{\pi}(x + iy))$$

for all pairs $(x, y) \in \mathfrak{R} \dotplus \mathfrak{R}$.

Example 15.4. According to the Corollary to Theorem 7.1 supra, scaled versions of the elementary hologram $H_1(H_0; ., .) = H_0 \circledcirc H_0$ can be implemented as diffraction HOEs (cf. Remark 4.5 supra) for the fundamental transverse mode of a coherent laser light beam. This implementation is performed with a CAD station by projecting layers of constant optical thickness of the rotationally symmetric Gaussian diffraction profile onto the symplectic hologram plane $\mathfrak{R} \oplus \mathfrak{R}$. In contrast to the Advanced Systems Analysis Package (ASAP) software procedure, however, the diffraction CGH is based on a quantum holographic description of the diffraction profile and therefore adapted to the purposes of amacronic sensor technology.

Corollary 15.5. By quantum complex linear superposition, the symplectic hologram plane $\mathfrak{R} \dotplus \mathfrak{R}$ can be realized as a neural plane of local neural networks.

In particular the quantum holographic approach to neural networks yields the following result:

Theorem 15.6. The intrinsic holographic interconnection patterns are determined by the representations of linear Schrödinger type whereas the extrinsic holographic interconnects are determined by the representations of linear Fraunhofer type of the Heisenberg nilpotent Lie group G.

Simulations of the synaptic strength patterns by conventional large-scale digital computers show that the self-organization of excited neural networks results in a cluster pattern of the neurons [132]; see Figure 15.1. The American artist Jackson Pollock has been motivated by excited neural networks to create his drip paintings (cf. Figure 15.2). Notice that the holographic theory of associative memory also leads to according prime place to the neuroglial cells rather than modifiable synaptic strengths in planar configurations of neurons [123].

Presently one of the most successful implementations of the symplectic hologram plane $\mathfrak{R} \oplus \mathfrak{R}$ as a neural plane is the Soffer optical resonator built at the Hughes Research Laboratories [126, 127, 129, 128, 169, 170]. The optical neurocomputer is formed by a coherent optical resonator cavity consisting of an optical hologram placed between two degenerate four-wavelet-mixing

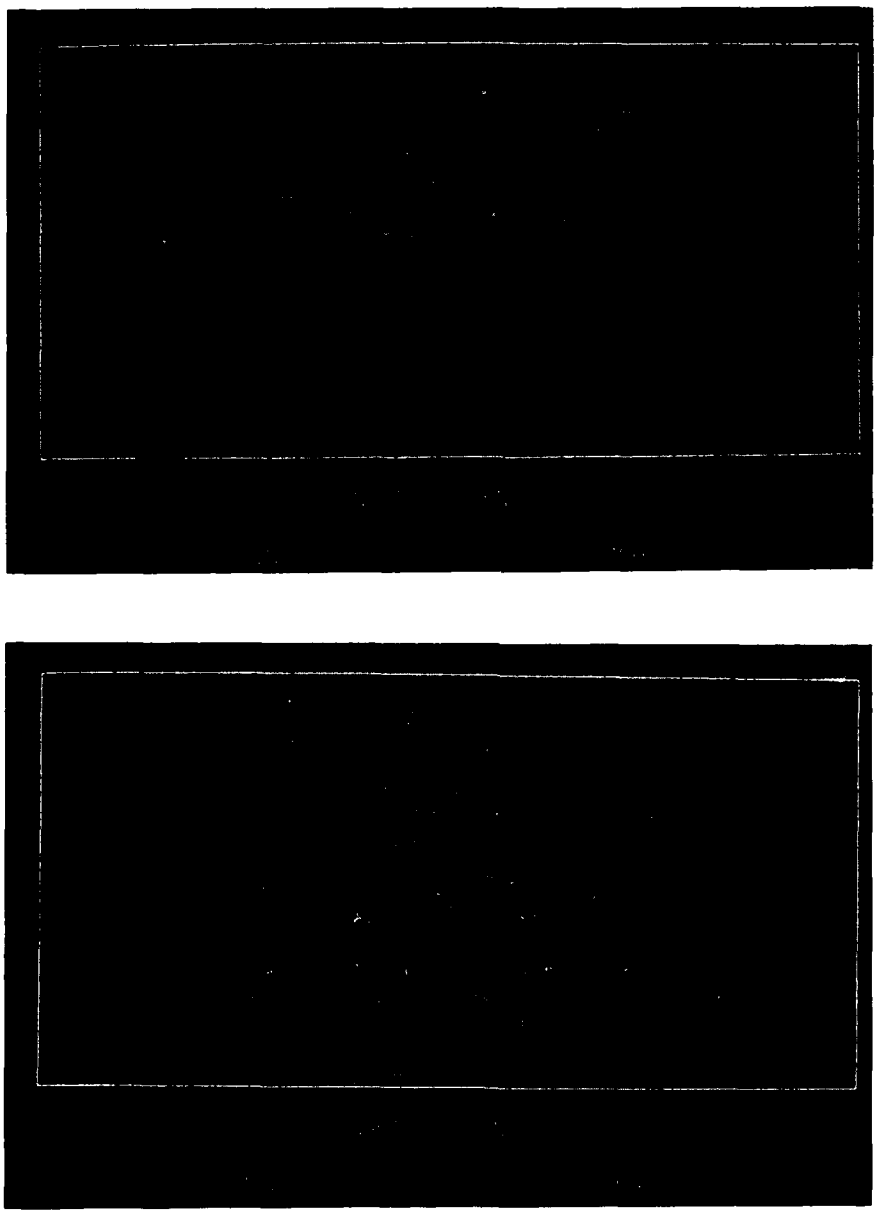

Figure 15.1

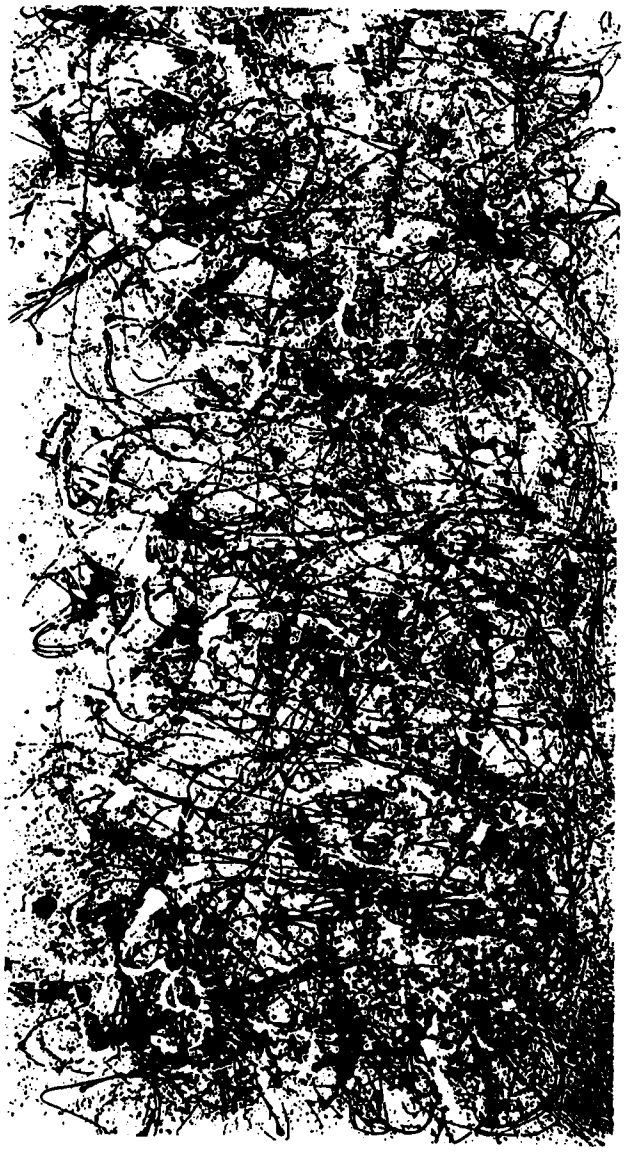

Figure 15.2: Jackson Pollock: *Autumn Rhythm*, 1950, Metropolitan Museum of Art

wavefront conjugate mirrors (PCMs). One of the wavefront conjugate mirrors is sesquilinear [30, 31, 49, 50] while the other one amplifies higher amplitude density signals more than lower amplitude density signals (see Theorem 7.1 supra). The optical hologram has multiple "example" images stored in it.

The neurocomputer is configured so that each example image is holographically encoded using a reference laser beam that impinges on the symplectic hologram plane $\mathfrak{R} \oplus \mathfrak{R}$ at a slightly different angle than the reference beams utilized for the other example patterns. After the neural system has been prepared, one can enter any image into the cavity by impinging it onto the optical hologram. The net result is that the holographically encoded image causes partial reconstruction of the reference beams. The complex-valued wavelet packet amplitude density of each reconstructed reference beam is proportional to the L^2 distance between the entered image and the example image associated with the reference. As the reference beams reverberate through the cavity the strongest (highest complex-valued wavelet packet amplitude density in the L^2 sense) one is incrementally amplified and the others are incrementally attenuated so that before long only the reference beam corresponding to the best matching example is left. In other terms, the stored image with the smallest distance to the input pattern survives in the mode competition at the expense of the more distant images. At the output port, i.e., the reconstructed real image port of the optical hologram, the best L^2 fitting example pattern then appears. Thus the optical neurocomputer functions as a nearest neighbour classifier for holographic imagery by recalling through a competitive memory.

The Soffer optical resonator can be viewed as an infinite-dimensional version of the Hopfield network. Or alternatively, if one envisions the optical elements of the neural system as consisting of small discrete optical units, then the Soffer optical resonator can be thought of as simply a large Hopfield network.

The second generation of Soffer optical resonators is based on a self-pumped wavefront conjugate mirror (SP-PCM) in conjunction with a SLM, CCD detector, frame grabber, and host computer [170]. Similar optical neurocomputers have also been recently built at the Department of Electrical Engineering of Caltech [145, 144, 143, 146] and the Joint Institute for Laboratory Astrophysics (JILA) of the University of Colorado [2, 3, 4, 5, 7]. These neural systems have also successfully demonstrated recording multiple patterns and functioning as a nearest neighbor associative memory. The day-dreaming phenomenon observed in a ring resonator memory reveals the quantum fluctuation as a consequence of the Heisenberg Uncertainty Principle (cf. Section 5 supra).

Mathematical models of neural networks are having a profound influence on current research in optical computing. This trend toward neural computing is motivated by the sophisticated control and information processing that occurs in biological systems. The basic model for a neural network is a large number of simple processing units (i.e., neurons) interacting with one another through weighted interconnections (i.e., synapses). A neural network is the finest grain parallel computer possible where information and program are stored in the weighted interconnections and the processors perform simple thresholding logic. It is this highly parallel nature that gives neural networks their computational power and makes them attractive for optical implementation.

H. John Caulfield (1989)

My interest is, to paraphrase a famous statement, not what mathematics can do for physics, but what physics can do for mathematics. That is my underlying motive.

Stanislaw M. Ulam (1986)

16. Artificial neural network identities

Theorem 15.3 supra implies the shift register identity $(m \geqslant n \geqslant 0)$

$$H_1(H_m, H_n; \mu, \mu') = \langle \delta_1(\mu, \mu', 0) w_1(H_m) | w_1(H_n) \rangle$$
$$= \frac{(-1)^n}{\sqrt{m!n!}} e^{-\pi(\mu^2 + \mu'^2)/2} \phi_{m,n}(\sqrt{\pi}(\mu + i\mu'))$$

for all points (μ, μ') of the quadratic hololattice $\mathcal{Z} \dotplus \mathcal{Z}$. In particular, the following result obtains:

Theorem 16.1. For $m \geqslant n \geqslant 0$ the identity

$$\sum_{(\mu,\mu') \in \mathcal{Z} \dotplus \mathcal{Z}} (-1)^{m+n} e^{-\pi(\mu^2 + \mu'^2)} \phi_{m,m}(\sqrt{\pi}(\mu + i\mu')) \phi_{n,n}(\sqrt{\pi}(\mu + i\mu'))$$
$$= \sum_{(\mu,\mu') \in \mathcal{Z} \dotplus \mathcal{Z}} e^{-\pi(\mu^2 + \mu'^2)} |\phi_{m,n}(\sqrt{\pi}(\mu + i\mu'))|^2$$

holds for the quadratic hololattice $\mathcal{Z} \dotplus i\mathcal{Z}$ of Gaussian integers inside the symplectic hologram plane $\mathfrak{R} \dotplus \mathfrak{R}$.

The preceding theorem gives rise to the following special identities for the odd powers of π in terms of theta-null values $\vartheta(0, 1) = \Sigma e^{-\pi\mu^2}$ [155, 154, 162] where

$$\Sigma := \sum_{\mu \in \mathfrak{Z}} :$$

$m = 1, n = 0$:

$$\pi = \frac{\Sigma e^{-\pi\mu^2}}{4\Sigma\mu^2 e^{-\pi\mu^2}}$$

$m = 2, n = 1$:

$$\pi^3 = \frac{15\,\Sigma\,(8\pi^2\mu^4 - 1)e^{-\pi\mu^2}}{32\Sigma\mu^6 e^{-\pi\mu^2}}$$

$m = 3, n = 2$:

$$\pi^5 = \frac{45\Sigma(16\pi^4\mu^8 - 140\pi^2\mu^4 + 21)e^{-\pi\mu^2}}{64\Sigma\mu^{10}e^{-\pi\mu^2}}$$

$m = 4, n = 3$:

$$\pi^7 = \frac{91\Sigma \text{ numerator } e^{-\pi\mu^2}}{1024\Sigma\mu^{14}}$$

where

$$\text{numerator} = 256\pi^6\mu^{12} - 15840\pi^4\mu^8 + 166320\pi^2\mu^4 - 25245.$$

Theorem 16.1 supra shows that the preceding identities for the theta-null values $\vartheta(0, 1)$ are of a combinatorial character.

Remark 16.2. The cardinal sine mother wavelet sinc mentioned in Example 6.4 supra, i.e., the univariate impulse response of the ideal lowpass filter, admits the Euler factorization

$$\text{sinc } x = \prod_{n \geqslant 1} \left(1 - \frac{x^2}{n^2}\right) \qquad (x \in \mathfrak{R}).$$

Its logarithmic derivative yields the identity

$$\pi x \,\text{cotan}\, \pi x = 1 - 2x^2 \sum_{n \geqslant 1} \left(\frac{1}{n^2} + \frac{x^2}{n^4} + \frac{x^4}{n^6} + \cdots\right).$$

A comparison with the generating function of the Bernoulli polynomials $B_n(X)$ of degree $n \geqslant 0$

$$\frac{we^{wX}}{e^w - 1} = \sum_{n \geqslant 0} \frac{1}{n!} B_n(X) w^n \qquad (w \in \mathfrak{C})$$

evaluated at $X = 0$ and $w = 2\pi ix$ yields the classical Euler formulae for the even powers of π:

$$\pi^{2n} = (-1)^{n+1} \frac{2(2n)!}{2^{2n} B_{2n}} \zeta(2n) \qquad (n \geq 1),$$

where ζ denotes the Riemann zeta-function and $B_{2n} = B_{2n}(0)$ are the Bernoulli numbers. In particular we get the special cases:

$n = 1$: $\pi^2 = 6\zeta(2)$
$n = 2$: $\pi^4 = 90\zeta(4)$
$n = 3$: $\pi^6 = 945\zeta(6)$
$n = 4$: $\pi^8 = 9450\zeta(8)$

The first identity belongs to the nicest formulae established by Leonhard Euler. It has been explicitly reproduced in the Encyclopedia Britannica (1963).

> *Hardly a week goes by without an article appearing on the front page of a national magazine or journal trumpeting yet another breakthrough in optical computing.*
>
> ***Lauren P. Silvernail (1990)***

> *Our ability to realize simple neural functions is strictly limited by our understanding of their organizing principles, and not by difficulties in implementation.*
>
> ***Carver A. Mead (1989)***

17. Synopsis

The computation of real world phenomena in real time requires computational power that exceeds by many orders of magnitude the capabilities of sequential digital computers presently available. Although the data transfer rate of biological neural networks is merely a few kilocycles, hence not very fast, biological wetware is able to solve tasks such as real-time pattern recognition or sound localization because it operates in analog mode which allows simultaneous summing of many inputs from interconnected units and permits massively parallel data processing without the need for iterative procedures. Extrapolation from simulations of simple neural circuits indicate that a sequential digital computer would have to operate at speeds of more than 10^{18} floating point operations per second in order to match the performance limit of the human brain. The implementation of artificial neural network models based on coherent optical processors and analog electronic circuits of neurons and synapses is currently being pursued in a number of laboratories

where several special purpose neurocomputer systems have been fabricated in holographic, optoelectronic, or CMOS VLSI electronic components. In the quantized theory of the electromagnetic field the bosons present in a coherent light beam travelling in a well-defined direction are the optical photons. The Kirillov quantization approach to the theory of the sesquilinear holographic transform $\psi(t')dt' \otimes \varphi(t)dt \mapsto H_1(\psi, \varphi; x, y) \cdot dx \wedge dy$ as outlined in this paper implies a link between elementary holograms and artificial neural networks. It allows to rigorously establish the quantum parallelism as a EPR-type phenomenon (Theorem 11.3 supra) and to recognize the symplectic hologram plane $\mathfrak{R} \oplus \mathfrak{R}$ as a neural plane (Corollary to Theorem 15.3 supra). It is the quantum theoretical base of the holographic transform $\psi(t')dt' \otimes \varphi(t)dt \mapsto H_1(\psi, \varphi; x, y) \cdot dx \wedge dy$ which allows to model three-dimensional planar optics [81, 89] by the unitary dual of the Heisenberg nilpotent Lie group G and to establish the universal validity of the quantum holographic concept from amacronic sensor technology to classical SAR image processing.

Wer spricht von Siegen. Überstehen ist alles.
Rainer Maria Rilke (1875–1926)

18. Bibliography

[1] T. Allen, C. Mead, F. Faggin, and G. Gribble. Orientation-selective VLSI retina. In T. Russel Hsing, editor, *Visual Communications and Image Processing'88*, number 1001 in Proc. SPIE, pages 1040–1046. SPIE, 1988.

[2] D.Z. Anderson. Coherent optical eigenstate memory. *Opt. Lett.*, 11:56–58, 1986.

[3] D.Z. Anderson. Nonlinear optical neural networks: Dynamic ring oscillators. In R. Eckmiller and C. v.d. Malsburg, editors, *Neural Computers*, pages 417–424. Springer-Verlag, Berlin, Heidelberg, New York, London, Paris, Tokyo, 1989.

[4] D.Z. Anderson. Competitive and cooperative dynamics in nonlinear optical circuits. In S.F. Zornetzer, J.L. Davis, and C. Lau, editors, *An Introduction to Neural and Electronic Networks*, pages 349–362. Academic Press, San Diego, New York, Berkeley, Boston, London, Sydney, Tokyo, Toronto, 1990.

[5] D.Z. Anderson and M.C. Erie. Resonator memories and optical novelty filters. *Opt. Eng.*, 26:434–444, 1987. Also [6].

[6] D.Z. Anderson and M.C. Erie. Resonator memories and optical novelty filters. In Caulfield and Gheen [24], pages 585–595.

[7] D.Z. Anderson and D.M. Lininger. Dynamic optical interconnects: Volume holograms as optical two-port operators. *Appl. Opt.*, 26:5031–5038, 1987.

[8] A. Aspect. Proposed experiment to test the nonseparability of quantum mechanics. *Phys. Rev.*, D 14:1944–1951, 1976. Also in [196], pp. 435–442.

[9] A. Aspect. Le théorème de Bell: vingt cinq ans après. In *51ième Rencontre entre Physiciens Théoriciens et Mathématiciens*, Université Louis Pasteur, Strasbourg, 1990. Institut de Recherche Mathématique Avancée.

[10] A. Aspect. Testing quantum mechanics in optics. In *15th Congress of the International Commission for Optics: Optics in Complex Systems*. International Commission for Optics, Garmisch-Partenkirchen, 1990.

[11] A. Aspect and P. Grangier. Experiments on einstein-podolsky-rosen-type correlations with pairs of visible photons. In R. Penrose and C.J. Isham, editors, *Quantum Concepts in Space and Time*, pages 1–15. Clarendon Press, Oxford, 1986.

[12] A. Aspect, P. Grangier, and G. Roger. Experimental tests of realistic local theories via Bell's theorem. *Phys. Rev.*, 47:460–463, 1981.

[13] R. Balian. Un principe d'incertitude fort en théorie du signal ou en mécanique quantique. *C.R. Acad. Sci. Paris*, 292:1357–1362, 1981.

[14] D.A. Baylor, T.D. Lamb, and K.-W. Yau. Responses of retinal rods to single photons. *J. Physiol.*, 288:613–634, 1979.

[15] J.J. Benedetto. Uncertainty principle inequalities and spectrum estimation. In J.S. Byrnes and Jennifer L. Byrnes, editors, *Recent Advances in Fourier Analysis and its Applications: Proceedings of the NATO Advanced Study Institute*, volume 315 of *NATO ASI series C: Mathematical and physical sciences*, pages 143–182, Dordrecht, Boston, London, 1990. Kluwer Academic Publishers Group. Held at Il Ciocco Resort Tuscany, Italy.

[16] A. Berthon. Operator groups and ambiguity functions in signal processing. In J.M. Combes, A. Grossmann, and Ph. Tchamitchian, editors, *Wavelets*, pages 172–180. Springer-Verlag, Berlin, Heidelberg, New York, London, Paris, Tokyo, Hong Kong, 1989.

[17] N. Bohr. Foundations of quantum physics (1926–1932). In J. Kalckar, editor, *Collected Works*, volume 6. North Holland-Elsevier Science Publishers, Amsterdam, New York, Oxford, 1985.

[18] D. Brady, X.-G. Gu, and D. Psaltis. Photorefractive crystals in optical neural computers. In *Neural Networks for Optical Computing*, volume 882, pages 132–136. SPIE, 1988.

[19] V. Braitenberg. Two visions of the cerebral cortex. In G. Palm and A. Aertsen, editors, *Brain Theory*, pages 81–96. Springer-Verlag, Berlin, Heidelberg, New York, London, Paris, Tokyo, Hong Kong, 1986.

[20] V. Braitenberg and C. Braitenberg. Geometry of orientation columns in the visual cortex. *Biological Cybernetics*, 33:179–186, 1979.

[21] J. Brezin. Geometry and the method of Kirillov. In J. Carmona, J. Dixmier, and M. Vergne, editors, *Non-Commutative Harmonic Analysis*, volume 466 of *Lecture Notes in Math.*, pages 13–25. Springer-Verlag, Berlin, Heidelberg, New York, London, Paris, Tokyo, Hong Kong, 1975.

[22] C.D. Cantrell, V.S. Letokhov, and A.A. Makarov. Coherent excitation of multilevel systems by laser light. In M.S. Feld and V.S. Letokhov, editors, *Coherent Nonlinear Optics*, pages 165–269. Springer-Verlag, Berlin, Heidelberg, New York, London, Paris, Tokyo, Hong Kong, 1980.

[23] P. Cartier. Quantum mechanical commutation relations and theta functions. In A. Borel and G.D. Mostow, editors, *Algebraic Groups and Discontinuous Subgroups*. pages 361–383, Providence, RI, 1966. Symp. in Pure Math. 9, Amer. Math. Soc.

[24] H.J. Caulfield and G. Gheen, editors. *Optical Computing*. SPIE Optical Engineering Press, Bellingham, WA, 1989.

[25] H. Chen, R.R. Hershey, and E.N. Leith. Diffractive optics with incoherent optical systems. In Ivan Cindrich, editor, *Holographic Optics: Design and Applications*, volume 883, pages 147–154. SPIE, 1988.

[26] T.W. Cole. Fourier theory in modern imaging. In J.F. Price, editor, *Fourier Techniques and Applications*, pages 185–199. Plenum Press, New York and London, 1985.

[27] G.D. Collins. *Temporally and spatially incoherent methods for Fourier transform holography and optical information processing*. PhD thesis, University of Michigan, Ann Arbor, MI, 1983.

[28] R.M.J. Cotterill. The brain: An intriguing piece of condensed matter. *Physica Scripta*, T 13:161–168, 1986.

[29] R.M.J. Cotterill. A possible role for coherence in neural networks. In R.M.J. Cotterill, editor, *Computer Simulation in Brain Science*, pages 164–188. Cambridge University Press, Cambridge, U.K., 1988.

[30] A. Cunha and E.N. Leith. One-way phase conjugation with partially coherent light and superresolution. *Opt. Lett.*, 13:1105–1107, 1988.

[31] A. Cunha and E.N. Leith. Generalized one-way phase conjugation systems. *J. Optical Society of America A*, B 6:1803–1812, 1989.

[32] L.J. Cutrona, E.N. Leith, C.J. Palermo, and L.J. Porcello. Optical data processing and filtering systems. *Trans. IRE*, IT-6:386–400, 1960.

[33] L.J. Cutrona, E.N. Leith, L.J. Porcello, and W.E. Vivian. On the application of coherent optical processing techniques to synthetic-aperture radar. *Proc. IEEE*, 54:1026–1032, 1966.

[34] C. Darmet, J.P. Gauthier, and F. Gourd. Elliptic and almost hyperbolic symmetries for the Woodward ambiguity function. To appear.

[35] J.G. Daugman. Two-dimensional spectral analysis of cortical receptive field profiles. *Vision Res.*, 20:847–856, 1980.

[36] J.G. Daugman. Uncertainty relation for resolution in space, spatial frequency, and orientation optimized by two-dimensional visual cortical filters. *J. Optical Society of America A*, A/2:1160–1169, 1985.

[37] J.G. Daugman. Complete discrete 2-d Gabor transforms by neural networks for image analysis and compression. *IEEE Trans. Acoustics, Speech, Signal Processing*, T-ASSP 36:1169–1179, 1988.

[38] J.G. Daugman. Relaxation neural network for complete discrete 2-d Gabor transforms. In T. Russel Hsing, editor, *Visual Communications and Image Processing'88*, number 1001 in Proc. SPIE, pages 1048–1061. SPIE, 1988.

[39] J.G. Daugman. Entropy reduction and decorrelation in visual cortex by oriented neural receptive fields. *IEEE Trans. Biomedical Eng.*, T-BME 36:107–114, 1989.

[40] D.L. Donoho and P.B. Stark. Uncertainty principles and signal recovery. *SIAM J. of Applied Math.*, 49:906–931, 1989.

[41] J.E. Dowling. *The Retina: An Approachable Part of the Brain*. The Belknap Press of Harvard University Press, Cambridge, MA and London, 1987.

[42] J.C. Eccles. New light on the mind-brain problem: How mental events could influence neural events. In H. Haken, editor, *Complex Systems: Operational Approaches*, pages 81–106. Springer-Verlag, Berlin, Heidelberg, New York, London, Paris, Tokyo, Hong Kong, 1985.

[43] J.C. Eccles. *Evolution of the Brain: Creation of the Self*. Routledge, London and New York, 1989.

[44] E. Elachi, T. Bicknell, R.L. Jordan, and C. Wu. Spaceborne synthetic-aperture imaging radars: Applications, techniques, and technology. *Proc. IEEE*, 70:1174–1209, 1982.

[45] N.H. Farhat, C.L. Werner, and T.H. Chu. Prospects for three-dimensional projective and tomographic imaging radar networks. *Radio Science*, 19:1347–1355, 1984.

[46] G.W. Farnell. Measured phase distribution in the image space of a microwave lens. *Can. J. Phys.*, 36:935–943, 1958.

[47] E.J. Farrell. An introduction to matching polynomials. *J. Combinat. Theory*, B 27:75–86, 1979.

[48] E. Feig and C.A. Micchelli. L^2-synthesis by ambiguity functions. In C.K. Chui, W. Schempp, and K. Zeller, editors, *Multivariate Approximation Theory IV*, pages 143–156. Birkhäuser Verlag, Basel, Boston, Berlin, 1989.

[49] J. Feinberg. Optical phase conjugation in photorefractive materials. In R.A. Fisher, editor, *Optical Phase Conjugation*, pages 417–463. Academic Press, Orlando, San Diego, New York, Austin, Boston, London, Sydney, Tokyo, Toronto, 1983.

[50] J. Feinberg. Applications of real-time holography. In Lloyd Huff, editor, *Holography*, volume 532, pages 119–135. SPIE, 1985.

[51] D.I. Feinstein. The hexagonal resistive network and the circular approximation. Technical Report Caltech-CS-TR-88-7, California Institute of Technology, Pasadena, CA, 1988.

[52] D.G. Feitelson. *Optical Computing*. MIT Press, Cambridge, Mass., London, 1988.

[53] M.R. Feldman and C.C. Guest. Holograms for optical interconnects for very large scale integrated circuits fabricated by electron-beam lithography. *Opt. Eng.*, 28:915–921, 1989.

[54] R. Felix. When is a Kirillov orbit a linear variety? *Proc. Amer. Math. Soc.*, 86:151–152, 1982.

[55] J.P. Fitch. *Synthetic Aperture Radar*. Springer-Verlag, Berlin, Heidelberg, New York, London, Paris, Tokyo, Hong Kong, 1988.

[56] G.B. Folland. Harmonic analysis in phase space. *Annals of Mathematics Studies*, 122, 1989.

[57] D. Gabor. Theory of communication. *J. Inst. Elec. Eng.*, 93:429–457, 1946.

[58] D. Gabor. Associative holographic memories. *IBM J. Res. Develop.*, 13:156–159, 1969.

[59] I. Gertner and R. Tolimieri. The group theoretic approach to image representation. *J. Visual Communication and Image Representation*, 1:67–82, 1990.

[60] C.D. Godsil and I. Gutman. On the theory of the matching polynomial. *J. Graph Theory*, 5:137–144, 1981.

[61] J.W. Goodman. Optics as an interconnect technology. In H.H. Arsenault, T. Szoplik, and B. Macukow, editors, *Optical Processing and Computing*, pages 1–32. Academic Press, Orlando, San Diego, New York, Austin, Boston, London, Sydney, Tokyo, Toronto, 1989.

[62] J.W. Goodman. A short history of the field of optical computing. In B.S. Wherett and F.A.P. Tooley, editors, *Optical Computing*, pages 7–21. Scottish Universities Summer School in Physics Publications, Edinburgh, 1989.

[63] P. Greguss. Manifestation of Gabor's holographic principle in various evolutionary stages of living material. In Jingtang Ke and Ryszard J. Pryputniewicz, editors, *International Conference on Holography Applications*, volume 673, pages 402–411. SPIE, 1987.

[64] P. Greguss. Nature and the holographic principle. In G. von Bally, editor, *Optics in Life Sciences*. Springer-Verlag, Berlin, Heidelberg, New York, London, Paris, Tokyo, Hong Kong, To appear.

[65] A. Grossmann and J. Morlet. Decomposition of functions into wavelets of constant shape, and related transforms. In L. Streit, editor, *Mathematics and Physics: Lectures on Recent Results*, volume 11, pages 135–165. World Scientific, Singapore, Philadelphia, 1985.

[66] J. Harrison. An introduction to fractals. In R.L. Devaney and L. Keen, editors, *Chaos and Fractals*, number 39 in Proc. Symp. in Appl. Math., pages 107–126, Providence, RI, 1989. American Mathematical Society.

[67] M.J. Hayford. Holographic optical design using CODE V. In Ivan Cindrich, editor, *Holographic Optics: Design and Applications*, volume 883, pages 2–7. SPIE, 1988.

[68] C. Heil and D. Walnut. Gabor and wavelet expansions. In J.S. Byrnes and Jennifer L. Byrnes, editors, *Recent Advances in Fourier Analysis and its Applications: Proceedings of the NATO Advanced Study Institute*, volume 315 of *NATO ASI series C: Mathematical and physical sciences*, pages 441–454, Dordrecht, Boston, London, 1990. Kluwer Academic Publishers Group. Held at Il Ciocco Resort, Tuscany, Italy.

[69] W. Heisenberg. *Physikalische Prinzipien der Quantenmechanik.* BI-Wissenschaftsverlag, Mannheim, Wien, Zürich, 1958.

[70] J.R. Higgins. Five short stories about the cardinal series. *Bull. (New Series) AMS,* 12:45–89, 1985.

[71] J. Hilgevoord and J. Uffink. A new view on the uncertainty principle. International School of History of Science, Second Course: *Sixty-Two Years of Uncertainty: Historical Philosophical and Physical Inquiries into the Foundations of Quantum Mechanics,* 1989. Erice, Sicily.

[72] J. Hilgevoord and J.B.M. Uffink. The mathematical expression of the uncertainty principle. In A. van der Merwe, F. Selleri, and G. Tarozzi, editors, *Microphysical Reality and Quantum Formalism,* pages 91–114. Kluwer Academic Publishers Group, Dordrecht, Boston, London, 1988.

[73] J. Hirsch and R. Hylton. Limits of spatial-frequency discrimination as evidence of neural interpolation. *J. Optical Society of America A,* 72:1367–1374, 1982.

[74] J. Hirsch and R. Hylton. Orientation dependence of visual hyperacuity contains a component with hexagonal symmetry. *J. Optical Society of America A,* A/1:300–308, 1984.

[75] J. Hirsch and R. Hylton. Quality of the primate photoreceptor lattice and limits of spatial vision. *Vision Res.,* 24:347–355, 1984.

[76] R.B. Holmes. Mathematical foundations of signal processing, ii: The role of group theory. Technical Report 781, Massachusetts Institute of Technology, Lincoln Laboratory, Lexington, MA, 1987.

[77] H. Hosoya. Matching and symmetry of graphs. *Comp. and Maths. with Appls.,* 12 B:271–290, 1986.

[78] R. Howe. Dual pairs in physics: Harmonic oscillators, photons, electrons, and singletons. In M. Flato, P. Sally, and G. Zuckerman, editors, *Applications of Group Theory in Physics and Mathematical Physics,* pages 179–207. American Mathematical Society, Providence, RI, 1985.

[79] A. Huang. Towards a digital optics platform. In F. Lanzl, H.-J. Preuss, and G. Weigelt, editors, *Optics in Complex Systems,* volume 1319 of *Proc. SPIE,* pages 156–160. SPIE, 1990.

[80] D.M. Hunten, L. Colin, T.M. Donahue, and V.I. Moroz. *Venus.* University of Arizona Press, Tucson, AZ, 1983.

[81] J. Jahns. Planar packaging of complex optical systems. In F. Lanzl, H.-J. Preuss, and G. Weigelt, editors, *Optics in Complex Systems,* volume 1319 of *Proc. SPIE,* pages 681–682. SPIE, 1990.

[82] J. Jahns, M.M. Downs, M.E. Prise, N. Streibl, and S.J. Walker. Dammann gratings for laser beam shaping. *Opt. Eng.*, 28:1267–1275, 1989.

[83] J.L. Jewell, Y.H. Lee, A. Scherer, S.L. McCall, N.A. Olsson, J.P. Harbison, and L.T. Florez. Surface-emitting microlasers for photonic switching and interchip connections. *Opt. Eng.*, pages 210–214, 1990.

[84] J.P. Jones and L.A. Palmer. An evaluation of the two-dimensional Gabor filter model of simple receptive fields in cat striate cortex. *J. Neurophysiology*, 58:1233–1258, 1987.

[85] J.P. Jones and L.A. Palmer. The two-dimensional spatial structure of simple receptive fields in cat striate cortex. *J. Neurophysiology*, 58:1187–1211, 1987.

[86] J.P. Jones, A. Stepnoski, and L.A. Palmer. The two-dimensional spectral structure of simple receptive fields in cat striate cortex. *J. Neurophysiology*, 58:1212–1232, 1987.

[87] F. Kiamilev, S.C. Esener, R. Paturi, Y. Fainman, P. Mercier, C.C. Guest, and S.H. Lee. Programmable optoelectronic multiprocessors and their comparison with symbolic substitution for digital optical computing. *Opt. Eng.*, 28:396–409, 1989.

[88] M. King. Fourier optics and radar signal processing. In H. Stark, editor, *Applications of Optical Fourier Transforms*, pages 209–251. Academic Press, Orlando, San Diego, New York, Austin, Boston, London, Sydney, Tokyo, Toronto, 1982.

[89] V.P. Koronkevich. Computer synthesis of diffraction optical elements. In H.H. A. Genault, T. Szoplik, and B. Macukow, editors, *Optical Processing and Computing*, pages 277–313. Academic Press, Orlando, San Diego, New York, Austin, Boston, London, Sydney, Tokyo, Toronto, 1989.

[90] A. Kozma, E.N. Leith, and N.G. Massey. Tilted-plane optical processor. *Appl. Opt.*, 11:1766–1777, 1972.

[91] R.E. Kronauer and Y.Y. Zeevi. Reorganization and diversification of signals in vision. *IEEE Trans. Systems, Man, and Cybernetics*, SMC-15:91–101, 1985.

[92] J. Lazzaro and C.A. Mead. A silicon model of auditory localization. *Neural Computation*, 1:47–57, 1989.

[93] E.N. Leith. Quasi-holographic techniques in the microwave region. *Proc. IEEE*, 59:1305–1318, 1971.

[94] E.N. Leith. Synthetic aperature radar. In D. Casasent, editor, *Optical Data Processing*, pages 89–117. Springer-Verlag, Berlin, Heidelberg, New York, London, Paris, Tokyo, Hong Kong, 1978.

[95] E.N. Leith. Incoherent optical processing and holography. In H.H. Arsenault, T. Szoplik, and B. Macukow, editors, *Optical Processing and Computing*, pages 421–440. Academic Press, Orlando, San Diego, New York, Austin, Boston, London, Sydney, Tokyo, Toronto, 1989.

[96] E.N. Leith. Fundamentals of modern holography. In *Annual International Symposium on Optical and Optoelectronic Applied Science and Engineering*, San Diego, CA, 1990. SPIE.

[97] E.N. Leith and D.K. Angell. Generalization of some incoherent spatial filtering techniques. *Appl. Opt.*, 25:499–502, 1986.

[98] E.N. Leith and A. Cunha. Holographic methods for imaging through an inhomogeneity. *Opt. Eng.*, 28:574–579, 1989.

[99] E.N. Leith and A.L. Inglis. Synthetic antenna data processing by wavefront reconstruction. *Appl. Opt.*, 7:539–544, 1968.

[100] E.N. Leith and C.-P. Kuei. Interferometric method for imaging through inhomogeneities. *Opt. Lett.*, 12:149–151, 1987.

[101] E.N. Leith and J. Upatnieks. Reconstructed wavefronts and communication theory. *J. Opt. Soc. Amer.*, 52:1123–1130, 1962.

[102] E.N. Leith and J. Upatnieks. Holography with achromatic-fringe systems. *J. Opt. Soc. Amer.*, 57:975–980, 1967.

[103] A.L. Lentine, H.S. Hinton, D.A.B. Miller, J.E. Henry, J.E. Cunningham, and L.M.F. Chirovsky. Symmetric self-electro-optic effect device: Optical set-reset latch. *Appl. Phys. Lett.*, 52:1419–1421, 1988.

[104] H. Lichte. Electron holography approaching atomic resolution. *Ultramicroscopy*, 20:293–304, 1986.

[105] E.H. Linfoot and E. Wolf. Phase distribution near focus in an aberration-free diffraction image. *Proc. Phys. Soc.*, B 69:823–832, 1956.

[106] R. Linsker. From basic network principles to neural architecture: Emergence of orientation-selective cells. *Proc. Natl. Acad. Sci. USA*, 83:8390–8394, 1986.

[107] R. Linsker. From basic network principles to neural architecture: Emergence of orientation columns. *Proc. Natl. Acad. Sci. USA*, 83:8779–8783, 1986.

[108] R. Linsker. From basic network principles to neural architecture: Emergence of spatial-opponent cells. *Proc. Natl. Acad. Sci. USA*, 83:7508–7512, 1986.

[109] R. Linsker. Development of feature-analyzing cells and their columnar organization in a layered self-adaptive network. In R.M.J. Cotterill, editor, *Computer Simulation in Brain Science*, pages 416–431. Cambridge University Press, Cambridge, U.K., 1988.

[110] R. Linsker. Self-organization in a perceptual network. *Computer*, 21:105–117, 1988.

[111] S. Marčelja. Mathematical description of the responses of simple cortical cells. *J. Opt. Soc. Amer.*, 70:1297–1300, 1980.

[112] W. Martienssen. Experiments on single photons. In *15th Congress of the International Commission for Optics: Optics in Complex Systems*. International Commission for Optics, Garmisch-Partenkirchen, 1990.

[113] B.R. Masters. Fractal analysis of human retinal blood vessel patterns: Developmental and diagnostic aspects. In B.R. Masters, editor, *Noninvasive Diagnostic Techniques in Opthalmology*, pages 515–527. Springer-Verlag, Berlin, Heidelberg, New York, London, Paris, Tokyo, Hong Kong, 1990.

[114] F.B. McCormick. Generation of large spot arrays from single laser beam by multiple imaging with binary phase gratings. *Opt. Eng.*, 28:299–304, 1989.

[115] C. Mead. *Analog VLSI and Neural Systems*. Addison-Wesley, Reading, MA, 1989.

[116] C. Mead and M. Ismail. *Analog VLSI Implementation of Neural Systems*. Kluwer Academic Publishers Group, Dordrecht, Boston, London, 1989.

[117] C.A. Mead and M.A. Mahowald. A silicon model of early visual processing. *Neural Networks*, 1:91–97, 1988.

[118] Y. Meyer. Principe d'incertitude, bases hilbertiennes et algèbres d'opérateurs, 1987.

[119] C.C. Moore and J.A. Wolf. Square integrable representations of nilpotent groups. *Trans. Amer. Math. Soc.*, 185:445–462, 1973.

[120] H. Moscovici. Coherent state representations of nilpotent lie groups. *Commun. Math Phys.*, 54:63–68, 1977.

[121] D.C. Munson, J.D. O'Brien, and W.K. Jenkins. A tomographic formulation of spotlight-mode synthetic aperture radar. *Proc. IEEE*, 71:917–925, 1983.

[122] H.L. Naparst. *Radar signal choice and processing for a dense target environment*. PhD thesis, University of California, Berkeley, CA, 1988.

[123] R. Nobili. Schrödinger wave holography in brain cortex. *Phys. Rev.*, 32:3618–3626, 1985.

[124] J. Ohta, M. Takahashi, Y. Nitta, S. Tai, K. Mitsunaga, and K. Kjuma. A new approach to a GaAs/AlGaAs optical neurochip with three layered structure. In *Proc. IJCNN International Joint Conference on Neural Networks*, volume II, pages 477–482, 1989.

[125] M. Ould-Beziou. PhD thesis, Université d'Orléans, 1989.

[126] Y. Owechko. Optoelectronic resonator neural networks. *Appl. Opt.*, 26:5104–5114, 1987. Also in [24], pp. 577–584.

[127] Y. Owechko. Holographic associative memories. In Uzi Efron, editor, *Spatial Light Modulators and Applications III*, volume 1150 of *Critical Reviews of Optical Science and Technology*, pages 164–176. SPIE, 1990.

[128] Y. Owechko, G.J. Dunning, E. Marom, and B.H. Soffer. Holographic associative memory with nonlinearities in the correlation domain. *Appl. Opt.*, 25:1900–1910, 1987. Also in [24], pp. 566–576.

[129] Y. Owechko, E. Marom, B.H. Soffer, and G. Dunning. Associative memory in a phase conjugate resonator cavity utilizing a hologram. In J. Shamir, A.A. Friesem, and E. Marom, editors, *Proc. SPIE*, volume 700, pages 296–300. IOCC-1986 International Optical Computing Conference, 1986.

[130] E.G. Paek, J.R. Wullert II, M. Jain, A. Von Lehmen, A. Scherer, J.Harbison, L.T. Florez, H.J. Yoo, J.L. Jewel, and Y.H. Lee. Compact and ultrafast holographic memory using a surface-emitting microlaser diode array. *Opt. Lett.*, 15:341–343, 1990.

[131] E.G. Paek, J.R. Wullert II, A. Von Lehmen, J.S. Patel, M. Jain, A. Scherer, J. Harbison, L.T. Florez, H.J. Yoo, and R. Martin. Implementation of neural network models by using coherent optics. In Uzi Efron, editor, *Spatial Light Modulators and Applications III*, volume 1150 of *Critical Reviews of Optical Science and Technology*, pages 192–203. SPIE, 1990.

[132] J.C. Pearson, L.H. Finkel, and G.M. Edelman. Plasticity in the organization of adult cerebral cortical maps: A computer simulation based on neuronal group selection. *J. Neurosci.*, 7:4209–4223, 1987.

[133] D.M. Pepper. Nonlinear optical phase conjugation. *Opt. Eng.*, 21:156–183, 1982.

[134] A. Peremolov. *Generalized Coherent States and Their Applications.* Springer-Verlag, Berlin, Heidelberg, New York, London, Paris, Tokyo, Hong Kong, 1986.

[135] R.L. Pfleegor and L. Mandel. Interference effects at the single photon level. *Phys. Lett.*, 24 A:766–767, 1967.

[136] J. Phillips. A note on square-integrable representations. *J. Functional Analysis*, 20:83–92, 1975.

[137] D.A. Pollen and S.F. Ronner. Phase relationships between adjacent simple cells in the visual cortex. *Science*, 212:1409–1411, 1981.

[138] K.H. Pribram, M. Nuwer, and R.J. Baron. The holographic hypothesis of memory structure in brain function and perception. In D.H. Krantz, R.C. Atkinson, R.D. Luce, and P. Suppes, editors, *Measurement, Psychophysics, and Neural Information Processing*, volume II of *Contemporary Developments in Mathematical Psychology*, pages 416–457. W.H. Freeman, San Francisco, New York, 1974.

[139] J.F. Price. Uncertainty principles and interference patterns. *Proc. Centre for Mathematical Analysis of the Australian National University*, 9:241–258, 1985.

[140] J.F. Price. Uncertainty principles and sampling theorems. In J.F. Price, editor, *Fourier Techniques and Applications*, pages 25–44. Plenum Press, New York and London, 1985.

[141] J.F. Price and A. Sitaram. Local uncertainty inequalities for locally compact groups. *Trans. Amer. Math. Soc.*, 308:105–114, 1988.

[142] D. Psaltis. Two-dimensional optical processing using one-dimensional input devices. *Proc. IEEE*, 72:962–974, 1984.

[143] D. Psaltis, D. Brady, X. Gu, and K. Hsu. Optical implementation of neural computers. In H.H. Arsenault, T. Szoplik, and B. Macukow, editors, *Optical Processing and Computing*, pages 251–276. Academic Press, Orlando, San Diego, New York, Austin, Boston, London, Sydney, Tokyo, Toronto, 1989.

[144] D. Psaltis, D. Brady, and K. Wagner. Adaptive optical networks using photorefractive crystals. *Appl. Opt.*, 27:1752–1759, 1988. Also in [24], pp. 603–610.

[145] D. Psaltis and N. Farhat. Optical information processing based on an associative-memory model of neural nets with thresholding and feedback. *Opt. Lett.*, 10:98–100, 1985. Also in [24], pp. 515–517.

[146] D. Psaltis, C.H. Park, and J. Hong. Higher order associative memories and their optical implementations. *Neural Networks*, 1:149–163, 1988.

[147] G. Ries. Rotationssymmetrische radar ambiguityfunktion. Manuskript, Lehrstuhl für Elektrotechnik VIII-Hochfrequenztechnik, Universität Siegen, 1989.

[148] B. Roberts, M.R. Taghizadeh, J. Turunen, and A. Vasara. Fabrication of space invariant fanout components in dichromatic gelatin. *Appl. Opt.*, 29:1134–1141, 1990.

[149] H.P. Robertson. The uncertainty principle. *Phys. Rev.*, 34:163–164, 1929.

[150] W. Schempp. Holographic fractals. To appear.

[151] W. Schempp. Phase anomalies in optical neural networks. To appear.

[152] W. Schempp. Gruppentheoretische aspekte der signalübertragung und der kardinalen interpolationssplines I. *Math. Meth. in the Appl. Sci.*, 5:195–215, 1983.

[153] W. Schempp. Radar ambiguity functions, the Heisenberg group, and holomorphic theta series. *P. ɔc. Amer. Math. Soc.*, 92:103–110, 1984.

[154] W. Schempp. Group theoretical methods in approximation theory, elementary number theory, and computational signal geometry. *J. Approx. Th.*, V:129–171, 1986.

[155] W. Schempp. Harmonic analysis on the Heisenberg nilpotent Lie group, with applications to signal theory. *Pitman Research Notes in Math.*, 147, 1986. Second edition under preparation.

[156] W. Schempp. Elementary holograms and 3-orbifolds. *C.R. Math. Rep. Acad. Sci. Canada*, 10:155–160, 1988.

[157] W. Schempp. Holographic grids. In T. Russel Hsing, editor, *Visual Communications and Image Processing'88*, number 1001 in Proc. SPIE, pages 116–120. SPIE, 1988.

[158] W. Schempp. The holographic transform. In G.V. Milovanovič, editor, *Numerical Methods and Approximation Theory*, volume III, pages 67–91. University of Niš, Niš, 1988.

[159] W. Schempp. The oscillator representation of the metaplectic group applied to quantum electronics and computerized tomography. In S. Albeverio, Ph. Blanchard, M. Hazewinkel, and L. Streit, editors, *Stochastic Processes in Physics and Engineering*, pages 305–344. D. Reidel, Dordrecht, Boston, Lancaster, Tokyo, 1988.

[160] W. Schempp. Extensions of the Heisenberg group and coaxial coupling of transverse eigenmodes. *Rocky Mountain J. Math.*, pages 383–394, 1989.

[161] W. Schempp. Holographic image processing, coherent optical computing, and neural computer architecture for pattern recognition. In K.B. Wolf, editor, *Lie Methods in Optics II*, volume 352 of *Lecture Notes in Physics*, pages 19–45. Springer-Verlag, Berlin, Heidelberg, New York, London, Paris, Tokyo, Hong Kong, 1989.

[162] W. Schempp. Neurocomputer architectures. *Results in Math.*, 16:345–382, 1989.

[163] D. Schreier. *Synthetische Holografie*. Fachbuchverlag, Leipzig, 1984.

[164] E.A. Schwartz. Phototransduction in vertebrate rods. *Annual. Rev. Neurosci.*, 8:339–367, 1985.

[165] I.E. Segal. Transforms for operators and symplectic automorphisms over locally compact abelian groups. *Math. Scand.*, 13:31–43, 1963.

[166] J. Shamir, H.J. Caulfield, and R.B. Johnson. Massive holographic interconnection networks and their limitations. *Appl. Opt.*, 28:311–324, 1989. Also in [24], pp. 546–559.

[167] A. Shimony. Recent quantum-mechanically significant optical experiments. In *Fundamental Aspects of Quantum Theory*, University of South Carolina, Columbia, SC, 1989. Conference on Foundations of Quantum Mechanics to Celebrate 30 Years of the Aharanov-Bohm Effect.

[168] D.S. Shucker. Square integrable representations of unimodular groups. *Proc. Amer. Math. Soc.*, 89:169–172, 1983.

[169] B.H. Soffer, G.J. Dunning, Y. Owechko, and E. Marom. Associative holographic memory with feedback using phase-conjugate mirrors. *Opt. Lett.*, 11:118–120, 1986.

[170] B.H. Soffer, Y. Owechko, and G.J. Dunning. A photorefractive optical neural network. In F. Lanzl, H.-J. Preuss, and G. Weigelt, editors, *Optics in Complex Systems*, volume 1319 of *Proc. SPIE*, pages 196–197. SPIE, 1990.

[171] C.T. Stansberg. Surface roughness measurements by means of polychromatic speckle patterns. *Appl. Opt.*, 18:4051–4060, 1979.

[172] C.T. Stansberg. On the first-order probability density function of integrated laser speckle. *Optica Acta*, 28:917–932, 1981.

[173] N. Streibl. Beam shaping with optical array generators. *J. Mod. Opt.*, 36:1559–1573, 1989.

[174] R.S. Strichartz. Sub-Riemannian geometry. *J. Diff. Geom.*, 24:221–263, 1986.

[175] G.J. Swanson. Binary optics technology: The theory and design of multi-level diffractive optical elements. Technical Report 854, Massachusetts Institute of Technology, Lincoln Laboratory, Lexington, MA, 1989.

[176] G.J. Swanson and W.B. Veldkamp. Diffractive optical elements for use in infrared systems. *Opt. Eng.*, 28:605–608, 1989.

[177] J.A. Titleer. Elementary quantum phenomenon as building unit. In P. Meystre and M.O. Scully, editors, *Quantum Optics, Experimental Gravity, and Measurement Theory*, pages 141–143. Plenum Press, New York and London, 1983.

[178] H.J. Tiziani. Real-time meteorology with bso crystals. *Optica Acta*, 29:463–470, 1982.

[179] A. Tonomura. Applications of electron holography. *Rev. Mod. Phys.*, 59.639–669, 1987.

[180] J. Uffink and J. Hilgevoord. Interference and distinguishability in quantum mechanics. *Physica*, B 151:309–313, 1988.

[181] J.B.M. Uffink and J. Hilgevoord. New bounds for the uncertainty principle. *Phys. Lett.*, 105 A:176–178, 1984.

[182] J. Uozumi, H. Kimura, and T. Asakura. Fraunhofer diffraction by Koch fractals. *J. Mod. Opt.*, 37:1011–1031, 1990.

[183] J. Uozumi, H. Kimura, and T. Asakura. Optical diffraction by regular and random Koch fractals. In F. Lanzl, H.-J. Preuss, and G. Weigelt, editors, *Optics in Complex Systems*, volume 1319 of *Proc. SPIE*, pages 11–12. SPIE, 1990.

[184] J.C. Várilly, J.M. Gracia-Bondía, and W. Schempp. The Moyal representation of quantum mechanics and special function theory. *Acta Applicandae Math.*, 11:225–250, 1990.

[185] W.B. Veldkamp, J.R. Leger, and G.J. Swanson. Coherent summation of laser beams using binary phase gratings. *Opt. Lett.*, 11:303–305, 1986.

[186] Jr. W. Miller. *Topics in Harmonic Analysis with Applications to Radar and Sonar.* Number 657 in Lecture Notes in Radar/Sonar. IMA Preprint Series, Minneapolis, MN, 1990.

[187] A. Weil. Sur certains groupes d'opérateurs unitaires. *Acta Math*, 111:143–211, 1964. Also in [188], pp. 1–69.

[188] A. Weil. *Collected Papers*, volume III. Springer-Verlag, Berlin, Heidelberg, New York, London, Paris, Tokyo, Hong Kong, 1980.

[189] N. Weste and K. Eshraghian. *Principles of CMOS VLSI Design*. Addison-Wesley, Reading, MA, 1985.

[190] J.A. Wheeler. The "past" and the "delayed-choice" double-slit experiment. In A.R. Marlow, editor, *Mathematical Foundations of Quantum Theory*, pages 9–48. Academic Press, Orlando, San Diego, New York, Austin, Boston, London, Sydney, Tokyo, Toronto, 1978.

[191] J.A. Wheeler. Frontiers of time. In G. Toraldo di Francia, editor, *Problems in the Foundations of Physics*, pages 395–497. Inter. School of Physics "Enrico Fermi", North Holland-Elsevier Science Publishers, 1979.

[192] J.A. Wheeler. Beyond the black hole. In H. Woolf, editor, *Some Strangeness in the Proportion: A Centennial Symposium to Celebrate the Achievements of Albert Einstein*, pages 341–375, Reading, MA, 1980. Addison-Wesley.

[193] J.A. Wheeler. The computer and the universe. *Int. J. Theor. Phys.*, 21:557–572, 1982.

[194] J.A. Wheeler. Particles and geometry. In *Unified Theories of Elementary Particles*, volume 160 of *Lecture Notes in Phys.*, pages 189–217, Berlin, Heidelberg, New York, London, Paris, Tokyo, Hong Kong, 1982. Heisenberg Symposium, Springer-Verlag.

[195] J.A. Wheeler. Law without law. In Wheeler and Zurek [196], pages 182–213.

[196] J.A. Wheeler and W.H. Zurek, editors. *Quantum Theory and Measurement*. Princeton University Press, Princeton, 1983.

[197] K. Wilber. *Das holographische Weltbild*. Scherz Verlag, Bern, München, Wien, 1986.

[198] R. Wilson and G.H. Granlund. The uncertainty principle in image processing. *IEEE Trans. on Pattern Anal. and Machine Intel.*, 6:758–767, 1984.

[199] W.K. Wooters and W.H. Zurek. Complementarity in the double-slit experiment: Quantum nonseparability and a quantitative statement of Bohr's principle. *Phys. Rev.*, D 19:473–484, 1979. Also in [196], pp. 443–454.

[200] A. Yariv. Phase conjugate optics and real-time holography. *IEEE J. Quantum Electronics*, QE 14:650–660, 1978.

[201] T. Yatagai. Cellular logic architectures for optical computers. *Appl. Opt.*, 25:1571–1577, 1986.

[202] J.A. Yeazell and C.R. Stroud. Rydberg-atom wave packets localized in the angular variables. *Phys. Rev.*, A 35:2806–2809, 1987.

[203] J.A. Yeazell and C.R. Stroud. Observation of spatially localized atomic electron wave packets. *Phys. Rev. Lett.*, 60:1494–1497, 1988.

[204] A.L. Yuille, D.M. Kammen, and D.S. Cohen. Quadrature and the development of orientation selective cortical cells by Hebb rules. *Biological Cybernetics*, 61:183–194, 1989.

Random surface geometries with applications to image processing†

Daniel Keenan
Department of Mathematics
University of Virginia
Charlottesville, VA 22903 USA
dmk7b@virginia.bitnet

Abstract A procedure is introduced for incorporating into image processing methods a priori 3-dimensional geometrical information about shapes of objects of interest. The information is built in by way of probability measures on deformations of a polyhedral "template." In order to understand the regularity of the resulting deformations, one needs a theory about the continuum which consists of probability measures on analogous deformations of a smooth compact 2-dimensional manifold template. The theory is constructed via Gaussian measures on an enlargement of the space of triplets of exact one-forms of M, such that with probability 1 the deformations are continous (and have additional regularity). The triplets can be viewed as a "generalized differential map."

1. Introduction

One would like to be able to incorporate *a priori* 3-D geometrical information into current image processing methods. For example, can one build into the taking of chest X-rays information concerning the shape of human lungs or into angiography the shape of arteries so that the various calculations which are typically made, and which are geometrical in nature (e.g., curvatures, diameter of certain cross sections, enclosed volume, surface area, etc.), can be automated and made less subjective?

In [2, 3, 1], the approach taken to incorporate geometrical information is that of a *deformable template*, where the template is an idealized prototype of the object of interest; for example, in the above, there would be lung and artery templates. The parameter space is viewed as having been created by the application of deformations to the template, very much in the spirit of having been swept out by a structure group. A *prior* probability measure

† Supported by Office of Naval Research Contract No. N00014-90-J-1007

J. S. Byrnes et al. (eds.), Probabilistic and Stochastic Methods in Analysis, with Applications, 469–477
© 1992 *Kluwer Academic Publishers. Printed in the Netherlands*

is then placed on such a space of deformations to describe the variations in form. The data is incorporated via a likelihood which describes the technology by which the images were acquired. The goal is the construction and justification of an algorithm for generating realizations from the posterior measure. When the template is a surface (in $\Re^3$) the realizations from the prior and posterior measures are "random surfaces."

In the above referenced works the templates were always polygons and polyhedra. In the present paper a model in the continuum is discussed; the necessity for such a construction is the result of such practical considerations as how to choose parameter values for the prior measure in order to obtain the desired regularity of the deformations.

What properties are important for an appropriate general formulation of deformations to a template? It seems quite reasonable to think of there first being a global similarity or affine transformation of the template which captures the location, orientation, and overall size, followed by local transformations which capture local structure. If M is the template and $\{f \in \mathcal{F}\}$ are the deformations, then the parameter space is:

$$\Theta = \{f(M),\ f \in \mathcal{F}\} \tag{1.1}$$

Ideally, one would like to have the parameter space characterized once one has specified the template M and several known functions defined on the template which would describe the allowable local variability/regularity mix; for example, these functions might specify that in certain regions of the template there will be little variability (i.e., the template is rather rigid there), whereas in other regions there might be much variability. Also, it is most important that the characterization of the deformations of the template be *constructive* in the sense that an operational procedure for actually constructing such deformations is available, as opposed to merely specifying an equivalence relationship; this is important from an algorithmic point of view.

In Section 2 a discrete (polyhedral) model is briefly described with the need for a theory in the continuum being suggested. In Section 3 a continuous theory is outlined, the full details being given in [5]. In the continuous model the template is a 2-dimensional submanifold M of $\Re^3$ and the above functions describing the variability/regularity mix (by which the deformations are created) are the coefficient functions of a second-order self-adjoint elliptic operator $\mathcal{L}$ on the one-forms of M. From $\mathcal{L}$ is constructed an operator Γ on an enlargement of the space of exact one-forms. In this paper $\mathcal{L}$ will be the Laplace-Beltrami operator on one forms. Triplets from this enlarged space can be thought of as identifying a "generalized differential map" from which the deformations are obtained by "integration"; in order to control the resulting geometry of the *deformed template* one must work at least at the differential level.

2. Polyhedral model

In the case of a polyhedral template the resulting geometry of the deformed polyhedral template is more naturally controlled by deforming edges rather than vertices. Heuristically speaking, the deformations will be constructed by first constructing their "differential maps." If P is a polyhedral template and $\{v_1, \ldots, v_m\}$ and $\{e_1, \ldots, e_n\}$ are, respectively, the vertices and edges of P, let matrices $(S_1, \ldots, S_n) \in [GL(3;\Re)]^n$ be "placed" on the n edges (S_i on edge i), vertex v_1 held fixed (for the moment). The matrices should be thought of as being "close" to the identity:

$$S_i = I + (S_i - I). \tag{2.1}$$

The S's are the discrete analogue of the differential map and the deformation f resulting from $(S_1, \ldots, S_n)$ being defined as: $v \in \{v_1, \ldots, v_n\}$.

$$f(v) = v_1 + \sum_{j=1}^{k} S_{i_j} e_{i_j} = v + \sum_{j=1}^{k} (S_{i_j} - I) e_{i_j} \tag{2.2}$$

where $\{e_{i_1}, \ldots, e_{i_k}\}$ is a path from v_1 to v. In order for this to make sense $f(v)$ must be independent of the path taken from v_1 to v. The independence of the path corresponds to the linear closure constraints imposed by the fixed edges of the polyhedral template. The parameter space in the polyhedral case is:

$$\Theta_n = \{f(P) \mid f \text{ created by (2.2)}, (S_1, \ldots, S_n) \in [GL(3)]^n, \text{ with path independence}\} \tag{2.3}$$

If the matrices S_i, $i = 1, \ldots, n$ were all the same matrix then we would be in the setting of the traditional geometries (Euclidean, Similarity, Affine groups); that is, Θ_n would be the orbit of figures equivalent (in the geometry) to the template. One only moves away from these traditional definitions of equivalence by allowing the matrices to be different on different edges. Loosely speaking, we will characterize *shapes via invariants not ordinarily* obtained by traditional geometries by judiciously "lumping" together orbits under traditional geometries.

Consider the following (simple) Gauss-Markov measure defined on $[GL(3)]^n$ via the density:

$$p(s_1, \ldots, s_n) \propto \prod_{(i_1, i_2)} \exp\left\{-\frac{1}{2\sigma^2}[\|s_{i_1} - I\|^2 - 2\rho(s_{i_1} - I, s_{i_2} - I) + \|s_{i_2} - I\|^2]\right\} \tag{2.4}$$

where the product is over all neighboring edges in the edge graph associated with the polyhedral template. There are just two parameters, ρ and σ. More precisely, we have a matrix-valued Gauss-Markov Random Field defined on

the edge graph associated with the polyhedral template. On closer examination the covariance structure of this measure is seen to be related to the Green's function for the discrete Laplacian on the edge graph. One must also condition on the S's, when applied to the fixed edges of the template, of producing deformed edges which "come back together"; these are the linear closure constraints which are equivalent to path independence. Conditioning the measure in expression (2.4) on these linear constraints, one obtains another Gaussian measure from which one can induce a measure on Θ_n; call it μ_n. The measure μ_n is our *prior* measure in the polyhedral case.

In practice one doesn't use just one polyhedral template but rather a sequence of polyhedral templates, allowing one to work at different scales; this sequence can be thought of as piecewise-flat approximations to a smooth manifold template M. As the polyhedral template approximations are refined, the covariance structure in expression (2.4) gets closer to (a function of) the inverse of the discrete Laplacian (on the edge graph) which one would suspect gets closer to the Green's function for the two-dimensional Laplacian, which because of its logarithmic singularity is only realizable as a covariance function on generalized functions. In our case the above covariance structure is for a measure on the "differential map" and not on the deformation itself, which would be obtained by an "integration." An important question is whether or not, in the continuum, the analogue of $f(\cdot)$ in expression (2.2) with the analogue of the above probability measure μ_n produces continuous deformations with probability one. This question is important because if one is to work at different scales it is crucial to know whether chaotic behaviour at a fine scale is due to an improper choice of parameters or to an inadequate theory (such as a certain probability measure only being realizable on generalized functions). In Section 3 it is shown that, in the continuum, the deformations are continuous (and more) with probability one.

What should be the analogue of the above discrete model in the continuum? If one thinks of the three rows of the matrices $(S_i - I)$, $i = 1, 2, \ldots, n$, in expression (2.1) as discrete versions of one-forms, then in expression (2.2), $f(\cdot)$ is created by "integrating" three one-forms over the path $\{e_{i_1}, \ldots, e_{i_k}\}$ from v_1 to v. The independence of the paths, which corresponds to the imposition of the linear closure constraints, is the discrete analogue of the one-forms being exact.

Consequently, a reasonable generalization of (2.1)–(2.4) would start with a smooth, compact, connected, oriented 2-dim submanifold M of $\mathfrak{R}^3$ as *template* with $B^1(M)$ being the exact one-forms of M. The matrices $(S_1, \ldots, S_n)$, $S_i = I + (S_i - I)$, $i = 1, \ldots, n$, the discrete analogue of a differential map, would be replaced by $(I + (\alpha_1, \alpha_2, \alpha_3))$, $\alpha_i \in B^1(M)$, $i = 1, 2, 3$. For $\alpha_i \in B^1(M)$, $i = 1, 2, 3$, and p_0 (fixed) $\in M$, define $f(\cdot)$ associated

with $(\alpha_1, \alpha_2, \alpha_3)$ as: $p \in M$

$$f(p) = p + \left(\int_{\gamma: p_0 \to p} \alpha_i(\gamma'(s))\, ds, \qquad i = 1,2,3 \right) \tag{2.5}$$

where γ is a path from p_0 to p in M. The parameter space Θ is thus:

$$\Theta = \{ f(M) \mid f \text{ created by (2.5)}, \alpha_i \in B^1(M),\ i = 1,2,3 \}. \tag{2.6}$$

One would first put a Gaussian measure on the space of one-forms with the covariance operator being the inverse of the Laplacian on one-forms, this is the analogue of the measure in expression (2.4). From this one would create the conditional measure, conditioning on the form being exact; this is the analogue of conditioning on the closure constraints. Finally, using this measure, one would induce a measure on the space Θ. Unfortunately, such measures cannot be realized on these spaces but only on "larger" spaces. In the next section we show that, probabilistically, this is inconsequential to our goal.

3. Smooth manifold template

Let (M, g) be a smooth, 2-dim compact, connected, oriented submanifold of $\mathfrak{R}^3$ where g is the Riemannian metric inherited from the dot product on $\mathfrak{R}^3$; M is our *template*. For the results presented in these proceedings the extrinsic geometry of M will not be exploited. Throughout this section all structure will be C^∞ unless otherwise specified. Let $\{U_\ell, \phi_\ell\}_{\ell=1}^N$ be a finite atlas on M with a subordinate partition of unity $\{U_\ell, h_\ell\}_{\ell=1}^N$. Let $\Lambda^{(k)}(M)$ be the k-forms on M, $k = 0, 1, 2$ and denote by $(\cdot,\cdot)_0^{(k)}$ the inner product:

$$(\alpha, \beta)_0^k = \int_M \alpha \wedge * \beta$$

where $\wedge$ and $*$ are the wedge and Hodge-star operators. The usual L^2 space is $\Lambda^{(k)}(M)$ completed with respect to $(\cdot,\cdot)_0^{(k)}$. Consider the family of norms $\{\rho_m^{(k)}\}_{m=0}^\infty$ on $\Lambda^{(k)}(M)$: $\alpha \in \Lambda^{(k)}(M)$

$$\rho_m^{(k)}(\alpha) = \sum_{\ell=1}^N \| \phi_{\ell,k}^* h_\ell \alpha \|_{m,k} \tag{3.1}$$

where $\phi_{\ell,k}^*$ is the induced map from $\Lambda^k(U_\ell)$ to the components of the form viewed as being defined on $\phi_\ell(U_\ell)$ and $\| \cdot \|_{m,k}$ is the usual Sobolev norm $\| \cdot \|_m$ on $D(\mathfrak{R}^2)$: $g \in D(\mathfrak{R}^2)$

$$\|g\|_m = \sum_{|\beta| \le m} \int_{\mathfrak{R}^2} |D^\beta g|^2\, dx$$

applied to the L(k) components of the k form, L(k) = 1 for k = 0 or 2 and L(1) = 2 (see [7] or [6]). It is shown in [4] that the family of separable Hilbertian norms $\{\rho_m^{(k)}\}_{m=0}^{\infty}$ determine the Schwartz topology $\tau^{(k)}$ on $\Lambda^{(k)}(M)$ and that the resulting countably Hilbertian space is nuclear.

Let $d^{(k)}$ and $\delta^{(k)}$ be the exterior derivative and boundary operator on $\{\Lambda^{(k)}(M),\ k = 0, 1, 2\}$ and define the Laplace-Beltrami operator as:

$$\Delta_{LB}^{(k)} = d^{(k-1)}\delta^{(k)} + \delta^{(k+1)}d^{(k)}$$

Let $B^{(k)}(M)$, $E^{(k)}(M)$, and $H^{(k)}(M)$ be respectively the exact, co-exact, and harmonic k-forms. The operator $\Delta_{LB}^{(k)}$ is invertible on $B^{(k)} \oplus E^{(k)}(M)$ and the inverse, denoted $\mathfrak{b}$, $\mathfrak{G}^{(k)}$, can be extended to $\Lambda^{(k)}(M)$ (w.r.t. L^2) by being set to zero on $H^{(k)}(M)$. Let $J^{(1)}$ be the projection in L^2 to the completion in L^2 of $B^1(M)$.

The full details for the following lemmas and theorem are given in [5].

Lemma 3.1. For the operator L given by

$$L = J^{(1)}G^{(1)}J^{(1)}$$

there exists an $m \geq 3$ such that the seminorm $p_L(\cdot)$:

$$p_L(\alpha) = (\alpha, L\alpha)_0^{(1)}$$

is the covariance functional for a mean zero Gaussian measure on $(\Lambda^{(1)}(M), \rho_m^{(1)})'$ concentrated on $(B^{(1)}(M), \rho_m^{(1)})'$, where $'$ denotes dual.

Remark 3.2. The measure in Lemma 3.1 is that obtained by first constructing a Gaussian measure on $(\Lambda^1(M), \rho_m^{(1)})'$ with covariance functional $p_G(\alpha) = (\alpha, G^{(1)}\alpha)_0^{(1)}$; the existence of $\rho_m^{(1)}$ and the Gaussian measure being the result of $G^{(1)}$ being continuous w.r.t. $\tau^{(1)}$ and known existence results [4]. The operator L is shown to be well-defined by using various results from the Hodge-DeRham Decomposition theory and various properties of G, δ and d. The operator L comes about because the condition $(I - d^{(0)}\delta^{(1)}G^{(1)})(\alpha) = 0$, $\alpha \in \Lambda^{(1)}(M)$, is equivalent to $\alpha \in B^{(1)}(M)$. The seminorm $\rho_L(\cdot)$ is shown to be Hilbert-Schmidt weaker than $\rho_m^{(1)}$. In [5] the conditioning is made precise. The measure in Lemma 3.1 is the "proper" realization of that suggested in Section 2: first obtain a Gaussian measure whose covariance operator is the inverse of the Laplacian on one forms, then condition on the form being exact.

Lemma 3.3. If $\eta = TM \times B^1(M) \to \mathfrak{R}$ is given by

$$\eta(p, Z_p)(\alpha) = \alpha_p(Z_p) \quad \alpha \in B^1(M),\ (p, Z_p) \in TM$$

and if $\{\gamma(s), 0 \leq s \leq t\}$ is a path in M, then the one parameter family $\{\eta(\gamma(s), \gamma'(s)), 0 \leq s \leq t\}$ is continuous in $(B^1(M), \rho_m^{(1)})'$.

Remark 3.4. Because of the nature of η, continuity in the dual space norm involves (a sup over) comparisons of one forms evaluated at different points of M; everything has to be parallel transported into the cotangent space at one point (that where continuity is to be shown, $\gamma(s)$). A Sobolev imbedding argument obtains boundedness of derivatives up to m ($m \geqslant 3$) for the components in local coordinates of α, $\rho_m^{(1)}(\alpha) \leqslant 1$. Using this boundedness, the continuity of the flow for parallel displacement, and the fact that the Levi-Civita connection is metric, the result is obtained.

Theorem 3.5. Let Y_i, $i = 1,2,3$ be independent Gaussian continuous linear random functionals from Lemma 3.1, extended to $\overline{(B^1(M), \rho_m^{(1)})}$, the completion w.r.t. $\rho_m^{(1)}$:

$$Y_i : \overline{(B^1(M), \rho_m^{(1)})} \to L^2(\Omega, A, P)$$

For $p \in M, \gamma = \{\gamma(s), 0 \leqslant s \leqslant t\}$ a path from p_o (fixed) to p, $\omega \in \Omega$

$$f(p,\omega) \stackrel{\text{def}}{=} p + \int_{\gamma: p_o \to p} Y_i(\eta(\gamma(s), \gamma'(s))(\omega)\, ds, \quad i = 1,2,3). \tag{3.2}$$

Then with probability one, $f(p,\omega)$ does not depend on the chosen path (for all p) and $f(\cdot,\omega) = M \to \mathfrak{R}^3$ is continuous. Defining $(Tf)(p,\omega) : T_pM \to T\mathbf{R}^3$ as:

$$(Tf)(p,\omega)(Z_p) \stackrel{\text{def}}{=} (f(p,\omega), Z_p + (Y_i(\eta(p, Z_p)(\omega), \quad i = 1,2,3) \tag{3.3}$$

then for $\{\xi(s), -\epsilon < s < \epsilon\}, \xi(0) = p, \xi'(0) = Z_p$

$$(Tf)(p,\cdot) = \lim_{s \to 0} \frac{f(\xi(s),\cdot) - f(\xi(0),\cdot)}{s} \tag{3.4}$$

the limit being in $L^2(\Omega, A, P)$ and w.p.1 (Tf) is a linear map for all $p \in M$ and

$$P[\omega | \nu[p] \dim\{Tf(p,\omega)(T_pM)\} \neq 2] = 0] = 1 \tag{3.5}$$

where ν is the volume element associated with g.

Remark 3.6. We will just give the flavor of the proof of the first part, expression (3.2); the other parts follow by similar arguments. Because of Lemma 3.3, the Cauchy-Bochner integral

$$\int_{\gamma: p_o \to p} \eta(\gamma(s), \gamma'(s))\, ds$$

is a well-defined element of $(B^1(M), \rho_m^{(1)})'$ and for $\alpha \in B^1(M)$

$$\left(\int_{\gamma: p_o \to p} \eta(\gamma(s), \gamma'(s))\, ds \right) \alpha = \int_{\gamma: p_o \to p} \alpha(\gamma'(s))\, ds$$

is independent of the path from p_0 to p. The integral in expression (3.2) is also a well-defined Cauchy-Bochner integral and the linearity of Y (between Banach spaces) results in the independence of the integral from the path chosen. Differences of integrals now reduce to integrals over "the path-difference of paths" which can be chosen to be a minimizing geodesic segment. Developing various bounds, one can eventually apply (a form of the) Kolmogorov continuous version theorem from which the continuity of $f(\cdot, \omega)$ follows. The other parts follow by similar arguments.

In the polyhedral model, there was a polyhedral template $\mathcal{P}$ and matrices $(S_1, \ldots, S_n)$, S_i "sitting" on edge i, where $S_i = I + (S_i - I)$ was designed to be a discrete analogue of a differential map. In the continuum the idea was to replace $\{S_i - I,\ i = 1, \ldots, n\}$ with a triplet of exact one forms. Expression (3.3) is the "proper" realization of this, where $(\alpha_1, \alpha_2, \alpha_3)$ is replaced by $\{(Y_i(\eta(p, Z_p)))(\omega),\ i = 1,2,3), p \in M\}$ for $\omega \in \Omega$. Expression (3.4) shows that (Tf), written in suggestive notation, acts (in an L^2 sense) much like a differential map. The deformations in the polyhedral model, expression (2.2), involved sums; in the continuum, the idea was to replace this with integrals of the triplets of exact one-forms, which, again, is properly realized by f in expression (3.2). The theorem shows that with probability one the image of M under f is continuous. One would like more regularity, at least locally. It would be impossible to rule out self-intersections, globally; it is hoped that the data would impose such consistencies. Ideally, one would like the images of M under f to be immersed submanifolds. Expression (3.5) can be thought of as a C^0 version of this. It says that with probability one the set of points $p(\in M)$ where the image of T_pM under (Tf) is not of full rank has volume measure zero.

4. Summary

In this paper both polyhedral and smooth manifold deformable template models were presented. The framework of Sections 2 and 3 will allow one to formulate and answer such questions, based upon observed noisy images, as how to construct good estimates of such geometrical entities as curvature and the location of its extrema, surface area, enclosed volume, and the diameter of a certain cross section of the object (or objects) in the images.

Also one should now be able to analyze how to choose and adapt (as $n \to \infty$) parameters for the sequence (in Section 2) of measures μ_n on the spaces $\Theta(\mathcal{P}^n)$, where $\mathcal{P}^n$ is the polyhedral template at refinement stage n, as $n \to \infty$, since in Section 3 for the smooth manifold template M we constructed $\Theta(M)$ and a measure μ (Theorem 3.5) which should be the "limits" of $\Theta(\mathcal{P}^n)$ and μ_n. Also it appears that the Laplace-Beltrami operator can be replaced by more general self-adjoint elliptic operators on

the space of one forms with the details going through; the parameters ρ and σ in expression (2.4) are replaced by functions.

Applications of the methods of this paper are currently underway to such problems as the estimation of the biparietal diameter of the fetal head based upon multiple ultrasound images (the biparietal diameter is a good measure of fetal growth) and the estimation of volumes in medical imaging.

5. Bibliography

[1] U. Grenander, Y. Chow, and D.M. Keenan. *HANDS: A Pattern-Theoretic Study of Biological Shapes.* Springer-Verlag, 1991.

[2] U. Grenander and D.M. Keenan. On the shape of plane images. Submitted, 1989.

[3] U. Grenander and D.M. Keenan. Understanding variables shapes in 3-d. Submitted, 1990.

[4] K. Ito. *Foundations of Stochastic Differential Equations in Infinite Dimensional Spaces.* Society for Industrial and Applied Mathematics, Philadelphia, 1984.

[5] D. Keenan. Random surface geometries constructed via exact one forms, 1991. Submitted.

[6] F.W. Warner. *Foundations of Differential Manifolds and Lie Groups.* Scott, Foresman, Glenview, Illinois, 1971.

[7] R.O. Wells. *Differentia nalysis on Complex Manifolds.* Prentice-Hall, Englewood Cliifs, N.J., 1973.

III

Applications in mathematics & computer science

Some continuations of the work of Paley and Zygmund on random trigonometric series

Jean-Pierre Kahane
Université de Paris-Sud à Orsay
Mathématiques—Bâtiment 425
91405 Orsay Cedex France
ulm0047@frors31.bitnet

Abstract We begin with a historical survey, describing sources and content of the fundamental papers of Paley and Zygmund about random trigonometric and Taylor series. Then, in a discussion of the recent and current research in this fertile area, we emphasize local properties of Brownian motion and some of its applications, the present theory of random trigonometric and Taylor series and some applications, Rademacher series in Banach spaces, Sidon sets, Riesz products, the Pisier algebra, and random coverings.

1. Our starting point

Under the cryptic title "On some series of functions," Paley and Zygmund published three papers, in 1930 and 1932, in the *Proceedings of the Cambridge Philosophical Society*. They were anticipated by two papers of Zygmund on lacunary trigonometric series in 1930, and followed in 1933 by a short article of Zygmund on continuability of power series, and a common work of Paley, Wiener and Zygmund, "Notes on random functions" (46, 47, 60, 42, 44, 65, and 67 in the bibliography of Zygmund's *Selected Papers*). The main content and the continuation of the paper of P.W.Z. can be found in the last chapters of the book of Paley and Wiener, *Fourier transforms in the complex domain* (1934).

The P.Z. papers consider series of the form

$$\sum c_n \epsilon_n(\omega) f_n(t) \tag{1.1}$$

where $\epsilon_n(\omega)$ are Rademacher functions, that is, essentially, independent random variables taking the values $+1$ and -1 with probability $1/2$ and, in particular, random trigonometric series

$$\mathrm{Re} \sum_0^\infty c_n \epsilon_n(\omega) e^{int} \tag{1.2}$$

J. S. Byrnes et al. (eds.), Probabilistic and Stochastic Methods in Analysis, with Applications, 481–515.
© 1992 *Kluwer Academic Publishers. Printed in the Netherlands.*

and random Taylor series

$$\sum_0^\infty c_n \epsilon_n(\omega) z^n \tag{1.3}$$

and the analogues when the $\epsilon_n(\omega)$ are replaced by $e^{2\pi i \omega_n}$, where the ω_n are independent random variables whose distribution is the Lebesgue measure on $[0,1]$. We call (1.1), (1.2), (1.3) Rademacher series, Rademacher trigonometric series, Rademacher Taylor series and

$$\sum c_n e^{2\pi i \omega_n} f_n(t) \tag{1.4}$$

$$\mathrm{Re} \sum_0^\infty c_n e^{2\pi i \omega_n} e^{int} \tag{1.5}$$

$$\sum_0^\infty c_n e^{2\pi i \omega_n} z^n \tag{1.6}$$

Steinhaus, Steinhaus trigonometric and Steinhaus-Taylor series.

The paper of P.W.Z. introduces Gaussian series

$$\sum_0^\infty c_n \xi_n f_n(t) \tag{1.7}$$

where the ξ_n are independent Gaussian normalized random variables (actually, it would have been fair to call them Wiener series), in particular Gaussian trigonometric series

$$\sum_0^\infty c_n (\xi_n \cos nt + \xi'_n \sin nt) \tag{1.8}$$

((ξ_n) and (ξ'_n) being two independent normal sequences) and—in a slightly different form—Gaussian Taylor series

$$\sum_0^\infty c_n \zeta^n z^n \tag{1.9}$$

where (ζ_n) is a complex normal sequence, for example $\zeta_n = \frac{1}{\sqrt{2}}(\xi_n + i\xi'_n)$. The case $r_n = \frac{1}{n}$ in (1.8) is essentially the Fourier-Wiener representation of Brownian motion, and the paper is concluded by a proof of the almost sure nowhere differentiability of the Wiener function.

We shall see that Rademacher series (1.1) play a fundamental role in the study of series of functions whose coefficients are independent random variables, in particular series (1.4) and (1.7). Steinhaus series (1.5) and (1.6) are more tractable than the Rademacher series (1.2) and (1.3) because

they are series of random translates; if they enjoy a property almost surely on an interval of values of t, the same holds on the whole circle. Gaussian series (1.8) are a way to study stationary Gaussian processes, and conversely Gaussian stationary processes are a way to study series (1.8); therefore, a difficult question like uniform convergence of random Fourier series is more tractable for Gaussian than for Steinhaus or Rademacher series.

On the other hand, Rademacher series (1.2) and (1.3) were used from the very start in order to provide examples and counterexamples in the theories of Fourier series and analytic functions in the unit disc. This is still the case now, and we shall discuss a few instances.

The introduction to P.W.Z. has a historical character. It describes two streams of ideas, from which P.Z. on the one hand and the work of Wiener on Brownian motion on the other are born, and it indicates that "the purpose of this paper is to bridge the gap between the P.Z. and the W. theories." Actually the purpose is not achieved, and can be considered as a permanent source of inspiration since then.

2. The two streams

Before going back to P.Z. and P.W.Z., let me develop the historical part, which is very much in the spirit of this conference. The probability theory of the twentieth century relies on *totally additive measures and Lebesgue* integration. It arose from very specific questions, and the two main streams are associated with two names: Borel and Einstein.

2.1. From Borel to P.Z.

"The introduction of the notion of random into analysis is in the first instance the work of Borel." This is the first sentence of P.W.Z., and they quote the theory of *probabilités dénombrables*, as expounded by Borel in Rendiconti di Palermo in 1904. Along the lines of questions considered by Borel they mention Rademacher (the so-called Rademacher functions were introduced in 1922) and Steinhaus. "To Steinhaus in particular is due the reduction of such questions to questions concerning the Lebesgue integral."

Let us be more specific. The problem of analytic continuation of a function defined by a Taylor series, raised by Weierstrass in 1880 (*Zur Functionenlehre*, Monatsberichte), became a very popular question in France in the 1890's. Following a seminal paper of Poincaré in 1892 ("Sur les fonctions à espaces lacunaires", *Amer. J. Math.*), and Hadamard's thesis on the relation between the coefficients of the Taylor series and the singularities of the function ("Essai sur l'étude des fonctions données par leur développement de Taylor", *Journal Math. pures et appliquées*, 1892), Borel wrote his thesis on a problem of continuation (not necessarily analytic continuation!) of some

analytic functions ("Sur quelques points de la théorie des fonctions", *Ann. Sc. Ecole Normale Supérieure*, 1895). At this time noncontinuable Taylor series appeared as a pathological situation. Examples were given by Poincaré ($\sum 2^{-n} z^{3^n}$) and by Hadamard ($\sum b_\mu z^{c_\mu}$, where $(c_{\mu+1} - c_\mu)/c_\mu$ is larger than some positive number). Then Borel published a note in the Comptes-Rendus in 1896 and an article in *Acta Mathematica* in 1897, with the same title "Sur les séries de Taylor", and a remarkable statement: "une série de Taylor admet, en général, son cercle de convergence comme coupure" (in general, the circle of convergence of a Taylor series is a natural boundary). Later on, in 1912, reviewing his previous work, he considered this statement as a most important result of his (cf. "Oeuvres", I, p. 154). Here is a translation of his comments.

> The main difficulty was to give a precise meaning before going to the proof...One can divide the series into an infinity of successive groups of terms, and assign to each group a point of the circle of convergence which depends only on the coefficients of this group; these points form a set E; each accumulation point of E is a singular point. Clearly now, if the successive coefficients are chosen randomly, that is, independently from the preceding coefficients, the probability that E is dense on the circle equals one.

I shall discuss this statement later. For the time being let me observe that random Taylor series appear as the initial motivation of Borel for probability theory. From the start it was the source of important probabilistic ideas. For example, here is the germ (actually, the first statement) of the so-called Borel-Cantelli lemma, in the 1897 article,

> on a donc sur le cercle une infinité d'arcs indépendants, dont la somme dépasse tout nombre donné, donc, en général, tout point du cercle appartiendra à une infinité d'arcs...

(Translation: one has infinitely many independent arcs on the circle and their sum exceeds any given number, therefore, in general, each point of the circle belongs to infinitely many arcs). Clearly "in general" means "with probability one," except that the notion of a totally additive probability was not available in 1897. Random Taylor series forced Borel, not only into the Borel-Cantelli lemma, but, what was much more important, into the ideas of totally additive measures and probabilities.

As far as I know, the topic was not discussed until 1929, when Steinhaus introduced series (1.6), which I called Steinhaus Taylor series. For Steinhaus the basic probability space was the interval $[0, 1]$ equipped with the Lebesgue

measure, and the standard model for the ω_n was given in this way: if

$$\omega = \sum_1^\infty \beta_m 2^{-m} \tag{2.1}$$

with $\beta_m = 0$ or 1 and, say, $\sum_1^\infty \beta_m = \infty$, then

$$\omega_n = \sum_{p=0}^\infty \beta_{(2p+1)m} 2^{-p-1}, \qquad m = 2^{n-1}. \tag{2.2}$$

In this way all problems on independent random variables can be reduced to estimates of Lebesgue measures or integrals on [0, 1]. For series (1.6) Borel's argument is correct and can be simplified by use of the zero-one law (but, again, the zero-one law of Kolmogorov was not available in 1929).

Steinhaus's article had a direct influence on Paley and Zygmund, but they first considered that Rademacher Taylor series (1.3) were a much more difficult matter than Steinhaus Taylor series (1.6); they announce the theorem on non-continuation at the end of their first paper, and postpone the proof until the last paper. A much simpler proof was given by Zygmund in 1933. Both proofs, the complicated and the simple, played a role in the development of their work which I gave in the 60's.

The main other sources of P.Z. are orthogonal series, in particular trigonometric series and Rademacher series. Lacunary trigonometric series provided methods and inspiration. Here is a comment of Zygmund (Oeuvres mathématiques de R. Salem, p. 24):

> on peut s'exprimer en disant que, tandis que le caractère aléatoire est intrinsèque dans les séries lacunaires, il est "greffé" dans les séries (1.2).

Lacunary trigonometric series go back to the Weierstrass example of a nowhere differentiable function. It became a real mathematical topic with Kolmogorov (1924), Sidon (1927), Banach (1930), Zygmund (1930 and 1932), and it so happened, that most theorems on sums of independent random variables were stated first for lacunary trigonometric series. This is true in particular for the integrability properties of the partial sums (boundedness in L^p) and the summability almost everywhere, established by Zygmund for lacunary trigonometric series before being stated by Paley and Zygmund for Rademacher series. Part of the influence of the Lebesgue integration theory on probability theory goes through trigonometric series.

As a conclusion, the stream of ideas coming from Borel started with a very specific problem: analytic continuation of random Taylor series. On one hand it developed probabilistic notions. On the other, via the Lebesgue theory, it renewed the study of trigonometric series and orthogonal systems,

and prepared the study of series of independent random variables. P.Z. realizes a new step in considering random series of functions, in particular random trigonometric series.

2.2. From Einstein to P.W.Z.

The Brownian motion (first discovered by the botanist Brown, and studied by several physicists during the 19th century) was rediscovered by Einstein as a necessary consequence of the assumption that statistical thermodynamics is valid for liquids as well as gas. Then he had the idea of using the quadratic variation property in order to derive the atomic dimensions from macroscopic observations (that is, the Brownian motion of a particle of which the mass is known). This was in the famous year 1905, and published in Annalen der Physik, as were his papers on relativity and on the photoelectric effect.

The program of Einstein was realized by Jean Perrin. From the physicist's point of view it was a triumph, leading to the attribution of the Nobel Prize to Jean Perrin. From a mathematical point of view an enormous task had still to be done, and it was performed by N. Wiener in different steps, starting with "Differential space" in 1923. In many papers on Brownian motion (including "Differential space", P.W.Z., and specially chapter IX of the book of Paley and Wiener), Wiener quotes Jean Perrin:

> ... it is impossible to fix a tangent, even approximately, and we are thus reminded of the continuous non differentiable functions of the mathematicians. It would be incorrect to regard such functions as mere mathematical curiosities, since indications are to be found in nature of nondifferentiable as well as differentiable processes ... *(P.W., p. 157)*

The program of Wiener was to define a process $X(t, \omega)$ with the properties pointed out by Einstein (independent increments, mean quadratic variation property) together with the almost sure properties suggested by Jean Perrin (continuity, nowhere differentiability). The definition of the process through measures and integration in function spaces appears already in "Differential space", and also the properties of the Fourier coefficients. The Hölder property of order $\frac{1}{4}$ appears in "Generalized harmonic analysis" in 1930. Only in P.W.Z. the nowhere differentiability is proved, in the stronger form

$$\text{a.s.}(\omega)\ \forall t \qquad \overline{\lim} \frac{|\, X(t+h,\omega) - X(t,\omega)\,|}{|\, h\,|^{\alpha}} = \infty \tag{2.3}$$

for every $\alpha > \frac{1}{2}$, and it is observed that the Hölder condition holds for every $\alpha < \frac{1}{2}$. Later on, in the book with Paley, Wiener introduces $X(t, \omega)$, called the *fundamental random function*, through the device of Steinhaus ((2.1),

(2.2)) and the Fourier series (the notation then is $\psi(x, \alpha)$), and gives a full explanation of the program and the results.

Though P.W.Z. also contains results on Gaussian Fourier series analogous to those of P.Z. on Rademacher and Steinhaus series, the main result is the almost sure nowhere differentiability of Brownian motion, that is, the final achievement of the program of Wiener coming from Einstein and Jean Perrin.

3. The situation in 1933

Let us go back to the Rademacher, Steinhaus and Gaussian series (1.1) to (1.9), and summarize what was known in 1933.

1) Suppose $\sum | c_n |^2 < \infty$ and $| f_n(t) | \leqslant 1$ for all n and $t \in [0, 1]$. Then the series (1.1), (1.4), (1.7) converge almost surely almost everywhere to a sum $F(t, \omega)$. Moreover

$$\int \exp(\lambda F^2(t, \omega))dt < \infty \qquad \text{a.s.}(\omega) \tag{3.1}$$

for each $\lambda > 0$, and it is a best possible result. The partial sums of the series (1.2), (1.5), (1.8) satisfy

$$\sup_t | S_n(t, \omega) | = O(\log^{3/2} n) \qquad \text{a.s.}(\omega)$$

and the sums of (1.3), (1.6), (1.9) are analytic functions satisfying

$$\sup | F(re^{i\theta}, \omega) | = o\left(\sqrt{\log \frac{1}{1 - r}}\right) \qquad \text{a.s.}(\omega),$$

this being best possible again.

2) Suppose $\sum | c_n |^2 = \infty$ and $\liminf \int_E f_n^2(t)dt > 0$ for all n and every Borel set E of measure > 0. Then the series (1.1), (1.4), (1.7) diverge almost surely almost everywhere. Moreover, given any process of summation T, each of these series is not T-summable almost surely almost everywhere. As a consequence, it is almost sure that none of the series (1.2), (1.5), (1.8) is a Fourier-Lebesgue (nor a Fourier-Stieltjes) series. Another consequence is that, assuming $\overline{\lim} | c_n |^{1/n} = 1$, the unit circle is a.s. a natural boundary for the random analytic functions (1.3), (1.6), (1.9).

3) From 1 and 2 we know the probability of the event that (1.2) represents an L^p-function when $1 \leqslant p < \infty$. This probability does not depend on p, and it is 1 or 0 according to the convergence or divergence of $\sum | c_n |^2$. This provides a new and beautiful proof of a theorem of Littlewood: no condition on the amplitudes of the coefficients of

a trigonometric series, strictly better than the Riesz-Fisher condition $\sum |c_n|^2 < \infty$, implies that the series is a Fourier-Lebesgue series. For changing the signs randomly, $\sum |c_n|^2 = \infty$ implies $\sum \pm c_n e^{int} \notin L^1$.

4) If $\sum |c_n|^2 \log^{1+\epsilon} |n| < \infty$ $(\epsilon > 0)$, (1.2) converges uniformly with respect to t a.s., and the same for (1.5) and (1.8). This is no longer true for $\epsilon = 0$. Moreover, writing

$$s_j = \left(\sum_{2^j \leq |n| < 2^{j+1}} |c_n|^2 \right)^{1/2}, \tag{3.2}$$

and assuming $\sum s_j = \infty$, (1.5) is Abel-divergent a.s. a.e., therefore (1.5) $\notin L^\infty$ (P.Z. states the result for (1.2) but proves it for (1.5), with a beautiful kind of martingale argument). We see that no explicit condition on the c_n is given for the series (1.2), (1.5) or (1.8) to represent continuous functions or bounded functions.

5) For the Brownian motion (or series (1.9) with $c_n = \frac{1}{n}$) we have continuity and nowhere differentiability in the strong form given above (see (2.3) and the Hölder condition).

The year 1933 is also the year when the Grundbegriffe der Wahrscheinlichkeitsrechnung of Kolmogorov and the Asymptotische Gesetze der Wahrscheinlichkeitsrechnung of Khintchin were published. The law of the iterated logarithm had been discovered a few years before. The new and majestic stream of modern probability theory was just born. At a first look P.Z. and P.W.Z. close a period, when probability should be reduced to the familiar Lebesgue measure on the line. They used the notations and language of analysis, they ignored the newborn foundations of probability theory, and they reached very sharp and sometimes final results on the specific problems which they considered.

However P.Z. and P.W.Z. were also the source of much subsequent work. In particular, I mention the study of Salem and Zygmund (1954) and the applications which I gave of their methods, the thesis of Billard (1963), the two editions of my book *Some random series of functions* (SRSF 1969 and 1985), and the book of Marcus and Pisier (1981). Here is a personal selection of themes.

4. The local behaviour of Brownian motion

Let me begin with the end of P.W.Z. The local version of the law of the iterated logarithm reads as follows:

$$\forall t \text{ a.s.} \qquad \limsup_{h \to 0} \frac{X(t+h) - X(t)}{\sqrt{2|h| \log\log 1/|h|}} = 1.$$

Therefore (Fubini) the t-set defined by

$$\text{a.s.} \qquad \limsup_{h\to 0} \frac{|X(t+h)-X(t)|}{\sqrt{2\,|h|\log\log 1/|h|}} = 1 \tag{4.1}$$

is of full Lebesgue measure. When (4.1) is satisfied we say that t is an ordinary point. Do there exist other points? This is not obvious, and Paul Lévy expressed the feeling that all t are ordinary (*Processus stochastiques et mouvement brownien*, 1948, p. 247).

The Hölder condition of order $\alpha < \frac{1}{2}$ was improved by Paul Lévy. One has a.s.

$$X(t+h) - X(t) = \mathcal{O}\left(\sqrt{|h|\log\frac{1}{|h|}}\right) \qquad (h \to 0) \tag{4.2}$$

uniformly on each bounded interval, and the $\mathcal{O}$ estimate can be made more precise.

There is also a stronger version of nowhere differentiability than (2.3), namely

$$\text{a.s. } \forall t \qquad \limsup_{h\to 0} \frac{|X(t+h)-X(t)|}{\sqrt{|h|}} > 0. \tag{4.3}$$

This is due to Dvoretzky (1963).

Not all points are ordinary points. There are rapid points, for which

$$\limsup_{h\to 0} \frac{|X(t+h)-X(t)|}{\sqrt{|h|\log\frac{1}{|h|}}} > 0 \tag{4.4}$$

and slow points, for which

$$\limsup_{h\to 0} \frac{|X(t+h)-X(t)|}{\sqrt{|h|}} < \infty. \tag{4.5}$$

Comparing (4.4) and (4.2) and (4.5) with (4.3), we see that all orders of magnitude are sharp. Rapid points were discovered by Orey and Taylor (1974) and slow points by me. There were further studies on slow points by Davis (1983), Perkins (1983), Davis and Perkins (1985), with more information on the law of the $\overline{\lim}$ in (4.5), and estimates for the Hausdorff dimension of the t's for which this $\overline{\lim}$ does not exceed a given number. Proofs of the existence of rapid and slow points can be found in SRSF 1985.

Let me explain how the existence of slow points in the zero-set of $X(\cdot)$ can be viewed. Let $E = X^{-1}(0)$ be the zero-set, and (I_j) the family of contiguous intervals, $I_j = (a_j, a_j + \ell_j)$. From Paul Lévy's construction the

restrictions of $X(\cdot)$ to the I_j are mutually independent and, when normalized in the form

$$Y_j(s) = \ell_j^{-1/2} X(a_j + \ell_j s),$$

they are independent from E as well. Given $\lambda > 0$, the t-set such that $X^2(t+h) < \lambda \mid h \mid$ for all h can be viewed as the set which stays illuminateded when the sun runs from direction $(1, \lambda)$ to direction $(-1, \lambda)$ and the sunlight is stopped by the graph of $X^2(\cdot)$. The shadowed interval corresponding to $Y_j^2(\cdot)$ is obtained from I_j by a random enlargement:

$$J_j = (a_j - \ell_j \beta_j, a_j + \ell_j + \ell_j \gamma_j),$$

where the couples (β_j, γ_j) are independent copies of a random couple (β, γ) whose law depends on λ only. It is rather intuitive and it can be proved that the J_j cover $\mathfrak{R}$ a.s. when λ is small enough, do not cover $\mathfrak{R}$ a.s. when λ is large, and moreover that $\mathfrak{R} \setminus \cup J_j$ has a Hausdorff dimension tending to 1/2 (the dimension of $E = \mathfrak{R} \setminus \cup I_j$) as $\lambda \to \infty$. My 1976 note contains the full proof.

This approach uses the Paul Lévy construction and cannot be applied for other processes. However analogues of formulas (4.1) to (4.5), including the existence of rapid and slow points, hold for many processes. For example, the whole is valid for fractional Brownian motion of index α $(-1/2 < \alpha < 1/2)$ when $\mid h \mid^{1/2}$ is replaced by $\mid h \mid^{1/2+\alpha}$. This extends to Gaussian Fourier series when

$$c_n \sim n^{-1-\alpha}$$

(meaning that the ratio is bounded above and below by positive numbers). (4.2) and (4.3) (with $\mid h \mid^{1/2+\alpha}$ in place of $\mid h \mid^{1/2}$) extends to all Rademacher, Steinhaus or Gaussian Fourier series for which

$$0 < \overline{\lim} \left(2^{j(1/2+\alpha)} s_j \right) < \infty$$

where

$$s_j = \left(\sum_{2^j \leqslant n < 2^{j+1}} \mid c_n \mid^2 \right)^{1/2}. \tag{4.6}$$

Proofs, references and comments can be found in SRSF 1968 and my paper in honour of A. Zygmund (1983). Slow points are not known for Rademacher or Steinhaus Fourier series.

It is natural and usual to compare random Fourier series and lacunary trigonometric series (I have already quoted Zygmund in this respect). To fix the ideas let us consider

$$f(t) = \sum_1^\infty 2^{-ja} \cos 2^j t \tag{4.7}$$

and series (1.8) with $c_n = n^{-1/2-a}, 0 < a \leqslant 1$. They have much in common. However, when $0 < a < 1$, the local behaviour of $f(\cdot)$ is the same at all points:

$$0 < \overline{\lim} \frac{|\, f(t+h) - f(t) \,|}{|\, h \,|^a} < \infty;$$

the function $f(\cdot)$ is more regularly irregular than the corresponding Gaussian process. On the other hand, when $a = 1$, $f(\cdot)$ satisfies

$$\begin{aligned} f(t+h) + f(t-h) - 2f(t) &= O(|\, h \,|) \\ f(t+h) - f(t) &= O\Big(|\, h \,| \log \frac{1}{|\, h \,|}\Big) \end{aligned} \tag{4.8.1}$$

uniformly with respect to t,

$$\overline{\lim_{h \to 0}} \frac{|\, f(t+h) - f(t) \,|}{|\, h \,| \log \frac{1}{|h|}} > 0 \tag{4.8.2}$$

for quasi all t (meaning except on a set of the first category of Baire),

$$0 < \overline{\lim_{h \to 0}} \frac{|\, f(t+h) - f(t) \,|}{|\, h \,| \sqrt{\log \frac{1}{|h|} \log \log \log \frac{1}{|h|}}} < \infty \tag{4.8.3}$$

for almost every t,

$$\overline{\lim_{h \to 0}} \frac{|\, f(t+h) - f(t) \,|}{|\, h \,|} < \infty \tag{4.8.4}$$

on a dense set of t, and

f is nowhere differentiable. (4.8.5)

Here (4.8.3) is the behaviour at ordinary points, (4.8.2) at rapid points, (4.8.4) at slow points. In this case, the lacunary series (4.7) has the same kind of irregular irregularity as the Brownian motion. These results on lacunary Fourier series are due to Geza Freud (1962,1966) (see also Izumi, Izumi, Kahane 1965 and Kahane 1986 where several other references can be found).

5. A few applications of Brownian motion and Gaussian processes to Fourier analysis

From P.Z. comes an important and general idea: in many circumstances it is hard to find a mathematical object with some prescribed properties, and pretty easy to exhibit a random object which enjoys these properties almost surely. I already insisted on the use of Rademacher trigonometric series in order to prove that no better condition than Riesz Fischer's on the moduli of

coefficients implies that a trigonometric series is a Fourier series. Let me give a few other examples using Brownian motion or Gaussian Fourier series.

1) A problem of Beurling on closed sets. Given a closed set $E \subset \mathfrak{R}^d$, with Hausdorff dimension α, no nonzero measure μ carried on E satisfies $\hat{\mu}(u) = O(|u|^{-\beta})$ with $\beta > \frac{\alpha}{2}$; this comes from potential theory. Is it possible to find E with a prescribed dimension α, carrying nonzero measures μ such that $\hat{\mu}(u) = O(|u|^{-\beta})$ for all $\beta < \frac{\alpha}{2}$? Let me remark that if $d \geqslant 2$ and $\alpha = d - 1$, the $d - 1$ dimensional sphere answers the question, and the boundary of the d-dimensional cube is not a solution, because $\hat{\mu}(u)$ cannot even tend to zero. The difficult situation is $d = 1$ and $0 < \alpha < 1$. Salem solved Beurling's problem by means of an ad hoc random construction (1950). The Brownian motion provides a simple solution: choose any closed set $F \subset \mathfrak{R}$, with dimension $\frac{\alpha}{2}$; then X(F) answers Beurling's problem a.s. In short, Brownian images of closed sets are Salem sets [26].
2) A problem on U-sets. A compact set $E \subset \mathfrak{R}^d$ is called a U-set if it carries no nonzero distribution whose Fourier transform tends to zero at infinity. For example, the boundary of the d-dimensional cube is a U-set. Salem introduced in 1944 an entropy condition which implies that E is a U-set, namely

$$\liminf_{\epsilon \to 0} \frac{N_\epsilon(E)}{\log 1/\epsilon} = 0$$

where $N_\epsilon(E)$ denotes the smallest number of balls of radius ϵ whose union contains E. Actually Salem's condition implies more, namely

$$\overline{\lim_{|u| \to \infty}} |T(u)| = \sup_u |T(u)|$$

for all pseudomeasures (distributions with bounded Fourier transforms) carried by E. Using Brownian images ($E = X(F)$) Salem's condition appears best possible in the following sense:

   a) given $\delta > 0$ there exists $E \subset \mathfrak{R}$ with $N_\epsilon(E) = O(\log \frac{1}{\epsilon})$, carrying a probability measure μ such that $\overline{\lim}_{|u| \to \infty} |\mu(u)| \leqslant \delta$.
   b) given any function $A(\epsilon)$ tending to ∞ as $\epsilon \to 0$ there exists a non-U-set E with $N_\epsilon(E) = O(A(\epsilon)\log \frac{1}{\epsilon})$ $(\epsilon \to 0)$ [27].

3) A problem on modifications of continuous functions. A famous theorem of Menšov says that, given a continuous function f on $\mathfrak{T}$, and $\epsilon > 0$, it is possible to change f on a set of Lebesgue measure $\leqslant \epsilon$ and get a "good" function; meaning that the Fourier series converges uniformly [2, p. 438-457]. Katznelson proved that "good" cannot mean that the Fourier series converges absolutely: there exists a continuous function

f such that no restriction of f to a set of positive Lebesgue measure can be represented by an absolutely convergent trigonometric series (1975). Olevskii was able to get such bad functions f in every Hölder class of index $\alpha < \frac{1}{2}$ (1978) and Hruščev had the idea of using Gaussian Fourier series in order to get these bad functions (1981). Actually the Brownian motion is an example [21].

4) Another problem on modifications of continuous functions. Given again a continuous function f on $\mathfrak{T}$, there exists a homeomorphism $\varphi : \mathfrak{T} \to \mathfrak{T}$ such that $f \circ \varphi$ has a uniformly convergent Fourier series. This is a theorem of Bohr and Pál for real valued functions, Saakian, Kahane and Katznelson for complex valued functions (for a history and comments, see Kahane 1982). Is it possible to replace uniformly convergent by absolutely convergent? The answer is negative (Olevskii 1981). Open question: does the Brownian motion provide an example? (Here as above, we subtract a linear term to the usual Brownian motion in order to have a continuous function on the circle).

5) The problem of spectral synthesis in $\ell^\infty(\mathbb{Z})$. It reads as follows: given $(a_n)_{n\in\mathbb{Z}}$ in $\ell^1(\mathbb{Z})$ and $(b_n)_{n\in\mathbb{Z}}$ in $\ell^\infty(\mathbb{Z})$, such that the function

$$f(t) = \sum_{n\in\mathbb{Z}} a_n e^{int}$$

vanishes on the support of the pseudomeasure

$$T(t) \sim \sum_{n\in\mathbb{Z}} b_n e^{int},$$

is it true that necessarily

$$\langle T, f\rangle = \sum_{n\in\mathbb{Z}} a_n b_{-n} = 0?$$

In 1959, Malliavin solved the question in a negative way, using a lacunary trigonometric series for the definition of f. Actually Gaussian trigonometric series give easier computations on applying Malliavin's idea, namely, to define T as $\delta'(f)$, δ' being the derivative of the Dirac measure. This is very much in the spirit of local time (which can be defined as $\delta(f)$).

6. Back to random Taylor series

A discussion of Borel's statement on random Taylor series

$$\sum_0^\infty X_n z^n \tag{6.1}$$

whose coefficients are independent complex random variables will show the crucial role of Rademacher series.

Let us start with Rademacher Taylor series (1.3), and suppose that $\overline{\lim} \mid c_n \mid^{1/n} = 1$, i.e., the circle of convergence is the unit circle $\mid z \mid = 1$. We want to prove that the unit circle is a natural boundary a.s. (theorem of P. Z., proved in their last paper). Suppose the contrary: there exists an arc I on the circle which consists of regular points (let us say: a regular arc) with a positive probability, and this probability is 1 by the zero-one law. The length of I exceeds $\frac{2\pi}{N}$ for N large enough.

Now we change signs in (1.3): we define $\epsilon_n^k = \epsilon_n$ when $n \equiv k \pmod N$ and $\epsilon_n^k = -\epsilon_n$ when $n \not\equiv k \pmod N$. The series

$$\sum_0^\infty c_n \epsilon_n^k z^n \tag{1.3*}$$

has the same almost sure properties as (1.3), and adding (1.3) and (1.3*) we obtain a function of the form $z^k H_k(z^N)$. Being regular on I, $H_k(z^N)$ is regular on the unit circle (a.s.). Now

$$\sum_{k=0}^{N-1} z^k H_k(z^N) = 2 \sum_0^\infty c_n \epsilon_n z^n,$$

therefore the unit circle is regular for (1.3), a contradiction. (In the 1968 edition of SRSF I thought that this proof was new. Actually it was given by Zygmund in 1933).

The unit circle plays no special role. What we proved is that the circle of convergence of (1.3), whenever it exists, is a natural boundary a.s.. This result extends to series (6.1) whenever the X_n are symmetric (same law for X_n and $-X_n$). Here is a way to see it. The X_n are defined on Ω. Let us introduce another probability space Ω' and a Rademacher sequence ϵ_n on Ω'. Now consider $\Omega \times \Omega'$ as our probability space, and the random series

$$\sum_0^\infty \epsilon_n(\omega') X_n(\omega) z^n. \tag{6.2}$$

For each given ω', (6.2) is nothing but another version of (6.1), therefore (6.2) has the same almost sure properties (on $\Omega \times \Omega'$) as (6.1) (on Ω). For each given ω, (6.2) is a Rademacher Taylor series, therefore has its circle of convergence as a natural boundary a.s. (on Ω'). Therefore the same holds a.s. on $\Omega \times \Omega'$, proving the result. Let me observe that the radius of convergence of (6.1) is a constant a.s.; we can speak of *the* circle of convergence of (6.1) whenever this constant is neither 0 nor ∞.

When the X_n are not symmetric, we use again $\Omega \times \Omega'$ and consider

$$\sum_0^\infty (X_n(\omega) - X_n(\omega'))z^n. \tag{6.3}$$

Now the coefficients are symmetric and independent, and we can apply the previous result. Either $|z| = \rho$ is a.s. a natural boundary for (6.1), or (6.3) has an a.s. radius of convergence $\rho' > \rho$. In this case a.s.(ω') a.s.(ω) the circle $|z| = \rho'$ is a natural boundary for (6.3) (with the obvious modification when $\rho' = \infty$). We can choose ω' in such a way that

1) the radius of convergence of $\sum_0^\infty X_n(\omega')z^n$ is ρ;
2) a.s.(ω) the circle of convergence of (6.3) is a natural boundary.

Writing $X_n(\omega') = x_n$, we decompose (6.1) in the form

$$\sum_0^\infty x_n z^n + \sum_0^\infty (X_n - x_n)z^n \tag{6.4}$$

and we obtain as a final statement something slightly different from Borel's, namely: either $|z| = \rho$ is a.s. a natural boundary for (6.1), or (6.1) can be decomposed in the form (6.4), where the first series converges for $|z| < \rho$ and the second a.s. in a larger disc $|z| < \rho'$, which is its domain of existence.

This is a theorem of Ryll-Nardzewski (1953), answering a question of Blackwell. The proof given here is taken from SRSF.

From the proof we can extract two principles which apply in more general situations, called the *principle of reduction* and the *device of symmetrization* in SRSF pp. 8,9. Now we consider independent random vectors in a linear space and we denote them by X_n. If the X_n are symmetric and $\epsilon_1^*, \epsilon_2^*, \cdots, \epsilon_n^*, \cdots$ is a fixed sequence with values $+1$ or -1, the random sequences (X_n) and $(\epsilon_n^* X_n)$ have the same distribution (that is what we used first). If the X_n are symmetric and (ϵ_n) is a Rademacher sequence independent from (X_n), the random sequences (X_n) and $(\epsilon_n X_n)$ have the same distribution. As an application, let us consider a property P which can be satisfied or not by any sequence of vectors, and suppose that, whenever (ϵ_n) is a Rademacher sequence and (x_n) is a constant sequence of vectors, $(\epsilon_n x_n)$ satisfies P a.s.; then, assuming that "(X_n) satisfies P" is an event, this event is almost sure. From this *principle of reduction* it appears that the Rademacher series of functions, or Rademacher series of vectors, plays a central role.

Now, given a random vector X defined on Ω, the random vector $\Psi(\omega, \omega') = X(\omega) - X(\omega')$ defined on the product space $\Omega \cdot \Omega$ is symmetric. When we know that Y enjoys a given property a.s. (on $\Omega \cdot \Omega$), it follows that there exists $\omega' \in \Omega$ and a fixed vector $x = X(\omega')$ such that $X - x$ enjoys the same property a.s. (in Ω). This is the *device of symmetrization*.

A third principle comes directly from the original proof of P.Z. of the non-continuation of series (1.3). Here is the idea: if a Taylor series $\sum a_n z^n$ is continuable across the circle of convergence to a point ζ, the series $\sum a_n \zeta^n$, though divergent, is summable by a convenient summation matrix. Now, given any summation matrix S (the exact definition is given in SRSF p. 12) and a series $\sum_1^\infty X_n$ of independent symmetric vectors in a Banach space, if the series is S-summable a.s., it converges a.s. This third principle (a.s. summability implies a.s. convergence) can be applied in many situations. It gives non continuation theorems for random Taylor series with several variables, for random Dirichlet series and for other series of analytic functions. Through Fejer's or Lebesgue-Fejer's theorem on Fourier series it has a key role in order to explain that (1.2) fails a.s. to represent an L^1 function when $(c_n) \notin \ell^2$.

7. Back to random trigonometric series

Let us consider Rademacher trigonometric series

$$\sum_0^\infty \epsilon_n r_n \cos(nt + \varphi_n) \tag{7.1}$$

where the amplitudes r_n and the phases φ_n are given, and Steinhaus trigonometric series

$$\sum_0^\infty r_n \cos(nt + 2\pi\omega_n) \tag{7.2}$$

where the r_n are given, and more generally

$$\sum_0^\infty X_n \cos(nt + \Phi_n) \tag{7.3}$$

where the $X_n e^{i\Phi_n}$ are independent symmetric complex variables.

Via the principle of reduction, the P.Z. theorems say that the following properties have the same probability, 0 or 1:

- (7.3) is a Fourier-Lebesgue series
- (7.3) represents a function which belongs to all L^p $(1 \le p < \infty)$
- (7.3) converges almost everywhere
- (7.3) is Abel-summable almost everywhere.

The case of uniform convergence is difficult, though a rather precise result can be given in terms of the

$$s_j = \left(\sum_{2^j \le n < 2^{j+1}} r_n^2 \right)^{1/2}$$

(already introduced in slightly different forms in (3.2) and (4.6)) for Rademacher and Steinhaus trigonometric series (7.1) and (7.2). Here is the result:

1) If $\sum_1^\infty s_j = \infty$, (7.1) and (7.2) fail a.s. to represent a bounded function.
2) If $\sum_1^\infty s_j < \infty$ and s_j is a decreasing sequence, (7.1) and (7.2) converge uniformly a.s., therefore represent continuous functions a.s.. The second statement is a corollary of a result of Salem and Zygmund (1954). The first was stated in P.Z. but proved only for Steinhaus series (7.2), as I already said. The first proof was given in Billard's thesis (1963).

Billard's idea was to derive properties of Rademacher series from properties of Steinhaus series, by means of a principle of contraction. We shall see a general form of the principle of contraction in the context of random series in Banach space. The initial inspiration was to prove that (7.1) and (7.2) fail to represent a bounded function with the same probability. Here is a consequence of Billard's theory: the following properties have the same probability, 0 or 1:

- (7.3) represents a bounded function
- (7.3) represents a continuous function
- (7.3) converges everywhere
- (7.3) converges uniformly.

Of course, the interest of Steinhaus trigonometric series is to involve random translations, and Billard's theory contains interesting statements on series of random translates.

Let me give an application of Rademacher trigonometric series to a property of Fourier coefficients of continuous functions. Is it true that, given a positive sequence (r_n) in ℓ^2, one can choose the phases φ_n in such a way that

$$\sum_0^\infty r_n \cos(nt + \varphi_n)$$

represents a continuous function? The answer is no, and given by a lacunary series. Is it true now that, given (r_n) in ℓ^2, one can enlarge the r_n (i.e., choose $r'_n \geq r_n$) and choose the φ_n in such a way that

$$\sum_0^\infty r'_n \cos(nt + \varphi_n)$$

represents a continuous function? The answer is yes, using an iterative randomization (De Leeuw, Kahane, Katznelson 1977).

8. Rademacher series in Banach space

My first motivation for considering Rademacher series in Banach spaces was to obtain the principle "summability implies convergence" , and the contraction principle, in this context. The contraction principle depends on an integrability property of the sum of Rademacher series, which I obtained as a consequence of the fact that, if the probability, that such a sum is large, is small, the probability that it is twice as large is very small:

$$\mathcal{P}(\| V \| > \tau) < \frac{\alpha}{2} \Rightarrow \mathcal{P}(\| V \| > 2\tau) < \alpha^2$$

(Kahane 1964).

As a consequence, not only $\| V \| \in L^1(\Omega)$, but $\exp \lambda \| V \| \in L^1(\Omega)$ when λ is small enough. Actually the final result in this direction is due to Kwapien (1976): $\exp \alpha \| V \|^2 \in L^1(\Omega)$ for all $\alpha > 0$.

The contraction principle expresses that the a.s. convergence (or boundedness) of a Rademacher series of vectors

$$\sum_1^\infty \epsilon_n u_n \tag{8.1}$$

implies the same for any series $\sum_1^\infty \epsilon_n \lambda_n u_n$, where λ_n is a given bounded sequence. As a consequence, the Rademacher series and the corresponding Steinhaus series

$$\sum_1^\infty e^{2\pi i \omega_n} u_n \tag{8.2}$$

have the same probability to converge (and also the same probability that the partial sums are bounded). In the case of trigonometric series in the space of continuous functions on $\mathcal{T}$, Billard's theorem is recovered. It is the way things are explained in SRSF.

There is now a huge literature on random series in Banach spaces, with a special interest on Rademacher series, which play a basic role in the relation between geometry and probability in Banach spaces (Hoffmann-Jørgensen 1974 and 1977, Maurey and Pisier 1976, Garling 1977, the book of Pisier 1989, the book of Ledoux and Talagrand 1991, where a very huge bibliography is given). Khintchin's inequalities, which express the behaviour of the norms $\| \sum \epsilon_n u_n \|$ in different $L^p(\Omega)$, appear as a consequence of the strong integrability (Pisier 1978). The notions of type and cotype express the behaviour of the expectation $E \| \sum \epsilon_n u_n \|$ with respect to the L^p norm of $\{\| u_n \|\}$ (Maurey and Pisier). Isoperimetric methods were developed (Talagrand).

Let me mention only one comparison theorem of Talagrand (Theorem 4.12 in Ledoux-Talagrand 1991). First, using duality, the norm of a Rademacher sum (say, of N terms), is expressed as

$$\left\| \sum_1^N \epsilon_i x_i \right\|_B = \sup_{t \in T} \left| \sum_1^N \epsilon_i t_i \right|$$

where $t = (t_1, \cdots, t_N) \in \mathfrak{R}^N$ and T is the image of the unit ball in B′ through the mapping $f \to \{f(x_i)\}$. The comparison theorem involves a convex and increasing function $F(\mathfrak{R}^+ \to \mathfrak{R}^+)$ and a sequence of contractions φ_i $(\mathfrak{R} \to \mathfrak{R})$ such that $\varphi_i(0) = 0$; it reads as

$$E\left(F\left(\frac{1}{2}\sup_{t\in T} \left| \sum_1^N \epsilon_i \varphi_i(t_i) \right|\right)\right) \leqslant E\left(F\left(\sup_{t\in T} \left| \sum_1^N \epsilon_i t_i \right|\right)\right).$$

Previously such an inequality was obtained when the Rademacher sequence ϵ_i is replaced by a normal sequence ξ_i, as a consequence of comparison theorems for Gaussian processes. Rademacher sums need a quite different treatment.

Open problems on Rademacher series in Banach spaces can be found in the book of Ledoux and Talagrand (section 12.3).

9. Back to P.W.Z.'s program ("to bridge the gap")

From the contraction principle Rademacher and Steinhaus series in Banach spaces behave in the same way. If now we consider, in addition to (8.1) and (8.2), a Gaussian series

$$\sum_1^\infty \xi_n u_n \tag{9.1}$$

where (ξ_n) is a normal sequence as in (1.7), the almost sure convergence of (8.1) by no means implies the same for (9.1).

However, if we consider Rademacher, Steinhaus and Gaussian Fourier series (1.2), (1.5), (1.8), they have the same probability to converge uniformly (which is the same as to represent a continuous function, or to represent a bounded function). This remarkable fact was discovered by Marcus and Pisier in 1978. The book of Marcus and Pisier "Random Fourier series with applications to harmonic analysis" contains the proof, together with an explicit condition on the c_n, and previous results of Pisier.

Here is the explicit condition. Consider

$$\psi(t) = \sum |c_n|^2 \sin^2 nt$$

and define

$$I(\psi) = \int_0^1 \frac{\sqrt{\psi^*(x)}}{\sqrt{\log 1/x}} dx$$

where ψ^* is the increasing rearrangement of ψ. Then

$$I(\psi) < \infty$$

is the necessary and sufficient condition for (1.2), (1.5), and (1.8), to converge uniformly, or represent a continuous function, or represent a bounded function, a.s.

Actually this is nothing but a reformulation of the Dudley-Fernique theorem for a stationary Gaussian processes. The usual form of the Dudley-Fernique theorem, for stationary Gaussian processes X_t defined on the circle $\mathfrak{T}$, involves the integral

$$I = \int \sqrt{\log N(\epsilon)} d\epsilon$$

where $N(\epsilon)$ is the minimum number of balls of radius ϵ covering $\mathfrak{T}$, in the metric defined by

$$d(t,t') = (E \mid X_t - X_{t'} \mid^2)^{1/2}.$$

The Dudley-Fernique theorem was the solution for stationary process of a long-standing problem of Kolmogorov: how to recognize, from the geometry of the Gaussian (centered) process $(X_t)_{t\in K}$ if there are a.s. bounded, or a.s. continuous, versions? Surprisingly, the general problem has a solution obtained by Talagrand (1987). Here is a simple and weak form of the result of Talagrand (Theorem 12.10 in Ledoux-Talagrand). Let me start with examples of Gaussian processes with bounded versions:

1) $(Y_n)_{n\in\mathbb{Z}}$ with $EY_n^2 = O\left(\frac{1}{\log n}\right)$ (because $\sum \mathcal{P}(\mid Y_n \mid > \lambda) < \infty$ when λ is large);
2) $(X_t)_{t\in K}$ in the convex hull of such a sequence (Y_n).

Theorem: example 2 is the general case.

There is a weakness however in this remarkable result, as well as in other versions of Talagrand's theorem: how to recognize the Y_n when (X_t) is given? Therefore, the interest of the theorem of Dudley and Fernique is not abolished with the theorem of Talagrand. It can be added that the necessary and sufficient condition of Marcus and Pisier does not suppress the interest of looking at the s_j $(= (\sum_{2^j\le|n|<2^{j+1}} \mid c_n \mid^2)^{1/2})$ in order to get easy information on local regularity or irregularity.

10. An open question: Bridging the gap for random Taylor series

I insisted on the non-continuation problem, but there are a lot of problems, works and results on random Taylor series; a partial bibliography can be found in SRSF 1985. I shall restrict myself to one question: what can be said on the range and the distribution of values of functions $F(z)$ which are sums of series (1.3) (Rademacher), (1.6) (Steinhaus), (1.9) (Gaussian) in the case when $\overline{\lim} \mid c_n \mid^{1/n} = 1$ (the unit disc is the domain of existence of the random analytic function $F(z)$) and $\sum_0^\infty \mid c_n \mid^2 = \infty$ (i.e., $F(z)$ does not belong to the Nevanlinna class)?

There is a very good information for Gaussian Taylor series (SRSF 1985, chap. 13, and Kahane 1987): the range of $F(z)$ ($\mid z \mid < 1$) is a.s. the whole plane $\mathbb{C}$. Moreover, for some fixed sequence $r_\nu \to 1$, we have a.s. estimates for the Nevanlinna function

$$N(r, b, F) = \int_0^r \frac{n(r, b, F)}{s} ds$$

where $n(r, b, F)$ is the number of zeros of $F(z) - b$ in the disc $\mid z \mid < r$, namely: *it is almost sure that for all* $b \in \mathbb{C}$,

1) $N(r_\nu, b, F) = N(r_\nu, 0, F) + O(1)$
2) $N(r_\nu, b, F) \geqslant \frac{1}{2} \log \rho(r_\nu)$ where

$$\rho(r) = \sum_0^\infty \mid c_n \mid^2 r^{2n} = E(\mid F(re^{i\alpha}) \mid^2).$$

For Steinhaus Taylor series the first part is known, namely, the range of $F(z)$ ($\mid z \mid < 1$) is a.s. the whole plane $\mathbb{C}$ (Offord 1972; also, for a far-reaching generalization, Murai 1978).

For Rademacher Taylor series the question is open as far as I know. The best result which I know is due to Jacob and Offord (1983): if $\log N = O(\sum_1^N \mid c_n \mid)$ $(N \to \infty)$, then the range is $\mathbb{C}$ a.s..

It should be added that the topic has a long history, going back to Littlewood and Offord 1948–1949, who considered the distributions of the zeros of $F(z) - a$ when $F(z)$ is a random entire function.

There is also a remaining question, even in the case of Gaussian Taylor series. Is it true that either such a series represents a.s. a continuous function on the closed disc $\mid z \mid \leqslant 1$, or that it maps a.s. the open disc $\mid z \mid < 1$ onto the whole plane $\mathbb{C}$?

11. Some applications to harmonic analysis: Sidon sets, the Pisier algebra, Riesz products

I have already given two applications of the P.Z. theory to Fourier series:

1) if $\sum |a_n|^2 = \infty$, $\sum \pm a_n e^{int} \in L^1$ for some choice of signs $\pm$;
2) if $\sum |a_n|^2 < \infty$, $\sum b_n e^{int} \in C$ for some sequence b_n, $|b_n| \geqslant |a_n|$.

Moreover, I gave a series of applications of Brownian motion and special Gaussian processes.

Let me concentrate on another aspect for a while: the use of random polynomials or random series in order to study lacunary sets. A theorem of Sidon says that, if Λ is a set of integers which is Hadamard-lacunary (the distance between two consecutive points is larger than some given fraction of their distances to the origin), and if a continuous function on $\mathfrak{T}$ has its frequencies in Λ, its Fourier series converges absolutely. With obvious and classical notations we have

$$C_\Lambda = A_\Lambda. \tag{11.1}$$

Now to take (11.1) as a definition of a *Sidon set* in $\mathfrak{Z}$.

A Sidon set has to be lacunary in some sense. The first method in order to see this is to use random trigonometric polynomials of the form

$$P(t) = \sum_{\lambda \in \Lambda} \pm c_\lambda e^{i\lambda t}, \qquad c_\lambda = 0 \text{ or } 1.$$

From the definition of a Sidon set there exists a constant $K = K(\Lambda)$ such that

$$\| P \|_A \leqslant K \| P \|_C .$$

We may have an estimate of the form

$$\mathcal{P}\left(\| P \|_C \leqslant B \left(\sum |c_\lambda|^2 \right)^{1/2} \right) > 0.$$

For example, from estimates of Salem and Zygmund we can take $B = \sqrt{\log N}$, N being the degree of P. Since

$$\sum |c_\lambda| = \sum |c_\lambda|^2 = \nu$$

(number of terms in P), a convenient choice of $\pm$ gives

$$\nu \leqslant KB\nu^{1/2}$$
$$\nu \leqslant K^2B^2.$$

Using the estimate of Salem and Zygmund we see that the number of points of Λ in $[-N, N]$ cannot exceed $K^2 \log N$. Using an estimate of the same kind for random trigonometric polynomials in several variables we have a more precise necessary condition: if Λ is a Sidon set, there exists a constant K' such that Λ contains at most $[K' s \log \nu]$ elements of the form

$$a + n_1\rho_1 + n_2\rho_2 + \cdots + n_s\rho_s$$

when $a, \rho_1, \cdots, \rho_s$ are given real numbers and $n_1, n_2, \cdots, n_s$ are integers such that $|n_1| + |n_2| + \cdots |n_s| \leqslant \nu$ (Kahane 1957).

In the opposite direction any quasi-independent set Λ is Sidon. Quasi-independent means that $\sum_{\lambda \in \Lambda} \alpha_\lambda \lambda = 0$ with $\alpha_\lambda = -1, 0, 1$ implies that all α_λ are 0. A finite union of quasi-independent sets is also Sidon. Until now it is not clear if this is also a necessary condition, nor if the necessary condition given above is also sufficient.

In 1960 Rudin introduced another kind of lacunary set, the so-called Λ_p-sets, and proved in this connection that the L^p-norms of functions with spectrum in a Sidon set behave like the L^p-norms of a Rademacher series, namely $O(\sqrt{p})$ $(p \to \infty)$.

A breakthrough in the theory of Sidon sets was made by Drury (1970) when he proved that a finite union of Sidon sets is a Sidon set; his method was to introduce $\Omega = \mathfrak{T}^{\mathfrak{C}}$, and harmonic analysis on Ω as well as $\mathfrak{T}$.

The next step was Rider 1975. Rider gives a new characterization of Sidon sets, which can be expressed as

$$C_{a.s.\,\Lambda} = A_\Lambda. \tag{11.2}$$

Here $C_{a.s.}$ is the space of functions

$$f \sim \sum \hat{f}_n e^{int}$$

such that, for almost all changes of signs,

$$\sum \pm \hat{f}_n e^{int}$$

represents a continuous function (if this is true for all changes of signs, then $f \in A$). Actually Rider considered Steinhaus and not Rademacher series; we now know that it is the same, and also the same as Gaussian series.

Finally, using (11.2), Pisier was able to prove the converse of Rudin's theorem (1978). It was the most spectacular use of random Fourier series in order to study lacunary sets. The whole theory is expounded in the book of Marcus and Pisier 1981.

Here is another spectacular result of Pisier using $C_{a.s.}$ (1979), also described in Marcus-Pisier. Let us consider

$$C \cap C_{a.s.}$$

that is, the space of continuous functions on $\mathfrak{T}$ such that a random change of signs of the Fourier coefficients gives a continuous function a.s.. Pisier proves that Lipschitz functions operate on $C \cap C_{a.s.}$ As a consequence $C \cap C_{a.s.}$ is a Banach algebra which is strictly contained in C and strictly contains A, such that the Lipschitz functions operate. This Pisier algebra gives a very neat answer to a problem of Katznelson (find homogeneous Banach algebras between C and A, on which not only analytic functions and not all continuous functions operate), and it is a remarkable object in harmonic analysis.

Let us go back to (11.1), the definition of Sidon sets, for a while. (11.1) expresses that C_Λ is isomorphic to A_Λ, which in turn is isomorphic to ℓ^1. Now, given vectors x_j in ℓ^1,

$$\left(\sum \| x_j \|^q \right)^{1/q} \leqslant C \left(E \| \sum \epsilon_j x_j \|^2 \right)^{1/2}$$

for all $q \geqslant 2$ (property of cotype 2).

Conversely, if C_Λ is isomorphic to ℓ^1, Λ is a Sidon set (Varopoulos 1976). If C_Λ has cotype 2, Λ is a Sidon set (Pisier 1978). If C_Λ has a finite cotype, Λ is a Sidon set (Bourgain-Milman 1985, developed in Prignot 1987). This is the best that we know on the geometric properties of C_Λ as a Banach space which are equivalent to the fact that Λ is Sidon.

New characterizations of Sidon sets were given by Pisier (1983) and Bourgain (1985); without answering the questions we raised they are currently the most powerful. Bourgain proves the following implications

$$(1) \Rightarrow (2) \Rightarrow (3) \Rightarrow (4) \Rightarrow (1)$$

where

(1): Λ is a Sidon set

(2): Λ has the Rudin property on L^p norms

(3): Λ has the Pisier property, meaning that there exists a $\delta > 0$ such that each finite subset A of Λ contains a quasi-independent subset B such that $| B | > \delta | A |$ ($| |$ is the cardinal)

(4) (Bourgain's property): there exists a $\delta > 0$ such that, given $(a_\lambda)_{\lambda \in \Lambda}$, vanishing outside a finite set, there exists a quasi-independent $A \subset \Lambda$ such that

$$\sum_{\lambda \in A} | a_\lambda | \geqslant \delta \sum_{\lambda \in \Lambda} | a_\lambda | .$$

Pisier already proved (1)⇔(2) as we saw, and also (1)⇔(3) (see the references in the announcement Pisier 1983). Bourgain's proof uses random sets of integers in order to get (2)⇒(3) and an elementary and clever argument to obtain (3)⇒(4). The last implication (4)⇒(1) is obvious when you are familiar with Riesz products.

Riesz products are of the form

$$\prod_{\lambda\in\Lambda}(1+\mathrm{Re}(c_\lambda e^{i\lambda t})) \tag{11.3}$$

where Λ is a quasi-independent set of integers, and $|c_\lambda| \leq 1$ for all λ. The condition on the coefficients guarantees that the partial products are positive, and the quasi-independence of Λ guarantees that their normalized L^1-norm is 1. When Λ is quasi-independent, Riesz products provide a way to express a bounded sequence $(c_\lambda)_{\lambda\in\Lambda}$ as the restriction to Λ of the Fourier transform of a bounded measure. Here is another way to express Bourgain's property: there exists $\delta > 0$ such that, given $(a_\lambda)_{\lambda\in\Lambda}$ with $|a_\lambda| \leq \delta$ $(\lambda \in \Lambda)$, there exists a measure μ in the σ-convex envelope of Riesz products of the form (11.3), such that

$$a_\lambda = \hat{\mu}_\lambda \qquad (\lambda \in \Lambda).$$

The classical Riesz products are of the form

$$\prod_{1}^{\infty}(1+\mathrm{Re}(c_j e^{i\lambda_j t})) \tag{11.4}$$

where the λ_j are positive integers, and

$$\lambda_{j+1}/\lambda_j \geq 3 \qquad (j = 1,2,\ldots). \tag{11.5}$$

The important property of the sequence (λ_j) is that it is dissociate, meaning that there is at most one way to express any integer n as a linear combination $\sum \alpha_j\lambda_j$, $\alpha_j = -1,0,1$. Dissociate means more than quasi-independent. There is an intimate relation between Riesz products and lacunary trigonometric series (see Peyrière 1991, Fan Ai-Hua 1989), and Riesz products are a mine for examples of measures in Fourier series, and, now, for multifractal analysis. Here is a basic problem: let us fix the λ_j and consider the measure defined by the Riesz product (11.4) as a function of the sequence $c = (c_j)$ (we always suppose $|c_j| \leq 1$), denoted by μ_c. Given c and c', is it true that either $\mu_c \perp \mu_{c'}$ or $\mu_c \sim \mu_{c'}$? How to express conditions of orthogonality or equivalence in terms of c and c'? The most promising result in this direction comes from Kilmer and Saeki 1985. They randomize (11.4) in the form

$$\prod_{1}^{\infty}(1+\mathrm{Re}(c_j e^{2\pi i\omega_j} e^{i\lambda_j t})) \tag{11.6}$$

where (ω_j) is a Steinhaus sequences, and get a random measure $\mu_{\omega,c}$. Given c and c', either $\mu_{\omega,c} \perp \mu_{\omega,c'}$ a.s. or $\mu_{\omega,c} \sim \mu_{\omega,c'}$ a.s.. Moreover, the explicit condition for the a.s. equivalence can be expressed as

$$\sum_1^\infty d^2(c_j, c'_j) < \infty,$$

d being the distance in the disc given by

$$ds^2 = d\theta^2 + (1-r)^{-1/2} dr^2 \qquad (z = re^{i\theta}).$$

It is quite possible that this holds also for (11.4) under the assumption (11.5). It can be checked that it holds if (11.5) is replaced by the stronger condition

$$\sum_1^\infty \left(\frac{\lambda_j}{\lambda_{j+1}}\right)^2 < \infty.$$

(11.6) is an example of a product of independent weight functions $P_j(t, \omega_j)$. The general frame is $P_j(t, \omega_j) \geqslant 0$ and $EP_j(t, \omega_j) = 1$ for every t. The random measures defined in this way have interesting properties (see for example Kahane 1989 or Kahane 1991).

12. Divergence everywhere, convergence everywhere, and random coverings

Let me turn to a topic which is very much in the spirit of P.Z. We consider a sequence of positive functions f_n on the circle $\mathbb{T}$ and consider the series of random translates

$$\sum_1^\infty f_n(t - \omega_n).$$

For simplicity let us assume $0 \leqslant f_n(t) \leqslant 1$ for all n and t. Convergence and divergence almost everywhere create no problem; either one is almost sure according to the convergence or divergence of

$$\sum_1^\infty \int_{\mathbb{T}} f_n(t)dt.$$

How to express the almost sure divergence resp. convergence on the whole of $\mathbb{T}$, or the almost sure divergence resp. convergence on a given part of $\mathbb{T}$?

The question of divergence is far from obvious even when $f_n = 1_{[0,\ell_n]}$ and there are considerable difficulties for $f_n = c_n 1_{[0,\ell_n]}$. Let me explain the situation in both cases.

For $f_n = 1_{[0,\ell_n]}$ the question is the condition of almost sure covering of $\mathfrak{T}$, or a given part of $\mathfrak{T}$, by random intervals

$$I_n = [0, \ell_n] + \omega_n.$$

For, if covering holds a.s., it holds infinitely many times. The question goes back to Dvoretzky, and there were contributions by Erdös (though no proof was published), Billard and myself; methods and results prior to 1968 are expounded in the first edition of SRSF. Here is an idea of what was known at this time:

- when $\ell_n = \frac{1-\epsilon}{n}$, covering of $\mathfrak{T}$ has probability 0, and the uncovered set has a.s. Hausdorff dimension ϵ; subsets of $\mathfrak{T}$ of dimension $< 1 - \epsilon$ are covered, subsets of dimension $> 1 - \epsilon$ are not covered a.s.;
- when $\ell_n = \frac{1+\epsilon}{n}$, covering of $\mathfrak{T}$ is almost sure;
- when $\ell_n = \frac{1}{n}$ it was undecided.
- writing

$$k(t) = \exp \sum_1^\infty (\ell_n - t)^+$$

($(\ )^+$ denoting the positive part),

$$\int_0^1 k(t)dt < \infty$$

implies that the probability of covering $\mathfrak{T}$ is 0, and

$$\int_0^1 k(t)\mu(dt) < \infty$$

where μ is a positive measure, implies that the probability of covering the support of μ is 0. Therefore, given a Borel set $A \subset \mathfrak{T}$

$$\mathrm{Cap}_k A > 0$$

implies that A is not covered a.s..

The topic moved suddenly in 1971. Independently, B. Mandelbrot and S. Orey solved the case $\ell_n = \frac{1}{n}$, and Shepp gave the final answer for the covering of $\mathfrak{T}$. a.s. covering holds if and only if

$$\int_0^1 k(t)dt = \infty,$$

and the condition can be expressed in the elegant form

$$\sum_1^\infty \frac{1}{n^2} \exp(\ell_1 + \ell_2 + \cdots + \ell_n) = \infty,$$

assuming, as we can, $\ell_1 \geqslant \ell_2 \geqslant \ell_3 \geqslant \cdots$. Coverings of other bodies were considered. A brief history of the topic up to 1985 is given in the second edition of SRSF, therefore I skip the references.

In 1987 I discovered at the occasion of a course in Urbana that

$$\mathrm{Cap}_k A = 0$$

is necessary and sufficient for the a.s. covering of A (in case the Lebesgue measure of A is positive, this means $k \notin L^1$). Different proofs (the initial proof being the shortest) are given in a recent paper (Kahane 1990) where also covering of $\mathfrak{T}^d$ by random translates of homothetic bodies is considered (final results are obtained in the case of simplexes; the cases of balls and cubes are still open).

Let me turn to the case $f_n = c_n 1_{[0,\ell_n]}$ now, $c_n \downarrow 0$. Of course, it is interesting only in the case of covering. When

$$\forall t \sum_1^\infty f_n(t - \omega_n) = \infty, \tag{12.1}$$

it means a kind of density (depending only on (c_n)) of the sets Λ_t of integers n (depending on t) such that $t \in I_n$. This problem is introduced in the thesis of Fan Ai-Hua (Orsay, 1989).

Fan Ai-Hua proved, in the case $\ell_n = \frac{1}{n}$, that (12.1) has probability 1 when $c_n = \frac{1}{\log\log n}$. On the other hand (12.1) has probability 0 when $\sum_1^\infty \frac{c_n}{n} < \infty$, from our first observation. There is a large gap and it does not seem easy to fill it.

Here is an addition in the case $\ell_n = \frac{1}{n}$. Now (12.1) has probability 0 when

$$\sum_1^\infty \frac{c_n}{n \log n} < \infty.$$

This can be seen by integrating the series in (12.1) against a convenient random measure. On the other hand, it has probability 1 when c_n decreases and satisfies

$$\sum_1^\infty c_{\varphi(n)} = \infty,$$

where $\varphi(1) = 2$ and $\varphi(n) = 2^{\varphi(n-1)}$. The gap is still larger in this case.

The random measure to be considered is associated with the f_n by means of the usual operator Q associated with a product of independent weights of the form

$$P_n(t,\omega) = \exp(-\lambda_n 1_{[0,\ell_n]}(t - \omega_n))/(\ell_n \exp(-\lambda_n) + 1 - \ell_n).$$

The choice of the λ_n has to obey two conditions: 1) Q should operate on the Lebesgue measure dt, and give a random measure Q(dt); 2) Q(dt) should integrate the series in (12.1). An exposition for random coverings and operators Q associated with a product of independent weights is given in (Kahane 1989) (MR 91e 60152).

Convergence everywhere is also interesting when $f_n = c_n 1_{[0,\ell_n]}$. When

$$\forall t \qquad \sum f_n(t - \omega_n) < \infty \tag{12.2}$$

it means a kind of scarcity of the sets Λ_t considered before.

Let me mention a remarkable result of Fan Ai Hua (unpublished) in the case $\ell_n = \frac{a}{n}$ $(a > 0)$: (12.2) holds a.s. whenever c_n decreases and $\sum n^{-1} c_n < \infty$. On the other hand, we know that $\sum n^{-1} c_n = \infty$ implies

$$\sum f_n(t - \omega_n) = \infty \qquad \text{a.e. a.s.}$$

Therefore, assuming $f_n = c_n 1_{[0,a/n]}$ *and* (c_n) decreasing, $\sum n^{-1} c_n = \infty$ is necessary and sufficient in order to have (12.2) a.s. The monotonicity condition on (c_n) is essential, as is clear by considering lacunary series of the type

$$\sum j^{-1} \sum_{n_{2j} < n \le n_{2j+1}} \chi_n(t - \omega_n)$$

($\chi_n = 1_{[0,\ell_n]}$ given such that $\ell_n \downarrow 0$, and n_j sparse enough).

13. Bibliography

[1] S. Banach. Uber eine eigenschaft der lakunären trigonometrischen reihen. *Studia Math.*, 2:207–220, 1930.

[2] Nina Bari. *Trigonometričeskie Ryadi.* Moscou, 1961.

[3] P. Billard. Séries de Fourier aléatoirement bornées, continues, uniformément convergentes. *Studia Math.*, 22:309–329, 1963.

[4] P. Billard. Séries de Fourier aléatoirement bornées, continues, uniformément convergentes. *Ann. Scient. Ec. Norm. Sup.*, 82:131–179, 1965.

[5] E. Borel. Sur les séries de Taylor. *C.R. Acad. Sci. Paris*, 123:1051–1052, 1896.

[6] E. Borel. Sur les séries de Taylor. *Acta Math*, 20:243–247, 1897.

[7] E. Borel. *Oeuvres.* CNRS Paris, 1972. Tome I.

[8] J. Bourgain. Sidon sets and Riesz products. *Ann. Inst. Fourier (Grenoble)*, 35(1):137–148, 1985.

[9] J. Bourgain and V. Milman. Dichotomie du cotype pour les espaces invariants. *C.R. Acad. Sci. Paris*, 300:263–266, 1985.

[10] B. Davis. On Brownian slow points. *Z. für Wahrscheinlichkeitstheorie*, 64:359–367, 1983.

[11] B. Davis and E. Perkins. Brownian slow points: the critical case. *Annals of Probability*, 13:779–803, 1985.

[12] S.W. Drury. Sur les ensembles de Sidon. *C.R. Acad. Sci. Paris*, 271:162–163, 1970.

[13] A. Dvoretzky. On the oscillation of the Brownian motion process. *Israël J. Math.*, 1:212–214, 1963.

[14] Fan Ai-Hua. Sur la convergence de séries trigonométriques lacunaires presque partout par rapport à des produits de Riesz. *C.R. Acad. Sci. Paris*, 309:295–298, 1989.

[15] G. Freud. Uber trigonometrische approximation und fouriersche reihen. *Math. Zeitschr*, 78:252–262, 1962.

[16] G. Freud. On Fourier series with Hadamard gaps. *Studia Math.*, 1:87–96, 1966.

[17] D.J.H. Garling. Sums of Banach space valued random variables. Mimeographed lecture notes, 1977.

[18] J. Hoffmann-Jørgensen. Sums of independent Banach space valued random variables. *Studia Math.*, 52:159–186, 1974.

[19] J. Hoffmann-Jørgensen. Probability in Banach spaces. In *Ecole d'été de probabilités de Saint-Flour 1976*, volume 598 of *Lecture Notes in Mathematics*, pages 1–186. Springer-Verlag, 1977.

[20] S.V. Hruščev. Teorema men'sova ob ispravlenii i Gaussovskie protsessi. *Trudy Matem. Inst. Steklov*, 155:151–181, 1981.

[21] S.V. Hruščev, J.-P. Kahane, and Y. Katznelson. Mouvement brownien et séries de Fourier absolument convergentes. *C.R. Acad. Sci. Paris*, 292:389–391, 1981.

[22] M. Izumi, S.I. Izumi, and J.-P. Kahane. Théorèmes élementaires sur les séries de Fourier lacunaires. *J. Anal. Math.*, 14:235–246, 1965.

[23] J.-P. Kahane. Sur les fonctions moyenne-périodiques bornées. *Ann. Inst. Fourier (Grenoble)*, 7:293–314, 1957.

[24] J.-P. Kahane. Sur un théorème de Paul Malliavin. *C.R. Acad. Sci. Paris*, 248:2943–2944, 1959.

[25] J.-P. Kahane. Sur les sommes vectorielles $\sum \pm u_n$. *C.R. Acad. Sci. Paris*, 259:2577–2580, 1964.

[26] J.-P. Kahane. Images browniennes des ensembles parfaits. *C.R. Acad. Sci. Paris*, 263:613–615, 1966.

[27] J.-P. Kahane. A metric condition for a circular set to be a set of uniqueness. *J. Approx. Th.*, 2:233–246, 1969.

[28] J.-P. Kahane. Sur l'irrégularité locale du mouvement Brownien. *C.R. Acad. Sci. Paris*, 278:331–333, 1974.

[29] J.-P. Kahane. Sur les zéros et les instants de ralentissement du mouvement brownien. *C.R. Acad. Sci. Paris*, 282:431–433, 1976.

[30] J.-P. Kahane. Sur les polynômes à coefficients unimodulaires. *Bull. London Math. Soc.*, 12:321–342, 1980.

[31] J.-P. Kahane. Quatre leçons sur les homéomorphismes du cercle et les séries de Fourier. In *Topics in modern harmonic analysis*, volume II, pages 956–990, May–June 1982. Proceedings of a seminar held in Torino and Milano.

[32] J.-P. Kahane. Slow points of Gaussian processes. In *Conference in harmonic analysis in the honour of Antoni Zygmund*, volume I, pages 67–83. Wadsworth, 1983.

[33] J.-P. Kahane. *Some random series of functions*. Cambridge University Press, 2nd edition, 1985.

[34] J.-P. Kahane. Geza Freud and lacunary Fourier series. *J. Approx. Th.*, 46(1):51–57, 1986.

[35] J.-P. Kahane. Distribution des valeurs des fonctions analytiques Gaussiennes. *Colloquium Math.*, 51:175–187, 1987.

[36] J.-P. Kahane. Random multiplication, random coverings, multiplicative chaos. In *Analysis at Urbana I (Urbana 1986-87)*, volume 137 of *London Math. Soc. Lect. Note Series*, pages 196–255. Cambridge University Press, 1989.

[37] J.-P. Kahane. Recouvrements aléatoires et théorie du potentiel. *Colloquium Math.*, 40–41:387–411, 1990.

[38] J.-P. Kahane. From Riesz products to random sets. Sendai conference, 1990, 1991.

[39] J.-P. Kahane and Y. Katznelson. Homéomorphismes du cercle et séries de Fourier absolument convergentes. *C.R. Acad. Sci. Paris*, 292:271–273, 1981.

[40] J.-P. Kahane and Y. Katznelson. Séries de Fourier des fonctions bornées. In *Studies in Pure Mathematics to the memory of Paul Turan*, pages 395–410. Birkhäuser Verlag, 1983. Preprint Orsay, 1978.

[41] Y. Katznelson. On a theorem of Menchoff. *Proc. Amer. Math. Soc.*, 53:396–398, 1975.

[42] S.J. Kilmer and S. Saeki. On Riesz product measures; mutual absolute continuity and singularity. *Ann. Inst. Fourier (Grenoble)*, 38(2):63–93, 1988.

[43] A. Kolmogoroff. Une contribution à l'étude de la convergence des séries de Fourier. *Fund. Math.*, 5:96–97, 1924.

[44] T.W. Körner. On a polynomial of J.S. Byrnes. *Bull. London Math. Soc.*, 12:219–224, 1980.

[45] S. Kwapien. A theorem on the Rademacher series with vector coefficients. In *Probability in Banach spaces*, volume 526 of *Lecture Notes in Mathematics*, pages 157–158. Springer-Verlag, 1976.

[46] M. Ledoux and M. Talagrand. Probability in Banach spaces. *Ergebnisse der Mathematik*, 23(3), 1991. 480 pages.

[47] K. De Leeuw, J.-P. Kahane, and Y. Katznelson. Sur les coefficients de Fourier des fonctions continues. *C.R. Acad. Sci. Paris*, 285:1001–1003, 1977.

[48] P. Lévy. *Processus stochastiques et mouvement Brownien*. Gauthier-Villars, Paris, 1948.

[49] J.E. Littlewood and C. Offord. On the distribution of zeros and a-values of a random integral function. *Annals of Mathematics*, 49:885–952, 1948.

[50] J.E. Littlewood and C. Offord. *Idem*, 50:990–991, 1949.

[51] P. Malliavin. Sur l'impossibilité de la synthèse spectrale sur la droite. *C.R. Acad. Sci. Paris*, 248:2155–2157, 1959.

[52] M.B. Marcus and G. Pisier. Necessary and sufficient conditions for the uniform convergence of random trigonometric series. In *Lecture notes series 50*. Aarhus, Denmark, 1978.

[53] B. Maurey and G. Pisier. Séries de variables aléatoires vectorielles indépendantes et géométrie des espaces de Banach. *Studia Math.*, 58:45–90, 1976.

[54] T. Murai. Une remarque sur la distribution des valeurs des séries de Taylor aléatoires. *C.R. Acad. Sci. Paris*, 287:931–934, 1978.

[55] T. Murai. Value distribution of random Taylor series in the unit disc. *Journal London Math. Soc.*, 24:480–494, 1981.

[56] C. Offord. The distribution of the values of a random function in the unit disc. *Studia Math.*, 41:71–106, 1972.

[57] A.M. Olevskii. Sučectvovanie funktsii s neustranimymi osobennostjami Carlemana. *Dokladi Akad. Nauk SSSR*, 238(4):796–799, 1978.

[58] A.M. Olevskii. Zamena peremennoy i absojutnaja shodimost pjada Fourier. *Dokladi Akad. Nauk SSSR*, 256:284–287, 1981.

[59] S. Orey and S.J. Taylor. How often on a Brownian path does the law of the iterated logarithm fail? *Proc. London Math. Soc.*, 28(3):174–192, 1974.

[60] R.E.A.C. Paley and N. Wiener. Fourier transforms in the complex domain. In *Coll. Amer. Math. Soc.* American Mathematical Society, 1934.

[61] R.E.A.C. Paley, N. Wiener, and A. Zygmund. Notes on random functions. *Math. Zeitschr*, 37:647–668, 1933.

[62] R.E.A.C. Paley and A. Zygmund. On some series of functions. In *Proceedings of the Cambridge Philosophical Society*, volume 26, pages 337–357, 458–474, 1930.

[63] R.E.A.C. Paley and A. Zygmund. On some series of functions. In *Proceedings of the Cambridge Philosophical Society*, volume 28, pages 190–205, 1932.

[64] E. Perkins. On the Hausdorff dimension of the Brownian slow points. *Z. für Wahrscheinlichkeitstheorie*, 64:369–399, 1983.

[65] J. Perrin. *Les atomes.* Paris, 1913.

[66] J. Peyrière. Almost everywhere convergence of lacunary trigonometric series with respect to Riesz products. *Australian J. Math.*, 1991.

[67] G. Pisier. Ensembles de Sidon et processus Gaussiens. *C.R. Acad. Sci. Paris*, 286:671–674, 1978.

[68] G. Pisier. Les inégalités de Khintchine-Kahane d'après C. Borell. In *Séminaire sur la géométrie des espaces de Banach 1977–78.* Ecole Polytechnique, 1978.

[69] G. Pisier. A remarkable homogeneous Banach algebra. *Israël J. Math.*, 34:38–44, 1979.

[70] G. Pisier. Arithmetic characterizations of Sidon sets. *Bull. AMS*, 8:87–89, 1983.

[71] G. Pisier. *The volume of convex bodies and Banach space geometry*. Cambridge University Press, 1989.

[72] P. Prignot. *Dichotomie du cotype pour les espaces invariants*. Number 87-02, I1-I50. Publications mathématiques d'Orsay, 1987.

[73] D. Rider. Randomly continuous functions and Sidon sets. *Duke Math. J.*, 42:759–764, 1975.

[74] W. Rudin. Trigonometric series with gaps. *J. Math. Mech.*, 9:203–227, 1960.

[75] C. Ryll-Nardzewski. D. Blackwell's conjecture on power series with random coefficients. *Studia Math.*, 13:30–36, 1953.

[76] A.A. Saakian. Integral'nie moduli gladkosti i koeffitsienti Fourier u superpozitsii funktsii. *Math. USSR Sbornik*, pages 597–608, 1979.

[77] R. Salem. Sets of uniqueness and sets of multiplicity 2. *Trans. Amer. Math. Soc.*, 56:32–49, 1944. See § 13.

[78] R. Salem. On singular monotonic functions whose spectrum has a given Hausdorff dimension. *Arkiv Math.*, 1:353–365, 1950.

[79] R. Salem. *Oeuvres mathématiques*. Hermann, Paris, 1967.

[80] R. Salem and A. Zygmund. Some properties of trigonometric series whose terms have random signs. *Acta Math*, 91:245–301, 1954.

[81] H. Steinhaus. Uber die wahrscheinlichkeit dafür, daßder konvergenzkreis einer potenzreihe ihre natürliche grenze ist. *Math. Zeitschr*, 21:408–416, 1929.

[82] S. Szidon. Verallgemeinerung eines satzes über die absolute konvergenz von Fourierreihen mit lücken. *Math. Ann.*, 97:675–676, 1927.

[83] S.J. Taylor. Regularity and irregularities on a Brownian path. *Ann. Inst. Fourier (Grenoble)*, 24:195–204, 1974.

[84] N. Wiener. Differential space. *Journal of Mathematics and Physics*, 2:131–174, 1923.

[85] N. Wiener. Generalized harmonic analysis. *Acta Math*, 55:117–258, 1930.

[86] A. Zygmund. On the convergence of lacunary trigonometric series. *Fund. Math.*, 16:90–107, 1930.

[87] A. Zygmund. On lacunary trigonometric series. *Trans. Amer. Math. Soc.*, 34:435–446, 1932.

[88] A. Zygmund. On continuability of power series. *Acta Litt. Sci. Szeged*, 6:80–84, 1933.

[89] A. Zygmund. On the continuability of power series. *Acta Litt. Sci. Szeged*, 6:80–84, 1933.

[90] Antoni Zygmund. *Selected papers of Antoni Zygmund.* Kluver, 1989. 3 volumes.

Empirical characteristic functional analysis and inference in sequence spaces

Uluğ Çapar
Department of Mathematics
Bilkent University
Ankara 06533 Turkey
capar@trbilun.bitnet

Abstract The concept of empirical characteristic functionals in certain sequence spaces is proposed. The convergence of the related empirical measures and processes are linked to the idea of weak convergence along projective systems. A review of multivariate empirical characteristic function techniques is included. Some hints are given for the statistical inference on probability distributions in sequence spaces.

1. Introduction

The empirical characteristic functions, following the initiation of their systematic study in the pioneering paper by Feuerverger and Mureika [9], have proved to be very efficient tools for stochastic analysis and inference problems. As many distributional properties such as stable distributions and distributions in abstract spaces can be characterized solely by characteristic functions (or functionals), it is natural that the inference problems related to such cases should be more favorably treated by empirical characteristic functions rather than empirical distribution functions or densities.

Let $(S, \mathcal{T}, \mathcal{P})$ be a probability space and let $\Theta = (\Theta_1, \cdots, \Theta_n)$ be an $\mathcal{T} \leftrightarrow \mathcal{B}^n$ measurable mapping of S into R^n, inducing a probability measure μ_n in $(R^n, \mathcal{B}^n)$. Then m independent observations $\Theta_j = (\Theta_{j1}, \cdots, \Theta_{jn})$, $(j = 1, 2, \cdots, m)$ of the random (finite) sequence $\Theta(\omega)$ will yield a tableau of the following form:

$$\begin{matrix} \theta_{11} & \theta_{12} & \theta_{1n} & \cdots \\ \theta_{21} & \theta_{22} & \theta_{2n} & \cdots \\ \vdots & \vdots & \vdots & \cdots \\ \theta_{m1} & \theta_{m2} & \theta_{mn} & \cdots \\ \vdots & \vdots & \vdots & \end{matrix} \tag{1.1}$$

J. S. Byrnes et al. (eds.), Probabilistic and Stochastic Methods in Analysis, with Applications, 517–534.
© 1992 *Kluwer Academic Publishers. Printed in the Netherlands.*

so that $\Theta_j(\omega) = (\theta_{j1}, \cdots, \theta_{jn})$, $(j = 1, \cdots, m)$. For increasing size of observations and the later reference to infinite sequences, the double array (1.1) has been viewed as an expansive one. The empirical characteristic function is defined by

$$\begin{aligned}\hat{\chi_{nm}}(t,\omega) &:= \int_{R^n} \exp(i(t \cdot x))\, d\lambda_{nm}(\omega, x) \\ &= \frac{1}{m} \sum_{j=1}^{m} \exp(i(t \cdot \Theta_j(\omega))) \\ &= \frac{1}{m} \sum_{j=1}^{m} \exp(i \sum_{s=1}^{n} t_s \theta_{js}), \qquad t \in R^n \end{aligned} \tag{1.2}$$

where λ_{nm} is the empirical distribution associated with (1.1), i.e.:

$$\lambda_{nm}(\omega) = \frac{1}{m} \sum_{j=1}^{m} \delta(\Theta_j(\omega)) \tag{1.3}$$

($\delta(x)$: concentrated unit mass at $x \in R^n$).

By the Glivenko-Cantelli theorem, λ_{nm} almost surely uniformly converges to μ_n on R^n. Furthermore it is well-known that on each bounded set $K \subset R_n$ that

$$\sup_{t \in S} |\hat{\chi_{nm}}(t) - \chi_n(t)| \to 0 \text{ a.s.} \tag{1.4}$$

where $\chi_n(t) = \int_{R^n} \exp(i(t \cdot x))\, d\mu_n(x)$. Furthermore if μ_n is singular with respect to Lebesgue measure on R^n, the supremum can be taken over all of R^n [4, 9]. Several estimates have been given for the rate of convergence in (1.4), cf. [4, 11]; see also Section 5.

More interesting and stronger modes of convergence occur in relation to certain stochastic processes (fields) associated with empirical characteristic functions. Two of the most important ones are:

1)

$$Y_m(t) = m^{\frac{1}{2}}(\hat{\chi_{nm}}(t) - \chi_n(t)) \qquad t \in R^n \tag{1.5}$$

2)

$$Z_m(t) = m^{\frac{1}{2}}\{|\hat{\chi_{nm}}(S_m^{-\frac{1}{2}} t)|^2 - |\chi_n(t)|^2\} \qquad t \in R^n \tag{1.6}$$

where in 2, S_m is the sample covariance matrix and $\hat{\chi_{nm}}(S_m^{-\frac{1}{2}}t)$ is the Mahalonobis transform of χ_{nm}, under the assumption that the appropriate conditions exist. 1 should be regarded as a complex-valued stochastic field. Finite dimensional distributions of the process $Y_m(t)$ converge by the multivariate central limit theorem to those of a complex valued n-variate Gaussian random field $Y^{\mu_n}(t)$, which can be represented by the stochastic integral

$$Y^{\mu_n}(t) = \int_{R^n} \exp(i(t \cdot x))\, dB^{\mu_n}(x), \qquad t \in R^n,$$

$B^{\mu_n}(x)$ being an n-variate Brownian bridge process associated with the measure μ_n. In other words B^{μ_n} is an n-variate Gaussian process satisfying for $x, y, x' \in R^n$:

$$E[B^{\mu_n}(x)] = 0$$

$$E[B^{\mu_n}(x)B^{\mu_n}(y)] = \mu_n[\{x' : x' \leqslant x \wedge y\}] - \mu_n[\{x' : x' \leqslant x\}]\mu_n[\{x' : x' \leqslant y\}]$$

$$\lim_{x_j \to -\infty} B^{\mu_n}(x_1, \cdots, x_n) = 0, \qquad j = 1, \cdots, n$$

$$\lim_{(x_1, \cdots, x_n) \to (\infty, \cdots, \infty)} B^{\mu_n}(x_1, \cdots, x_n) = 0.$$

It is shown that $Y^{\mu_n}(t)$ has the same covariance structure as $Y_m(t)$, i.e., $E[Y^{\mu_n}(t)\overline{Y^{\mu_n}(s)}] = \chi_n(t-s) - \chi_n(t)\chi_n(-s)$ and $EY^{\mu_n}(t) = 0$.

For $T > 0$ let a compact set K_n be given by $K_n = [-T, T]^n$. The processes $Y_m(t)$ induce probability measures in $\mathcal{C}^2(K_n)$. These measures will not converge weakly to the distribution of $Y^{\mu_n}(t)$ unless the latter process has continuous paths. As worked out in [4, 12], Y_m converges weakly to Y^{μ_n} in $\mathcal{C}^2(K_n)$ if and only if

$$\int_0^{\frac{1}{2}} \frac{\psi_n(s)}{s(\log \frac{1}{s})^{\frac{1}{2}}}\, ds < \infty \tag{1.7}$$

where $\psi_n(s)$ is the non-decreasing rearrangement of $(1 - \mathrm{Re}\chi_n(t))^{\frac{1}{2}}$.

To work out the weak limit of the process in 2 is much more difficult than that of 1. Under the null hypothesis "the measure μ_n is normal with some expected value vector and some non-singular covariance matrix," however, the process becomes

$$Z_m(t) = m^{\frac{1}{2}}\{|\hat{\chi_{nm}}(S_m^{-\frac{1}{2}}t)|^2 - e^{-(t \cdot t)}\} \tag{1.8}$$

and it converges weakly in $\mathcal{C}(K_n)$ to the sample continuous Gaussian process $Z^{\mu_n}(t)$ satisfying $Z^{\mu_n}(t) = Z^{\mu_n}(-t)$, $E[Z^{\mu_n}(t)] = 0$ and having the covariance structure

$$\rho_{st} = E[Z^{\mu_n}(s)Z^{\mu_n}(t)] = 4e^{-(s \cdot s)-(t \cdot t)}\{\cosh((s \cdot t)) - 1 - \frac{1}{2}(s \cdot t)^2\}, \tag{1.9}$$

(cf. [4]). $Z(t)$ has the further property that $Z(s)$ and $Z(t)$ are independent for any pair of orthogonal vectors s and t.

There has been little effort so far to generalize the empirical characteristic function methods to infinite dimensional spaces, perhaps mainly due to the fact that it is difficult to find genuine examples whereby random elements of such spaces can be observed. Feuerverger and McDunnough [8] considered an extension to strictly stationary ergodic time series and introduced the concept of poly-characteristic functions and their empirical version. This is, for fixed k, basically the characteristic function of the finite dimensional random vectors $(\Theta_r, \Theta_{r-1}, \cdots, \Theta_{r-k})$ related to a discrete-time stationary process $\Theta = (\Theta_1, \Theta_2, \ldots)$.

Çapar in [3] attempted a further generalization to discrete-time non-stationary processes. Partially observed trajectories of such processes will yield, in a limiting sense, random elements of certain sequence spaces. In Sections 2 and 3 we outline the formalism and the basic properties related to such a generalization.

2. Empirical characteristic functionals in sequence spaces and related properties

Let E be a real sequence space with a specified topology and let $\mathcal{B}_E$ be its Borel σ-field. The *characteristic functional* of a probability distribution μ on $(E, \mathcal{B}_E)$, is given by

$$\chi^{\mu}(f) := \int_E \exp(i < f, x >) d\mu(x), f \in F$$

Here F will be

1) the sequence space G if E satisfies $E = G^*$ ($(\cdot)^*$: continuous dual)
2) E^* if 1 does not hold.

Some examples of (E, F) pairs would be (R^N, R_0^N), (l_1, c_0), (l_∞, l_1), (l_p, l_q), (c_0, l_1) etc. (R_0^N : the space of all sequences with finite length, $c_0 = \{x \in R^N : \lim_i x_i = 0\}$, $1/p + 1/q = 1$).

If E is reflexive, 1 and 2 yield the same F. Also for certain E spaces, the values of χ^{μ} on G may uniquely determine its values on the whole E^*, (e.g., $E = l_1$). The canonical projection onto the first n coordinates will be indicated by π_n. The projection of μ on $(R^n, \mathcal{B}^n)$ and its restriction to $\pi_n^{-1}(\mathcal{B}^n)$ are denoted by $\tilde{\mu}_n$ and μ_n respectively. A superscript $(\cdot)^\circ$ on a finite sequence will indicate augmentation to an infinite sequence by filling out the rest of the positions by zero.

Now let Θ be an $\mathcal{T} \leftrightarrow \mathcal{B}_E$ measurable mapping of S into E, or more generally into R^N (the space of all real sequences), such that one of the sufficient conditions for the induced probability measure to be concentrated on

the particular sequence space is satisfied. We may suppose that the random sequence $\Theta(\omega)$ is generated by a non-stationary random process or by any other source which can be observed any number of times independently under identical conditions. Such observations will yield a double array of the same form as (1.1), where the rows represent the observed components of independent random sequences $\Theta_m(\omega)$ $(m = 1,2,\ldots)$. By assumption, Θ and Θ_m $(m = 1,2,\ldots)$ induce the same probability distribution, say μ, on $(E,\mathcal{B}_E)$.

Definition 2.1. The *empirical characteristic distribution* λ_{nm} associated with (1.1) is the random probability measure

$$\lambda_{nm}(\omega) := \frac{1}{m}\sum_{j=1}^{m}\delta(\pi_n^{-1}\pi_n\Theta_j(\omega))$$

defined on $(E,\pi_n^{-1}(\mathcal{B}^n))$ and concentrated on m atoms $\pi_n^{-1}\pi_n\Theta_j(\omega)$, for $(j = 1,\cdots,m)$. (Thus $\tilde{\lambda}_{nm} := \pi_n\lambda_{nm}$ is concentrated on m points in R^n.)

Definition 2.2. The *empirical characteristic functional* (e.c.fl.) $\hat{\chi}_{nm}$ associated with (1.1) is defined as:

$$\hat{\chi}_{nm}(f,\omega) := \int_E \exp(i\langle(\pi_n f)^\circ, x\rangle)\lambda_{nm}(\omega, dx), \qquad f \in F$$

The e.c.fl. can alternatively be expressed as:

$$\hat{\chi}_{nm}(f,\omega) = \int_{R^n}\exp[i((\pi_n f)\cdot y)]\tilde{\lambda}_{nm}(\omega, dy) = \frac{1}{m}\sum_{j=1}^{m}\exp(i\sum_{k=1}^{n} f_k\theta_{jk})$$

where $\langle .,. \rangle$ denotes the bilinear form of the E,F duality. In the following Glivenko-Cantelli type theorem $\chi_n^\mu(f)$ is the characteristic functional of the projected destribution, i.e.:

$$\chi_n^\mu(f) := \int_E \exp(i < (\pi_n f)^\circ, x >)\, d\mu_n(x)$$

$$= \int_{R^n}\exp[i((\pi_n f)\cdot y)]\mu_n(dy) \qquad f \in F. \quad (2.1)$$

Theorem 2.3.

- **i:** $\lim_{n\to\infty}\chi_n^\mu(f) = \chi^\mu(f)$, for $f \in F$. The convergence is uniform on compact subsets of F if (E,F) : (R^N, R_0^N) or (l_1, c_0) or (l_p, l_q), $(p \geq 1)$. (R_0^N: The space of all sequences with finite length).
- **ii:** $\lim_{n,m\to\infty}\hat{\chi}_{nm}(f) = \chi^\mu(f)$ a.s., if $(E,F) = R^N, R_0^N)$ or if Θ is a.s. bounded and $(E,F) = (c_0, l_1), (l_p, l_q), (l_\infty, l_1)$.
- **iii:** The convergence in ii) is uniform on compact subsets of F if $(E,F) = (R^N, R_0^N)$ or (l_p, l_q).

Proof. [2, 3] ∎

The study of convergence of empirical measures in sequence spaces and convergence of measures induced by the empirical process create some difficulty. For λ_{nm} (or $\tilde{\lambda}_{nm}$) and μ are not defined on a common underlying measurable space. There is a similar situation for the measures induced by the finite dimensional empirical processes and the distribution of the limiting process.

In such instances the abstract concept of 'weak convergence along a projective system', which is outlined in the next section, has proved to be useful. Alternative treatments via cylindrical measures or set martingales in the limit can also be given.

3. Weak convergence of probability measures along a projective system

Following the notation and the terminology of [15], we consider projective systems of Hausdorff topological spaces of the form

$$\{(\Omega_\alpha, \pi_{\alpha\beta})_{\alpha \preceq \beta} : \alpha, \beta \in D\}$$

having the projective limit $\Omega = \varprojlim(\Omega_\alpha, \pi_{\alpha\beta})$ with continuous canonical mappings $\pi_\alpha : \Omega \to \Omega_\alpha$. The right-filtering partially ordered set D and all other symbols are assumed to have their usual meaning and properties.

In relation with such a projective system we consider two hypotheses:

Hypothesis R_1: $\pi_\alpha^{-1}, (\alpha \in D)$ commutes with the operation of forming the rim, i.e., $\pi_\alpha^{-1}(rA) = r(\pi_\alpha^{-1}A)$, where $r(A) = A \cap \overline{A^c}$.

Hypothesis R_2: For every $\alpha \in D, \pi_\alpha \mathcal{B} \subset \mathcal{B}_\alpha$ holds, where $\mathcal{B}$ and $\mathcal{B}_\alpha$ are Borel σ-fields in Ω and Ω_α respectively, the former being with respect to the projective limit topology.

Hypothesis R_1 is satisfied by many important projective systems including those where each $\pi_\alpha (\alpha \in D)$ is an open mapping. (In this case Hypothesis R_1 is actually equivalent to the stronger property $\pi_\alpha^{-1}(bA) = b(\pi_\alpha^{-1}A) (b(\cdot) = \text{boundary})$. This would be the case if for instance the projective limit topology coincides with the product topology.

Hypothesis R_2 would be ensured, e.g., if Ω and $\Omega_\alpha (\alpha \in D)$ are Polish spaces and $\mathcal{B}$ and $\mathcal{B}_\alpha$ are replaced by σ-fields of subsets which are measurable for the completion of probability measures on Borel sets, thus containing anaytic sets. (cf. [7, pp. 391]).

Definition 3.1. Let $\mathcal{P} = \{(\Omega_\alpha, \pi_{\alpha\beta})_{\alpha \preceq \beta} : \alpha, \beta \in D\}$ be a projective system of metrizable spaces with the projective limit $\Omega = \varprojlim(\Omega_\alpha, \pi_{\alpha\beta})$ furnished with the projective limit topology and let the σ-fields $\mathcal{B}_\alpha$ and $\mathcal{B}$, in Ω_α and

Ω respectively, satisfy Hypothesis R_2. If $\{\mu_\alpha, \alpha \in D\}$ is a net of probability measures defined on measurable spaces $(\Omega_\alpha, \mathcal{B}_\alpha), \alpha \in D$, we say that μ_α *converges weakly along the projective system* $\mathcal{P}$ *to a probability measure* μ *on* $\mathcal{B}$ denoted by $\mu_\alpha \overset{w-\mathcal{P}}{\to} \mu$, if for every μ-continuity set $B \in \mathcal{B}$

$$\lim_\alpha \mu_\alpha(\pi_\alpha B) = \mu(B)$$

holds.

Note. In the case of a Polish projective limit, $\mathcal{B}$ and $\mathcal{B}_\alpha$ may be chosen as the σ-fields obtained by the completion of Borel probability measures μ and $\pi_\alpha(\mu)$ respectively.

The following version of Alexandroff's second theorem is valid for this type of convergence.

Theorem 3.2. Let $\{\mu_\alpha, \alpha \in D\}$ be a net of probability measures on a projective system $\mathcal{P}$ as described in Definition 3.1, satisfying further hypothesis R_1. If Ω is sufficiently rich, (i.e., $\pi_\alpha \Omega = \Omega_\alpha$) and μ is tight on Ω, then the following are equivalent:

1) $\mu_\alpha \overset{w-\mathcal{P}}{\to} \mu, \alpha \in D$.
2) Let $f \in C(\Omega_\beta), \beta \in D$ and if $\alpha \in D, \alpha \succeq \beta$, let f^α and f^Ω be the lifts of f to Ω_α and Ω respectively, (i.e., $f^\alpha(x) = f(\pi_{\beta\alpha} x)$, $f^\Omega(x) = f(\pi_\beta x)$). Then $\lim_{\alpha \succeq \beta} \mu_\alpha(f^\alpha) = \mu(f^\Omega)$.
3) The same conclusion as in 2, $C(\Omega_\beta)$ being replaced by the set of bounded uniformly continuous functions.
4) For $\beta \in D$, let $F \in \mathcal{B}_\beta$ be a closed subset of Ω_β, then

$$\limsup_{\alpha \succeq \beta} \mu_\alpha(\pi_{\beta\alpha}^{-1} F) \leqslant \mu(\pi_\beta^{-1} F).$$

5) For $\beta \in D$, let $G \in \mathcal{B}_\beta$ be an open subset of Ω_β, then

$$\liminf_{\alpha \succeq \beta} \mu_\alpha(\pi_{\beta\alpha}^{-1} G) \geqslant \mu(\pi_\beta^{-1} G).$$

Proof. [2]. ∎

We can also state the following tightness versus relative compactness type result.

Theorem 3.3. Let the projective system $\mathcal{P}$ as described in Definition 3.1. have a separable, metrizable projective limit. Further assume that for each $\epsilon > 0$, there exists a compact subset K_ϵ of Ω such that $\mu_\alpha(\pi_\alpha K_\epsilon) \geqslant 1 - \epsilon$ for every

$\alpha \in D$ is satisfied by a net $\{\mu_\alpha\}_{\alpha\in D}$ of probability measures. Then $\{\mu_\alpha\}$ has a subnet converging along the projective system $\mathcal{P}$.

Proof. Let μ_α be the image of μ_α on $\pi_\alpha^{-1}\mathcal{B}_\alpha$, i.e., $\mu_\alpha \circ \pi_\alpha^{-1} = \mu_\alpha$ and let $\mu_\alpha^*(\alpha \in D)$ be any set of extensions of μ_α to $(\Omega, \mathcal{B})$. Such extensions always exist but may consist of measures which are only finitely additive. On the other hand Ω can be imbedded topologically into a compact metric space $\hat{\Omega}$. For any μ_α^*, let m_α be the measure on $\hat{\Omega}$ defined by $m_\alpha(B) = \mu_\alpha^*(B \cap \Omega)$ for all Borel subsets of $\hat{\Omega}$. The net $\{m_\alpha\}$ has a subnet, say $\{m_{N_\alpha}\}_{\alpha\in D}$ converging weakly to a σ-additive measure ν on $\hat{\Omega}$. For any index α, let $C_{\epsilon,\alpha} = \pi_\alpha^{-1}\pi_\alpha K_\epsilon$, which is compact in $\hat{\Omega}$. Let β be a fixed index, then by the ordinary weak convergence of measures and the fact that $C_{\epsilon,\alpha} \downarrow$:

$$\begin{aligned}\nu(C_{\epsilon,\beta}) &\geqslant \limsup_{\alpha \succeq \beta} m_{N_\alpha}(C_{\epsilon,\beta}) \geqslant \limsup_{\alpha \succeq \beta} m_{N_\alpha}(C_{\epsilon,N_\alpha}) \\ &= \limsup_{\alpha \succeq \beta} \mu_{N_\alpha}(\pi_{N_\alpha} K_\epsilon) \geqslant 1 - \epsilon.\end{aligned}$$

By considering a sequence $\epsilon_n \downarrow 0$, this set of inequalities implies along the same line as in the proof of Theorem 6.7 of [14], that there exists a measure μ on Ω such that $\nu(B) = \mu(B \cap \Omega)$ for any Borel set $B \subset \hat{\Omega}$. Let now F be any closed subset of Ω_β. There exists a closed set D in $\hat{\Omega}$ such that $\pi_\beta^{-1}F = D \cap \Omega$. As $m_{N_\alpha} \xrightarrow{w} \nu$ on $\hat{\Omega}$, we have $\limsup_\alpha m_{N_\alpha}(D) \leqslant \nu(D)$. This is the same thing as stating $\limsup_\alpha \mu_{N_\alpha}^*(\pi_\beta^{-1}F) \leqslant \mu(\pi_\beta^{-1}F)$. Now for $N_\alpha \succeq \beta$:

$$\begin{aligned}\limsup_\alpha \mu_{N_\alpha}^*(\pi_\beta^{-1}F) &= \limsup_\alpha \mu_{N_\alpha}(\pi_{N_\alpha}^{-1}\pi_{\beta N_\alpha}^{-1}F) \\ &= \limsup_{N_\alpha \succeq \beta} \mu_{N_\alpha}(\pi_{\beta N_\alpha}^{-1}F) \leqslant \mu(\pi_\beta^{-1}F).\end{aligned}$$

Then by part 3 of Theorem 3.2, $\mu_{N_\alpha} \xrightarrow{w-\mathcal{P}} \mu$. ∎

In the definition of convergence along projective systems, measures can be replaced by measurable mappings. Thus if $(S, \mathcal{T}, P)$ is a probability space, $\mathcal{P}$ a projective system and $U_\alpha : S \to \Omega_\alpha (\alpha \in D)$ is a net of $\mathcal{T} \leftrightarrow \mathcal{B}_\alpha$ measurable mappings we say that U_α converges to an $\mathcal{T} \leftrightarrow \mathcal{B}$ measurable mapping $U : S \to \Omega$ along the projective system $\mathcal{P}$, and let $\lim_\alpha U_\alpha \xrightarrow{w-\mathcal{P}} U$ if the probability measures μ_α induced by U_α on $(\Omega_\alpha, \mathcal{B}_\alpha)$ converge weakly along $\mathcal{P}$ to the measure induced by U on $(\Omega, \mathcal{B})$.

4. Weak convergence of empirical measures and processes in the sequence spaces

Returning to the probabilistic scheme and terminology of Section 2, we can describe the convergence of empirical measures as follows.

Theorem 4.1. Let μ be a probability measure induced on R^N by Θ and let $(R^n, \mathcal{B}^n, \tilde{\mu}_n)$ and $(R^n, \mathcal{B}^n, \lambda_{nm})$ extend over all analytic sets (e.g., obtained by completion). If $m_n \to \infty$ as $n \to \infty$, then $\lambda_{nm_n} \overset{w-\mathcal{P}}{\to} \mu$ a.s. along the projective system $\mathcal{P} = \{(R^n, \pi_{n_1 n_2})_{n_1 < n_2} : n_1, n_2 \in N\}$.

Proof. Let $\lambda^*_{nm_n}$ $(n = 1, 2, \ldots)$ be a set of arbitrary extensions of λ_{nm_n} from $\pi_n^{-1}(\mathcal{B}^n)$ to $\mathcal{B}_{R^N}$ (such extensions always exist). Since $\hat{\chi}_{nm_n}(f)$ depend only on finite dimensional restrictions of measures, except on a null set we have by Theorem 2.3,

$$\lim_{n\to\infty} \int_{R^N} \exp(i < f, x > \lambda^*_{nm_n}(\omega, dx) = \chi^\mu(f), \quad f \in R^N_0.$$

By the analogue of Lévy-Cramer theorem (cf. [17], Theorem 1.2.8.) $\lambda^*_{nm_n} \overset{w}{\to}$ μ a.s. as $n \to \infty$. If B is a finite dimensional set, then for large n : $\pi_n^{-1}\pi_n B = B, \lambda_{nm_n}(\pi_n B) = \lambda^*_{nm_n}(B)$ and the conclusion follows immediately. If B is an infinite dimensional set, it will have no interior with respect to Tikhonov's topology, thus $\mu(B) = 0$. As $\{\pi_n^{-1}\pi_n B\}$ is a decreasing sequence of universally measurable sets, letting $C = \bigcap_{n=1}^{\infty} \pi_n^{-1}\pi_n B$, we have $B \subset C \subset \bigcap_{n=1}^{\infty} \pi_n^{-1}\pi_n B = B$ and thus $\lim_{n\to\infty} \mu(\pi_n^{-1}\pi_n B) = \mu(C) = 0$. There exists a sequence $\{n_k\}$ of positive integers and a decreasing sequence $\{C_k\}$ of μ-continuity sets satisfying:

1) $C_k \supset \pi_{n_k}^{-1}\pi_{n_k} B$
2) $\lim_{k\to\infty} \mu(C_k) = 0$

The double limit $\lim_{n,k\to\infty} \lambda^*_{nm_n}(C_k)$ exists and is equal to zero. For there are positive integers k_ϵ and n_ϵ such that for $k \geq k_\epsilon$ and $n \geq n_\epsilon$ we have $|\mu(C_k) - \mu(B)| = \mu(C_k) < \frac{\epsilon}{2}$ and $|\lambda^*_{nm_n}(C_{k_\epsilon}) - \mu(C_{k_\epsilon})| < \frac{\epsilon}{2}$, therefore $|\lambda^*_{nm_n}(C_{k_\epsilon}) - \mu(B)| < \epsilon$. But $\lambda^*_{nm_n}(C_k) \leq \lambda^*_{nm_n}(C_{k_\epsilon})$ and $\mu(B) = 0$. Therefore $\lim_{k\to\infty} \lambda^*_{km_k}(C_k) = 0$ and this implies $\lambda^*_{nm_n}(\pi_n^{-1}\pi_n B) - \lambda_{nm_n}(\pi_n B) \to 0 = \mu(B)$ a.s. ∎

In order to suppress path dependence of the convergence consider λ_{nm} as random measures, i.e., as measurable mappings $S \to M_n$, where M_n denotes the set of all probability measures on $(R^n, \mathcal{B}^n)$. Let also the set of all probability measures on $(R^N, \mathcal{B}^N)$ be denoted by M. Then

Theorem 4.2. For every sequence m_n of positive integers tending to infinity as $n \to \infty$, we have $\lim_{n\to\infty} \lambda_{nm_n} \overset{w-\mathcal{P}}{\to} \Delta_\mu$ where $\Delta_\mu : S \to M$ is the measurable mapping with distribution degenerate at $\mu \in M$.

Proof. 3] ∎

Note. Another viewpoint for the convergence of measures in Theorem 4.1 and Theorem 4.2 could be suggested via the concept of set martingale in the limit. Let

$$\mathcal{P} = \{(\Omega_\alpha, \Sigma_\alpha, P_\alpha, \pi_{\alpha\beta})_{\alpha \preceq \beta}, \alpha, \beta \in D\}$$

be a projective system of probability measures having the property of sequential maximality. It is well-known that with such a system there is associated a set martingale [15, Section 3.1, Proposition 7]). In parallel to Blake's definition of a 'weak martingale in the limit' [1], one can introduce the concept of a 'weak set martingale in the limit' for a system $\{(\Omega_\alpha, \Sigma_\alpha, \nu_{m\alpha}) : m = 1, 2, ..\}$ of probability spaces if $\nu_{m\alpha} \xrightarrow{w} P_\alpha$ as $m \to \infty (\alpha \in D)$, where $\{P_\alpha, \alpha \in D\}$ is a set martingale with base $\{\Sigma_\alpha, \alpha \in D\}$. Then Theorem 4.1 can be rephrased as: $\{(\lambda_{nm_n}, R^n, \mathcal{B}^n) : m = 1, 2, \ldots\}$ is a set martingale in the limit with the underlying set martingale $\{\mu_n : n = 1, 2, ..\}$ which has the base $\{\pi_n^{-1}\mathcal{B}^n : n = 1, 2, \ldots\}$.

Now the empirical process given by (1.5) and (1.6) are modified for sequence spaces as:

$$Y_{nm}(f) := m^{\frac{1}{2}}(\hat{\chi_{nm}}(\pi_n f) - \chi_n^\mu(\pi_n f)), f \in F \tag{4.1}$$

$$Z_{nm}(f) := m^{\frac{1}{2}}\{|\hat{\chi}_{nm}(S_{nm}^{-\frac{1}{2}}(\pi_n f))|^2 - |\chi_n^\mu(f)|^2\}, f \in F. \tag{4.2}$$

These should be regarded as processes ((4.1) is complex-valued and (4.2) real) with a generalized index set. (Here F is in general a topological vector space). Like in the ordinary cases, as given by (1.5) and (1.6), the weak convergence of processes should be restricted to compact subsets. Now if $(E, F) = (R^N, R_0^N)$, the compact sets in F consist of elements that have their lengths bounded by a common integer, say d, and their first d coordinates determining a compact set in R^d. Then for $n \geq d$

$$Y_{nm}(f) = m^{\frac{1}{2}}(\hat{\chi}_{nm}(f) - \chi_d^\mu(f)) \tag{4.3}$$

where f runs over a compact subset K of $R_{0,d}^N$ (set of sequences with lengths bounded by d). Since for all $n \geq d$, $\hat{\chi}_{nm}(f)$ is essentially the same as the empirical characteristic function obtained by m independent observations of the d-long random vector, (4.3) is equivalent to a d-dimensional multivariate process as outlined in the introduction. In particular if $K \equiv K_d$, then the conclusion regarding the weak conergence in $\mathcal{C}^2(K_d)$ will be valid under the condition (1.7). Note that this condition is satisfied uniformly in d if

$$\int_\Omega \log^+(\| \Theta(\omega) \|_2)^{1+\epsilon} dP(\omega) < \infty \tag{4.4}$$

for small ϵ. (cf. [5]).

Similarly the multivariate results can be applied to the process (4.2) whenever $K \equiv K_d \subset R_0^N = F$.

For fixed n and arbitrary dual pairs (E, F), the process (4.1) (resp. (4.2)) can be restricted, in view of (4.3) to compact (bounded) subsets of R^n, thus converges weakly in $\mathcal{C}^2(K_n)$(resp.$\mathcal{C}(K_n)$) to the Gaussian processes as described in the introduction. (In (4.2) χ_n^μ is replaced by $e^{-\sum_1^n f_j^2}$).

The measures induced by the processes Y_{nm} (or Z_{nm}) are not defined on a common underlying measurable space, neither do they form an inverse system since they are not necessarily compatible. We investigate their convergence behavior within the concept of weak convergence along projective systems as described in Section 3. For the multicubes $K_n = [-T, T]^n, (T > 0)$, we define projection mappings $\gamma_{n_1 n_2} : \mathcal{C}(K_{n_2}) \to \mathcal{C}(K_{n_1})(n_1 < n_2)$ by:

$$(\gamma_{n_1 n_2} f)(x_1, \cdots, x_{n_1}) = f(x_1, \cdots, x_{n_1}, 0, \cdots, 0) \qquad \forall f \in \mathcal{C}(K_{n_2}) \quad (4.5)$$

The mappings $\gamma_{n_1 n_2}$ are continuous and satisfy $\pi_{n_3 n_2} \circ \pi_{n_2 n_1} = \pi_{n_3 n_1}$ for $n_1 < n_2 < n_3$. (For complex-valued functions $\gamma_{n_1 n_2} : \mathcal{C}^2(K_{n_2}) \to \mathcal{C}^2(K_{n_1})$). On the other hand if λ is a measure on $(\mathcal{C}(K_2), \mathcal{B}_{\mathcal{C}(K_2)}), \gamma_{n_1 n_2}(\lambda)$ is defined as the ordinary image measure.

Now reconsider the processes Y_{nm} and Z_{nm}, the former being given by (4.1) and the latter by:

$$Z_{nm} = m^{\frac{1}{2}}\{|\chi_{nm}(S_{nm}^{-1}(\pi_n f))|^2 - e^{-\sum_1^n f_j^2}\}, f \in F \quad (4.6)$$

For fixed n they converge weakly in $\mathcal{C}(K_n)$ and $\mathcal{C}^2(K_n)$ to the centered Gaussian processes Y^{μ_n} and Z^{μ_n} having the covariance structures

$$E[Y^{\mu_n}(f)\overline{Y^{\mu_n}(g)}] = \chi_n^\mu(f - g) - \chi_n^\mu(f)\chi_n^\mu(-g) \qquad f, g \in F \quad (4.7)$$

$$E[Z^{\mu_n}(f)Z^{\mu_n}(g)] = 4e^{-\sum_1^n f_j^2 - \sum_1^n g_j^2}\{\cosh(\sum_1^n f_j g_j) - 1 - \frac{1}{2}(\sum_1^n f_j g_j)^2\}$$

$$f, g \in F \quad (4.8)$$

provided that conditions (1.7) or (4.4) are satisfied.

Let ν_n^Y and ν_n^Z be the probability measures representing the distributions of the limiting processes Y^{μ_n} and Z^{μ_n} respectively.

Theorem 4.3.

1)

$$\mathcal{P}^Y = \{(\mathcal{C}^2(K_n), \mathcal{B}_{\mathcal{C}^2(K_n)}, \nu_n^Y, \gamma_{n_1 n_2})_{n_1 < n_2}; n_1, n_2 \in N\}$$
$$\mathcal{P}^Z = \{(\mathcal{C}(K_n), \mathcal{B}_{\mathcal{C}(K_n)}, \nu_n^Z, \gamma_{n_1 n_2})_{n_1 < n_2}; n_1, n_2 \in N\}$$

are topological projective systems of Gaussian probability spaces.

2) The projective limits $(\mathcal{C}^2(K_\infty), \mathcal{B}_{\mathcal{C}^2(K_\infty)}, \nu^Y)$ and $(\mathcal{C}(K_\infty), \mathcal{B}_{\mathcal{C}(K_\infty)}, \nu^Z)$ of the projective systems in 1 exist and are unique. (K_∞: product of infinite copies of $[-T, T]$).
3) Let either the condition (1.7) (for every n) or (4.4) be satisfied. Then for any sequence m_n such that $m_n \to \infty$ as $n \to \infty$, the process Y_{nm_n} has a subsequence converging weakly to ν^Y along the projective systems $\mathcal{P}^Y$. Furthermore for such a sequence the process Z_{nm_n} has a subsequence converging weakly to ν^Z along $\mathcal{P}^Z$.

Proof.

1) As $\gamma_{n_1 n_2}$ are continuous, we only need to show that the measures ν_n^Y and ν_n^Z are compatible with respect to the mappings $\gamma_{n_1 n_2}$. We restrict the proof to ν_n^Z, a similar argument applies to ν_n^Y. We have to prove $\nu_{n_1}^Z = \nu_{n_2}^Z \circ \gamma_{n_1 n_2}^{-1}$ for $n_1 < n_2$. The measure on the righthand-side is obtained by the extension of family of distributions of the type

$$\{\mathcal{L}(Z^{\mu_{n_2}}(g^{(1)}), \cdots Z^{\mu_{n_2}}(g^{(s)}))\} \tag{4.9}$$

where $\mathcal{L}(\cdot)$ denotes the law of a random vector and

$$g^{(i)} = (g_1^{(i)}, \cdots, g_{n_1}^{(i)}, 0, \cdots, 0) \in \mathcal{C}(K_{n_2}),$$
$$(i = 1, \ldots, s; s = 1, 2, \ldots).$$

But (4.9) is Gaussian and completely determined by the covariance structure given by (4.8). Also the right-hand side of (4.8) (as well as of (4.7)) has the property that projections on lesser dimensions yield the same type of expressions. Thus we have

$$E[Z^{\mu_{n_2}}(g^{(i)})Z^{\mu_{n_2}}(g^{(j)})] =$$
$$E[Z^{\mu_{n_1}}((g_1^{(i)}, \cdots, g_{n_1}^{(i)}))Z^{\mu_{n_1}}((g_1^{(j)}, \cdots, g_{n_1}^{(j)}))]$$

which implies $\nu_{n_1}^Z$ and $\nu_{n_2}^Z \circ \gamma_{n_1 n_2}^{-1}$ are obtained by the extension of the same family of finite dimensional distributions, hence they should be equal.

2) Let $\gamma_n : \mathcal{C}(K_\infty) \to \mathcal{C}(K_n)$ be defined as

$$(\gamma_n g)(x) = g(x^n), g \in \mathcal{C}(K_\infty), \qquad x \in R^n,$$

γ_n verifies the relation $\gamma_{n_1} = \gamma_{n_1 n_2} \circ \gamma_{n_2}$ for $n_1 < n_2$ and has the three properties: 1) linear; 2) $g \in \mathcal{C}(K_\infty), g \neq 0 \Rightarrow \exists n$, such that $\gamma_n g \neq 0$; 3) $\cap_{n=1}^{\infty} \gamma_n^{-1}(0) = \{0\}$.

Then by [16, Proposition 11, pp. 84] the projective limit topology of $\mathcal{C}(K_\infty)$ has a base of closed neighborhoods consisting of the finite intersections of the sets $\gamma_n^{-1}(B_{\epsilon,n}), \epsilon > 0, (n = 1, 2, \ldots), B_{\epsilon,n}$ being

closed balls in $\mathcal{C}(K_n)$. This is usually coarser than the norm topology of $\mathcal{C}(K_\infty)$. But if V_ϵ is a closed ball in the norm topology of $\mathcal{C}(K_\infty)$, as $V_\epsilon = \cap_{n=1}^{\infty} \gamma_n^{-1}(B_{\epsilon,n})$, the projective limit topology generates the same σ-field in $\mathcal{C}(K_\infty)$. Since each measure ν_n^Z is Radon on $(\mathcal{C}(K_n), \mathcal{B}_{\mathcal{C}(K_n)})$ and the projective system obviously satisfies the condition of sequential maximality, the conclusion follows from [15, Theorem 5, pp. 121]. The proof for the other process is the same.

3) Again restricting our discussion to Z_{nm_n}, we first note $\gamma_n[\mathcal{C}(K_\infty)] = \mathcal{C}(K_n)$, $n = 1, 2, \ldots$ is a direct result of Tietze's extension theorem. Let $(\nu_n^Z)^*$ be the image of ν_n^Z on $\mathcal{B}_n^* = \gamma_n^{-1}(\mathcal{B}_{\mathcal{C}(K_n)})$, i.e. $(\nu_n^Z)^* \circ \gamma_n^{-1} = \nu_n^Z$. Since the system in 1) admits a projective limit as given in 2), there exist σ-extensions $\overline{(\nu_n^Y)}^*$ of $(\nu_n^Z)^*$ to $\mathcal{B}_{\mathcal{C}(K_\infty)}$ such that $\overline{(\nu_n^Y)}^* \to \nu^Z$ strongly, i.e., $\|\overline{(\nu_n^Z)}^* - \nu^Z\| \to 0$, where the norm denotes the total variation. (cf. [15, Theorem 8, pp. 134]). Therefore the family $\{\overline{(\nu_n^Y)}^*\}, (n = 1, 2, \ldots)$ is tight, implying that given $\epsilon > 0$, there exists a compact set $K_\epsilon \in \mathcal{B}_{\mathcal{C}(K_\infty)}$ (which is also compact in the projective limit topology) such that $\overline{(\nu_n^Y)}^*(K_\epsilon) \geq 1 - \frac{\epsilon}{2}$. Let ν_{nm_n} denote the measure induced on $\mathcal{C}(K_n)$ by the process Z_{nm_n}. Since $\nu_{nm_n} \xrightarrow{w} \nu_n^Z$ as $n \to \infty$, in view of nondegeneracy of ν_n^Z there exists n_0 such that for $n \geq n_0$, $|\nu_{nm_n}(\gamma_n K_\epsilon) - \nu_n^Z(\gamma_n K_\epsilon)| < \frac{\epsilon}{2}$. On the other hand we have $\nu_n^Z(\gamma_n K_\epsilon) = \overline{(\nu_n^Y)}^*(\gamma_n^{-1}\gamma_n K_\epsilon) \geq \overline{(\nu_n^Y)}^*(K_\epsilon) \geq 1 - \frac{\epsilon}{2}$. This, along with the previous inequality implies that $\nu_{nm_n}(\gamma_n K_\epsilon) \geq 1 - \epsilon$, for $n \geq n_0$. Now the conclusion follows from Theorem 3.3. A parallel argument applies to the process Y_{nm_n}.

∎

Remark 4.4. It can be shown that Hypothesis R_1 of Theorems 3.2 and 3.3 is verified for the above projective systems. Hypothesis R_2 is assumed to have been taken care of as in Theorem 4.1.

Remark 4.5. Without the null hypothesis on normality, the limiting distributions ν_n^Z of the processes Z_{nm} will not in general form a projective system with $\gamma_{n_1 n_2}$ as functional morphisms. For instance, for arbitrary μ_n distributions and under some additional assumptions of independence and finite fourth moments, ν_n^Z is found to be Gaussian on $\mathcal{C}(K_n)$ with the following covariances (cf. [6]):

$$E[Z^{\mu_n}(f)Z^{\mu_n}(g)] = 2\mathrm{Re}\{\chi_n^{\mu}(-f)\chi_n^{\mu}(-g)\rho(f,g) + \chi_n^{\mu}(f)\chi_n^{\mu}(-g)\rho(-f,g)\},$$
$$f, g \in R^n$$

where

$$\rho(f,g) = \chi_n^{\mu}(f+g) - \chi_n^{\mu}(f)\chi_n^{\mu}(g) + \frac{1}{2}\{f\nabla^2\chi_n^{\mu}(f)\nabla\chi_n^{\mu}(g) + g\nabla^2\chi_n^{\mu}(g)\nabla\chi_n^{\mu}(f) + \chi_n^{\mu}(g)[f(\nabla\chi_n^{\mu}(g)] + \chi_n^{\mu}(f)[g\nabla\chi_n^{\mu}(g)]\} + \ldots$$

It is clear that taking projections will not give, in the presence of Laplacian factors, the covariance structure of lower dimensions.

5. On inference problems

In view of the convergence of characteristic function(al)s and weak convergence properties of the related processes, different functionals of empirical processes lend themselves as potential statistics in inference problems. Some examples are:

1) Univariate distributions

   a) For testing the symmetry about the origin in univariate distributions, the statistic $T_m = \int_R [\mathrm{Im}\hat{\chi}_{1m}(t)]^2 dG(t)$ is suggested [9]. Here G is taken to be a distribution function symmetric about the origin. When the center of symmetry is specified, T_m can be modified as $\inf_a \int [\mathrm{Im}\{e^{iat}\chi_{1m}(t)\}]^2\, dG(t)$.

   b) For simple goodness of fit $R_m = \sqrt{m}\max\{|\hat{\chi}_{1m}(t_j) - \chi_0(t_j)|, j = 1,\cdots,s\}$, where χ_0 is a specified univariate characteristic function, is studied in [10]. A Cramér-von Mises-type statistic $M_m^w = m\int_{-\infty}^{\infty} |\hat{\chi}_{1m}(t) - \chi_0(t)|^2\, dw(t)$, with w being some weight function on the line, can be used for the same purpose [11].

   c) For testing normality (with some mean and variance) in one dimension, Murota-Takeuchi [13] proposes $Z_m(t), (n = 1)$, (cf. (1.6)), evaluated at some point selected in an interval $[-T, T]$, i.e., $Z_m(t) = \sqrt{m}\{|\hat{\chi}_{1m}(\frac{t}{\sqrt{s}})|^2 - e^{-t^2}\}$.

2) Multivariate distributions

   a) K-sample homogeneity: Let $\Theta_1^{(j)},\ldots,\Theta_{m_j}^{(j)}, j = 1,\cdots,K, K \geqslant 1$ be a set of K independent observations with sizes $m_1,\cdots,m_K$ of K n-dimensional random vectors $\Theta^{(1)},\ldots,\Theta^{(K)}$ with corresponding characteristic functions $\chi^{(1)}(t),\ldots,\chi^{(K)}(t)$. Let $\hat{\chi}_{nm_j}^{(j)}(t)$ be the empirical characteristic function of the j-th sample. Then the characteristic homogeneity process

$$S_N(t) = \sum_{j=1}^{K} a_j(N)\sqrt{m_j}\hat{\chi}_{nm_j}^{(j)}(t)$$

where $N = (m_1, \cdots, m_j)$ and $a_j(N)$ are properly selected constants, can be used to test homogeneity [5].

b) Independence: For

$$n \geq 2, S_m(t) = \sqrt{m}(\hat{\chi_{nm}}(t) - \prod_{k=1}^{n} \hat{\chi}_{nm,k}(t_k)),$$

$$t = (t_1, \ldots, t_n),$$

(the empirical characteristic independence process) is proposed to test the independence of the components of Θ.($\hat{\chi}_{nm,k}(t_k) = \hat{\chi_{nm}}(0, t_k, 0)$: the empirical characteristic function of the k-th components) [5].

c) Testing for normality in arbitrary dimensions: Various extensions of n-dimensional Murota-Takeuchi statistic, as given by (1.6) or (1.8), can be proposed.

i) Consider nonzero vectors $t_1, \cdots, t_L$ in a neighborhood of the origin, such that the $L \times L$ matrix $[\rho_{t_i,t_j}]$ be nonsingular. ($\rho_{s,t}$ is given by (1.9)). Then the quadratic form $Q_m = Q_m(t_1, \cdots, t_L) = z'_m R^{-1} z_m$, where $z'_m = (z_m(t_1), \cdots, z_m(t_L))$ with an asymptotic chi-square distribution of L degrees of freedom under the null-hypothesis, can be used to test normality.

ii) For nonzero pairwise orthogonal n-dimensional vectors $t_1, \cdots, t_n$

$$N_m^{(n)} = \max\{|Z_m(t_1)|, \cdots, |Z_m(t_m)|\}$$

forms another extension of the Murota-Takeuchi statistic.

iii)

$$M_m^{(n)}(T) = \sup_{t \in [-T,T]^n} |Z_m(t)|$$

$$= \sup_{t \in [-T,T]^n} ||\hat{\chi_{nm}}(S_m^{-\frac{1}{2}} t)|^2 - e^{-|t|^2}|$$

is a refinement of ii. Procedures to estimate or approximate the critical tail values of ii and iii are suggested in [6].

Any kind of inferential study regarding the unkown distributions on sequence spaces, such as the distribution induced by a non-stationary process has to be carried out in finite dimensions, with some large n. The rationale behind doing this by utilizing the empirical characteristic functionals and the related processes, is provided by Theorems 2.3 and 4.3. According to Theorem 2.3, $\lim_{n\to\infty} \chi_n^{\mu}(f) = \chi^{\mu}(f), f \in F$ and the convergence is uniform

on compact subsets of F for certain dual pairs (E, F), including (l_p, l_q). On compact subsets of l_q Hölder's inequality yields:

$$|\chi_n^\mu(f) - \chi^\mu(f)| \leqslant \int_{l_q} |\exp\{i[M(\sum_{k=n+1}^{\infty} |x_{k+1}|^p)^{\frac{1}{p}}\} - 1| d\mu(x) \qquad (5.1)$$

for some constant $M > 0$. (Similar inequalities hold for other dualities).

In some special cases (5.1) can be utilized (at least in principle) to approximate $\chi^\mu(f)$ uniformly on compact subsets of F. Two such cases would be:

1) The image of Θ in l_p is almost surely contained in some particular compact set, e.g., subsets of the type $K_{M,k} = \{x : x \in l_p, |x_n|^p n^k \leqslant M, n = 1, 2, \ldots; k > 1\}$
2) μ is a Gaussian distribution with a given covariance operator. If for some $n_0, n \geqslant n_0 \Rightarrow |\chi_n^\mu(f) - \chi^\mu(f)| < \epsilon$, then functionals of the empirical processes indexed by R^{n_0} and given under 1 and 2 above, can be used for different inference problems.

The following iterated logarithm result [4] may give a clue for the right sample size in each dimension:

$$\limsup_{m\to\infty} \left(\frac{m}{2\log\log m}\right)^{\frac{1}{2}} \sup_{t\in[-T,T]^n} |\chi_{nm}(t) - \chi_n(t)| = K \qquad \text{a.s.}$$

with $K = \sup\{\sup_{t\in[-T,T]^n} |k(t)| : \mathcal{K}_{\mu_n}\}$, where $\mathcal{K}_{\mu_n}$ is the generalized Finkelstein set corresponding to distribution μ_n which has the characteristic function $\chi_n(t)$.

For testing normality with an arbitrary covariance operator, the generalized Murota-Takeuchi statistic of 2-c-i as applied to $[-T, T]^n$ will be suitable. In this regard, a sequential scheme of tests of normality in increasing number of dimensions by using the expansive set of data given by (1.1) can also considered. The acceptance and rejection of the hyptothesis of normality in the sequence space should be based, in some way, on the length of runs of acceptance and rejection in finite dimensional tests. However one should expect a substantial difficulty in introducing measures of performance for such a test.

6. Bibliography

[1] L.H. Blake. Weak submartingales in the limit. *Bull. London Math. Soc.*, 2:573–5, 1979.

[2] U. Çapar. Weak convergence along a projective system and some of its applications. In *Abs. of 53rd IMS Annual Meeting and 2nd Bernoulli Congress World Congress*, volume 99, 1990.

[3] U. Çapar. An introduction to empirical characteristic functionals and measures in sequence spaces. *Int. J. of Management and Systems*, 7(1):67–81, January–April 1991.

[4] S. Csörgő. Testing by the empirical characteristic functions. *Z. für Wahrscheinlichkeitstheorie*, 55:203–229, 1981.

[5] S. Csörgő. Testing by the empirical characteristic function: a survey. *Asymptotic Statistics*, pages 45–56, 1984. Kutná Hora 1983.

[6] S. Csörgő. Testing for normality in arbitrary dimensions. *Annals of Statistics*, 14(2):708–723, 1986.

[7] R.M. Dudley. *Real Analysis and Probability*. Math. Ser. Wadsworth and Brooks-Cole, 1989.

[8] A. Feuerverger and P. McDunnough. On some Fourier methods for inference. *J. American Statistical Association*, 76(374):379–387, June 1981. Theory and Methods Section.

[9] A. Feuerverger and R.A. Mureika. The empirical characteristic function and its applications. *Annals of Statistics*, 5:88–97, 1977.

[10] H.D. Keller. *Einige untersuchungen zur empirischen charakteristischen funktion und deren anwendungen*. PhD thesis, Univ. of Dortmund, Dept. of Statistics, September 1979.

[11] J. Kellermeier. The empirical characteristic function and large sample hypothesis testing. *J. Multivariate Analysis*, 10:78–87, 1980.

[12] M.B. Marcus. Weak convergence of the empirical characteristic function. *Annals of Probability*, 9(2):194–201, 1981.

[13] K. Murota and K. Takeuchi. The studentized empirical characteristic function and its application to test for the shape of distribution. *Biometrika*, 68:55–65, 1981.

[14] K.R. Parthasaraty. *Probability measures on metric spaces*. Academic Press, Orlando, San Diego, New York, Austin, Boston, London, Sydney, Tokyo, Toronto, 1967.

[15] M.M. Rao. *Foundations of stochastic analysis.* Academic Press, Orlando, San Diego, New York, Austin, Boston, London, Sydney, Tokyo, Toronto, 1981.

[16] A.P. Robertson and W.C. Robertson. *Topological vector spaces.* Cambridge University Press, Cambridge, U.K., 1966.

[17] N.N. Vakhania. *Probability distributions on linear spaces.* North Holland-Elsevier Science Publishers, Amsterdam, New York, Oxford, 1981.

Is probability a part of mathematical truth?

Donald J. Newman
Department of Mathematics
Temple University
Philadelphia, PA 19122 USA
v5531e@vm.temple.edu
Also at Prometheus Inc.

Abstract We wish to look to using probabilistic methods in what some may view as the "strange new" mathematics. If nature uses probability in quantum physics, then why shouldn't mathematicians? The possibilities abound. Perhaps "undecidable propositions" should be looked at as statements with probabilistic truth values, perhaps "NP-complete" problems should be attacked probabilistically, and perhaps "chaos" is merely the picture of probability in what used to be thought of as "deterministic reality."

Or perhaps this is all nutty, but let's have a look.

1. Introduction

The dawn of Quantum Theory shook the scientific world with the stunning message that the elementary particles were really not *stuff* at all, but "pieces of probability." Believe it or not, understand it or not, this description of the elementary particles as having only a probabilistic reality is a highly functional and useful picture of the subatomic universe. It works!

The great Albert Einstein never "believed" this probability picture of matter, but that didn't stop his using it with incredible effectiveness. Indeed, it was for *this* that he earned his Nobel prize: the prize was given him for the photoelectric effect, not for the monumental relativity theory.

So, this *second* 20th-century revolution in physics carried the message that the truth in science was more "fuzzy" than had been thought. The first revolution—relativity theory—merely said that we had been mistaken in our picture of truth, but did not deny the sharpness of it. Truth under Einstein was just as sharp and hard-edged as it had been under Newton. But truth under Bohr and the quantum theory gang was different, fuzzy, soft-edged—and very involved with probability theory. This is not to say that physicists were unable to get answers to problems. A whole new mechanics—quantum mechanics—evolved and answers continued to be cranked out. A *new attitude*, but business as usual.

J. S. Byrnes et al. (eds.), Probabilistic and Stochastic Methods in Analysis, with Applications, 535–542.
© 1992 *Kluwer Academic Publishers. Printed in the Netherlands.*

This new attitude seemed to be everywhere. The great writer Virginia Woolf made an important discovery about one of her characters, a Mrs. Brown. "My name is Brown," said she, "catch me if you can." The important discovery of Woolf was that *you can't*! Mere words were insufficient to *catch* anything as overwhelming as a human character. But Woolf's acknowledgement of this impossibility was a tremendous breakthrough! She showed us the infinitude of the human soul. A powerful message!

Even the pristine Queen—Mathematics herself—succumbed to new order. Old things we counted on gave way to the new *fuzzier* ones. One old thing that gave way, under Gödel, was decidability. The cherished belief had always been that a meaningful mathematical statement was either provably true or provably false. This belief, however attractive and "convincing," simply had to be given up when an example was produced which was meaningful, but not provably true and not provably false! When this example was translated into its arithmetical counterpart, it turned out to be so convoluted and endlessly "boring" that mathematicians simply laughed and scoffed. "Oh, who cares about that silly isolated counterexample," they said.

You'd think that mathematicians would know better! You'd think they learned their lesson from Pythagoras. The irrationality of the "silly number" $\sqrt{2}$ also appeared to be an isolated example. Now we know the irrationals are all about us; they are in every sense more numerous than the rationals. No, no, mathematicians should never make fun of the isolated counterexample. It will—like $\sqrt{2}$ did, and like the Gödel undecidable—emerge as the *overwhelming norm*. Yes, it is now known that *most* statements are undecidable. Our cherished provably true (or provably false) statements are the silly ones, being in the infinitesimal minority.

Gödel's example—aside from its 100 pages of very ponderous details which show that that it *is* a meaningful statement (in the system of integers)—is reducible to a Kindergarten version which the reader might enjoy. He also would probably be horrified by it because it appears dangerously close to the obviously contradictory and senseless childhood joke, "This statement is false." But this close resemblance is really not so significant. The words "true" or "false" are not really definable in the system, whereas the word "provable," meaning having a proof, is definable—as a moment's thought (or 100 pages of genuine mathematics) will convince you. At any rate, our Kindergarten Gödel statement is:

This statement is unprovable.

which we have "framed" for reference's sake. We will call it the "statement in the frame" (SIF) and at other times we will read it and observe what it says.

So, now for the undecidability proof:

STEP 1 Suppose the SIF *had a proof.* Then it would be true, but taking it out of its frame, it would be unprovable (because that's what it says). This is a contradiction! So, *it cannot have a proof.*

STEP 2 We now know from step 1 that the SIF cannot have a proof, so taking it out of its frame, we see that it is making a true statement. So, *it is true.*

STEP 3 Since the SIF is true, by step 2, we may conclude that the SIF *cannot be proven false.*

Okay then, steps 1 through 3 do the job. Step 1 shows that the SIF cannot be proved true and step 3 shows that the SIF cannot be proved false. So, indeed the SIF is an undecidable proposition!

A general underlying theme seems to run in the examples thus far: that the sharp, hard-edged notion of truth isn't adequate any longer. Indeed, it never was. Elementary particles existed long before their subtleties were recorded by the quantum theorists, Mrs. Browns *were* indescribable long before Virginia Woolf pointed it out to us, and undecidable propositions were always so.

The probability aspect of this "fuzz" is not really apparent, except perhaps in quantum theory, where even Einstein had some doubts. But let us turn now to other examples where probability is more obvious.

There is much current interest in J.P. Kahane's construction of the *ultra-flat polynomials.* He answers thereby many questions of Hardy, Littlewood, and Erdös by a clever use of probability methods in Fourier analysis. At any rate, Kahane *produced* a polynomial of each degree with certain remarkable properties; the word "produced" must be emphasized because his methods involve probabilistic, and therefore not explicit, constructions. To some of us, this nonexplicitness is quite acceptable—and in fact quite beautiful. It is very exciting to prove the existence of something which nobody has the vaguest notion of how to locate!

Thus, a real number exists which is "normal" in every base. Expanded in base 2, it has asymptotically as many 0's as it does 1's; in base 3, as many 0's as it does 1's or 2's; in base 4, as many 0's as it does 1's, 2's, or 3's, and so on. Such a real number exists because almost all numbers have this property (the probability argument!), but so far no such number has been explicitly produced. It is even conceivable that no such explicit number *can* ever be produced. Undoubtedly, numbers such as π or $\sqrt{2}$ are normal in every base, but it may well be undecidable that they are so.

Probability methods are in fact the direct successors of counting arguments and the nonconstructive nature of these are often quite amusing. For instance, one can prove that there are two people in New York City with the same number of hairs on their heads (there are more than 7,000,000 people there and are less than 200,000 hairs on any head). This counting argument is

an excellent example of a situation where explicit construction is impossible. Even the "totally bald" heads have a few hundred tiny hairs on them and the sought-after couple is a time-varying function, hairs constantly growing in and falling out. Explicit construction is impossible, but the counting argument is absolutely convincing!

Erdös loves to stand up in a crowded room and boldly announce: "There are two people here who have exactly the same number of *friends* in this room." This proof, albeit a counting argument, has a slight twist to it (a slight nontriviality, of course, coming from Erdös), but again it is not at all based on any explicit knowledge of the people involved. We *know* much more than we know!

So, sometimes the probability argument is a pure delight and we couldn't desire any more. Who cares, after all, which two New Yorkers have the same number of hairs on their heads? But there are times when we do desire more: we would love to see an *explicit* display of a Kahane ultraflat polynomial—and at least *one* explicit example of a normal number.

There is, however, one area in mathematics where the probabilistic is the *only* choice, where any *constructive* choice is, by its very nature, counterindicated. This is in game theory, where much of the battle is to make unpredictable moves!

In Wilson's very nice book, *The Selfish Gene*, a remarkable connection is disclosed between game theory and evolution—another demonstration of how our very existence is connected to probabilistic mathematics. Williams points to an actual species of rodents which are competitive for their food supply. The game is: to fight or not to fight. If both participants elect to not fight (i.e., they are *pacifists*), then the food is shared. If one decides to fight (i.e., is a *warrior*) and the other decides to not fight, then the food goes entirely to the warrior. And if both decide to fight, then both lose by being hurt in their battle. Note then that this is not a zero-sum game, but nonetheless there is a solution. With the appropriate numerical parameters estimated, this solution turns out to be roughly: be a warrior 32% of the time, and be a pacifist 68% of the time. Remember, we are describing an actual species and actual parameters. What is amazing is that in this species it is observed that 32% of the members are warriors and 68% are pacifists! No individual varies his play—the species as a whole solved the game. Evolution does probability!

2. Probability in our thought processes

Whether or not we are conscious of it, our reasoning is at least partially subject to randomness. The longer and more complicated a proof, the less we *really* do believe it. Intuitively, we don't fully (i.e., with probability $p = 1$)

believe any single step, so that a combination of, e.g., 100 steps has only a probability p^{100}—and this might be quite far from 1.

My favorite example of this built-in probability-in-reasoning is the famous short story of Robert Louis Stevenson's, "The Imp in the Bottle". According to the story, there is an *Imp*, a magical wish-granting genie, trapped inside a bottle. If you buy this bottle, you own the Imp and it will grant you wealth, love, and power. The catch is that you must sell it before you die for strictly less than you bought it for, or else you are doomed to roast in hell for all eternity.

To make this precise, let us mandate that the purchase price of the Imp must be a *positive integer* number of *cents*, American funds.

SO: Would you buy it for 1¢? No, of course not. You could not ever sell it for less than you bought it for; you would surely lose!

NEXT: Would you buy it for 2¢? (Now the thought process is slower.) But again the answer is "*No.*" By the previous argument you know that nobody would ever buy it from you for 1¢. So, indeed you still could never sell it before you die.

The mathematician sees the obvious induction in the above and (sort of) agrees that therefore he would never buy the Imp for any n¢.

BUT: I would surely buy this Imp for $1,000.00—and feel totally sure of selling it for, say, $999.00.

Nobody really believes a proof of 100,000 steps! (And rightfully so, if nobody believes a proof of 99,900 steps!)

(In the actual Stevenson tale, the protagonist buys the bottle for (the equivalent of) 2¢ and is able to sell it to a drunken sailor for 1¢. The sailor is delighted, since he knows that he is already damned to spend eternity in hell!)

There is another example of lack of belief in a long proof. This is the infamous four-color problem, which has been solved by a computer. A computer proof (?) based on firings—and perhaps misfirings—of electrons? Why should I believe such a proof, especially this proof which has had to be "repaired" several times when errors were found?

These are all valid objections, but then again are firings and misfirings of electrons in a machine any less convincing than firings or misfirings of neurons in a human brain? Are any long proofs by a computer or from a person totally believable? Or are they all just probable?

Are there any mathematical truths, or only things of probability $1 - 10^{-100}$? Perhaps anything with probability $\geq 1 - 10^{-100}$ is as true as you can ever get.

So, *truth* is like elementary particles. It isn't *stuff* at all, but only probability. Yes, Mr. Einstein, not only does God play dice, *God is dice*!

3. P = NP?

We hinted at the "mentality" of the computer in connection with the four-color problem, but major questions remain: Does a computer have mentality? Does it have consciousness? Does it have strokes of genius? This last question has been formalized into the well-known P = NP problem. In simplified nontechnical terms, this problem exemplifies the familiar situation in which we say to ourselves, "Oh, of course; why didn't I think of that?" It is the situation where an answer to a question is so easy to *check* that we feel that it should have been easy to *find*.

(Is 4294967297 composite? Yes, it's divisible by 641. Oh, why didn't I see that? I don't know Mr. Fermat you should have.)

At any rate, this is the P = NP problem. Can *all* easily checked answers to a question be easily discovered?

The thought process we want is a little like: "Why don't I try ... Oh, of course, it works!" In short, if we guarantee the "Oh, of course, it works," then all we need supply is the "Why don't I try..." but that's the genius part; that's the flash of the idea. There seems little reason to believe that the hunch presents itself to us just because it will be easy to check—*except* that we have all seen it happen and too often to consider it an accident. It is with great delight that we witness strokes of genius—even when (as is usual) they are from others.

- When a 12-year-old boy makes a queen sacrifice and wins a championship chess game, all the world rejoices (well, except for the one who lost to him)!
- When Sue Shapiro (a friend of the family) unerringly picks out the four-leaf clover from a field of clover, the witnesses are both stunned and delighted.
- When that little boy on television solves all those complicated mazes with no apparent effort, we are again quite delighted.

These are perfect examples of solutions which are easy to check. Once made, Bobby Fischer's brilliancy of the century is quickly seen to force a checkmate. Once drawn, a successful maze path is also quickly seen to succeed. A four-leaf clover is a palpable reality. There are, of course, many other examples. There seem to be very special people with very special talents, but what is being suggested is that *yes*, P = NP—that any question which has an easily checked solution also has an easy path to that solution (the discovery process being available to a special-purpose mind).

And now comes the fuzziness. We seem to be on the brink of another *undecidability*. If indeed P = NP, we undoubtedly could never prove it. For a proof would involve a production of an algorithm (the proof itself), and such an algorithm could be programmed into a computer. The computer

could have strokes of genius! The great boon to mankind! Of course, this is the reason for the great interest in the P = NP problem in the first place.

Well, why not? It's about time that something good happened to mankind. Why not have the computer become a true thinker? ('tis a consummation devoutly to be wished)

The negative answer, however, is very convincingly put forth in Penrose's marvelous book, *The Emperor's New Mind*. Penrose's thesis is simply that computers are not—and never can become—conscious, and that therefore they can never become true thinkers.

We seem to be led to the conclusion that P = NP is undecidable. It is, as with the SIF of Gödel, *true* (because of the Bobby Fischers), but *unprovable* (because of Penrose's thesis).

4. Chaos: The third 20th century revolution in science

The message of this paper and of this "new science" is that we are living not in a universe of sharp, clear realities, but rather in one of probabilities (what we have been calling *fuzzy* instead of what we have been calling *sharp*). The germ of this new attitude came from the discovery of huge discontinuities in nature: the *butterfly effect*, in popular terminology. The scenario is that of a butterfly flapping its wings in Tokyo causing a slight dislocation of air particles, thereby causing a slight motion of leaves on a tree, and so on and on, . . ., ending in a cyclone somewhere. The point is that such a slight perturbation could—and often does—cause large changes at large distances. The mathematical notion of discontinuity is certainly not a new one. What is new is the realization that discontinuity is prevalent in nature.

If indeed the flutter of a butterfly's wing in Tokyo could cause a cyclone in Timbuktu, then we must conclude that that cyclone's cause was *probability*. It was not a large physical force that caused the butterfly to wave its wings, but only a random (probability!) whim. The butterfly effect was possibly first discovered by Edward Lorentz, who was doing some computer experiments in meteorology. Lorentz would feed into a computer some descriptive weather parameters and then read out some weather predictions. Quite by accident, he fed in some parameters which differed only very slightly from the ones he had used the week before, and was shocked to find that the new week's predictions were *markedly* different from the earlier ones. "I only changed the parameters in the fourth decimal place; no instruments ever detect better than that." If such "unnoticeable" errors produce such an enormous cumulative effect, then we have been all wrong looking for a sensible method of weather prediction! It doesn't even exist in nature!

Lorentz went on to build his famous mathematical model, which showed the truly explosive property of the iterative procedures present in nature. Lorentz's finding was not restricted just to meteorology. Similar

phenomena were discovered in, e.g., the gypsy moth population, shapes of clouds, the intertwining of blood vessels, heart troubles—even the stock market variations. The word spread like wildfire! All is discontinuity, and hence *all is probability.*

5. Bibliography

[1] J. Gleick. *Chaos.* 1988.

[2] Roger Penrose. *The Emperor's New Mind.* 1989.

[3] E.R. Wilson. *The Selfish Gene.* 1978.

Extension of radial positive-definite distributions in $\mathfrak{R}^n$ and maximum entropy†

Jean-Pierre Gabardo
Department of Mathematics and Statistics
McMaster University
Hamilton, Ontario, L8S 4K1 Canada
gabardo@sscvax.cis.mcmaster.ca

Abstract Positive-definite functions or distributions appear naturally in the theory of homogeneous random fields and, in particular, in the definition of their correlation functionals. We consider the problem of extending a radial positive-definite function, or distribution, defined in a ball centered at the origin of $\mathfrak{R}^n$ to one defined in the whole space. Such an extension was shown to exist by W. Rudin (in the case of a continuous function) and, later on, by A.E. Nussbaum (in the case of a distribution). Our goal in this paper is to explain how the maximum entropy principle can be used to obtain explicit solutions of the n-dimensional radial extension problem via a reduction to a one-dimensional one. We also investigate the question of uniqueness of the extension.

1. Notation

We will denote by $\mathfrak{R}^n$ the n-dimensional Euclidean space and by $\hat{\mathfrak{R}}^n$ its dual group. If f is a function defined on $\mathfrak{R}^n$, we will denote by $\check{f}$ the function defined by $\check{f}(x) = f(-x)$, for x in $\mathfrak{R}^n$. If $f : \mathfrak{R} \to \mathfrak{C}$ is a function, we denote its Fourier transform by $\hat{f}$ or $\mathcal{F}_1 f$. It is defined by

$$\hat{f}(\gamma) = (\mathcal{F}_1 f)(\gamma) = \int_{\mathfrak{R}} e^{-2\pi i \gamma x} f(x)\, dx, \qquad \gamma \in \hat{\mathfrak{R}}.$$

If $f : \mathfrak{R}^n \to \mathfrak{C}$, its Fourier transform $\mathcal{F}_n f : \hat{\mathfrak{R}}^n \to \mathfrak{C}$ is defined by

$$(\mathcal{F}_n f)(\xi) = \int_{\mathfrak{R}^n} e^{-2\pi i \langle \xi, y \rangle} f(y)\, dy, \qquad \xi \in \hat{\mathfrak{R}}^n.$$

† The author was supported by NSERC grant OGP0036564.

J. S. Byrnes et al. (eds.), Probabilistic and Stochastic Methods in Analysis, with Applications, 543–554.
© 1992 *Kluwer Academic Publishers. Printed in the Netherlands.*

Note that we reserve the notation $\hat{f}$ for functions f defined on $\mathfrak{R}$. If $g : \hat{\mathfrak{R}}^n \to \mathfrak{C}$, its inverse Fourier transform is

$$(\mathcal{F}_n^{-1} g)(x) = \int_{\mathfrak{R}^n} e^{2\pi i \langle x, \xi \rangle} g(\xi)\, d\xi, \qquad x \in \mathfrak{R}^n.$$

Of course, as usual, the Fourier transform is first defined for functions in the Schwartz class $\mathcal{S}(\mathfrak{R}^n)$ and then, by duality, to the class $\mathcal{S}'(\mathfrak{R}^n)$ of tempered distributions. We will denote by the bracket $\langle T, \phi \rangle$ the duality between a distribution (or a generalized random field) T and a test function ϕ. $C_o^\infty(\Omega)$ is the class of infinitely differentiable functions with compact support in Ω. $B_n(R)$ and S_n are defined by $B_n(R) = \{x \in \mathfrak{R}, |x| < R\}$ and $S_n = \{\xi \in \hat{\mathfrak{R}}^n, |\xi| = 1\}$. We also denote by $d\sigma$ the $(n-1)$-dimensional Lebesgue measure on S_n and, if ϕ is a function on $\mathfrak{R}^n$, we define its spherical average ϕ° by the formula

$$\phi^\circ(x) = \frac{1}{|S_n|} \int_{S_n} \phi(|x|\sigma)\, d\sigma, \qquad x \in \mathfrak{R}^n.$$

2. Introduction

Let us consider a complex-valued generalized random field Φ defined on $\mathfrak{R}^n$. If we pick any $\phi_1, \ldots, \phi_n \in C_o^\infty(\mathfrak{R}^n)$, then $\langle \Phi, \phi_1 \rangle, \ldots, \langle \Phi, \phi_n \rangle$ are random variables with a well-defined joint probability distribution. We will assume in the following that, for all $\phi \in C_o^\infty(\mathfrak{R}^n)$, the expected value $E(\langle \Phi, \phi \rangle) = 0$ and also that $E(|\langle \Phi, \phi \rangle|^2) < \infty$. The generalized random field Φ is called homogeneous if, for any $\phi_1, \ldots, \phi_k \in C_o^\infty(\mathfrak{R}^n)$ and any point $h \in \mathfrak{R}^n$, the k-dimensional random variables $(\langle \Phi, \phi_1 \rangle, \ldots, \langle \Phi, \phi_k \rangle)$ and $(\langle \Phi, \phi_1(\cdot + h) \rangle, \ldots, \langle \Phi, \phi_k(\cdot + h) \rangle)$ are identically distributed. This is, of course, the n-dimensional analogue of a generalized stationary stochastic process (see [9, 16, 17] for more details). The correlation functional of the generalized random variable Φ is the sesquilinear form B defined on $C_o^\infty(\mathfrak{R}^n) \times C_o^\infty(\mathfrak{R}^n)$ by the formula

$$\forall \phi_1, \phi_2 \in C_o^\infty(\mathfrak{R}^n), \quad B(\phi_1, \phi_2) = E(\langle \Phi, \phi_1 \rangle \overline{\langle \Phi, \phi_2 \rangle}). \tag{2.1}$$

In the case where Φ is homogeneous, the sesquilinear form B is translation invariant and one can show the existence of a unique distribution (in the sense of Schwartz) $Q \in \mathcal{S}'(\mathfrak{R}^n)$ such that

$$\forall \phi_1, \phi_2 \in C_o^\infty(\mathfrak{R}^n), B(\phi_1, \phi_2) = \langle Q, \dot{\phi}_1 * \overline{\phi_2} \rangle. \tag{2.2}$$

The distribution Q is clearly positive-definite on $\mathfrak{R}^n$, i.e., for all $\phi \in C_o^\infty(\mathfrak{R}^n)$, we have $\langle Q, \dot{\phi} * \overline{\phi} \rangle \geq 0$ since

$$\langle Q, \dot{\phi} * \overline{\phi} \rangle = E(|\langle \Phi, \phi \rangle|^2) \geq 0.$$

Conversely, it is known that every positive-definite distribution $Q \in \mathcal{S}'(\mathfrak{R}^n)$ arises in the definition of the correlation functional of some generalized homogeneous random field Φ. Thus, Q controls the "second-order theory" of Φ and, in fact, if Φ is Gaussian, it is completely determined by Q. By the Bochner-Schwartz theorem [15], the Fourier transform of Q is a positive tempered measure μ on $\hat{\mathfrak{R}}^n$, i.e., $\mu \geqslant 0$ and for some integer $m \geqslant 0$, we have

$$\int_{\hat{\mathfrak{R}}^n} (1 + |\xi|^2)^{-m} \, d\mu(\xi) < \infty.$$

This yields the following representation for the correlation functional:

$$\forall \phi_1, \phi_2 \in C_o^\infty(\mathfrak{R}^n), B(\phi_1, \phi_2) = \int_{\hat{\mathfrak{R}}^n} (\mathcal{F}_n \phi_1)(\xi) \overline{(\mathcal{F}_n \phi_2)(\xi)} \, d\mu(\xi).$$

The measure μ is called the *spectral measure* of the generalized random field Φ. In the case where the positive-definite distribution Q associated with Φ is radial, i.e., if

$$\forall \phi \in C_o^\infty(\mathfrak{R}^n), \langle Q, \phi \rangle = \langle Q, \phi^\circ \rangle,$$

where ϕ° is the spherical average of ϕ, we say that Φ is homogeneous and isotropic.

In the following, we will be dealing with a basic extension problem: we will assume that the values of the correlation functional of a homogeneous and isotropic random field, $B(\phi_1, \phi_2)$, are only known to us when ϕ_1, ϕ_2 are supported in some finite ball centered at the origin, and we will try to construct explicitely spectral measures consistent with the given correlation data. We will also look at the question as to when a spectral measure consistent with the given correlation data is unique and explain the relation with the concept of maximum entropy.

3. Extension of distribution positive-definite in a ball

We need the following definition.

Definition 3.1. Let R be such that $0 < R \leqslant \infty$ and suppose that Q is a distribution (in the sense of Schwartz) on $B_n(R)$. We say that Q is positive-definite on $B_n(R)$ if

$$\forall \phi \in C_o^\infty(B_n(R/2)), \quad \langle Q, \phi * \tilde{\phi} \rangle \geqslant 0 \tag{3.1}$$

In that case, we will write $Q \gg 0$ on $B_n(R)$.

Let us remark that if Q is actually a continuous function on $B_n(R)$ (i.e., Φ is a "standard" homogeneous random field), (3.1) is equivalent to

$$\sum_{i,j} Q(x_i - x_j) \xi_i \overline{\xi_j} \geqslant 0$$

for all $x_1, \ldots, x_k \in B_n(R/2)$, all $\xi_1, \ldots, \xi_k \in \mathbb{C}$, and all $k \geq 1$.

The basic extension problem stated above can be rephrased in terms of distributions in the following way: given $Q \gg 0$ on $B_n(R)$, we try to construct $Q_1 \gg 0$ on $\mathfrak{R}^n$ such that $Q_1 = Q$ on $B_n(R)$, or, equivalently, we try to find a positive measure $\mu \in \mathcal{S}'(\mathfrak{R}^n)$ such that $\mathcal{F}_n^{-1}(\mu) = Q$ on $B_n(R)$. In the case $n = 1$, M.G. Krein [10] showed that such an extension was always possible. However, when $n > 1$ and $B_n(R)$ is replaced by an n-dimensional cube centered at the origin, the extension problem does not always have a solution, as was shown by W. Rudin [13]. Nevertheless, it was shown, again by W. Rudin [14], that if $Q \gg 0$ on $B_n(R)$ is a radial continuous function, the extension was always possible. Rudin's work was later generalized by A.E. Nussbaum [12] to include the case of radial positive-definite distributions. As far as the uniqueness problem is concerned, necessary and sufficient conditions were given in the one-dimensional case by M.G. Krein [10] and E.J. Akutowicz ([1]; see also [2]) for continuous functions, but they are not easy to check in practice. Recently, the author [8] found another necessary and sufficient condition for nonuniqueness in the one-dimensional case, given in terms of the continuity of a linear functional, which is valid for distributions.

Theorem 3.2. Let $T \gg 0$ on $(-R, R)$. Then the extension problem for T has a nonunique solution if and only if, for some $\lambda \in \mathbb{C}$, with $\operatorname{Im}\lambda \neq 0$, there exists $C > 0$ such that

$$\forall \varphi \in C_0^\infty((0,R)), \quad |\hat{\varphi}(\lambda)| \leq C\left[\langle T, \check{\varphi} * \overline{\varphi}\rangle\right]^{1/2} \tag{3.2}$$

It can be shown that if (3.2) holds for some λ with $\operatorname{Im}\lambda \neq 0$, then, in fact, it holds for all $\lambda \in \mathbb{C}$ (with the constant C dependent on λ). Using this fact, one can extend the definition of the Fourier transform to the completion of $C_0^\infty((0,R))$ with respect to the norm

$$\|\varphi\| = \sqrt{|\langle T, \check{\varphi} * \overline{\varphi}\rangle|},$$

defined for all $\varphi \in C_0^\infty((0,R))$. If we denote by H that completion, then the Fourier transform of an element $u \in H$, denoted by $\hat{u}$, is an entire analytic function of exponential type less than or equal to $2\pi R$. Of course, H is a Hilbert space with inner product defined for the elements $\varphi, \psi \in C_0^\infty((0,R))$ by $[\varphi, \psi] = \langle T, \check{\varphi} * \overline{\psi}\rangle$ and extended by continuity to all of H. It is immediate that if $S \gg 0$ on $\mathfrak{R}$ and $S = T$ on $(-R, R)$, then

$$[\varphi, \psi] = \int_{\mathfrak{R}} \hat{\varphi}(\gamma)\,\overline{\hat{\psi}(\gamma)}\,d\mu(\gamma),$$

for all $\varphi, \psi \in C_0^\infty((0,R))$ where $\mu = \hat{S}$ and this integral representation of the inner product in H extends immediately to all of H. It turns out that the uniqueness problem is closely related to the notion of entropy.

Definition 3.3. Let $\mu \geqslant 0$ be a tempered measure on $\hat{\mathfrak{R}}$ with $\mu = w + \mu_s$, where $w \in L^1_{loc}(\hat{\mathfrak{R}})$ and μ_s is singular. Then μ is said to have finite entropy if

$$\int_{\hat{\mathfrak{R}}} \frac{\log w(\gamma)}{1+\gamma^2}\, d\gamma > -\infty.$$

One can show (see [8]) that if μ is a measure with finite entropy and $\mathcal{F}_1^{-1}(\mu) = T$ on $(-R, R)$, then the extension problem for T always has more than one solution. Conversely, if the extension is nonunique, there exist positive-definite extensions whose Fourier transforms are measures with finite entropy and, in fact, the entropy maximizers corresponding to certain logarithmic integrals depending on the complex parameter λ can be computed explicitly. More precisely, if $\lambda \in \mathbb{C}$ and $\operatorname{Im} \lambda > 0$, let us denote by u_λ the unique element of H satisfying

$$\forall \varphi \in C_0^\infty((0,R)), \quad \hat{\varphi}(\bar{\lambda}) = [\varphi, u_\lambda]. \tag{3.3}$$

It can be shown that $\hat{u}_\lambda$ does not vanish on the real axis and thus one can define the weight ν_λ by the formula

$$\forall \gamma \in \hat{\mathfrak{R}},\ \nu_\lambda(\gamma) = \frac{\operatorname{Im}\lambda\, \|u_\lambda\|^2}{\pi |\hat{u}_\lambda(\gamma)|^2 |\lambda - \gamma|^2}. \tag{3.4}$$

We have the following theorem.

Theorem 3.4. Let $T \gg 0$ on $(-R, R)$ satisfy (3.2) and, if $\operatorname{Im}\lambda > 0$, let ν_λ be the weight defined by (3.3) and (3.4). Then $\nu_\lambda \in \mathcal{S}'(\hat{\mathfrak{R}})$, $\mathcal{F}_1^{-1}\nu_\lambda = T$ on $(-R, R)$, and, furthermore, if $\mu \geqslant 0$ is any measure in $\mathcal{S}'(\hat{\mathfrak{R}})$ with absolutely continuous part w and $\mathcal{F}_1^{-1}\mu = T$ on $(-R, R)$, we have the entropy inequality

$$\frac{\operatorname{Im}\lambda}{\pi} \int_{\hat{\mathfrak{R}}} \frac{\log w(\gamma)}{|\lambda - \gamma|^2}\, d\gamma \leqslant \frac{\operatorname{Im}\lambda}{\pi} \int_{\hat{\mathfrak{R}}} \frac{\log \nu_\lambda(\gamma)}{|\lambda - \gamma|^2}\, d\gamma$$

with equality if and only if $\mu = \nu_\lambda$.

This theorem was proved in [8]. A version of it was proved independently by H. Dym (see [7]), but in the case of matrix-valued functions and with stronger assumptions on T. Let us mention here that the concept of maximum entropy in connection with the extension problem was introduced by J.P. Burg ([5]; see also [3, 11]) in the discrete case and by J. Chover [6] in the continuous one. Another interesting version of the entropy inequality stated above can be found in [4].

4. Higher dimension: the radial case

As mentioned earlier, the n-dimensional extension problem was solved in the radial case by W. Rudin [14] for continuous positive-definite functions on $B_n(R)$ and by A.E. Nussbaum [12] for positive-definite distributions on $B_n(R)$. However, the existence of the extension is obtained by Rudin via a Hahn-Banach argument and by Nussbaum via an abstract spectral theorem in nuclear spaces. This, of course, makes it difficult to obtain explicit formulas for possible extensions. Since such formulas are available in the one-dimensional case (by the maximum entropy method, for example), it is of practical interest to try to reduce the study of the n-dimensional radial case, which is essentially "one-dimensional," to the one-dimensional one. It turns out that such a reduction is possible and an important ingredient for doing so is the following lemma used by W. Rudin in [14].

Lemma 4.1 (W. Rudin). Let $\phi \in C_0^\infty(B_n(R))$ with ϕ radial and suppose that $\mathcal{F}_n\phi \geq 0$. Then there exist a sequence $\{\phi_k\}$ with $\phi_k \in C_0^\infty(B_n(R/2))$ such that

$$\phi = \sum_k \check{\phi}_k * \overline{\phi_k} \tag{4.1}$$

in the sense of convergence in $C_0^\infty(B_n(R))$.

Remark 4.2. The ϕ_k's in the previous lemma are not radial in general. Lemma 4.1 is the most technical part of Rudin's proof of the existence of the extension in the radial case and its proof uses the Hadamard factorization theorem. Rudin only mentions the uniform convergence of the series in (4.1) (since this is all he needs), but the convergence in $C_0^\infty(B_n(R))$ follows easily from his argument.

Rudin's lemma will allow us to associate with any radial distribution $Q \gg 0$ on $B_n(R)$ an even one-dimensional distribution $T \gg 0$ on $(-R, R)$.

Lemma 4.3. Let $Q \gg 0$ on $B_n(R)$ be radial. Then the distribution T defined on $(-R, R)$ by the formula

$$\forall \varphi \in C_0^\infty((-R, R)), \quad \langle T, \varphi \rangle = \langle Q, \mathcal{K}\varphi \rangle, \tag{4.2}$$

where

$$\mathcal{K}\varphi = \mathcal{F}_n^{-1}\left[\frac{\hat{\varphi}(|\xi|) + \hat{\varphi}(-|\xi|)}{2}\right],$$

is even and positive-definite on $(-R, R)$.

Proof. Since, by the Paley-Wiener theorem (see [15]), $\hat{\varphi}$ is the restriction to $\mathbb{R}$ of an entire function of exponential type less than $2\pi R$, it follows easily

that the function $\psi(\xi) = [\hat{\varphi}(|\xi|) + \hat{\varphi}(-|\xi|)]/2$ for $\xi \in \hat{\mathfrak{R}}^n$, is the restriction to $\hat{\mathfrak{R}}^n$ of an entire function of exponential type less than $2\pi R$ defined on $\mathbf{C}^n$. Hence, by the Paley-Wiener theorem again, $\mathcal{K}\varphi$ belongs to $C_o^\infty(B_n(R))$ and (4.2) is well defined. It is also easily checked that the mapping $\mathcal{K}$: $C_o^\infty((-R,R)) \to C_o^\infty(B_n(R))$ is continuous. Thus (4.2) defines a distribution T on $(-R,R)$ which is clearly even. Let us show that $T \gg 0$ on $(-R,R)$. If $\varphi \in C_o^\infty((0,R))$,we have

$$\mathcal{F}_n\mathcal{K}(\dot{\varphi} * \overline{\varphi}) = \left[|\hat{\varphi}|^2(|\xi|) + |\hat{\varphi}|^2(-|\xi|)\right]/2 \geqslant 0$$

and thus, by Lemma 4.1, there exists a sequence $\{\phi_k\}$ in $C_o^\infty(B_n(R/2))$ such that $\mathcal{K}(\dot{\varphi} * \overline{\varphi}) = \sum_k \dot{\phi}_k * \overline{\phi_k}$ in the sense of convergence of test functions in $C_o^\infty(B_n(R))$. Therefore,

$$\langle T, \dot{\varphi} * \overline{\varphi}\rangle = \langle Q, \mathcal{K}(\dot{\varphi} * \overline{\varphi})\rangle = \sum_k \langle Q, \dot{\phi}_k * \overline{\phi_k}\rangle \geqslant 0,$$

which proves the lemma. ∎

Our next goal is to solve the extension problem for Q, taking for granted that we can do it for T. We need to introduce the following definition.

Definition 4.4. In the following, we will denote by Ω a measurable subset of S_n having the property that

$$\sigma \in \Omega \text{ if and only if } -\sigma \notin \Omega \tag{4.3}$$

for a.e.$(d\sigma)\,\sigma \in S_n$. We define the function $\operatorname{sign}_\Omega$ by $\operatorname{sign}_\Omega(0) = 0$ and, if $\xi \neq 0$, $\operatorname{sign}_\Omega(\xi) = 1$ for $\xi/|\xi| \in \Omega$, and $\operatorname{sign}_\Omega(\xi) = -1$ for $\xi/|\xi| \notin \Omega$.

Theorem 4.5. Let $R > 0$, let $Q \gg 0$ on $B_n(R)$ be radial and consider the distribution $T \gg 0$ on $(-R,R)$ defined by (4.2). Suppose that the positive measure $\nu \in \mathcal{S}'(\hat{\mathfrak{R}})$ satisfies $\mathcal{F}_1^{-1}\nu = T$ on $(-R,R)$. Then, the measure $\mu \in \mathcal{S}'(\hat{\mathfrak{R}}^n)$ defined by the formula

$$\forall \phi \in C_o^\infty(\hat{\mathfrak{R}}^n), \langle \mu, \phi\rangle = \int_{\mathfrak{R}} \left[2|S_n|^{-1} \int_\Omega \phi(r\sigma)\, d\sigma\right] d\nu(r) \tag{4.4}$$

satisfies $\mathcal{F}_n^{-1}\mu = Q$ on $B_n(R)$.

Proof. We first remark that if $\phi \in C_o^\infty(B_n(R))$, if $\sigma \in S_n$, and if we denote by dS the $(n-1)$-dimensional Lebesgue measure on the hyperplane $\{u \in \mathfrak{R}^n, \langle \sigma, u\rangle = 0\}$, the function ϕ_σ defined by

$$\forall t \in \mathfrak{R}, \phi_\sigma(t) = \int_{\langle \sigma, u\rangle = 0} \phi(\sigma t + u)\, dS(u),$$

belongs to $C_o^\infty((-R,R))$. Furthermore, it follows easily from Fubini's theorem that $\hat{\phi}_\sigma(r) = (\mathcal{F}_n\phi)(r\sigma)$, for all $r \in \hat{\mathbb{R}}$, and it is clear that $\check{\phi}_\sigma = \phi_{-\sigma}$. Hence, we have

$$\begin{aligned}
\int_{\hat{\mathbb{R}}^n} (\mathcal{F}_n\phi)(\xi)\,d\mu(\xi) &= 2|S_n|^{-1}\int_{\hat{\mathbb{R}}}\left[\int_\Omega (\mathcal{F}_n\phi)(r\sigma)\,d\sigma\right]dv(r)\\
&= 2|S_n|^{-1}\int_\Omega\left[\int_{\hat{\mathbb{R}}}\hat{\phi}_\sigma(r)\,dv(r)\right]d\sigma\\
&= 2|S_n|^{-1}\int_\Omega \langle T,\phi_\sigma\rangle\,d\sigma\\
&= |S_n|^{-1}\int_\Omega \langle T,\phi_\sigma+\check{\phi}_\sigma\rangle\,d\sigma \qquad \text{(since } T \text{ is even)}\\
&= |S_n|^{-1}\int_\Omega \langle T,\phi_\sigma+\phi_{-\sigma}\rangle\,d\sigma\\
&= |S_n|^{-1}\int_{S_n} \langle T,\phi_\sigma\rangle\,d\sigma\\
&= |S_n|^{-1}\int_{\hat{\mathbb{R}}}\left(\int_{S_n}\hat{\phi}_\sigma(r)\,d\sigma\right)dv(r).
\end{aligned}$$

Now, it is clear that the function ψ defined by

$$\psi = \mathcal{F}_1^{-1}\left[|S_n|^{-1}\int_{S_n}\hat{\phi}_\sigma(r)\,d\sigma\right]$$

belongs to $C_o^\infty((-R,R))$ and is even. Using the previous computation, we have thus

$$\begin{aligned}
\langle\mu,\mathcal{F}_n\phi\rangle &= \langle T,\psi\rangle = \langle Q,\hat{\psi}(|\xi|)\rangle\\
&= \langle Q,\mathcal{F}_n^{-1}[(\mathcal{F}_n\phi)^\circ]\rangle\\
&= \langle Q,\phi^\circ\rangle = \langle Q,\phi\rangle,
\end{aligned}$$

since the Fourier transform commutes with orthogonal transformations and Q is radial. This shows that $\mathcal{F}_n^{-1}\mu = Q$ on $B_n(R)$. ∎

Remark 4.6. If $dv = v(r)\,dr$ where v is a positive function, then $d\mu = w(\xi)\,d\xi$ where $w(\xi) = 2|S_n|^{-1}v(|\xi|\,\mathrm{sign}_\Omega(\xi))\,|\xi|^{-(n-1)}$.

It should be pointed out that the measure μ constructed above is not radial in general, unless v is even. In that case, μ can be defined by the formula

$$\forall\,\phi \in C_o^\infty(\hat{\mathbb{R}}^n),\ \langle\mu,\phi\rangle = \int_{\hat{\mathbb{R}}}\left[|S_n|^{-1}\int_{S_n}\phi(r\sigma)\,d\sigma\right]dv(r). \tag{4.5}$$

Conversely, if μ is radial, it can be written in the form (4.5) where ν is defined by the formula

$$\forall \varphi \in C_0^\infty(\hat{\mathfrak{R}}),\ \langle \nu, \varphi \rangle = \int_{\mathfrak{R}^n} \frac{\varphi(|\xi|) + \varphi(-|\xi|)}{2}\, d\mu(\xi).$$

Therefore, by Theorem 4.5, there is a one-to-one correspondence between radial positive-definite extensions of Q and even positive extensions of T One obtains in this way, using Theorem 3.2, the following characterization for the "nonuniqueness" of the radial positive-definite extensions of Q.

Corollary to 4.6. Let $R > 0$ and let $Q \gg 0$ on $B_n(R)$ be radial. Then, there exists a nonunique radial distribution $Q_1 \gg 0$ on $\mathfrak{R}^n$ with $Q_1 = Q$ on $B_n(R)$ if and only if the associated one-dimensional distribution T defined by (4.2) satisfies (3.2).

5. Maximum entropy

It is now clear that, when the n-dimensional radial extension problem has a nonunique solution, we can use the maximum entropy method (i.e., Theorem 3.4) to provide us with explicit solutions by using Theorem 4.5. More explicitely, if ν_λ is the weight defined in (3.4), we know that $\mathcal{F}_1^{-1}\nu_\lambda = T$ on $(-R, R)$ and therefore the weight w_λ^Ω defined by

$$\forall \xi \in \hat{\mathfrak{R}}^n,\ w_\lambda^\Omega(\xi) = 2|S_n|^{-1}\nu_\lambda(|\xi| \operatorname{sign}_\Omega(\xi))\,|\xi|^{-(n-1)}$$

satisfies $\mathcal{F}_n^{-1} = Q$ on $B_n(R)$ for all choices of Ω satisfying (4.3). Of course, one can wonder, in view of Theorem 3.4, if the weights w_λ^Ω are the entropy maximizers associated with certain n-dimensional logarithmic integrals. This turns out to be the case, but in order to obtain a result valid in full generality, one has to restrict the complex parameter λ to vary on the positive imaginary axis. Furthermore, in that case the associated weight w_λ^Ω turns out to be radial (and thus independent of Ω) and the logarithmic integral considered has a much nicer form. We need the following lemma.

Lemma 5.1. Let $R > 0$ and let us assume that the distribution $T \gg 0$ on $(-R, R)$ associated with Q satisfies (3.2). Let $t > 0$ and consider u_{it}, the unique element of H satisfying (3.3) with $\lambda = it$. Then, we have

$$\forall \gamma \in \hat{\mathfrak{R}},\ |\hat{u}_{it}(-\gamma)| = |\hat{u}_{it}(\gamma)| \tag{5.1}$$

and, in particular, the weight W_t defined by

$$\forall \xi \in \hat{\mathfrak{R}}^n,\ W_t(\xi) = 2|S_n|^{-1}\nu_{it}(|\xi|)\,|\xi|^{-(n-1)}$$

satisfies $\mathcal{F}_n^{-1}(W_t) = Q$ on $B_n(R)$.

Proof. Since $T \gg 0$ on $(-R, R)$ and T is even, T must be real. In particular, this implies that if $u \in H$, then $\bar{u} \in H$ and $\|\bar{u}\| = \|u\|$. Now by definition of u_{it}, we have that, for all $\varphi \in C_0^\infty((0,R))$,

$$[u_{it}, \varphi] = \langle T, (u_{it})^\vee * \bar{\varphi} \rangle = \int_{\mathfrak{R}} e^{-2\pi x} \overline{\varphi(x)}\, dx$$

$$= \overline{\int_{\mathfrak{R}} e^{-2\pi x} \varphi(x)\, dx} = \overline{\langle T, (u_{it})^\vee * \varphi \rangle}$$

$$= \langle T, (\overline{u_{it}})^\vee * \bar{\varphi} \rangle = [\overline{u_{it}}, \varphi].$$

Hence, $\overline{u_{it}} = u_{it}$ by uniqueness, and thus, $\overline{\hat{u}_{it}(-\gamma)} = \hat{u}_{it}(\gamma)$, which proves (5.1). This clearly implies that ν_{it} defined by (3.4) is even and thus $\mathcal{F}_n^{-1}(W_t) = Q$ on $B_n(R)$ by Theorem 4.5. ∎

We can now state a maximum entropy theorem for extensions of radial positive-definite distributions.

Theorem 5.2. Consider a radial distribution $Q \gg 0$ on $B_n(R)$, $0 < R < \infty$ and suppose that the associated distribution T satisfies (3.2). Let μ be a positive tempered measure on $\hat{\mathfrak{R}}^n$ with $\mu = w + \mu_s$, where $w \in L^1_{loc}(\hat{\mathfrak{R}}^n)$ and μ_s is singular. Then, if $\mathcal{F}_n^{-1}(\mu) = Q$ on $B_n(R)$ and $t > 0$, we have the entropy inequality

$$\int_{\mathfrak{R}^n} \frac{\log w(\xi)}{(t^2 + |\xi|^2)|\xi|^{n-1}}\, d\xi \leq \int_{\mathfrak{R}^n} \frac{\log W_t(\xi)}{(t^2 + |\xi|^2)|\xi|^{n-1}}\, d\xi \tag{5.2}$$

with equality if and only if $\mu = W_t$.

Proof. We note first that

$$\int_{\mathfrak{R}^n} \frac{2t}{\pi |S_n| (t^2 + |\xi|^2)|\xi|^{n-1}}\, d\xi = 1.$$

Therefore we obtain, using Jensen's inequality and Lemma 5.1, that

$$\exp\left[\int_{\mathfrak{R}^n} \frac{2t \log(w(\xi)/W_t(\xi))}{\pi |S_n| (t^2 + |\xi|^2)|\xi|^{n-1}}\, d\xi\right]$$

$$\leq \int_{\mathfrak{R}^n} \frac{2t\, w(\xi)}{\pi |S_n| (t^2 + |\xi|^2)|\xi|^{n-1} W_t(\xi)}\, d\xi$$

$$= \int_{\mathfrak{R}^n} \frac{t\, w(\xi)}{\pi (t^2 + |\xi|^2) \nu_{it}(|\xi|)}\, d\xi$$

$$= \int_{\mathfrak{R}^n} |\bar{u}_{it}(|\xi|)|^2\, w(\xi)\, d\xi\, \|u_{it}\|^{-2}$$

$$\leq \int_{\mathfrak{R}^n} |\hat{u}_{it}(|\xi|)|^2\, d\mu(\xi)\, \|u_{it}\|^{-2}$$

$$= \langle T, (u_{it})^\vee * \overline{u_{it}} \rangle \|u_{it}\|^{-2}$$

$$= \|u_{it}\|^2 \|u_{it}\|^{-2} = 1,$$

and (5.2) follows. Since equality in Jensen's inequality only occurs for constant functions, an equality in (5.2) implies that $\mu_s = 0$ and $w = W_t$. ∎

Remark 5.3. The measure μ in Theorem 5.2 need not be radial. Let us also mention that some of the computations involving u_{it} in the proof above are a bit formal, but they can be easily justified by considering a sequence in $C_o^\infty((0,R))$ converging to u_{it} in H.

6. Bibliography

[1] E.J. Akutowicz. On extrapolating a positive-definite function from a finite interval. *Math. Scand.*, 7, 1959.

[2] E.J. Akutowicz. Sur l'approximation par certaines fonctions entières. *Ann. Scient. Ec. Norm. Sup.*, 3e série:281–301, 1960. t. 77.

[3] J. Benedetto. Fourier uniqueness criteria and spectrum estimation theorems. In J. Price, editor, *Fourier Techniques and Applications*, pages 149–170. Plenum, New York, 1985.

[4] J. Benedetto. A qualitative maximum entropy theorem for the real line. *Integral Equations and Operator Theory*, 10:761–779, 1987.

[5] J.P. Burg. *Maximum Entropy Spectral Analysis*. PhD thesis, Stanford University, 1975.

[6] J. Chover. On normalized entropy and the extensions of a positive-definite function. *J. Math. Mech.*, 19:927–945, 1961.

[7] H. Dym. *J contractive matrix functions, reproducing kernel Hilbert spaces and interpolation*, volume 71 of *CBMS Regional conference Series in Mathematics*, pages 157–169. AMS, Providence, RI, 1989.

[8] J.-P. Gabardo. Extension of positive-definite distributions and maximum entropy. Preprint.

[9] I.M. Gel'fang and N. Ya Vilenkin. *Generalized Functions*, volume 4 of *Applications to Harmonic Analysis*. Academic Press, New York, 1964–68.

[10] M.G. Krein. Sur le problème de prolongement des fonctions Hermitiennes positives et continues. *C.R. (Doklady) Acad. Sci. U.S.S.R.*, 26:17–22, 1940.

[11] H.J. Landau. Maximum entropy and the moment problem. *Bull. AMS*, 16:47–77, 1987.

[12] A.E. Nussbaum. Integral representation of functions and distributions positive-definite relative to the orthogonal group. *Trans. Amer. Math. Soc.*, 175:355–387, 1973.

[13] W. Rudin. The extension problem for positive-definite functions. *Ill. J. Math*, 7:532–539, 1963.

[14] W. Rudin. An extension theorem for positive-definite functions. *Duke Math. J.*, 37:49–53, 1970.

[15] L. Schwartz. *Théorie des Distributions.* Hermann, Paris, 1966.

[16] M.I. Yadrenko. *Spectral Theory of Random Fields.* Translations series in mathematics and engineering. Optimization Software, INC., Publications Division, New York, 1983.

[17] A.M. Yaglom. *Correlation Theory of Stationary and Related Random Functions I, Basic Results.* Springer-Verlag, New York, 1987.

The phase behaviour of ultraflat unimodular polynomials

B. Saffari
Département de Mathématiques
Université de Paris-Sud
91405 Orsay France
saffari@matups.matups.fr
Also at Prometheus Inc.

1. Introduction

In Sections 4 through 11 of this paper we study the phase behaviour, on the unit circle, for the so called "ultraflat unimodular polynomials" the existence of which is known since Kahane's celebrated 1980 paper [7]. Before doing so we recall, in Sections 2 and 3, some definitions and historical background.

Throughout this paper, the implied constants in the O notation of Landau are understood as absolute. A notation such as O_δ means that the implied constant depends only on the parameter δ.

2. Some historical background

As in Littlewood [9], let $\mathcal{S}_n$ denote the class of those polynomials $P(z) = \sum_{k=0}^{n} a_k z^k$ which are unimodular, i.e., all of whose coefficients are complex numbers of modulus 1:

$$|a_k| = 1 \qquad \text{for all } k = 0, 1, \ldots, n.$$

By Parseval's formula $\int_0^1 |P(e^{2i\pi\theta})|^2 d\theta = n + 1$, we then have (for $n \geq 1$)

$$\min_{|z|=1} |P(z)| < \sqrt{n+1} < \max_{|z|=1} |P(z)|. \tag{2.1}$$

An old problem (or rather an old *theme*) is this:

Problem (Littlewood's flatness problem). How close can such a unimodular polynomial come to satisfying

$$|P(z)| \equiv \sqrt{n+1} \text{ on the whole unit circle } |z| = 1? \tag{2.2}$$

We insist on the (obvious) fact that (2.2) is impossible if $n \geq 1$. So one must look for less than (2.2), but then there are various ways of seeking

J. S. Byrnes et al. (eds.), Probabilistic and Stochastic Methods in Analysis, with Applications, 555–572.
© 1992 *Kluwer Academic Publishers. Printed in the Netherlands.*

such an "approximate situation." One way is this: in 1966 Littlewood [9] conjectured the existence of unimodular polynomials of arbitrarily large degrees which are *flat* on the unit circle, that is, such that

$$B\sqrt{n+1} \leqslant |P(z)| \leqslant A\sqrt{n+1} \qquad \text{(whenever } |z| = 1\text{)} \tag{2.3}$$

where A and B are positive *absolute* constants (satisfying, of course, $0 < B < 1 < A$). We do not know who coined the term "flat," nowadays commonly used to describe those $P \in \mathcal{G}_n$ which satisfy (2.3): it was not mentioned by Littlewood [9], but became customary after Körner [8] proved, in 1980, Littlewood's conjecture on the existence of such polynomials.

Let us emphasize that the important aspect of the above conjecture of Littlewood (now Körner's theorem) is really the *lower* bound $B\sqrt{n+1}$ in (2.3). Indeed, if we just require polynomials $P \in \mathcal{G}_n$ with the *upper* bound condition

$$\max_{|z|=1} |P(z)| \leqslant A\sqrt{n+1} \qquad (A = \text{some absolute constant}), \tag{2.4}$$

then as early as 1914 Bernstein [3] proved in essence, as a lemma for the study of absolute convergence of Fourier series, that the polynomial

$$G(z) = \sum_{k=0}^{n} e^{i\alpha k^2/(n+1)} \cdot z^k \qquad (\alpha = \text{real constant} \neq 0) \tag{2.5}$$

indeed satisfies the upper-bound inequality (2.3), with $A = A(\alpha)$ depending only on α. See Bari's book [1] for a simplified version of Bernstein's proof. In particuliar the constant A becomes absolute in the case of

$$G_1(z) = \sum_{k=0}^{n} e^{i\pi k^2/(n+1)} \cdot z^k \tag{2.6}$$

and

$$G_2(z) = \sum_{k=0}^{n} e^{i\pi k(k+1)/(n+1)} \cdot z^k = G_1(ze^{i\pi/(n+1)}). \tag{2.7}$$

The polynomials $G(z)$, $G_1(z)$, and $G_2(z)$ are often called Gauss polynomials because of their obvious connection with Gauss sums. Since Bernstein's early work, various examples of $P \in \mathcal{G}_n$ satisfying (2.4) have been found and much research has been done on them. (For an account of some of the work done till the mid 1960's, see Littlewood's book [10, pp. 25–32]. A fairly complete account of this topic alone would require a respectable expository paper. Yet, in this paper, I will resist the temptation to digress into any example other than the already mentioned Gauss polynomials and the example given by relation (2.10) below.

What led to Körner's existence proof for (2.3) has a rather interesting history. It was known to Littlewood [9] that the (special) Gauss polynomials $G_1(z)$ and $G_2(z)$ defined by (2.6) and (2.7) have the following surprising properties: for any δ with $0 < \delta < 1/2$, we have

$$|G_1(e^{it})| = \sqrt{n+1} + O_\delta(n^\delta) \qquad \text{outside } 0 \leqslant |t| \leqslant n^{-\delta} \tag{2.8}$$

and (equivalently) a similar estimate for $|G_2(e^{it})|$, but we also have

$$\min_t |G_1(e^{it})| = \min_t |G_2(e^{it})| = O_\delta(n^\delta). \tag{2.9}$$

Thus, because of (2.8), the Gauss polynomials G_1 and G_2 almost satisfy Littlewood's condition (2.3) with nearly optimal constants but, because of (2.9), they just fail to satisfy the lower bound condition in (2.3). In his 1977 paper [4], Byrnes proved that the unimodular polynomial (of degree $n^2 - 1$)

$$B(z) := \sum_{k\ 0}^{n-1} \sum_{r\ 0}^{n-1} \omega^{kr/n} z^{k+rn} \qquad (\omega = e^{2i\pi/n}) \tag{2.10}$$

has properties remarkably similar to those of $G_1(z)$ and $G_2(z)$. In particular he proved, for $B(z)$, estimates somewhat sharper than (2.8) and (2.9), with much simpler proofs, and also extended his estimates to arbitrary degrees. In addition Byrnes used the same method to prove that by suitably "perturbing" $O(n^{3/4})$ terms of $P(e^{it})$ for some $P \in \mathcal{S}_n$, one obtains a function $f(t)$ such that, for every real t,

$$|f(t)| = \sqrt{n+1} + O(n^{1/4}) \qquad \text{(uniformly in } t \text{ and } n). \tag{2.11}$$

Then Körner [8] proved, via a modification of Byrnes's last construction together with the use of a probabilistic idea, the existence of some $P \in \mathcal{S}_n$ satisfying (2.3).

3. Ultraflat polynomials

In the same 1966 paper [9], Littlewood had also suggested that, conceivably, there might even exist a sequence (P_m) of polynomials in $\mathcal{S}_n$ (possibly even with coefficients all equal to $+1$) such that $(n+1)^{-1/2}|P(e^{it})|$ converges to 1 uniformly in t. We shall call such sequences of unimodular polynomials "ultraflat." More precisely, we shall give the following definition:

Definition. Given a sequence (ϵ_n) of positive numbers tending to zero, we shall say that a sequence (P_m) of unimodular polynomials is (ϵ_n)-*ultraflat* if $\deg P_m \to \infty$ as $m \to \infty$ and if, for $|z| = 1$,

$$(1-\epsilon_n)\sqrt{n+1} \leqslant |P_m(z)| \leqslant (1+\epsilon_n)\sqrt{n+1} \qquad (\text{where } n = \deg P_m) \tag{3.1}$$

or, equivalently,

$$\max_{|z|=1} \left| |P(z)| - \sqrt{n+1} \right| \leqslant \epsilon_n \sqrt{n+1} \qquad (n = \deg P_m). \tag{3.2}$$

In looser terms, we shall simply say that a unimodular polynomial $P(z)$ of large degree (i.e., going to infinity) is *ultraflat* if $P = P_m$ for some m, where (P_m) is an (ϵ_n)-ultraflat sequence for some suitable (ϵ_n) tending to zero.

Despite Körner's above-mentioned result on the existence of "flat" unimodular polynomials, the existence of *ultraflat* unimodular polynomials seemed very unlikely, in view of a 1957 conjecture of P. Erdös (problem 22 in [5]) asserting that, for all $P \in \mathcal{S}_n$ with $n \geqslant 1$,

$$\max_{|z|=1} |P(z)| \geqslant (1 + C)\sqrt{n+1} \tag{3.3}$$

where C is some positive absolute constant. Yet, shortly after Körner's proof, Kahane [7] further refined Körner's method and proved that there exists a sequence $(P_n)_{n \geqslant 1}$, with $P_n \in \mathcal{S}_n$, which is (ϵ_n)-ultraflat, where

$$\epsilon_n = O\left(n^{-1/17}\sqrt{\log n}\right). \tag{3.4}$$

Thus theErdös conjecture (3.3) was disproved (in the case of the class $\mathcal{S}_n$). For the more restricted class $\mathcal{T}_n$ of those $P(z)$, all of whose coefficients are ± 1; the analogous Erdös conjecture remains unsettled to this date (end of 1991). We conjecture that, for the ± 1 polynomials, it is true, and consequently we conjecture that there are no ultraflat polynomials with only ± 1 coefficients.

Some additional remarks on Kahane's breakthrough are made in Section 12. For the moment let us insist that the ultraflat polynomials $P \in \mathcal{S}_n$ whose phase behaviour we shall be studying below are not necessarily those of Kahane's paper [7]: we shall consider *arbitrary* ultraflat polynomials $P \in \mathcal{S}_n$, only assumed to satisfy (3.1) or (3.2) for *some* sequence (ϵ_n) tending to zero.

4. The phase problem: the main conjectures

We shall henceforth suppose that $P \in \mathcal{S}_n$, $(n \to \infty)$, is (ϵ_n)-ultraflat, that is, satisfies (3.1). Write

$$P(e^{it}) = R(t)e^{i\alpha(t)} \qquad \text{with } R(t) = |P(e^{it})|. \tag{4.1}$$

We think of t as time. The ultraflatness condition (3.1) means that the mobile point $P(e^{it})$ moves inside a narrow annulus centered at the origin and of inner (resp. outer) radius $(1 - \epsilon_n)\sqrt{n+1}$ (resp. $(1 + \epsilon_n)\sqrt{n+1}$). Our

purpose is the *phase problem*, i.e., the study of the phase $\alpha(t)$, or rather the (instantaneous) angular speed $\alpha'(t)$. Writing

$$P(e^{it}) = \sum_{k=0}^{n} \exp(ikt + i\theta_k) \qquad (\theta_k \in \mathfrak{R} \text{ for all } k),$$

we see that we have $n+1$ unit vectors whose endpoints $\exp(ikt+i\theta_k)$ rotate along the unit circle with (respective) constant angular speeds $0, 1, 2, \ldots, n$. That $P(z)$ is ultraflat is equivalent to saying that there is a choice of the initial positions $\exp(i\theta_k)$, $(k = 0, 1, 2, \ldots, n)$ so that the resultant vector has endpoint $P(e^{it})$ moving in the above-mentioned narrow annulus. Our intuition tells us (or at least mine did, when I considered the problem) two things. First that, since the "components" $\exp(ikt + i\theta_k)$ have (respective) angular speeds $0, 1, 2, \ldots, n$, then the "resultant angular speed" is approximately their average; in other words we, *might expect* to have

$$\alpha'(t) = n/2 + o(n). \tag{4.2}$$

We shall see that (4.2) is trivially true *in average*, that is,

$$\frac{1}{2\pi}\int_0^{2\pi} \alpha'(t)dt = n/2 + O(n\epsilon_n) \tag{4.3}$$

but that (4.2) itself is far from being true. Indeed we shall prove (Theorem 5.2) that $\alpha'(t)$ takes values at least as large as $2n/3 + O(n\epsilon_n)$ and as small as $n/3 + O(n\epsilon_n)$.

Secondly, our intuition tells us that, since all the components $\exp(ikt + i\theta_k)$ turn counter-clockwise, then so does their resultant $P(e^{it})$, modulo negligible fluctuations; in other words,

$$\min_{0 \leqslant t \leqslant 2\pi} \alpha'(t) \geqslant o(n). \tag{4.4}$$

Now (4.4) is indeed true: we shall prove (Theorem 5.2) that

$$O(n\epsilon_n) \leqslant \alpha'(t) \leqslant n + O(n\epsilon_n). \tag{4.5}$$

Actually we *conjecture* that

$$\min_{0 \leqslant t \leqslant 2\pi} \alpha'(t) = O(n\epsilon_n), \qquad \max_{0 \leqslant t \leqslant 2\pi} \alpha'(t) = n + O(n\epsilon_n), \tag{4.6}$$

and even something much more specific, namely that the normalized angular speed $\alpha'(t)/n$ is, *asymptotically*, uniformly distributed in $[0, 1]$. (The precise definition is given below).

At this point let us formulate the main conjecture and, in Section 5, our partial results that support it. (Recall that $P \in \mathcal{G}_n$ is supposed (ϵ_n)-ultraflat, i.e., that (3.1) holds).

Conjecture (Uniform distribution conjecture for the angular speed). In the interval $0 \leqslant t \leqslant 2\pi$, the distribution of the normalized angular speed $\alpha'(t)/n$ converges to the uniform distribution as $n \to \infty$. More precisely, for any $x \in [0,1]$ we have

$$\text{meas}\{t \in [0,2\pi] : 0 \leqslant \alpha'(t) \leqslant nx\} = 2\pi x + O(\epsilon_n). \tag{4.7}$$

For the special ultraflat polynomials produced by Kahane [7], (4.7) is indeed true. (See [11]).

In the general case (4.7) can, by integration, be reformulated (equivalently) in terms of the moments of the angular speed $\alpha'(t)$:

Conjecture (Reformulation of the uniform distribution conjecture). For any $q > 0$ we have

$$\frac{1}{2\pi}\int_0^{2\pi} |\alpha'(t)|^q dt = \frac{n^q}{q+1} + O(n^q \epsilon_n). \tag{4.8}$$

We also have the following closely related (and, in some sense, *stronger)* conjecture. It says that the angular acceleration $\alpha''(t)$ and the other higher derivatives of $\alpha(t)$ are L^2-negligible, i.e., have very small L^2 norms on $[0,2\pi]$:

Conjecture (Negligibility conjecture for higher derivatives). For every integer $r \geqslant 2$, the derivative $\alpha^{(r)}$ of order r satisfies

$$\frac{1}{2\pi}\int_0^{2\pi} |\alpha^{(r)}(t)|^2 dt = O_r(n^{2r}\epsilon_n). \tag{4.9}$$

One can prove that (4.9) implies (4.8), but with error $O_q(n^q \epsilon_n)$. The above conjectures (4.7), (4.8) and (4.9) suggest that, very roughly speaking, the unit circle can be divided into a small number of arcs ("small" meaning bounded or $O_\delta(n^\delta)$ for all $\delta > 0$) such that, on each such arc S, the circular motion of $e^{i\alpha(t)}$ is either (approximately) uniformly accelerated or uniformly retarded; in other words, the angular speed might have the form

$$\alpha'(t) = ant + b + \nu(t) \qquad (\text{for } t \in S) \tag{4.10}$$

where $a = a(S)$ and $b = b(S)$ are "constants" depending only on S, and $\nu(t) = \nu(S,t)$ is a "noise term" all of whose derivatives have negligible L^2 norms.

For the special ultraflat polynomials produced by Kahane [7], the phenomenon (4.10) is indeed the case. (See [11]).

The results we state in the next section, and prove in Sections 6 through 11, *partially* confirm the above conjectures.

5. The phase problem: statements of results

In this section, we state some results which will be proved in Sections 6 through 11. We keep all the notation of the previous sections. In particular $P \in \mathcal{S}_n$ is (ϵ_n)-ultraflat.

Theorem 5.1. Let $\mathcal{C}$ denote the (closed) trajectory of $P(e^{it})$ as t runs over $[0, 2\pi]$. Then the average value of the angular speed $\alpha'(t)$ on $[0, 2\pi]$ (which is also the winding number of $\mathcal{C}$ with respect to the origin) is given by

$$\frac{1}{2\pi}\int_0^{2\pi} \alpha'(t)dt = \frac{1}{2\pi}\int_0^{2\pi} \frac{e^{it}P'(e^{it})}{P(e^{it})}dt = \frac{n}{2} + O(n\epsilon_n). \tag{5.1}$$

Theorem 5.2. We have

$$O(n\epsilon_n) \leqslant \min_{0\leqslant t\leqslant 2\pi} \alpha'(t) \leqslant n/3 + O(n\epsilon_n) \tag{5.2}$$

and

$$2n/3 + O(n\epsilon_n) \leqslant \max_{0\leqslant t\leqslant 2\pi} \alpha'(t) \leqslant n + O(n\epsilon_n). \tag{5.3}$$

Remark 5.3. If the "uniform distribution conjecture" (4.7) is true, then it immediately follows that (5.2) and (5.3) can be improved to

$$\min_{0\leqslant t\leqslant 2\pi} \alpha'(t) = O(n\epsilon_n) \text{ and } \max_{0\leqslant t\leqslant 2\pi} \alpha'(t) = n + O(n\epsilon_n). \tag{5.4}$$

Theorem 5.4. Put $\|\varphi\|_q = \left(\frac{1}{2\pi}\int_0^{2\pi} |\varphi(t)|^q dt\right)^{1/q}$ if $\varphi \in L^q(0, 2\pi)$ and $q \geqslant 1$. Then

$$\|\alpha'\|_2^2 = n^2/3 + O(n^2\epsilon_n) \tag{5.5}$$

and

$$\|\alpha'\|_4^4 + \|\alpha''\|_2^2 = n^4/5 + O(n^4\epsilon_n). \tag{5.6}$$

We see that the relations (5.1), (5.2), (5.3) and (5.5) are all partial confirmations of the "uniform distribution conjectures" (4.7) and (4.8). Relation (5.6) is also consistent with the conjectures (4.8) and (4.9). Indeed, (4.8) and (4.9) would respectively imply

$$\|\alpha'\|_4^4 = n^4/5 + O(n^4\epsilon_n) \qquad \text{(case } q = 4 \text{ of Conjecture (4.8))} \tag{5.7}$$

and

$$\|\alpha''\|_2^2 = O(n^4\,\epsilon_n) \qquad \text{(case } r = 2 \text{ of Conjecture (4.9))} \tag{5.8}$$

and we see that *theorem* (5.6) is obtained by adding up the conjectural relations (5.7) and (5.8).

Now (5.5) and the trivial inequality $\|\alpha'\|_4 \geqslant \|\alpha'\|_2$ imply:

$$\|\alpha'\|_4^4 \geqslant n^4/9 + O(n^4\,\epsilon_n) \tag{5.9}$$

and, *equivalently*, in view of (5.6)

$$\|\alpha''\|_2^2 \leqslant \frac{4}{45}n^4 + O(n^4\epsilon_n). \tag{5.10}$$

Of course (5.9) and (5.10) are very poor compared to the optimal (conjectural) relations (5.7) and (5.8). But one further "partial confirmation" of our above conjectures is the following improvement of the trivial inequalities (5.9) and (5.10):

Theorem 5.5. There is an (effectively computable) absolute constant $\gamma > 0$ such that the trivial inequalities (5.9) and (5.10) can be improved to the respective (equivalent) relations

$$\|\alpha'\|_4^4 \geqslant \left(\frac{1}{9} + \gamma\right) n^4 + O(n^4\epsilon_n) \tag{5.11}$$

and

$$\|\alpha''\|_2^2 \leqslant \left(\frac{4}{45} - \gamma\right) n^4 + O(n^4\epsilon_n). \tag{5.12}$$

In Section 11 we shall prove the existence of such a constant γ, but will not compute a numerical value for it, because further refinements of our present method (to be written out later) will provide better numerical values.

6. Some preliminary estimates

We first show that the sequence (ϵ_n) in the flatness condition (3.1) necessarily satisfies

$$\epsilon_n \geqslant n^{-1} + O(n^{-2}). \tag{6.1}$$

(This can be improved, but all we need here is to know that $\epsilon_n \geqslant Kn^{-1}$ for some absolute constant $K > 0$). To prove (6.1), write

$$f(t) = |P(e^{it})|^2 = \sum_{k=-n}^{n} c_k e^{ikt} \qquad (c_{-k} = c_k) \tag{6.2}$$

and note that $c_0 = n + 1$ and $c_n = \bar{a}_0 a_n$, so $|c_n| = 1$. Also write

$$g(t) = |P(e^{it})|^2 - (n+1) = \sum_{1 \leqslant |k| \leqslant n} c_k e^{ikt} \tag{6.3}$$

and

$$\begin{aligned} h(t) &= \frac{1}{n} \sum_{r=0}^{n-1} g\left(t + \frac{2r\pi}{n}\right) \\ &= c_n e^{int} + \bar{c}_n e^{-int} = 2\cos(nt + \varphi) \end{aligned} \tag{6.4}$$

where $c_n = e^{i\varphi}$. Then by (6.3), (6.4) and (3.1),

$$2 = \|h\|_\infty \leqslant \|g\|_\infty \leqslant (n+1)(2\epsilon_n + \epsilon_n^2), \tag{6.5}$$

whence

$$\epsilon_n \geqslant \left(1 + \frac{2}{n+1}\right)^{1/2} - 1 = n^{-1} + O(n^{-2}) \tag{6.6}$$

which proves (6.1).

In all the O estimates below, we are using the fact that, by (6.1), uniformly bounded functions are $O(n\epsilon_n)$. First rewrite (3.1) in the cruder form

$$R(t) = \sqrt{n} + O(\sqrt{n}\epsilon_n) \qquad \text{where } R(t) = |P(e^{it})|. \tag{6.7}$$

We shall also need estimates for $R'(t)$ and $R''(t)$. (In the rest of this paper we suppose n large enough so that $P(z)$ has no root on the unit circle: $P(e^{it}) \neq 0$, so $R(t) > 0$ and $f(t) > 0$). Once again, by (3.1) or (6.7),

$$f(t) = n + O(n\epsilon_n) \text{ and } g(t) = O(n\epsilon_n), \tag{6.8}$$

so Bernstein's inequality applied to the trigonometric polynomial $g(t)$ implies

$$\|f'\|_\infty = \|g'\|_\infty = O(n^2\epsilon_n) \text{ and } |f''\|_\infty = \|g''\|_\infty = O(n^3\epsilon_n). \tag{6.9}$$

Now $R(t) = \sqrt{f(t)}$, hence

$$R'(t) = \frac{f'(t)}{2\sqrt{f(t)}} = \frac{O(n^2\epsilon_n)}{2\sqrt{n} + O(\sqrt{n} \cdot \epsilon_n)} = O(n^{3/2}\epsilon_n) \tag{6.10}$$

and similarly

$$\begin{aligned} R''(t) &= \frac{2f(t)f''(t) - (f'(t))^2}{4(f(t))^{3/2}} \\ &= \frac{O(n^4\epsilon_n)}{4n^{3/2} + O(n^{3/2}\epsilon_n)} = O(n^{5/2}\epsilon_n). \end{aligned} \tag{6.11}$$

7. Proof of Theorem 5.1

Differentiate (4.1):

$$ie^{it}P'(e^{it}) = R'(t)e^{i\alpha(t)} + i\alpha'(t)R(t)e^{i\alpha(t)} \tag{7.1}$$

whence

$$\alpha'(t) = \frac{e^{it}P'(e^{it})}{P(e^{it})} + i\frac{R'(t)}{R(t)}. \tag{7.2}$$

Since $\alpha'(t)$ is real, on integrating (7.2) over $[0, 2\pi]$ we have

$$\frac{1}{2\pi}\int_0^{2\pi} \alpha'(t)dt = \frac{1}{2\pi}\int_0^{2\pi} \frac{e^{it}P'(e^{it})}{P(e^{it})}dt \tag{7.3}$$

(winding number of $\mathcal{C}$ around the origin). Of course (7.3) is a well known elementary result. We now prove (5.1). By (3.1) and by Bernstein's inequality applied to our (ϵ_n)-ultraflat polynomial

$$P(z) = \sum_{k=0}^{n} a_k z^k \in \mathcal{G}_n, \tag{7.4}$$

we have

$$e^{it}P'(e^{it})\overline{P(e^{it})} = O(n^2), \tag{7.5}$$

hence by (6.1), (6.8), (7.3) and (7.4),

$$\begin{aligned}\frac{1}{2\pi}\int_0^{2\pi} \alpha'(t)dt &= \frac{1}{2\pi}\int_0^{2\pi} \frac{e^{it}P'(e^{it})\overline{P(e^{it})}}{n + O(n\epsilon_n)}dt \\ &= \frac{1}{n}\cdot\frac{1}{2\pi}\int_0^{2\pi} e^{it}P'(e^{it})\overline{P(e^{it})}dt + O(n\epsilon_n) \\ &= \frac{1}{n}\sum_{k=1}^{n} k|a_k|^2 + O(n\epsilon_n) \\ &= \frac{1}{n}\cdot\frac{n(n+1)}{2} + O(n\epsilon_n) = \frac{n}{2} + O(n\epsilon_n)\end{aligned}$$

which proves (5.1) and Theorem 5.1.

8. Proof of part of Theorem 5.2

Here we only prove the inequalities

$$O(n\epsilon_n) \leqslant \min_{0\leqslant t\leqslant 2\pi} \alpha'(t) \leqslant \max_{0\leqslant t\leqslant 2\pi} \alpha'(t) \leqslant n + O(n\epsilon_n). \tag{8.1}$$

(The proof of the rest of Theorem 5.2 uses Theorem 5.4, and will be given in Section 10. By (6.7), (7.2) and Bernstein's inequality applied to P, we have

$$\begin{aligned} \alpha'(t) = \Re e\left(\frac{e^{it}P'(e^{it})}{P(e^{it})}\right) &\leqslant \left|\frac{P'(e^{it})}{P(e^{it})}\right| \\ &\leqslant \frac{n^{3/2} + O(n^{3/2}\epsilon_n)}{\sqrt{n} + O(\sqrt{n}\epsilon_n)} = n + O(n\epsilon_n) \end{aligned} \tag{8.2}$$

which proves the rightmost inequality in (8.1). Now consider the "inverse" P^* of P, i.e., the polynomial

$$P^*(z) = \sum_{k=0}^{n} a_{n-k} z^k = z^n \overline{P(1/z)}. \tag{8.3}$$

Obviously $P^* \in \mathcal{G}_n$ and is also (ϵ_n)-ultraflat, since $|P^*(z)| = |P(z)|$ on the unit circle $|z| = 1$. By (8.3),

$$P^*(e^{it}) = R(t)e^{int - i\alpha(t)}. \tag{8.4}$$

So, by applying the conclusion of (8.2) to P^*, with $\alpha(t)$ of course replaced by $nt - \alpha(t)$, we have

$$n - \alpha'(t) \leqslant n + O(n\epsilon_n)$$

which proves the leftmost inequality in (8.1).

9. Proof of Theorem 5.4

By (7.1) we have

$$|P'(e^{it})|^2 = |R(t)\alpha'(t)|^2 + |R'(t)|^2. \tag{9.1}$$

Now, by (7.4),

$$\frac{1}{2\pi}\int_0^{2\pi} |P'(e^{it})|^2 dt = \sum_{k=1}^{n} k^2 |a_k|^2 = n(n+1)(2n+1)/6$$

while, by (6.7) and (6.10),

$$\frac{1}{2\pi}\int_0^{2\pi} (|R(t)\alpha'(t)|^2 + |R'(t)|^2)\, dt = n(1 + O(\epsilon_n)) \cdot \|\alpha'\|_2^2 + O(n^3\epsilon_n^2).$$

Comparing the last two equalities yields (5.5). To prove (5.6), differentiate again (7.1) and then take the squares of the moduli of both sides, to obtain

$$\begin{aligned} &|P'(e^{it}) + e^{it}P''(e^{it})|^2 \\ &\quad = |R''(t) - (\alpha'(t))^2 R(t)|^2 + |2\alpha'(t)R'(t) + \alpha''(t)R(t)|^2. \end{aligned} \tag{9.2}$$

Integrate both sides of (9.2) over $[0, 2\pi]$ (with respect to $dt/2\pi$). By (7.4), the integral of the left side is

$$\frac{1}{2\pi}\int_0^{2\pi}\left|\sum_{k=0}^{n} k^2 a_k e^{ikt}\right|^2 dt = \sum_{k=1}^{n} k^4 = n^5/5 + O(n^4) \tag{9.3}$$

while that of the right hand side is

$$(\|\alpha'\|_4^4 + \|\alpha''\|_2^2)\cdot n(1 + O(\epsilon_n)) + O(n^5\epsilon_n) \tag{9.4}$$

in view of (6.7), (6.10), (6.11), (8.1) and the estimate $\alpha''(t) = O(n^2)$ which can be obtained by differentiating (7.2) and by using Bernstein's inequality. Comparing (9.3) and (9.4) yields (5.6) and completes the proof of Theorem 5.4.

10. End of proof of Theorem 5.2

We adopt an idea already used in [12]. Write

$$\mu = \min_{0\le t\le 2\pi} \alpha'(t) \text{ and } M = \max_{0\le t\le 2\pi} \alpha'(t). \tag{10.1}$$

To finish the proof of Theorem 5.2, it remains to show that

$$\mu \le n/3 + O(n\epsilon_n) \text{ and } M \ge 2n/3 + O(n\epsilon_n). \tag{10.2}$$

Put $\psi(t) = \alpha'(t) - \mu$ for $0 \le t \le 2\pi$. Then, by (5.1), (5.5) and (8.1),

$$\begin{aligned} \frac{1}{2\pi}\int_0^{2\pi}|\psi(t)|^2 dt &= \|\alpha'\|_2^2 + \mu^2 - 2\mu\cdot\frac{1}{2\pi}\int_0^{2\pi}\alpha'(t)dt \\ &= n^2/3 + \mu^2 - n\mu + O(n^2\epsilon_n). \end{aligned} \tag{10.3}$$

Now, since $0 \le \psi(t) \le M - \mu$, we have by (5.1):

$$\begin{aligned} \frac{1}{2\pi}\int_0^{2\pi}|\psi(t)|^2 dt &\le (M-\mu)\cdot\frac{1}{2\pi}\int_0^{2\pi}\psi(t)dt \\ &= (M-\mu)(n/2 - \mu + O(n\epsilon_n)). \end{aligned} \tag{10.4}$$

Comparing (10.3) and (10.4), we have again by (8.1)

$$n^2/3 - n\mu/2 \le (n/2 - \mu)M + O(n^2\epsilon_n) \tag{10.5}$$

and since by (5.1) we have $\mu \le n/2 + O(n\epsilon_n) \le M$, (10.5) implies (10.2) and completes the proof of Theorem 5.2.

11. Proof of Theorem 5.5

The proof is based on the following lemma.

Lemma. (Concentration on low degrees for real trigonometric polynomials with small L^4 norms). For every $\delta_1 > 0$ and $\delta_2 > 0$, no matter how small, there exists an effectively computable $\epsilon = \epsilon(\delta_1, \delta_2) > 0$ and an integer $m_0 = m_0(\delta_1, \delta_2)$ such that whenever a real trigonometric polynomial

$$F(t) = \sum_{k=0}^{m} (A_k \cos kt + B_k \sin kt)$$

satisfies $m \geqslant m_0$ and

$$\|F\|_4 \leqslant (1+\epsilon)\|F\|_2, \tag{11.1}$$

then

$$\sum_{k<\delta_1 m} (A_k^2 + B_k^2) \leqslant \delta_2 \sum_{k=0}^{m} (A_k^2 + B_k^2). \tag{11.2}$$

Proof (of the lemma). It is more convenient to rewrite $F(t)$ in the form

$$F(t) = \sum_{k=-m}^{m} b_k e^{ikt} \qquad (b_k \in \mathbb{C},\ b_{-k} = b_k)$$

and put $F_\rho(e^{it}) = \sum_{k=-m}^{m} b_k \rho^k e^{ikt}$ where $\rho = e^{\lambda/m}$ and λ is a real parameter at our disposal. Write also:

$$(F(t))^2 = \sum_{h=-2m}^{2m} d_h e^{iht} \qquad (d_{-h} = d_h \text{ for all } h)$$

Then $d_0 = \sum_{k=-m}^{m} |b_k|^2 = \|F\|_2^2$ and

$$\|F\|_4^4 = \sum_{h=-2m}^{2m} |d_h|^2 = d_0^2 + \sum_{h=1}^{2m} |d_h|^2.$$

Thus (11.1) can be rewritten as

$$2\sum_{h=1}^{2m} |d_h|^2 \leqslant \epsilon_1 d_0^2 \text{ with } \epsilon_1 = (1+\epsilon)^4 - 1. \tag{11.3}$$

Now $(F_\rho(e^{it}))^2 = \sum_h^{2m}{}_{-2m} d_h \rho^h e^{iht}$, whence

$$\begin{aligned} \|F_\rho\|_4^4 &= \sum_{h=-2m}^{2m} |d_h|^2 \cdot \rho^{2h} \\ &= d_0^2 + 2\sum_{h=1}^{2m} |d_h|^2 (\rho^{2h} + \rho^{-2h}) \\ &\le d_0^2 + 2(\rho^{4m} + \rho^{-4m}) \sum_{h=1}^{2m} |d_h|^2 \\ &\le d_0^2 (1 + 2\epsilon_1 \cosh(4\lambda)) \end{aligned} \tag{11.4}$$

assuming (11.1) and therefore (11.3). Also

$$\begin{aligned} \|F_\rho\|_4^2 \ge \|F_\rho\|_2^2 &= \sum_{k=-m}^{m} b_k^2 \cdot \rho^{2k} \\ &\ge \sum_{k=-m\delta_1}^{m\delta_1} b_k^2 \cdot \rho^{2k} \\ &= \sum_{k=-m\delta_1}^{m\delta_1} b_k^2 (\rho^{2k} + \rho^{-2k}) - 2 \\ &\ge \left(\sum_{k=-m\delta_1}^{m\delta_1} b_k^2 \right) (\rho^{2m\delta_1} + \rho^{-2m\delta_1}) - 2 \\ &\ge \left(\sum_{k=-m\delta_1}^{m\delta_1} b_k^2 \right) \cosh(2\lambda\delta_1). \end{aligned} \tag{11.5}$$

By (11.4) and (11.5), we see that (11.1) implies

$$\left(\sum_{k=-m\delta_1}^{m\delta_1} b_k^2 \right) \Big/ \|F\|_2^2 \le \frac{(1 + 2\epsilon_1 \cosh(4\lambda))^{1/2}}{\cosh(2\lambda\delta_1)}. \tag{11.6}$$

For any fixed $\epsilon_1 > 0$ and any fixed δ_1, $(0 < \delta_1 < 1)$, the right hand side of (11.6) tends to infinity as $\lambda \to +\infty$; therefore, as λ varies in $\mathfrak{R}$, the right hand side of (11.6) has a minimum $M(\epsilon, \delta_1)$. For fixed δ_1, we have $\lim_{\epsilon \to 0} M(\epsilon, \delta_1) = 0$. So, for any fixed $\delta_2 > 0$ and any $\epsilon > 0$ *sufficiently small* the right hand side of (11.6) is $< \delta_2$ for some choice of $\lambda = \lambda(\epsilon, \delta_1, \delta_2) < \infty$. This completes the proof of the lemma. ∎

Proof (of Theorem 5.5). The idea is to use the fact that

$$\alpha'(t) = F(t) + O(n\epsilon_n) \text{ and } \alpha''(t) = F'(t) + O(n^2\epsilon_n) \tag{11.7}$$

where *here* $F(t)$ is the trigonometric polynomial $n^{-1}\Re e(e^{it}P'(e^{it})\overline{P(e^{it})})$, and to apply the lemma to *this* F, (of degree $m = 2n$). The two estimates (11.7) follow from (7.2) and the error estimates of § 6 via Bernstein's inequality. The proof of Theorem 5.5 is by contradiction.

Suppose Theorem 5.5 is not true. Then, for any fixed $\delta_1 > 0$ and $\delta_2 > 0$, and any δ with $0 < \delta < \epsilon(\delta_1, \delta_2)$ [where $\epsilon = \epsilon(\delta_1, \delta_2)$ is that of the lemma] and any sufficiently large n, we have the (equivalent) inequalities

$$\begin{aligned} \|\alpha'\|_4^4 &\leqslant \left(\frac{1}{9} + \delta\right) n^4 + O(n^4\epsilon_n) \\ &= (1 + 9\delta)\|\alpha'\|_2^4 + O(n^4\epsilon_n) \end{aligned} \tag{11.8}$$

and

$$\|\alpha''\|_2^2 \geqslant \left(\frac{4}{45} - \delta\right) n^4 + O(n^4\epsilon_n). \tag{11.9}$$

For sufficiently small δ and sufficiently large $m = 2n$, we have, by (11.7), (11.8) and the lemma,

$$\begin{aligned} \|F'\|_2^2 = \sum_{k=1}^{m} k^2(A_k^2 + B_k^2) &= \sum_{k \leqslant m\delta_1} + \sum_{k > m\delta_1} \\ &\leqslant m^2\delta_1^2 \sum_{k \leqslant m\delta_1} (A_k^2 + B_k^2) + m^2 \sum_{k > m\delta_1} (A_k^2 + B_k^2) \\ &\leqslant n^2\delta_1^2\|F\|_2^2 + m^2\delta_2\|F\|_2^2 = 4n^2(\delta_1^2 + \delta_2)\|F\|_2^2 \end{aligned}$$

and therefore, by (11.7) again,

$$\begin{aligned} \|\alpha''\|_2^2 &\leqslant 4n^2(\delta_1^2 + \delta_2)\|\alpha'\|_2^2 + O(n^4\epsilon_n) \\ &= 4(\delta_1^2 + \delta_2)n^4/3 + O(n^4\epsilon_n), \end{aligned}$$

which contradicts (11.9) for sufficiently small δ, δ_1 and δ_2. This proves Theorem 5.5. ∎

12. Miscellaneous remarks

Remark 12.1. In the fall of 1979 J.-P. Kahane gave me a preprint of his paper [7] (I already had a preprint of Körner [8]). I immediately coined the term "flat" for Körner-type polynomials and "ultraflat" for Kahane-type ones. But afterwards I heard exactly these same terms from such unrelated sources that obviously several people must have coined these same words at the same time!

Remark 12.2. The (a priori arbitrary) (ϵ_n)-ultraflat polynomials $P \in \mathcal{G}_n$ have hidden and interesting properties worth studying. (Those produced by Kahane [7] are excellent models for testing ideas and conjectures). Let $P \in \mathcal{G}_n$ be (ϵ_n)-ultraflat, let $P^* \in \mathcal{G}_n$ denote its "inverse" and ${}^*P \in \mathcal{G}_n$ its "reverse" [cf. (8.3)]:

$$P^*(z) = \sum_{k=0}^{n} a_{n-k} z^k = z^n \overline{P(1/z)}$$

$${}^*P(z) = \sum_{k=0}^{n} a_{n-k} z^k = z^n P(1/z).$$

Clearly both P^* and ${}^*P$ are (ϵ_n)-ultraflat, and we conjecture the following "near orthogonality" properties of the pairs (P, P^*) and $({}^*P, P)$:

$$\sum_{k=0}^{n} a_k a_{n-k} = o(n) \qquad (\text{as } n \to \infty) \tag{12.1}$$

$$\sum_{k=0}^{n} a_k a_{n-k} = o(n) \qquad (\text{as } n \to \infty). \tag{12.2}$$

Conjectures (12.1) and (12.2) are much stronger than are the respective statements:

1) "P is nowhere near being self-inversive" (P self-inversive means $P = P^*$, that is, $a_{n-k} = a_k$ for all k).
2) "P is nowhere near being symmetric (or palindromic)" (P symmetric (or palindromic) means $P = {}^*P$, that is, $a_{n-k} = a_k$ for all k).

The truth of Item 1 is a consequence of our paper [6]. In fact, a trivial corollary to the results of [6] is that, if $P \in \mathcal{G}_n$ is ultraflat, then

$$\sum_{k=0}^{n} a_k a_{n-k} \leq \frac{5}{6} n + o(n) \qquad (n \to \infty) \tag{12.3}$$

and I can further decrease the constant $5/6$ in (12.3) (though I am unable to replace it by zero, otherwise I would have a proof of (12.1)). But (2) is an open problem, and so is its following consequence:

Conjecture (Weak form of Item 2 of Remark 12.2). An ultraflat $P \in \mathcal{G}_n$ cannot be symmetric (or palindromic), i.e., we cannot have $P = {}^*P$.

Remark 12.3. Here is another type of open problem:

Conjecture. Let E be any fixed subset of the unit circle which is *not* everywhere dense. Then there cannot exist ultraflat polynomials all of whose coefficients are in E.

It would be most desirable to have a proof of this conjecture for E *finite,* or even when E is the group of d-th roots of 1 for some $d \geqslant 2$. (This is not known for *any* $d \geqslant 2$. The case $d = 2$ is that of the ± 1 polynomials). But J. Beck [2] has combined the existence of Kahane's ultraflat polynomials with other ingenious ideas to give a proof of the following improvement of Körner's theorem:

Theorem 12.4 (Beck). [2]. For fixed $d \geqslant 300$ and sufficiently large n, there are polynomials (of degree n) all of whose coefficients are d-th roots of 1 and which satisfy Littlewood's condition (2.3).

Remark 12.5.

Conjecture (A very general one (containing the previous one)). Let $E \subset \mathbb{C}$, $E \neq \{0\}$, be such that the closure $\bar{E}$ of E contains no circle of centre origin and radius > 0. (For example, any finite set not reduced to the origin.) Let P be any polynomial all of whose coefficients are in E and having at least two nonzero coefficients. Put

$$\|P\|_q = \left(\frac{1}{2\pi} \int_0^{2\pi} |P(e^{it})|^q dt \right)^{1/q} \quad \text{if } -\infty < q < \infty \text{ and } q \neq 0$$

$$\|P\|_\infty = \max_{0 \leqslant t \leqslant 2\pi} |P(e^{it})|\,, \quad \|P\|_{-\infty} = \min_{0 \leqslant t \leqslant 2\pi} |P(e^{it})|$$

$$\|P\|_0 = \exp\left(\frac{1}{2\pi} \int_0^{2\pi} \log|P(e^{it})| dt \right).$$

I conjecture that, whenever $-\infty \leqslant p < q \leqslant \infty$, we have

$$\frac{\|P\|_q}{\|P\|_p} \geqslant 1 + C(p,q) \tag{12.4}$$

where $C(p,q) > 0$ depends only on p and q.

Remark 12.6. There are several other related matters, in particular some interesting problems of D.J. Newman about ultraflat polynomials. I shall deal with them elsewhere.

13. Last minute addendum

A few days after submitting this paper, I made these three observations:

1) Theorem 5.5, as it is stated, is not interesting unless the actual value of γ is computed. Indeed, Hölder's inequality implies the statement

of Theorem 5.5 with $\gamma = 1/27$. But in a forthcoming paper, we shall see that the method of proof of Theorem 5.5 gives a constant γ larger than 1/27.

2) One can obtain (10.2) in a straightforward manner, just by the "degenerate Hölder inequality" majorizing the 2-norm in terms of the 1-norm and the sup-norm.
3) The "negligibility conjecture" for the acceleration alone (case $r = 2$) implies the negligibility conjecture for all $r > 2$, because of Bernstein's inequality, and the approximation relation (11.7) and its analogues for higher derivatives. It would therefore suffice to settle the case $r = 2$.

14. Bibliography

[1] N.K. Bari (Bary). *A treatise on trigonometric series*, volume II. Pergamon, New York, 1964.

[2] J. Beck. "flat" polynomials on the unit circle—on a problem of Littlewood. To appear.

[3] S.N. Bernstein. Sur la convergence absolute des séries trigonométriques. *C.R. Acad. Sci. Paris*, pages 1661–1663, 1914.

[4] J.S. Byrnes. On polynomials with coefficients of modulus one. *Bull. London Math. Soc.*, 9:171–176, 1977.

[5] P. Erdös. Some unsolved problems. *Michigan Mathematical Journal*, 4:291–300, 1957.

[6] M.L. Fredman, B. Saffari, and B. Smith. Polynômes réciproques. *C.R. Acad. Sci. Paris*, 308:461–464, 1989.

[7] J.-P. Kahane. Sur les polynômes à coefficients unimodulaires. *Bull. London Math. Soc.*, 12:321–342, 1980.

[8] T. Körner. On a polynomial of J.S. Byrnes. *Bull. London Math. Soc.*, 12:219–224, 1980.

[9] J.E. Littlewood. On polynomials $\sum \pm z^m$, $\sum \exp(\alpha_m i) z^m$, $z = e^{\theta i}$. *Journal London Math. Soc.*, 41:367–376, 1966.

[10] J.E. Littlewood. *Some problems in real and complex analysis*. Heath, 1968.

[11] H. Queffelec and B. Saffari. On Kahane's ultraflat polynomials. Preprint.

[12] B. Saffari. Cross-means and functions of mean value zero. In *Proc. of Symposium in honour of H. Delange*, Orsay, 1982.

Fixed points in mixed spectrum analysis†

Benjamin Kedem
Department of Mathematics and Systems Research Center
University of Maryland
College Park, Maryland 20742 USA
bnk@gertrude.umd.edu

Silvia Lopes
Department of Statistics
Institute of Mathematics
UFRGS
Campus do Vale
91500 Porto Alegre RS Brazil

Abstract. Families and sequences of zero-crossing counts generated by parametric time invariant linear filters are called higher order crossings or HOC. Because of the close relationship between zero-crossing counts and first order autocorrelations, families of first order autocorrelations are also referred to as HOC. We investigate the HOC from some particular families of linear filters applied in the problem of multiple frequency detection in noise. Viewing the cosine of each discrete frequency as a fixed point of a certain mapping, it is shown how to construct HOC sequences that converge to the fixed points. A faster convergence rate is achieved by controlling the bandwidth of the parametric filters.

1. Introduction

1.1. The general idea of HOC

In general, when a filter is applied to a time series, it changes the series mode of oscillation. Thus, when a bank of filters is applied to the same series, we obtain a sequence or family of oscillation patterns. The resulting family of zero-crossing counts is referred to as *higher order crossings* or simply HOC. The corresponding first order autocorrelations are referred to as *higher order correlations*, or simply HOC again. Because the first order autocorrelation

† Work supported by grants AFOSR-89-0049 and ONR-89-J-1051.

J. S. Byrnes et al. (eds.), Probabilistic and Stochastic Methods in Analysis, with Applications, 573–591.
© 1992 *Kluwer Academic Publishers. Printed in the Netherlands.*

and the expected zero-crossing rate of a real valued stationary time series are essentially equivalent, using the same acronym is quite tolerable. The particular HOC under consideration should be clear from the context.

This paper shows how to construct convergent HOC sequences for the purpose of multiple frequency estimation in the presence of ambient noise.

The gist of the idea is to employ HOC sequences in the fine tuning of parametric filters. This is done iteratively as follows. A time series is filtered by a parametric filter, and the resulting first order autocorrelation is immediately used in adjusting the filter parameter. The adjusted filter is then applied again, giving rise to a new first order autocorrelation, and the procedure is repeated. By choosing the filters appropriately, the scheme gives convergent sequences of higher order correlations, or equivalently, convergent sequences of higher order crossings, depending on what one chooses to observe, correlations or zero-crossing counts. From a statistical point of view, under appropriate conditions, the method guarantees the strong consistency (almost sure convergence) of the estimating HOC sequences.

To express the same idea in symbols, let $\{Z_t\}$, $t = 0, \pm 1, \pm 2, \cdots$, be a zero-mean stationary time series, and let $\{\mathcal{L}_\theta\}$, $\theta \in \Theta$, be a parametric family of time invariant linear filters. Denote by $\{Z_t(\theta)\}$ the filtered series,

$$Z_t(\theta) = \mathcal{L}_\theta(Z)_t$$

Then $\{\rho_1(\theta)\}$, $\theta \in \Theta$, defined by

$$\rho_1(\theta) = \frac{\Re\{E[Z_t(\theta)\overline{Z_{t+1}(\theta)}]\}}{E|Z_t(\theta)|^2}$$

is a HOC family defined from a parametrized first order autocorrelation. Here and elsewhere, a bar denotes complex conjugate. For a real valued process $\{Z_t(\theta)\}$, let $I_{[A]}$ be the indicator of the event A, and define,

$$D_\theta = \sum_{t=2}^{N} I_{[Z_t(\theta)Z_{t-1}(\theta)<0]}$$

as the number of zero-crossings observed in $Z_1(\theta), Z_2(\theta), \cdots, Z_N(\theta)$. This is the corresponding HOC family from zero-crossings. When $\{Z_t\}$ is a strictly stationary pure sinusoid, or when $\{Z_t\}$ is Gaussian, then

$$\rho_1(\theta) = \cos\left(\frac{\pi E(D_\theta)}{N-1}\right) \tag{1.1}$$

and we can see that in this real case knowing $\rho_1(\theta)$ is equivalent to knowing $E(D_\theta)$. The right hand side being an *expected rate*, is *independent* of N. More examples that relate ρ_1 to $E(D)$ by a simple formula are given in [1]. For

example, let $\{Z_t\}$ be a real valued zero mean stationary Gaussian process, and define

$$Y_t = Z_t^3$$

Then $\{Y_t\}$ is still stationary with mean zero, but it is no longer Gaussian. Let $\rho_1(y)$ be the first order autocorrelation of $\{Y_t\}$, and let $D(y)$ be the zero-crossing count in $Y_1, Y_2, \cdots, Y_N$. Then,

$$\rho_1(y) = \frac{9}{10}\cos\left(\frac{\pi E(D(y))}{N-1}\right) + \frac{1}{10}\cos\left(\frac{3\pi E(D(y))}{N-1}\right)$$

Thus, from $E(D(y))$ we can get $\rho_1(y)$. Going in the reverse direction requires the solution of a third degree equation.

Inspired by the algorithm presented in [2], we shall be concerned with fixed points of $\rho_1(\theta)$ obtained from the recursion,

$$\theta_{j+1} = \rho_1(\theta_j) \tag{1.2}$$

for some specific families of parametric filters. As it turns out, *by controlling the filter bandwidth, the fixed points can be made to coincide with the cosines of the frequencies in the discrete spectrum of* $\{Z_t\}$.

1.2. The problem

Consider the mixed spectrum model for $t \in \{0, \pm 1, \pm 2, \cdots\}$,

$$Z_t = \sum_{j=1}^{p} A_j \cos(\omega_j t + \phi_j) + \zeta_t = X_t + \zeta_t \tag{1.3}$$

where p is not necessarily known, $A_1, \cdots, A_p$, are unknown constants, $\omega_1, \cdots, \omega_p$ are unknown frequencies with values in $(-\pi, \pi]$, $\{\zeta_t\}$ is white noise with mean 0 and variance σ_ζ^2, and $\phi_1, \cdots, \phi_p$, are independent random variables uniformly distributed in $(-\pi, \pi]$, and are independent of $\{\zeta_t\}$. The assumption of white noise is not really needed, but it simplifies the exposition. In fact, any continuous spectrum noise will do just as well.

The problem is to estimate $\omega_1, \cdots, \omega_p$ from recursive HOC sequences of the form (1.2).

For this goal, we investigate the HOC sequences $\rho_1(\theta_j)$ from two parametric families of filters, loosely referred to as the "alpha filter" and the "complex filter." We also discuss briefly a third parametric filter to which we refer as the "exponential filter."

2. Two useful parametric families of filters

2.1. The alpha filter

The alpha filter is defined by the time invariant linear transformation for $\alpha \in (-1, 1)$,

$$Z_t(\alpha) = Z_t + \alpha Z_{t-1}(\alpha)$$

so that,

$$Z_t(\alpha) = Z_t + \alpha Z_{t-1} + \alpha^2 Z_{t-2} + \cdots$$

From this the impulse response is,

$$h(n;\alpha) = \begin{cases} \alpha^n, & n \geq 0 \\ 0, & \text{otherwise} \end{cases}$$

and the squared gain is,

$$|H(\omega;\alpha)|^2 = \frac{1}{1 - 2\alpha\cos(\omega) + \alpha^2}$$

for $\omega \in (-\pi, \pi]$. The corresponding higher order correlation is given by

$$\rho_1(\alpha) = \frac{E[Z_t(\alpha)Z_{t+1}(\alpha)]}{E[Z_t^2(\alpha)]} = \frac{\sum_{j=1}^{p} \frac{A_j^2}{2} \frac{\cos(\omega_j)}{1-2\alpha\cos(\omega_j)+\alpha^2} + \sigma_\zeta^2 \frac{\alpha}{1-\alpha^2}}{\sum_{j=1}^{p} \frac{A_j^2}{2} \frac{1}{1-2\alpha\cos(\omega_j)+\alpha^2} + \sigma_\zeta^2 \frac{1}{1-\alpha^2}} \qquad (2.1)$$

An easily proven important fact, referred to as the *fundamental property*, is that α is precisely the first order autocorrelation of the filtered noise $\zeta(\alpha)$ [2],

$$\alpha = \frac{\int_{-\pi}^{\pi} \cos(\omega)|H(\omega;\alpha)|^2 d\omega}{\int_{-\pi}^{\pi} |H(\omega;\alpha)|^2 d\omega} \qquad (2.2)$$

We can see that $\rho_1(\alpha)$ is a weighted average of $\cos(\omega_1), \cdots, \cos(\omega_p)$, and α, and therefore it must fall between the smallest and largest of these parameters. This is the key observation on which the HK algorithm is based.

2.2. The complex filter

The complex filter is defined by the transformation,

$$Z_t(\alpha; M) = \left(1 + e^{i\theta(\alpha)}\mathcal{B}\right)^M Z_t$$

where M is a positive integer, $\alpha \in (-1, 1)$, and $\theta(\alpha) \in (-\pi, \pi]$. Think of M as being sufficiently large (e.g., $M = 20$) so that we can entertain the

approximation $\theta(\alpha) \approx \cos^{-1}(\alpha)$. This will be made more palatable in a moment. Clearly,

$$Z_t(\alpha; M) = \sum_{n=0}^{M} \binom{M}{n} e^{i\theta(\alpha)n} Z_{t-n}$$

and the impulse response is,

$$h(n; \alpha, M) = \begin{cases} \binom{M}{n} e^{i\theta(\alpha)n}, & n = 0, \ldots, M \\ 0, & \text{otherwise} \end{cases}$$

The corresponding squared gain is

$$|H(\omega; \alpha, M)|^2 = 4^M \cos^{2M}\left(\frac{\omega - \theta(\alpha)}{2}\right)$$

for $\theta, \omega \in (-\pi, \pi]$, and $\alpha \in (-1, 1)$. Mimicking the fundamental property (2.2) for the alpha filter, we *define* α by the equation,

$$\alpha = \frac{\int_{-\pi}^{\pi} \cos^{2M}\left(\frac{\lambda - \theta(\alpha)}{2}\right) \cos(\lambda) d\lambda}{\int_{-\pi}^{\pi} \cos^{2M}\left(\frac{\lambda - \theta(\alpha)}{2}\right) d\lambda} \tag{2.3}$$

As such, α is the real part of the first order autocorrelation of the filtered white noise, which is not white anymore. As $M \to \infty$,

$$\alpha = \frac{\int_{-\pi}^{\pi} \cos^{2M}\left(\frac{\lambda - \theta(\alpha)}{2}\right) \cos(\lambda) d\lambda}{\int_{-\pi}^{\pi} \cos^{2M}\left(\frac{\lambda - \theta(\alpha)}{2}\right) d\lambda} \to \cos(\theta(\alpha)) \tag{2.4}$$

so that the approximation $\theta(\alpha) \approx \cos^{-1}(\alpha)$ makes sense. In fact, already with $M = 20$, the approximation is excellent. We think of $\theta(\alpha)$ as the "center of the filter."

From [2] we obtain the higher order correlation,

$$\rho_1(\alpha, M) = \frac{\Re\{E[Z_t(\alpha, M)\overline{Z_{t-1}(\alpha, M)}]\}}{E|Z_t(\alpha, M)|^2} =$$

$$\frac{\sum_{j=1}^{p} \frac{A_j^2}{2}\left[\cos^{2M}\left(\frac{\omega_j + \theta(\alpha)}{2}\right) + \cos^{2M}\left(\frac{\omega_j - \theta(\alpha)}{2}\right)\right]\cos(\omega_j) + \frac{\sigma_\varepsilon^2}{\pi}\int_{-\pi}^{\pi} \cos^{2M}\left(\frac{\lambda - \theta(\alpha)}{2}\right)\cos(\lambda)\, d\lambda}{\sum_{j=1}^{p} \frac{A_j^2}{2}\left[\cos^{2M}\left(\frac{\omega_j + \theta(\alpha)}{2}\right) + \cos^{2M}\left(\frac{\omega_j - \theta(\alpha)}{2}\right)\right] + \frac{\sigma_\varepsilon^2}{\pi}\int_{-\pi}^{\pi} \cos^{2M}\left(\frac{\lambda - \theta(\alpha)}{2}\right) d\lambda} \tag{2.5}$$

or, from (2.3),

$$\rho_1(\alpha, M) = \frac{\sum_{j=1}^{p} \frac{A_j^2}{2}\left[\cos^{2M}\left(\frac{\omega_j+\theta(\alpha)}{2}\right)+\cos^{2M}\left(\frac{\omega_j-\theta(\alpha)}{2}\right)\right]\cos(\omega_j) + \left[\frac{\sigma_\zeta^2}{\pi}\int_{-\pi}^{\pi}\cos^{2M}\left(\frac{\lambda-\theta(\alpha)}{2}\right)d\lambda\right]\alpha}{\sum_{j=1}^{p} \frac{A_j^2}{2}\left[\cos^{2M}\left(\frac{\omega_j+\theta(\alpha)}{2}\right)+\cos^{2M}\left(\frac{\omega_j-\theta(\alpha)}{2}\right)\right] + \frac{\sigma_\zeta^2}{\pi}\int_{-\pi}^{\pi}\cos^{2M}\left(\frac{\lambda-\theta(\alpha)}{2}\right)d\lambda} \tag{2.6}$$

Again, from (2.6), as with the alpha filter, $\rho_1(\alpha, M)$ is a weighted average of $\cos(\omega_1), \cdots, \cos(\omega_p)$, and α—a crucial observation that helps in recovering all the ω_j.

We think of $\rho_1(\alpha, M)$ as a function of α with parameter M.

3. The HK algorithm

The HK algorithm is best described in terms of the alpha filter for the case $p = 1$. So, let $p = 1$, and consider the alpha filter. It is convenient to define the weight function,

$$C(\alpha) \equiv \frac{\mathrm{Var}(\zeta_t(\alpha))}{\mathrm{Var}(Z_t(\alpha))} = \frac{\sigma_\zeta^2}{\frac{A_1^2}{2}\frac{1-\alpha^2}{1-2\alpha\cos(\omega_1)+\alpha^2}+\sigma_\zeta^2} \tag{3.1}$$

Clearly, $0 < C(\alpha) < 1$, and we obtain,

$$\rho_1(\alpha) = (1 - C(\alpha))\cos(\omega_1) + C(\alpha)\alpha \tag{3.2}$$

This weighted average implies that $\rho_1(\alpha)$ must be between α and $\cos(\omega_1)$. Choose any $\alpha_0 \in (-1, 1)$ and, without loss of generality, suppose $\alpha_0 < \cos(\omega_1)$. Then,

$$\alpha_0 < \rho_1(\alpha_0) < \cos(\omega_1)$$

Define the recursion [2]

$$\alpha_{k+1} = \rho_1(\alpha_k) \tag{3.3}$$

It follows from (3.2) that,

$$\alpha_0 \leqslant \alpha_1 \leqslant \alpha_2 \leqslant \cdots \leqslant \cos(\omega_1)$$

The sequence $\{\alpha_k\}$ is monotone and bounded, and hence it converges to α^*, say. However, from (3.3)

$$\rho_1(\alpha^*) = \alpha^* = \cos(\omega_1)$$

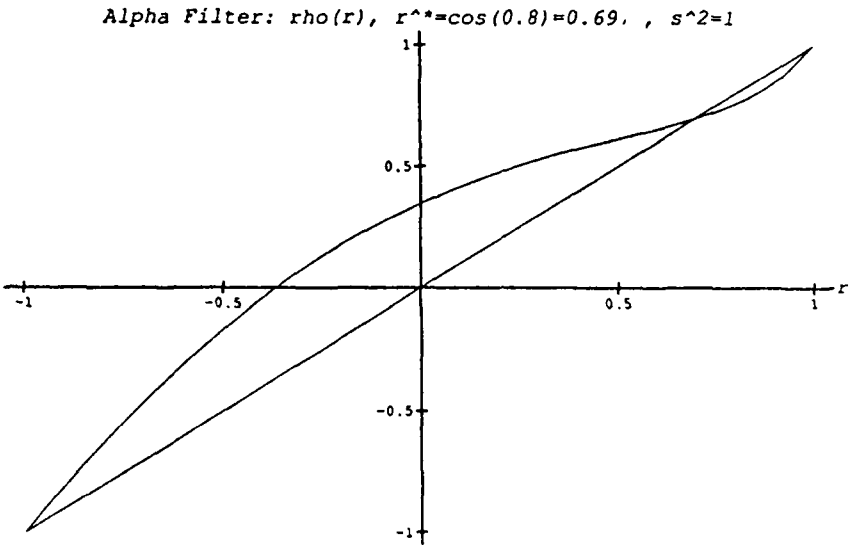

Figure 3.1: An attracting fixed point $\alpha* = \cos(0.8)$ of $\rho_1(\alpha)$ from the alpha filter. $\rho = 1$, $\omega_1 = 0.8$, $A_1 = \sqrt{2}$, $\sigma_\xi^2 = 1$.

Thus, $\cos(\omega_1)$ *is obtained as a fixed point of the mapping* $\rho_1(\alpha)$, *and* $\omega_1 = \cos^{-1}(\alpha^*)$.

Figure 3.1 shows the fixed point in $\rho_1(\alpha)$ for $\omega_1 = 0.8, A_1 = \sqrt{2}, \sigma_\xi^2 = 1$.

It has been observed in [2] and [5] that any filter that satisfies the fundamental property (2.2), gives rise to the same algorithm, and the same solution, as above. In many cases all that is needed is a reparametrization that guarantees (2.2).

An extension of the HK algorithm to the general multiple frequency case is possible, but for this we need different families of filters, as done in the next section. The alpha filter, without any modification, cannot be applied in multiple frequency detection. If the recursion (3.3) is applied to $\rho_1(\alpha)$ in (2.1) when $p \geq 2$, the sequence $\{\alpha_k\}$ converges to a point between the lowest and highest $\cos(\omega_i)$.

4. Multiple frequency estimation using the complex filter

The HK algorithm can be extended to the multiple frequency case when the generated HOC are obtained from bandpass filters. The complex filter falls in this category when M is large enough. This fact is illustrated in Figure 4.1

which shows the graph of the normalized squared gain,

$$\cos^{2M}\left(\frac{\omega-\theta}{2}\right), \quad -\pi \leq \omega \leq \pi$$

with $\theta = 2.0$, and $M = 40, 100$.

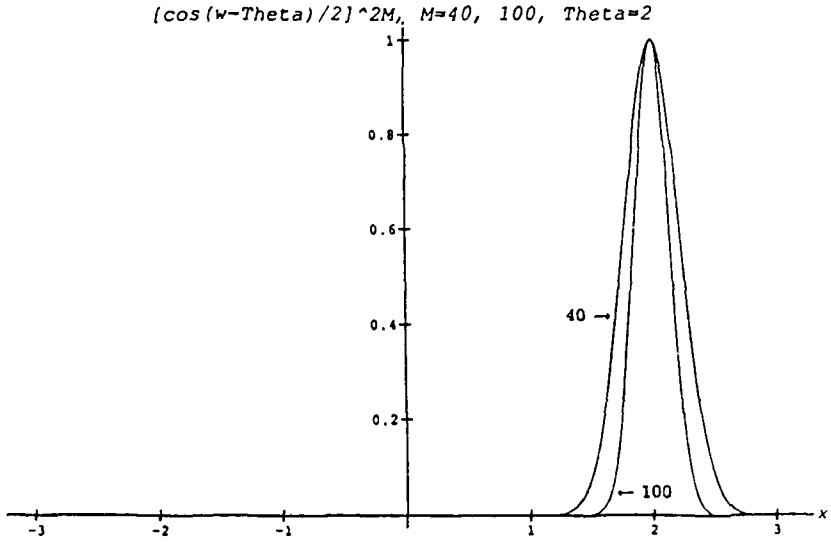

Figure 4.1: The normalized complex filter, with $M = 40, 100$, acts as a bandpass filter passing frequencies in a neighborhood of $\tau = 2.0$.

We can see that by increasing M, it is possible to discount the power associated with the entire spectral support except for a small band in a neighborhood of θ. This means that we can practically filter out any desired band of frequencies, and at the same time amplify frequencies in a small neighborhood of θ, the "center" of the filter. Based on (2.4), we shall assume that M_0 is sufficiently large so that the approximation

$$\theta(\alpha) \doteq \cos^{-1}(\alpha) \tag{4.1}$$

holds for all $M > M_0$.

Choose $\alpha_0 \in (-1, 1)$ closer to $\cos(\omega_1)$ than to any other $\cos(\omega_j)$, $j \neq 1$. Assume that $\alpha_0 \in (-1, 1)$ is sufficiently close to $\cos(\omega_1)$ so that

$$\alpha_0 < \cos(\omega_1)$$

and such that $\theta(\alpha_0)$ is closest to ω_1, and $\omega_1 < \theta(\alpha_0)$. This is possible due to (4.1). Then as $M \to \infty$,

$$\frac{\cos^{2M}\left(\frac{\omega_1+\theta(\alpha_0)}{2}\right)+\cos^{2M}\left(\frac{\omega_j-\theta(\alpha_0)}{2}\right)}{\cos^{2M}\left(\frac{\omega_1-\theta(\alpha_0)}{2}\right)} \to 0, \qquad j \neq 1$$

and

$$\frac{\cos^{2M}\left(\frac{\omega_1+\theta(\alpha_0)}{2}\right)}{\cos^{2M}\left(\frac{\omega_1-\theta(\alpha_0)}{2}\right)} \to 0$$

Therefore, by dividing both the numerator and denominator in (2.6) by $\frac{A_1^2}{2}\cos^{2M}\left(\frac{\omega_1-\theta(\alpha_0)}{2}\right)$, one obtains, for sufficiently large M,

$$\rho_1(\alpha_0, M) = \frac{\cos(\omega_1) + \text{terms that go to } 0 + \left\{\frac{\left[\frac{\sigma^2}{\pi}\int_{-\pi}^{\pi}\cos^{2M}\left(\frac{\lambda-\theta(\alpha_0)}{2}\right)d\lambda\right]}{\frac{A_1^2}{2}\cos^{2M}\left(\frac{\omega_1-\theta(\alpha_0)}{2}\right)}\right\}\alpha_0}{1 + \text{terms that go to } 0 + \frac{\frac{\sigma^2}{\pi}\int_{-\pi}^{\pi}\cos^{2M}\left(\frac{\lambda-\theta(\alpha_0)}{2}\right)d\lambda}{\frac{A_1^2}{2}\cos^{2M}\left(\frac{\omega_1-\theta(\alpha_0)}{2}\right)}}$$

Evidently, as M increases, $\rho_1(\alpha_0, M)$ becomes arbitrarily close to being a weighted average of $\cos(\omega_1)$ and α_0. Thus, because $\alpha_0 < \cos(\omega_1)$, we can find a sufficiently large M_0 so that

$$\alpha_0 < \rho_1(\alpha_0, M_0) < \cos(\omega_1).$$

Now let $\alpha_1 = \rho_1(\alpha_0, M_0)$ and repeat the argument for $M_1 > M_0$. Then,

$$\alpha_0 < \alpha_1 < \rho_1(\alpha_1, M_1) < \cos(\omega_1).$$

In general, define

$$\alpha_{k+1} = \rho_1(\alpha_k, M_k).$$

corresponding to the sequence $M_0 < M_1 < M_2 < \cdots$, to obtain a sequence

$$\alpha_0 < \alpha_1 < \alpha_2 < \cdots < \cos(\omega_1).$$

It follows that as $k \to \infty$,

$$\alpha_k \uparrow \alpha^* \leq \cos(\omega_1).$$

On the other hand, for M_k large enough, we can find small $\epsilon, \epsilon_1, \epsilon_2$, such that $\omega_1 + \epsilon < \theta(\alpha_k)$, and $\theta(\alpha_k) \in (\omega_1 - \epsilon_1, \omega_1 + \epsilon_2)$, so that

$$\rho_1(\alpha_k, M_k) \geq \frac{\cdots + \frac{A_1^2}{2}\cos^{2M_k}\left(\frac{\omega_1 - \theta(\alpha_k)}{2}\right)\cos(\omega_1) + \alpha_k \frac{\sigma_z^2}{\pi}\int_{\omega_1}^{\omega_1+\epsilon}\cos^{2M_k}\left(\frac{\omega-\theta(\alpha_k)}{2}\right)d\omega}{\cdots + \frac{A_1^2}{2}\cos^{2M_k}\left(\frac{\omega_1 - \theta}{2}\frac{\alpha_k}{2}\right)\frac{\sigma_z^2}{\pi}\int_{\omega_1-\epsilon_1}^{\omega_1+\epsilon_2}\cos^{2M_k}\left(\frac{\omega-\theta}{2}\frac{\alpha_k}{2}\right)d\omega}$$

It is now clear that there are $\eta_1(k), \eta_2(k)$ that go to zero with k, such that

$$\alpha_{k+1} = \rho_1(\alpha_k, M_k) \geq \frac{\cos(\omega_1) + \text{terms that go to } 0 + \alpha_k\eta_1(k)}{1 + \text{terms that go to } 0 + \eta_2(k)}$$

It follows that as $k \to \infty$,

$$\alpha_k \to \alpha^* \geq \cos(\omega_1)$$

and we have proved the convergence of α_k to $\cos(\omega_1)$. The same argument can be used when $\alpha_0 > \cos(\omega_1)$. Thus $\alpha^* = \cos(\omega_1)$ becomes a fixed point of $\rho_1(\alpha, M)$, as $M \to \infty$. We have proved the following fact.

Theorem 4.1. Suppose $\{Z_t\}$ is the harmonic process (1.3), and suppose $\alpha_0 \in (-1, 1)$ is in a small neighborhood of $\cos(\omega_1)$ that contains no other $\cos(\omega_j)$, $j \neq 1$. Then there exists an increasing sequence $\{M_k\}$ such that

$$\alpha_{k+1} = \rho_1(\alpha_k, M_k) \to \alpha^* = \cos(\omega_1)$$

and α^* becomes a fixed point of $\rho_1(\alpha, M)$ as M increases.

Remark 4.2. A somewhat different approach, leading to a sequence of fixed points, is to obtain for each fixed M a fixed point α_M^* of $\rho_1(\alpha, M)$, from the iterations $\alpha_{k+1} = \rho_1(\alpha_k, M)$, and then show that $\alpha_M^* \to \cos(\omega_1)$, as $M \to \infty$. The validity of this approach is demonstrated in Figure 4.2 which illustrates the existence of fixed points in $\rho_1(\alpha, 10)$, $\rho_1(\alpha, 100)$, for $p = 2$, and $\omega_1 = 0.8$, $\omega_2 = 2.1$. The approach adopted above is that of shrinking the effective bandwidth (by increasing M) at each iteration of $\alpha_{k+1} = \rho_1(\alpha_k, M_k)$, and is in the spirit of Kedem and Yakowitz [4]. It can be argued that the convergence, toward the cosine of the frequency to be detected, achieved for a variable bandwidth is much faster.

Remark 4.3. It is easy to see from (2.6) that for sufficiently large M, and when the filter is centered near ω_1 (that is, the filter passes ω_1), we essentially have the representation,

$$\rho_1(\alpha, M) = \cos(\omega_1) + C(\alpha, M)(\alpha - \cos(\omega_1))$$

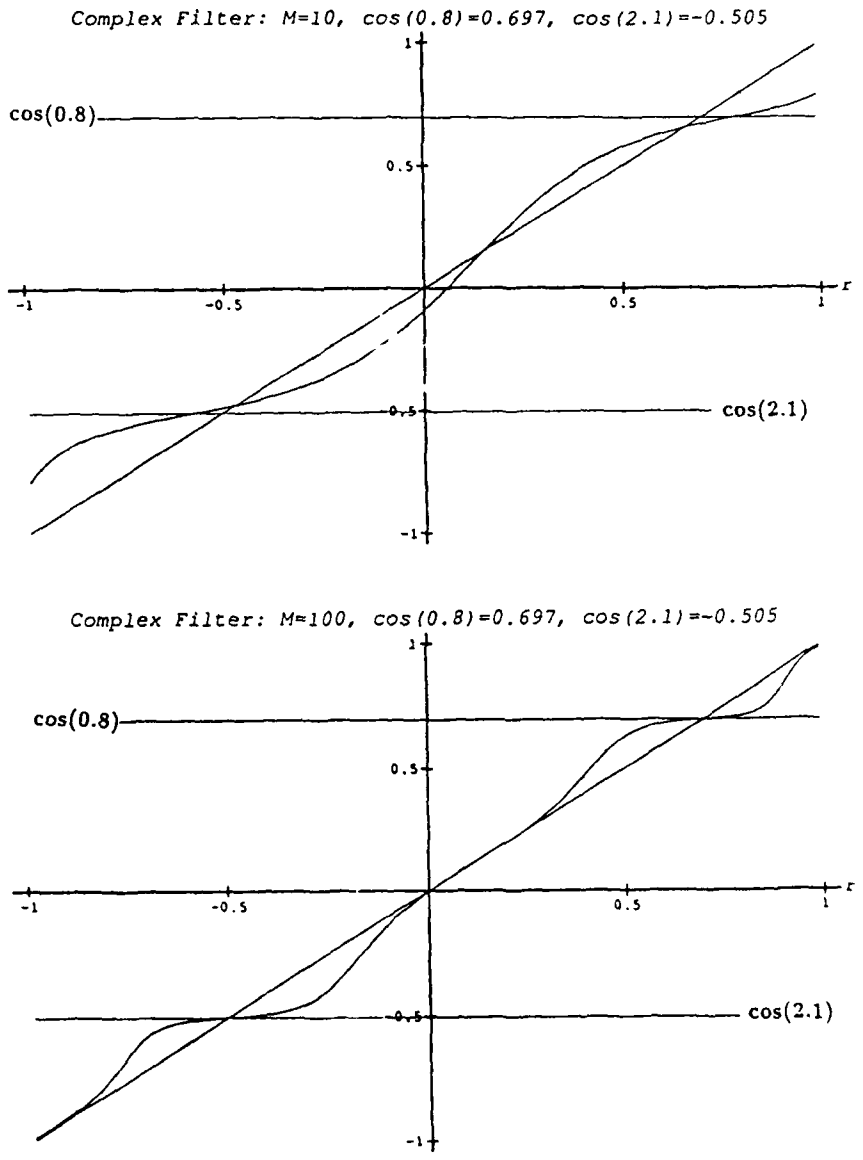

Figure 4.2: Fixed points in $\rho_1(\alpha, 10)$, $\rho_1(\alpha, 100)$, from the complex filter for $p = 2$, $\omega_1 = 0.8$, $\omega_2 = 2.1$.

where

$$0 < C(\alpha, M) = \frac{E|\zeta_t(\alpha)|^2}{\frac{A_1^2}{4}|H(\omega_1; \alpha, M)|^2 + E|\zeta_t(\alpha)|^2} < 1$$

and $|H(\omega; \alpha, M)|^2 = 4^M \cos^{2M}((\omega - \theta(\alpha))/2)$. This is the general form used in [4]. This form shows clearly that $\rho_1(\alpha, M)$ is essentially a contraction at $\cos(\omega_1)$, and that the convergence rate of $\alpha_{k+1} = \rho_1(\alpha_k, M)$ depends on the contraction factor $C(\alpha, M)$. As M increases with each iteration, $C(\alpha, M)$ decreases (as long as the filter passes ω_1) and we obtain a speeded up rate of convergence.

4.1. Examples

To demonstrate the plan given in Theorem 4.1, we resort to some examples with simulated data. In practice $\rho_1(\alpha)$ must be estimated, and we use the estimate obtained from zero-crossings,

$$\hat{\rho}_1(\alpha) = \cos\left(\frac{\pi D_\alpha}{N-1}\right) \tag{4.2}$$

The choice of this estimate is justified because we deal with narrow band (large M) cases where the "cosine formula" (1.1) holds to a great degree. Observe that in (4.2) the dependence on M is suppressed for simplicity.

The zero-crossing count D_α is defined for real data, a fact which is not compatible with the complex-valued output of the complex filter. To overcome this technicality, a reasonable modification is to use the real counterpart defined by

$$h(n; \alpha, M) = \begin{cases} \binom{M}{n} \cos(\theta(\alpha)n), & n = 0, \ldots, M \\ 0, & \text{otherwise} \end{cases}$$

For long data records, the modification is inconsequential. In the examples we use the approximation $\theta(\alpha) = \cos^{-1}(\alpha)$.

It is convenient to introduce the observed zero-crossing rate,

$$\hat{\gamma}_{\alpha_k} \equiv \frac{\pi D_{\alpha_k}}{N-1}$$

Then the algorithm becomes,

$$\alpha_{k+1} = \cos(\hat{\gamma}_{\alpha_k}) \tag{4.3}$$

where the parameter M increases with each iteration.

The examples below pertain to N = 2000 (more precisely, 2000 plus the maximum M used), and various SNR's (SNR: signal to noise ratio). The

noise was generated from independent $\mathcal{N}(0, \sigma_\zeta^2)$ random variables. In each case, we also report the performance of the periodogram for comparison.

The examples convey the potential of the algorithm (4.3) for frequency detection in ambient noise. From an applications point of view, it is interesting to note that once a true discrete frequency is "captured" in the bandpass, it is not lost throughout the procedure as long as M increases judiciously. The examples indicate that linear growth is appropriate.

4.1.1. Example 1: p = 1

In this example, $\omega_1 = 0.91$, $A_1 = -0.390676$, $B_1 = -0.938528$, and $\sigma_\zeta^2 = 1$. With $\theta(\alpha_0) = 1.21$, the normalized HOC sequence $\{\hat{\gamma}_{\alpha_k}\}$ converges to 0.909946. By comparison, the corresponding periodogram estimate is $\omega_1 = 0.91419$.

		$\omega_1 = 0.91, \theta(\alpha_0) = 1.21$
k	M_k	$\hat{\gamma}_{\alpha_k}$
0	5	1.05453
1	7	0.96652
2	9	0.94766
3	11	0.92566
4	13	0.91938
5	15	0.91623
6	17	0.91309
7	19	0.90366
8	21	0.90995
9	23	0.90995
		$\hat{\omega}_1 = 0.90995$

4.1.2. Example 2: p = 2, moderate SNR

In this example p = 2, $\omega_1 = 0.5$, $\omega_2 = 1.2$, $A_1 = 1.68853$, $B_1 = -1.64565$, $A_2 = -1.59479$, $B_2 = 0.238443$, and $\sigma_\zeta^2 = 1$. With $\alpha_0 = 0.8$, the normalized HOC sequence $\{\hat{\gamma}_{\alpha_k}\}$ converges to 0.49976. For $\theta(\alpha_0) = 2.0$, the convergence is toward 1.20069. This is to be compared with the corresponding periodogram estimates 0.50325 and 1.20304.

		$\omega_1 = 0.5, \theta(\alpha_0) = 0.8$	$\omega_2 = 1.2, \theta(\alpha_0) = 2.0$
k	M_k	$\hat{\gamma}_{\alpha_k}$	$\hat{\gamma}_{\alpha_k}$
0	15	0.60349	1.69102
1	17	0.50605	1.31227
2	19	0.50134	1.19597
3	21	0.50134	1.18812
4	23	0.50134	1.18812
5	25	0.49976	1.20069
6	27	0.49976	1.20069
7	29	0.49976	1.20069
8	31	0.49976	1.20069
		$\hat{\omega}_1 = 0.49976$	$\hat{\omega}_2 = 1.20069$

4.1.3. Example 3: Detecting a weak component

Here we have two sinusoidal components where the first one is relatively weak. The parameters are $p = 2$, $\omega_1 = 0.97$, $\omega_2 = 2.1$, $A_1 = -0.699457$, $B_1 = -0.116106$, $A_2 = -1.15000$, $B_2 = 2.45159$, $\sigma_\xi^2 = 2$. With $\theta(\alpha_0) = 0.85$, the normalized HOC sequence $\{\hat{\gamma}_{\alpha_k}\}$ converges to 0.97281. For $\theta(\alpha_0) = 1.8$, the convergence is toward 2.09963. This is to be compared with the corresponding periodogram estimates which are 0.97240 and 2.13928.

		$\omega_1 = 0.97, \theta(\alpha_0) = 0.85$	$\omega_2 = 2.1, \theta(\alpha_0) = 1.8$
k	M_k	$\hat{\gamma}_{\alpha_k}$	$\hat{\gamma}_{\alpha_k}$
0	20	0.92566	2.09492
1	22	0.96652	2.10121
2	24	0.97281	2.10121
3	26	0.96967	2.10121
4	28	0.97281	2.09963
5	30	0.97595	2.09963
6	32	0.97281	2.09963
7	34	0.97281	2.09963
		$\hat{\omega}_1 = 0.97281$	$\hat{\omega}_2 = 2.09963$

5. A brief look at the complex exponential filter

Clearly, the preceding development can be repeated with numerous families of bandpass filters. A particularly good choice, in terms of the rate of convergence toward the fixed points, is the parametric complex exponential filter defined by the impulse response,

$$h(n;\alpha,M) = \begin{cases} \exp(in\theta(\alpha))/\sqrt{2M+1}, & |n| \leq M \\ 0, & |n| > M \end{cases}$$

corresponding to the squared gain,

$$|H(\omega;\alpha,M)|^2 = \frac{1}{2M+1}\frac{\sin^2[\frac{1}{2}(2M+1)(\omega-\theta(\alpha))]}{\sin^2[\frac{1}{2}(\omega-\theta(\alpha))]},\quad -\pi \leqslant \omega \leqslant \pi$$

where M is a positive integer. This parametric filter was considered in [4]. The fundamental property is manifested through the relationship [4],

$$\alpha = \Re\left\{\frac{E[\zeta_t(\alpha,M)\overline{\zeta_{t-1}(\alpha,M)}]}{E|\zeta_t(\alpha,M)|^2}\right\}$$

It holds exactly for

$$\theta(\alpha) = \cos^{-1}\left(\frac{2M+1}{2M}\alpha\right)$$

when $|\alpha| \leqslant 2M/(2M+1)$. Again, as M increases, $\theta(\alpha) \doteq \cos^{-1}(\alpha)$, and $\alpha \in (-1,1)$. The corresponding α_k sequence converges very fast, provided α_0 is sufficiently close to $\cos(\omega_j)$ for some j. This is illustrated graphically in Figure 5.1. The figure shows the existence of fixed points α^*_M in

$$\rho_1(\alpha,M) = \frac{\Re\{E[Z_t(\alpha,M)\overline{Z_{t-1}(\alpha,M)}]\}}{E|Z_t(\alpha,M)|^2}$$

for $M = 10, 20$, and $\omega_1 = 0.8$, $\omega_2 = 2.1$, the case considered earlier. Near $\cos(0.8)$, $\cos(2.1)$, the derivative of $\rho_1(\alpha,M)$, $M = 10, 20$, is essentially 0 and the convergence of $\alpha_k = \rho_1(\alpha_{k-1},M)$ toward α^*_M is very fast. Already with $M = 20$, it is difficult to see a significant difference between α^*_{20} and the cosine of the frequency of interest.

As expected, a much faster rate of convergence is provided by the iterates of $\rho_1(\alpha,M)$ for fixed M, and the "basin of convergence" becomes more pronounced. This can be seen very clearly in Figure 5.2 which shows the graph of 10 iterates $\rho_1^{10} \equiv \rho_1 \circ \rho_1^9 = \rho_1 \circ \rho_1 \cdots \circ \rho_1$. This means that the procedure of increasing M with each iteration leads to a speeded up rate of convergence of the HK algorithm, a fact highlighted already in [4].

5. Example 4: use of the exponential filter

To illustrate the performance of the HK algorithm using the complex exponential filter, we resort again to HOC from zero -crossings obtained from the real counterpart of $h(n;\alpha,M)$,

$$h(n;\alpha,M) = \begin{cases} \cos(in\theta(\alpha))/\sqrt{2M+1}, & |n| \leqslant M \\ 0, & |n| > M \end{cases}$$

The following table gives the observed zero-crossing rate $\hat{\gamma}_{\alpha_k}$ obtained from the recursion $\alpha_{k+1} = \cos(\hat{\gamma}_{\alpha_k})$, using the exact same data as in Example 3 above. The results in both cases are quite comparable.

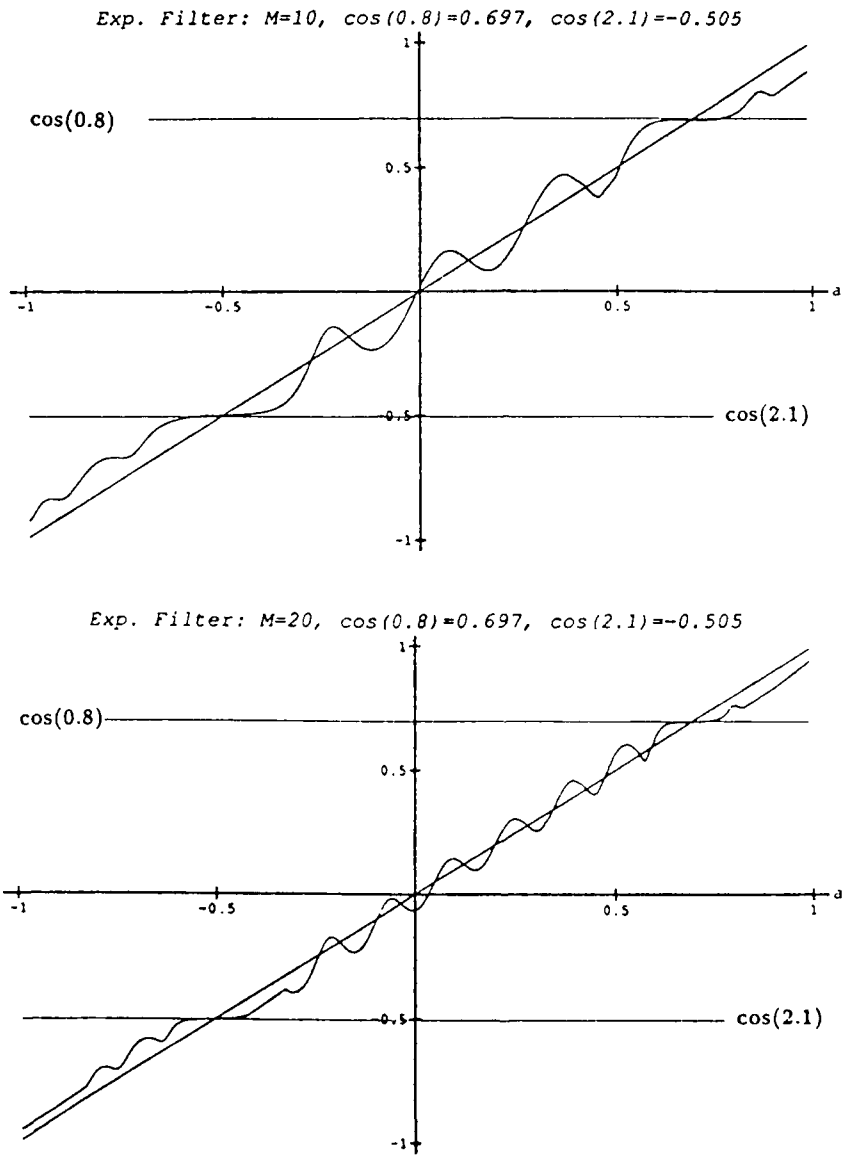

Figure 5.1: Fixed points in $\rho_1(\alpha, 10)$, $\rho_1(\alpha, 20)$, from the complex exponential filter for $p = 2$, $\omega_1 = 0.8$, $\omega_2 = 2.1$.

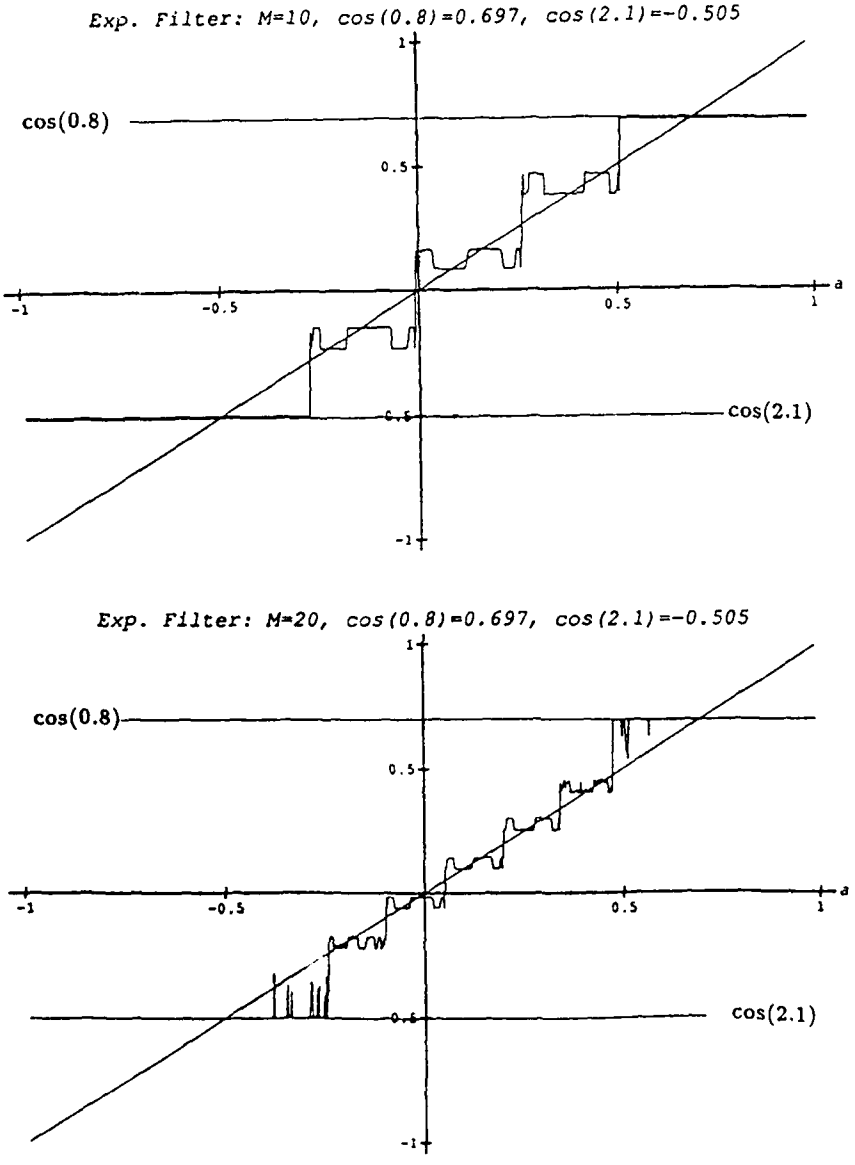

Figure 5.2: The graph of 10 iterates $\rho_1 \circ \rho_1 \cdots \rho_1$ of $\rho_1(\alpha, 10)$, $\rho_1(\alpha, 20)$, from the complex exponential filter for $p = 2$, $\omega_1 = 0.8$, $\omega_2 = 2.1$.

		$\omega_1 = 0.97, \theta(\alpha_0) = 0.85$	$\omega_2 = 2.1, \theta(\alpha_0) = 1.8$
k	M_k	$\hat{\gamma}_{\alpha_k}$	$\hat{\gamma}_{\alpha_k}$
0	10	0.95709	1.83718
1	20	0.97281	2.02891
2	30	0.96967	2.09963
3	40	0.96967	2.10121
4	50	0.96967	2.10121
5	60	0.96967	2.10121
		$\hat{\omega}_1 = 0.96967$	$\hat{\omega}_2 = 2.10121$

6. Summary

The HK algorithm for multiple frequency detection in noise has been described in terms of some parametric families of filters. It has been demonstrated with the help of artificial data that the algorithm, when following the particular form

$$\alpha_{k+1} = \cos(\hat{\gamma}_{\alpha_k})$$

using (real) bandpass filters to generate HOC from zero-crossings, performs quite remarkably. The examples indicate that only a few iterations are needed in order to achieve a very satisfactory precision. Equally good results were obtained using a variety of other bandpass filters, such as the sine Butterworth bandpass filter constructed from lowpass and highpass filters. Under some assumptions, including the assumption that the cosine formula (1.1) holds, we can show that as $N \to \infty$, the sequence α_k converges with probability one to the cosine of the desired frequency. The two main ingredients needed in order to establish this, are a well behaved (close to zero) derivative of $\rho_1(\alpha, M)$ near the cosine of the frequency of interest, and the fact that the asymptotic zero-crossing rate lies between the highest and lowest nonnegative frequencies in the spectral support [3]. This matter will be taken up elsewhere.

7. Bibliography

[1] J. Barnett and B. Kedem. Zero-crossing rates of functions of Gaussian processes. *IEEE Trans. Infor. Th.*, 1991. To appear.

[2] S. He and B. Kedem. Higher order crossings of an almost periodic random sequence in noise. *IEEE Trans. Infor. Th.*, 35:360–370, March 1989.

[3] B. Kedem and E. Slud. On autocorrelation estimation in mixed-spectrum Gaussian processes. Submitted 1991.

[4] B. Kedem and S. Yakowitz. A contribution to frequency detection. Submitted 1990.

[5] S. Yakowitz. Some contributions to a frequency location method due to He and Kedem. *IEEE Trans. Infor. Th.*, 1991. To appear.

Monte Carlo periodograms†

T.W. Körner
Prometheus Inc.
21 Arnold Avenue
Newport, RI 02840 USA
twk@moa.dpmms.cambridge.ac.uk
Permanent address: Trinity Hall, Cambridge University

Abstract Hidden periodicities may be more easily detected if sampling takes place at random times.

1. Introduction

In this paper we consider the following natural problem. Suppose $f : \mathfrak{R} \to \mathfrak{C}$ is a function of the form

$$f(x) = \sum_{m=1}^{M} a_m \exp(i\lambda_m x) \tag{1.1}$$

with $a_m \in \mathfrak{C}$ and $\lambda_m \in \mathfrak{R}$ $[1 \leqslant m \leqslant M]$, but that we do not know the values of the a_m and λ_m or even of M. The result of making an observation at a point $x_n \in \mathfrak{R}$ is given by

$$\tilde{f}(x_n) = f(x_n) + e_n \tag{1.2}$$

where e_n is some unknown random error. We are allowed to make observations at $x_1, x_2, \ldots, x_N$ and wish to estimate the a_m and λ_m from the resulting observations $\tilde{f}(x_1), \tilde{f}(x_2), \ldots, \tilde{f}(x_N)$.

As it stands the question is not fully defined. We make the following remarks.

1) Unless the error e_n is zero it is unreasonable to expect to recover those λ_m for which the associated a_m are very small. Even if there is no error we would expect a method which claimed to recover λ_m for all nonzero a_m to be numerically unstable.

† This work was supported by AFOSR, under contract F49620-90-C-0023.

J. S. Byrnes et al. (eds.), Probabilistic and Stochastic Methods in Analysis, with Applications, 593–604.
© 1992 *Kluwer Academic Publishers. Printed in the Netherlands.*

2) It is unreasonable to expect to recover those λ_m outside a previously specified set Λ composed of a finite number of intervals. Dirichlet's theorem (see, e.g., [2], pp. 177–178) tells us that, given any function f of the form

$$f(x) = \sum_{m=1}^{M} a_m \exp(i\lambda_m x)$$

with $a_m \in \mathfrak{C}$ and $\lambda_m \in \mathfrak{R}$ $[1 \leqslant m \leqslant M]$, together with $x_1, x_2, \ldots, x_N \in \mathfrak{R}$, and any $\epsilon > 0$ and $K > 0$, we can find $\lambda'_m \in \mathfrak{R}$ such that

$$|\lambda'_m - \lambda_m| > K$$

but

$$\left| \sum_{m=1}^{M} a_m \exp(i\lambda'_m x_n) - \sum_{m=1}^{M} a_m \exp(i\lambda_m x_n) \right| < \epsilon$$

for all $1 \leqslant n \leqslant N$.

3) Next we observe that if f is given by

$$f(t) = \exp(i\lambda t) - \exp(i(\lambda + \eta)t)$$

then $|f(t)| < \epsilon$ for all $|t| < |\eta|^{-1}\epsilon/2$. It is thus unreasonable to seek a method which does not require previous knowledge of

$$\lambda^* = \min_{r \neq s} |\lambda_r - \lambda_s|.$$

4) We also need to know something about the errors e_n. In what follows we shall assume that the e_n are independent identically distributed random variables with mean $\mathcal{E}e_n = 0$ and variance $\mathcal{E}e_n^2 = \sigma^2$. We shall further assume that the distribution of e_n is Gaussian (since we work in $\mathfrak{C}$ this means that $\arg e_n$ is uniformly distributed on $[0, 2\pi)$ and $\mathrm{Re}\ e_n$ is a real Gaussian random variable) but our arguments apply, with hardly any change, whenever the distribution of e_n is reasonably well behaved. More complicated models of errors exist in which the e_n are not independent. I believe that the method proposed will produce similar results for some of these as well.

5) We must have some idea, not only of the cost of single computation, but of the cost of making a single observation. The relative cost may lead us to prefer a method requiring many computations but few observations or vice versa. The absolute cost may make some methods impractical.

So far the considerations we have raised apply to all methods. Our discussion will make two specific assumptions which will not always be satisfied in practice.

6) We assume that the choice of $x_1, x_2, \ldots, x_N$ precedes any of the observations. In other words our method is not adaptive (though, of course, it could be incorporated into an adaptive scheme).
7) Finally we assume that the $x_1, x_2, \ldots, x_N$ may be chosen freely from the reals.

In order to illustrate the remarks above and to provide a comparison with the methods we shall propose, consider the following standard procedure. Suppose that f is as in equation (1.1) and we know that the λ_m all lie well within $\Lambda = [-\alpha, \alpha]$. Choose $T > 0$ and set

$$x_n = -T + 2\pi T/N.$$

We now obtain the observations $\tilde{f}$ given by equation (1.2) and compute the *Fourier transform*

$$\tilde{F}(-\alpha + 2\pi\alpha/N) = N^{-1} \sum_{n=1}^{N} \tilde{f}(x_n) \exp\{-i(-\alpha + 2\pi\alpha/N)x_n\}$$

for $r = 1, 2, \ldots, N$, using the fast Fourier transform. Provided that N is reasonably large (specifically, $N^{1/2}/\log N$ is large compared with $\sigma/\min_{1 \le m \le M} |a_m|$) it is clear that $\tilde{F}(-\alpha + 2\pi\alpha/N)$ will not differ appreciably from

$$F(-\alpha + 2\pi\alpha/N) = N^{-1} \sum_{n=1}^{N} f(x_n) \exp\{-i(-\alpha + 2\pi\alpha/N)x_n\}.$$

In particular, provided that $\lambda^* T$ is large, the graph of F will exhibit M typical regions of disturbance centered on the λ_m of maximum amplitude $|a_m|$ and typical width of the order T^{-1}. Thus, provided we take N roughly of the same size as $T\alpha$, we can locate the λ_m to a precision of about T^{-1}. This method thus requires of the order of $\alpha\delta^{-1}$ observations and $\alpha\delta^{-1} \log(\alpha\delta^{-1})$ computations to locate the frequences λ_m to within δ.

In the next section we give an informal description of our proposed method along the same lines. Section 3 compares our method with the one just described. The final section contains further extensions of our method. In particular we show there that (provided we are prepared to accept a certain probability of error, which may be as small as we please) we can locate the frequences λ_m to within δ using only of the order of $\log \delta^{-1} \log\log \delta^{-1}$ observations and $\log \delta^{-1} \log\log \delta^{-1}$ computations.

While the full strength of this last result is unlikely to be attainable in practice, the underlying method is easy to implement and does give substantial savings (at least compared to the standard procedure outlined above).

2. Description

Choose $T > 0$ and a reasonably large integer N (for simple problems $N = 400$ might be sufficient). Choose $x_1, x_2, \ldots, x_N$ *at random* in the interval $[-T, T]$. More formally, set $x_n = X_n$ where $X_1, X_2, \ldots, X_N$ are independent, identically distributed random variables each uniformly distributed on $[-T, T]$. (Of course, the interval $[-T, T]$ may be replaced by any other interval of length $2T$.)

Now suppose that f is as in equation (1.1) and we have the observations $\tilde{f}$ given by equation (1.2). We define an *approximate Fourier transform* $\tilde{F}(\lambda)$ for a frequency λ by

$$\tilde{F}(\lambda) = N^{-1} \sum_{n=1}^{N} \tilde{f}(X_n) \exp(-i\lambda X_n).$$

Observe that (keeping λ fixed) $\tilde{F}(\lambda)$ is a random variable given by

$$\tilde{F}(\lambda) = N^{-1} \sum_{n=1}^{N} Y_n$$

where the

$$Y_n = (f(X_n) + e_n) \exp(-i\lambda X_n)$$

are themselves independent, identically distributed random variables taking values in $\mathbb{C}$. We note that

$$\mathcal{E}Y_n = \mathcal{E}(f(X_n) \exp(-i\lambda X_n)) = F(\lambda)$$

where

$$F(\lambda) = \frac{1}{2T} \int_{-T}^{T} f(t) \exp(-i\lambda t) dt$$

and that

$$\begin{aligned} \mathcal{E}|Y_n|^2 &= \mathcal{E}(|f(X_n)|^2 + e_n^* f(X_n) + e_n f(X_n)^* + |e_n|^2) \\ &= \mathcal{E}|f(X_n)|^2 + \mathcal{E}|e_n|^2. \end{aligned}$$

If $\lambda^* T$ is sufficiently large the cross terms in the evaluation of $\mathcal{E}|f(X_n)|^2$ will be negligible, and so setting $\tau^2 = \mathrm{var}(Y_n)$, we will have

$$\tau^2 \leqslant \sum_{m=1}^{M} |a_m|^2 + \sigma^2 + \eta \tag{2.1}$$

where η is negligible.

Applying the central limit theorem we see that

$$N^{1/2}(\tilde{F}(\lambda) - F(\lambda)) = N^{-1/2} \sum_{n=1}^{N} (Y_n - \mathcal{E}(Y_N))$$

is approximately Gaussian with mean 0 and variance τ^2. In other words

$$\tilde{F}(\lambda) = F(\lambda) + E(\lambda) \tag{2.2}$$

where $E(\lambda)$ is approximately normal with mean zero and variance $\tau^2 N^{-1}$. I think of $E(\lambda)$ as noise which is partly natural, coming from the errors e_n, and partly artificially induced by the random choice of the sample points. In the same way I interpret the inequality (2.1) by saying that the variance τ^2 has a natural component σ^2 and an artificially induced component $\tau^2 - \sigma^2$. Because of the nature of the Gaussian distribution we would not be surprised to find $|E(\lambda)|$ of size about $\tau N^{-1/2}$ or even about $2\tau N^{-1/2}$ but it would be extremely surprising to find $|E(\lambda)|$ of size $5\tau N^{-1/2}$ or greater.

With this in mind let us fix a $K \geqslant 3$. The probability that $|Z| \geqslant K\tau N^{-1/2}$ is $p(K)$ with $p(K)$ approximately given by

$$\frac{2}{\sqrt{2\pi}} \int_K^\infty \exp(-x^2/2)dx.$$

Since

$$F(\lambda) = \frac{1}{2T} \int_{-T}^{T} f(t) \exp(-i\lambda t)\, dt$$

$$= \sum_{m=1}^{M} a_m \frac{\sin((\lambda_m - \lambda)T)}{(\lambda_m - \lambda)T} \tag{2.3}$$

we see that, if $|\lambda_m - \lambda|$ is reasonably large compared with T^{-1} for all m, then $|\tilde{F}(\lambda)|$ will be smaller than $(K+1)\tau N^{-1/2}$ with probability at least $1 - p(K)$. On the other hand, provided that $\lambda^* T$ is reasonably large, if $|a_r| \geqslant 3K\tau N^{-1/2}$ then for λ close to λ_r the term

$$\frac{\sin((\lambda_r - \lambda)T)}{(\lambda_r - \lambda)T}$$

will dominate in the expansion

$$\tilde{F}(\lambda) = \sum_{m=1}^{M} a_m \frac{\sin((\lambda_m - \lambda)T)}{(\lambda_m - \lambda)T} + E(\lambda)$$

with probability at least $1 - p(K)$.

So far we have looked at $\tilde{F}(\lambda)$ for a single value of λ. Now suppose that we are given Λ, the union of a finite number of disjoint intervals of total length $|\Lambda|$. Provided R is reasonably large compared with the number of intervals making up Λ, we can find R points $\nu_1, \nu_2, \ldots, \nu_R \in \Lambda$ such that if $\lambda \in \Lambda$ then $|\lambda - \nu_r| < |\Lambda|/R$ for some r, $1 \leqslant r \leqslant R$. It is, of course, not true that the 'errors' $E(\nu_r)$ are mutually independent but the simplest possible estimate shows that

$$|E(\nu_r)| \leqslant K\tau N^{-1/2} \qquad \text{for all } 1 \leqslant r \leqslant R \tag{2.4}$$

with probability at least $1 - Rp(K)$. If equation (2.4) holds then the same kind of considerations as applied in the previous paragraph and in the penultimate paragraph of the introduction will apply, provided we have $|\Lambda|R^{-1}$ of size about $(6T)^{-1}$ or smaller. If $|a_m| \geqslant 3\tau N^{-1/2}$ and λ_m is well within Λ we shall see a typical region of disturbance centered on λ_m of amplitude roughly $|a_m| \pm K\tau N^{-1/2}$ and width of the order T^{-1} standing out from the surrounding noise. We may or may not detect regions associated with smaller $|a_m|$ but, provided we ignore all ν_r with $|\tilde{F}(\nu_r)| \leqslant (K+1)\tau N^{-1/2}$ we shall not obtain any 'false positives'.

A well-known estimate gives

$$\frac{2}{\sqrt{2\pi}} \int_K^\infty \exp(-x^2/2)dx \leqslant \frac{2}{K\sqrt{2\pi}} \int_K^\infty x \exp(-x^2/2)dx$$
$$= \frac{2}{K\sqrt{2\pi}} \exp(-K^2/2).$$

Thus the procedure of the last paragraph will locate all the λ_m in the search region for which $|a_m| \geqslant a^*$ to a precision of about δ (and not produce false positives) with a probability of failure less than ϵ provided the following relations hold. (Here $u \succeq v$ is to be read as $u \geqslant Cv$ for some numerical constant C.)

$$\delta \succeq T^{-1}$$
$$T^{-1} \succeq |\Lambda|R^{-1}$$
$$a^* \succeq K\tau N^{-1/2}$$
$$\epsilon \succeq RK^{-1} \exp(-K^2/2).$$

Thus we need

$$\epsilon N^{1/2} a^* \tau^{-1} \exp(N(a^*\tau^{-1})^2/2) \succeq R \succeq |\Lambda|\delta^{-1} \tag{2.5}$$

for our method to perform as desired. The inequality (2.5) tells us how we must vary N, the number of sample points. Since the sample points are not in arithmetical progression we can not use the fast Fourier transform, and our method will require of the order of RN computations.

3. Discussion

The reader who is worried by the probability ϵ of error should observe that, if we fix the other parameters, and seek to reduce ϵ by increasing N then N need only increase slower than $\log(\epsilon^{-1})$. Thus an essentially trivial increase in the number of sample points and computations will reduce the probability of failure inherent in the method below, e.g., the probability of some serious undetected computer error. It should also be noted that if $\sigma > 0$ then *any* method must inevitably have a strictly positive probability of error.

Let us now compare our method with that discussed at the end of the introduction. Let us fix ϵ and a^* (for example we might take $a^* = \min_{1 \leqslant m \leqslant M} |a_m|$). In the introduction we took $\Lambda = [-\alpha, \alpha]$ and saw that the standard method required of the order of $|\Lambda|\delta^{-1}$ sample points and $|\Lambda|\delta^{-1}\log(|\Lambda|\delta^{-1})$ computations to locate the frequencies λ_m to within δ. Our method, which allows Λ to be the finite union of intervals, requires, at most, of the order of $\log(|\Lambda|\delta^{-1})$ sample points and of the order of $|\Lambda|\delta^{-1}\log(|\Lambda|\delta^{-1})$ computations. We note, for later use, that the choice of Λ can be made *after* the observations.

There are various remarks we should make at this stage.

1) Although we have achieved a substantial reduction in the number of sample points required, the number of computations has not been reduced. In Section 4 we shall see that this weakness can, to a large extent, be overcome.
2) If we keep $a_1, a_2, \ldots, a_M$ fixed but allow the λ_m to vary, it is not hard to see that the accuracy δ and the power of discrimination λ^* vary in step with each other. Thus our method requires, at most, of the order of $\log(|\Lambda|\lambda^{*-1})$ sample points and of the order of $|\Lambda|\lambda^{*-1}\log(|\Lambda|\lambda^{*-1})$ computations. Although we have chosen the random variables X_n to have uniform probability distribution on $[-T, T]$, smoothing them might well produce better discrimination in practice. For example, if we take the X_n to be independent, identically distributed random variables each with density function

$$g(x) = \begin{cases} T^{-1}|T - x|, & \text{for all } |T - x| \leqslant T \\ 0, & \text{otherwise} \end{cases}$$

and proceed as before, our method and the supporting argument are essentially unchanged except that equation (2.3) becomes

$$F(\lambda) = \sum_{m=1}^{M} a_m \frac{(\sin((\lambda_m - \lambda)T/2))^2}{((\lambda_m - \lambda)T/2)^2}.$$

We have thus localised the disturbance associated with the frequency rather better than before.

3) The 'detection/noise' ratio

$$\rho^* = \frac{a^*}{N^{1/2}(\sum_{m=1}^{M} |a_m|^2 + \sigma^2)^{1/2}}$$

only decreases as fast as $N^{-1/2}$. Thus to reduce ρ^* by a factor of L whilst keeping everything else unchanged requires us to multiply the number of sample points, and so, also, the number of computations by a factor of order L^2.

At first sight this does not seem very good, but a simple example shows that the rates of growth in the last sentence can not be improved. Suppose that we simplify our problem so that equation (1.1) becomes

$$f(x) = a$$

with $a \in \mathbb{C}$. Then equation (1.2) gives

$$\tilde{f}(x_n) = a + e_n$$

and our problem reduces to finding whether $a = 0$ or not. Simple statistical considerations show that, in order to be reasonably confident of detecting $a \neq 0$ when $|a| \geq a^*$ and not declaring $a \neq 0$ when, in fact, $a = 0$, we need a 'detection/noise' ratio

$$\rho^{**} = \frac{a^*}{N^{1/2}\sigma}$$

rather larger than 1. Since we must read the values of $\tilde{f}(x_n)$ in order to use them we must make at least N computations. Just as before, to reduce ρ^{**} by a factor of L whilst keeping everything else unchanged requires us to multiply the number of sample points, and so, also, the number of computations by a factor of order L^2. It is, of course, true that ρ^{**} only involves the 'natural noise level' σ whilst ρ^* involves a noise level with an 'artificial component' of order $(\sum_{m=1}^{M} |a_m|^2)^{1/2}$. In Section 4 we shall sketch a way of getting round this.

4) We turn now to the estimation of a_m. The obvious way of doing this is to guess $a_m = \tilde{F}(\nu_j)$ where ν_j is the point at which $|\tilde{F}(\nu_k)|$ is largest within the disturbance associated with λ_m. Other schemes are possible, but the reader should remember that the random errors $E(\nu_k)$ of equation (2.2) are are not independent. With our simple scheme there are two sources of error. The first source is the distance of ν_j from λ_m. This error will be of order $|a_m|\delta^2$ and, provided δ has already been chosen quite small, will not be important. (In any case, once we have located λ_m as lying near ν_k we can always calculate $\tilde{F}(\nu)$ for a group of closely spaced points near ν_k without adding noticeably to

the computational load. We shall develop this idea substantially in Remark 4.2 of the next section.)

We are thus only worried by the second source of error, to wit the noise $E(\lambda)$. Almost exactly the same considerations as applied to the problem of detection in note 3 show that this error will be of the order of $N^{-1/2}\tau$ for our method and that any method whatsoever must have errors in the estimation of a_m of order at least $N^{-1/2}\sigma$. The last sentence of 3 thus applies with ρ^* and ρ^{**} replaced by

$$\epsilon^* = \frac{\text{error level}}{N^{1/2}\tau} \quad \text{and} \quad \epsilon^{**} = \frac{\text{error level}}{N^{1/2}\sigma}.$$

4. Multistage searching

Suppose as usual that f is as in equation (1.1) and that we have chosen ϵ and a^* once and for all. Suppose further that we know a $\delta > 0$ such that $\lambda^* = \min_{1 \leqslant s < r \leqslant M} |\lambda_r - \lambda_s|$ is substantially larger than δ. Let us say that λ_j is an *important frequency* if $|a_j| \geqslant a^*$. We also fix $\epsilon > 0$ which will correspond to a desired upper bound for the probability of error and a length $\alpha > 0$. For the purposes of this section, the information we shall require about the method discussed in the previous sections can be summarised as follows.

Summary. There exists a constant $P > 0$ and numbers $N, L > 1$ depending on a^*, ϵ and δ with the following property. Suppose $\delta \geqslant \eta' > 0$ and that $k \geqslant 2$ is an integer. Suppose further that $T'\eta' = P$ and that $N' = \lfloor N \log k \rfloor$ (i.e., N' is the integer part of $N \log k$. Let us take a set E' of N' points at random on $[-T', T']$. Suppose we are now given Λ' a union of intervals each of length greater than η', and such that their total length $|\Lambda|$ satisfies $|\Lambda|\eta^{-1} = 2\alpha\delta^{-1}$. Then the method of the previous sections will locate all important frequencies lying in Λ' (together, possibly, with other frequencies but without false positives) to within η' with probability at least $1 - \epsilon/k$. The number of computations required will be no greater than $L \log k$.

In the theoretical discussion that follows k will be a large integer; in practice there are useful gains even with $k = 2$ or 3. To check the summary it suffices to look at the inequalities preceding inequality (2.5) and recall that the 'noise level' τ is a constant of the system.

Now suppose we are given $\Lambda = [-\alpha, \alpha]$ (or, more generally, a reasonable set of intervals of total length 2α). We suppose further that $M\delta/(2\alpha)$ is small compared with 1. Let us set $\Lambda(0) = \Lambda$, $\eta(1) = \delta$, and define $\eta(j)$ inductively for each $2 \leqslant j \leqslant k$ by

$$M\eta(j-1)\eta(j)^{-1} = 2\alpha\delta^{-1}.$$

Let $T(j)$ be chosen so that $T(j)\eta(j) = P$ and chose a set $E(j)$ of $N' = [N \log k]$ points at random on $[-T(j), T(j)]$.

Referring to the summary we see that we can use the method of the previous sections applied to $E(1)$ to locate the, at most, M important frequencies in a set $\Lambda(1)$ consisting of, at most, M intervals each of length $2\eta(1)$. Now, using this knowledge, we may apply the method to $E(2)$ to locate the, at most, M important frequencies in a subset $\Lambda(2)$ of $\Lambda(1)$ consisting of, at most, M intervals each of length $2\eta(2)$.

Continuing through k stages we arrive at a set $\Lambda(k)$ consisting of at most M intervals of length $2\eta(k)$. Provided that nothing has gone wrong, each interval contains exactly 1 frequency $\lambda(s)$ and each important frequency lies in an interval. There is, of course, a positive probability of failure at each step, but, looking at the summary we see that this is less than ϵ/k. The probability that anything has gone wrong, and that the second half of the second sentence of this paragraph could be false, is thus less than ϵ.

We have thus used $kL \log k$ computations and $kN \log k$ sample points to locate all important frequencies (and, possibly, some others) to within $\delta(M\delta/2a)^{-k+1}$ with a probability of error of less than ϵ. In other words, with probability at least $1 - \epsilon$ we have achieved an accuracy of η in locating important frequencies, using only of the order of $\log \eta^{-1} \log\log \eta^{-1}$ computations and of the order of $\log \eta^{-1} \log\log \eta^{-1}$ sample points. Provided we know $\min |a_j|$ (and provided that this minimum is nonzero) we can choose a^* sufficiently small that all the frequencies λ_m are important frequencies. In this way we have fulfilled the promise made in the penultimate paragraph of Section 1.

We conclude with a series of remarks.

Remark 4.1. Although we can locate the λ_m to arbitrarily high *accuracy* by increasing k, the power of *discrimination* of the method (i.e., the smallest value of $\lambda^* = \min_{1 \leqslant r < s \leqslant M} |\lambda_r - \lambda_s|$ with which it is guaranteed to cope) is of the order of $\eta(1) = \delta$. The number of operations and observations required for a given power δ of discrimination remain governed by the estimates of Section 3.

Remark 4.2. So far we have concentrated on obtaining good estimates for the frequencies λ_m and more or less ignored the associated amplitudes a_m. However once the frequencies are known to high accuracies the amplitudes are easily obtained using the method of least squares. In particular, suppose we are given a T such that $T \min_{1 \leqslant r < s \leqslant M} |\lambda_r - \lambda_s|$ is very large. Choose N points $X_1, X_2, \ldots, X_N$ at random on $[-T, T]$. Suppose we have estimates λ'_m of λ_m for $1 \leqslant m \leqslant P$ which are sufficiently good to make $T|\lambda_m - \lambda'_m|$ very small. Then similar arguments to those we used in Section 2 show that, with a probability of error less than some bound fixed in advance, we can

estimate the a_m for $1 \leqslant m \leqslant P$ to within an order of $\tau^* N^{-1/2}$ where

$$\tau^{*2} = \sigma^2 + \sum_{j=P+1}^{M} |a_j|^2.$$

For the sake of theoretical simplicity let us suppose that we use a completely different set of random points to estimate amplitudes from the set of points that we used to estimate the frequencies. If we use the same number of points in each of the two sets we add hardly anything to the number of computations (and in particular we do not change its order of magnitude). The errors in our estimates of amplitudes will be of the order of τ^* divided by the square root of the total number of observations.

Remark 4.3. The idea of Remark 4.2 can be taken slightly further. Once we have good estimates λ'_m and a'_m for the λ_m and a_m with $1 \leqslant m \leqslant P$ we can apply our method (possibly using a different set of observations) to g defined by

$$g(x) = f(x) - \sum_{m=1}^{P} a'_m \exp(i\lambda'_m x).$$

Since, in the spirit of Section 3, we could say that g is associated with a lower artificially induced noise level (at least, if we restrict the range over which we take observation points appropriately) we should expect to be able to estimate further frequencies λ_m and amplitudes a_m for which $|a_m|$ is smaller than before. However the new frequency and amplitude estimates will be less accurate than those previously obtained. If we take $|a_1| \geqslant |a_2| \geqslant \ldots \geqslant |a_M|$ then this sort of idea will only enable us to estimate frequencies λ_m and amplitudes a_m for $1 \leqslant m \leqslant Q$ using a total of N observations on condition that $|a_Q|^2$ is reasonably large compared with $(\sigma^2 + \sum_{j=Q+1}^{M} |a_j|^2)/N^{1/2}$.

Remark 4.4. If we consider the multidimensional generalisation of our problem to a function $f : \mathfrak{R}^n \to \mathfrak{C}$ given by

$$f(\mathbf{x}) = \sum_{m=1}^{M} a_m \exp(i\boldsymbol{\lambda}_m \cdot \mathbf{x})$$

with $a_m \in \mathfrak{C}$ and $\boldsymbol{\lambda}_m \in \mathfrak{R}^n$ $[1 \leqslant m \leqslant M]$, then our methods can be applied essentially unchanged and retain their advantages.

Remark 4.5. It would be in keeping with the philosophy of this paper to suggest that if a long term sequence of expensive observations is to be made the times of observation should be chosen according to a Poisson process.

Remark 4.6. It is not hard to produce rigorous proofs of the statements of this paper using the methods of [1] (see in particular pages 67 to 70). However the constants so obtained are misleadingly pessimistic. In practice it seems best to 'tune' the method on some particular problem. (If you graph the output the 'noise level' can be seen very clearly.) Once this is done the formulae of this paper show how the number of sample points, etc., need to be changed for other problems.

Remark 4.7. Simple numerical experimentation at Prometheus Inc. suggests that the methods of this paper are impractical without a modern desktop computer, but that, once a speed of 10^6 operations per second is available, realistic problems can be tackled. They are easy to program and I suggest that interested readers try them for themselves.

5. Bibliography

[1] J.-P. Kahane. *Some Random Series of Functions.* Cambridge University Press, Cambridge, U.K., 2nd edition, 1985.

[2] J.-P. Kahane and R. Salem. *Ensembles Parfaits et Séries Trigonometriques.* Hermann, Paris, 1963.

A class of equivalent measures

Stamatis Koumandos
Department of Mathematics
University of Thessaloniki
54006 Thessaloniki Greece
ck@grathun1.bitnet

Abstract We give sufficient conditions for one generalized Rademacher-Riesz product to be equivalent to another. Also, we discuss criteria for mutual singularity of these measures.

1. Introduction

In this talk, we deal with Riesz product type measures based on a certain sequence of independent random variables with zero mean. A particular case of these measures are the Rademacher-Riesz products on $[0, 1]$, that is, measures of the form:

$$d\mu = \lim_{n\to\infty} \prod_{k=1}^{n} (1 + a_k r_k)\, dx,$$

where $|a_k| \leqslant 1$ and the limit is taken in the weak* sense. As it is known the Rademacher function r_k is defined by $r_k(x) = 1 - 2\epsilon_k$, where ϵ_k is the k-th digit of the dyadic expansion of x.

Generalized Rademacher-Riesz products have been introduced in [3] and the entropy of such a measure has been determined. This problem was reduced to the calculation of the Hausdorff dimension of the support of this measure; the support of a generalized Rademacher-Riesz product is under some circumstances of fractal type. Exact knowledge of these circumstances depends on some criteria for singularity or absolute continuity of these measures. Thus, it is natural to ask whether the supports of two generalized Rademacher-Riesz products coincide or are disjoint.

In this work, our main purpose is to give some simple criteria for equivalence or mutual singularity of two generalized Rademacher-Riesz products, so that, the results obtained will be immediately adaptable for the case of ordinary Rademacher-Riesz products.

Some central results concerning mutual singularity or equivalence for the classical trigonometric Riesz products have been derived by several authors. In [6] Peyrière gives a very simple criterion for two Riesz product

J. S. Byrnes et al. (eds.), Probabilistic and Stochastic Methods in Analysis, with Applications, 605–613.
© 1992 *Kluwer Academic Publishers. Printed in the Netherlands.*

measures to be mutually singular. A little later, in [1], Brown and Moran obtained, among other things, sufficient conditions for equivalence of Riesz products and their result was improved by Ritter in [7]. In addition, Kilmer and Saeki (cf. [4]) have contributed to the study of the same subject. More recently, Parreau (cf. [5]) gave a criterion for the equivalence of generalized trigonometric Riesz products.

Here, we treat measures of a different kind from those mentioned above by means of novel methods. The main results are derived via probabilistic tools, namely, martingale theory. We note also that, though our measures are closely related to infinite product measures, in the sense of [2], the results are obtained without any use of Kakutani's well known criterion for comparing product measures.

In the next section we give some preliminary notions and we recall the definition of the generalized Rademacher-Riesz product measure. Also, we state the propositions which are the key in our method.

2. Preliminaries

Let r be a positive integer ($r \geqslant 2$) and let ϵ_n be the n-th digit of the expansion of $x \in [0, 1)$ in the base r. We shall call a cylinder of order n an r-adic interval of the form:

$$E_{n,j} = \left[\frac{j-1}{r^n}, \frac{j}{r^n}\right) \qquad \text{for } j = 1, 2, \ldots, r^n.$$

We define the sequences of functions $(R_k^i)_{k=1}^{\infty}$ for $i = 0, 1, \ldots, r-1$ on $[0, 1]$ as follows:

$$R_k^i(x) = 1 - r\delta_{\epsilon_k, i},$$

where $\delta_{\epsilon_k,i}$ is the usual Kronecker's symbol and R_k^i is zero on each r-adic rational. We call the sequence $(R_k^i)_{k=1}^{\infty}$ the system of r-adic Rademacher functions associated with the digit i.

Let $(a_n^{(0)}), (a_n^{(1)}), \ldots, (a_n^{(r-1)})$ be sequences of real numbers, satisfying $a_n^{(i)} > 0$ and $\sum_{i=0}^{r-1} a_n^{(i)} = 1$, for all n. We define the sequence of random variables $(X_k)_{k=1}^{\infty}$ on $[0, 1]$ as follows :

$$X_k = \sum_{i=0}^{r-1} a_k^{(i)} R_k^i \qquad \text{for } k = 1, 2, \ldots$$

It is plain that $(X_k)_{k=1}^{\infty}$ are independent random variables with zero mean on the usual probability space of $[0, 1]$.

Let $E_n(x)$ be the cylinder of order n which contains x for $n = 1, 2, \ldots$ and let $E_0(x) = [0, 1]$. We define

$$\mu(E_n(x)) = \frac{1}{r^n} \prod_{k=1}^{n} (1 - X_k(x)).$$

If $E_{n,j} = \bigcup_{s=0}^{r-1} E_{n+1,s}$ is the partition of $E_{n,j}$ into cylinders of order $n + 1$, it is easy to see that the set function μ satisfies the conditions:

1)

$$\mu(E_{n,j}) = \sum_{s=0}^{r-1} \mu(E_{n+1,s}) \qquad \text{for every } n \text{ and } j = 1, 2, \ldots, r^n.$$

2)

$$\sum_{j=1}^{r^n} \mu(E_{n,j}) = 1 \qquad \text{for all } n.$$

Therefore, μ may be extended to a Borel probability measure on $[0, 1]$ in a unique manner. It is clear that μ is the weak* limit of the sequence of measures μ_n defined by $d\mu_n = \prod_{k=1}^{n} (1 - X_k)\, d\lambda$, where λ is the Lebesgue measure on the σ-algebra B of the Borel subsets of $[0, 1]$. We call such a measure μ a *generalized Rademacher-Riesz product (R.R. product)* associated with the sequences $(a_n^{(i)})$, and in what follows we shall employ the notation

$$d\mu = \prod_{n=1}^{\infty} (1 - X_n)\, d\lambda. \tag{2.1}$$

Remark 2.1. In the case where $r = 2$ we have $R_n^1 = r_n$ and $R_n^0 = -r_n$, where $(r_n)_{n=1}^{\infty}$ are the usual Rademacher functions on $[0, 1]$. If we take $a_n^{(0)} = \frac{1+a_n}{2}$, $a_n^{(1)} = \frac{1-a_n}{2}$, where $|a_n| \leqslant 1$, the measure (2.1) has the form

$$d\mu = \prod_{n=1}^{\infty} (1 + a_n r_n)\, d\lambda,$$

which is an ordinary Rademacher-Riesz product on $[0, 1]$.

One can prove easily the following elementary lemma:

Lemma 2.2. Let μ be a generalized R.R. product as in (2.1). Then, we have the following conclusions:

1) The random variables $(R_n^i)_{n=1}^{\infty}$ are independent on the probability space $([0, 1], B, \mu)$.

2) Let

$$\xi_n = c_n + \sum_{i=0}^{r-1} c_n^{(i)} R_n^i,$$

where (c_n), $(c_n^{(i)})$ are sequences of real numbers such that at least one $c_n^{(i)} \neq 0$ and one $c_n^{(i)} \neq 1$ for every n. Then the random variables ξ_n are independent on the probability space $([0,1], B, \mu)$.

3) We further have

$$\int_0^1 R_n^i \, d\mu = 1 - ra_n^{(i)}.$$

We also need the following proposition which is a simple corollary of the martingale convergence theorem:

Proposition 2.3. Let $(f_n, F_n)_{n\geq 1}$ be a martingale on a probability space (Ω, F, P). *We suppose that*

$$\sup_n \int_\Omega |f_n|^a \, dP < +\infty \qquad \text{for some } a > 1.$$

Then, there exists a function f such that:

1)

$$\int_\Omega |f| \, dP < +\infty,$$

2)

$$f_n(x) \to f(x), \qquad P\text{-almost everywhere, and}$$

3)

$$\int_\Omega |f_n - f| \, dP \to 0 \qquad \text{as } n \to \infty.$$

For a proof see [8, p. 477-478].

3. Criterion for equivalence of two generalized R.R. products

We shall prove the following proposition:

Proposition 3.1. Let $d\mu = \prod_{n=1}^{\infty}(1 - X_n)\,d\lambda$ and $d\nu = \prod_{n=1}^{\infty}(1 - Y_n)\,d\lambda$, where $X_n = \sum_{i=0}^{r-1} a_n^{(i)} R_n^i$, and $Y_n = \sum_{i=0}^{r-1} b_n^{(i)} R_n^i$. If

$$\sum_{n=1}^{\infty}\sum_{i=0}^{r-1}\frac{(a_n^{(i)} - b_n^{(i)})^2}{a_n^{(i)} b_n^{(i)}} < +\infty, \tag{3.1}$$

then μ, ν are equivalent measures (i.e, $\mu \ll \nu$ and $\nu \ll \mu$).

Proof. It is enough to show that $\mu \ll \nu$. We consider the sequence of functions:

$$F_n = \prod_{k=1}^{n}\left(\frac{1 - X_k}{1 - Y_k}\right) \qquad \text{for } n = 1, 2, \ldots \tag{3.2}$$

Let B_n be the σ-algebra generated by $\{E_{n,j} : 1 \leqslant j \leqslant r^n\}$. It is easy to see that the stochastic sequence $(F_n, B_n)_{n\geqslant 1}$ is a martingale on the probability space $([0, 1], B, \nu)$. We observe that

$$\frac{1 - X_k}{1 - Y_k} = 1 + \frac{1}{r}\sum_{i=0}^{r-1}\left(\frac{a_k^{(i)} - b_k^{(i)}}{b_k^{(i)}}\right)(1 - R_k^i). \tag{3.3}$$

We can further have

$$\begin{aligned}\left(\frac{1 - X_k}{1 - Y_k}\right)^2 = 1 &+ \frac{1}{r}\sum_{i=0}^{r-1}\left(\frac{a_k^{(i)} - b_k^{(i)}}{b_k^{(i)}}\right)^2 (1 - R_k^i) \\ &+ \frac{2}{r}\sum_{i=0}^{r-1}\left(\frac{a_k^{(i)} - b_k^{(i)}}{b_k^{(i)}}\right)(1 - R_k^i).\end{aligned} \tag{3.4}$$

Using (3.4) and Lemma 2.2, we obtain

$$\int_0^1 F_n^2\,d\nu = \prod_{k=1}^{n}\left(1 + \sum_{i=0}^{r-1}\frac{(a_k^{(i)} - b_k^{(i)})^2}{b_k^{(i)}}\right) \tag{3.5}$$

It follows from our assumption (3.1) that

$$\sum_{n=1}^{\infty}\sum_{i=0}^{r-1}\frac{(a_n^{(i)} - b_n^{(i)})^2}{b_n^{(i)}} < +\infty;$$

and finally from (3.5) and the above we have

$$\sup_n \int_0^1 F_n^2\,d\nu < +\infty. \tag{3.6}$$

Now, according to Proposition 2.3, relation (3.6) implies that F_n converges in $L^1(\nu)$. Furthermore, F_n converges ν-almost everywhere. Let $F = \lim_{n\to\infty} F_n$ (ν – a.e). Since, by (3.3)

$$\int_0^1 F_n \, d\nu = 1,$$

it follows that

$$\int_0^1 F \, d\nu = 1. \tag{3.7}$$

If $\mu = \mu_1 + \mu_2$ is the Lebesgue decomposition of μ into absolutely continuous and singular parts, respectively, with respect to ν, it is well-known that (see [8, p. 493])

$$\mu_1(A) = \int_A F \, d\nu \qquad \text{for every } A \in B. \tag{3.8}$$

Combining (3.7) with (3.8) it follows that $\mu_2 = 0$, therefore $\mu \ll \nu$, and the proof is complete. ∎

Remark 3.2. It is an immediate consequence of the proposition just proved that if for two generalized R.R. products μ, ν associated with $a_n^{(i)}$ and $b_n^{(i)}$ respectively,

$$\sum_{n=1}^{\infty} \sum_{i=0}^{r-1} (a_n^{(i)} - b_n^{(i)})^2 < +\infty$$

and

$$\liminf_{n\to\infty} B_n > 0, \qquad \text{where } B_n = \min_{0\le i\le r-1} b_n^{(i)} \tag{3.9}$$

hold true, then μ, ν are equivalent. It is remarkable that one can prove this assertion without the application of the Lebesgue decomposition used above. It suffices to observe that (3.9) implies $\limsup_{n\to\infty} B_n^* < 1$, where $B_n^* = \max_{0\le i\le r-1} b_n^{(i)}$ which in turn implies that ν is a continuous measure. Hence, the sequence of measures ω_n defined by, $d\omega_n = F_n \, d\nu$, converges to μ in the weak* topology. This and the convergence of F_n in $L^1(\nu)$ yield $\mu \ll \nu$.

In the case where μ, ν are two ordinary R.R. products associated with $(a_n), (b_n)$ respectively, Proposition 3.1 is stated as follows:

Corollary 3.3. Let $d\mu = \prod_{n=1}^{\infty} (1 + a_n r_n) \, d\lambda$ and $d\nu = \prod_{n=1}^{\infty} (1 + b_n r_n) \, d\lambda$. If

$$\sum_{n=1}^{\infty} \frac{(a_n - b_n)^2}{(1 - a_n^2)(1 - b_n^2)} < +\infty,$$

then μ, ν are equivalent measures.

Proof. It suffices to observe that in this case (3.5) has the form:

$$\int_0^1 F_n^2 \, d\nu = \prod_{k=1}^{n} \left(1 + \frac{(a_k - b_k)^2}{1 - b_k^2}\right)$$

■

Remark 3.4. It is now clear that for two R.R. products μ, ν associated with $(a_n), (b_n)$ respectively, if $\sum_{n=1}^{\infty}(a_n - b_n)^2 < +\infty$ and $\limsup_{n\to\infty} |b_n| < 1$, then μ, ν are equivalent measures. By virtue of Corollary 3.3, μ, ν may be equivalent in some cases where $\sum_{n=1}^{\infty}(a_n - b_n)^2 < +\infty$ whereas $|a_n|, |b_n|$ approach 1. Consider, for example, $a_n = 1 - c_n - c_n^2$, $b_n = 1 - c_n$, where $c_n > 0$ and $\sum_{n=1}^{\infty} c_n^2 < +\infty$. However, as we shall see in the next section, in the case where $\sum_{n=1}^{\infty}(a_n - b_n)^2 < +\infty$ and $|a_n|, |b_n|$ approach 1, μ, ν may be mutually singular under some further assumptions for (a_n) and (b_n).

4. Mutual singularity of generalized R.R. products

It can be easily shown that if μ, ν are generalized R.R. products associated with $(a_n^{(i)})$, and $(b_n^{(i)})$ respectively and $\sum_{n=1}^{\infty}\sum_{i=0}^{r-1}(a_n^{(i)} - b_n^{(i)})^2 = +\infty$ then μ, ν are mutually singular. This may happen in some cases where the above series converges, provided of course that the condition (3.9) is dropped. The following proposition gives us further information about mutual singularity of generalized R.R. products:

Proposition 4.1. We suppose $d\mu = \prod_{n=1}^{\infty}(1 - X_n)\, d\lambda$ and $d\nu = \prod_{n=1}^{\infty}(1 - Y_n)\, d\lambda$, where $X_n = \sum_{i=0}^{r-1} a_n^{(i)} R_n^i$, $Y_n = \sum_{i=0}^{r-1} b_n^{(i)} R_n^i$. Let us put

$$\sigma_n^2 = \sum_{i=0}^{r-1} \frac{(a_n^{(i)} - b_n^{(i)})^2}{b_n^{(i)}},$$

$$M_n = \max_{0 \le i \le r-1} \frac{a_n^{(i)}}{b_n^{(i)}}.$$

If

$$\sup_n M_n < +\infty \quad \text{and} \quad \sum_{n=1}^{\infty} \sigma_n^2 = +\infty,$$

then μ, ν are mutually singular.

Proof. There exists a sequence of real numbers (u_n) such that

$$u_n > 0, \quad \sum_{n=1}^{\infty} \sigma_n^2 u_n = +\infty, \quad \sum_{n=1}^{\infty} \sigma_n^2 u_n^2 < +\infty.$$

We define the sequence of random variables

$$\xi_n = \frac{Y_n - X_n}{1 - Y_n} u_n \qquad \text{for } n = 1, 2, \ldots$$

Using Lemma 2.2 stated above and formula (3.3) it follows that $(\xi_n)_{n=1}^{\infty}$, are independent random variables with respect to ν, such that

$$\int_0^1 \xi_n \, d\nu = 0.$$

From formula (3.4) we obtain

$$\int_0^1 \xi_n^2 \, d\nu = u_n^2 \sigma_n^2.$$

Now, we define

$$\zeta_n = \xi_n - u_n \sigma_n^2 \qquad \text{for } n = 1, 2, \ldots$$

We observe that $(\zeta_n)_{n=1}^{\infty}$ are independent random variables with respect to μ, and using again (3.3), (3.4) and Lemma 2.2, we obtain

$$\int_0^1 \xi_n \, d\mu = u_n \sigma_n^2, \quad \text{hence} \quad \int_0^1 \zeta_n \, d\mu = 0.$$

It is not hard to see that

$$\int_0^1 \zeta_n^2 \, d\mu < u_n^2 \sigma_n^2 M_n.$$

Thus, by the Khinchin-Kolmogorov Theorem (see [8, p. 359]) we conclude

$$\sum_{n=1}^{\infty} \xi_n(x) \qquad \text{converges } \nu\text{-a.e.}$$

and

$$\sum_{n=1}^{\infty} \zeta_n(x) \qquad \text{converges } \mu\text{-a.e.}$$

If there is some x_0 such that both $\sum_{n=1}^{\infty} \xi_n(x_0)$, and $\sum_{n=1}^{\infty} \zeta_n(x_0)$ converge, it follows that $\sum_{n=1}^{\infty} \sigma_n^2 u_n < +\infty$; contradiction. This proves that μ and ν are mutually singular, as claimed. ∎

For the case of two ordinary Rademacher-Riesz products μ and ν we have the following:

Corollary 4.2. Let $d\mu = \prod_{n=1}^{\infty}(1 + a_n r_n)\, d\lambda$, and $d\nu = \prod_{n=1}^{\infty}(1 + b_n r_n)\, d\lambda$; if

$$\sum_{n=1}^{\infty} \frac{(a_n - b_n)^2}{1 - b_n^2} = +\infty \quad \text{and} \quad \sup_n \frac{1 - a_n^2}{1 - b_n^2} < +\infty,$$

then μ and ν are mutually singular.

This follows from the proof of Proposition 4.1 under some minor modifications.

We complete this paper with the promised example of mutually singular Rademacher-Riesz products μ, ν associated with $(a_n), (b_n)$, in the case where $\sum_{n=1}^{\infty}(a_n - b_n)^2 < +\infty$ and $|a_n|, |b_n|$ approach 1. According to the Corollary 4.2, it suffices to take $a_n = 1 - c_n$, $b_n = 1 - 2c_n$, where $0 < c_n < \frac{1}{2}$, $\sum_{n=1}^{\infty} c_n = +\infty$, $\sum_{n=1}^{\infty} c_n^2 < +\infty$. Notice also that these measures μ and ν are continuous.

5. Bibliography

[1] G. Brown and W. Moran. On orthogonality of Riesz products. *Math. Proc. Camb. Phil. Soc.*, 76:173–181, 1974.

[2] S. Kakutani. On equivalence of infinite product measures. *Annals of Mathematics*, 49:214–224, 1948.

[3] C. Karanikas and S. Koumandos. On a generalized entropy's formula. *Results in Math.*, 18:254–263, 1990.

[4] S.J. Kilmer and S. Saeki. On Riesz product measures; mutual absolute continuity and singularity. *Ann. Inst. Fourier (Grenoble)*, 38(2):63–93, 1988.

[5] F. Parreau. Ergodicité et pureté des produits de Riesz. *Ann. Inst. Fourier (Grenoble)*, 40(2):391–405, 1990.

[6] J. Peyriére. Étude de quelques propriétés des produits de Riesz. *Ann. Inst. Fourier (Grenoble)*, 25(2):127–169, 1975.

[7] G. Ritter. Unendliche Produkte unkorrelierter Funktionen auf kompakten abelschen Gruppen. *Math. Scand.*, 42:251–270, 1978.

[8] A.N. Shiryayev. *Probability*. Springer-Verlag, Berlin, Heidelberg, New York, London, Paris, Tokyo, Hong Kong, 1984.

IV

Stochastic calculus

Second order Hamilton-Jacobi equations in infinite dimensions and stochastic optimal control problems

P. Cannarsa
Dipartimento di Matematica
Università di Roma Tor Vergata
Via O. Raimondo
00173 Roma Italy
cannarsa@icnucevm.cnuce.cnr.it

G. Da Prato
Scuola Normale Superiore
Piazza dei Cavalieri 7
56126 Pisa Italy

Abstract Second order Hamilton-Jacobi equations in infinite dimensions are semilinear parabolic equations in which the unknown function $u(t,x)$ is defined for real t and x belonging to a Hilbert space X. Our presentation will focus on the relationship between such equations and stochastic optimal control of distributed parameter systems.

Perturbation methods can be used to study Hamilton-Jacobi equations. Such methods are based on a detailed analysis of the linearized problem, which is related to solutions of some stochastic partial differential equations. We will describe two different approaches to the linearized equation: one is based on the probabilistic representation formula for the solution, the other uses just functional analysis.

1. Finite dimensional optimal control

Let us consider a free terminal point problem of Mayer type. More precisely, one is given a complete separable metric space U (the *control space*) and a system $x(\cdot)$ governed by the *state equation*

$$\begin{cases} x'(t) = f(t, x(t), u(t)), & t_0 \leqslant t \leqslant T \\ x(t_0) = x_0 \in \mathbf{R}^n \end{cases} \tag{1.1}$$

Here u is a measurable map $u : [0,T] \to U$ (usually called a *control*) and $f : [0,T] \times \mathbf{R}^n \times U \to \mathbf{R}^n$ is a continuous vector field satisfying

$$\begin{cases} \|f(t,x,u)\| \leqslant C(1 + \|x\|) \\ \|f(t,x,u) - f(t,y,u)\| \leqslant C\|x - y\| \end{cases} \tag{1.2}$$

J. S. Byrnes et al. (eds.), Probabilistic and Stochastic Methods in Analysis, with Applications, 617–629.
© 1992 *Kluwer Academic Publishers. Printed in the Netherlands.*

for all $x, y \in R^N, t \in [0,T]$, and $u \in U$. Notice that, under the above assumptions, for any initial data $(t_0, x_0) \in [0,T] \times R^N$ and control u the state equation (1.1) has a unique solution $x(\cdot; t_0, x_0, u) \in C([0,T]; R^N)$.

Given a Lipschitz continuous function $g : R^n \to R$, our optimal control problem consists of

$$\text{minimizing } g(x(T; t_0, x_0, u)) \text{ over all controls } u. \tag{1.3}$$

A control $\bar{u}$ at which the minimum is attained is said to be an *optimal control* and the corresponding trajectory $x(\cdot)$ is called an *optimal trajectory*.

The ultimate goal of optimal control theory is to give conditions for optimality. The following is just an example of a result that states the existence of optimal controls (see for instance [11]).

Proposition 1.1. Assume (1.2) and suppose further that $f(t,x,U)$ is compact and convex for all $(t,x) \in [0,T] \times R^n$. Then, problem (1.1)–(1.3) has at least one optimal solution.

Let now f be differentiable with respect to x and g be differentiable. Fix a control $\bar{u}$ and set $\bar{x}(\cdot) = x(\cdot; t_0, x_0, \bar{u})$.

Definition 1.2. The adjoint state of the pair $\bar{u}, \bar{x}$ is the solution $\bar{p}$ of the adjoint system

$$\begin{cases} -pU(t) = [D_x f(t, \bar{x}(t), \bar{u}(t))]^* p(t) \\ -p(T) = Dg(\bar{x}(T)) \end{cases}$$

A useful tool in the construction of optimal trajectories is the *value function* defined as

$$V(t_0, x_0) = \inf \{ g(x(T; t_0, x_0, u)) \mid u : [0,T] \to U \text{ measurable} \}$$

Under assumptions (1.2), it is easy to see that V is Lipschitz continuous in $[0,T] \times R^n$. However, V is not differentiable in general (see, e.g., [11]).

For any $(t,x,p) \in [0,T] \times R^n \times R^n$ let us set

$$H(t,x,p) = \sup_{u \in U} p \cdot f(t,x,u). \tag{1.4}$$

Proposition 1.3. Assume (1.2) and suppose further that f be differentiable with respect to x and g be differentiable. Let $\{\bar{u}, \bar{x}\}$ be a control-trajectory pair, and let $\bar{p}$ be the corresponding adjoint state. Then, $\bar{u}$ is optimal if and only if

$$\bar{p}(t) \cdot f(t, \bar{x}(t), \bar{u}(t)) = H(t, \bar{x}(t), \bar{p}(t)) \tag{1.5}$$

and[2]

$$(H(t,\bar{x}(t),\bar{p}(t)),-\bar{p}(t)) \in D^+V(t,\bar{x}(t)) \tag{1.6}$$

for a.e. $t \in [t_0, T]$.

Equation (1.5) above is the well-known Pontryagin Maximum Principle (see, e.g., [11]). The inclusion (1.6) is the result of the work of several authors (see, e.g., [4] and the references cited therein).

The above proposition explains the importance of the value function, as noted first by Bellmann who established the so-called dynamic programming approach to optimal control. This approach tries to characterize the value function without computing the infimum in its definition and then derives information on optimal controls and optimal trajectories using, e.g., (1.6). The independent characterization of the value function is usually provided by the Hamilton-Jacobi-Bellmann equation

$$-v_t + H(t,x,-D_x v) = 0, \tag{1.7}$$

which V satisfies for a.e. $(t,x) \in [0,T] \times R^n$. Equation (1.7), however, has no classical solutions, in general, and indeed we have already noted that V can fail to be differentiable. On the other hand, the Cauchy problem consisting of (1.7) and the terminal condition

$$v(T,x) = g(x) \tag{1.8}$$

has nonunique solutions in the class of Lipschitz continuous functions. The problem of finding a suitable class of weak solutions to (1.7)–(1.8), in which one has both existence and uniqueness of solutions, has been solved by Crandall and Lions in [7] by considering the so-called *viscosity solutions*.

In order to give the definition of these solutions, let us introduce first the super- and subdifferential of a given function. Let $\Omega \subset R^N$ be an open domain, $x_0 \in \Omega$ and $\varphi : \Omega \to R$.

Definition 1.4. The (possibly empty) sets

$$D^+\varphi(x_0) = \left\{ p \in R^N \mid \limsup_{x \to x_0} \frac{\varphi(x) - \varphi(x_0) - p \cdot (x - x_0)}{|x - x_0|} \leqslant 0 \right\}$$

$$D^-\varphi(x_0) = \left\{ p \in R^N \mid \liminf_{x \to x_0} \frac{\varphi(x) - \varphi(x_0) - p \cdot (x - x_0)}{|x - x_0|} \geqslant 0 \right\}$$

are called, respectively, the *superdifferential* and the *subdifferential* of φ at x_0.

The following is one of the possible definitions of viscosity solution, see [6].

[2] This set denotes the superdifferential defined below, see Definition 1.4.

Definition 1.5. A function $v \in C(]0,T[\times R^n)$ is said to be a viscosity solution of (1.7) if, for all $(t,x) \in]0,T[\times R^n$,

$$-p_t + H(t,x,-p_x) \leqslant 0 \qquad \forall (p_t,p_x) \in D^+ v(t,x)$$
$$-p_t + H(t,x,-p_x) \geqslant 0 \qquad \forall (p_t,p_x) \in D^- v(t,x).$$

The following result is proved in [6].

Proposition 1.6. Assume (1.2) and define H as in (1.4). Then, the terminal value problem (1.7)–(1.8) has a unique viscosity solution $v \in C([0,T] \times R^n)$. Moreover, v coincides with the value function V of problem (1.1)–(1.3).

2. Control of distributed parameter systems

In order to motivate the analysis of infinite dimensional systems, let us discuss the following example.

Example 2.1. Let $\Omega \subset R^N$ be an open bounded domain, $\xi \in \Omega$, and fix $x_0 \in L^2(\Omega)$. Let $\phi : R \to R$ be a given Lipschitz function.

For any $u \in L^\infty([t_0,T] \times \Omega)$ we denote by $x(t,\xi;t_0,x_0,u)$ the solution of the parabolic equation

$$\begin{cases} x_t(t,\xi) = \Delta_\xi x(t,\xi) + u(t,\xi) \text{ in }]t_0,T] \times \Omega \\ x(t,\xi) = 0 \text{ on }]t_0,T] \times \partial\Omega \\ x(t_0,\xi) = x_0(\xi) \end{cases} \tag{2.1}$$

Given $M > 0$, the problem of minimizing $\int_\Omega \phi(x(T,\xi;t_0,x_0,u))d\xi$ over all controls $u \in L^\infty([t_0,T] \times \Omega)$ satisfying $|u(t,\xi)| \leqslant M$, is an infinite-dimensional equivalent of the Mayer problem (1.1)–(1.3). A more realistic situation than the one described in (2.1), occurs when the control is concentrated at the boundary of the domain, i.e., enters the state equation as a boundary data of Dirichlet (resp. Neumann) type as follows:

$$\begin{cases} x_t(t,\xi) = \Delta_\xi x(t,\xi) \text{ in }]t_0,T] \times \Omega \\ x(t,\xi) = u(t,\xi) (\text{resp. } \frac{\partial x}{\partial \nu}(t,\xi) = u(t,\xi)) \text{on}]t_0,T] \times \partial\Omega \\ x(t_0,\xi) = x_0(\xi) \end{cases} \tag{2.2}$$

Boundary control problems can be also given an abstract formulation as we will see below.

Let the state space be a separable Hilbert space X, with scalar product $\langle \cdot,\cdot \rangle$ and norm $\| \cdot \|$, and let the control space be a complete separable metric space U.

Let $A : D(A) \subset X \to X$ be the generator of a strongly continuous semigroup of bounded linear operators on X, that will be denoted by e^{tA}, $t \geqslant 0$, with $\|e^{tA}x\| \leqslant \|x\|, \forall x \in X$. By the Hille-Yosida Theorem this assumption

is equivalent to requiring that A be a densely defined closed linear operator, whose resolvent set contains the positive real axis, satisfying $\|(\lambda - A)^{-1}x\| \leqslant \frac{1}{\lambda}\|x\|, \forall \lambda > 0, \forall x \in X$.

Let $f : [0, T] \times X \times U \to X$ be a continuous map satisfying the following assumptions, that are the analogue of (1.2):

$$\begin{cases} \|f(t,x,u)\| \leqslant C(1 + \|x\|) \\ \|f(t,x,u) - f(t,y,u)\| \leqslant C\|x - y\| \end{cases} \tag{2.3}$$

for all $x, y \in X, t \in [0, T]$, and $u \in U$.

Under the above assumptions, for any $x_0 \in X$ and measurable map $u : [0, T] \to X$, the state equation

$$\begin{cases} x'(t) = Ax(t) + f(t, x(t), u(t)), \qquad t_0 \leqslant t \leqslant T \\ x(t_0) = x_0 \end{cases} \tag{2.4}$$

has a unique *mild* solution $x(\cdot; t_0, x_0, u) \in C([0, T]; X)$, i.e.,

$$x(t) = e^{(t-t_0)A}x_0 + \int_{t_0}^{t} e^{(t-s)A} f(x(s), u(s))ds$$

for all $t \in [0, T]$.

Given a Lipschitz function $\varphi : X \to R$, we are interested in the problem of

$$\text{minimizing } \varphi(x(T; t_0, x_0, u)) \text{ over all controls } u. \tag{2.5}$$

Remark 2.2. Returning to the example above, it is easy to set problem (2.1) in the abstract framework (2.4) taking

$$\begin{cases} X = L^2(\Omega) \\ U = \{u \in L^\infty(\Omega) \mid |u(\xi)| \leqslant M, \xi \in \Omega \text{ a.e.}\} \\ f(t,x,u) = u \\ D(A) = H^2(\Omega) \cap H_0^1(\Omega), \qquad Ax(\xi) = \Delta x(\xi) \\ \varphi(x) = \int_\Omega \phi(x(\xi))d\xi. \end{cases}$$

The assumptions of the Hille-Yosida Theorem are easily checked since A is self-adjoint and dissipative (see, e.g., [17]).

The boundary control problem (2.2) in the Dirichlet case can also be given an abstract setup by choosing X, A, and φ as above and taking $U = \{u \in L^\infty(\partial\Omega) \mid |u(\xi)| \leqslant M, \xi \in \partial\Omega \text{ a.e.}\}$. The state equation is of the form (2.4) with a *discontinuous* f as follows:

$$\begin{cases} x'(t) = Ax(t) - ADu(t) \\ x(t_0) = x_0 \end{cases}$$

where $D : U \to X$ is the so-called Dirichlet map defined as

$$Du = w \Leftrightarrow \begin{cases} \Delta w = 0 & \text{in } \Omega \\ w = u & \text{on } \partial\Omega. \end{cases}$$

By similar methods one can also treat problem (2.2) in the Neumann case.

The value function of problem (2.4)–(2.5) is defined as

$$V(t_0, x_0) = \inf\{\varphi(x(T; t_0, x_0, u)) \mid u : [0, T] \to U \text{ measurable }\}.$$

for all $(t_0, x_0) \in [0, T] \times X$ and the corresponding Hamilton-Jacobi equation is the following

$$\begin{cases} -v_t + H(t, x, -D_x v) - \langle Ax, D_x v \rangle = 0, \\ v(T, x) = \varphi(x) \end{cases} \tag{2.6}$$

where

$$H(t, x, p) = \sup_{u \in U} \langle p, f(t, x, u) \rangle. \tag{2.7}$$

Comparing equation (2.6) with (1.7), it is easy to realize that it presents additional difficulties: indeed the term $\langle Ax, D_x v \rangle$ is discontinuous in X, as A is an unbounded operator. Nevertheless, after the pioneering work [1] concerning the linear-convex case, several results have been obtained to extend the viscosity solution approach to infinite dimensions, see [7, 13, 18]. The Hamilton-Jacobi equation related to the boundary control problem (2.2) in the Neumann case is studied in [5].

3. Stochastic optimal control

Let now Q be a positive nuclear operator in X, so that there exists a complete orthonormal system in X, $\{e^k\}$, and a sequence of nonnegative real numbers, $\{\lambda_k\}$, such that

$$\begin{cases} \text{(i) } Qe^k = \lambda_k e^k, & k \in \mathbf{N} \\ \text{(ii) } \sum_{k=1}^{\infty} \lambda_k < \infty \end{cases} \tag{3.1}$$

Let $\{\Omega, \mathcal{F}, \mathbf{P}\}$ be a complete probability space and $W(t)$ a Q-Wiener process in X, i.e.,

$$W(t) = \sum_{k=1}^{\infty} \sqrt{\lambda_k}\beta_k(t)e^k, \tag{3.2}$$

where β_k are mutually independent standard Brownian motions.

For any $t \geqslant 0$ let $\mathcal{F}_t$ be the σ-algebra generated by $\{\beta_k(s) \mid k \geqslant 1, 0 \leqslant s \leqslant t\}$ and let $M_W^2(t_0, T; X)$ denote the space of the X-valued processes $x(\cdot)$ such that $x(t)$ is $\mathcal{F}_t$-measurable for all $t_0 \leqslant t \leqslant T$ and

$$\mathbf{E}\left(\int_{t_0}^{T} \|x(t)\|^2 dt\right) < \infty$$

where $\mathbf{E}$ denotes the expectation.

Under assumptions (2.3), for any $u \in M_W^2(t_0, T; X)$ the state equation

$$\begin{cases} dx(t) = [Ax(t) + f(t, x(t), u(t))]dt + dW(t), \quad t_0 \leqslant t \leqslant T \\ x(t_0) = x_0 \end{cases} \tag{3.3}$$

has a unique mild solution $x(\cdot; t_0, x_0, u)$, i.e.,

$$\begin{aligned} x(t) &= e^{(t-t_0)A}x_0 + \int_{t_0}^{t} e^{(t-s)A} f(x(s), u(s))ds + W_A(t), \\ W_A(t) &= \int_{t_0}^{t} e^{(t-s)A} dW(s). \end{aligned} \tag{3.4}$$

for all $t \in [0, T]$. Moreover, $x(\cdot; t_0, x_0, u)$ is continuous with probability one.

Remark 3.1. When $\{e^k\}$ are eigenvectors of A, i.e.,

$$e^k \in D(A), \quad Ae^k = -\alpha_k e^k, \qquad \alpha_k > 0,$$

the stochastic convolution can be expressed in the form

$$W_A(t) = \sum_{k=1}^{\infty} \sqrt{\lambda_k} e^k \int_{t_0}^{t} e^{-(t-s)\alpha_k} d\beta_k(s). \tag{3.5}$$

Notice that, in this case, operators Q and e^{tA} commute.

Given a Lipschitz function $\varphi : X \to R$, let us consider the problem of

$$\text{minimizing } \mathbf{E}[\varphi(x(T; t_0, x_0, u))] \text{ over all } u \in M_W^2(t_0, T; X) \tag{3.6}$$

in which, for simplicity, we have assumed the state space to coincide with the control space. The value function of problem (3.3)–(3.6) is defined, as usual, by

$$V(t_0, x_0) = \inf\{\mathbf{E}[\varphi(x(T; t_0, x_0, u))] \mid u \in M_W^2(t_0, T; X)\}.$$

The Hamilton-Jacobi equation related to the stochastic optimal control problem (3.3)-(3.6) is the following semilinear parabolic equation in infinitely many variables

$$\begin{cases} v_t + \frac{1}{2}\operatorname{Tr}(QD_x^2 v) + \langle Ax, D_x v\rangle - H(t, x, -D_x v) = 0, \\ v(T, x) = \varphi(x) \end{cases} \tag{3.7}$$

where Tr denotes the *trace*, $D_x^2 v$ the second derivative with respect to x (which is an operator in X) and H is still given by (2.7).

Remark 3.2. It is very interesting for applications to consider the case of a cylindrical Wiener process, i.e., of a process of the form (3.2) with $\lambda_k = 1, \forall k$ or, equivalently, $Q = I$. In this case, W is usually referred to as a *white noise*. Although W is not a Gaussian process in X, one can show that under suitable assumptions the convolution process W_A in (3.4) is Gaussian (see the next section).

In [3] the Hamilton-Jacobi equation (3.7) is studied by perturbation methods. For this purpose, it is essential to solve a linearized form of (3.7). While we refer the reader to [10] for a probability approach to linear equations, in the next section we will explain a different method just based on functional analysis. To simplify the exposition, we will describe this technique in the case of a nuclear Q. Different approaches to (3.7) are developed in [8, 12, 15], and [14].

4. A functional analysis approach

In this section we consider the problem

$$\begin{cases} v_t = \frac{1}{2}\,\mathrm{Tr}(QD_x^2 v) + \langle Ax, D_x v\rangle, \\ v(0,x) = \varphi(x) \end{cases} \tag{4.1}$$

where Q is a linear bounded self-adjoint operator in X satisfying (3.1) and A is the infinitesimal generator of a strongly continuous semi-group in X. We begin our analysis with the case of $A = 0$, i.e., with the infinite dimensional heat

$$\begin{cases} v_t = \frac{1}{2}\,\mathrm{Tr}(QD_x^2 v), \\ v(0,x) = \varphi(x) \end{cases} \tag{4.2}$$

We define $C_b(X)$ to be the Banach space of all functions $\varphi : X \to R$ which are uniformly continuous on X and such that

$$\|\varphi\|_0 = \sup_{x\in X} |\varphi(x)| < \infty.$$

For $k \in \mathbf{N}$, we denote by $C_b^k(X)$ the set of all functions $\varphi : X \to \mathbf{R}$ which are uniformly continuous and bounded on X, together with all their Fréchet derivatives up to the order k. We set

$$C_b^\infty(X) = \bigcap_{k=1}^{\infty} C_b^k(X).$$

It is well known that, if X is finite-dimensional, then all spaces $C_b^k(X), k = 1, 2, \ldots, \infty$, are dense in $C_b(X)$. If X is infinite-dimensional, on

the contrary, then the density of $C_b^k(X)$ in $C_b^0(X)$ fails to be true for $k \geqslant 2$, see [16, Section 7]. For this reason we introduce the space $\tilde{C}_b^0(X)$ to denote the closure of $C_b^\infty(X)$ in the topology of $C_b(X)$.

Let us define the operator Δ_Q by

$$\Delta_Q \varphi = \tfrac{1}{2} \operatorname{Tr}(QD_x^2\varphi), \qquad \forall \varphi \in C_b^2(X).$$

If we regard an element $\varphi \in C_b^2(X)$ as a function of infinitely many variables

$$\varphi(x) = \varphi(x_1, x_2, \ldots, x_n, \ldots), x_n = \langle x, e^n \rangle$$

then the operator Δ_Q may be represented as follows

$$\Delta\varphi = \frac{1}{2} \sum_{k=1}^{\infty} \lambda_k \frac{\partial^2 \varphi}{\partial x_k^2},$$

where $\frac{\partial \varphi}{\partial x_k} = \langle D_x \varphi, e^k \rangle$ and $\frac{\partial^2 \varphi}{\partial x_k^2} = \langle D_x^2 \varphi e^k, e^k \rangle$.

It is well known that if the dimension of X is finite, then the linear operator Δ_Q is not closed in $\tilde{C}_b^0(X)$. However, we have the following result proved in [2].

Theorem 4.1. The linear operator Δ_Q is closable and its closure is the generator of a strongly continuous semigroup of contractions $S_Q(\cdot)$ in $\tilde{C}_b^0(X)$.

Clearly, the semigroup S_Q provides a notion of solution to problem (4.2), which is classical for $\varphi \in C_b^2(X)$. Concerning the approximation of the semigroup S_Q by its finite-dimensional projections we have the following result. Let us introduce the heat semigroups in $\tilde{C}_b^0(X)$, with respect to the k^{th} component, which is defined as

$$(T_k(t)\varphi)(x) = \frac{1}{\sqrt{2\pi\lambda_k t}} \int_{-\infty}^{+\infty} e^{-\frac{(x_k - \xi)^2}{2\lambda_k t}} \varphi(x_1, \ldots, x_{k-1}, \xi, x_{k+1}, \ldots)\, d\xi,$$

$\forall x \in X$. It is easy to show that

$$\|T_k(t)\varphi\|_0 \leqslant \|\varphi\|_0. \tag{4.3}$$

Lemma 4.2. Assume (3.1), then the product $\prod_{k=1}^{n} T_k(t)\varphi$ converges in $\tilde{C}_b^0(X)$ as $n \to \infty$, for all $\varphi \in \tilde{C}_b^0(X)$, uniformly on the bounded sets of $[0, \infty[$. Moreover, the operator

$$S_Q(t)\varphi := \lim_{n \to \infty} \prod_{k=1}^{n} T_k(t)\varphi, \qquad \varphi \in \tilde{C}_b^0(X) \tag{4.4}$$

is a strongly continuous semigroup of contractions in $\tilde{C}_b^0(X)$. Furthermore, for any $k \in \mathbf{N}$, the semigroup $S_Q(t)$ maps $C_b^k(X)$ into itself, and the restriction of $S_Q(t)$ to $C_b^k(X)$ is again a strongly continuous semigroup of contractions.

Proof. We first consider $\varphi \in C_b^\infty(X)$. In this case we have

$$\begin{aligned}
&\left\| \prod_{k=1}^{n+1} T_k(t)\varphi - \prod_{k=1}^{n} T_k(t)\varphi \right\|_0 \\
&\leqslant \left\| \prod_{k=1}^{n} T_k(t) \right\|_{\mathcal{L}(C_b(X))} \|T_{n+1}(t)\varphi - \varphi\|_0 \\
&\leqslant \left\| \int_0^t \frac{\partial T_{n+1}(s)\varphi}{\partial t} ds \right\|_0 \leqslant \frac{\lambda_{n+1}}{2} \left\| \int_0^t \frac{\partial^2 T_{n+1}(s)\varphi}{\partial x_{n+1}^2} ds \right\|_0 \\
&\leqslant \frac{\lambda_{n+1}}{2} t \|\varphi\|_2.
\end{aligned}$$

Therefore, recalling that Q is nuclear, we conclude that $\{\prod_{k=1}^{n} T_k(t)\varphi\}_{n\in\mathbf{N}}$ is a Cauchy sequence for all $\varphi \in C_m^\infty(X)$. Since

$$\left\| \prod_{h=1}^{n} T_h(t) \right\|_{\mathcal{L}(C_b^0(X))} \leqslant 1$$

and $C_b^\infty(X)$ is dense in $\tilde{C}_b^0(X)$, the first part of the conclusion follows. The general case is easily checked. ∎

We now turn to the general equation (4.1). Let us first proceed formally, by assuming that $v(t,x)$ is a solution to (4.1). Setting

$$v(t,x) = u(t, e^{tA}x) \tag{4.5}$$

then

$$\begin{aligned}
&v_t(t,x) = u_t(t,e^{tA}x) + \langle Ae^{tA}x, D_x u(t,e^{tA}x)\rangle; \qquad x \in D(A) \\
&D_x v(t,x) = e^{tA^*} D_x u(t,e^{tA}x) \\
&D_x^2 v(t,x) = e^{tA^*} D_x^2 u(t,e^{tA}x) e^{tA}.
\end{aligned}$$

It follows that

$$u_t(t,e^{tA}x) = \frac{1}{2} \operatorname{Tr}\left[e^{tA} Q e^{tA^*} D_x^2 u(t,e^{tA}x)\right],$$

thus u is a solution of the problem

$$\begin{cases} u_t(t,x) = \frac{1}{2}\operatorname{Tr}[e^{tA}Qe^{tA^*}D_x^2 u(t,x)] & \text{in }]0,T] \times X \\ u(0,x) = \varphi(x), & \varphi \in \tilde{C}_b^0(X). \end{cases} \tag{4.6}$$

In the following, we will first solve (4.6) by using an abstract result [9], then we will show that formula (4.5) gives a solution of our problem.

We write problem (4.6) in abstract form in the Banach space $\mathcal{X} = \tilde{C}_b^0(X)$, as follows

$$\begin{cases} u'(t) = \overline{\Delta(t)}u(t) \\ u(0) = \varphi \end{cases} \tag{4.7}$$

where $\overline{\Delta(t)}$ is the closure of the operator

$$\Delta(t)\varphi = \frac{1}{2}\operatorname{Tr}(e^{tA}Qe^{tA^*}D_x^2\varphi); \qquad \forall \varphi \in C_b^2(X),\ t \in [0,T] \tag{4.8}$$

By Theorem 2.1, $\overline{\Delta(t)}$ is the generator of a strongly continuous semigroup in $\mathcal{X}$. More generally, we consider the problem

$$\begin{cases} u'(t) = \overline{\Delta(t)}u(t) + f(t) \\ u(0) = \varphi \end{cases} \tag{4.9}$$

where $f \in L^p(0,T;\mathcal{X}), p \geq 1$. We recall that $u \in L^p(0,T;\mathcal{X})$ is a strong solution of (4.9) if there exists a sequence u_n in $W^{1,p}(0,T;\mathcal{X})$ such that

1) $u_n \to v$ in $C([0,T];\mathcal{X})$
2) $u_n'(\cdot) - \overline{\Delta(\cdot)}u_n \to f(\cdot)$ in $L^p(0,T;\mathcal{X})$
3) $u_n(0) \to \varphi$ in $\mathcal{X}$

Moreover, u is a *strict* solution of (4.9) if

1) $u \in W^{1,p}(0,T;\mathcal{X})$,
2) $u(t) \in D(\overline{\Delta(t)})$ for a.e. $t \in [0,T]$ and $\overline{\Delta(\cdot)}u(\cdot) \in L^p(0,T;\mathcal{X})$,
3) problem (4.9) is fulfilled.

The following result is a special case of Theorem 3 in [9].

Proposition 4.3. *Let $\mathcal{X}, \mathcal{Y}$ be Banach spaces with $\mathcal{Y} \subset \mathcal{X}$ continuously and densely. Let $\{\mathcal{A}(t)\}_{t\in[0,T]}$ be a family of linear operators in $\mathcal{X}$ such that*

1) *$\mathcal{A}(t)$ is a generator of a strongly continuous semigroup in $\mathcal{X}$, with*
$$\|e^{s\mathcal{A}(t)}\|_{\mathcal{L}(X)} \leq e^{\omega_1 t}$$
2) *$Y \subset D(\mathcal{A}^2(t))$ for all $t \in [0,T]$*
3) *$\mathcal{A}(\cdot)y \in C([0,T];\mathcal{X})$, for all $y \in \mathcal{Y}$*
4) *The part $\mathcal{A}_y(t)$ of $\mathcal{A}(t)$ in $\mathcal{Y}$ is the generator of a contraction semigroup in $\mathcal{Y}$ with*
$$\|e^{s\mathcal{A}(t)}\|_{\mathcal{L}(Y)} \leq e^{\omega_y t}.$$

Then, $\forall x \in \mathcal{X}, \forall f \in L^p(0,T;\mathcal{X}), p \leq 1$, problem (4.9) has a unique strong solution u. Moreover, $u \in C([0,T];\mathcal{X})$ and there exists a constant $K > 0$, depending only on $\omega_{\mathcal{X}}$ and $\omega_{\mathcal{Y}}$ such that

$$|v(t)| \leq K\{\|\varphi\|_{\mathcal{X}} + \|f\|_{L^p(0,T;\mathcal{X})}\} \tag{4.10}$$

We now solve problem (4.6). By a strong solution of (4.6) we mean a strong solution of (4.7) in $L^p(0,T;\mathcal{X})$, $\forall p \geqslant 1$. For the following result see [2].

Proposition 4.4. Assume (3.1) and (2.3) and let $\varphi \in \tilde{C}_b^0(X)$. Then problem (4.6) has a unique strong solution u which, in addition, belongs to $C([0,T];\tilde{C}_b^0(X))$. Moreover, if $\varphi \in C_b^2(X)$ then $u \in C^1([0,T];\tilde{C}_b^0(X)) \cap C([0,T];C_b^2(X))$, and equation (4.6) is fulfilled. Furthermore, there exists a constant C, depending only on ω_X and ω_Y such that

$$\|u'(t,\cdot)\|_0 + \|v(u,\cdot)\|_2 \leqslant C\|\varphi\|_2 \tag{4.11}$$

for all $t \in [0,T]$.

5. Bibliography

[1] V. Barbu and G. da Prato. *Hamilton-Jacobi equations in Hilbert spaces.* Pitman, Boston, 1982.

[2] P. Cannarsa and G. da Prato. On a functional analysis approach to parabolic equations in infinite dimensions. Preprint.

[3] P. Cannarsa and G. da Prato. Second-order Hamilton-Jacobi equations in infinite dimensions. *SIAM J. Control Optim.*, 29:474–492, 1991.

[4] P. Cannarsa and H. Frankowska. Some characterizations of optimal trajectories in control theory. *SIAM J. Control Optim.* To appear.

[5] P. Cannarsa, F. Gozzi, and H.M. Soner. A dynamic programming approach to nonlinear boundary control problems of parabolic type. Preprint.

[6] M.G. Crandall, L.C. Evans, and P.L. Lions. Some properties of viscosity solutions of Hamilton-Jacobi equations. *Trans. Amer. Math. Soc.*, 282:487–502, 1984.

[7] M.G. Crandall and P.L. Lions. Viscosity solutions of Hamilton-Jacobi equations. *Trans. Amer. Math. Soc.*, 277:1–42, 1983.

[8] G. da Prato. Some results on Bellman equations in Hilbert spaces. *SIAM J. Control Optim.*, 23:61–71, 1985.

[9] G. da Prato and M. Iannelli. On a method for studying abstract evolution equation in the hyperbolic case. *Comm. in Partial Differential Equations*, 1:586–608, 1976.

[10] G. da Prato and J. Zabczyk. Smoothing properties of the Kolmogoroff semigroups in Hilbert spaces. *Stochastic Systems and Appl.* To appear.

[11] W.H. Fleming and R.W. Rishel. *Deterministic and stochastic optimal control.* Springer-Verlag, Berlin, Heidelberg, New York, London, Paris, Tokyo, Hong Kong, 1975.

[12] T. Havârneanu. Existence for the dynamic programming equation of control diffusion processes in Hilbert space. *Nonlinear Anal., Theory, Methods and Applications*, 9:619–629, 1985.

[13] H. Ishii. Viscosity solutions for a class of Hamilton-Jacobi equations in Hilbert spaces. Preprint.

[14] H. Ishii. Viscosity solutions of nonlinear second-order partial differential equations in Hilbert spaces. Preprint.

[15] P.L. Lions. Viscosity solutions of fully nonlinear second-order equations and optimal stochastic control in infinite dimensions. Part III: Uniqueness of viscosity solutions for general second-order equations. *J. Functional Analysis*, 86:1–18, 1989.

[16] A.S. Nemirovski and S.M. Semenov. The polynomial approximation of functions in Hilbert spaces. *Math. USSR Sbornik*, 92:257–281.

[17] A. Pazy. *Semigroups of Linear Operators and Applications to Partial Differential Equations.* Springer-Verlag, Berlin, Heidelberg, New York, London, Paris, Tokyo, Hong Kong, 1983.

[18] D. Tataru. Viscosity solutions of Hamilton-Jacobi equations with unbounded nonlinear terms. *J. Math. Appl. Anal.* To appear.

Nuclear space-valued stochastic differential equations with applications†

Gopinath Kallianpur
Center for Stochastic Processes
Department of Statistics
University of North Carolina at Chapel Hill
Chapel Hill, NC 27599-3260 USA
Also at Prometheus Inc.

Abstract Stochastic differential equations governing processes taking values either in Hilbert spaces or in duals of nuclear spaces arise in studying stochastic models of the behavior of voltage potentials of spatially extended neurons. A brief survey of the theory developed so far will be given in as self-contained a manner as possible. The asymptotic behavior of large systems of interacting neurons will also be considered.

1. Introduction

In this article, my aim is to present a brief survey of recent advances in infinite dimensional stochastic differential equations (SDE's). I shall naturally be concerned with the work that a number of my colleagues and students of mine and I have been doing over the last several years. The work originated in attempts to find suitable SDE models to describe the space-time fluctuation of voltage potentials of spatially extended neurons. The idea of finding stochastic partial differential equations (SPDE's) sprang from the efforts to introduce randomness into the Hodgkin-Huxley theory in which a system of nonlinear partial differential equations (PDE's) plays a fundamental role in this part of neurophysiology. Our work led us to investigate both linear and certain types of nonlinear SDE's governing stochastic processes taking values in a particular type of infinite dimensional space, namely, the dual of a nuclear space.

A brief account of the principal results will be presented in which the emphasis will be rather on the manner in which the problems are formulated and the SDE's derived than on the proofs. The reader interested in the latter

† This research was supported by the Air Force Office of Scientific Research Contract No. F-90-0030.

J. S. Byrnes et al. (eds.), Probabilistic and Stochastic Methods in Analysis, with Applications, 631–647.
© 1992 *Kluwer Academic Publishers. Printed in the Netherlands.*

will find them in the cited papers which have either been already published or are being prepared for publication.

As a result of this preoccupation with nuclear space-valued SDE's several important developments will not be discussed, notably, measure-valued SDE's and especially, the Fleming-Viot model for population genetics and the theory of SDE's in Banach spaces (see [2, 9]) and [11]). Since my object is to give a basic introduction to these equations, it will take me too far afield to consider applications to chemical kinetics or to include recent work on interacting neuronal systems. The reader is referred to [10, 6] and [1] for an account of these developments.

In what follows (particularly in Sections 2 and 3) applications to neuronal cell behavior will be kept in mind. However, the SDE's presented here have applications to other areas such as chemical reaction diffusions, random strings and fluctuation limit theorems of interacting particle diffusions. The important problem of diffusion approximation is introduced in Section 4.

It is by now well-recognized in the neurophysiological literature that a neuron cell is spatially extended and hence a realistic mathematical description of neuronal activity would have to take into account synaptic inputs that occur randomly in time as well as randomly at different locations on the neuron's surface. If $\mathcal{X}$ denotes the cell membrane, the voltage potential associated with the neuron cell may be regarded as a random field, indexed both by time $t \geqslant 0$ and by location $x \in \mathcal{X}$. The importance of the study of the fluctuation of the voltage potential consists in the fact that information is transmitted through the changing amplitudes of the electric potential across the cell membrane.

Let $u(t, x)$ represent the difference of the voltage potential at time t and site x from the resting potential of about -60mV. The evolution of u can be ascribed to two causes:

1) Diffusion and leaks due essentially to "deterministic" causes. In the two examples of the next section, these will be represented by a PDE (suggested by core conductor theory) with Neumann or insulating boundary conditions. More generally (as is explained in Section 2) it is abstractly described by a Hilbert space $L^2(\mathcal{X}, \mu)$ and a semigroup defined on it possessing certain properties.
2) Random fluctuations: When a burst of neurotransmitter hits some place on the membrane, the potential will jump up or down by a random amount at a random time and location. It is reasonable to model this randomness by a Gaussian space-time process. Alternatively, since the arrivals of the impulses at distant locations or in disjoint time intervals are believed to be approximately independent, they may be modeled as a mixture of Poisson processes or as a generalized Poisson process.

These questions form the basis of the linear SDE's of the next section which, in turn, lead to more general classes of nuclear space-valued SDE's.

2. Linear SPDE's

It is convenient to begin with the following class of examples. Consider the cable equation

$$\frac{\partial u}{\partial t} = -\alpha u + \beta \frac{\partial^2 u}{\partial x^2} \qquad t > 0, 0 < x < b \tag{2.1}$$

$$u(0, x) = u_0(x) \tag{2.2}$$

where α, β are positive constants and the initial value is a smooth function u_0 on $[0, b]$. (2.1) is the PDE that governs $u(t, x)$, the value of the membrane potential (more precisely, the difference between the membrane potential and the resting potential) in the absence of external impulses. One way to convert (2.1) into a model that permits randomness in the phenomenon being investigated is formally, to add Gaussian white noise in space time to get

$$\frac{\partial u}{\partial t} = -\alpha u + \beta \frac{\partial^2 u}{\partial x^2} + \dot{W}_{tx}. \tag{2.3}$$

The new term $\dot{W}_{tx}$ is the fictitious derivative of the space-time Wiener process or Brownian sheet W_{tx}. The latter (along with its variants) is an important and basic process in the theory of SPDE's. The spatial variable x can be n-dimensional. $W_{t,x_1,\ldots,x_n}$, $(t \geq 0, x_i \in [0, b], i = 1, \ldots, n)$ is a family of random variables defined on a probability space $(\Omega, \mathcal{F}, P)$, with the following properties:

(i): For every $(t, x_1, \ldots, x_n)$, $W_{t,x_1,\ldots,x_n}$ is a Gaussian random variable with mean 0 and covariance

(ii): $E(W_{t,x_1,\ldots,x_n} W_{s,y_1,\ldots,y_n}) = (t \wedge s)(x_1 \wedge y_1) \ldots (x_n \wedge y_n)$.

(iii): For each ω or P-a.e. ω in Ω, the paths $(t, x_1, \ldots, x_n) \to W_{t,x_1,\ldots,x_n}(\omega)$ are continuous.

It is well known that as a function of $(t, x_1, \ldots, x_n)$, the function in (iii) is almost nowhere differentiable. Hence (taking $n = 1$), (2.3) cannot be regarded as a PDE with a random term $\dot{W}_{tx}$ added on. A rigorous reformulation of (2.3) involves the extension to PDE's of Itô's theory of (ordinary) SDE's. Once this is done, the rich theory of stochastic calculus is available as a powerful apparatus for solving (2.3). (However, the fact that we are dealing with multiparameter processes or random fields and

partial differential operators imposes limitations on this approach, as we shall see below.)

Prior to rewriting (2.3) as an Itô type SPDE let us note that the Green function of the Neumann problem for ((2.1), (2.2)) is given by

$$G(x,y;t) = \sum_{n=0}^{\infty} e^{-\lambda_n t}\phi_n(x)\phi_n(y), (t>0) \tag{2.4}$$

where

$$\lambda_0 = \alpha, \lambda_n = \alpha + \beta(\frac{n\pi}{b})^2$$

for $n \geq 1$ and

$$\phi_0(x) = b^{-1/2},$$
$$\phi_n(x) = 2^{1/2}b^{-1/2}\cos\frac{n\pi x}{b} \qquad (n \geq 1).$$

For any $f \in H = L^2([0,b], dx)$ if we define

$$(T_t f)(x) = \int_0^b G(x,y;t)f(y)\,dy \qquad \text{for } t>0 \text{ and } T_0 = I, \tag{2.5}$$

it is easily verified that T_t is a contraction semigroup on H. The generator $-L$ has dense domain and agrees with $-\alpha I + \beta\frac{\partial^2}{\partial x^2}$ on smooth functions. L, of course, is a positive operator. (2.3) can be rewritten as

$$du(x,t;\omega) = -Lu(x,t;\omega)dt + dW_{tx}(\omega)$$

$$u(0,x,\omega) = u_0(x). \tag{2.6}$$

The above is an example of the Ornstein-Uhlenbeck (OU) SPDE. What we mean by a solution of this equation will be made clear in Section 3 where a general definition is given.

By substituting the expression for G into the RHS of

$$u(t,x,\omega) = \int_0^t G(x,y;t)u_0(x)u_0(x)\,dx + \int_0^t\int_0^b G(x,y;t-s)\,dW_{sy}(\omega), \tag{2.7}$$

it can be seen that (2.7) solves (2.6). The L.H.S. of (2.7) is an example of a Gaussian random field, i.e., a Gaussian process of the two parameters t and x. Various regularity properties of u can be derived (see [14]). In particular, $u(t,x,\omega)$ is, for almost all ω, a continuous function of (t,x). One may hence regard $u(t,\cdot,\omega)$ as a process depending on the single parameter

t and taking values in the Banach space $C[0,b]$. It is possible, but not particularly illuminating to look upon $u(t,\bullet)$ as the solution of an infinite dimensional SDE.

The situation changes radically when we go from one space dimension to two. The following example is due to J.B. Walsh [15]. Replace (2.3) by

$$\frac{\partial u(t;x,y)}{\partial t} = (\Delta u - u)(t;x,y) + \dot{W}_{txy} \tag{2.8}$$

with initial and boundary conditions

$$\frac{\partial u}{\partial x}(t;0,y) = \frac{\partial u}{\partial x}(t;\pi,y) = \frac{\partial u}{\partial y}(t,x,0) = \frac{\partial u}{\partial y}(t,x,\pi) = 0$$

and $u(0;x,y) = 0$ for all x and y. (Here, we have taken $b = \pi$ for convenience). As in the previous problem, we have a contraction semigroup T_t on $L^2([0,\pi]^2)$ with generator $-L$ which coincides with $\Delta - I$ on the smooth functions on $[0,\pi]^2$. The eigenfunctions and eigenvalues of L are $\phi_{jk}(x,y) = \phi_j(x)\phi_j(y)$ where $\phi_j(x)$ is the same as in the previous example (with $b = \pi$) and $\lambda_{jk} = 1 + j^2 + k^2$. The method for obtaining a random field solution to the corresponding SPDE fails because $\sum_{j,k} \frac{1}{\lambda_{jk}}$ diverges.

We shall return to this example later in this section.

Equations of the kind introduced above were studied in [7] as SDE's governing processes taking values in duals of nuclear spaces. The spaces which we will be chiefly concerned with will be denoted by Φ and Φ' where Φ is a countable Hilbertian nuclear space (CHNS) and Φ' is its topological dual. By a CHNS we mean a linear vector space whose topology is given by an increasing family of Hilbertian norms or seminorms $\|\cdot\|_r$ such that if Φ_r denotes the $\|\cdot\|_r$-completion of Φ, then

$$\Phi \subset \ldots \subset H_1 \subset H_0 = H_0' \subset H_{-1} \subset \ldots \subset \Phi'$$

and $\Phi = \bigcap_r \Phi_r$. Furthermore $r \leqslant s$ implies $\Phi_s \subseteq \Phi_r$. The property of nuclearity says that for every integer r, there exists $s > r$ such that the injection map from $\Phi_s \hookrightarrow \Phi_r$ is Hilbert-Schmidt.

A typical example of Φ is the space $\mathcal{S}(\mathbf{R}^d)$ of rapidly decreasing functions on $\mathbf{R}^d$. The dual Φ' then consists of the Schwarz distributions. In applications, duals of nuclear spaces other than Schwarz distributions are sometimes encountered. While most SPDE's or infinite dimensional SDE's have Gaussian white noise as the driving term, there are examples such as applications to fluctuations of the voltage potentials of cells of the central nervous system where it seems natural to assume that the random impulses arise from a Poisson random measure. This is the motivation for the definition of a Φ'-valued martingale. A Φ'-valued stochastic process $M_t(t \geqslant 0)$ is a martingale relative to a filtration $(\mathcal{F}_t)$ if for each $\varphi \in \Phi$, $M_t[\varphi]$ is a real-valued martingale.

For convenience, we will deal here only with square integrable martingales, i.e., such that $EM_t[\varphi]^2 < \infty$ for each φ. The reader will find properties of Φ'-valued martingales and the existence of a cadlag (= right continuous with left limits) version as well as properties of stochastic integrals w.r.t. (M_t) in [12], and [6].

An important example of a Φ'-valued martingale is the Wiener process W_t which is a Φ'-valued process such that $t \to W_t$ is continuous, $EW_t[\varphi] = 0$ and $EW_t[\varphi]W_s[\psi] = (t \wedge s)Q(\varphi, \psi)$ where $\varphi, \psi \in \Phi$ and Q is a bilinear form continuous on $\Phi \times \Phi$. Any such Wiener process actually lives in $C(\mathbf{R}_+, H_{-q})$ for some $q > 0$. An example of a discontinuous martingale defined by a Poisson random measure will be encountered in Section 3.

Definition 2.1 (Ornstein-Uhlenbeck Φ'-SDE's). The *SDE* is given by

$$d\xi_t = A(t)'\xi_t dt + dM_t \quad (t > 0) \tag{2.9}$$

$$\xi_0 = \eta \tag{2.10}$$

where

(i): $M = (M_t)_{t \in \mathbf{R}_+}$ is a Φ'-valued martingale,
(ii): η is a Φ'-valued random variable independent of M and
(iii): $A(t)$ is the generator of a Kolmogorov type evolution semigroup on Φ defined as follows: $\{S(s,t), 0 \leqslant s \leqslant t < \infty\}$ is a semigroup on Φ satisfying the conditions given below for each $T > 0$.

- **(a):** There exists $q_0 \geqslant 0$ such that for all $q \geqslant q_0$ $\| S(s,t)\varphi \|_q \leqslant \alpha_q e^{\sigma_q(t-s)} \| \varphi \|_q$, ($\varphi \in \Phi, \alpha_q, \sigma_q$ positive constants which, together with q_0 may depend on T).
- **(b):** $\frac{d}{dt} S(s,t)\varphi = S(s,t)A(t)\varphi$
- **(c):** $\frac{d}{ds} S(s,t)\varphi = -A(s)S(s,t)\varphi$ $(0 \leqslant s \leqslant t \leqslant T)$.
  $A'(t)$ is the adjoint of $A(t)$ defined by $(A'(t)u)[\varphi] = u[A(t)\varphi]$.

Theorem 2.2. [6] Let $M_0 = 0$ a.s. and $EM_t[\varphi]^2 < \infty$. Further, let $E\|\eta\|^2_{-r} < \infty$ for some $r > 0$. Then for each $T > 0$, there exists $p_T > 0$ such that $(\xi_t)_{0 \leqslant t \leqslant T} \in D([0,T], H_{-p_T})$ a.s. and

$$\xi_t[\varphi] = \eta[S(0,t)\varphi] + \sum_{j=1}^{\infty} \int_0^t \langle S(s,t)\varphi, \varphi_j \rangle_{p_T} dM[\varphi_j] \tag{2.11}$$

is the unique solution of (2.9)-(2.10). Here (φ_j) is a CONS in H_{p_T}.

Nuclear spaces Φ, Φ' occur in connection with a rigged Hilbert space. We are given a separable Hilbert space H, a CHNS Φ and its dual Φ' s.t.

$$\Phi \hookrightarrow H \hookrightarrow \Phi'$$

where the injection maps are continuous. H itself may or may not coincide with H_0.

In many practical problems (including the examples at the beginning of this section) one is given a Hilbert space (usually an L^2-space) and a continuous semigroup T_t on it which is naturally specified in the problem. The space Φ is not given in advance. For a wide class of problems, the generator $-L$ has the Hilbert-Schmidt property that $(I + L)^{-r_1}$ is a Hilbert-Schmidt operator on H for some $r_1 > 0$. A CHNS space Φ, appropriate to the problem can be constructed in the following manner. Let (φ_j) and (λ_j) be the eigenfunctions and eigenvalues respectively, of L. The Hilbert-Schmidt condition implies that (φ_j) is a CONS in H. Define

$$\Phi = \left\{ \varphi \in H : \sum_{j=1}^{\infty} (1 + \lambda_j)^{2r} (\varphi, \varphi_j)_H^2 < \infty \qquad \forall r \geqslant 0 \right\} \tag{2.12}$$

Let H_r be the completion of Φ under the Hilbertian norm $\| \varphi \|_r^2 = \sum_{j=1}^{\infty} (1 + \lambda_j)^{2r} (\varphi, \varphi_j)_H^2$. Then $\Phi = \bigcap H_r$ and $H_0 = H$. For any $r \geqslant 0$, the injection map $H_s \hookrightarrow H_r$ is Hilbert-Schmidt for $s > r + r_1$. We shall refer to (H, T_t, Φ) as a compatible family.

Suppose that W_t is a Φ'-valued Wiener process with covariance kernel Q and such that $W_\cdot \in C(\mathbf{R}_+, H_{-q})$. The next result is a useful special case of Theorem 2.2.

Theorem 2.3. Consider the Ornstein-Uhlenbeck SDE

$$d\xi_t = -L'\xi_t dt + dW_t, \tag{2.13}$$

$E \| \eta \|_{-r_2}^2 < \infty$ for some $r_2 > 0$, $\xi_0 = \eta$ where η is a Gaussian random variable independent of W. Then (2.13) has a unique solution $\xi_\cdot = (\xi_t)_{t \in \mathbf{R}}$, such that

$$\xi_\cdot \in C(\mathbf{R}_+, H_{-p}) \qquad \text{for } p \geqslant \max(q + r_1, r_2) \tag{2.14}$$

and is a Gaussian process;

$$\xi_t = \sum_{j=1}^{\infty} \xi_t^j \varphi_j, \tag{2.15}$$

the series converging uniformly a.s. in $0 \leqslant t \leqslant T$ in the H_{-p}-topology. The coefficient processes ξ_t^j are real-valued Ornstein-Uhlenbeck processes

satisfying $d\xi_t^j = -\lambda_j \xi_t^j dt + W_t^j, \xi_j^0 = \eta_j$ where $W_t^j = W_t[\varphi_j]$ and $\xi_t^j = \xi_t[\varphi_j]$. The coefficient processes are independent iff $Q(\varphi_i, \varphi_j) = \delta_{ij}$.

We shall now apply this theorem to complete the solution to Walsh's example. (In [15], the existence of a distribution value solution is discussed). Write $D = [0, \pi]^2$ and $H = L^2(D)$ with inner product denoted by $\langle\ ,\ \rangle_0$. With appropriate notational changes in our definition,

$$\| \varphi \|_r^2 = \sum_{j,k} (1 + \lambda_{jk})^{2r} \langle \varphi, \varphi_{jk} \rangle_0^2$$

and

$$\Phi = \{\varphi \in L^2(D) : \| \varphi \|_r < \infty \forall r \geq 0\}.$$

Φ is nuclear and can be identified with the space $\mathcal{D}(D)'$ of Schwarz distributions. The generator L satisfies the Hilbert-Schmidt condition with $r_1 > -\frac{1}{2}$ (the smallest integer r_1, therefore is 0). For $\varphi \in \Phi$, let $\dot{W}_t(\varphi) = \int\int_D \varphi(x, y) d_{xy} W_{txy}$. Then $\dot{W}_t(\varphi), \varphi \in \Phi$ is a Gaussian system of random variables with $E\dot{W}_t(\varphi) = 0$ and $E\dot{W}_t(\varphi)\dot{W}_s(\psi) = (t \bigwedge s)\langle \varphi, \psi \rangle_0$. $\dot{W}_t$ is thus not an $L^2(D)$-valued random variable but a cylindrical Brownian motion (c.B.m.) on $L^2(D)$. Now, $E\dot{W}_t(\varphi)^2 = t \| \varphi \|_0^2 \leq t \| \varphi \|_1^2$ and the injection map from $H_{-1} \hookrightarrow H_0$ is Hilbert-Schmidt. The latter follows from the fact that $\varphi_{jk}^{(1)} = (1 + \lambda_{jk})^{-1} \varphi_{jk}$ forms a CONS in H_1 and

$$\sum_{j,k} \| \varphi_{jk}^{(1)} \|_0^2 = \sum_{j,k} (1 + \lambda_{jk})^{-2} = \sum_{j,k} (1 + j^2 + k^2)^{-2} < \infty.$$

It then follows that there exists a Φ'-valued Wiener process W_t which actually lives in H_{-1} such that

$$EW_t[\varphi]W_s[\psi] = (t \bigwedge s)\langle \varphi, \psi \rangle_0.$$

We can now apply Theorem 2.3 to our example noting that $r_1 = 0, q = 1$ and $r_2 = 0$ since $\eta = 0$. Thus the SDE (2.13) which is a rigorous form of the SPDE (2.8) has a unique Gaussian solution $\xi_\cdot \in C(\mathbf{R}_+, H_{-1})$. In addition, the Ornstein-Uhlenbeck coefficient processes ξ_t^j in (2.15) are independent.

3. General Φ'-valued SDE's

Many physical problems often involve nonlinearities which require more realistic stochastic models than the linear SDE's considered so far. The Hodgkin-Huxley theory of neuronal behavior is a good example. Even a relatively simple stochastic description of the theory has to take into account some important nonlinear features such as the reversal (or equilibrium) potentials.

As an illustration, let us consider a "point" neuron, where the spatial extension of the neuron is ignored. The reversal potentials are simply two nonrandom constants, $V_e > 0$ and $V_i < 0$ which are introduced to control the behavior of the potential V_t (strictly speaking, V_t is the difference of the potential from some resting value), i.e., to prevent it from assuming two high a positive or negative value.

If $\gamma > 0$ denotes the rate at which the potential decays while in a quiescent state and if a_e and a_i are the magnitudes of the excitatory and inhibitory impulses arriving in independent Poisson processes N_e and N_i, then V_t satisfies the SDE

$$dV_t = -\gamma V_t dt + (V_e - V_t)a_e dN_e(t) + (V_i - V_t)a_i dN_i(t) \tag{3.1}$$

$$(V_0 = \text{given initial value}). \tag{3.2}$$

It has been shown that if a_e and a_i are small (which is the case in practice), under suitable conditions involving γ, a_e, a_i, f_e and f_i (the last two quantities denoting the respective intensities of N_e and N_i), the above SDE approximates a diffusion SDE. More precisely, if the solution of the n^{th} approximating equation is given by V_t^n, then for some sequence of constants c_n, δ_n, the discontinuous process $X_t^n = c_n(V_t^n - \delta_n)$ converges in distribution to the solution X_t of the diffusion equation

$$dX_t = -\beta X_t dt + \sigma(X_t)dW_t. \tag{3.3}$$

In (3.3), $\beta > 0$ is a constant, W is the standard, one-dimensional Wiener process and the diffusion coefficient σ is given by $\sigma^2(x) = \alpha_0 + \alpha_1 x + \alpha_2 x^2$ where the α's are certain real constants, with $\alpha_2 > 0$. The presence of the nonconstant diffusion coefficient makes X_t a non-Gaussian process and (3.3) a nonlinear SDE. For more details see [8] and the references therein.

The above discussion forms the motivation for the study of Φ'-valued diffusion SDE's and SDE's that generalize (3.1). The study of these equations, of course, has a much wider purpose. For both types of SDE's we make the basic assumption on Φ that there exists $(h_n) \in \Phi$ such that (h_n) is a CONS in H_0 and is a COS in each H_n.

Definition 3.1 (Poisson martingale driven SDE). Let $(U, \mathcal{U}, \mu)$ be a σ-finite measure space such that $L^2(U, \mu)$ is separable. Let $N(du ds)$ be a Poisson random measure on $\mathbf{R}_+ \times U$ with intensity measure $\mu(du)ds$ and its compensator $\tilde{N}(du\, ds) = N(du\, d) - \mu(du)ds$. The Φ'-valued SDE is given

by

$$dX_t = A(t, X_t)dt + \int_U G(t, X_{t-}, u)\tilde{N}(dudt), \tag{3.4}$$

$$X_0 = 0.$$

The coefficient processes A and G satisfy the conditions given below:

- $A : \mathbf{R}_+ \times \Phi' \to \Phi'$,
- $B : \mathbf{R}_+ \times \Phi' \to L(\Phi', \Phi')$, the family of continuous linear operators from Φ' to itself.
- For each $T > 0$, there exists $p_0 = p_0(T) \in \mathbf{N}^+$ such that for every $p \geq p_0$ there is a $q \geq p$ and a constant $K = K(p, q)$ such that for $t \in [0, T]$ and $u \in U$,

$$A(t, \cdot) : H_{-p} \to H_{-q}, \; G(t, \cdot, u) : H_{-p} \to H_{-p} \tag{3.5}$$

and for every $\varphi \in \Phi$,

$$A(t, \nu)[\varphi], \int_U |G(t, \nu, u)[\varphi]|^2 \mu(d\mu)$$

are continuous in $\nu \in H_{-p}$.

- (Coercivity) For $\varphi \in \Phi (\subset H_{-p})$

$$2A(t, \varphi)[\varphi] + \int_U \| G(t, \varphi, u) \|^2_{-p} \, \mu(du) \leq K(1 + \| \varphi \|^2_{-p}); \tag{3.6}$$

- (Growth) For $\nu \in H_{-p}$,

$$\| A(t, \nu) \|^2_{-q} + \int_U \| G(t, \nu, u) \|^2_{-p} \, \mu(du) \leq K(1 + \| \nu \|^2_{-p}). \tag{3.7}$$

Definition 3.2 (Solution). The notion of *solution* of an SPDE or a Φ'-valued SDE has to be clarified. For both the SDE (3.4) and the diffusion equation to be given below as well as for all SDE's we have two distinct definitions of solution. We give below the definitions for (3.4).

Definition 3.3 (Strong solution). Let a probability basis $(\Omega, (\mathcal{F}_t), \mathbf{P})(t \geq 0)$ satisfying the usual conditions be given and let N be a Poisson random measure adapted to the filtration $(\mathcal{F}_t)$ and with intensity measure $\mu(du)ds$. A

$(\mathcal{F}_t)$-adapted process $(X_t)_{0\leqslant t\leqslant T} \in D([0,T],\Phi')$ (Skorohod space) is a strong solution of (3.4) if for each $\varphi \in \Phi$,

$$X_t[\varphi] + \int_0^t A(s,X_s)[\varphi]ds + \int_0^t\int_U G(s,X_{s-},u)[\varphi]\tilde{N}(du\,ds). \tag{3.8}$$

We also assume that the Φ'-valued random variable X_0 satisfies

$$E \parallel X_0 \parallel^2_{-p} < \infty \qquad \text{for some } p. \tag{3.9}$$

(X_t) is said to be the unique strong solution if the following is true: If (Y_t) is another strong solution, then

$$P(X_t = Y_t \ \ \forall t \in [0,T]) = 1.$$

For most statistical purposes, the distributional properties of a solution are more relevant than the requirement that it be produced as a random function on an arbitrarily chosen probability space. This leads to the concept of a weak solution. A weak solution of an SPDE (or an infinite dimensional SDE) should not be confused with a weak or generalized solution of a PDE.

Definition 3.4 (Weak solution). By a weak solution of (3.4) we mean a Φ'-valued process (X_t) defined on some probability space $(\Omega,\mathcal{F},P)$ with a reference filtration $(\mathcal{F}_t)_{t\geqslant 0}$ such that

1) there exists an $(\mathcal{F}_t)$-adapted Poisson random measure N with intensity measure $\mu(du)ds$,
2) $(X_t)_{0\leqslant t\leqslant T} \in D([0,T],\Phi')$ and the map $\omega \mapsto X(t,\omega)$ is measurable with respect to the natural σ-fields provided in the problem;
3) (3.8) and (3.9) are satisfied.

Our aim in studying these nonlinear SDE's has been to concentrate on the weak solution. We have been able to obtain the existence of a weak solution under conditions which do not include the so-called monotonicity condition stated below. For $t \in [0,T], \nu_1, \nu_2 \in H_{-p}$,

$$2\langle A(t,\nu_1)-A(t,\nu_2),\nu_1-\nu_2\rangle_{-q} + \int_U \parallel G(t,\nu_1,u)-G(t,\nu_2,u) \parallel^2_{-q} \mu(du)$$
$$\leqslant K \parallel \nu_1 - \nu_2 \parallel^2_{-q}.$$

However, we can prove uniqueness only by assuming the monotonicity condition, in which case, the solution turns out also to be strong. The problem of proving uniqueness of weak solution without assuming the monotonicity condition is open. We will not discuss these questions further in this article.

Our main result concerning (3.4) is

Theorem 3.5. Under conditions (3.5)-(3.7) and (3.9), the equation (3.4) has a weak solution. Furthermore, there exists an integer p (possibly depending on T) such that $(X_t)_{0\leqslant t\leqslant T} \in D([0,T], H_{-p})$ a.s.

The proof of Theorem 3.5 and the existence of a weak solution in $D(\mathcal{R}_+, \Phi')$ for all $t > 0$ as well as other properties of these SDE's are given in a forthcoming paper [3].

Remark 3.6. In the SDE's (3.4) and (3.10) below it is tacitly assumed that the stochastic integrals

$$\int_0^t\int_{\mathbf{R}_+\times U} G(s, X_{s-}, u)\tilde{N}(du\, ds) \quad \text{and} \quad \int_0^t B(s, X_s)dW_s$$

are defined and belong to Φ'. A demonstration of this fact (as well as many other details in this exposition) would take up far too much space and is therefore omitted.

Definition 3.7 (Diffusion equation). The *diffusion equation* in Φ' is of the form

$$dX(t) = A(t, X_t)dt + B(t, X_t)dW_t, (t > 0)$$

$$X_0 \quad = \xi, \tag{3.10}$$

a Φ'-valued random variable independent of (W_t), a Wiener process which is a martingale with respect to the filtration $(\mathcal{F}_t)$ and has Q as its covariance kernel. We will not repeat here the definitions of weak and strong solution which, with appropriate changes, are the same as the ones given earlier for the discontinuous SDE.

The theory of equation (3.10) on the existence and uniqueness of solution has been worked out in detail in [5].

The drift coefficient A maps $\mathcal{R}_+ \times \Phi'$ into Φ' and the diffusion coefficient B (which is the new feature here) is operator-valued, i.e.,

$$B : \mathcal{R}_+ \times \Phi' \to L(\Phi', \Phi')$$

where L is the space of continuous linear mappings from Φ' to Φ'. Let $q > 0$ be such that $W \in C(\mathcal{R}_+, H_{-q})$. Then clearly $W_t \in H_{-r}$ for any $r \geqslant q$. In stating the conditions let us fix $r \geqslant q$. The quadratic form Q, defined on $\Phi \times \Phi$ then has a continuous extension to a nuclear form on $H_r \times H_r$. The finite quantity

$$|Q|_{-r,-r} = \sum_j Q[h_j^r, h_j^r]$$

is the trace norm of Q, (h_j^r) being a CONS in H_r. For any $A \in L(\Phi', \Phi')$ let $A^* \in L(\Phi, \Phi)$ be the usual adjoint of A. Denote the quadratic form $Q[A^*\varphi, A^*\psi]$ by $Q_A[\varphi, \psi]$.

The coercivity, growth and monotonicity conditions now take the following form. For each $T > 0$, and sufficiently large $m \geqslant r$, there exists a constant $\theta > 0$ and an index $p \geqslant m$ such that for $t \in [0, T]$,

(Coercivity) $2A(t, \varphi)[\varphi] + |Q_{B(t,\varphi)}|_{-m,-m} \leqslant \theta(1 + \| \varphi \|^2_{-m})$ for $\varphi \in \Phi (\subset H_{-m})$;

(Growth) If $u \in H_{-m}$ then $A(t, u) \subset H_{-p}$ and

$$\| A(t,u) \|^2_{-p} + |Q_{B_t(u)}|_{-m,-m} \leqslant \theta(1 + \| u \|^2_{-m})$$

(Monotonicity) For $u, v \in H_{-m} (\subset H_{-p})$

$$\langle A(t,u) - A(t,v), u - v \rangle_{-p} + |Q_{B_t(u)-B_t(v)}|_{-p,-p} \leqslant \theta \| u - v \|^2_{-p} .$$

In addition to the joint continuity of A and B it is further assumed that $B_t(u)v \in H_{-m}$ if $u, v \in H_{-m}$ and $Q[B_t^*(u)\varphi, B_t^*(u)\varphi]$ is continuous in $u \in \Phi'$ for each $\varphi \in \Phi$. The condition on the initial variable X_0 takes the form $E \| X_0 \|^{2+\delta}_{-m} < \infty$ for $\delta > 0$.

Theorem 3.8. Under the above conditions and a slightly weaker initial condition, it is shown in [5] that the SDE has a unique strong solution (X_t) which has the further property that $(X_t)_{0 \leqslant t \leqslant T} \in C([0, T], H_{-p})$.

Remark 3.9. In the case of both equations (3.4) and (3.10) we have obtained solutions over a finite interval $[0, T]$ and in this case, the paths lie in $D([0, T], H_{-p})$ and $C([0, T], H_{-p})$ respectively. H_{-p} is a much smaller space than Φ'. As we increase the time interval, the indices p increase to ∞ in general.

If we are interested in a solution to (3.10) for all $t \geqslant 0$, then using Theorem 3.8 with $T = 1, 2, \ldots$ and "pasting" together the solutions on $[0, n] (n = 1, 2, \ldots)$ we obtain the unique solution $X_\cdot = (X_t)_{0 \leqslant t < \infty}$ to (3.10) which has the property $X_\cdot \in C(\mathbf{R}_+, \Phi')$ a.s. It is not true in general, that there is an integer p such that $X_\cdot \in C(\mathbf{R}_+, H_{-p})$ a.s. An example, due to S. Ramaswamy and me is given in [4].

We might also mention here a technical advantage in working with the dual of a CHNS Φ rather than with a Hilbert or Banach space specified in advance in which the solution has to live. It is that Φ' belongs to a class of infinite dimensional linear topological spaces which have the property (possessed by finite dimensional Euclidean spaces) that bounded, closed subsets are compact. A paper of Mitoma's gives criteria for tightness of sequences of probability measures on Φ' that are easier to use than tightness conditions for Hilbert and Banach spaces [13].

4. Diffusion approximation [3]

Let

$$X_t^n = X_0^n + \int_0^t A^n(s, X_s^n)ds + \int_0^t \int_U G^n(s, X_{s-}^n, u)\tilde{N}(duds) \tag{4.1}$$

and let

$$\sup_{n \geq 1} E \parallel X_0^n \parallel_{-p}^2 < \infty \qquad \text{for some } p \tag{4.2}$$

Assume the same condition on (4.1) as in the previous section with the proviso that the constants appearing in the coercivity, growth and monotonicity conditions do not depend on n.

Proposition 4.1. Let $\{X_0^n\}$ be tight in H_{-p}. Then $\{X^n\}$ is tight in $\mathbf{D}([0,T], H_{-p})$.

Let Q be a continuous, quadratic form on Φ and let $A : \mathbf{R}_+ \times \Phi' \to \Phi'$, $B : \mathbf{R}_+ \times \Phi' \to L(\Phi', \Phi')$ satisfy the following conditions: For each $\varphi \in \Phi$, as $n \to \infty$

$$X_0^n \overset{D}{\Longrightarrow} X_0 \tag{4.3}$$

$$A^n(s,\nu)[\varphi] \to A(s,\nu)[\varphi], \tag{4.4.1}$$

and

$$\int_U G^n(s,\nu,u)[\varphi]^2 \mu^n(du) \to Q[B_s(\nu)^*\varphi, B_s^*(\nu)\varphi] \tag{4.4.2}$$

$$\int_U |G^n(s,\nu,u)[\varphi]|^3 \mu^n(du) \to 0, \tag{4.4.3}$$

uniformly in $(s,\nu) \in [0,T] \times A_M^p$ where $A_M^p = \{\nu \in H_{-p} : \parallel \nu \parallel_{-p} \leqslant M\}$.

$$\sup_n E \parallel X_0^n \parallel_{-p}^2 < \infty. \tag{4.5}$$

Under these conditions we have the following result.

Proposition 4.2. If P^* is a cluster point of P^n, the probability measure induced by X^n of Proposition 4.1 on $D([0,T], H_{-p})$, then

$$P^*(C([0,T], H_{-p})) = 1. \tag{4.6}$$

We now wish to relate P^* to the diffusion equation

$$dX_t = A(t, X_t)dt + B(t, X_t)dW_t \tag{4.7}$$

with initial condition X_0 independent of $W_\cdot$. Let $\mathcal{D}_0^\infty(\Phi') = \{F : \Phi' \to \mathbf{R}$, $F(\nu) = h(\nu[\phi])$ for $h \in C_0^\infty(\mathbf{R})$, and $\phi \in \Phi$. For $F \in \mathcal{D}_0^\infty(\Phi')$ define

$$\mathcal{L}_s F(\nu) = A(s,\nu)[\varphi]h'(\nu[\varphi]) + 1/2h''(\nu[\varphi])Q[B_s^*(\nu)\varphi, B_s^*(\nu)\varphi]$$

and let

$$M^F(Z)_t := F(Z_t) - F(Z_0) - \int_0^t \mathcal{L}_s F(Z_s)ds.$$

Denoting by $(\mathcal{B}_{t+})$ the canonical filtration in $D([0,T],H_{-p})$, we define a probability measure P on $(C([0,T],H_{-p}), \mathcal{B}_{t+} \cap C([0,T],H_{-p}))$ as a solution of the $\mathcal{L}$-martingale problem if for each $F \in \mathcal{D}_0^\infty(\Phi')$, $M^F(Z)_t$ is a P-martingale.

Our next proposition is:

Proposition 4.3. P^* is a solution of the $\mathcal{L}$-martingale problem.

To get our final result, we assume the monotonicity condition for A and B:

For all

$$\nu, \nu' \in H_{-p},\ t \in [0,T], \tag{4.8}$$

for some $q \geq p$ $\langle A_t(\nu) - A_t(\nu'), \nu - \nu' \rangle_{-q} + |Q_{B_t(\nu)-B_t(\nu')}|_{-q,-q} \leq K|\nu - \nu'|^2_{-q}$.

Theorem 4.4 (Diffusion approximation). Under the conditions of the preceding section on X_0^n, A^n and G^n and conditions (4.1) (4.8), we have that P^n converges weakly to P^* where P^* is the probability law of the unique strong solution of the diffusion SDE

$$dX_t = A(t,X_t)dt + B(t,X_t)dW_t \tag{4.9}$$

with X_0 independent of W where (W_t) is a Φ'-valued Wiener process with $EW_t[\varphi]W_s[\psi] = (t \wedge s)Q(\varphi,\psi)$.

Remark 4.5. Actually it can be shown that $(X_t)_{0 \leq t \leq T}$ lies in $C([0,T],H_{-r})$ a.s. where the index r will, in general, depend on T.

4.1. Application

We will give just one application of Theorem 4.4 to obtain the approximation of the Poisson Ornstein-Uhlenbeck S.D.E. to the usual (i.e., Wiener) Ornstein-Uhlenbeck SDE. (see [7]). As before, let $-L$ be the generator of the semigroup T_t on $H = L^2(\mathcal{X})$ (where (H, T_t, Φ) is a compatible family). The Poisson Ornstein-Uhlenbeck SDE's are given by

$$\xi_t^n = \xi_0^n - \int_0^t L'\xi_s^n ds + X_t^n$$

where

$$X_t^n[\varphi] = tm^n[\varphi] + \int_0^t \int_{\mathcal{R}\times\mathcal{X}} a\varphi(x)\{N^n(da\,dx\,ds) - \mu^n(da\,dx)\,ds\}$$
$$= tm^n[\varphi] + M_t^n[\varphi].$$

Then

$$\langle M^n[\varphi]\rangle_t = tQ^n(\varphi,\varphi)$$

where

$$Q^n(\varphi,\varphi) = \int_{\mathcal{R}\times\mathcal{X}} a^2\varphi(x)^2\mu^n(da\,dx).$$

Suppose the following conditions are satisfied.

- $m^n \in \Phi'$ and Q^n is continuous on $\Phi' \times \Phi'$;
- $\sup_n E \parallel \xi_0^n \parallel^2_{-r_2} < \infty$ and $\xi_0^n \overset{\mathcal{D}}{\Rightarrow} \xi_0$
- $m^n[\varphi] \to m[\varphi]$,
- $Q^n[\varphi,\psi]$ converges to a continuous limit $Q[\varphi,\psi]$,
- $\int_{\mathcal{R}_+\times\mathcal{X}} |a\varphi(x)|^3\mu^n(da\,dx) \to 0$.

Then the conditions of Theorem 4.4 hold and ξ^n converges weakly to ξ, the strong solution of $d\xi_t = -L'\xi_t\,dt + dW_t$, ($\xi_0$ initial value independent of W) where W is a H_{-r}-valued Wiener process with covariance kernel Q.

5. Bibliography

[1] T.S. Chiang, G. Kallianpur, and P. Sundar. Propagation of chaos and the McKean-Vlasov equation in duals of nuclear spaces. *Applied Mathematics and Optimization*, 24:55–83, 1991.

[2] W.H. Fleming and M. Viot. Some measure-valued Markov processes in population genetics theory. *Indiana Univ. Math. J.*, 30:925–935, 1981.

[3] G. Hardy, G. Kallianpur, S. Ramasubramanian, and J. Xiong. Nuclear space valued stochastic differential equations driven by poisson random measures. Submitted, 1991.

[4] G. Kallianpur. Infinite dimensional stochastic differential equations with applications. In *Proceedings of the 1989 COSMEX Meeting*, pages 227–238. World Scientific, 1990.

[5] G. Kallianpur, I. Mitoma, and R.L. Wolpert. Diffusion equations in duals of nuclear spaces. *Stochastics and Stochastic Reports*, 29:285–329, 1990.

[6] G. Kallianpur and V. Perez-Abreu. Stochastic evolution equations driven by nuclear space-valued martingales. *Applied Mathematics and Optimization*, 17:237–272, 1988.

[7] G. Kallianpur and R. Wolpert. Infinite dimensional stochastic differential equation models for spatially distributed neurons. *Applied Mathematics and Optimization*, 12:125–172, 1984.

[8] G. Kallianpur and R. Wolpert. Weak convergence of stochastic neuronal models. In M. Kimura, G. Kallianpur, and T. Hida, editors, *Lecture Notes in Biomathematics*, volume 70, pages 116–145. 1987.

[9] N. Konno and T. Shiga. Stochastic partial differential equations for some measure-valued diffusions. *Prob. Th. Rel. Fields*, 79:201–225, 1988.

[10] P. Kotelenez. Law of large numbers and central limit theorem for chemical reactions with diffusions. Technical report, U. Bremen, 1982.

[11] N.V. Krylov and B.L. Rozovskii. Stochastic evolution equations. *J. of Soviet Mathematics*, 16:1233–1277, 1981.

[12] I. Mitoma. Martingales of random distributions. *Mem. Fac. Sci. Kyushu Univ.*, 35:185–197, 1981.

[13] I. Mitoma. Tightness of probabilities on $C([0,1];S')$ and $D([0,1];S')$. *Annals of Probability*, 11:989–999, 1984.

[14] J.B. Walsh. A stochastic model of neural response. *Adv. Appl. Prob.*, 13:231–281, 1981.

[15] J.B. Walsh. An introduction to stochastic partial differential equations. In P.L. Hennequin, editor, *Lecture Notes in Mathematics*, volume 1180, pages 266–437. 1986.

A basic view of stochastic integration

Ron C. Blei
Department of Mathematics
University of Connecticut
Storrs, CT 06269 USA
blei@uconnvm.bitnet

Abstract. Outlined is a bi-measure theoretic framework, including the fundamental Grothendieck inequality and factorization theorem of which self-contained proofs are presented. Stochastic integrators have a natural description in this framework.

1. The problem of stochastic integration—a (biased) overview

Let $\Omega = (\Omega, \mathcal{U}, \mathbf{P})$ be a probability space and let

$$X = \{X_\omega(t) : \omega \in (\Omega, \mathcal{U}, \mathbf{P}), t \in [0,1]\}$$

be a stochastic process. We often encounter processes almost all of whose sample paths are of unbounded variation. This property, effectively conveying the non-deterministic nature of a stochastic model, naturally brings up the issue of stochastic integration. The basic question is this: given a real-valued process X almost all ($\mathbf{P}$) of whose sample paths $X(t)(t \in [0,1])$ are of unbounded variation, how can we make sense of an integral (a random variable on $(\Omega, \mathcal{U}, \mathbf{P})$)

$$\int F_\omega(t)dX_\omega(t) =: \int F(t)dX(t) \tag{1.1}$$

where $F_\omega(t)$ $(\omega \in \Omega, t \in [0,1])$ is a "random" function, and integration is performed over $[0,1]$?

The obvious difficulty is that for almost all $\omega, F_\omega(t)$ cannot be integrated against $dX_\omega(t)$ in the ordinary Riemann-Stieltjes sense. To negotiate this obstacle, one usually follows a functional analytic approach. We start with a *simple* function on $\Omega \times [0,1]$ (a *simple* process)

$$F_\omega(t) = \sum_i a_i \mathbf{1}_{A_i \times [s_i, t_i]}(\omega, t), \qquad A_i \in \mathcal{U}, 0 \leqslant s_i \leqslant t_i \leqslant 1, \tag{1.2}$$

J. S. Byrnes et al. (eds.), Probabilistic and Stochastic Methods in Analysis, with Applications, 649–662.
© 1992 *Kluwer Academic Publishers. Printed in the Netherlands.*

and define its integral with respect to X by

$$\int_0^1 F dX =: \sum_i a_i 1_{A_i}(X(t_i) - X(s_i)). \tag{1.3}$$

In order to obtain a larger class of integrands and a corresponding extension of (1.3), we

1) make some (reasonable) assumptions about X, and then
2) propose an appropriate metric on simple processes, convergence in which will imply convergence, in some sense, of the respective random variables in (1.3).

N. Wiener was first to integrate deterministic L^2-functions with respect to Brownian motion [21, 17]. K. Itô, a pioneer in the area of stochastic calculus, replaced the deterministic integrands in Wiener's integral with *random* functions (e.g., [9, 10]). Itô's construct, recast in a framework of martingales [6], has evolved into a stochastic integral where X is a *semimartingale* (=: martingale + a finite variation process) and the integrand is *predictable* (see [5, 12, 15, 19]).

To motivate our point of view, we note that the Itô integral is based on a crucial L^2-isometry between simple predictable processes (in (1.2) above, A_i is $X(s_i)$-measurable) and their respective stochastic integrals (e.g., [5], Theorem 2.3). In this sense, the summation method underlying the Itô integral is analogous to conditional summability of series. Integrals involving predictable processes and semimartingales are thus stochastic *Riemann-Stieltjes* integrals, inextricably linked to the idea of filtration. A hypothesis of increasing σ-fields is certainly natural when a stochastic model is indexed by *time*. In a general format, however, "filtrations" do not always play an obvious role—e.g., processes indexed by spatial parameters. In the specific context of stochastic integration, consider for example any L^2-bounded process with orthogonal increments; it need not be a semimartingale, but still qualifies as an integrator (see Example 5.2 in Section 5).

In this paper, which focuses on Item 1 above, stochastic integration is viewed on a primal level: a process X will be an *integrator* if bounded deterministic functions are integrable with respect to X (the notion of *integrability* will be made precise in due course). The idea of an integrator generalizes the role assigned to Brownian motion in the Wiener integral. Since deterministic functions are adapted to every filtration, a semimartingale [19] will *a fortiori* be an integrator in our sense. However, filtrations and related analysis of "time" do not have preassigned roles in our setting. Indeed, their absence at the outset facilitates constructions of *Lebesgue-Stieltjes* stochastic integrals (Item 2 above), which will be described in a later paper.

This article, which is an overview of three previous papers [2, 3, 4], outlines a format of bi-measure theory, including the fundamental Grothendieck

inequality and factorization theorem (Theorems 3.1 and 3.5 in Section 3). Stochastic integrators are then naturally viewed in this framework. Examples are described in the last section of the paper.

The next two questions of interest—how to deal with integrators in several parameters and how to deal with *random* integrands—will be discussed in subsequent work.

2. The framework

Let $(\mathcal{X},\mathcal{A})$ and $(\mathcal{Y},\mathcal{B})$ be measurable spaces. A $\mathbb{C}$-valued function μ on measurable rectangles in $\mathcal{X}\times\mathcal{Y}$ is a bimeasure if μ is $\mathbb{C}$-measure separately in each coordinate, i.e., for each $E\in\mathcal{A}$ and $F\in\mathcal{B}$, $\mu(E\times\cdot)$ and $\mu(\cdot\times F)$ are $\mathbb{C}$-measures on $(\mathcal{Y},\mathcal{B})$ and $(\mathcal{X},\mathcal{A})$, respectively. The term *bimeasure* originates in the works of Morse and Transue (e.g., [16]); in [1] we refer to these and more general set functions as Fréchet pseudomeasures. We proceed to catalogue below, without proofs, some basic facts regarding bimeasures.

1) The Fréchet variation of a bimeasure μ is defined as

$$\|\mu\| = \sup\left\{\left\|\sum_{i,j=1}^{N}\mu(E_i\times F_j)r_i\otimes r_j\right\|_\infty : \{E_i\}_i,\{F_j\}_j \right.$$
$$\left.\text{measurable partitions of } \mathcal{X} \text{ and } \mathcal{Y}, \text{ respectively, } N>0\right\}. \qquad (2.1)$$

In (2.1), $\{r_i\}_{i\in\mathfrak{N}}$ denotes the usual system of Rademacher functions on $[0,1]$, and $r_i\otimes r_j(s,t) = r_i(s)r_j(t), (s,t)\in[0,1]^2, (i,j)\in\mathfrak{N}^2$. The Rademacher system here is merely a convenient device generating arbitrary choices of signs: given any $\varepsilon_i = \pm 1, i\in\mathfrak{N}$, there is $t\in[0,1]$ so that $r_i(t) = \varepsilon_i, i\in\mathfrak{N}$. The starting point of multi-measure theory is the assertion: if μ is a bimeasure, then $\|\mu\|$ is finite. This statement, verified by applying the machinery of vector valued measures (e.g., [7], IV.10), is of course the two-dimensional extension of the statement that the total variation of every $\mathbb{C}$-measure is finite.

2) Let f and g be bounded measurable functions on $\mathcal{X}$ and $\mathcal{Y}$, respectively, and define $\mu_f(F) = \int_{\mathcal{X}} f(x)\mu(dx\times F)$, and $\mu_g(E) = \int_{\mathcal{Y}} g(y)\mu(E\times dy), E\in\mathcal{A}, F\in\mathcal{B}$. We deduce that μ_f and μ_g are $\mathbb{C}$-measures on $\mathcal{Y}$ and $\mathcal{X}$, respectively, and then define the integral of $f\otimes g$ with respect to μ by

$$\int_{\mathcal{X}\times\mathcal{Y}} f\otimes g\,d\mu = \int_{\mathcal{Y}} g(y)\mu_f(dy) = \int_{\mathcal{X}} f(x)\mu_g(dx). \qquad (2.2)$$

We have the following estimates:

$$\|\mu_f\|\le\|f\|_\infty\|\mu\|,\quad \|\mu_g\|\le\|g\|_\infty\|\mu\|, \qquad (2.3)$$
$$\left|\int_{\mathcal{X}\times\mathcal{Y}} f\otimes g\,d\mu\right|\le\|f\|_\infty\|g\|_\infty\|\mu\|.$$

3) The estimates in (2.3) easily imply that for all $\varepsilon > 0$ and all bounded measurable functions f and g on $\mathcal{X}$ and $\mathcal{Y}$, respectively, there are simple functions φ and ψ on $\mathcal{X}$ and $\mathcal{Y}$, respectively, so that

$$\left|\int_{\mathcal{X}\times\mathcal{Y}} f \otimes g \, d\mu - \int_{\mathcal{X}\times\mathcal{Y}} \varphi \otimes \psi \, d\mu\right| < \varepsilon. \tag{2.4}$$

3. Some basic tools (with proofs)

Theorem 3.1 (a version of Grothendieck's fundamental inequality [8]). Let $\mathcal{X}$ and $\mathcal{Y}$ be measurable spaces and let μ be a bimeasure on $\mathcal{X} \times \mathcal{Y}$. Let $\{f_k\}_{k\in\mathfrak{N}}$ and $\{g_k\}_{k\in\mathfrak{N}}$ be sequences of bounded measurable functions on $\mathcal{X}$ and $\mathcal{Y}$, respectively, satisfying

$$\left\|\sum_{k\in\mathfrak{N}} |f_k|^2\right\|_\infty < 1, \qquad \left\|\sum_{k\in\mathfrak{N}} |g_k|^2\right\|_\infty < 1. \tag{3.1}$$

Then

$$\sum_{k\in\mathfrak{N}} \left|\int_{\mathcal{X}\times\mathcal{Y}} f_k \otimes g_k \, d\mu\right| \leq K\|\mu\|, \tag{3.2}$$

where $K > 0$ is a universal constant.

Proof 3.2. Fix an arbitrary $\varepsilon > 0$. For each $k \in \mathfrak{N}$, choose simple functions φ_k on $\mathcal{X}$ and ψ_k on $\mathcal{Y}$ so that

$$\left|\int_{\mathcal{X}\times\mathcal{Y}} f_k \otimes g_k \, d\mu - \int_{\mathcal{X}\times\mathcal{Y}} \varphi_k \otimes \psi_k \, d\mu\right| < \varepsilon/2^k \tag{3.3}$$

and

$$\left\|\sum_{k\in\mathfrak{N}} |\varphi_k|^2\right\|_\infty < 1, \qquad \left\|\sum_{k\in\mathfrak{N}} |\psi_k|^2\right\|_\infty < 1. \tag{3.4}$$

To establish the theorem, it suffices to verify

$$\sum_{k\in\mathfrak{N}} \left|\int_{\mathcal{X}\times\mathcal{Y}} \varphi_k \otimes \psi_k \, d\mu\right| \leq K\|\mu\|. \tag{3.5}$$

But the implication (3.4) $\Rightarrow$ (3.5), in view of the definition of $\|\mu\|$, is equivalent to the usual formulation of the Grothendieck inequality (cf. [13]), which we state and prove below (the verification of the equivalence is a simple exercise in transcribing notation from one framework to another). ∎

Fact 3.3 (Grothendieck's inequality (the usual formulation)).
Let $(a_{mn})_{m,n\in\mathfrak{N}}$ be an array of complex scalars so that for all sequences of complex scalars $(s_m)_{m\in\mathfrak{N}}$ and $(t_m)_{m\in\mathfrak{N}}$ $(|s_m| \leqslant 1, |t_m| \leqslant 1, m \in \mathfrak{N})$,

$$\left|\sum_{m,n=1}^{N} a_{mn}s_m t_n\right| \leqslant 1 \qquad \text{for all } N > 0. \tag{3.6}$$

Then, for some universal constant $K > 0$ and for all $(\mathbf{x}_m)_{m\in\mathfrak{N}}$ and $(\mathbf{y}_n)_{n\in\mathfrak{N}}$, sequences of vectors in the unit sphere of l^2,

$$\left|\sum_{m,n=1}^{N} a_{m,n}\langle \mathbf{x}_m, \mathbf{y}_n\rangle\right| \leqslant K \qquad \text{for all } N > 0 \tag{3.7}$$

($\langle\ \rangle$ denotes the usual inner product in l^2).

Proof 3.4 (of the usual formulation of Grothendieck's inequality). We can assume that $\mathbf{x}_m$ and $\mathbf{y}_m$ are vectors with real-valued coordinates.

Step 1: $\left|\sum_{m,n=1}^{N} a_{mn}e^{i\langle \mathbf{x}_m, \mathbf{y}_n\rangle}\right| \leqslant e.$

Verification Let $(Z_k)_{k\in\mathfrak{N}}$ be a sequence of independent standard normal variables. We shall make use of the following identity (an exercise): let $\mathbf{x}$ and $\mathbf{y}$ be real vectors on the unit sphere of l^2, then

$$eEe^{i\Sigma x(k)Z_k}e^{-i\Sigma y(k)Z_k} = e^{\langle x,y\rangle}. \tag{3.8}$$

We estimate

$$\begin{aligned}
&\left|\sum_{m,n=1}^{N} a_{mn}e^{i\langle \mathbf{x}_m, \mathbf{y}_n\rangle}\right| \qquad (3.9)\\
&= e\left|\sum_{m,n=1}^{N} a_{mn}Ee^{i\Sigma x_m(k)Z_k}e^{-i\Sigma y_n(k)Z_k}\right| \qquad \text{by (3.8)}\\
&\leqslant eE\left|\sum_{m,n=1}^{N} a_{mn}e^{i\Sigma x_m(k)Z_k}e^{-i\Sigma y_n(k)Z_k}\right| \leqslant e \qquad \text{by (3.6).}
\end{aligned}$$

Step 2: There is a mapping Ψ from l^2 into l^2 so that

$$\langle \Psi(\mathbf{x}), (\mathbf{y})\rangle = \sum_{j=2}^{\infty} (\langle \mathbf{x}, \mathbf{y}\rangle)^j/j!, \tag{3.10}$$

and

$$\|\Psi(\mathbf{x})\|_2^2 = e^{\|\mathbf{x}\|_2^2} - \|\mathbf{x}\|_2^2 - 1, \qquad \mathbf{x} \in l^2. \tag{3.11}$$

Verification Merely observe that

$$(\langle \mathbf{x}, \mathbf{y} \rangle)^j = \sum_{k_1 \in \mathfrak{N}, \ldots, k_j \in \mathfrak{N}} \mathbf{x}(k_1) \cdots \mathbf{x}(k_j) \mathbf{y}(k_1) \cdots \mathbf{y} k_j)$$

and that

$$\sum_{k_1 \in \mathfrak{N}, \ldots, k_j \in \mathfrak{N}} |\mathbf{x}(k_1) \cdots \mathbf{x}(k_j)|^2 = (\|\mathbf{x}\|_2^2)^j.$$

Step 3: Let $b = (e-2)^{\frac{1}{2}}$, and define $\Psi_b(\mathbf{x}) = \Psi(\mathbf{x})/b$. Then, for all $\mathbf{x}$ and $\mathbf{y}$ in the unit sphere of l^2,

$$\langle \mathbf{x}, \mathbf{y} \rangle = \sum_{j=0}^{\infty} (-1)^j b^{2j} (e^{\langle \Phi_b^{\{j\}}(\mathbf{x}), \Phi_b^{\{j\}}(\mathbf{y}) \rangle} - 1) \tag{3.12}$$

($\Phi_b^{\{j\}}$ denotes the j-th iterate of Φ_b).

Verification Observe that Φ_b maps the unit sphere into itself. The iteration of the identity

$$\langle \mathbf{x}, \mathbf{y} \rangle = e^{\langle \mathbf{x}, \mathbf{y} \rangle} - 1 - b^2 \langle \Phi_b(\mathbf{x}), \Phi_b(\mathbf{y}) \rangle$$

implies (3.12).

Combining Step 1 and Step 3, we deduce (3.7) as follows:

$$\begin{aligned}
&\left| \sum_{m,n=1}^{N} a_{mn} \langle \mathbf{x}_m, \mathbf{y}_n \rangle \right| \\
&= \left| \sum_{m,n=1}^{N} a_{mn} \sum_{j=0}^{\infty} (-1)^j b^{2j} (e^{\langle \Phi_b^{\{j\}}(\mathbf{x}_n), \Phi_b^{\{j\}}(\mathbf{y}_m) \rangle} - 1) \right| \\
&\leqslant \sum_{j=0}^{\infty} b^{2j} \left| \sum_{m,n=1}^{N} a_{mn} (e^{\langle \Phi_b^{\{j\}}(\mathbf{x}_n), \Phi_b^{\{j\}}(\mathbf{y}_m) \rangle} - 1) \right| \\
&\leqslant (e+1)/(3-e).
\end{aligned}$$

The proof of Theorem 3.1 is complete. ∎

Theorem 3.5 (Grothendieck's Factorization Theorem, e.g., [18]). Let $\mathcal{X}$ be a locally compact Hausdorff space, and let $\mathcal{Y}$ be a measurable space. For every bimeasure μ on $\mathcal{X} \times \mathcal{Y}$ there is a probability measure ν on the Borel σ-field of $\mathcal{X}$ so that for all $f \in C_0(\mathcal{X})$ and $g \in L^\infty(\mathcal{Y})$ (=bounded measurable functions on $\mathcal{Y}$),

$$\left| \int_{\mathcal{X} \times \mathcal{Y}} f \otimes g \, d\mu \right| \leqslant K \|f\|_{L^2(\mathcal{X}, \nu)} \|g\|_\infty \|\mu\| \tag{3.13}$$

for some universal constant $K > 0$.

Proof 3.6. Consider the Banach space $C_0(\mathcal{X}) \times L^\infty(\mathcal{Y})$ normed by

$$\|(f,g)\| = \max\{\|f\|_\infty, \|g\|_\infty\}, f \in C_0(\mathcal{X}), g \in L^\infty(\mathcal{Y}).$$

Without loss of generality, assume that $\|\mu\| = 1$ and let K be the constant in Theorem 3.1 above. Let $\mathcal{W}$ be the set consisting of all elements $(f,g) \in C_0(\mathcal{X}) \times L^\infty(\mathcal{Y})$ which can be written as

$$(f,g) = \left(\sum_{k\in\mathfrak{N}} |f_k|^2, \sum_{k\in\mathfrak{N}} |g_k|^2\right),$$

so that

$$\sum_{k\in\mathfrak{N}} \left|\int_{\mathcal{X}\times\mathcal{Y}} f_k \otimes g_k d\mu\right| \leqslant K.$$

Theorem 3.1 implies the convex set $\mathcal{W}$ is disjoint from the open convex set

$$O = \{(f,g) \in C_0(\mathcal{X}) \times L^\infty(\mathcal{Y}) : \max\{\sup_{x\in\mathcal{X}} f(x), \sup_{y\in\mathcal{Y}} g(y)\} < 1\}.$$

Therefore, by the Hahn-Banach theorem, there is a bounded linear functional on $C_0(\mathcal{X}) \times L^\infty(\mathcal{Y})$ which "separates" O from $\mathcal{W}$. In particular (by the Riesz representation theorem) we obtain a regular Borel measure ν on $\mathcal{X}$ and a bounded linear functional γ on $L^\infty(\mathcal{Y})$ (a regular Borel measure on the maximal ideal space of $L^\infty(\mathcal{Y})$) so that

$$\int_{\mathcal{X}} f d\nu + \gamma(g) < 1 \qquad \text{for all } (f,g) \in O, \tag{3.14}$$

and

$$\int_{\mathcal{X}} f d\nu + \gamma(g) \geqslant 1 \qquad \text{for all } (f,g) \in \mathcal{W}. \tag{3.15}$$

Since O contains the cone for all "negative" elements as well as the open unit ball in $C_0(\mathcal{X}) \times L^\infty(\mathcal{Y})$, we deduce from (3.14) that ν and γ are positive measures and that $\|\nu\| + \|\gamma\| \leqslant 1$. Let $f \in C_0(\mathcal{X})$ and $g \in L^\infty(\mathcal{Y})$ be arbitrary, and assume that $\mu(f,g) = \int_{\mathcal{X}\times\mathcal{Y}} f \otimes g d\mu$ is nonzero. We have

$$(K/|\mu(f,g)|)(|f|^2, |g|^2) \in \mathcal{W},$$

and therefore, by (3.15),

$$|\mu(f,g)| \leqslant K\int_{\mathcal{X}} |f|^2 d\nu + \gamma(|g|^2). \tag{3.16}$$

Now define

$$F = \left((\gamma(|g|^2))^{\frac{1}{4}} / \left(\int_X |f|^2 d\nu \right)^{\frac{1}{4}} \right) f,$$

$$G = \left(\left(\int_X |f|^2 d\nu \right)^{\frac{1}{4}} / (\gamma(|g|^2))^{\frac{1}{4}} \right) g.$$

In (3.16), replace f by F and g by G, and thus obtain

$$\left| \int_{X \times Y} f \otimes g \, d\mu \right| \leq K \|f\|_{L^2(X,\nu)} (\gamma(|g|^2))^{\frac{1}{2}}. \tag{3.17}$$

Replace ν by $\nu/\|\nu\|$ (clearly, $\nu \neq 0$), and deduce (3.13). ∎

Remark 3.7. Grothendieck's fundamental inequality is a generalization of Littlewood's classical "mixed norm" inequality [14], and has enjoyed several proofs (e.g., [18]). The self-contained proof given here is a version of the proof in [2]; the novelty in the argument given above is Step Step 1.

The proof of Theorem 3.5 is a transcription of the proof of a more general statement [3], Theorem 3.2. It is an adaptation of the argument used to prove the Pietsch factorization theorem (cf. [13], Prop. 3.1).

4. Integrators

Let $X = \{X(t) : 0 \leq t \leq 1\}$ denote a $\mathfrak{R}$-valued stochastic process defined on a probability space $(\Omega, \mathcal{U}, \mathbf{P})$, and assume that $\mathbf{E}|X(0)| < \infty$. We norm X

$$\|X\| = \sup \left\{ \mathbf{E} \left| \sum_{j=1}^{N} \varepsilon_j \Delta X([t_{j-1}, t_j]) \right| : N > 0, \right.$$

$$\left. \varepsilon_j = \pm 1, 0 \leq t_{j-1} < t_j \leq 1, j = 1, \ldots, N \right\} \tag{4.1}$$

($\Delta X(I) =: X(b) - X(a)$ where I is an interval with end points $a \leq b$). Observe that for each $Y \in L^\infty(\Omega, \mathbf{P})$, the total variation of the function $\mathbf{E}YX(t)(t \in [0,1])$ is bounded by $\|Y\|_\infty \|X\|$. We shall call X an *integrator* if $\|X\| < \infty$. Indeed, define $F_X(A,t) = \mathbf{E}1_A X(t)$ and

$$\mu_X(A \times (s,t]) = F_X(A,t^+) - F_X(A,s^+), \qquad A \in \mathcal{U}, 0 \leq s < t \leq 1. \tag{4.2}$$

Observe that $\|X\| < \infty$ if and only if μ_X is a bimeasure on $\Omega \times [0,1]$, i.e., μ_X is a signed measure in the first coordinate and determines a Borel measure in the second. A statement equivalent to $\|X\| < \infty$ is that $X(1)$, the outcome at $t = 1$, does not depend on the way the "past" is arranged. To be precise,

let $\|X\| < \infty$, and assume without any loss of generality that $\lim_{t \to 1-} X(t) = X(1)$, (weak limit in $L^1(\Omega, \mathbf{P})$, i.e., $\lim_{t \to 1} \mathbf{E}1_A X(t) = \mathbf{E}1_A X(1)$ for all $A \in \mathcal{U}$). Let $t_0 = 0, t_j \uparrow 1$, and $I_j = (t_{j-1}, t_j]$. Then for all permutations τ of $\mathfrak{N}$,

$$X(1) - X(0) = \sum_{j=1}^{\infty} \Delta X(I_{\tau(j)}), \tag{4.3}$$

(weak convergence in $L^1(\Omega, \mathbf{P})$).

Theorem 4.1 (Interchangeability of stochastic increments). Suppose that $E|X(t)| < \infty$ for every $t \in [0, 1]$. Then, X is an integrator if and only if (4.3) holds for all $t_j \uparrow 1$ and all permutations τ of $\mathfrak{N}$.

If X is an integrator, then for every bounded measurable function f on $[0, 1]$, $\int_0^1 f(t)\mu_X(\cdot \times dt)$ is a signed measure on $(\Omega, \mathcal{U})$ which is absolutely continuous with respect to $\mathbf{P}$. We define

$$\int_0^1 f(t)dX(t) = \frac{d}{d\mathbf{P}} \left(\int_0^1 f(t)\mu_X(\cdot \times dt) \right) \tag{4.4}$$

(Radon-Nikodym derivative) and obtain

$$\mathbf{E}\left| \int_0^1 f(t)dX(t) \right| \leq \|f\|_\infty \|X\|. \tag{4.5}$$

The Grothendieck factorization theorem (Theorem 2 in Section 3) implies

Corollary to 4.1. Let X be a process with $\|X\| < \infty$. Then, there exists a probability measure ν on $[0, 1]$ so that for all $f \in L^2([0, 1], \nu)$, the stochastic integral $\int_0^1 f(t)dX(t)$, extending the definition in (4.4), is a well defined random variable in $L^1(\Omega, \mathbf{P})$, and

$$\mathbf{E}\left| \int_0^1 f(t)\, dX(t) \right| \leq K\|f\|_{L^2(\nu)}\|X\|. \tag{4.6}$$

(A probability measure ν for which (4.6) holds will be called a factorizing measure for X.)

In the case that μ_X is extendable to a signed measure on $\Omega \times [0, 1]$, stochastic integration of random integrands with respect to X proceeds in the usual framework of measure theory. In this case, ν of Corollary to 4.1 is of course the total variation measure $|\mu_X|$. Stochastic integration has a life of

its own precisely because in most cases μ_X is *not* extendable to a bona fide measure on $\Omega \times [0,1]$, i.e.,

$$\|X\|_{(\tau)} =: \sup\left\{\sum_{i,j} |\mu_X(A_i \times I_j)|;\ \Sigma \mathbf{1}_{A_i} \leqslant 1, \Sigma \mathbf{1}_{I_j} \leqslant 1\right\}$$

("total variation" of μ_X)

$$= \sup\left\{\sum_j E|\Delta X(I_j)| : \Sigma \mathbf{1}_{I_j} \leqslant 1\right\} = \infty. \tag{4.7}$$

A process X for which $\|X\| < \infty$ and $\|X\|_{(\tau)} = \infty$ will be called a *stochastic integrator.*

The Corollary to 4.1 implies a series representation of an integrator X. Let $\{\varphi_k\}_{k\in\mathfrak{N}}$ be an orthonormal basis of $L^2([0,1],\nu)$, define $\hat{X}(k) = \int_{[0,1]} \varphi_k dX$, and write

$$X \sim \sum_{k\in\mathfrak{N}} \hat{X}(k)\varphi_k. \tag{4.8}$$

Corollary to 4.1. For all $f = \Sigma \hat{f}(k)\varphi_k \in L^2([0,1],\nu)$

$$\int_{[0,1]} f dX = \lim_{N\to\infty} \sum_{k=1}^{N} \hat{f}(k)\hat{X}(k) \tag{4.9}$$

(weak convergence in $L^1(\Omega, \mathbf{P})$).

5. Some examples

Example 5.1. Let X be an L^2-bounded martingale process defined on $[0,1]$ and let $v(t) = E|X(t)|^2, (t \in [0,1])$. Then, X is an integrator with a factorizing measure dv (an application of Grothendieck's factorization theorem is not needed here). If X is a non-constant *continuous* L^2-bounded martingale, then the sample paths of X are almost surely of unbounded variation (cf. [19], Corollary 1, p. 64), implying in particular that X is a stochastic integrator.

Example 5.2. More generally, any L^2-bounded process with orthogonal increments is an integrator. In this general case, in contrast with the specific case of L^2-bounded martingales, a factorizing measure is produced by an application of the Grothendieck theorem. An L^2-bounded process X with orthogonal increments is a *stochastic* integrator if X has factorizing measure

ν which is absolutely continuous with respect to Lebesgue measure, and which satisfies

$$\mathbf{E}\left|\int_{[0,1]} f\,dX\right| \geqslant \kappa\|X\|\,\|f\|_{L^2(\nu)} \tag{5.1}$$

for all $f \in L^2([0,1],\nu)$ and some fixed constant $\kappa > 0$. A class of such processes is canonically produced as follows: Let $(\Omega,\mathbf{P}) = ([0,1]),dx)$ (dx = Lebesgue measure), and fix a set of "random variables" $\{\cos 2\pi nt\}_{n\in S}$ with the property that the L^1-closure and the L^2-closure of the span of $\{\cos 2\pi nt\}_{n\in S}$ are equal (sets S with this property are called $\Lambda(2)$-sets, e.g., [20]). Denote this closure by L^2_S. Fix any unitary equivalence U between $L^2([0,1],dx)$ and L^2_S, and define $X(t) = U1_{[0,t]}$. One now verifies that X is an integrator ($\int_{[0,1]} f dX = Uf, f \in L^2([0,1],dx)$), that Lebesgue measure is a factorizing measure for X, and that (5.1) is satisfied.

Example 5.3. Any L^1-bounded process with independent increments is an integrator. In this case, in the absence of any other data about the process, we require an application of Grothendieck's theorem to produce a factorizing measure.

In a specific case, when $p > 1$, p-stable motion is a stochastic integrator with a factorizing Lebesgue measure (p-stable motion means that increments are independent symmetric p-stable variables). This is obtained directly by use of properties of p-stable distributions, without the use of the Grothendieck theorem.

Example 5.4. Finally, we indicate how to construct stochastic integrators by methods which are amenable to computer simulations. The strategy is

1) to produce processes X over finite probability spaces so that $\|X\|$ is "small" and $\|X\|_{(\tau)}$ is "large", and then
2) "paste" together these processes. We briefly describe the first step.

Theorem 5.5 ([11], Chapter 6). Let $A_1,\ldots,A_k$ be finite subsets of $\mathfrak{N}$. There exists (with "high" probability) a choice of signs $\varepsilon_{i_1\ldots i_k} = \pm 1, (i_1,\ldots,i_k) \in A_1 \times \cdots \times A_k$, so that

$$\left\| \sum_{(i_1,\ldots,i_k)\in A_1\times\cdots\times A_k} \varepsilon_{i_1\ldots i_k} r_{i_1} \otimes \cdots \otimes r_{i_k} \right\|_\infty \leqslant D|A_1 \times \cdots \times A_k|^{\frac{1}{2}}(|A_1| + \cdots + |A_k|)^{\frac{1}{2}}, \tag{5.2}$$

for some numerical constant $D > 0$ which depends only on k.

Corollary to 5.5. Let m be an arbitrary positive integer and let Ω_m denote the uniform probability space $\{1,\dots,2^m\}$. There are processes X on Ω_m so that $\|X\| \leqslant 1$, and $\|X\|_{(\tau)} \geqslant \kappa_m$, where $\lim_{m\to\infty} \kappa_m = \infty$.

Proof 5.6. We think of Ω_m as the compact abelian group $\{-1,1\}^m$ with its usual normalized Haar measure. Let $F_m \subset \hat{\Omega}_m$ be arbitrary and let σ be an injection from F_m onto $\{1,\dots,|F_m|\}$. Define a process X on Ω_m by

$$X_\omega(t) = \frac{1}{|F_m|^{1/2}} \sum_{\chi\in F_m} \mathbf{1}_{[0,t]}(\sigma(\chi)/_{|F_m|})\chi(\omega),\ t \in [0,1],\ \omega \in \Omega_m. \quad (5.3)$$

The definition of X and harmonic analysis on Ω_m imply

$$\|X\|_{(\tau)} \geqslant |F_m|^{1/2} \quad \text{and} \quad \|X\| \leqslant 1.$$

■

Proof 5.7. Let $F_m \subset \{1,\dots,2^m\}$ be arbitrary. By Theorem 5.5, we find (with "high" probability) $\varepsilon_{i\omega} = \pm 1, i \in F, \omega \in \Omega_m$, so that

$$\left\| \sum_{i\in F_m,\omega\in\Omega_m} \varepsilon_{i\omega} r_i \otimes r_\omega \right\|_\infty \leqslant C|F_m|^{1/2}2^m, \quad (5.4)$$

where C is a positive constant that is independent of m. Define a process X on Ω_m by

$$X_\omega(t) = \frac{1}{4C|F_m|^{\frac{1}{2}}} \sum_{i=1}^{|F_m|} \mathbf{1}_{[0,t]}(i/_{|F_m|})\varepsilon_{i\omega}, \qquad t \in [0,1],\ \omega \in \Omega_m.$$

The definition of X and (5.4) imply

$$\|X\|_{(\tau)} \geqslant 4C|F_m|^{1/2} \quad \text{and} \quad \|X\| \leqslant 1. \quad (5.5)$$

■

Remark In the case of explicit constructions of X (Proof 5.6), the uniform probability measure on F_m is a factorizing measure. In the case of random constructions of X (Proof 5.7), a factorizing measure is obtained by an application of Corollary to 4.1.

6. Bibliography

[1] R.C. Blei. Fractional dimensions and bounded fractional forms. *Mem. Am. Math Soc.*, 57(331), 1985.

[2] R.C. Blei. An elementary proof of the Grothendieck inequality. *Proc. Amer. Math. Soc.*, 100:58–60, 1987.

[3] R.C. Blei. Multi-linear measure theory and the Grothendieck factorization theorem. *Proc. London Math. Soc.*, 56:529–546, 1988.

[4] R.C. Blei. Multi-linear measure theory and multiple stochastic integration. *Prob. Th. Rel. Fields*, 81:569–584, 1989.

[5] K.L. Chung and R.J. Williams. *Introduction to Stochastic Integration.* Birkhäuser Verlag, Basel, Boston, Berlin, 1983.

[6] J.L. Doob. *Stochastic Processes.* John Wiley & Sons, New York, London, Sydney, 1967.

[7] N. Dunford and J.T. Schwartz. *Linear Operators, Part I.* Interscience Publishers, New York, 1958.

[8] A. Grothendieck. Resumé de la théorie metrique des produits tensoriels topologique. *Bol. Soc. Matem. Saõ Paulo*, 8, 1956.

[9] K. Itô. Stochastic integral. *Proc. Imp. Acad. Tokyo*, 20:519–524, 1944.

[10] K. Itô. Stochastic differential equations. *Mem. Am. Math Soc.*, 4, 1951.

[11] J.-P. Kahane. *Some Random Series of Functions.* Cambridge University Press, Cambridge, U.K., second edition, 1985.

[12] P.E. Kopp. *Martingales and Stochastic Integrals.* Cambridge University Press, Cambridge, U.K., 1984.

[13] J. Lindenstrauss and A. Pelczynski. Absolutely summing operators in $\mathcal{L}^p$-spaces and their applications. *Studia Math.*, 29:275–326, 1968.

[14] J.E. Littlewood. On bounded bilinear forms in an infinite number of variables. *Quarterly J. of Math. Oxford*, 1:164–174, 1930.

[15] M. Métivier. *Semimartingales—a Course on Stochastic Processes.* Walter de Gruyter, New York, 1982.

[16] M. Morse and W. Transue. Functionals of bounded Fréchet variation. *Canadian J. Math.*, 1:153–165, 1949.

[17] R.E.A.C. Paley, N. Wiener, and A. Zygmund. Notes on random functions. *Math. Zeitschr*, 37:647–668, 1933.

[18] G. Pisier. Factorization of linear operators and geometry of Banach spaces. In *CBMS Regional Conf. Ser. in Math*, volume 60, Providence, RI, 1986. American Mathematical Society.

[19] P. Protter. *Stochastic Integration and Differential Equations—A new Approach*. Springer-Verlag, Berlin, Heidelberg, New York, London, Paris, Tokyo, Hong Kong, 1990.

[20] W. Rudin. Trigonometric series with gaps. *J. Math. Mech.*, 9:203–227, 1960.

[21] N. Wiener. Differential-space. *J. Math and Physics*, 2:131–174, 1923.

On the entropy of certain stochastic measures

A. Bisbas
Department of Mathematics
University of Thessaloniki
Thessaloniki 54006 Greece
ck%grathun1.bitnet

C. Karanikas
(same address)

Abstract We give a formula for the Hausdorff dimension of certain fractals obtained by a weakly ergodic Markovian process. This result is closely related with the entropy of certain ergodic measures.

1. Introduction

To understand our problem we recall some elementary results. We consider a Bernoulli trial on the two-state space described by the following sequence of transition matrices:

$$P^{(n)} = \begin{pmatrix} \frac{1+a_n}{2} & \frac{1-a_n}{2} \\ \frac{1+a_n}{2} & \frac{1-a_n}{2} \end{pmatrix} \tag{1.1}$$

where $0 \leqslant a_n \leqslant 1, n = 1, 2, \ldots$ The measure μ on $[0,1]$ corresponding to this process can be considered as an infinite product called the *Rademacher-Riesz product (R.R product)*

$$d\mu = \lim_{N \to \infty} \prod_{n=1}^{N} (1 + a_n r_n(x))\, dx,$$

where $r_n(x)$ is the Rademacher function associated with the positive integer n and the limit is in the weak* sense.

In the case where $a_n = a$, for any n, it is easy to estimate the Hausdorff dimension, dim M (cf. [1]), of a Borel set M of positive measure. In fact by a well-known formula it suffices to estimate

$$\liminf \frac{\log \mu(E_n(x))}{-n \log 2}$$

J. S. Byrnes et al. (eds.), Probabilistic and Stochastic Methods in Analysis, with Applications, 663–668.
© 1992 *Kluwer Academic Publishers. Printed in the Netherlands.*

x a.e. with respect to μ, where $E_n(x)$ is the segment $[\frac{k}{2^n}, \frac{k+1}{2^n})$ containining x for some $k = 0, 1, \ldots, 2^n - 1$.

We sketch a proof based on the Birkhoff Ergodic Theorem. By elementary calculations this is equal to

$$\frac{\log \prod_{k=1}^{n}(1 + a r_k(x))2^{-n}}{-n \log 2} = 1 - \frac{1}{\log 2}\frac{1}{n}\sum_{k=1}^{n}\log(1 + a r_k(x))$$

For any $x \in [0, 1]$ let the decimal expansion of $x = x_1 x_2 \cdots x_n \cdots$ and

$$Tx = T(x_1 x_2 \cdots x_n \cdots) = x_2 x_3 \cdots x_n \cdots$$

be the shift operator. Since $r_n(x) = 1 - 2x_n$, $n = 1, 2, \ldots$,the last formula can be written:

$$1 - \frac{1}{\log 2}\frac{1}{n}\sum_{k=1}^{n}\log\left(1 + a r_1\left(T^k x\right)\right)$$

one can easily show that T is a measure-preserving transformation, and by Birkhoff's Theorem (cf. [8]) the limit of the last expresion is equal to

$$1 - \frac{1}{\log 2}\int_0^1 \log(1 + a r_1(x))d\mu(x) = 1 - \frac{1}{\log 4}\log(1 + a)^{1+a}(1 - a)^{1-a}.$$

The right hand side of this is the entropy of this process and so, in this case the Hausdorff dimension is equal to the degree of the entropy. This is a special case of the Shannon-McMilan Theorem, which states that for ergodic measures the Hausdorff dimension is equal to the degree of the entropy [1].

In this work we shall show that for a wide class of non-ergodic non-homogeneous Markovian measures this theorem applies. More precisely, we state:

2. The main result

Let

$$P^{(0)} = (p_1, p_2, \ldots, p_r),\ P^{(n)} = (p_{ij}^n), \qquad n = 1, 2, \ldots,\ 1 \leqslant i, j \leqslant r$$

be a non-homogeneous Markovian stochastic process. Let for any n the *ergodic index* (see [5]):

$$\delta\left(P^{(n)}\right) = \frac{1}{2}\sup_{i,k}\sum_{j=1}^{r}\left|p_{ij}^n - p_{kj}^n\right|$$

We suppose that,

$$\frac{1}{N^2}\sum_{n,m=1}^{N}\delta\left(P^{(m+1,n-1)}\right)\to 0, \tag{2.1}$$

$(N\to\infty)$, where

$$P^{(m+1,n-1)}=P^{(m+1)}P^{(m+2)}\dots P^{(n-1)}.$$

We denote by μ the measure associated with this process; then the Hausdorff dimension of μ is:

$$\dim(\operatorname{supp}\mu)\leqslant -\lim_{N\to\infty}\inf\frac{1}{N}\sum_{n=0}^{N}\frac{1}{\log r}\sum_{i,j}^{r}\mu\left(E_{ij}^{(n)}\right)\log p_{ij}^{n} \tag{2.2}$$

where $\mu(E_{ij}^{(n)})=p_{ij}^{n}P^{(0,n-1)}L_i$ and $L_i=(0,\dots,1,\dots,0)^T$ (1 is in position i).

A sufficient condition for the equality in (2.2) can be given by a weak convergence of the left hand side of (2.1) as is $0((\log N)^{-2})$.

In a sense this is the entropy of this process. This result is more general than the previous works in [2] and [6] as well as the Shannon-McMilan-Breiman Theorem on the entropy of Markovian processes [1].

In the first work we dealt with the Bernoulli schema described by the sequence of matrices $P^{(n)}$ as in (1.1). As before we write:

$$\frac{\log\mu(E_n(x))}{-n\log 2}=1-\frac{1}{\log 2}\frac{1}{n}\sum_{k=1}^{n}\log(1+a_k r_k(x))$$

$$=1-\frac{1}{\log 4}\frac{1}{n}\sum_{k=1}^{n}\left[\log(1-a_k^2)+r_k(x)\log\left[\frac{1+a_k}{1-a_k}\right]\right].$$

Then because the Rademacher functions are independent random variables $d\mu$, we use Kolmogorov's law of large numbers to obtain formula (2.2) for the special cases where $r=2$, $p_{i1}^{n}=(1+a_n)/2$, $p_{i2}^{n}=(1-a_n)/2$.

In the second work we considered a Bernoulli schema on the r-state space $(r\geqslant 2)$. We described the measure μ as a generalized R.R. product and derived (2.2).

Here we have to note the works of J. Peyriére [7] and G. Brown W. Moran and C.E. Pearce [3] on the Hausdorff dimension of trigonometric Riesz products $\prod_{n=1}^{\infty}(1+a_n\cos\lambda_n x)dx$, where λ_n is a sequence of integers satisfying a condition such as for any $n\lambda_n$ divides λ_{n+1} or $\lambda_n/(\lambda_{n+1})\to 0$, $n\to\infty$.

Next we describe the proof of the main result and in the last section we describe our representative example. It seems to us that a probabilistic approach to the Hausdorff dimension of trigonometric Riesz products is possible; we hope to deal with this in another work.

2.1. The Hausdorff dimension of a Markovian process

We describe the measure μ associated with the non-homogeneous Markovian stochastic process determined by a sequence of matrices:

$$P^{(0)}, P^{(1)}, \ldots, P^{(n)}, \ldots.$$

We assume that all matrices have dimension $r \times r$ except $P^{(0)}$ which has dimension $1 \times r$. Notice that our result is still valid under the more general assumption that all matrix multiplication involved are performable.

As in [6] we use generalized Rademacher functions. For each $i = 1, 2, \ldots, r$ we define the sequence of Rademacher functions associated with i: $R_n^i(x) = 1 - r\delta_{x_n,i}$, where $\delta_{\cdot,\cdot}$ is the Kronecker delta and $x_1 x_2 \cdots x_n \cdots$ is the r-adic expansion of $x \in [0, 1]$.

Observation 2.1. The measure μ associated with the stochastic Markovian process matrices $P^{(0)}, P^{(1)}, \ldots, P^{(n)}, \ldots$, is a product,

$$d\mu = \prod_{n=0}^{\infty} G_n(x)\, dx,$$

where

$$G_0(x) = 1 + (p_r^0 - p_1^0)R_1^1(x) + \cdots + (p_r^0 - p_{r-1}^0)R_1^{r-1}(x)$$

and for any $n \geq 1$:

$$G_n(x) = \sum_{i=1}^{r} \frac{1 - R_{n-1}^i(x)}{r} \left[1 + (p_{ir}^n - p_{i1}^n)R_n^1(x) + \cdots \right.$$
$$\left. \cdots + (p_{ir}^n - p_{i(r-1)}^n)R_n^{r-1}(x)\right]$$

Proof. It is easy to check. ∎

Observation 2.2.

$$\log G_n(x) = \sum_{i,j=1}^{r} \frac{1 - R_{n-1}^i(x)}{r} \frac{1 - R_n^j(x)}{r} \log r p_{ij}^n$$
$$= \frac{1}{r^2} \sum_{i,j=1}^{r} f_{i,j}^n(x) \log r p_{ij}^n,$$

where $f_{i,j}^n = 1 - R_{n-1}^i - R_n^j + R_{n-1}^i R_n^j; i, j = 1, 2, \ldots, r.$

Observation 2.3.

1) First,

$$\int_0^1 R_n^i(x)d\mu(x) = P^{(0,n-1)}I_iE$$

2) Second,

$$\int_0^1 R_m^i(x)R_n^j d\mu(x) = P^{(0,m-1)}I_iP^{(m,n-1)}I_jE$$

where $P^{(0,n-1)} = P^0P^1 \dots P^{n-1}$, $E = (1,1,\dots,1)^T$ and I_i is equal with the identity matrix $(r \times r)$ in all elements except in the position (i,i) where 1 is replaced by $r-1$.

Proof. Easy. ∎

Proof (of the main result). We estimate the lim inf of

$$\frac{\log \mu(E_N(x))}{N \log r} = 1 - \frac{\sum_{n=1}^N \log G_n(x)}{N \log r} = 1 - \frac{1}{r^2}\sum_{i,j}^r \frac{\sum_{n=1}^N f_{ij}^n(x)\log rp_{ij}^n}{N \log r}$$

For each pair of (i,j) we shall apply the law of large numbers for $\frac{1}{N}\sum_{n=1}^N g_{ij}^n(x)$ where $g_{ij}^n(x) = (f_{ij}^n(x)\log rp_{ij}^n)/r^2$.

It suffices to show that for $N \to \infty$ the variance:

$$V\left(\frac{1}{N}\sum_{n=1}^N g_{ij}^n(x)\right) \to 0. \tag{2.3}$$

Then by Chebyshev's inequality we have (2.2). Thus for (2.3) we show

$$|\mu(g_{ij}^m)\mu(g_{ij}^n) - \mu(g_{ij}^n g_{ij}^m)| < \text{const}\,\delta(P^{(m,n)}) \tag{2.4}.$$

In fact from Observation 2.3 the left hand side of (2.4) is

$$\begin{aligned}
&|(p_{ij}^m \log rp_{ij}^m)(p_{ij}^n \log rp_{ij}^n)P^{(0,m-1)}B_{ij} \\
&\qquad \left[E, P^{(0,n-1)}B_{ij}E \cdots P^{(m+1,n-1)}B_{ij}E\right]| \\
&\leqslant \text{const}\left|P^{(0,m-1)}B_{ij}\left[Ec - (c-\delta\left(P^{(m,n)}\right)E\right]\right| \\
&\leqslant \text{const}\,\delta\left(P^{(m,n)}\right),
\end{aligned}$$

where the matrix B_{ij} is equal with the zero matrix in all elements except in the position (i,j) instead of 0 it has 1, and where c is a constant depending on i, j, m and n.

For the equality of (2.2) one can use:

Theorem 2.4 (Davenport, Erdös and Leveque). *If $x_n \geqslant 0$ and the series: $\sum_{n=1}^\infty x_n/n$ converges,then there exists an increasing subsequence n_k such that $n_{k+1}/n_k \to 1$ and the series $\sum_{k=1}^\infty x_{n_k}$ converges.*

∎

3. Application: Measures on the Poisson boundary of the free group of two generators

This was our initial example for this work. We describe the non-homogeneous Markovian process on the tree that represends the reduced words on the free group of two generators $\{a, b\}$. Let $\{1, 2, 3, 4\}$ be the state space. We assume that on each state there correspond the generators $\{a, a^{-1}, b, b^{-1}\}$ respectively. The transition matrix $P^{(n)}$, $n = 1, 2, \ldots$ is the following:

$$P^{(n)} = \begin{pmatrix} \frac{1+a_n}{3+a_n} & 0 & \frac{1+a_n}{3+a_n} & \frac{1-a_n}{3+a_n} \\ 0 & \frac{1-a_n}{3-a_n} & \frac{1+a_n}{3-a_n} & \frac{1-a_n}{3-a_n} \\ \frac{1+a_n}{3+a_n} & \frac{1-a_n}{3+a_n} & \frac{1+a_n}{3+a_n} & 0 \\ \frac{1+a_n}{3-a_n} & \frac{1-a_n}{3-a_n} & 0 & \frac{1-a_n}{3-a_n} \end{pmatrix},$$

where $0 \leqslant a_n$ and $\sup a_n < 1$. It is not difficult to see that the ergodic index $\delta(P^{(n)}) < \text{const} < 1$ and by an easy argument (cf. Lemma V.2.3 [5]) we have $\delta(P^{(m,n)}) \leqslant \prod_{k=m}^{n} \delta(P^{(k)})$. Thus condition (2.1) is satisfied and so the Hausdorff dimension of the boundary of this tree (cf. [4]) is given by the equality of (2.2).

4. Bibliography

[1] P. Billingsley. *Ergodic Theory and Information*. John Wiley & Sons, New York, London, Sydney, 1965.

[2] A. Bisbas and C. Karanikas. On the Hausdorff dimension of Rademacher-Riesz products. *Monatsh. für Math.*, 110:15–21, 1990.

[3] G. Brown, W. Moran, and C.E. Pearce. Riesz products, Hausdorff dimension and normal numbers. *Math. Proc. Camb. Phil. Soc.*, 101:529–540, 1987.

[4] A. Figa-Talamanca and C. Nebbia. Harmonic analysis and representation theory for groups acting on homogeneous trees. To appear.

[5] D. Isaacson and R. Madsen. *Markov Chains Theory and Applications*. John Wiley & Sons, New York, London, Sydney, 1976.

[6] C. Karanikas and S. Koumandos. On a generalized entropy's formula. *Results in Math.*, 18:254–263, 1990.

[7] J. Peyriére. Étude de quelques proprietés des produits de Riesz. *Ann. Inst. Fourier (Grenoble)*, 25(2):127–169, 1975.

[8] A.N. Shiryayev. *Probability*. Springer-Verlag, Berlin, Heidelberg, New York, London, Paris, Tokyo, Hong Kong, 1984.

The geometry of attractors for a class of iterated function systems

Mauro Piccioni
Dipartimento di Matematica Pura e Applicata,
Universitá di L'Aquila, Italy
Centro Matematico Vito Volterra,
Universitá di Roma Tor Vergata Italy
piccioni@vaxtvm.infn.it

Massimo Regoli
Centro Matematico Vito Volterra,
Universitá di Roma Tor Vergata Italy
regoli@mat.utovrm.it

Abstract An iterated function system (IFS) on a compact metric space is a finite collection of mappings of the space into itself. Under suitable conditions, an attractor for the IFS can be defined in a natural way. If the mappings depend on a parameter, the subset of the parameter space for wich the corresponding attractor is connected is called the Mandelbrot set of the family. Under some suitable symmetry conditions, it can be shown that, for parameter values not in the Mandelbrot set, the attractor is homeomorphic to the Cantor set. We determine the Mandelbrot set for a family of nonlinear IFS's on the unit triangle obtained from the problem of filtering the noise from a Markov chain signal model.

1. Introduction

Let us consider a finite set of transformations $\mathcal{I} = \{I_i, i = 1, \ldots, m\}$ acting on a complete metric space K. For any input sequence $\{i_n\}$ taking values in $I_m = \{1, \ldots, m\}$ the sequence $\{s_n\}$ is generated through the recursion $s_{n+1} = I_{i_n}(s_n)$, from any chosen initial point $s_0 \in K$. We refer to the collection of all these sequences as the iterated function system generated by $\mathcal{I}$ [2, 1].

If these transformations are contractive, i.e., Lipschitz with a Lipschitz constant strictly smaller than one, it is easy to show that the IFS has an attractor S, which is a subset of K approached by $\{s_n\}$ as n increases, independently of the initial point and the input sequence [2, 7, 8]. For the precise definition see the next section. Such an attractor S is characterized as the unique compact subset of K which is $\mathcal{I}$-self-similar, that is $S = \bigcup_{i=1}^{m} I_i(S)$.

J. Cornes et al. (eds.), *Probabilistic and Stochastic Methods in Analysis, with Applications*, 669–685
© 1992 *Kluwer Academic Publishers. Printed in the Netherlands*

Whenever each point $s \in S$ can be uniquely decoded, that is there exists only one input sequence $\{i_n\}$ such that s is the limit of $F_{i_1}(F_{i_2}(\ldots(F_{i_n}(x))))$ (which in any case will not depend on $x \in K$), then the attractor is totally disconnected. Under some symmetry condition on $\mathcal{F}$ the converse is also true. Hence a remarkable connection is established between geometry and dynamics.

If the input at time n is chosen at random from a probability distribution P_{s_n} depending on the current value of s_n, but not on the previous ones, the sequence $\{s_n\}$ is turned into a Markov process $\{S_n\}$. The study of such a class of processes started with [12], [4] and later their asymptotic behaviour has been investigated in [10], [11], with motivations arising from the theory of learning. In particular the romanian school [9] contributed to this field [9] giving them the name of random systems with complete connections (to which we will prefer the more recent one of iterated function systems with place-dependent probabilities [3]). The main result of this theory is that if the convergence to S is exponential (as in the case of contractive transformations) and a uniform positivity condition on the family of conditional probabilities P_s holds, then $\{S_n\}$ has a unique stationary probability law which is easily seen to be supported by the attractor S. Thus the relevant dynamics takes place on S and, if S is totally disconnected, it is possible to extract from S_n the whole sequence of inputs applied up to time n.

In this paper we are interested in an important class of IFS on a compact set K with place-dependent probabilities which are obtained from some problems of recursive estimation of Markov chains, already introduced in [5]. Let $\{X_n\}$ be an irreducible and aperiodic Markov signal on the state space I_d and $\{Y_n\}$ be an observation process coming from a noisy memoryless channel with values in I_m.

Let $P = \{p_{ij}\}$ be the transition matrix of $\{X_n\}$ and $\varepsilon_{ij} > 0$ be the probability of an observation $i \in I_m$ given that the signal at the same time is $j \in I_d$.

The predictive sequence:

$$S_n(i) = P(X_n = i | Y_j, j = 1, \ldots, n-1), i = 1, \ldots, d, \tag{1.1}$$

is then an IFS with values in the unit d-dimensional simplex Σ_d, since it is possible to write as $S_{n+1} = F_{Y_n}(S_n)$ where:

$$F_i(s)(h) = \frac{\sum_1^d p_{jh}\varepsilon_{ji}s_j}{\sum_1^d \varepsilon_{ji}s_j} \tag{1.2}$$

and

$$P(Y_n = i | S_n, S_{n-1}, \ldots) = \pi_i(S_n) = \sum_1^d \varepsilon_{ji}s_j. \tag{1.3}$$

It is immediately checked that in general not all of the F_i's will be contractive transformations on Σ_d. Nonetheless the existence of the attractor S can be shown only by using the weaker condition:

$$\operatorname{diam}(F_{i_1} \circ \ldots \circ F_{i_n})(\Sigma_d) \to 0 \tag{1.4}$$

which holds uniformly in the input sequence, as $n \to \infty$. Moreover such a convergence is exponentially fast, which implies the uniqueness of the stationary law for $\{S_n\}$ and the fact that it is supported by S. These results can be found in [5].

The previous analysis allow one to study the extent of the memory of the predictor through the geometry of the attractor. Under suitable symmetry conditions such an attractor is totally disconnected if and only if the predictor has infinite memory, i.e., $Y_{n-1}, Y_{n-2}, \ldots$, can be extracted from S_n (and such a relation is continuous). Our interest is to identify the values of the parameters for which this happens, at least for some family of prediction problems.

Such a program has been completely pursued when both $\{X_n\}$ and $\{Y_n\}$ are binary, in which case the attractor is either perfect and totally disconnected, or it is an interval. For the ternary case we extend the results contained in [5] which is the original contribution of the paper.

The organization of the paper is as follows. In Section 2 the basic theory of attractors for IFS on a compact set is reviewed starting from the assumption (1.4). In section 3 we completely classify the connectedness of the attractor in the ternary completely symmetric case, that is

$$\begin{aligned} p_{ij} &= (1-p)\delta_{ij} + \frac{p}{2}(1-\delta_{ij}), \\ \varepsilon_{ij} &= (1-\varepsilon)\delta_{ij} + \frac{\varepsilon}{2}(1-\delta_{ij}), \qquad i,j = 1,2,3, \end{aligned} \tag{1.5}$$

with the only assumption thet $0 \leq \varepsilon \leq 2/3$.

2. IFS on a compact set and their attractors

Let K be a compact metric space and $\mathcal{F} = \{F_i, i \in I_m\}$ a family of continuous transformations of K into itself. Let us denote by $F_{i_1, \ldots, i_n}$ the composition $F_{i_1} \circ \ldots \circ F_{i_n}$ and let

$$\mathcal{F}^n = \{F_{i_1, \ldots, i_n}, (i_1, \ldots, i_n) \in I_m^n\}. \tag{2.1}$$

Now suppose that

$$\lim_n \sup_{F \in \mathcal{F}^n} \operatorname{diam} F(K) = 0. \tag{2.2}$$

Such a condition is obviously satisfied whenever

$$d(F_i(x), F_i(y)) \leq r_i d(x, y) \tag{2.3}$$

for some $r_i < 1, i \in I_m$, but on a compact set is obviously weaker. The goal of this section is to review the by now classical theory of attractors for IFS [2, 7, 8] starting from (2.2) rather than (2.3).

It is an immediate consequence of (2.2) that for any sequence $\{i_n\} \in I_m^\infty$, the sequence of transformations $\{F_{i_1,\ldots,i_n}\}_{n=1,\ldots}$ converges uniformly to the constant

$$\Phi(\{i_n\}) = \bigcap_{n=1}^{\infty} F_{i_1,\ldots,i_n}(K).$$

The mapping $\Phi : I_m^\infty \to K$ is clearly continuous so the range of Φ is a compact set called the attractor of the IFS $\mathcal{F}$.

Theorem 2.1. Let S be the attractor of $\mathcal{F}$. Then

i: For any nonempty compact set C in K

$$\mathcal{F}^n(C) = \bigcup_{(i_1,\ldots,i_n)\in I_m^n} (F_{i_1,\ldots,i_n})(C) \to S \tag{2.4}$$

as $n \to \infty$, in the Hausdorff metric;

ii: S is the unique compact subset of K such that

$$S = \mathcal{F}(S) = \bigcup_{i=1}^{m} F_i(S); \tag{2.5}$$

iii: For any $s \in S$ the set $\{F_{i_1,\ldots,i_n}(s) : (i_1,\ldots,i_n) \in I_m^n, n = 0, 1, \ldots\}$ is dense in S;

iv: if $s^*_{i_1,\ldots,i_n}$ is the unique fixed point of $F_{i_1,\ldots,i_n}$ then S is the closure of $\{s^*_{i_1,\ldots,i_n} : (i_1,\ldots,i_n) \in I_m^n, n = 1, 2, \ldots\}$.

Proof. i) is straightforward since both $\mathcal{F}^n(K)$ and $\mathcal{F}^n(\{x\})$, for any $x \in K$, are in a ball of arbitrarily small radius around S in the Hausdorff metric for n sufficiently large. By the definition of Φ, since each F_i is continuous, it is $F_i(S) \subset S, \forall i \in I_m$. On the other hand if $s = \Phi(\{i_n\})$ then $s \in F_{i_1}(S)$. This shows (2.5). Uniqueness follows from (2.4). iii) follows by taking $C = \{s\}$ in (2.4) and observing that (2.5) implies $S = \mathcal{F}^n(S)$, for any integer n. To establish iv) first note that (2.2) makes impossible the existence of more than one fixed point for each $F_{i_1,\ldots,i_n}$. Hence iv) esults from the continuity of Φ, since any sequence $\{i_n\} \in I_m^\infty$ can be approximated by a periodic one and the Φ–images of periodic sequences are precisely all the fixed points of $F_{i_1,\ldots,i_n}$, for any integer n and $i_k \in I_m, k = 1, \ldots, n$. ∎

We will be particularly interested in characterizing those situations in which Φ is invertible, that is from each point s in the attractor we can recover in a unique way its code that is the whole sequence of inputs $\{i_n\}$ which has produced it through the mapping Φ.

Theorem 2.2. Φ is invertible if and only if for each $i \in I_m$, F_i restricted to S is one-to-one and for $i_1 \neq i_2$, $F_{i_1}(S) \cap F_{i_2}(S) = \emptyset$. In this case S is perfect and totally disconnected.

Proof. The necessity is evident. For the sufficiency observe that i_n can be read observing to which of the mutually disjoint sets $F_i(S)$, $i \in I_m$, the point $(F_{i_{n-1}}^{-1} \circ \ldots \circ F_{i_1}^{-1})(s)$ belongs. Finally, if Φ is invertible it is a homeomorphism between I_m^∞ and S, hence the former being perfect and totally disconnected S is such. ∎

It should be clear that the previous theorem cannot be used to establish that Φ is invertible if, as usual, S is unknown. For this reason the following corollary, whose proof is immediate, is more useful in practice.

Corollary to 2.2. Let C be a compact subset of K such that $F_i(C) \subset C$ for each $i \in I_m$. Then $S \subset C$, hence the conditions of Theorem 2.2 are satisfied if they hold in C.

Unfortunately, S can be perfect and totally disconnected without Φ being invertible [7]. However the following result can be used in many cases to rule out this possibility. To any family $\{B_i\}_{i=1}^m$ of m subsets of K we associate an undirected graph $\Gamma_m(\{B_i\}_{i=1}^m)$ on the vertex set I_m, called the intersection graph, having an edge connecting j and k if and only if $B_j \cap B_k \neq \emptyset$. The proof of the next result is taken from that of [7] for the case of weak contractions but again it relies only on (2.2).

Theorem 2.3. The attractor S is connected if and only if the graph

$$\Gamma_m(\{F_i(S)\}_{i=1}^m)$$

is connected.

Proof. The proof consists of showing that S is well-chained, that is for any $\varepsilon > 0$ and any choice of s and $t \in S$ there exists a chain $\{s_k\}_{k=0}^{l}$ with $s_0 = s$ and $s_l = t$, such that $d(s_k, s_{k-1}) < \varepsilon$, for $k = 1, \ldots, l$. This will follow once we prove that for any integer n the intersection graph $\Gamma_m(\{F_{i_1 \ldots i_n}(S)\}_{i_1, \ldots, i_n \in I_m})$ is connected. In fact then a chain connecting s and t can be built in such a way that for $k = 1, \ldots, l$, s_{k-1} and s_k both belong to some common $F_{i_1 \ldots i_n}(S)$ hence their distance is smaller then ε, for n sufficiently large.

Finally such an intersection graph can be easily proved to be connected by induction, observing that for any integer n and any choice of $(i_1,\dots,i_n) \in I_m^n$ the intersection graph $\Gamma_m(\{F_{i_1,\dots,i_n,i}(S)\}_{i=1}^m)$ is again irreducible. Since the union of the above family is $F_{i_1,\dots,i_n}(S)$ it is easy to build a path connecting $(i_1,\dots,i_n,i_{n+1})$ and $(j_1,\dots,j_n,j_{n+1}) \in I_m^{n+1}$ from one connecting $(i_1,\dots,i_n)$ and $(j_1,\dots,j_n) \in I_m^n$. ∎

The last two theorems allow one to obtain the following alternative whenever some symmetry argument can be used to show that the assumption is fulfilled.

Corollary to 2.3. Let us a consider an IFS $\mathcal{F}(\alpha) = \{F_i(\alpha), i \in I_m\}$ made by one-to-one maps which satisfies (2.2) for any value of α and call S_α its attractor. Suppose that whenever there exists i and j, different from i, such that $F_i(\alpha)(S_\alpha) \cap F_j(\alpha)(S_\alpha) \neq \emptyset$, then the whole graph $\Gamma_m(\{F_i(\alpha)(S_\alpha)\}_{i=1}^m)$ is connected. Then S_α is either perfect and totally disconnected or connected, and this happens when Φ_α is invertible or it is not, respectively.

With terminology taken from [1] we can call the set of all values of α for which S_α is connected the Mandelbrot set of the family of IFS $\mathcal{F}(\alpha)$. Our main interest is to investigate such a set for families of IFS which will be introduced in the next section.

Let us also remark that, by a general result in [6], the invariant measure μ of a Feller-Markov process $\{S_n\}$ on a compact state space, can be approximated by the empirical measure, that is $\frac{1}{n}\sum_{k=1}^n \delta_{S_k}$ converges in distribution to μ with probability one, for any possible starting point $s_0 \in K$. This allows to get an approximate picture of the measure μ, hence of its support, by simulating $\{S_n\}$, moreover, if $s_0 \in S$, then such an empirical measure is supported by points belonging to S (e.g., the fixed point of some F_i). This has been used to get the pictures shown in the paper.

3. Ternary case

In this final section we consider the IFS (1.2) with parameter values as in (1.5).

The mappings F_i can be rewritten as:

$$F_i(s)(i) = \phi(s_i), \qquad i = 1,2,3 \tag{3.1}$$

$$F_i(s)(j) = \psi(s_i, s_j), \qquad i = 1,2,3, j \neq i, \tag{3.2}$$

where:

$$\phi(s_1) = \frac{(1-p)(1-\varepsilon)s_1 + \frac{p\varepsilon}{4}(1-s_1)}{(1-\varepsilon)s_1 + \frac{\varepsilon}{2}(1-s_1)}, \qquad 0 \leqslant s_1 \leqslant 1,$$

$$\psi(s_1, s_2) = \frac{\frac{(1-\varepsilon)p}{2}s_1 + \frac{(1-p)\varepsilon}{2}s_2 + \frac{p\varepsilon}{4}(1-s_1-s_2)}{(1-\varepsilon)s_1 + \frac{\varepsilon}{2}(1-s_1)},$$

for $s_1, s_2 \geqslant 0$ and $s_1 + s_2 \leqslant 1$. The trivial case in which $p = 2/3$ is excluded in the sequel, hence we can assume that the mappings F_i are one-to-one.

Remark 3.1. We will have to check that the image under F_i of some polygon G, with edges parallel to those of Σ_3, is contained in another polygon G_0 of the same kind. Since F_i maps Σ_3 homeomorphically onto its image it will be enough to check that $F_i(\partial G) = \partial F_i(G) \subset G_0$, since in each case it can be trivially established that G it is mapped into the appropriate side of the boundary. Moreover since each component of F_i is monotone on every segments, it will be enough to verify that the vertices of G are mapped into G_0 by F_i.

It is immediately checked that:

$$F_j = \pi_{i,j} \circ F_i \circ \pi_{j,i},$$

where $\pi_{i,j}$ exchanges the j-th with the i-th coordinate, leaving the other fixed. This implies that the attractor S is invariant under coordinate permutations. Therefore Corollary 2.5 holds.

Now let us suppose that the signal chain is persistent, that is $0 < p < 2/3$. This case has been already covered by [5], but for the sake of completeness we report the full proof here.

Each F_i is one-to-one onto the triangle with vertices $(1-p, p/2, p/2)$ and its permutations and its fixed point has the form

$$s_i^*(j) = (1-\zeta)\delta_{ij} + \frac{\zeta}{2}(1-\delta_{ij}), 0 < \zeta < \frac{2}{3}. \tag{3.3}$$

In fact, s_1^* being the normalized eigenvector associated to the largest eigenvalue of the matrix $P^T D_1$, it is

$$(1-p)(1-\varepsilon) + \frac{p\varepsilon}{4}\zeta/(1-\zeta) = p(1-\varepsilon)(1-\zeta)/\zeta + \left(1-\frac{p}{2}\right)\frac{\varepsilon}{2}.$$

Since the l.h.s. is increasing and the r.h.s. is decreasing in ζ, and the former exceeds the latter for $\zeta = 2/3$ by the positive amount $(1-\frac{3}{2}\varepsilon)(1-\frac{3}{2}p)$ (3.3) is proved. Hence the triangle

$$J_1 = \{(s_1, s_2, s_3) : \zeta/2 \leqslant s_i \leqslant 1-\zeta, i = 1,2,3\}$$

with vertices s_1^*, s_2^* and s_3^* is not empty and has the property

$$F_i(J_1) \subset J_1, i = 1,2,3. \tag{3.4}$$

It suffices to show this for $i = 1$. In view of the preceding Remark we have only to show that $F_1(s_2^*)$ is in J_1 (in which case also $F_1(s_3^*)$ will be in J_1 by symmetry). First, since $1 - \zeta$ is the fixed point of the increasing function ϕ, it is

$$\zeta/2 \leqslant F_1(s_1, s_2, s_3)(1) \leqslant 1 - \zeta$$

for $\zeta/2 \leqslant s_1 \leqslant 1 - \zeta$. Moreover for $0 < p < 2/3$ it is $F_1(s_2^*)(2) > F_1(s_2^*)(3)$. Finally

$$F_1(s_2^*)(3) > \zeta/2 \tag{3.5}$$

holds if and only if $\zeta > p$ as it results by taking into account that $F_1(s_1^*)(3) = \zeta/2$ and subtracting each side from the corresponding one in (3.5). But since $\zeta > p$ in the range of values of p and ε we are considering (3.4) is proved.

By (3.4) and Corollary 2.3 it is necessarily $S \subset J_1$. But (3.5) also ensures that we will never get the equality in (3.4), hence S will never coincide with J_1 and it will never be a triangle, either. We can now prove the following theorem:

Theorem 3.2. The attractor S for the IFS (1.2) and (1.4) is perfect and totally disconnected if and only if

$$p < \frac{\varepsilon(1-\varepsilon)}{(1-\varepsilon^2)}, \tag{3.6}$$

otherwise it is connected.

Proof. We will show that S is perfect and totally disconnected if and only if

$$F_2(s_1^*)(2) > F_2(s_1^*)(1) \tag{3.7}$$

which, once written down explicitly, is shown to be equivalent to $\zeta > \varepsilon$. This happens if and only if by replacing ζ with ε in (3.3) the r.h.s. exceeds the l.h.s. After a number of simplifications (3.6) is obtained. ∎

Now assume (3.7). For any $s \in J_1$ denote by Q_s and P_s the sets

$$Q_s = \{y \in J_1 : y_2 \geqslant s_2, y_1 \leqslant s_1\} \tag{3.8}$$

$$P_s = \{y \in J_1 : y_2 \leqslant s_2, y_1 \geqslant s_1\}. \tag{3.9}$$

Then

$$F_1(P_s) \subset P_{F_1(s)}, F_2(Q_s) \subset Q_{F_2(s)}. \tag{3.10}$$

By the introductory Remark it suffices to prove (3.10) with P_s and Q_s replaced by the segments forming their boundary. Next the first is verified

by using the monotonicity of the components of F_1 on each segment and checking that both

$$\frac{d}{d\alpha}F_1(s_1, s_2 - \alpha, s_3 + \alpha)(i)|_{\alpha=0}$$

and

$$\frac{d}{d\alpha}F_1(s_1 + \alpha, s_2, s_3 - \alpha)(i)|_{\alpha=0}, \qquad i = 1, 2,$$

have the right signs. The second follows by symmetry. In particular for $s = s_2^*$ and $s = s_1^*$ we get

$$F_1(I_1) \subset P_{1,(s_2^*)}, F_2(I_1) \subset Q_{1,(s_1^*)}.$$

Since $F_1(s_2^*)(2) = F_2(s_1^*)(1)$, from (3.7) it follows that $P_{1,(s_2^*)}$ and $Q_{1,(s_1^*)}$ are disjoint, from which

$$F_1(I_1) \cap F_2(I_1) = \emptyset.$$

Hence for $i \neq j$

$$F_i(I_1) \cap F_j(I_1) = \emptyset,$$

which implies by Corollary 2.3 that S is perfect and totally disconnected.

Suppose now

$$F_2(s_1^*)(1) \geq F_2(s_1^*)(2) = F_1(s_2^*)(1). \tag{3.11}$$

we will construct a sequence $x_k = F_{i_1 \ldots i_k}(s_1^*) = \Phi(i_1, \ldots, i_k\bar{1})$ of points in I converging to a point s in $M = \{x : x(1) = x(2)\}$, where each of i_k is either 1 or 2. The construction builds successively the digits i_k in the *code* of s. Let us start from the *code* $\bar{1}$ of the periodic point s_1^* and begin to substitute, starting from the left, the symbol 1 with 2 and conversely until it will happen that

$$\Phi(\sigma 1) \in I \text{ but } \Phi(\sigma 2\bar{1}) \in R$$

where σ is a list of 1 and 2 (for the first step it consists only of 2's but we need it for the sequent steps).

It's clear that sooner or later this will happen, since substituing all the symbols of the address of s_1^* we obtain $s_2^* \in R$.

Now we keep the first digit that changed will lead us in R, and keep on trying to change the following digit in the code. Now the procedure ends in a finite number of steps at a point in M, or an infinite number of digits will not be changed (because when changed the corresponding point will be in R) and by continuity of ϕ this will prove the convergence to a point in M. The above statement is etablished provided we show

$$\Phi(\sigma 2\bar{1}) \in R \Rightarrow \Phi(\sigma 1\bar{2}) \in R,$$

that is keeping the symbol that once changed would lead us in R and changing all the following we come back in R.

Let $z_1 = F_2(s_1^*)$ and $z_2 = F_1(s_2^*)$ because of (3.11) we will have that: $z_2 \in Q_{z_1}$ or equivalently $z_1 \in P_{z_2}$.

Let $G(x) \equiv F_\sigma(x)$. Then $G(z_2) \in Q_{G(z_1)}$ (equivalently $G(z_1) \in P_{G(z_2)}$). It is clear that since $G(z_1) = \Phi(\sigma 2\bar{1}) \in R$ then by (3.10) we obtain $G(z_2) = \Phi(\sigma 1\bar{2}) \in Q_{G(z_1)} \subset R$;

It is clear that this argument, with the appropriate choice of G as a composition of F_1 and F_2 allows to construct the desired sequence $x_k = \Phi(\sigma_k \bar{1})$.

Now let us consider the repulsive case when

$$\frac{2}{3} < p < 1 \tag{3.12}$$

Since the triangle having the fixed points of the F_i's as vertices is not invariant anymore, we turn our attention to the fixed points of the composition $F_i \circ F_j$, s_{ij}^* for $i \neq j$.

Let $s_{23}^* = (x^*, y^*, z^*)$; since

$$F_3(s_{23}^*) = s_{32}^* = (x^*, z^*, y^*);$$

then:

$$\begin{aligned} z^* &= \psi(z^*, y^*) \\ y^* &= \phi(z^*) \\ x^* &= \psi(z^*, x^*). \end{aligned} \tag{3.13}$$

First of all, notice that:

$$(1-p) \leqslant y^* \leqslant x^* \leqslant z^* \leqslant \frac{p}{2}; \tag{3.14}$$

for the range of parameter values we are considering.

To establish this observe first that z^* is the unique solution of the equation:

$$z = \psi(z, \phi(z)).$$

Such an equation can be written as:

$$\phi(z) - \frac{(p - 2z)[(2 - 3\epsilon)z + \epsilon]}{\epsilon(3p - 2)} = r(z), \tag{3.15}$$

where:

$$r(0) = \frac{p}{3p-2} > \phi(0) = \frac{p}{2};$$

and

$$r(1) < 0.$$

At the unique fixed point $1-\zeta$ of ϕ it is:

$$(1-\epsilon)(1-\zeta)^2 + \frac{\epsilon}{2}\zeta(1-\zeta) = (1-p)(1-\epsilon)(1-\zeta) + \frac{p\epsilon}{4}\zeta;$$

hence by substituting into the r.h.s. of (3.15) we get:

$$r(1-\zeta) = \frac{(1-\epsilon)}{\epsilon/2}(1-\zeta) > 1-\zeta;$$

from which it follows $z^* > 1-\zeta$. Since $y^* = \phi(z^*)$ and ϕ is decreasing, then $y^* < 1-\zeta$.

By subtracting the first from then third of (3.13) we get that $z^* - x^*$ and $x^* - y^*$ have the same sign, hence (3.14) is established. It is clear now that the hexagon:

$$J_2 = \{s : y^* \leq s_i \leq z^*\}, \tag{3.16}$$

having $\{s^*_{ij} : i \neq j\}$ as vertices is nonempty.

Let us show the following:

Theorem 3.3. For each i it is

$$F_i(J_2) \subset J_2 \tag{3.17}$$

Proof. By symmetry we need to show this only for the case $i = 3$.

By the introductory remark, it is enough to look at the images of each of the segments of the boundary of J_2. Since $\psi(s,t)$ being nonincreasing in t for any s, F_3 maps L inside R: hence it suffices to look at the part of the boundary of J_2 which is inside L.

By the uniqueness of the fixed point of ϕ, $1-\zeta$, the interval $[y^*, z^*]$ is invariant under ϕ. ∎

Let us now consider the images of the oriented segments $[s^*_{23}, s^*_{21}]$. First of all:

$$\phi(x^*) < x^*, \tag{3.18}$$

this is proved in the following way. The solution of $\psi(z,x) = x$ is

$$x = \frac{p[(2-3\epsilon)z + \epsilon]}{2(2-3\epsilon)z + 3\epsilon p}$$

which is increasing in z and is $\frac{1}{3}$ in $z = 0$. Therefore $x > \frac{1}{3} > 1 - \zeta$ from which (3.18) follows.

From (3.18)

$$F_3(s^*_{21})(3) < s^*_{21}(3),$$

moreover it is easy to verify that:

$$\frac{d}{d\alpha} F_3((1-\alpha)s^*_{23} + \alpha s^*_{21})(2)\Big|_{\alpha=0} < 0,$$

from which

$$F_3(s^*_{21})(2) < F_3(s^*_{23})(2) = s^*_{32}(2) = z^*,$$

which finally shows that $F_3([s^*_{23}, s^*_{21}]) \subset I_2$.

Now look at $[s^*_{21}, s^*_{31}]$. It is enough to verify that:

$$F_3(s^*_{31})(2) < \psi(y^*, z^*) < y^* < \phi(z^*).$$

It is immediately checked that the opposite inequality holds for denominator, whereas the correct inequality holds for the numerator as soon as

$$\frac{z^*}{\psi(z^*)} < \frac{p-2}{1-p}$$

which is always satisfied.

Finally observe that $[s^*_{23}, s^*_{13}]$ is mapped by F_3 into the segment $[s^*_{32}, s^*_{31}]$, and the latter is mapped into a segment having third component costant with endpoints internal to I_2.

Let us work out the condition:

$$F_1(s^*_{13})(1) > F_1(s^*_{31})(1) \tag{3.19}$$

which will be shown to be necessary and sufficient for disconnectedness.

For the moment notice that the above is equivalent to:

$$\psi(y^*, z^*) > \phi(y^*)$$

which after some algebraic manipulations become:

$$(1-\epsilon)(1-\frac{3}{2}p)y^* < (1-\frac{3}{2}p)\frac{\epsilon}{2}z^* \iff y^* - \phi(z^*) > \frac{\epsilon}{2(1-\epsilon)}z^*$$

where z^* is the unique solution of $\phi(z) = r(z)$.

Let us set $l(z) = \frac{\epsilon}{2(1-\epsilon)}z$.

Now r is a quadratic polynomial with $r(0) > 0$ and $r(\frac{p}{2}) = 0$, hence the equation

$$r(z) = l(z)$$

has an unique positive solution in z, with:

$$0 < z < \frac{p}{2}$$

Now ϕ and l are monotone and continuous, $\phi(0) = p/2 < r(0)$ hence ϕ and r meet necessarily at a point in which r decreases and afterwards ϕ dominates r, which implies:

$$\phi(z) > l(z) \iff z^* < z \iff \phi(z^*) > l(z^*).$$

So it is sufficent to find when the first inequality is true.
The relations:

1) $r(z) = l(z)$
2) $\phi(z) > l(z)$

can be rewritten as:

$$2(1-\epsilon)(p-2z)[(2-3\epsilon)z+\epsilon] = \epsilon^2(3p-2)z \tag{3.20}$$

$$[p\epsilon+(4-4\epsilon-4p+3p\epsilon)z](1-\epsilon) > \epsilon z[2-3\epsilon)z+\epsilon] \tag{3.21}$$

Now, multiplying the both sides of (3.20) by ϵ and both sides of (3.21) by $4(1-\epsilon)$ and then summing we obtain:

$$r(\xi) < l(\xi) \tag{3.22}$$

with:

$$\xi = \frac{2(1-\epsilon)\epsilon p}{Ap+B} \tag{3.23}$$

and

$$A = 3\epsilon^2 - 8\epsilon + 8$$
$$B = 6\epsilon^2 - 12\epsilon + 8$$

After some algebraic manipulations, we finally get that 3.19 is equivalent to:

$$p < \frac{4(3\epsilon^2-6\epsilon+4)}{(2-\epsilon)(3\epsilon^2-8\epsilon+8)} \tag{3.24}$$

This consideration led us to:

Theorem 3.4. The attractor of the IFS (3.1), (3.2) with $2/3 < p < 1$, is totally disconnected and perfect if and only if (3.24) holds.

First of all we establish

$$F_1(P_s) \subset Q_{I_1(s)}, \quad F_1(Q_s) \subset P_{I_1(s)} \tag{3.25}$$

where P_s and Q_s are defined as in (3.9) and (3.8) with I_1 replaced by I_2. Because of our introductory Remark it is suffices to check that

1) $\frac{d}{d\alpha} F_1(s(1), s(2) - \alpha, s(3) + \alpha)(i)\big|_{\alpha = 0}$
2) $\frac{d}{d\alpha} F_1(s(1) + \alpha, s(2), s(3) - \alpha)(i)\big|_{\alpha = 0}$

have the right sign for $i = 1, 2$.

By symmetry one obtains:

$$F_2(P_s) \subset Q_{I_2(s)}, \quad F_2(Q_s) \subset P_{I_2(s)}. \tag{3.26}$$

Now it is immediately seen that:

$$F_2(I_2) \subset F_2(Q_{s^*_{21}}) \subset P_{I_2(s^*_{21})}, \quad F_1(I_2) \subset F_1(P_{s^*_{12}}) \subset Q_{I_1(s^*_{12})}$$

and since (3.19) is equivalent to

$$P_{I_2(s^*_{21})} \cap Q_{I_1(s^*_{12})} = \emptyset$$

and by symmetry, for each $i \neq j$:

$$F_i(I_2) \cap F_j(I_2) = \emptyset,$$

hence the attractor is totally disconnected and perfect.

For the case

$$F_1(s^*_{12})(2) \leq F_1(s^*_{12})(1) \tag{3.27}$$

we will construct again a sequence $x_k = F_{i_1 \ldots i_k}(s^*_{21})$ of points in I converging to a points s in M, where each of i_h is either 1 or 2. The construction builds successively the digit i_k in the *code* of s. Let us start from the *code* 21 of the periodic point s^*_{21} and begin to substitute, starting from the left, the symbol 1 with 2 and conversely until either

1) $\Phi(\sigma 11\bar{2}\bar{1}) \in L$ but $\Phi(\sigma 12\bar{2}\bar{1}) \in R$, or
2) $\Phi(\sigma\bar{2}\bar{1}) \in L$ but $\Phi(\sigma 1\bar{1}\bar{2}) \in R$

will happen, where σ is an even list if digits 1 and 2.

It's clear that sooner or later this will happen, since substituing all the symbols of the address of s^*_{21} we obtain $s^*_{12} \in R$.

Now we keep the first digit that changed will lead us in R. (1 in case 1., 2 in case 2.) and keep on trying to change the following digit in the code. Now, either the procedure ends in a finite number of steps at a point in M, or an infinite number of digits will not be changed (because when changed the corresponding point will be in R) by continuity of Φ.

This is proved once it established that:

1) $\Phi(\sigma 12\bar{2}\bar{1} \in R \Rightarrow \Phi(\sigma 11\bar{1}\bar{2})) \in R$
2) $\Phi(\sigma 1\bar{1}\bar{2} \in R \Rightarrow \Phi(\sigma 22\bar{1}\bar{1})) \in R$

that is, keeping the symbol that changed lead us in R and changing all the following we come back in R.

Let $z_1 = F_1(s^*_{12})$ and $z_2 = F_2(s^*_{21})$ because of (3.27) we will have that: $z_1 \in P_{z_2}$ or equivalently $z_2 \in Q_{z_1}$.

1) Let $G(x) \equiv F_\sigma(F_1(x))$. It is clear that since $G(z_2) = \Phi(\sigma 12\overline{21} \in R$ then, since the number of the maps is odd and by (3.25) and (3.26), we obtain $G(z_1) = \Phi(\sigma 11\overline{12}) \in Q_{G(z_2)} \subset R$;
2) Let $G(x) \equiv F_\sigma(x)$. It is clear that $G(z_1) = \Phi(\sigma 1\overline{12}) \in R$ then, since the number of the maps is even and by (3.25) and (3.26), we obtain $G(z_2) = \Phi(\sigma 2\overline{21}) \in Q_{G(z_1)} \subset R$;

The interested reader will raise the question: what happens for $2/3 < \varepsilon < 1$. In this case we have not been able to find a simple invariant set I as in the previous case. However by a numerical experience we conjecture that for $2/3 < p < 1$ the attractor is always totally disconnected and perfect, whereas for $0 < p < 2/3$ both cases should appear, but the codes of contact points ($\overline{12}$ and $\overline{21}$ in the persistent and $1\overline{12}$ and $2\overline{21}$ in the repulsive case) seem to vary from case to case, suggesting the possibility of a more complicated behaviour.

4. Bibliography

[1] M.F. Barnsley. *Fractals Everywhere*. Academic Press, New York, 1989.

[2] M.F. Barnsley and S.G. Demko. Iterated function systems and the global construction of fractals. *Proc. Roy. Soc. London*, A(399):243–275, 1985.

[3] M.F. Barnsley, S.G. Demko, J.H. Elton, and J.S. Geronimo. Invariant measures for Markov processes arising from iterated function systems with place-dep. prob. *Ann. Inst. Henri Poincaré*, 24:367–394, 1988.

[4] W. Doeblin and R. Fortet. Sur les chaînes à liaisons complètes. *Bull. Soc. Math. France*, 65:132–148, 1937.

[5] J.H. Elton and M. Piccioni. Iterated function system arising from recursive estimation problems. Submitted, 1991.

[6] H. Furstenberg and V. Kifer. Random matrix products and measures on projective spaces. *Israël J. Math.*, 46:12–32, 1983.

[7] M. Hata. On the structure of self-similar sets. *Japan J. Appl. Math.*, 2:381–414, 1985.

[8] J.E. Hutchinson. Fractals and self-similarity. *Indiana Univ. Math. J.*, 30:713–747, 1981.

[9] M. Iosifescu and Theodorescu. R. *Random Processes and Learning.* Springer-Verlag, New York, 1969.

[10] S. Karlin. Some random walks arising in learning models. *Proc. J. Math.*, 3:725–756, 1953.

[11] J. Lamperti and P. Suppes. Chains of infinite order and their application to learning theory. *Proc. J. Math.*, 15:739–754, 1959.

[12] O. Onicescu and G. Mihoc. Sur les chaînes statistiques. *C.R. Acad. Sci. Paris*, 200:511–512, 1935.

A. Figures

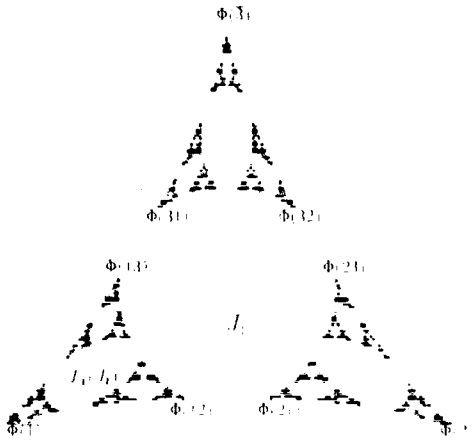

Figure A.1: Persistent chain.

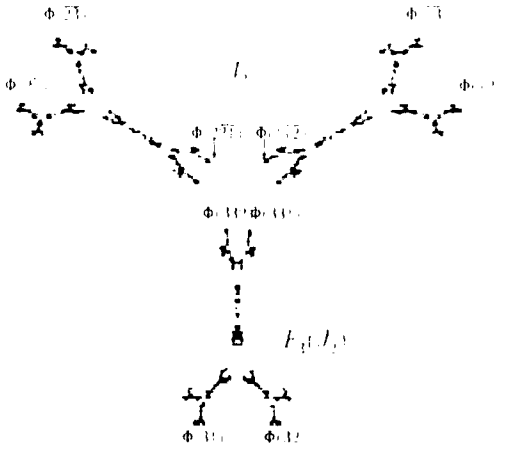

Figure A.2

Problems

1. Wavelets on H^2 (Stéphane Jaffard)

Recall that the Hardy space H^2 is the subspace of L^2 composed of functions whose Fourier transforms vanish for $\xi \leqslant 0$. The problem is to find an orthonormal basis of H^2 of the form $2^{j/2}\psi(2^j x - k)$ where ψ would be smooth and well localized (the maximal localization and smoothness possible would also have to be determined). Such a construction would be useful in mathematical analysis and signal analysis. One of the difficulties lies in the following result (cf. [2, Chapter 3]):

Theorem 1.1. There exists no multiresolution analysis on H^2 which would give a wavelet ψ such that $\hat{\psi}$ is continuous and

$$|\hat{\psi}| \leqslant C\,|\xi|^{-\alpha} \qquad \text{for any } \alpha > 1/2.$$

Thus the difficulty, if such a basis exists, lies in constructing a wavelet basis which could not be obtained through a multiresolution analysis. Such examples, even for L^2, have not been found (to our knowledge).

2. Wavelets on domains (Stéphane Jaffard)

A key point for the resolution of PDE's using wavelets is to construct wavelets which are an orthonormal basis of $L^2(\Omega)$ and bases of Sobolev spaces on the domain. The existing results are the following:

On a segment (or a square, a cube, ...) there exists an orthonormal basis of compactly supported wavelets of the form $2^{j/2}\psi(2^j x - k)$, except for N functions at each level j localized near the end points of the segment, where the function ψ has to be modified (cf. [5]). There exists such bases which are also bases for the H^s spaces or for the H^s_0 spaces; but for no other spaces (such as $H^1_0 \cap H^s$, for instance). For a general domain, there exists a similar basis with exponential decay, but all the wavelets have to be modified (though the correction exponentially decreases as a function of $2^j \operatorname{dist}(k2^{-j}, \partial\Omega)$), and they are bases of the H^s_0. A non-smooth basis which works for H^1_0 also exists (cf. [1, 4]).

Bases of the first kind which would work for more general domains, and bases, even of the second kind, but which would work for a given Sobolev space, or could be adapted to mixed boundary conditions, would be extremely useful.

J. S. Byrnes et al. (eds.), Probabilistic and Stochastic Methods in Analysis, with Applications, 687–690.
© 1992 *Kluwer Academic Publishers. Printed in the Netherlands.*

3. Bibliography

[1] S. Jaffard. Wavelet methods for fast resolution of elliptic problem. *SIAM Journal of Numerical Analysis*. To appear.

[2] S. Jaffard. PhD thesis, Ecole Polytechnique, France, 1989.

[3] S. Jaffard and Y. Meyer. Bases d'ondelettes dans des ouverts de $\mathbb{R}^n$. *Journal de Mathématiques Pures et Appliquées*, 68:95–108, 1989.

[4] P.G. Lemarié. Deux bases d'ondelettes pour un polygone de $\mathbb{R}^2$. Preprint, 1991.

[5] Y. Meyer. Ondelettes sur l'intervalle. Preprint, 1990.

4. (Hervé Queffelec)

Let N be an integer ≥ 1. Does there exist a sequence $c_1, \ldots, c_N$ with $|c_i| = 1$ and $\sup_{|z|=1} |\sum_1^N c_i z^{i^2}| \leq B\sqrt{N}$ where B is a numerical constant? Or even

$$\sup_{|z|=1} \left|\sum_1^N c_i z^{i^2}\right| = o(\sqrt{N \log N})$$

(If one takes random signs for the c_i, one gets $O(\sqrt{N \log N})$.) Or (still less demanding) can one find a sequence λ_N of positive integers, with $\lambda_{n+1} > \lambda_n$, $\lambda_{n+1} - \lambda_n \to \infty$, and for each N a sequence $(c_i)_{1 \leq i \leq N}$ of complex numbers of modulus one such that

$$\sup_{|z|=1} \left|\sum_1^N c_i z^{\lambda_i}\right| = o(\sqrt{N \log N})$$

Remark 4.1. The modified Rudin-Shapiro sequence $P_0 = Q_0 = 1$ and

$$P_{n+1}(z) = P_n(z) + z^{2^n} Q_n(z)$$
$$Q_{n+1}(z) = P_n(z) - z^{2^n} Q_n(z)$$

provides examples of sequences of integers $(\lambda_n)_{n \geq 1}$ with density zero for which there exists (c_i) with

$$\sup_{|z|=1} \left|\sum_1^N c_i z^{\lambda_i}\right| = O(\sqrt{N})$$

5. One-sided sampling (Harold Shapiro)

When a bandlimited function $f(t)$ on $\mathfrak{R}$ is sampled at equally-spaced values of t, faster than the Nyquist rate, than f (assumed, say, to belong to $L^2(\mathfrak{R})$) can be reconstructed from these samples, as is well-known, by a procedure that is stable with respect to small fluctuations in the data. Actually, the redundancy of the sampled information is so great that even the *one-sided samples*, i.e., the sample values $f(t)$ for $t > T$ (where T is any prescribed number) suffice in principle for the reconstruction of f; but now the reconstruction process leads to an ill-posed problem in the sense of Hadamard, i.e., tiny changes in the sampled values can lead to huge changes in the reconstructed f, and this instability gets worse the larger T is, and the closer the sampling rate to the Nyquist rate. The situation seems reminiscent of reconstructing a hologram from its fragment.

Before posing our question, let us recapitulate the (very well-known) ideas that substantiate what has just been said. As our basic setup, let us consider the case $T = 0$, and assume

$$f(t) = \frac{1}{2\pi}\int_{-a}^{a} \phi(\omega)e^{-i\omega t}\,d\omega$$

where a, with $0 < a < \pi$ is given and $\phi \in L^2(-a, a)$, and that the numbers

$$c_n = f(n) = \frac{1}{2\pi}\int_{-a}^{a} \phi(\omega)e^{-in\omega}\,d\omega$$

are given for integral $n \geq 0$, and that we wish to calculate f (or, what is equivalent, and more convenient for us, ϕ).

Let us define

$$\phi(\omega) = \begin{cases} \phi(\omega) & |\omega| < a \\ 0 & a \leq |\omega| \leq \pi \end{cases}$$

Then, the *uniqueness* of the reconstruction is easy: for, if $c_n = 0$ for $n \geq 0$, the Fourier coefficients of ϕ, which is in $L^2(\Pi)$ (Π being the interval $[-\pi, \pi]$, identified as the unit circle) vanish for positive n, so ϕ is the complex-conjugate of a function in the Hardy space $H^2(\Pi)$ and, vanishing for $a < |\omega| < \pi$, it vanishes identically.

To perform the reconstruction, let $\psi \in H^2(\Pi)$ be the function with Fourier expansion

$$\psi \sim \sum_{n=1}^{\infty} c_n e^{inw}.$$

Our problem is to find $\phi \in L^2(\Pi)$ such that

1) ϕ vanishes a.e. on the arc $\Gamma: a < |\omega| < \pi$ of the unit circle;
2) $\psi - \phi$ has vanishing Fourier coefficients of positive index (and hence, is of the form h where $h \in H^2(\Pi)$).

Thus, the problem reduces to finding $h \in H^2(\Pi)$ which, on the given proper sub-arc Γ of the unit circle, is equal a.e. to the known function $\psi \in L^2(\Gamma)$. This is a case of the classical problem of Carleman, to reconstruct an analytic function in a plane domain, in terms of the values on a proper part of its boundary. Many papers have been devoted to this question. It is a well-known "badly posed problem" and can be attacked numerically, e.g., by use of Tikhonov's method of regularization.

We now come to our questions. First of all, can anything similar be done if the one-sided samples are not equally spaced (but, sufficiently dense to imply uniqueness of f; conditions for this are known)? Also, how is the above-sketched solution (even in the equally-spaced case) to be modified if f is not a deterministic function but a stationary Gaussian process, and noise is present?

Index